PETROLOGICAL STUDIES OF IGNEOUS ROCKS, MAINLY FROM CONTINENTAL EXTENSIONAL ZONES

Raymond Macdonald

Doctor of Science

University of Edinburgh

1987

(Volume 1)

ABSTRACT

51 papers are presented, covering a wide range of interests in the petrology and geochemistry of igneous and metamorphic rocks. Studies on the alkaline rocks of the Gardar Province, SW Greenland, focussed on the role of the volatile phase in effecting chemical modifications during the later stages of crystallization. Volatiles also played a major role during the complex evolution of trachytic caldera volcanoes and rhyolitic dome fields of the Kenya Rift Valley. Several differentiation processes acted on magmas derived from both mantle and crust at these centres.

Work on Permo-Carboniferous volcanism in the U.K. included a review of the petrology of the Scottish lava suites; time-controlled changes in basalt chemistry; compositional heterogeneity in the mantle sources; and the geochemistry and tectonic significance of the end-Carboniferous quartz dolerite suite and the Derbyshire and Cockermouth lavas.

A major study of the chemical variation in subalkaline rhyolitic glasses examines tectonic and petrogenetic influences on the compositions of silicic melts. Studies of rhyolitic volcanism in the Coso field, California were partly aimed at determining the eruptive potential of a possible caldera-forming system. A role for selective assimilation of the magma chamber walls is invoked in the genesis of the basalt-rhyolite suite of the 1875 Askja eruption, Iceland.

Anomalous limestone-pelite successions of the northern Highlands have been assigned to a separate lithostratigraphic group, the Albynian, on petrographic and geochemical grounds. Its status to the other Caledonian supergroups is unknown. A widespread suite of metabasites within the Moines of northern Scotland is the result of a major, possibly Grenvillian, magmatic event.

Two papers deal with the distribution of types of tholeiitic basalts in southern Africa; some adjustments to the concept of Karoo geochemical provinces are made. A further two examine lamprophyric magmatism in the Southern Uplands and Lake District, discussing the likely complexity of the mantle sources for the mafic rocks, and the genetic relationships between the lamprophyres and the associated granitic rocks.

Other studies include the effects of magma rheology on xenolith transport; a review of the physical aspects of volcanic eruptions; a review of silicon geochemistry in igneous and metamorphic rocks; and various papers on igneous rocks in Maine, U.S.A., Trinidad and Saudi Arabia.

CONTENTS

	Page
INTRODUCTION	1
Statement of contributions to joint research	1
SUMMARY OF RESEARCH RESULTS	1
Alkaline rocks of the Gardar Province, SW Greenland	1
Peralkaline volcanism of the Kenya Rift Valley	3
General studies of alkaline and peralkaline rocks	6
Permo-Carboniferous volcanism in Northern Britain	6
Chemistry and petrogenesis of rhyolitic volcanic rocks	8
Igneous and metamorphic rocks of the Scottish Highlands	9
Karoo basalts of southern Africa	11
Lamprophyre dykes of northern Britain	11
Others	12
BIBLIOGRAPHY	14
SUBMITTED PUBLICATIONS	20

INTRODUCTION

The largest part of my research work has been in the petrology of igneous rocks, with smaller contributions to metamorphic and sedimentary geology. I have maintained an interest in many aspects of igneous rocks, e.g. volcanology, mineralogy, geochemistry, and the properties of magmas, and I have worked on extrusive and intrusive rocks in Greenland, Kenya, the western U.S.A. and Iceland, as well as the U.K. I summarize below the main results of my research work. This submission is made partly on the basis of the breadth of my studies.

Statement of contributions to joint research

Much of my work has been done in collaboration with various colleagues and a general statement of the nature of my contribution to such work is perhaps relevant here.

In all papers of which I am the first author, I made the largest scientific contribution, which normally involved a major role in the establishment of the project, the leading role in data interpretation and the writing of the first draft of the paper. For papers in which I am the second (or later) author, my role was varied, from supplying field or analytical data to data interpretation and/or writing of the paper. The nature of my contribution in such papers is specified below.

SUMMARY OF RESEARCH RESULTS

Alkaline rocks of the Gardar Province, SW Greenland

The basis of this work was my Ph.D. studies at Edinburgh, supervised by Dr. B.G.J. Upton, concerning the petrology and geochemistry of trachybasaltic - peralkaline rhyolitic dykes of the Tugtûtòq area. The main feature was the recognition of the importance of post-emplacement modifications of peralkaline rock chemistry, especially the loss or gain of alkalies and loss of halogens, which were poorly

appreciated at the time (Macdonald, 1969 [p. 22]; Macdonald and Edge, 1970 [p. 48]). These modifications set severe constraints on assessing petrogenetic mechanisms. Liquid lines of descent may be impossible to define quantitatively and the isotopic signatures of the source regions may be lost during isotopic exchange with groundwaters.

A natural example of a fugitive volatile phase from a peralkaline granite, frozen into gabbroic rocks of the Kûngnât complex, allowed Macdonald et al. (1973 [p. 76]) to show that it was notably enriched in K, F and H_2O, and in LREE, Li, Pb, Rb, Y, Zn, Cs, U, Th and Zr. The paper was the first record of a hydrous phase of this composition coexisting with natural peralkaline granite. In a related study, Upton et al. (1971 [p. 82]) used a series of Gardar intrusions to show that faster cooling rates had resulted in a more complete preservation of magmatic chemistry. This study was an outgrowth of ideas presented in my doctorate thesis, using a larger data base. Reaction between quartz dioritic basement rocks and alkaline solutions fugitive from a comenditic intrusion on Igdlutalik island generated a rheomorphic fenite in which grew the rare mineral, narsarsukite. Upton et al. (1976 [p.104]) described the occurrence, noting that the narsarsukite formed short prisms elongate parallel to c, in contrast to the tabular habit of earlier described occurrences. I contributed field observations and analytical data to this study.

Another mineralogical study prompted by my Ph.D. work concerned chemical variation in minerals of the astrophyllite group (Macdonald and Saunders, 1973 [p. 114]). This paper probably still stands as the most complete statement on the chemistry of this rare, but interesting, mineral; much of the credit must go to the superb analytical data of M.J. Saunders.

Peralkaline volcanism of the Kenya Rift Valley

My doctoral studies convinced me that potentially the most valuable information on peralkaline magma compositions would come from non-hydrated obsidians. At an early stage of my Postdoctoral Fellowship at the University of Reading, Dr. D.K. Bailey and I planned a programme to collect and analyze a wide range of peralkaline salic glasses and their phenocrysts, as a first step to understanding crystal $\rightleftharpoons$ liquid $\rightleftharpoons$ vapour equilibria in such rocks. Our work was concentrated in the Kenya Rift Valley and we are still actively involved in research there.

A first step was to devise projections in the system Na_2O-K_2O-Al_2O_3-SiO_2 to accommodate these complex rock compositions (Bailey and Macdonald, 1969 [p. 130]). The projections were largely developed by Dr. Bailey. My role was to test them against natural rocks. Our 1970 paper (Bailey and Macdonald, 1970 [p. 137]) used the projections to show fundamental differences between continental and oceanic comendites, the former showing quartz-feldspar cotectic characteristics indicative of an origin by crustal remelting. The oceanic varieties were probably derived by fractional crystallization and/or partial melting of basaltic rocks.

Macdonald et al. (1970 [p.150]) examined a series of peralkaline trachytic and rhyolitic obsidians from the central rift and showed that crystal $\rightleftharpoons$ liquid equilibria were alone unable to account for the compositional variation in the series. A role for an alkali-bearing vapour phase during both melting of mafic lower crust and subsequent magmatic evolution was invoked. Further information on the nature of the volatile phase was provided by Bailey and Macdonald (1975 [p. 161]). They considered it to be rich in halogens, with the metallic elements forming preferred 'complexes' with either F (e.g. Zr, Rb) or Cl (e.g. Nb, Y). This paper made the very clear suggestion that the volatile phase plays a critical, buffering role on the composition of peralkaline,

salic magmas at all stages of their generation and evolution.

Since 1970, both Lancaster and Reading have continued work in the central rift, focussing on different volcanoes but maintaining close scientific contact. With my research students, I have studied the rhyolitic dome field at Naivasha, and with Dr. L.A.J. Williams and research students, the trachytic caldera volcanoes Silali, Menengai and Suswa. Our publication rate for this work has been relatively low, for two main reasons. Firstly, its scope has been large, involving the production of large scale geological maps, and detailed petrochemical and isotopic analyses. Secondly, the exciting developments in our understanding of caldera volcanism and pyroclastic deposits over the last decade have led to continuous revision and widening of our ideas as to how these volcanic systems evolve.

Williams et al. (1984 [p.179]) reviewed information on the seven major, late Quaternary trachytic caldera volcanoes in the Rift Valley, broadly distinguishing two groups. In a northern group, basalts and mugearites form bimodal associations with trachytes. Caldera formation was accompanied by sparse pyroclastic activity and collapse may have been initiated by withdrawal of magma from depth. A southern group are overwhelmingly of trachytic composition. Krakatau-style caldera formation was accompanied by the eruption of voluminous ash flow and airfall tuffs. This paper was largely the work of Dr. Williams; I contributed the geochemical sections.

In a recent review (Macdonald, 1987 [p.197]), I summarized the philosophy of our petrological studies in the caldera volcanoes and the rhyolitic dome fields. Only by putting the complexes into a thoroughly documented time-space-composition framework, such as that of Williams et al. (1984 [p. 179]), can we hope to understand how they have evolved, and what their future eruptive history is likely to be.

The caldera volcanoes have evolved by complex interplays of crystal fractionation, magma mixing, volatile transfer and possibly liquid-state differentiation processes. The dominant process is related to the stage of structural evolution of each centre. The complexity is shown by Leat et al's (1984 [p. 218]) study of the Menengai trachytic caldera volcano. Detailed mapping, tied to a geochemical and mineralogical study of all the eruptive products, including a suite of plutonic nodules, permitted a very full reconstruction of Menengai's geochemical and structural evolution. Of particular interest was the recognition of ash flow tuffs which are extremely zoned compositionally (more than any known single eruptive unit), inferred convective rehomogenization in the magma, the rapid rates of differentiation in the reservoir, and the ubiquity of compositional zonation. This study stands as the most detailed analysis of the geochemical evolution of a peralkaline trachyte volcano yet published. Although most of the work was Leat's, my contribution was in guiding the direction of the project, and in aspects of interpretation of the chemical data, e.g. the role of magma mixing.

Macdonald (1987 [p. 218]) has proposed that the main difference between the development of the northern and southern groups of calderas was in the formation of a stable, volatile-rich cap in the latter. This influenced the types of differentiation which were operative, and hence the geochemical evolution and eruptive styles of the calderas.

In a recent attempt to promote further the role of the volatile phase, Bailey and Macdonald (1987 [p. 240]) have suggested that a wide range of peralkaline felsic magmas from the central rift were generated by melting of different sources during the influx of a CO_2 rich fluid. Trachytes, pantellerites and comendites are the products of a flux/melting cycle climbing progressively through mantle, mafic deep crust, and sialic crust. I contributed data and some ideas to this project,

but the philosophy and insight are undoubtedly Ken Bailey's.

General studies of alkaline and peralkaline rocks

My experience with peralkaline rocks led in the mid-70's to a series of review articles. Macdonald and Bailey (1973 [p. 262]) compiled, for the U.S. Geological Survey Data of Geochemistry Series, analytical data for peralkaline silicic obsidians. It aimed to provide a sound basis for further studies of peralkaline silicic magmatism.

At the IAVCEI meeting in Catania, 1971, D.K. Bailey, F. Barberi and I were invited to put together a special issue of the Bulletin Volcanologique on peralkaline silicic magmatism (Bailey et al., 1974). The roles of commissioning and editing the papers, and writing an overview paper (Macdonald et al., 1974 [p. 301]), were divided between the three editors. I also wrote two reviews for the volume [pp. 310, 339], one on the chemistry and classification of peralkaline oversaturated rocks, the other on their tectonic setting, showing that although such rocks occur predominantly in continental rift settings, they are also found in a wide range of other settings, such as subduction zones and oceanic islands.

In 1974, I published, in H. Sørensen's "The Alkaline Rocks", a review of the role of fractional crystallization in the genesis of alkaline rocks [p. 358]. The review drew heavily on my Greenland studies, and on the obsidian work at Reading, to show that crystal $\rightleftharpoons$ liquid processes have had a major role in generating the spectrum of common alkaline rocks.

Permo-Carboniferous volcanism in Northern Britain

This research was, in one sense, a continuation of the Greenland and Kenyan work, i.e. alkaline volcanism in a rift valley setting (the Scottish Midland Valley). In 1972, I initiated a geochemical programme

on the Upper Palaeozoic volcanic rocks of central and southern Scotland. Though these rocks represent one of the most diverse suites of igneous rocks in any magmatic province of comparable size, little chemical research on these rocks post-dated 1940. In 1982, the study was extended into N. England, partly in collaboration with colleagues at the Open University.

Macdonald (1975 [p. 378]), an invited Carnegie review article, outlined the multi-lineage character of the Scottish Dinantian suites, the evidence for polybaric chemical evolution, and the petrological character of the rocks in modern terms. It has fulfilled its aim as the basis of all subsequent geochemical studies. Time-controlled changes in basalt chemistry in the Midland Valley province in the Carboniferous and Permian were related by Macdonald et al. (1977 [p. 424]) to two thermal cycles, each of which produced a similar trend towards increasing silica-undersaturation with time.

The paper by Macdonald (1980 [p. 436]) presented the first trace element data for the Midland Valley volcanic rocks. The spectrum of mafic rocks from hypersthene-normative basalts to strongly undersaturated, nephelinitic varieties was formed by varying degrees of equilibrium partial melting of a phlogopite peridotite mantle which was broadly similar to that from which oceanic alkaline basalts are currently being generated. The mantle sources were heterogeneous as regards distribution of the incompatible trace elements. The first modern geochemical study of the late Carboniferous quartz dolerite dyke swarms (Macdonald et al., 1981 [p. 449]) revealed evidence for the polybaric evolution of the magmas; variable source compositions; along- and across-dyke compositional variations; and compositional links with the lowest "Permian" lavas of the Oslo Rift, Norway.

Geochemical studies of the classic Carboniferous sequences of Derbyshire (Macdonald et al., 1984 [p.467]) established that the basalts ranged from nepheline - to quartz - normative types and were derived by varying degrees of partial melting of heterogeneous mantle sources followed by final equilibration within the lower crust. Magmas generated in isolated mantle pockets rose to the surface through crust attenuated by lithospheric stretching. A compositionally similar sequence of lavas is exposed near Cockermouth, Cumbria (Macdonald and Walker, 1985 [p.480]), dominated by quartz-normative tholeiites. Minor tholeiitic andesites were recorded for the first time in the English Carboniferous. There is no evidence in the chemistry of the Cockermouth lavas that the Iapetus suture underlies the Northumberland Basin.

Thorpe and Macdonald (1985 [p.486]) used trace element evidence to show that the Whin Sill complex of northern England was fed by a large number of compositionally distinct magma pulses. Certain of the associated "whin dykes" may have formed feeders for the Sill. The research for this project was equally shared by the two authors, Dr. Thorpe wrote the first draft of the manuscript.

Chemistry and petrogenesis of rhyolitic volcanic rocks

Since 1975, I have worked with the U.S. Geological Survey in a study, financed by them, of the chemical variation in rhyolitic glasses and its significance for their origin. The work has assembled the largest data base of its kind, and the study will be published as a USGS Professional Paper (Macdonald et al., in press, [p.495]). We feel that it is the most detailed assessment of the factors providing the spectrum of rhyolite compositions. The paper includes: tectono-magmatic discrimination diagrams for high-silica rhyolites based on stable element distributions; chemical variations related to increasing

maturity of continental crust; assessment of variations related to different genetic mechanisms; chemical criteria distinguishing crystal $\rightleftharpoons$ liquid dominated systems from more complex systems involving a volatile phase; systematic element by element description, providing a 'magmatic' data base for further studies. We hope that this paper will prove to be a starting point for geochemical studies of the granite clan.

As a spin-off from this programme, I collaborated with USGS geologists on studies of the geochemical evolution of the Coso volcanic field, California (Bacon et al., 1981 [p. 501]). The high-silica rhyolite domes and lava flows of this complex are an example of the early stages of evolution of a silicic magmatic system of substantial size and longevity. The field is potentially hazardous and may evolve to the stage of catastrophic caldera collapse. My main roles in the project were provision of analytical data and helping to interpret the geochemical information.

Another coproject with the USGS, and with the Universities of Cambridge, Rhode Island and the Open University, was a study of the products of the 1875 eruption of Askja, Iceland (Macdonald et al., 1987 [p. 520]). Perhaps the most interesting result was that the rhyolitic members of the eruption had formed by a dual process; fractional crystallization of the associated mafic rocks plus selective assimilation of elements (e.g. Rb, Cs, ^{18}O) from the hydrothermally altered granitoid wall rocks at the magma chamber walls. This is apparently the first record of such contamination in the silicic products of an oceanic island.

Igneous metamorphic rocks of the Scottish Highlands

This work has been conducted in collaboration with the British Geological Survey. My role was to provide, and to help interpret,

the analytical data for a wide-ranging series of projects. These included the first detailed description of one of the granitoid, late Caledonian vein complexes of the Great Glen (Fettes and Macdonald, 1978 [p.568]). We stressed, inter alia, the role of accessory phases in granite evolution, and compositional modifications resulting from loss of a volatile phase.

Rock et al. (1985 [p.592]) synthesized the geology and geochemistry of widespread metabasites in the Moinian outcrop of northern Scotland, the results of a major, possibly Grenvillian, magmatic event (or events) not perhaps fully appreciated yet in U.K. geology.

In a set of papers, Rock et al. (1984 [p.611], 1986a,b [pp. 640,664]) discussed the problem of anomalous local limestone-pelite successions within the Moine outcrop. Metamorphic limestones of the Great Glen area were shown by Rock et al. (1984 [p. 611]) to be neither Dalradian, Moinian or Lewisian in age. They were assigned to a separate, provisional lithostratigraphic assemblage, whose relationship to the above supergroups remained to be established. Rock et al. (1986 [p. 640]) termed this separate unit the "Albynian", suggesting that it might lie between (or be diachronous with) some part of the Moine or Dalradian successions. They showed that the Glen Urquhart pelite-metamorphic complex probably belonged to the Albynian. Rock et al. (1986 [p. 664]) extended the geochemical study of the pelites to other Highland occurrences. Some were assigned to the Dalradian, others to the Albynian, while certain sillimanite-gneisses were shown to be restites.

The status of the Albynian is an exciting question in Highland geology. For example, if it is transitional between the Moine and Dalradian, it may begin to solve the difficult problem of the 'Old Moine'/'Young Moine'/Dalradian controversy.

Rock and Macdonald (1986 [p.684]) report on a lens of pelites, carbonate rocks and amphibolites from the Moines of the Ross of Mull. They may represent a hot spring environment during deposition of the Moine.

Karoo basalts of southern Africa

Cox et al. (1967 [p.695]) recognized that the Karoo basalts are divisible into two distinct provinces. A southern province consists of normal tholeiitic basalts, while a northern province contains tholeiites abnormally high in K, Ti, P, Ba, Sr and Zr. Whether the differences were due to variations in the source materials or to differing magmatic histories, was not known. Later workers ascribed them to heterogeneous mantle sources, a point pursued by Macdonald et al. (1983 [p.719]) in a study of Karoo basalts of southern Malawi. The Malawi data also required a modification of the concept of Karoo provinces. The northern province may now be seen as areas where the K-enriched rocks occur, even though they may be accompanied by 'normal' (southern province) tholeiites. My role in Cox et al. (1967 [p. 695]) was essentially analytical, providing chemical data on northern province lavas.

Lamprophyre dykes of northern Britain

A recent interest has been in Caledonian lamprophyric dykes of southern Scotland and northern England. These dykes represent an important, but neglected, aspect of Caledonian magmatism, providing information on such topics as the nature of the mantle sources of Caledonian magmas, the genesis of the granites, and the position of the Iapetus suture. Macdonald et al. (1985 [p.729]) provided the first published attempt to analyze in detail the nature of the mantle sources of mafic lamprophyres of calc-alkaline affinity. A multi-component origin was

proposed, with contributions from a depleted mantle source, an H_2O-rich subduction zone component, and a CO_2-rich phase thought to result from the degassing of the mantle after ocean closure.

The Newmains dyke, near Dumfries, is a differentiated intrusion which carries, in miniature, petrogenetic implications widely applicable to the British Caledonian granites. The lamprophyric components of the dyke possibly represent the mafic precursors to the silicic rocks; they generated syenitic and granitic residua mainly by crystal fractionation, though a volatile phase separated and metasomatically enriched the country rocks in K, Ba and Rb. The residua were themselves contaminated by ^{87}Sr from these country rocks (Macdonald et al., 1986 [p. 739]).

Others

The paper by Sparks et al. (1977 [p.751]) and Wilson et al. (1987 [p. 756]) represent an interest with which I have flirted for many years and which will certainly be a major, future research concern - physical volcanology. Sparks et al. (1977 [p. 751]) examined some of the consequences for the transport of xenoliths in magmas if a Bingham model is assumed for magma rheology. One such consequence is that xenolith transport is favoured by slow rates of ascent, appropriate to development of a yield strength, rather than the fast rates commonly assumed. I contributed the petrological sections of this paper.

Wilson et al. (1987 [p. 756]) is a review invited by the Annual Review of Earth and Planetary Sciences. It is a concise, but we feel comprehensive, outline of how the physical sciences have contributed to our understanding of magmatic, especially eruptive, processes. The paper was largely written by Dr. Wilson. My main contributions were in the section on magma availability and eruption onset.

The article on silicon geochemistry (Macdonald, 1983 [p. 768]) was an invited book chapter. It assesses the major processes which result in Si transport from mantle to crust, and within the crust, and describes Si distribution in mantle and crustal rocks and minerals.

"The Evolution of the Crystalline Rocks" (Bailey and Macdonald (eds.), 1976 [p. 806]) was an attempt to review developments in the experimental petrology of igneous and metamorphic rocks up to the mid-70s. The rationale of the book is discussed in the preface.

Among "one-off" studies may be included that on the Old Red Sandstone of Kintyre (Friend and Macdonald, 1968 [p.810]), an outgrowth of my B.Sc. mapping project: a study of minor intrusions in Maine, USA (Gottfried et al., 1984 [p.828]), in which I interpreted the geochemical data: and Cretaceous tholeiites from Trinidad (Wadge and Macdonald, 1985 [p. 853]) for which I supplied the geochemistry. The paper on the Jebel Thurwah ophiolite complex (Nassief et al., 1984 [p.865]) was based on a Ph.D. thesis which I supervised, but owes much to Professor Gass's knowledge of Saudi Arabian geology.

PUBLICATIONS*

1967 Cox, K.G., Macdonald, R., Hornung, G. Petrographic and geochemical provinces of the Karroo basalts of Southern Africa. Amer. Miner., v. 52, 1451-74. [p.695]

1968 Friend, P.F., Macdonald, R. Stratigraphy, volcanic sediments and tectonic setting of the Lower Old Red Sandstone of Southern Kintyre. Scott. J. Geol. v. 4, 265-82. [p.810]

1969 Bailey, D.K., Macdonald, R. Alkali-feldspar fractionations trends and the derivation of peralkaline liquids. Amer. J. Sci., v. 267, 242-8. [p.310]

Macdonald, R. The petrology of the alkaline dykes of the Tugtutôq area, S. Greenland. Bull. geol. Soc. Denmark, v. 19, 257-82. [p.22]

Macdonald, R., Gibson, I.L. Pantelleritic obsidians from the volcano Chabbi (Ethiopia). Contr. Min. Petrol., v. 24, 239-44. [p.255]

1970 Bailey, D.K., Macdonald, R. Petrochemical variations among mildly peralkaline (comendite) obsidians from the oceans and continents. Contr. Min. Petrol., v. 28, 340-51. [p.137]

Macdonald, R. Mid-Gardar feldspathoidal dykes from the Tugtutoq area, S. Greenland. Bull. geol. Soc. Denmark, v. 20, 64-66. [p.74]

Macdonald, R., Bailey, D.K., Sutherland, D.S. Oversaturated peralkaline glassy trachytes from Kenya. J. Petrol., v. 11, 507-17. [p.150]

Macdonald, R., Edge, R.A. Trace element distribution in alkaline dykes of the Tugtutoq region, S. Greenland. Bull. geol. Soc. Denmark, v. 20, 38-58. [p.48]

Macdonald, R., Parker, A. Zirconium in alkaline dykes from the Tugtutoq region, S. Greenland. Bull. geol. Soc. Denmark, v. 20, 59-63. [p.69]

* page no. in square brackets refer to thesis

1971 Upton, B.G.J., Thomas, J.E., Macdonald, R. Chemical variation within three alkaline complexes in South Greenland. Lithos. v. 4, 163-84. [p.82]

1973 Macdonald, R., Bailey, D.K. The chemistry of the peralkaline oversaturated obsidians. U.S. Geol. Surv. Prof. Paper (Data of Geochemistry Series). 440-N. Part 1. [p.262]

Macdonald, R., Saunders, M.J. Chemical variations in minerals of the astrophyllite group. Miner. Mag., v. 39, 97-111. [p.114]

Macdonald, R., Upton, B.G.J., Thomas, J.E. Potassium and fluorine-rich hydrous phase coexisting with peralkaline granite in South Greenland. Earth Planet, Sci. Letters, v. 18, 217-222. [p.76]

1974 Bailey, D.K., Barberi, F. and Macdonald, R. (editors). Oversaturated peralkaline silicic rocks. Bull. Volcanol. 38, Part 3 (Special Issue).

Macdonald, R., Bailey, D.K., and Barberi, F. Recommendations for further studies on the peralkaline oversaturated volcanic rocks. Bull. Volcanol. 38, 828-836. [p.301]

Macdonald, R. The role of fractional crystallisation in the origin of the alkaline rocks. In Sørensen, H., editor, The Alkaline Rocks. John Wiley & Sons, London and New York, 442-459. [p.358]

Macdonald, R. Nomenclature and petrochemistry of the peralkaline oversaturated volcanic rocks. Bull. Volcanol. 38, 498-516. [p.310]

Macdonald, R. Tectonic setting and magma associations. Bull. Volcanol. 38, 575-593. [p.339]

1975 Bailey, D.K., Macdonald, R. Fluorine and chlorine in peralkaline liquids and the need for magma generation in an open system. Miner. Mag. 40, 405-414. [p.161]

Macdonald, R. Review article: Petrochemistry of the Early Carboniferous (Dinantian) lavas of Scotland. Scott. J. Geol. 11, 269-314. [p.378]

Upton, B.G.J., Macdonald, R. The Garleton Hills, Traprain Law and Kidlaw, East Lothian. in G.Y. Craig and P. McL. D. Duff (eds) The Geology of the Lothians and South East Scotland, p. 69-78. Scottish Academic Press, Edinburgh.

1976 Bailey, D.K., Macdonald, R. (editors). Experimental Petrology. Academic Press, London. [p.806]

Upton, B.G.J., Macdonald, R., Hill, P.G., Jefferies, B. and Ford, C.E. Narsarsukite: a new occurrence in peralkaline trachyte, South Greenland. Miner. Mag. 40, 737-746. [p.104]

1977 Macdonald, R., Thomas, J.E. and Rizzello, S.A. Variations in basalt chemistry with time in the Midland Valley province during the Carboniferous and Permian. Scott. J. Geol. 13, 11-22. [p.424]

Sparks, R.S.J., Pinkerton, H. and Macdonald, R. The transport of xenoliths in magmas. Earth Planet. Sci. Letters 35, 234-238. [p.751]

1978 Fettes, DJ., and Macdonald R. The Glen Garry vein complex, Inverness-shire. Scott. J. Geol. 14, 335-58. [p.568]

1980 Macdonald, R. Trace element evidence for mantle heterogeneity beneath the Scottish Midland Valley in the Carboniferous and Permian. Phil. Trans. R. Soc. Lond. A297, 245-57. [p.436]

1981 Bacon, C.R., Macdonald, R., Smith, R.L., Baedecker, P.A. Pleistocene high-silica rhyolites of the Coso volcanic field, Inyo County, California. J. geophys. Res. 86, 10223-41. [p.501]

Macdonald, R., Gottfried, D., Farrington, M.J., Brown, F.W., Skinner, N.G. Geochemistry of a continental tholeiite suite: late Palaeozoic quartz dolerite dykes of Scotland. Trans. R. Soc. Edinb.: Earth Sci. 72, 57-74. [p.449]

1983 Macdonald, R. Silicon in igneous and metamorphic rocks. In Aston, S.R. editor, Silicon Geochemistry and Biogeochemistry, 1-37. Academic Press, London. [p.768]

Macdonald, R., Crossley, R ., Waterhouse, K.S. Karroo basalts of southern Malawi and their regional petrogenetic significance. Miner. Mag. 47, 281-9. [p.719]

Williams, L.A.J., Macdonald, R., Leat, P.T. Magmatic and structural evolution of the central part of the Kenya Rift. Proc. Regional Seminar on Geothermal Energy in E. and S. Africa, 61-67. UNESCO/USAID. [p.171]

1984 Gottfried, D., Macdonald, R., Sutter, J., Pavlides, L. Geochemical features and $^{40}Ar/^{39}Ar$ age of tholeiitic and mafic-alkaline dikes from Aroostook County, north east Maine. U.S. Geol. Surv. Bull. 1612, 23 p. [p.828]

Leat, P.T., Macdonald, R., Smith, R.L. Geochemical evolution of the Menengai caldera volcano, Kenya. J. geophys. Res. 89, 8571-92. [p.218]

Macdonald, R., Gass, K.N., Thorpe, R.S., Gass, I.G. Geochemistry and petrogenesis of the Derbyshire Carboniferous basalts. J. geol. Soc. London 141, 147-159. [p.467]

Nassief, M.O., Macdonald, R., Gass, I.G. The Jebel Thurwah upper Proterozoic ophiolite complex, western Saudi Arabia. J. geol. Soc. London 141, 537-546. [p.865]

Rock, N.M.S., Jeffreys, L.A., Macdonald R. The problem of local anomalous limestone-pelite successions within the Moine outcrop. I. Limestones of the Great Glen area, from Ardgour to Nigg. Scott. J. Geol. 20, 283-306. [p.611]

Williams, L.A.J., Macdonald, R., Chapman, G.R. Quaternary caldera volcanoes of the Kenya rift. J. geophys. Res. 89, 8553-70. [p.179]

1985 Macdonald, R., Thorpe, R.S., Gaskarth, J.W. and Grindrod, A.R. Multi-source origin of Caledonian lamprophyres of N. England. Miner. Mag. 49, 485-494. [p.729]

Macdonald, R. and Walker, B.H. Geochemistry and tectonic significance of the Lower Carboniferous Cockermouth lavas, Cumbria. Proc. Yorks. Geol. Soc. 45, 141-146. [p.480]

Rock, N.M.S., Macdonald, R., Walker, B.H., May, F., Peacock, J.D., Scott, P. Intrusive metabasite belts within the Moine assemblage, west of Loch Ness, Scotland: evidence for metabasite modification by country rock interactions. J. geol. Soc. London 142, 643-661. [p.592]

Thorpe, R.S. and Macdonald, R. Geochemical evidence for the emplacement of the Whin Sill complex of northern England. Geol. Mag. 12, 389-396. [p.486]

Wadge, G. and Macdonald, R. Cretaceous tholeiites of the northern continental margin of South America: the Sans Souci Formation of Trinidad. J. geol. Soc. London 142, 297-308. [p.853]

1986 Macdonald, R., Rock, N.M.S., Rundle, C.C., Russell, O.J. Relationships between late Caledonian lamprophyric, syenitic and granitic magmas in a differentiated dyke, southern Scotland. Miner. Mag. 50. [p.739]

Rock, N.M.S. and Macdonald, R. Petrology, chemistry and origin of a peculiar lens of pelites, 'limestones' and possible paraamphibolites from the Moines of the Ross of Mull, Scotland. Proc. Geol. Assoc. 97, 249-258. [p.684]

Rock, N.M.S., Macdonald, R., Drewery, S.E., Pankhurst, R.J., Brook, M. Pelites of the Glen Uquhart serpentinite-metamorphic complex, west of Loch Ness (Anomalous local limestone-pelite successions within the Moine outcrop: III). Scott. J. Geol. 22, 179-202. [p.611]

Rock, N.M.S., Macdonald, R., Jeffreys, L.A. Metamorphic limestones of the Great Glen area: a reply. Scott. J. Geol. 22, 140-144. [p.635]

Rock, N.M.S., Macdonald, R., Szucs, T., Bower, J. The comparative geochemistry of some Highland pelites (Anomalous local limestone-pelite successions within the Moine outcrop: II). Scott. J. Geol. 22, 107-126. [p.664]

n press

Bailey, D.K. and Macdonald, R. Dry peralkaline felsic liquids and carbon dioxide flux through the Kenya rift zone. In Mysen, B.O., editor, Magmatic Processes: Physiochemical Principles. The Geochemical Society Spec. Publ. 1 (1987). [p.240]

Macdonald, R. Quaternary peralkaline silicic rocks and caldera volcanoes of Kenya. In Fitton, J.G. and Upton, B.G.J., editors, Alkaline Igneous Rocks. Geol. Soc. London Spec. Publ., 329-349 (1987). [p.218]

Macdonald, R., Smith, R.L. and Thomas, J.E. The chemistry of the subalkaline silicic obsidians. U.S. Geol. Surv. Prof. Paper. [p.495]

Macdonald, R., Sparks, R.S.J., Sigurdsson, H., Mattey, D.P., McGarvie, D.W., Smith, R.L. The 1875 eruption of Askja volcano, Iceland: fractional crystallization and selective contamination in rhyolite genesis. Miner. Mag. 51 (June, 1987). [p.520]

Wilson, L., Pinkerton, H., Macdonald, R. Physical processes in volcanic eruptions. Ann. Rev. Earth Planet. Sci. 15, 73-95 (1987). [p.756]

SUBMITTED PUBLICATIONS

ALKALINE ROCKS OF THE GARDAR PROVINCE, SW GREENLAND

THE PETROLOGY OF ALKALINE DYKES FROM THE TUGTUTOQ AREA, SOUTH GREENLAND

RAYMOND MACDONALD

MACDONALD, R.: The petrology of alkaline dykes from the Tugtutôq area, South Greenland. *Bull. geol. Soc. Denmark*, vol. 19, pp. 257–282. Copenhagen, December 17th, 1969.

Intermediate to acid alkaline dykes of Gardar age from the Tugtutôq region, South Greenland, form an almost continuous series from trachydolerites through hastingsite- and riebeckite-bearing microsyenites to riebeckite and aegirine microgranites. Chemically, the series shows a transition from anorthite- and nepheline-normative types to acmite- and quartz-normative varieties. Though the dykes are thought to have been ultimately derived by fractionation of basaltic magma, several processes have tended to alter the original liquid compositions, including loss of a vapour phase, devitrification of the acid dykes, alkali-ion exchange effects and alteration of amphibole. The evolutionary trends of the magmas cannot therefore be closely defined.

The rocks which form the basis of the study were collected on the islands of the Tugtutôq region, South Greenland (figs 1 a, b) where they occur as dykes, intruded during the *Gardar* period, the youngest division of the Precambrian in South Greenland. Reviews of the chronology and geological history of the Precambrian in this part of Greenland have been presented by Bridgwater (1965), Berthelsen and Noe-Nygaard (1965) and details of Gardar igneous activity in the Tugtutôq area were given by Upton (1962, 1964 a); the sequence of events is summarised in table 1.

Intrusion of the various Gardar igneous rocks was connected with large-scale faulting of the region. The dyke swarms which are of particular interest here, those trending NE-ENE, are parallel to pre-existing structures in the granitic basement and show no radial grouping around any plutonic centre. The complexes were formed at high crustal level and probably underlay alkaline central volcanoes, while the dykes, in view of their abundance, almost certainly acted as feeders to surface volcanism. Trachytic lava flows (rhomb-porphyries) have been described by Stewart (1964) from the Ilímaussaq peninsula, occurring near the top of a thick sequence of mildly alkaline olivine basalts. These Gardar lavas, preserved in the eastern part of the province, represent relatively early Gardar volcanism. It is not yet clear whether the trachytic lavas were produced by fissure eruption or from one of the central volcanoes.

Gardar volcanism involved generation and uprise of olivine basalt magma much of which had a composition close to the critical plane of silica-undersaturation (Upton, in press). The dykes under discussion are the

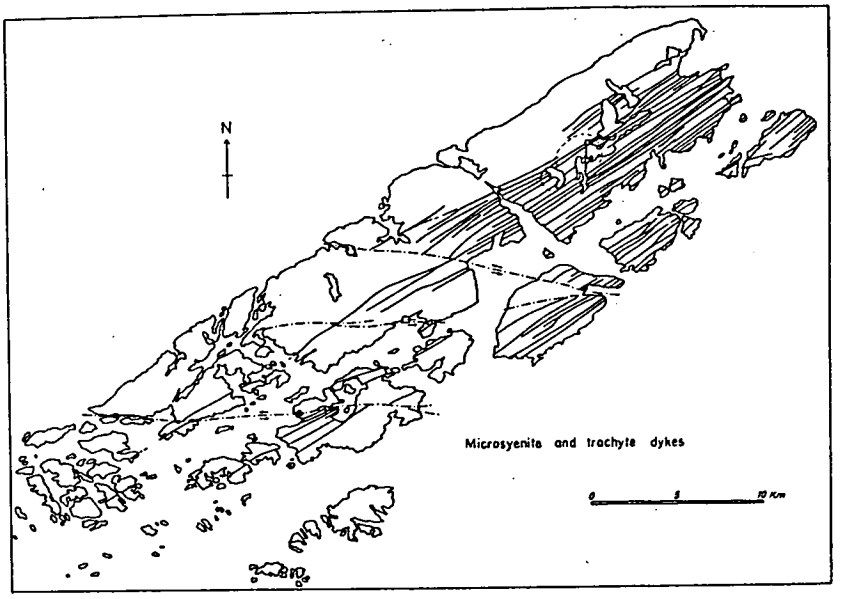

a

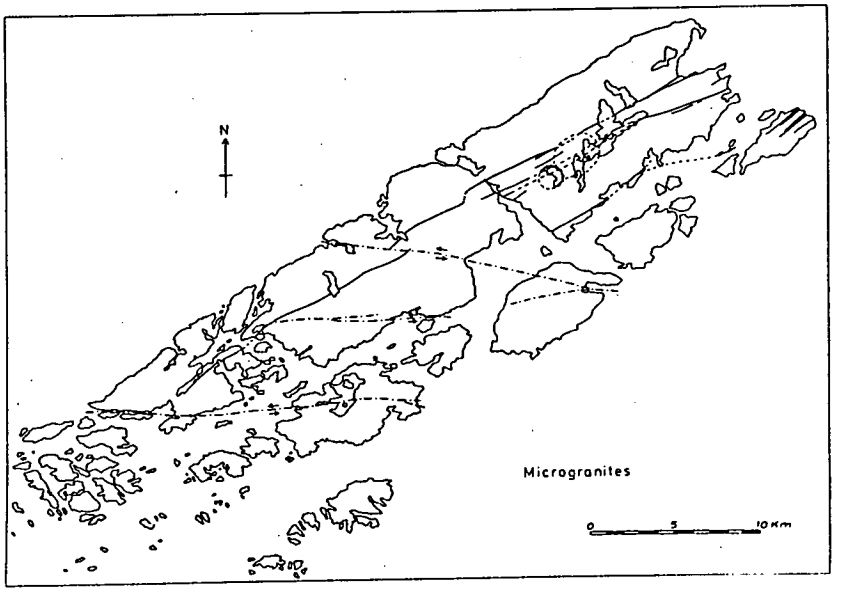

b

Fig. 1. Distribution of (a) microsyenite and (b) microgranite dykes on Tugtutôq. From Upton (1964a).

Table 1. Sequence of Gardar igneous events in the Tugtutôq region

Late	Camptonitic dolerite dykes Small trachytes Intrusion of Central Complex ? Formation of diatremes
Mid	Large numbers of dykes on ENE trend Krydsø and Assorutit intrusions Doleritic/gabbro dykes, including 'giant-dykes'
Early	Hviddal composite dyke Thin ENE-WSW dolerites NW–SE olivine dolerites

more salic representatives of the intense dyke swarm encountered in granitic basement rocks on and around the eastern part of Tugtutôq. The abundant basic dykes of the region are not considered further, although it is assumed that the basaltic magmas that fed them were parental to the salic magmas, and that olivine-plagioclase fractionation plus subordinate clinopyroxene-ilmenomagnetite fractionation within the crust have played a major part in their evolution. Trachydoleritic dykes compositionally intermediate between the dolerite/gabbroic dykes and the microsyenitic (or trachytic) dykes also occur in considerable abundance. Generally these, and the dolerite/gabbro dykes, are found to precede the salic dykes.

One aim of this study was to examine closely evolutionary trends in the acid dykes, when alkali feldspar is thought to have been the dominant fractionating phase. Thirty new analyses of the dyke rocks and six new analyses of alkali feldspar phenocrysts have been made. In terms of composition the analysed dykes form an almost continuous series from the rocks of trachydoleritic affinities, through microsyenites (or trachytes) to riebeckite and aegirine microgranites. The normal index minerals of peralkalinity, such as riebeckite, are entirely absent from the more basic members of the suite, and chemically the series passes from silica-undersaturated to -oversaturated types and from anorthite-normative to acmite-normative varieties. Despite their continuity as a series, the dykes may have been intruded over a considerable time interval, very approximately around 1150 m. y. ago (Bridgwater, 1965) and certainly belong to a number of swarms. It is a basic assumption of this paper in grouping together members of different swarms, that each swarm has been derived from a similar source and shared a common evolutionary history.

Field data for the dykes may be found in Upton (1962, 1964 a). The dykes normally have chilled margins except in composite dykes where they have been intruded into a still-hot earlier component, and no evidence has been found for metamorphosed contacts, or for wall-rock contamination. In the composite dykes, with the exception of the remarkable feldspathic dykes or 'big feldspar dykes' (BFDs) (Bridgwater 1967, Bridgwater &

Harry, 1968), the younger central components are invariably more acidic than the initial intrusion.

No work on the BFDs of the Tugtutôq area has been done, in order to avoid overlap with Dr Bridgwater's study. These large, composite dykes are unusual in that they have earlier, alkali-rich (microsyenite) margins and later more basic (trachydoleritic or doleritic) centres. Though the centre may be chilled against the margins, normally there is complete gradation across the dykes. The chemical trends across the dykes are closely comparable to those in the other Gardar bodies, as shown on Σ Fe-Mg-alkalis diagrams (Bridgwater & Harry, 1968), and the BFDs seem to provide evidence of the existence of magma bodies differentiated prior to intrusion of the dykes.

Petrography

The petrography of the dykes is summarised in table 2 and modes of analysed specimens listed in table 3 (pp. 275–276). Reaction series in the ferromagnesian minerals of the dykes are shown in fig. 2.

The trachydolerites used in this work, which are virtually aphyric, are not typical of the Gardar trachydolerites, which normally contain phenocrysts of sodic plagioclase, clinopyroxene and ore.

The trachydolerites and more basic microsyenites are typically holocrystalline except for the fine-grained marginal facies that are suspected of having originally been glass. With increasing richness in silica, however, increasing degrees of supercooling seem to have characterised the dykes, and the more acid dykes commonly show felsitic or spherulitic textures suggesting that they were predominantly glassy at first, acquiring their present textures by subsequent devitrification. The centres of the thicker acid dykes show microgranitic or granophyric textures.

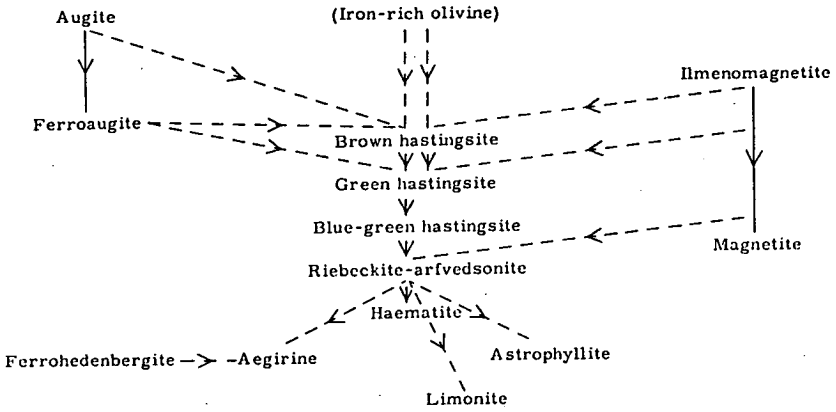

Fig. 2. Reaction series in the ferromagnesian minerals of the dykes.

Table 2. Summary of petrography of Tugtutôq alkaline dykes

Rock Group	Phenocrysts	Groundmass
Trachydolerites	Scarce apatites	Cryptoperthitic feldspar (occasional oligoclase cores,) biotite, augitic pyroxene, ore, apatite. Textures – generally orthophyric.
Hastingsite microsyenites	Alkali feldspar (anorthoclase microperthite), fayalite pseudomorphs, pyroxene (augite-ferroaugite), ore, apatite, scarce hastingsite	Microantiperthitic feldspar, with occasional albite rims, hastingsite, riebeckite-arfvedsonite, limonite, ore, quartz, pyroxene, apatite, carbonate. Occasional vugs. Textures – trachytic.
Riebeckite microsyenites	Microperthitic feldspar Ore	Microantiperthitic feldspar, riebeckite-arfvedsonite, ore, limonite, quartz, zircon. Textures – trachytic, felsitic, spherulitic.
Riebeckite microgranites	Antiperthitic feldspar, quartz, ore, riebeckite-arfvedsonite (or aegirine aggregates pseudomorphing it).	Microantiperthitic feldspar, riebeckite-arfvedsonite, aegirine, ore, zircon, limonite, fluorite, astrophyllite. Textures – trachytic, spherulitic, felsitic, granophyric, microgranitic.
Aegirine microgranites	Antiperthitic feldspar, quartz, hedenbergite, fayalite pseudomorphs	Aegirine, microperthitic feldspar, quartz, riebeckite-arfvedsonite, astrophyllite. Textures – felsitic, trachytic, spherulitic.

Petrochemistry

The distribution of the major elements in the dyke suite has been summarised in variation diagrams (fig. 3), using as abcissa the sum of the normative components, q + or + ab+ ac+ ns, which for convenience is termed the Fractionation Index (FI). This expression is merely a modification of the Differentiation Index of Thornton and Tuttle (1960), and reflects the observation of Bailey and Schairer (1964) that peralkaline felsic liquids fractionate not towards petrogeny's residua system but towards eutectics enriched in alkali silicate relative to that system.

The variation diagrams (fig. 3) show that with increasing Fractionation Index there is a regular decrease of MgO, CaO, TiO_2, and P_2O_5, and an overall decrease in $FeO+Fe_2O_3$ and MnO. Al_2O_3 falls steadily from the point where alkali feldspar first occurs as phenocrysts. The distribution of the alkalis is complex and is discussed in detail below. SiO_2 shows an overall increase from 49 to 76 %, but reaches a maximum in the riebeckite microgranites and declines slightly in the aegirine microgranites. The curve shows scarcity of specimens in the range 66–71 % SiO_2. As only 33 analyses of the dykes have been plotted in fig. 3, it might be argued that the composition gap is the result of insufficient sampling. A histogram for

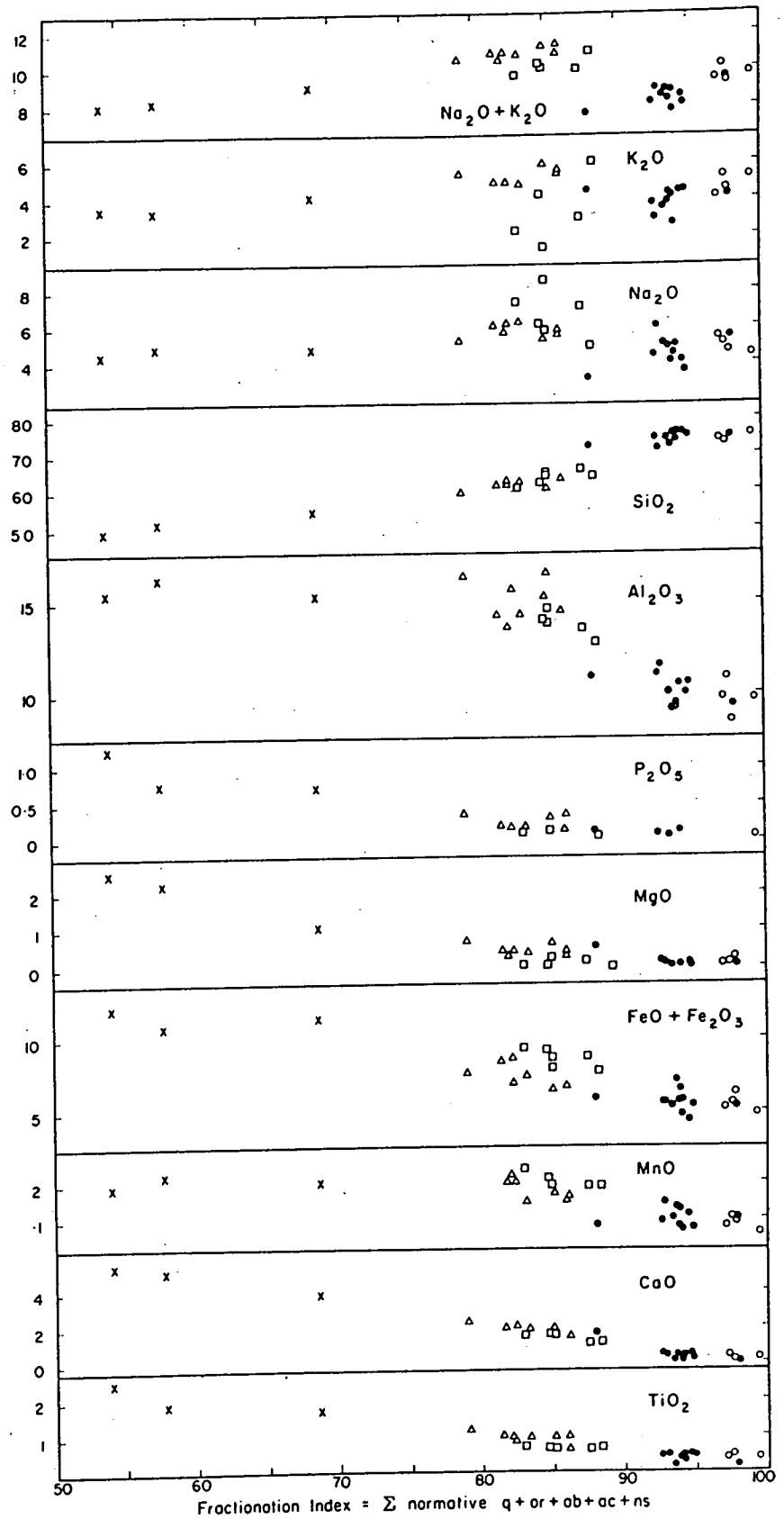
$Na_2O + K_2O$
K_2O
Na_2O
SiO_2
Al_2O_3
P_2O_5
MgO
$FeO + Fe_2O_3$
MnO
CaO
TiO_2
50
60
70
80
90
100
Fractionation Index = Σ normative q + or + ab + ac + ns

all Gardar rocks (99 analyses, fig. 4) shows a minimum in the range 70–72 %, suggesting that there may be a significant gap. However, in the case of the rocks from the various central complexes 10 of the samples (between 70–74 %) come from a single member of the Ilímaussaq intrusion (Hamilton, 1964). Of the dyke analyses shown in fig. 4, 35 are from the Tugtutôq area. Any sample bias shown in the Tugtutôq series will obviously strongly bias the form of the histogram. In fact, the microgranites (15 analyses in table 4, pp. 277–278) have been grossly oversampled for analysis compared to the microsyenites (14 analyses in table 4), considering the inferred volume relationships in the area (fig. 1). The histogram gives a completely inaccurate picture of relative volumes of trachytic magma (with $SiO_2 > 60$ %) and rhyolitic magma, and many more analyses of Gardar acid rocks are needed to establish whether or not the silica-gap really exists.

Origin of the dyke series

Apart from the alkalis, the major elements show smooth and regular trends in the variation diagrams, and appear, in a qualitative way at least, to be explicable in terms of fractionation of the observed phenocryst minerals from trachytic magma (table 2). An origin by crystal fractionation has already been proposed by Upton (1964 a), by analogy with the rocks of the Kûngnât complex. The Kûngnât trachytic magma is thought to have fractionated as a result of bottom-accumulation of feldspar, olivine, clinopyroxene and ilmenomagnetite to yield a layered series of syenites with peralkaline granitic residua (Upton, 1960). The volume relationships of the trachytic and rhyolitic magmas in the Tugtutôq area, inferred from their relative outcrops (fig. 1), are also consistent with this hypothesis. However, the distribution of Na and K, described below, is not readily explicable in terms of derivation of the series by simple crystal fractionation, mainly due to the fact that the alkali contents of the magmas intruded to form the dykes have probably been affected by several processes other than fractional crystallisation, namely loss of a vapour phase, devitrification, alkali-ion exchange effects and hydrothermal alteration. The present Na_2O/K_2O ratios of the dykes cannot therefore be taken as those of the liquids, and the fractionation path (or paths) of the dyke magmas cannot be accurately deduced. The effects of these various processes are described below.

Distribution of Na_2 and K_2O

The behaviour of the alkalis in relation to Al_2O_3 and SiO_2 can conveniently be examined in two projections recently devised by Bailey & Macdonald

Fig. 3. Variation diagram for the dykes, using Fractionation Index as abcissa (see text for explanation). Crosses – trachydolerites, triangles – hastingsite microsyenites, squares – riebeckite microsyenites, closed circles – riebeckite microgranites, open circles – aegirine microgranites.

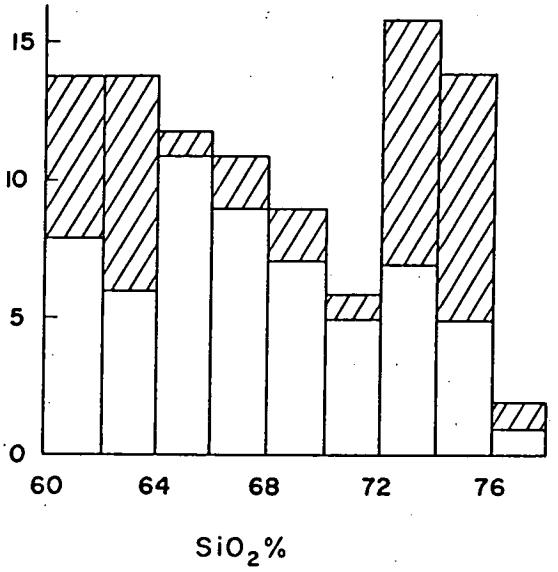

Fig. 4. Frequency of SiO_2 values in Gardar alkaline rocks having $SiO_2 > 60$ %. Blank columns – central complexes, striped columns – dyke swarms. Data from Upton (1960), Hamilton (1964), Watt (1966), this paper (table 4), and Macdonald (unpublished data).

(1969). The first of these (fig. 5 a) is a simple triangular diagram plotting molecular SiO_2 and Al_2O_3 against (Na_2O + K_2O). The alkali feldspar compositional join plots as a point, and any plane radiating from that join projects as a line. For example, Or-Ab-P"–P' is a plane in the peralkaline oversaturated volume of the system Na_2O–K_2O–Al_2O_3–SiO_2 (fig. 5 b) and it is represented in fig. 5 a by the line Feldspar – P'P". A deficiency of this projection is that it cannot be used to show the alkali ratio of rocks. The conventional granite system, Q–Or–Ab, does not share this deficiency, but is of limited value in plotting the compositions of peralkaline rocks as it assumes a 1 : 1 ratio of alkalis : alumina (Bailey & Schairer, 1964, Thompson & Mackenzie, 1967). The ratio Na_2O/K_2O can, however, be shown in projection on planes such as Or–Ab–P"–P' (fig. 5 c), since lines of constant Na_2O/K_2O ratio can be drawn crossing the plane. Trends in magma series can be shown in terms of decreasing Al_2O_3 and correct alkali ratio. Feldspar compositions and tie-lines to rocks can also be shown.

An important feature that can be demonstrated using a SiO_2–Al_2O_3-alkalis diagram (fig. 6) is that fractionation of alkali-feldspar alone from any slightly peralkaline oversaturated liquid (e.g. X) must drive the residual liquid towards feldspar-poorer compositions along the projection of F–X, i.e. towards X'. With further feldspar fractionation the liquid will persist along the projection of F–X until another process intervenes, such as crystallisation of another phase. For example, fractionation of quartz is

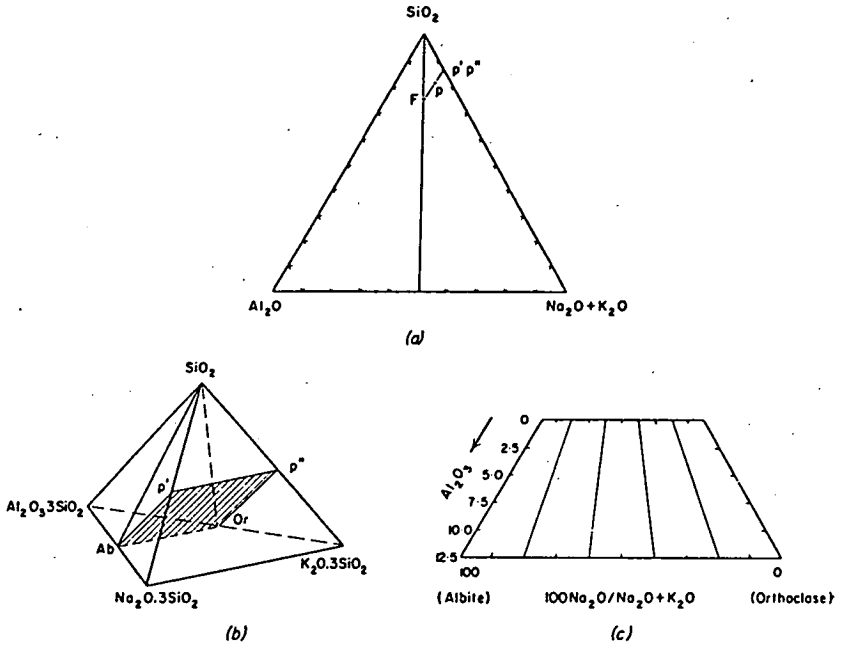

Fig. 5. (a) SiO_2–Al_2O_3–(Na_2O+K_2O) diagram. F = alkali feldspar. P = hypothetical peralkaline composition. P'P", the intersection of F–P on the alkali-silica sideline, measures the alkali-silica index of composition P.
(b) The oversaturated volume of the system Na_2O–K_2O–Al_2O_3–SiO_2, showing the plane Ab–Or–P"–P'. This plane is equivalent to F–P–P'P" in (a).
(c) Quadrilateral representing any plane in the peralkaline volume of (b), such as Ab–Or–P"–P'.

possible when the quartz-feldspar cotectic is reached. In fig. 6 have been plotted the quartz-potash feldspar (K–K') and quartz-albite (N–N') cotectics from the system K_2O–Al_2O_3–SiO_2 and Na_2O–Al_2O_3–SiO_2 both at 1 atmosphere (Schairer & Bowen, 1955 and 1956). The cotectic relevant to the Tugtutôq dyke series is chemically restrained into the zone defined by K–K' and N–N', and the fractionation trend must be within that zone, i.e. at a large angle to any earlier fractionation path.

The Tugtutôq peralkaline dykes lie on a trend initially similar to F–X–X', but the microgranites show a clustering around 85 % silica, the aegirine microgranites lying further down the quartz-feldspar cotectic zone, i.e. at SiO_2- and Al_2O_3-poorer positions, than the riebeckite microgranites (fig. 7). This trend is consistent with fractionation of feldspar in the microsyenites followed by feldspar plus quartz fractionation in the microgranites, i.e. by removal of the most abundant phenocryst phases.

In detail, the trend of the hastingsite microsyenites in fig. 7 does not pass on extrapolation through the alkali feldspar composition, but some point slightly richer in Al_2O_3. This probably reflects the operation of the pla-

gioclase effect of Bowen (1945) and is a measure of the amount of Al associated with Ca in the feldspar phenocrysts.

The plagioclase effect is potentially feasible in any magmas containing normative diopside. The trachydolerites and hastingsite microsyenites of Tugtutôq suite all carry this normative constituent. The feldspar phenocrysts from 50226, a non-peralkaline hastingsite microsyenite, carry appreciable amounts of anorthite molecule, 7 % by weight (Upton, 1964 a), and those from Gardar microsyenite dykes reported by Scharbert (1966) up to 14 % An by weight. Fractionation of such feldspars could result in fractionally removing Al_2O_3 relative to alkalis.

In the peralkaline dykes, the effect of Ca-entry into the feldspars is greatly diminished, and there is usually less Ca in the phenocrysts than in the rock. However, in such Al_2O_3-deficient compositions, the fractionation of any feldspar will accentuate the peralkalinity, and the plagioclase effect must still be considered operative.

The Tugtutôq peralkaline dyke rocks have been plotted in fig. 8, with tie-lines to their respective feldspar phenocrysts. There is an irregular, but strong increase in Na_2O/Na_2O+K_2O ratio from the hastingsite microsyenites to the riebeckite microsyenites, but a regular decrease in progressively more acid dykes. It is clear from the attitude of the feldspar/rock tie-lines, however, which show that the phenocrysts are in all cases more potassic relative to soda than the whole rocks, that fractionation of feldspar

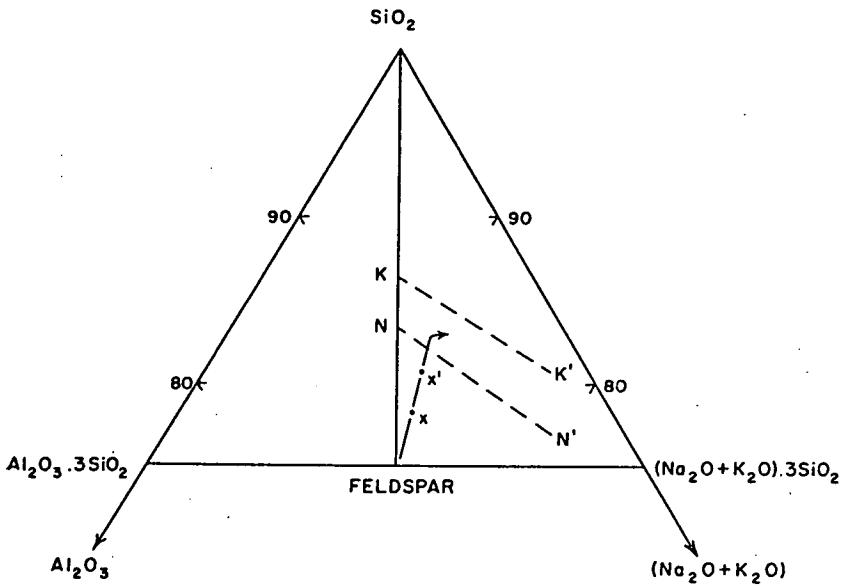

Fig. 6. SiO_2–Al_2O_3–(Na_2O+K_2O) diagram, in which have been plotted the quartz-albite (N–N') and quartz-potash feldspar (K–K') experimental cotectics at 1 atmosphere. A possible fractionation path of a peralkaline trachyte (X) is shown.

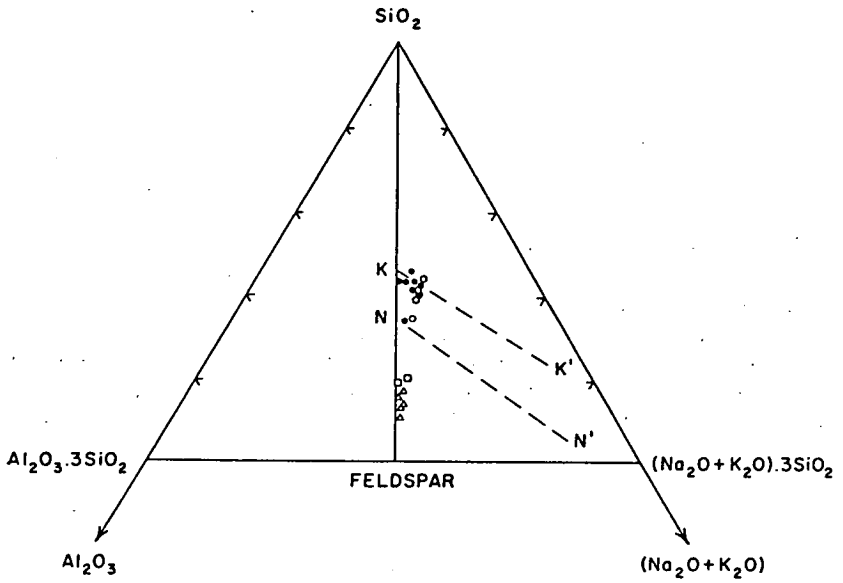

Fig. 7. Analyses of Tugtutôq peralkaline dykes in a SiO_2–Al_2O_3–(Na_2O+K_2O) diagram. Symbols as in fig. 3.

(± quartz) should *at all stages* produce residual liquids enriched in soda. The trend towards decreasing $Na_2O/Na_2O + K_2O$ ratio in the microgranites cannot therefore be a result of simple feldspar (± quartz) fractionation, although the distribution of the analyses in the SiO_2–Al_2O_3–($Na_2O + K_2O$) diagram (fig. 7) was consistent with this origin.

If the analyses of the dykes are taken to represent original liquid composition, and if the chemical variation in the series is a result solely of crystal fractionation, then the trend of alkali ratios in the microgranites must be a result of fractionation of another alkali-bearing phase with feldspar, one rich in Na relative to K, and poor in Al. The only mineral in the phenocryst assemblage of the riebeckite microgranites is riebeckite-arfvedsonite, which if removed in sufficiently large amounts *relative to feldspar* could result in lowered Na_2O/K_2O ratios of residual liquids. However, the amphibole phenocrysts are present in the dykes in only very minor amounts compared to the feldspar phenocrysts (table 3, pp. 275–276) and any effect of fractionating amphibole must have been slight compared to that of feldspar crystallisation. Furthermore, the trend in the microgranites is towards enrichment in normative acmite (table 5, pp. 279–280), whereas fractionation of large amounts of riebeckite- arfvedsonite could initiate a miaskitic from a peralkaline trend. The riebekite-arfvedsonite phenocrysts in the Tugtutôq dykes commonly enclose magnetite, and, although magnetite phenocrysts are common in the more basic rocks, they are generally absent in the most acid dykes, suggesting that there is a reaction relationship between magnetite and liquid to produce amphibole. It is likely that

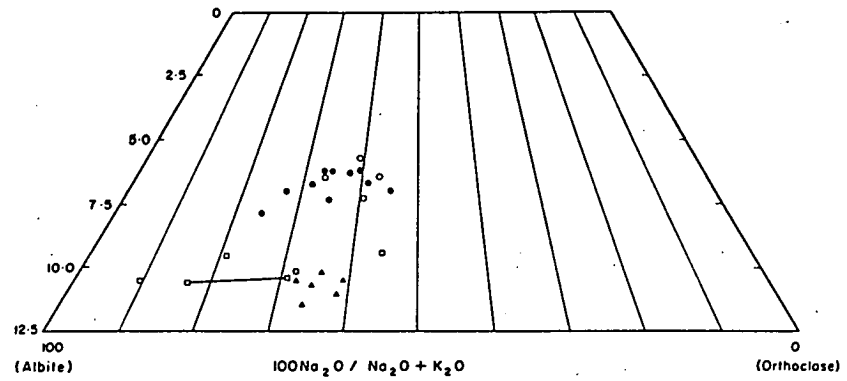

a

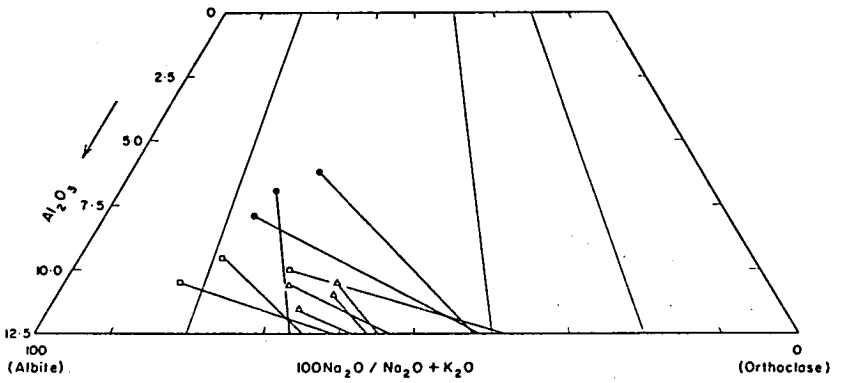

b

Fig. 8. (a) Analyses of Tugtutôq peralkaline dykes plotted in a quadrilateral representing a plane in the volume Na_2O–K_2O–Al_2O–SiO_2, such as Ab–Or–P"–P' in fig. 5b. Symbols as in fig. 3. Heavy line joins the margins (50050) and centre (50051) of a riebeckite microsyenite dyke. (b) Same plot, with compositions of dykes tied to their feldpar phenocrysts (in terms of Or/Or + Ab mol. per cent).

magnetite fractionated from those peralkaline rhyolites during magma ascent, but that amphibole commenced crystallisation giving phenocrysts only at high crustal levels, shortly before final emplacement and consolidation of the dykes. A comparable situation is found in the Kûngnât complex (Upton, 1960), where there is some evidence from magnetite-rich schlieren in the riebeckite granites, that while magnetite acted as an accumulitic phase, there is no direct evidence that riebeckite-arfvedsonite ever behaved similarly.

It is suggested that the alkali distribution in the acid dykes cannot be explained simply in terms of fractionation of the observed phenocryst assemblages. Several alternative processes may now be considered.

Loss of vapour phase

Where the vapour pressure in a magma exceeds the external pressure, a volatile phase will separate, which may or may not be above its critical point, depending on the type and amount of solutes in it (Krauskopf, 1967). The critical point of water is lowered by the addition of solutes of greater volatility, but raised by involatile elements. In the first case, the volatile phase may remain above its critical point until after consolidation of the magma, and the maximum number of fluid phases is two. In case two, the separating phase may be rich in dissolved salts (geological evidence such as liquid inclusions and volcanic emanations indicates that NaCl is especially common) and may fall below its critical point, where yet another fluid phase may separate, richer in water and halogens. A natural example of this second case has been described by Roedder & Coombs (1967), working on fluid inclusions in peralkaline granites from Ascension Island. Great importance attaches to these dense, supercritical fluids, because they are strong solvents and are a potent mechanism for removing Na and to a lesser extent K from silicate melts.

It is possible that the magmas which formed the Tugtutôq dyke series underwent continuous loss of a supercritical vapour phase during their ascent and emplacement. Further, if it is assumed that volatiles were enriched in residual liquids during fractionation, then the volatile pressure may have been sufficiently high to allow escape of a vapour phase only in the rhyolitic magmas. If this fugitive fluid phase contained a high proportion of Na relative to K, then the process could have had the effect of decreasing the Na_2O/K_2O ratios determined by fractional crystallisation. Unfortunately, it is impossible to make even qualitative estimates of the alkalis lost during this process.

Loss of alkalis on magmatic crystallisation or devitrification

The vapour phase discussed above was that separating from the essentially liquid magma during its ascent and emplacement. A further fluid phase may escape from the cooling magma – during magmatic crystallisation, or in the case of magma chilled to a glass, during subsequent devitrification. In these latter cases, the magma may be considered essentially solidified.

There is much recent evidence on the chemical changes affecting peralkaline acid lavas during magmatic crystallisation or devitrification (Carmichael, 1962; Noble, 1965, 1967; Noble, Smith and Peck, 1967; Ewart, Taylor and Capp, 1968). The most marked effects are loss of alkalis, especially Na, and halogens, but Al may be gained and Si gained or lost. The alkalis lost in this way are those left after feldspar plus aegirine (or amphibole) formation, i.e. those normally expressed as normative sodium metasilicate. Noble (1965), for example, found that more than one-quarter of the Na_2O originally present in a pantellerite tuff was lost on devitrification.

It is clear that the alkalis : alumina : silica ratios in the Tugtutôq dykes cannot safely be assumed to be those of the liquids immediately prior to solidification, and that late-stage alkaline fluids probably escaped from the

dykes, presumably also enriched in halides and water. There is unfortunately no indication of where they have escaped to, as there is no evidence of wall-rock contamination. One must assume that these residual fluids streamed up the dykes and were lost to the surface, or alternatively that they were removed at a much later stage by groundwater leaching. That alkali loss has been operative in at least some of the peralkaline Gardar intrusives is shown by the alkali metasomatism of wall-rocks seen in the intrusive complexes at Kûngnât, Ilímaussaq and central Tugtutôq.

The feldspar phenocrysts of the peralkaline Tugtutôq dykes all have lower ratios of $Na_2O/Na_2O + K_2O$ than the host rocks, suggesting operation of the orthoclase effect (Bailey & Schairer, 1964). Successive residual liquids after feldspar fractionation should contain larger amounts of excess alkalis with increasing Na_2O/K_2O ratio. On devitrification, progressively larger amounts of Na should be lost relative to K, and the result could be that the rock series showed a trend of decreasing Na_2O/K_2O ratio in more acid dykes (fig. 8).

One effect of devitrification would be to cause a scatter of analyses of acid dykes in the SiO_2–Al_2O_3-alkalis diagram (fig. 7). Alkali loss will trend to drive the projected *liquid* compositions away from the alkali apex and towards the Al_2O_3–SiO_2 side-line. Since more acid dykes always show increasing proportions of aegirine : feldspar (table 5), despite devitrification, the composition trend can never cross to the Al_2O_3-rich side of the Al_2O_3 : alkalis = 1 : 1 line i. e. to a miaskitic trend, as a result of this process.

Alkali-ion exchange effects

A further complication to the alkali balance is that unequal distribution of Na and K in various parts of the same dyke may be common, especially between chilled margins and coarser centres. The only available data are for the riebeckite microsyenite, 50050 (chill) and 50051 (centre). The zones have similar total alkali contents (9.7 % and 10.4 % respectively), but different Na_2O/K_2O ratios, 3.25 and 1.48 by weight. It is unlikely that the zones in this dyke represent different pulses from magma body differentiated prior to intrusion because the bulk chemistry of chill and centre are almost identical, apart from alkalis (table 4). The data are consistent, however, with exchange of alkali ions across the dyke, presumably migrating along a temperature gradient during the cooling of the dyke. The two compositions are joined by a heavy line in fig. 8 a and there is a marked difference in plotted position. Many more analyses are required to determine whether this situation is general, but it may mean that the distribution of points in fig. 8 is partly a result of sampling within the dykes, and further work may modify the trends quite considerably.

Loss of Na on alteration of amphibole

There is evidence that alteration of soda-amphibole can lead to decreased Na_2O/K_2O ratios in the Tugtutôq dykes. In the large composite micro-

granite dyke which extends through central Tugtutôq (Upton, 1964, p. 16–17) two main acid facies are present: a normal riebeckite-arfvedsonite bearing variety, and a more oxidised variety, in which haematite is the sole coloured mineral. There are transitional types, with amphibole largely replaced by magnetite. The Na_2O/K_2O ratios of oxidised and normal facies are 0.65 and 0.73 respectively. Locally, presumably attendant upon high oxidation conditions, magnetite and finally haematite became the stable Fe-bearing mineral rather than amphibole. Na must have been released during this oxidation, possibly to the wall-rock, and the normative result was the appearance of a small amount (0.8 %) of corundum (table 7).

Whereas such a small amount of normative corundum could be due to analytical error, the analysis of a porphyritic rhyolite sill from the south side of the Narssaq valley (GGU 61848, table 7, p. 281) which Upton (1962, p. 36) suggested could have been fed by the Tugtutôq dyke, also contains normative corundum (1.2 %). The sill has similar chemistry to the dyke and it seems likely that the excess of Al is real.

The riebeckitic facies of this big dyke is itself relatively alkali-deficient, and despite the presence of soda-iron amphibole it contains a small amount of normative anorthite (2.2 %). The appearance of corundum on alteration of the amphibole is to be expected only from dykes containing low potential acmite, but the process can affect Na_2O/K_2O ratios in more strongly peralkaline dykes. The alteration of amphibole to limonite in the Tugtutôq microsyenites has probably resulted in a decrease in Na/K ratios, and may explain, at least in part, the spread of points in the lower part of fig. 8.

Divergence of fractionation trends

The evidence of possible alkali migration in the riebeckite microsyenite dyke 50050/50051 suggests that the high Na contents of some of these dykes may be a post-intrusion effect. It is assumed here, for sake of discussion, that the high Na_2O/K_2O ratios of certain of the riebeckite microsyenites is a primary feature of the magmas. Since the feldspar phenocrysts in the dykes are always more potassic than the liquids, feldspar fractionation alone would tend to produce progressively more sodic residual liquids. Since the riebeckite microsyenites have $Na_2O/Na_2O + K_2O$ ratios of up to 90 %, it is clear that the rhyolite magmas would have been enriched in Na almost to the exclusion of K by this process. In a literature survey of all peralkaline acid lavas, the author was unable to find a description of a suite of rocks so enriched in Na relative to K. It seems doubtful that the highly sodic riebeckite microsyenites could have been parental to the microgranites, even assuming loss of large amounts of Na from the rhyolite magmas in residual fluid phases during consolidation and/or subsequent devitrification.

An alternative solution may be that microgranites have been derived from a hastingsite microsyenite stem with low Na_2O/K_2O ratio (e.g. 50169, table 4), and that the Na-rich riebeckite microsyenites represent a separate evolutionary branch. Some support for this is found in the feldspar phenocryst compositions.

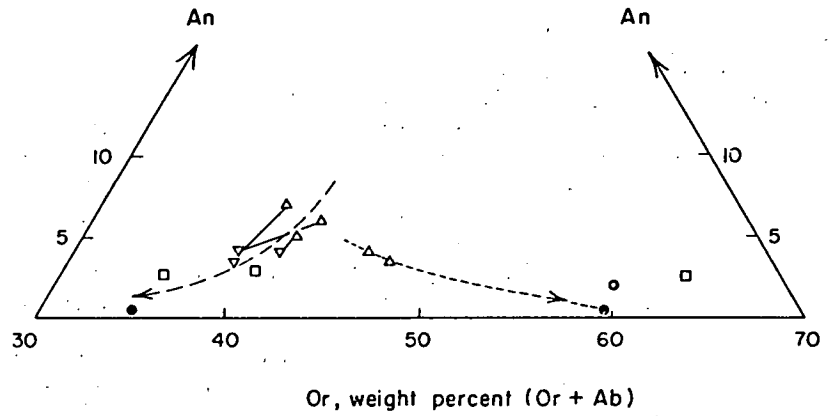

Fig. 9. Part of an Or–Ab–An diagram. Triangles – feldspar phenocrysts from hastingsite microsyenites (inverted = groundmass feldspars), squares – from riebeckite microsyenites, circles – from riebeckite microgranites. Tie-lines connect phenocryst and groundmass feldspars from same rock. Inferred trends towards Ab- and Or-enrichment are shown by dashed lines. Data from this paper and from Upton (1964a).

The gabbroic and syeno-gabbroic intrusions of Tugtutôq show a range in feldspar composition from circa $An_{70}Ab_{30}$ through K-rich oligoclase to Ca-bearing alkali feldspar (Upton, 1964b). There is no clear evidence that two feldspars were coprecipitating at any stage; a single continuous feldspar sequence is observed with a change from triclinic to monoclinic symmetry inferred at approximately Or_{20-25}.

The trend shown by the feldspar phenocrysts of the hastingsite microsyenite dykes of Tugtutôq is towards Or-enrichment at the expense of Ab and An (fig. 9), and strong K-enrichment is also shown in two of the microgranites (Or_{59}). The feldspars of the riebeckite microsyenites do not lie on this trend; whereas two plot at more sodic compositions, one has the maximum Or content (Or_{62}) of any of the analysed feldspars. The feldspars from a third microgranite, 50187, has the lowest Or-content of any analysed specimen (Or_{35}). The behaviour of the feldspar phenocrysts is therefore not simple, and once again an origin of the dyke series by continuous crystal fractionation must be questioned. There is, however, some support for the idea that there has been a divergence in the hastingsite microsyenites towards, on the one hand, the riebeckite microsyenites and on the other, the microgranites. Where data are available, the groundmass feldspars of the hastingsite microsyenites are slightly enriched in Ab relative to the phenocrysts (Upton, 1964 a). It is therefore possible to group these feldspar phenocrysts with those of the riebeckite microsyenites into a series showing Ab-enrichment with decreasing An-content, and to link the other two hastingsite microsyenites with the microgranites (fig. 9). This theory leaves unexplained the anomalously high and low Or contents of the microsyenite 50167 and the microgranite 50187 respectively, but has the

advantage of being open to test; the groundmass feldspars of the microsyenite dyke 50169 should be slightly richer in Or than the phenocrysts.

If this divergence is accepted, it is a short step to viewing the series as comprising a large number of separate trends, or "bundle of liquid lines of descent", only approximating a single fractionation series. This effect has been termed "proliferation of liquid lines of descent" by Cox (1967). Consider a basaltic magma ascending through the crust, crystallising on a cotectic equilibrium. If it ascends reasonably slowly, the magma may never leave the cotectic condition, that is crystallisation may keep pace with the changing pressure conditions. In this case, the magma gives rise to a series of residual liquids which define a unique fractionation trend. During rapid magma ascent, however, involving sudden changes of pressure, the magmas may leave the higher pressure cotectic equilibria and pre-existing phenocrysts will tend to be resorbed. Under the new pressure-temperature conditions, different phenocryst assemblages will separate, and each member of the original series of magmas can itself be parental to a series of derivatives. Crystal/liquid processes tend to drive a fairly wide range of basic liquids towards similar end-points on fractional crystallisation. The residua produced by the proliferated magma series may therefore be compositionally very similar, and it may prove impossible to tell that they had had rather different evolutionary histories. The dyke magmas intruded in the large Gardar province were derived from several batches supplied over long periods of time, and the assumption made earlier that they can be considered as a single petrochemical series was perhaps naive.

Conclusions

There is reasonable evidence from various sources that the Tugtutôq acid dykes were formed from trachytic magmas dominantly by fractionation of alkali feldspar, accompanied by quartz in the rhyolites. However, the Na_2O/K_2O ratios of the original magmas have probably been modified by several processes, including loss of a vapour phase, devitrification, alkali-ion exchange effects and secondary alteration of amphibole. It is thus impossible to describe closely the evolutionary trend (or trends) of the magmas. Further, the dykes were intruded as a number of swarms over a considerable period of time, and probably did *not* initially represent a single evolutionary sequence.

The study of all crystalline peralkaline rocks is open to the problems of interpretation met during this work, and answers to the problems of the petrogenesis of peralkaline magmas must be sought in glassy lavas.

Acknowledgments

This study was carried out at the Grant Institute of Geology, University of Edinburgh during the tenure of a N. E. R. C. Research Studentship, which is gratefully acknowledged. Thanks are due to Professor F. H. Stewart for laboratory facilities, and to the Director of the Geological Survey of Greenland, K. Ellits-

gaard-Rasmussen, for enabling me to partake in the Survey's summer expedition to South Greenland in 1966.

I gratefully thank my supervisor, Dr B. G. J. Upton, for providing me with his Tugtutôq collections, for introducing me to the geology of South Greenland in the field, and for patient help at all stages of the work. Dr Upton and Mr J. E. Thomas read the manuscript and offered several useful suggestions for its improvement.

Warm thanks are extended to Messrs M. J. Saunders, G. R. Angell and R. L. Bennett for training and help in chemical, X-ray and mineral separation techniques respectively, and to Drs E. L. P. Mercy and N. B. Price for making these facilities available.

Finally, I should like to thank Drs D. K. Bailey, I. G. Meighan and B. G. J. Upton for several stimulating discussions on the petrogenesis of alkaline rocks.

Department of Geology,
University of Reading, Whiteknights Park,
Reading RG62AB, England
April 17th, 1969

Appendix

Methods of analysis

The rock samples were analysed for Si, Ti, Al, Fe, Mn, Mg and Ca by X-ray fluoresence spectroscopy, using Philips XRF equipment (PW 1310/50 generator with PW 1320 control cabinet). The rock powder was diluted with La_2O_3 and $Li_2B_4O_7$ in order to minimise matrix absorption effects, fused, crushed and briquetted using boric acid as a binder. Calibration curves were drawn up for each element using the international rock standards (G1, W1, S1 etc.). Na and K were determined by flame photometer, P by spectrophotometer, and Fe" by titration with dichromate. H_2O was determined gravimetrically, and F by the spectrophotometric method of Peck and Smith (1964, Talanta, Vol. 11, 1343–1347).

In the feldspar samples, Na and K were determined by flame photometer, Ca by titration with EDTA, and Fe (as Fe_2O_3) by titration with $K_2Cr_2O_7$, using the $SnCl_2$ reduction technique recommended by Mercy & Saunders (1966, Earth Planet. Sci. Letters, Vol. 1, 169–182).

Dansk sammendrag

Intermediære til sure alkaline gange af Gardar alder fra Tugtutôqområdet i Sydgrønland danner en næsten fuldstændig serie fra trakydoleriter over hastingsit- og riebeckitbærende mikrosyeniter til riebeckit- og ægirinmikrograniter. Kemisk viser serien en overgang fra anortit- og nefelin-normative typer til acmit- og kvarts-normative typer. Selvom gangene antages oprindeligt at være afledt fra basaltisk magma ved fraktionering, har flere processer tjent til at ændre den oprindelige væskesammensætning, heri medregnet tab af en dampfase, afglasning af sure gange, udbytning af alkaline ioner og omdannelse af amfibol. Mønsteret for magmaernes udvikling kan derfor ikke fastlægges nøjagtigt.

Table 3. Modes of analysed specimens.

	Trachydolerites			Hastingsite microsyenites								Riebeckite microsyenites					
	40471	50093	50149	30713	40429	40433	40462	40498	40570	50169	50226	30645	30739	50050	50051	50136	50167
Phenocrysts																	
Feldspar	–	–	–	32.2	30.0	12.1	16.2	26.2	5.4	25.2	24.6	18.0	–	tr.	tr.	10.5	16.4
Quartz	–	–	–	–	–	–	–	–	–	–	–	–	–	–	–	–	–
Apatite	tr.	–	tr.	0.1	tr.	–	tr.	tr.	–	–	–	–	–	–	–	–	–
Ore	–	–	–	0.2	tr.	–	tr.	tr.	–	–	0.2	0.3	–	1.6	–	–	–
Olivine	–	–	–	–	–	–	0.8	tr.	–	–	0.6	–	–	–	–	–	–
Pyroxene	–	–	–	–	–	0.1	–	–	tr.	tr.	0.6	–	–	–	–	–	–
Amphibole	–	–	–	–	–	–	–	–	–	0.6[1]	–	–	–	–	–	–	–
% phenocrysts	–	0.0	–	32.5	30.0	12.2	17.0	26.2	5.4	25.8	26.0	18.3	0.0	1.6	0.0	10.5	16.4
Groundmass																	
Feldspar	60.6	64.1	73.6	44.5	49.1	58.7	56.8	53.3	68.9	51.9	52.1	–	–	51.1	70.0	40.3	40.4
Quartz	–	–	–	–	–	0.6	2.7	tr.	1.9	4.5	–	–	–	tr.	0.8	–	–
Apatite	1.9	–	0.9	–	tr.	–	–	–	tr.	–	–	–	–	–	–	–	–
Ore	7.1	5.1	6.2	0.9	1.9	1.9	1.5	1.6	2.0	0.3	–	–	–	4.6	5.2	–	0.4
Biotite	20.7	1.8	9.6	–	–	–	–	–	–	–	–	–	–	–	–	–	–
Pyroxene	9.7	8.2	8.4	–	5.5	tr.	–	–	–	–	–	–	–	–	–	–	–
Amphibole	–	–	–	6.6[1] / 6.0[2]	5.4	18.7[1] / 3.0[2]	11.3[1] / 6.7[2]	14.9	16.8	16.8	8.9	–	–	41.8	22.8	42.1	42.2
Limonite	–	–	–	8.0	6.1	4.9	3.9	4.0	5.0	0.7	13.0	–	–	0.9	1.2	7.1	–
Zircon	–	–	–	–	–	–	–	–	–	–	–	–	–	–	–	–	0.6
Carbonate	–	–	–	1.4	–	tr.	–	–	tr.	–	–	–	–	–	–	–	–
Fluorite	–	–	–	–	–	–	–	–	–	–	–	–	–	–	–	–	–
Vugs	–	–	–	–	2.0	–	–	–	–	–	–	0.3	–	–	–	–	–
% groundmass	100.0	79.2	98.7	67.4	70.0	87.8	82.9	73.8	94.6	74.2	74.0	81.7	100.0	98.4	100.0	89.5	83.6

[1] = hastingsite, [2] = riebeckite-afvedsonite. 50093 – plus chlorite (16.6%) and epidote (4.2%), 50149 – plus chlorite (1.3%).

Table 3 (contd.)

	Riebeckite microgranites											Aegirine microgranites			
	30685	30758	40427	40449	40493	40495	40575	50163	50181	50187	50237	30691	40554	40600(a)	50197
Phenocrysts															
Feldspar.....	4.3	–	18.0	2.2	3.7	17.6	10.6	–	18.1	20.0	–	4.1	8.4	20.3	16.1
Quartz.....	5.2	–	8.7	4.1	1.4	17.0	9.4	–	10.9	14.0	tr.	4.4	2.3	20.2	4.5
Apatite.....	–	–	–	–	–	–	–	–	–	–	–	–	–	–	–
Ore.....	–	–	–	–	–	–	2.5	2.6	–	–	–	–	–	–	–
Olivine.....	–	–	–	tr.	–	–	–	–	–	–	–	tr.	–	tr.	–
Pyroxene.....	–	–	–	–	–	1.9	1.5	–	–	–	–	tr.	0.2	tr.	1.2
Amphibole....	–	–	0.8	–	0.8	tr.	–	–	3.6	–	–	–	–	–	–
% phenocrysts.	9.5	0.0	27.5	6.3	5.9	36.5	23.0	2.6	32.6	34.0	0.0	8.5	10.9	40.5	21.8
Groundmass															
Feldspar.....	64.5	51.1	33.0	45.5	46.0	33.0	51.0	–	33.3	–	48.9	52.3	41.5	–	27.2
Quartz			24.0	26.2	27.8	16.5			22.2		32.6				22.3
Apatite.....	–	–	–	–	–	–	–	–	–	–	–	–	–	–	–
Ore.....	–	tr.	tr.	3.8	–	–	–	–	0.9	–	tr.	–	–	–	1.3
Biotite.....	–	–	–	–	–	–	–	–	–	–	tr.	–	–	–	–
Pyroxene.....	15.9	27.7	3.9	–	6.7	12.0	–	–	tr.	–	–	39.2	42.6	–	26.1
Amphibole....	9.8	21.2	11.5	17.2	12.8	1.5	24.8	–	11.0	–	18.5	–	3.9	–	–
Limonite.....	–	–	–	1.0	–	–	–	–	–	–	–	–	–	–	1.3
Zircon.....	–	–	–	–	–	–	0.7	–	–	–	tr.	–	–	–	–
Carbonate.....	–	–	–	–	–	–	–	–	–	–	–	–	–	–	–
Fluorite.....	0.3	–	–	–	–	–	–	–	–	–	tr.	–	–	–	–
Vugs.....	–	–	–	–	–	–	0.5	–	–	–	–	–	1.1	tr.	–
% groundmass.	90.5	100.0	72.4	93.7	93.3	63.0	77.0	97.4	67.4	66.0	18.5	91.5	89.1	59.5	78.2

40495 – plus pyrochlore? (0.5%).

Table 4. Analyses of dykes from the Tugtutôq area

	Trachydolerites			Hastingsite microsyenites								Riebeckite microsyenites					
	40471	50093	50149	30713	40429	40433	40462	40498	40570	50169	50226	30645	30739	50050	50051	50136	50167
SiO_2.....	49.2	51.6	54.4	61.1	59.1	61.1	62.1	62.9	62.5	63.8	60.4	66.0	63.8	62.2	62.3	64.2	65.2
TiO_2.....	2.49	1.91	1.70	0.83	1.15	1.00	0.96	0.98	0.94	0.65	0.98	0.67	0.90	0.76	0.66	0.73	0.66
Al_2O_3.....	15.40	16.30	15.30	15.60	16.34	14.20	13.60	15.30	14.30	14.53	16.55	13.50	14.60	14.30	14.00	12.87	13.95
Fe_2O_3.....	3.20	2.92	5.93	2.61	4.13	2.68	3.18	2.33	1.78	2.81	2.66	4.04	3.35	4.44	5.08	3.57	2.95
FeO.....	8.93	7.90	5.48	4.36	3.44	5.82	5.35	4.43	5.69	4.04	3.91	4.73	5.27	4.96	4.16	4.18	5.13
MnO.....	0.19	0.22	0.20	0.20	0.15	0.20	0.22	0.16	0.19	0.15	0.17	0.19	0.19	0.24	0.21	0.19	0.21
MgO.....	2.56	2.29	1.03	0.41	0.67	0.38	0.24	0.40	0.35	0.23	0.63	0.14	0.25	0.05	0.04	0.00	0.02
CaO.....	5.54	5.05	3.62	2.19	2.32	1.96	2.18	1.51	1.89	1.61	1.87	1.09	1.68	1.68	1.58	1.21	1.58
Na_2O.....	4.58	4.93	4.86	6.16	5.19	6.02	5.66	5.89	6.24	5.54	5.36	7.15	8.65	7.42	6.19	4.93	5.89
K_2O.....	3.60	3.43	4.25	4.82	5.31	4.78	4.80	5.54	4.54	5.34	5.84	2.92	1.39	2.28	4.18	6.03	4.18
P_2O_5.....	1.24	0.74	0.71	0.15	0.34	0.18	0.15	0.35	0.18	0.13	0.29	<0.05	0.13	0.09	0.15	0.06	0.08
H_2O^+.....	1.17	1.66	1.50	0.56	0.86	0.45	0.46	0.60	0.48	0.29	0.78	0.45	0.42	0.48	0.28	0.59	0.36
F.....	0.18	0.12	0.12	0.10	0.09	0.15	0.18	0.12	0.20	0.14	0.09	0.18	0.03	0.23	0.26	0.11	0.19
	98.28	99.07	99.10	99.09	99.09	98.92	99.08	100.51	99.28	99.26	99.53	101.06	100.66	99.13	99.09	98.67	100.40
$O \equiv F$....	0.08	0.05	0.05	0.04	0.04	0.06	0.00	0.05	0.08	0.06	0.04	0.07	0.01	0.10	0.11	0.05	0.08
Total.....	98.20	99.02	99.05	99.05	99.05	98.86	99.00	100.46	99.20	99.20	99.49	100.99	100.65	99.03	98.98	98.62	100.32
F. I. ...	53.9	57.7	68.6	82.3	79.0	81.5	82.1	86.0	83.2	85.9	85.0	87.5	85.0	83.0	84.7	88.3	95.0

F. I. = Fractionation Index, Σ norm q + or + ab + ac + ns; 50136, 50187, 50226 – from Upton (1964a), except for F; 50136 – CO_2 = 1.14%; 50226 – CO_2 = 0.44%.

Table 4 (contd.)

	Riebeckite microgranites											Aegirine microgranites			
	30685	30758	40427	40449	40493	40495	40575	50163	50181	50187	50237	30691	40554	40600(a)	50197
SiO_2.....	71.5	73.7	74.4	72.5	75.3	74.6	75.8	72.7	75.6	75.9	74.6	75.7	73.9	73.1	74.6
TiO_2.....	0.43	0.42	0.19	0.65	0.36	0.18	0.40	0.35	0.43	0.32	0.45	0.36	0.34	0.42	0.21
Al_2O_3.....	11.50	9.28	10.00	10.95	9.15	9.35	10.55	9.06	10.10	10.47	11.00	9.70	9.65	10.90	8.45
Fe_2O_3.....	3.42	4.14	2.55	3.77	3.02	4.84	3.44	4.96	2.32	2.27	2.63	4.45	4.57	4.31	5.86
FeO.....	2.16	2.25	2.65	2.10	2.59	0.41	1.90	2.19	2.01	2.44	2.94	0.27	0.58	1.12	0.13
MnO.....	0.14	0.12	0.10	0.08	0.08	0.10	0.07	0.13	0.11	0.07	0.09	0.06	0.08	0.10	0.09
MgO.....	0.06	0.03	0.00	0.51	0.00	0.02	0.00	0.04	0.07	0.00	0.10	0.00	0.00	0.05	0.19
CaO.....	0.34	0.10	0.09	1.59	0.12	0.05	0.21	0.34	0.48	0.29	0.43	0.24	0.29	0.15	0.18
Na_2O.....	5.99	4.55	5.05	3.22	4.17	5.40	3.65	4.92	4.14	5.04	4.48	4.55	5.36	5.01	4.67
K_2O.....	2.91	4.19	3.50	4.39	4.19	4.08	4.50	3.86	4.38	2.71	3.66	5.11	4.04	5.17	4.53
P_2O_5.....	<0.05	0.10	0.05	0.12	<0.05	<0.05	<0.05	<0.05	<0.05	<0.05	0.07	<0.05	<0.05	<0.05	<0.05
H_2O^+.....	0.48	0.22	0.19	0.82	0.16	0.10	0.21	0.15	0.19	0.26	0.07	0.21	0.05	0.39	0.08
F.....	0.20	0.08	0.26	0.41	0.16	0.16	0.11	0.52	0.17	0.20	0.25	0.15	0.29	0.25	0.08
	99.13	99.18	99.03	101.11	99.30	99.29	99.78	99.22	100.00	99.97	100.77	100.80	99.15	100.97	99.07
$O \equiv F$....	0.08	0.03	0.11	0.17	0.07	0.07	0.05	0.22	0.07	0.08	0.11	0.06	0.12	0.11	0.03
Total.....	99.05	99.15	98.92	100.94	99.23	99.20	99.73	99.00	99.93	99.89	100.66	100.74	99.03	100.86	99.04
F. I.....	92.8	93.9	93.3	88.0	93.8	97.8	94.7	93.6	94.5	94.0	92.6	99.3	97.1	97.4	97.7

Table 5. CIPW norms of analyses of dykes. 50136, 50187, 50226, from Upton (1964a).

	Trachydolerites			Hastingsite microsyenites								Riebeckite microsyenites					
	40471	50093	50149	30713	40429	40433	40462	40498	40570	50169	50226	30645	30739	50050	50051	50136	50167
Quartz.....	–	–	2.7	2.0	3.9	2.8	6.5	3.7	4.1	7.7	3.0	10.9	4.1	7.1	8.4	10.7	10.9
Orthoclase.....	21.1	20.0	25.0	28.4	31.1	28.4	28.4	32.8	26.7	31.7	35.6	17.2	8.3	13.3	24.5	36.4	24.5
Albite.....	32.8	37.7	40.9	51.9	44.0	46.1	43.0	47.7	48.2	45.1	46.4	52.9	67.1	60.8	48.7	33.2	48.7
Anorthite.....	10.8	12.2	7.5	0.8	5.6	–	–	–	–	–	4.0	–	–	–	–	–	–
Na_2SiO_3.....	–	–	–	–	–	–	–	–	–	–	–	–	–	–	–	–	–
Acmite.....	–	–	–	–	–	4.2	4.2	1.8	4.2	1.4	–	6.5	5.5	1.8	3.2	8.0	0.9
Diopside Wollastonite	3.5	3.4	2.4	3.5	1.4	3.2	3.6	2.1	2.9	2.6		1.6	3.0	2.4	2.1		2.7
Diopside Enstatite...	1.4	1.3	1.2	0.6	0.8	0.4	0.3	0.4	0.3	0.3	4.4	0.1	0.3	0.1	0.1	5.7	0.1
Diopside Ferrosilite..	2.1	2.1	1.2	3.2	0.5	3.2	3.7	1.8	2.9	2.5		1.7	3.0	2.6	2.2		2.9
Opx Enstatite...	–	–	1.4	0.4	0.9	0.5	0.3	0.6	0.6	0.3		0.3	0.3	–	0.1		–
Opx Ferrosilite..	–	–	1.6	1.8	0.8	5.1	3.4	3.6	5.3	2.1	0.3	4.9	4.4	2.4	1.5	3.4	3.7
Magnetite.....	4.6	4.2	8.6	3.7	6.0	1.9	2.6	2.6	0.5	3.5	3.8	2.6	2.1	5.6	5.8	1.2	3.7
Haematite.....	–	–	–	–	–	–	–	–	–	–	–	–	–	–	–	–	–
Ilmenite.....	4.7	3.6	3.2	1.5	2.1	2.0	1.8	1.8	2.7	1.2	1.8	1.2	1.7	1.5	1.2	1.4	1.2
Apatite.....	3.0	1.7	1.7	0.3	0.7	0.3	0.3	0.7	0.3	0.3	0.7	–	0.3	0.3	0.3	–	–
CaF_2.....	0.2	0.2	0.2	0.2	0.2	0.3	0.4	0.2	0.5	0.3	–	0.4	0.1	0.5	0.5	–	0.4
Varia.....	1.2	1.7	1.5	0.5	0.9	0.5	0.5	0.6	0.5	0.3	0.8	0.5	0.4	0.5	0.3	0.6	0.4

Addenda: 40471 Nepheline = 3.3, forsterite = 3.5, fayalite = 6.1;
50093 Nepheline = 2.3, forsterite = 3.1, fayalite = 5.7;
30662 Wollastonite = 3.8.

Table 5 (contd.)

	Riebeckite microgranites											Aegirine microgranites			
	30685	30758	40427	40449	40493	40495	40575	50163	50181	50187	50237	30691	40600(a)	40554	50197
Quartz	25.7	32.8	32.8	34.7	36.2	33.3	37.4	31.3	34.7	35.5	33.3	34.4	27.1	32.0	35.2
Orthoclase	17.2	24.5	20.6	26.1	24.5	23.9	26.7	22.8	25.6	16.2	21.7	30.0	30.6	23.9	26.7
Albite	43.0	24.6	32.0	27.2	24.1	25.7	28.8	25.2	27.8	39.1	36.2	21.5	27.2	27.2	18.3
Anorthite	–	–	–	2.2	–	–	–	–	–	–	–	–	–	–	–
Na_2SiO_3	–	–	0.5	–	0.2	1.0	–	–	–	–	–	0.5	0.2	0.6	0.4
Acmite	6.9	12.0	7.4	–	8.8	13.9	1.8	14.3	6.5	3.2	1.4	12.9	12.5	13.4	17.1
Opx.Diopside Wollastonite	–	–	–	0.7	–	–	0.1	–	0.5	1.3	0.1	–	–	–	0.1
Opx.Diopside Enstatite	–	–	–	0.6	–	–	–	–	0.2		–	–	–	–	0.1
Opx.Diopside Ferrosilite	–	–	–	–	–	–	0.1	–	0.3		0.1	–	–	–	–
Opx. Enstatite	0.2	0.1	–	0.7	–	0.1	–	0.1	0.1	2.5	0.2	–	0.1	–	0.3
Opx. Ferrosilite	2.8	3.7	4.8	–	4.2	0.7	0.4	3.7	2.8		2.9	–	1.7	0.7	–
Magnetite	1.4	–	–	5.1	–	–	4.2	–	0.2	1.6	3.0	–	–	–	–
Haematite	–	–	–	0.3	–	–	–	–	–	–	–	–	–	–	–
Ilmenite	0.7	0.8	0.3	1.2	0.8	0.3	0.8	0.6	0.8	0.6	0.9	0.8	0.8	0.6	0.5
Apatite	–	0.3	–	0.3	–	–	–	–	–	–	–	–	–	–	–
CaF_2	0.5	–	0.2	0.9	0.2	0.1	0.2	0.5	0.4	–	0.5	0.3	0.2	0.4	0.2
Varia	0.5	0.3	0.4	0.8	0.3	0.2	0.2	0.5	0.2	0.3	0.1	0.2	0.5	0.1	0.1

Table 6. Analyses of feldspar phenocrysts from Tugtutôq dykes

	Na_2O	K_2O	CaO	Fe_2O_3	Or	Ab	An
40570.....	5.82	7.84	0.72	–	46.6	49.8	3.6
50169.....	5.83	7.48	0.81	0.46	45.2	50.7	4.1
50167.....	3.92	9.95	0.53	0.45	62.4	35.0	2.6
50050.....	5.75	5.79	–	–	40.0	57.0	3.0
50187.....	7.34	5.62	0.10	–	34.9	64.5	0.6
40495.....	4.37	9.25	0.09	–	59.2	40.3	0.4

40570, 50169, hastingsite microsyenites
50050, 50167, riebeckite microsyenites
50187, 40495, riebeckite microgranites
50187, 40495, separated feldspar contained <20% quartz impurity
Or, Ab, An – as weight percent.

Table 7. Analyses of a microgranite dyke and a rhyolite sill from the Tugtutôq-Narssaq area

40435 – oxidised facies of acid member of composite dyke, central Tugtutôq (Upton, 1964a, p. 16); analyst R. Macdonald.
61848 – quartz porphyry sill, Narssaq (from Watt, 1966, analysis 10).

	40435	61848		40435	61848	Mode 40435	
SiO_2....	76.2	73.98					
TiO_2....	0.35	0.37	q	41.6	41.0	Phenocrysts:	
Al_2O_3...	10.50	11.39	or	26.7	21.5	Feldspar	2.0
Fe_2O_3...	5.05	4.72	ab	24.6	25.4	Quartz	1.6
FeO....	0.09	1.15	an	–	3.6		
MnO...	0.05	0.15	c	0.8	1.2	Groundmass:	
MgO ...	0.04	0.06	hy	0.1	0.2	Feldspar	56.3
CaO....	0.30	0.72	mt	–	3.1	Quartz	29.4
Na_2O...	2.90	3.00	il	0.3	0.7	Haematite	9.1
K_2O....	4.49	3.63	hm	5.1	2.6	Zircon	1.3
P_2O_5....	<0.05	0.03	CaF_2	0.2	–	Fluorite	0.2
H_2O^+...	0.94	0.83	tn	0.6	–		
F.....	0.18	–	CIPW NORMS				
	101.09	100.03					
O ≡ F..	0.08	–					
Total...	101.01	100.03					

References

Bailey, D. K. & Macdonald, R. 1969: Alkali-feldspar frationation trends and the derivation of peralkaline liquids. *Amer. J. Sci.* **267**, 242–248.
Bailey, D. K. & Schairer, J. F. 1964: Feldspar-liquid equilibria in peralkaline liquids – the orthoclase effect. *Amer. J. Sci.* **262**, 1198–1206.
Berthelsen, A. & Noe-Nygaard, A. 1965: The Precambrian of Greenland, *In* Rankama, K. (edit.) *The Precambrian*, Vol. 2, 113–262. London and New York.

Bowen, N. L. 1945: Phase equilibria bearing on the origin and differentiation of the alkaline rocks. *Amer. J. Sci.* **243A**, 75–89.

Bridgwater, D. 1965: Isotopic age determinations from South Greenland and their geological setting. *Bull. Grønlands geol. Unders.* **53** (also *Meddr Grønland* **179**, Nr. 4), 56 pp.

Bridgwater, D., 1967: Feldspathic inclusions in the Gardar igneous rocks of South Greenland and their relevance to the formation of major anorthosites in the Canadian Shield. *Canad. Jl Earth Sci.* **4**, 955–1014.

Bridgwater, D. & Harry, W. T. 1968: Anorthosite xenoliths and plagioclase megacrysts in Precambrian intrusions of South Greenland. *Bull. Grønlands geol. Unders.* **77** (also Meddr *Greenland* **185**, Nr. 2), 243 pp.

Carmichael, I. S. E. 1962: Pantelleritic liquids and their phenocrysts. *Miner. Mag.* **33**, 86–113.

Cox, K. G. 1967: Proliferation of liquid lines of descent in basaltic magmas. *Proc. geol. Soc. London* **1637**, 49 only.

Ewart, A., Taylor, S. R. & Capp, A. C. 1968: Geochemistry of the pantellerites of Mayor Island, New Zealand. *Contr. Mineral. Petrol.* **17**, 116–140.

Hamilton, E. I. 1964: The geochemistry of the northern part of the Ilimaussaq intrusion, S. W. Greenland. *Bull. Grønlands geol. Unders.* **42** (also *Meddr Grønland* **162**, Nr. 10), 104 pp.

Krauskopf, K. B. 1967: *Introduction to geochemistry*. McGraw-Hill, New York.

Noble, D. C. 1965: Gold Flat member of the Thirsty Canyon Tuff – a pantellerite ash-flow sheet in southern Nevada. *U. S. geol. Surv. Prof. Pap.* **525 – B**, 85–90.

Noble, D. C. 1967: Sodium, potassium, and ferrous iron contents of some secondarily hydrated natural silicic glasses. *Amer. Min.* **52**, 280–286.

Noble, D. C., Smith, V. C., and Peck, L. C. 1967: Loss of halogens from crystallised and glassy silicic volcanic rocks. *Geochim. et cosmochim. Acta* **32**, 215–224.

Roedder, E & Coombs, D. C. 1967: Immiscibility in granitic melts, indicated by fluid inclusions in ejected granitic blocks from Ascension Island. *J. Petrol.* **8**, 417–451.

Schairer, J. F. & Bowen, N. L. 1955: The system K_2O–Al_2O_3–SiO_2. *Amer J. Sci.* **253**, 681–746.

Schairer, J. F. & Bowen, N. L. 1956: The system Na_2O–Al_2O_3–SiO_2. *Amer. J. Sci.* **254**, 129–195.

Scharbert, H. G. 1966: The alkali feldspars from microsyenitic dykes of southern Greenland. *Miner. Mag.* **35**, 903–919.

Stewart, J. W. 1964: The earlier Gardar igneous rocks of the Ilimaussaq area, S. Greenland. Unpublished Ph. D. thesis, University of Durham.

Thompson, R. N. & Mackenzie, W. S. 1967: Feldspar-liquid equilibria in peralkaline acid liquids: an experimental study. *Amer. J. Sci.* **265**, 714–734.

Thornton, C. P. & Tuttle, O. F. 1960: Chemistry of igneous rocks. 1. Differentiation index. *Amer. J. Sci.* **258**, 664–684.

Upton, B. G. J. 1960: The alkaline igneous complex of Kûngnât Fjeld, South Greenland. *Bull. Grønlands geol. Unders.* **27** (also *Meddr Grønland* **123**, Nr. 4), 145 pp.

Upton, B. G. J. 1962: Geology of Tugtutôq and neighbouring islands, South Greenland. Pt. I. *Bull. Grønlands geol. Unders.* **34** (also *Meddr Grønland* **169**, Nr. 8), 60 pp.

Upton, B. G. J. 1964a: Geology of Tugtutôq and neighbouring islands, South Greenland. Pt. II. Nordmarkitic syenites and related alkaline rocks. *Bull. Grønlands geol. Unders.* **44** (also *Meddr Grønland* **169**, Nr. 2), 62 pp.

Upton, B. G. J. 1964b: Geology of Tugtutôq and neighbouring islands, South Greenland. Pt III. Olivine gabbro, syeno-gabbros, and anorthosites. *Bull. Grønlands geol. Unders.* **48** (also *Meddr Grønland* **169**, Nr. 3, 1–47).

Upton, B. G. J. *in press:* South-West Greenland. *In* Sørensen, H., (edit.) *The Alkaline Rocks.* John Wiley and Son, New York.

TRACE ELEMENT DISTRIBUTION IN ALKALINE DYKES FROM THE TUGTUTÔQ REGION, SOUTH GREENLAND

RAYMOND MACDONALD AND R. A. EDGE

MACDONALD, R. and EDGE, R. A.: Trace element distribution in alkaline dykes from the Tugtutôq region, South Greenland. *Bull geol. Soc. Denmark*, vol. 20, pp. 38–58. Copenhagen, July 9th, 1970.

The intermediate to acid alkaline dykes of the Tugtutôq area, South Greenland, are characterised by high concentrations of Li, Rb, Y, La, Ce, Nb and Pb, and by intense depletion in Sr, Ba and Cr. The distribution of the trace elements is consistent with the theory that the dykes evolved by fractional crystallisation, though part of the original Cl, H_2O, Li and Ga contents of the rhyolitic magmas was lost on devitrification of the dykes.

F, Cl, Li, Rb, Sr, Ba, Sc, Y, La, Ce, Nb, Cr, Cu, Ga and Pb have been determined in a suite of alkaline dykes from the Tugtutôq region, South Greenland. The dykes are of mid-Gardar age and were intruded into basement granites approximately 1150 m.y. ago (Bridgwater, 1965). Details of the geological setting and igneous activity of this area have been given by Upton (1962, 1964a), and an account of the petrology of the alkaline dykes, including major element analyses, has been prepared (Macdonald, 1969).

The dykes studied form an almost continuous series from trachydolerites through hastingsite- and riebeckite-bearing microsyenites to riebeckite- and aegirine-bearing microgranites (table 1). They are thought to represent a fractionation series, ultimately derived from alkali basalt magma. The fractionating phases, all of which occur as phenocrysts in the dykes, were as follows:

hastingsite microsyenites: alkali feldspar, smaller amounts of olivine, clinopyroxene, Fe-Ti oxides, apatite;
riebeckite microsyenites: alkali feldspar, minor Fe-Ti oxides;
riebeckite microgranites: alkali feldspar, quartz, minor Fe-Ti oxides.

The analysed trachydolerites are virtually aphyric; by analogy with other Gardar trachydolerites, it is assumed that the phenocryst assemblage was sodic plagioclase, olivine, ore, clinopyroxene and apatite.

The dykes show a transition from anorthite- and nepheline-normative varieties to acmite- and quartz-normative types, and the agpaitic index (Na + K/Al) increases steadily towards the microgranites. The series is

closely comparable to the augite syenite-alkali granite sequence of western Kûngnât, except that modal olivine and pyroxene are more abundant in the Kûngnât syenites, a result of the drier and more reduced nature of these magmas (Upton, 1964a).

Though the dykes are thought to be derived dominantly by fractional crystallisation, post-emplacement processes have tended to alter the original liquid compositions. Most important of these is devitrification of the microgranites, where Na was lost relative to K, resulting in a lowering of the Na_2O/K_2O ratios compared to the rhyolite magmas. According to Noble (1965, 1968) and Noble, Smith & Peck (1967), these late-stage fluids which are lost on devitrification of peralkaline rhyolitic glass may also be enriched in halogens and certain trace metals, especially the alkaline earths. There is also an increase in Fe^{3+}/Fe^{2+} ratios. The fluids are probably comparable to those which have caused the large-scale metasomatism round several of the Gardar central complexes, such as Ilímaussaq, Kûngnât and central Tugtutôq.

Secondly, there is limited evidence that alkali ion exchange has taken place between centres and margins of certain microsyenite dykes. In particular, the very high Na_2O/K_2O ratios of some riebeckite microsyenites *may* be a result of this process. No other major element seems to have migrated with the alkali ions.

The trace element study has been made to determine whether or not the distribution of these elements is consistent with the ideas of the origin and evolution of the dykes proposed from the petrological study.

Data

32 dykes have been analysed for F (spectrophotometrically) and for Cl, Rb, Sr, Ba, Y, Ce, Nb and Pb by X-ray fluorescence spectroscopy, while 16 selected dykes were analysed for Li, Sc, La, Cr, Cu and Ga by emission spectroscopy (table 1). Data are also presented for Li, Cu and Ga (emission spectroscopy) and Rb, Sr, Ba and Y (X-ray fluorescence) in the alkali feldspar phenocrysts of 6 rocks (table 4). Details of the analytical methods may be found in the appendix. H_2O, Na_2O and K_2O values have been taken from Macdonald (1969).

Distribution of the elements

Following Macdonald (1969), the trace element data have been plotted in variation diagrams (figs 1 a, b) against a Fractionation Index, F. I., the sum of the normative components, q+or+ab+ac+ns.

Table 1. Trace element data for Tugtutôq

	Trachydolerites			Hastingsite microsyenites								Riebeckite microsyenites					
GGU coll.no	40471	50093	50149	30713	40429	40433	40462	40498	40570	50169	50226	30645	30739	50050	50051	50136	50167
F	0.18	0.12	0.12	0.10	0.09	0.15	0.18	0.12	0.20	0.14	0.09	0.18	0.03	0.23	0.26	0.11	0.19
Cl....	800	290	230	360	305	550	545	625	415	540	–	155	95	145	200	–	220
Li....	7	–	20	–	29	29	38	–	36	40	–	48	–	–	–	–	–
Rb ...	70	55	55	100	90	110	170	110	90	150	115	80	25	100	180	170	170
Sr....	820	630	200	155	260	50	50	160	70	100	255	50	85	60	55	70	80
Ba ...	2880	3525	3990	650	1360	50	35	700	290	225	1170	n.d.	20	10	n.d.	190	80
Sc....	37	–	36	–	17	19	14	–	10	11	–	7.5	–	–	–	–	–
Y	50	40	65	45	30	65	65	45	65	70	40	120	80	120	130	80	75
La ...	125	–	50	–	65	150	200	–	215	140	–	245	–	–	–	–	–
Ce ...	195	150	90	115	140	230	280	175	285	255	95	480	300	520	470	300	230
Nb ...	45	75	25	20	30	70	85	35	70	65	30	185	95	170	180	120	105
Cr....	385	–	255	–	100	125	95	–	90	60	–	60	–	–	–	–	–
Cu ...	43	–	13	–	7.1	39	17	–	14	14	–	27	–	–	–	–	–
Ga ...	26	–	25	–	19	28	20	–	31	33	–	40	–	–	–	–	–
Pb ...	n.d.	n.d.	n.d.	n.d.	n.d.	15	n.d.	n.d.	n.d.	n.d.	n.d.	40	n.d.	30	20	–	n.d.
K/Rb.	427	508	653	400	501	354	235	426	408	296	425	303	444	189	195	294	204
F.I....	53.9	57.7	68.6	82.3	79.0	81.5	82.1	86.0	83.2	85.9	85.0	87.5	85.0	83.0	84.7	88.3	85.0

n.d. = not detected. F.I. = Fractionation Index, Σ norm. q + or + ab + ac + ns.
Analysts: Li, Sc, La, Cr, Cu, Ga – R. A. Edge; others – R. Macdonald.

Fluorine, chlorine and water

The distribution of H_2O in the dykes may also be discussed here, as it is related to that of the halogens. Although H_2O decreases regularly with increasing F.I. (fig. 1 a) there is a considerable spread of F and Cl values, and no obvious trends are shown in the diagram. Significant trends may be seen, however, by averaging the F and Cl values for each rock group (table 3). F is enriched in more acid dykes, with a slight decrease between riebeckite- and aegirine-bearing microgranites, whereas there is an overall decrease in Cl with fractionation. The Cl trend contrasts with the general observation that both F and Cl are enriched in lower-temperature, more alkaline liquids (Fleischer & Robinson, 1963; Johns & Huang, 1967). It is possible that Cl and H_2O in the trachydolerites and hastingsite microsyenites were being removed by apatite fractionation, but apatite is absent as a phenocryst phase in more acid dykes, and another explanation is required for the decrease in Cl and H_2O.

The distribution of the F, Cl and H_2O in the dykes seems instead to be related to the mineralogy, which is summarised in table 2. It is suggested

alkaline dykes, in p.p.m. except F (wt. %)

Riebeckite microgranites											Aegirine microgranites			
30685	30758	40427	40449	40493	40495	40575	50163	50181	50187	50237	30691	40554	40600(a)	50197
0.20	0.08	0.26	0.41	0.16	0.16	0.11	0.52	0.17	0.20	0.25	0.15	0.29	0.25	0.08
95	50	140	340	85	300	325	55	235	–	90	120	110	75	350
95	167	–	–	–	244	77	–	89	178	–	–	238	–	25
110	260	555	300	365	460	325	360	250	175	265	300	365	400	590
50	60	45	90	50	45	55	50	65	55	70	50	50	50	60
n.d.	20	n.d.	100	25	n.d.	n.d.	n.d.	85	25	30	n.d.	n.d.	n.d.	n.d.
4.7	4.6	–	–	–	3.7	2.8	–	3.0	2.9	–	–	8.8	–	5.0
120	115	135	140	85	180	110	200	85	130	125	130	145	105	425
265	260	–	–	–	505	340	–	180	420	–	–	505	–	820
770	570	860	540	620	730	650	935	400	600	550	950	755	705	1340
330	270	505	190	190	450	200	275	120	200	200	205	220	230	695
35	30	–	–	–	10	25	–	25	30	–	–	30	–	15
6.5	3.8	–	–	–	5.2	11	–	5.2	8.3	–	–	9.0	–	5.0
35	29	–	–	–	48	34	–	21	40	–	–	30	–	22
100	20	95	225	65	120	60	90	20	–	55	105	85	70	70
224	134	52	121	96	74	115	89	144	129	114	141	92	107	64
92.8	93.9	93.3	88.0	93.8	97.8	94.7	93.6	94.5	94.0	92.6	99.3	97.1	97.4	97.7

that Cl entered into groundmass biotites and amphiboles of the trachydolerites and hastingsite microsyenites in fairly large amounts but that in more acid dykes it was excluded from amphibole lattices by the preferential entry of F and lost from the dykes. It may be significant that in those two trachydolerites where the biotite has been largely altered to chlorite, Cl is considerably lower (50149 = 230 p.p.m., 50093 = 290 p.p.m., table 1) than in the unaltered trachydolerite (40471 = 800 p.p.m.), suggesting that Cl was partially lost on alteration of the biotite. In this case the average Cl content for the trachydolerites given in table 3 is too low, and may actually be nearer 800 p.p.m.; the decrease of Cl with increasing F.I. would thus be more regular.

This explanation of Cl distribution could also be applied to H_2O; as F-rich riebeckite-arfvedsonite became more abundant, the tendency for Cl and H_2O to be excluded from the rock-forming minerals was increased. Indirect evidence for this hypothesis comes from the analysis of the riebeckite-arfvedsonite from the Central Complex sill 40595, which shows considerable enrichment of F over H_2O, 2.75 % and 0.30 % by weight respectively. In the hastingsitic and riebeckitic amphiboles of the Younger Granites of Nigeria, Borley (1963) and Borley & Frost (1963) have shown

a

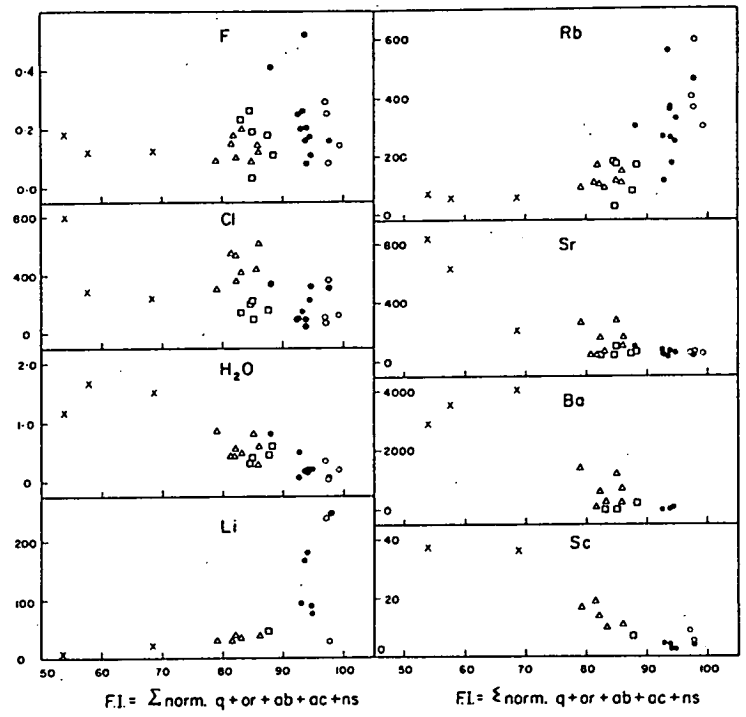
F
Cl
H_2O
Li
Rb
Sr
Ba
Sc
F.I. = Σ norm. q + or + ab + ac + ns
F.I. = Σ norm. q + or + ab + ac + ns

b

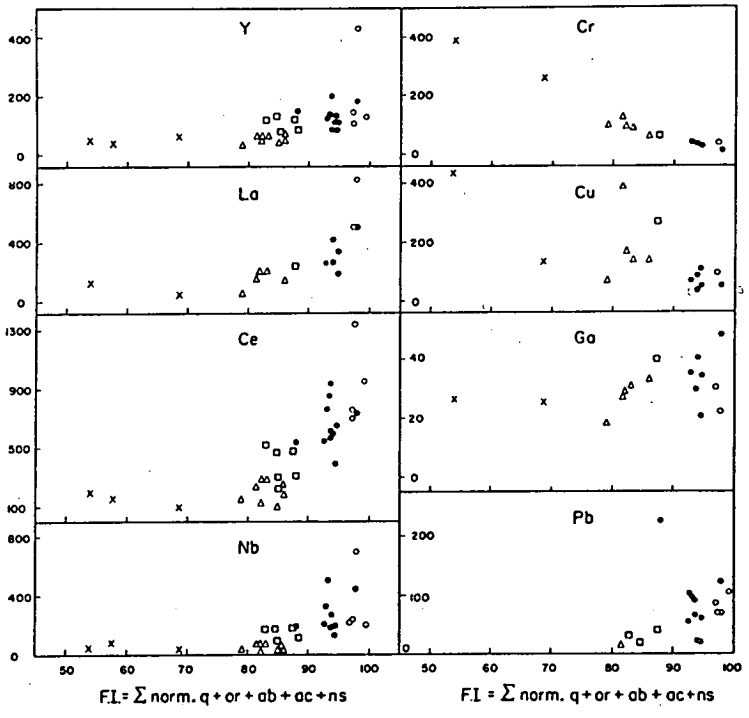
Y
La
Ce
Nb
Cr
Cu
Ga
Pb
F.I. = Σ norm. q + or + ab + ac + ns
F.I. = Σ norm. q + or + ab + ac + ns

Table 2. Summary of petrography of Tugtutôq alkaline dykes

Rock Group	Phenocrysts	Groundmass
Trachydolerites	Scarce apatites.	Cryptoperthitic feldspar (occasional oligoclase cores), biotite, augitic pyroxene, ore, apatite. Textures – generally orthophyric.
Hastingsite microsyenites	Alkali feldspar (anorthoclase → microperthite), fayalite pseudomorphs, pyroxene (augite → ferroaugite), ore, apatite, scarce hastingsite.	Microantiperthitic feldspar, with occasional albite rims, hastingsite, riebeckite-arfvedsonite limonite, ore, quartz, pyroxene, apatite, carbonate. Occasional vugs. Textures – trachytic.
Riebeckite microsyenites	Microperthitic feldspar. Ore.	Microantiperthitic feldspar, riebeckite-arfvedsonite, ore, limonite, quartz, zircon, Textures – trachytic, felsitic, spherulitic.
Riebeckite microgranites	Antiperthitic feldspar, quartz, ore, riebeckite-arfvedsonite (or aegirine aggregates pseudomorphing it).	Microantiperthitic feldspar, riebeckite-arfvedsonite, aegirine, ore, zircon, limonite, fluorite, astrophyllite. Textures – trachytic, spherulitic, felsitic, granophyric, microgranitic.
Aegirine microgranites	Antiperthitic feldspar quartz, hedenbergite, fayalite pseudomorphs.	Aegirine, microperthitic feldspar, quartz, riebeckite-arfvedsonite, astrophyllite. Textures – felsitic, trachytic, spherulitic.

Table 3. Average F and Cl values for the dykes

Rock type	No. of analyses	Avge F wt. %	(range)	Avge Cl p.p.m.	(range)
Trachydolerites.....	3	0.14	(0.12–0.18)	440	(230–800)
Hastingsite microsyenites.....	8	0.13	(0.09–0.20)	418	(305–625)
Riebeckite microsyenites.....	6	0.17	(0.03–0.26)	163	(95–220)
Riebeckite microgranites.....	11	0.23	(0.08–0.52)	172	(50–340)
Aegirine microgranites.....	4	0.19	(0.08–0.29)	164	(75–350)

Fig. 1. Variation diagram a) for F, Cl, H_2O, Li, Rb, Sr, Ba, Sc, and b) for Y, La, Ce, Nb, Cr, Cu, Ga and Pb using Fractionation Index (F. I.), the sum of the normative components q+or+ab+ac+ns as abcissa. Crosses: trachydolerites, triangles: hastingsite microsyenites, squares: riebeckite microsyenites, closed circles: riebeckite microgranites, open circles: aegirine microgranites.

that Cl and H_2O are concentrated in the hastingsitic varieties, while the riebeckitic types are F-rich.

In the aegirine-rich dykes, all three elements are partially excluded, due to the scarcity of suitable lattice sites, and the average values are lower than in the riebeckite microgranites (table 3). The fugitive halogens presumably were lost from the dykes in the late-stage fluids which carried the excess alkalis. Earlier workers (e.g. Noble, 1965, Noble et al., 1967) have stressed the loss of large amounts of halogens on devitrification of peralkaline rhyolitic glass.

In summary, F, Cl and H_2O were enriched in residual liquids during fractionation of the Tugtutôq alkaline magmas. Their present distribution reflects however the number of available lattice sites in the rock-forming minerals. F was preferentially accepted into the amphiboles of more acid dykes and increasing proportions of Cl and H_2O were lost on crystallisation.

Lithium

Fig. 1a shows that there is a mild increase in Li between the trachydolerites and the microsyenites and a very strong enrichment in the microgranites, up to 245 p.p.m. The aegirine microgranite 50197 has an anomalously low Li content of 25 p.p.m. (fig. 1 a). Strong Li enrichment in the Kûngnât granites has been recorded by Upton (1960), one specimen (26498) having the very high value of 900 p.p.m. Bowden (1966) has found Li contents up to 630 p.p.m. in Nigerian riebeckite granites, and has suggested that Li is enriched in residual liquids in the series amphibole granites → riebeckite granites. The Mayor Island pantellerites (Ewart, Taylor & Capp, 1968) and the nordmarkites and ekerites of Oslofjord (Dietrich, Heier & Taylor, 1965) are relatively low in Li, with ranges of 56–79 and 15–63 p.p.m. respectively.

Li does not tend to enter alkali feldspars, as for example, in the phenocrysts from the Tugtutôq dykes (table 4) or the feldspars from the Kûngnât complex (Upton, 1960) where the maximum value is only 10 p.p.m. In peralkaline acid rocks, it seems instead to be concentrated in riebeckite-arfvedsonite. Borley (1963) reports Li values up to 1.02 % by wt. from Nigerian amphiboles, and two riebeckite-arfvedsonites from Kûngnât have 1300 and 2000 p.p.m. Li (B.G.J. Upton, pers. comm.). This concentration of Li into the Na-Fe amphibole may explain the anomalously low value of 25 p.p.m. in the aegirine microgranite, 50197. That rock is unique among the analysed microgranites in having no modal amphibole and there may have been a lack of suitable lattice sites to hold the Li, the major part escaping in the alkaline late-stage fluids on crystallisation of the dyke.

Table 4. Trace element data for alkali feldspar phenocrysts from Tugtutôq dykes

Specimen	Or	Ab	An	Li	Rb	Sr	Ba	Y	Cu	Ga	K/Rb
Hastingsite microsyenites											
*50226	39.5	53.5	7.0	–	60	760	2900	–	–		881
*40498	42.0	52.0	6.0	–	85	335	2300	–	–		660
*30713	41.0	54.0	5.0	–	105	375	2300	–	–		544
50169	45.2	50.7	4.1	2.8	175	215	1055	10	10	39	355
40570	46.6	49.8	3.6	2.1	–	215	1310	–	31	13	–
Riebeckite microsyenites											
50050	40.0	57.0	3.0	10	–	–	–	–	58	41	–
50167	62.4	35.0	2.6	–	390	155	415	20	–	–	212
Riebeckite microgranites											
50187	34.9	64.5	0.6	2.2	310	25	230	25	6.3	52	150
40495	59.3	40.3	0.4	13	1100	15	100	60	5.2	29	70

* – from Upton (1964a).

Rubidium

Rb values vary from 25 p.p.m. to 590 p.p.m. and show an overall increase with F.I. (fig. 1a). They can be compared with Rb data for several alkaline and peralkaline suites, e.g. western Kûngnât (62–375 p.p.m., Upton, 1960), Ilímaussaq (150–623 p.p.m., Hamilton, 1964), the syenites and granites of the New Hampshire White Mountain Magma series (87–370 p.p.m., Butler & Smith, 1962), the Paresis complex South-West Africa (120–550 p.p.m., Siedner, 1965) and the Hviddal giant dyke (80–300 p.p.m., Upton, 1964a) but do not reach the concentrations (1400 p.p.m.)

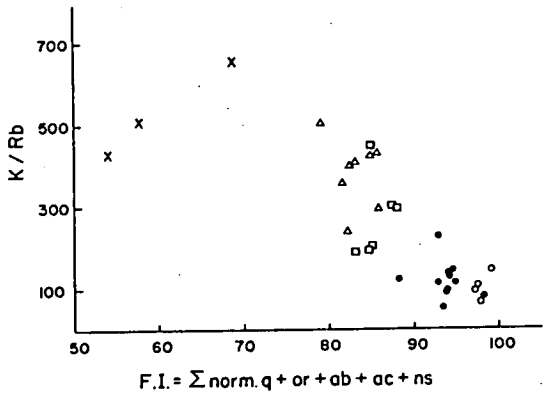

Fig. 2. K/Rb against F. I. in Tugtutôq dykes. Symbols as in fig. 1.

reported by Butler et al. (1962) for Nigerian albite-riebeckite granites, or the value of 950 p.p.m. in a Nevadan pantellerite glass (Noble, 1965). Rb also increases steadily with F.I. in the feldspar phenocrysts (table 4) from 60 p.p.m. in the hastingsite microsyenite 50226 to ~ 1100 p.p.m. in the aegirine microgranite 40495. Similar behaviour is observed in the feldspars of the Kûngnât (Upton, 1960) and Hviddal (Upton, 1964b) intrusions.

The K/Rb ratio drops steadily with increasing F.I. from 653 in a trachydolerite to 52 in a microgranite (fig. 2). This behaviour parallels that in many other alkaline complexes and has been attributed to the slight size difference between the K^+ ion (1.35Å) and the Rb^+ ion (1.47 Å), leading to an enrichment of Rb relative to K during fractionation dominated by feldspar crystallisation (Taylor, 1965). Very low values of K/Rb are characteristic of strongly fractionated rocks. The K/Rb ratio of the feldspar phenocrysts in the dykes also decreases with increasing F.I.

Strontium and barium

Sr falls from 820 p.p.m. in the trachydolerites to 100 p.p.m. in the hastingsite microsyenites, and thence to values close to 50 p.p.m. in the microgranites (fig. 1a). Sr is concentrated in the feldspar phenocrysts relative to the groundmass of porphyritic microsyenites but is present in decreasing amounts in the feldspars of more acid dykes, and the microgranite feldspar phenocrysts actually contain less Sr than the groundmass (cf. tables 1 and 4, using bulk rock compositions as approximate »liquid« compositions).

Similar behaviour is shown by Ba, except that there is an initial build-up in the trachydolerites (fig. 1a). Ba is known to concentrate in residual liquids during differentiation of basic magmas until an alkali feldspar begins to crystallise (Taylor, 1965) and its behaviour in the Tugtutôq rocks would seem normal on those grounds. That Sr shows steady decrease in this range (fig. 1a) indicates that it was being fractionally removed by feldspar and perhaps apatite at a stage when Ba was still being allowed to concentrate in the residual liquids. Like Sr, Ba concentrates in the feldspar phenocrysts, and the ratio Ba feldspar phenocrysts/Ba whole rock decreases with in-

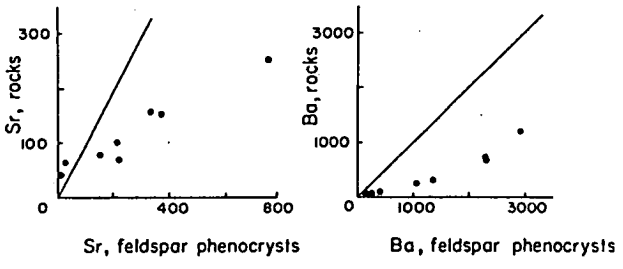

Fig. 3. Comparison of Sr and Ba in feldspar phenocrysts and their host rocks.

creasing F.I. (fig. 3). In contrast to Sr however, the ratio is never less than 1.

Very rapid decrease of Ba with increasing differentiation is common in trachyte-rhyolite and trachyte-phonolite associations, due to fractionation of alkali feldspar. The range of values in the syenite-granite sequence of western Kûngnât (Upton, 1960) is 4100–48 p.p.m., in the nordmarkites and ekerites of Oslofjord, 890–11 p.p.m. (Dietrich et al., 1965), in the Ilímaussaq augite syenite → lujavrite series 5000–10 p.p.m. (Hamilton, 1964) and in the Hviddal giant dyke, 6000–9 p.p.m. (Upton, 1964b).

Scandium

The geochemical behaviour of Sc has recently been reviewed by Norman & Haskin (1968) who suggested a) that Sc decreases with fractionation and b) that there is no good evidence of a close geochemical relationship between Sc and any major element. Sc had previously been found to substitute for Fe^{2+} in pyroxenes (Wager & Mitchell, 1951; Borisenko, 1959), but was not detected in co-existing olivines, an anomaly attributed to the difficulty of balancing charges in the olivines (Taylor, 1965). Presumably for similar reasons, the element was also absent from opaque iron ores. Wager & Mitchell (1951) record Sc in the apatites of the later basic differentiates of Skaergaard, presumably replacing Ca, but on the other hand, it has not been found to replace Ca in feldspar. Sc was not found in apatites by Nockolds & Mitchell (1948) but it did enter sphene and hornblende, possibly substituting for Ti rather than Ca.

In the Tugtutôq dykes, Sc drops off sharply with differentiation, with perhaps a slight enrichment in the most fractionated microgranites (fig. 1a). The behaviour of Sc is clearly complex, and in the absence of data of Sc abundances in the minerals, comments on Sc distribution in the dykes and on the phases which removed it during magmatic evolution would be speculative.

Yttrium, lanthanum and cerium

Although Y, La and Ce can replace Ca in the 9-coordination site in apatite and to a lesser extent in pyroxene and feldspar, they are generally concentrated in residual liquids (Taylor, 1965). This is the behaviour demonstrated in the Tugtutôq dykes (fig. 1b). Ce and La show considerably more enrichment than Y, and Ce is by far the most abundant of the three elements in the intermediate to acid dykes, ranging from 100–200 p.p.m. in the trachydolerites to a maximum of 1340 p.p.m. in one of the aegirine microgranites (50197).

Table 5. Some comparative data for Y, La and Nb in alkaline rocks

Locality	Rock types (end-members)	Range of Y values	Range of La values	Range of Nb values	Reference
Tugtutôq area	trachydolerite→aegirine microgranites	30–425	50–820	20–695	This work
Hviddal dyke	augite → foyaites syenites	57–105	detected in two rocks 210, 280	44–150	Upton (1964b)
Central Complex, Tugtutôq	oversaturated syenites and alkali granites	60–290	–	50–260	Macdonald (unpublished data)
Ilímaussaq	augite syenites → lujavrites / alkaline granites	0<1000 1000	0<3000 2500	0<1400 1100	Hamilton (1964)
Qagssimiut	trachytic dykes, generally cf. Tugtutôq	50–240	40–500	10–160	Ayrton & Burri (1967)
Oslofjord province	nordmarkites and ekerites	79–130	32–150	115–250	Dietrich et al. (1965)
Pantelleria	pantellerites	85–180	–	250–400	Butler & Smith (1962)
Nevada	pantelleritic tuffs and glasses	73–450	110–610	70–640	Noble (1965)
Mayor Island, New Zealand	pantellerites	140–190	93–130	63–81	Ewart et al. (1968)
White Mountain Magma Series	over- and under-saturated syenites, alkali granites (gabbro included for Nb)	b.s-90	–	15–330	Butler & Smith (1962); Gottfried, Jenkins, & Grimaldi (1961)

Some recent data for Y and La in alkaline rocks are listed in table 5. The level of concentration of Y in the Tugtutôq rocks compares very closely with those from alkaline volcanic rocks reported by Butler & Smith (1962) and for Norwegian peralkaline granites (»ekerites«) (Dietrich et al., 1965), but never reaches the striking degree of enrichment of the Ilímaussaq granites and lujavrites, 1000 p.p.m. (Hamilton, 1964). It is rather surprising that Y was not detected in the Kûngnât rocks (Upton, 1960), though the emission spectrographic method used may have been rather insensitive or the analysis line employed may have been subjected to interference. The concentration of Y in residual liquids is seen in alkaline rock suites to a much greater extent than in acid rocks of tholeiitic or calc-alkaline suites (Nockolds

& Allen, 1954). The data for the alkaline complexes presented in table 5 include, therefore, some of the highest Y concentrations reported for igneous rocks. The value of 425 p.p.m. for the aegirine microgranite 50197 (table 2) is very high when compared to other alkali granitic rocks, which themselves are considerably enriched in Y relative to the crustal granite average, 40 p.p.m. (Taylor, 1964).

Unlike Y, data for Ce and La in alkaline rocks are scarce and comparisons are not easily made. Ce was not detected in the Kûngnât rocks by emission spectroscopy (Upton, 1960) and there are no published data for the Ilímaussaq rocks. 3200 p.p.m. Ce has been reported from rockallite by Washington (1914), which is considerably higher than any Tugtutôq rock.

Taylor (1964) has suggested that the average concentration of La in the crust is 30 p.p.m. and in granitic rocks is 50 p.p.m. This being so, the degree of enrichment of La in several of the alkaline rock complexes listed in table 5, especially the peralkaline suites, is striking. In the Ilímaussaq complex, the agpaites show an enrichment of $\times$ 60 over the augite syenites, while in the Tugtutôq dykes, the microgranites are about $\times$ 10 richer in La than the trachydolerites.

Niobium

Although niobium can replace titanium in titanium minerals, it is generally concentrated in the residual liquids (Taylor, 1965). This is the behaviour demonstrated in the Tugtutôq dykes (fig. 1b). Previous workers have established that the highest concentrations of Nb in igneous rocks are in alkaline rocks, especially nepheline syenites, alkali granites and in carbonatites (Parker & Fleischer, 1968). The Tugtutôq microgranites ($<$ 695 p.p.m.) and the Ilímaussaq granites and lujavrites ($<$ 1400 p.p.m.) are much enriched in Nb compared to the various alkaline rocks listed in table 5.

Chromium

Cr decreases very regularly from 385 p.p.m. in the trachydolerite 40471 to values $<$ 20 p.p.m. in the aegirine microgranites (fig. 1b). The phases which fractionated Cr were presumably pyroxenes and ore in the trachydolerites and hastingsite microsyenites, and ore alone in the more acid dykes. Cr tends to be intensely depleted in peralkaline rocks; it is below the limit of detection in the Kûngnât (Upton, 1960) and Mayor Island (Ewart et al., 1968) series and is just detectable in the nordmarkites and ekerites of Oslofjord (Dietrich et al., 1965).

Copper

Cu is present in small amounts (< 50 p.p.m.) in all the dykes, showing an overall depletion with increasing F.I. (fig. 1b). Upton (1960) reported a similar decrease in the western Kûngnât syenites and granites, but in some alkaline series, such as the Hviddal dyke, the nordmarkites and ekerites of Oslofjord and the pantellerites of Mayor Island, Cu does not display a regular distribution with fractionation.

The geochemistry of Cu is complicated. It enters Ca-bearing minerals, such as apatite and plagioclase, and can substitute for Fe^{2+} (Taylor, 1965). Cu also forms sulphide phases. It is clear from the data of Upton (1960, tables 11 and 12) that Cu is generally concentrated in the feldspars of the Kûngnât syenites; the distribution is very irregular, however, and Upton suggested that Cu is actually present in the feldspars as submicroscopic sulphide. The decreasing Cu content in more acid dykes from Tugtutôq is refected in the feldspar phenocrysts (table 4), though the feldspars from 50050 have an anomalously high value of 58 p.p.m., perhaps indicating the presence of sulphide. It is, therefore, impossible without further mineral analyses (especially of apatite and pyroxene phenocrysts) to decide which phases have fractionated Cu from the liquids, and whether the phase was a silicate, sulphide or even oxide.

Gallium

Ga values drop between the trachydolerites and the most basic hastingsite microsyenite, increase through the microsyenites, and then show a considerable scatter in the microgranites (fig. 1b). This scatter contrasts with the fairly regular distribution of Ga in the Kûngnât and Hviddal intrusions (Upton, 1960; Upton, 1964b), and seems to be due to loss of Ga in the late-stage, Na-rich fluids during devitrification. The evidence for this is briefly discussed below.

During fractionation of peralkaline acid magma, the ratio Na_2O/K_2O generally increases in residual liquids (Bailey & Schairer, 1964, Noble, 1968, Ewart et al., 1968), and it may be assumed that the Tugtutôq rhyolitic magmas also showed this trend. As mentioned earlier, however, the Na_2O/K_2O ratios of the acid dykes were considerably lowered on devitrification, Na being lost in the late-stage fluids probably comparable to those responsible for the albitisation of alkaline granites. If it can be assumed that the *original* Na_2O/K_2O ratios of the rhyolite magmas were reasonably constant, then the *present* Na_2O/K_2O ratios of the dykes give a crude estimate of the amount of Na lost relative to K. This assumption is probably justifiable: the ratio in the Mayor Island pantellerite obsidians varies from

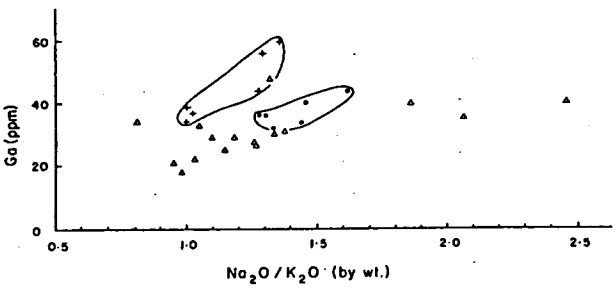

Fig. 4. Ga against Na_2O/K_2O ratio in albitised (plus signs), pantellerite obsidi, ans closed circles) and Tugtutôq dykes (triangles). Data for granites from Bowden (1964) and Upton (1960), for pantellerites from Noble (1965) and Ewart et al., (1968).

1.28 to only 1.46 and in the Pantellerian pantellerite obsidians from 1.33 to 1.48 (Ewart et al., 1968; Carmichael, 1962; Chayes & Zies, 1962, 1964).

Accordingly, Ga values in the microgranites have been plotted against Na_2O/K_2O ratio (fig. 4). There seems to be a significant decrease in Ga with decreasing Na_2O/K_2O ratio, suggesting that the scatter of Ga values in the microgranites is at least partly due to the fact that some proportion of the original Ga content has been lost in the Na-rich fluids on devitrification.

On this basis, the distribution of Ga in the Tugtutôq dykes can be compared with that of other peralkaline suites. It may be assumed that the behaviour of Ga in pantellerite obsidians has been determined solely by crystal fractionation. Using Na_2O/K_2O as a fractionation index (fig. 4) it can be seen that Ga increases with fractionation in these Mayor Island and Nevadan pantellerites (data from Ewart et al., 1968, Noble, 1965). For any given value of Na_2O/K_2O, the Tugtutôq dykes show lower values of Ga than the pantellerites, as would be expected from the proposal that the dykes have lost some proportion of their original Na content.

It follows from the suggestion made above, that Ga will be enriched in albitising fluids, and Ganeyev & Sechina (1962) and Bowden (1964) have previously shown that Ga is indeed enriched in albitised granites. The granites from Kûngnât are more or less albitised, and analyses of them have been plotted in fig. 4 along with analyses of albitised granites from Northern Nigeria (Bowden, 1964). Since some of the Na content of these granites has been secondarily derived for any given Na_2O/K_2O the Ga content may be expected to be higher than those in the pantellerites or Tugtutôq dykes. This effect is shown in fig. 4. Despite the crudity of the basis of comparison, a series does emerge from these observations: Na-Ga enriched albitised granites, "normal" pantellerites where crystal fractionation has determined the Ga/Na ratio, and the Na-Ga depleted Tugtutôq microgranites.

There is no obviously regular distribution of Ga in the feldspar phenocrysts of the dykes with increasing fractionation. There is evidence, however, from these feldspars and those from the western Kûngnât syenites and

EX. BIBL. UNIV. EDINBURGEN.

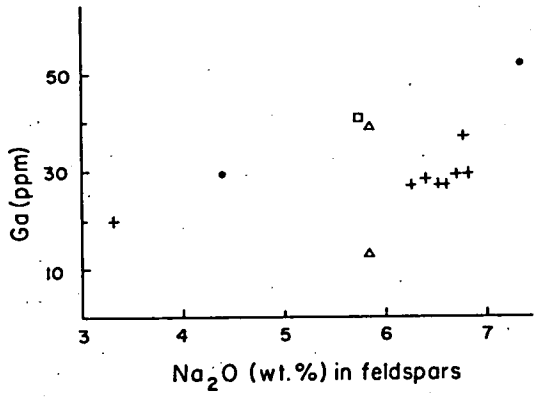

Fig. 5. Ga against Na_2O in feldspar phenocrysts from Tugtutôq dykes and from western Kûngnât syenites and granites (crosses). Kûngnât data from Upton (1960, table 12).

granites (Upton, 1960) that Ga is concentrated in the most sodic feldspars (fig. 5). A similar graph and distribution were presented by Ganeyev & Sechina (1962) for feldspars from albitised Russian granites, and Bowden (1964) has reported that Ga is highest in the feldspars of the albite-riebeckite granites of Northern Nigeria.

The Tugtutôq work confirms that of earlier workers, that the Ga distribution is closely linked with that of Na and that it is highly soluble in alkaline fluids.

Lead

Although on the basis of geometric characteristics Pb might be expected to substitute for K in alkali feldspars and micas and for Ca in plagioclases and apatites, it is generally accepted that Pb is concentrated in residual melts (Taylor, 1965). This is the behaviour demonstrated in the Tugtutôq dykes, where Pb is below the limit of detection (13 p.p.m.) until the riebeckite microsyenite stage, and then increases to nearly 120 p.p.m. in the microgranites. (The high value of 225 p.p.m. for 40449 is not accompanied by anomalously high values for other trace elements and may be the result of contamination.)

The Pb content of the trachytic dykes of the Qagssimiut region (Ayrton & Burri, 1967) compares closely to those from Tugtutôq, varying from the limit of detection, 10 p.p.m., to 35 p.p.m. Dietrich et al. (1965) report late-stage enrichment in ekerites (35–45 p.p.m. Pb) relative to nordmarkites (trace Pb) from the Oslofjord province. In the Paresis complex, South-West Africa, Pb shows strong concentration (< 154 p.p.m.) in the latest comendites of the volcanic cycle and also increases with fractionation in the later, syenitic intrusive cycle up to 93 p.p.m. (Siedner, 1965).

The Pb values of 120 and 154 p.p.m. quoted for peralkaline rhyolites from Tugtuôq and Paresis respectively are considerably enriched when compared, for example, with Turekian & Wedepohl's (1961) average of 19 p.p.m. for "low-calcium" granites and of 12 p.p.m. for syenites, and with Taylor's (1964) crustal granite average af 20 p.p.m.

Alkali ion exchange effects

Macdonald (1969) has suggested that alkali ion exchange may have taken place between the margins and centres of certain of the dykes probably while the dyke was either still molten or glassy. The evidence for this suggestion is limited: a riebeckite microsyenite dyke from eastern Tugtutôq (50050/50051) has centre and margins showing closely comparable major element chemistry apart from Na_2O/K_2O ratios (margin = 3.25, centre = 1.48). The trace elements are also very similar, only Rb and perhaps Cl showing significant differences (table 1). Though Rb is enriched in the central zones of the dyke, the K/Rb of centre and margins are virtually the same, 195 and 189 respectively. It seems likely that Rb followed K (cf. similar ionic radii and charges of K and Rb) during any ion-exchanging across the dyke, but that the other trace metals are fairly evenly distributed through the dyke. This effect obviously requires further investigation, and may have resulted in sampling errors.

Conclusions

The distribution of the trace elements is generally as expected in a fractionation series from classical considerations, and the very high concentrations of Li, Rb, Y, La, Ce, Nb and Ga, and the strong depletion in Sr, Ba and Cr are also typical of highly fractionated alkaline magmas. Part of the original Cl, F, H_2O, Ga and Li contents of the acid dykes is thought to have escaped in a Na-rich residual fluid phase on crystallisation. The trace element study stresses certain features shown by the major element work, namely that the present compositions of crystallised peralkaline acid rocks cannot safely be regarded as those of the original magmatic liquids. Consequently the behaviour of certain trace elements during differentiation of such magmas can be ascertained only by analysing obsidians and their phenocryst phases.

Appendix

Analytical Methods

X-ray fluorescence spectroscopy

The samples were analysed for Cl, Rb, Sr, Ba, Y, Ce, Nb and Pb by X-ray fluorescence spectroscopy using Philips equipment (PW 1310/50 generator with PW 1320 control cabinet). The rock powders (-120 mesh) were held against mylar film for all elements except Cl, where the powder was briquetted at a pressure of 15 tons/sq. in. in order to increase the counting rate. The operating condition for the analyses are given in table A 1 and the precision of the methods in table A 2. International standards G-1 and W-1 were used in all cases to construct calibration curves, supplemented in some cases by new U.S.G.S. standards (G-2, GSP-1 and AGV-1), C.A.A.S. syenite-1, "seeded" rocks and synthetic powders. Values of standards employed are given in table A 3.

Emission spectroscopy

Li, Cu, Ga, Cr, La and Sc were determined using d.c. arc emission spectroscopy by the procedures of Ahrens & Taylor (1961) on a Hilger large quartz and glass spectrograph with a seven-step (2:1 ratio) sector. For the determination of Cr, La and Sc, samples were mixed with twice their weight of a carbon-palladium mixture containing 1 % Pd, the palladium serving as internal standard, and arced to completion at 6.8 amps. For the determination of Li, Cu and Ga, the unmixed samples were arced at 4.4 amps until the end of the alkali element distillation period. Sodium served as a variable internal standard. All determinations were made in duplicate.

Lines read (using a Joyce-Loebl Mark IIIC, double-beam recording microdensitometer) were Li 6707, Na 5682, Cu 3274, Ga 4172, Na 3303, Sc 4246, Cr 4254, La 4333 and Pd 3959. Background corrections were made for Li, Sc, Cr and La.

Granite G-1, diabase W-1 and the C.A.A.S. syenite-1 were used as standards. The concentration values adopted are given in table A 3. Analytical precision expressed as the coefficient of variation (C), was calculated from all duplicate determinations by the method of Youden (1959), and is given in table A 2.

Fluorine was determined spectrophotometrically by the method of Peck & Smith (1964).

Table A1. Operating conditions for x-ray fluorescence spectroscopy

Element	Line	2θ Peak	2θ Background	Tube	Tube running conditions KV	Amps.	Atmosphere	Collimator	Crystal	Counter	EHT (volts)	Discrimination LL	CW	Att.
Rb	Kα1	26.52	27.52	W	40	20	Air	F	LiF	S	800	5	24	2³
Sr	Kα1	37.65	38.65	W	40	20	Air	F	Topaz	S	890	6	22	2⁴
Ba	Kα1	16.32	15.32	W	55	20	Air	F	Topaz	S	750	14	14	2³
			17.32											
Y	Kα1	23.69	23.19	W	40	20	Air	F	LiF	S	800	5	24	2³
			24.19											
Ce	Kα1	15.10	14.70	Cr	70	20	Air	F	Topaz	S	800	9	23	2⁴
			15.50											
Nb	Kα1	21.30	20.80	Cr	40	20	Air	F	LiF	S	710	4	16	2²
Pb	Lα1	51.60	51.10	W	60	32	Air	F	Topaz	S	850	12	22	2³
			52.10											
Cl	Kα1	35.45	38.45	Cr	55	28	Vac.	C	P.E.	FP	1800	15	14	2⁶

Vac = vacuum; F = fine, C = course collimators; LL = lower level; CW = counter window; Att. = attenuation in discrimination; S = scintillation; FP = flow proportional; P.E. = penta erythritol.

Table A2. Analytical precision

Element	Cl	Rb	Sr	Ba	Y	Ce	Nb	Pb	Li	Cu	Ga	Cr	La	Sc
C (%)	10	2	2	2	5	5	5	7	4	9	6	9	9	13

Table A3. Geochemical standards and concentration values (p.p.m.)

Element	G-1	W1	Syenite-1	Others
Na	24,620 (F)	15,350 (F)	24,030 (W)	–
Li	24 (F)	12 (F)	126 (W)	–
Cu	13 (F)	110 (F)	25 (W)	–
Ga	18 (F)	16 (F)	18 (W)	–
Cr	22 (F)	120 (F)	–	–
La	120 (F)	–	243 (W)	–
Sc	3 (F)	34 (F)	14 (W)	–
Rb	220 (F)	22 (F)	–	G-2 170 (E); GSP-1 260 (E)
Sr	280 (E)	220 (E)	–	G-2 500 (E); AGV-1 660 (E)
Ba	1220 (F)	215 (E)	273 (W)	AGV-1 1420 (E)
Y	13 (F)	25 (F)	–	Synthetics
Ce	200 (F)	25 (F)	–	,,
Nb	20 (F)	10 (F)	146 (W)	,,
Pb	49 (F)	8 (F)	315 (E)	,,
Cl	A basalt of known Cl content was "seeded" with various amounts of NaCl			

Sources: F (Fleischer, 1965); W (Webber, 1965); E (Preferred values, Geology Department, Edinburgh University).

Acknowledgements. The XRF data presented here formed part of a Ph. D. thesis submitted by one of us (R. M.) to the University of Edinburgh. Thanks are due to Professor F. H. Stewart and Dr. N. B. Price for laboratory facilities, to Dr. Price and Mr. G. R. Angell for training, help and advice during the analytical work and to Dr. B. G. J. Upton who supervised the study. Dr. I. G. Meighan was a welcome companion in the laboratory. The material was collected in Greenland under the auspices of the Geological Survey of Greenland, and the results are published by permission of the Director of the Survey.

Dansk sammendrag

De intermediære til sure gange i Tugtutôq-området i Sydgrønland karakteriseres af et højt indhold af grundstofferne Li, Rb, Y, La, Ce, Nb og Pb samt ved udbredt mangel på Sr, Ba og Cr. Fordelingen af sporeelementerne er i overensstemmelse med gangenes dannelse ved fraktioneret krystallisation. En del af det oprindelige indhold af Cl, H_2O, Li og Ga i det rhyolitiske magma forsvandt ved gangenes devitrifikation.

Department of Geology, University of Reading,
Whiteknights Park, Reading, RG6 2AB, England
April 15th, 1969

References

Ahrens, L. H. & Taylor, S. R. 1961: *Spectrochemical analysis.* (2nd ed.), Pergamon, Oxford.

Ayrton, S. N. & Burri, M. 1967: L'évolution du socle précambrien dans la region de Qagssimiut. *Bull. Grønlands geol. Unders.* **66** (also *Meddr Grønland*, **175**, 2), 90 pp.

Bailey, D. K. & Schairer, J. F. 1964: Feldspar-liquid equilibria in peralkaline liquids – the orthoclase effect. *Am. J. Sci.* **262**, 1198–1206.

Borisenko, L. F. 1959: On the distribution of scandium in igneous rocks from the example of some massifs of the Soviet Union. *Geochemistry* **7**, 770–777.

Borley, G. D. 1963: Amphiboles from the Younger Granites of Nigeria. Part 1. Chemical classification. *Mineralog. Mag.* **33**, 358–376.

Borley, G. D. & Frost, M. T. 1963: Some observations on igneous ferrohastingsites. *Mineralog. Mag.* **33**, 646–662.

Bowden, P. 1964: Gallium in Younger Granites of Northern Nigeria. *Geochim. cosmochim. Acta* **28**, 1981–1988.

Bowden, P. 1966: Lithium in Younger Granites of Northern Nigeria. *Geochim. cosmochim. Acta* **30**, 555–564

Bridgwater, D. 1965: Isotopic age determinations from South Greenland and their geological setting. *Bull. Grønlands geol. Unders.* **53** (also *Meddr Grønland* **179**, 4), 56 pp.

Butler, J. R., Bowden, P. & Smith, A. Z. 1962: K/Rb ratios in the evolution of the Younger Granites of Northern Nigeria. *Geochim. cosmochim. Acta* **26**, 89–100.

Butler, J. R. & Smith, A. Z. 1962: Zirconium, niobium, and certain other trace elements in some alkali igneous rocks. *Geochim. cosmochim. Acta* **26**, 945–953.

Carmichael, I. S. E. 1962: Pantelleritic liquids and their phenocrysts. *Mineralog. Mag.* **33**, 86–113.

Chayes, F. & Zies, E. G. 1962: Sanidine phenocrysts in some peralkaline volcanic rocks. *Yb. Carnegie Instn Wash.* **61**, 112–118.

Chayes, F. & Zies, E. G. 1964: Notes on some Mediterranean comendite and pantellerite specimens. *Yb. Carnegie Instn Wash.* **63**, 186–190.

Dietrich, R. V., Heier, K. S. & Taylor, S. R. 1965: The igneous rock complex of the Oslo region. 20: Petrology and geochemistry of ekerite. *Skr. norske Vidensk. Akad. I. Mat.-naturv. Kl.* **19**.

Ewart, A., Taylor, S. R. & Capp, A. C. 1968: Geochemistry of the pantellerites of Mayor Island, New Zealand. *Contr. Mineral Petrol.* **17**, 116–140.

Fleischer, M. 1965: Summary of new data on rock samples G–1 and W–1, 1962–1965. *Geochim. cosmochin. Acta* **29**, 1263–1283.

Fleischer, M. & Robinson, W. O. 1963: Some problems on the geochemistry of fluorine. *Royal Soc. Canada Special Publn* **6**, 58–75.

Ganeyev, I. G. & Sechina, N. P. 1962: Geochemical characteristics of albitised granites. *Geochemistry* **2**, 158–165.

Gottfried, D., Jenkins, L. & Grimaldi, F. S. 1961: Distribution of niobium in three contrasting comagmatic series of igneous rocks. *Prof. Pap. U. S. geol. Surv.* **424–B**, 256–258.

Hamilton, E. I. 1964· The geochemistry of the northern part of the Ilímaussaq intrusion, S. W. Greenland. *Bull. Grønlands geol. Unders.* **42** (also *Meddr Grønland* **162**, 10), 104 pp.

Johns, W. D. & Huang, W. H. 1967: Distribution of chlorine in terrestrial rocks. *Geochim. cosmochim. Acta* **31**, 35–50.

Macdonald, R. 1969: The petrology of alkaline dykes from the Tugtu:ôq area, South Greenland. *Bull. geol. Soc. Denmark* **19**, 257–282.

Noble, D. C. 1965: Gold Flat member of the Thirsty Canyon Tuff – a pantellerite ash–flow sheet in southern Nevada. *Prof. Pap. U.S. geol. Surv.* **525–B**, 85–90.

Noble, D. C. 1968: Systematic variation of major elements in comendite and pantellerite glasses. *Earth Planet Sci. Letters* **4**, 167–172.

Noble, D. C., Smith, V. C. & Peck, L. C. 1967: Loss of halogens from crystallised and glassy silicic volcanic rocks. *Geochim, cosmochim. Acta* **31**, 215–224.

Nockolds, S. R. & Allen, R. 1954: The geochemistry of some igneous rock series: Part 2. *Geochim. cosmochim. Acta* **4**, 105–142.

Nockolds, S. R. & Mitchell, R. L. 1948: The geochemistry of some Caledonian plutonic rocks. *Trans. R. Soc. Edinb.* **61**, 535–575.

Norman, J. C. & Haskin, L. A. 1968: The geochemistry of Sc: A comparison to the rare earths and Fe. *Geochim. cosmochim. Acta* **32**, 93–108.

Parker, R. L. & Fleischer, M. 1968: Geochemistry of niobium and tantalum. *Prof. Pap. U.S. geol. Surv.* **612**, 1–43.

Peck, L. C. & Smith, V. C. 1964: Spectrophotometric determination of F in silicate rocks. *Talanta* **11**, 1343–1347.

Siedner, G. 1965: Geochemical features of a strongly fractionated alkali igneous suite. *Geochim. cosmochim. Acta* **29**, 113–137.

Taylor, S. R. 1964: Abundance of chemical elements in the continental crust: a new table. *Geochim. cosmochim. Acta* **28**, 1273–1285.

Taylor, S. R. 1965: The application of trace element data to problems in petrology. *Phys. Chem. Earth* **6**, 133–213.

Turekian, K. K. & Wedepohl, K. H. 1961: Distribution of some major elements in some units of the earth's crust. *Bull. geol. Soc. Am.* **72**, 175–192.

Upton, B. G. J. 1960: The alkaline igneous complex of Kûngnât Fjeld, South Greenland. *Bull. Grønlands geol. Unders.* **27** (also *Meddr Grønland* **123**, 4), 145 pp.

Upton, B. G. J. 1962: Geology of Tugtutôq and neighbouring island, South Greenland. Pt. I. *Bull. Grønlands geol. Unders.* **34** (also *Meddr Grønland* **169**, 8), 60 pp.

Upton, B. G. J. 1964 a: Geology of Tugtutôq and neighbouring islands, South Greenland. Pt. II. Nordmarkitic syenites and related alkaline rocks. *Bull. Grønlands geol. Unders.* **44** (also *Meddr Grønland* **169**, 2), 62 pp.

Upton, B. G. J. 1964 b: Geology of Tugtutôq and neighbouring islands, South Greenland. Pt. IV. The nepheline syenites of the Hviddal composite dyke. *Bull. Grønlands geol. Unders.* **48** (also *Meddr Grønland* **169**, 3II), 49–80.

Wager, L. R. & Mitchell, R. L. 1951: The distribution of trace elements during strong fractionation of a basic magma, a further study of the Skaergaard intrusion, East Greenland. *Geochim. cosmochim. Acta* **5**, 129–208.

Washington, H. S. 1914: The composition of rockallite. *Q. Jl geol. Soc. Lond.* **70**, 294–302.

Webber, G. R. 1965: Second report of analytical data for C. A. A. S. syenite and sulphide standards. *Geochim. cosmochim. Acta* **29**, 229–248.

Youden, W. J. 1959: *Statistical methods for chemists.* Wiley, New York.

ZIRCONIUM IN ALKALINE DYKES FROM THE TUGTUTÔQ REGION, SOUTH GREENLAND

RAYMOND MACDONALD AND A. PARKER

MACDONALD, R. & PARKER, A.: Zirconium in alkaline dykes from the Tugtutôq region, South Greenland. *Bull. geol. Soc. Denmark*, vol. 20, pp. 59–63. Copenhagen, July 9th, 1970.

Zr values are reported for 30 alkaline dykes from the Tugtutôq area, South Greenland. Concentrations increase in the fractionation series trachydolerite → aegirine microgranite to a maximum of 7175 p.p.m., but it is not yet clear how Zr is distributed between the various minerals in the silicic dykes.

The rocks occur as swarms of dykes of Gardar age intruded into basement granites some 1150 m years ago (Bridgwater, 1965). The geological setting and details of the igneous activity have been given by Upton (1962, 1964a), while Macdonald (1969) has described the petrology of the dykes, giving 33 rock-analyses. Macdonald & Edge (1970) have presented data for F, Cl, Rb, Sr, Ba, Sc, Y, La, Ce, Nb, Cr, Cu, Ga and Pb in the analysed specimens.

The dykes form a series from trachydolerites through hastingsite- and riebeckite-microsyenites to devitrified microgranites and rhyolites. Though the dykes are thought to represent the products of the extreme fractionation of alkali basalt magma, the compositions of the acid types have been modified by devitrification, resulting in a loss of Na (and to a lesser extent K), Cl, H_2O, Li and Ga (Macdonald, 1969; Macdonald & Edge, 1970).

Results

The results of the analyses are given in table 1, and values are plotted against a Fractionation Index (F.I. = Σ normative q + or + ab + ac + ns) in fig. 1. The determinations were made by X-ray fluorescence, using the following technique.

After grinding to -125 mesh in an agate "Pulverisette", two 2.5 g splits of each rock were fused with lithium tetraborate (Parker, 1968). The resulting beads were then analysed for zirconium on a Philips PW1540 X-ray spectrometer with: a tungsten anode tube operated at 50 kV, 40 mA; fine colli-

4*

Table 1. Zr concentrations in Tugtutôq alkaline dykes

Rock types and GGU collection nos	Zr p.p.m.	F.I.	Rock types and GGU collection nos	Zr p.p.m.	F.I.
Trachydolerites			Riebeckite microgranites		
40471	305	53.9	30685	1255	92.8
50093	335	57.7	30758	1770	93.9
50149	230	68.6	40427	4450	93.3
			40449	1990	88.0
Hastingsite microsyenites			40493	1895	93.8
30713	190	82.3	40495	4045	97.8
40429	175	79.0	40575	1960	94.7
40433	435	81.5	50163	2630	93.6
40462	435	82.1	50181	1120	94.5
40498	190	86.0	50187	1985	94.0
40570	415	83.2	50237	1810	92.6
50169	460	85.9			
			Aegirine micro-granites		
Riebeckite microsyenites			30691	2135	99.3
30645	1160	87.5	40554	2305	97.1
30739	515	85.0	40600(a)	2390	97.4
50050	1430	83.0	50197	7175	97.7
50051	1485	84.7			
50167	590	85.0			

F.I. = Fractionation Index – Σ norm. q + or + ab + ac + ns (Macdonald, 1969).
Values are averages of four determinations.
Analysts: A. Parker, G. J. Smith and J. Ward.

mator; LiF 200 analysing crystal; and scintillation counter. Duplicate determinations were made on each bead, making a total of four per rock. The method was calibrated using a number of international rock standards together with artificial mixtures of "specure" oxides approximating in composition to the rocks being analysed. Corrections were made for strontium interference using the values quoted in Macdonald & Edge (1970). The estimated precision of the method is ± 2.5 % relative.

The absolute values may be compared with those from other Gardar intrusive rocks, which are among the most Zr-rich in the world: trachytic dykes from the Qagssimiut region, 890–3880 p.p.m. (Ayrton & Burri, 1967); the differentiated nepheline syenites of the Hviddal composite dyke, 360–750 p.p.m. (Upton, 1964b); and the syenite-granite suite of the Kûngnât intrusion, 52 – approx. 7000 p.p.m. (Upton, 1960). The Tugtutôq microgranites are analogous to the highly differentiated lujavrites of the

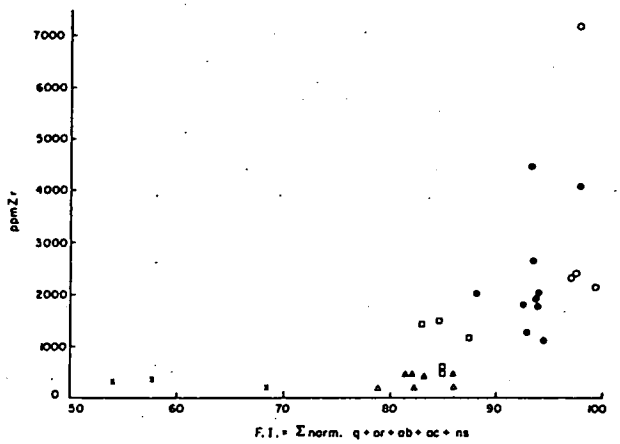

Fig. 1. Variation diagram for Zr in alkaline dykes from the Tugtutôq region. Crosses: trachydolerites; triangles: hastingsite microsyenites; squares: riebeckite microsyenites; closed circles: riebeckite microgranites; open circles: aegirine microgranites.

Ilímaussaq intrusion, which contain up to 12 000 p.p.m. Zr (Ussing, 1912, Gerassimovsky & Kuznetsova, 1967).

Discussion

Goldschmidt's (1954) studies on the geochemistry of Zr established that Zr becomes concentrated in the late magmatic and pegmatitic stages of fractionation, especially in highly alkaline melts. Degenhardt (1957) pointed out that alkaline rocks contain on average twice as much Zr as calc-alkaline types. Further, though zircon is a common accessory in calc-alkaline granites, it is remarkably scarce in peralkaline, Zr-rich rocks, (Mathew & Watson, 1953; Chao & Fleischer, 1960; Siedner, 1965; Bowden, 1966). This feature has been attributed to the high solubility of Zr in alkaline melts and the subsequent restriction of zircon crystallisation. Many data are now available to show that Zr can enter alkali amphiboles and pyroxenes to a large extent, and Bowden (1966), for example, has concluded that most of the Zr in the riebeckite-granites of the Northern Nigerian ring-complexes is present in the lattices of aegirine and riebeckite. Bowden was able to demonstrate that the concentation of Zr in the Younger Granites varies sympathetically with the alkalinity of the liquids, expressed as the agpaitic coefficient.

Similar behaviour is shown by the Tugtutôq dykes. There is an overall increase in Zr concentration in more peralkaline rocks, i.e. with increasing F.I. (fig. 1). This regular behaviour suggests that unlike Li and Ga, Zr was not expelled to any great extent during devitrification of the dykes.

The distribution of Zr among the minerals of the silicic dykes is not well understood at present. Zircon is rare in the peralkaline dykes and is restricted to certain riebeckite-rich varieties. It appears to be completely absent

from rocks containing normative sodium metasilicate. Furthermore, in zircon-free dykes, Zr is not all held in the pyroxenes or amphiboles, as might be expected from the experience of previous workers. In the microgranite 40495, the aegirine aggregates replacing amphibole phenocrysts have 1400 ± 150 p.p.m. Zr, the rock 4045 p.p.m. The riebeckite-arfvedsonite phenocrysts of the microgranite 40427 carry 760 ± 100 p.p.m. Zr, whereas the rock has 4450 p.p.m. Assuming fairly comparable concentrations in the groundmass amphiboles and pyroxenes, which is reasonable especially in the former case since pyroxene aggregates and groundmass pyroxene must have formed more or less contemporaneously, these minerals do not carry anywhere near the bulk of the Zr in these rocks. It is possible that submicroscopic Zr-rich accessory minerals are present in the silicic dykes. In the more coarsely crystalline granite sheets of western Kûngnât (Upton, 1960), which are chemically very similar to the Tugtutôq microgranites, zircon and pyrochlore are common accessories, and indeed pyrochlore has been recorded from two microgranite dykes. The crystallisation of zircon in the Kûngnât granites apparently contradicts previous observations that zircon is absent from strongly peralkaline rocks.

Acknowledgements. The material was collected under the auspices of the Geological Survey of Greenland, and the results are published by permission of the Director, K. Ellitsgaard-Rasmussen. For assistance during the laboratory work we are grateful to G. J. Smith and Mrs J. Ward.

Dansk sammendrag

Zr-indhold opgives for 30 alkaline gange i Tugtutôq-området i Sydgrønland. I fraktioneringsserierne trachydolerit ægirin mikrogranit ses Zr-koncentrationen at stige til maksimalt 7175 p.p.m. Zr-fordelingen mellem de forskellige mineraler i de sure gange er dog endnu uklar.

Department of Geology, University of Reading,
Whiteknights Park, Reading RG6 2AB
August 29th, 1969.

References

Ayrton, S. N. & Burri, M. 1967: L'évolution du socle précambrien dans la région de Qagssimiut. *Bull. Grønlands geol. Unders.* **66** (also *Meddr Grønland* **175**, 2), 90 pp.

Bowden, P. 1966: Zirconium in Younger Granites of Northern Nigeria. *Geochim. cosmochim. Acta* **30**, 985–993

Bridgwater, D. 1965: Isotopic age determinations from South Greenland and their geological setting. *Bull. Grønlands geol. Unders.* **53** (also *Meddr Grønland* **179**, 4), 56 pp.

Chao, E. C. T. & Fleischer, M. 1960: Abundance of zirconium in igneous rocks. *Rept 21st Intern. Geol. Congr. Norden,* Part 1, 106–131.

Degenhardt, H. 1957: Untersuchungen zur geochemische Verteilung des Zirconiums in der Lithosphäre. *Geochim cosmochim. Acta* **11**, 279–309.

Gerassimovsky, V. I. & Kuznetsova, S. Ya. 1967: On the petrochemistry of the Ilímaussaq intrusion, South Greenland. *Geochemistry* **3**, 236–246.

Goldschmidt, V. M. 1954: *Geochemistry*. Oxford University Press.

Macdonald, R. 1969: The petrology of alkaline dykes from the Tugtutôq area, South Greenland. *Bull. geol. Soc. Denmark* **19**, 257–282.

Macdonald, R. & Edge, R. A. 1970: Trace element distribution in alkaline dykes from the Tugtutôq region, South Greenland. *Bull. geol. Soc. Denmark* **20**, 38–58.

Mathews, W. H. & Watson, K. D. 1953: Spherulitic alkali rhyolite dikes in the Atsutla Range, Northern British Columbia. *Am. Miner.* **38**, 432–447.

Parker, A. 1968: An electron-microprobe study of the homogeneity of glass discs for X-ray fluorescence analysis. *Anal. Chim. Acta* **40**, 513–514.

Siedner, G. 1965: Geochemical features of a strongly fractionated alkali igneous suite. *Geochim. cosmochim. Acta* **29**, 113–137.

Upton, B. G. J. 1960: The alkaline igneous complex of Kûngnât Fjeld, South Greenland. *Bull. Grønlands geol. Unders.* **27** (also *Meddr Grønland* **123**, 4), 145 pp.

Upton, B. G. J. 1962: Geology of Tugtutôq and neighbouring islands, South Greenland. Part I. *Bull. Grønlands geol. Unders.* **34** (also *Meddr Grønland* **169**, 8), 59 pp.

Upton, B. G. J. 1964a: Geology of Tugtutôq and neighbouring islands, South Greenland. Part II. Nordmarkitic syenites and related alkaline rocks. *Bull. Grønlands geol. Unders.* **44** (also *Meddr Grønland* **169**, 2) 62 pp.

Upton, B. G. J. 1964 b: Geology of Tugtutôq and neighbouring islands South Greenland. Part IV. The nepheline syenites of the Hviddal composite dyke. *Bull. Grønlands geol. Unders.* **48** (also *Meddr Grønland* **169**, 3) 50–80.

Ussing, N. V. 1912: The geology of the country around Julianehaab, Greenland. *Meddr* Grønland 38, 426 pp.

MID-GARDAR FELDSPATHOIDAL DYKES IN THE TUGTUTÔQ REGION, SOUTH GREENLAND

RAYMOND MACDONALD

Bull. geol. Soc. Denmark, vol. 20, pp. 64–66. Copenhagen, July 9th, 1970.

During the course of a Ph.D. study on the petrology of the mid-Gardar alkaline dykes of the Tugtutôq region, four feldspathoid-bearing dykes were found in material collected by B.G.J. Upton during mapping for the Geological Survey of Greenland, but not microscopically examined by him. These dykes were analysed, but eventually were not included in the text of the thesis. Subsequently, at least three further feldspathoidal dykes were collected during the summer of 1966 (86006–9, 85952, 86080), of which two have now been analysed. Since these are the only recorded examples of undersaturated syenitic rocks intruded in the Tugtutôq area after the consolidation of the giant gabbro dykes, it was felt worthwhile to present the analyses and modes.

In table 2, the terms "augite" and "aegirine-augite" are used in the general sense to indicate colourless, purple and pinkish pyroxenes of the augite-ferroaugite series and green pyroxenes of the hedenbergite-aegirine-augite series respectively. 85952 includes small amounts of an as yet unidentified colourless mineral, prismatic, length-slow and with virtually straight extinction. In these fine-grained rocks, the identification of the feldspathoids and their breakdown products is rather difficult; the figures given in table 2 must therefore be taken as approximate.

Dansk sammendrag

I tabelform præsenteres analyser af nogle undermættede, feldspatoidførende dykes fra Tugtutôq området.

Department of Environmental Sciences
University of Lancaster
Bailrigg, Lancaster
August 29th, 1969.

Table 1. Analyses of feldspathoidal dykes from the Tugtutôq area

	50104	50121	50193	50195	86080	85952
SiO_2	54.3	53.6	54.1	56.9	60.6	54.5
ZrO_2	0.15	0.26	0.16	0.20	0.43	0.54
TiO_2	1.35	1.02	1.01	0.87	0.18	0.26
Al_2O_3	14.81	15.24	16.80	15.56	16.82	13.13
Fe_2O_3	3.71	2.53	3.71	3.21	3.60	11.28
FeO	8.12	9.10	6.10	6.61	1.55	0.30
MnO	0.28	0.34	0.27	0.28	0.12	0.32
MgO	1.15	0.90	1.06	0.38	0.39	0.12
CaO	3.70	3.44	2.48	2.12	1.58	1.24
Na_2O	5.51	6.93	6.82	6.70	8.74	9.97
K_2O	4.72	4.83	5.03	4.67	4.66	3.53
P_2O_5	0.42	0.31	0.32	0.23	0.08	0.17
H_2O+	1.60	0.70	0.97	1.16	0.83	3.20
F	0.26	0.35	0.27	0.30	0.77	0.82
Cl	0.05	0.17	0.23	0.08	0.07	0.01
	100.13	99.72	99.33	99.27	100.42	99.39
≡ F, Cl	0.12	0.19	0.16	0.15	0.34	0.35
Total	100.01	99.53	99.17	99.12	100.08	99.04
Agp. Ix	0.96	1.09	0.99	1.03	1.16	1.55
F.I.	70.6	73.9	76.7	79.5	92.9	91.5
Rb	160	235	180	190	–	610
Sr	120	95	75	115	–	85
Ba	290	175	100	175	–	195
Y	105	150	100	125	–	635
Nb	165	280	280	240	–	1065

50104. Pink, non-porphyritic microsyenite dyke (10 m), Niaqornaq.
50121. Light grey, non-porphyritic microsyenite dyke (8 m), Niaqornaq.
50193. Central part of dark, non-porphyritic microsyenite dyke (6 m), island between Qangue and Tugtutôq, Skovfjord.
50195. Dark grey microsyenite dyke, island in Skovfjord between Qangue and Tugtutôq. Described by Upton as sparsely porphyritic, but analysed specimen aphyric.
86080. Central part of greenish-grey, non-porphyritic 'felsite' dyke, Central Tugtutôq fjord.
85952. Centre of 1.5 m, green, non-porphyritic dyke. Igdlutalik.
Includes La = 1830 p.p.m. and Li = 350 p.p.m.

Analysts: 50104, 50121, 50193, 50195 – R. Macdonald (except Zr, X-Ray Unit, Department of Geology, University of Reading).
86080, 85952 – S. A. Malik, Geochemistry Unit, Reading (major elements) and X-ray Unit (trace elements).

EARTH AND PLANETARY SCIENCE LETTERS 18 (1973) 217–222. NORTH-HOLLAND PUBLISHING COMPANY

POTASSIUM- AND FLUORINE-RICH HYDROUS PHASE COEXISTING WITH PERALKALINE GRANITE IN SOUTH GREENLAND

R. MACDONALD
Department of Environmental Sciences, University of Lancaster, U.K.

B.G.J. UPTON
Grant Institute of Geology, University of Edinburgh, U.K.

and

J.E. THOMAS
Department of Geology, University of Reading, U.K.

Received 19 September 1972
Revised version received 6 January 1973

A record of the composition of a hydrous phase coexisting with peralkaline granite has been found in the Kûngnât Fjeld syenite complex, S. Greenland. Troctolitic gabbros immediately adjacent to thin granite sheets have been severely altered, with addition of notable amounts of K, F and H_2O. The granite sheets represent the residue of the strong fractionation of trachytic magma, and the K and F bearing aqueous solutions are thought to have separated from them at a relatively late stage in the crystallisation history. This appears to be the first record of a hydrous phase of this composition coexisting with natural peralkaline granite.

1. Introduction

Luth and Tuttle [1] have recently stressed the important role played by the vapour phase coexisting with hydrous granite magmas and rocks in such processes as granitization, feldspathization, metamorphism, and pegmatite and ore genesis. They point out the need for further data on the composition and physical nature of these vapours, since these data will place important restrictions on the type and extent of the processes which such vapours may effect. The composition of these vapour phases is likely to be highly variable, depending not only on the composition of the host rocks, but also on the P–T environment, on local P–T and chemical gradients, and on the stage of crystallisation of the melt [1–3]. Consequently, chemical data on vapour phases from a range of specific geological situations are required before an overall understanding of their behaviour will be possible.

In this paper, we provide qualitative information on a K- and F-rich aqueous phase which separated from a suite of peralkaline granite sheets. No record of a similar phase has previously been published, to our knowledge. It is not yet possible to specify whether the fluids were above or below their critical point.

2. Geology

Kûngnât Fjeld is a deeply dissected alkaline complex in South Greenland approximately 1250 my old, intrusive into amphibolite facies gneisses [4]. The complex is some 5 km across and consists of two intersecting stocks of hypersolvus syenite, each with

late-stage acid sheets. These sheets cross-cut an alkali olivine gabbro ring-dyke which is itself younger than the syenites.

Since the granite sheets associated with both stocks are believed to be products of extreme fractionation processes within the magmas responsible for the syenites, the fact that they cut the gabbro is taken as evidence that, firstly, emplacement of the syenite stocks and ring-dyke occurred within a short time interval, and secondly, that both syenite bodies remained above their solidus temperatures as the time of ring-dyke emplacement.

The western syenite stock is rhythmically layered and shows upward progression from larvikitic syenites (with small amounts of normative nepheline) to quartz-bearing nordmarkites (3–4% normative quartz). The sequence has been subdivided [4] into a "lower layered series" and an "upper layered series", separated by a zone of gneiss inclusions.

The lower layered series evolved by slow crystallisation of trachytic magma, accompanied by convective circulation within the stock, which resulted in the gravitational settling of alkali feldspar (Or_{34-42} wt.%), Fe-rich olivines and clinopyroxenes, Fe–Ti oxide solid solutions, and apatite. The magma is believed to have completed crystallisation as an essentially closed system producing a suite of peralkaline acid rocks during the final stages of consolidation. These peralkaline residua are seen as several thin (< 5 m) sheets cutting the gneisses near the southern and western margins of the western stock.

The conclusion that the sheets represent the residua of the trachyte magma after large-scale extraction of syenitic cumulates was initially based on field, mineralogical and chemical considerations [4]. It has since been supported by isotopic studies (5) in which it has been shown that the initial $^{87}Sr/^{86}Sr$ ratios of the peralkaline granites lie close to 0.704, similar to those yielded by the syenites and lower than would have been expected had the sheets had a rheomorphic origin.

In connection with the sheets, the following points of broad petrogenetic interest may be made:

(i) The lower layered series, which includes nepheline-normative syenites, and the peralkaline acid sheets provide an example of a transition from undersaturated to oversaturated compositions.

(ii) The granites have an exposed volume of < 1% of the syenites.

3. The acid sheets

The late transgressive sheets of the western stock may be conveniently divided into four groups which, judging from cross-cutting and petrographic relationships represent the order of emplacement and possibly reflect falling temperatures during final solidification of the stock: (a) quartz syenites, (b) granite with anhedral amphibole, (c) micro-granites with idiomorphic (acicular) riebeckitic amphibole, and (d) aplites and zoned pegmatite-aplites bearing aegirine.

The zonal features shown by rocks of groups (d) tend to show bilateral symmetry, while the fact that the veins leading from inner zones may penetrate outer zones whereas the reverse relationship has not been observed, implies that crystallisation proceeded principally from the walls inwards. The concentric zoned structures of these pegmatite-aplite bodies are inferred to be evidence of convective stirring within the granite magmas, a process apparently facilitated by their peralkaline character [1].

The syenite sheets consist of antiperthite with interstitial hastingsite and quartz. Passage to the granites of groups (b) and (c) involves not only an increase in model quartz, but replacement of hastingsite by riebeckite-arfvedsonite. Astrophyllite, fluorite, zircon, magnetite, biotite and aenigmatite are accessories. Aegirine occurs in some of the marginal facies of these granites, but becomes an essential component in the aplitic and complex aplite-pegmatite sheets.

Seven new chemical analyses are given in table 1. Rocks of groups (c) and (d) are characterised by higher Na_2O/K_2O ratios and higher agpaitic indices (molecular $[Na_2O + K_2O]/Al_2O_3$) than rocks of groups (a) and (b). Y, Zn, and Zr appear to be enriched in the group (d) intrusives. K/Rb ratios, in each case < 180, reach extremely low values [22] in group (d) rocks. These chemical features are consistent with the theory that the sheets evolved by a continuous crystal fractionation process.

4. Metasomatism of gabbros adjacent to the acid sheets

Whereas gneisses and syenites alongside the acid

Table 1
Analyses of granitic rocks from western Kûngnât. Groups a–d refer to intrusive sequence (see text). Specimen numbers are those of the Greenland Geological Survey.

Collection No.	86176	86158	86159	86163	86157	86190	86178
Group	a	b	c	c	d	d	d
SiO_2	69.2	73.6	77.3	75.2	63.9	75.3	64.9
TiO_2	0.38	0.23	0.08	0.16	0.24	0.30	0.34
Al_2O_3	14.35	12.58	11.24	8.67	14.79	11.10	13.76
Fe_2O_3	2.32	2.59	1.61	2.65	4.05	3.80	4.03
FeO	2.12	1.52	1.32	4.63	2.77	0.36	2.72
MnO	0.08	0.03	0.03	0.06	0.14	0.16	0.13
MgO	0.03	0.02	0.02	0.02	0.02	0.03	0.01
CaO	0.64	0.36	0.06	0.17	0.85	0.15	0.77
Na_2O	5.05	4.19	4.97	4.32	7.93	7.95	7.31
K_2O	5.22	5.26	3.43	3.75	4.23	0.26	4.47
P_2O_5	0.04	0.02	0.01	0.01	0.04	0.08	0.02
H_2O^+	0.40	0.09	0.04	0.10	0.28	0.21	0.22
F	0.23	0.31	0.15	0.50	0.84	0.07	–
Cl	0.015	0.005	0.007	0.003	0.006	0.48	0.015
Sum	100.08	100.81	100.27	100.24	100.09	99.82	98.70
O = F, Cl	0.10	0.13	0.06	0.21	0.36	0.04	–
Total	99.98	100.68	100.21	100.03	99.73	99.78	98.70
Na_2O/K_2O (wt.)	0.97	0.80	1.45	1.15	1.87	30.58	1.63
Agpaitic index	0.97	1.00	1.05	1.28	1.19	1.20	1.24
Ba	140	90	55	65	45	75	–
Ce	920	240	< 20	140	1550	940	–
La	515	135	< 25	100	805	420	–
Li	–	95	150	380	180	65	–
Pb	40	20	< 10	10	60	770	–
Rb	245	380	280	325	470	95	–
Sr	20	30	< 10	< 10	30	80	–
Th	60	60	10	15	55	360	–
U	15	< 5	< 5	5	30	110	–
Y	130	125	55	80	220	480	–
Zn	190	200	230	470	490	590	–
Zr	815	970	530	335	2440	3140	–
K/Rb	177	115	102	96	75	22	–

Cs in all samples less than 20 ppm. Sn in all samples below detection (–20 ppm) except 86190 (analysis 6) where it is estimated at 500 ppm.

Analysts. Major elements – S.A. Malik, D.A. Bungard, J.M.C. Palmer. Trace elements – D. Gillies, G. Smith, J. Ward (University of Reading), G.R. Angell (University of Edinburgh): XRF. (Li-atomic absorption spectroscopy, S.A. Malik.)

sheets show little sign of metasomatic change, the olivine gabbros of the ring-dyke are wholly reconstituted for widths of up to 4 cm away from the contacts with the granitic, aplitic and aplite-pegmatite sheets. The unaltered gabbro is a strikingly fresh troctolitic rock composed of labradorite zoned through andesine, interstitial alkali feldspar, olivine, titanaugite, ilmenite, magnetite, ulvospinel, biotite and apatite. In the contact metasomatised facies adjacent to the acid sheets, however, the olivine, titanaugite, opaque oxides as well as the original lepidomelane biotite are replaced by fine-grained aggregates of green or brown biotites. The apatites have acquired pale brownish colouration and the

Table 2
Analyses of unaltered (26040, 86186) and metasomatised gabbros from the western sector of the Kûngnât ring-dyke. Analysts as in table 1. 26040 from Watt (10, No. 107).

	26040	86186	86180 (a)	86184	86191 (a)
SiO_2	45.38	44.6	41.2	43.4	45.5
TiO_2	3.19	2.69	2.22	2.37	1.60
Al_2O_3	17.99	17.41	14.76	14.97	12.87
Fe_2O_3	3.09	1.90	1.22	2.70	1.19
FeO	11.92	13.58	12.35	12.72	10.80
MnO	0.18	0.19	0.17	0.19	0.19
MgO	5.10	7.45	6.92	7.60	6.54
CaO	7.65	7.58	6.30	6.03	5.32
Na_2O	3.70	3.21	2.68	3.13	3.09
K_2O	0.91	0.78	6.44	3.88	6.90
P_2O5	0.25	0.30	0.36	0.38	0.42
H_2O^+	0.35	0.41	2.49	1.47	0.93
F	0.03	0.06	4.29	1.98	5.41
Cl	–	0.006	0.008	0.059	0.009
Sum	99.89	100.11	101.41	100.88	100.77
$O \equiv F, Cl$	0.01	0.03	1.81	0.85	2.28
Total	99.88	100.08	99.60	100.03	98.49
Ba	–	1200	1075	1140	1055
Ce	–	< 20	40	100	360
La	–	< 25	55	60	145
Li	–	n.d	450	220	1025
Pb	–	< 10	50	90	150
Rb	–	10	1680	325	4920
Sr	–	585	600	455	495
Th	–	–	< 5	< 5	140
U	–	–	< 5	< 5	30
Y	–	< 10	55	45	315
Zn	–	< 5	180	200	530
Zr	–	95	55	125	925
K/Rb	–	656	32	99	12

Cs less than 20 ppm except for 86180 (a), estimated at 50–100 ppm, and 86191 (a), estimated at 100–200 ppm.

feldspars are rendered turbid by an abundance of minute fluorite inclusions.

Two analyses of the fresh gabbro (table 2, nos. 1,2) and three of the metasomatized gabbros (table 2, nos. 3–5) are now available. The metasomatism clearly involved notable addition of K, F and H_2O, with concomitant dilution of the other major constituents. Ce, La, Li, Pb, Rb, Y and Zn are also enriched in the altered gabbros, and one sample (86191(a)) also shows concentrations of Cs, Th, U and Zr. In addition, there appears to have been a real, and as yet unexplained loss of Ca from the gabbros.

5. Discussion

The evidence indicates the loss from the acid sheets of hydrous fluids rich in K and F. The fluids were transferred to the gabbros but not to the syenites and gneisses adjacent to the sheets, and this may be due to the existence at the granite-grabbro contacts of strong chemical gradients. It may well be that these compositional gradients played a controlling role during the initiation of the metasomatism.

There is no evidence that the alteration of the gabbros was a secondary, post-magmatic effect, atten-

dant perhaps upon a reheating event or a shearing episode. It seems more reasonable to assume that the fluids escaped from the granites during the magmatic stages.

At present it is not possible to say whether the hydrous phase escaped as supercritical fluids or aqueous solutions or as vapours below their critical point, though studies of fluid inclusions in the feldspars may provide interesting information in this regard. There are unfortunately very few published data on the composition of the hydrous phase coexisting with granites and granite magmas with which to compare the Kûngnât sheets.

Dense, saline aqueous fluids found as fluid inclusions in granite blocks on Ascension Island [6] are Na and Cl rich. Noble [7] records the loss of large amounts of Na and Cl (and lesser amounts of F) at least partly as a volatile phase during primary crystallisation and devitrification of a wide range of peralkaline acid rocks. In the case of the Kûngnât sheets, however, there is no evidence for the transference of either Na or Cl, and if the aqueous fluids released by these sheets did contain substantial concentrations of Na and Cl in addition to K and F, then these former elements were wholly lost from the system, leaving no record of their passing.

It would appear that, at whatever stage of consolidation of the sheets the hydrous phase escaped, there was a remarkably complete separation of Na from K. A possible explanation may be found in the work of Orville [3], who demonstrated in synthetic alkali feldspar-alkali chloride systems a tendency for alkalis to migrate through the vapour phase in such a way that K is concentrated in cooler, and Na in hotter, environments. It may be that there is at Kûngnât a natural example of the migration of K into cooler country rocks while Na was concentrated in the granites.

An alternative explanation of the apparently anomalous behaviour of the Kûngnât sheets finds some support in recent experimental work in the systems $NaAlSi_3O_8$–NaF–H_2O(8) and $NaAlSi_3O_8$–NaCl–H_2O(9) at 1 kb. pressure, which has shown that whereas F tends to remain concentrated in the liquid during crystallisation of these melts, Cl is preferentially partitioned into the fluid phase. It is conceivable, therefore, that during the cooling of the Kûngnât granite magmas, a (supercritical?) Na- and Cl-rich phase separated at an early stage and was expelled from the melt, while F (and K) tended to remain in the liquid until a later stage in the crystallisation history, and were finally expelled as a dense (subcritical?) fluid.

During the period of emplacement of the sheets, the Kûngnât Fjeld complex was undoubtedly cooling and contracting. It probably was heavily jointed and cracked, and these fractures may have provided easy routes of exit by which the Na- and Cl-rich vapours made their way towards the surface.

Acknowledgements

We thank K. Ellitsgaard-Rasmussen, Director of the Geological Survey of Greenland, for permission to publish this paper. We also wish to thank S.A. Malik, D.A. Bungard and J.M.C. Palmer (Geochemistry Unit), D. Gillies, G. Smith and J. Ward (X-ray Unit) of the University of Reading and G.R. Angell (University of Edinburgh), for making the new analyses quoted here. Dr. M. Stone, University of Exeter, kindly arranged facilities for lithium determination by atomic absorption spectroscopy.

References

[1] W.C. Luth and O.F. Tuttle, The hydrous vapor phase in equilibrium with granite and granite magmas, Geol. Soc. Am. Mem. 115 (1969) 513.

[2] O.F. Tuttle and N.L. Bowen, Origin of granite in the light of experimental studies in the system $NaAlSi_3O_8$–$KAlSi_3O_8$–SiO_2–H_2O, Geol. Soc. Am. Mem. 74 (1958).

[3] P.M. Orville, Alkali ion exchange between vapor and feldspar phases, Am. J. Sci. 261 (1963) 201.

[4] B.G.J. Upton, The alkaline complex of Kûngnât Fjeld, South Greenland, Bull. Grønlands Geol. Unders. 27 (1960).

[5] O. van Breemen and B.G.J. Upton, Age of some Gardar intrusive complexes, S. Greenland, Geol. Soc. Am. Bull. 83 (1972) 3381.

[6] E. Roedder and D.S. Coombs, Immiscibility in granite melts indicated by fluid inclusions in ejected granite blocks from Ascension Island, J. Petrol. 8 (1967) 417.

[7] D.C. Noble, Loss of sodium from crystallised comendite welded tuffs of the Miocene Grouse Canyon Member of the Belted Range Tuff, Nevada, Geol. Soc. Am. Bull. 81 (1970) 2677.

[8] A.F. Koster van Groos and P.J. Wyllie, Melting relationships in the system $NaAlSi_3O_8$–NaF–H_2O to 4 kilobars pressure, J. Geol. 76 (1968) 50.

[9] A.F. Koster van Groos and P.J. Wyllie, Melting relationships in the system $NaAlSi_3O_8$–NaCl–H_2O at one kilobar pressure, with petrological applications, J. Geol. 77 (1969) 581.

[10] W.S. Watt, Chemical analyses from the Gardar Igneous Province, South Greenland, Geol. Surv. Greenland Report 6 (1966).

Lithos 4, 1971, 163–84

CHEMICAL VARIATION WITHIN THREE ALKALINE COMPLEXES IN SOUTH GREENLAND

BRIAN G. J. UPTON, JOHN E. THOMAS & RAYMOND MACDONALD

Upton, B. G. J., Thomas, J. E. & Macdonald, R. 1971: Chemical variation within three alkaline complexes in south Greenland. *Lithos 4*, 163–84.

Comparison is made between three hypersolvus alkaline complexes of Precambrian age occurring in the same igneous province. Two represent the cores of deeply eroded central volcanoes; the third comprises a suite of trachytic and rhyolitic dykes. In each complex a similar suite of trachytic and comenditic magmas was intruded and the gross mineralogy and chemistry are closely comparable. However, such differences as exist are explicable in terms of variation in cooling rates, controlling the degree to which the rocks represent cumulates and the extent to which excess alkalis in liquid residua were lost to the atmosphere and wall-rocks. In the Kûngnât Fjeld complex where cooling was slowest, alkali loss is inferred to have been greatest and the bulk of the constituent syenites are mildly peraluminous in consequence. In the dyke complex cooling was rapid and alkali loss less severe; the majority of the trachyte/rhyolite dyke rocks are mildly peralkalic. The central ring-complex of Tugtutôq represents an intermediate situation in relation to Kûngnât Fjeld and the dyke complex.

B. G. J. Upton, Grant Institute of Geology, University of Edinburgh, Scotland.
J. E. Thomas, Department of Geology, University of Reading, England.
R. Macdonald, Department of Environmental Sciences, University of Lancaster, England.

The chemical variations within and between three silica-saturated to silica-oversaturated igneous complexes belonging to the Gardar volcanic province of south Greenland, are discussed. A general review of this Precambrian alkaline igneous province is being published elsewhere (Upton, in press). Although both undersaturated (feldspathoidal) and oversaturated syenitic and granitic rocks are abundantly represented in the region, only the oversaturated intrusions are discussed below.

In addition to the larger quartz-syenite/granite complexes at Nunarssuit and Dyrnaes-Narssaq ('N' and 'D.N' on Fig. 1), there occur four smaller central complexes displaying generally similar rock-types and internal structures. These are (a) the Kûngnât Fjeld complex (5 × 2 km); (b) the Puklen complex (4 × 2 km), satellitic to the Nunarssuit complex; (c) the central ring complex on Tugtutôq (henceforth abbreviated to central Tugtutôq complex) (4 × 2 km) and (d) the Klokken complex (2 × 2 km), denoted by 'Ku.', 'P', 'C.T.' and 'Kl' respectively in Fig. 1. Although the dominant rock type in each of these is quartz syenite grading to granite, the full range of lithologies includes also troctolitic gabbro, syeno-gabbro, and larvikitic syenite, and cor-

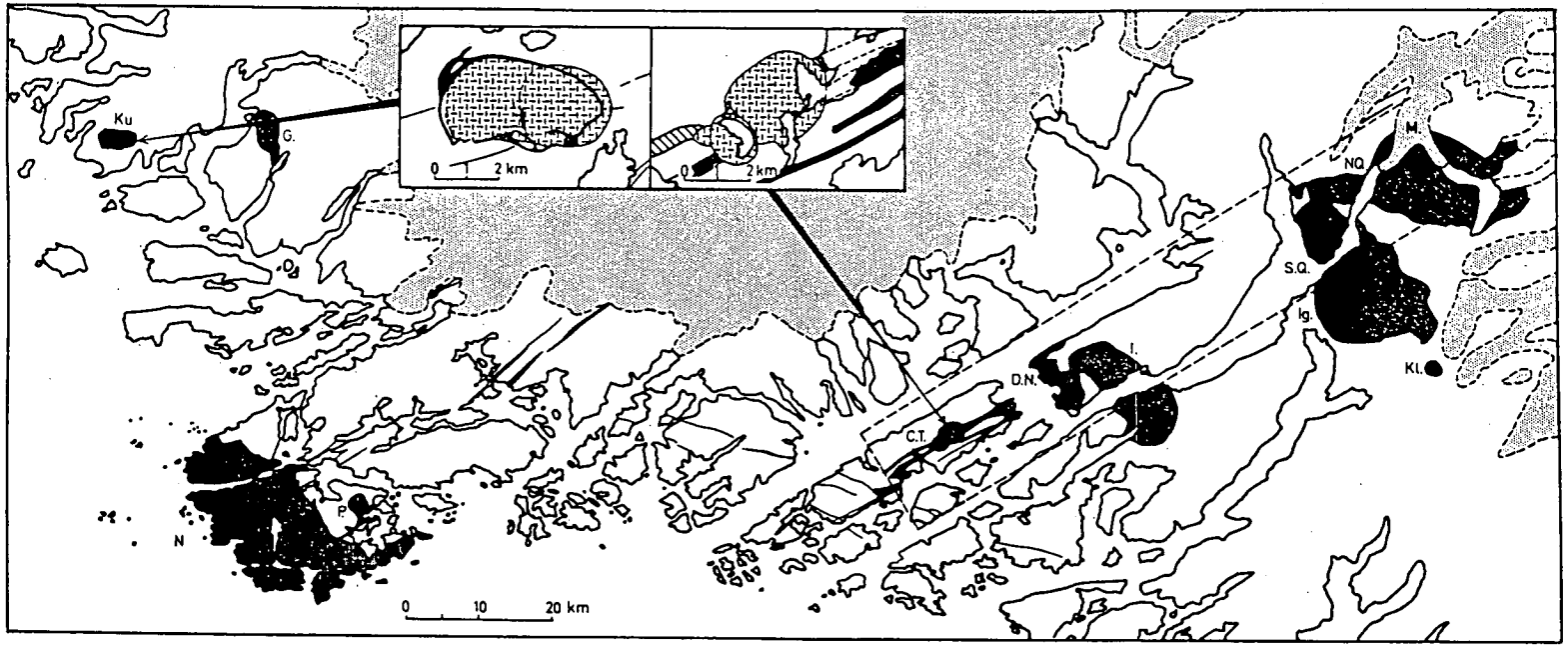

Fig. 1. Sketch map of the Gardar province. Inland-ice, fine stipple, Intrusive complexes, black (Ku, Kûngnât Fjeld; G, Grønnedal-Ika; N, Nunarssuit; P, Puklen; C. T., central Tugtutôq; D. N., Dyrnaes–Narssaq; I, Ilímaussaq; Ig, Igdlerfigssalik; S. Q. South Qoroq; N. Q., North Qoroq; M, Motzfeldt; Kl, Klokken). The country rock is Precambrian granites, gneisses and schists. The Dyke Complex occurs principally within the area enclosed by the dashed line. Inset maps of Kûngnât Fjeld and central Tugtutôq; gabbro, black; syenite, quartz syenite and granite, cross-hatch; nepheline syenite, oblique hatching.

responds to a magmatic suite grading from alkali basalt through trachyte to comendite.

The central Tugtutôq complex is known to be younger than the Dyrnaes-Narssaq complex since a swarm of ENE trending dykes cut the latter but are truncated by the former. This dyke-swarm includes trachydolerites (some composite with trachytic margins), trachytes (or microsyenites), and comenditic 'quartz porphyries' or microgranites and is thought to have involved a magmatic suite closely comparable to those responsible for the central complexes listed above. The swarm is concentrated in a zone extending from eastern Tugtutôq into the Johann Dahls Land region adjoining the inland ice-sheet.

The three complexes discussed in further detail below are: (1) the Kûngnât Fjeld complex, (2) the central Tugtutôq complex, and (3) the ENE dyke-swarm referred to above. This swarm, intruded in the time interval separating the formation of the central Tugtutôq and Dyrnaes-Narssaq complexes will, from here on, be referred to, as 'the Dyke Complex'.

Thirty-one analyses of the salic rocks from the Kûngnât Fjeld complex, twenty-three from the central Tugtutôq complex and forty-two from the Dyke Complex are available. The dyke-rock analyses are published in Macdonald (1969) and Scharbert (1968). The new analyses of Kûngnât Fjeld and central Tugtutôq rocks are presented in Tables 1 and 2. (One of the Kûngnât Fjeld analyses (26042) utilised in the diagrams is from Upton (1960).)

Analytical methods

Si, Al, total iron (as Fe_2O_3), Ti, P, Mn, F and Cl in the Kûngnât Fjeld rocks and in certain central Tugtutôq complex specimens were determined colorimetrically using a Technicon Autoanalyser (Thomas & Malik, in preparation). Ca and Mg were determined by atomic absorption spectroscopy and alkalis by flame emission techniques, on a Unicam SP90 atomic absorption spectrophotometer. A modification of Wilson's method (Wilson 1955, 1960) was used to determine ferrous iron and H_2O^+ was determined by a modified Penfield method, employing a mixture of lead oxide and lead chromate as flux.

The basic colorimetric methods adapted and modified for automation are given in Table 3.

The following standard reference samples were run as control samples during analysis of the Gardar rocks: U.S.G.S. peridotite PCC–1, Nancy granite GA, Nancy basalt BR, Msusule tonalite T–1 and C.A.A.S. syenite S–1.

The Tugtutôq central complex rocks (analyst, Macdonald) were analysed by a combination of X-ray fluorescence and 'rapid' wet chemical methods (Macdonald 1969).

The Kûngnât Fjeld complex

This is the most north-westerly of the major intrusions assigned to the Gardar period; it consists of two intersecting syenite stocks, each approximately 3 km in diameter, penetrating Ketilidian (or possibly preKetilidian) gneisses. Strontium/rubidium datings on biotites from the Kûngnât Fjeld complex indicate an age of 1240±150 my (Moorbath et al. 1960). Since neither of the syenites shows any clear signs of chilling against either the country rocks or each other it is inferred that the surrounding rocks were already pre-heated when the two syenites were emplaced in rapid succession. A narrow and essentially complete ring-dyke of gabbroic and syeno-gabbroic rocks was intruded after the consolidation of the syenites. However, the very high degree of back-veining and rheomorphic phenomena associated with this ring-dyke indicate that this too was emplaced while the syenites were still at an elevated temperature. The ring-dyke gabbros are cut by thin granitic sheets that have been interpreted as late-stage differentiates derived from both of the syenite masses (Upton 1960).

The earlier, western, stock has been sub-divided into upper and lower units separated by a diffuse, horizontal zone or raft of gneiss inclusions. Both the upper and lower units (or series) are layered, displaying rhythmic and cryptic layering as well as igneous lamination. The layering has been attributed to the gravitative settling of alkali feldspars in the range Or_{34-42} (wt. %), (originally sanidines that subsequently unmixed to perthites), with iron-rich olivines and clinopyroxenes, together with subordinate Fe-Ti oxide solid-solutions and apatite. The crystal settling is believed to have accompanied two successive episodes of convective activity, the first and more vigorous episode declining during the growth of the lower layered series and the second, less vigorous episode commencing after a detached layer of roofing rocks had subsided into the magma chamber. The upper layered series accumulated during this later phase, above the xenolithic zone formed by the roof subsidence. Although the top of this upper layered series has been lost through erosion, it is probable, from the presence of large horn-felsed basic xenoliths, that the magma that produced this series penetrated and stoped a cover of basaltic lavas. The drusy or variolitic texture of the uppermost rocks also suggests that they crystallised at a relatively shallow level in the crust.

In the lower layered series the cumulus feldspars show some increase in K content, and a concomitant decrease in Ca, with increasing fractionation. Clinopyroxene optics indicate a trend from ferroaugites to hedenbergites with some increase in aegirine-augite solid solution in the lower layered series but not in the upper. The olivines become increasingly fayalitic. There is petrographic evidence indicating that the pyroxenes, olivines and oxides enter into reaction relationships with the liquid at an advanced state of fractionation. The biotites, hastingsitic amphiboles and quartz in the syenites are believed to be wholly of intercumulus origin.

The lower layered series, together with the adjacent country rocks and the later ring-dyke, are cut by a profusion of granitic and microgranitic sheets less than 5 m thick, showing little or no marginal chilled facies. These acid rocks are interpreted as low temperature residues from the lower layered succession, in which pyroxenes again became stable. The suite is characterised by the presence of riebeckite-arfvedsonite solid solutions, aegirine and astrophyllite, with very subordinate appearance of aenigmatite.

Although the upper layered series, like the lower, shows upward gradation into increasingly leucocratic rocks, no granitic differentiates are seen and the highest rocks preserved are perthositic syenites with some interstitial quartz.

The younger syenite stock to the east is also composed of hypersolvus syenites and quartz syenites. The feldspars range from Or_{30} to Or_{35} (wt. %) reaching Or_{45} in associated pegmatites. Fayalitic olivines, clinopyroxenes, hornblendes, biotite and Fe-Ti oxides are also present. Indications of layering occur at many parts of the stock but differentiation throughout the intrusion is relatively slight and strong fractionation by gravitative removal of cumulus crystals is absent. Nevertheless this intrusion also produced a suite of late microgranites in the form of thin sheets, probably resulting from a filter-press process, cross-cutting the syenites, ring-dyke gabbro and surrounding gneisses. Intersections between these sheets and those associated with the western lower layered series have not been observed. The acid differentiates of the two syenite stocks are readily distinguished petrographically: these eastern sheets are composed of biotite/hornblende microgranites in which riebeckite-arfvedsonite, aegirine and astrophyllite are totally absent. A further distinction between east and west Kûngnât is that whereas carbonates (calcite + siderite) occur abundantly in the east Kûngnât syenite pegmatites, they are relatively rare components in those of the western syenites. The reverse is true in the case of fluorite.

Mackenzie & Smith (1962) noted that there is a significant difference between the unmixing products of the feldspars in the two stocks. The west Kûngnât feldspars contain both monoclinic and triclinic potassium feldspar phases together with a sodic phase approaching low temperature albite. Those of east Kûngnât show two sodic phases and a potassic phase that is either wholly or dominantly monoclinic. This difference is most reasonably accounted for by supposing that the western syenites had a significantly slower cooling history than those of the younger eastern stock.

The central Tugtutôq complex

This complex lies across the path of the main Tugtutôq dyke-swarm, postdating the emplacement of the great majority of the ENE dykes. After the initial intrusion of small stocks (or ring-dykes?) of microsyenite, an annular ring-complex, approximately 3×2.5 km, developed by four further episodes

Table 1. Analyses and C.I.P.W. norms of rocks from the Kûngnât Fjeld complex.

G.G.U. spec. no.	26473	26004	26005	26470	26255	26427	26436	27647	27648	27654
SiO_2	65.6	53.9	56.7	58.1	59.6	61.0	61.4	63.9	63.3	64.0
TiO_2	0.24	2.23	1.75	1.34	0.86	0.77	0.80	0.47	0.43	0.46
Al_2O_3	15.15	12.99	14.45	15.56	15.69	15.27	16.46	16.83	16.50	16.20
Fe_2O_3	1.63	2.02	1.90	2.24	1.32	1.50	1.71	1.07	1.12	1.19
FeO	4.53	12.90	10.33	7.78	7.45	6.51	5.19	3.84	3.88	3.09
MgO	.41	.89	.68	.60	.41	.32	.28	.12	.06	.16
CaO	1.26	5.08	3.99	3.47	3.06	3.26	2.28	1.69	1.53	1.43
Na_2O	5.81	4.58	4.73	4.91	5.09	5.29	5.24	5.66	5.87	6.06
K_2O	4.93	4.35	4.90	5.23	5.59	5.43	5.90	6.06	6.06	5.94
H_2O+	.52	.46	.50	.51	.37	.49	.85	.44	.35	.46
P_2O_5	.03	.57	.45	.39	.17	.13	.12	.05	.05	.05
MnO	.15	.30	.25	.19	.19	.17	.13	.10	.12	.08
F	.11	–	.16	.13	.11	.08	.10	.15	.12	.09
Cl	.07	–	.05	.07	.06	.07	.08	.05	.02	.05
	100.44	100.27	100.84	100.52	99.97	100.29	100.54	100.43	99.41	99.26
O≡F, Cl	0.06	–	0.06	0.07	0.06	0.05	0.06	0.07	0.05	0.05
Total	100.38	100.27	100.78	100.45	99.91	100.24	100.48	100.36	99.36	99.21
q	8.2	–	–	.2	–	1.3	2.1	3.4	1.7	3.1
or	28.9	25.7	28.9	30.6	32.8	32.2	35.0	36.1	36.1	35.0
ab	48.7	35.5	39.6	40.9	42.4	44.0	43.5	47.2	49.3	50.3
an	1.1	2.0	3.9	5.6	3.9	2.2	4.4	2.8	.8	–
ne	–	1.8	–	–	–	–	–	–	–	–
ac	–	–	–	–	–	–	–	–	–	.5
co	–	–	–	–	–	–	–	–	–	–
di	3.6	17.1	10.7	7.3	8.3	11.0	4.6	3.2	5.5	5.1
hy	5.9	–	4.5	8.4	6.4	4.7	5.3	4.0	2.9	1.8
ol	–	9.3	5.0	–	1.5	–	–	–	–	–
il	.5	4.2	3.3	2.6	1.7	1.5	1.5	.9	.8	.9
mt	2.3	2.9	2.8	3.2	1.9	2.1	2.6	1.6	1.6	1.6
ap	–	1.3	1.1	1.0	.3	.3	.3	.3	–	.3
CaF_2	.2	–	.3	.2	.2	.2	.2	.3	.2	.2
NaCl	.1	–	.1	.1	.1	.1	.1	.1	.1	.1
Fractionation Index	85.8	61.2	68.5	71.7	75.1	77.5	80.6	86.7	87.1	88.9

Analysts: S. A. Malik, D. A. Bungard, J. M. C. Palmer. * includes H_2O.

of fracturing and roof-collapse concentrically disposed around a single centre. The intrusions comprising this ring-complex show a small compositional variation from quartz syenite to riebeckite-arfvedsonite granite. The mineralogy of these rocks is broadly similar to that seen in western Kûngnât, i.e. they are hypersolvus quartz-bearing rocks containing perthites in the range Or_{25}–Or_{56} (wt. %) (Macdonald 1968), fayalite, ferrohedenbergite–aegirine–augite solid solutions, blue-green hornblendes, biotite and scarce aenigmatite, with riebeckite and astrophyllite in the more acid facies.

Apart from masses of the country-rock granites, the various syenite units

27692	26094	27677	27700	27699	26231	27683	27696A	27324	81128	81144
61.6	62.0	62.6	63.2	64.0	65.8	62.9	56.4	61.6	71.8	74.0
0.16	0.31	0.31	0.71	0.11	0.14	0.39	1.66	0.57	0.33	0.20
15.69	17.02	15.57	16.24	16.28	17.50	15.74	15.94	16.70	14.57	13.64
1.91	1.55	2.81	2.16	2.14	1.63	1.69	1.99	2.11	.47	.52
5.72	4.00	4.67	4.63	3.58	.90	4.98	7.82	4.47	1.98	1.12
.17	.16	.13	.09	.10	.03	.07	1.50	.33	.32	.16
1.80	1.55	1.98	1.33	1.40	.21	1.26	4.20	2.14	1.34	.79
5.45	6.25	5.66	6.29	6.31	6.82	6.20	4.89	5.64	4.37	4.19
5.59	5.81	5.17	5.24	5.25	5.92	5.28	4.74	5.88	5.09	4.99
.65	.50	.69	.37	.66	.43	.41	.39	.39	.16	.31
.07	.02	.07	.05	.08	.03	.12	.55	.10	.05	.02
.23	.17	.18	.15	.15	.04	.16	.19	.16	.04	.03
.06	–	.07	.06	.05	–	.16	.09	.04	.12	.12
.06	–	.03	.07	.05	–	.04	.02	.04	.06	.04
99.16	99.34	99.94	100.59	100.16	99.45	99.40	100.38	100.17	100.70	100.13
0.04	–	0.04	0.04	0.03	–	0.08	0.04	0.03	0.07	0.06
99.12	99.34	99.90	100.55	100.13	99.45	99.32	100.34	100.14	100.63	100.07
2.5	–	5.0	2.3	3.7	3.1	2.7	–	1.0	23.2	29.7
32.8	34.5	30.6	31.1	31.1	35.0	31.1	27.8	34.5	30.0	29.5
45.6	51.1	47.2	53.4	52.9	57.1	51.4	40.9	47.2	36.2	35.1
2.2	1.1	2.2	.3	.8	–	–	7.8	3.3	5.6	.6
–	1.0	–	–	–	–	–	–	–	–	–
–	–	–	–	–	.5	.5	–	–	–	–
	–	–	–							1.1
5.1	5.9	5.9	4.4	4.2	1.0	3.6	7.8	5.4	.2	–
6.6	–	3.2	3.5	3.0	–	5.8	2.0	3.8	3.6	1.6
–	2.3	–	–	–	–	–	6.1	–	–	–
.3	.6	.6	1.4	.2	.3	.8	3.2	1.1	.6	.5
2.8	2.3	4.2	3.2	3.0	2.1	2.3	3.0	3.0	.7	.7
.3	–	.2	.3	.3	–	.3	1.3	.3		–
.2	–	.2	.2	.2	–	.3	.2	.2	.2	.5
.1	–	.1	.1	.1	–	.1	.1	.06	.1	.1
80.9	85.6	82.8	86.8	87.7	95.7	85.7	68.7	82.7	89.4	94.3

contain xenoliths of basalt and quartzite derived from the early Gardar Eriksfjord Formation, and also fragments of the earlier Gardar ENE dykes.

The youngest component of the central Tugtutôq complex, the Blå Månesø stock (1.5 × 1.25 km), cuts the ring-complex on its south-western side. This stock is perthositic, consisting principally of antiperthitic feldspar ($Or_{32.5-36.5}$) (Macdonald 1968), with interstitial biotite, quartz, aegirine-augite, soda-hornblende, astrophyllite and aenigmatite.

The contacts of the central Tugtutôq intrusions against the country rock granites are knife-sharp, with moderately fine-grained chilled facies and

Table 2. Analyses and C.I.P.W. norms of syenites and granites from the central Tugtutôq complex.

	50291	50296	40503	40513	40514	40590	50256	50263	40593
SiO_2	65.3	63.9	69.2	65.1	67.1	65.5	69.2	66.4	63.2
TiO_2	0.27	0.30	0.34	0.55	0.24	0.41	0.32	0.47	0.41
Al_2O_3	16.16	15.77	13.50	16.20	14.27	15.41	14.55	15.30	17.40
Fe_2O_3	1.90	1.86	2.04	1.56	2.22	1.55	1.88	2.17	1.33
FeO	2.34	4.11	2.08	2.87	2.18	3.55	1.73	2.77	3.35
MnO	0.10	0.19	0.09	0.11	0.13	0.18	0.07	0.09	0.13
MgO	0.06	0.03	0.04	0.20	0.09	0.05	0.04	0.16	0.18
CaO	1.07	1.28	1.03	1.45	0.77	1.34	0.98	1.29	1.50
Na_2O	6.29	6.65	4.95	5.66	6.69	6.19	5.47	5.89	6.24
K_2O	5.57	5.32	6.32	5.83	4.50	5.47	5.09	5.34	6.18
H_2O^+	0.20	0.48	0.43	0.47	0.35	0.39	0.46	0.42	0.37
P_2O_5	0.05	0.11	<0.05	0.08	<0.05	<0.05	<0.05	0.13	0.05
F	0.34	0.28	0.39	0.20	0.57	0.20	0.42	0.44	–
Cl	0.04	0.04	0.07	0.09	0.03	0.08	0.03	0.05	–
Sum	99.69	100.32	100.48	100.37	99.14	100.32	100.24	100.92	100.34
O≡F, Cl	0.15	0.13	0.18	0.10	0.25	0.10	0.18	0.20	–
Total	99.54	100.19	100.30	100.27	98.89	100.22	100.06	100.72	100.34
q	5.8	1.9	16.1	6.8	11.3	5.8	16.9	9.7	–
or	33.1	31.5	37.3	34.5	26.9	32.3	30.1	31.4	36.5
ab	52.4	51.6	34.2	47.5	48.9	48.8	46.2	48.7	52.0
an	–	–	–	1.8	–	–	0.2	–	1.2
ne	–	–	–	–	–	–	–	–	0.4
ac	0.8	4.0	5.9	–	6.5	2.8	–	0.5	–
ns	–	–	0.1	–	0.2	–	–	–	–
di	2.9	3.7	2.4	3.3	0.5	4.7	1.9	2.9	5.2
hy	1.4	5.1	2.2	2.1	3.9	3.3	0.3	1.7	–
ol	–	–	–	–	–	–	–	–	1.8
il	0.5	0.6	0.7	1.1	0.5	0.8	0.6	0.9	0.8
mt	2.4	0.7	–	2.3	–	0.9	2.7	2.9	1.9
ap	0.1	0.3	0.1	0.2	0.1	0.1	0.1	0.3	0.1
CaF_2	0.7	0.6	0.8	0.4	1.2	0.4	0.9	0.9	–
NaCl	0.1	0.1	0.1	0.2	0.1	0.1	0.1	0.1	–

Analysts: 50296, 40514, 40590, 30722, 40590 and 50292 – S. A. Malik, D. A. Bungard, J. M. C. Palmer, R. Mac-

little evidence of thermal metamorphism or metasomatism. The earliest components of the complex (Unit 1) consist of fine-grained porphyritic microsyenite (feldspar phenocrysts Or_{34-5}), presumably intruded into cold surroundings and rapidly quenched. The time gap separating this event from the succeeding units 2 and 3 was probably brief and there are no internal chilled contacts between these units. The Unit 4 ring-dyke and, finally the Blå Månesø perthosite (Unit 5), were probably intruded after somewhat longer time intervals to judge by their sharper and more distinct contacts against preceding members.

Unit 3 and, to some extent, Unit 2 rocks show a crudely porphyritic texture and it is possible to distinguish larger alkali feldspars (showing complex compositional zoning (Or_{25-40}) that was not obliterated by the perthitic unmixing) from the perthitic feldspars in the rock matrix.

50276	50280	40500	30722	40595	50299	30699	50228	50242	50292
42.9	41.5	64.9	72.3	73.9	68.2	62.4	64.8	67.6	63.2
0.86	1.15	0.30	0.18	0.10	0.26	0.35	0.28	0.10	0.28
5.90	5.75	15.02	13.14	13.06	15.70	14.95	16.40	17.15	16.55
3.30	12.60	2.37	1.60	1.05	1.46	3.03	2.98	1.21	1.81
37.5	28.3	3.49	1.50	1.32	2.15	4.47	2.04	0.58	3.38
1.50	1.35	0.13	0.07	0.04	0.07	0.17	0.09	0.05	0.18
0.14	0.26	0.06	0.01	0.02	0.04	0.07	0.02	0.00	0.02
2.06	2.44	0.97	0.21	0.16	0.55	1.55	0.58	0.62	1.48
2.61	2.51	5.99	5.93	5.70	6.35	7.08	7.64	7.38	6.82
2.02	1.77	5.10	4.62	4.53	5.21	4.62	4.85	4.95	5.43
0.58	1.02	0.35	0.20	0.03	0.12	0.60	0.38	0.25	0.48
0.06	0.23	0.05	<0.05	0.07	<0.05	<0.05	<0.05	<0.05	0.08
0.35	0.10	0.19	0.29	0.26	0.16	0.46	0.12	0.32	0.27
0.08	0.06	0.03	0.03	0.03	0.02	0.04	0.02	0.05	0.01
99.86	99.04	98.95	100.08	100.27	100.29	99.79	100.20	100.26	99.99
0.17	0.06	0.09	0.13	0.12	0.07	0.20	0.05	0.13	0.11
99.69	98.98	98.86	99.95	100.15	100.22	99.59	100.15	100.13	99.88
–	–	8.2	22.0	24.7	9.9	0.9	1.6	5.8	–
12.0	10.7	30.6	27.4	26.8	30.7	27.5	28.6	29.2	32.2
19.2	20.1	49.6	42.0	41.9	51.5	51.5	57.3	60.6	55.1
–	–	–	–	–	–	–	–	–	–
–	–	–	–	–	–	–	–	–	–
2.3	1.1	1.5	4.6	3.0	1.6	7.5	6.3	1.3	2.4
–	–	–	0.7	0.6	–	–	–	–	–
7.2	9.2	3.2	–	–	1.4	4.4	1.7	1.0	4.9
11.7	33.3	3.2	2.6	2.4	2.6	5.8	2.3	–	1.8
41.2	4.4	–	–	–	–	–	–	–	0.9
1.6	2.2	0.6	0.3	0.2	0.5	0.7	0.5	0.2	0.5
3.7	18.1	2.7	–	–	1.3	0.6	1.1	1.1	1.4
0.1	0.6	0.1	0.1	0.2	0.1	0.1	0.1	0.1	0.2
0.7	0.2	0.4	0.6	0.5	0.3	1.0	0.2	0.7	0.6
0.1	0.1	0.1	0.1	0.1	–	0.1	–	0.1	–

donald. Remainder – R. Macdonald.

Thin layers and schlieren of hedenbergite and fayalite-rich rock which occur sporadically in Units 2 and 3 are attributed to crystal winnowing by magmatic currents. However, well-layered structures such as are shown by rocks of similar composition at Kûngnât Fjeld, are absent.

The Dyke Complex

After the intrusion of large gabbroic dykes and, where these show composite nature, their associated syenitic rocks, large numbers of smaller dykes, rarely exceeding 20 m in width, were emplaced along the ENE trend during an episode marked by intermittent left-lateral displacements along roughly E–W trending faults.

In spite of some order-reversals there is a general tendency for trachy-

Table 3. Summary of basic colorimetric methods.

Element	Colorimetric method
Si	Molybdenum blue method using 1-amino-2-naphthol-4-sulphonic acid as reductant (Shapiro & Brannock 1962).
Al	Solochrome cyanine R with ascorbic acid to suppress iron interference (Hill 1959).
Ti	Tiron method as modified by Rigg & Wagenbauer (1961).
Total iron as Fe_2O_3	2, 2'-dipyridyl method (Riley 1958).
P	Molybdivanadophosphoric acid complex method (Shapiro & Brannock 1956).
Mn	Permanganate method with ammonium persulphate as oxidant and silver nitrate as catalyst (Shapiro & Brannock 1962).
F	Determined utilizing the bleaching action of fluorine on the xylenol orange-zirconium complex (Fuge 1969, unpublished manuscript)
Cl	Determined utilizing the stable coloured iron (III) thiocyanate complex (Huang & Johns 1967; Fuge 1969, unpublished manuscript).

dolerite dykes to be followed by trachyte dykes interspersed with relatively scarce comenditic rhyolite dykes. Whereas the trachytes and comendites are variable in texture and mineralogy, the following generalisations can be made:

(a) They are well chilled against the country-rock granites and the large gabbro and syenite dykes. The contact facies are frequently spherulitic suggesting initial quenching to a glass followed by later devitrification. The readiness to quench to glass rather than to a holocrystalline product was increasingly pronounced in the more acid dykes and many of the rhyolitic dykes are spherulitic throughout.

(b) They are commonly vesicular or drusy indicating that the magmas at current levels of erosion, were at relatively low pressures at the time of quenching.

(c) Metasomatism or metamorphism of wall-rocks is minimal.

(d) Whereas a few dykes have up to 40% of phenocrysts (modally), the majority have less than 30% and dykes with less than 5% are abundant. Feldspar phenocrysts of the trachytes and comendites fall in the range Or_{35-62} (wt. %) (Bondam 1955, Upton 1964, Scharbert 1966, Macdonald 1969). Scharbert describes the phenocrysts from some of the trachytes as being intermediate between the sanidine-anorthoclase cryptoperthite and orthoclase microperthite series, with a potassium-rich phase that is either monoclinic or showing only slight obliquity. Clinopyroxenes (augite-hedenbergite), Fe-Ti oxides and, in the more rhyolitic compositions, riebeckite-arfvedsonite and quartz occur as phenocryst phases. Aggregates of aegirine in some of the comendites appear to be pseudomorphous after riebeckite-arfvedsonite. Fayalitic olivine phenocrysts also occur in some of the trachytes and comendites although this mineral is normally pseudomorphed by iddingsite. Biotite and apatite are occasionally present as phenocrysts in the more basic trachyte dykes.

Development of the three complexes

The Kûngnât Fjeld and central Tugtutôq complexes are of similar overall dimensions and must also have involved magmas of closely allied composition. However, whereas the Kûngnât Fjeld magmas were intruded into hot rocks, the ambient temperature of the country rocks in the vicinity of the central Tugtutôq complex must have been considerably lower, judging by the nature of the contacts and the porphyritic textures of some of the intrusive units and the pronounced compositional zoning preserved in the pyroxenes and feldspars. The difference is probably accounted for, at least in part, by the different erosional levels at which the two centres are now seen (Upton, in press).

In the slow-cooled magma chambers at Kûngnât Fjeld, convection was able to occur and to facilitate the strong fractionation exhibited by the western centre. By analogy, a deeper level section through central Tugtutôq would probably show similar layered structures and evidence of the differentiation processes that yielded the observed variation in the higher level intrusions. There is a general textural and compositional similarity between the Blå Månesø perthosites of central Tugtutôq and the highest rocks exposed in the western upper layered series at Kûngnât Fjeld and there is thus a reasonable likelihood that a similar series underlies the visible Blå Månesø rocks.

From the fact that both complexes contain inclusions of basalt or basalt and quartzite believed to be derived from the Gardar 'supracrustal series', it is evident that both penetrated to high crustal levels and probably fed surface volcanoes comparable in type to the recent pantellerite/trachyte volcanoes of the Ethiopian rift.

Although data are insufficient to estimate the average compositions of the Kûngnât Fjeld intrusions that might relate to 'initial liquid' compositions, it nevertheless appears likely that the three principal intrusive events (namely emplacement of western stock, eastern stock and ring-dyke) involved successively more basic magmas ranging from quartz trachyte to hawaiite/alkali basalt. This in turn prompts the suggestion that the earliest stage in the evolution of the complex involved the production of a differentiated magma chamber with trachytic compositions overlying more basic magma at depth (cf. Socorro volcano, Bryan 1966) and that the three progressively deeper level portions of this magma worked their way towards the surface, separated by short time intervals. On this hypothesis it is to be anticipated that gravity surveys of the complex should show strong positive anomalies relating to dominantly gabbroic rocks underlying the syenites. Independent evidence for the reality of such differentiated magma columns in the Gardar volcanism is available from study of other intrusions, particularly the 'big feldspar dykes' (Bridgwater & Harry 1968).

The trachytic and comendite dykes of the Dyke Complex are densely distributed over a zone between 5–10 km broad and approximately 90 km

Table 4. The samples; localities and height above sea-level.

Kûngnât Fjeld samples	
26473	Quartz syenite. South-west Kûngnât Fjeld, c. 520 m.
26004	Syenite. Western lower layered series (lower banded group), SE bank of river draining main glacier, c. 450 m.
26005	Syenite. Western lower layered series (lower banded group), SE bank of river draining main glacier, c. 450 m.
26470	Syenite. Western lower layered series, NW bank of river draining main glacier, c. 450 m.
26255	Syenite. Western lower layered series (laminated group), E face of 920 m peak, c. 690 m.
26427	Syenite. Western lower layered series (laminated group), close to ridge crest S of 920 m peak, c. 885 m.
26436	Syenite. Western lower layered series (laminated group), ridge crest N of 920 m peak, c. 760 m.
27647	Quartz syenite. Western lower layered series (unlaminated group) exposure within main glacier, c. 620 m.
27648	Quartz syenite. Western lower layered series (unlaminated group), foot of spur beneath Röverborgen, main glacier, c. 670 m.
27654	Quartz syenite. Western lower layered series (unlaminated group) foot of Röverborgen wall, c. 800 m.
27692	Quartz syenite. Western upper layered series, NNW of Röverborgen summit, c. 990 m.
26094	Syenite. Western upper layered series, SE of Röverborgen, c. 1040 m.
27677	Syenite. Western upper layered series, ridge crest N of Röverborgen summit, c. 1130 m.
27700	Quartz syenite. Western upper layered series, ridge crest S of Röverborgen summit, c. 1175 m.
27699	Quartz syenite. Western upper layered series, ridge crest S of Röverborgen summit, c. 1215 m.
26231	Quartz syenite. Western upper layered series, Röverborgen summit, 1280 m.
27683	Quartz syenite. Western upper layered series, S end of Nisseborgen ridge, c. 1050 m.
27696A	Syenite. Eastern syenite intrusion, just E of glacier on Röverborg-Kûngnât Fjeld coll, c. 1100 m.
27324	Syenite. Eastern syenite intrusion, SW side of river draining Röverborg-Kûngnât Fjeld coll, c. 790 m.
81128	Microgranite. ½m sheet cutting eastern syenite and ring-dyke gabbro, SE of Kûngnât Fjeld, c. 250 m.
81144	Microgranite. 1m sheet cutting eastern syenite and ring-dyke gabbro, gully NE of Kûngnât Fjeld, c. 400 m.
Central Tugtutôq samples	
50291	Quartz syenite, Unit II, stream section W of Stor Pele Sö, c. 190 m.
50296	Quartz syenite, Unit II, hillside west of Stor Pele Sö, c. 280 m.
40503	Quartz syenite, Unit III, summit of 200 m hill, SE side of Stor Pele Sö, c. 200 m.
40513	Quartz syenite, Unit III, east coast of Stor Pele Sö, c. 85 m.
40514	Quartz syenite, Unit III, north end of peninsula in Stor Pele Sö, c. 120 m.
40590	Quartz syenite, Unit III, river slabs above Blå Måne Sö, c. 290 m.
50256	Quartz syenite, Unit III, summit of 280 m hill between Stor Pele Sö and Blå Måne Sö, c. 280 m.
50263	Quartz syenite, Unit III, W of summit of Syenittinde, c. 400 m.
40593	Quartz syenite, Unit III, hillside E of Stor Pele Sö, c. 150 m.
50276	Mafic syenite facies in Unit III, west of Stor Pele Sö, c. 320 m.
50280	Mafic syenite facies in Unit III, west of Stor Pele Sö, c. 320 m.
40500	Quartz syenite, unit IV, S coast of Stor Pele Sö, c. 90 m.

long, coincident with the chain of Gardar central complexes that includes, from WSW to ENE, (a) central Tugtutôq, (b) Dyrnaes-Narssaq, (c) Ilímaussaq (northern part) (d) North and South Qoroq, and (e) Motzfeldt. The Dyke Complex is intermediate in age between the older complexes (b), (d) and (e), and the younger complexes such as (a) and (c). It has previously been proposed (Upton 1964) that the dyke magmas were developed during the evolution of an oversaturated complex at depth from which they were supplied, in intermittent batches, during a period of crustal extension. The postulated deep-seated complex may have had the form similar to the giant composite dykes now exposed in the Tugtutôq, Isortoq and Ilordleq areas. The process of progression from giant dyke form to 'central complex' form has been outlined by Upton (in press) and it is suggested that the central Tugtutôq complex was produced at a later stage, from the same source, when the period of crustal extension had terminated.

In summary, one sees in central Tugtutôq, Kûngnât Fjeld and the Dyke Complex, the products of what were closely similar suites of trachyte to comendite magmas, crystallised under differing conditions. At Kûngnât Fjeld accumulitic sequences were formed under conditions of slow cooling and, in the case of the western lower layered series, beneath a considerable cover (4–5 kms?). In central Tugtutôq, a succession of relatively small magma batches already at or below their liquidus temperatures were intruded into cold country rocks and cooled at a notably faster rate than at Kûngnât Fjeld. Consequently crystal fractionation in situ was negligible at this centre. The level of exposure is higher than at Kûngnât Fjeld, probably little over 3 km below the contemporary land surface.

The Dyke Complex, similarly, was intruded into cold country rocks at, or above (e.g. the dykes of the north-western Ilímaussaq peninsula) the erosion level of the central Tugtutôq complex. The initial magma pulses (at least) of these dykes were quenched to glasses, normally porphyritic, which subsequently devitrified.

Petrochemistry

The variation diagrams presented in Figs. 2 and 3 show the major oxides (+F and Cl) plotted against the 'Fractionation Index' (Macdonald 1969). This 'F.I.' index is a modification of the Thornton and Tuttle differentiation

---

30722 Microgranite sheet cutting Unit III, E face of 280 m hill, c. 200 m.
40595 Microgranite sheet cutting Unit III, E face of 280 m hill, c. 200 m.
50299 Poikilitic quartz syenite, Unit V, ridge between streams, north side of complex, c. 150 m.
30699 Syenite, Blå Måne Sö intrusion, coll between Hviddal and Blå Måne Sö, c. 190 m.
50228 Syenite, Blå Måne Sö intrusion, west of Blå Måne Sö, c. 120 m.
50242 Syenite, Blå Måne Sö intrusion, foot of cliffs on NW shore of Blå Måne Sö, c. 90 m.
50292 Trachyte dyke, 1 m, 180° cutting Unit II syenite, stream-section west of Stor Pele Sö, c. 150 m.

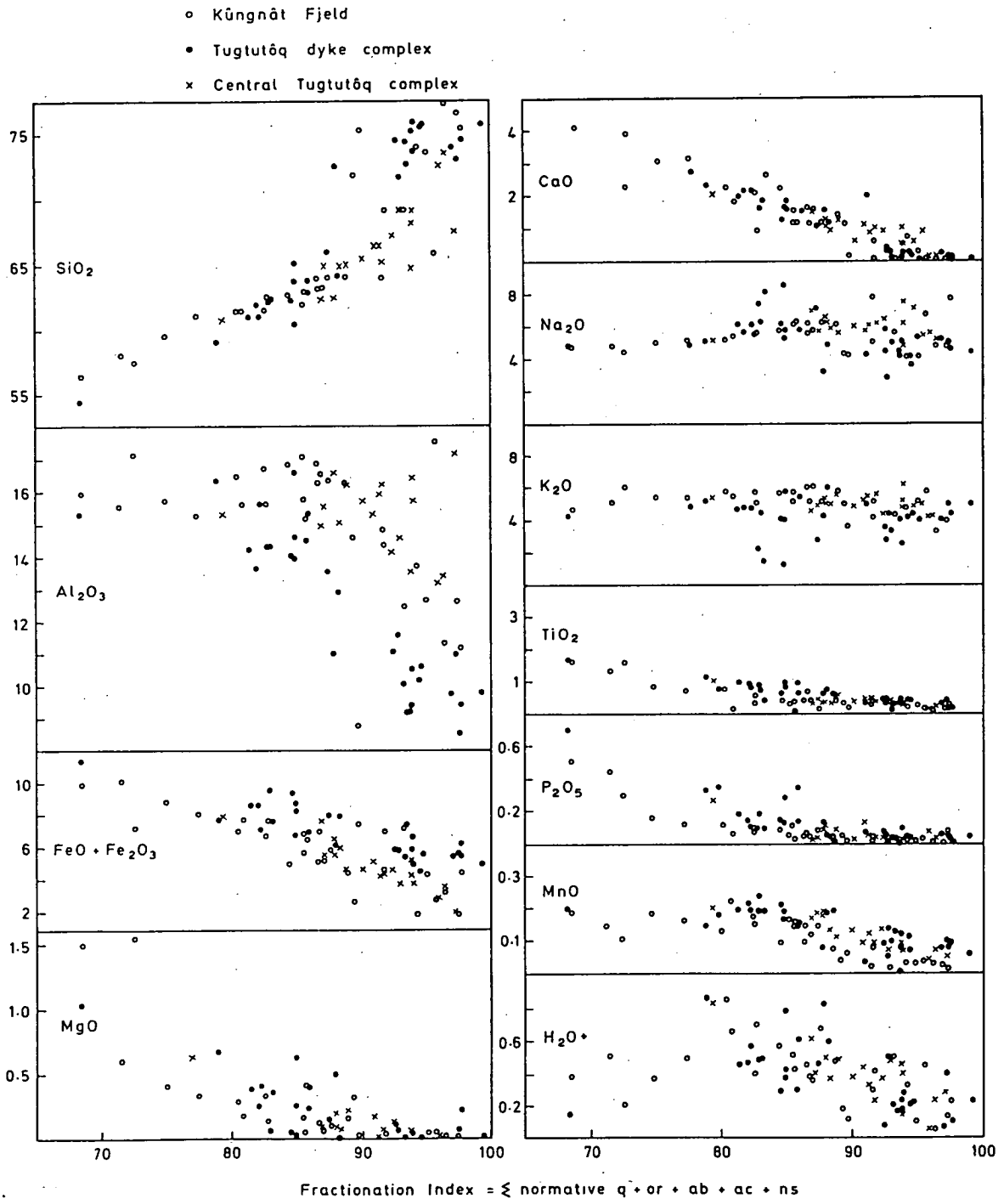

Fig. 2. Chemical variation within the salic rocks of the three complexes.

Fig. 3. Chemical variation within the principal salic units of the Kûngnât Fjeld complex. →

o Western lower layered series and associated minor intrusions.

• Western upper layered series.

× Eastern syenites and associated minor intrusions.

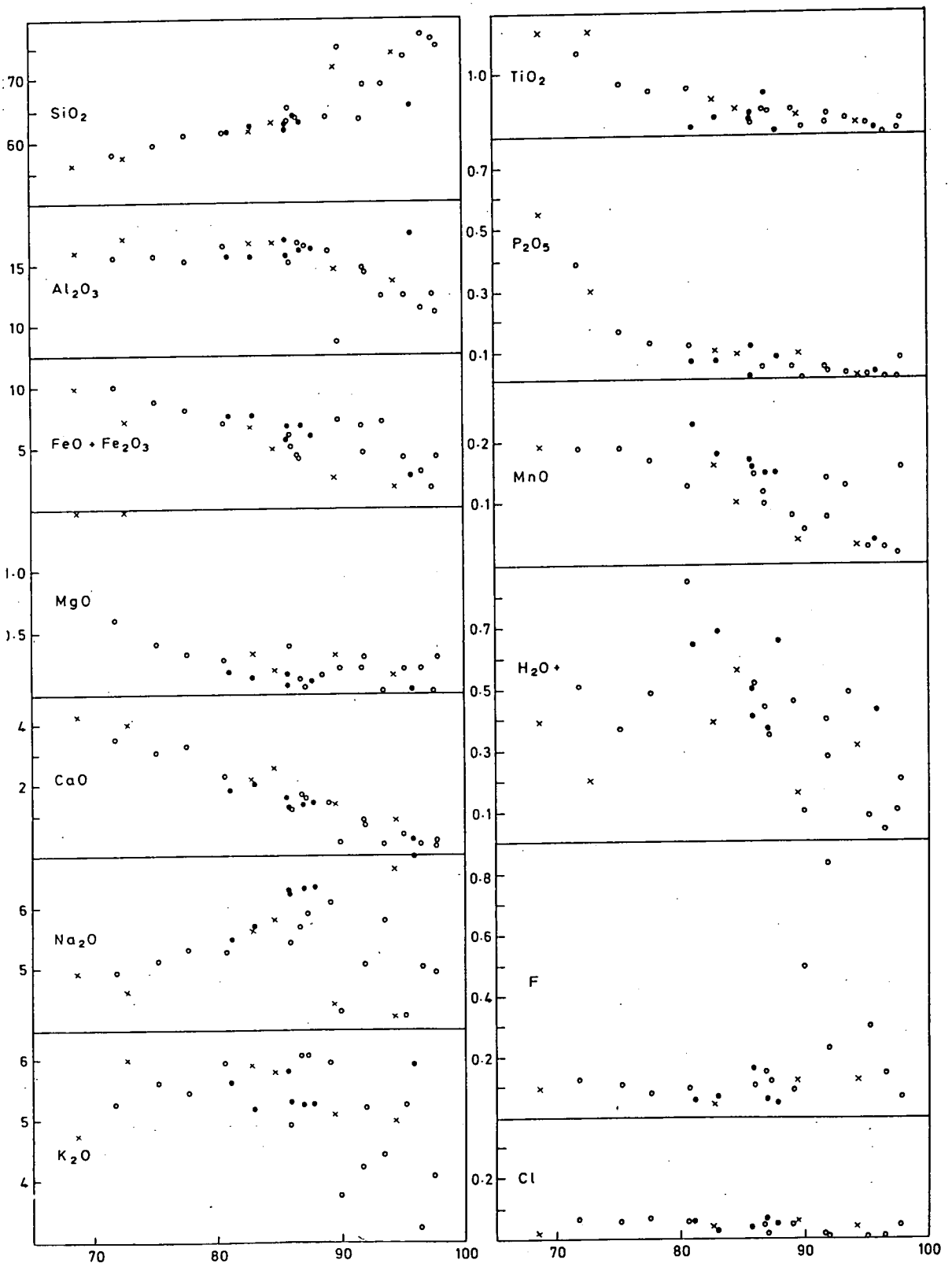

Fractionation Index = Σ normative q + or + ab + ac + ns

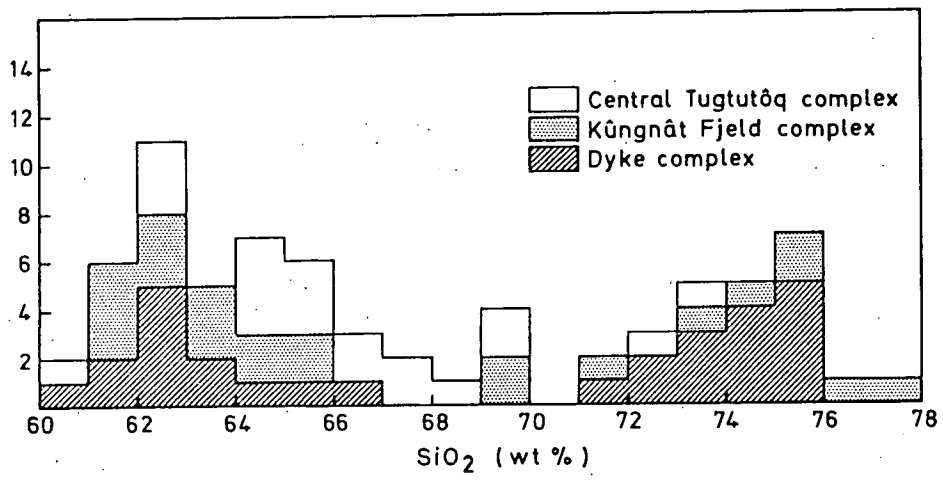

Fig. 4. Silica-frequency histogram for the salic rocks.

index and is the sum of the normative salic components + normative acmite and sodium metasilicate. In all three complexes the silica curve rises steeply beyond 'F.I.' values around 90, and simultaneously aluminium and alkalis begin to decrease, the latter very irregularly. This is readily explicable for the Kûngnât Fjeld analyses where the rocks are largely feldspathic cumulates until the liquids encountered the feldspar/silica phase boundary and quartz commenced co-precipitation with feldspar. Consequently a large jump in the bulk-rock silica contents at the stage of quartz separation is to be expected. However, in corresponding quenched liquid compositions a levelling off in silica content with continued fractionation would be anticipated after the composition encountered the feldspar/silica boundary curve, rather than any further silica increase.

Silica frequency histograms (Fig. 4) for the three complexes indicate a distinct scarcity of rocks with silica values intermediate between 67–72%. This could be construed as grounds for considering the granitic rocks to have had a different origin from the syenitic rocks as, for example, they would if they were due to rheomorphism of the country-rock granites and acid gneisses. However, there is no independent evidence to suggest that this was so and, on the contrary, the geochemical features of the acid rocks (in particular their K/Rb values) suggest that they are fractional crystallisation products from trachytic magmas. One possible explanation for this 'silica gap' (which is wholly distinct from the so-called 'Daly-gap' displayed at more basic compositions in the province (Upton, in press)), is that the liquids in this composition range were too viscous to separate and erupt with any facility. Viscosities were lower in the higher temperature trachytic magmas and it is tentatively suggested that this increasing viscosity with falling temperature and increasing silica content was counterbalanced and eventually reversed by the rising water, halogen and excess alkali content of the liquid residues. The behaviour of aluminium in the three groups

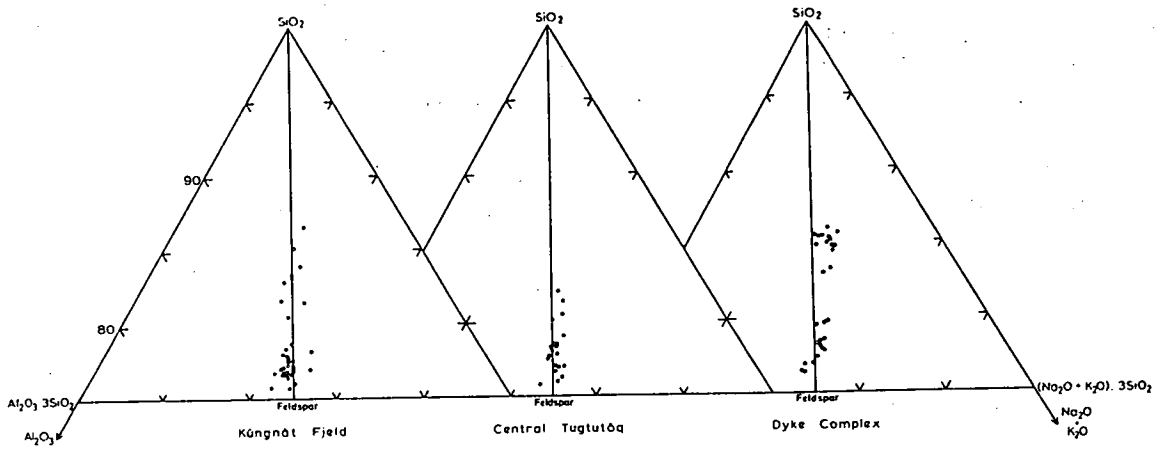

Fig. 5. Silica-alumina-alkali plots for the three complexes.

of rocks is comparable. Al_2O_3 in the various syenites and trachytes remains roughly constant at approximately 16% implying that the fractionating crystal assemblage (principally of feldspar, clinopyroxene and olivine) also had a mean content of approximately 16% Al_2O_3. At silica values >65%, alumina falls to values between 11–12% in the granites and rhyolites, almost certainly due to an increase in the Al content of the fractionating assemblage, i.e. by a rise in the feldspar/ferromagnesian ratio in the latter.

Molecular SiO_2, Al_2O_3, Na_2O and K_2O constitute more than 80% of all the analyses of the central complex and dyke complex rocks discussed here and it is appropriate that the relative proportions of these elements should be examined to reveal any important chemical differences between the suites. Recently Bailey & Macdonald (1969) have advocated the use of a ternary plot of the molecular percentages of SiO_2, Al_2O_3 and Na_2O+K_2O for displaying the proximity or otherwise of rock analyses to the simple 'granite system', in which there is excess of neither Al_2O_3 nor alkalis. The projection still suffers the inevitable drawback of ignoring those components not involved in the simple salic quaternary system but, none the less, it involves no distortions due to omission of excess alkalis or alumina. Fig. 5 shows these plots for the Kûngnât Fjeld, central Tugtutôq and the Dyke Complex analyses respectively.

In each case there is a roughly linear trend of points away from the alkali feldspar point, the trend commencing at a point equivalent to a Ca-bearing alkali feldspar with about 10–15% An. It is known that this feldspar lies in the range Or_{25-35}, with the equilibrium feldspar tending to become increasingly potassic as the bulk rock compositions become increasingly silicic. Points for Kûngnât Fjeld fall close to the feldspar-silica join but the majority of points lie to the peraluminous side of it. Most of the central Tugtutôq rocks are mildly peralkaline, while, in the Dyke Complex, the more siliceous types are strongly peralkaline, showing a transition towards pantelleritic composition (Bailey & Macdonald 1969). The differing degrees

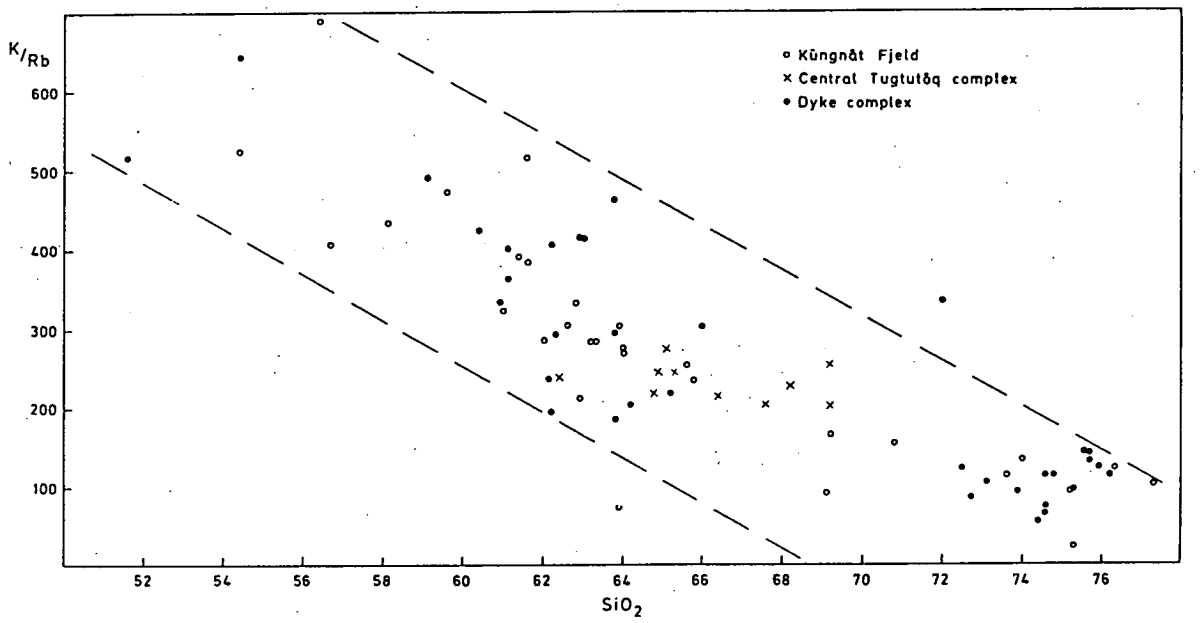

Fig. 6. K/Rb versus SiO_2 (wt. %) plot.

of peralkalinity are also shown in the normative ac+ns contents. No rock from either central complex has >10% ac+ns, while comenditic dykes from Tugtutôq contain up to 17.5 ac+ns (Macdonald 1969).

These features can be related to the geology. The Kûngnât Fjeld rocks are largely cumulates of Ca-bearing alkali-feldspar and thus plot at more Al-rich positions than the theoretical alkali feldspar point. Much of the peralkaline potential of the Kûngnât magmas may have been lost as surface exhalations and to some extent by diffusion of excess alkalis into the hot country rocks. The higher-level rocks of the central Tugtutôq complex may also have lost alkalis in this manner and since feldspar accumulation has not operated significantly in these rocks, their compositions now plot near to the feldspar-silica join. The Dyke Complex represents the nearest approach to 'liquid' compositions since the magmas experienced very rapid chilling, frequently to glasses. Even here significant alkali loss can be expected to have occurred, partly through surface loss of vapour and partly as a result of devitrification processes modifying the bulk compositions long after the initial cooling event (Macdonald 1969).

It has been inferred therefore, that the original magma in all cases was a slightly peraluminous trachyte which became peralkaline almost certainly by operation of the plagioclase effect (Bowen 1945, Macdonald 1969) and that the build-up of excess alkalis has been prevented to varying degrees in these three rock complexes in a manner roughly proportional to their cooling rates.

The potassium versus fractionation index plot (Figs. 2, 3) shows pronounced scatter in the most fractionated rocks. Here explanation in terms of the

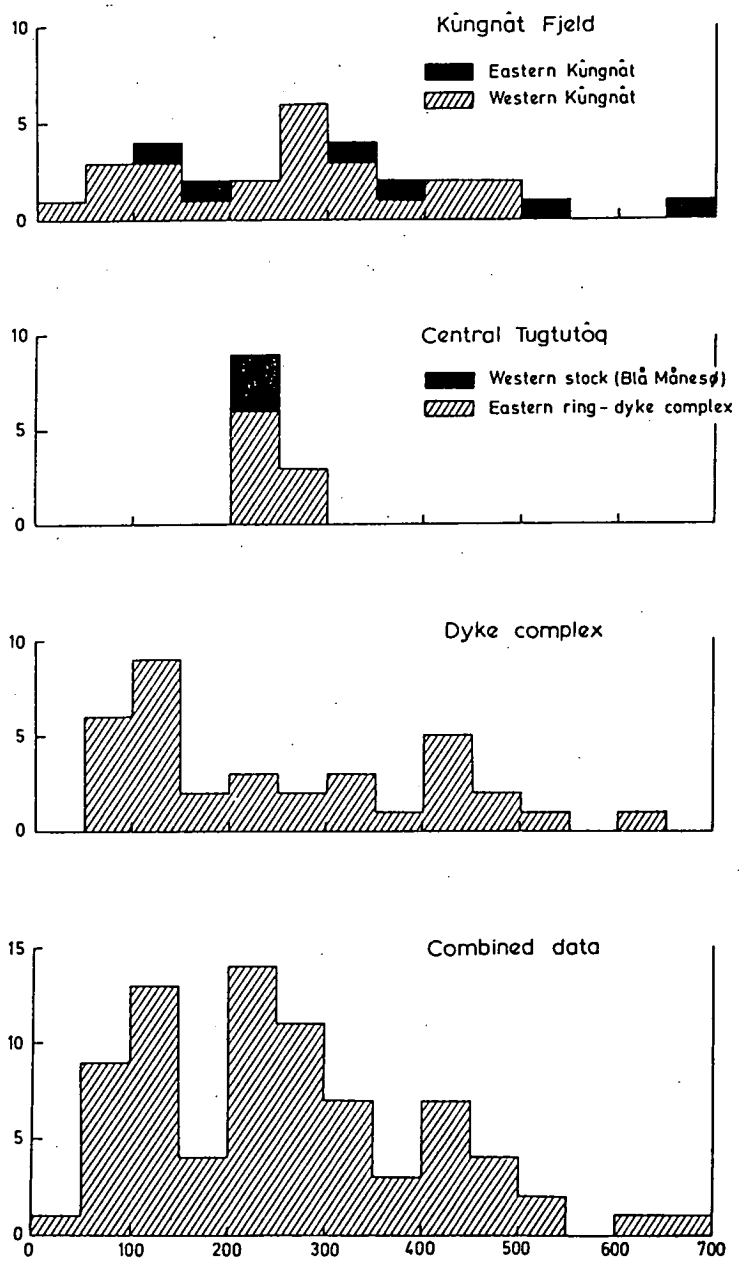

Fig. 7. K/Rb frequency diagram.

differential loss of K in the various late-stage fugitive solutions is acceptable as there is tangible evidence for loss of K to the K-rich metasomatic zones adjacent to some of the western Kûngnât Fjeld peralkaline granites.

One of the reasons for ascribing much of the compositional variation in these complexes to crystal fractionation, or at least to crystal-liquid equili-

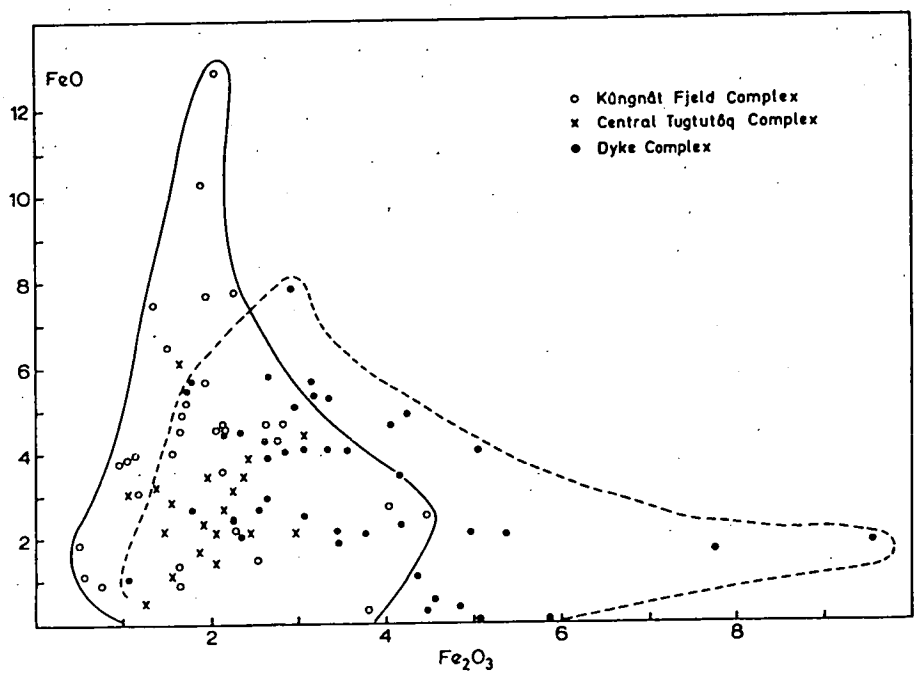

Fig. 8. FeO versus Fe_2O_3 (wt. %) plot. Full line outlines the field of the Kûngnât Fjeld and central Tugtutôq complex rocks; the dashed line, that of the Dyke Complex.

bria, is the progressive increase in concentration of such elements as Rb, Zr, U, Th, rare earths and others (Upton 1960, Macdonald 1968). These could be expected to behave as incompatible elements not readily incorporated in the lattices of the principal phenocryst/cumulus minerals identified in these rocks. Strong fractionation was inferred to be the reason for falling K/Rb and Al/Ga values at Kûngnât Fjeld. K/Rb values for the Kûngnât Fjeld syenites and granites (Fig. 6) vary widely (23–690), decreasing with rising SiO_2 content. Since there was a strong enrichment of Rb relative to K in the metasomatising fluids expelled from the rhyolite magmas (Upton et al. in prep.), the original K/Rb ratios must have been even lower than the present values. It can be seen that for the syenites with K/Rb 400–200, SiO_2 values lie in the range 60–68%; values greater than 400 are confined to rocks with less than 64% and values less than 200 are confined to rocks over 62% SiO_2. A far narrower spread of values is seen at central Tugtutôq (205–277). The Dyke Complex shows a spread of values (59–640) comparable to that seen at Kûngnât Fjeld. These data are displayed on a frequency histogram in Fig. 7 where it can be seen that the lowest Kûngnât Fjeld values are shown by the rocks from the western stock. The slight tendency to a bimodal distribution of K/Rb values brought out in the histogram combining data from the three complexes, relates to the bimodal distribution of the silica contents shown in Fig. 4.

There is no obvious relationship between oxidation state as reflected by FeO/Fe_2O_3 ratios and fractionation in the three complexes. There is, however, a significant difference between the two central complexes and the Dyke Complex in that the latter analyses show a distinct tendency to be more oxidised, with ratios between .2 and 3.0 compared with ratios of .55–6.5 for the central complexes (Fig. 8). This relates well to the freshness of fayalitic olivines in the syenites as compared with iddingsite pseudomorphs after fayalite seen in the corresponding trachytic dyke rocks. The greater degree of oxidation in the dyke rocks could be due to influx of water from the wall-rocks either during the initial cooling phase or subsequently during devitrification processes.

Acknowledgements: – We thank the Director of the Greenland Geological Survey for permission to work on survey material and to publish this paper. We also thank S. A. Malik, D. A. Bungard, J. M. C. Palmer and Mrs. L. Porteous of the Geochemistry Unit, University of Reading, who made most of the analyses quoted here. Details of automated procedures for the determination of F and Cl were provided by Dr. R. Fuge, University College, Aberystwyth whose cooperation is gratefully acknowledged.

May 1970, revised November 1970

REFERENCES

Bailey, D. K. & Macdonald, R. 1969: Alkali-feldspar fractionation trends and the derivation of peralkaline liquids. *Am. Jour. Sci. 267*, 242–8.

Bondam, J. 1955: Petrography of a group of alkali-trachyte dyke rocks from the Julianehaab District, South Greenland. *Meddelelser om Grönland 135*, No. 2, 1–31.

Bowen, N. L. 1945: Phase equilibria bearing on the origin and differentiation of alkaline rocks. *Am. Jour. Sci. 243A*, 75–89.

Bridgwater, D. & Harry, W. T. 1968: Anorthosite xenoliths and plagioclase megacrysts in Precambrian intrusions of south Greenland. *Bull. Grönlands geol. Unders. 77*, 243 pp. (also *Meddelelser om Grönland 185*, No. 2, 243 pp.).

Bryan, W. B. 1966: History and mechanism of eruption of soda-rhyolite and alkali basalt, Socorro Island, Mexico, *Bull. volcanologique 29*, 453–80.

Hill, U. T. 1959: Photometric determination of aluminium in steel. *Anal. Chem. 31*, 429–31.

Huang, W. H. & Johns, W. D. 1967: Simultaneous determination of fluorine and chlorine in silicate rocks by a rapid spectrophotometric method. *Anal. Chim. Acta 37*, 508–15.

Macdonald, R. 1968: Petrological studies of some peralkaline acid rocks from the Gardar province, south Greenland. Unpub. Ph.D. thesis. Edinburgh.

Macdonald, R. 1969: The petrology of alkaline dykes from the Tugtutôq area, south Greenland. *Bull. geol. Soc. Denmark 19*, 256–81.

Mackenzie, W. S. & Smith, J. V. 1962: Single crystal x-ray studies of crypto- and microperthites. *Norsk geol. tidsskr. 42*, (feldspar vol.) 72–103.

Moorbath, S., Webster, R. K. & Morgan, J. W. 1960: Absolute age determination in South-West Greenland. The Julianehaab granite, the Ilímaussaq batholith and the Kûngnât syenite complex. *Bull. Grönlands geol. Unders. No. 25*, 14 pp. (also *Meddelelser om Grönland 169*, No. 9, 14 pp.).

Rigg, T. & Wagenbauer, H. A. 1961: Spectrophotometric determination of titanium in silicate rocks. *Anal. Chem. 33*, 1347–49.

Riley, J. P. 1958: The rapid analysis of silicate rocks and minerals. *Anal. Chim. Acta 19*, 413–28.

Scharbert, H. G. 1966: The alkali feldspars from microsyenite dykes of Southern Greenland. *Mineralog. Mag. 35*, 903–19.

Scharbert, H. G. 1968: Microsyenitic dykes from the Northern part of the Ilímaussaq peninsula, Southern Greenland. *Tschermaks miner. petrogr. Mitt. 12*, No. 4, 443–62.

Shapiro, L. & Brannock, W. W. 1956: Rapid analysis of silicate rocks. *U. S. Geol. Surv. Bull. 1036C*, 56 pp.

Shapiro, L. & Brannock, W. W. 1962: Rapid analysis of silicate, carbonate and phosphate rocks. *U. S. Geol. Surv. Bull. 1144–A*, 56 pp.

Upton, B. G. J. 1960: The alkaline igneous complex of Kûngnât Fjeld, south Greenland: *Bull. Grönlands geol. Unders. 27*, 145 pp. (also *Meddelelser om Grönland 123*, No. 4, 145 pp.).

Upton, B. G. J. 1964: The geology of Tugtutôq and neighbouring islands, south Greenland. Pt. II. Nordmarkitic syenites and related alkaline rocks: *Bull. Grönlands geol. Unders. No. 44*, 62 pp. (also *Meddelelser om Grönland 169*, No. 2, 62 pp.).

Upton, B. G. J. in press: The Alkaline Province of South West Greenland, *in* Sørensen, H. (ed.) *Alkaline Rocks*, Interscience.

Wilson, A. D. 1955: A new method for the determination of ferrous iron in rocks and minerals. *Bull. Geol. Surv. G. B. 9*, 56–8.

Wilson, A. D. 1960: The micro-determination of ferrous iron in silicate minerals by a volumetric and a colorimetric method. *Analyst 85*, 823–7.

Accepted for publication December 1970 Printed April 1971

MINERALOGICAL MAGAZINE, SEPTEMBER 1976, VOL. 40, PP. 737–46

Narsarsukite: a new occurrence in peralkaline trachyte, south Greenland

B. G. J. UPTON, R. MACDONALD*, P. G. HILL, B. JEFFERIES, AND C. E. FORD

Department of Geology, Edinburgh, EH9 3JW

*Department of Environmental Sciences, Lancaster, LA1 4YR

SUMMARY. A flinty, spherulitic dyke of peralkaline trachyte in a Precambrian dyke-swarm consists mainly of albite and aegirine. Within this, euhedral crystals of narsarsukite, $Na_2(Ti,Fe)Si_4O_{10}(F)$, occur as short prisms elongate parallel to *c*. This distinguishes them from all previously described narsarsukites, which have tabular habits. Minor phases present include micas, apatite, quartz, pectolite, nordite, and a thorium silicate. Probe analyses are presented for narsarsukite, aegirine, albite, biotite, apatite, pectolite, nordite, and the thorium silicate.

On mineralogical and geochemical grounds it is unlikely that the narsarsukite-bearing dyke is a differentiate of supposedly mantle-derived basalt–trachyte–comendite magmas in the region. The dyke is colinear with a comendite dyke exposed at lower altitude and it is suggested that the narsarsukite-bearing dyke developed as a rheomorphic fenite generated by reaction between quartz diorite basement and fugitive alkaline solutions from the subjacent comendite.

NARSARSUKITE is a rare titanosilicate known only in close association with highly alkaline igneous intrusions and is generally confined to silica-oversaturated granites, syenites, and fenites. It is a chain silicate with tetragonal symmetry and a composition of approximately $Na_2(Ti,Fe)Si_4O_{11}$ with four formula units per unit cell (Warren and Amberg, 1934; Pyatenko and Pudovkina, 1961). It may, however, contain some hydroxy and/or halide ions and the formula is quoted by Vlasov *et al.* (1966) as $Na_2(Ti,Fe)Si_4O_{10}(OH,F)$ and by Semenov (1969) as $Na_8Ti_3FeSi_{15}O_{43}F$.

The localities from which it has hitherto been recorded include the type locality at Narssarssuk, South Greenland (Flink, 1901; Bøggild, 1953), Ilímaussaq, South Greenland (Semenov, 1969), Montana (Graham, 1935; Stewart, 1959), Sudan (Jérémine and Christophe-Michel-Lévy, 1961), Oslofjord (Saebø, 1966), Quebec (Rajasekaran, 1966), Kola Peninsula (Vlasov *et al.*, 1966), and East Greenland (Bearth, 1959).

This account concerns a previously undescribed locality on the island of Igdlutalik some 45 km west of the type locality and approximately 12 km west of the Ilímaussaq complex, in which the mineral occurs as euhedral crystals within a dyke of peralkaline trachyte.

Field occurrence. The narsarsukite-bearing dyke occurs among a prominent swarm of ENE.-WSW. trending alkaline dykes that extends through the Ilímaussaq peninsula and the Tugtutôq district (Upton, 1974). The swarm involves dykes of alkali olivine basaltic and trachybasaltic composition together with trachytes, phonolites,

© Copyright the Mineralogical Society.

quartz trachytes, and comendites. All are part of the Gardar alkaline province and are believed to have been intruded between 1150 and 1200 Myr ago.

The narsarsukite-bearing dyke crops out within a gully at a height of approximately 220 m. The dyke is some 20 m wide and the outcrop can be traced not more than 50 m

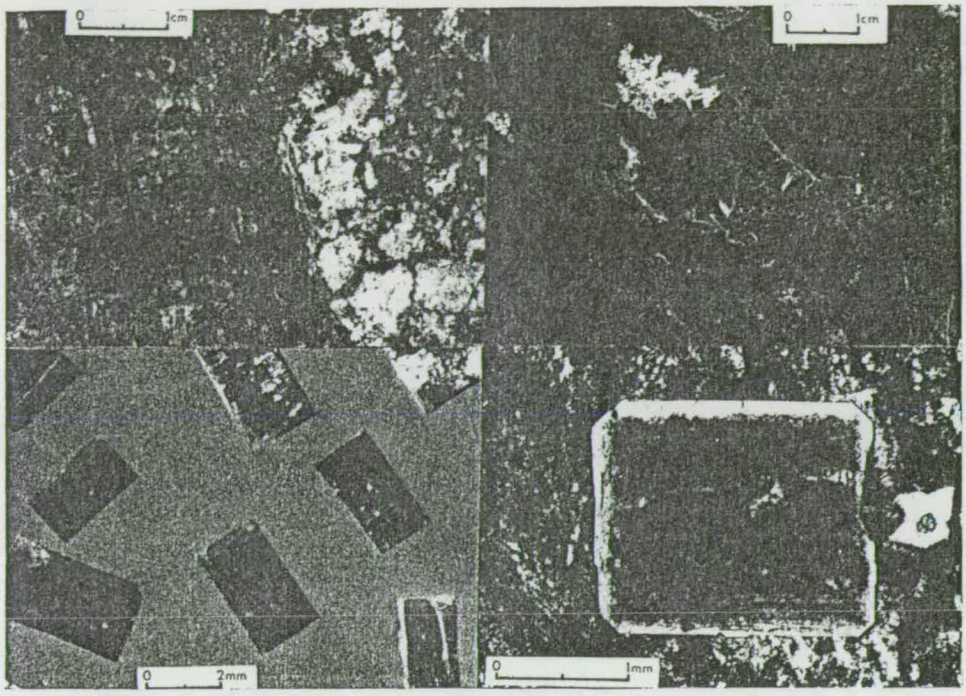

FIGS. 1 to 4: FIG. 1 (top left). Polished surface showing contact of the peralkaline dyke (left) and the country-rock (right). Ovoid spherulites can be seen in the dyke as well as small (<1 mm) dark aggregates of biotite apparently pseudomorphous after a mineral with approximately square cross-section. FIG. 2 (top-right). Polished surface of dyke-rock showing spherulites. The light-coloured area within the larger spherulite in the upper part of the plate consists of pectolite. Narsarsukite crystals (with light-coloured rims) may be seen as square/rectangular sections at top left, centre, and lower right. FIG. 3 (bottom left). Separated narsarsukite crystals showing elongation parallel to the *c*-axis and slight curvature of the prism faces. FIG. 4 (bottom right). Photomicrograph of a narsarsukite crystal viewed (approximately) along the *c*-axis, showing the clouded interior and clear rims.

along the length of the dyke. The southern contact, against the country-rock quartz diorite, is well exposed and shows a reddish-brown fine-grained flow-banded marginal dyke facies (fig. 1). The interior of the dyke is heterogeneous but composed mainly of dull greenish-grey flinty rock. Spherulitic structures up to 2 cm diameter are common (fig. 2). Narsarsukite crystals are abundant in the dyke interior, occurring as deep-green square-sectioned prisms up to 6 mm long. The prisms faces exhibit slight concavity (fig. 3).

The narsarsukite-bearing dyke lies on strike with a comendite dyke that is seen at lower altitude (*c.* 50m), to the ENE. The alignment of these two dykes suggests that

they may be intimately connected and that possibly the narsarsukite-bearing rock represents a higher-level facies of a dyke that either grades down or is abruptly underlain by comendite.

Analytical techniques. Microprobe analyses were performed on a Cambridge Scientific Instruments Microscan 5 Electron Probe Microanalyser. The more common elements were measured against well-established standards of simple composition. The rare earths were determined against synthetic glass standards described by Drake and Weill (1972). Corrections for atomic number, absorption, and characteristic fluorescence differences between standard and unknown are essentially those described by Sweatman and Long (1969). A correction for 'dead-time' counting losses was also made.

Probe-analyses of albite, aegirine, apatite, biotite, and nordite are presented in Table II. Light-brown veinlets and patches developed within some of the aegirine-rich spherulites consist of acicular pectolite, apatite, and interstitial quartz. Analyses of the apatite and pectolite are also given in Table II.

The habit of the Igdlutalik narsarsukite appears to be unique (fig. 3). The crystals occur as stumpy prisms approximately twice as long as they are broad, while narsarsukites described from other localities are invariably tabular parallel to {001}. Some crystals exhibit geniculate twinning. The forms {100} and {001} are dominant, with slender prism faces of the form {110}; {210} and {111} forms, common at Narssarssuk and elsewhere, are not developed. The simple, nearly rectangular habit is shared by those at Mont St. Hilaire (Rajasekaran, 1966), although the latter retain the usual tabularity. The deep-green colour is a further unusual feature, narsarsukite being typically a pale-yellow mineral. {100} cleavage is well developed.

The crystal cores are cloudy and contain an abundance of small inclusions (mainly aegirine and albite), while the crystal rims are clear (fig. 4). This zonation is abrupt and not gradational from core to margin. The presence of some 30 wt. % of inclusions consisting of a 3:2 (approximate) ratio of albite and aegirine would account for the bulk compositional differences between the clear rims and the inclusion-rich central parts shown in Table I. In thin-section the narsarsukite is colourless and the colour exhibited by the crystals as a whole is probably governed by the high content of included aegirine. The narsarsukite is uniaxial positive: ω 1·604±0·002, ϵ 1·657± 0·002.

Probe-analyses of the narsarsukites show them to be essentially homogeneous, the compositional differences between cores and rims being wholly attributable to the inclusions in the former. Niobium is a significant minor component of the narsarsukites. Separated crystals (with contained inclusions) were analysed for H_2O, Cl, and F. Whereas H_2O and Cl were so low as to be indeterminable, 0·73 % F was determined. Since the inclusions are essentially albite and aegirine, this figure is clearly a minimum value for F in the narsarsukite.

An accelerating potential of 20 kV and a probe current of 30 nA measured by a Faraday Cage were the general operating conditions and ensured reasonable counting statistics for all the elements.

With the exception of narsarsukite, stability of the minerals examined under the

electron beam was not a problem. Sodium volatilization in the narsarsukite was overcome by the use of a de-focused beam.

Rock-sample[1] GGU 50176 was analysed using the wet-chemical methods described by Upton *et al.* (1971, p. 165), except that F and Cl were determined by the spectrophotometric method of Peck and Smith (1964). In GGU 50177, SiO_2 was determined

TABLE I

Narsarsukite analysis			Atomic Ratios based on 11 Oxygens+Fluorine				
	1	2		1		2	
SiO_2	62·01	61·89	Si	4·00		4·05	
TiO_2	15·59	10·87	Ti	0·76		0·53	
Nb_2O_5	1·31	1·00	Nb	0·04		0·03	
Al_2O_3	0·43	4·18	Al	0·03		0·32	
FeO	3·20*	5·07*	Fe	0·17	1·03	0·28	1·17
MnO	0·11	0·10	Mn	0·01		0·01	
MgO	0·20	0·14	Mg	0·02		0·01	
CaO	0·01	0·13	Ca	0·00		0·01	
Na_2O	16·04	15·35	Na	2·01	2·02	1·95	1·96
K_2O	0·06	0·06	K	0·01		0·01	
F	1·0†	n.d.‡	F	0·20		—	
	99·96	98·79					
$O \equiv F$	0·44						
	99·52						

1. Mean of seven analyses of clear rims in GGU 86012, Igdlutalik.
2. Mean of six analyses of inclusion-rich cores in GGU 86012, Igdlutalik.

* Total iron as FeO.

† Adjusted for 0·73 % F in separated narsarsukite crystals containing *c.* 30 % (wt.) of albite and aegirine inclusions. H_2O^+ and Cl in specimen not detected. F and Cl analyses by S. Rizzello using method of Huang and Johns (1967).

‡ n.d. not detected.

gravimetrically, Al_2O_3 by the method of Mercy and Saunders (1966), total iron, CaO, MgO, and MnO by atomic absorption spectrometry, TiO_2 and P_2O_5 spectrophotometrically, F by the method of Peck and Smith (1964), FeO and H_2O as for GGU 50176, and Na_2O and K_2O by flame-photometry.

Petrography and mineralogy. The flow-banded selvedge of the narsarsukite-bearing dyke consists of finely disseminated albite, aegirine, hematite, (green) biotite, and opaque oxides. The flow-banding is defined by modal variation within these components on a mm scale.

The quartz diorite within a few cm of the dyke possess a granoblastic texture and consists of quartz, andesine, and microperthite. The crystals are strained and fractured. Fine-grained aggregates of aegirine, green biotite, and blue-green amphibole, patchily distributed along the crystal boundaries, imply some degree of metasomatic recrystallization and introduction of Fe and Na.

Samples from the dyke interior display textural and modal inhomogeneity. They

[1] Sample numbers refer to the Geological Survey of Greenland collection.

are typically fine-grained rocks composed principally of aegirine and albite. Typically the albite is anhedral and less than 100 μm across. However, albite crystals up to 1 cm occur in some coarser more leucocratic facies. Aegirine generally occurs as short prisms 50 to 100 μm long but is seen as longer acicular prisms within spherulites. Other components include green biotite, white mica, riebeckite, opaque oxides, calcite, apatite, zircon, and nordite.

TABLE II. *Electron-probe analyses of accompanying minerals*

	1	2	3	4	5	6	7	8	9	10	11	12
SiO_2	68·51	68·50	52·51	52·88	52·50	35·60	36·55	0·06	0·52	53·65	46·48	43·47
TiO_2	n.d.	n.d.	2·03	0·77	1·70	0·93	1·20	n.d.	n.d.	n.d.	n.d.	n.d.
Al_2O_3	19·05	19·30	1·24	1·65	1·00	13·16	16·35	n.d.	n.d.	0·02	n.d.	0·29
FeO*	0·06	0·08	26·41	27·12	25·52	29·28	10·00	n.d.	0·22	0·05	0·22	1·29
MnO	n.d.	n.d.	0·10	0·02	0·13	0·47	0·69	n.d.	0·02	n.d.	n.d.	3·16
MgO	0·02	0·02	0·62	0·68	1·40	4·89	9·26	n.d.	0·02	0·56	0·13	0·50
CaO	0·01	0·03	1·01	3·12	3·36	0·08	0·03	45·27	54·91	31·93	1·48	n.d.
Na_2O	11·83	11·72	13·73	12·32	12·00	0·05	0·02	1·35	n.d.	9·79	11·15	n.d.
K_2O	n.d.	0·13	n.d.	n.d.	n.d.	9·60	9·57	n.d.	n.d.	n.d.	n.d.	n.d.
	99·48	99·78	97·65	98·56	97·61	94·06	92·67	96·48	96·64	96·00	101·12	90·37

1. Albite in GGU 101201.
2. Albite in GGU 101204: Mean of 2 analyses.
3. Aegirine in GGU 101201: Mean of 3 analyses.
4. Aegirine in GGU 101202: Mean of 3 analyses.
5. Aegirine in GGU 101204: Mean of 5 analyses.
6. Biotite in GGU 101202: Mean of 3 analyses.
7. Biotite in GGU 101204.
8. Apatite in GGU 101201: Total includes: P_2O_5 = 40·89; SrO = 3·74; La_2O_3 = 1·03; CeO_2 = 3·04; Pr_2O_3 = 0·18; Nd_2O_3 = 0·92; Mean of 2 analyses.
9. Apatite in GGU 101204: Total includes: P_2O_5 = 40·95; Mean of 4 analyses.
10. Pectolite in GGU 101201: Mean of 4 analyses.
11. Nordite in GGU 86012: Total includes BaO = 8·99; SrO = 9·73; ZnO = 9·74; La_2O_3 = 8·48; CeO_2 = 11·37; Nd_2O_3 = 1·35; Mean of 8 analyses.
12. Unknown thorian mineral in GGU 86012: Total includes: ZnO = 0·63; ThO_2 = 35·12; Mean of 10 analyses.

* Total iron as FeO. n.d. = not detected.

The Igdlutalik narsarsukite has a distinctly high Ti/Fe ratio compared with those from Ilímaussaq and Narssarssuk, and falls into the category of titanian narsarsukite (Semenov, 1969). In this respect it most closely resembles the Sweet Grass, Montana narsarsukites (Stewart, 1959).

Small euhedral crystals (<0·5 mm), occurring in rectilinear, square-sectioned prisms, occur both within the narsarsukite crystals and the groundmass. These are brown (with conspicuous colour zonation) isotropic and, where included in narsarsukite, surrounded by radiating fractures. Probe-analyses show these to contain approximately 35 % ThO_2 (Table II). Their composition, form and isotropy suggest that they are an alteration product, probably hydrated, of thorite.

A further accessory mineral sparsely distributed through the groundmass is a member of the nordite group. It occurs as colourless prismatic euhedra with pyramidal terminations, up to 0·4 mm long. These are biaxial negative, with a small 2V and are length slow with extinction onto prism edges of *c.* 36°. They show shadowy zonation, a prismatic cleavage and birefringence of 0·020±0·002 (γ 1·646±0·002: α 1·628± 0·002). The refractive indices are slightly higher than those quoted for nordite from

the type locality in Lovozero (Vlasov *et al.*, 1966) and the birefringence of the Igdlutalik material is marginally lower. The composition of nordite according to Bakakin *et al.* (1970) is $Na_3Ce(Sr,Ca)(Mn,Mg,Fe,Zn)_2Si_6O_{18}$. While Bakakin *et al.* report ZnO up to 3·9 % in nordite from Lovozero, the Igdlutalik material contains over 9 % of this component.

TABLE III. *Whole-rock analyses*

Major elements (Wt %)			CIPW Norms			Trace elements (ppm)	
	50176	50177		50176	50177		50176
SiO_2	62·4	62·3	qz	3·92	4·60	Rb	560
TiO_2	1·01	1·05	or	24·18	11·82	Zn	445
Al_2O_3	12·54	12·73	ab	42·07	55·22	Yt	70
Fe_2O_3	7·67	5·29	ac	22·31	15·51	Ce	970
FeO	0·30	0·37	hy	1·34	3·44	Zr	500
MnO	0·13	0·18	di	1·33	2·96	Sr	585
MgO	0·78	1·91	il	0·92	1·17	Ba	15
CaO	1·36	2·50	ap	0·83	1·44	Nb	940
Na_2O	8·46	9·35	tn	1·31	1·09	K/Rb	60·4
K_2O	4·07	1·98	hl	0·01	—		
H_2O^+	0·19	0·18	ns	1·42	1·70		
P_2O_5	0·35	0·61	fr	0·36	0·88		
F	0·19	0·42					
Cl	<0·01						
	99·45	98·87					
O ≡ F	0·08	0·18					
	99·37	98·69					

Analysts: 50176, S. A. Malik and R. Macdonald; 50177, Sheila Rizzello and R. Macdonald.

Apatite is a ubiquitous minor accessory throughout the dyke. Analyses of apatite prisms occurring in sample GGU 101204 (Table II), an albite–aegirine–calcite-rich facies, show no unusual features while the apatite from GGU 101201, associated with late pectolite-rich veins and patches, has a significant content of Sr, Na, and rare-earth elements.

Whole rock composition. Analyses of two samples of the narsarsukite-bearing rock are presented in Table III. These, and the accompanying norm, show the rocks to be silica-oversaturated trachyte containing *c.* 1–2·5 % of normative Na_2SiO_3 (ns). The analyses do not differ greatly from those of fourteen trachytic (or microsyenitic) dyke-rocks occurring within the Tugtutôq swarm, (Macdonald, 1969). These contain 59 to 66 % SiO_2 and 6·5–9·3 % $FeO+Fe_2O_3$ while the dyke under consideration has some 62 % SiO_2 and 5·5–8 % total iron oxides. An excess of wt. % Na_2O over K_2O is a feature the dyke has in common with all but three of the other fourteen trachytic analyses but the narsarsukite-bearing dyke is exceptionally sodic, containing *c.* 9 % Na_2O as compared to a range of 5·1–7·4 % in the other analysed (narsarsukite-free) dykes. Furthermore, with >1 % TiO_2, the narsarsukite-bearing dyke is among the most titaniferous of the analysed dykes. The iron is predominantly in the ferric state and is mainly contained within the aegirine component.

While eleven of the fourteen trachytes possess normative acmite, none has a molecular excess of alkalis over alumina leading to normative 'ns'. Upton *et al.* (1971) proposed that many of the salic dykes in the Tugtutôq swarm may initially have been strongly persodic but lost alkalis during magmatic crystallization or subsequent devitrification. Despite the evidence for some metasomatic sodium loss to wall-rocks the Igdlutalik dyke retained a peralkaline character as a result of its modal content of such persodic minerals as narsarsukite and nordite.

In comparison with the other analysed dykes the narsarsukite-bearing dyke also shows anomalously high contents of Sr, Zn, Ce, La, and Nb. The Sr, Zn, and rare-earth elements are accommodated principally within the nordite. Nb and Ti are contained mainly within the narsarsukite; the associated analysed aegirines contain less than 4 % TiO_2.

Melting relations. Melting experiments were carried out on two samples of the dyke. One of these, sample GGU 101201, is from a narsarsukite-rich sample from the dyke interior, texturally similar to the analysed sample GGU 50176. The other, GGU 101202, is from chilled marginal-facies material.

This, though free of narsarsukite, contains small rectangular biotite aggregates, which are conceivably pseudomorphous after narsarsukite. The experiments were carried out at 1 kb P_{H_2O} in sealed $Ag_{70}Pd_{30}$ alloy tubes, with oxygen fugacity buffered by the $Fe_2O_3+Fe_3O_4+H_2O$ assemblage. Approximately 10 wt. % of water was added to the samples.

Crystallization of GGU 101201 commences with appearance of aegirine somewhat above 950 °C. Magnetite crystallizes with aegirine between 950 and 900 °C. Between 850 and 800° albite begins to crystallize while magnetite is resorbed. From 750 to 700°, nepheline crystallizes together with aegirine and albite. At 700° there is only a trace of liquid (glass) remaining. Magnetite appears as the liquidus phase of GGU 101202 at over 950 °C, with albite and aegirine crystallizing between 900 and 850 °C. From 750 to 700° magnetite is replaced by ilmenite and nepheline commences crystallization.

Narsarsukite crystallized from neither composition; it is consequently thought unlikely that narsarsukite could have crystallized from any liquid with a composition similar to GGU 101201, above 700 °C. However, GGU 101201 could conceivably represent a residual composition after the loss of some considerable quantity of fugitive components (H_2O,Na_2O,SiO_2?).

The occurrence of nepheline (identified optically and by X-ray diffraction), is difficult to reconcile with the quartz-normative character of the trachyte and known phase relations in the system $NaAlSiO_4$–SiO_2–H_2O. It may suggest either that the primary phase volume of nepheline extends into quartz-normative regions under conditions of excessive peralkalinity, or that in these experiments the water-vapour phase dissolved sufficient silica to shift the remaining bulk composition into the nepheline-normative region.

Paragenesis of narsarsukite. Growth of narsarsukite, according to Stewart (1959), requires an excess of silica, high partial pressure of oxygen, and an abundance of Ti and Na. Stewart considered that at lower P_{O_2} neptunite, $Na_2FeTiSi_4O_{12}$, would be

generated. However, Rajasekaran (1966) demonstrated the apparently stable co-existence of narsarsukite and neptunite at St. Hilaire, Quebec. All known occurrences of narsarsukite are in silica-oversaturated environments in close association with alkaline intrusive roacks that have crystallized at relative low pressures (<2 kb).

Flink (1901) gave the first precise description of the mineral, which occurs abundantly as one of the earliest phases in an assemblage including quartz, microcline, albite, aegirine, and taeniolite at the type locality of Narssarssuk, in a marginal facies of the Igdlerfigssalik alkaline complex (Emeleus and Harry, 1970). An extensive list of minerals from this locality was presented by Gordon (1924). At Ilímaussaq (Semenov, 1969), narsarsukite occurs in a quartz-bearing contact zone between naujaite and alkaline granite. Narsarsukite is also known from quartz-bearing pegmatites in the Werner Bjerge alkaline complex, East Greenland (Bearth, 1959) and, according to Gerasimovskii (in Vlasov *et al.*, 1966), narsarsukite occurs along metasomatized (albitized) zones between alkali syenite and plagioclase gneiss, at the margin of the Lovozero complex (Kola, U.S.S.R.). The mineral is also well known from quartz veins cutting a syenitic stock in the Sweetgrass Hills, Montana (Graham, 1935). In a fuller description of a second occurrence (Sage Creek) in the Sweetgrass area, Stewart (1959) wrote of narsarsukite occurring in close-spaced veinlets within highly brecciated metamorphosed rocks, intimately intruded by syenite. This hybrid host rock is composed of orthoclase, albite, aegirine, quartz, biotite, apatite, calcite, and pectolite and is, like the Igdlutalik host rock, a greenish-grey flinty material. The veinlets comprise both manganpectolite and narsarsukite, with later galena, calcite, and quartz. Pectolite is also associated with narsarsukite in the Lovozero occurrence (Vlasov *et al.*, 1966).

The Mont St. Hilaire (Quebec) occurrence appears closely comparable to that of Sage Creek. Rajasekaran (1966) described narsarsukite forming euhedral prisms within a greenish-grey metasomatized hornfels in the aureole of the Mont St. Hilaire alkaline stock, and concluded that the narsarsukite had grown as porphyroblasts in a matrix of albite, aegirine, apatite, and opaque oxides. The Mont St. Hilaire narsarsukites, like those from Igdlutalik, have cores crowded with inclusions (albite and an unidentified green mineral) and clear rims devoid of inclusions.

Brief descriptions have been furnished by Saebø (1966) and Jérémine and Christophe-Michel-Lévy (1961) of accessory narsarsukite in peralkaline granites at Gjerdingen (Oslo District) and Gouré (Sudan) respectively. The Gjerdingen occurrence is of particular interest in that the narsarsukite is accompanied by ramsayite ($Na_2Ti_2Si_2O_9$). An illustration of the Gouré material shows that, like the Igdlutalik crystals, inclusion-rich cores are surrounded by clear narsarsukite margins.

At Igdlutalik the flow-banding and spherulitic structure, together with the sharp and apparently chilled margin, seemingly provide clear evidence that the body is a magmatic dyke that congealed as a glass of extreme and unusual composition which later devitrified. The high values for Zn, Zr, Rb, Nb, and rare earths, together with high (Na+K)/Al and strikingly low K/Rb could have arisen from extreme fractionation of feldspar from more basic magmas. One sample of the dyke was analysed for strontium isotopes by Mr. A. B. Blaxland. On the assumption that the dyke is older than 1144 Myr (which would be the case if the dyke is coeval with the main ENE.-WSW.

alkaline dyke swarm) the initial $^{87}Sr/^{86}Sr$ ratio was less than 0·7040. This too is compatible with an origin by crystal fractionation of (mantle-derived) basaltic parental magma.

The relatively low Si and high Ca and Sr values are, however, less readily explicable on a crystal fractionation basis. Furthermore if the narsarsukite euhedra in an (originally) glassy matrix are interpreted as phenocrysts, the absence of any feldspar (or other) phenocryst minerals is a further feature difficult to explain by a fractionation hypothesis. Thus, from both petrochemical and mineralogical viewpoints it appears improbable that such a magma could have arisen by crystal fractionation from any of the trachytic, comenditic, or other magma types represented in the Tugtutôq–Ilímaussaq dyke swarm.

Stewart (1959) pointed out that the requisite conditions for narsarsukite growth may be obtained where emanations from alkaline magmas react with siliceous wall-rocks. The origin of the Iglutalik dyke-rock may well be bound up with reaction between emanations from the comendite dyke seen outcropping to the ENE. and the country-rock quartz-diorites. We suggest that a peralkaline acid magma was injected into a dyke fissure during the development of the regional dyke swarm. As it ascended, a fugitive volatile phase preceded it, rich in Na, Fe, Ti and in Sr, Zn, and rare-earth elements, reacting with the quartz diorite to create a zone of fenite above the acid magma. With rising temperature and lowering of melting-point as metasomatism proceeded, a rheomorphic fenite was generated and driven ahead of the (comenditic) magma. This, in turn, was responsible for some metasomatism of wall-rocks with which it came into contact. The bulk composition of the rheomorphic fenite magma was similar to that of the metasomatized hornfels described by Rajasekaran (1966) from the Mont St. Hilaire aureole.

While the Mont St. Hilaire narsarsukites are clearly porphyroblasts, this is less obviously so on Igdlutalik. The spherulitic flow-banded matrix must have been largely or wholly molten and it is improbable that porphyroblasts grown at sub-solidus temperatures during a temperature rise would have survived extensive melting.

Whereas aenigmatite ($Na_4(Fe_{10}Ti_2)Si_{12}O_{40}$) is well known as a phenocryst phase in peralkaline magmas (pantellerites), other NaFeTi silicates such as titanian acmite, ramsayite, neptunite, and narsarsukite have not been recorded as phenocrysts in fast-chilled eruptives or intrusives and it seems improbable that the Igdlutalik narsarsukites are true phenocrysts grown from an unusual Fe-Ti-rich persodic magma. However, on textural evidence it is not possible to decide whether the narsarsukite euhedra crystallized from the magma or from a glass at sub-solidus temperatures, although it appears certain that the crystals grew before the devitrification leading to spherulite formation. Failure to grow narsarsukite in the experimental runs may be due to lack of correspondence between the starting materials used and the original magma (or glass) composition, arising from loss of fugitive components during cooling and devitrification.

Acknowledgements. The dyke was found during the 1 : 20 000 reconnaissance mapping of the Julianehaab area by the Greenland Geological Survey. We are grateful to K. Ellitsgaard-Rasmussen. Director, Greenland Geological Survey, for permission to publish. S. A. Malik

(University of Reading) and Sheila Rizzello (University of Lancaster) kindly provided the whole-rock analyses.

REFERENCES

BAKAKIN (V. V.), BELOV (N. V.), and SOLOYEVA (L. P.) [Бакакин (В. В.), Белов (Н. В.) и Солоева (Л. П.)], 1970. The crystal structure of nordite and its relationship to melilite and datolite—gadolinite. *Amer. Min.* **55**, 1167–81.

BEARTH (P.), 1959. On the alkali massif of the Werner Bjerge in East Greenland. *Medd. Grønland.* **153**, 62 pp.

BØGGILD (O. B.), 1953. *The Mineralogy of Greenland.* Copenhagen.

DRAKE (M. J.) and WEILL (D. F.), 1972. New rare earth element standards for electron microprobe analysis. *Chem. Geol.* **10**, 179–81.

EMELEUS (C. H.) and HARRY (W. T.), 1970. The Igaliko nepheline syenite complex. *Grønlands Geol. Unders. Bull.* **85**.

FLINK (G.), 1901. On the minerals from Narsarsuk on the Firth of Tunugdliarfik in southern Greenland, *Medd. Grønland*, **1**.

GORDON (S. G.), 1924. Minerals obtained in Greenland on the second Academy-Vaux Expedition 1923. *Proc. Acad. Nat. Sci. Philadelphia*, **76**, 249–68.

GRAHAM (W. A. P.), 1935. An occurrence of narsarsukite in Montana. *Amer. Min.* **20**, 598–601.

HUANG (W. G.) and JOHNS (W. D.), 1967. Simultaneous determination of fluorine and chlorine in silicate rocks by a rapid spectrophotometric method. *Anal. Chim. Acta*, **37**, 508–15.

JÉRÉMINE (E.) and CHRISTOPHE-MICHEL-LÉVY (M.), 1961. Un nouveau gisement de narsarsukite (Identification d'un mineral denomme provisiorement 'gouréite' par A. Lacroix en 1934). *Bull. Soc. franç. Min. Crist.* **84**, 191–4.

MACDONALD (R.), 1969. The petrology of alkaline dykes from the Tugtutoq area, south Greenland. *Medd. Dansk geol. Foren.* **19**, 257–82.

MERCY (E. L. P.) and SAUNDERS (M. J.), 1966. Precision and accuracy in the chemical determination of total Fe and Al in silicate rocks. *Earth Planet. Sci. Lett.* **1**, 169–82.

PECK (L. C.) and SMITH (V. C.), 1964. Spectrophotometric determination of fluorine in silicate rocks. *Talanta*, **11**, 1343–7.

PYATENKO (Yu. A.) and PUDOVKINA (Z. V.) [Пятенко (Ю. А.) и Пудовкина (З. В.)], 1961. *Crystal structure of narsarsukite* in *Crystal Chemistry of Large Cation Silicates* (ed. Belov). (Transl. 1963) 128–36 N.Y.

RAJASEKARAN (K. C.), 1966. Narsarsukite from Mont St. Hilaire, Quebec, Canada. *Canad. Min.* **8**, 506–14.

SAEBØ (P. C.), 1966. A short comment on some Norwegian mineral deposits within the igneous rock complex of the Oslo Region. *Norsk geol. Tidsskrift*, **46**, 260–1.

[SEMENOV (E. I.)] Семенов (Е. И.), 1969. Минер. щелочного массива Илимаусак (*Mineralogy of the Ilimaussaq alkalic massif*). Moscow, Изд. Наука.

STEWART (D. B.), 1959. Narsarsukite from Sage Creek, Sweet Grass Hills, Montana. *Amer. Min.* **44**, 265–73.

SWEATMAN (T. R.) and LONG (J. V. P.), 1969. Quantitative electron-probe microanalysis of rock-forming minerals. *Journ. Petrology*, **10**, 332–79.

UPTON (B. G. J.), 1974. *The alkaline province of south-west Greenland* in *The Alkaline Rocks* (ed. Sørensen), 221–37, Wiley.

—— THOMAS (J. E.), and MACDONALD (R.), 1971. Chemical variation within three alkaline complexes in south Greenland. *Lithos*, **4**, 163–84.

VLASOV (K. A.), KUZ'MENKO (M. V.), and ES'KOVA (E. M.) [Власов (К. А.), Кузьменко (М. В.) и Еськова (Е. М.)], 1966. *The Lovozero alkali massif.* (Transl. from U.S.S.R. Acad. Sci. Press, Moscow, 1959) Edinburgh (Oliver & Boyd).

WARREN (B. E.) and AMBERG (C. R.), 1934. X-ray study of narsarsukite, $Na_2(TiFe)Si_4O_{11}$. *Amer. Min.* **19**, 546–8.

[*Manuscript received 4 July 1975, revised 11 November 1975*]

MINERALOGICAL MAGAZINE, MARCH 1973, VOL. 39, PP. 97–111

Chemical variation in minerals of the astrophyllite group

R. MACDONALD
Department of Environmental Sciences, University of Lancaster

M. J. SAUNDERS
Grant Institute of Geology, University of Edinburgh

SUMMARY. Eight new and fourteen published analyses of astrophyllites are used to examine chemical variation within the group. Al, Ca, Cs, F, Mg, Mn, Nb, Rb, Sn, Zn, and Zr may all substitute in moderate to large amounts in the unit cell, whose basic formula is $(K,Na)_3Fe_7Ti_2Si_8(O,OH)_{31}$; the natural Mn- and Nb- analogues of astrophyllite have been recorded. Ba, Cl, Cu, Li, P, Pb, Sr, and Ta are present, but in smaller amounts. The majority of specimens show appreciable cation deficiencies, up to 5 % of sites remaining vacant. Astrophyllites from undersaturated igneous rocks are characterized by higher Al, Ca, Mg, Mn, (OH+F), (K+Na), and Zr, and lower Li, Pb, and Zn contents than those from oversaturated igneous rocks. A 'high-alkali' type of astrophyllite is distinguished. A new occurrence of nigerite is noted.

ASTROPHYLLITE is a rare mineral, being restricted to alkaline, and usually peralkaline, salic rocks. It has most commonly been recorded as an accessory in peralkaline nepheline syenites and granites and their associated pegmatites, but occurs more rarely in fenites and other metasomatic rocks. Minerals of the astrophyllite group have also been found in metamorphic parageneses, such as riebeckite gneisses and pegmatites from N.W. Spain (Floor, 1961, 1966), in nepheline–syenite gneiss from Finland (Eskola and Sahlstein, 1930), and in paragneiss from Labrador (Nickel *et al.*, 1964).

Though astrophyllite has been known for nearly 130 years, having been discovered in 1844 by Weibye on the island of Låven, Norway, very few complete analyses have been made of the mineral, causing Butler *et al.* (1962) to call astrophyllite 'analytically neglected'. It is known that a number of minor elements, such as Zr, Nb, and Cs, can enter into the astrophyllite structure in moderate to large amounts, yet few published analyses contain determinations of more than one or two of these elements. As a result, it has not been possible to give a complete account of chemical variation within the group, or to comment unreservedly on such features as the approach to stoichiometry (Nickel *et al.*, 1964). Accordingly, we have analysed eight samples of astrophyllite from various localities for 26 elements, as a first step towards further elucidating the group's chemistry. We have checked that no other element is present in the specimens in more than trace amount, and feel therefore that these eight analyses can be considered practically complete.

© Copyright the Mineralogical Society.

Formula. Woodrow (1967) has shown that the structure of astrophyllite is similar to that of the trioctahedral micas, except that it contains octahedrally coordinated Ti in the tetrahedral layer. The basic unit consists of a continuous sheet of $(Fe,Mn)O_6$ octahedra between two sheets consisting of chains of SiO_4 tetrahedra linked by TiO_6 octahedra in the ratio 4:1. These composite sheets are separated by sheets of alkali ions, where K occurs in 13-fold coordination and Na in 10-fold coordination. The general formula has been adjusted to $(K,Na)_3Fe_7Ti_2Si_8(O,OH)_{31}$ or $A_3B_7C_2D_8X_{31}$, and unit-cell contents are based on 31 anions (Nickel *et al.*, 1964; Woodrow, 1967).

Two major substitutions have been distinguished, Mn for Fe in the *B*-group, resulting in the Mn-analogue of astrophyllite, *kupletskite* (Semenov, 1956), and Nb for Ti in the *C*-group, giving the Nb-analogue, *niobophyllite* (Nickel *et al.*, 1964). It is clear from table III (sample nos. 19–21, 22, 17) that the natural examples of kupletskite, niobophyllite, and the type astrophyllite from Låven, Norway, are rather removed from their end-member compositions, though more nearly 'pure' astrophyllites have been found in Colorado and S. Greenland (table II, nos. 1, 2, 3).

Analytical data. Eight samples of astrophyllite were available to us for this study (table I). Samples 2 and 7 were supplied pure. The relatively large crystals in specimens 1, 4, 5, and 6 were flaked from the rocks and hand-picked to purity. Pure astrophyllite in sample 3 was electromagnetically separated from amphibole with no difficulty, whereas final purification of specimen 8 from the astrophyllite/amphibole mixture supplied to us was possible only by hand-picking.

During analysis, a small amount (0·38 wt. %) of a red mineral forming hexagonal tablets, and insoluble in HF, HNO_3, and H_2SO_4 was found in sample 7, from La Guia, Vigo, Spain. This mineral has been identified as *nigerite* $(Zn,Fe,Mg)(Sn,Zn)_2(Al,Fe^{3+})_{12}O_{22}(OH)_2$, by Miss E. E. Fejer, Department of Mineralogy, British Museum (Natural History), to whom we extend our grateful thanks. The effect of the nigerite on the chemical determinations, especially on the Zn and Sn values, is unknown. However, the Zn content of sample 7 is low compared to most of our analyses, suggesting that contamination may not have been appreciable. All other samples were $\geqslant$ 99 % pure.

An initial qualitative analysis of about 0·01 g of each sample was performed using X-ray fluorescence. The presence of Nb, Rb, Zn, and Zr was confirmed in all samples, and a useful assessment of their relative quantities made by comparing appropriate peak heights on the recorder scans. The following elements were especially sought, but were not found in appreciable quantity: Bi, Ce, Ga, Ge, Mo, Sb, Th, U, W, and Yt. There may be a relatively high rare-earth content in specimen 8. The presence of B could not be confirmed using insensitive qualitative chemical tests. Be was not sought, but other elements not recorded were apparently absent.

Maxwell (1968, p. 314) has recently made a plea for more published descriptions of wet-chemical procedures used for the analysis of uncommon minerals, suggesting that these will be of use not only to intending analysts, but also in allowing an assessment of the validity of the analytical results presented. Accordingly, we have outlined in some detail the methods used here (Appendix). In some cases, these methods proved to be not entirely satisfactory, and we recommend alternative procedures that we have

not yet fully investigated. However, we believe that our results (tables I and II) are as reliable as any yet published for astrophyllite. They contain the most complete information available on Ba, Cl, Cu, Nb, Sn, Sr, Ta, and Zn in astrophyllites, and the first determinations of Pb, to our knowledge. They show that the mineral is a strong concentrator of Sn and Zn, and earlier reports that it is enriched in Cs, Nb, Rb, Ta, and Zr were confirmed on all samples.

The unit-cell contents of 14 published analyses of astrophyllite, kupletskite, and niobophyllite are given in table III. We have included here all fairly complete, reliable analyses of which we are aware. Early analyses of astrophyllite from El Paso County, Colorado by Koenig (1877) and Eakins (1891) have been omitted because new and more complete data (table I, no. 1) are now available for material from this locality.

Substitutions. These are conveniently considered in terms of replacement in the astrophyllite formula $(K,Na)_3Fe_7Ti_2Si_8(O,OH)_{31} = A_3B_7C_2D_8X_{31}$.

A-group. Ca is the most important substitute for alkalis, up to a maximum of 0·83 atoms, i.e. some 28 % of available sites, in kupletskite from Kuivchorr, Kola. Ba and Sr are both very low, Ba tending to be the more abundant. Rb is also generally low, less than 0·15 atom, though Ganzeev *et al.* (1969) report astrophyllites from Russian alkaline granites with rather higher Rb (wt. %) values than our specimens. Despite the fact that it is only a minor substituent, Rb still shows strong enrichment relative to K compared to common terrestrial rocks and minerals (Butler *et al.*, 1962). K/Rb ratios (wt.) are always less than 30, and range down to 2 (data from this paper and from Ganzeev *et al.*, 1969). There is no correlation between K and Rb.

Cs is also concentrated in astrophyllite, and a caesian specimen from alkaline granite from Dara Pioz in the Alai range, Kirgiz SSR, containing 10·80 % Cs (wt.) has been described by Ganzeev *et al.* (1969). The full analysis of this mineral has not yet been published: however, the atomic ratio 100 Cs: (Cs+Na+K) is 45·5; hence the mineral should not be given species status, for which Cs should be > Na+K. The data given in table IV indicate that many more analyses are needed to ascertain the degree of isomorphism between astrophyllite and its Cs-enriched variety.

Analyses for rare earths are very scarce. Nickel *et al.* (1964) report 1·50 % (wt.) $(Ln,Yt)_2O_3$ in niobophyllite with Ce and La oxides predominant. Assuming all the rare-earths to be Ce, this gave a unit-cell content of 0·123 atom. Dietrich *et al.* (1965) report semi-quantitative spectrographic results for two astrophyllites from Norwegian alkaline granites (ekerites): La, 250, 130 ppm; Nd, 700, 420 ppm; Yt 200, 250 ppm.

B-group. The most important substitution is of Mn for Fe, resulting in the Mn end-member, kupletskite, and complete solid solution almost certainly exists between astrophyllite and kupletskite (Semenov, 1956; Nickel *et al.*, 1964) (fig. 1a). Mg is also an important substitute for Fe, occupying up to 30 % of *B*-sites in kupletskite from the Sea of Azov region, U.S.S.R. (table III, no. 19).

Zn ranges from 0·02 atom in the Spanish astrophyllites to 0·31 atom in the Colorado specimen, which is the most Zn-enriched astrophyllite yet recorded. Borley (1963) has described the entry of Zn into riebeckite–arfvedsonites from the Younger Granites of

TABLE I. *New analyses of astrophyllite from various localities. M. J. Saunders, anal.*

	1	2	3	4	5	6	7	8
SiO_2	35·41	34·71	35·79	34·18	35·99	35·86	34·81	33·93
Al_2O_3	0·40	0·89	0·72	1·54	3·46	2·61	2·00	1·46
TiO_2	9·92	8·90	9·88	9·04	8·15	10·14	10·48	8·87
ZrO_2	0·99	1·38	1·74	3·70	4·53	1·89	0·40	1·60
Nb_2O_5	2·76	2·58	1·87	1·07	1·25	0·78	1·22	3·45
Ta_2O_5	0·26	0·29	0·16	0·06	0·10	0·04	0·13	0·46
SnO_2	0·40	0·30	0·07	0·14	0·04	0·01	0·20	0·38
FeO	29·56	35·23	33·11	27·02	20·91	22·65	34·35	30·59
Fe_2O_3	0·76	0·70	1·76	0·67	1·48	0·87	0·89	3·80
MnO	4·16	1·02	1·70	7·41	8·14	9·10	2·00	2·10
MgO	0·11	0·08	0·21	0·97	0·87	1·49	0·10	0·19
ZnO	1·88	0·76	0·58	0·24	0·18	0·34	0·12	0·11
PbO	0·43	0·37	0·10	< 0·01	< 0·01	< 0·01	0·15	0·06
Li_2O	0·181	0·051	0·050	0·036	0·016	0·015	0·198	0·028
CuO	0·005	0·010	0·013	0·005	0·017	0·004	0·012	0·022
Na_2O	2·97	2·72	2·83	2·19	2·46	2·57	2·15	2·00
K_2O	5·04	5·57	5·48	5·98	6·03	6·06	4·91	4·99
Rb_2O	1·10	0·38	0·19	0·31	0·41	0·20	0·36	0·49
Cs_2O	0·08	0·07	< 0·01	0·15	0·12	< 0·01	0·06	0·19
CaO	0·23	0·28	0·46	1·43	1·56	1·60	1·15	0·82
SrO	0·007	0·003	0·008	0·034	0·020	0·022	0·018	0·009
BaO	0·120	0·020	0·050	0·035	0·097	0·069	0·091	0·053
P_2O_5	0·04	n.f.†	n.f.	0·01	0·04	0·01	n.f.	n.f.
F	1·15	1·24	1·38	1·26	1·22	1·27	1·29	0·90
H_2O^+	2·70	2·60	2·49	2·80	2·91	2·71	2·79	3·37
Cl	< 0·01	< 0·01	< 0·01	< 0·01	< 0·01	< 0·01	< 0·01	< 0·01
Sum	100·66	100·15	100·64	100·28	100·00	100·31	99·88	99·87
$O \equiv (F,Cl)_2$	0·48	0·52	0·58	0·53	0·51	0·53	0·54	0·38
Total	100·18	99·63	100·06	99·75	99·49	99·78	99·34*	99·49

* Acid insoluble 0·38 %. † Not found.

Key to Tables I and II; 1, 2, 3 from oversaturated rocks, 4, 5, 6, from undersaturated, and 7, 8 from metamorphic.

1. Astrophyllite, pegmatite, St. Peter's Dome, El Paso County, Colorado. Occurs as crystals up to 7 cm × 2 cm × 1 cm embedded in quartz. The geology and mineralogy of these pegmatites have been described by Gross and Heinrich (1966), who give the following optical data for the astrophyllite: α 1·695, red-orange, β 1·725, lemon-yellow, γ 1·755, dark yellow-green; $2V_\gamma$ large.
2. Astrophyllite from peralkaline granite sheet (Greenland Geol. Surv. no. 26272), Kûngnât complex, South Greenland. White homogeneous rock consisting of euhedral antiperthite (65·5 % modally), anhedral quartz (29·0), riebeckite or arfvedsonite (4·5), zircon (tr.), opaque ore (tr.), and astrophyllite (0·8). Latter has α 1·695, orange, β 1·715, yellow, γ 1·751, lemon-yellow; $2V_\gamma$ 66 to 70° (B. G. J. Upton, pers. comm.).
3. Astrophyllite from peralkaline granite sill (G.G.U. no. 40595/86114), Central Complex, Tûgtutoq, South Greenland. Anhedral crystals up to 1 mm long (0·6 % modally), occur in association with alkali feldspar (76·3), quartz (18·4), riebeckite or arfvedsonite (4·7), and fluorite (trace). α bright-orange, β 1·721, orange-yellow, γ 1·751, yellow; $2V_\gamma$ 69 to 75°.
4. Astrophyllite, pegmatite, Barkevik, Langesundfjord, Norway, from the collections of the Department of Geology, University of Edinburgh. Associated minerals in hand specimen used for mineral separation include perthitic feldspar, nepheline, aegirine, riebeckite or arfvedsonite, and zircon. Astrophyllite occurs as flakes up to 7 cm × 2 cm, sometimes intergrown with pyroxene or amphibole. α orange, β 1·710, orange-yellow, γ 1·740, lemon-yellow. $2V_\gamma$ large.

TABLE II. *Unit-cell contents, based on 31 anions, of new analyses of astrophyllites*

	1	2	3	4	5	6	7	8
Na	1·277	1·182	1·208	0·940	1·030	1·076	0·916	0·854
K	1·426	1·591	1·538	1·691	1·661	1·667	1·377	1·402
Rb	0·147	0·054	0·026	0·045	0·057	0·029	0·050	0·069
Cs	0·003	0·005	—	0·013	0·010	—	0·005	0·019
Ca	0·055	0·067	0·108	0·339	0·361	0·369	0·270	0·193
Sr	0·001	0·001	0·001	0·004	0·003	0·003	0·003	0·001
Ba	0·011	0·001	0·004	0·003	0·008	0·005	0·008	0·004
A	2·920	2·901	2·885	3·035	3·130	3·149	2·629	2·542
Fe^{2+}	5·484	6·600	6·088	5·007	3·776	4·087	6·316	5·631
Fe^{3+}	0·128	0·118	0·291	0·112	0·241	0·070	0·147	0·630
Mn	0·781	0·194	0·317	1·391	1·488	1·663	0·372	0·391
Mg	0·036	0·027	0·069	0·321	0·280	0·480	0·033	0·062
Li	0·163	0·046	0·045	0·032	0·013	0·013	0·174	0·024
Zn	0·308	0·125	0·094	0·039	0·029	0·054	0·020	0·019
Cu	0·003	0·001	0·003	0·001	0·003	0·001	0·003	0·004
Pb	0·025	0·023	0·005	—	—	—	0·009	0·004
B	6·928	7·134	6·912	6·903	5·830	6·368	7·074	6·765
Ti	1·656	1·500	1·634	1·506	1·324	1·645	1·733	1·468
Zr	0·107	0·151	0·186	0·399	0·478	0·198	0·042	0·172
Nb	0·277	0·261	0·185	0·107	0·122	0·075	0·121	0·344
Ta	0·016	0·019	0·010	0·003	0·005	0·003	0·008	0·026
Sn	0·036	0·027	0·001	0·012	0·004	0·001	0·017	0·033
C	2·092	1·958	2·016	2·027	1·933	1·922	1·921	2·043
Al	0·104	0·234	0·188	0·402	0·880	0·664	0·519	0·378
Si	7·855	7·777	7·869	7·572	7·772	7·736	7·653	7·468
D	7·959	8·011	8·057	7·974	8·652	8·400	8·172	7·846
OH	3·996	3·885	3·652	4·138	4·192	3·899	4·090	4·949
F	0·806	0·879	0·959	0·883	0·833	0·866	0·894	0·627
O	26·198	26·236	26·389	25·979	25·975	26·235	26·016	25·424
Σ cations	19·899	20·004	19·870	19·939	19·545	19·839	19·796	19·196
Fe^{2+}/Fe^{3+}	42·84	55·9	20·9	44·7	15·7	58·4	43·0	8·9
K/Na	1·12	1·35	1·27	1·80	1·61	1·55	1·50	1·64
K/Rb (wt)	4	13	26	18	13	27	12	9
Nb/Ta (wt)	9·1	7·6	10·0	15·2	10·7	16·6	8·0	6·4

5. Astrophyllite, Narssarssuk, S. Greenland (G.G.U. no. 63785A). From pegmatite cutting SI–4 syenite, Igaliko Complex (see Emeleus and Harry, 1970, p. 70). Pegmatite contains abundant aegirine, perthitic alkali feldspar, natrolite (in granular aggregates), cancrinite, and (?) zircon. Optical data on astrophyllite, kindly supplied by Dr. C. H. Emeleus: β 1·710, γ 1·735, $2V_\gamma$ 84 ± 1·5°.
6. Astrophyllite, microfoyaite dyke, Mirala Estate, Zomba, Malawi. (Coll. no., Malawi Geol. Surv. is K.B. 1689.) This dyke described by Bloomfield, 1965, p. 142. Dyke also contains aegirine, nepheline, alkali feldspar and alkali amphibole, titanomagnetite, fluorite, rutile, and zircon. Astrophyllite occurs as narrow, bronzy yellow flakes up to 4 × 40 mm in size, enclosing feldspar, and showing the pleochroic scheme α bright orange, β yellow, γ pale lemon-yellow.
7. Astrophyllite from riebeckite-gneiss of Galiñeiro type, south of La Guia, Vigo, Spain (Floor, 1966, coll. no. 61 cor 20). Crystals up to 2 mm in length in association with quartz, albite, microcline ($Or_{99\cdot6}Ab_{0\cdot4}An_{0\cdot0}$), riebeckite, lepidomelane, aegirine, zircon, fluorite, and trace amounts of nigerite. α orange, β 1·722, yellow, γ 1·757, lemon-yellow; $2V_\gamma$ 88·4° in red light, 81·9° in green light.
8. Astrophyllite from non-deformed pegmatite, 10 cm thick, south of Monte Galiñeiro, Vigo, Spain (Floor, 1966, pegmatite of col 602 m., p. 59). Floor describes the geology and mineralogy of this pegmatite, which contains quartz, microcline, albite, astrophyllite, riebeckite, zircon, xenotime, and pyrochlore. Astrophyllite forms thin crystals up to 5 mm long, and with α orange-red, β 1·726, yellow, γ 1·758, lemon-yellow; $2V_\gamma$ 78·6° in red light, 67·2° in green light.

TABLE III. *Unit-cell contents, based on 31 anions, of minerals of the astrophyllite group, calculated from published analyses (refs. below). 9—from oversaturated igneous, 10–21—from undersaturated igneous, 22—from metamorphic, parageneses; 23–24, 'high-alkali' astrophyllites*

	9	10	11	12	13	14	15	16	17	18	19	20	21	22	23	24
Na	1·274	0·936	1·265	0·983	1·259	1·264	1·177	1·259	1·352	1·308	1·211	0·892	0·892	1·079	2·146	1·860
K	1·421	1·876	1·637	1·630	1·578	1·814	1·617	1·636	1·713	1·661	1·245	1·547	1·202	1·572	1·911	1·791
Rb	—	—	—	—	—	—	—	—	—	—	—	0·052	—	—	—	—
Ca	0·158	0·282	0·375	0·402	0·298	0·239	0·296	0·169	0·273	0·293	0·242	0·335	0·830	0·173	0·253	0·966
Sr	—	—	0·007	0·005	—	—	—	—	—	—	—	—	—	—	—	—
Ba	—	—	0·013	—	—	—	—	—	—	—	—	0·027	—	—	—	—
Ln	—	—	—	—	—	—	—	—	—	—	—	—	—	0·123	—	—
A	2·853	3·094	3·297	3·020	3·135	3·317	3·090	3·064	3·338	3·262	2·698	2·853	2·924	2·947	4·310	4·617
Fe^{2+}	4·131	5·471	4·859	3·592	4·124	4·189	3·989	3·699	3·042	2·561	1·342	0·964	0·979	4·439	3·081	2·970
Fe^{3+}	1·714	0·644	0·452	1·062	0·443	0·459	0·416	0·656	0·720	0·232	0·146	1·262			0·457	0·317
Mn	0·254	0·521	1·225	1·241	1·338	1·970	2·220	2·407	2·821	2·965	3·436	4·303	5·040	1·862	0·696	0·532
Mg	0·214	0·294	0·499	0·376	0·307	0·313	0·300	0·349	0·206	0·121	2·108	0·523	0·956	0·053	1·959	1·749
Li	—	—	—	—	—	—	—	—	—	—	—	0·083	—	—	—	—
Zn	—	—	—	—	—	—	—	—	—	0·033	—	—	—	—	—	—
B	6·313	6·930	7·035	6·271	6·212	6·931	6·925	7·111	6·789	5·912	7·032	7·135	6·975	6·354	6·193	5·568
Ti	1·560	2·014	1·940	2·126	1·520	1·553	1·831	1·476	1·323	1·521	0·850	1·723	1·949	0·494	1·884	1·870
Zr	0·346	0·086	0·060	0·000	—	0·493	0·390	0·416	0·571	0·262	0·311	0·000	0·125	—	—	—
Nb	0·077	—	—	—	0·120	—	—	—	—	0·476	0·059	0·241	0·065	1·492	—	—
Ta	0·008	—	—	—	0·003	—	—	—	—	—	—	—	—	0·032	—	—
Sn	—	—	—	—	—	—	—	—	—	—	—	—	—	—	—	—
C	1·991	2·100	2·000	2·126	1·643	2·046	2·221	1·892	1·894	2·259	1·220	1·964	2·139	2·018	1·884	1·870
Al	0·147	0·311	0·154	0·583	1·259	0·425	0·253	0·337	0·445	0·516	1·324	0·254	0·427	0·235	0·269	0·220
Si	7·830	7·485	7·567	7·200	7·257	7·397	7·237	7·500	7·416	7·656	7·423	7·220	7·015	7·467	7·812	7·943
D	7·977	7·796	7·721	7·783	8·516	7·822	7·490	7·837	7·861	8·172	8·747	7·474	7·442	7·702	8·081	8·163
OH	3·717	4·835	4·330	5·032	5·773	5·074	5·078	5·297	5·024	4·251	5·597	5·600	5·503	5·429	4·724	4·683
F	1·104	—	0·592	0·885	0·429	—	0·673	—	0·485	0·450	0·650	—	0·830	0·325	0·293	0·331
Cl	—	—	0·129	0·000	—	—	—	—	—	—	—	—	—	—	—	0·038
O	26·179	26·165	25·949	25·083	24·798	25·926	25·249	25·703	25·491	26·299	24·753	25·400	24·667	25·246	25·983	25·948
Σ cations	19·134	19·920	20·053	19·200	19·506	20·116	19·726	19·904	19·882	19·605	19·697	19·426	19·480	19·021	20·268	20·118
Fe^{2+}/Fe^{3+}	2·41	8·50	10·75	3·38	9·31	9·13	9·59	5·64	4·23	11·04	9·19	0·76	—	—	6·74	9·37
K/Na	1·12	2·00	1·29	1·66	1·25	1·44	1·37	1·30	1·27	1·27	1·03	1·73	1·35	1·46	0·90	0·96
K/Rb (wt.)	—	—	—	—	—	—	—	—	—	—	—	14	—	—	—	—
Nb/Ta (wt.)	4·6	—	—	—	35·6	—	—	—	—	—	—	—	—	24·2	—	—

Nigeria, where it occurs up to a maximum of 0·10 atom per unit-cell (0·93 % wt. ZnO), and has suggested that this represents an unusually large amount of Zn to be found in silicate lattices. Astrophyllite must therefore be considered a strong Zn-concentrator.

TABLE IV. *Data indicating the degree of solid substitution between astrophyllite and Cs-kupletskite.*

Locality	$\frac{Cs \times 100}{Cs+Na+K}$ (atomic)	
Lovozero, U.S.S.R.	0·03	Ganzeev *et al.*, 1969
Kûngnât, S. Greenland	0·20	This paper
Narsarssuaq, S. Greenland	0·40	This paper
Tuva, U.S.S.R.	1·18	Ganzeev *et al.*, 1969
Burpala, U.S.S.R.	2·00	Ganzeev *et al.*, 1969
Burpala, U.S.S.R.	4·33	Ganzeev *et al.*, 1969
Dara Pioz, U.S.S.R.	7·56	Ganzeev *et al.*, 1969
Dara Pioz, U.S.S.R. (Cs-kupletskite)	45·51	Ganzeev *et al.*, 1969

The Colorado specimen is also the most Pb-enriched of our samples (0·03 atom), though this element normally occurs in only very minor amounts, being below the limit of detection (0·01 % wt.) in three of the samples. Cu is also a relatively unimportant minor substituent for Fe. Koenig (1877) reported a CuO value of 0·42 % (wt.) in astrophyllite from El Paso co., Colorado, but the new data (table I) suggest that his figure may be in error. Li is present in our samples up to a maximum of 0·17 atoms in a Spanish astrophyllite, though Ganzeev *et al.* (1969) have recorded astrophyllites richer in Li from several Russian localities, ranging up to 0·59 % Li (wt.).

Fe^{2+}/Fe^{3+} ratios in the new and published analyses vary widely, from 0·8 to 58·4, but the new analyses generally show the Fe to be present mostly in the divalent form.

Source of analyses used in table 3

Specimens 9–18, astrophyllite; 19–21, kupletskite; 22—niobophyllite; 23, 24 high-alkali astrophyllite.

9—post-Jurassic alkaline granite, Maritime Province, U.S.S.R. (Perchuk and Zyryanov, 1965, table 1, no. 10);
10—Naujakasik, Tunugdliarfik, S. Greenland (Kunitz, 1936, table 9);
11—Kukisvumchorr, Chibina Tundra, Kola, U.S.S.R. (Bonshtedt, 1931);
12—Yukspor, Chibina Tundra, Kola, U.S.S.R. (Bonshtedt, 1931);
13—Central Turkestan–Alay Range, U.S.S.R. (Perchuk, 1964, p. 204);
14—Brevik, Norway (Kunitz, 1936, table 9);
15—Island of Eikaholm, Norway (Brøgger, 1890);
16—Rume, Los Archipelago (Kunitz, 1936, table 9);
17—Låven, Langesundfjord, Norway (Gossner and Reindl, 1934, p. 165);
18—Middle Tatarsk massif, U.S.S.R. (Sveshnikova, 1960, table 1);
19—Sea of Azov region, U.S.S.R. (Valter *et al.*, 1965, p. 251);
20—Mt. Nephka, Lovozero, Kola, U.S.S.R. (Semenov, 1956, 1960);
21—Mt. Kuivchorr, Lovozero, Kola, U.S.S.R. (Semenov, 1956);
22—Seal Lake, Labrador (Nickel *et al.*, 1964);
23—U.S.S.R., (Peng and Ma, 1963);
24—Pegmatite, Yukspor, Khibina, U.S.S.R. (Dorfman, 1962, p. 54).

From a spectral study of astrophyllite from El Paso County, Colorado, Manning (1969, p. 672) has suggested that Fe^{3+} ions are not located in the octahedral layer, despite the presence in Koenig's (1877) analysis of material from this locality of significant Fe_2O_3 (Fe^{2+}/Fe^{3+}(atomic) = 4·4). The new analysis of Colorado astrophyllite (spec. 1) has a value of this ratio of 42·8. These features combined suggest that Fe^{3+} is relatively minor in the astrophyllite structure, and that many of the older analyses may be in error in this regard.

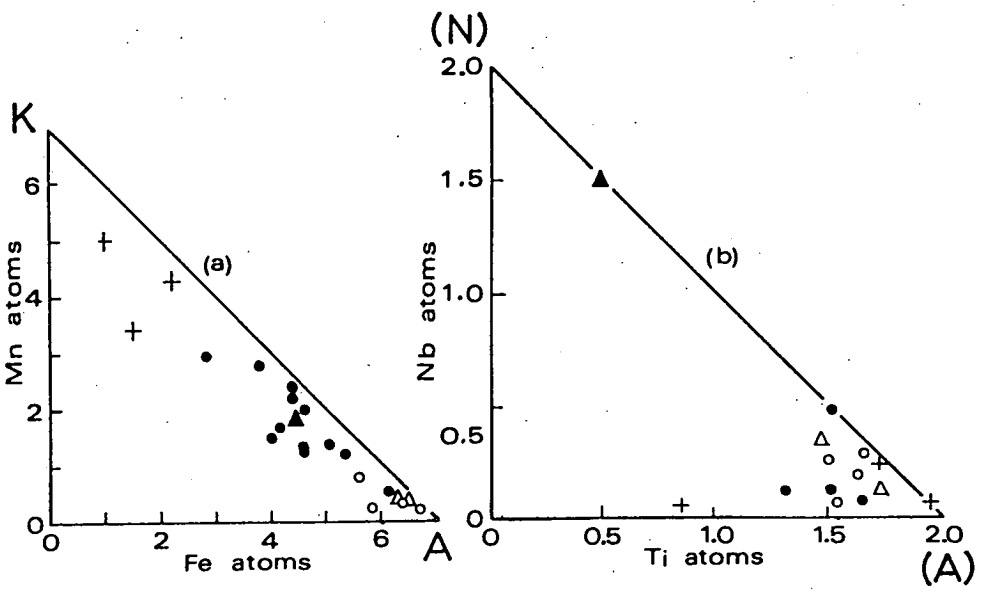

FIG. 1. Degree of solid substitution between (a) theoretical astrophyllite (A) and kupletskite (K) compositions, and (b) astrophyllite and niobophyllite (N). Open circles—astrophyllites from oversaturated rocks; closed circles—astrophyllites from undersaturated rocks; open triangles—astrophyllites from Spanish metamorphic rocks; closed triangle—niobophyllite; crosses—kupletskite.

Dietrich *et al.* (1965, table 4) found Cr, Sc, and V below the limits of detection in astrophyllite from two Norwegian ekerites, while Ni was detectable at 75 and 90 ppm.

C-group. Due to an inadequate number of available analyses, Nickel *et al.* (1964) were unable to draw any conclusions about the degree of solid solution between astrophyllite and its Nb-analogue, niobophyllite. Data now available (fig. 1b) indicate that Nb replaces Ti in astrophyllite up to some 24 % of available sites, but that there is still a considerable composition gap between astrophyllite and niobophyllite. Hansen (1968) has given values of 4·2–7·1 % Nb_2O_5 (wt.) for niobophyllite from the Ilimaussaq intrusion, S. Greenland, and, although the full analysis of this mineral has not yet been published, it seems likely that it will fall in the composition gap of fig. 1b.

Ta is a very minor substitute for Ti, occurring up to 0·03 atom (table III). The Nb/Ta ratio varies from 5 to 36 (wt. %). The importance of Zr replacing Ti in astro-

phyllite was recognized by Kunitz (1936); Zr ranges from 0·00 to 0·57 atoms, that is, it occupies up to 28 % of the theoretical *C*-sites. The most Zr-rich specimens are those from the nepheline syenite pegmatites of the Permian Oslofjord alkaline province.

Sn is present in only trace amounts, up to 0·04 atom. The only determination of Hf in astrophyllite is from the Kangerdlugssuaq alkaline intrusion, E. Greenland, where Brooks (1970) records Hf 0·2 %, Zr 1·13 %, and a Zr/Hf (wt.) ratio of 5·7.

D-group. Al is an important substitute for Si in the tetrahedral sites, occupying up to 16 % of the *D*-sites.

X-group. The main substituent is F, which reaches 1·1 atoms. Cl is very low (< 0·01 % wt.) in all our specimens. The only other determinations, in two astrophyllites from Kola, U.S.S.R (Bonshtedt, 1931), gave 0·00 and 0·35 % wt. Cl, the latter equivalent to 0·129 atom Cl in the unit cell. OH has a fairly small range, some 3·5 to 6 atoms.

Stoichiometry. Nickel *et al.* (1964) found appreciable departures from the ideal $A_3B_7C_2D_8X_{31}$ formula in kupletskite, niobophyllite, and astrophyllite from Colorado, and suggested that non-stoichiometry may be a characteristic feature of the group. This prediction appears to be borne out by the larger body of data (tables II and III). All but three of the analyses show cation deficiencies ranging up to 0·98 atoms per unit cell, or some 5 % of available sites. This feature is partly due to failure in most cases to analyse for all possible substituting elements. Of the 8 new analyses, 6 have total cations equal to or greater than 19·8 per unit cell, suggesting perhaps that many astrophyllites will prove to be nearly stoichiometric when fully analysed. However, the Spanish astrophyllite F92 (spec. 8) contains only 19·2 cations per unit cell, exhibiting one of the largest deficiencies of all specimens we have examined.

There is no preferential tendency towards either cation excess or deficiency in the *A*, *C*, and *D* groups, but in the *B*-group deficiency of cations is more common than excess. There is also no strong correlation between cation deficiency in one group and cation excess in another.

Relationship between composition and parageneses

Igneous rocks. Systematic differences between astrophyllites found in granitic rocks (oversaturated parageneses) and those from feldspathoidal rocks (undersaturated parageneses) can be readily detected by inspection of tables II and III. Compared to the 'oversaturated' types, astrophyllites from undersaturated rocks show higher Na+K, Ca, Sr, Mn, Mg, Zr, Al, and OH+F and lower Zn, Pb, and Li contents. The data of Ganzeev *et al.* (1969) suggest that the highest concentrations of Rb and Cs are also found in astrophyllites from granitic rocks, and this is in accord with the high values for those elements found in the Colorado specimen during this study.

There is also a strong tendency for K/Na ratios to be higher in 'undersaturated' types, and the increased Na+K content usually results in a cation excess in the *A*-group, while 'oversaturated' astrophyllites usually have a cation deficiency in this group (tables II and III). Between 'oversaturated' and 'undersaturated' types, there is,

therefore, increasing replacement of Mn and Mg for Fe, Ca for alkalis, Zr for Ti, Al for Si, and (OH+F) for O. There is no obvious connection between the Nb-content of astrophyllite and the type of rock in which it is found.

It seems clear that the relatively open structure of astrophyllite allows it to accept a large number of minor elements; the mineral acts as a 'soak' for the residual elements during magmatic crystallization and its composition varies with the composition of the residual solutions. Ganzeev *et al.* (1969) have already suggested that the enrichment of the alkali metals in various Russian astrophyllites closely reflects the concentration of these elements in the host-rock.

Metamorphic rocks. The two Spanish astrophyllites are found in association with quartz and are generally similar in composition to the astrophyllites from oversaturated rocks, except that the contents of Ca and Al and the K/Na ratios are more similar to those from undersaturated parageneses. Both show a large cation deficiency in the *A*-group, and also Zn is particularly low. The composition of astrophyllites will depend on the composition of the host-rock, but further analyses may show that it also varies with the type of metamorphism and the pressure–temperature conditions.

Niobophyllite, found in association with albite and arfvedsonite in paragneiss (Nickel *et al.*, 1964) is as yet unique in the astrophyllite group, and perhaps owes its unusual composition to the unique nature of the Seal Lake deposit.

High alkali astrophyllites. Woodrow (1967, p. 678) has pointed out that the composition and structure of an astrophyllite studied by Peng and Ma (1963) may indicate the occurrence of several other varieties of the mineral. The analysis of Peng and Ma's specimen and that of a closely similar astrophyllite studied by Dorfman (1962), are included in table III (nos. 23 and 24). They are characterized by being very Mg-rich (up to 2 atoms per unit-cell), and by having a large excess of cations in the *A*-group, very low K/Na ratios (< 1), and an overall excess of cations per unit-cell. To distinguish them from other members of the group, we have termed them 'high-alkali' astrophyllites. The extra Na atoms and the high Mg contents have resulted in structural modifications compared to the structure of the Colorado astrophyllite studied by Woodrow (1967) and Woodrow has suggested that other varieties, with different Ti/Si ratios in the tetrahedral layers, may also be possible.

Acknowledgements. Drs. C. H. Emeleus, P. Floor, D. Gould (Uganda Geological Survey), F. Habgood (Director, Malawi Geol. Survey), and B. G. J. Upton generously provided specimens.

REFERENCES

BLOOMFIELD (K.), 1965. *Bull. Geol. Surv. Malawi*, 16.
[BONSHTEDT (E.)], Бонштедт (Э.), 1931. Зап. Росс. мин. общ. (*Mém. Soc. Russe Min.*), ser. 2, 60, 280 [MA 5–232].
BORLEY (G. D.), 1963. *Min. Mag.* 33, 358.
BRØGGER (W. C.), 1890. *Zeits. Krist.* 16, 1.
BROOKS (C. K.), 1970. *Geochimica Acta*, 34, 411 [MA 21–2364].
BUTLER (J. R.), BOWDEN (P.), and SMITH (A. Z.), 1962. Ibid. 26, 89.

DIETRICH (R. V.), HEIER (K. S.), and TAYLOR (S. R.), 1965. *Skr. norske Vidensk. Akad. Mat. Naturv. Kl.*, 19.

[DORFMAN (M. D.)] Дорфман (М. Д), 1962. Минералогия пегматитов и зон выветривания в ийолит-уртитах Юкспор Хибинского массива [*Mineralogy of the pegmatites and areas of wind erosion in ijolite-urtite of the Yukspor peak in Khibiny mountain range*] Изд. АН СССР (Akad. nauk U.S.S.R. Press), Moscow [MA 16–557].

EAKINS (L. G.), 1891. *Amer. Journ. Sci.*, ser. 3, **42**, 35.

EMELEUS (C. H.) and HARRY (W. T.), 1970. *Medd. Grønland*, **186**, nr. 3.

ESKOLA (P.) and SAHLSTEIN (Th. G.), 1930. *Bull. Comm. Géol. Finlande*, **92**, 77.

FLOOR (P.), 1961. *Notas Com. Inst. Geol. Min. España*, **62**, 59.

—— 1966. *Leidse Geol. Medd.* **36**, 1.

[GANZEEV (A. A.), EFIMOV (A. F.), and SEMENOVA (N. G.)] GANZEYEV (A. A.), YEFIMOV (A. F.), and SEMENOVA (N. G.) [Ганзеев (А. А.), Ефимов (А. Ф.), и Семенова (Н. Г.)], 1969. [Геохимия, 335] transl. as *Geochem. Intern.* **6**, 295.

GOSSNER (B.) and REINDL (E.), 1934. *Centr. Min. Abt. A*, 161.

GROSS (E. B.) and HEINRICH (E. W.), 1966. *Amer. Min.* **51**, 299.

HANSEN (J.), 1968. *Rept. 23rd Intern. Geol. Congr., Czechoslovakia*, **7**, 263.

KOENIG (G. A.), 1877. *Zeits. Kryst. Min.*, **1**, 423.

KUNITZ (W.), 1936. *Neues Jahrb. Min. Abt. A, Beil.-Bd.* **70**, 429.

MANNING (P. G.), 1969. *Canad. Min.* **9**, 663 [M.A. 21–1553].

MAXWELL (J. A.), 1968. *Rock and mineral analysis.* New York and London (Wiley: Interscience). [M.A. 20–1897].

NICKEL (E. H.), ROWLAND (J. F.), and CHARETTE (D. J.), 1964. *Canad. Min.* **8**, 40.

PENG (CHIH-CHUNG) and MA (CHE-SHENG), 1963. [*Scientia Sinica*, **12**, 272]; Min. Abstr. **16**–611.

[PERCHUK (L. L.)] Перчук (Л. Л.), 1964. [*Physico-chemical petrology of the granite and alkaline intrusions of the Central Turkestan–Alay Range.*] (In Russian.) Moscow (Akad. nauk U.S.S.R. Press).

—— and ZYRYANOV (V. N.) [Зырянов (В. Н.)], 1965. Doklady Acad. Sci. U.S.S.R., Earth Sci. Sect. **162**, 200, transl. from Докл. Акад. наук СССР, **162**, 671 [M.A. **19**–139].

[SEMENOV (E. I.)] Семенов (Е. И.), 1956. Доклады Акад. наук СССР (*Compt. Rend. Acad. Sci. USSR*), **108**, 933 [M.A. **13**–384].

[——] —— 1960. Труды Инст. мин., геохим. крист. редк. элем. (*Trans. Inst. Min., Geochem. Cryst. Rare Elements*), **4**, 20.

[SVESHNIKOVA (E. V.)] Свешникова (Е. В.), 1960. Геология и Геофизика, **2**, 142.

[VALTER (A. A.), EREMENKO (G. K.), and LYSENKO (G. A.)] Вальтер (А. А.), Еременко (Г. К.) и Лысенко (Г. А.), 1965. Мин. Сборник Львов геол. общ. (*Min. Mag. Lvov Geol. Soc.*), **19**, 248.

WOODROW (P. J.), 1967. *Acta Cryst.* **22**, 673.

Appendix on analytical methods

M. J. SAUNDERS

(Brief notes are given on the analytical procedure for each element. Details of the procedures, instrumental conditions, standard materials, etc., may be obtained from M. J. Saunders.)

Sample attack. Samples were easily and completely attacked by evaporating with HF, HNO_3, and H_2SO_4 in the usual manner. Residues were easily soluble in dil. H_2SO_4 to give a clear solution initially, but after a few minutes, especially with more prolonged heating, Sn, Ta, and Nb precipitated.

If HF, HNO_3, and $HClO_4$ were used, although attack appeared to be complete, the residues produced were often insoluble in dil. HCl, a white precipitate presumably containing Ta, Nb, Ti, and Sn remaining. Some MnO_2 was produced with sample weights of 0·1 g and over for those samples with high Mn. It was dissolved by adding dil. H_2O_2.

Silicon. This was determined using the Jeffery and Wilson (1960) method. The method was slightly modified, only 0·3–0·4 g sample being used, to keep Ti below the level at which it interfered. A Palau crucible was used for the Na_2CO_3 fusion. The melt was dissolved in 9 ml HCl. Impure SiO_2 was ignited at 1200 °C before weighing. The residue after volatilization of SiO_2 was large, containing

most of the Sn, Ti, Nb, and Ta present; it was therefore ignited at the same temperature as the impure SiO_2 before weighing. It was fused with the minimum quantity of $KHSO_4$, the melt dissolved by warming with 1 ml HCl and water (Sn, Nb, and Ta remain insoluble here and were ignored), and added to the filtrate from the gravimetric SiO_2 determination which was then diluted to 200 ml. The residue containing Nb, Ta, Sn, Pb, and Ba was allowed to settle and SiO_2 in the filtrate determined colorimetrically as soon as possible after the gravimetric determination. Small amounts of Sn and Pb present in the samples should not affect the accuracy of this determination.

Aluminium, calcium, magnesium, and manganese. These were determined in the filtrate from the SiO_2 determination. The insoluble material containing Nb, Pb, Sn, Ta, and Ba was allowed to settle before taking aliquots.

Al_2O_3. $LaCl_3$ was added to a 25 ml aliquot which was then diluted to 50 ml. Standards contained $LaCl_3$, NaCl, and HCl in similar concentrations to those in sample solution. Determination was by A.A. using a N_2O–C_2H_2 flame.

MnO. An aliquot of between 25 and 50 ml of the silica filtrate was diluted to 100 ml and Mn determined by A.A. using an air–C_2H_2 flame. NaCl was not added to standards. As a check on the accuracy of these determinations in the samples containing most Mn, Mn was also determined colorimetrically as permanganate using periodate as an oxidizing agent (Sandell, 1959, p. 608), and by the titrimetric method of Lingane and Karplus (1946).

The results by the three methods for MnO in sample 4 were: A.A. 7·33 %. Colorimetric 7·41, 7·51 %. Titrimetric 7·44 %.

CaO, MgO. For Ca a 25 ml, and for Mg a 5 or 10 ml aliquot of the SiO_2 filtrate were used. Aliquots were diluted to 100 ml and Ca and Mg determined by A.A. using N_2O–C_2H_2 and air–C_2H_2 flames respectively. Sample and standard solutions contained like amounts of $LaCl_3$, NaCl, and HCl.

Iron. This was determined using $SnCl_2$ reduction (Mercy and Saunders, 1966). A 0·08 to 0·1 g sample was attacked with HNO_3, HF, and $HClO_4$ in a P.T.F.E. crucible. The crucible and residue were placed in a conical beaker, 5 ml of HCl and 20 ml water added, and the beaker and contents heated to give maximum solution. The insoluble residue was ignored and Fe^{3+} reduced with $SnCl_2$ in a CO_2 atmosphere in the usual manner. $K_2Cr_2O_7$ (0·03 N) was used to titrate Fe^{2+}; sodium diphenylamine sulphonate was used as indicator and a blank was determined.

$SnCl_2$ reduction is probably quite accurate applied to astrophyllite analysis as there is no V or Mo present. Results obtained suggested that there was no reduction of Nb and Ta present in the insoluble residue.

Titanium. This was determined colorimetrically as the peroxide. A 0·025 g sample was attacked with HF, HNO_3, and H_2SO_4. The residue was dissolved in dilute H_2SO_4 and the peroxide immediately developed. The final volume of dilution was 50 ml. Sulphuric acid (7 ml 1+1) was added to sample and standard solutions to buffer any effect due to sulphate in sample solutions. Phosphoric acid (10 ml 25 %) was added to all solutions to decolorize Fe. Tests showed that it was not fully effective and Fe equivalent to 30 % Fe_2O_3 in a sample gave an absorbance equivalent to about 0·05 % TiO_2.

In the presence of Fe, H_3PO_4, and H_2SO_4 similar in concentration to those in sample solutions, the Nb interference was proportional to the concentration of Nb, 0·25 mg Nb_2O_5 being equivalent to 0·021 mg TiO_2. To make a valid correction for this interference Ti–peroxide was developed before Nb hydrolysed. Nb is then kept in solution as the peroxide.

Niobium was determined colorimetrically as the peroxide (Palilla *et al.*, 1953), after separation from Ta and Ti, etc., using ion-exchange according to the Kallman *et al.* (1962) method. 0·1 g of sample was attacked with HF, HNO_3, and H_2SO_4, dissolved in HF–HCl mixture and transferred to a column of Amberlite CG 400 resin, 12 inches long, contained in a flexible PVC tube of 1 cm internal diameter and supported by a disc of Perspex. The maximum flow rate possible with this column was slower than that described by the above workers. The column was washed with HF–HCl to elute Ti, Zr, Fe, etc., from Nb and Ta. Niobium was eluted from Ta by washing with NH_4Cl–HF mixture, H_3BO_3 and 10 mg Zr (as $ZrOCl_2$) added to the eluate and Nb+Zr precipitated with cupferron. Paper pulp was added and the precipitate filtered on a Whatman No. 40 paper and ignited in a Vitreosil crucible. The use of paper pulp here left ignited oxides easily attacked subsequently by fusing with 1·5 g of $KHSO_4$; the melt was dissolved in concentrated H_2SO_4, transferred to a 50 ml flask and Nb determined as the peroxide in 96 % H_2SO_4. The absorbance of a reagent blank containing $KHSO_4$ was also

measured. Tin, the only element present in astrophyllite that accompanies Nb through the ion-exchange separation was assumed not to interfere in the peroxide determination.

Tantalum was eluted from the resin column using NH_4Cl–NH_4F mixture and determined colorimetrically using pyrogallol (B.I.S.R.A. 1967). 10 mg of Zr (as $ZrOCl_2$) were added to the eluate and Ta+Zr precipitated using cupferron. Paper pulp was added, the precipitate filtered, ignited in a Vitreosil crucible, and attacked, fusing with 1·5 g of $KHSO_4$. The melt was dissolved in 4 % ammonium oxalate and the colorimetric procedure applied. The sensitivity of this procedure is adequate for the determination of Ta in astrophyllite; 0·25 mg Ta_2O_5/50 ml gave an absorbance of 0·4 in 4 cm cells at 400 nm. A reagent blank containing $KHSO_4$ and Zr was measured, and found to be about 0·17, decreasing the accuracy of the Ta results obtained. Only Bi accompanies Ta through the ion exchange separation and it was absent in astrophyllite.

Iron, ferrous. Fe^{2+} was determined using a slightly modified version of Wilson's (1955) method. About 0·1 g NH_4VO_3, accurately weighed, and 10 ml HF were added to 0·1 g sample in a Pt crucible, and the mixture left for 2 days. The crucible and contents were placed in H_2SO_4–H_3BO_3 solution, avoiding a washing operation, and unreduced NH_4VO_3 titrated with ferrous ammonium sulphate in the presence of H_3PO_4, using sodium diphenylamine sulphonate as the indicator.

Zirconium was determined gravimetrically as the phosphate using the method described by Kolthoff and Sandell (1952, p. 725), with a little modification.

About 0·1 to 0·2 g of sample (depending on availability) were fused with K_2CO_3 in a Palau crucible and the melt extracted with water; Zr remains in the residue, and most of the Nb, Ta, Pb, and Sn present should pass into solution (cf. Schoeller and Powell, 1955, p. 200). The residue was dissolved in H_2SO_4. If necessary Ba and Sr sulphates were filtered off, and Zr phosphate precipitated in the usual way in the presence of a very large excess of H_2O_2 to keep Ti and possible traces of Nb and Ta in solution. Precipitation was allowed to take place overnight. Paper pulp was added before filtration and the precipitate ignited in a Pt crucible taking the usual precautions in the presence of phosphate.

Qualitative X.R.F. analyses of the Zr phosphate precipitates indicated that only traces of Nb, Ta, and Ti were present, the major contaminant being iron, which must have been present only in small amounts as the precipitates were pure white.

Copper, zinc, potassium, lithium, sodium (manganese). A 0·1 g sample (0·05 g if material is scarce) was attacked with HF, HNO_3, and H_2SO_4, dissolved in dilute H_2SO_4 and diluted to 50 ml (25 ml if using the smaller sample wt.). Cu, Zn, and Li were normally determined in this solution, though the concentration of Zn was in some cases too high. A 10 ml aliquot was diluted to 100 ml for Na and K determinations, and for Zn where appropriate.

Na_2O and K_2O were determined directly using the EEL flame photometer. The concentrations of Na and K in the sample solutions were such that their mutual enhancement could be ignored.

For Na_2O determination, Ca interferes only if there is more than 2 % CaO in the sample. Cs, Fe, and Mn can interfere but probably not in the concentrations found in astrophyllite; any enhancement due to Rb was ignored.

There are few interferences in the potassium determination. A correction was made for rubidium emission passing through the K filter (a wide spectral band-width gelatine filter was used). Interference in the determination of from 10 to 15 ppm K_2O was proportional to the Rb concentration, 1 ppm Rb_2O was equivalent to 0·6 ppm K_2O. Any enhancement due to Rb and Cs was ignored.

ZnO was determined using A.A. and a C_2H_2–air flame. It was assumed that there were no interferences (Abbey, 1967, p. 14), but it is not known whether Nb or Zr interfere.

CuO was determined by A.A. using a C_2H_2–air flame. There should be few interferences (Slavin, 1968, p. 103).

Li_2O was determined using A.A. and a C_2H_2–air flame. It was assumed that there were no interferences (Slavin, 1968, p. 123). Standard solutions contained Na and K equivalent to 2·5 % Na_2O and 5·5 % K_2O in a sample.

MnO can be easily determined using A.A. in the solution used for Na and K analyses.

Rubidium and caesium were determined using the Unicam SP 900 flame photometer (C_2H_2–air flame). We would have preferred to use propane as fuel, but did not possess a suitable burner. 0·1 g of sample was attacked with HF, HNO_3, and H_2SO_4, dissolved in HCl, diluted to 40 ml and a double precipitation of the R_2O_3 group made with NH_4OH in the presence of NH_4Cl (Peck, 1964), with the reagent

quantities scaled down. The filtrate was evaporated to small bulk and ammonium salts destroyed with HNO_3 (Smith, 1853), as the NH_4^+ ion interferes (Dean, 1961, p. 178). The residue was fumed with H_2SO_4 to remove nitrates, dissolved in dilute H_2SO_4, and diluted to 25 ml.

For Rb, standard solution contained Na and K equivalent to 2·5 % Na_2O and 5·5 % K_2O in a sample.

Cs standards also contained Na and K in appropriate amounts. The background radiation when measuring Cs in samples was rather high, probably due to Ca and Mg, which are not separated using NH_4OH precipitation.

Cs_2O contents below 0·01 % could not be detected. Duplicate determinations agreed for sample 4.

Little Rb and Cs should be lost in the double NH_4OH precipitation in the presence of excess NH_4Cl (cf. Kolthoff and Sandell, 1952, p. 312).

Water was determined using the rapid method of Shapiro and Brannock (1955, 1962), but with the more efficient flux recommended by Peck (1964, p. 18). Sample weights of 0·1–0·2 g were used. Duplicate determinations using a small and large weight of sample agreed; results were precise to within 0·1 % H_2O absolute. Fluorine should not interfere, as it will be held by the flux.

Fluorine was determined by the method of Huang and Johns (1967) with modification to the procedure for measuring the absorbance of coloured solutions. 0·025 g of sample were attacked as described by the above workers and the sample solution diluted to 50 ml. A 5 ml aliquot was taken for the colour determination.

The following results were obtained over a period for % F in astrophyllite 2 using a variety of methods:

Titrimetric (Kolthoff and Sandell, 1952, p. 721)	1·20
Colorimetric (Huang and Johns), modified	1·28
Colorimetric (Peck and Smith, 1964)	1·24

Results reported here for % F in astrophyllite are therefore probably accurate to within ±0·10 % absolute. The method used was selected because of its sensitivity, so that only a small sample weight was required, and because Cl may be easily determined at the same time.

Chlorine was sought using the method of Huang and Johns (1967) but was not detected in any of the samples.

Lead, barium, and strontium were determined in the same solution to conserve sample. A 0·05 g sample was attacked with HNO_3, HF, and $HClO_4$ and the residue dissolved in HCl. $LaCl_3$ and 0·01 g NaCl (KCl may precipitate K perchlorate) were added and the solution diluted to 10 ml. Any insolubie material was allowed to settle before A.A. determinations.

PbO was determined using A.A. and a C_2H_2–air flame. Standards contained appropriate amounts of NaCl and $LaCl_3$. If there is sufficient sample the determination is best made in the absence of NaCl and $LaCl_3$ as they tend to cause unsteady readings. The absorbance of 10 ppm Pb, similar to the highest sample concentration of Pb measured, added to a solution of sample 6 which contains negligible Pb, was compared with that of a pure 10 ppm Pb solution. A relative enhancement of about 7·5 % was indicated under the conditions of the determination. Results for Pb were corrected by this factor.

BaO was determined by A.A. using a N_2O–C_2H_2 flame. NaCl and $LaCl_3$ were added to standard solutions. Calcium may interfere (Kerber and Barnett, 1969), but it was assumed that interference was negligible as Ca is low in astrophyllite.

SrO was determined using A.A. and a N_2O–C_2H_2 flame. NaCl and $LaCl_3$ were added to standard solutions.

Tin was determined colorimetrically using 2 : 3 : 7 trihydroxy-9-phenyl-6-fluorone following the method of Luke, described by Sandell (1959, p. 862). From 0·01 to 0·02 g of sample containing less than 40 μg Sn were attacked with proportionately small volumes of HNO_3, HF, and H_2SO_4, dissolved in H_2SO_4 and the whole of the solution taken for the colour determination. The calibration graph, 0 to 80 μg Sn taken through the procedure, was linear to 40 μg Sn, then flattened quickly. The absorbance of a reagent blank taken through the whole procedure was measured. Best quality reagents (such as 'Aristar' grade) are necessary to keep the blank absorbance low.

Phosphorus was determined using the method of Murphy and Riley (1958) in samples where there was plenty of material. A turbidity developed in coloured solution on standing overnight. The precipitate, presumably of Sn, Ta, Nb, was allowed to settle before absorbance measurements.

Rare earths. These were sought in sample 5 by standard methods (Schoeller and Powell, 1955; Groves, 1951) using the silica filtrate after determining Al, Ca, Mg, and Mn and the eluate from the determination of Nb. Rare earth contents were too low for their determination gravimetrically. An X.R.F. qualitative comparison of Ln contents indicated that similarly low amounts were present in all samples.

REFERENCES

Abbey (S.), 1967. *Geol. Surv. Canada, Paper* 67-37, 35 pp. [M.A. 21-1064].

B.I.S.R.A., 1967. Open report MG/D/556/67.

Dean (J. A.), 1960. *Flame Photometry.* New York (McGraw-Hill).

Groves (A. W.), 1951. *Silicate Analysis*, 2nd edn, London (Allen and Unwin).

Huang (W. H.) and Johns (W. D.), 1967. *Anal. Chim. Acta*, **37**, 508.

Jeffrey (P. G.) and Wilson (A.D.), 1960. *Analyst*, **85**, 478–86.

Kallman (S.), Oberthin (H.), and Liu (R.), 1962. *Anal. Chim. Acta*, **34**, 609.

Kerber (J. D.) and Barnett (W. B.), 1969. *Perkin Elmer Atomic Absorption Newsletter*, **8**, 113.

Kolthoff (I. M.) and Sandell (E. B.), 1952. *A textbook of quantitative inorganic analysis*, 3rd edn, New York (Macmillan).

Lingane (J. J.) and Karplus (R.), 1946. *Ind. Eng. Chem. Anal. Ed.* **18**, 191.

Mercy (E. L. P.) and Saunders (M. J.), 1966. *Earth Planet. Sci. Letters*, **1**, 169.

Murphy (J.) and Riley (J. P.), 1958. *Journ. Marine Biol. Ass. U.K.* **37**, 9.

Palilla (F. C.), Adler (N.), and Hiskey (C. F.), 1953. *Anal. Chem.* **25**, 926.

Peck (L. C.), 1964. *Bull. U.S. Geol. Surv. 1170.*

—— and Smith (V. C.), 1964. *Talanta*, **11**, 1343.

Sandell (E. B.), 1959. *Colorimetric determination of traces of metals*, 3rd edn, New York and London (Wiley: Interscience).

Schoeller (W. R.) and Powell (A. R.), 1955. *The analysis of minerals and ores of the rarer elements*, 3rd edn, London (Griffin).

Shapiro (L.) and Brannock (W. W.), 1955. *Anal. Chem.* **27**, 560.

—— —— 1962. *Bull. U.S. Geol. Surv.* **1114-A**, 46.

Slavin (W.), 1968. *Atomic absorption spectrometry.* New York (Interscience).

Smith (J. L.), 1853. *Amer. Journ. Sci.*, ser. 2, **15**, 234.

Wilson (A. D.), 1955. *Bull. Geol. Surv. Gt. Britain*, **9**, 56.

[*Manuscript received 24 March 1971; revised 29 June 1972*]

PERALKALINE VOLCANISM OF THE KENYA RIFT VALLEY

[AMERICAN JOURNAL OF SCIENCE, VOL. 267, FEBRUARY 1969, P. 242-248]

ALKALI-FELDSPAR FRACTIONATION TRENDS AND THE DERIVATION OF PERALKALINE LIQUIDS

D. K. BAILEY and R. MACDONALD

University of Reading, Reading, England

ABSTRACT. Two new ways have been devised for comparing the compositions and possible differentiation trends of alkaline felsic rocks. Plotting a series of compositions in a triangular diagram in terms of molecular alumina, silica and total alkalis will reveal any consistent trend in silica and total alkali variation such as might be expected by feldspar fractionation. A quadrilateral diagram in which molecular alumina is plotted against soda/potash ratio can then be employed to show the variation in alkali ratio in whole rocks (and their feldspars) with changes in silica content and peralkalinity. Many of the pantellerites examined in this way appear to be on a quartz-feldspar crystallization path. Moreover, there is no strong indication that they have been simply derived from a trachytic parent by feldspar fractionation.

FELDSPAR FRACTIONATION IN THE SYSTEM Na_2O–K_2O–Al_2O_3–SiO_2

Of all the problems connected with the peralkaline rhyolites, perhaps the most tantalizing is their relationship to the more abundant subaluminous magmas. Some form of crystallization differentiation, producing an alumina-deficient residual magma, is a favorite mechanism because it is relatively simple and, perhaps, because we have been conditioned into giving this mechanism pride of place in igneous petrogenesis. In the case of peralkaline rhyolite a natural choice of parental magma seems to be a slightly peralkaline quartz-trachyte, which by fractionating alkali feldspar, yields a strongly peralkaline rhyolite. A simple test of this hypothesis is to project the rhyolite and trachyte compositions into the oversaturated part of "Petrogeny's Residua System", $NaAlSi_3O_8$–$KAlSi_3O_8$–SiO_2 (Bowen, 1937) to see if the compositions define a "trend". But this projection cannot show the degree of peralkalinity of the compositions used, and we have been examining other projections in which this factor can be shown.

In order to simplify the problem we have considered first the results of feldspar fractionation in the system Na_2O–K_2O–Al_2O_3–SiO_2, shown in tetrahedral form in figure 1. One fact of immediate significance emerges when feldspar fractionation is considered in three dimensions. Any given liquid composition in the system must, together with the two feldspar end-members, Ab and Or, define a plane within the system. Because this plane includes the feldspar join, the separation of feldspar from the initial liquid cannot remove the residual liquid from the plane. This must apply even if the feldspar is changing composition continuously during crystallization. The resulting liquid can leave the plane only when another process, for example, crystallization of a second phase, intervenes.

This condition is shown in figure 2 for the oversaturated peralkaline volume, where a liquid of composition P lies in the plane Or–Ab–P′–P″. The position of this plane can be described by the molecular ratio of

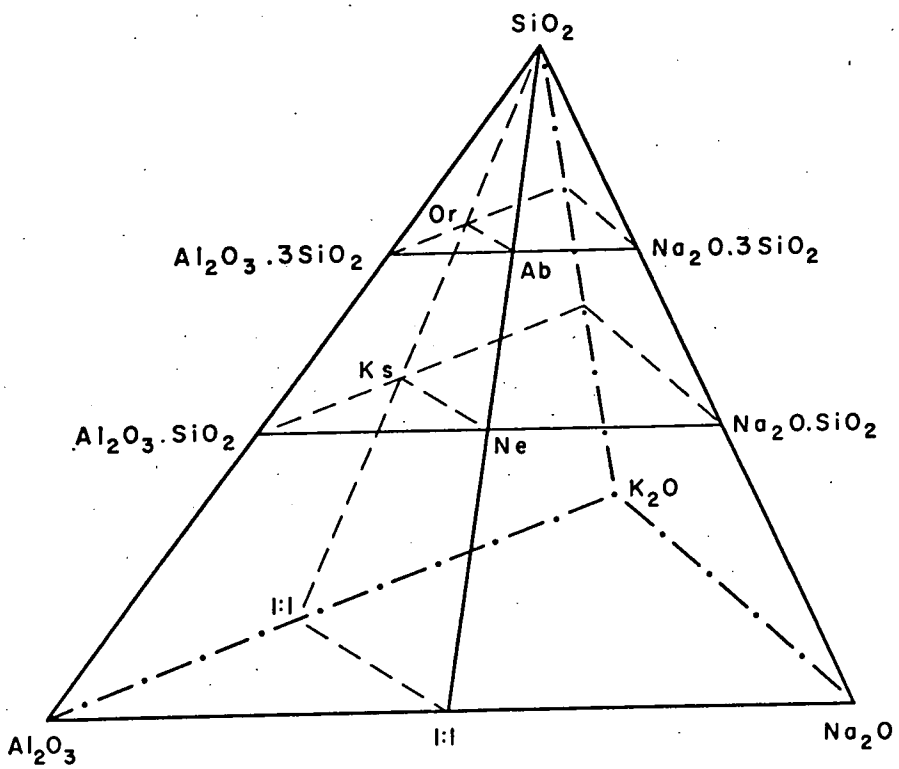

Fig. 1. Tetrahedral diagram of the system Na_2O–K_2O–Al_2O_3–SiO_2 showing the alkali feldspar join and the form and positions of the surrounding composition volumes.

excess alkalis: excess silica after deduction of molecular feldspar from the composition P, that is, the function:

$$\frac{\text{Mole } (Na_2O + K_2O - Al_2O_3)}{\text{Mole } (SiO_2 - 6Al_2O_3)}$$

or, more simply, by the intercept of the plane with the silica-alkali sidelines (P′ or P″). This value, which we call the "alkali-silica" index, must remain constant through a series of compositions linked solely by crystallization of alkali feldspar. Similar functions can be applied to felsic compositions in volumes other than the oversaturated peralkaline volume.

Because any parental liquid crystallizing only alkali feldspar is constrained to a plane radiating from the feldspar join, it is possible to project peralkaline compositions into a triangular plane in which the three variables are molecular SiO_2, Al_2O_3, and total alkalis, as shown in figure 3.

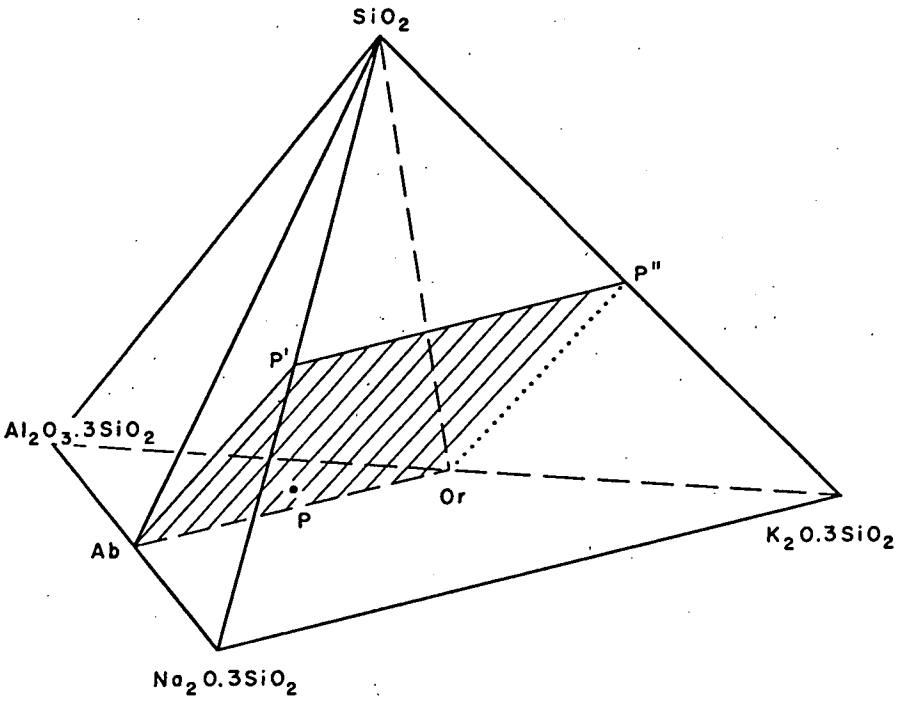

Fig. 2. The oversaturated volume of the system Na_2O–K_2O–Al_2O_3–SiO_2 showing the peralkaline composition P lying in the plane Or–Ab–P′–P″.

In this the feldspar join projects as a point and any plane radiating from the join projects as a line. The plane Or–Ab–P′–P″ in figure 2 thus appears in figure 3 as a line "Feldspar–P′P″", and fractionation of feldspar from a liquid in this line will drive the residual liquid along it, as shown by the arrow. It is clear from figure 3 that every peralkaline liquid has its own fixed "feldspar-fractionation" plane, and there can be no single low-temperature channel to which all peralkaline liquids converge by precipitating feldspar. On the contrary, liquids with different "alkali-silica" indices will diverge with separation of feldspar.

FELDSPAR FRACTIONATION IN MAGMAS

If peralkaline rhyolites are derived by alkali-feldspar fractionation from a less siliceous parent, the "alkali-silica" index for a given magma series should be constant, that is, the rocks should show a distinct trend from the feldspar-point when plotted in figure 3.

To test this, and other characteristics, we have compiled all the available data on peralkaline rocks. The results of the larger study will be presented in later papers, but the techniques, and the tests on some selected series, are given here because we feel they will be immediately useful to petrologists working in this field.

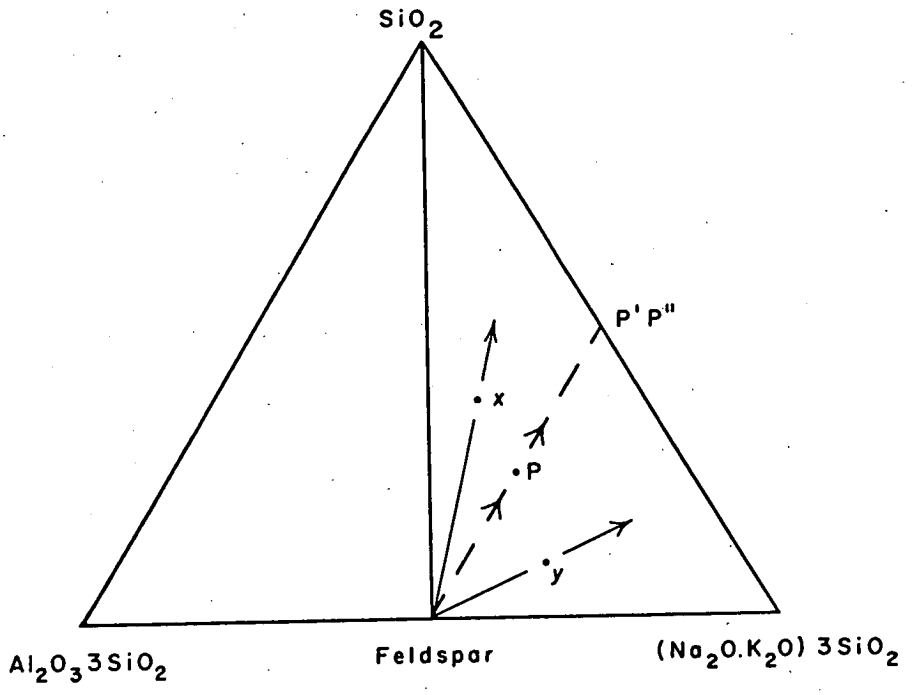

Fig. 3. SiO_2–Al_2O_3–total alkali diagram in which the feldspar join projects as a point and the plane Or–Ab–P′–P″ as the line "Feldspar-P′P″". Separation of feldspar from a liquid of composition P must drive it toward P′P″. Separation of feldspar from compositions x and y must develop divergent trends as indicated by the arrows.

In figure 4 the compositions of two series of pantellerite glasses and two series of comendites are plotted in terms of molecular SiO_2, Al_2O_3, and total alkalis. The comendite series have low "alkali-silica" indices and appear to trend from the alkali-feldspar composition. The pantellerites form a separate group in which the points are more dispersed and could not be said to be on a clearly defined path from the alkali feldspar composition. These are all felsic rocks, the components used in figure 4 constituting over 80 percent of the total rock composition in each case, and there can be little question that the differences observed are real. On this evidence pantellerites show no clear sign of derivation from a trachytic source (compare Noble, 1965). The scattering of the points is inexplicable in terms of alkali feldspar fractionation alone. Another process, or processes, must be involved. From the position of the pantellerite points in figure 4, co-precipitation of quartz is one possibility, and we have therefore plotted the quartz-potash feldspar and quartz-albite cotectics from K_2O–Al_2O_3–SiO_2 and Na_2O–Al_2O_3–SiO_2 (Schairer and Bowen, 1955 and 1956) in figure 4. It is immediately apparent that part of the spread of pantellerite points (and comendites) is along the zone defined by these two cotectics, and it is no coincidence that where data

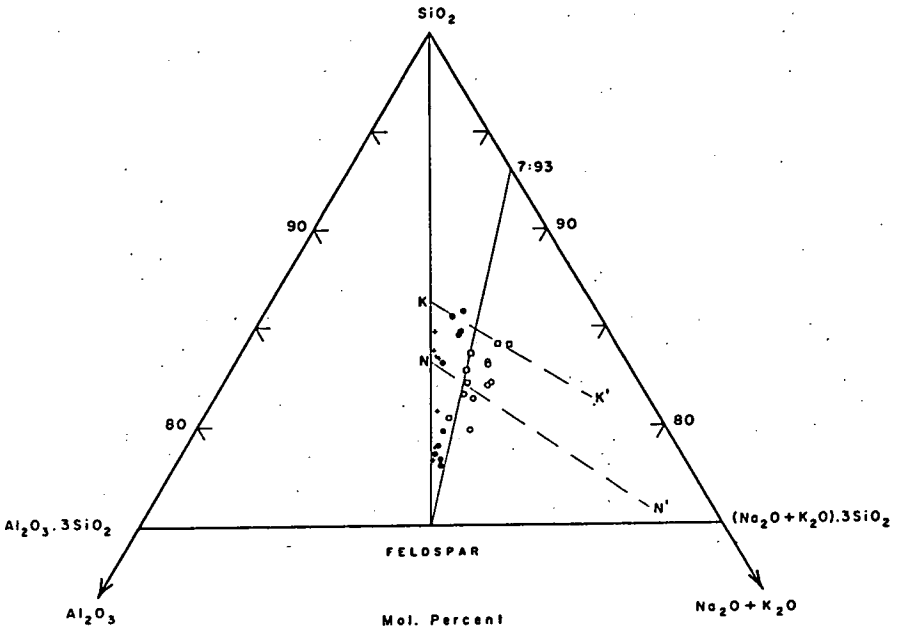

Fig. 4. SiO_2–Al_2O_3–total alkali diagram showing two series of comendites (Tugtutoq, solid circles; Korea, crosses), and two series of pantellerites (Pantelleria, open circles; Fantale, Ethiopia, squares). Line K-K′ is the quartz-potash feldspar cotectic: line N-N′ is the quartz-albite cotectic. The line of "alkali-silica" index 7:93 is that chosen for comparison of the pantellerites in figure 5.

are available the pantellerites in this zone are quartz–feldspar–phyric. Once the condition of co-precipitation of quartz and feldspar is achieved the liquid-trend must be along the zone, that is, approximately at right angles to any earlier feldspar-fractionation path. For this reason some comendites and pantellerites in this zone may appear transitional. When all rock series are taken into account there may be additional complications due to series with "alkali-silica" indices intermediate between comendites and pantellerites. In the majority of cases, however, comendites and pantellerites can be distinguished on the basis of their total chemistry. This will be elaborated in a subsequent paper.

ALKALI RATIOS IN LIQUIDS AND CRYSTALS

The chief deficiency of figures 3 and 4 is that the alkali ratio, Na_2O/K_2O, is lost in this projection. But once a series of compositions has been found to lie within, or close to a specific "alkali-silica" plane in this projection, a simple device can be used to show liquid trends in terms of Al_2O_3 and alkali-ratio. The method is illustrated in figure 5. The quadrilateral in figure 5 represents a plane such as Or–Ab–P″–P′ (figure 2) in which the Al_2O_3 (as percentage molecular $SiO_2 + Al_2O_3 + Na_2O + K_2O$) varies from 12.5 to 0 mole percent between the lower and upper edges, and the ratio of soda to total alkalis ($Na_2O/Na_2O +$

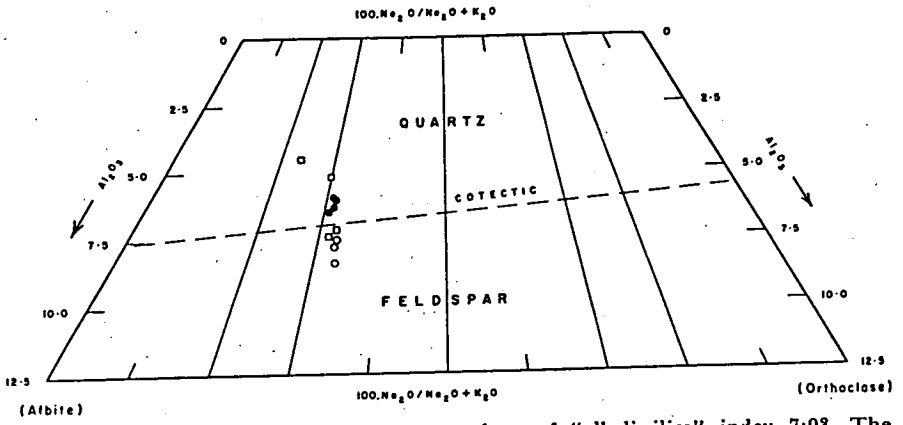

Fig. 5. Quadrilateral representing the plane of "alkali-silica" index 7:93. The quartz-feldspar cotectic is interpolated between the intercepts of the Na_2O side-line with the quartz-albite cotectic and the K_2O side-line with the quartz-potash feldspar cotectic. Pantellerites from Pantelleria on which there are modal data are shown by circles (filled where quartz-phyric) and those from Fantale by squares. One specimen from Fantale containing 6.5 percent Al_2O_3 coincides with a Pantellerian specimen.

$K_2O \times 100$ percent) increases progressively from right to left. To depict the variation of alkali ratio only, with respect to Al_2O_3, it is not necessary to specify the "alkali-silica" index of the quadrilateral, but for any comparison of rocks to be meaningful they should lie within, or close to, the same "alkali-silica" plane. Furthermore, if we wish to include experimental data in the same diagram this, too, can only be made strictly comparable if the "alkali-silica" index is the same. A plane having an "alkali-silica" index of 7:93 was chosen for figure 5 to handle the pantellerite data, because the pantellerite compositions shown in figure 4 are close to but on the silica-depleted side of this plane.

From the experimental data on K_2O–Al_2O_3–SiO_2 and Na_2O–Al_2O_3–SiO_2 (Schairer and Bowen, 1955 and 1956) it is possible to plot the positions of the quartz-potash feldspar and quartz-albite cotectics where they intersect the sidelines of figure 5. Between these the trace of the alkali feldspar-quartz cotectic surface has been interpolated as shown by the dashed line. Figure 5, in its simplest form, is a section of the four-component system, Na_2O–K_2O–Al_2O_3–SiO_2, seen in figures 1 and 2, which must intersect the feldspar-quartz cotectic surface. It would not be appropriate to plot comendites in figure 5 because they have different "alkali-silica" indices, and the appropriate section of the cotectic surface would lie nearer to the feldspar join. Most of the pantellerite compositions fall "within" the primary phase-field of quartz, as defined by the interpolated cotectic. It must be remembered, of course, that only part of their total composition has been used to plot their position, and there may be some distortion because they lie off the plane of the diagram. But their position cannot be simply dismissed as a distortion produced by the projection, because where the modes of these rocks are known they are quartz–feldspar–phyric. By analogy with the simple

system Na_2O–K_2O–Al_2O_3–SiO_2, these compositions may be thought of as lying outside the plane of the diagram on the quartz-feldspar cotectic surface. The "trend" shown by these compositions veers toward the Na_2O sideline and is presumably a projection of their trend across the quartz-feldspar surface. It is distinctly different, in its nature and in its direction, from any simple feldspar-fractionation trend.

Three general attributes of figure 5 make it especially useful in the examination of peralkaline rocks. First, it is possible to represent compositions of salic rocks with minimum ambiguity; second, feldspar composition, and tie-lines to rocks or liquids, can be shown; and third, any trends in a magma series will be unequivocally shown in terms of increasing silica, decreasing alumina, and correct alkali ratio. In the majority of cases, total alkalis will decrease across the plane from the feldspar join. Total alkalis will increase across the plane only if its "alkali-silica" index exceeds the ratio of the alkali:silica in the feldspar, namely, 12.5:87.5.

We are currently exploring the applications of these new projections to the published data on peralkaline rocks, coupled with appropriate experimental studies. The results of the data study will be available shortly. In the meantime we would welcome any new information on the rocks, both analytical and modal, from fellow-workers in this field.

ACKNOWLEDGMENT

We would like to thank Dr. P. M. Orville for his constructive criticisms of the manuscript.

REFERENCES

Bowen, N. L., 1937, Recent high-temperature research on silicates and its significance in igneous geology: Am. Jour. Sci., 5th ser., v. 33, p. 1-21.

Noble, D. C., 1965, Gold Flat member of the Thirsty Canyon tuff—a pantellerite ash-flow sheet in southern Nevada: U.S. Geol. Survey Prof. Paper 525-B, p. B85-B90.

Schairer, J. F., and Bowen, N. L., 1955, The system K_2O–Al_2O_3–SiO_2: Am. Jour. Sci., v. 253, p. 681-746.

———— 1956, The system Na_2O–Al_2O_3–SiO_2: Am. Jour. Sci., v. 254, p. 129-195.

Contr. Mineral. and Petrol. 28, 340—351 (1970)
© by Springer-Verlag 1970

Petrochemical Variations among Mildly Peralkaline (Comendite) Obsidians from the Oceans and Continents

D. K. Bailey and R. Macdonald *
Department of Geology, University of Reading, England

* Present address: Department of Environmental Sciences, University of Lancaster.

Abstract. Eleven new analyses and modes of comendite obsidians are presented, and compared with all available data on similar rocks. Most specimens are aphyric or contain only sparse phenocrysts, most commonly alkali feldspar. The oxides SiO_2, Al_2O_3, Na_2O and K_2O total over ninety percent by weight in all analyses. Iron, as FeO, is the only other constituent rising above one percent by weight. When the analyses are projected into the system Na_2O-K_2O-Al_2O_3-SiO_2, oceanic and continental samples group differently. Oceanic specimens have a compositional spread ranging from trachytic to the quartz-feldspar cotectic zone, consistent with derivation through a trachyte magma stem. Continental comendites show a strong correlation with the experimentally determined quartz-feldspar minima along a path of increasing peralkalinity. These differences presumably reflect the contrasting environments of magma generation, and suggest an origin by partial melting within the continental crust for the continental comendite obsidians.

Introduction

Peralkaline rhyolites are a varied group of rocks, in which the agpaitic index (molecular $Na_2O + K_2O/Al_2O_3$) ranges from 1.00 to 2.50. In the mildly peralkaline range, the rocks called comendites have compositions transitional towards normal rhyolites in which molecular alumina exceeds total molecular alkalis. Comenditic rhyolites are frequently referred to simply as alkali rhyolites, and are sometimes treated as if they were merely a slightly aberrant form of the more common aluminous rhyolites. But the peralkaline condition can not be disregarded, because it is abnormal for the rocks of the Earth's crust and there is no known way in which simple melting of common sialic materials could yield peralkaline liquids (Bailey and Schairer, 1964, 1966). To account for peralkaline magmas Bowen (1945) suggested a crystal fractionation mechanism by which peralkalinity might develop in residual liquids — namely the "plagioclase effect", whereby alumina is fractionated with calcium in early-formed plagioclase. This appears to be a feasible mechanism in alkali basalts, and it is generally supposed that subalkaline basalts can yield peralkaline rhyolite residua (Coombs, 1963) although an example of the process has yet to be described. In the light of present knowledge therefore it is clearly desirable to maintain a clear distinction between comendite and rhyolite. The main objective of the present paper is to present eleven new analyses of comendite obsidians and to scrutinise the available data on comendites in an effort to discern any other significant characteristics.

As comendites become increasingly peralkaline they approach the pantellerite composition. We have found that the division proposed by Lacroix (1927) at 12.5 % total normative femics (comendite less, pantellerite greater) is a sound, working classification, which usefully separates two chemically distinct groups. Other

chemical characteristics of this boundary have been elaborated elsewhere (Macdonald and Bailey, *in press*), the chief of these are that in comendites, total iron (as FeO) is normally less than four percent (weight), alumina is greater than eleven percent (weight), and the soda: potash ratio is generally lower.

Two aspects of our approach to peralkaline rhyolite problems deserve comment.

1. As total alkalis, alkali ratio, and the alkali: alumina ratio are critical we have restricted our study to obsidians, because there is good reason to suppose that devitrified and crystalline rocks have lost alkalis (Noble, 1968).

2. Because the total chemical variation is largely determined by variations in SiO_2, Al_2O_3, Na_2O and K_2O, we put special emphasis on projections in the system Na_2O-K_2O-Al_2O_3-SiO_2 as a means of examining peralkaline compositions (Bailey and Macdonald, 1969).

Petrography

Most comenditic obsidians are either aphyric or contain only sparse phenocrysts — the modal data available to us are given in the Tables. Only one specimen has phenocrysts in any abundance, Kenya S85, and these appear to be an accumulation of quartz and feldspar. It is the only unquestionable comendite obsidian containing quartz phenocrysts that has come to our notice.

The only phenocryst analyses that are available, a few feldspar compositions, are also reported in Table 1.

Major Oxide Chemistry

Eleven new analyses of comendite obsidians are given in Table 1. The oxides of Si, Al, Na and K make up more than 90 percent by weight, and bulk even more largely in molecular percentage. Of the other constituents only FeO and Fe_2O_3 reach levels greater than 1 percent by weight. In the case of comendites, therefore, it is most appropriate to examine their chemical variation in terms of the system Na_2O-K_2O-Al_2O_3-SiO_2. Recalculations of these four oxides to 100 molecular percent, and the alkali ratios, are given in Table 1 for the new analyses. In Table 2 the same recalculations are given for all other acceptable comendite analyses known to us. The final figures in Table 2 refer to the type comendite from Sardinia. This is included for comparison, but it differs from other comenditic *glasses* in its grey colour, lower Na_2O, and higher H_2O and oxidation state. Noble and Haffty (1969) suggest that it has suffered alkali loss and its position in the figures supports this opinion. The molecular values in Tables 1 and 2 are plotted in Fig. 1 and 2, which are projections in the system Na_2O-K_2O-Al_2O_3-SiO_2 (Bailey and Macdonald, 1969).

Fig. 1 examines the variation in SiO_2, Al_2O_3 and combined alkalis. Oceanic and continental samples are shown as triangles and circles, respectively, and the difference in their chemical variations is readily apparent. Continental comendites are closely grouped within and along a quartz-feldspar cotectic zone defined by the field boundaries of Or-silica and Ab-silica, taken from the systems K_2O-Al_2O_3-SiO_2 and Na_2O-Al_2O_3-SiO_2 at 1 atms. (Schairer and Bowen, 1955, 1956). This distribution is parallelled by the alignment of quartz-feldspar minima (A, B and C) determined in three sections of the system Ab-Or-Q-Ac-Ns-H_2O

Table 1

Analysis No.	1	2	3	4	5	6	7	8	9	10	11
SiO_2	71.4	70.2	69.5	72.3	72.6	72.7	74.3	75.8	73.6	74.2	72.8
ZrO_2	0.18	0.21	0.20	0.11	0.14	0.14	—		—	—	0.18
TiO_2	0.23	0.31	0.32	0.21	0.20	0.20	0.15	0.09	0.20	0.20	0.24
Al_2O_3	12.40	12.55	13.25	13.18	12.78	12.87	12.01	12.14	12.04	10.84	12.32
Fe_2O_3	1.22	1.14	1.05	0.82	0.88	0.86	0.88	0.80	1.26	1.23	1.30
FeO	2.14	3.10	3.21	2.25	2.02	2.06	1.46	0.94	1.87	1.86	2.14
MnO	0.13	0.11	0.12	0.08	0.08	0.07	0.08	0.06	0.07	0.06	0.13
MgO	0.03	0.02	0.02	0.01	0.01	0.01	0.00	0.01	0.05	0.02	0.02
CaO	0.47	0.77	0.88	0.84	0.69	0.62	0.32	0.30	0.38	0.30	0.50
Na_2O	5.90	5.72	5.87	5.83	5.77	5.76	5.36	5.22	5.74	5.17	5.66
K_2O	4.70	4.82	4.93	3.78	3.84	3.89	4.58	4.48	4.51	4.53	4.56
P_2O_5	0.03	0.03	0.03	0.01	0.02	0.01	0.00	0.00	0.01	0.01	0.04
H_2O^+	0.20	0.25	0.13	0.22	0.31	0.27	0.23	0.12	0.00	0.30	0.05
H_2O^-	—	—	—	—	—	—	0.22	0.14	0.18	0.09	—
F	0.23	0.18	0.16	0.18	0.19	0.18	0.34	0.29	0.26	0.30	0.22
Cl	0.26	0.31	0.25	0.20	0.21	0.20	0.17	0.25	0.19	0.18	0.26
CO_2	—	—	—	—	—	—	—	—	—	—	—
Sum	99.52	99.72	99.92	100.02	99.74	99.84	100.10	100.64	100.36	99.29	100.42
$O \equiv F, Cl$	0.16	0.15	0.12	0.12	0.13	0.12	0.18	0.18	0.15	0.17	0.15
Total	99.36	99.57	99.80	99.90	99.61	99.72	100.02	100.46	100.21	99.12	100.27
Agpaitic Index	1.19	1.16	1.13	1.04	1.07	1.06	1.15	1.10	1.20	1.24	1.15
Fe as FeO	3.24	4.13	4.16	2.99	2.81	2.83	2.25	1.66	3.00	2.97	3.31
$FeO/FeO + Fe_2O_3$	0.64	0.73	0.75	0.73	0.70	0.71	0.62	0.54	0.60	0.60	0.62
Na_2O/K_2O	1.26	1.19	1.19	1.54	1.50	1.48	1.17	1.16	1.27	1.14	1.24

Molecular											
SiO_2	81.6	81.4	80.7	82.1	82.4	82.3	83.0	83.4	82.6	83.9	82.3
Al_2O_3	8.4	8.6	9.1	8.8	8.5	8.6	7.9	7.9	7.9	7.2	8.2
$Na_2O + K_2O$	10.0	10.0	10.2	9.1	9.1	9.1	9.1	8.7	9.5	8.9	9.5
$\frac{100\ Na_2O}{Na_2O + K_2O}$	65.5	64.3	64.6	70.1	69.4	69.4	63.7	63.7	66.0	63.4	65.5
Q	22.7	20.5	17.1	23.0	24.1	24.1	28.9	31.0	27.0	31.9	24.9
or	27.8	28.4	28.9	22.2	22.8	22.8	27.2	26.7	26.7	26.7	26.7
ab	37.7	37.7	40.9	46.6	44.0	44.5	36.2	37.2	36.7	30.4	38.3
ac	3.7	3.2	3.2	0.9	2.5	2.3	2.8	2.3	3.7	3.7	3.7
ns	1.5	1.1	0.9	—	0.1	—	0.7	0.1	1.3	1.5	0.8
di wo	0.2	1.1	1.4	1.2	0.8	0.8	—	—	—	—	0.2
di en	0.1	0.1	0.1	—	—	—	—	—	—	—	0.1
di fs	0.1	1.2	1.5	1.3	0.9	0.9	—	—	—	—	0.2
hy en	—	—	—	—	—	—	—	—	0.1	0.1	—
hy fs	3.7	4.2	4.2	2.2	2.6	2.6	2.5	1.7	3.2	3.2	3.6
mt	—	—	—	0.7	—	—	—	—	—	—	—
il	0.5	0.6	0.6	0.4	0.4	0.5	0.3	0.2	0.5	0.4	0.5
ap	—	—	—	—	—	—	—	—	—	—	0.1
Z	0.3	0.3	0.3	0.2	0.2	0.2	—	—	—	—	0.3
CaF_2	0.5	0.4	0.3	0.4	0.4	0.4	0.5	0.4	0.6	0.4	0.5
NaCl	0.4	0.5	0.4	0.4	0.4	0.4	0.2	0.5	0.4	0.3	0.4
NaF	—	—	—	—	—	—	0.3	0.3	—	0.3	—
∑femics	10.3	11.8	12.2	7.1	7.7	7.5	6.8	4.7	9.4	9.3	9.7

Spec. 1. Ascension Island, Atlantic. Scarce phenocrysts of alkali felspar (< 1.0%). (No. 15,375).
Spec. 2. Bouvet Island, Atlantic. Scarce phenocrysts of anorthoclase (< 1.0%). (No. B2).
Spec. 3. Bouvet Island. Phenocrysts of alkali felspar Or_{30} (2.5%). (No. WT 18B).
Spec. 4. Easter Island (Motu Iti), Pacific. Aphyric (No. 17,525).
Spec. 5. Easter Island (Rana Kau), Pacific. Very scarce microphenocrysts of (?) zircon. (No. 17,518).
Spec. 6. Easter Island (Cero Orito), Pacific. Aphyric. (No. 17,691).
Spec. 7. Iceland (Ljosufjoll) Atlantic. Scarce alkali felspar phenocrysts (1%), and trace pyroxene, olivine and (?) plagioclase. (No. 491).
Spec. 8. Iceland (Midhyrna) Atlantic. Less than 1% alkali felspar phenocrysts (Or_{35}). Trace of pyroxene and ore. (No. 295).
Spec. 9. Iceland (Hrafntinnusker) Atlantic. Aphyric. (No. 423).
Spec. 10. Kenya rift valley (L. Naivasha), Africa. Felspar phenocrysts (including graphic intergrowths) 10.2%; quartz 1.3%; clinopyroxene trace; vesicles 29.2% (Mode by F. E. Lloyd). (No. 43/3/S/85).
Spec. 11. Kenya rift valley (unlocalised). Aphyric. (No. EAK 7).
Analysts. S. A. Malik, D. A. Bungard, Department of Geology, University of Reading.

Table 2. *Data on comendite obsidians used in figures; analyses taken from other sources*

No.	Fe as FeO	Molecular SiO_2	Molecular Al_2O_3	Molecular $Na_2O + K_2O$	Molecular 100 $Na_2O/Na_2O + K_2O$	Molecular Agpaitic Index	Source	Locality	Orig. spec. number	Phenocrysts
12	4.97	81.2	8.8	10.0	64.1	1.13	Broch (1946)	Bouvet	2	Anorthoclase (<5%)
—[a]	3.39	81.9	9.0	9.1	72.1	1.01	Carmichael (1967)	E. Iceland	2	Plagioclase (2.1%) Pyroxene (0.3%) Olivine (0.3%) Oxide (0.1%)
13	3.17	81.40	9.33	9.26	72.7	0.99	Lacroix (1936)	Easter	Orito	No data
14	2.88	83.4	8.1	8.5	67.2	1.04	Lacroix (1936)	Easter	Rana Kau	No data
15	5.64	77.1	11.4	11.5	65.6	1.01	Carmichael (1962)	Pitcairn	12,095	Felspar (0.6%). Traces olivine, pyroxene, and opaques
16	4.91	77.4	10.6	12.0	65.5	1.14	Edwards (1938)	Kerguelen	—	Felspar and pyroxene
17	3.03	79.9	10.0	10.1	67.3	1.01	Morgan (1966)	New Guinea	2	Trace anorthoclase and aegirine augite
18	2.86	79.9	9.9	10.3	67.8	1.04	Morgan (1966)	New Guinea	1	No data
19	1.79	83.6	8.1	8.2	59.3	1.02	Bowen (1937)	Kenya	248	Rare anorthoclase, v. rare fayalite
20	3.02	83.9	7.3	8.8	63.1	1.19	Bowen (1937)	Kenya	246	Aphyric
21	3.44	83.4	7.6	9.0	65.4	1.19	Bowen (1937)	Kenya	249	Aphyric
22	2.88	83.4	7.8	8.8	63.4	1.12	Lacroix (1934)	Tibesti	L. 1	Felspar, fayalite, hedenbergite, magnetite
23	2.30	82.9	8.0	9.1	60.7	1.13	Merlin (1953)	Ethiopia		Aphyric
24	1.62	83.8	8.1	8.1	56.6	1.01	Noble (1968)	Idaho	D101,042	No data
25	2.2	83.4	8.0	8.6	60.2	1.08	Noble *et al.* (1968)	Nevada	Average 1	—
26	2.06	83.6	7.9	8.5	60.6	1.08	Noble (1968)	Nevada	D100,737	No data
27	3.34	83.4	7.5	9.1	64.2	1.21	Noble (1968)	Nevada	D100,317	No data
28	3.3	83.3	7.5	9.2	64.4	1.22	Noble *et al.* (1968)	Nevada	Average 2	—
29	1.91	83.7	8.15	8.15	58.0	1.00	Sutherland (unpublished)	Kenya	43/3/S/87	Aphyric
30	3.70	85.4	6.9	7.7	56.6	1.11	Chayes and Zies (1962)	Sardinia	40B5	Sanidine (9.3%) Quartz (6.0%) Tridymite and others (0.3%)

[a] Overlooked in original compilation. This Eastern Iceland analysis differs from the others from Iceland (Table 1) but is very similar to 13, Table 2 (Easter Island). It plots close to 13 in the Easter Island group in Figs. 1, 2, 3 and 4 and the same considerations may apply.

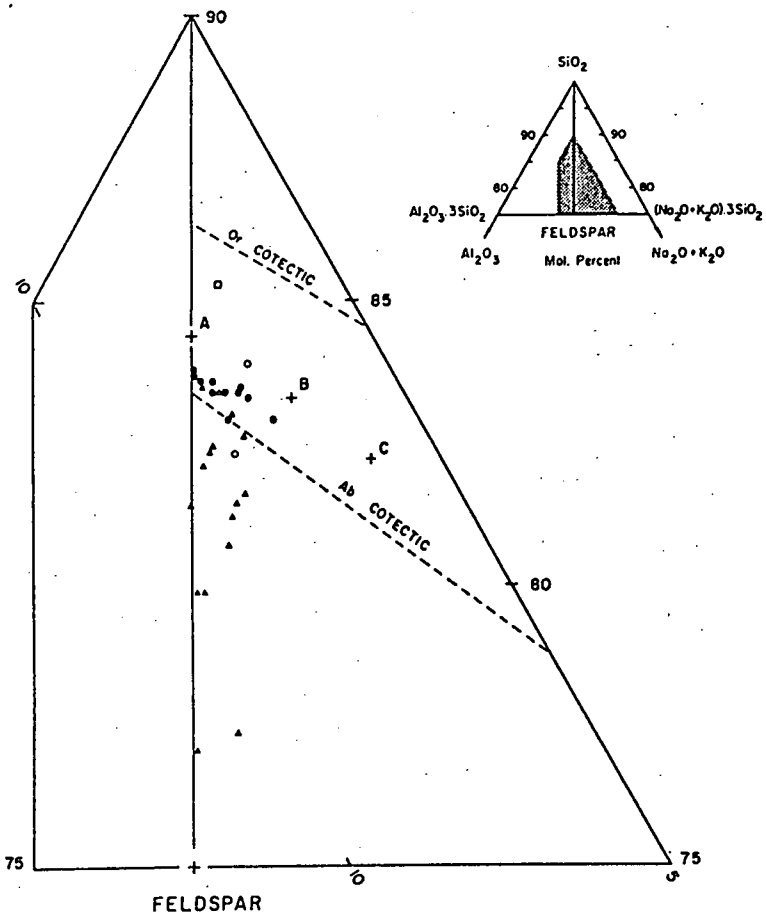

Fig. 1. An enlarged portion of the triangular variation diagram for molecular SiO_2, Al_2O_3 and $(Na_2O + K_2O)$ (shaded portion of inset). New analyses shown by open symbols. Oceanic obsidians as triangles. Continental obsidians as circles. The quartz-feldspar cotectic zone is defined by the broken lines which are the albite-silica and orthoclase-silica field boundaries, converted into molecular amounts, from Schairer and Bowen (1955, 1956). The quartz-feldspar minima compositions A, B, and C are calculated from Carmichael and MacKenzie (1963). The open square is the type-comendite from Sardinia

at 1 kilobar water pressure by Carmichael and MacKenzie (calculated from Table 3, p. 391, 1963). The similarity can hardly be fortuitous. It strongly suggests that these continental comendites, whatever their origin, are quartz-feldspar minima compositions of increasing peralkalinity.

Two of the three newly analysed comendite obsidians from Iceland fall within the cotectic zone of Fig. 1. An older analysis from Easter Island also falls within the zone, but the three new analyses of Easter Island obsidians are less siliceous and contribute to the scattered spread of oceanic samples between the cotectic zone and the feldspar point (simple trachyte composition).

The different distribution of oceanic and continental obsidians is even more marked in Fig. 2, which displays variation in alkali ratio with alumina content.

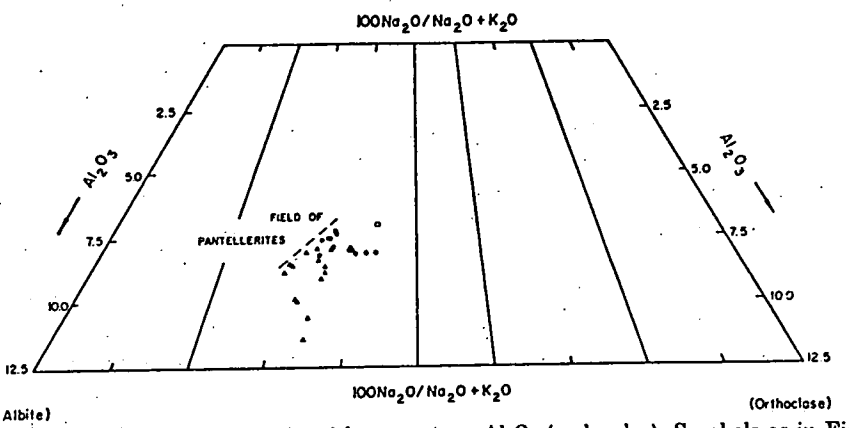

Fig. 2. Variation of alkali ratio with percentage Al_2O_3 (molecular). Symbols as in Fig. 1

The higher, and more varied, alumina contents of oceanic obsidians produce a dispersed pattern, in contrast to the tight grouping of the continental samples.

When total iron as FeO is plotted against agpaitic index in Fig. 3 iron shows a fairly regular increase with peralkalinity in the continental group whereas the oceanic samples are widely scattered.

In the light of the evidence presented above it is worthwhile examining the two groups separately, and in more detail.

Oceanic Comendites

When the oceanic obsidians are projected in Figs. 1 and 2 they are spread between the quartz-feldspar cotectic region and trachytic compositions. In Fig. 4 the oceanic samples have been replotted in an enlarged portion of Fig. 2 to illustrate locality differences. The numbers of analyses from each locality are insufficient for firm conclusions to be drawn about each individual set, but the overall distribution calls for comment.

With the exception of the Easter Island[1] obsidians the distribution pattern of the oceanic comendites in Fig. 4 (and in Fig. 1) is consistent with derivation by fractional crystallization of alkali feldspar, with a composition in the polybaric feldspar minima range Or_{30-35} (Tuttle and Bowen, 1958), from trachytic parental magmas. This pattern would also be consistent with partial melting along an oversaturated trachytic stem. In either case, minor differences between volcanic centres could be attributed to slight variations in starting materials (source heterogeneity) and physical controls such as total pressure. Differences in degree of peralkalinity, for instance, are easily discernible in Fig. 1. The three Bouvet analyses are notewothy because, although they group neatly with the Ascension sample in Figs. 1, 2 and 4 they are distinctly richer in iron than any other comenditic obsidian (the two trachytes from Pitcairn and Kerguelen, as would be expected, are richer in cafemic constituents) (see Fig. 3 and Tables 1 and 2).

The five obsidians from three closely related centres on Easter Island (Baker, 1967) lie outside the composition band of the other oceanic obsidians, because they have higher soda-potash ratios[1]. This is entirely due to their low potash

1 See footnote Table 2.

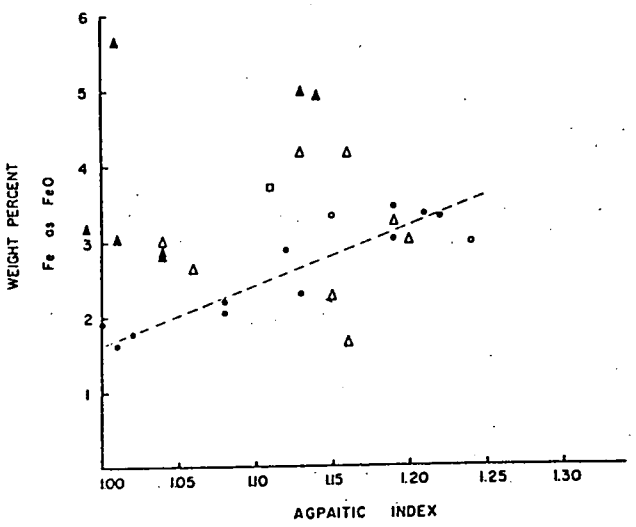

Fig. 3. Variation of total iron (as FeO) with agpaitic index (molecular Na_2O+K_2O/Al_2O_3). The thin broken line is merely to indicate the axis of distribution of the continental obsidians. Symbols as in Figs. 1 and 2

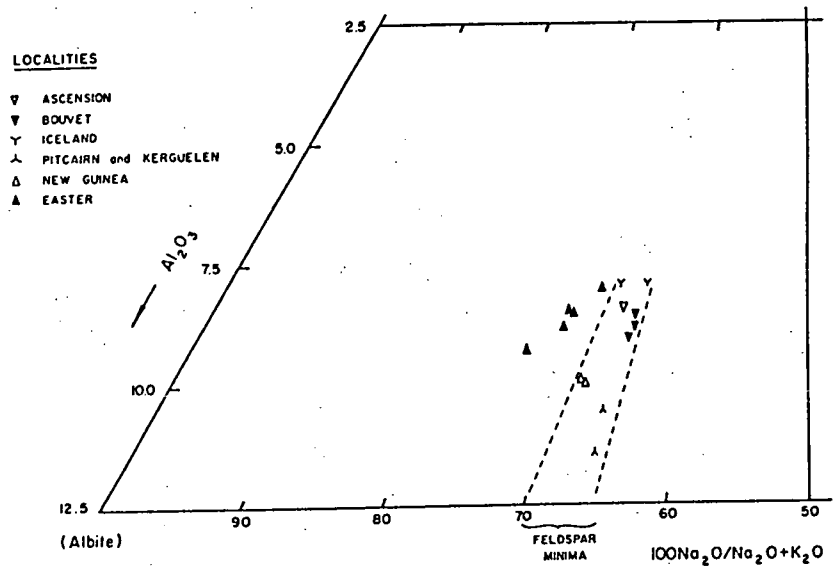

Fig. 4. An enlarged version of Fig. 2 showing the relationship of obsidians from different oceanic volcanoes. The broken lines indicate a compositional band between the feldspar minima compositions and the quartz-feldspar cotectic zone

contents compared with other comendites (Table 1). We can only assume, in the light of evidence available at present, that this is a peculiarity of the Easter Island magmatism. Analyses of the basic lavas from this centre do not appear to have abnormal alkali ratios. Low potash contents are, however, a feature of oceanic metaluminous obsidians, and one of the Easter Island samples is marginally metaluminous (Table 2). It is possible, therefore, that the Easter Island rocks have a different derivation from the other oceanic samples, possibly through a metaluminous trachyte stem.

Continental Comendites

In Figs. 1, 2 and 3 the continental obsidians plot in an ordered array, showing clear correlation in Fig. 1 with the quartz-feldspar cotectic zone. Fig. 5 is an expanded portion of Fig. 2 in which the relationships among the continental samples can be shown in more detail.

In Fig. 1 the three quartz-feldspar minima (A, B, and C) determined by Carmichael and MacKenzie (1963) show a trend within, and parallel to the 1 atms. cotectic zone, and there is a sympathetic distribution of continental comendite obsidians. When these minima are plotted in Fig. 5 it is seen that this pattern is maintained in terms of alkali ratio. It is particularly well-shown by the series of samples from Nevada and Idaho, and is remarkably re-enforced when the pantellerite from Nevada is taken into consideration. This series follows a curved path close to, and roughly parallel with the arc A-B-C defined by the experimental results. The near-correspondence of the two curves strongly suggests that these obsidians are quartz-feldspar minima compositions along a path of increasing peralkalinity. Noble (1968) has already shown that in this series peralkalinity increases with increasing sodicity, which is precisely the condition along the curve A-B-C. There is also a general increase in total iron along both curves with increasing peralkalinity and sodicity.

It should be noted that the least peralkaline obsidian at the right-hand end of the natural curve, has a lower soda-potash ratio than the synthetic minimum A, i.e. the starting points of the two curves are different. Various factors may account for this but possibly the most important difference between the two curves is that the experiments were conducted in the presence of excess H_2O, whereas the natural obsidians are essentially dry. The compositions A, B, and C represent total anhydrous compositions, the compositions of co-existing liquids and vapours during the experiments being unknown.

The remaining comendite obsidians are from African volcanoes, and show a similar distribution but with a little more scatter. All except one (Analysis 11, Table 1) lie in the 1 atmosphere cotectic zone, and the scatter may represent differences in the chemistry of the source materials or the physical conditions of magma generation.

We had not expected, and indeed, we are still a little surprised by the separation of available oceanic and continental comendite obsidians. It is difficult to see why some continental comendites should not have the same origins and petrochemistry as the oceanic samples. It may be that the Kenyan specimen which plots outside the cotectic zone is an inkling that such somendites may yet be reported from continental provinces. The excess of Cl over F in this specimen is also exceptional for a continental comendite.

The clustering of continental comendites in the peralkaline cotectic region strongly suggests that they do not owe their origin to fractional crystallization or partial melting of a trachytic parent, as could be suggested for the oceanic samples. It is difficult to avoid the conclusion that the different crustal environments of the two groups is reflected in their different petrochemical patterns. The quartz-feldspar cotectic trend of the continental obsidians is compatible with partial melting of source materials having silica in excess throughout, the constraint

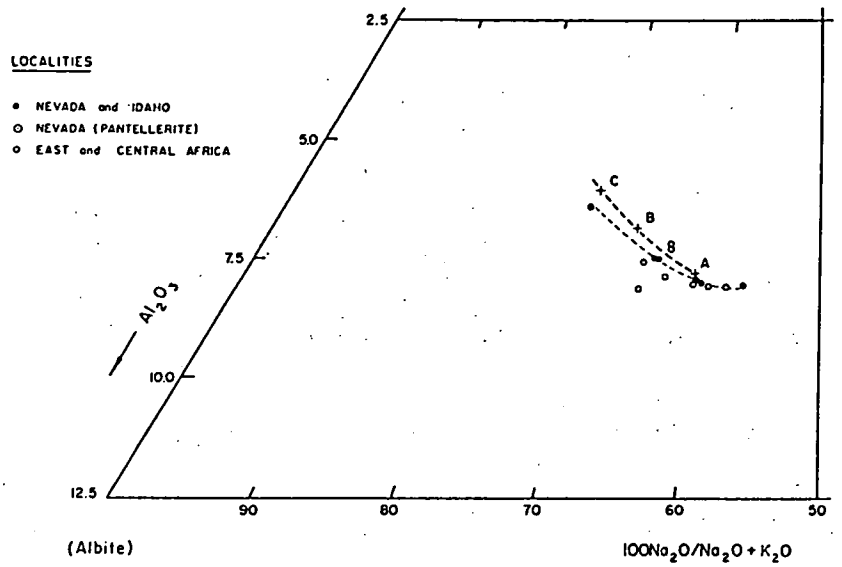

Fig. 5. Enlarged version of Fig. 2 showing the relationships of continental obsidians and the experimentally determined quartz-feldspar minima with increasing peralkalinity (A, B, C). The thin broken line picks out the trend of the Nevada and Idaho obsidians for comparison

being that successive melts must be in equilibrium with quartz. Within the continental crust this is feasible: in the oceanic environment it is much less likely to apply. Peralkalinity in melts generated within the continental crust is much more problematical. Arguments have been presented elsewhere (Bailey, 1970) to show that isochemical melting is improbable, and that influx of volatiles is to be expected, and, indeed, would promote melting. Given this premise it is to be expected that mobile alkalis would be an important part of the volatile phase and may influence the generation of peralkaline melts. If the extent of melting outstrips the influx of volatiles, successive melts will be less peralkaline and eventually may achieve the metaluminous quartz-feldspar minimum condition.

Summary

Available analyses of mildly peralkaline (comendite) obsidians are divisible into two groups, oceanic and continental.

When projected into the system Na_2O-K_2O-Al_2O_3-SiO_2 the oceanic samples cover a broad range from trachytic compositions to the quartz-feldspar cotectic zone, while the continental obsidians approximate to a quartz-feldspar minima path of increasing peralkalinity. The only other major constituent, iron, increases steadily with peralkalinity in the continental series, but shows a broad scatter among oceanic samples. Fluorine is normally more abundant than chlorine in the continental rocks.

With the exception of the Easter Island samples, the oceanic pattern is consistent with derivation of comendites through a trachytic magma stem by fractional crystallization of alkali feldspar in the minima range Or_{30-35}. The Easter Island samples are abnormally low in K_2O for peralkaline obsidians and appear to have a different origin possibly related to that of oceanic metaluminous obsidians[2].

The continental comendite obsidians form a pattern consistent with derivation along a quartz-feldspar minima path. It is suggested that this may represent a path of increasing partial melting within the continental crust, in the presence of alkali-bearing vapour.

Acknowledgements. We are particularly grateful to the following for kindly donating specimens for analysis: Dr. J. D. Bell (Ascension), Dr. P. E. Baker (Easter Island), Dr. D. S. Sutherland (Kenya) and Dr. W. J. Verwoerd (Bouvet). The Iceland samples and their modes (quoted in Table 1) were generously provided by Dr. H. Sigurdsson.

References

Bailey, D. K.: Volatile flux, heat-focusing and the generation of magma. Geol. J. Special. Issue 2, 177—186 (1970).
— Macdonald, R.: Alkali-feldspar fractionation trends and the derivation of peralkaline liquids. Am. J. Sci. 267, 242—248 (1969).
— Schairer, J. F.: Feldspar-liquid equilibria in peralkaline liquids — the orthoclase effect. Am. J. Sci. 262, 1198—1206 (1964).
— — The system Na_2O-Al_2O_3-Fe_2O_3-SiO_2 at 1 atmosphere, and the petrogenesis of alkaline rocks. J. Petrol. 7, 114—170 (1966).
Baker, P. E.: Preliminary account of recent geological investigations on Easter Island. Geol. Mag. 104, 116—122 (1967).
Bowen, N. L.: Recent high-temperature research on silicates and its significance in igneous geology. Am. J. Sci. 33, 1—21 (1937).
— Phase equilibria bearing on the origin and differentiation of alkaline rocks. Am. J. Sci., Daly Vol. 243-A, 75—89 (1945).
Broch, O. A.: Lavas of Bouvet Island. In: Two contributions to Antarctic petrography. Scient. Results Norw. Antarct. Exped., No. 25, 3—26 (1946).
Carmichael, I. S. E.: Pantelleritic liquids and their phenocrysts. Mineral. Mag. 33, 86—113 (1962).
— The iron-titanium oxides of salic volcanic rocks and their associated ferromagnesian silicates. Contr. Mineral. and Petrol. 14, 36—64 (1967).
— MacKenzie, W. S.: Feldspar-liquid equilibria in pantellerites an experimental study. Am. J. Sci. 261, 382—396 (1963).
Chayes, F., Zies, E. G.: Sanidine phenocrysts in some peralkaline volcanic rocks. Ann. Rept. Geophys. Lab. Yearbook 61, 112—118 (1962).
Coombs, D. S.: Trends and affinities of basaltic magmas and pyroxenes as illustrated on the diopside-olivine-silica diagram. Mineralog. Soc. Am. Spec. Papers 1, 227—250 (1963).
Edwards, A. B.: Tertiary lavas from the Kerguelen archipelago. B.A.N.Z. Antarctic Res. Exped. (1929—1931) 2, 69—100 (1938).
Lacroix, A.: Les rhyolites et les trachytes hyperalcalins quartzifères á propos de ceux de la Corée. Compt. Rend. 185, 1410—1415 (1927).
— Volcanisme et lithologie. Mission au Tibesti (1930—1931) dirigée par M. Dalloni. Mém. Acad. Sci. (Paris) 61, 169-(1934).
— Composition chimique des laves de l'Ile de Pâques. Compt. Rend. 202, 601—605 (1936).
Macdonald, R., Bailey, D. K.: The chemistry of peralkaline oversaturated obsidians. U. S. Geol. Survey, Profess. Papers 440-N, part 1 (in press).
Merlin, O. H.: Le vulcaniti acide dell'Africa Orientale. Centro Studi Pet. Geol. dell Cons. Naz. Richerche, Univ. Padova (1953).

2 See footnote Table 2.

Morgan, W. R.: A note on the petrology of some lava types from East New Guinea. J. Geol. Soc. Aust. 13(2), 583—591 (1966).
Noble, D. C.: Gold Flat Member of the Thirsty Canyon Tuff — a pantellerite ash-flow sheet in southern Nevada. U.S. Geol. Survey, Profess. Papers 525-B, 85—90 (1965).
— Systematic variation of major elements in comendite and pantellerite glasses. Earth and Planet. Sci. Letters 4, 167—172 (1968).
— Hafity, J.: Minor-element and revised major-element contents of some Mediterranean pantellerites and comendites. J. Petrol. 10, 502—509 (1969).
— Sarjent, K. A., Mehnert, H. H., Ekren, E. B., Byers, F. M., Jr.: Silent Canyon Volcanic Centre. In: Eckel, E. B. (ed.), Nevada Test Site. Geol. Soc. Am. Mem. 110, 65—75 (1968).
Schairer, J. F., Bowen, N. L.: The system K_2O-Al_2O_3-SiO_2. Am. J. Sci. 253, 681—746 (1955).
— The system Na_2O-Al_2O_3-SiO_2. Am. J. Sci. 254, 129—195 (1956).
Tuttle, O. F., Bowen, N. L.: Origin of granite in the light of experimental studies in the system $NaAlSi_3O_8$-$KAlSi_3O_8$-SiO_2-H_2O. Geol. Soc. Am. Mem. 74, 1—153 (1958).

Dr. D. K. Bailey
Department of Geology
University of Reading
Reading, England

Universitätsdruckerei H. Stürtz AG Würzburg
Printed in Germany

Oversaturated Peralkaline Glassy Trachytes from Kenya

by R. MACDONALD,[1] D. K. BAILEY,[1] *and* D. S. SUTHERLAND[2]

[1]*Department of Geology, University of Reading and* [2]*Department of Geology, University of Leicester*

(*Received 9 September 1969; in revised form 9 January 1970*

ABSTRACT

Peralkaline felsic lavas from the central part of the Kenya Rift Valley were used by Bowen as an illustration of the final stages of fractional crystallization in nature. Despite the importance of trachyte to this and other theories on the evolution of peralkaline rhyolites, only one analysis of a pantelleritic trachyte obsidian is available from the literature. Comparison of four newly analysed trachyte obsidians, from the Menengai volcano, with the pantellerites from other centres in the Kenyan province shows that they form a chemically coherent group. Plotting the analyses in the system Na_2O–K_2O–Al_2O_3–SiO_2 reveals that the pantelleritic trachytes cannot be related to the pantellerites simply by crystal ⇌ liquid equilibria. At least in the case of the Kenyan specimens the conventional theory of fractional crystallization from trachyte to rhyolite needs re-examination. Data on the Kenyan rocks suggest that alkali feldspar ⇌ liquid ⇌ alkali-bearing vapour equilibria have controlled their evolution.

INTRODUCTION

PERALKALINE trachytes and rhyolites are typical minor members of the alkali basalt association, in which they are commonly regarded as products of fractional crystallization from an alkali basalt parent magma. Such a derivation seems not unreasonable where alkali basalt predominates, but in some of the major continental provinces large volumes of peralkaline felsic magmas have been erupted with little associated basalt. Alkaline magmatism of this type is characteristic of many continental rift zones, and the origin and evolution of these magmas is clearly a crucial part of stable continent geology. Where fractional crystallization from an alkali basalt parent becomes questionable, the relationship between trachyte and rhyolite must also be re-examined.

Other possibilities have been suggested, ranging from an origin for the rhyolites by fractional crystallization from a more basic parent without passing through a trachyte stage (Noble, 1965), to crustal anatexis around basaltic intrusions (Romano, 1968; Villari, 1968). The range of hypotheses indicates that although a considerable volume of analytical data is available, the relationships are still unclear. It may be that each hypothesis is applicable only to a particular group of rocks, but the distinctive chemical peculiarities of pantelleritic rhyolites make this unlikely, and suggest that their origin is subject to special controls. We believe that the cause of much of the uncertainty lies in sampling. At first sight it seems pedantic to say that in any petrogenetic study it is vital that the magma compositions be preserved as nearly as possible in the rocks, but for peralkaline rocks this cannot be too strongly emphasized. Rhyolite and

[Journal of Petrology, Vol. 11, Part 3, pp. 507–17, 1970]

trachyte magmas are largely composed of SiO_2, Al_2O_3, Na_2O, and K_2O and it is essential that these four components be accurately preserved in the lavas sampled. When these magmas have alkalis in excess of alumina they are particularly susceptible to alkali losses during and after crystallization (Romano, 1969). Experience shows that quenched liquids (fresh, non-hydrated glasses) are the only satisfactory samples of peralkaline liquids. When this criterion is applied, the volume of available data is greatly diminished; pantellerite glasses are not common, and only one genuine pantelleritic trachyte obsidian (with less than 10 per cent normative quartz) has been specified in the literature, from the Menengai volcano, Kenya (McCall, 1967, p. 19). In this paper we present analyses of four further pantelleritic trachyte glasses from Menengai. Using these and other published and unpublished analyses of pantellerite glasses from the same province it is possible to assess some of the mechanisms suggested for the derivation of these magmas.

GEOLOGY

The central sector of the Rift Valley of Kenya is characterized by an abundance of felsic peralkaline volcanics with only minor basalts. The felsic rocks comprise trachytes (ranging from alkaline to strongly peralkaline pantelleritic trachytes) and the more silicic pantellerites, comendites, and alkali rhyolites. The most conspicuous development of pantellerites and pantelleritic trachytes is found in the volcanic massif of Eburru (Sutherland, in preparation) but pantelleritic rocks also occur over a wider area within the Kinangop Tuffs and as lava flows and intrusions in these tuffs to the south of Eburru (west and south-west of Lake Naivasha). To the south, the volcano of Longonot consists largely of trachytes, some of which are of peralkaline type. North of Eburru the volcano of Menengai is similarly trachytic (McCall, 1967) and peralkaline types may well predominate.

The age of the volcanics is still uncertain. McCall (1967, p. 39) has suggested that the early Menengai volcanics were erupted in the Pliocene, but he has also adopted a similar age for the Kinangop Tuffs which are regarded by Thompson & Dodson (1963) as Pleistocene. The activity of Menengai continued in the Pleistocene with the formation of the caldera, and more recent activity has given rise to the flows of the caldera floor. The volcanics of Eburru and the area around Lake Naivasha range from Pleistocene to Recent.

Analyses of glassy rocks from the caldera wall, and from associated deposits of ejectamenta outside the caldera of Menengai are given in Table 1 (together with a Recent trachytic obsidian from the caldera floor (McCall, 1967, p. 19)). The rocks plotted in Figs. 1 and 2 comprise these glassy trachytes and published and unpublished analyses of glassy trachytes and pantellerites from the Eburru–Naivasha area.

Petrographically as well as chemically the pantelleritic trachytes and pantellerites form a coherent suite. They are undoubtedly related to the phonolitic

trachytes and phonolites that are conspicuously abundant throughout the Rift zone, and they are also associated with the less peralkaline comendites and rhyolites occurring in the Naivasha area. This paper, however, confines attention to the pantelleritic trachytes and their relationship with the pantellerites. The trachytes are defined as having less than 10 per cent normative quartz, but an almost continuous series extends from 4 to 29 per cent Q.

A complete range of textures is represented from aphyric obsidian, through porphyritic obsidian to partly and wholly crystalline rocks. In the porphyritic rocks, phenocrysts of alkali feldspar are always present. They appear to have a restricted range of composition, from 35 to 42 weight per cent Or. Quartz is recognizable among the phenocrysts of silicic pantellerites (24 per cent normative Q). Fayalitic olivine is present as occasional phenocrysts in most trachytes and in pantellerites containing up to 16 per cent normative Q. It is usually accompanied by opaque oxide. In the more silicic rocks olivine and opaque oxide are absent, and aenigmatite appears as a phenocryst phase. Pyroxene (hedenbergite or aegirine–augite) occurs as sparse phenocrysts throughout the series. Aenigmatite and alkali amphibole form phenocrysts in the more silicic pantellerites. The amphibole is variable. An olive to brownish type (near kataphorite?) forms phenocrysts, and often occurs in the groundmass of trachytes and pantellerites, but the more common variety seen in the groundmass of crystalline rocks throughout the group is a greenish-blue 'arfvedsonite'.

The distribution of phenocrysts is sometimes irregular, possibly through the movements of a lava prior to consolidation and occasionally owing to the acquisition of crystals along with xenolithic fragments. Alien feldspar such as labradorite in a trachyte must be assumed to be of xenocrystic origin, but it is more difficult to assess in cases where trachytes or pantellerites contain variable amounts of the common alkali feldspar, how much of the feldspar crystallized from the enclosing liquid.

The analysed pantelleritic trachyte obsidians of Table 1

43/1/S/5. Sparse phenocrysts and aggregates of slightly rounded euhedral and subhedral anorthoclase (1–3 per cent), approximately 0·8 mm, enclosing occasional apatite. Set in finely banded glass, pale yellow in section. Banding consists of layers rich in minute microlites, and ranges in scale from thin streaks to layers of more opaque glass 2–3 mm thick.

43/1/S/6. Very sparse phenocrysts of anorthoclase ($\leqslant$ 1 per cent), singly and in groups of stout crystals up to 0·6 mm. Set in pale greenish-yellow glass containing few greenish rod-shaped microlites and many near-spherical vesicles.

43/1/S/6a. Anorthoclase phenocrysts more abundant than mode (below) would suggest. More than 11 000 points were counted, but limitation is imposed by the size of the thin section. (Visual estimate of specimen analysed is 10 per cent feldspar.) Feldspar is euhedral, up to 3 mm in length. Sparse green pyroxene

($z \wedge c$ 46°), 0·3 mm, forms slightly rounded subhedra intergrown with opaque oxide. The latter forms crystals up to 0·15 mm. Pale yellow fayalitic olivine (0·5 mm) as somewhat broken crystals, also encloses opaque oxides. Matrix is yellow glass virtually free from microlites but full of vesicles which occasionally show marginal development of dark minerals.

Mode (volume per cent):

Phenocrysts				Matrix		
Feldspar	*Olivine*	*Pyroxene*	*Oxides*	*Glass*	*Others*	*Pores*
3·9	0·3	0·3	0·2	56·6	0·1	38·6
6·4	0·4	0·4	0·4	92·2	0·2	—

43/1/S/11. Heterogeneous rock, with irregular bands and lenses on a macroscale (several centimetres thick). Heterogeneity comprises black obsidian separated by scoriaceous layers containing numerous small lithic and crystal fragments. Whilst fragmental material may well be derived, the feldspar is the common alkali feldspar. It shows irregular distribution, but specimen analysed was clean-looking obsidian whose feldspars appeared to be indigenous. Thin section of obsidian shows only a few phenocrysts of anorthoclase set in pale yellow glass containing a few microlites and numerous flattened vesicles in pronounced layers. More turbid layers of the rock, which were avoided in analysis, are rich in microlites, crystals of feldspar and green pyroxene, and small lithic fragments of syenitic to trachytoid texture.

COMPARISON OF ANALYSES

Four major variables, SiO_2, Al_2O_3, Na_2O, and K_2O, need comparison in this suite of analyses. In Fig. 1 the molecular percentages of SiO_2, Al_2O_3, and total alkalis are compared in a triangular diagram, in the manner suggested in an earlier paper (Bailey & Macdonald, 1969). With the exception of one specimen, the distribution of analyses is parallel to the feldspar–quartz axis of the diagram, but well off-set towards the peralkaline side. The slightly higher peralkalinity in the rhyolites is easily verified in this diagram by projecting lines from the SiO_2 apex through the sample points onto the alkali–alumina base-line. A normal sub-aluminous trachyte would plot at the feldspar point in this diagram and it should be noted that the pattern of Kenyan analyses shows no connection with this point.

The variation in alkali ratios with alumina content is shown in Fig. 2 (Bailey & Macdonald 1969). This diagram could be visualized as a section of the system Na_2O–K_2O–Al_2O_3–SiO_2 with an alkali:silica index 11:89, as depicted in Fig. 1. It should be emphasized that projection of sample points into this plane involves no distortion of alkali ratios and, therefore, direct comparison with conjugate feldspar compositions is possible. With the same exception noted above, the analyses again fall in a band, showing slight decrease in Na_2O/K_2O ratio at the rhyolite end. The two diagrams together show a marked regular

TABLE 1

Chemical analyses and CIPW norms of glass peralkaline trachytes from the Menengai Volcano, Kenya

	43/1/S/5	*43/1/S/6*	*43/1/S/6a*	*43/1/S/11*	*43/1192*
SiO_2	63·1	62·7	62·5	62·8	63·4
TiO_2	0·69	0·69	0·75	0·70	0·73
Al_2O_3	12·41	12·50	15·21	12·36	12·06
Fe_2O_3	2·05	2·04	1·15	2·11	3·50
FeO	6·97	6·90	5·55	6·94	5·70
MnO	0·35	0·35	0·28	0·36	0·40
MgO	0·16	0·18	0·33	0·18	0·31
CaO	1·12	1·20	1·45	1·13	0·99
Na_2O	8·43	8·52	7·18	8·42	7·95
K_2O	4·57	4·72	5·20	4·54	4·55
P_2O_5	0·09	0·10	0·14	0·09	0·10
H_2O^+	0·14	0·19	0·30	0·05	0·24
F	0·36	0·34	0·17	0·36	—
Cl	0·23	0·22	0·10	0·23	—
Sum	100·67	100·65	100·31	100·27	99·93
Less O ≡ F, Cl	0·20	0·19	0·09	0·20	—
Total	100·47	100·46	100·22	100·07	99·93
Q	6·9	6·1	0·3	6·8	7·45
or	27·2	27·8	30·6	26·7	26·7
ab	38·3	38·3	49·3	38·8	37·2
hl	0·4	0·4	0·2	0·4	—
ac	6·0	6·0	3·2	6·0	5·7
ns	5·7	5·9	1·7	5·5	4·5
di	1·9	2·1	4·6	1·9	3·7
hy	11·7	11·4	7·9	11·5	8·8
il	1·4	1·4	1·4	1·4	1·4
ap	0·3	0·3	0·3	0·3	0·2
CaF_2	0.7	0·7	0·3	0·7	—

43/1/S/5, 43/1/S/6, 43/1/S/6a: blocks in agglomerate, north-east of Menengai.
43/1/S/11: lava exposed in caldera wall below Valley Farm, west side of Menengai.
Analyst: S. A. Malik, Geochemistry Unit, Department of Geology, University of Reading.
43/1192: Recent lava, Menengai caldera floor (McCall, 1967, table II, no. N).
Analysts: Min. Res. Div., Overseas Geological Survey.
Al_2O_3 values not corrected for minor element interference.

TABLE 2

Partial chemical analyses of alkali feldspar phenocrysts

	43/1/S/6a	*43/1/S/11*
CaO	0·56	0·46
Na_2O	6·52	6·47
K_2O	6·77	6·78
Or	41·3	40·8
Ab	56·4	56·3
An	2·3	2·9
(wt. per cent)		

Analyst: S. A. Malik
The third natural feldspar composition used in Fig. 2 is of the phenocrysts from a pantellerite from the Eburru massif (43/3/S/46): X-ray determination by D. S. Sutherland, $Or_{35}Ab_{65}$ (wt. per cent).

variation in the four major components in these rocks, the rhyolites being slightly more peralkaline *and* more potassic than the trachytes. The one exception from these generalizations is a specimen which is abnormally rich in feldspar phenocrysts (43/1/S/6a). It is probably no coincidence that the feldspar tie-lines to this specimen in both Figs. 1 and 2 project into the zone of the other

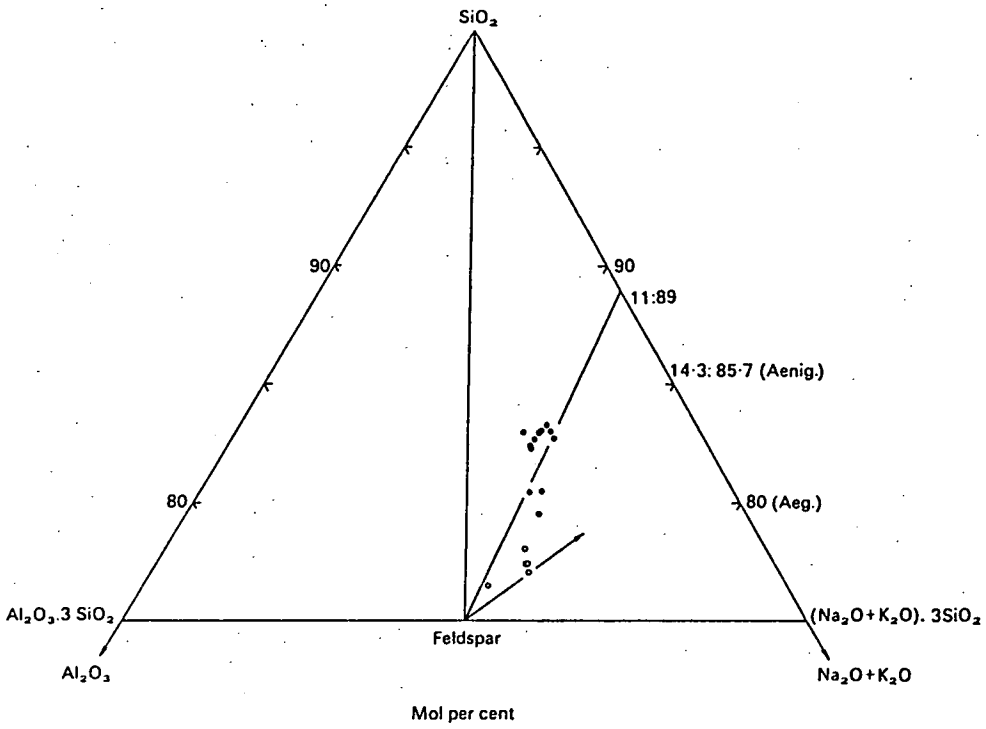

FIG. 1. Triangular diagram showing variation in molecular SiO_2, Al_2O_3 and $(Na_2O + K_2O)$. Open circles—pantelleritic trachytes, closed circles—pantellerites. Data sources are: this paper, Table 1; Prior (1903, pp. 245–6); Bowen (1937, no. NLB 230); Nicholls & Carmichael (1969, no. 121–R); unpublished analyses (D. S. Sutherland). Aeg. = aegirine. Aenig. = aenigmatite.

specimens, suggesting that the rock is feldspar–cumulitic. Moreover, this lava is highly vesicular (38·6 vol. per cent) and it is probable that part of the shift in Figs. 1 and 2 is a result of devolatilization.

The distinct pattern of regular variation in the four major oxides implies that this suite of Kenyan rocks forms a coherent group, chemically as well as geologically. It would be straining coincidence to suppose that the relationships among these lavas are random. Their close spatial and temporal development coupled with this regular variation suggest a consistent process or processes operating in the magma development. In trying to discern a controlling process we must first examine some of the suggestions that have already been proposed for the origins of peralkaline acid rocks.

DISCUSSION

1. *Melting of country rocks at the margins of a basic intrusion.* This mechanism has been suggested by Villari (1968) and Romano (1968) for the formation of pantellerite in the type-area, Pantelleria. We believe that such a process could not yield strongly peralkaline melts from aluminous crustal rocks, and over a whole province would hardly yield a series of peralkaline magmas showing

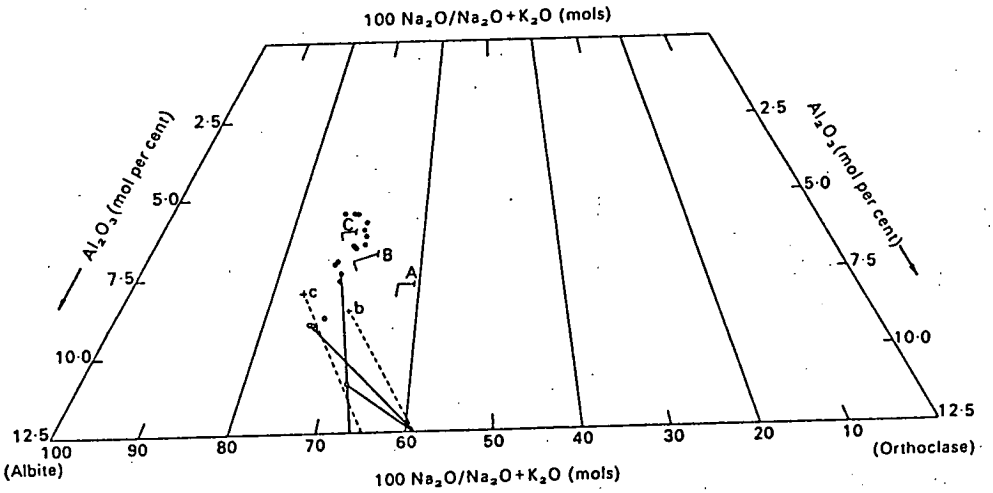

FIG. 2. Quadrilateral showing the variation in alkali ratio and Al_2O_3. Symbols and data sources as before. A, B, and C—quartz-feldspar minima recalculated to actual compositions from data in Carmichael & Mackenzie (1963, table 3). A—in the 'granite system': B—with 4·5 per cent Ac and 4·5 per cent Ns added to the system: C—with 8·3 per cent Ac and 8·3 per cent Ns. (Note that the trend of the minima A–B–C is contrary to the distribution of the Kenyan peralkaline obsidians.) A small segment of the quartz–feldspar field boundary to the left of each minimum is shown as far as the intersection with the low-temperature zone on the feldspar liquidus. Crosses show compositions lying in the experimental low-temperature zone (Carmichael & Mackenzie 1963, tables 1B, 2D), with tie-lines (broken) to the conjugate feldspars. b—from the '4·5' join, c—'8·3' join. The solid tie-lines relate to natural samples. (N.B. the position of the minimum in the granite system determined by Carmichael & Mackenzie (1963) differs from that of Tuttle & Bowen (1958). For sake of consistency we have used the former point.)

regular variation. The close similarity of pantellerites from many regions makes this hypothesis exceedingly dubious even for the province for which it is proposed.

2. *Fractional crystallization*

(*a*) Noble's suggestion (1965) that pantellerites are the end-product of a fractional crystallization series that does not pass through a trachytic stage cannot be applied to the Kenyan suite where peralkaline trachytes are so well represented.

(*b*) Normative alkali feldspar is the main constituent of trachytes and rhyolites, and alkali feldspar is the most common and the most abundant phenocryst. Crystallization or melting of alkali feldspar is therefore a logical contender for

the controlling process in their evolution. Several authors have proposed that pantellerites are derived from trachytes by fractional crystallization of alkali feldspar (Carmichael & Mackenzie 1963; Thompson & Mackenzie 1967; Ewart *et al.*, 1968; Noble 1968), and the methods of projection used in Figs. 1 and 2 provide a good test of this hypothesis (Bailey & Macdonald, 1969). Tie-lines from the feldspar point in Fig. 1 to the sample compositions show quite plainly that the distribution cannot be explained in terms of feldspar fractionation. Such a process would drive successive residual liquids along a path that maintained a constant alkali: silica ratio determined by the peralkalinity of the original liquid. In Fig. 2 alkali feldspar compositions can be plotted in the baseline (12·5 per cent mol. Al_2O_3) and the trachyte feldspar phenocryst compositions show even more emphatically that fractionation of feldspar would produce a residual liquid trend almost at right-angles to the pattern shown by the Kenyan obsidians. Both Figs. 1 and 2, therefore, indicate that feldspar fractionation is inadequate to explain the Kenyan pattern.

It has been suggested from experimental results (Carmichael & Mackenzie, 1963; Thompson & Mackenzie, 1967), that pantelleritic rocks lie in a low temperature zone analogous to the thermal valley in the 'granite' system (Tuttle & Bowen, 1958). Crystallization of feldspar would drive residual liquids along this zone until the quartz-feldspar field boundary was intersected, and thence by crystallization to the quartz-feldspar minimum. The compositions of the quartz–feldspar minima determined by Carmichael & Mackenzie (1963) and the intersections of the low-temperature zone with the quartz feldspar boundary are shown in Fig. 2. We had hoped to show the position of the low-temperature zone also, but this is not possible. From the Thompson & Mackenzie (1967) experiments the zone cannot be precisely located but Carmichael & Mackenzie (1963) list a composition in each of their joins which they believe to lie in the zone. Each of these compositions has the property of precipitating feldspar of constant compositions over a wide range of temperature, and the feldspar tie-line should define the trace of the low-temperature zone. Unfortunately, when these compositions are plotted in Fig. 2 the feldspar tie-lines are not colinear with the intercepts of the low-temperature zone on the quartz–feldspar boundary. This relationship is inexplicable solely in terms of constant feldspar precipitation along the low-temperature zone: the intervention of some other factor would be necessary to keep the liquid compositions in such a zone. It may be that a more complex relationship between liquids and feldspars, such as that shown by the Kenyan suite, has been simulated but hitherto unrecognized in the experiments.

3. *Partial melting of basaltic materials.* This process has been suggested (Bailey, 1964; Bailey & Schairer, 1966) as the converse of fractional crystallization—chiefly to resolve the problem of large volumes of felsic magma in provinces deficient in basic magma. Regarded simply, in terms of feldspar $\rightleftharpoons$ liquid

equilibria, partial melting would be subject to the same criticisms as fractional crystallization as far as the Kenyan suite is concerned. Another factor besides feldspar ⇌ liquid equilibria is required to describe the pattern of Kenyan analyses.

4. *A third factor.* The pattern of analyses in Fig. 1 suggests that the rocks are products of a general process operating in this province, and the regular distribution implies that this is an equilibrium-controlled process.[1] If we assume for the moment that trachyte represents the higher temperature magma, then the series of points to rhyolite might represent a cooling-solidification path. As was pointed out before, the major crystallizing phase is feldspar but the feldspar tie-lines are strongly transverse to the trachyte–rhyolite distribution. If feldspar ⇌ liquid equilibria have influenced the distribution, a third phase must also be involved. This phase would have to have a composition that would project to the right of the trachyte–rhyolite analyses in Fig. 1, i.e. it would be strongly deficient in Al_2O_3. If it were a phase separating from the liquid simultaneously with feldspar, and generating the series from trachyte to rhyolite, its composition would have to plot on the SiO_2-poor side of a line from the feldspar point through the trachyte compositions. Among the possible alkali–iron silicates that might be considered only aegirine has a $Na_2O:SiO_2$ ratio that is adequate, and even this is marginal. The phenocryst pyroxene found as traces in the trachytes is not rich enough in alkali to account for the observed trend. It is necessary, therefore, to consider the possible effect of alkalis in the vapour phase. Such a vapour is not necessarily rich in water (cf. Nicholls & Carmichael, 1969, p. 288).

If we allow for participation of the vapour phase, the requirement would be that while feldspar is separating, alkalis or alkalis plus silica would be simultaneously separating into the vapour. Consideration of Fig. 2, where the conjugate feldspars are more potassic than the liquids, shows that the alkalis moving into the vapour would need to have a higher $Na_2O:K_2O$ ratio than the liquid. The total situation would be a liquid line of descent controlled by simultaneous separation of potassic feldspar and sodic vapour. There need not necessarily be an extreme build-up of alkalis in the vapour phase—this could be 'buffered' by reaction with the wall-rocks, producing an aureole of alkali metasomatism.

The above discussion describes a cooling path from trachyte to rhyolite, but the converse, progressive melting, is equally valid and, in view of the abundance of felsic volcanics relative to basic rocks in the more recent history of the Rift may be applicable in the Kenya province. Melting of alkali basalt composition at depth could be initiated by influx of alkali-rich juvenile vapours (cf. Bailey, 1970), and a pattern such as that shown by the Kenyan analyses would describe

[1] An analysis of a newly acquired specimen of trachyte obsidian from the rim of the crater Longonot was completed, except for Cl and F, during revision of the manuscript. It is very similar to the Menengai samples and plots close to them in Figs. 1 and 2. Longonot is at the opposite (southern) end of the Kenyan province from Menengai.

a rising temperature path from pantellerite to trachyte. In this system, as more of the potassic feldspar component melted its effect would be balanced by more soda from the vapour passing into the liquid. Buffering would be achieved by the continued influx of vapour into the zone of melting. The general arguments favouring progressive melting rather than fractional crystallization, especially under the influence of volatiles, have been given elsewhere (Bailey, 1964 and in press).

CONCLUSIONS

The lavas, ranging from peralkaline trachyte to pantellerite, erupted in the central part of the Kenyan rift cannot be explained in terms of a simple fractional crystallization sequence, nor, unless the individual rocks are totally unrelated, in terms of simple crystal ⇌ liquid equilibria. Ironically, it was mainly rocks from this province which Bowen (1937) used as the prime natural examples of Petrogeny's Residua System. He believed that because their compositions projected into the low temperature region of the system $NaAlSiO_4$–$KAlSiO_4$–SiO_2, they must be products of crystal ⇌ liquid equilibria, thus representing the end-products of fractional crystallization from basalt. We suggest that the regular variation in the chemistry of this suite can be explained essentially in terms of feldspar ⇌ liquid ⇌ alkali-bearing vapour equilibria. The ultimate derivation of the felsic liquids is still an open question.

ACKNOWLEDGEMENTS

D. S. Sutherland's work at the University of Leicester is financed by N.E.R.C. in connection with the research project directed by Professor B. C. King (Bedford College, University of London), which is investigating the structure and petrology of the central and northern Rift of Kenya. Analyses quoted in this paper were carried out on material collected by D. S. Sutherland.

We thank S. A. Malik (University of Reading), who made the analyses and J. E. Thomas for making the analytical facilities available. R. Macdonald gratefully acknowledges the tenure of a University of Reading Research Fellowship during the period 1967–9.

REFERENCES

BAILEY, D. K., 1964. Crustal warping—a possible tectonic control of alkaline magmatism. *J. geophys. Res.* 69, 1103–11.

—— 1969. Volatile flux, heat-focusing and the generation of magma. *Geol. Jr. Special Issue*, No. 2, 177–86.

—— in press. Melting in the deep crust. In Sørensen, H. (ed.), *The alkaline rocks*. New York: John Wiley and Sons.

—— & MACDONALD, R., 1969. Alkali–feldspar fractionation trends and the derivation of peralkaline liquids. *Am. J. Sci.* 267, 242–8.

—— & SCHAIRER, J. F., 1966. The system Na_2O–Al_2O_3–Fe_2O_3–SiO_2 at 1 atmosphere, and the petrogenesis of alkaline rocks. *J. Petrology*, 7, 114–70.

BOWEN, N. L., 1937. Recent high-temperature research on silicates and its significance in igneous geology. *Am. J. Sci.* 33, 1–21.

CARMICHAEL, I. S. E., & MACKENZIE, W. S., 1963. Feldspar-liquid equilibria in pantellerites: an experimental study. Ibid. **261**, 382–96.

EWART, A., TAYLOR, S. R., & CAPP, A. C., 1968. Geochemistry of the pantellerites of Mayor Island, New Zealand. *Contr. Miner. Petrol.* **17**, 116–40.

MCCALL, G. J. H., 1967. Geology of the Nakuru–Thomson's Falls–Lake Hannington area. *Report No. 78, Geol. Surv. Kenya.*

NICHOLLS, J., & CARMICHAEL, I. S. E., 1969. Peralkaline acid liquids: a petrological study. *Contr. Miner. Petrol.* **20**, 268–94.

NOBLE, D. C., 1965. Gold Flat Member of the Thirsty Canyon Tuff—a pantellerite ash-flow sheet in Southern Nevada. *Prof. Pap. U.S. geol. Surv.* **525–B**, 85–90.

—— 1968. Systematic variation of major elements in comendite and pantellerite glasses. *Earth planet. Sci. Lett.* **4**, 167–72.

PRIOR, G. T., 1903. Contributions to the petrology of British East Africa. *Mineralog. Mag.* **13**, 228–63.

ROMANO, R., 1968. New petrochemical data on volcanites from the island of Pantelleria (Channel of Sicily). *Geol. Rundsch.*, **57**, 773–83.

—— 1969. Sur l'origine de l'excès de sodium dans certaines laves de l'Île de Pantelleria. *Bull. volcan.* **33**, 1–7.

THOMPSON, A. O., & DODSON, R. G., 1963. Geology of the Naivasha Area. *Report N. 55, Geol. Surv. Kenya.*

THOMPSON, R. N., & MACKENZIE, W. S., 1967. Feldspar–liquid equilibria in peralkaline acid liquids: an experimental study. *Am. J. Sci.* **265**, 714–34.

TUTTLE, O. F., & BOWEN, N. L., 1958. Origin of granite in the light of experimental studies in the system $NaAlSi_3O_8$–$KAlSi_3O_8$–SiO_2–H_2O. *Mem. geol. Soc. Am.* **74**.

VILLARI, L., 1968. On the geovolcanological and morphological evolution of an endogenous dome (Pantelleria, Mt. Gelkhamar). *Geol. Rundsch.*, **57**, 784–95.

MINERALOGICAL MAGAZINE, DECEMBER 1975, VOL. 40, PP. 405–14

Fluorine and chlorine in peralkaline liquids and the need for magma generation in an open system

D. K. BAILEY

Department of Geology, University of Reading, Reading, RG6 2AB

AND R. MACDONALD

Department of Environmental Sciences, University of Lancaster, Bailrigg, Lancaster

SUMMARY. Fluorine, chlorine, zinc, niobium, zirconium, yttrium, and rubidium have been determined on fifteen obsidians from Eburru volcano (Kenya Rift Valley), spanning the range from pantellеritic trachyte to pantellerite. All pairs of elements show positive correlation coefficients, ranging between 0·769 and 0·998, but with most values better than 0·900. In spite of some very high correlations, only two of the twenty-one best-fit lines pass near the origin of the Cartesian coordinates. Linear distributions are found *within* two separate groups of elements: F, Zr, Rb; and Cl, Nb, Yt. Zn behaves in general as a member of the second group but seems to be subject to an additional variation. When an element from the fluorine group is plotted against one from the chlorine group the resulting pattern is non-linear. Therefore, although the elements in both groups would generally be considered 'residual' (partition coefficients between crystals and liquid approaching zero) there are clearly detectable differences in their variation, and hence their behaviour.

Major-element variations in the obsidians are such that a vapour (fluid) phase would be needed to account for any magma evolution. The trace-element patterns are also impossible by closed-system crystal fractionation and suggest that this fluid may have been rich in halogens, with the metallic elements forming preferred 'complexes' with either F or Cl. The F–Zr–Rb 'complex' also varies quite independently of the important major oxides (e.g. Al_2O_3) in the rocks. In the case of Rb this is but one aspect of a more significant anomaly, in which there is no sign of any influence of alkali feldspar (which partitions Rb) in the variation. This is remarkable because trachytes and rhyolites have normative $ab+or > 50$ %, and any evolutionary process *controlled* by crystal $\rightleftharpoons$ liquid interactions must be dominated by the melting or crystallization of alkali feldspar. The results on the Eburru obsidians show that *if they are an evolutionary series* then *either*, the process was not crystal $\rightleftharpoons$ liquid controlled, *or* that any such process has been overriden (or buffered) by other processes that have superimposed the observed trace-element patterns. In the latter event, the buffering phase may have been a halogen-bearing vapour.

The same considerations must apply to other pantellerite provinces where Rb appears to have behaved as a 'residual' element.

IN recent years we have compiled all the available data on oversaturated peralkaline obsidians (Macdonald and Bailey, 1973) and set in train an analytical programme on all new samples that we have been able to obtain. Our own field sampling has been focused on the Nakuru–Naivasha region of Kenya, the topographic culmination of the East African rift, where there is an unparalleled development of Quaternary–Recent peralkaline volcanoes. In the trachyte to pantellerite composition range it had been demonstrated previously that the obsidians from different volcanoes showed systematic variations in major-element chemistry, but these variations were not consistent with

© Copyright the Mineralogical Society.

a fractional-crystallization model involving the observed phenocryst phases (Macdonald *et al.*, 1970). The best development of pantellerite magmatism is found in the Eburru volcano (Sutherland, 1971) just north-west of Lake Naivasha. Trace-element analyses of some of Sutherland's samples by Weaver *et al.* (1972) were used (with data from five other volcanoes) to argue that the relationships between trachytes and pantellerites are most reasonably explained by fractional crystallization. Subsequent examination has revealed, however, that the 'Eburru' specimens used by Weaver *et al.* were a mixed population (Bailey *et al.*, 1975).

Since 1970 we have collected and analysed obsidians from Eburru, which span the composition range from quartz-trachyte to pantellerite, and the major-element variation within this one volcanic pile cannot be explained by fractional crystallization of the phenocryst phases. The major-element evidence on quenched liquids is thus in direct conflict with the conclusions reached through the trace elements by Weaver *et al.* (1972). Trace-element analyses of our own Eburru samples form part of the long-term study of peralkaline obsidians, and they are now sufficiently far advanced to demonstrate that fractional crystallization *cannot* explain the variations. This demonstration, however, is only a subsidiary aim of the present article—our chief concern is to describe some unexpected relationships (especially involving halogens) which may provide some real clues to the secrets of this magmatism.

We shall look at a small group of trace elements (F, Cl, Zn, Nb, Zr, Yt, and Rb), which includes the two (Nb and Zr) considered most significant by Weaver *et al.* (1972). Our population is fifteen obsidians from quartz-trachyte to rhyolite: we are unable to include any basalts because we are restricting our study to glasses (quenched liquids). Actually, there are no contemporaneous basalts in the Eburru pile, although there is a Recent basalt field in the lowlands just to the north. We believe it would be begging the question to include these basalts with the Eburru magmatism until we have evidence other than geographic proximity to indicate that the two may be cogenetic (this problem is currently being studied by A. W. H. Bowhill, University of Reading: see also Bailey *et al.*, 1975, fig. 1). Correlations among the selected trace elements are moderately to strongly positive, whereas their correlations with major elements are generally poor. Although the major element ranges in the population are small (e.g. SiO_2 range from 66·2 to 72·0 per cent) the trace element ranges are large (e.g. Zr range from 1038 to 3058 ppm). Samples with essentially identical major-element chemistry show widely different trace-element levels, and the impossibility of reconciling these facts with simple fractional crystallization has been noted elsewhere (Bailey, 1973).

Trace-element relations. The limits, means, and concentration factors are listed in Table I. Trace-element values, sample points, rock names, and age relations are given in the Appendix.

The absence of basic rocks, with very low levels of the selected trace elements, is not a serious drawback to correlation analysis because in the case of the strongly concentrated elements, F, Zr, and Rb, the obsidian values span two-thirds of the possible range from the maximum observed down to zero. The results of the correlation analysis are given in matrix form in Table II.

TABLE I. *Limits, means, and concentration factors in 15 obsidians from Eburru, Kenya. Values in ppm*

	F	Cl	Zn	Nb	Zr	Yt	Rb
Minimum (m)	2910	2090	333	230	1038	195	131
Maximum (M)	7800	4290	537	542	3058	410	417
Mean	4900	3300	457	388	1910	307	252
Standard Deviation	1660	630	58	96	671	63	98
Maximum concentration factor (M/m)	2·68	2·05	1·61	2·36	2·95	2·10	3·18

TABLE II. *Correlation matrix for trace elements in the Eburru obsidians (all coefficients are positive). Plus or minus indicates the sign of the intercept of the best-fit line (reduced major-axis equation: Till, 1973) on the axis of the second variable in those cases where the 95 % confidence limits do not include the origin. Zero indicates that the origin falls within the 95 % confidence limits*

	F	Cl	Zn	Nb	Zr	Yt	Rb
F	1·000						
Cl	0·862(+)	1·000					
Zn	0·769(+)	0·879(+)	1·000				
Nb	0·955(+)	0·943(−)	0·909(−)	1·000			
Zr	0·994(0)	0·876(−)	0·817(−)	0·972(−)	1·000		
Yt	0·932(+)	0·954(0)	0·928(−)	0·995(+)	0·951(+)	1·000	
Rb	0·996(−)	0·853(−)	0·790(−)	0·959(−)	0·998(−)	0·937(−)	1·000

Implications of the trace-element distributions

The central tenet of the trace-element argument with respect to magma evolution, as propounded by Weaver *et al.* (1972), is that in a series of peralkaline liquids certain elements will be unable to enter the crystallizing phases, and will become progressively concentrated in the residual liquids. This assumes that the liquids are related by a process dominated by crystal ⇌ liquid interactions: we would claim that this itself needs to be proven, but for the moment let us examine the rest of the case. Zr is chosen as the prime example of a residual element because of: its high solubility in peralkaline melts (and insolubility in the major crystalline phases); its impassiveness to late-stage 'volatile effects'; and its abundance and high-precision determination by XRF (Weaver *et al.*, 1972). Consequently Zr is claimed to be a more useful index of differentiation than the more commonly used major-element indices. More assumptions are, of course, compounded in this claim. In the case of the Eburru rocks we cannot reconcile the claim with the major-element patterns (Bailey, 1973) and, moreover, we now cannot find support for it in our trace-element data.

Weaver *et al.* (1972) state that in the six volcanic centres they have tested the graphical plots of each of the elements Ce, La, Nb, and Rb against Zr are linear, and

project through the origin. They deduce from this (assuming that Zr is the archetype residual element) that the other four elements also have bulk distribution-coefficients (element concentration in combined crystal phases/concentration in liquid) close to zero. Compared with their data on Eburru (kindly provided by S. D. Weaver) our

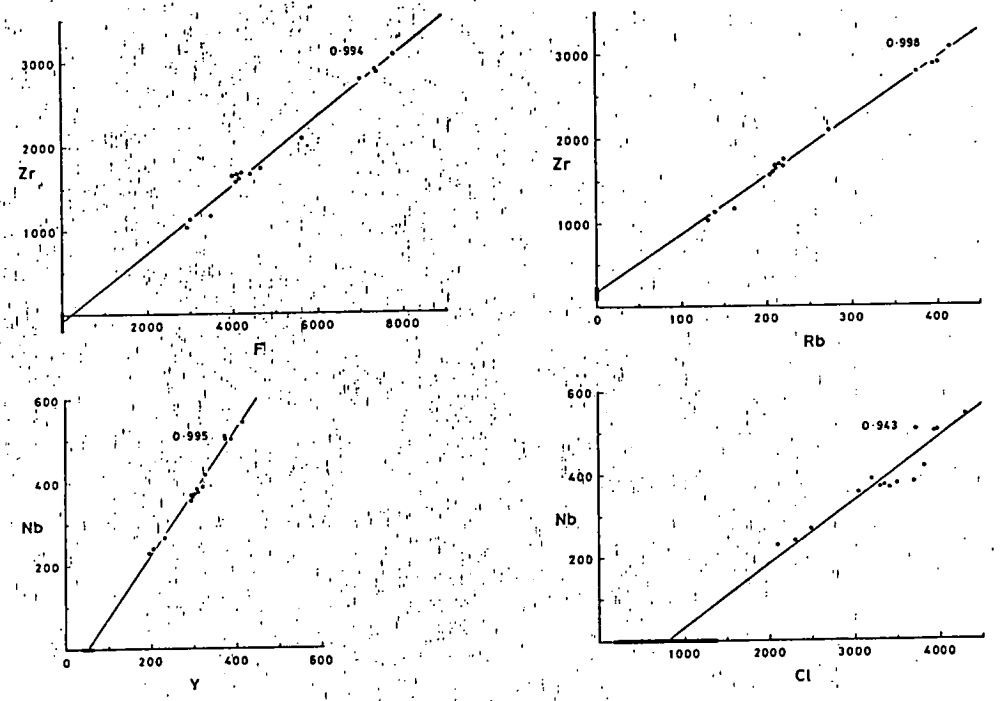

FIG. 1. Four examples of linear correlations of element pairs in the Eburru obsidians (solid circles). In every case the line is the computed reduced major-axis line and the heavy bar on the axis shows the 95 % confidence limits on the intercept. All values in ppm.

obsidian analyses show far less 'noise', more systematic variations, and higher correlation coefficients throughout. Our distribution patterns are quite different. Many are not linear, and most do not project through the origin. The latter are shown in Table II by plus and minus signs, to indicate the sign of the intercept on the axis of the second variable when the first variable reaches zero. Only those pairs of variables with a correlation coefficient better than 0·990 appear to be convincingly linear; these four are examined first.

Fluorine, zirconium, and rubidium. These three elements are the most strongly correlated, each pair providing a linear plot, two of which are shown in fig. 1.

In the case of F and Zr the calculated best-fit line passes close to the origin, which falls within the 95 % confidence limits. Assuming that Zr is the archetype residual element, then F too would have a bulk distribution coefficient close to zero, and constant throughout the series. The consistent behaviour of F would also indicate that the

population of obsidians is free of vagarious late-stage volatile losses, because our tests confirm the findings of Noble *et al.* (1967) that fluorine-loss is one of the most conspicuous effects of devitrification in this sort of lava.

The correlation of Rb with Zr, however, destroys the primacy of Zr as a residual element. The line misses the origin, making a positive intercept on Zr when Rb runs to zero. If this distribution is generated by crystal ⇌ liquid relations in a closed system then Zr must be fractionated (at a constant distribution coefficient) in the solid phases throughout the lava series. If Zr is held to have a distribution coefficient close to zero then the *system must be open to Rb.* Because, if the data are fitted to a fractional-crystallization model, then Rb increases in the residual liquids at a greater rate than Zr: if a fractional-melting model is adopted then the level of Rb must fall faster than Zr as the liquid volume increases. Either way, Rb has to move in or out of the system if Zr is behaving as a residual element. The same deduction, but without the precision, could have been made from the concentration factors in Table I.

In fact, the covariance of Rb and Zr shown in this range of obsidians is even more dramatic, because if the liquids were generated by fractional crystallization about two-thirds of the separating crystals would have to be alkali feldspar (based on normative *ab*+*or* in the trachytes) and the partition coefficient for Rb between alkali feldspar and liquid must be greater than zero. Relevant partition coefficients are available from Noble and Hedge (1970) for alkali feldspar phenocrysts and glassy matrices from peralkaline volcanics. They give values for the Rb partition coefficients in eleven peralkaline rocks, ranging from 0·25 to 0·45. Two of these determinations were made directly on separated phenocrysts and glass, giving values of 0·32 and 0·38 (1970, p. 235, Table, Samples 4 and 11*b*). Determinations of Rb have also been made on separated feldspars and glass from two Eburru rocks (PCO 134 and 135) giving partition coefficients of 0·41 and 0·31, respectively (Geochemistry Unit, Reading: analysts S. A. Malik and D. A. Bungard). Taking the average partition coefficient for Rb of 0·35 for alkali-feldspars/peralkaline-liquids, fractional crystallization (from a trachytic parent) in which 70 % of the separating crystals were alkali feldspar would result in a *bulk distribution coefficient* for Rb of 0·25. Fig. 2 is a graphical plot for Rb *v.* Zr to show the curve that would be generated by fractional crystallization when the bulk distribution coefficients for Rb and Zr are 0·25 and zero, respectively. The curve is calculated from a starting-point at 100 ppm Rb on the *actual* line and is developed by

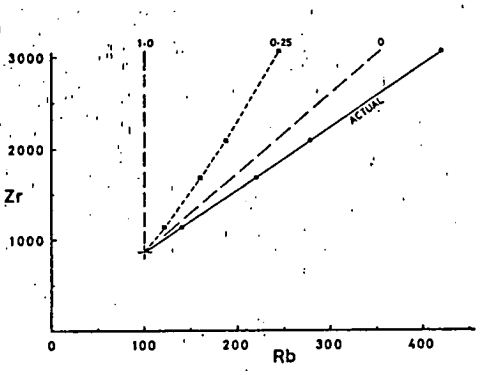

FIG. 2. Showing the difference between the actual array line for Rb *v.* Zr and that expected by fractional crystallization if the bulk distribution coefficient for Rb is finite whilst that for Zr is zero. In the latter case, taking a starting concentration of 100 ppm Rb, the points should lie between the broken lines 0 and 1·0 (if there is to be any concentration of Rb). The line 0·25 represents a reasonable case calculated on the basis of four-stage fractionation (solid squares) at intervals defined by Zr concentrations (solid circles) in the actual array.

four successive crystal crops at stages marked by *actual* Zr contents in the Eburru rocks. The highest calculated Rb value on the 'fractionation' curve is 244 ppm, which is only a little more than half the actual value (417 ppm) for the same Zr content. It is glaringly obvious from fig. 2 that either Zr is *not* a reliable index of differentiation, or fractional crystallization *cannot* account for the covariance of Rb and Zr, or *both*. All evidence available to us favours the third conclusion!

Niobium, yttrium, and chlorine. There is good correlation between Nb and Yt; the plot, shown in fig. 1, is linear within the limits of experimental error, with a narrow 95 % confidence band. The calculated line does not pass through the origin. If it were assumed that crystal fractionation controls the series, and Nb has a distribution coefficient close to zero, the sample array might be explained by Yt having a significantly higher distribution coefficient. The only phase that might be separating throughout the whole series is alkali feldspar, which would not normally be suspected of fractionating Yt with respect to Nb. Furthermore, neither Nb nor Yt shows a simple linear relation with Zr, which adds further complications to the model.

Nb and Yt both show reasonably linear correlations with Cl. The graphical plot for Nb *v.* Cl, shown in fig. 1, reveals a high positive intercept of the computed line on the Cl axis. This has the same implications for fractional crystallization as the Nb *v.* Yt array. It should be noted that if a fractional-melting evolution model is applied to these data, and Nb is taken to have a distribution coefficient of zero, then the system must be open to the ingress of Yt and Cl.

Yt *v.* Cl gives a similar pattern to Nb *v.* Cl but the line runs through the origin (within the 95 % confidence band).

Non-linear patterns, and covariance with fluorine and chlorine. Examination of the correlation matrix (Table II) shows that in addition to the four coefficients better than 0·990, there are a further ten better than 0·900. Nb and Zr are the best of this group with a coefficient of 0·972. But when graphical plots of these pairs of variables are made it emerges that many of these correlation coefficients are not lower (i.e. $< 0{\cdot}990$) due to random deviations from the line (as might be argued, for instance, for Nb *v* Cl, fig. 1). The lower coefficients for many pairs of elements result from *patterned*, but *non-linear* arrays of points. Examples are depicted in fig. 3, in which it may be seen that each computed best-fit line has been achieved by balancing a cluster of points in the middle of the array against points at the extremities. These are certainly not random patterns. The most obvious case is F *v.* Cl, with a relatively low correlation coefficient of 0·862, where a better description of the array would be an inflected line. The fact that this pattern is matched by Nb *v.* Zr, elements of a completely different kind, determined by a completely different method, must rule out the possibility that the arrangement is fortuitous. Fig. 3 confirms what was implicit from fig. 1 and the earlier discussion, namely, that Zr varies linearly with F (and Rb), that Nb varies linearly with Cl (and Yt), but between these groups of elements there is a marked inflection in the pattern of distribution. The complexity of the element covariances within these two groups, coupled with this additional complication of the relationships between the groups, rules out any rational *closed-system* (isochemical) evolutionary model. Such a conclusion is entirely consonant with those reached earlier on the

basis of major-element variations (Macdonald *et al.*, 1970) and comparisons of major and trace elements (Bailey, 1973).

Before considering alternative explanations for the chemical variations in the Eburru obsidians, the anomalously high, and seemingly erratic, zinc distribution needs comment (fig. 3). Firstly, Zn can be determined with high precision by XRF.

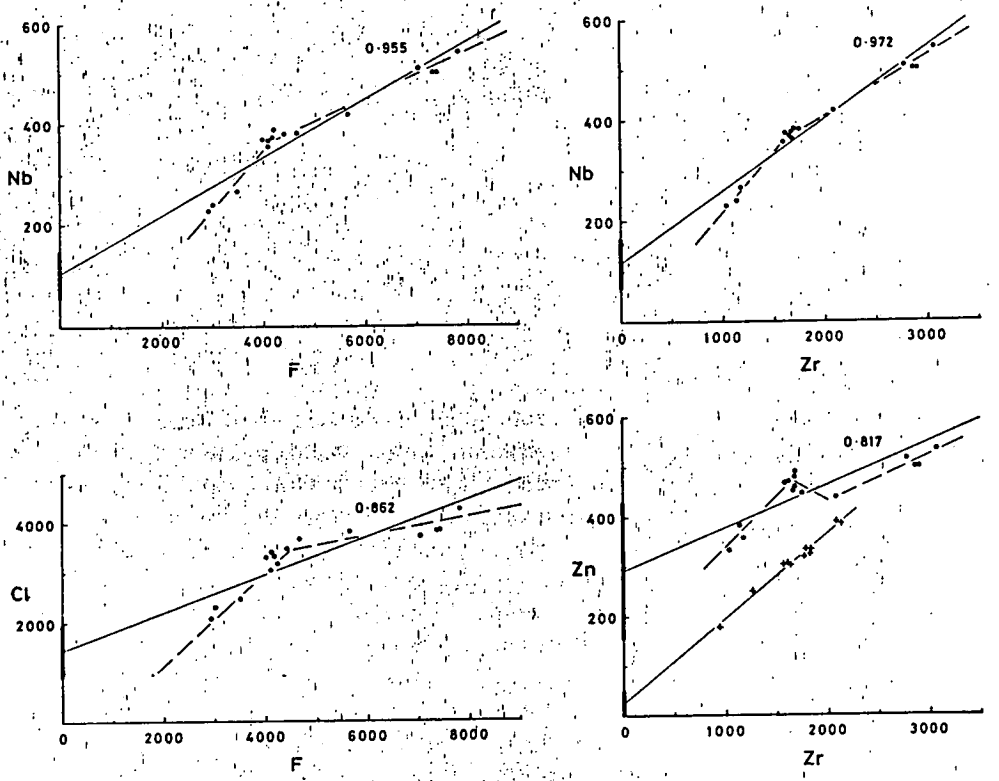

FIG. 3. Four examples of non-linear arrays in the Eburru obsidians. Solid circles, continuous lines, and heavy bars as in fig. 1. The broken lines represent preferred descriptions of the variation in each case. In the Zn *v.* Zr plot the plus signs are comendite obsidians from the Naivasha volcanic area (see text).

Secondly, the limiting Zn values in fig. 3 were checked by atomic absorption, with good agreement. Thirdly, the high levels, and the variability, of the Zn values in the Eburru samples, are not due to vagaries of sampling, sample preparation, or analytical method, because the second data set (plus signs) in fig. 3 represent comendite obsidians from the Naivasha volcanic area, just south of Eburru. These were collected, prepared, and analysed with the Eburru samples, so we are seeing a genuine Zn anomaly in the Eburru rocks. Fourthly, the broad scatter of the Zn values about the best-fit line in fig. 3 is confirmed by later results on other samples (not yet analysed for F and Cl)—the impression given by this pattern is of a second-order fluctuation in Zn concentration superimposed on a main trend indicated by the line. The general

form of the Zn distribution, when plotted against Zr, resembles that of Yt, Nb, and Cl against Zr, except that the general high levels of Zn are more obvious. Indeed, Zn shows its strongest correlations with Yt, Nb, and Cl, in that order (see Table II) so that similar factors, either at source or during magma generation, or both, have presumably influenced all four elements, but to different degrees. At present we have no evidence to suggest possible causes of the second-order fluctuations in the Zn pattern.

As a final point it should be noted that inflected patterns similar to those among the trace elements (shown in fig. 3) also emerge when some major elements (and their functions) are plotted against Zr. Examples are Al_2O_3, TiO_2, and agpaitic index $(Mol(Na_2O+K_2O)/Al_2O_3)$.

An open-system model

In our earlier paper on the major-element patterns in the range pantelleritic trachyte to pantellerite (Macdonald *et al.*, 1970) we had to conclude that *if the rocks were an evolutionary series* a phase now missing from the rocks must have played a major part in the evolutionary process. The Eburru obsidians fall into the previously defined major-element patterns and the same conclusion applies. Furthermore, the trace-element patterns are now found to be incompatible with closed-system evolution. We concluded from the earlier major-element studies that if the rocks had been generated by a series of melting episodes then a separate vapour (fluid) phase had contributed Na (and possibly Si and Fe) to successive silicate liquids. Our reasons for preferring a fractional-melting model were given in that account (Macdonald *et al.*, 1970): a further reason in the Eburru rocks is that the chemical variations do not seem to fit any regular pattern in the development of the volcano. It would be premature to try to elaborate this model much further until all our data are in, but some additional conclusions from the present trace-element distributions are in order.

It is clear that a simple fractional-melting model could not generate most of the observed trace-element patterns. For instance, most of the correlation lines do not pass through the origin, which would be the first requirement for 'residual' elements. In such cases, where the correlation is linear (fig. 1) the line could be interpreted as a product of simple mixing, but the true picture must be more complex because some patterns are inflected (fig. 3). The most significant feature is the affinity of Zr and Rb with F, and the *separate* affinity of Nb, Yt, and Zn with Cl: judging by the inflected variation patterns between these two groups they would seem to have some degree of independence throughout the rock series. One possibility is that the metallic elements form preferred complexes with either fluorine or chlorine, and the partitioning of these complexes between vapour (fluid) and silicate melt varies with the melting conditions (e.g. relative volumes of melt to vapour, variations in melt or vapour compositions, temperature, and pressure). We are investigating this and other possibilities by: further analyses of Eburru rocks and extracted gases; experimental determination of melting, crystallization, and volatile exsolution; and by studies of obsidian suites from other volcanoes.

Another remarkable feature of the Eburru rocks is the Rb variation, which shows no recognizable contribution from alkali feldspars in contact with the melt (yet

alkali-feldspar phenocrysts are normal). If a coexisting vapour phase contributing Rb (and Zr and F) is accepted, the Rb patterns in the rocks suggest that the effect of this vapour is paramount. It is as if the melts were buffered for Rb. The fact that a key major element such as Al gives inflected variation patterns when plotted against Zr, Rb, and F also suggests that the concentrations of these elements are controlled by some factor other than those that determine the major-element distributions in the magmas.

Finally, one general point may be made concerning F and Cl in peralkaline magmas. It is commonly argued by advocates of fractional crystallization, that the high concentrations of Zr that distinguish peralkaline from subaluminous magmas are due to the solubility of Zr in peralkaline melts, and their consequent failure to precipitate zircon during crystallization. But how, then, is it possible to account for the high concentrations of F and Cl that equally distinguish these same peralkaline melts from other oversaturated magmas? We believe that the very high correlation of Zr and F in our samples exposes this as an artificial dilemma, and we appeal to fellow petrologists and petrochemists to critically reappraise some of the time-honoured concepts of magma evolution.

Acknowledgements. Wet chemical analyses for F and Cl were made by S. A. Malik and D. A. Bungard; XRF analyses for Zn, Nb, Zr, Yt, and Rb by G. J. Smith and N. I. Tarrant. We are indebted, too, to Dr. A. Parker who set up the XRF routines, calibration methods, and computations, and to Dr. R. Till and Mrs. J. Webber for the correlation programme and its operation. A. Parker, J. E. Thomas, and R. Till improved the final manuscript by their valuable comments on the first draft.

REFERENCES

BAILEY (D. K.), 1973. *Journ. geol. Soc. Proc.* **129**, 649.
—— WEAVER (S. D.), and SUTHERLAND (D. S.), 1975. *Contr. Min. Petr.* **50**, 47–8.
MACDONALD (R.) and BAILEY (D. K.), 1973. *U.S. Geol. Surv. Prof. Paper*, 440N–1.
—— —— and SUTHERLAND (D. S.), 1970. *Journ. Petrology*, **11**, 507–17.
NOBLE (D. C.) and HEDGE (C. E.), 1970. *Contr. Min. Petr.* **29**, 234–41.
PARKER (A.) (unpubl.). *Geol. Dept. Univ. of Reading.*
SUTHERLAND (D. S.), 1971. *Journ. geol. Soc. Proc.* **127**, 417.
THOMAS (J. E.), BUNGARD (D. A.), and MALIK (S. A.), 1975. *Univ. Reading Geol. Reports*, 6.
TILL (R.), 1973. *Area (Inst. of Brit. Geographers)*, **5**, 303–8.
WEAVER (S. D.), SCEAL (J. S. C.), and GIBSON (I. L.), 1972. *Contr. Min. Petr.*, **36**, 181–94.

[*Manuscript received 21 August 1974; revised 5 June 1975*]

APPENDIX. *Trace-element values (ppm) in 15 Eburru obsidians*

Sample	F	Cl	Zn	Nb	Zr	Yt	Rb	Co-ordinates	Age group
PCO082	4000	3300	454	370	1653	294	212	AK 966 332	c
PCO083	4100	3400	467	367	1664	296	211	AK 956 323	c
PCO084	3000	2300	384	240	1137	203	139	AK 971 329	b–c
PCO129	4650	3680	448	381	1748	305	220	AK 943 297	d
PCO130	4200	3190	491	389	1697	318	213	AK 933 363	b
PCO131	7020	3710	519	508	2776	371	377	BK 001 398	a–b
PCO132	4400	3480	480	379	1679	305	218	AK 950 279	d
PCO133	4150	3330	472	372	1608	300	208	AK 954 295	d
PCO134	5630	3810	440	419	2091	324	273	AK 965 242	d
PCO135	4090	3040	469	357	1593	292	206	AK 974 229	a?
PCO161	7390	3930	501	502	2865	383	397	BK 037 323	a
PCO162	7370	3930	503	502	2880	375	402	BK 039 329	a
PCO163	7800	4290	537	542	3058	410	417	BK 022 263	a
PCO164	3480	2480	359	269	1168	230	162	AK 910 362	b
PCO165	2910	2090	333	230	1038	195	131	AK 905 374	b

Methods: F and Cl; determined colorimetrically (Thomas *et al.*, 1975). Zn, Nb, Zr, Yt, Rb; determined by XRF (Parker, unpub.), using U.S.G.S. Standard Rocks (G2, GSP1, AGV1, PCC1, DTS1, BCR1) for calibration.

Co-ordinates: 1000 m Universal Transverse Mercator Grid Clarke 1880 (Modified) Spheroid. Grid Zone Designation 37 M. The 100 000 m Sq Identification is given by the prefix letters: easting and northing by the final six digits. As used on Survey of Kenya maps.

Age groups: a–d: oldest–youngest. Broad groupings only are possible because many flows do not overlap to give precise relationships.

Rock descriptions. The suffix (P) signifies rare feldspar phenocrysts: in such rocks there are usually abundant microphenocrysts. Full modal data will be published later, with the major element analyses.

PCO082 See Macdonald and Bailey (1973), Anal. 82.
PCO083 See Macdonald and Bailey (1973), Anal. 83.
PCO084 See Macdonald and Bailey (1973), Anal. 84.
PCO129 Obsidian
PCO130 Obsidian (P)
PCO131 Obsidian
PCO132 Obsidian
PCO133 Obsidian
PCO134 Glassy lava with abundant phenocrysts of feldspar, quartz, and aenigmatite, and rare clinopyroxene.
PCO135 Glassy lava with phenocrysts of feldspar, aenigmatite, and clinopyroxene.
PCO161 Obsidian
PCO162 Obsidian
PCO163 Obsidian. Same locality as Anal. 89, Macdonald and Bailey (1973).
PCO164 Obsidian (P)
PCO165 Obsidian (P)

Proceedings of the Regional Seminar on

GEOTHERMAL ENERGY

in Eastern and Southern Africa

15-21 June 1982
Nairobi, Kenya

Full Proceedings

United Nations Educational Scientific and Cultural Organisation
United States Agency for International Development

(1983)

Magmatic and Structural Evolution of the Central Part of the Kenya Rift

L.A.J. Williams, R. MacDonald and P.T. Leat

or the purpose of this paper, the central part of the ift is taken to be the NNW-trending section between °S and the equator. A long history of volcanism in iis region, spanning some 1.5 million years, ulminated in intense Quaternary activity.

In view of their importance in determining the ost favourable sites for geothermal exploration, ie Quaternary silicic complexes in the floor of the ift demand special consideration in a review of ie magmatic evolution of the region. This contribu- on provides, therefore, a brief commentary on field nd laboratory investigations being carried out by ie authors in collaboration with Professor D. K. ailey (University of Reading).

The Lancaster-Reading work overlaps and extends wider project in northern and southern Kenya (East frican Geological Research Unit) directed by rofessor B. C. King (formerly Bedford College, niversity of London) and one of the present authors LAJW). Detailed maps and memoirs covering some 0,000 km² of the Rift north of the equator will be ublished in the near future by the Geological Survey f Kenya.

Valuable information on the south of the present egion comes from a reassessment of the strati- raphy, geochronology and evolution of the eastern ift margin (Baker and Mitchell, 1976; Baker, rossley and Goles, 1978) and the western side of he Magadi trough between the Mau Range and the anzanian border (Crossley and Knight, 1981). here are no published accounts of the volcanics orming the Mau highlands, but the results of a apid survey carried out 20 years ago will appear oon (Williams, Report 96, Geological Survey of enya).

HYSIOGRAPHY AND STRUCTURAL SETTING

ver much of the region under discussion, the Rift is well-defined 70-km wide trough bounded on its astern side by the NNW-SSE Sattima fault, and to ie west by faults and monoclinal flexures which ombine to form the Mau Escarpment. The latter ies out as a distinct feature at about the latitude of akuru, and between there and the equator the estern margin is more difficult to define. The chief structural element in this part of the area is a long-active flexure, but downwarping outpaced volcanic accumulation only at a very late stage so that the present slope into the Rift is a recent feature (Jones and Lippard, 1979). Near the equator, Londiani and other Tertiary volcanoes mask the junction between the main Rift and the Nyanza (formerly Kavirondo) trough which branches westwards to Lake Victoria.

The most recent volcanics are largely confined to an inner graben about 30 km wide (the Naivasha-Nakuru trough) which is separated from the eastern boundary of the Rift by the Bahati-Kinangop step-fault platform (Figures 1 and 2). The Bahati block is terminated by N-S faults near Nakuru, a change to NNE trends at the equator marking the beginning of what is conveniently termed the northern section of the Rift. At 1°S, faults swing to nearly meridional trends as the structures pass southwards into the Magadi trough.

The Rift floor reaches its maximum altitude of some 2000 m between Naivasha and Nakuru. It declines southwards to about 1500 m at 1°S, and it slopes down to a similar elevation just north of the equator. The topographic culmination is undoubtedly in part a consequence of the rapid accumulation of volcanics from closely-spaced centres. On a regional scale, however, the floor continues to descend, standing at an altitude of about 600 m at the Tanzanian border in the south and below 300 m at Lake Turkana (Rudolf) in the north. Quaternary volcanics extend along the full length of the Rift depression, but the extent to which they thicken towards the Naivasha-Nakuru section has yet to be demonstrated. It is unwise, therefore, to reject tectonic processes as contributory factors involved in the production of the topographic culmination in the Rift floor. Tilting caused by late-stage differential movements on the Rift boundary faults would provide one plausible explanation for the sloping floors. This mechanism, rather than regional doming, was preferred by Crossley (1979) in a discussion of the southern part of the Rift.

The shoulders of the Rift rise to altitudes of over 3000 m in the Mau Range to the west, and to nearly 4000 m at peaks in the Aberdare Range beyond the

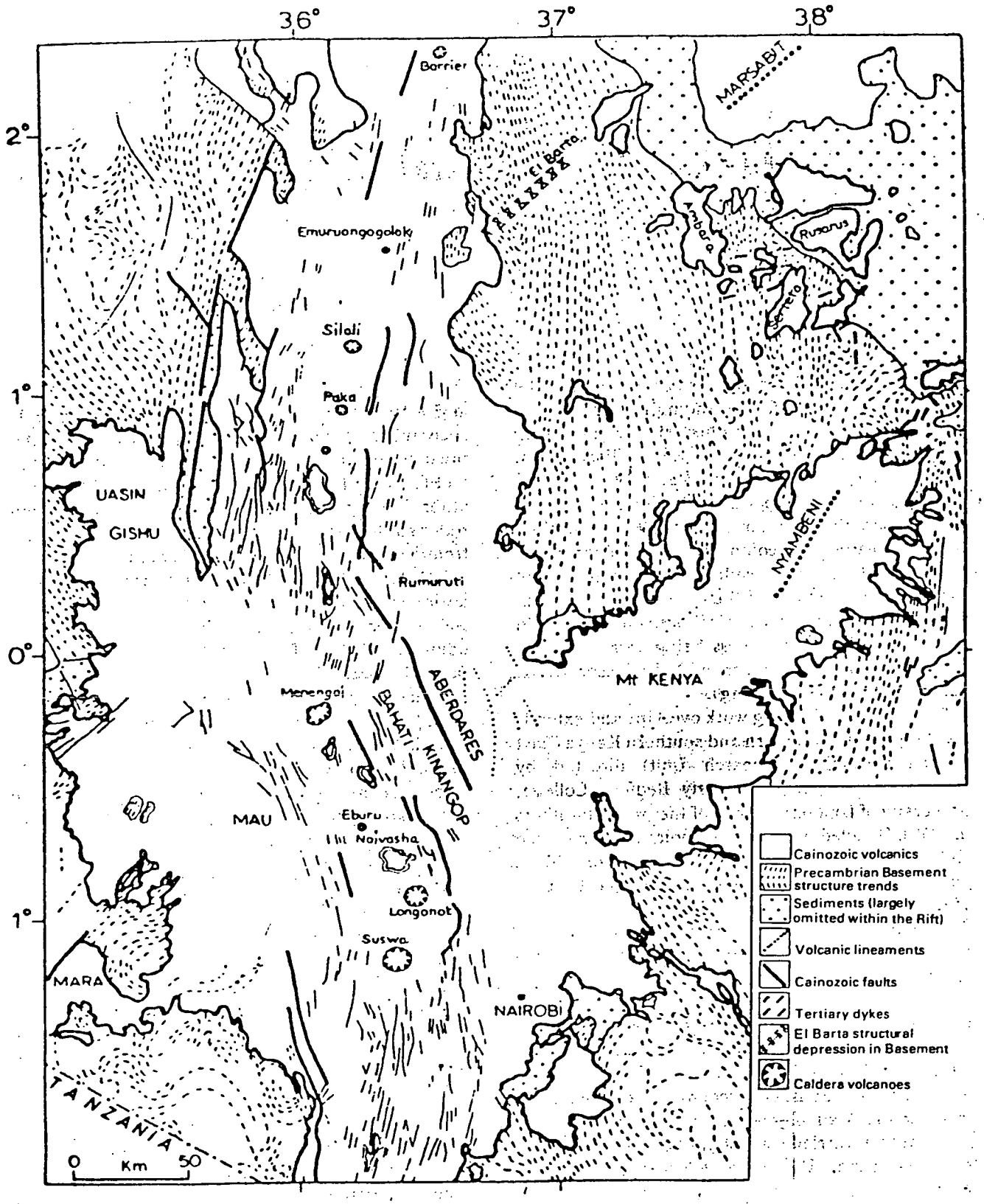

Figure 1. Structural Map of the Kenya Rift

Kinangop-Bahati platform; much of the latter stands above 2500 m. All the high ground flanking the Rift in this part of the country is made up of Cenozoic volcanics. The underlying Precambrian basement rocks are not exposed in the boundary scarps or within the trough in central Kenya. Moreover, the basement gneisses have not been encountered in boreholes drilled to depths of 1300 m in the Rift floor.

West of the Rift, inliers of basement at the southern end of the Mau Range show that the altitude of the sub-volcanic surface is about 1800 m, and that it declines steadily inwards before being lowered by faults defining the margin of the trough. An inward slope of the basement surface can also be demonstrated on the eastern side of the Rift from borehole evidence in the Nairobi area, about 60 km SE of

Longonot. The basement rocks there lie beneath some 500 m of volcanics, the contact occurring at an altitude of nearly 1200 m. Although the basement probably continues to descend westwards towards the Rift margin, thickening of the volcanics to possibly 1500 m causes the present ground surface to rise steadily in that direction. The depth to basement beneath the Aberdare Range, east of the Sattima faults, is unknown, but the total thickness of volcanics forming this major basaltic complex must amount to at least 2000 m.

Detailed mapping north of the equator has shown that basement within the Rift probably lies at about 2500 m below sea level. The displacement between flanks and floor in central Kenya is, therefore, at least 4000 m, much of this being attributable to downward movements (King, 1978).

The highland regions bordering the central section of the Rift constitute part of what has become known as the 'Kenya dome'. Early views (e.g. Baker and Wohlenberg, 1971) favoured an origin through pulses of domal uplift but, for reasons mentioned above, the term is now commonly used to describe a topographic feature produced more by volcanic accumulation than vertical uplift (King, 1978). It is important to realize, however, that late uplifts and tilts of the Rift shoulders have never been rejected as important events: such movements are demanded by geomorphological as well as structural evidence.

TERTIARY VOLCANISM AND STRUCTURAL HISTORY

Much of the evidence bearing on the early history of the Rift in this region lies concealed beneath a thick cover of young volcanics and sediments, but it is clear that the initial depression was a broad downwarp along the crest of previously uparched basement rocks. This depression was certainly in existence by 15 Ma, but it was subsequently infilled by Miocence phonolites. Around 12—13 Ma, these voluminous and extremely fluid lavas spilled over to flow eastwards through the Nairobi region, and westwards across at least part of the Mau-Molo area. Published maps show representatives of the 'plateau' phonolites in the Bahati area, but current studies suggest that at least some of these flows belong to younger groups. It follows, therefore, that the total thickness of Rift infill is much greater than was envisaged during reconnaissance investigations. This has proved to be the case farther north where the Tertiary sequence alone is some 3000 m thick (Chapman, Lippard and Martyn, 1978).

The precise age-range of the predominantly basaltic volcanics of the Aberdares remains unknown. In eastern outcrops, agglomeratic units on the fringes of this massive complex rest on an extensive flow of Miocene phonolite (13 Ma), but it is not unlikely that early activity of the Aberdare volcano preceded or accompanied the period of plateau phonolite overspill from the Rift. An upper age limit

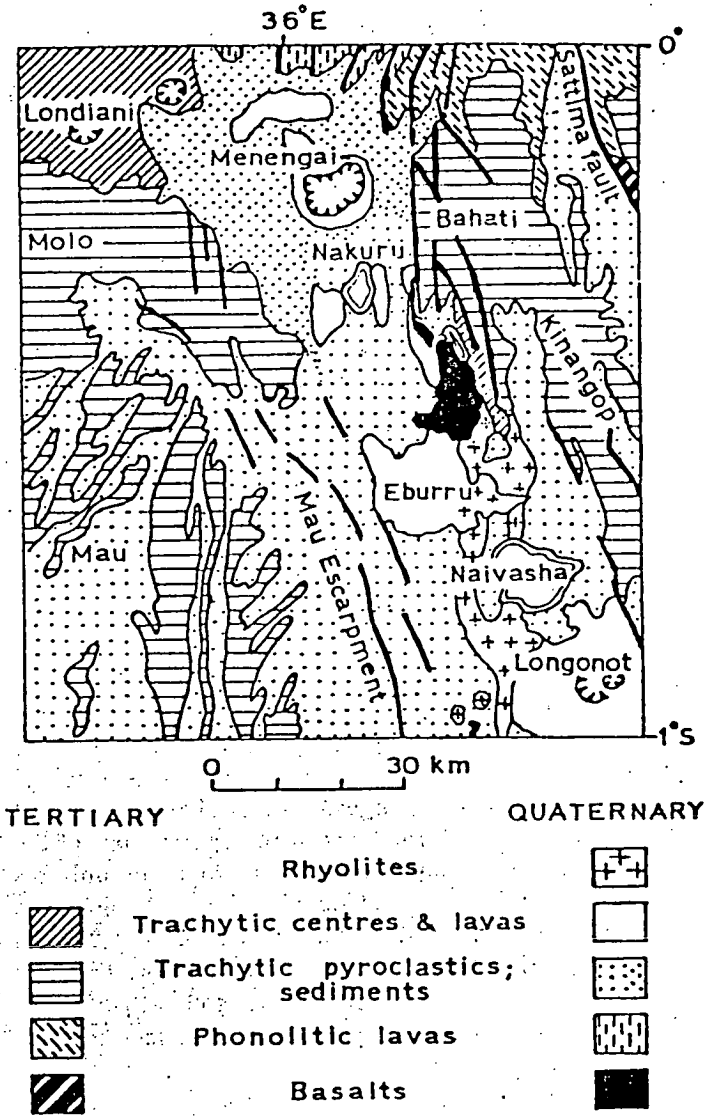

Figure 2. Simplified Geological Map of the Central Part of the Kenya Rift.
(Close stipple = Menengai ignimbrite)

of about 7 Ma for the main basaltic pile can be inferred from relationships on the northern flanks of the volcano, but renewed activity in the Pliocene left a widespread veneer of basalts derived from numerous vents. These younger (Laikipian) basalts are underlain locally by trachytic flows (Sattima series), closely related to intrusive sheets emplaced in the older (Simbara) basalts of the complex (Shackleton, 1945). The significance of trachytic tuffs at the northern end of the Aberdare Range is discussed later.

The Sattima fault-scarp reveals thick trachyphonolite (Thomson's Falls phonolites) banked against the Simbara basalts. Similar phonolitic lavas exposed west of the fault pass beneath extensive welded tuffs of the Bahati platform. McCall (1967) reported difficulty in distinguishing the Thomson's Falls flows from what he mapped as local representatives of the Miocene (Rumuruti) phonolites, concluding that interdigitation of the two units occurs near the top of the plateau phonolite sequence. The Rumuruti phonolites in the type region much farther

north have yielded dates in the range 10—12 Ma, but a single determination on the Thomson's Falls lava gave a result of about 6.5 Ma (Baker et al., 1971). A possible explanation for the apparent discrepancy in the dates comes from detailed mapping in the Lake Bogoria (Hannington) area north of the equator (Griffiths, 1977). It was shown that some of the phonolitic lavas previously considered to belong to the Rumuruti group are in fact members of a formation which had not been recognized during the earlier reconnaissance work. This Tasokwan Formation (6.5—7.5 Ma) consists essentially of phonolitic trachytes which rest unconformably on the Rumuruti phonolites and underlying Samburu basalts. The Tasokwan lavas were traced into the Marmanet region, about 20 km north of the equator, but their distribution between there and the northern parts of Bahati has yet to be established. The view that at least some of the lavas underlying Bahati are of Tasokwan age is supported by a K-Ar date of 6.2±0.2 Ma for the 'Rumuruti' phonolitic trachyte at Sabukia, NE of Menengai.* It follows that basalts patchily exposed beneath the phonolitic lavas do not necessarily belong to the Samburu group as suggested on published maps.

The Pliocene formations in the central part of the Rift are made up largely of trachytic ignimbrites which have yet to be subjected to detailed study. The Bahati tuffs from the eastern flank of the Nakuru trough, rising some 800 m above the floor. They are heavily mantled with red lateritic soils attributed to prolonged 'end-Tertiary' erosion. The lack of thick red soils across the Kinangop platform shows that the uppermost pyroclastics there are younger than those of Bahati. A K-Ar date of 3.3 Ma (Baker et al., 1971) suggests that the lower part of the Kinangop sequence is broadly equivalent to the Lower (lava) and Middle (ignimbrite) trachyte divisions of the Nairobi area (Saggerson, 1970) lying outside the Rift to the SE. Thus, by mid-Pliocene times, the Rift depression had been largely infilled by trachytic volcanics which spread far beyond the margins. The Aberdare complex remained a substantial barrier but tuffs, tentatively correlated with those of the Bahati area, are preserved on the northern flanks.

Overspill of trachytic volcanics on the eastern side of the Rift culminated in the eruption of lavas (Limuru trachytes; about 2 Ma), the uppermost flows of which passed unhindered eastwards to Nairobi. They are exposed in the scarps framing the Kedong embayment, just east of the map area at 1°S, but they never flooded the Kinangop; the present platform must have started to form at the end of the Pliocene. The arcuate Kedong scarps are quite unlike structures seen elsewhere in the Rift. One interpretation (Williams, 1978a) of the fault pattern invokes control by a Plio-Pleistocene caldera some 35 km across, taking the Nairobi and Kinangop trachytic volcanics as the eastern and northern flanks of a gigantic shield.

Pliocene ignimbrites are well represented in sequences on the western side of the Rift, and they can be traced from Molo southwards across the Mau. In westernmost outcrops, beyond the area covered by Figure 2, welded tuffs rest on Miocene plateau phonolites, overstepping locally on to basement rocks. Near Molo, the trachytic ignimbrites overlie older phonolitic tuffs (8 Ma), the youngest unit of a long-active Miocene strongly alkaline complex centred on Timboroa (Jones and Lippard, 1979). In this area, the Mau tuffs yielded dates of about 6 Ma, but some of the ignimbrites at the southern end of the Mau Range can be correlated with units in the Narok area which were erupted over the period 2—4 Ma (Crossley and Knight, 1981). Most of the Mau tuffs probably came from now-concealed sources within the Rift. Some of the northern flows may have been erupted during early activity at Londiani trachyte volcano, but the present low-angle cone consists chiefly of lavas (3 Ma). Summit calderas are preserved on Londiani and the nearby Kilombe trachytic centre (2 Ma); both volcanoes are tilted gently towards the Rift.

CHRONOLOGY OF FAULTING

A first major episode of faulting at about 7 Ma has been demonstrated in widely separated areas along the western side of the Rift, the movements coinciding with important changes in the compositions of the volcanics. North of the equator, phonolites and subordinate basanites were followed by members of basalt-trachyte suites (Chapman, Lippard and Martyn, 1978). The trachytic volcanism of the Londiani-Molo region replaced nephelinite-phonolite activity after Miocene faulting at the eastern end of the Nyanza (Kavirondo) trough (Jones and Lippard, 1979). In southern Kenya, nephelinites and phonolites were largely superseded by basalts and trachytes, though some strongly alkaline activity continued after faulting at approximately 7 Ma.

The timing of early faulting along the eastern side of the Rift can be defined with some precision north of the equator where formations dating back to at least 17 Ma have now been mapped in considerable detail (for references see King, 1978; Williams and Truckle, 1980). Faulting commenced during eruptions of the oldest (Samburu) basalts, and continued through the period of subsequent plateau phonolite activity which extended to 10 Ma along the eastern margin of the Rift. Major faulting, broadly corresponding to the 7 Ma event on the western side of the Rift, occurred before eruption of the Tasokwan phonolitic trachytes. Eastward flow of these lavas was restricted by fault-scarps at the latitude of Lake Bogoria, but farther south the Thomson's falls trachyphonolites of about the same age flowed around the northern end of the Aberdares. It is un-

*Dr J. G. Mitchell, University of Newcastle upon Tyne, personal communication.

kely, therefore, that the Sattima fault existed as a ignificant feature at that time. Some movement on he fault may have taken place before eruption of the 3ahati-Kinangop ignimbrites (age-range unknown, ut probably 3—4 Ma), judging by the attenuated equence of trachytic tuffs preserved on the NW lanks of the Aberdares: but the main displacement ccurred during the Pleistocene.

The Sattima fault dies out at about 0°45'S, and arther south the boundary scarps of the Rift are a ranching continuation of the fault system which harply defines the western margin of the Kinangop lateau near Naivasha. In common with many other arts of the Rift, the youngest major movements on hese boundary faults are demonstrably of Pleisocene age. Baker and Mitchell (1976) concluded that aults displacing the Limuru trachyte west of Nairobi vere active during the period 1.65—1.9 Ma. They lso argued that an earlier movement on the fault runcating the Ngong nephelinitic volcano (not preisely dated, but probably about 6 Ma) took place etween 2.3 and 3.3 Ma. The lower age limit is somehat equivocal, and further work could well lead to lownward adjustment. It is quite possible that some f the early movements on the Ngong and Sattima aults were broadly synchronous with an important ost-Tasokwan event (4—6 Ma) in the Lake Bogoria rea north of the equator (Griffiths, 1977).

A thick cover of late Quaternary ashes across the Mau makes it extremely difficult to establish the full ectonic history of the western margin of the Nakuru-Naivasha trough. Nevertheless, the evolution of lrainage patterns on the ash surface is instructive in roving the recent age of much of the uplift and ilting of the Rift shoulders (Williams, 1978a).

Though detailed discussion of the evidence bearng on fault chronology in the floor of the Rift is eyond the scope of this article, it is important to ealize that several episodes of Quaternary faulting an be demonstrated locally. For instance, facing tructures SE of Nakuru show that basalts and rachytes erupted within the trough were banked gainst pre-existing scarps and were subsequently runcated by renewed faulting, one major event ccurring post-1.2 Ma.

LATE QUATERNARY VOLCANISM

ntense Quaternary volcanism along the Nakuru-Naivasha trough culminated in the construction of rachytic caldera volcanoes at Menengai and Longonot, and the emplacement of silicic complexes in the ntervening area around Eburru and Naivasha. Subrdinate basaltic activity occurred on the flanks of Eburru. Over the last decade, much of this region as been studied in detail by teams from the universities of Lancaster and Reading.

Scott (1980) recognized the following sequence of vents at Longonot:

. Construction of a large peralkaline trachyte composite cone having a basal diameter of some 30 km and a volume of about 280 km³.
2. Caldera collapse accompanied by pyroclastic activity.
3. Eruption of interesting mixed lavas (hawaiite-peralkaline trachyte).
4. Growth of a trachyte lava cone, about 10 km across, on the eastern side of the caldera.
5. Explosive eruption of ash and pumice from the cone, followed by summit collapse.
6. Eruption of mixed hawaiite-trachyte lavas within the crater.
7. Lateral eruption of two trachyte lava flows 200—300 years ago.

Further geochemical and mineralogical studies are in progress. One of us (PTL) recently supplemented Scott's study by tracing an ash-flow tuff erupted during collapse of the early caldera at Longonot.

West of Longonot, the Lake Naivasha field (Bliss, 1979) consists of a series of comendite flows, domes and pyroclastics representing the voluminous (13 km³) eruption of rhyolitic magma over about the last 20,000 years. A full report on the geology, geochemistry and evolution of the Naivasha complex is in the final stages of preparation by one of the present authors (RM). One significant conclusion of this work is that the area is underlain by a substantial magma chamber which may eventually evolve to the stage of caldera collapse. Moreover, collaboration between Bliss and Scott made it possible to establish a direct correlation between units in the Longonot and Naivasha sequences.

Beyond Lake Naivasha, Eburru stands out as a buttress from the Mau Escarpment. The complex trachyte-rhyolite massif is surmounted by a multiple crater system, but it has no recognizable caldera. The western parts of the volcano are thickly mantled with ashes, but rhyolite domes form prominent features on the eastern side. To the north, the youngest basalt flows surround and engulf older faulted cinder cones, some of which have large explosion craters produced by phreatic eruptions. Here and elsewhere along the floor of the Rift, relationships between volcanics and lake sediments have proved important for purposes of correlation. Eburru formed an effective barrier separating the Nakuru and Naivasha lake basins, and complete understanding of the evolution of the complex is essential in attempts to relate events in other parts of the trough. The most recent investigations of the Eburru volcanics, involving comparisons with those at Naivasha and Longonot, show that the three complexes are chemically distinct.*

One of the authors (PTL) is studying Menengai and adjacent parts of the Nakuru area. An important

*Professor D. K. Bailey, University of Reading, personal communication.

feature of the work has been the recognition of an extensive ignimbrite flow (Figure 2) covering 1000 km² of the floor of the trough, and extending locally on to its flanks. Geochemical and mineralogical studies of the Menengai volcanics revealed a complex magmatic evolution of a type unique to these central Kenya volcanoes. A proposed model involves phases of magma mixing, crystal fractionation and thermo-gravitational diffusion.

DISTRIBUTION OF VOLCANICS AND MAGMATIC EVOLUTION

The following points deserve consideration in efforts to unravel the complex evolutionary patterns displayed by the volcanics of the Kenya Rift:

1. Along the entire length of the Rift, there are no strongly undersaturated phonolites younger than 7 Ma, apart from the distinctive types (phonolitic nephelinites) associated with nephelinite volcanoes. Moreover, between 2°S and about 1° 30'N, there are few exposed trachytes and no rhyolites older than 7 Ma. Important changes in magmatic compositions coincided with a widespread episode of major faulting (King and Chapman, 1972).
2. Trends of decreasing undersaturation with time in basic volcanics are reported in well-calibrated Miocene-Quaternary sequences in the northern part of the Rift (Truckle, 1980). A different structural regime in central Kenya and periodic overtopping of the Rift depression by volcanics combine to conceal many of the older formations, making it difficult to establish temporal trends.
3. Voluminous Quaternary rhyolites of the central section of the Rift are sandwiched between two zones in which undersaturated salic volcanics occur in late Miocene-Pleistocene sequences (Figure 3). South of 1°S, phonolitic trachytes and trachyphonolites are well represented in successions of the Nairobi region, and some flows of these compositions may lie deeply buried beneath Longonot. Nearby, the Quaternary caldera volcano of Suswa owes its unique phonolitic composition to its position on the fringe of this southern undersaturated zone. North of the equator, trachyphonolites and phonolitic trachytes were erupted in two main events, the earlier at some 6—7 Ma (Tasokwan formation) and the later at about 0.5—1 Ma (Hannington formation). Flows belonging to both these formations found their way into the central part of the Rift, but they probably terminate at about the latitude of Menengai which, contrary to a former belief, consists entirely of oversaturated trachytes.
4. The absence of late Quaternary caldera volcanoes south of Suswa, and a substantial gap in their distribution between the equator and 0°45'N, have long been puzzling features of Rift volcanology. It so happens that these gaps in the line of axial caldera volcanoes correspond closely to the regions of undersaturated salic volcanism mentioned above, and also broadly to the latitudes of nephelinitic activity in southern and central Kenya (Williams, 1978b). This strongly alkaline volcanism spanned the period 2.5—15 Ma at around 1°30'S, but across the border in Tanzania it persists to the present day. Near the junction of the Nyanza trough and the main Rift, members of nephelinite-phonolite suites in an equatorial zone were erupted earlier but over a similar period of time (8—20 Ma).
5. The concentration of young peralkaline silicic

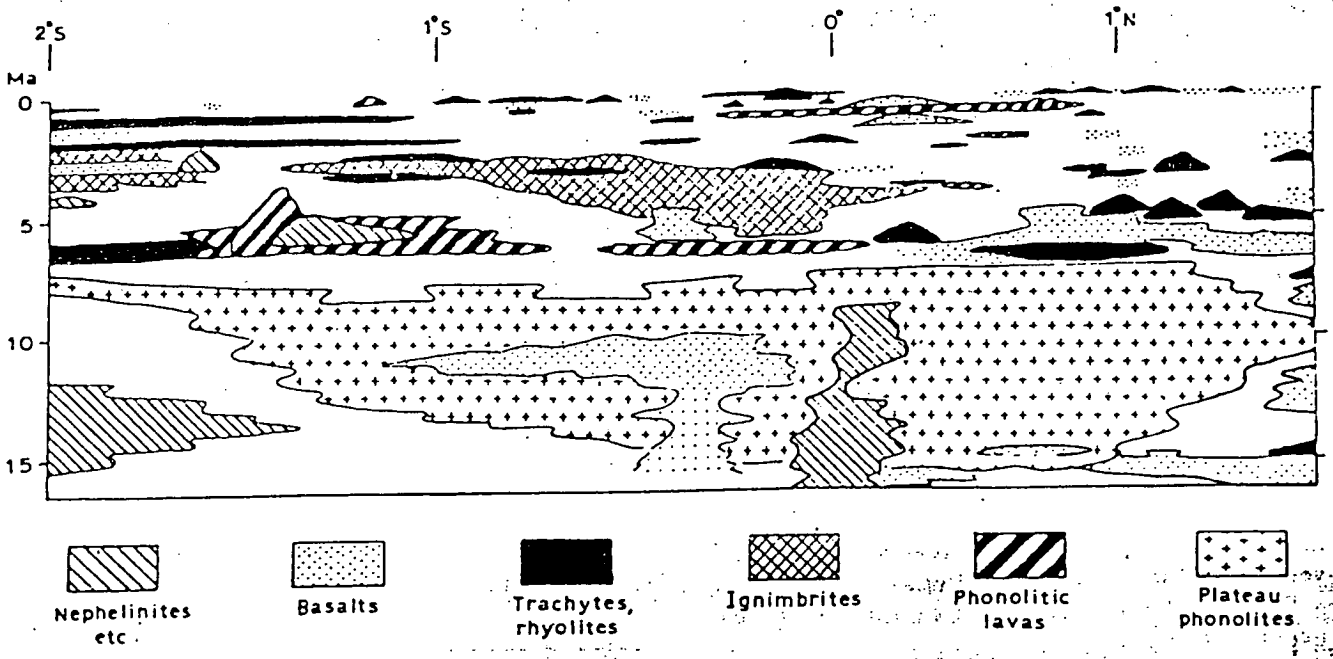

Figure 3. Schematic Representation of the Volcanic Stratigraphy along the Kenya Rift.

volcanoes between the equator and 1°S occurs in a region dominated by earlier (Pliocene) massive eruptions of ignimbrites (Figure 3). It is of interest to note that, following a gap north of Menengai, there is a further cluster of silicic volcanoes between 0°45′ and 1°30′N. This is a region of overlapping Pliocene trachyte volcanoes (2—6 Ma) which are the time equivalents of the central Rift ignimbrites.

6. The Quaternary silicic volcanoes of central Kenya have larger calderas and they erupted more abundant pyroclastics than their counterparts farther north (Williams, 1978a). A similar marked contrast in the style of activity throughout the Pliocene shows that the present unique character of volcanism in the central section of the Rift is a reflection of a long-standing pattern. This should be borne in mind in considering potential sites for geothermal energy exploitation.

ACKNOWLEDGEMENTS

One of us (PTL) was awarded a Natural Environment Research Council Studentship to support the work on Menengai volcano. We gratefully acknowledge financial assistance from the Research Grant Fund and the Department of Environmental Sciences, University of Lancaster.

REFERENCES

Baker, B. H., Williams, L. A. J., Miller, J. A. and Fitch, F. J. 1971. Sequence and geochronology of the Kenya rift volcanics. *Tectonophysics* 11:191—215.

Baker, B. H. and Wohlenberg, J. 1971. *Nature* 229:538—542.

Baker, B. H. and Mitchell, J. G. 1976. Volcanic stratigraphy and geochronology of the Kedong-Olorgesailie area and the evolution of the south Kenya rift valley. *J. Geol. Soc. Lond.* 132: 467—484.

Baker, B. H., Crossley, R. and Goles, G. G. 1978. Tectonic and magmatic evolution of the southern part of the Kenya rift valley. In: *Petrology and Geochemistry of Continental Rifts*, eds. E. -R. Neumann and I. B. Ramberg, pp. 29—50. NATO Advanced Study Institutes Series, D. Reidel, Dordrecht, Holland.

Bliss, C. M. 1979. Geology and petrochemistry of the Naivasha area, Kenya Rift Valley. Unpublished Ph.D. thesis, University of Lancaster.

Chapman, G. R., Lippard, S. J. and Martyn, J. E. 1978. The stratigraphy and structure of the Kamasia Range, Kenya Rift Valley. *J. Geol. Soc. Lond.* 135:265—281.

Crossley, R. 1979. The Cenozoic stratigraphy and structure of the western part of the rift valley in southern Kenya. *J. Geol. Soc. Lond.* 136:393—405.

Crossley, R. and Knight, R. M. 1981. Volcanism in the western part of the rift valley in southern Kenya. *Bull. Volcanol.* 44: 117—128.

Griffiths, P. S. 1977. The geology of the area around Lake Hannington and the Perkerra River, Rift Valley Province, Kenya. Unpublished Ph.D. thesis, University of London.

Jones, W. B. and Lippard, S. J. 1979. New age determinations and the geology of the Kenya Rift—Kavirondo Rift junction, W. Kenya. *J. Geol. Soc. Lond.* 136:693—704.

King, B. C. 1978. Structural and volcanic evolution of the Gregory Rift Valley. In: *Geological Background to Fossil Man*, ed. W. W. Bishop, pp. 29—54. Scottish Academic Press, Edinburgh.

McCall, G. J. H. 1967. Geology of the Nakuru—Thomson's Falls—Lake Hannington area. *Geol. Surv. Kenya Rep. 78.*

Saggerson, E. P. 1970. The structural control and genesis of alkaline rocks in central Kenya. *Bull. Volcanol.* 34:38—76.

Scott, S. C. 1980. The geology of Longonot volcano, Central Kenya: a question of volumes. *Phil. Trans. Roy. Soc. Lond.* 296 (A. 1420):437—465.

Shackleton, R. M. 1945. Geology of the Nyeri area. *Geol. Surv. Kenya Rep. 11.*

Truckle, P. H. 1980. Variation of basic lava petrology of the Kenya Rift Valley. In: *Geodynamic Evolution of the Afro-Arabic Rift System*, pp. 133—142. Accademia Nazionale dei Lincei, Rome.

Williams, L. A. J. 1978a. Character of Quaternary volcanism in the Gregory Rift Valley. In: *Geological Background to Fossil Man*. ed. W. W. Bishop, pp. 55—69. Scottish Academic Press, Edinburgh.

Williams, L. A. J. 1978b. The volcanological development of the Kenya rift. In: *Petrology and Geochemistry of Continental Rifts*, eds. E. -R. Neumann and I. B. Ramberg, pp. 101—121. NATO Advanced Study Institutes Series, D. Reidel, Dordrecht, Holland.

Williams, L. A. J. and Truckle, P. H. 1980. Volcanic sequences in the Kenya rift. In: *Geodynamic Evolution of the Afro-Arabic Rift System*, pp. 123—132. Accademia Nazionale dei Lincei, Rome.

JOURNAL OF GEOPHYSICAL RESEARCH, VOL. 89, NO. B10, PAGES 8553-8570, SEPTEMBER 30, 1984

LATE QUATERNARY CALDERA VOLCANOES OF THE KENYA RIFT VALLEY

L. A. J. Williams and Ray Macdonald

Department of Environmental Sciences, University of Lancaster, United Kingdom

G. R. Chapman

British Geological Survey, London, United Kingdom

Abstract. There are seven major, late Quaternary (≤1 m.y.), trachytic caldera volcanoes in the Kenya Rift Valley; the Barrier, Emuruangogolak, Silali, Paka, Menengai, Longonot, and Suswa. These are situated in the inner troughs of the rift. Their positions are not apparently related to transverse lineaments or basement structures. The structural development was complex, involving combinations of the formation of large calderas and small calderas/pit craters, the growth of lava and tuff cones and the eruption of fissure basalts. Two groups of volcanoes are broadly distinguished. A southern group, comprising Suswa, Longonot, and Menengai, are overwhelmingly of trachytic composition. Krakatau-style formation of calderas approaching 100 km^2 in area was accompanied by the eruption of voluminous ash flow and airfall tuffs (20-50 km^3). In the remaining, more northerly volcanoes, basalts and mugearites form bimodal associations with trachytes. Caldera formation was accompanied by only sparse pyroclastic activity and the collapse may have been initiated by withdrawal of magma from depth. Knowledge of the geochemical evolution of the complexes is limited by the scarcity of published analytical data. The only detailed study is that of Menengai, where chemical variations were caused, at different structural stages, by magma mixing, crystal fractionation and various liquid-state differentiation processes.

Introduction

Some 15 years have elapsed since McCall (1968b) drew attention to five caldera volcanoes in the central part of the Kenya Rift, the centers concerned being Suswa, Longonot, Menengai, Kilombe, and Silali. The next decade brought a spate of review articles dealing with aspects of rift volcanism and structure (Williams, 1969, 1970, 1972, 1978a, b; King, 1970, 1978; King and Chapman, 1972; King and Williams, 1976; Baker et al., 1971, 1972). All mention a chain of trachytic caldera volcanoes along the rift floor, and they add to McCall's list further examples from northern Kenya, notably Emuruangogolak and a center at the southern end of Lake Turkana known as the "Barrier." Two volcanoes between Menengai and Silali are traditionally regarded as members of the chain, though one (Paka) barely qualifies for inclusion as a caldera volcano, and the other (Korosi) has no caldera at all. Similarly, the Eburru complex south of Menengai is frequently listed with the caldera volcanoes, though it is surmounted only by a few small craters.

Copyright 1984 by the American Geophysical Union.

Paper number 4B0420.
0148-0227/84/004B-0420$05.00

The young trachytic centers along the floor of the rift receive little more than a passing reference in these reviews so that important differences in their compositions, size, general morphology, evolution, and structural setting have not been placed on record. All that has been attempted so far is a broad subdivision of the volcanoes into two groups (Williams, 1978a, b, 1982). The centers south of the equator have calderas at least 10 km across, and they are the likely sources for voluminous airfall pyroclastics which can be traced up to 100 km west of the axial line of the rift. In contrast, the centers in a northern group are surmounted by calderas which are rarely more than 8 km and generally less than 5 km across. They have much more restricted spreads of pyroclastics than the volcanoes to the south, and they also differ in having prominent basalts. The basaltic contributions came mainly from late fissures which opened up across the trachytic volcanoes and intervening areas of the rift floor.

Recent mapping has provided more detail on the geology of the Kenyan caldera volcanoes, although much of it remains unpublished in Ph.D. theses. This review aims, first, to summarize available information and, second, to note those areas where major gaps in knowledge still remain. Menengai is not included, in deference to studies by Leat (1983) and Leat et al. (this issue).

Structural Setting of Quaternary Volcanism

Along the greater part of its length, the Kenya Rift shows distinct structural asymmetry in cross section (Figure 1). One margin is commonly defined by a major fault scarp, whereas the opposite side is marked by a combination of downwarping and step faulting. The gross structure is thus a half-graben. Both tectonic and volcanic activity tended to migrate inward with time, leading to the formation of narrow troughs 25-35 km wide in which Quaternary volcanics and sediments overlie Tertiary formations at least 3 km thick. Attenuated Tertiary volcanic sequences are exposed along the margins of the rift depression which is generally about 70 km across in central Kenya, splaying out in the north where the rift tends to lose its identity in a broad depression several hundred kilometers wide. The rift narrows in southern Kenya but across the border in Tanzania the structures diverge through a region of scarps and tilted blocks. The Tertiary formations cover considerable areas on both sides of the rift zone, resting on late Precambrian-early Palaeozoic metamorphic basement. To the east, Tertiary volcanic rocks derived from the rift coalesce with contributions from numerous Pliocene and Quaternary centers.

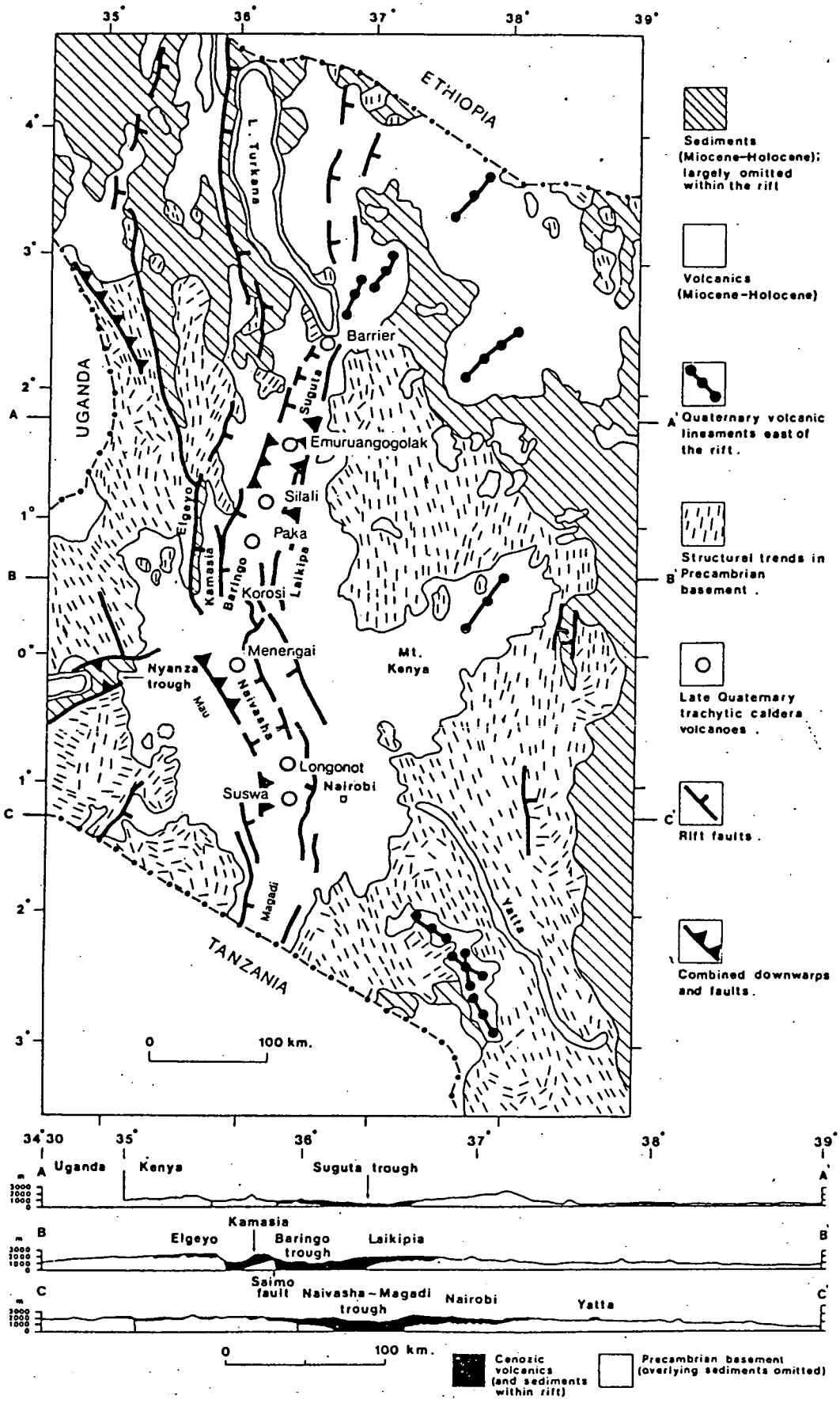

Fig. 1. Outline map of the Kenya Rift showing the chain of late Quaternary caldera volcanoes in the narrow inner troughs of the rift depression. All structural lines ar greatly simplified.

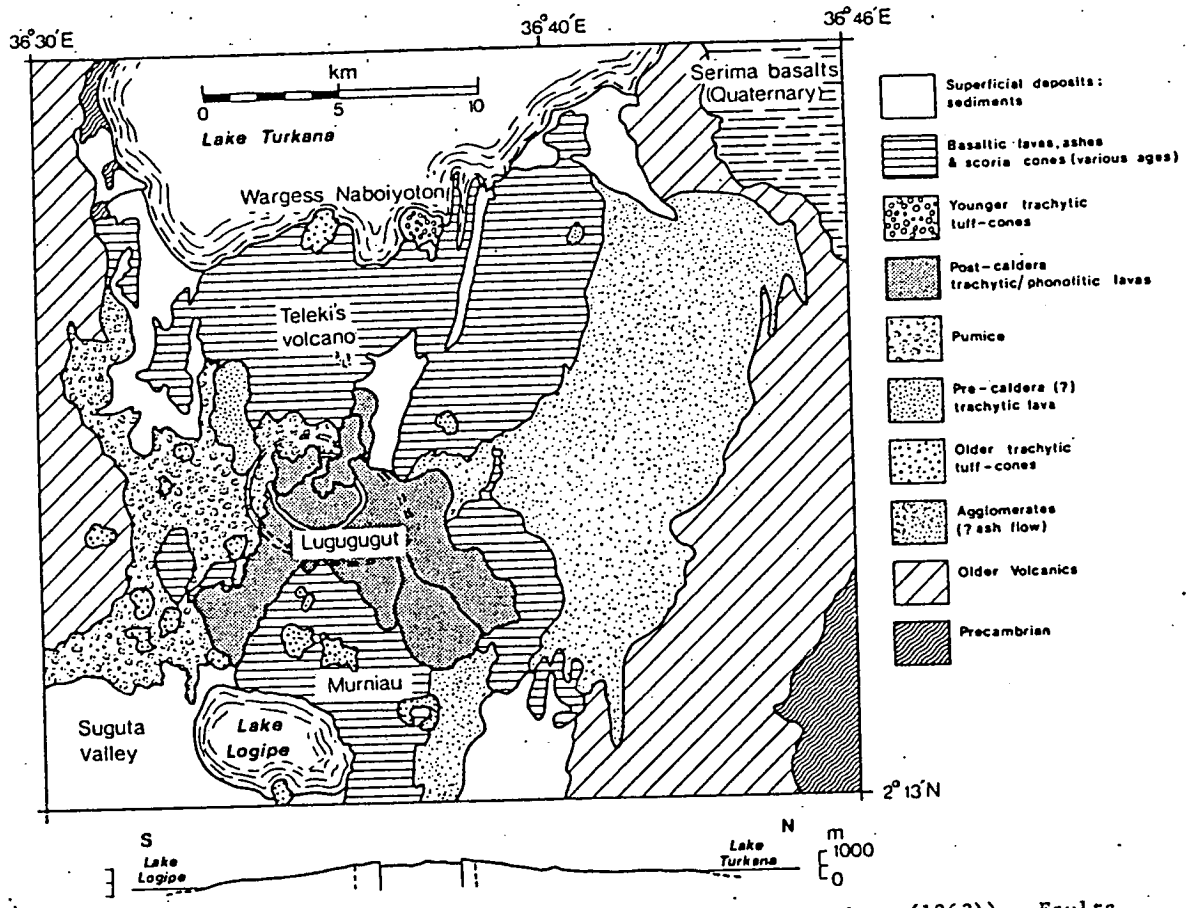

Fig. 2. Simplified map of the Barrier volcano (modified from Dodson (1963)). Faults are omitted; trends N-NNE.

The most recently active troughs are not situated axially within the rift depression. They tend to lie closer to downwarped margins and to be separated from major boundary faults on the opposite side of the rift by platforms, ramps, tilted blocks or uparched structures, all of which display pre-Quaternary sequences. These are particularly rewarding regions for study because they provide the only conclusive evidence of the nature and thickness of deep rift infill beneath the Quaternary deposits of the inner troughs. The volcanics exposed along and beyond the rift margins are commonly those emplaced at times when accumulation outpaced subsidence. Two main periods of overspill are recognized. The first led to vast spreads of "plateau" phonolites following complete infill of the rift in the mid-Miocene (12-14 Ma), and the second to overtopping of the southern part of the rift by trachytic lavas and ignimbrites in the Pliocene (2-6 Ma). The present morphology of the rift was determined mainly by a major episode of faulting in early Pleistocene times, and subsequent volcanism within the rift was largely confined to the inner troughs which were belts of closely spaced faults.

Marked changes in the orientation of the rift, possibly reflecting control by structures in the basement, provide a basis for subdivision of the inner troughs into three segments. From Lake Turkana to the equator, the Suguta-Baringo trough (NNE-SSW) runs close to the eastern margin of the rift, and its course is not influenced by diverging fault patterns on the western side. The Naivasha trough (NNW-SSE) lies on the western sid of the rift zone, swinging southward to pass into the Magadi segment which is situated more central in the rift depression between latitude 1°S and t Tanzanian border. There are no caldera volcanoes in the Magadi trough, and it does not warrant treatment in this account.

Description of Individual Complexes

The Barrier

Structural setting and topography. The Barrier complex (Figure 1) is so named because it separates Lake Turkana (altitude 370 m) and the Suguta Valley, the site of a former lake. The volcanic pile is nearly symmetrical in N-S sections (Figure 2), with slopes of 4°-5°. Flatter E-W profiles may be attributable to a thick pyroclastic cover lapping on to steeply inclined Tertiary basalts at the margins of a downwarped trough some 18 km across. The wester rim of the inner caldera stands nearly 700 m above Lake Logipe (altitude 250 m) and the wall of the outer caldera rises a further 80 m (Baker and Lovenbury, 1971).

Span of activity. The only evidence relating to the earliest activity at the Barrier is that by 9600 years B.P. the volcano was apparently separating Lake Turkana and Lake Suguta (Truckle 1976). An ash eruption at Teleki's volcano on the northern slopes of the Barrier was observed in 1888 (see summary and references in the work

of Dodson (1963)). Five basaltic flows from the cone were sampled in the course of studies of recent secular variation in geomagnetic declination and inclination (Skinner et al., 1975), giving estimated dates of extrusion ranging from the year 1030 to the time of the observed eruption.

Evolution. Reexamination of aerial photographs in conjunction with consideration of relationships shown on Dodson's (1963) map suggests the following sequence in the evolution of the Barrier:

1. Basal formations are now totally concealed, but they probably formed a low-angle lava shield with a maximum thickness of some 500 m.
2. A thick sheet (? ash flow) of trachytic agglomerate was emplaced on the eastern flanks of the shield.
3. Trachytic tuff cones were built mainly on the western and southern flanks.
4. The first major eruptions of basaltic lavas occurred on the SE flanks of the shield. These are indistinguishable from faulted basalts which are exposed for 20 km along the eastern side of the Suguta Valley, and activity was undoubtedly related to extensive fissure systems. Dodson maintains that these olivine basalts and basanites, together with similar flows on the NW flanks of the Barrier which rest locally on Tertiary basalts and basement gneisses, were extruded after emplacement of phonolites and trachytes of the summit region. It seems likely, however, that basaltic activity spanned a much longer time range.
5. Subsidence of the first caldera probably occurred after the eruption of sparsely porphyritic trachytes on the NW flanks, for these lavas are apparently truncated by the ring fracture.
6. Phonolitic lavas erupted within the early caldera spread over a large area on the southern flanks, presumably exploiting a wide breach in the caldera rim. A narrower breach in the NE part of the wall can be inferred from a tongue of phonolite resting on agglomerates. The lavas also flowed eastward across a flatter surface of agglomerates, apparently unimpeded by any caldera rim which was either poorly defined or reduced by erosion.
7. Collapse of the inner caldera truncated the phonolitic flows which evidently form the entire succession in walls estimated to be 150 m high. The map shows equivalent phonolites in the floor of the caldera, but the morphology of these flows suggests that they are younger lavas. A pumice mantle to the north and west is tentatively regarded as a syn-caldera formation. Pumice and ash beds extend across the first caldera rim to form the greater part of the western flanks of the complex, resting ultimately on Tertiary basalts. Detailed mapping of this ground will be required to establish relationships of the pumice mantle to tuff cones and various basalts.
8. The most recent activity in the caldera was concentrated around the northern rim where greenish grey trachytic lavas are banked against and overtop the wall. Naboiyoton tuff cone, which rises more than 180 m above the level of Lake Turkana, may be somewhat older than the summit lavas, but it is a young feature lacking strand lines corresponding to flights of terraces found elsewhere around the lake.
9. The final event at the Barrier produced spreads of basaltic lavas and pyroclastics on the northern and southern slopes. Teleki's volcano is situated well down the flanks, but one of the older basaltic scoria cones in a cluster higher up the slopes could be located on the first caldera ring fracture. Lugugugut (Andrew's volcano) undoubtedly owes its position to activity on the early caldera fracture.

Dimensions and orientations of the calderas. The first ring fracture probably passes beneath the source of the porphyritic trachyte flow on the SE flanks, suggesting a slightly oval form with NW-SE long axis about 6 km long and the short axis 5 km. The inner caldera is nearly circular and has a diameter of about 3 km.

A minimum subsidence of 230 m for the outer caldera can be inferred from the claim that phonolitic lavas exposed in the walls (150 m high) of the inner structure all belong to a single eruptive episode, together with the known difference in altitude of the two caldera rims (80 m). The displacement on the inner caldera fault exceeds the height of the walls by an unknown amount.

Composition of volcanics. Only nine analyses of Barrier rocks have been published. Smith (1938) presented three analyses of lavas from the northern flanks, including two from Teleki's volcano, and analyses of a lava and pyroclastic material from Andrew's volcano.

To standardize the chemical nomenclature for all the caldera complexes, we have employed the terminology of Coombs and Wilkinson (1969) for alkali rock suites. The Teleki rocks are thus ne-normative hawaiites ("soda-trachybasalts" of Smith (1938)), the other specimens alkali olivine basalts. Normative ne is in the range 1-4%, so that all specimens are mildly Si undersaturated.

By contrast, the four analyses given by Brown and Carmichael (1971) (two basanites, one feldspathoidal trachybasalt, and one phonolite) are more strongly undersaturated, suggesting the presence of a range of mafic magmas at the Barrier. Unfortunately, Brown and Carmichael's (1971) specimens were not located either geographically or stratigraphically and are thus of limited use.

Emuruangogolak

Structural setting and topography. Emuruangogolak is located at the narrowest sector of the Baringo-Suguta trough. At this waist, outcrops of downwarped and faulted Miocene formations on the eastern side of the depression are separated by little more than 20 km from tilted Pliocene trachytes on the western side. The eastern flanks of the volcano are involved in closely spaced, young, NNE faults along the margin of the trough. Trachytes of the Emuruagiring Plateau (Figure 3) are provisionally regarded as upfaulted parts of the Emuruangogolak shield.

The volcano rises to an altitude of 1130 m (Emuruepoli), some 750 m above the floor of the Suguta Valley (to the north) and about 500 m above the low-lying ground flanking Silali (to the south).

Span of activity. Two K/Ar age determinations suggest that activity commenced little more than 1 m.y. ago. A specimen of trachyte lava from the SE part of the early shield yielded a date of 0.9 ± 0.1 Ma; this came from one of the oldest exposed flows. Another trachyte, collected beneath tuffs in the wall of a pit crater inside the first caldera, gave a date of 0.5 ± 0.1 Ma. Weaver

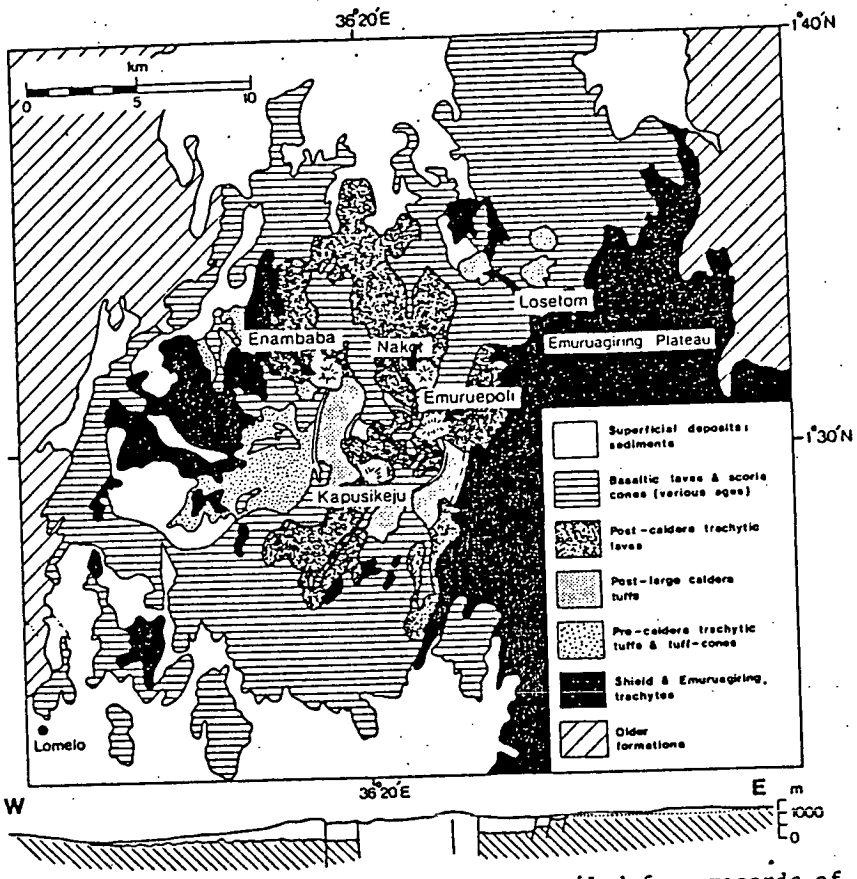

Fig. 3. Simplified map of Emuruangogolak volcano compiled from records of the East African Geological Research Unit Expedition of 1973. All faults and fissures are omitted for clarity; trends N-NNE.

(1978) considers this lava to be the youngest part of the main shield, but it is more likely to represent part of the first caldera infill.

The youngest flows on Emuruangogolak are not more than a few centuries old. Charcoal extracted from tree molds on a basalt from the southern margin of the inner caldera and from charred wood fragments on the surface nearby yielded ^{14}C dates of 230 ± 100 and 270 ± 100 years (Shotton et al., 1974). This basalt passes beneath a small cone which was the source of the youngest trachyte flow of the complex.

Evolution. The earliest activity led to the construction of a broad, low-angle shield about 30 km across, consisting predominantly of trachyte lavas (Figure 4a). The flanks of the shield dip at no more than 5° and the maximum thickness is 600 m. Subordinate ignimbrites are exposed low down on the SE flanks.

The shield lavas were disrupted by minor NNE faults before the outbreak of intense pyroclastic activity on the western and southern flanks of the volcano which produced clusters of coalescing trachytic pumice tuff cones. These may have extended across the summit region, but there are no traces of the distinctive yellow pyroclastics on the eastern flanks.

The development of the pumice tuff cones was followed by the first caldera collapse (Figure 4b). Only the western rim is now exposed intact. To the north, the ring fracture is buried beneath later lavas, mainly those erupted from two prominent trachyte cones (Enambaba and Nakot). Weaver (1978) considered these lava cones to be post-second caldera, but it is more likely that they contributed flows infilling the earlier caldera. Whatever the source of the first caldera infill, it is clear that the flows were impounded to the south by a rim which was subsequently removed by erosion: friable pumice tuffs, similar to those forming the preserved portion of the caldera wall, would have been particularly susceptible to rapid erosion. Removal of such a rim offers a plausible explanation for a marked break in slope which is taken to represent inversion of the original topography (Figure 4c). The precise location of the ring fracture cannot be defined to the east where it is probably masked by later tuffs. Several arcuate faults are visible on aerial photographs, and it is quite possible that the ring fracture bifurcates and that the total displacement was less than elsewhere around the rim.

Green and brown tuffs containing trachytic pumice lapilli mantle much of the ground inside the first caldera. The tuffs were truncated by the second caldera, which exposes a thin cover above trachytic flows forming the greater part of the wall, and they were probably derived from a low cone in the summit region (Figure 4c). Two pit craters between the first and second caldera faults on the western side of the volcano expose a thin layer of basaltic scoria beneath green tuffs. The basaltic material rests conformably on yellow pumice tuffs resembling those of the western

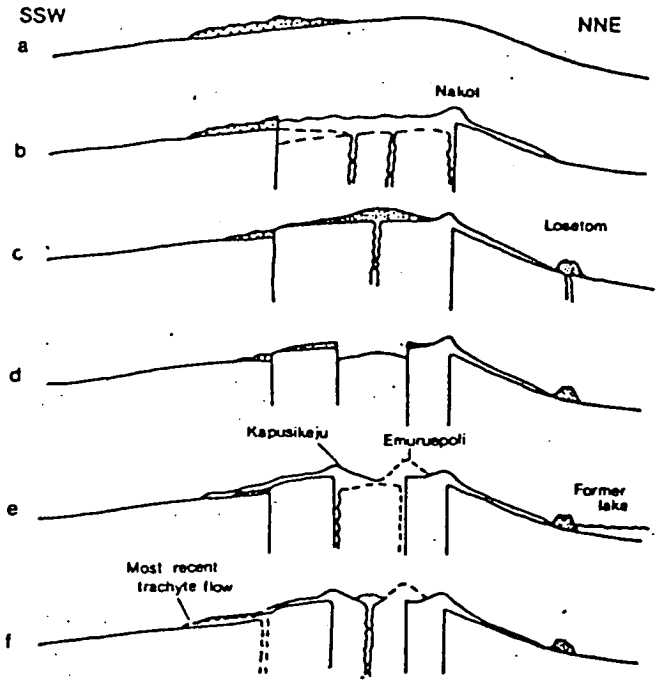

Fig. 4. Schematic diagram illustrating the evolution of Emuruangogolak. (a) Trachytic lava shield surmounted by tuff cones. (b) Subsidence of first caldera. Infilled by trachytes, in part derived from lava cones on northern section of ring fracture. (c) Erosion of tuffs on southern flanks. Tuff cones developed in summit region and on north flanks. (d) Collapse of inner caldera. (e) Trachytic lava cones developed on inner ring fracture. Lake Suguta submerged lower northern flanks, cutting cliff line on cones. (f) Trachytes erupted in arc across inner caldera floor. To south, flank eruptions from cones on first caldera fracture. Note that basalts are omitted for clarity.

flanks. A dated trachyte flow (0.5 Ma) apparently underlies these yellow pyroclastics: it has been taken (Weaver, 1978) to represent the top of the shield succession, but the altitude of the exposure (higher than the projected level of the shield surface outside the caldera) casts doubt on this interpretation unless it represents the top of a buried lava cone. The flow could well be related to the sequence exposed in the inner caldera wall, in which case the date gives some idea of the interval separating the first and second episodes of caldera subsidence.

Three pumice tuff cones low on the NE flanks probably formed at about the same time as the green and brown tuffs of the summit area. The largest (Losetom, 775 m) stands some 270 m above outcrops of trachyte lavas which are tentatively assigned to the shield.

Weaver (1978) maintains that eruptions of some of the earliest basalts occurred soon after collapse of the second caldera, basing this observation on the fact that basaltic flows underlie trachyte flows from Enambaba and Nakot. The ages of these lava cones remain controversial: they developed on the rim of the first caldera and probably predated the formation of the inner structure. Similarly, the upper age limit of basalts and hawaiites on the western flanks of the volcano cannot be established conclusively. They occupied valleys cut deeply in a formerly more extensive cover of yellow pumice tuffs. Locally, the superimposed drainage cut down into the underlying shield trachytes. The valleys passed undeflected across even east facing fault scarps, showing that the drainage pattern was inherited from the tuff cover. Subsequent erosion of the yellow tuffs caused inversion of the original topography and left many of the basalt flows perched above the present surface. These basaltic lavas came from sources on the first caldera rim where a thin veneer over the tuffs was largely responsible for preservation of the wall. The flows were erupted before the construction of Enambaba cone and are therefore probably pre-second caldera.

The inner caldera (Figure 4d) exposes up to 75 m of trachyte lavas, the upper part of the succession infilling the earlier structure. The flows are capped by green and brown tuffs which are overlain in the western wall by an obsidian 5 m thick. Following callapse of the second caldera, major trachyte eruptions on or close to the ring fracture led to the construction of a lava cone (Kapusikeju, 1234 m) on the SW rim and a cone (Emuruepoli, 1328 m) and dome on the NE side (Figure 4e). Lavas from these centers flooded most of the caldera floor, and massive flows poured down the flanks of the volcano. The Kapusikeju flow spread over the gently inclined surface of green tuffs and then cascaded between high levees down the steeper slope marking the margin of the first caldera infill. The narrow stream then widened in the terminal portion of the flow which rests on a thin veneer of earlier basalts covering shield trachytes. These trachyte eruptions were followed by the maximum development of Lake Suguta which lapped around the northern flanks of the volcano.

The final episode of trachytic volcanism took the form of the emission of steep-sided, disc-shaped bodies in an arc across the caldera floor and two flank eruptions from cones situated on the first caldera fracture (Figure 4f). The flow which had its source at the foot of the slope south of Kapusikeju rests on the flows which yielded young ^{14}C dates.

The full chronology of basaltic eruptions cannot be established at present, and the tripartite division of the postcaldera basalts proposed by Weaver (1978) may be an oversimplification. The youngest basalts were erupted along a NNE-SSW fissure system passing nearly through the center of the inner caldera, culminating in activity near Kapusikeju which produced the dated flow mentioned earlier. It is understandably difficult to relate precisely events on the northern and southern flanks of the volcano. Locally around the northern fringes of the outcrop, sediments are banked against minor fault scarps in basalts: at other localities, young flows rest on lake sediments.

Dimensions and orientations of the calderas. The shape of the first caldera cannot be specified precisely, but the ring fracture probably passes beneath the lava cones of Enambaba and Nakot to the north and beneath the two youngest trachyte cones on the southern flanks. The likely dimensions are thus 9 x 7 km, and the long axis trends NNW-SSE. The inner caldera measures 4.5 x 3.5 km and it is elongated NW-SE. The ring fracture splits into three faults on the eastern side, to form a stepped margin, and it is possible that the

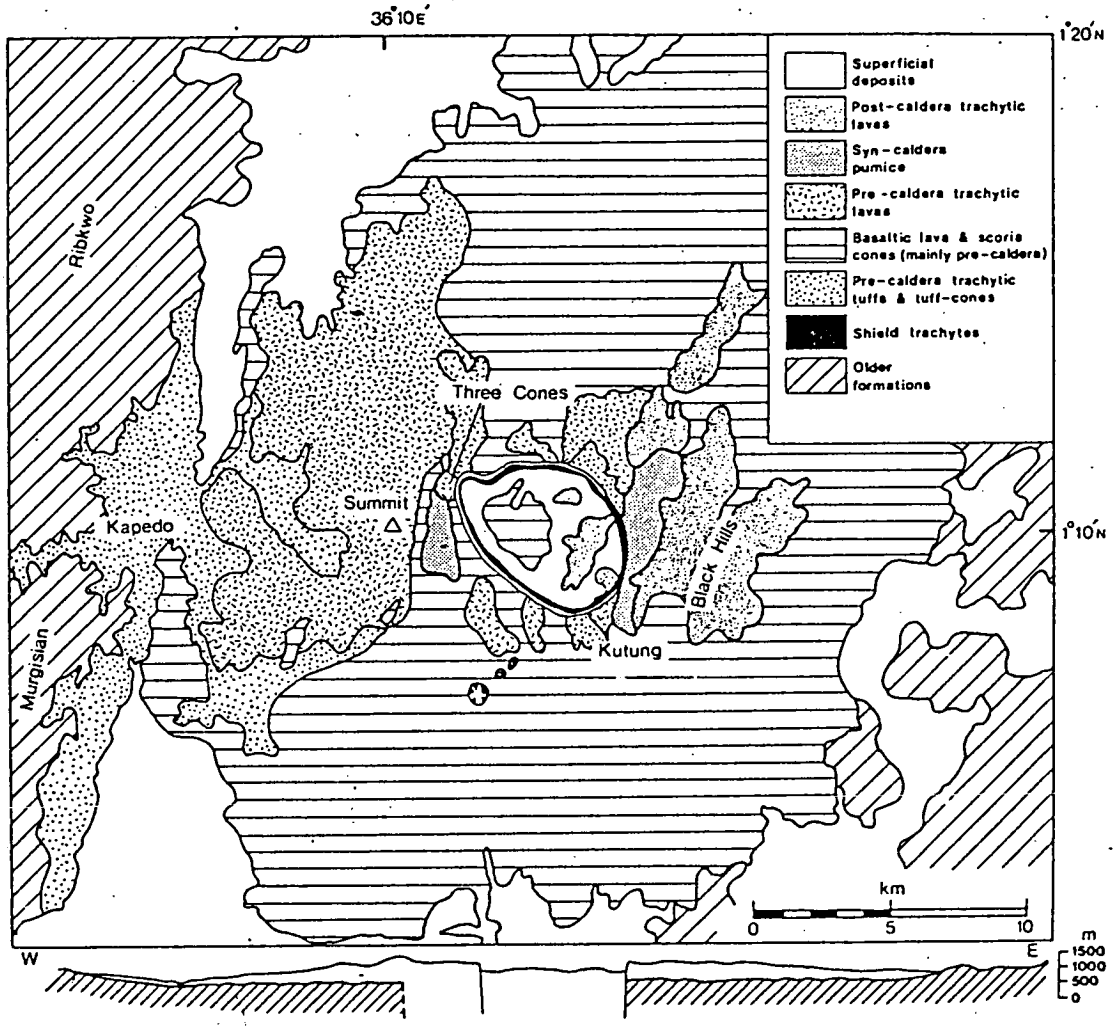

Fig. 5. Simplified map of Silali volcano compiled mainly from an unpublished map and report by G. J. H. McCall. All faults and fissures are omitted (north trending on south flanks; NNE trending on north flanks).

first caldera also had a complex eastern rim.

The amount of subsidence is difficult to estimate. The thickness of flows infilling the first caldera is at least 200 m, and this provides a minimum figure for the displacement on the outer ring fault. The inner caldera wall has a maximum height of 75 m, but there could well be a substantial thickness of postcaldera volcanics unexposed in the floor.

Compositions of the Emuruangogolak volcanics. Although over 80 analyses of Emuruangogolak rocks have been made (Weaver, 1978), only 12 have been published. Furthermore, all analyzed rocks are lavas or coarse-grained nodules; apparently, no pyroclastic rocks have yet been analyzed. Our knowledge of the geochemical evolution of the complex is thus limited. Volcanism at Emuruangogolak was bimodal. No rock with SiO_2 between 49% and 59% has yet been found (Weaver, 1978). The basaltic lavas are mildly alkaline ferrobasalts, with ne between 1% and 4%, and have distinctly high Fe and Ti contents. The silicic members are oversaturated trachytes, with q in the range 0-12%. Both metaluminous and peralkaline types have been recorded. Weaver (1978) claims that there is no simple variation of trachyte composition with time. Syenite and microsyenite bombs ejected during the second caldera collapse have compositions very similar to the lavas.

Weaver (1978) suggests that there was a long-term change in the trace element chemistry of the Emuruangogolak lavas. The Zr/Nb ratio changed from 4.0 to 3.6 to 3.3, the changes being associated with intense pyroclastic activity and caldera collapse, respectively. Some doubt is cast on the existence of these changes by the uncertainties of stratigraphic relationships noted above.

Silali

Structural setting and topography. The volcano is situated centrally in a trough 30 km wide flanked by downwarped Pliocene volcanics on the west and tilted and faulted Miocene formations on the east.

The summit of Silali rises to 1528 m, standing some 800 m above the floor of the trough which declines gently northward from an altitude of about 800 m at 1°00'N to 600 m between Silali and Emuruangogolak. The summit is located on massive precaldera flows of trachyte which form much of the western flanks of the volcano, imparting marked asymmetry in east-west profiles (Figure 5).

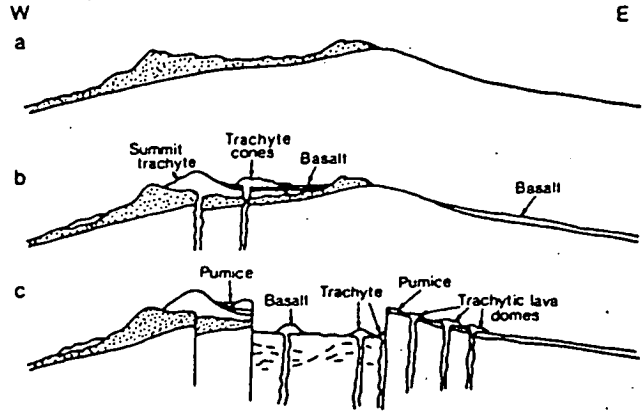

Fig. 6. Schematic diagram illustrating the authors' interpretation of the evolution of Silali. (a) Trachytic lava shield surmounted by tuff cones. (b) Summit trachytes erupted from arcuate fracture. Widespread fissure basalts followed by construction of trachytic lava cones. (c) Caldera collapse accompanied by deposition of pumice mantle. Formation of trachytic lava domes east of caldera, and eruption of trachytes and basalts in caldera floor.

Span of activity. The age of initial activity at Silali cannot be estimated because exposures of the shield lavas are restricted to the caldera walls.

Faulted basalts covering the slopes of Silali are certainly late Quaternary flows. The general impression is that historic activity on Silali was mainly confined to the emplacement of some discoid flows of glassy trachyte/trachyphonolite to the east of the caldera; lack of vegetation led McCall (1968a) to conclude that these can be little more than a few hundred years old.

Evolution. The earliest activity at Silali undoubtedly produced a trachyte lava shield (Figure 6a) which must have had a maximum thickness of at least 500 m. The shield probably has a basal diameter of some 25-30 km.

Construction of the shield was followed by voluminous eruptions of yellowish trachytic pumice tuffs (Kapedo tuffs) from predominantly pyroclastic cones on the western flanks. Similar tuffs are exposed above shield trachytes in the caldera walls, and remnants of cones stand above the rim toward the eastern end of the caldera. Correlation with the Kapedo tuffs (McCall and Hornung, 1972) of the western slopes is based entirely on characteristics such as color, and the possibility of a later pyroclastic episode at the summit of the shield cannot be ruled out. A basalt flow (Mission basalt) exposed along the Suguta River north of Kapedo is intercalated in the Kapedo tuffs.

Deposition of the Kapedo tuffs was followed by major eruptions of trachytic lavas (Summit trachytes) which cover most of the western slopes of the volcano (Figure 6b). There is no single cone source, and the lavas evidently rose up along a fault (perhaps an early ring fracture). They now form a summit ridge with steep eastern and western slopes. The flows extended eastward into the region of the present caldera where they have been identified in the walls. There followed a major basaltic phase during which all but the western slopes were mantled by flows erupted fr numerous fissures. These Katenmening basalts lapped against the Summit trachytes, but they n dip at about 30° eastward in the vicinity of th contact where they were apparently downwarped w the trachytes. McCall and Hornung (1972) sugge that the volcano "suffered sagging along a medi meridional zone" to account for the steep dips the basalts. Elsewhere, G.J.H. McCall (unpublished report, 1969) refers to possible major graben subsidence after eruption of the Summit trachytes.

The likelihood of sagging at the margin of an early caldera has not been considered, though th Summit trachytes were erupted along an arcuate fissure. A break in slope on the northern basal covered flanks, some 3 km beyond the present caldera rim, provides slender evidence for a con tinuation of an early ring fracture, though inversion of topography following erosion would have to be invoked (see discussion of Emuruangogolak). Evidence for a former caldera rim across the southern flanks is even more tenuous; a large sink crater in the basalts coul conceivably be related to a fracture. To the ea the line of recent trachyte mounds is the most likely position for an early fracture system. T case for early caldera collapse on Silali is debatable, but such a structure would have a diameter of about 12 km, which is roughly the si of the calderas on the Menengai-Longonot-Suswa group of volcanoes south of the equator.

After eruption of the Katenmening basalts, thr trachyte cones developed near the foot of the ea facing summit scarp. Lava flows were directed mainly northward. Subsidence of the caldera truncated the "Three Cones" trachyte, exposing t underlying sequence of shield lavas, yellow pumi tuffs, Summit trachytes, and Katenmening basalts A thin syn-caldera pumice mantle was deposited between the western rim and the summit ridge and also on the eastern side of the caldera (Figure 6c).

The final events were the emplacement of the domelike mounds of trachytes/trachyphonolites (Black Hills) on the upper eastern flanks of the mountain, the eruption of trachytes which flowed down the NE slopes from small cone sources, and the eruption of both trachytes and basalts in th caldera floor. One trachyte flow cascaded down the lower part of the caldera Wall. McCall regarded the basalts as part of the Katenmening formation, but the cones and flows show no signs of disruption and are here considered to be post caldera features, probably of the same age as a few scattered basaltic eruptions on the flanks o the volcano.

Dimensions and orientation of caldera. Silali caldera is the most spectacular of the structures described in this account. It measures 7.5 x 5 k with the long axis trending NW-SE. The precipito walls are up to 300 m high. The caldera has an embayment at the NW end and a stepped feature at the SE margin. The total thickness of infill is unknown so that subsidence can only be estimated from wall height, but it must exceed 300 m.

Composition of Silali volcanics. The following comments are based on 50 analyses of Silali rocks kindly made available by G. J. H. McCall, of whic only a handful have been published (McCall and Hornung, 1972). No analyses of the voluminous

pyroclastic rocks are available. As at Emuruangogolak, volcanism at Silali was bimodal, but the compositional range was larger. Both hy- and ne-normative basalts are present, while the trachytes comprise q- and ne- and an- and ac-normative varieties.

The shield trachytes include q- + an, q + ac, and ne + ac bearing types. Some of the ne-normative rocks are phonolites, but as noted above, these particular rocks may represent a postshield phase of activity. The succeeding Kapedo Tuff contains q + ac and ne + ac trachytes; no metaluminous types have yet been recorded. The intercalated Mission Basalt is hy-normative. The Summit trachytes are apparently all oversaturated, with both peralkaline and metaluminous types. Although McCall and Hornung (1972) record the presence of q-normative rocks in the Katenmening basalts, the q disappears when allowance is made for postmagmatic oxidation of specimens. The range of mafic compositions is thus from hy- to ne-normative varieties; the presence of hawaiites and mugearites may also be noted. The Three Cones trachyte is q + an bearing and the Black Hills trachyte comprises q + an and ne + ac bearing specimens.

The close stratigraphic association of this wide range of trachytes is fascinating. Detailed evaluation of magma compositions in relation to the volcanological development of Silali may provide real information on the origin of such trachytes.

Paka

The main eruptive events at Paka (Sceal, 1974) and Korosi (Carney, 1972) volcanoes were probably broadly synchronous. Although the latter has no recognizable caldera, some aspects of its development are considered here insofar as they throw light on the evolution of the former. Both volcanoes are covered by a simplified map (Figure 7).

Structural setting and topography. At the latitude of Paka, the eastern margin of the rift is essentially a step-faulted flexure in which the exposed formations (mainly Miocene basaltic, phonolitic and trachytic lavas and tuffs) commonly dip at 5°-10° inward toward the most recent depression (Baringo trough). West of Paka, a faulted NNE trending anticlinal structure (the Kaparaina arch) runs through the foothills of the Kamasia Range, separating the Baringo trough from a major fault (Kito Pass fault with throw exceeding 2000 m) about 18 km west of the meridian 36°00'E (Chapman et al., 1978). The margin of the rift lies a further 25 km to the west where another major fault forms the Elgeyo Escarpment.

The summit of Paka (1700 m) stands some 800 m above the plains to the west. The slopes of the outer flanks of the volcano rarely exceed 3°-4°, but the western slopes steepen to 10°-15° near the caldera rim (section, Figure 7).

Span of activity. The Nginyang basalt, which came from a source between Paka and Korosi, flowed northwestward to pass across the northern end of an extensive outcrop of Layamarok trachyphonolite (~0.5 Ma). Shield trachytes on the NE flanks of Korosi (and probably some early Paka flows) rest locally on formations belonging to an older trachytic caldera volcano (Chepchuk; K-Ar dates in the range 1.13-1.22 Ma), the western part of which was downfaulted and is now concealed. This evidence strongly suggests that activity at both Paka and Korosi commenced about 1 m.y. ago. Eruptions continued until very recent times, the youngest flows in this region being some of the basalts between Paka and Korosi, and on the NE flanks of Paka. The trachyte at Muruese (cone and flow extremely well preserved) and the trachyte and basalt erupted in Paka caldera are clearly Holocene, but they remain undated.

Evolution of Paka. Until more detailed information on the pyroclastics is forthcoming, it will be exceedingly difficult to make further progress in working out the precise stratigraphy and evolutionary history of this center. Examination of the aerial photographs suggests that it is well nigh impossible at present to distinguish shield trachytes from other precaldera flows: no attempt is made to do so in the map (Figure 7).

The following provisional sequence of eruptive events is proposed:

1. A trachytic lava shield developed with a basal diameter of 18-25 km.
2. Trachytic tuff cones were built mainly on the western side of the shield; examples are the cones truncated by the caldera. The cluster of tuff cones NNE of the caldera could well include representatives of this phase of activity, but many probably belong to a later episode.
3. By analogy with Korosi, the mugearites of Katalim and Mundi are provisionally listed at this stage in the sequence. They were erupted either on the lower western flanks of the shield or just beyond the limits of the shield. Some basalts on the eastern and southern sides of Paka underlie precaldera trachytes, resting locally on flows which are possibly the only exposed portions of the primitive shield.
4. Most of the precaldera trachytes were erupted from now concealed sources across the summit and flanks of the volcano. Some have been exposed by erosion of overlying tuffs (e.g., a prominent flow NE of Muruese); others, mainly the uppermost flows on the southern flanks, conceivably belong to a postcaldera phase of activity, but they are not distinguished on the map (Figure 7).
5. Much of the volcano is covered by pumice tuffs and intercalated agglomerates. Some of these deposits were probably derived from a large explosion crater just before caldera collapse. Others may have been associated with the formation of the caldera. The tuff cones of the NE flanks (see point 2 above) possibly provided some of the widespread late pyroclastics, but the history of this region is difficult to unravel.
6. The most recent eruptive events produced trachyte followed by basalt in the caldera, a trachyte flow from a cone low on the SW flanks (Muruese), and basalts on both sides of the volcano on a line running NNE through the caldera.

Dimensions of the caldera. The near-circular structure is about 1.5 km across. A small embayment in the SE margin corresponds to the end of an ENE trending explosion crater measuring 1 x 0.5 km. The caldera rim is breached on the northern side. The thickness of trachytes and basalts erupted in the caldera floor cannot be determined with precision, but subsidence must have exceeded 200 m.

Composition of volcanics. Sceal and Weaver (1971) have provided analyses of seven Paka rocks: three basalts, three trachytes, and one mugearite.

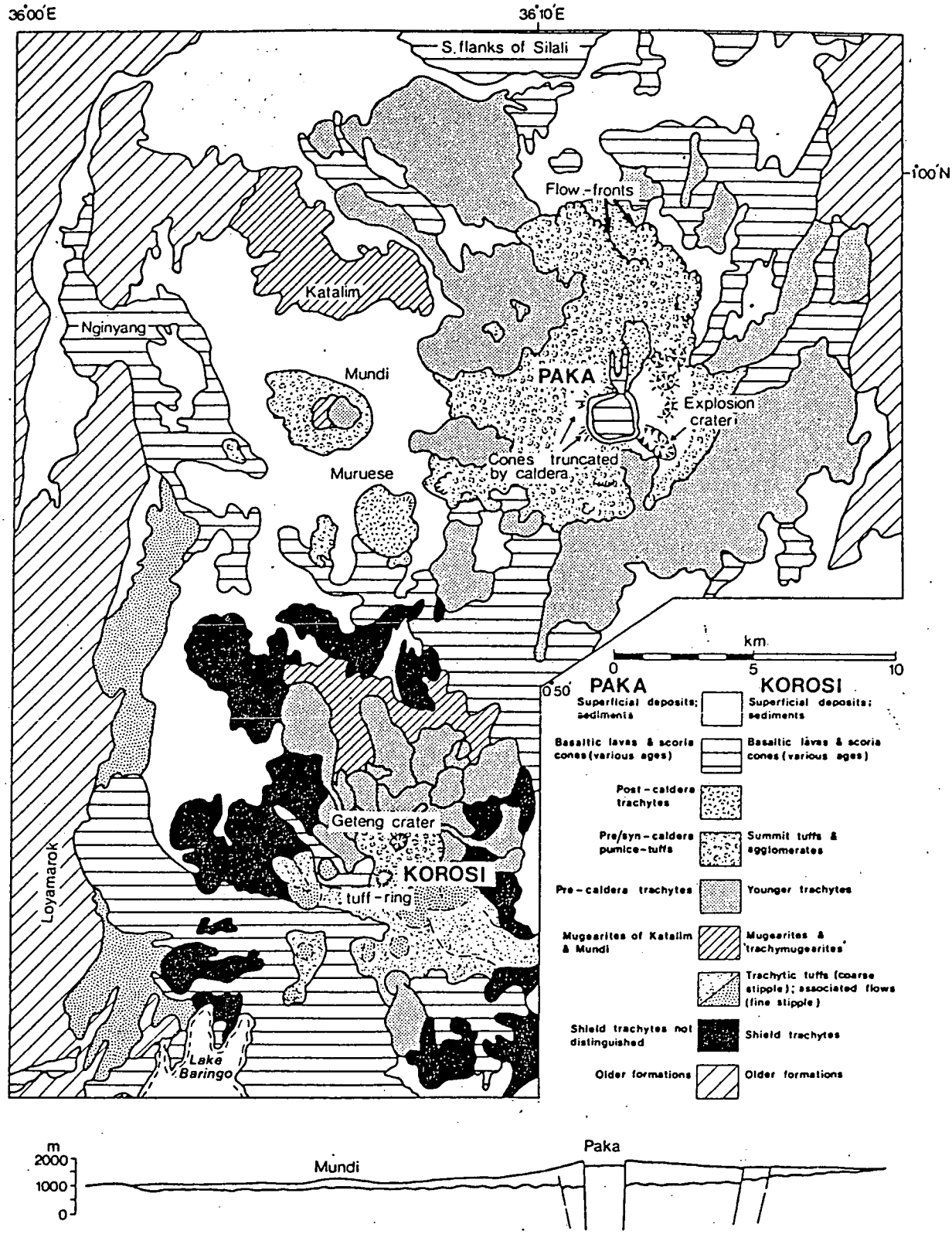

Fig. 7. Simplified map of Paka caldera volcano (modified from Sceal (1974)) and the adjacent Korosi center (modified from Carney (1972)) which has no recognizable caldera. Faults and fissures are omitted for clarity; trends NNE.

When allowance is made for posteruptive oxidation, the basalts are mildly undersaturated, with ne < 5%. A precaldera trachyte (4/L) from a flow on the plains on the NW side of the volcano is q-normative. Another (4/M) trachyte overlain by tuffs on the northern flanks of Paka is ne-normative, and the young flow at Muruese is also ne-normative.

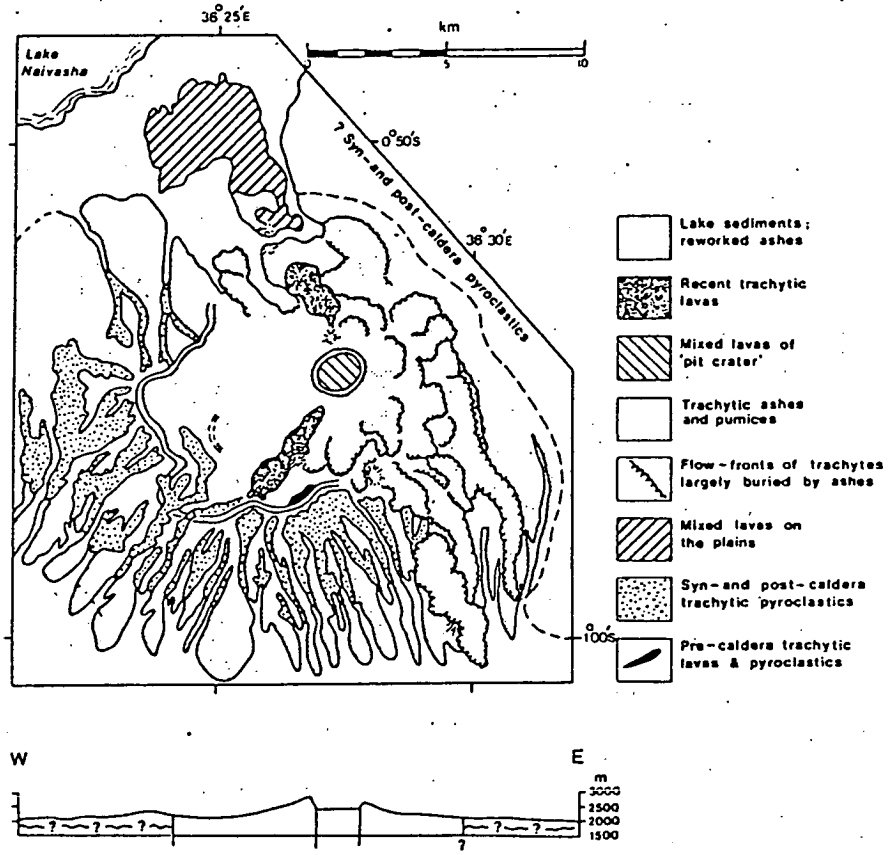

Fig. 8. Simplified map of Longonot volcano (after Scott, 1980).

Longonot

This volcano has been described recently by Scott (1980), and it is treated only briefly in this account. Work is still in progress, and no attempt is made here to summarize unpublished geochemical data bearing on the compositions of the volcanics.

Structural setting and topography. Longonot is situated toward the southern end of the Naivasha trough (Figure 1), whose eastern margin is a step fault platform exposing Pliocene volcanics and sediments (Baker and Mitchell, 1983). The western margin (Mau Escarpment) is essentially a faulted monocline and is mantled by thick Quaternary ashes. There is mounting evidence to show that thick Quaternary silicic formations and largely unexposed basalts occupy much of the inner trough in this region. Deep (2500 m) geothermal wells immediately west of Longonot are providing vital information about the formations infilling the Naivasha trough (Ogoso Odongo, 1983): we are now engaged in a detailed study of material from the boreholes.

The summit of Longonot (2780 m) is on the rim of a pit crater/small caldera surmounting a prominent lava cone. Nearby, between Longonot and Menengai, the floor of the Kenya Rift attains its maximum altitude (2000 m).

Span of activity. Concealment of the foundation rocks and the primitive Longonot shield by pyroclastics and lake sediments (Figure 8) makes it impossible at present to provide a reliable estimate for the lower age limit of activity at Longonot. It is not unlikely, however, that future work will confirm the suggestion by Scott (1980) that, like Suswa, this volcano developed over not more than the last 400,000-500,000 years. The most recent activity has not been dated, but some flows are clearly only a few centuries old. Some interdigitation of Longonot and Suswa units can be expected, while recognition of syncaldera ash flows in the Hell's Gate area south of Lake Naivasha permits the correlation of Longonot eruptives with those of the Naivasha comenditic field (University of Lancaster, unpublished work, 1981).

Evolution. Scott (1980) recognized the following seven major eruptive episodes at Longonot:

1. An early peralkaline trachyte composite volcano developed with a basal diameter of about 30 km and dips on the flanks of 20°-25°. From knowledge of other centers, we prefer to view this very poorly exposed composite cone as a feature which developed on an unseen low-angle trachytic lava shield about 25-30 km across at the base.
2. Pyroclastic flow, base surge, and airfall ash/pumice eruptions accompanied the later stages of caldera collapse; the deposits mantled the slopes of the volcano and almost infilled the caldera. From the exposed remnants of a western rim, Scott suggests that the embayed caldera is about 7.5 km across. This figure was evidently based largely on the assumption that a later lava pile was centered on the caldera margin. We do not see any objection to a caldera with an ENE-WSW long axis up to 10-12 km and short axis of 7.5-8 km.
3. Mixed hawaiite-peralkaline trachyte lava flows were erupted on the northern slopes.
4. A peralkaline trachyte lava pile was built

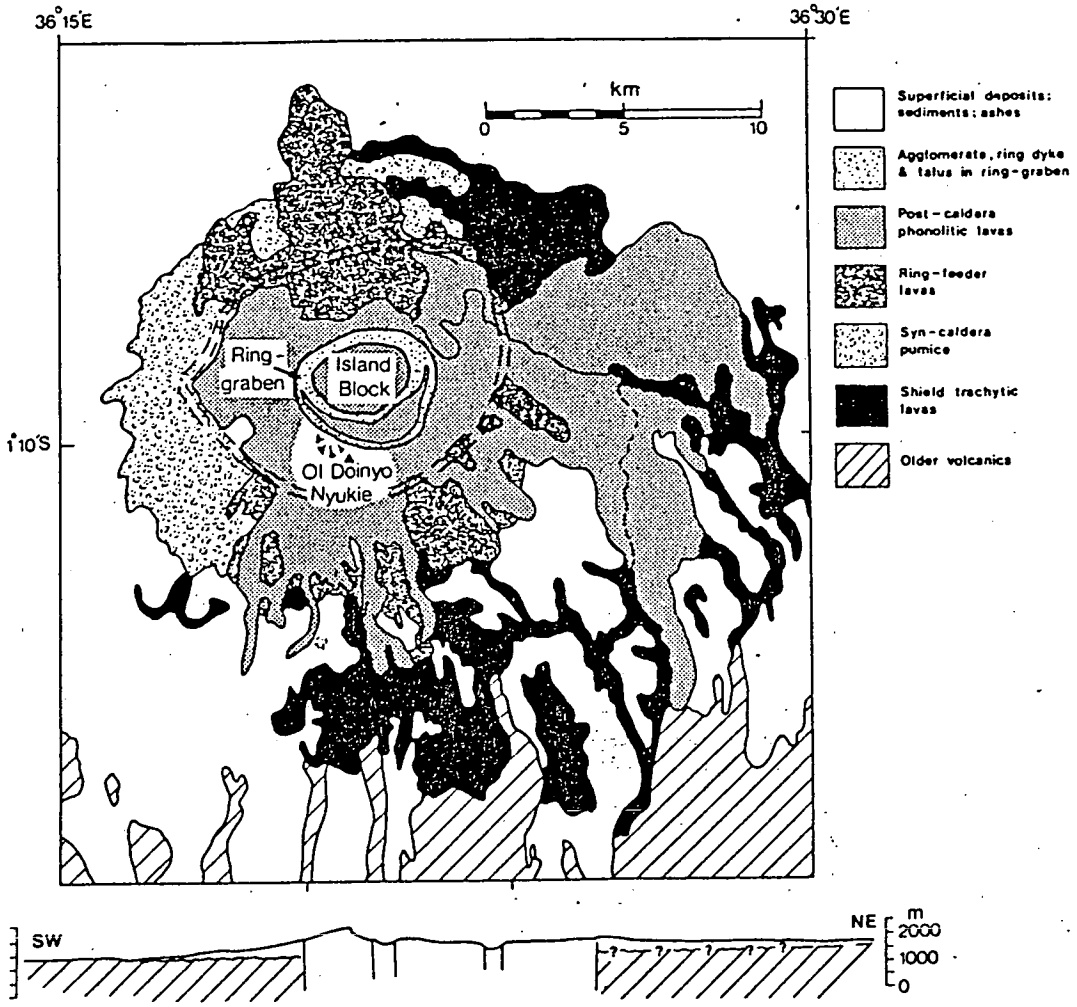

Fig. 9. Simplified map of Suswa volcano (after Johnson, 1969). Faults are omitted; trends N-NNW.

"from a source region situated on the infilled, eastern caldera floor."

5. Strong explosive activity produced thick ash and pumice deposits, followed by asymmetric collapse of the summit region to form a circular pit crater 1.8 km in diameter.

6. Mixed hawaiite-peralkaline trachyte lavas were erupted in the pit crater floor.

7. Peralkaline trachyte lavas issued from the northern and southwestern slopes of the lava pile. Fumarolic activity persists in the pit crater.

Suswa

Structural setting and topography. Suswa is the southernmost caldera volcano in the Kenya Rift. It is situated in an area where the NNW trending Naivasha trough passes southward into the nearly meridional Magadi depression. Arcuate scarps defining the eastern margin of the rift pass southward into a step fault platform (Baker and Mitchell, 1976, 1984). The western margin of the rift at the latitude of Suswa is a continuation of the Mau downwarp.

The summit of Suswa (2358 m) is the rim of a crater on a prominent lava cone (Ol Doinyo Nyukie). The rift floor stands at around 1650 m north of the volcano (an almost unbroken ash/sediment mantle) and about 1350 m to the south (horst and graben structures in intensely fractured trachytes).

Span of activity. Along the southern flanks of the volcano, early trachytic lavas (0.4 Ma) of Suswa rest conformably on Plateau trachytes (0.8-1.4 Ma), flood lavas which covered a substantial part of the rift floor in southern Kenya (Baker and Mitchell, 1976, 1984). Caldera collapse occurred shortly before 0.24 Ma (Baker and Mitchell, 1984). The youngest Suswa lavas have only a sparse cover of vegetation, and they cannot be older than a few centuries. Fumarolic activity on Suswa is more widespread than on any of the other caldera volcanoes.

Evolution. The history of Suswa is described in a well-illustrated account by Johnson (1969), who defined three major eruptive episodes (primitive shield construction; syn-caldera pumice and ring feeder "lavas"; postcaldera lavas). For a petrological study (Nash et al., 1969) the postcaldera lavas were divided into two groups to separate earlier flows, which spread across the caldera floor and through a breached eastern rim, from later distinctive lavas forming Ol Doinyo Nyukie cone which overwhelmed the southern wall of the caldera (Figure 9). The following are the main events in the evolution of the center:

1. A low-angle shield developed by eruption of sodalite-bearing trachyte lavas. Johnson maintains that the shield is oval with a ENE trending long axis of 20 km and a short axis of 17 km. Reexamination of maps and aerial photographs suggests that these figures are minima (see Table 1). The primitive shield probably has a maximum thickness of 500–600 m and average slopes of 3°. Sediments and pumiceous ashes are interbedded with shield lavas low on the northern flanks of Suswa. The source of the pumice is unknown. An origin from explosive activity on the shield cannot be discounted, but some could well have come from Longonot which has a similar time span of activity and where early pyroclastics are abundant.

2. Collapse of the caldera was accompanied by eruptions of pumice and ring feeder lavas, the latter coming from fractures outside and concentric with the caldera wall. The earliest pumiceous deposits (not distinguished from ring feeder "lavas" in Figure 9) were emplaced before extrusion of the ring feeder "lavas." Lack of sorting and occasional inclusions of vesicular glassy lava led Johnson to conclude that the sheets were emplaced as lahars; an ash flow origin was not considered but cannot be ruled out. In the NE wall of the caldera, these deposits grade into well-laminated accretionary lapilli tuffs which appear to be truncated by the caldera fault.

The ring feeder "lavas," now interpreted as agglutinates (B. H. Baker, personal communication, 1984), drape over much of the caldera rim, rarely flowing more than 3 km down the outer slopes. On steeper portions of the wall, the lower parts of the inwardly dipping sheets collapsed leaving truncated remnants on the caldera scarp. The ring fracture zone is about 750 m wide on the northern side of the volcano, where upwelling of lava occurred along the caldera fault and on one or two subsidiary fractures set back from the scarp. Bedded pumice deposits from a mantle up to 60 m thick on the western flanks of the volcano, and a thinning sequence can be traced around the northern part of the southern slopes; deposition was probably controlled largely by prevailing easterly winds. The deposits include airfall and ash flow pyroclasts, with some surge deposits (B. H. Baker, personal communication, 1984). Intercalation of pumiceous deposits and ring feeder lavas can be demonstrated at the western rim of the caldera, early and late predominantly lava successions being separated by the main pumice units. The source of the pumice remains speculative. Some may have come from the caldera fracture zone, but Johnson points out that an origin from now buried vents inside the caldera cannot be discounted.

Numerous occurrences of spatter/welded agglutinate 1–1.5 m thick were observed on the caldera walls, many having a basal layer of pumice breccia. Some units can be traced laterally for more than a kilometer; others extend for only a few meters. One of the most prominent beds of "spatter" at the western end of the caldera is intercalated in the pumice mantle, dipping into the embayment. At another locality in this region, what is considered to be similar material uniformly covers pumice (here banked against the scarp), locally extending down to the caldera floor. There was no significant subsidence of the caldera after deposition of the pumice mantle.

3. Exposed postcaldera lavas belong to two main groups. The earlier sequence consists of aphyric or sparsely porphyritic phonolitic flows which flooded the caldera and spilled through a breach in the eastern rim. Later trachytes and phonolites were associated with the growth of a major cone (Ol Doinyo Nyukie) on the southern side of the caldera. Activity at the summit of Ol Doinyo Nyukie ended with collapse to form what has been termed a pit crater with a WNW-ESE long axis of 1.6 km. The present funnel-shaped depression, truncated by the ring graben on its northern side, is 460 m deep.

4. The precise mechanism which produced the annular trench in the central part of the main caldera is still speculative. Models range from those in which the trench represents subsidence of arcuate slices followed by tilt of the island block (hence the term "ring graben") to more elaborate processes involving formation of a caldera and subsequent uprise of an inner cylindrical block (a spectacular form of resurgence). Access to the island block is difficult, and its structure remains largely unknown. The surface consists of lavas resembling those of Ol Doinyo Nyukie, but the sequence does not match that exposed in the outer wall of the trench; this lack of correlation lends some support to the resurgence model, the surface flows on the block being members of a sequence initially confined within a caldera at the foot of Ol Doinyo Nyukie.

Rare outcrops of nonvesicular crystalline phonolite in the northeastern part of the trench have a flow lamination dipping northward at 20° to 50°. These are considered to be part of a ring intrusion emplaced before formation of the trench. The laminated rocks, together with Ol Doinyo Nyukie lavas and earlier aphyric phonolites, occur as subrounded blocks up to 3 m across in agglomerates which coat parts of the walls of the trench. The mode of occurrence of these coarse agglomerates has yet to be fully explained. Johnson thought they were formed by explosive activity along ring fractures and that they owe their present disposition to subsequent collapse along the same fractures. The most prominent developments of th agglomerates seem to be on the inner walls of the trench, so that acceptance of a resurgence model to account for the island block presumably implie upward transport of these agglomerates by the rising block. They have an earthy matrix, and their survival poses problems if substantial move ment of the block is envisaged. No remnants of pyroclastic cones occur around the margins of the island block as might be expected if the agglomerates had any surface expression on the presen lava cap.

A plausible sequence of events would appear to be formation of a shallow caldera and emplacemen of ring dykes, explosive activity near the margi of the caldera and emplacement of agglomerates i the ring fracture zone, eruption of lavas in the floor of the caldera, and formation of a ring graben, accompanied by tilting of a central bloc The sequence envisaged combines many of the features in the three models put forward by Johnson but leaves undecided the question of a uplift of the island block which can only be settled by further field work. Johnson undoubt exaggerated all vertical movements in his diagr matic illustrations, and this tends to conceal fact that a very shallow initial caldera, toget

with near-complete infill by lavas, considerably reduces the amount of subsequent uplift of the central block; indeed, uplift may be quite unnecessary.

5. A final eruptive episode, probably only a few hundred years ago, produced a flow from a concealed source in the southern part of the ring graben and a lava eruption from a fissure on the southern outer flanks of Suswa. The lavas resemble those of Ol Doinyo Nyukie in containing numerous phenocrysts of anorthoclase.

Dimensions and orientations of the caldera and ring graben. The outer caldera has a ENE axis about 12 km long and a short axis of some 8 km. The walls rise locally 200 m above the present floor but are generally 110-160 m high. Exposures in the ring graben fail to locate the base of lavas occupying the floor of the main caldera which therefore have a minimum thickness of 100 m. Johnson argues that the primitive shield lavas must have risen to an altitude of about 2100 m, indicating subsidence exceeding 700 m. The reasoning is not altogether clear because the altitude of the caldera floor is not quoted. If it is taken to be 1800 m, Johnson's figure for caldera subsidence would imply infill with a total thickness of more than 400 m.

The fracture zone defining the ring graben and island block is 5-5.5 km across. The precipitous annular trench is 0.5 km wide in the north, but a marked embayment in the southern part of the outer wall increases the width to 1.8 km. The depth of the trench ranges from 90 to 215 m, though truncation of the Ol Doinyo Nyukie center leaves a steep outer wall 520 m high beneath the summit. The island is an oval block with ENE long axis measuring nearly 4 km and short axis measuring about 2.5 km. The flat lava surface dips a few degrees to the NW, with slight upwarping at the SE and NW margins. Most of the surface of the block lies below the level of the outer rim of the ring graben.

Composition of Suswa volcanics. The most detailed geochemical study is that of Nash et al. (1969), who analyzed only 10 specimens, all lavas. Reference to Figure 3 of Leat et al. (this issue) will amply demonstrate the dangers of restricting sampling in this way. Precaldera and syn-caldera flows are mildly undersaturated, peralkaline trachytes. The two samples of early postcaldera lavas are peralkaline phonolites. The Ol Doinyo Nyukie flows are of great interest: with time, they evolved from undersaturated, metaluminous trachytes to strongly peralkaline phonolites.

Summary View of the Development of the Caldera Complexes

In Table 1 are summarized most of the critical features of the evolution of the caldera volcanoes. It must be stressed that certain features are based on scanty field evidence or aerial photograph interpretation only and that some numerical values are "best estimates." We feel, nevertheless, that the data are a faithful summary of the present state of knowledge.

Figure 10 is an attempt to explore, in schematic form, common links in the evolution of each center. The centers are arranged essentially in south to north order, except that Paka and Korosi are displaced, to emphasize their differences to the other centers. The information is presented as a series of evolutionary stages. There is no implication that the same time span is involved in each complex, or that the length of arrows indicates specific lengths of time. Certain features may be selected for discussion from Table 1 and Figure 10.

A trachytic lava shield is undoubtedly common to all complexes. They are low-angle structures, of similar dimensions, except that Paka and Korosi are somewhat smaller. Pyroclastic deposits are sparse at this stage, and it is important to note that no basalts have been conclusively recognized in the shields.

The volcanoes north of the equator, i.e., Korosi northward to the Barrier, tended to develop on the shield prominent trachytic tuff cones, with associated wide spreads of pyroclastic deposits and minor flows. These cones developed, or are preserved, especially on the western sides of the shields, for some reason as yet not understood. Easterly prevailing winds contribute to, but do not offer a full explanation for, the distribution of the pyroclastic deposits. The most obvious remnants of large calderas at the Barrier and Emuruangogolak also occur on the western sides. This might be related simply to thicker accumulations of pyroclastics on the west. Alternatively, there may be fundamental differences in the nature of the ring fractures, i.e., single fracture on the west and bifurcation of fractures (and hence stepped margins) in the east.

There are no directly comparable features in the southern set, although the composite cone at Longonot and the cones of the northern flanks of Menengai (Leat, 1983) may be counterparts. The presence at this stage of the Summit Trachyte at Silali is a point of fundamental difference to the other centers.

Only at Silali is there irrefutable evidence of pre-large caldera basaltic activity. We believe that some basalts at the Barrier and Emuruangogolak probably belong to the pre-large caldera stage. Paka has precaldera basalts but is not directly comparable because it lacks a large caldera.

All the volcanoes except Paka and Korosi evolved to a stage of large caldera collapse. The differences in caldera size, shape, nature of margin, and amount of subsidence are documented in Table 1. A critically important distinction between the northern and southern sets is in the nature of the syn-caldera eruptives. Voluminous ash flow and airfall tuffs accompanied the collapse of the Menengai and Longonot calderas and probably that of Suswa also. By contrast, large caldera formation at the northern volcanoes was accompanied by the extrusion of, at best, sparse pyroclastic rocks. The significance of this is discussed later. The two stages of caldera collapse at Menengai inferred by Leat (1983) are probably justified but are currently unique to that complex.

Post-large caldera activity at Suswa and Longonot showed common stages characterized by the growth of a single major lava cone within the caldera, followed by pit crater development at the summit. Their subsequent evolutions differed. The formation of the hypothetical small caldera at Suswa was not paralleled at Longonot, while the ring graben at Suswa has no counterpart in any Kenyan complex. Menengai had a less complicated post-large caldera history. The dominant activity has

TABLE 1. Summary of Principal Events in the Evolution of the Late Quaternary Caldera Volcanoes, Kenya Rift

	Suswa	Longonot	Menengai*	Paka†	Silali*	Emuruangogolak	Barrier
			Trachytic Shield				
Basal diameter, km	25-30	25-30	22 X 15	18-25	25-30	30	?20-25
Height, m	500-600	?	+300	?400	500	600	?
Slopes of flanks, deg	3	?	2-8	?3-4	?2-3	2-5	?
			Postshield, Precaldera Volcanics				
Trachytic tuff cones	...	composite cone may be equivalent	cones/craters of NW may be equivalent	prominent; some syn-caldera	prominent	prominent	prominent
Trachytic lavas	...	...	...	prominent but some probably shield	summit and cones near caldera	...	NW flanks
Basalts/ mugearites	...	...	...	mugearites	copious basalts	...	?basalts
			Large Caldera				
Size, km	12 X 8	10-12 X 7.5-8	hypothetical earlier ?8; later 12 X 8		7.5 X 5	9 X 7	6 X 5
Elongation	ENE-WSW	?ENE-WSW	NE-SW		NW-SE	NNW-SSE	NW-SE
Subsidence, m	probably less than reported + 700	600 reported	~ 400 in each caldera		+300	+200	+230
			Syn-Caldera Volcanics				
	pumice; ring feeder lavas and agglutinate sheets	ash flow and air fall tuffs/pumice	two major ash flow sheets		thin pumice mantle	...	...
			Post-Large Caldera Events				
	phonolitic lavas and lava cone in caldera	tuffs/pumice continued; mixed lavas on N flanks; trachyte lava cone in caldera; ash/ pumice from cone				trachytes in caldera and from cones on ring fracture; tuffs in caldera and on N flanks; basalts on W flanks	phonolitic lavas in caldera
			Small Caldera/Pit Crater				
Size, km	pit crater 1.6; hypothetical caldera 5-5.5	pit crater 1.8		1.5		4.5 X 3.5	3
Shape/ elongation	?	circular		circular; embayment in SE margin		NW-SE	circular
Subsidence, m	?	+350		+200		+75	+150
			Late Events				
	formation of ring graben; tilting of island block; phonolitic lavas of ring graben and S flanks	mixed lavas in pit crater; trachytes on flanks	pumice locally intercalated with trachytes in caldera	basalts and trachytes in caldera and on flanks	trachytic lavas E and NE of caldera; basalts in caldera and low on flanks	trachyte cones on both caldera fractures; trachytes in caldera; widespread fissure basalts	trachytic lavas in caldera; basanites and basalts on flanks

* No small caldera
† No large caldera

been eruption of lavas and pyroclastics, with no further collapse.

Discussion

This review of the late Quaternary caldera volcanoes of the Kenya Rift has assessed not only the substantial contributions made in the last 20 years, but also the very large areas where field, stratigraphical, and geochemical data are lacking. Figure 10 must be seen as a preliminary framework on which to base attempts at understanding the undoubted links between the complexes. Certain general points relevant to the study of caldera volcanism may perhaps be made here, however.

1. The area of each of the southern calderas is about 100 km^2. At Menengai and Longonot, the volumes of syn-caldera deposits are between 20 and about 50 km^3 (Scott, 1980; Leat et al., this issue). These centers are thus in the intermediate size range of silicic caldera-forming volcanoes, being comparable, for example, to Crater Lake, Oregon (Smith, 1979). It may be noted, however, that they are very youthful structures, probably less than 0.5 m.y. old. This indicates very rapid growth of these trachytic centers, high overall

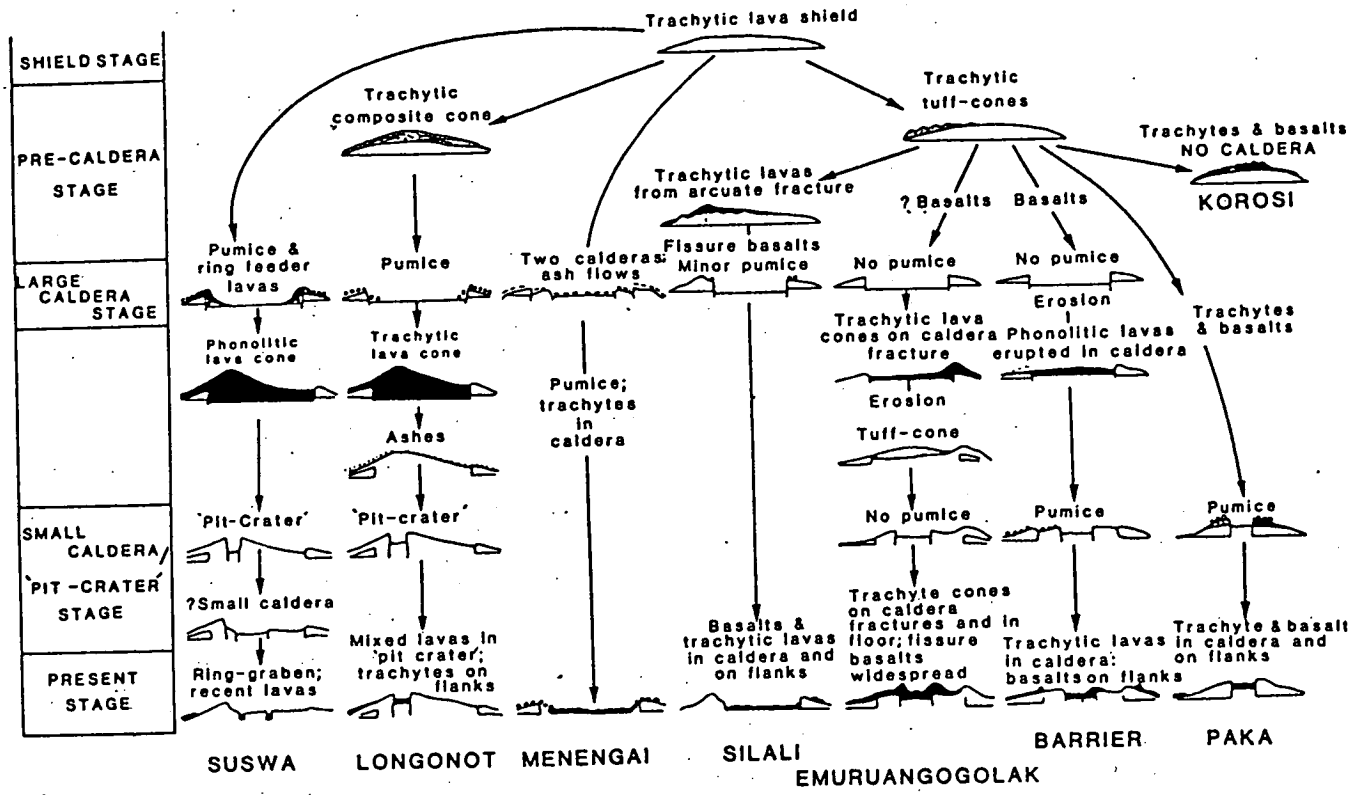

Fig. 10. Diagrammatic overview of the evolution of the late Quaternary caldera volcanoes of the Kenya Rift.

effusion rates, and rapid magmatic differentiation mechanisms (Leat et al., this issue).

The northern centers have smaller calderas and are possibly slightly longer lived (~1 m.y.?). Firmer data on volumes of syn-caldera pyroclastics and ages of shield rocks are required to place these centers in the hierarchy of Smith (1979).

2. The positions of the volcanoes within the rift show no obvious relationship to transverse lineaments, bends in the rift structure, or to basement structures. The situation of Menengai close to the junction between the main rift and a west branch (Nyanza trough) is considered to be fortuitous, though we obviously cannot rule out the possibility that its unique structural setting had some bearing on events in its evolution.

3. The calderas of Longonot, Menengai, and probably Suswa are of Krakatau type, associated with the eruption of voluminous ash flow tuffs. The northern centers show a notable scarcity of syn-caldera rocks. In the case of Silali, voluminous basaltic fissure eruptions preceded caldera collapse. There is the possibility that the caldera formed by withdrawal of basaltic magma from the underlying reservoir along the fissure swarms, in the manner proposed for the Askja volcano, Iceland (Sparks et al., 1981). The model is certainly worth exploring for the northern centers when the stratigraphies are better understood. The exciting possibility exists, therefore, of testing genetic models of two types of caldera structure within a closely related suite of trachytic complexes.

4. Only three generalizations can be made about magma compositions in the late Quaternary caldera volcanoes of Kenya. First, the southern complexes show a decrease in the proportion of basaltic eruptives, to the point of nonappearance at Menengai and Suswa. The absence of basalt from these volcanic systems is probably not real, however. The presence of mixed hawaiite-trachyte flows at Longonot (Scott, 1980), seen only after caldera collapse, suggests that basaltic magma is present at depth under all the complexes. The ability of mafic magma to reach the surface may be related to the stage of development of the overlying silicic magma chamber, in particular its size and structural coherence. Second, the salic products of Emuruangogolak, Silali, Menengai, and Suswa contain metaluminous and peralkaline varieties. Scott (1980) consistently refers to the Longonot trachytes as peralkaline, while insufficient data are available for the Barrier rocks to comment on the degree of Al_2O_3 saturation. We appreciate that many metaluminous samples may well have been peralkaline prior to alkali loss during crystallization or hydration; caution is required in interpretation. Nevertheless, the trend in time from metaluminous to peralkaline among the Ol Doinyo Nyukie lavas of Suswa and the zonation in the second Menengai ash flow from metaluminous (last erupted part) to peralkaline (Leat et al., this issue) suggest that the peralkaline varieties have been derived from metaluminous parents and that metaluminous trachytic magma was present in all the caldera systems. Third, the trachytic products of each center tend to be consistently either Si oversaturated or undersaturated. One exception is Silali where ne- and q-normative trachytes are intimately associated stratigraphically. It may eventually be possible to relate magma compositions to the structural history of Silali in sufficient detail to isolate the controls of the

degree of Si saturation. Another exception is Paka where geochemical data are sparse and where it is particularly difficult to unravel the stratigraphy.

5. Knowledge of the magmatic evolution of the caldera volcanoes is very limited at present. Lack of geochemical data and/or poor sampling of the pyroclastic deposits for all centers except Menengai mean that realistic assessments of differentiation mechanisms and how they relate to volcano development are not yet possible. Judging from the Menengai data (Leat et al., this issue), the evolutionary histories are complex: magma mixing, fractional crystallization, and liquid state differentiation processes have probably operated in all centers, though the importance of each mechanism has undoubtedly varied with the type of center.

Acknowledgments. Many of the data summarized here were collected by P. T. Leat and G. H. J. McCall, S. C. Scott and members of the East African Geological Research Unit (Directors B. C. King, Bedford College, London, and L.A.J.W.; funded by Overseas Development Administration, United Kingdom, and Government of Kenya). Part of the support for the Kenya work is provided by the Natural Environment Research Council. We thank B. H. Baker and C. A. Wood for constructive criticism of the manuscript, Peter Mingins for drafting the diagrams, and Jackie Dixon for typing the paper. G.R.C. publishes by permission of the Director, British Geological Survey.

References

Baker, B. H., and J. G. Mitchell, Volcanic stratigraphy and geochronology of the Kedong-Olorgesailie area and the evolution of the South Kenya Rift Valley, J. Geol. Soc. London, 132, 467-484, 1976.

Baker, B. H., and J. G. Mitchell, Stratigraphy, geochronology and volcano-tectonic evolution of the Kedong-Naivasha-Kinangop region, Gregory Rift Valley, Kenya, J. Geol. Soc. London, in press, 1984.

Baker, B. H., L. A. J. Williams, J. A. Miller, and F. J. Fitch, Sequence and chronology of the Kenya rift volcanics, Tectonophysics, 11, 191-215, 1971.

Baker, B. H., P. A. Mohr, and L. A. J. Williams, Geology of the Eastern Rift System of Africa, Spec. Pap. Geol. Soc. Am., 136, 67 pp., 1972.

Baker, M. J., and H. T. Lovenbury, The South Turkana Expedition scientific papers, VII, The 1969 season survey, Geogr. J., 137, 349-360, 1971.

Brown, F. H., and I. S. E. Carmichael, Quaternary volcanoes of the Lake Rudolf region, II, The lavas of North Island, South Island and the Barrier, Lithos, 4, 305-323, 1971.

Carney, J. N., The geology of the area east of Lake Baringo, Kenya Rift Valley, Ph.D. thesis, Univ. of London, London, United Kingdom, 1972.

Chapman, G. R., S. J. Lippard, and J. E. Martyn, The stratigraphy and structure of the Kamasia Range, Kenya Rift Valley, J. Geol. Soc. London, 135, 265-281, 1978.

Coombs, D. S., and J. F. G. Wilkinson, Lineages and fractionation trends in undersaturated volcanic rocks from the East Otago Volcanic Province (New Zealand) and related rocks, J. Petrol., 10, 440-501, 1969.

Dodson, R. G., Geology of the South Horr area, Rep. 60, Geol. Surv. of Kenya, Nairobi, 1963.

Johnson, R. W., Volcanic geology of Mount Suswa, Kenya, Philos. Trans. R. Soc. London Ser. A, 265, 383-412, 1969.

King, B. C., Vulcanicity and rift tectonics in East Africa, in African Magmatism and Tectonics, edited by T. N. Clifford and I. G. Gass, pp. 263-282, Oliver and Boyd, Edinburgh, 1970.

King, B. C., Structural and volcanic evolution of the Gregory Rift Valley, in Geological Background to Fossil Man, edited by W. W. Bishop, pp. 29-54, Scottish Academic Press, Edinburgh, 1978.

King, B. C., and G. R. Chapman, Volcanism of the Kenya Rift Valley, Philos. Trans. R. Soc. London Ser. A, 271, 185-208, 1972.

King, B. C., and L. A. J. Williams, The East African Rift System, in Geodynamics: Progress and Prospects, edited by C. L. Drake, pp. 63-74, AGU, Washington, D. C., 1976.

Leat, P. T., The structural and geochemical evolution of Menengai caldera volcano, Kenya Rift Valley, Ph. D. thesis, Univ. of Lancaster, Lancaster, United Kingdom, 1983.

Leat, P. T., R. Macdonald, and R. L. Smith, Geochemical evolution of the Menengai caldera volcano, Kenya, J. Geophys. Res., this issue.

McCall, G. J. H., Silali, another major caldera volcano in the rift valley of Kenya, Geol. Soc. London Proc., 1644, 267-268, 1968a.

McCall, G. J. H., The five caldera volcanoes of the central rift valley in Kenya, Geol. Soc. London Proc., 1647, 54-59, 1968b.

McCall, G. J. H., and G. Hornung, A geochemical study of Silali volcano, Kenya, with special reference to the origin of the intermediate-acid eruptives of the central rift valley, Tectonophysics, 15, 97-113, 1972.

Nash, W. P., I. S. E. Carmichael, and R. W. Johnson, The mineralogy and petrology of Mount Suswa, Kenya, J. Petrol., 10, 409-439, 1969.

Ogoso-Odongo, M. E., Petrography of well samples from the Okaria geothermal field: Its use as a tool in geothermal resource development, in Proceedings of the Regional Seminar on Geothermal Energy in Eastern and Southern Africa, 1982, Nairobi, pp. 76-79, UNESCO/USAID, Nairobi, Kenya, 1983.

Sceal, J. S. C., The geology of Paka volcano and the country to the east, Baringo District, Kenya, Ph. D. thesis, Univ. of London, London, United Kingdom, 1974.

Sceal, J. S. C., and S. D. Weaver, Trace element data bearing on the origin of salic rocks from the Quaternary volcano Paka, Gregory Rift, Kenya, Earth Planet. Sci. Lett., 12, 327-331, 1971.

Scott, S. C., The geology of Longonot volcano, central Kenya: A question of volumes, Philos. Trans. R. Soc. London Ser. A, 296, 437-465, 1980.

Shotton, F. W., R. E. G. Williams, and A. S. Johnson, Birmingham University radiocarbon dates, VIII, Radiocarbon, 16, 285-303,

Skinner, J. J., W. Iles, and A. Brock, The Recent secular variation of declination and inclination in Kenya, Earth Planet. Sci. Lett., 25, 338-346, 1975.

Smith, R. L., Ash-flow magmatism, Spec. Pap. Geol. Soc. Am., 180, 5-27, 1979.

Smith, W. C., Petrographic description of volcanic rocks from Turkana, Kenya Colony, with notes on their field occurrence from the manuscript of Mr. A. M. Champion, Q. J. Geol. Soc. London, 94, 507-550, 1938.

Sparks, R. S. J., L. Wilson, and H. Sigurdsson, The pyroclastic deposits of the 1875 eruption of Askja, Iceland, Philos. Trans. R. Soc. London Ser. A, 299, 241-273, 1981.

Truckle, P. H., Geology and late Cainozoic lake sediments of the Suguta Trough, Kenya, Nature, 263, 390-383, 1976.

Weaver, S. D., The Quaternary caldera volcano Emuruangogolak, Kenya Rift, and the petrology of a bimodal ferrobasalt-pantelleritic trachyte association, Bull. Volcanol., 40, 209-230, 1978.

Williams, L. A. J., Volcanic associations in the Gregory Rift Valley, East Africa, Nature, 224, 61-64, 1969.

Williams, L. A. J., The volcanics of the Gregory Rift Valley, East Africa, Bull. Volcanol., 34, 439-465, 1970.

Williams, L. A. J., The Kenya Rift volcanics: A note on volumes and chemical composition, Tectonophysics, 15, 83-96, 1972.

Williams, L. A. J., The volcanological development of the Kenya Rift, in Petrology and Geochemistry of Continental Rifts, edited by E-R. Neumann and I. B. Ramberg, pp. 101-121, D. Reidel, Hingham, Mass., 1978a.

Williams, L. A. J., Character of Quaternary volcanism in the Gregory Rift Valley, in Geological Background to Fossil Man, edited by W. W. Bishop, pp. 56-69, Scottish Academic Press, Edinburgh, 1978b.

Williams, L. A. J., Physical aspects of magmatism in continental rifts, in Continental and Oceanic Rifts, Geodynamics Ser., vol. 8, edited by G. Palmason, pp. 193-222, AGU, Washington, D. C., 1982.

G. R. Chapman, British Geological Survey, Exhibition Road, London SW7 2DE, United Kingdom.

R. Macdonald and L. A. J. Williams, Department of Environmental Sciences, University of Lancaster, Lancaster LA1 4YQ, United Kingdom.

(Received October 4, 1983;
revised March 6, 1984;
accepted March 9, 1984.)

Quaternary peralkaline silicic rocks and caldera volcanoes of Kenya

R. Macdonald

SUMMARY: The late-Quaternary trachytic caldera volcanoes of the Kenya rift provide an unrivalled opportunity for studying the mechanisms of evolution of large peralkaline volcanic complexes and assessing the fundamental problems of magma genesis and chemical differentiation. In a northern set of centres (the Barrier, Emuruangogolak, Silali and Paka) basalt is a major component and mugearites, while scarce, may also be present. Caldera collapse was possibly of Kilauean type. Geochemical variations and the relationships between eruptive rocks and suites of plutonic nodules are consistent with fractional crystallization as the dominant differentiation mechanism in these centres.

The southern basalt-absent centres (Menengai, Longonot and Suswa) show Krakatoa-style collapse. The pyroclastic sequences, especially syncaldera ash-flow deposits, indicate the ubiquity of striking compositional zonations within the magma chambers. Chemical variations in these centres have been ascribed to complex interplays of side-wall crystallization, magma mixing and liquid-state differentiation processes, especially involving volatile complexing. The ultimate origin of the trachytes at these centres is still debatable; crystal fractionation and partial melting of basalt are both viable mechanisms. The different development of the two types of centre may be related to the growth of a volatile-rich cap, which profoundly influences the types of differentiation mechanism.

Recent developments in igneous petrology have focussed attention on the differentiation mechanisms that generate highly evolved volcanic rocks such as peralkaline trachytes and rhyolites. A vigorous debate is in progress on the relative importance of magma mixing, partial melting, assimilation, crystal settling, sidewall crystallization, thermodiffusion, volatile complexing and vapour-phase transport in the development of the strong compositional zoning that characterizes many evolved volcanic systems. Volcanological studies of young centres, geochemical studies of their products, and experimental and theoretical work in geological fluid mechanics have identified new concepts for the evolution of magmatic systems. The most valuable progress will now be made by integrated studies of selected complexes to collect the geological, geochemical and geophysical data specifically designed to test the various competing hypotheses.

Caldera volcanoes are particularly useful in such studies. Compositional and mineralogical variations within eruptive units, especially of pyroclastic type, record the common occurrence of zonation within magma chambers at single points of time, while the sequence of eruptive units marks the chemical evolution of the chamber with time. The relationship between the eruptive rocks and associated suites of coarse-grained nodules provides insights into plutonic processes while the volcano is at the magmatic stage.

In Kenya the late-Quaternary caldera volcanoes (Fig. 1) provide an excellent opportunity for placing the high-level stages of peralkaline silicic magmatism into a time–volume–compositional context. The centres are young (less than 1 Ma) and well preserved. Although many problems remain, their stratigraphy is fairly well known. It should be possible to establish rates of magmatic and structural evolution. The presence of zoned phenocrysts and extensive suites of plutonic nodules are evidence of fractional crystallization at various stages during their growth. Magma mixing has been recorded at several complexes and is probably ubiquitous. The importance of the volatile phase in magma genesis and differentiation in this province has been persistently advocated by D. K. Bailey and his colleagues (see below).

Despite their potential importance, progress in the study of the caldera volcanoes has been uneven. Much of the large-scale mapping and preliminary geochemical data are in unpublished Ph.D theses, many of which were completed before the impressive developments in physical volcanology of the last 10 years. Although extensive geochemical and isotopic programmes are under way, little has yet been published.

In this review geological and geochemical evidence of the origin and evolution of the peralkaline silicic rocks is related to the structural development of the caldera complexes. Attention is focussed on the seven centres of the inner trough of the Kenya rift (Fig. 1) but, where relevant, information from slightly older complexes, e.g. Kilombe (about 2 Ma), and non-caldera complexes, e.g. Eburru and Naivasha, is also included. The Suswa volcano consists of undersaturated trachytes but is an integral part of the province.

From: FITTON, J. G. & UPTON, B. G. J. (eds), 1987, *Alkaline Igneous Rocks*, Geological Society Special Publication No 30, pp 329–349

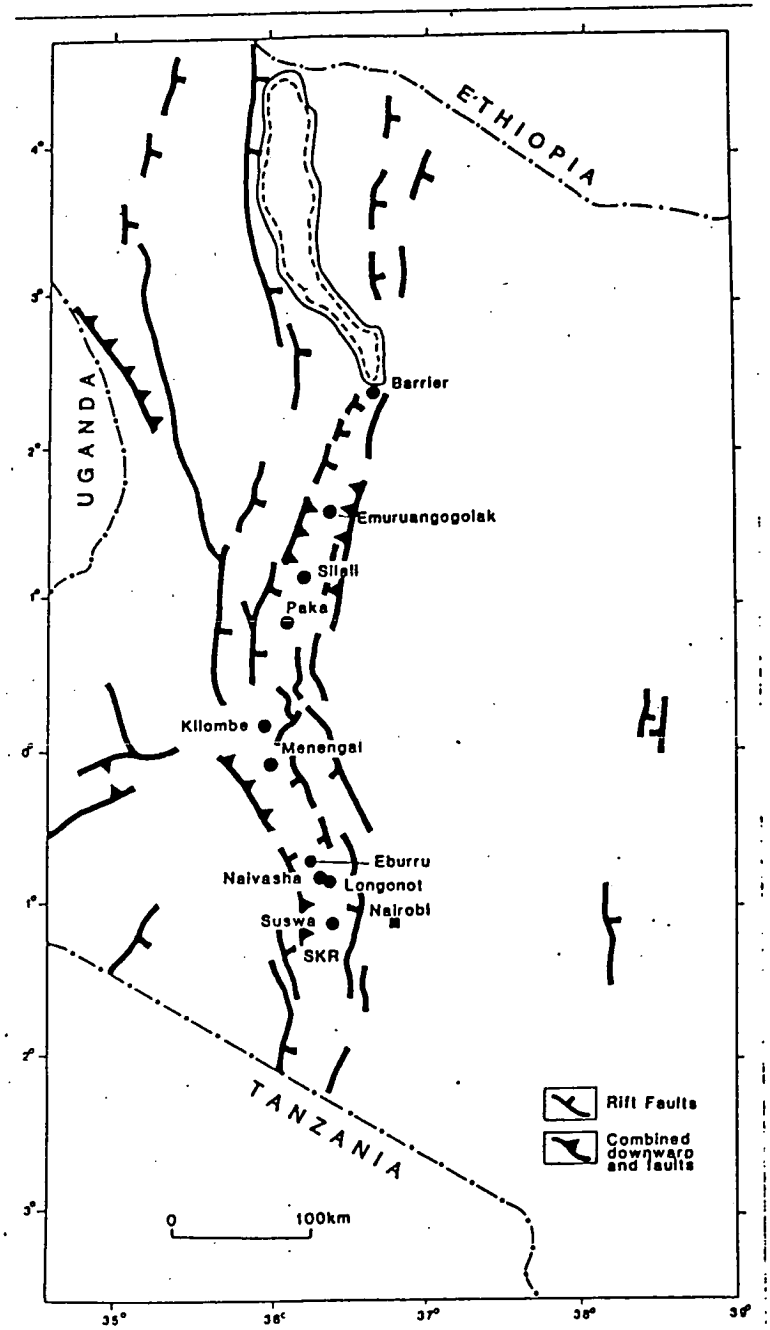

FIG. 1. Locality map of the late Quaternary trachytic caldera volcanoes, the Eburru and Naivasha complexes, the Kilombe volcano and the area of the sourthern part of the Kenya rift (SKR) studied by Baker *et al.* (1977).

The caldera volcanoes

The structural development of each of the seven major late-Quaternary trachytic caldera volcanoes has been complex and, to varying degrees, unique. McCall (1968), Williams (1978a, b, 1982) and Williams *et al.* (1984) have broadly distinguished two groups.

In a northern group comprising the Barrier, Emuruangogolak, Silali and Paka, basalts are

important components of the magma series. Intermediate rock types, such as mugearites and trachybasalts, are less common or absent. At Paka, Sceal & Weaver (1971) estimate the proportions of rock types to be 25% basalt, 5% mugearite and 70% trachyte. Weaver (1978) records 20% basalt and 80% trachyte at Emuruangogolak, with a complete absence of rocks in the range 49%–59% SiO_2. Using calculations of 'percentage crystallized' based on incompatible-trace-element (ITE) abundances, Weaver (1978) considers this gap to represent 25% of the crystallization range. A smaller, but real, composition gap is also present at Silali (McCall and Hornung 1972), but no data are presented on the relative proportions of rock types.

An important feature of the northern calderas (Williams *et al.* 1984) is that caldera formation was accompanied by sparse pyroclastic activity, suggesting that caldera collapse was initiated by withdrawal of magma at depth (*cf.* McCall 1968). In the case of Silali, it is possible that withdrawal of basalt magma from the sub-volcanic reservoir and its eruption as the extensive Katenmening Basalts from fissures and fractures on the shield flanks triggered the collapse.

The southern group of calderas (Menengai, Longonot and Suswa) is almost entirely of trachytic composition. Although basalts have erupted between the centres, in the only mafic magma recorded in the calderas occurs as mixed trachyte–basalt flows on Longonot (Scott 1980; Scott & Bailey, in press). The occurrence is important, however, in that it suggests that basalt is probably present beneath all the southern centres but normally has been unable to penetrate through lower-density trachytic caps. So far no mugearitic or trachybasaltic rocks have been found at these complexes. This may reflect physical discrimination against such compositions by the eruptive system, or may equally well indicate generation of the mafic and salic members from different source rocks.

In contrast with the northern centres, caldera collapse in the southern complexes was of Krakatoan type (Leat 1984; Williams *et al*, 1984) and was accompanied by the eruption of voluminous air-fall and ash-flow tuffs. The differing structural styles and the contrasting proportions of the major rock types in the two caldera groups suggest that the main fractionation mechanisms were different either in style or effect. Relevant evidence is discussed below.

The rock types

The range of rock types found in the caldera centres is summarised in Table 1. The salic products of these complexes are trachytes, with maximum SiO_2 contents of about 64%. Rhyolites of recent age are restricted to the dome field of Naivasha and Eburru, neither of which has evolved to the stage of caldera collapse. The trachytes may be entirely oversaturated (Emuruangogolak, Menengai and Longonot), undersaturated (the Barrier?, Suswa) or contain both varieties (Silali, Paka). They are overwhelmingly

TABLE 1. *Selected features of the trachytic caldera volcanoes*

Caldera volcano	Range of rock types	Maximum SiO_2 (eruptives) (%)	SiO_2 gap (eruptives) (%)	Types of nodule	Relative volume of pyroclastics (%)
The Barrier	Basanites, U bas, U haw, U tbas, P phon		?		?
Emuruangogolak	U bas, OP trach, OS trach	64	49–59	Gabbro, syenite	
Silali	O bas, U bas, U haw, O mug, OS trach, OP trach, UP trach, P phon	63	50–56	Gabbro, 'diorite', syenite	<10?
Paka	U bas, O mug, OP trach, UP trach	61	?	Syenite	
Menengai	OP trach*, OS trach	68*	No rock <60	Syenite	53
Longonot	OP trach, mixed haw–trach flows	64	No rock < 61†	Syenite	>20
Suswa	Up trach, US trach, P phon	59	No rock <56	None recorded	

Bas, basalts; haw, hawaiites; mug, mugearite; tbas, trachybasalt; trach, trachyte; phon, phonolite; U, undersaturated; O, oversaturated (*hy* ± *q* normative); P, peralkaline; S, subalkaline.
* Strictly speaking, some rocks are rhyolitic.
† Excluding mixed flows.

peralkaline, although subalkaline varieties have been recorded at Emuruangogolak, Silali, Menengai and Suswa and are invariably less evolved than the associated peralkaline trachytes.

Selected analyses are given in Table 2. The Kenyan rocks show the strong enrichments in Zr, Hf, Nb, Ta, Zn, Y, rare-earth elements (REE), F and Cl typical of peralkaline rocks. The enrichments are extreme in certain rhyolitic obsidians from Eburru and Naivasha. The F contents are among the highest recorded in silicic obsidians, and the Kenyan province can be regarded as the

TABLE 2. *Representative analyses of Kenyan peralkaline trachytes and rhyolites*

	Trachyte Emuruangogolak S72	Trachyte Paka 4/L	Trachyte Menegai K1A1	Pantellerite Eburru KE-12	Comendite Naivasha 565	Trachyte SKR KLR-54
SiO_2 (wt. %)	63.22	59.45	63.2	70.30	72.5	63.65
TiO_2 (wt. %)	0.78	0.83	0.59	0.33	0.24	0.94
Al_2O_3 (wt. %)	12.54	14.89	10.53	7.62	10.32	14.12
Fe_2O_3 (wt. %)	3.96	4.14	—	2.36	1.93	2.01
FeO (wt. %)	4.50	3.78	9.02*	6.24	2.25	6.03
MnO(wt. %)	0.38	0.30	0.34	0.26	0.06	0.27
MgO (wt. %)	0.27	0.92	0.13	0.02	0.02	0.04
CaO (wt. %)	1.31	2.32	0.83	0.35	0.15	1.31
Na_2O (wt. %)	6.55	6.00	5.19	7.28	5.86	6.34
K_2O (wt. %)	4.56	4.84	4.67	4.27	4.39	5.22
P_2O_5 (wt. %)	0.06	0.09	—	0.02	—	o.07
H_2O^+ (wt. %)	1.28	1.41	—	0.10	0.23	—
F (wt. %)	—	—	—	0.42	0.95	—
Cl (wt. %)	—	—	—	0.33	0.47	—
Subtotal (wt. %)	99.41	98.97	—	99.90	99.40	—
O≡F, Cl	—	—	—	0.26	0.51	—
Total (wt. %)	99.41	98.97	—	99.64	98.89	—
Ba (ppm)	176	174	6	—	3	160
Cr (ppm)	4	—	<1	—	—	—
Hf (ppm)	—	—	34.5	34.2	60.5	17.7
Nb (ppm)	167	155	369	372	590	207
Pb (ppm)	10	—	36	—	68	—
Rb (ppm)	116	110	216	208	637	115
Sr (ppm)	18	42	3	—	<2	10
Ta (ppm)	—	—	22.3	21.1	49.4	11.1
Th (ppm)	14	—	40.6	32.5	124	19.4
U (ppm)	—	—	7.8	7.3	25.1	—
Y (ppm)	112	81	210	300	296	93
Zn (ppm)	254	—	416	472	448	—
Zr (ppm)	556	663	1356	1608	2018	764
La (ppm)	99	102	296	246	153	152
Ce (ppm)	172	202	541	463	310	185
Nd (ppm)	—	96	208	195	151	91
Sm (ppm)	—	—	38.6	44.4	36.8	17.9
Eu (ppm)	—	—	2.37	3.71	0.47	3.17
Gd (ppm)	—	—	39.4	40.0	42.2	—
Tb (ppm)	—	—	4.84	8.14	8.22	2.4
Tm (ppm)	—	—	2.70	3.82	4.61	—
Yb (ppm)	—	—	21.0	25.1	34.6	8.9
Lu (ppm)	—	—	3.05	3.50	4.33	1.64
K/Rb	326	365	179	170	57	547
Rb/Sr	6.4	2.6	72	—	1200	12
Eu/Eu*	—	—	0.19	0.27	0.04	0.58
Ce_N/Yb_N	—	—	6.6	4.7	2.3	5.4

Data sources: S72, Weaver 1978; 4/L, Sceal & Weaver 1971; K1A1, Leat *et al.* 1984; KE-12, Bailey & Macdonald 1975, and unpublished data; 565, Macdonald, unpublished data; KLR-54, Baker *et al.* 1977.

F-rich end-member of the natural spectrum of suites of ranging F:Cl ratios (Bailey 1980; Hildreth 1981).

There is a broad, positive correlation between peralkalinity and concentrations of ITE such as Zr (Fig. 2). The scatter in this diagram is due to several effects: (i) post-emplacement losses or gains of alkalis, affecting the magmatic values of the agpaitic index; (ii) inter-suite variations in Zr abundances; (iii) non-linear relationships between Zr and the agpaitic index in certain suites, e.g. Eburru.

It has been noted that differing values of ITE ratios, such as Zr/Nb (Fig. 3), characterize separate volcanoes within the rift (Weaver *et al.* 1972; Bailey & Macdonald 1975; Baker *et al.* 1977; Jones 1981). Weaver *et al.* (1972) thought that the differences reflect changes in the ITE content of the basaltic parents with time, while Bailey & Macdonald (1975) related the trace-element patterns to buffering by vapour phases of variable F/Cl ratio during magmatic evolution. Changes in Zr/Nb ratio during the development of Emuruangogolak coincided with intense pyroclastic activity or caldera collapse. Weaver (1978) has explained this in terms of volatile degassing, with partitioning of Zr towards the vapour phase being slightly higher than that of Nb.

An important observation is the wide compositional range within rock types. Thus, specimens KLR-54 and K1A1 (Table 2) are peralkaline trachytes with almost identical SiO_2 contents. K1A1 has a considerably more evolved character, as indicated by such ratios as K/Rb, Rb/Sr and Eu/Eu* and the chondrite-normalized REE patterns (Fig. 4), in keeping with its more strongly peralkaline character. In contrast, the peralkaline rhyolite 565, by the same criteria is more evolved than rhyolite KE12 despite being considerably less peralkaline.

Although mafic rocks are abundant in the northern centres, only 19 major element analyses, indicating a range from basanites to *hy*-normative basalt, have been published (Smith 1938; McCall 1970; Brown & Carmichael 1971; Sceal & Weaver 1971; McCall & Hornung 1972; Weaver 1978). Therefore it is not yet possible to assess their petrogenesis. One point deserves preliminary comment, however. Norry *et al.* (1980) note that the Sr, Nd and Pb isotopic compositions of mafic lavas from northern Kenya are comparable with those in oceanic regions, implying not only an insignificant role for contamination by ancient sialic rocks but also that the sources had been impoverished in ITE for much of their history. Metasomatism of the sub-Kenya mantle by CO_2-rich fluids in relatively recent times (less than

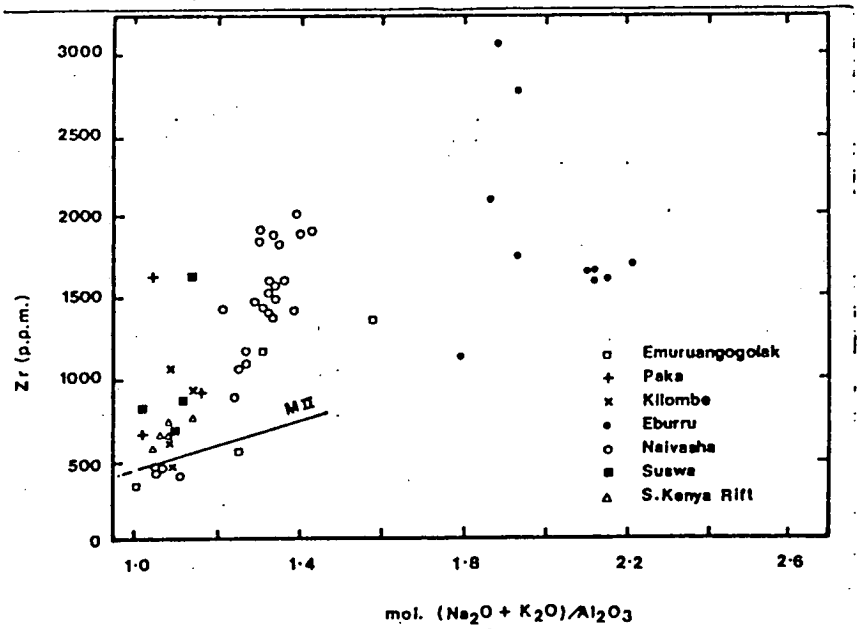

FIG. 2. Zr-mol. $(Na_2O + K_2O)/Al_2O_3$ (agpaitic index) plot for paralkaline trachytes and rhyolites. Data sources: Emuruangogolak, Weaver (1978); Paka, Sceal & Weaver (1971); Kilombe, Jones (1981); Menengai, Leat *et al.* (1984); Eburru, Bailey & Macdonald (1975, and unpublished data); Naivasha, Macdonald (unpublished data); southern Kenya Rift, Baker *et al.* (1977); Suswa, Nash *et al.* (1969).

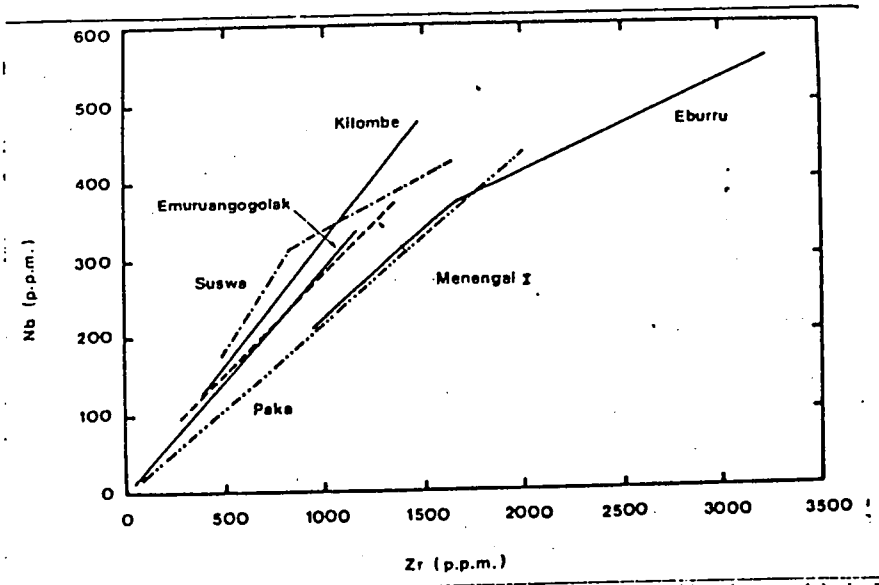

FIG. 3. Zr-Nb plot for basalt-trachyte suites of Paka and Emuruangogolak (post-caldera lavas only), the Kilombe trachytes, the first Menengai trachytic ash-flow sheet and the pantelleritic trachyte–pantelleritic obsidians of Eburru. Data sources as for Fig. 2.

100 Ma ago?) was invoked as a source of ITE in the rift basalts.

Nevertheless, the abundances of the ITE remained low for alkali basalts. For example, plots of Ce, Zr and Rb against $(Fe_2O_3+FeO)/(FeO+Fe_2O_3)+MgO$ (Thompson 1982a, Fig. 34.3) reveal that the *ne*-normative basalts of Paka (Sceal & Weaver 1971), Emuruangogolak (Weaver 1978), Naivasha and Silali (University of Lancaster, unpublished data) have levels of ITE much more characteristic of olivine tholeiites than alkali basalts. In this respect the Kenyan rocks compare with the *ne*- normative members of the Skye Main Lava Series (Thompson *et al.* 1980; Thompson 1982a, b). This effect is particularly marked for Zr, a feature also noted by Pearce (1983) on the basis of MORB-normalized trace-element patterns (MORB, mid-ocean ridge basalt).

It is curious that the basalts associated with some of the most ITE-enriched silicic rocks in the world are relatively ITE impoverished. An important implication is that, if the higher-silica Kenyan rocks are related to the basalts by simple closed-system fractional crystallization, the liquid lines of descent were extremely long. Baker *et al.* (1977, p. 328) calculate from major-element modelling that the 'commonest' (*not* the most fractionated) type of Plateau trachyte lava in the southern Gregory rift represents about 3% by volume of residual liquid derived from the putative parental basalt. That trachyte contains 63% SiO_2. For high-silica rhyolites (76% SiO_2 or less) of the Naivasha area, which show Rb enrichments of up to 80 relative to possible parental basalts, the calculated volume is around 1%. Such values place constraints on the time–space evolution of the magmatic systems which are as yet unconsidered in most models of fractional crystallization.

Geological evidence for depths of magmatic differentiation

On the basis of the approach of Mahood (1984), several lines of evidence combine to suggest that the magma reservoirs beneath the caldera complexes lie at relatively shallow depths.

Plutonic nodules

There can be little doubt that these nodules are the sub-volcanic, crystallized equivalents of the basalts and trachytes of the Kenyan calderas (McCall 1970; McCall & Hornung 1972; Weaver 1978; Jones 1979a; Leat *et al.* 1984). The presence of medium-grained varieties of syenite at Emuruangogolak (Weaver 1978) and at the 2 Ma centre Kilombe (Jones 1979a) and of miarolitic gabbros with interstitial glass at Silali (McCall 1970) suggests that crystallization took place at shallow levels.

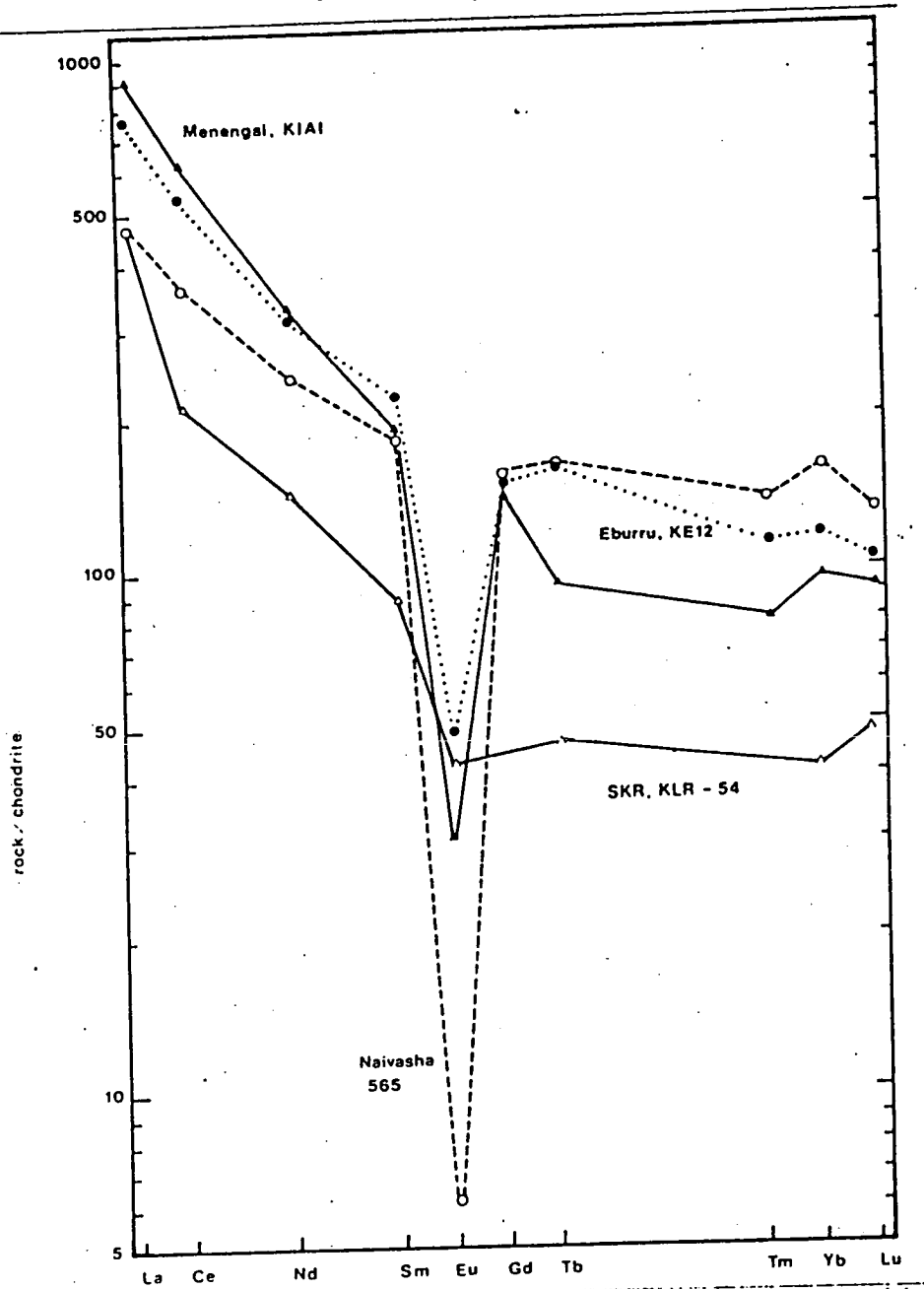

FIG. 4. Chondrite-normalized REE patterns for selected peralkaline trachytes (KIAI and KLR-54) and rhyolites (KE12 and 565). Data and localities are given in Table 2. The normalizing values are from Nakamura (1974), except for Tb and Tm which are from Thompson (1982b).

Distribution of recent faults

The inner trough of the Gregory rift is cut by swarms of closely spaced normal faults, whose development has overlapped that of the late-Quaternary calderas. Evidence from Suswa (Johnson 1969) and from Longonot and Menengai (McCall 1967) shows that these faults virtually die out on the shields of those centres. Mahood (1984) has noted that this is a general feature of Quaternary pantelleritic or trachytic shields and suggests that it indicates the existence at shallow

depths of partially molten zones which cannot support brittle fracture.

The situation in the southern centres contrasts with that in the northern group. At both Silali (McCall & Hornung 1972) and Emuruangogolak (Weaver 1978) closely spaced faults and open fissures cut the shields virtually to the caldera rims. This raises the interesting possibility that the northern complexes are underlain by smaller or deeper chambers than those further S.

Experimental studies

Phase equilibrium studies on pantellerites and trachytes from central Kenya have provided preliminary information on pressures of equilibration of the magmas. Liquidus data for a halogen-rich (F+Cl=0.75 wt. %) water-poor (H_2O^+ =0.10%) pantelleritic obsidian from Eburru (Bailey *et al.* 1974) show that alkali feldspar is the liquidus phase to pressures of about 1 kb, where it is joined by quartz. At higher pressures quartz is on the liquidus. Since quartz phenocrysts are relatively uncommon in pantellerites (Mahood 1984; Sutherland 1974) and virtually always occur in association with alkali feldspar, an upper limit of 1 kb is set for the pressure at which the pantellerites equilibrated. Since liquidi temperatures for pantellerites and trachytes converge at higher pressures (Bailey *et al.* 1974, Fig. 3), low pressures of equilibration probably also characterize the Kenyan trachytes.

Caldera collapse

On the basis of studies of the Sierra La Primavera caldera complex, Mexico, Mahood (1981) has argued that the formation of a caldera 11 km in diameter on eruption of only 20 km^3 of magma as the caldera-forming unit requires a magma chamber with a shallow roof (2–6 km?). If eruption had proceeded from a greater depth, collapse would have been accommodated more easily along regional normal faults than along circular ring fractures. Mahood (1984) applies this line of reasoning to peralkaline volcanoes in general, including the Kenyan centres, most of which occur in areas of extensional tectonics.

With specific reference to Menengai, the high eruption rates required for the emplacement of two chemically zoned voluminous ash-flow tuffs as single flow units also suggest that, prior to eruption, the magma resided in a shallow reservoir (Leat 1984).

Although magmatic differentiation involving the salic rocks apparently proceeded at shallow depths, the sizes and shapes of the magma chambers are not known. It is assumed here that the area of the top of each chamber is no smaller than the area of the caldera above it, and that the chambers have the mushroom shape currently widely accepted (Smith 1979; McBirney 1980; Hildreth 1981) for high-level salic reservoirs.

Basalt–trachyte relationships

Fractional crystallization of basaltic magma

This has been favoured by Sceal & Weaver (1971), Weaver *et al.* (1972), Baker *et al.* (1977), Weaver (1978), Jones (1979b), Norry *et al.* (1980) and Baker (1986) as the dominant mechanism producing trachyte in the Pleistocene–Recent sequences of the rift. *Prima facie* evidence for crystallization processes within the magma chambers of the northern caldera centres is provided by plutonic nodules.

McCall (1970) and McCall & Hornung (1972) have described a series of gabbroic and syenite blocks from Silali volcano which are mineralogically and compositionally equivalent to the eruptive rocks and clearly represent the 'plutonic' stage of evolution. A feature of the nodules is their extraordinary abundance: '. . . the surface of the basalt is littered with a profusion of blocks and bombs, and these are far more conspicuous than outcrops of the basalt' (McCall 1970, p. 257). Their size is also notable: the largest gabbroic block has dimensions in excess of 6 m, thicker than the flow which apparently carried it. McCall suggests that they represent parts of the magma chamber disrupted and detached by gas-coring during a terminal phase of ascent of volatile-charged magma which erupted as the pre-caldera Katenmening basalts.

The gabbroic nodules contain olivine + titan-augite + plagioclase + Fe–Ti oxides + phonolitic interstitial glass, which in some samples is miarolitic. Some specimens are slightly more evolved, exhibiting a 'dioritic' character, with biotite instead of olivine and plagioclase of andesine composition. Syenite nodules are also mentioned, but few details are given.

The Silali nodules are a very important suite, recording conditions in the pre-caldera magma chamber. The simplest interpretation of the relationships is that the interstitial phonolitic liquid in the mafic blocks formed by fractional crystallization and was expelled from the crystallizing wall-rocks to form part of a salic cap to the chamber.

Weaver (1978) reports that small gabbroic nodules are occasionally found in the late basaltic fissure eruptions of Emuruangogolak. Some are mineralogically equivalent to the basalts, while

others are cumulate rocks rich in plagioclase, sometimes with well-developed igneous lamination. One flow contains up to 30% nodules in various states of disaggregation. Most are plagioclase–clinopyroxene–magnetite aggregates; others are dunitic. Weaver infers the presence of layered gabbros at high levels in the Emuruangogolak system. As at Silali, the nodules provide direct evidence of fractional crystallization at depth.

Another approach to basalt–trachyte relationships has been by geochemical modelling. The most detailed analysis is that by Baker *et al.* (1977) of a Plio-Pleistocene basalt–benmoreite–trachyte suite from the southern part of the rift which shows compositional similarities to the northern centres. They used mass-balance calculations for major-element compositions and Rayleigh-law modelling of trace-element contents to show that compositional variations within the suite resulted from closed-system fractionation of the observed phenocryst phases or of phases reasonably inferred to have existed at higher-pressure stages of evolution. A 10% SiO_2 gap which exists between benmoreites and basalts was considered to result from physical discrimination against the relevant magmas by the eruptive system. The eruption of the lavas spanned a considerable period of time (0.8 Ma or less) and took place from several vents. As appreciated by Baker *et al.* (1977, p. 315), the rocks cannot be placed in a rigorous time–composition–space context.

Sceal & Weaver (1971), Weaver *et al.* (1972), Ferrara & Treuil (1974) and Baker *et al.* (1977) have used linear correlations of ITE in Kenyan basalt–trachyte sequences to suggest that the linearity is best explained by fractional crystallization. The argument is that processes such as volatile transfer and crustal melting are unlikely to add the ITE to the melts in exactly the right proportions and amounts to maintain the linear correlations. In fact it remains an open question whether high ITE correlations can or cannot result from the generation of basalts from the upper mantle and trachytes from the lower crust during the same volatile-induced melting cycle, especially if halogens $\pm CO_2$ have a dominant control over trace-element distribution.

The question of the linearity of ITE correlations deserves examination, however. Zr–Rb co-variations for two Kenyan suites are shown in Fig. 5. One is Paka, where the data are taken (Sceal & Weaver 1971) to be most consistent with a fractional-crystallization origin for the trachytes. The other is a pantelleritic trachyte–pantellerite suite from Eburru used by Bailey & Macdonald (1975) to invoke the necessity of a halogen-bearing vapour phase in magma generation. The Eburru rocks show considerably less scatter than the supposedly linear Paka sequence. Further problems relating to the Paka rocks are as follows.

1 The complete body of analytical data, and the petrographic and stratigraphic details, have not been published. Judging from the few published analyses (Sceal & Weaver 1971), the Paka suite contains *ne*- and *hy*-normative basalts and *ne*- and *q*-normative trachytes. The suite clearly represents more than one lineage, yet these

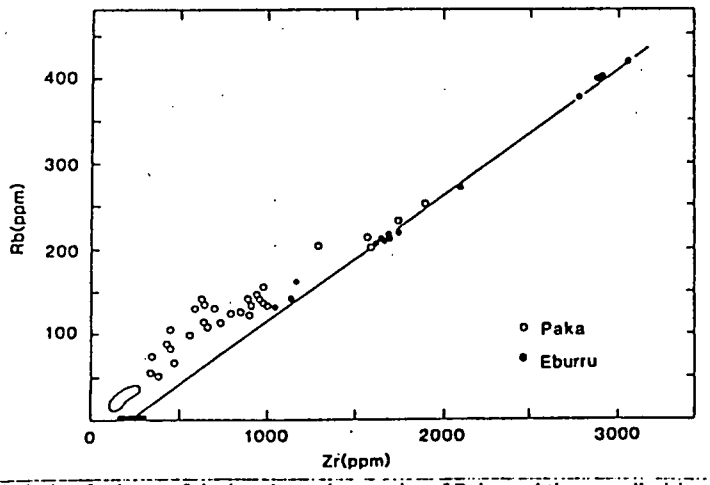

FIG. 5. Zr–Rb co-variation for lavas of the basalt-trachyte series of Paka and the pantelleritic obsidians of Eburru. Data sources are given in Fig. 2. Paka basalts are shown as field. The full line is the computed reduced major-axis line for the Eburru data, and the heavy bar on the axis shows the 95% confidence limits on the intercept.

complexities are not explored by Sceal & Weaver (1971).

2 In certain graphs, e.g. Zr–REE (including Y) plots, the more mafic rocks are clearly not collinear with the trachytes.

3 No pyroclastic rocks were included in the analysed sample. The significance of the linearity at Paka cannot therefore be assessed, and these remarks also apply to all the Kenya centres used by Sceal & Weaver (1971) & Weaver *et al* (1972).

A rather stronger case for linearity is presented by Weaver (1978). On a Zr–Nb plot (Fig. 6) the Emuruangogolak trachytes fall on three distinct lines, in accord with stratigraphy. Even here, two of the lines are not truly collinear with the basalt analyses and do not, on extrapolation, pass through the origin. These features may be compatible with different ITE partitioning into the crystallizing phases but a case has not yet been made.

Significance of composition gaps

As noted earlier, a scarcity of intermediate rock types is present at all the northern set centres, accompanied by a distinct gap over part of the compositional range. This may reflect the following.

1 Some sort of physical control in which rise to the surface is prevented by high viscosity and/or density (Baker *et al.* 1977; Jones 1979b). Thus, four flows of the Kilombe volcano contain blebs of anorthoclase-phyric benmoreite within trachyte (Jones 1979b). The blebs range in volume from less than 1% to 10% and in size up to 30 cm in diameter. Benmoreite lavas are not present at the surface, so the blebs bridge the composition gap in an otherwise complete sequence of lavas from basalt to trachyte. Jones argues that the benmoreite magmas had high viscosity, which was perhaps due to the anorthoclase phenocrysts, and were discriminated against during eruption.

At the Longonot volcano basaltic magma has been erupted only as mixed lavas with peralkaline trachyte (Scott 1980; Scott & Bailey, ~~in press~~ 1984). These lavas were the first products following each of three caldera collapses, and Scott & Bailey (~~in press~~ 1984) argue that input of basalt magma into a root zone underlying a trachyte magma chamber initiated each pre-caldera pyroclastic event and subsequent caldera formation. Again, the volcano has been an imperfect sampler of its magmatic

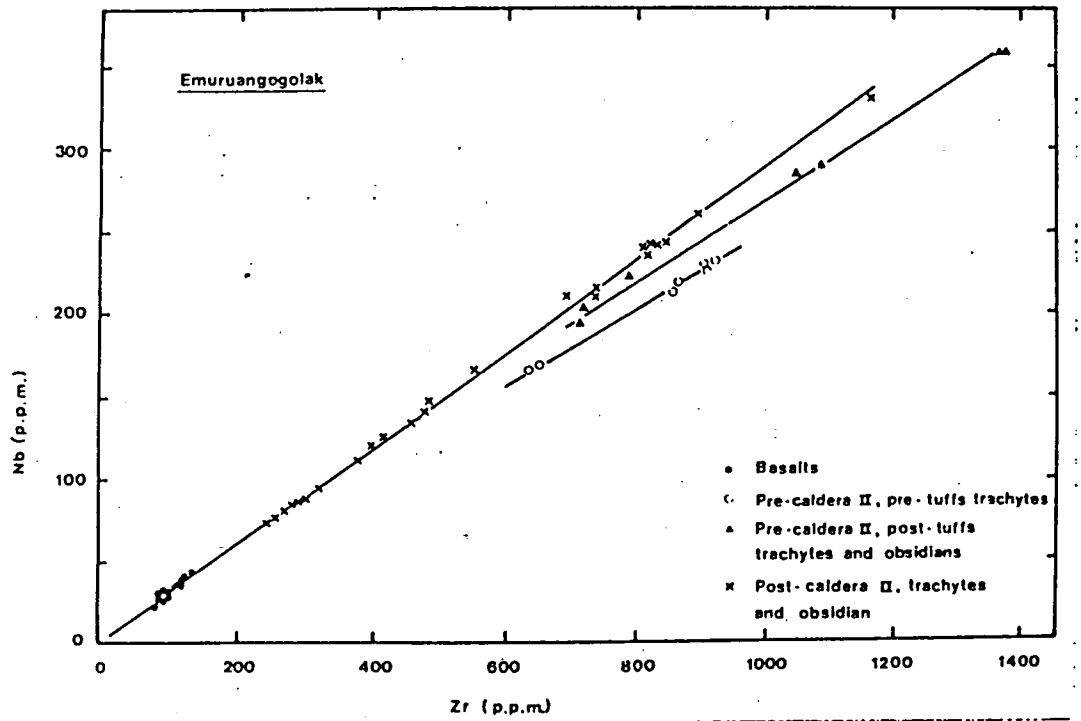

FIG. 6. Zr–Nb plot for lavas of Emuruangogolak showing, in slightly simplified form, the three groups identified by Weaver (1978, Fig. 6).

UPPER4 M21155$15A 10-07-86 15-55-13 Alkaline Igneous Rocks7
UPPER4 M21155$15A 10-07-86 15-55-13 Alkaline Igneous Rocks8

components. A requirement for the Kenyan suites is that the compositions being discriminated against are variable: hawaiites and mugearites (5.1%–2.4% MgO) in the Pleistocene sequence of the southern rift studied by Baker *et al.* (1977), hawaiites to benmoreites (3.9%–0.8% MgO) at Emuruangogolak (Weaver 1978), and benmoreites (about 1%MgO) at Kilombe (Jones 1979b). Therefore it cannot be said that a certain compositional range has less potential to erupt.

2 A control related to the crystallization process itself, where the intermediate composition range is seen as one of rapid crystallization over a narrow temperature interval producing low volumes of melt (Weaver 1978). The appropriate compositions are then found, perhaps exclusively, as margins to the major crystallizing phases within the chamber. Direct evidence of this is found in the nodule suite at Silali; the interstitial glass in certain gabbroic cumulates is of phonolitic composition (unpublished data). One untested possibility is that the onset of crystallization of Fe–Ti oxides produces rapid changes in major-element composition, especially SiO_2. Using calculations of 'percentage crystallized' based on ITE abundances, Weaver (1978) considered that the composition gap between 49% and 59% at Emuruangogolak represented only 25% of the crystallization range between basalt and trachyte. In a similar study Clague (1978) suggested that the transition 50%–57% SiO_2 in the basalt–trachyte sequence of Reunion represented only about 15% of the total range. Both workers related the SiO_2 jump to Fe–Ti oxide precipitation. The position of the composition gap in a magmatic series would then be critically dependent on the point at which oxides began to precipitate, which is itself perhaps a function of pO_2.

Such a mechanism might account for a relative scarcity of intermediate lavas but not for their complete absence, as at Emuruangogolak and Silali, unless a particularly efficient combination of 2 and 3 were operating.

3 A real absence of intermediate materials in the erupted and subjacent parts of the volcanoes would cast serious doubt on a fractional-crystallization hypothesis. This plus the relatively high ratio of salic-to-mafic products at even the northern centres has encouraged the idea that the basalts and trachytes have had different sources.

Partial melting of mafic deep continental crust

The basis of this process (Bailey 1964; Bailey & Schairer 1966; Macdonald *et al*, 1970; Bailey 1974) is that a mantle-derived halogen $\pm CO_2$-rich volatile phase promotes melting of the lower basaltic parts of the continental crust, trachytes representing greater degrees of melting than rhyolites. The vapour buffers the composition of the melts because it controls the temperature of melting and the proportions of solid phases entering the liquid. It also maintains a buffering action on the melt during its subsequent ascent via crystal $\rightleftharpoons$ liquid $\rightleftharpoons$ vapour equilibrium (Bailey 1980).

A problem with this model is that it is, as yet, difficult to test quantitatively. Little is known about the way in which elements partitition between crystal, liquid and vapour during melting and subsequent ascent. Similar lack of information has not dissuaded petrologists from a general acceptance of partial melting of metasomatized mantle as a mechanism for generating alkaline basalts.

Isotopic data which might point to different sources for the basalts and trachytes are available only for the Emuruangogolak volcano (Norry *et al.* 1980). The $^{87}Sr/^{86}Sr$ ratios of the trachytes ($0.703\,72 \pm 0.000\,04$–$0.705\,78 \pm 0.000\,03$) are higher than those of the basalts ($0.703\,38 \pm 0.000\,06$–$0.703\,43 \pm 0.000\,06$, which requires either contamination of the trachytes or derivation from a different source. However, Pb and Nd isotope compositions have mantle values and show no consistent differences between the rock groups, and Norry *et al.* (1980) prefer the explanation that the trachytes were derived from the basalts by fractional crystallization but were contaminated by continental crust.

In summary, several features of the northern set of centres are consistent with a fractional crystallization origin of the salic rocks: the presence of plutonic nodules, in some cases spanning the compositional range of the lavas and containing trachyte glass, the relatively complete range of rock types and the high proportion of lavas compared with pyroclastic rocks. It must be noted, however, that the few available isotope data seem to require trachyte–crust interactions; there are important composition gaps at each centre and the pyroclastic rocks in these complexes have been analytically neglected.

Trachyte–trachyte and trachyte–rhyolite relationships

One view is to see the *crystal–fractionation* mechanisms which produced the trachytes from parental basalts as continuing and controlling compositional variation within the trachytes. One proponent (Weaver 1978, p. 111) acknowledges that at Emuruangogolak, '. . . in detail the

validity of the crystal fractionation process is difficult to assess owing to the cumulophyric nature of many rocks and the loss of alkalis during post-eruptive processes. A favoured mechanism for generating peralkaline from subalkaline melts in the Kenyan sequences (Nash *et al.* 1969; Baker *et al.* 1977; Weaver 1978) is the plagioclase effect (Bowen 1945), a process exacerbated by entry of Al into coexisting clinopyroxene. The transition to peralkalinity within one-feldspar trachytes, lacking discrete plagioclase, is possible only where the feldspar phenocrysts are relatively calcic, i.e. where they have higher normative *an* than the liquid. The peralkalinity is exacerbated by removal of alkali-feldspar-dominated assemblages, with minor clinopyroxene, fayalite and Fe–Ti oxides. If the assemblage is *ne* normative, it may drive mildly undersaturated trachytic magmas towards silica oversaturation.

As noted earlier for the gabbros, there is direct evidence of crystallization processes within the subjacent trachytic magmas in the form of plutonic nodules. At Emuruangogolak, for example, syenite blocks occur in pyroclastic rocks associated with the collapse of caldera II. They are mineralogically similar to the trachyte lavas, although somewhat more leucocratic.

The volcano Kilombe (about 2 Ma old) is older than the other caldera centres discussed here but contains an important suite of syenite nodules (Jones 1979a). The nodules are found only in post-caldera flows and range in size up to some metres. Four classes are recognised.

1 Most abundant, and forming all the large blocks, are coarse-grained syenites. These are formed by nearly complete solidification of batches of trachytic liquid, although a small proportion of residual liquid has escaped from these rocks.

2 Fine-grained syenites, which represent essentially solidified trachyte magma.

3 Aplitic syenites, which occur as veins in the other syenites and are again interpreted as essentially crystallized trachyte.

4 Melasyenites which are found in very-late-stage post-caldera tuffs and are interpreted as Na–Fe–Nb–Y–REE-enriched residual fluid from the crystallization of coarser-grained syenites.

Phenocrysts of nepheline occur in some fine-grained syenites, and groundmass nepheline and zeolites are common in coarse- and fine-grained varieties. However, all the analysed lavas are slightly SiO_2-oversaturated. Furthermore, Jones (1979a) claims that fractional crystallization in the magma chamber has produced more evolved compositions than in the lavas. The general point is that the nodules provide evidence of compositions at depths either not represented in the extrusive rocks or not yet sampled. They record a stage or stages in the evolution of the magma chamber which is not available in the surface rocks.

Syenite blocks or nodules at Menengai were first described by McCall (1967). Their place in the evolutionary history of the centre has been elucidated by Leat *et al.* (1984). Nodules are found in the second ash-flow sheet, whose eruption accompanied collapse of the Menengai caldera. They are thought to represent crystallization against the roof and sides of the chamber of a trachytic magma formed by rehomogenization of the upper part of the chamber after euption of the first ash-flow sheet. This magma was apparently never tapped by the volcano so, as at Kilombe, an important evolutionary stage is recorded only in the plutonic nodules.

Syenites are also found in the Rupfx Tuff, a post-caldera phreatomagmatic deposit. Leat *et al.* (1984) suggest that these formed by 75% crystallization of a Ba-rich trachytic magma against the roof; the chemical effects of this crystallization episode can be recognized in the erupted products.

The evidence from the nodules is that fractional crystallization was intermittently active at Menengai. Other differentiation processes have also been recognized.

Trachyte–trachyte mixing occurred at several stages during the growth of Menengai (Leat *et al.* 1984). The only direct evidence of mixing is in certain small-volume pre-caldera tuffs. These show distinctive compositional variations which are similar to those of the pre-caldera lavas (Fig. 7). It is suggested that the lavas (about 30 km^3 volume) also represent a mixing sequence, although pre-eruptive mixing obliterated petrographic evidence of the end-members. Leat *et al.* (1984) see this process as being consistent with structural stage: the magma chamber was growing by the addition of two or more trachyte magmas.

There is also some evidence that in very recent post-caldera times trachytic magmas from deeper in the magma chamber penetrated into the volatile-rich cap to the chamber, resulting in the formation of mixed magma.

Pantellerite–pantellerite and comendite–trachyte–basalt mixing have been noted at Eburru (D. K. Bailey, personal communication) and Naivasha (R. Macdonald, unpublished data) respectively, suggesting that mixing of salic magmas may be ubiquitous in the rift volcanoes. However, other than at Menengai, its effect as a differentiation mechanism has yet to be assessed.

Leat (1983) and Leat *et al.* (1984) have

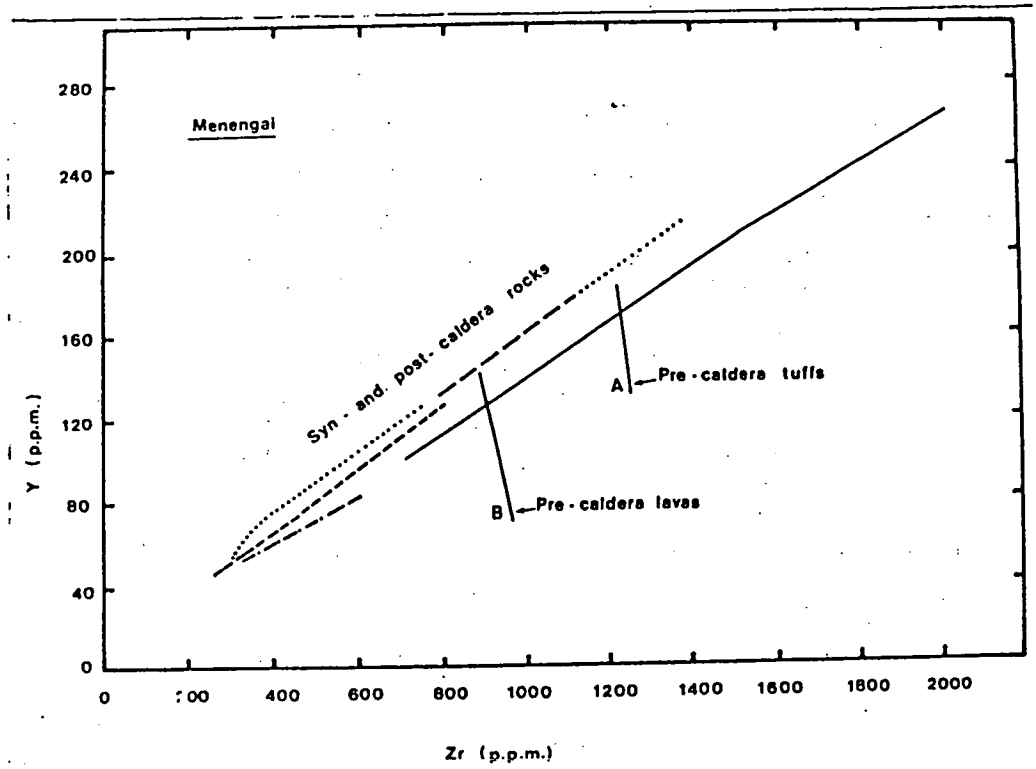

FIG. 7. Zr contents plotted against Y contents in Menengai volcanic rocks (after Leat *et al.* 1984). The pre-caldera tuff trend A represents a single zoned air-fall tuff which is megascopically mixed. Trend B is generalized for the pre-caldera lavas. Both are at a high angle to the trends of syn-caldera and post-caldera units, which was were interpreted by Leat *et al.* as resulting mainly from combinations of liquid-state differentiation processes and crystal fractionation.

identified a further process, rehomogenization of magma by convective overturn (Fig. 8) which contributed to magma evolution at the Menengai volcano. Calculations showed that the density of the trachyte melts was controlled mainly by Fe and volatile contents. Prior to eruption of the first ash-flow sheet, a roofward decrease in density of at least the upper parts of the pre-eruptive column was caused by an increase in volatile concentrations, outweighing the contrary effects of an increase in Fe and a decrease in temperature. Following eruption of the ash-flow, and probably accompanying caldera collapse, volatiles were lost to the atmosphere via fractures in the cauldron block. One result was that the Fe-rich magma in the upper zone of the chamber now had a density similar to, or greater than, that of the underlying lower-Fe trachyte. Convective mixing was promoted, producing a homogenized magma.

This effect may be common in peralkaline systems, where Fe contents generally increase in more differentiated, more peralkaline liquids. However, a good understanding of the time–composition–space relationships at the volcano is necessary to be able to distinguish the homogenized magma chemically.

Further complexity in the interplay of processes during the development of Menengai was revealed by detailed studies of the two ash-flow and air-fall tuff sequences which accompanied caldera collapse. Leat *et al.* (1984) have recorded pre-eruptive gradients in magmatic composition of the kind well known in calc-alkaline systems (Smith 1979; Hildreth 1981) and increasingly recognized on peralkaline systems (Gibson 1970; Noble *et al.* 1979; Hildreth 1981; Mahood 1981; Wolff & Wright 1982). At Menengai there was roofward enrichment in Na, Fe, Mn, F, Cl, Rb, Cs, Pb, Th, U, Nb, Ta, Zr, Hf, REE, Y, Zn and Ni, and roofward depletion in Mg, Al, K, Ca, Ti, P, Sc, Ba and possibly Sr (Fig. 9).

One important observation at Menengai is the ubiquity of compositional zonation in the pyroclastic units. Even thin (a few metres) post-caldera tuffs may show substantial gradients; Zr

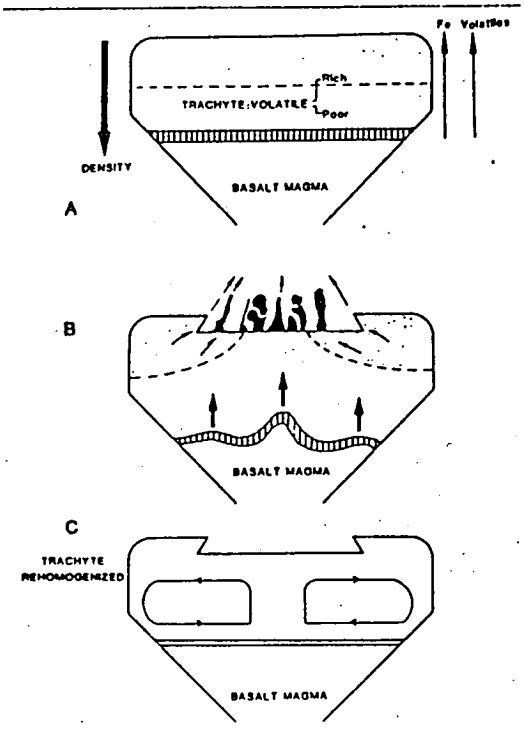

FIG. 8. Diagrammatic representation (much simplified after Leat *et al.* (1984), Fig. 15)) to show the effects of convective overturn on rehomogenizing trachytic magma. A, Prior to major ash-flow eruption, a stable-density interface separates volatile-rich and volatile-poor layers within the trachytic cap to the chamber. B, Following caldera collapse, volatiles in upper parts of the chamber are easily lost through the fractured roof and the magma becomes more dense. Convective overturn promotes mixing with underlying trachyte and perhaps also with magma (striped) from deeper in the chamber, rising buoyantly towards the roof zone. C, Convection proceeds within the upper chamber until a volatile-rich cap is re-established.

abundances in tuff G, for example, vary from 1215 to 1769 ppm. Another is that the variations may be extreme; enrichment factors exceeding 5 for some elements in the first ash-flow sheet are about the maximum yet recorded in a single zoned eruptive unit.

Preliminary study of the Hell's Gate green tuff, a syn-caldera ash-flow of the Longonot volcano, shows that it also is compositionally zoned, although less strongly than the Menengai sheet (enrichment factor 2). It is probable that such zonations are characteristic of all the pyroclastic phases in the southern calderas at least, and further study should document them.

As is the case for the calc-alkaline examples (Hildreth 1983; Michael 1983; Miller & Mittlefehldt 1984), the origin of the compositional zonations is contentious. One possibility can immediately be ruled out at Menengai. Figure 10 is a section of the SiO_2–Al_2O_3–(Na_2O+K_2O) system (Bailey & Macdonald 1969) on which are shown the compositional range of the second Menengai ash-flow tuff and a feldspar control line constructed by connecting the last-erupted least-differentiated tuff to its coexisting alkali feldspar phenocrysts. Clearly, feldspar fractionation by itself could not have produced the trend towards strong enrichment in peralkalinity shown by the tuff magmas (*cf* Macdonald *et al.* 1970; Bailey & Macdonald 1975). Addition of clinopyroxene to the fractionating assemblage is of little help because the hedenbergitic phenocrysts in the sheet are peralkaline, in the sense of having molecular Na_2O greater than Al_2O_3 (Leat 1983).

A further problem regarding fractional crystallization is shown in Fig. 11. Generalized trends for the northern centres Emuruangogolak and Paka show the decrease in K/Rb ratio almost invariably shown with increasing differentiation. The last-erupted parts of the Menengai ash-flows have K/Rb ratios greatly in excess of the trachytes at these centres and, in the case of the first sheet, of any Quaternary basalt in the rift valley. This is quite different to normal geochemical experience and would imply a fractionation mechanism of K and Rb different to that involving crystal ⇌ liquid processes.

Leat *et al.* (1984) used trace-element data to suggest that poorly specified liquid-state differentiation processes had operated, in combination with minor crystal fractionation, in the upper parts of the Menengai chamber. Their model could not be tested rigorously because of lack of information on mineral–liquid partition coefficients in the Menengai samples and because it is currently impossible to disentangle the relative roles of volatile complexing, vapour-phase transport and, for certain elements, fractional crystallization in the differentiation of peralkaline silicic magmas.

A role for volatile complexing in the evolution of the Kenyan salic magmas has been repeatedly championed by D. K. Bailey and his colleagues (Bailey 1986).

Using the composition of non-hydrated glassy pantelleritic trachytes from Menengai, Macdonald *et al.* (1970) suggested that the transition from pantelleritic trachyte to pantellerite in the Kenyan volcanoes was achieved, not by simple crystal fractionation, but by alkali feldspar ⇌ liquid ⇌ alkali-bearing vapour equilibria. In a study of pantellerites from Eburru, Bailey & Macdonald (1975) showed that major- and trace-element variations were incompatible with closed-system

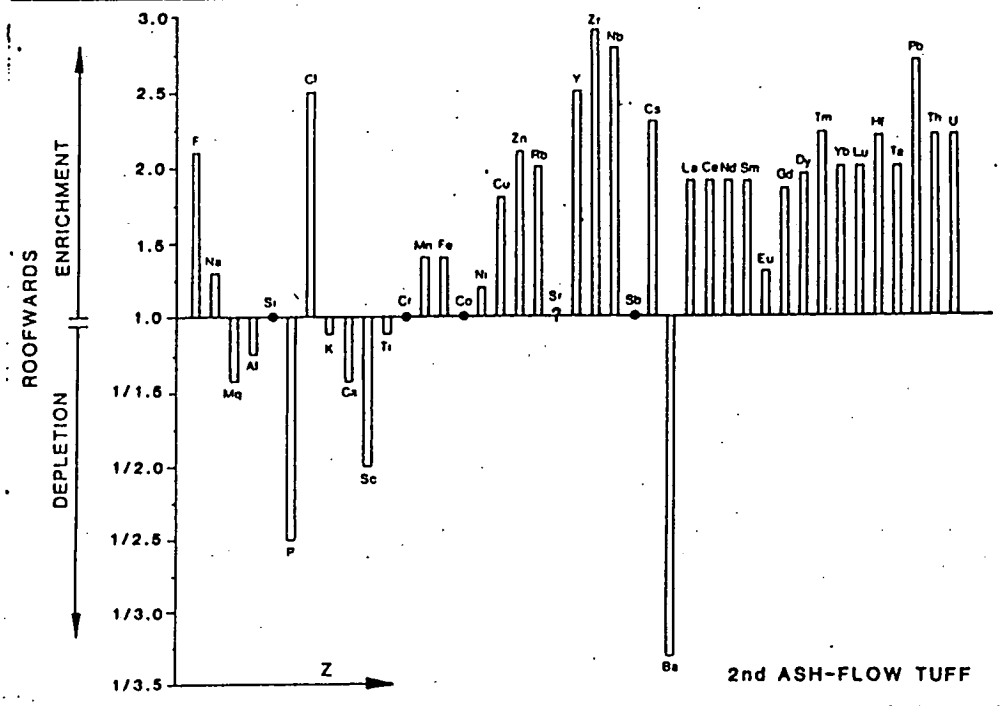

42 FIG. 9. Observed enrichment factors in the second Menengai ash-flow tuff (Leat *et al.* 1984, Fig. 8), calculated by
43 dividing the compositions of the early-erupted by the late-erupted parts of the tuff.

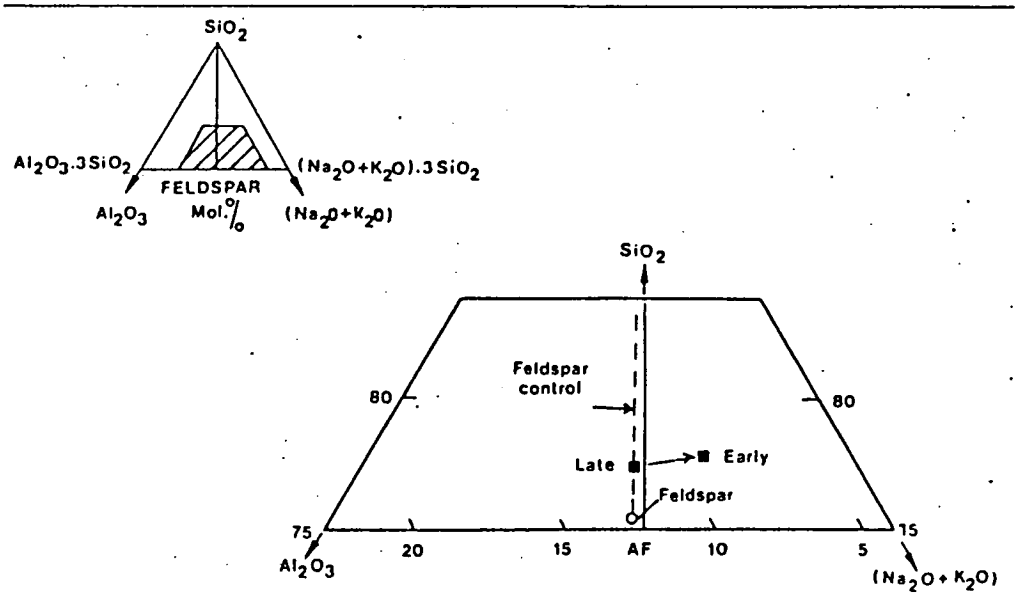

44 FIG. 10. Enlarged portion of the variation diagram for molecular SiO_2, Al_2O_3 and $(Na_2O + K_2O)$ (shaded area in
45 inset). AF is the stoichiometric Ca-free alkali feldspar composition. A tie-line connects the compositions of the
46 early- and late-erupted parts of the second Menengai ash-flow tuff (■). The open circle is the composition of
47 feldspar phenocrysts in the late-erupted part of the tuff. Data from Leat (1983).

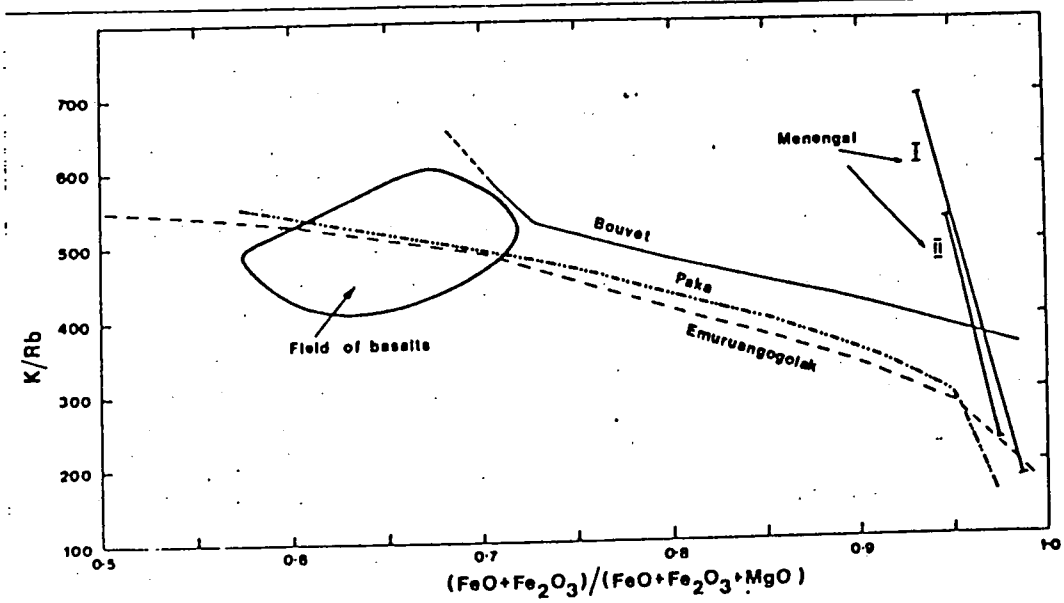

FIG. 11. K/Rb ratio plotted against $(FeO + Fe_2O_3)/(FeO + Fe_2O_3 + MgO)$ ratio for the basalt-trachyte suites of Emuruangogolak and Paka, and for the first and second Menengai trachytic ash-flow sheets. Data sources as for Fig. 2. The generalized trend for the oceanic Bouvet Island basalt-comendite sequence is also shown (Imsland *et al.* 1977). Additional rocks in the field of basalts from Pleistocene-Recent basalts of the Eburru and Naivasha areas (D.K. Bailey and R. Macdonald, unpublished data).

crystal fractionation and invoked the role of a halogen-rich vapour phase in magmatic evolution. They suggested that in this phase Zr and Rb complexed preferentially with F and Nb, and Y and Zn complexed preferentially with Cl (Fig. 12).

As Mahood (1981) has noted, acceptance of a role for volatile complexing in the evolution of peralkaline silicic magmas does not disguise the fact that the mechanisms are speculative and, as yet, not verified experimentally. We have little information on the nature of the inferred complexes: very high correlations of trace metals with F or Cl in the Eburru obsidians may indicate complexing with halogens (Bailey & Macdonald 1975). However, Scott (1982) presents petrographic evidence that a low-solubility CO_2-rich vapour phase coexisted with peralkaline trachyte magma at Longonot, raising the possibility of a role for dissolved carbonate complexes (*cf* Bailey 1980). Bailey (1978) suggests that the vapour coexisting with the silicic magmas was also rich in N and H. However, Kenyan silicic magmatism generally appears to have been very low in H_2O (Bailey 1978, 1980).

Little is known of the way in which the volatile complexes operate. They possibly migrate along *P–T* gradients within the magmas. Alternatively, the complexing of a trace metal with a volatile phase may lower its chemical potential in the liquid, thereby lowering the likelihood of it entering the crystallizing phases.

Continued studies of trace-element patterns in relation to measured halogen, CO_2 and H_2O contents in the Kenyan centres will provide some insight into this thorny aspect of alkaline rock genesis.

The Menengai study has raised several points of general importance in the study of peralkaline volcanic rocks.

1 Whatever the mechanism, it appears that extreme compositional zonations were developed repeatedly through tens of cubic kilometres of magma in times of 10^2–10^4 years (Leat *et al.* 1984). These rates are high when compared with large-volume nonperalkaline systems and must be related to the high Fe and high halogen contents and the relatively low viscosity of the magmas.

2 The most mafic trachytes erupted at Menengai, certain high-Ba post-caldera tuffs, are thought to have compositions partly controlled by processes other than crystal fractionation. They have covered their genetic tracks and cannot therefore be used to model likely mafic source rocks or possible liquid lines of descent from basaltic magma. Leat *et al.* (1984) claim

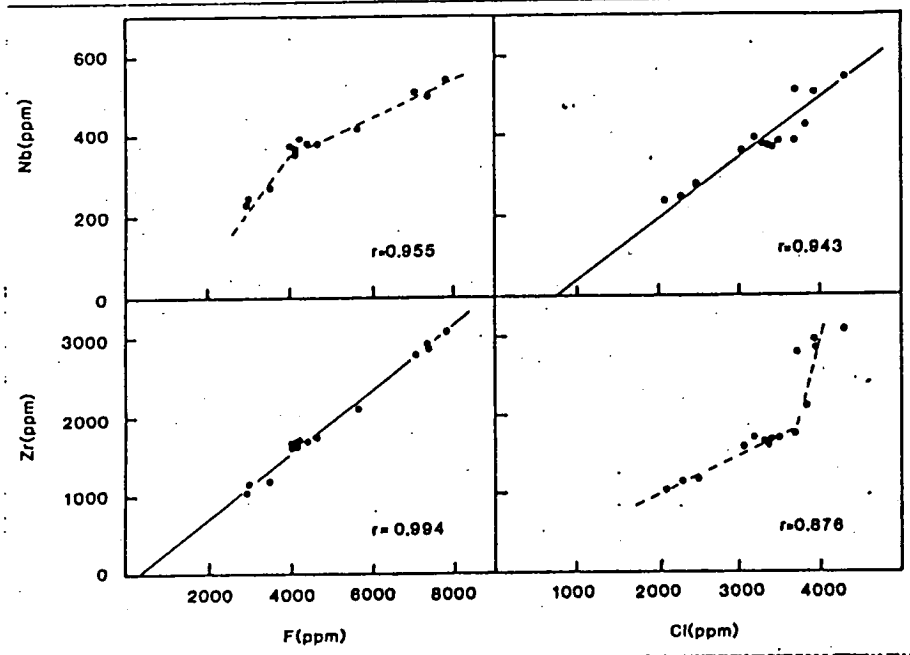

FIG. 12. Examples of linear and non-linear arrays in the Eburru pantelleritic obsidians (from data in Bailey & Macdonald (1975)). Nb is thought to have formed preferred complexes with Cl, and Zr with F, during magmatic evolution.

that parental trachytes have not been recognized at Menengai. The general implication is that indiscriminate use of the chemistry of erupted rocks, without due regard to their place in the evolutionary history of the complex, may lead to spurious petrogenetic conclusions.

3 The inference from the Menengai data (Leat *et al.* 1984) is that the peralkalinity resulted at least in part from processes involving a volatile phase. The antipathetic behaviour of Na and Al resulted in those magmas in the upper part of the chamber achieving critical undersaturation in Al_2O_3 (*cf* Mahood (1981) for the zoned Tala Tuff, Sierra La Primavera, Mexico). The plagioclase effect cannot be uncritically assumed to have promoted peralkalinity in any of the caldera complexes and especially in the southern set where liquid-state processes may have been important.

4 The evolutionary complexity of volcanoes such as Menengai is unlikely to be recognized unless the pyroclastic rocks are included in the geochemical work. Analyses of lavas only would reveal a relatively limited range of compositions, and genetic models based on these data would be wholly inadequate to explain the total compositional range. The analysed sample automatically biases the genetic conclusions. This has been a weakness of several studies of the Kenyan peralkaline rocks (Sceal & Weaver 1971; McCall & Hornung 1972; Weaver *et al.* 1972; Bailey & Macdonald 1975; Baker *et al.* 1977; Weaver 1978).

Generalized models

It was accepted earlier that crystal–liquid processes may have dominated the chemical evolution of the northern set of centres. The development of the southern centres was clearly more complex, if Menengai is typical. Here a model for the evolution of both sets is presented. It is highly speculative but it is hoped that it will help to focus future research on the calderas.

Leat *et al.* (1984) suggest that liquid–crystal–volatile processes became dominant over crystal–liquid processes at Menengai only when a strong volatile gradient had become established in the magma chamber. The volatile-rich cap provided the environment wherein volatile complexing and possibly vapour-phase transport acted most effectively. Conversely, crystallization was suppressed throughout much of the cap by lowering liquidus temperatures, and magma mixing was inhibited by the inability of more mafic magma to penetrate into the lower-density cap. Therefore it may be no coincidence that those centres

(Emuruangogolak and Paka) where no role for volatile complexing has been invoked are from the northern group of caldera where caldera collapse was accompanied by only sparse pyroclastic activity. These centres have not (yet) established volatile-rich caps of sufficient size or stability to permit the operation of volatile-dominated processes.

The reasons for this difference cannot yet be isolated. The size or geometry of the magma chambers, the rate of magma throughput, the local rate of crustal extension (and thus the leakiness of the roof) and the volatile contents of the magmas may all be contributory factors.

Figure 13 attempts to present, in simplified form, the salient features of the evolution of the two sets of caldera complexes as viewed prior to caldera collapse. The general features of the magma chambers follow models of Smith (1979), Hildreth (1981) and McBirney (1980).

In the northern centres a relatively small trachytic cap overlies a dominant volume of basaltic magma, the layers being separated by a mugearitic layer. During periods of eruptive quiescence there are stable density interfaces between the main rock types. Each crystallizes against the side-walls and possibly the roof to form cumulates. The evidence from the intersti-

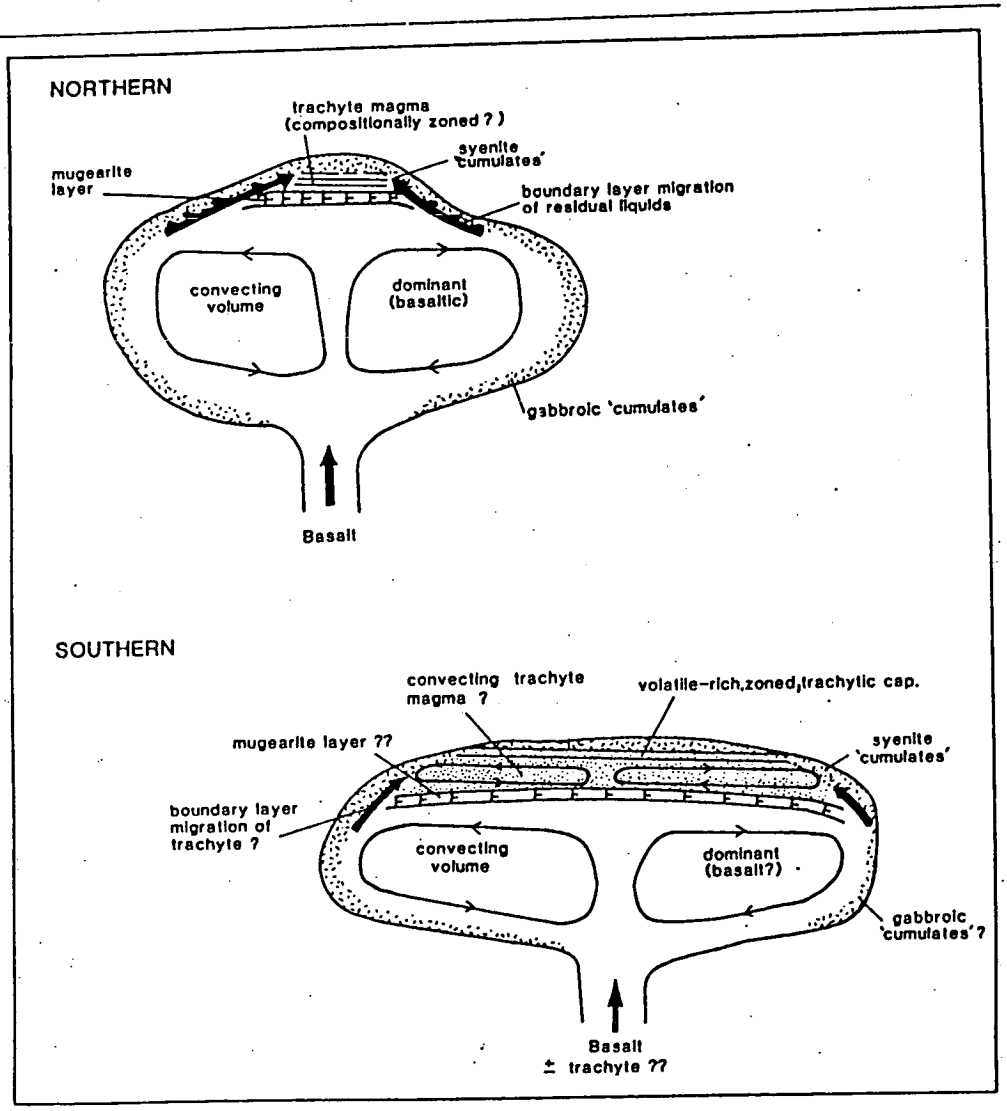

FIG. 13. Generalized models to show relationships in northern and southern set calderas prior to caldera collapse.

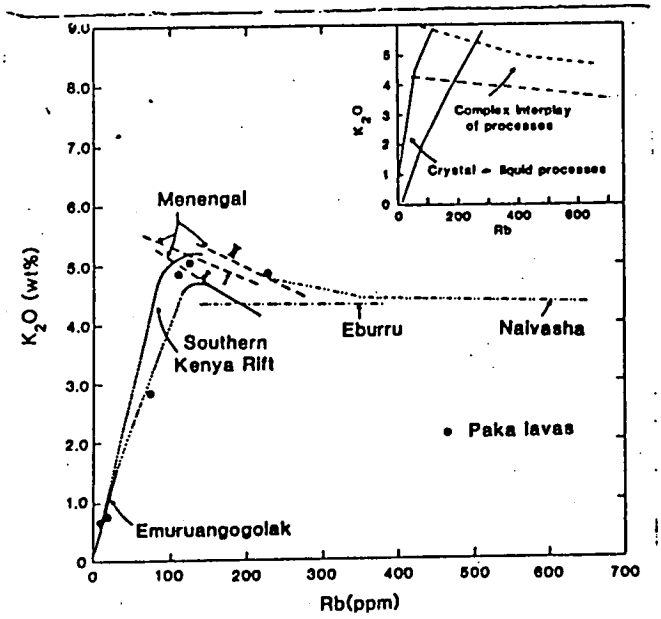

FIG. 14. K_2O–Rb relationships in Kenya basalt–trachyte ± rhyolite suites. Generalized trends for the Emuruangogolak and southern Kenya rift sequences are shown as dotted lines where composition gaps exist. Menengai I, II and III are the trends for the first and second ash-flow sheets and the post-caldera pyroclastic rocks respectively. Data sources are as for Fig. 2. K–Rb space is divided into two overlapping areas where different genetic mechanisms are dominant (inset).

tial glasses in the Silali nodules is taken to show that the trachytes (and probably mugearites) formed by fractional crystallization within these cumulate zones. They rose by boundary-layer migration (McBirney 1980; Turner & Gustafson 1981) towards the chamber roof where they were arrested at a level controlled by their density. The cap was probably compositionally zoned. No substantial volatile-rich cap was established. Caldera collapse was achieved mainly by lateral migration of basalts along fissures, disrupting the caldera walls. Small volumes of trachyte were erupted explosively to form a thin pumice mantle.

The model of the southern centres is even more hypothetical. The dominant volume of basalt is based on thermal considerations and on the presence of small-volume mixed flows at Longonot. Most of the basalt may actually be stored in interconnecting dykes and sills, rather than as a single body. The gabbroic cumulates are hypothetical, as is the mugearite layer. No attempt is made to prejudge the origin of the trachyte magmas. Some may have come from fractional crystallization of basalt and some from deeper sources, e.g. by partial melting of the mafic lower crust.

A critical feature is that the trachyte layer eventually splits into a volatile-rich upper layer and a volatile-poor (convecting?) lower layer. A complex interplay of processes within the cap produces extremely differentiated residua and may ultimately lead to Krakatoa-type caldera formation.

Figure 14 is a preliminary attempt to summarize in terms of K_2O and Rb the compositional fields in which each differentiation mechanism plays a dominant, or important, role. The Emuruangogolak, Paka and southern Kenya rift suites are taken to show positive correlations over most of their range, although the very marked K_2O gaps in each case must be noted. These suites are used to define a field of crystal⇌liquid processes, the main mechanisms being partial melting and crystal fractionation, although magma mixing can produce spread within the field. In the case of fractional crystallization the inflection in the magmatic trends is probably due to a change of plagioclase-dominated to alkali-feldspar-dominated fractionating assemblages. Where partial melting is dominant, the inflection may reflect the differing partitioning of K and Rb into the volatile phase buffering the melting or the disappearance of a potassic phase from the crystalline residue.

A second field encompasses the range of the Menengai zoned ash-flow sheets, the Menengai post-caldera tuffs, pantelleritic trachytes and pantellerites from Eburru, and the Naivasha comendites. In this compositional range complex interplays of volatile complexing, vapour-phase

transport, crystal fractionation, magma mixing and crustal contamination have occurred, probably within the volatile-rich caps to the magma chambers. This diagram is almost certainly also applicable to the peralkaline silicic rocks of other petrographic provinces.

ACKNOWLEDGMENTS Thanks are due to Dr. P. T. Leat, Dr. S. C. Scott, Dr. R. S. J. Sparks and Dr. L. A. J. Williams for constructive criticism of the manuscript, and to Professor D. K. Bailey and Dr. L. A. J. Williams for guidance over many years. The Natural Environment Research Council has supported our Kenyan work via research studentships.

References

BAILEY, D. K. 1964. Crustal warping—a possible tectonic control of alkaline magmatism. *J. geophys. Res.* 69, 1103–11.

—— 1974. Melting in the deep crust. *In*: SØRENSEN, H. (ed.) *The Alkaline Rocks*, pp. 436–42. Wiley, London.

—— 1978. Continental rifting and mantle degassing. *In* NEUMANN, E. R. & RAMBERG, I. B. (eds) *Petrology and Geochemistry of Continental Rifts*, pp. 1–13, Reidel, Dordrecht.

—— 1980. Volcanism, Earth degassing and replenished mantle lithosphere. *Phil. Trans. R. Soc. Lond.*, Ser. A, 297, 309–22.

—— & MACDONALD, R. 1969. Alkali feldspar fractionation trends and the derivation of peralkaline liquids. *Am. J. Sci.* 267, 242–8.

—— & —— 1975. Fluorine and chlorine in peralkaline liquids and the need for magma generation in an open system. *Mineral. Mag.* 40, 405–14.

—— & SCHAIRER, J. F. 1966. The system Na_2O–Al_2O_3–Fe_2O_3–SiO_2 at 1 atmosphere, and the petrogenesis of alkaline rocks. *J. Petrol.* 7, 114–70.

——, COOPER, J. P. & KNIGHT, J. L. 1974. Anhydrous melting and crystallization of peralkaline obsidians. *Bull. Volcanol.* 38, 653–65.

BAKER, B. H. 1986. Outline of the volcanology and petrology of the Kenya rift alkaline province. *In*: FITTON, J. G. & UPTON, B. G. J. (eds.) *Alkaline Igneous Rocks, Geol. Soc. Publ.* (10) pp. 111–116.

——, GOLES, G. G., LEEMAN, W. P. & LINDSTROM, M. M. 1977. Geochemistry and petrogenesis of a basalt-benmoreite-trachyte suite from the southern part of the Gregory Rift, Kenya. *Contrib. Mineral. Petrol.* 64, 303–32.

BOWEN, N. L. 1945. Phase equilibria bearing on the origin of the alkaline rocks. *Am. J. Sci.* 243A, 75–89.

BROWN, F. H. & CARMICHAEL, I. S. E. 1971. Quaternary volcanoes of the Lake Rudolf region, II, The lavas of North Island, South Island and the Barrier. *Lithos* 4, 305–23.

CLAGUE, D. A. 1978. The oceanic basalt-trachyte association an explanation of the Daly gap. *J. Geol.* 86, 739–43.

FERRARA, G. & TREUIL, M. 1974. Petrological implications of trace element and Sr isotope distributions in basalt-pantellerite series. *Bull. Volcanol.* 38, 548–74.

GIBSON, I. L. 1970. A pantelleritic welded ash-flow from the Ethiopian Rift Valley. *Contrib. Mineral. Petrol.* 28, 89–111.

HILDRETH, W. 1981. Gradients in silicic magma chambers: implications for lithospheric magmatism. *J. geophys. Res.* 86, 10153–92.

—— 1983. Comment on 'Chemical differentiation of the Bishop Tuff and other high-silica magmas through crystallization processes'. *Geology* 11, 622–3.

IMSLAND, P., LARSEN, J. G., PRESTVIK, T. & SIGMOND, E. M. 1977. The geology and petrology of Bouvetøya, south Atlantic Ocean. *Lithos* 10, 213–34.

JOHNSON, R. W. 1969. Volcanic geology of Mount Suswa. *Phil. Trans. R. Soc. Lond. Ser.* A26, 383–421.

JONES, W. B. 1979a. Syenite boulders associated with Kenyan trachyte volcanoes. *Lithos* 12, 89–97.

—— 1979b. Mixed benmoreite/trachyte flows from Kenya and their bearing on the Daly Gap. *Geol. Mag.* 116, 487–9.

—— 1981. Chemical effects of deuteric alteration in some Kenyan trachyte lavas. *Mineral. Mag.* 44, 279–85.

LEAT, P. T. 1983. The structural and geochemical evolution of Menengai Caldera Volcano, Kenya Rift Valley. *PhD thesis*, University of Lancaster (Unpublished).

—— 1984. Geological evolution of the trachytic caldera volcano Menengai, Kenya Rift Valley. *J. geol. Soc. Lond.* 141, 1057–69.

——, MACDONALD, R. & SMITH, R. L. 1984. Geochemical evolution of the Menengai caldera volcano. *J. geophys. Res.* 89, 8571–92.

MCBIRNEY, A. R. 1980. Mixing and unmixing of magmas. *J. Volcanol. geotherm. Res.* 7, 357–71.

MCCALL, G. J. H. 1967. Geology of the Nakuru-Thompson's Falls-Lake Hannington area. *Rep. geol. Surv. Kenya*, 78.

—— 1968. The five caldera volcanoes of the central rift valley in Kenya. *Geol. Soc. London Proc. 1647*, pp 54–9.

—— 1970. Gabbroic and ultramafic nodules: high level intracrustal nodular occurrences in alkalic basalts and associated volcanics from Kenya, described and compared with those of Hawaii. *Phys. Earth planet. Inter.* 3, 255–72.

—— & HORNUNG, G. 1972. A geochemical study of Silali volcano, Kenya, with special reference to the origin of intermediate-acid eruptives of the central rift valley. *Tectonophysics* 15, 97–113.

MACDONALD, R., BAILEY, D. K. & SUTHERLAND, D. S. 1970. Oversaturated peralkaline glassy trachytes from Kenya. *J. Petrol.* 11, 507–17.

MAHOOD, G. A. 1981. The chemical evolution of a late Pleistocene rhyolitic centre: The Sierra La Primav-

era, Jalisco, Mexico. *Contrib. Mineral. Petrol.* 77, 129–49.

—— 1984. Pyroclastic rocks and calderas associated with strongly peralkaline magmatism. *J. geophys. Res.* 89, 8540–52.

MICHAEL, P. J. 1983. Reply to comment on 'Chemical differentiation of the Bishop Tuff and other high-silica magmas through crystallization processes'. *Geology*, 11, 623–4.

MILLER, C. F. & MITTLEFEHLDT, D. W. 1984. Extreme fractionation in felsic magma chambers: a product of liquid-state diffusion or fractional crystallization? *Earth planet. Sci. Lett.* 68, 151–8.

NAKAMURA, N. 1974. Determination of REE, Ba, Fe, Mg, Na and K in carbonaceous and ordinary chondrites. *Geochim. cosmochim Acta*, 38, 757–75.

NASH, W. P., CARMICHAEL, I. S. E. & JOHNSON, R. W. 1969. The mineralogy and petrology of Mount Suswa, Kenya. *J. Petrol.* 10, 409–39.

NOBLE, D. C., RIGOT, W. L. & BOWMAN, H. R. 1979. Rare-earth-element content of some highly differentiated ash-flow tuffs and lavas. *Spec. Pap. geol. Soc. Am.* 180, 77–85.

NORRY, M. J., TRUCKLE, P. J., LIPPARD, S. J., HAWKESWORTH, C. J., WEAVER, S. D. & MARRINER, G. F. 1980. Isotopic and trace element evidence from lavas, bearing on mantle heterogeneity beneath Kenya. *Phil. Trans. R. Soc. Lond. Ser. A*, 297, 259–71.

PEARCE, J. A. 1983. Role of the sub-continental lithosphere in magma genesis at active continental margins. *In*: HAWKESWORTH, C. J. & NORRY, M. J. (eds) *Continental Basalts and Mantle Xenoliths*, pp. 230–49. Shiva, Orpington.

SCEAL, J. S. C. & WEAVER, S. D. 1971. Trace element data bearing on the origin of salic rocks from the Quaternary volcano Paka, Gregory Rift, Kenya. *Earth planet. Sci. Lett.* 12, 327–31.

SCOTT, S. C. 1980. The geology of Longonot volcano, central Kenya: a question of volumes. *Phil. Trans. R. Soc. Lond. Ser. A*. 296, 437–65.

—— 1982. Evidence from Longonot volcano, Central Kenya, lending further support to the argument for a coexisting CO_2 rich vapour in peralkaline magma. *Geol. Mag.* 119, 215–7.

—— & BAILEY, D. K. 1984. Coeruption of contrasting magmas and temporal variations in magma chemistry at Longonot volcano, Central Kenya. *in press.*

SMITH, R. L. 1979. Ash flow magmatism. *Spec. Pap. geol. Soc. Am.* 180, 5–27.

SMITH, W. C. 1938. Petrographic description of volcanic rocks from Turkana, Kenya Colony, with notes on their field occurrence from the manuscript of Mr. A. M. Champion. *Q. J. geol. Soc. Lond.* 94, 507–50.

SUTHERLAND, D. S. 1974. Petrography and mineralogy of the peralkaline silicic rocks. *Bull. Volcanol.* 38, 517–47.

THOMPSON, R. N. 1982a. Geochemistry and magma genesis. *In* SUTHERLAND, D. S. (ed.) *Igneous Rocks of the British Isles*, pp 461–77. Wiley, London.

—— 1982b. Magmatism of the British Tertiary Province. *Scott. J. Geol.* 18, 49–107.

——, GIBSON, I. L., MARRINER, G. F., MATTY, D. P., MORRISON, M. A. 1980. Trace-element evidence of multistage mantle fusion and polybaric fractional crystallization in the Palaeocene lavas of Skye, NW Scotland. *J. Petrol.* 21, 265–93.

TURNER, J. S. & GUSTAFSON, L. B. 1981. Fluid motions and compositional gradients produced by crystallization or melting at vertical boundaries. *J. Volcanol. geotherm. Res.* 11, 93–125.

WEAVER, S. D. 1978. The Quaternary caldera volcano Emuruangogolak, Kenya Rift, and the petrology of a bimodal ferrobasalt–pantelleritic trachyte association. *Bull. Volcanol.* 40, 209–30.

——, SCEAL, J. S. C. & GIBSON, I. L. 1972. Trace element data relevant to the origin of trachytic and pantelleritic lavas in the East African Rift System. *Contrib. Mineral. Petrol.* 36, 181–94.

WILLIAMS, L. A. J. 1978a. The volcanological development of the Kenya Rift. *In*: NEUMANN, E. R. & RAMBERG, I. K. (eds) *Petrology and Geochemistry of Continental Rifts* pp. 101–21. Reidel, Dordrecht.

—— 1978b. Character of Quaternary volcanism in the Gregory Rift Valley. *In*: BISHOP, W. W. (ed.) *Geological Background to Fossil Man*, pp. 56–69. Scottish Academic Press, Edinburgh.

—— 1982. Physical aspects of magmatism in continental rifts. *In:* PALMASON, G. (ed.) *Continental and Oceanic Rifts. Geodynamics Series 8*, pp. 193–222. American Geophysical Union, Washington, DC.

——, MACDONALD, R. & CHAPMAN, G. R. 1984. Late Quaternary caldera volcanoes of the Kenya Rift Valley. *J. geophys. Res.* 89, 8553–70.

WOLFF, J. A. & WRIGHT, J. V. 1982. Formation of the Green Tuff, Pantelleria. *Bull. volcanol.* 44, 681–90.

Bull. volcanol. 47, 944-73.

R. MACDONALD, Department of Environmental Sciences, University of Lancaster, Bailrigg, Lancaster LA1 4YQ, U.K.

JOURNAL OF GEOPHYSICAL RESEARCH, VOL. 89, NO. B10, PAGES 8571-8592, SEPTEMBER 30, 1984

GEOCHEMICAL EVOLUTION OF THE MENENGAI CALDERA VOLCANO, KENYA

Philip T. Leat and Ray Macdonald

Department of Environmental Sciences, University of Lancaster, England

Robert L. Smith

U.S. Geological Survey, Reston, Virginia

Abstract. The Menengai volcano is composed almost entirely of strongly peralkaline, Si-oversaturated trachytes. No mafic or intermediate products have yet been identified. The volcano has had a complex geochemical evolution, resulting from the interplay of magma mixing, crystal fractionation and liquid state differentiation. The controlling mechanism at any time was related to the growth stage of the complex, the presence of volatile gradients in the chamber, and the distribution of magma densities in the chamber. Prior to a major ash flow eruption, the magma reservoir was growing by the addition and mixing of two or more trachytic melts, only slightly different in composition. A volatile-rich cap eventually separated from the lava-forming zone and became compositionally zoned by liquid state processes. In late precaldera times, trachyte magma was able to penetrate into the cap zone, resulting in the eruption of mixed magma. The first Menengai ash flow tuff was erupted from a compositionally zoned magma chamber which showed strong roofward enrichment in Fe, Mn, Cs, Hf, Nb, Ni, Pb, Rb, Ta, Th, U, Y, Zn, Zr, and the REE (including Eu) and probably also Na, Cl, and F, and roofward depletion in Al, Mg, Ca, K, Ti, P, Ba, and Sc. Observed enrichment factors of up to 5 make this one of the most strongly zoned ash flow units yet recorded. Zonation was achieved by liquid state differentiation, probably involving volatile transfer and thermodiffusion, and minor crystal fractionation. After a period of rehomogenization of the magma remaining in the upper parts of the chamber, the second Menengai ash flow tuff was erupted, with formation of the present caldera. This unit is also compositionally zoned, although with lower observed enrichment factors than the first sheet. Caldera collapse was followed by convective overturn within the magma chamber and the rise to the roof zone of a Ba-rich magma from a level not tapped by the ash flow. Enrichment of volatiles in this zone resulted in the establishment of a stable density interface between an upper, tuff-producing zone and the lower, lava-forming zone. In the latter, 25% crystallization of syenite took place against the side walls. Crystallization in the tuff-forming zone was more extensive (75%) and produced a series of chemically evolved tuffs. At some critical stage, liquid state processes became dominant in both zones and compositional variations comparable to those in the ash flow sheets were established. Some mixing of the upper and lower zone magmas may have occurred relatively recently. The Menengai volcano provides evidence of the development by liquid state mechanisms of extensive compositional zonations through thicknesses in excess of 10^2 m in times of 10^2-10^3 years. It also gives unique information on the senses and amounts of elemental enrichments and depletions during liquid state differentiation of trachytic magma.

Copyright 1984 by the American Geophysical Union.

Paper number 4B0305.
0148-0227/84/004B-0305$05.00

Introduction

In the central Kenya Rift Valley, a unique petrographic province comprises at least five Quaternary to Recent volcanic complexes (Menengai, Eburru, SW Naivasha, Longonot, and Suswa) which overlap in time and space. The rocks are overwhelmingly peralkaline, ranging from Si oversaturated and undersaturated trachyte to rhyolite compositions. Adjacent complexes may be less than 10 km apart, but petrographic and chemical features indicate that all five complexes are distinct and derived from separate magma chambers.

Detailed studies, referred to below, of Menengai, Eburru, SW Naivasha, and Longonot reveal the complexities of the structural and chemical evolution of each center. In this report the geochemistry of the eruptive rocks of the Menengai caldera volcano is related to the geological history to demonstrate the complex interaction of petrogenetic processes which occurred as the volcano grew and evolved.

Summary of Geological History

Activity at Menengai (latitude 0°12'S, longitude 36°04'E) started about 0.2 m.y. ago, with the growth of a 30-km^3 lava shield. Subordinate pyroclastics include strombolian-style cinder cones, which form the NW part of the shield, and plinian-style pumice falls, which were erupted in late precaldera times. Syn-caldera activity is represented by two ash flow tuffs, which were both preceded by pumice falls. The first (representing about 20 km^3 of magma) is separated from the second (representing about 30 km^3 of magma) by sediments up to 4 m thick. Both ash flows were emplaced as single flow units and have outflow sheet aspect ratios of about 1:4,000. Half the volume of the combined ash flow sheet was ponded in the caldera. The present (77 km^2, 12 x 8 km) caldera formed in association with the eruption of the second ash flow tuff. Well-developed sector graben, embayed caldera walls, and apparently random spacing of some postcaldera vents indicate piecemeal (Krakatoan) collapse. Twenty-three cubic kilometers of magma was erupted as >70 postcaldera lava flows which cover the caldera floor. Cinder cones are rare and plinian-style pumice falls represent about 2 km^3 of magma. Most lavas and pumice falls were erupted from vents located

near the center of the caldera. Correlations with dated fluctuations of nearby soda lakes indicated dates of 29,000 and about 14,000 for the eruptions of the two ash flows. Intracaldera lake sediments prove the existence (from 10,300 to 8300 years B.P.) of a lake which flooded the NE part of the caldera, through which a prominent phreatomagmatic deposit, the Ruplax Tuff, was erupted. All Menengai eruptives are trachytes, phenocryst contents ranging from 6% (by volume) to almost zero. The most porphyritic rocks are the last erupted parts of the ash flow tuffs which are both zoned from a near-aphyric first erupted part. Alkali feldspar, which comprises some 92% of the assemblage, ranges from Ab55 Or43 An2 to Ab67 Or33 An0, the higher Ab feldspars generally occurring in Na-rich rocks. Hedenbergitic pyroxene and Ti-Fe oxides are ubiquitous phenocryst phases; fayalite, aenigmatite, and amphibole (mainly arfvedsonite) are rare.

Analytical Methods

We have sampled all the main eruptive units at Menengai. All analyzed ash flow samples were single pumice clasts of large size, to avoid problems caused by crystal enrichment effects during eruption and deposition. For airfall tuffs, original magma compositions can usually be sampled only if the pumice clasts are large in relation to enclosed crystals. Many Menengai airfall pyroclastics are aphyric; for the porphyritic varieties, the above condition is thought to have been met. Lava samples represent single specimens from each analyzed flow.

All but 8 rocks were ground in an agate mortar to avoid contamination. The remaining 8 were ground in Colmonoy: Cr and Ni values are not reported for those rocks. Major elements except FeO, F, Cl, and H_2O were determined by XRF using glass fusion discs prepared from dried rock powder and $LiBO_2$: $2Li_2B_4O_7$ flux. F was determined by specific ion electrode; Cl, spectrophotometrically; H_2O+, gravimetrically; and FeO, by a modified version of Wilson's (1955) method. The abundances of Ba, Cu, Nb, Ni, Pb, Rb, Sr, Y, Zn and Zr were obtained by XRF, holding sample powder on mylar film. Co, Cr, Cs, Hf, Sb, Ta, Th, U, and the REE were determined by instrumental neutron activation analysis. Estimates of the analytical precision for the trace element determinations are similar to those in the work of Bacon et al. (1981, Table 1).

Results

Chemical Composition

The Menengai trachytes are dominantly quartz-normative, strongly peralkaline rocks, which are sodic and F rich, in the sense of having $Na_2O > K_2O$ and F > Cl. Subalkaline varieties are rare but of petrogenetic importance (see later). In terms of Macdonald's (1974) classification of the peralkaline silicic rocks (Figure 1), the Menengai samples range from comenditic trachyte through pantelleritic trachyte to pantellerite, the spread of points paralleling those of such comparable suites as the Longonot and Eburru complexes in the central Kenya Rift and Pantelleria. Although the more evolved members are rhyolitic, the suite is, for simplicity, here referred to as trachytic.

A striking feature of the Menengai rocks is the restricted range of major element compositions (Table 1). SiO_2, for example, varies only from 60% to 67.5%. The detailed sampling of all the eruptive units of the center's 100-km^3 volume indicates that this range is real. In common with many other caldera-forming continental volcanoes (Smith, 1979; Hildreth, 1979, 1981), the modest range of major element compositions at Menengai is accompanied by strong gradients in minor and trace element abundances, e.g., Zr 168 to 2017 ppm and Ba < 5 to 1316 ppm. The very high abundances of certain "incompatible" elements, including Nb, Y, Zn, Zr, Hf, Ta, and the REE, are more comparable to those in pantellerites than to most trachyte suites (Macdonald and Bailey, 1973) but are in line with the high agpaitic indices (mol $(Na_2O + K_2O)/Al_2O_3 < 1.69$).

The extreme depletion in Ba and Sr is remarkable for rocks with such relatively low SiO_2 contents. Two "end-member" compositions may broadly be distinguished among the erupted products of Menengai: Si-poor, subalkaline trachyte, with higher Al, Ca, Mg, K, Ti, P, Ba, Sc, Sr, and a strongly peralkaline rhyolite, enriched in Na, Fe, Mn, Rb, Y, Zr, Nb, Pb, REE, Hf, Ta, Cs, Th, U, Ni, F, and Cl.

The elemental enrichments are selective. While abundances of the K-related elements, Cs, Pb, Rb, Th, and U are high, they do not show the extreme enrichments of such elements as Nb and Zr. This tends to distinguish peralkaline from subalkaline rock suites (Figure 2) and may be related to the role of halogens in volatile complexing in peralkaline magmas (Bailey and Macdonald, 1975; Hildreth, 1981; Mahood, 1981).

Most of the analyzed rocks are either secondarily hydrated or crystalline, and the effects of these processes on the chemistry must be evaluated. The highly systematic geochemical variation in the suite can be used to show that most samples have lost up to half their original Na_2O contents, an effect typical of peralkaline rocks (Noble, 1970; Macdonald and Bailey, 1973; Baker and Henage, 1977; Jones, 1981). There is no evidence, however, of any other major influence on rock chemistry, although some samples have unsystematic abundances of Cl, F, Cs, U, and Fe_2O_3/FeO ratios believed to result from crystallization and/or secondary hydration.

Complexity of the Geochemical Evolution of Menengai

Zr is used as an index of fractionation because of its wide range (168 to 2017 ppm), its high solubility in peralkaline melts (Dietrich, 1968; Watson, 1979), and precedence in Kenyan geochemical studies (Sceal and Weaver, 1971; Bailey and Macdonald, 1975; Baker, 1975). A plot of Zr concentrations against time (Figure 3) neatly summarizes variations in chemistry as related to structural events in the evolution of the volcano. The complex geochemical evolution of Menengai has been revealed only by detailed sampling of all eruptive units within a firm stratigraphic framework. In the next sections the data are discussed in greater detail and attempts are made to identify the main petrogenetic processes operative in the Menengai magma chamber.

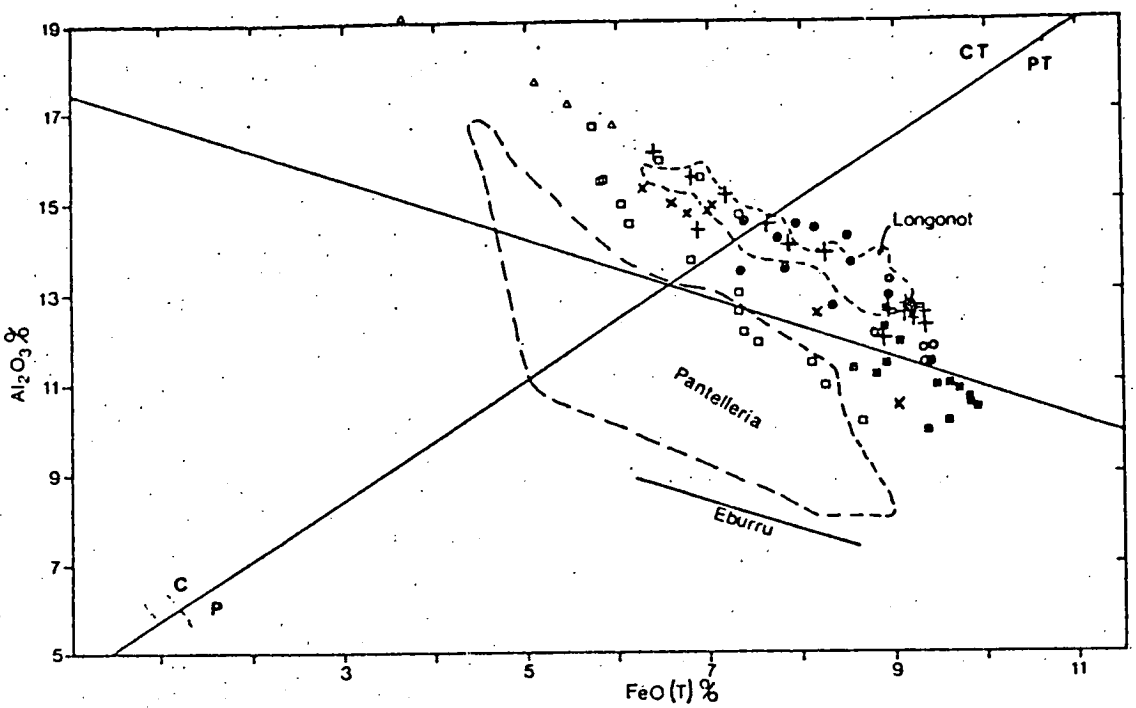

Fig. 1. Menengai rocks plotted in Macdonald's (1974) classificatory scheme for peralkaline, quartz-normative extrusive rocks, based on Al_2O_3 and iron ($FeO_{(T)}$) contents. C, comendite; P, pantellerite; CT, comenditic trachyte; PT, pantelleritic trachyte. Symbols: solid circles, precaldera lavas; open circles, precaldera tuffs; multiplication signs, first ash flow tuff; plus signs, second ash flow tuff; solid squares, postcaldera lavas; open squares, postcaldera tuffs; triangles, syenite clasts. Note that certain tuffs and the syenites are marginally subalkalic but are plotted here for completion. Fields or range of trachytes from Longonot and of pantellerites from Eburru and Pantelleria (Macdonald and Bailey, 1973) given for comparison.

Geochemical Variations and Differentiation Mechanisms

Precaldera Lavas: Chemistry

Ten of the 11 analyzed precaldera lavas were collected from the Lion's Head cliff, the highest part of the caldera wall. The samples are numbered, from oldest to youngest, 1 to 15, with the prefix KOL. Sample K1L4, collected from the southwest caldera wall, was selected as the only glassy precaldera lava. Unfortunately, it proved to be secondarily hydrated.

The oldest exposed flow, KOL1, has been dated at 180,000 years by the K-Ar method (Leat, 1983). The youngest lavas must have predated eruption of the first Menengai ash flow tuff at around 29,000 years B.P. The precaldera lavas were thus erupted over a period of some 150,000 years, to form a volume of about 30 km^3.

Abundances of most major elements and many trace elements, namely, Nb, Rb, Th, and Ni, show little variation (<x1.25) in the lavas. Other trace elements show somewhat wider ranges (>x1.5), including Sr, Y, Zn, and the REE. Two compositional end-members may be distinguished. One, higher in Ca, Fe, Sr, Y, Zn, and the REE the other with slight enrichment in Al, K, Zr, Nb, and Th.

Early precaldera lavas have compositions closer to the lower-Y type, while, with time, flows increased in Y and related elements. The increase was not continuous; frequent reversals toward the lower-Y end-member apparently took place (Figure 4). Considering the evolutionary stage of the system we suggest that these reversals most probably represent periodic addition of new magma batches to the growing Menengai chamber.

Precaldera Tuffs: Chemistry

The six analyzed samples were taken from the western caldera wall. Although they probably represent late precaldera activity, their exact age relationship to the lavas is not known. The rocks are pantelleritic trachytes (Figure 1). Chemical variation within the sequence is similar to that in the lavas, but on average, the tuffs have higher concentrations of Zr, Nb, and most other incompatible trace elements, lower abundances of P, Mg, Al, and Sr, and similar amounts of K, Ti, and Ca. Certain important features of tuff chemistry can be shown on a Zr-Y plot (Figure 5):

1. The tuff compositions are displaced to higher Zr and Y contents relative to the lavas.
2. The oldest analyzed tuff (K1A8) is the most evolved, as witnessed by the high Zr and Y contents.
3. The three tuff samples K1A12, K1A11, and K1A13 lie on a trend which is parallel to that of the precaldera lavas. All three samples come from a single airfall unit. They show that at least some precaldera tuffs were erupted from a compositionally heterogeneous chamber.

These tuffs provide critical evidence of the origin of the compositional variations in the

TABLE 1. Representative Analyses of

	Precaldera Lavas				Precaldera Tuffs		First Ash Flow Tuff						Second Ash			
	KOL1	KOL8	KOL13A	KOL15	K1A12	K1A13	K1A1	K1A4	K1A32/1	K1A32/5	K1A32/8	K1A32/6	K1A15	K1A19	K1A20	H4
Chemical Analyses (wt %)																
SiO_2	63.9	62.4	65.5	63.2	61.0	64.2	63.2	63.4	62.7	63.2	61.0	62.5	64.6	63.2	62.9	63.5
Al_2O_3	14.48	14.18	13.09	12.85	11.77	11.75	10.53	12.51	14.90	14.70	14.94	15.23	12.28	11.91	13.85	16.02
Fe_2O_3	-	-	-	-	-	-	-	-	-	-	-	-	2.21	-	2.15	-
FeO	7.40*	8.50*	8.97*	8.95*	9.42*	9.36*	9.02*	8.17*	7.03*	6.75*	6.65*	6.30*	7.31	8.87*	6.29	6.44*
MgO	0.26	0.33	0.25	0.25	0.13	0.08	0.13	0.20	0.36	0.67	0.43	0.46	0.32	0.36	0.33	0.37
CaO	1.06	1.24	1.01	1.40	1.03	1.00	0.83	1.01	1.49	1.66	1.57	1.53	1.01	1.00	1.18	1.39
Na_2O	7.05	6.04	5.99	6.60	6.08	7.23	5.19	6.27	6.05	5.36	6.63	5.32	4.89	7.34	5.41	6.11
K_2O	5.00	4.86	4.69	4.68	4.40	4.46	4.67	4.90	5.35	5.31	5.84	5.53	4.34	4.46	4.79	5.23
H_2O+	0.81	0.54	0.31	1.18	-	-	-	1.29	0.00	0.23	0.56	0.00	0.14	0.00	0.00	-
TiO_2	0.67	0.71	0.77	0.74	0.68	0.68	0.59	0.66	0.77	0.76	0.81	0.82	0.71	0.71	0.74	0.80
P_2O_5	0.03	-	0.05	0.04	0.01	<0.01	-	-	-	-	-	-	-	0.05	-	0.12
MnO	0.16	0.45	0.22	0.26	0.42	0.40	0.34	0.35	0.29	0.24	0.30	0.28	0.40	0.40	0.36	0.28
Cl	0.004	0.04	-	0.02	-	-	-	0.15	0.01	0.03	0.26	0.20	0.20	0.15	0.12	-
F	0.14	0.08	-	0.16	-	-	-	0.16	0.12	0.17	0.24	0.09	0.27	0.26	0.20	-
Subtotal	100.96	99.37	100.85	100.33	-	-	-	99.07	99.07	99.08	99.23	98.26	98.68	98.71	98.32	-
$O\equiv F_1Cl$	0.06	0.06	-	0.07	-	-	-	0.12	0.05	0.08	0.16	0.08	0.16	0.14	0.11	-
Total	100.90	99.31	100.85	100.26	-	-	-	98.95	99.02	99.00	99.07	98.18	98.52	98.57	98.21	-
Trace Elements (ppm)																
Ba	<5	<5	<5	<5	<5	5	6	8	10	15	15	17	6	8	<5	21
Co	0.5	0.7	0.4	0.3	-	-	0.5	0.5	0.7	0.6	0.7	0.7	0.4	0.3	0.3	-
Cr	<1	<1	<1	<1	<1	1	<1	<1	1	1	<1	<1	1	1	1	1
Cs	1.3	2.4	0.6	1.5	-	-	2.6	1.2	0.3	0.6	0.2	0.3	1.6	1.5	1.1	-
Cu	11	10	13	11	6	6	13	11	12	18	10	11	9	10	9	6
Hf	23.0	23.8	25.0	22.0	-	-	34.5	19.4	9.4	8.8	7.6	6.5	21.2	19.6	14.9	-
Nb	291	293	302	271	346	337	369	227	114	106	95	89	275	253	198	100
Ni	9	13	12	11	13	15	17	11	10	10	5	6	12	9	8	9
Pb	34	31	49	35	32	31	36	25	26	14	15	11	35	27	27	13
Rb	173	168	158	156	140	186	216	133	81	82	60	66	165	152	123	82
Sb	0.4	0.4	0.5	0.5	-	-	0.9	0.5	0.4	0.4	0.4	0.2	0.5	0.3	0.4	-
Sc	3.3	3.7	3.7	3.4	-	-	0.93	3.2	7.6	8.0	8.8	8.5	3.3	3.6	5.0	-
Sr	6	7	2	9	6	2	3	<2	<2	3	<2	<2	<2	<2	<2	2
Ta	17.0	18.4	17.9	16.5	-	-	22.3	13.0	6.50	6.08	5.32	4.78	16.1	14.9	11.5	-
Th	30.3	27.2	33.7	32.1	-	-	40.6	22.6	10.5	10.9	7.0	7.8	31.0	28.5	21.4	-
U	2.8	5.1	3.5	5.3	-	-	7.8	4.0	0.8	1.8	4.1	4.6	5.5	5.0	3.6	-
Y	71	172	83	129	130	181	210	127	66	70	51	49	130	121	93	51
Zn	240	323	298	292	340	382	416	258	163	146	128	126	316	284	314	151
Zr	953	908	948	797	1236	1201	1356	750	378	333	296	271	804	736	561	282
La	133	268	193	222	-	-	296	174	96	90	82	72	214	201	146	-
Ce	229	584	337	404	-	-	541	330	183	173	142	136	386	360	280	-
Nd	92	181	134	149	-	-	208	130	75	74	59	56	142	135	103	-
Sm	15.5	34.1	23.3	26.1	-	-	38.6	22.9	14.0	12.8	10.6	10.0	24.9	24.1	18.7	-
Eu	0.86	2.01	1.71	2.05	-	-	2.37	1.62	1.39	1.48	1.56	1.60	2.02	1.93	1.67	-
Gd	16.0	34.4	21.0	31.2	-	-	39.4	23.0	12.0	14.0	7.4	7.9	20.2†	19.7†	15.6†	-
Tb	2.11	4.90	2.96	3.31	-	-	4.84	2.91	1.77	1.72	1.47	1.20	-	-	-	-
Tm	<1.00	2.25	<2.00	1.71	-	-	2.70	2.04	0.76	0.95	0.61	0.58	1.93	1.49	0.90	-
Yb	7.5	23.0	10.0	14.9	-	-	21.0	13.5	6.4	7.2	5.0	4.8	13.3	12.9	10.8	-
Lu	1.15	3.14	1.38	2.10	-	-	3.05	1.90	1.09	1.09	0.80	0.74	2.02	1.84	1.45	-

Additional data: Dy (ppm); K1A15 = 21.6, K1A19 = 20.6, K1A20 = 15.8, ET = 11.0, K1A38 = 11.3.
*Total Fe as FeO.
†Gd values determined by Inductively coupled plasma spectrometry at King's College, London.

precaldera suites. Zr-Y and Zr-$FeO_{(T)}$ plots (Figures 5 and 10) reveal that the genetic mechanisms in the precaldera rocks were different, either in type or effect, from those in syncaldera and postcaldera rocks, judging from the high angles between the generalized trends. Petrographically, tuff K1A12 is a mixture of two trachytes (Leat, 1983), and the trend from K1A13 to K1A12 is almost certainly a mixing trend.

We suggest, therefore, that the precaldera lavas also represent a mixing sequence, though in this case, preeruptive mixing was sufficiently thorough that no petrographic evidence of the process remains. Such a mechanism would be consistent with the evolutionary stage of the volcano: the chamber was growing by addition of mixing of two, or more, slightly different trachytic magmas.

This model leaves unexplained the origin of tuffs such as K1A8. Relative to the highest-Fe lavas, these plot along trends similar to those of the syncaldera and postcaldera suites (Figure 5). We consider them to have formed from precaldera lava-type magma by the same mechanisms that were dominant during syncaldera and postcaldera times, namely, liquid state differentiation, the evidence for which is given later. In the context of the

the Main Eruptive Units of Menengai

Flow Tuff				Postcaldera Lavas						Postcaldera Tuffs				
K1S8	ET	K1A38	K1A28	K1R4	K1R1	KOR32	KOR23	K1R5	KOR18	A2	K1A34/1	G3	B	D
Chemical Analyses (wt %)														
62.5	62.6	62.9	62.4	65.2	64.0	66.1	65.2	65.0	65.5	61.9	63.4	-	60.4	63.0
12.59	15.13	14.35	12.69	11.27	11.83	10.49	12.21	10.58	10.94	16.64	15.44	11.84	14.67	12.98
2.08	1.31	0.82	2.03	-	-	-	2.11	-	2.14	-	-	-	-	-
7.34	5.99	6.13	7.28	8.55*	9.05*	9.90*	6.97	9.83*	7.66	5.72*	5.84*	7.52*	7.35*	7.33*
0.24	0.39	0.38	0.23	0.23	0.22	0.11	0.17	0.19	0.13	0.58	0.35	0.31	0.45	0.18
1.04	1.33	1.29	1.04	0.98	1.06	0.84	1.14	0.91	0.93	1.84	1.06	0.73	1.16	0.81
7.71	6.66	6.99	8.18	7.48	7.16	7.92	7.66	5.96	7.92	5.49	5.90	3.22	6.70	6.37
4.58	5.26	5.25	4.59	4.47	4.60	4.29	4.55	4.36	4.26	5.38	5.36	4.49	4.97	4.73
0.00	0.16	0.19	0.02	0.25	0.00	0.12	0.00	0.20	0.09	-	0.18	3.72	1.86	1.88
0.72	0.76	0.75	0.72	0.71	0.77	0.73	0.78	0.73	0.75	0.96	0.64	0.49	0.72	0.47
-	-	-	-	-	-	<0.01	0.02	-	<0.01	0.23	-	-	-	-
0.40	0.34	0.31	0.41	0.38	0.41	0.29	0.26	0.40	0.28	0.26	0.24	0.32	0.35	0.32
0.16	0.09	0.08	-	-	0.16	0.18	0.12	0.15	0.15	-	0.03	0.23	0.17	0.26
0.26	0.13	0.13	-	-	0.29	0.30	0.23	0.27	0.28	-	0.13	0.50	0.33	0.52
99.62	100.15	99.57	99.59	99.52	99.55	101.28	101.42	98.58	101.04	-	98.57	-	99.13	98.85
0.14	0.08	0.07	-	-	0.16	0.17	0.12	0.15	0.15	-	0.06	0.25	0.18	0.28
99.48	100.07	99.50	99.59	99.52	99.39	101.11	101.30	98.43	100.89	-	98.51	-	98.95	98.57
Trace Elements (ppm)														
<5	14	<5	<5	<5	5	<5	<5	<5	<5	1316	54	<5	110	<5
0.3	0.3	0.4	0.3	0.3	<0.3	-	0.4	0.2	0.3	-	1.1	-	1.5	0.5
<1	<1	<1	1	1	<1	<1	<1	<1	<1	<1	<1	<1	<1	1
1.5	0.8	0.7	1.5	1.3	1.4	-	1.4	1.8	1.7	-	0.7	-	1.5	3.0
11	12	12	9	11	10	10	11	10	9	4	13	7	11	11
21.0	9.8	9.8	20.9	23.3	22.5	-	22.3	28.1	28.6	-	15.7	-	21.1	41.7
272	137	137	275	271	257	318	257	310	302	61	210	513	275	492
11	8	6	10	11	7	13	11	13	13	8	9	21	9	20
26	15	16	25	24	31	34	26	32	26	9	20	47	66	51
158	98	97	161	145	142	178	140	166	165	55	136	277	147	257
1.2	0.4	0.6	0.6	0.9	1.0	-	0.4	0.6	0.9	-	0.5	-	0.4	0.9
3.3	6.6	6.3	3.2	3.4	3.8	-	3.8	2.4	2.6	-	3.9	-	3.4	1.1
<2	<2	<2	<2	<2	<2	<2	<2	<2	<2	27	11	7	23	3
16.1	7.85	7.88	16.1	16.0	15.6	-	15.1	18.7	19.1	-	12.2	-	15.7	29.8
31.1	14.2	14.1	30.6	28.2	27.7	-	26.9	34.2	34.8	-	23.4	-	30.6	59.8
5.1	2.6	2.5	5.5	4.9	4.7	-	4.9	6.1	6.0	-	3.6	-	5.3	10.8
128	67	67	129	143	142	178	138	167	166	36	89	240	125	224
291	167	166	299	291	318	381	293	370	362	110	167	369	218	360
787	385	383	794	880	871	1118	836	1050	1021	168	630	1769	885	1676
219	109	110	217	217	215	-	213	266	263	-	157	-	189	363
395	203	198	385	380	397	-	390	484	489	-	277	-	327	643
150	76	74	139	144	146	-	151	186	180	-	104	-	121	228
25.4	13.5	13.2	25.1	25.4	25.5	-	26.6	32.7	32.5	-	17.4	-	21.9	38.2
2.03	1.55	1.57	1.98	2.63	2.70	-	2.69	3.18	3.19	-	1.69	-	2.16	2.05
-	11.2†	10.9†	-	12.0	25.0	-	29.0	34.0	35.3	-	17.0	-	22.0	42.4
-	-	-	-	3.20	3.16	-	3.22	4.29	3.98	-	1.75	-	2.35	4.37
1.87	0.84	0.88	1.99	2.29	1.86	-	1.90	3.04	2.41	-	0.96	-	<2.00	3.15
13.6	6.9	6.6	13.7	15.6	16.0	-	14.4	19.5	18.1	-	10.2	-	12.4	23.7
2.07	1.04	1.00	2.01	2.21	2.21	-	2.18	2.68	2.73	-	1.39	-	1.84	3.41

precaldera suite, it seems likely that a low-density, volatile-rich cap became separated from the main lava-producing zone by a stable interface. Within that cap, liquid state processes became dominant, to produce the tuffs from a high-Fe lava parent. Later penetration of trachytic magma into the cap resulted in the trend between K1A13 and K1A12.

Syncaldera Eruptive Rocks: The Menengai Ash Flow Tuffs

Seven samples from the first ash flow tuff have been analyzed. Two represent composites from several small pumice lumps from the basal air fall unit; the other five are single pumice clasts from the ash flow. Stratigraphic positions within the sheet are given in Figure 6, along with data for six elements. There is continuous chemical variation throughout the airfall-ash flow sequence, which is particularly strong in the airfall pumices and in the early erupted part of the ash flow. Also, the behavior of Al_2O_3, K_2O, and Ba are antipathetic to $FeO_{(T)}$, Nb, and Zr. The sequence thus shows an orderly progression from most to least evolved compositions, and it seems that the eruption tapped a compositionally zoned magma chamber (Smith, 1979; Hildreth, 1979, 1981, and references therein).

Field evidence (Leat, 1983) suggests that the

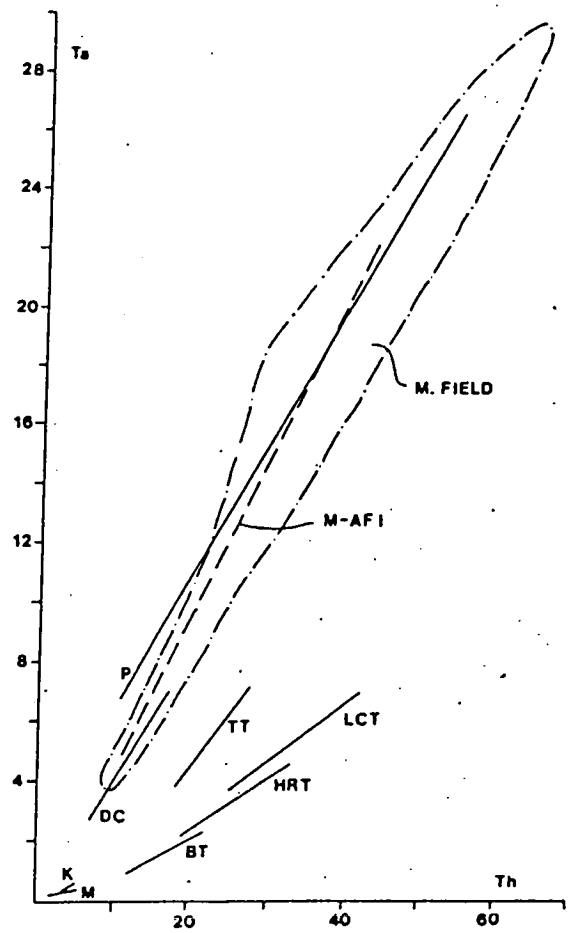

Fig. 2. Generalized plot (after Hildreth, 1981, Figure 2) of Ta and Th contents of the Menengai volcanic rocks and of comparative, large eruptive units. Field encloses all Menengai data; M-AFI is the trend of the second ash flow tuff (data, this paper). M, climatic eruption of Mount Mazama, Crater Lake; K, 1912 eruption in the Valley of the Ten Thousand Smokes, Alaska; BT, Bishop Tuff, California; HRT, Huckleberry Ridge Tuff, Yellowstone; LCT, Lava Creek Tuff, Yellowstone; TT, Tala Tuff, Jalisco; DC, Devine Canyon tuff, Oregon; P, trend of silicic rocks of Pantelleria (all from Hildreth (1981)). The Menengai data follow the general case of steeper slopes and higher Ta contents with increasing alkalinity. Note the close similarity of the Menengai rocks to the more silicic Pantellerian volcanics.

ash flow tuff was emplaced as a single flow unit, at least in the caldera wall exposures. Most compositionally zoned ash flow tuffs were erupted as multiple flow units, e.g., the Bandelier Tuff (Smith and Bailey, 1966), the Bishop Tuff (Hildreth, 1979), and the Fantale Tuff (Gibson, 1970). At least one other example of compositional zonation preserved in a single flow unit has been described, in the Acatlan ignimbrite (Wright and Walker, 1977, 1981).

Table 2 and Figure 7 summarize the chemical variation in the first Menengai ash flow tuff, the figure being based on Hildreth's (1979) use of a similar diagram for the Bishop Tuff. "Enriched" elements are those which concentrated upward (roofward) in the preeruptive magma chamber; "depleted" elements were concentrated downward, either actively and/or passively by dilution. Several features are noteworthy:

1. Fe and Mn were enriched roofward, and Al, Mg, Ca, K, Ti, and P depleted roofward. Enrichment and depletion factors for most major elements were small, however.
2. With the exception of Ba, Sc, and Co (and perhaps Sr; see below), all trace elements were concentrated upward, though the observed enrichment factors are very variable.
3. Na has been lost from all samples. Judging from its distribution in the second ash flow tuff (Table 2), it probably also concentrated upward in the first sheet.
4. The low abundances ($\leq$3 ppm) of Sr mean that analytical imprecision masks its sense of enrichment.
5. F and Cl show erratic variations when plotted against stratigraphic height within the sheet. These almost certainly resulted from posteruptive processes.
6. The REE were all upward concentrating, the observed enrichment factors for all but Eu being about 4. It is significant that the differentiation mechanism(s) within the ash flow magma did not fractionate the REE (excluding Eu) from each other.
7. The high enrichment factor for Cs (8.7) must be treated with great caution, since analytical problems are severe at low concentrations.
8. The antipathetic behavior of K and Rb resulted in a very sharp drop in the K/Rb ratio in roof zone rocks. The ratio (696) in the late erupted part of the sheet is remarkably high for such a highly differentiated rock, as judged by the low CaO, MgO, Ba, and Sr contents.
9. Small, but real, decreases in the ratios of such geochemically coherent elements as Zr and Hf, and Nb and Ta match the behavior of such ratios in zoned subalkaline systems (Macdonald et al., 1984).
10. The maximum reliable enrichment factor for an upwardly concentrated element in the first ash flow is 5 for Zr. This compares closely to factors of 4-5 observed for certain elements in the Tshirege Member of the Bandelier Tuff (R. L. Smith, unpublished data, 1983) and is about the maximum yet recorded in a single, zoned eruptive unit, excluding mixed eruptions. Observed enrichment factors are critically dependent on depth of drawdown into the magmatic system, however, and the total enrichment factor, measuring the total amount of differentiation within the zoned part of the system, is perhaps never observed in single, large-volume silicic eruptions.

Seventeen samples of the second Menengai ash flow tuff have been analyzed. Sample K1A31 was prepared from several pumice lumps from the basal pumice fall. K1A15 (oldest) through K1A20 and H7 (oldest) through H3 represent stratigraphic sections collected from coarse breccia facies of the ash flow, the former in the caldera wall and the latter 2 km NE of the caldera. Stratigraphic positions of the other samples within the sheet cannot be determined. K1S8 and K1S10 were collected from a fines-enriched facies of the sheet (the Olongai Tuff (Leat, 1983)) and ET from a welded airfall facies. K1A38, K1B10, and K1A28 are from separate sites NE of the caldera.

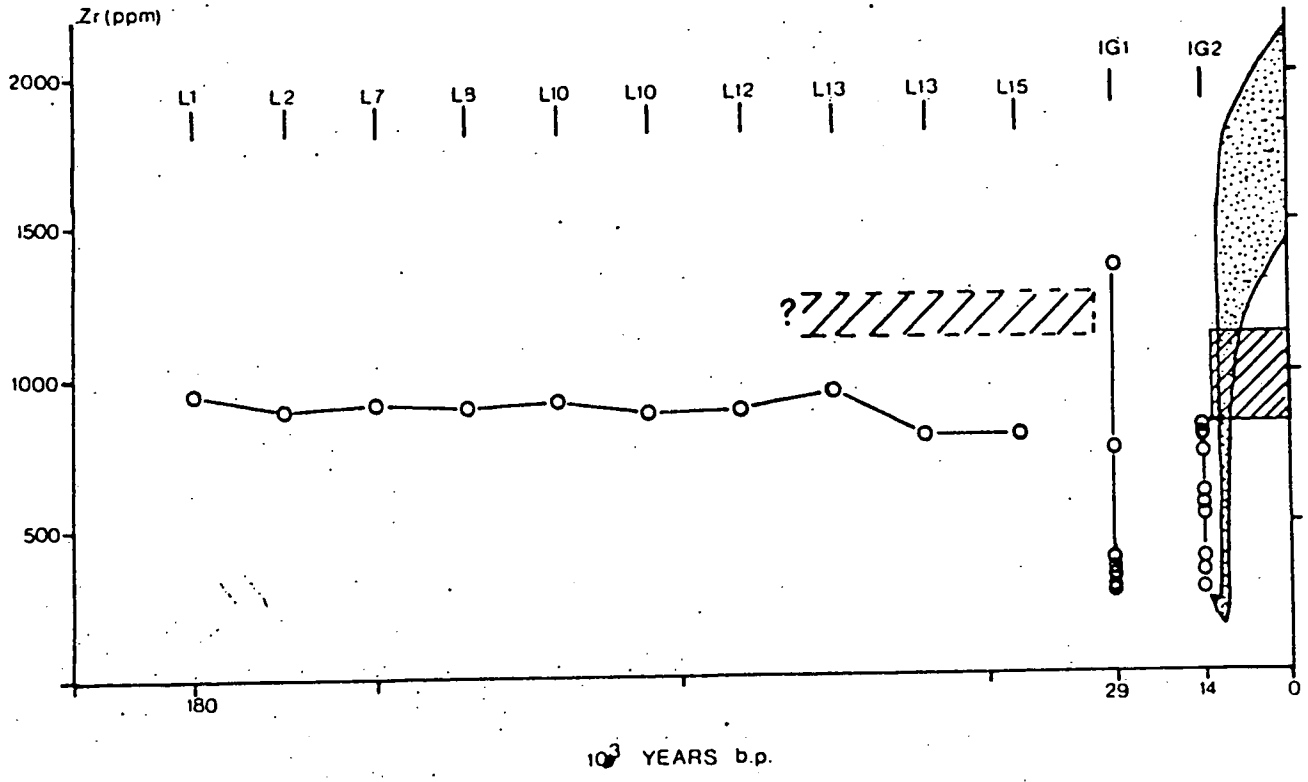

Fig. 3. Variation in Zr concentrations with time. Precaldera lavas L1 to L15 are arbitrarily spaced at regular intervals along the time axis. Approximate position of precaldera tuffs shown by widely spaced diagonal lines. First and second ash flow tuffs plotted at 29,000 years B.P. and 14,000 years B.P., respectively. Fields of postcaldera lavas and tuffs shown by closely spaced diagonal lines and stipple, respectively.

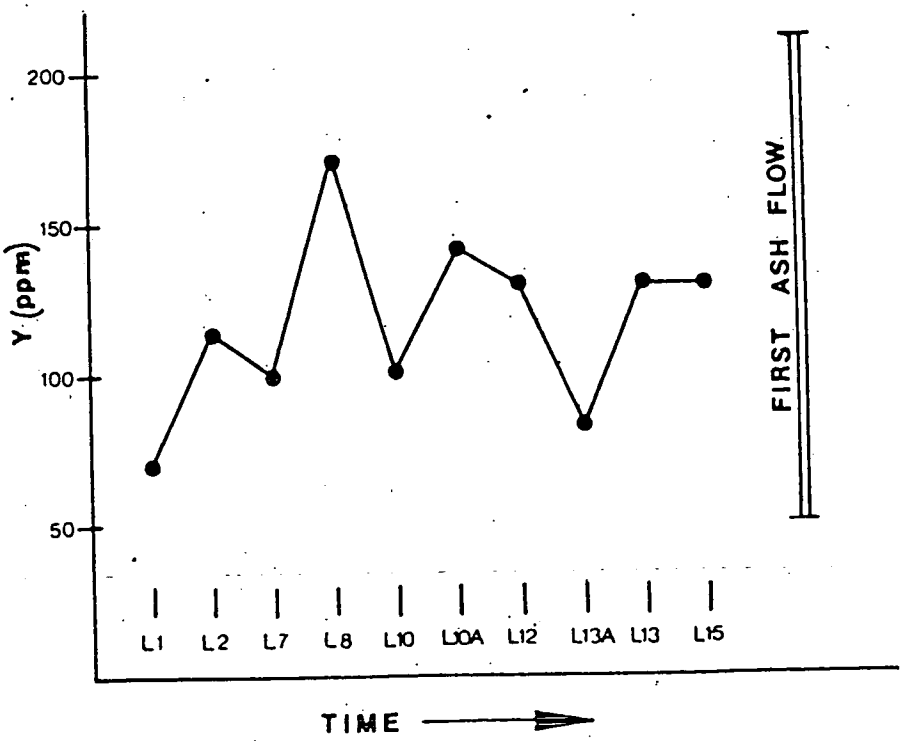

Fig. 4. Y concentration-time plot for precaldera lavas. Lavas are arbitrarily spaced evenly along the time axis. L1 to L15 are sample numbers.

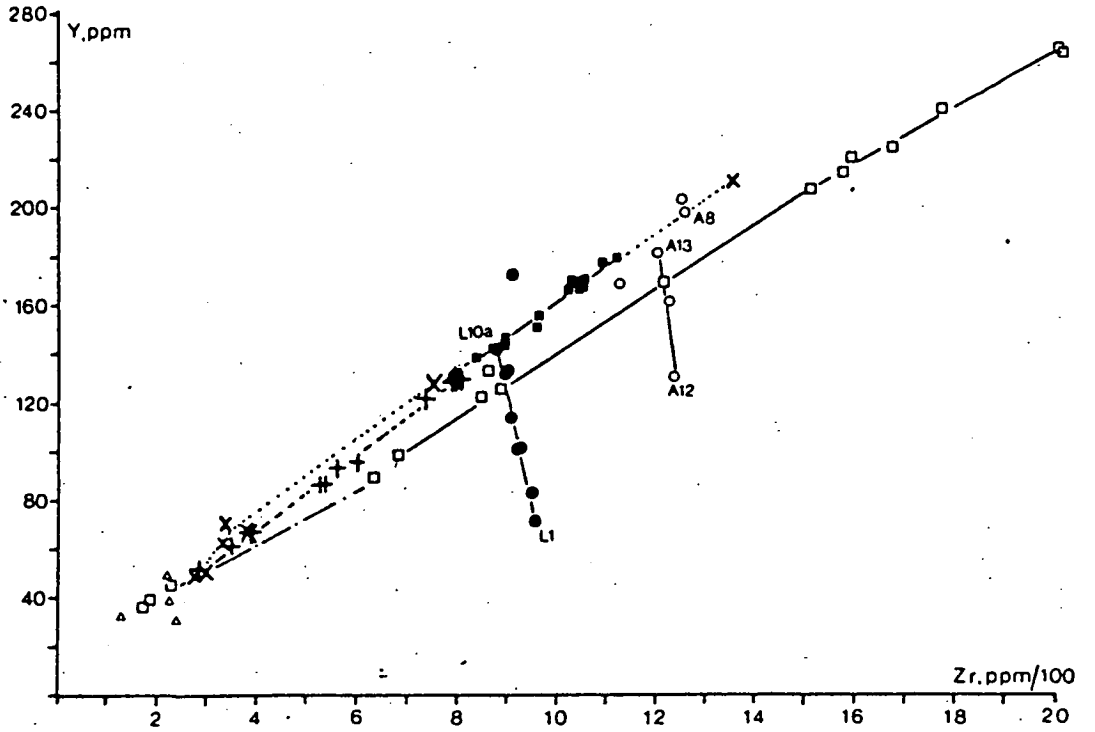

Fig. 5. Zr contents plotted against Y contents in Menengai volcanic rocks. Symbols as in Figure 1. A generalized trend of the precaldera lavas is drawn between KOL1 and KOL10A. Three precaldera tuffs on the trend K1A12 to K1A13 represent a single, zoned airfall tuff. Note that both these trends are at a high angle to trends of syn-caldera and postcaldera units.

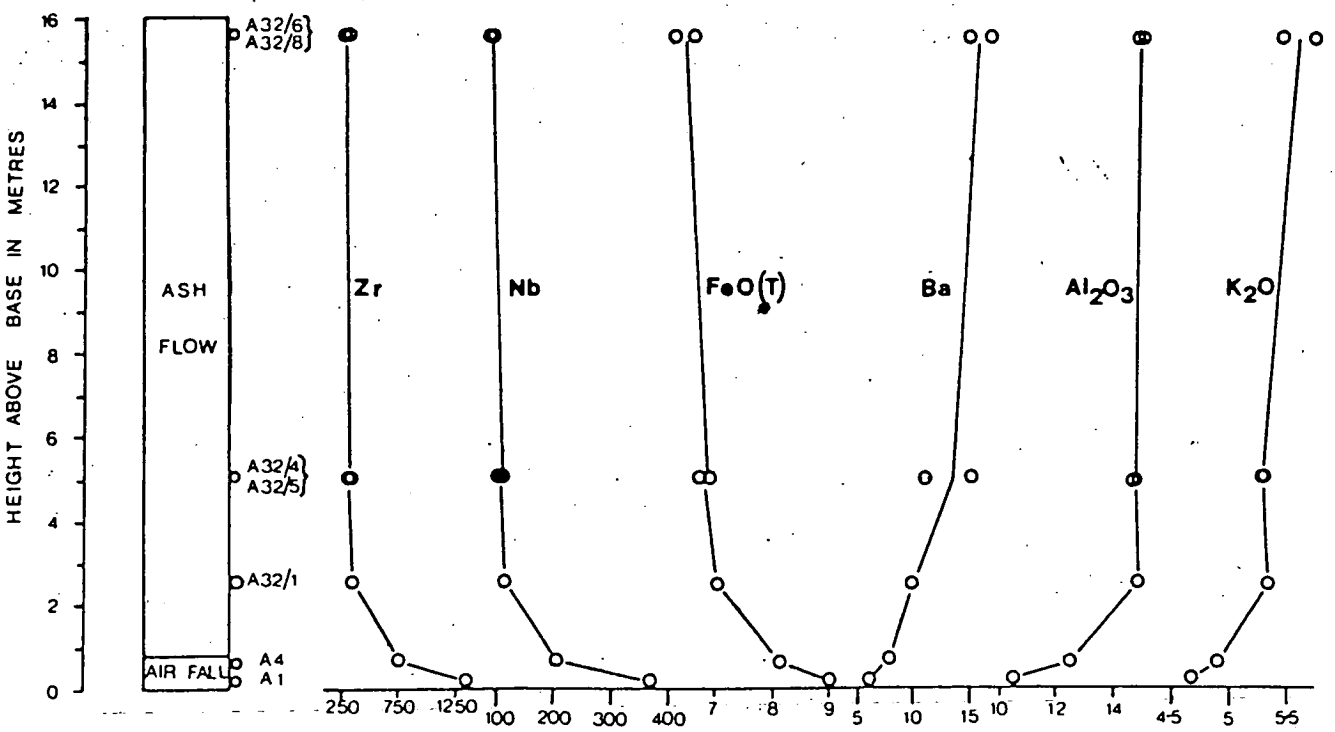

Fig. 6. Stratigraphic relationships of, and selected chemical variations in, analyzed samples of the first Menengai ash flow tuff. Height scale approximate. $FeO_{(T)}$, Al_2O_3, and K_2O in weight percent; Ba, Nb, and Zr in ppm.

TABLE 2. Summary of Compositional Variations in the Main Eruptive Units of Menengai

	Precaldera Lavas		First Ashflow Tuff			Second Ashflow Tuff			Postcaldera Lavas			Postcaldera Tuffs		
	Higher-Y Type	Lower-Y Type	Early Erupted	Late Erupted	Early/ Late	Early Erupted	Late Erupted	Early/ Late	"Evolved"	"Primitive"	Evolved/ Primitive	"Evolved"	"Primitive"	Evolved/ Primitive
Chemical Analyses (wt %)														
SiO_2	63.2	63.9	63.2	62.5	1.0	62.5	63.5	1.0	66.1	65.2	1.0	61.6	63.4	1.0
Al_2O_3	12.85	14.48	10.53	15.23	0.7	12.28	16.02	0.8	10.49	12.21	0.9	12.98	15.44	0.8
$FeO_{(T)}$	8.95	7.40	9.02	6.30	1.4	9.30	6.44	1.4	9.90	8.88	1.1	7.33	5.84	1.3
MgO	0.25	0.26	0.13	0.46	0.3	0.25	0.37	0.7	0.11	0.17	0.6	0.18	0.35	0.5
CaO	1.40	1.06	0.83	1.53	0.5	1.01	1.39	0.7	0.84	1.14	0.7	0.81	1.06	0.8
Na_2O	-	-	-	-	-	7.96	6.11	1.3	7.92	7.66	1.0	-	-	-
K_2O	4.68	5.00	4.67	5.53	0.8	4.56	5.23	0.9	4.29	4.55	0.9	4.73	5.36	0.9
TiO_2	0.74	0.67	0.59	0.82	0.7	0.71	0.80	0.9	0.73	0.78	0.9	0.47	0.64	0.7
P_2O_5	0.04	0.03	<0.12	<0.25	< 1	~0.05	0.12	~0.4	<0.01	0.05	<0.2	<0.09	~0.05	?
MnO	0.26	0.16	0.34	0.28	1.2	0.40	0.28	1.4	0.29	0.26	1.1	0.32	0.24	1.3
Cl	0.02	0.004	-	-	-	0.20	0.08	2.5	0.18	0.12	1.5	0.26	0.03	8.7
F	0.16	0.14	-	-	-	0.27	0.13	2.1	0.30	0.23	1.3	0.52	0.13	4.0
Trace Elements (ppm)														
Ba	<5	<5	6	17	0.4	6	21	0.3	<5	<5	?	<5	54	<0.1
Co	0.3	0.5	0.5	0.7	0.7	0.4	0.4	1.0	0.2	0.4	0.5	0.5	1.1	0.5
Cr	<1	<1	<1	<1	?	1	1	1.0	<1	<1	?	1	<1	?
Cs	1.5	1.3	2.6	0.3	8.7	1.6	0.7	2.3	1.8	1.4	1.3	3.0	0.7	4.3
Cu	11	11	13	11	1.2	11	6	1.8	10	11	0.9	11	11	1.0
Hf	22.0	23.0	34.5	6.5	5.3	21.2	9.8	2.2	28.1	22.3	1.3	41.7	15.7	2.7
Nb	271	291	369	89	4.1	275	100	2.8	318	257	1.2	492	210	2.3
Ni	11	9	17	6	2.8	11	9	1.2	13	11	1.2	20	9	2.2
Pb	35	34	36	11	3.3	35	13	2.7	34	26	1.3	51	20	2.6
Rb	156	173	216	66	3.3	165	82	2.0	178	140	1.3	257	136	1.9
Sb	0.5	0.4	0.9	0.3	3.0	0.6	0.6	1.0	0.6	0.4	1.5	0.9	0.5	1.8
Sc	3.4	3.3	0.9	8.5	0.1	3.3	6.3	0.5	2.4	3.8	0.6	1.1	3.9	0.3
Sr	9	6	3	<2	?	<2	2	?	<2	<2	?	3	11	0.3
Ta	16.5	17.0	22.3	4.78	4.7	16.1	7.88	2.0	18.7	15.1	1.2	29.8	12.2	2.4
Th	32.1	30.3	40.6	7.8	5.2	31.0	14.1	2.2	34.2	26.9	1.3	59.8	23.4	2.6
U	5.3	2.8	7.8	1.8	4.3	5.5	2.5	2.2	6.1	4.9	1.2	10.8	3.6	3.0
Y	129	71	210	49	4.3	130	51	2.5	178	138	1.3	224	89	2.5
Zn	292	240	416	126	3.3	316	151	2.1	381	293	1.3	360	167	2.2
Zr	797	953	1356	271	5.0	804	282	2.9	1118	836	1.3	1676	630	2.7
La	222	133	296	72	4.1	214	110	1.9	266	213	1.2	363	157	2.3
Ce	404	229	541	136	4.0	386	198	1.9	484	390	1.2	643	277	2.3
Nd	149	92	208	56	3.7	142	74	1.9	186	151	1.2	228	104	2.2
Sm	26.1	15.5	38.6	10.0	3.9	24.9	13.2	1.9	32.7	26.6	1.2	38.2	17.4	2.2
Eu	2.05	0.86	2.37	1.60	1.5	2.02	1.57	1.3	3.18	2.69	1.2	2.05	1.69	1.2
Gd	31.2	16.0	39.4	7.9	5.0	20.2	10.9	1.9	34.0	29.0	1.2	42.4	17.0	2.5
Tb	3.31	2.11	4.8	1.2	4.0	-	-	-	4.29	3.22	1.3	4.37	1.75	2.5
Tm	1.71	<1.00	2.7	0.58	4.7	1.93	0.88	2.2	3.04	1.90	1.6	3.15	0.96	3.3
Yb	14.9	7.5	21.0	4.8	4.4	13.3	6.6	2.0	19.5	14.4	1.4	23.7	10.2	2.3
Lu	2.10	1.15	3.05	0.74	4.1	2.02	1.00	2.0	2.68	2.18	1.2	3.41	1.39	2.5
Rocks used	KOL15	KOL1	K1A1	K1A 32/6		K1A15	K1A38 H4		KOR32 K1R5	KOR23		D	K1A34/1	

Additional data: Dy (ppm); K1A15 = 21.6, K1A38 = 11.0.

Like the first sheet, the second is chemically zoned, the senses of elemental enrichments and depletions being comparable (Table 2 and Figure 8). A more complete data set is available, however. Na, F, and Cl show systematic upward enrichments, because posteruptive processes have not significantly altered magmatic abundances. Only for Sr, where abundances are very low, ≤2 ppm, is the sense of enrichment unknown. Observed enrichment factors are generally lower than for the first ash flow, and a comparison can be drawn with the Valles system, New Mexico, where the first (Otowi) ash flow tuff had a more evolved early erupted part than the second (Tshirege) member (Smith, 1979). Importantly, the second Menengai ash flow is zoned from a strongly peralkaline early erupted

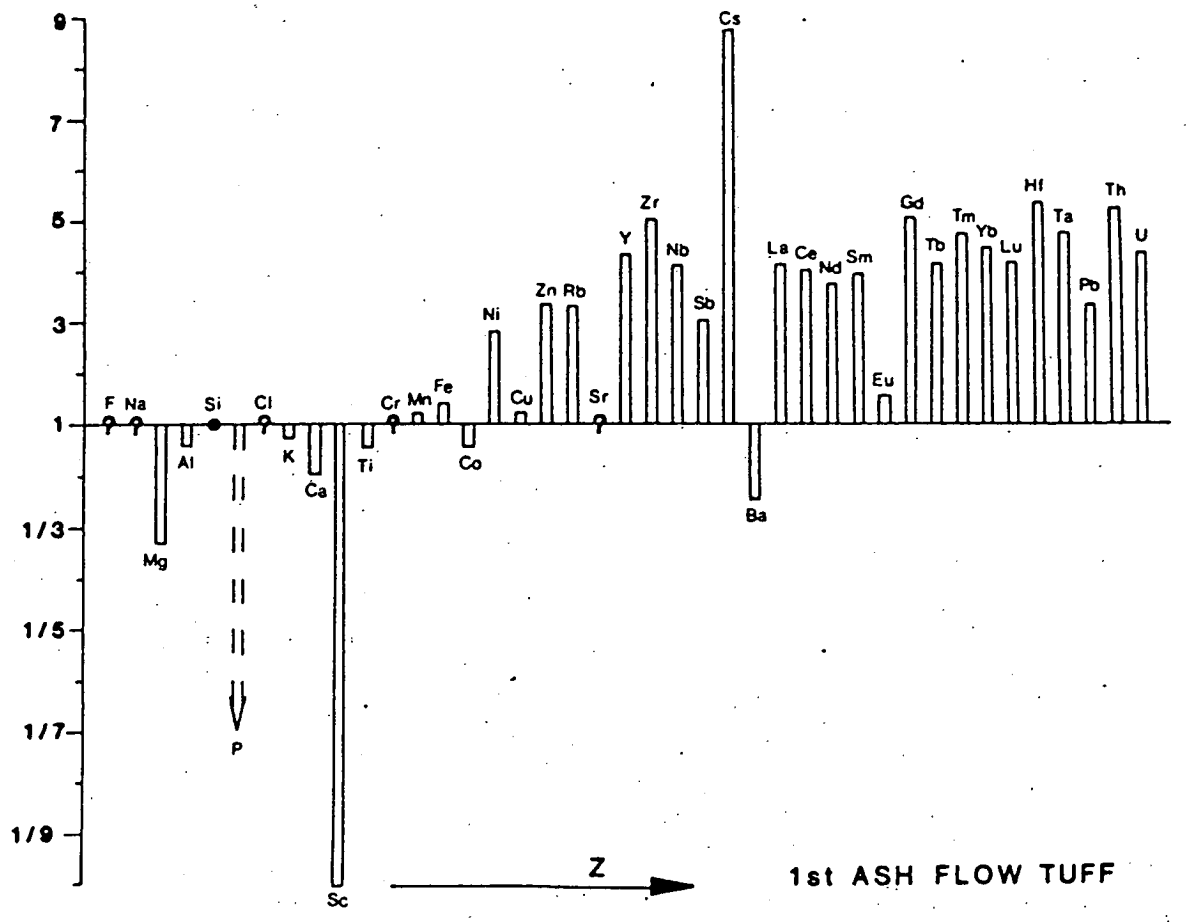

Fig. 7. Observed enrichment factors in the first Menengai ash flow tuff, arranged by atomic number. Factors as in Table 2.

material (agpaitic index, 1.44) to a subalkaline last erupted part (0.98).

Postcaldera Lavas: Chemistry

Thirteen samples of postcaldera lavas have been analyzed. Added to this group is an analysis of a caldera floor cone tuff (K1R7), whose chemical affinities are with the lavas rather than the other postcaldera tuffs. The probable stratigraphic order, interpreted from field evidence, forms the basis of the chemical variations-time plot (Figure 9). There are overall increases, with time, in the concentrations of Ce, Zr (and related elements) and decreases in Ca, Al (and related elements). The reversals of the overall trends, notably that at KOR32, could be results of periodic mixing of the evolving postcaldera magma with another melt. We prefer a different explanation. Chemical variations in the postcaldera lavas (Table 2, Figure 10) are similar to those in the ash flow tuffs, which were palpably erupted from a zoned chamber, a view strengthened by field evidence that flows KOR23 and KOR32, compositional extremes in the lavas, were erupted at about the same time. The fluctuations shown in Figure 9 thus record the range of compositional levels from which the lavas were erupted. We thus infer that individual flows show a range in composition; at present, we do not have the data to test this. The high Fe-Zr nature of sample KOR32 suggests that the complete zonation had been established relatively early in postcaldera times, but note that an unknown, but probably thick, sequence of postcaldera eruptives is buried under the presen exposures (Leat, 1983).

Postcaldera Tuffs: Chemistry

Most of the 17 analyzed postcaldera tuffs wer prepared from several pumice lumps from each tephra layer. The feldspar-rich tuff A3 was separated into glass (A3G) and feldspar (A3F) components. The two samples of Ruplax Tuff (K1A34/1 and K1A34/2) are single pumice clasts. Samples G1, G2 and G3 are from the same 2-m-thic tephra layer, tuff G.

As a group the postcaldera tuffs show strikin chemical variations. The early tuff, A2, has a Zr content of 168 ppm, which is the lowest for a Menengai eruptive rock. The late erupted tuff L has, by contrast, the highest Zr (2017 ppm), the range thus being 12X. Individual tephra layers also show a range of compositions. Zr concentra tions within tuff G vary from 1215 to 1769 ppm. This is evidence that at least some of the post-caldera tuffs were erupted from a compositionall zoned chamber. The directions and amounts of elemental enrichments and depletions (Table 2) a comparable to those in the ash flow tuffs and postcaldera lavas and were almost certainly produced by the same differentiation mechanisms. The tuffs are not, however, completely similar t those earlier units; on a Zr-$FeO_{(T)}$ plot (Figure

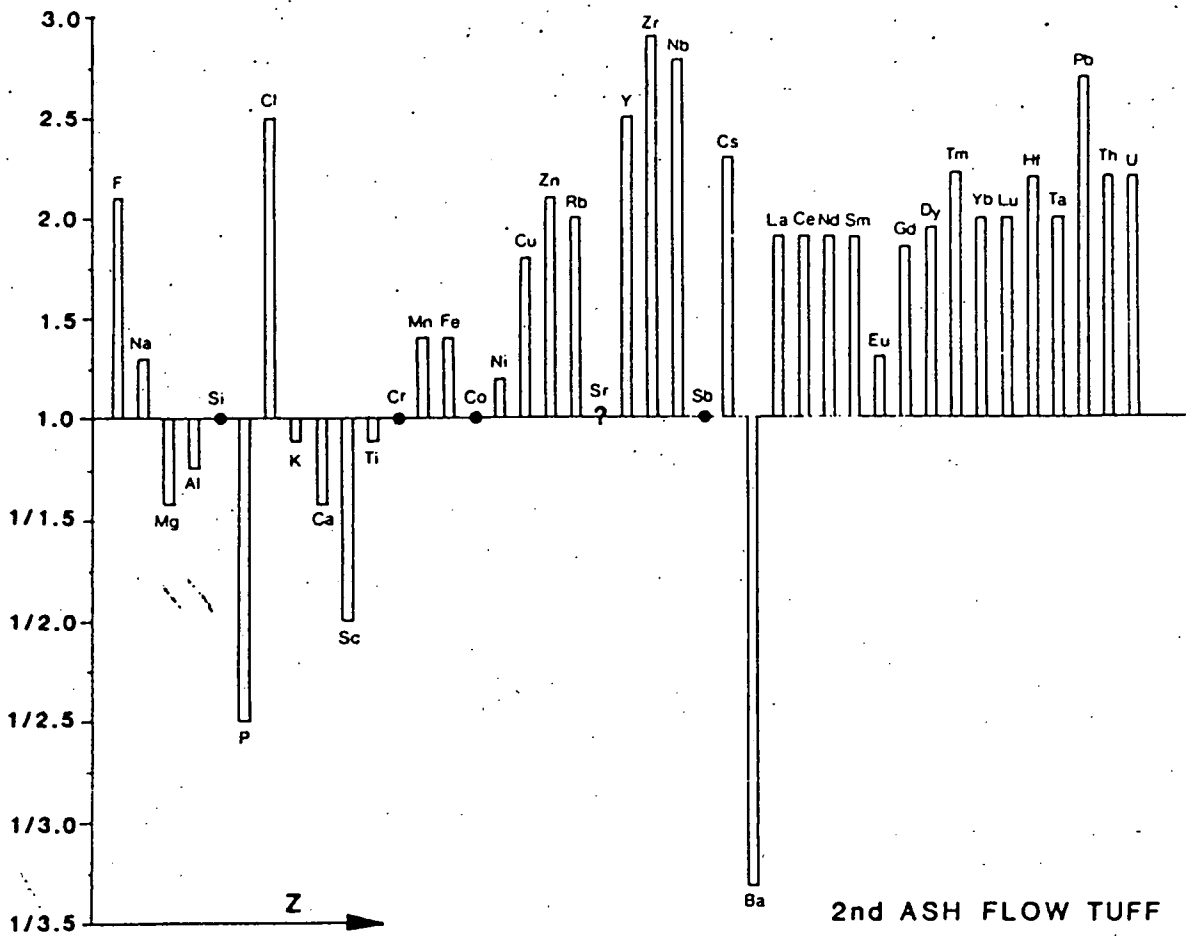

Fig. 8. Observed enrichment factors in the second Menengai ash flow tuff. Factors as in Table 2.

10), for example, they plot on a separate, though subparallel, low-Fe trend. Furthermore, the trend is not linear. We shall speculate later that the early and late postcaldera tuffs were generated by a different mechanism than the main sequence between the Ruplax Tuff and tuff G3.

Four syenites occurring as lithic clasts in the Ruplax Tuff (samples K1XA-D) have compositions broadly similar to those of the early postcaldera tuffs such as A2, except that the concentrations of Zr and the related incompatible elements are rather lower.

Differentiation Mechanisms: Syncaldera and Postcaldera Rocks

The four main eruptive units show zonation patterns which are similar (Figures 5 and 10). They plot as parallel, but separate, trends on many variation diagrams (e.g., Figure 10). It is likely that the zonations shown by these units were produced by a common mechanism, with intermittent returns to geochemical controls by other mechanisms to generate the different "starting" compositions.

The roofward enrichment of Ni and depletion in K argue against mixing with basalt, or partial melting of more mafic sources, to explain the observed zonations. Liquid immiscibility is also unlikely to have played a significant role because the trachytic compositions in question lie outside the two liquid fields on the modified Greig diagram (Philpotts, 1982) and because no petrographic evidence for the process exists in the Menengai rocks. Contamination of trachytic magma by crystalline roof material is discounted as a major mechanism because the rate with which the zonations developed in the chamber (10^2-10^4 years) is probably too high to be explained in this way and because the four main trends do not converge, at evolved compositions, on a single possible contaminant; rather, they diverge from similar "starting" compositions (Figure 10).

Fractional crystallization, volatile complexing, and thermogravitational diffusion, acting either alone or in combination, appear to be the most likely differentiation mechanisms in the upper parts of the Menengai chamber.

Petrographic evidence of crystal fractionation is found in the alkali feldspars of the second ash flow tuff. Within the pumices, phenocrysts range from euhedral to well rounded. Compositional zoning is minor but ubiquitous; rims are enriched either in Or or Ab relative to the cores. In the Menengai suite as a whole, evolved rocks generally contain high Ab feldspars (Leat, 1983). The relationships between feldspar composition, rock composition (as expressed by Zr contents) and thus inferred depth within the preeruptive magma chamber of the second ash flow tuff, are shown in Figure 11. Clearly, the relationships are not simple.

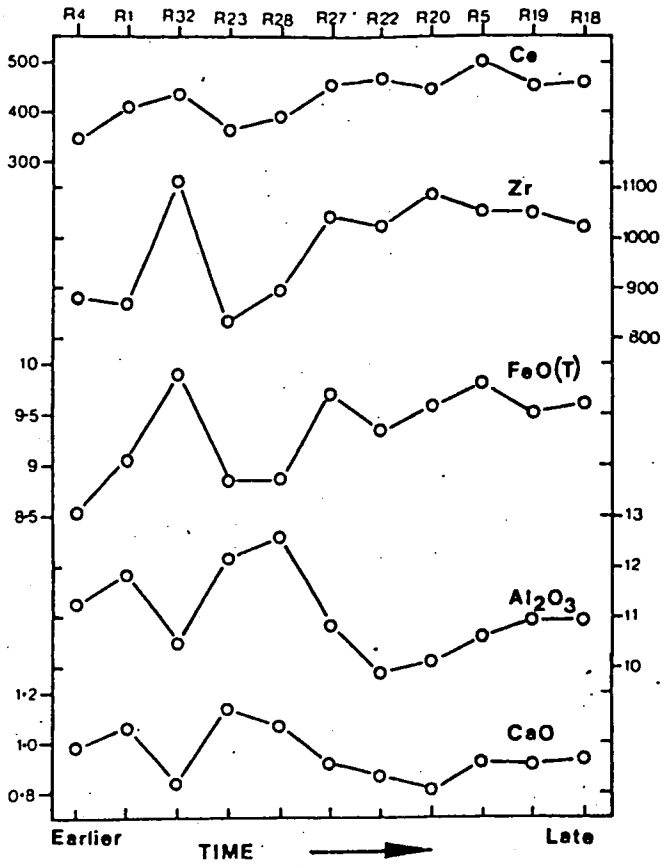

Fig. 9. Time-concentration variations for selected elements in the postcaldera lavas. $FeO_{(T)}$, Al_2O_3, and CaO in weight percent, Ce and Zr in ppm. R4 to R18 are specimen numbers. Lavas arbitrarily spaced evenly along time axis.

A-B is taken to be the trend of feldspars in equilibrium with liquids of respective Zr concentration, i.e., at the appropriate depth. The suggestion is that feldspars plotting below the line have sunk through the magma. Feldspars in pumice K1A38 for example, might have formed in magma which, just prior to eruption, contained 700-800 ppm Zr and sank to a level in the chamber with only 380 ppm Zr. Sinking of crystals may have been density controlled, as calculated magma densities (Bottinga and Weill, 1970) are less than feldspar densities.

It is more difficult to explain the compositions of the feldspars in pumice K1A19 which plot above A-B, pointing to rise of phenocrysts through the magma. This presumably indicates at least local convective motion within the chamber. As the preeruptive magma column must have been stably density stratified in order to develop the described chemical gradients, the only possible cause of motion would have been double diffusive effects (Turner and Gustafson, 1978). Phenocrysts able to penetrate the boundary layer might be able to ascend through the chamber.

Whatever the detailed explanation, the resorbed form, the zonation, and the lack of systematic relationship between feldspar and rock compositions indicate that the feldspars and liquids were not in equilibrium, providing a priori evidence of crystal fractionation in the magma chamber of the second ash flow tuff.

The lack of trace element data for the mafic phenocryst minerals in the trachytes is a serious obstacle to testing petrogenetic models. The great variations in the values of partition coefficients of most trace elements between unzoned phenocrysts and silicic glasses (Mahood and Hildreth, 1983) mean that it is dangerous to

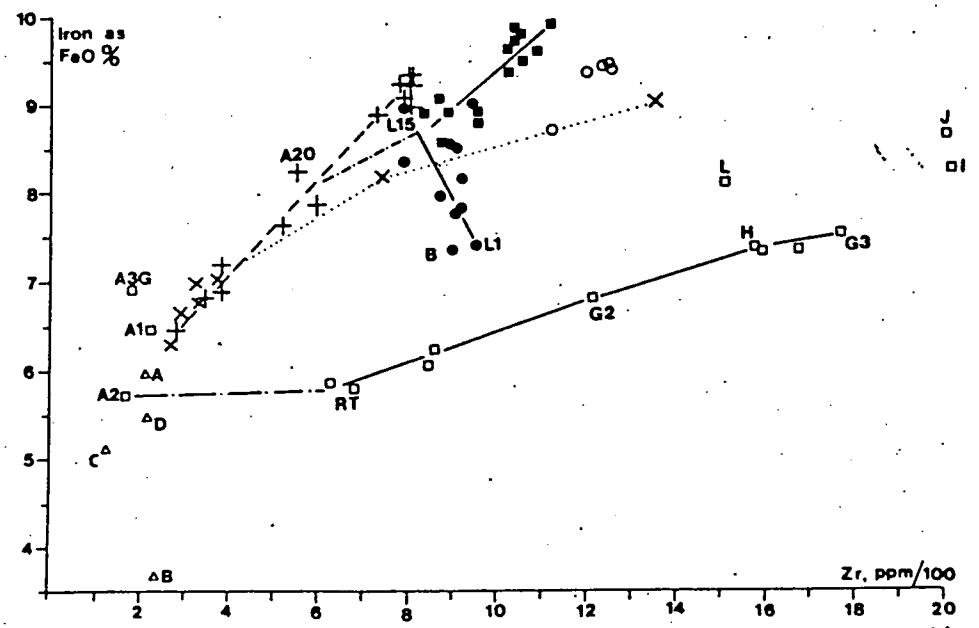

Fig. 10. Zr-$FeO_{(T)}$ plot. Symbols as in Figure 1. RT, Ruplax Tuff. Generalized trend of precaldera lavas drawn between samples KOL1 and KOL15. Trends of the first and second ash flow tuffs shown as dotted and dashed lines, respectively. Solid line through solid squares is trend of postcaldera lavas. Dot-short dash line indicates suggested origin of postcaldera lavas from a composition close to K1A20 (see text for details). The long dash-dot part of the postcaldera tuff trend is thought to have been derived by a different mechanism from the solid line part, as explained in the text.

attempt quantitative modelling of crystal fractionation schemes using data from even closely similar suites. Nevertheless, available data for the Menengai rocks and minerals place constraints on likely differentiation mechanisms, and, in particular, on the role of crystal fractionation. These constraints apply whether the fractionation is thought to have proceeded by crystal settling or by the filling-box mechanism (Turner and Gustafson, 1978, 1981; Turner, 1980).

It is possible to devise a scheme involving fractionation of observed phenocryst phases that could generate the major element variations in the syn-caldera and postcaldera eruptive units. Leat (1983), for example, has satisfactorily modelled the derivation of tuff G3 by 64% crystallization of the Ruplax Tuff, using the assemblage alkali feldspar (88-96%), clinopyroxene (3-7%), Ti-magnetite (2-4%), and apatite (trace), with mineral compositions derived by microprobe.

Several aspects of the trace element geochemistry of the postcaldera tuffs suggest, however, that crystal fractionation by itself might not have been the only differentiation mechanism:

1. Enrichment factors of Cl and F (8.7 and 4.0) in the same suite of rocks not believed to have been affected by posteruptive halogen loss are higher than those indicated by the modelling (2.8). This would require an independent mechanism enriching halogens by different amounts in the upper part of the chamber.

2. Some transition elements, especially Ni, enriched roofward despite the likelihood of high bulk partition coefficients. Ni concentrates in clinopyroxene (Villemant et al., 1981) and has a K^{Ni}_{Af} of 0.7 for some Menengai feldspars (Leat, 1983). Available evidence suggests that Ni would be depleted in roof zone magmas. The antipathetic behavior of Ni and Sc (and Mg and Ca) is also difficult to explain by fractionation of the observed ferromagnesian phenocrysts.

3. In order to explain the roofward depletion of Ba using the above model, the bulk partition coefficent for Ba would have to be >3.3. The K^{Ba}_{Af} value measured on alkali feldspar phenocrysts from sample A3 is 1.6. Since feldspar is the only Ba-carrying phase, it is possible that Ba depletion was not the result of crystal fractionation alone.

4. Eu is an upward concentrating element in all four units, requiring that its bulk partition coefficient be less than unity and its K^{Eu}_{Af} considerably less than 1. This requirement is at odds with published values of K^{Eu}_{Af} in Si-saturated systems which range from 1.23 (Chaine des Puys, France (Villemant et al., 1981)) to 9.06 (Yellowstone rhyolites (Leeman and Phelps, 1981)). The distribution of Eu, antipathetic to that of Ba, casts reasonable doubt against alkali feldspar-dominated crystal fractionation.

5. All REE, except Eu, are enriched roofward by similar amounts, but less than Zr, in each of the four main units. Crystal fractionation would require that all REE had the same bulk partition coefficients, less than that of Zr. Mahood and Hildreth (1983) have shown that partition coefficients for REE in all mineral phases in the Bishop Tuff, California and La Primavera volcanic rocks, Mexico, vary systematically with atomic weight, and that most minerals have partition coefficients for the LREE larger than those for the HREE. In all suites known to us, protracted crystal fractionation has resulted in partitioning of the REE.

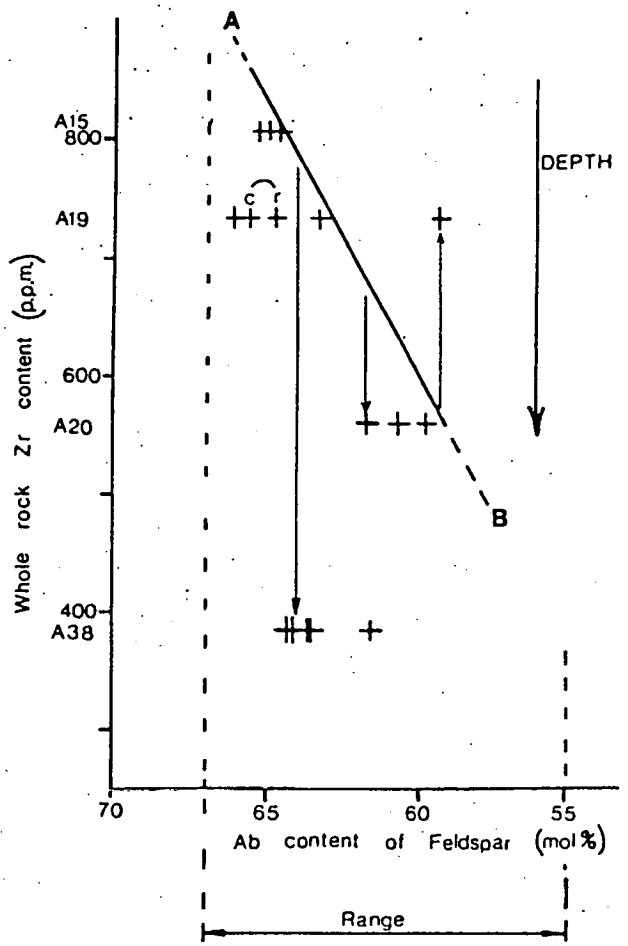

Fig. 11. Ab content of alkali feldspars from second ash flow tuff plotted against whole-rock Zr contents of enclosing pumices. Sample numbers shown on ordinate. Depth in magma chamber is considered to be an inverse function of Zr content. Range is the total range of Menengai feldspars. C and R represent core and rim compositions of phenocrysts in K1A19.

6. The Menengai volcanic rocks contain 0.01% to 0.23% P_2O_5. Individual zoned units cover much of this range, showing (Figure 12), smooth negative relationships between Zr and P_2O_5. Also shown on the diagram are the mean and lowest apatite saturation limits experimentally determined in synthetic "granitic," peralkaline melts by Watson and Capobianco (1981). Assuming that the Menengai magmas are satisfactorily modelled by the synthetic melts in the levels of P needed to form apatite, it is unlikely that apatite was in equilibrium with liquids containing less than about 0.14% P_2O_5 and highly unlikely that it could have existed in liquids with 0.04% P_2O_5. Such considerations agree with the observed rarity of apatite in the rocks. The behavior of P at low levels in the Menengai magmas contrasts with the apparent buffering (Figure 12) at 0.08% P_2O_5 in the trachytes of the Sao Miguel, Azores (Storey, 1981), where P abundances may have been controlled by apatite saturation. One interpretation is that

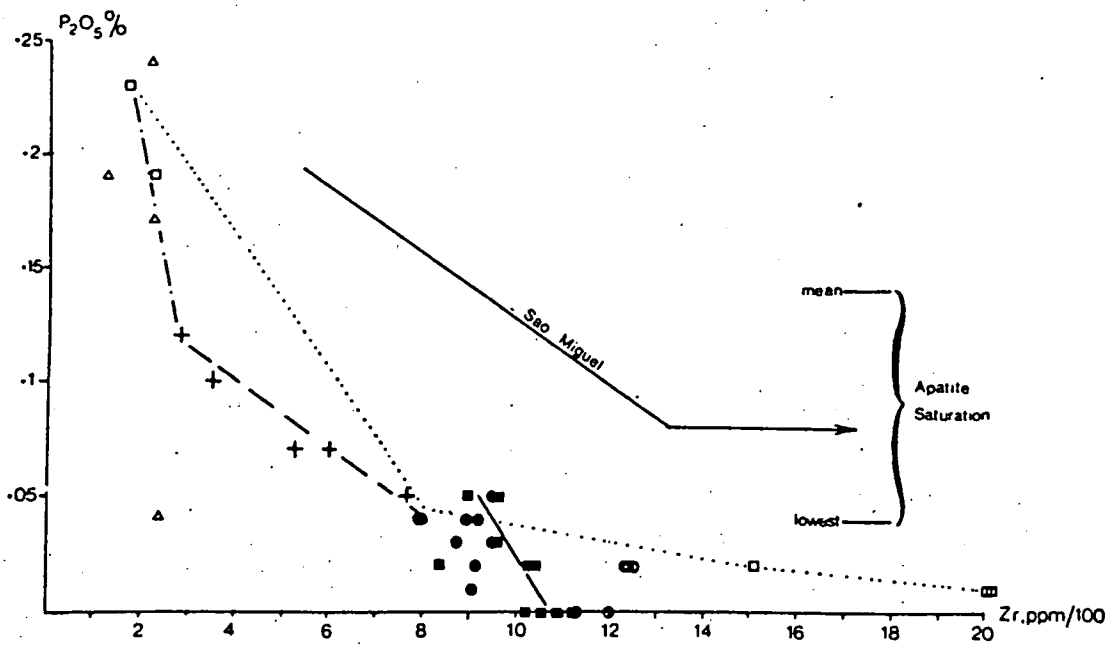

Fig. 12. Zr-P_2O_5 plot. Symbols as in Figure 1. The dot-dash line is the trend of postcaldera regression (see text for detail). Solid and dotted lines are the trends of postcaldera lavas and tuffs, respectively. The mean and lowest limits of apatite saturation in synthetic, peralkaline granite melts are those determined by Watson and Capobianco (1981). The Sao Miguel (Azores) trend, drawn from data of Storey (1981), was apparently controlled by apatite saturation, in contrast to the Menengai trends.

the roofward depletion of P in zoned Menengai units was not the result of crystal fractionation.

These constraints cannot be tested more rigorously until further trace element data become available. Taken together, however, they seem to suggest that fractional crystallization might not have been the sole process operative in the chamber, and it is assumed that other processes, in particular, liquid state mechanisms, were intermittently dominant. Two mechanisms may have been important: volatile complexing and thermodiffusion.

The concept that the upper parts of silicic magma chambers can be enriched in trace metals by the upward migration of volatile complexes, especially involving F and Cl, has been applied to the Kenyan peralkaline centers by Bailey and Macdonald (1970, 1975), Macdonald et al. (1970) and Bailey (1980). Enrichment pattern in eruptive units are thought to be related to the abundances and proportions of F, Cl, CO_2, and H_2O and to the varying ways in which trace metals preferentially complex with the volatiles. Mahood (1981) has also invoked volatile complexing as a dominant mechanism in the evolution of the mildly peralkaline Tala Tuff, a zoned ash flow sheet of the La Primavera complex, Mexico. She notes, however, that direct evidence relating to the existence of such volatile complexes and to their senses and rates of migration within magma chambers is very scanty.

The concept of liquid state thermodiffusion in silicic systems has been developed chiefly by Hildreth (1979, 1981), Mahood (1981), and Mahood and Hildreth (1983) as an outgrowth of the thermogravitational diffusion hypothesis (Shaw et al., 1976). It involves the diffusion migration, presumably by Soret effects, of trace elements to structurally more favorable melts, gradients in melt structure within the magma chamber being produced by the combined effects of gradients in temperature, bulk composition, and volatile concentration. As admitted by the major proponents (Mahood and Hildreth, 1983), the mechanisms are poorly understood and difficult to test rigorously. Furthermore, thermodiffusion may accompany volatile complexing as a differentiation mechanism, and the relative effects of each process may be impossible to disentangle.

In the light of our assumption that crystal fractionation cannot explain the major chemical variations in the main syn-caldera and postcaldera units at Menengai, we suggest that the zonations within the magma chamber might have resulted from two linked liquid state processes: roofward migration of metals as halide, carbonate, and perhaps hydroxyl and alkali silicate complexes and upward and downward enrichment of elements by ionic thermodiffusion.

A Model for the Evolution of the Menengai Magma Chamber

An attempt is now made to relate the geochemical variations to the structural development of the volcano, taking rather more account of volcanological and physical considerations. Much of the discussion is necessarily speculative but will hopefully provide some insight into the evolution of large, peralkaline trachytic systems. Whatever the fractionation mechanisms, the chemical variations (Figures 3 and 10) indicate that the evolution of the magma chamber was complex and dynamic.

The precaldera chamber grew by mixing of batches of chemically similar higher-Y and lower-Y magma. The precaldera tuffs seem to record a high-volatile cap which stabilized, became

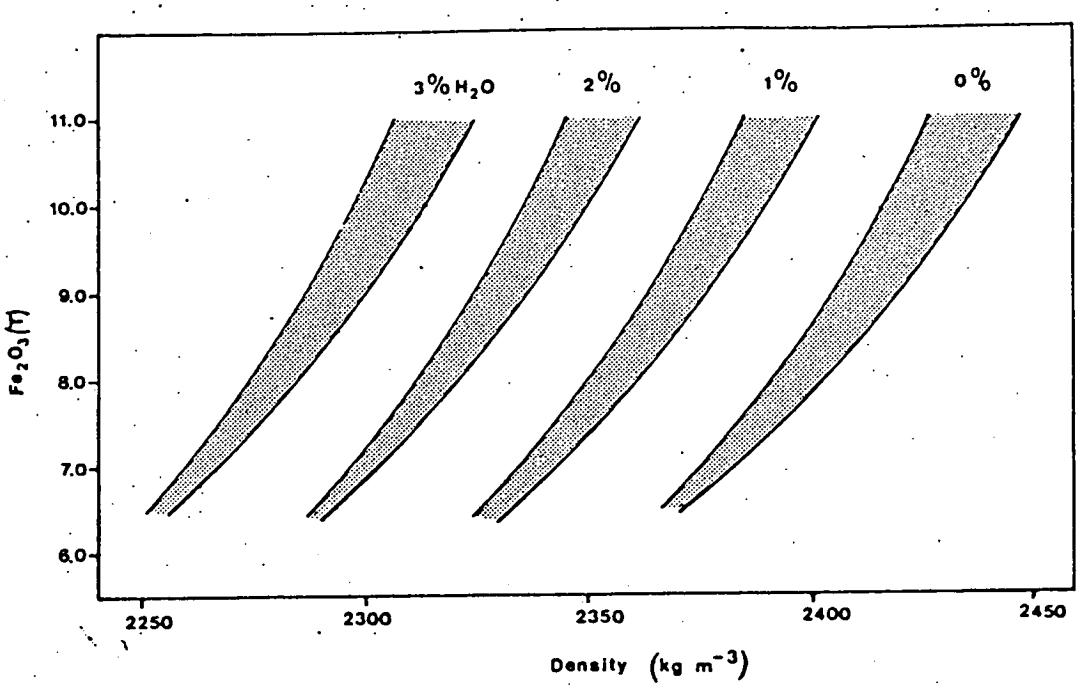

Fig. 13. Calculated densities of Menengai magmas as a function of $Fe_2O_{3(T)}$ content at four values of H_2O^+. Method of Bottinga and Weill (1970) was followed, with pressure taken to be 1.5 kbar.

separated from the underlying magma, and evolved by liquid state processes.

Before the eruption of the first ash flow tuff, the whole of the upper part of the chamber was gravitationally stable, and liquid state processes were dominant. This column was partly erupted as the first ash flow tuff.

Chemical variation in the second ash flow tuff is slightly different from that in the first (Figure 10). While the late erupted parts of both sheets are similar, the early erupted magmas of the second sheet were more Fe rich and less Zr rich than their counterparts in the first. There is an apparent lack of mixing between the two ash flow forming magmas (Figure 10). Zonation in the second sheet may have evolved from a bulk magma which had remained in the chamber after the eruption of the earlier unit. We suggest that this occurred by rehomogenization as follows.

Figure 13 shows that the density of the Menengai melts was controlled mainly by Fe and volatile concentrations. There is no evidence for changes in the Fe contents of the magmas which formed the two ash flows, but volatile losses may have changed the densities. A roofward decrease in density in at least the upper parts of the preeruptive column was caused by a roofward increase in volatile content, which outweighed the contrary effect of decrease in temperature (e.g., Hildreth, 1979, 1981) and increase in Fe. After ash flow eruption and caldera collapse, fractures in the cauldron block permitted easy transport of volatiles out of the magma chamber to be lost to the atmosphere. Fe-rich magma in the upper parts of the chamber was rendered of similar density to the underlying lower Fe magma, promoting convective mixing of the top zones of the chamber.

The homogenized magma seems to have had a uniform composition ($FeO_{(T)}$ ≈ 6.5%, Zr ≈ 250 ppm) which was never tapped by the volcano but perhaps is represented by syenitic lithic clasts, not yet analyzed, found in the second sheet. They may have formed by crystallization against the roof and/or sides of the syenites chamber, although we cannot identify the chemical effects of such a crystallization episode.

The homogenized magma evolved, dominantly by liquid state differentiation processes but with minor crystal settling, into the zoned column later erupted as the second ash flow.

Postcaldera volcanism at Menengai produced the twin series of lavas and tuffs. These show subparallel, but separated, trends on variation diagrams (Figure 10), the main differentiation mechanisms in each case probably involving liquid state processes. Detailed examination of the chemistry of the postcaldera tuffs reveals a rather complicated picture, however. The main tuff trend subparallel to that of the lavas has as its end-members the Ruplax Tuff and sample G3 (Figure 10). The Ruplax Tuff has low $FeO_{(T)}$ (≈5.8%) and Zr (≈650 ppm) contents and relatively high Sr content (∿10 ppm) and is taken to be the parental magma of the main tuff series. Its composition is similar to the magma erupted to form the later parts of the second ash flow tuff, and the Ruplax Tuff is inferred to have originated at depth in the preeruptive chamber of the second sheet.

The tuffs A1, A2, and A3 are thought, on scanty field evidence, to predate the Ruplax Tuff. They represent the most primitive magma yet erupted from Menengai and, as shown on Figure 10, are taken to be the parent of the Ruplax Tuff and thus of all the postcaldera tuffs. Their significance is clearly shown on a Zr-Ba plot (Figure 14). The second ash flow is zoned from <5 ppm Ba in its first erupted part to 21 ppm in the last erupted. Tuff A1, probably the earliest postcaldera tuff, contains 100 ppm Ba, while A2 and A3 have 1000 ppm Ba. This dramatic increase in Ba is accompanied

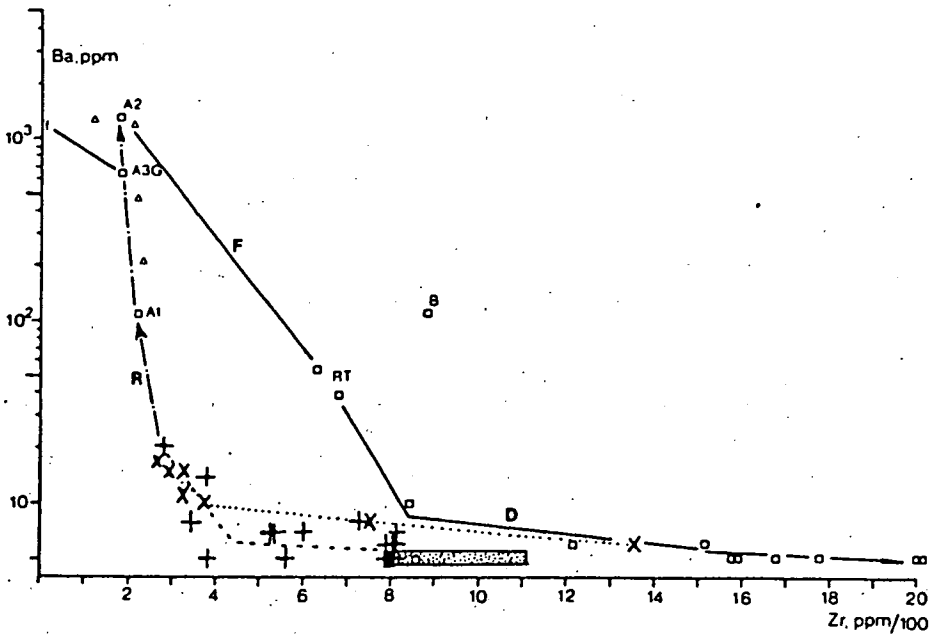

Fig. 14. Zr-Ba plot, used to explore certain aspects of the syn-caldera and postcaldera magmatism. Symbols as in Figure 1. Stippled box is the field of precaldera and postcaldera lavas. Dotted and dashed lines are the trends of the first and second ash flows. Arrowed dash-dot line is the trend of postcaldera regression from the second ash flow tuff to tuff A2, passing through tuffs A1 and A3G. Syenites plot along this trend. Line F is the trend from tuff A2 to the Ruplax Tuff (RT). D indicates the trend of evolved postcaldera lavas.

by increased Al, Mg, Ca, Ti, and Sr and decreased trace elements such as Zr and Nb.

The situation is analogous to the Valles caldera, New Mexico, where the immediately postcaldera eruptives are more primitive than the last erupted part of the Tshirege Member of the Bandelier Tuff (Smith, 1979, pp. 13-15). Smith called this phenomenon postcaldera regression, and it seems to have also occurred at Fantale, Ethiopia (Gibson, 1972), Yellowstone, Wyoming (Hildreth et al., 1980), and La Primavera, Mexico (Mahood, 1981).

The Ba-rich magma which formed tuffs A1, A2, and A3 originated at a deeper level in the chamber than that tapped by the second ash flow. It is tempting to see that level as a repository of downward concentrating elements from earlier differentiation episodes. The ascent of the Ba-rich magma into the top of the chamber is thought to have been caused by density changes resulting from volatile loss into the roof rocks, as follows. After eruption of the second ash flow, volatiles were lost into the freshly fractured cauldron block. The density of the Fe-rich magma near the chamber roof increased to a point where it was greater than that of underlying magma. The column became gravitationally unstable, and a batch of Ba-rich magma rose buoyantly, by gravitational overturn, to a position just below the roof of the chamber (Figure 15). It is possible that ascent was aided by earlier upwarping beneath the eruptive vents of the second ash flow tuff, owing to the way in which magma is drawn from the chamber toward the eruptive conduits.

The Ba-rich magma was emplaced as a layer between the cool, crystalline chamber roof and the relatively low temperature, Fe-rich magma formerly at the roof. A density contrast immediately formed between them and was to persist through much of the postcaldera activity. The Ba-rich magma lost heat, and its low volatile content (~0.04% F + Cl, judging from concentrations in the Ruplax Tuff, with perhaps a similar amount of H_2O) did not prevent rapid crystallization. Three of the four analyzed syenites found as lithic clasts in the Ruplax Tuff are compositionally similar to tuffs A1, A2, and A3, suggesting that they represent crystallized Ba-rich magma, though low contents of Zr and other residual elements indicate some partitioning of such elements into the melt. Thus a period of crystal fractionation plastered a syenitic layer onto the chamber roof and generated the compositional trend from tuff A2 to the Ruplax Tuff. These rocks contain 168 ppm and 650 ppm Zr, respectively, indicating about 75% crystallization of the Ba-rich magma.

A small volume of Ba-rich magma was involved in the process of convective overturn. About 2 km^3 of magma was erupted as postcaldera tuffs (Leat, 1983). Assuming that a similar amount remained in the chamber, the volume of postcaldera tuff producing magma was ~4 km^3. If the 75% crystallization figure deduced above is correct, 16 km^3 of Ba-rich magma rose to the chamber roof, to form a 100-m-thick layer. This may represent the whole of the Ba-rich zone at depth (Figure 15).

Crystallization against the chamber roof, diking, and geothermal effects eventually sealed the roof against large-scale volatile loss. Possible upward migration of volatiles, coupled with the crystallization of anhydrous phases, led to the reestablishment of volatile gradients in the chamber. This prevented further crystallization but promoted differentiation by liquid-state processes. The magma at this point has evolved to the composition of the Ruplax Tuff. Further

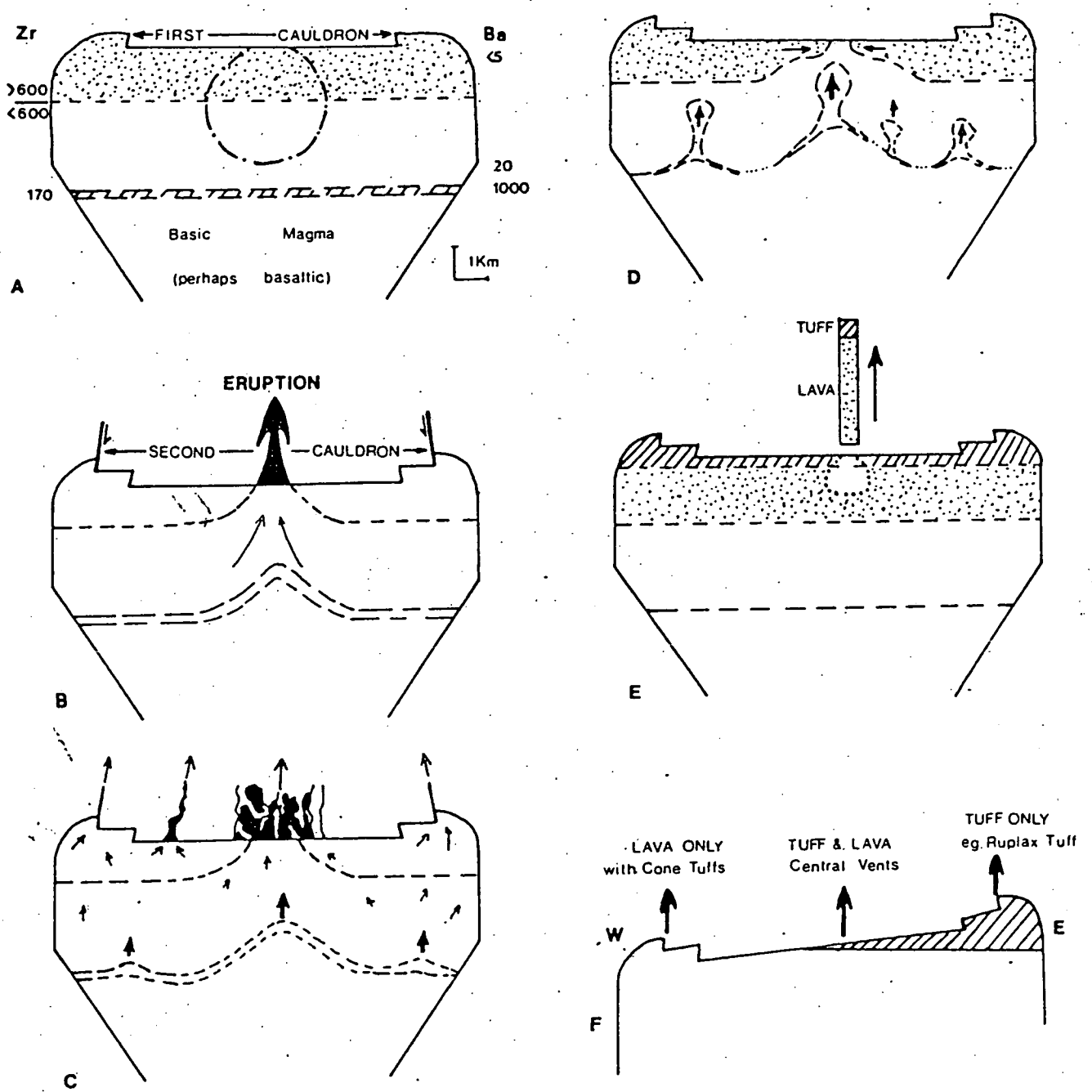

Fig. 15. Diagrammatic representation of the evolution of the Menengai magma chamber from before the eruption of the second ash flow to the present day. (a) Prior to the second ash flow. The existence of the first cauldron is speculative, but realistic. (b) Eruption of the second ash flow tuff. Activity is shown at one central vent but is equally likely to have taken place from several vents along the caldera fracture. The dotted line indicates the possible batch of magma actually erupted, after Blake (1981). The dashed lines indicate the inferred position of the previously horizontal isochemical zones after the eruption. The outward dip of the ring fracture seems likely to promote descent of the dense cauldron block, cause the observed (Leat, 1983) rapid increase in eruption rate, and result in the formation of a ring dike; the fracture may dip inward near the surface, however. (c) Escape of volatiles after eruption of second ash flow. Small arrows show volatile migration. Heavy arrows show buoyant ascent of the Ba-rich layer resulting from volatile loss. (d) Ba-rich layer ascends as diapirs toward the chamber roof. (e) Newly stabilized chamber after Ba-rich magma (diagonal rule) forms layer at roof zone. This Ba-rich magma evolves to the tuff-forming magma, while magma formerly at the top of the chamber forms the lava-producing zone (stippled). The dotted line encloses the volume of magma tapped in a single postcaldera eruption, with an initial pyroclastic phase and a later lava phase. (f) The idealized situation shown in Figure 15e is complicated by a westerly tilt of the chamber roof. Volcanic eruptions of varying combinations shown.

fractionation was to produce the later tuffs and the postcaldera lavas.

It is clear from volcanological and stratigraphic considerations (Leat, 1983) that the lavas and tuffs were erupted over the same period from the caldera floor; so their chemical differences cannot be explained by eruption from separate magma chambers. Rather, they seem to have been erupted from discrete zones in a single, stratified chamber. The best interpretation is that the tuff-producing magma occupied an upper, volatile-rich zone of the chamber which capped an underlying, volatile-poor, lava-producing zone. The volumes of tuff and lava erupted during any postcaldera eruption are variable and depend on the geometry of the chamber roof (Figure 15), but there is overall a greater volume of lavas.

There appears to have been abrupt transitions from pyroclastic to effusive phases in individual eruptions which coincided with the change in chemical type. Early tuffs in the sequence show no evidence of mixing of tuff- and lava-forming magmas, interpreted to result from the sharp density interface between the two zones. The tuff-producing magma was poorer in Fe and almost certainly richer in volatiles than the lava-forming magma and must have been considerably less dense (Figure 13). The density contrast (perhaps 120 kg m^{-3}) was enough to prevent physical mixing.

The postcaldera lavas developed from magma which had occupied a near-roof position in the preeruptive chamber of the second ash flow, and the chemical variations in both units were produced by similar, liquid state differentiation mechanisms. Figure 10 indicates, however, that the lava suite is more Zr rich than the second ash flow and that an additional mechanism is required to produce the least evolved lava-forming magmas from any ash flow magma. We speculate that this mechanism was crystal fractionation. The trend drawn from ash flow sample K1A20 to lava sample KOR23 (Figure 10) was modelled by 25% crystallization of an alkali feldspar + minor clinopyroxene + sparse Fe-Ti oxides assemblage, which is consistent with petrography. This fairly high degree of crystallization may have been promoted by loss of volatiles after ash flow eruption. The paucity of phenocrysts in postcaldera lavas suggests that crystallization took place on the side walls of the chamber.

Subsequently, both layers fractionated internally by liquid state processes. The sense of enrichment and depletion were similar for almost all elements. The layers had slightly different bulk compositions. The tuff-producing zone was poorer in Fe and perhaps Si and richer in Al and K. This is evident on the $FeO_{(T)}$-Al_2O_3 plot (Figure 1), where the tuffs are more comenditic than the pantelleritic lavas.

Some indirect evidence relating to possible mixing of the two zones during late postcaldera times is found in the compositions of the late tuffs I, J, and L (Figure 10), which have chemical characteristics consistent with their being mixtures of lava-forming magma and, as yet unidentified, highly evolved, tuff-forming magma. Continued eruption of tuffs might have led to a considerable reduction in thickness of the tuff-forming zone, permitting entry by, and mixing with, lava-forming magma from below. Tuff B has an unusual high-Fe chemistry (Figure 10) demanding a special genesis, discussed by Leat (1983).

The westerly tilt of the roof of the magma chamber (Figure 15) was deduced as follows:

1. Postcaldera strombolian cones occur only in the western part of the caldera, while tuffs erupted from the center and eastern parts are sheet forming. This suggests that the west side of the caldera floor is directly underlain by magma poorer in volatiles and thus denser, representing deeper levels in the magma column than that directly underlying the center and east of the caldera floor.
2. An analyzed sample of strombolian cone tuff has a lava-type, rather than a tuff-type, composition, while all analyzed sheet-forming tuffs have tuff-type chemistry. Since the tuff-forming magma was less dense than the lava-forming type, it seems that the tuff-forming magma did not spread under the western part of the chamber roof.

Figure 16 provides a summary of the petrogenetic model. The main features are as follows: 1, evolution of the precaldera lavas by mixing of magmas in the growing chamber; 2A, stabilization of a volatile-enriched cap; development of the tuffs by liquid state processes; 2B, penetration of trachytes into the roof zone, resulting in magma mixing; 3, establishment of a strongly zoned upper part of the chamber by liquid state processes ± minor crystal fractionation; eruption of first ash flow tuff; possible caldera formation (?); 4A, rehomogenization of magma remaining in upper part of chamber; 4B, reestablishment of zonation by liquid state differentiation ± minor crystal fractionation; eruption of second ash flow tuff; formation of caldera; 5A, convective overturn and rise of Ba-rich magma to roof zone; establishment of stable density interface between tuff- and lava-forming zones; 5B, in upper zone, crystallization of syenites against roof generates trend toward Ruplax Tuff composition; in lava-producing zone, 25% crystallization against sidewalls; 5C, liquid state differentiation in tuff-forming zone generates trend toward G3 composition; same mechanism in lower zone produces other lava compositions; 6, possible mixing of upper and lower zone magmas to form late tuff magmas.

Discussion

In this section we discuss a miscellany of topics where the Menengai data have provided information of general interest to the study of large-volume, silicic, volcanic systems, including the senses of elemental enrichments in a strongly peralkaline magma chamber, the time scale over which the compositional zonations developed, and possible controls of the various differentiation mechanisms.

Crystal Fractionation and Liquid State Differentiation

Reasoned accounts of the evolution of large-volume silicic systems (Pitcher, 1979; Smith, 1979; Hildreth, 1981; Smith and Macdonald, 1979; Macdonald et al., 1984) note that different fractionation mechanisms dominate at different stages of a system's development. We have claimed that, at Menengai, there is evidence for magma mixing, rehomogenization, crystal fractionation, and various liquid state

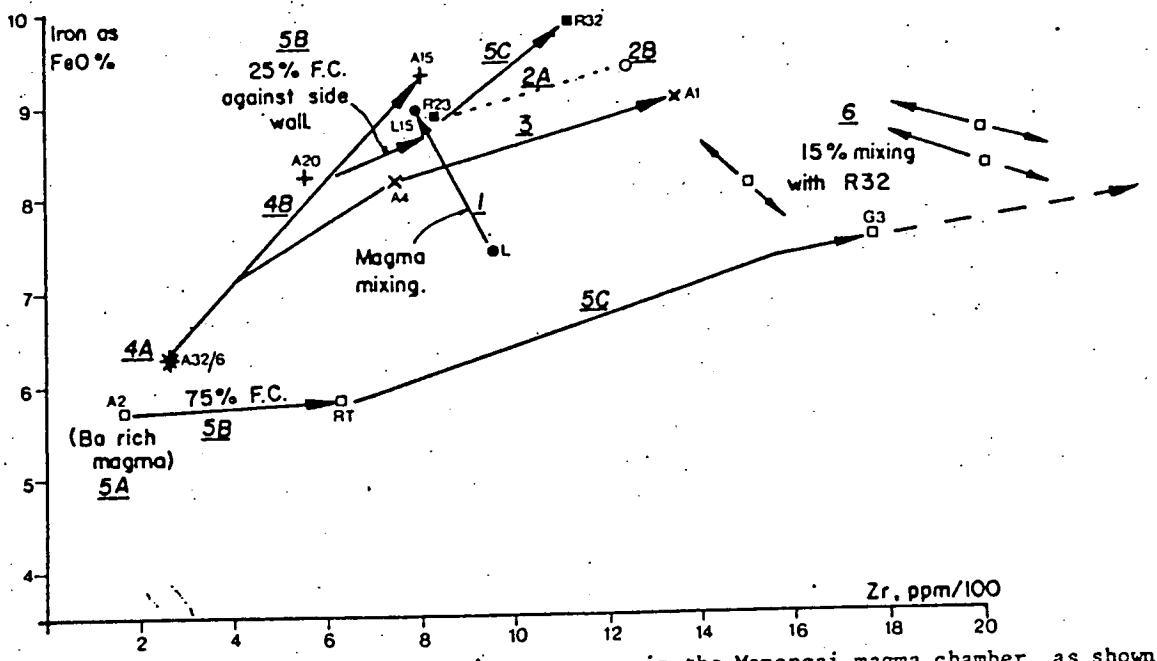

Fig. 16. Summary of the petrogenetic processes in the Menengai magma chamber, as shown by their influence on Zr-$FeO_{(T)}$ relationships. Stages 1 to 6 as explained in text.

mechanisms, such as volatile transfer and thermo-diffusion.

Magma mixing apparently occurred during the devleopment of the precaldera lavas and tuffs. There is no explicit evidence of its operation in syn-caldera and postcaldera times, but it is implicit in our understanding of how such volcanic systems work that magma mixing was certainly occurring at depths greater than those tapped by the Menengai eruptives (Smith, 1979). Such mixing of magmas has been recorded at the Longonot trachytic caldera volcano (Scott, 1980).

Syn-caldera and postcaldera magmatism in the upper parts of the chamber was dominated by liquid state differentiation, with intermittent periods of crystal fractionation. It is of interest to speculate on the conditions which favor each mechanism. At Menengai the following evidence seems to suggest that liquid state processes were promoted by the establishment of strong volatile gradients (Shaw et al., 1976; Smith, 1979; Hildreth, 1979, 1981; Mahood, 1981):

1. The latest precaldera materials tended to be emplaced as sheet-forming tuffs, suggesting elevated volatile concentrations.

2. Syncaldera eruptions showed a progression from plinian-type airfalls to voluminous ash flows.

3. Roofward enrichment of F and Cl can be demonstrated in the second Menengai ash flow (Table 2). This could, of course, be the result, rather than a promoter, of liquid state differentiation.

It may be that the critical parameter determining whether volatile gradients can be established is chamber size. As the chamber grows, the input of magma, and also the erupted portions, becomes a smaller part of the total volume. Progressively, eruptions have a smaller degassing effect, and volatile enrichment toward the chamber roof may take place.

Development of Compositional Zonations in the Menengai Magma Chamber

Testing and refinement of models of the differentiation of silicic magma chambers will require information on the time and magmatic volumes over which differentiation takes place. As a contribution, we summarize here relevant data from Menengai.

Compositions showed little variation over the 150,000-year eruptive period of the precaldera lavas. We have ascribed this to the growing of the magma chamber by the periodic mixing of two similar trachytic magmas. The more evolved nature of the precaldera tuffs is taken to show that liquid state processes operated in the roof zone. The zonation of individual tephra layers is ascribed to renewed magma mixing in the alread zoned, volatile-rich cap.

This phase of activity was ended by the eruption of the first ash flow tuff from a zoned, upper part of the chamber. The volume of the zoned magma must have exceeded the 20 km^3 of erupted magma. Eruption of the second ash flow followed within 16,000 years, by which time compositional zonation had been reestablished. Lower observed enrichment factors cannot be taker to mean that the real factors within the chamber were lower. Assuming that the area of the top o the magma chamber was no smaller than that of th caldera, i.e., 77 km^2, and using Leat's (1983) estimate of 30 km^3 for the volume of the second ash flow tuff magma, a minimum value of 400 m fo the thickness of the zoned part of the system ca be derived.

Eruption of the second ash flow tuff was followed by convective overturn, rise of the Ba-rich magma, and the crystallization of the syenites against the chamber roof. The thickness of the zone of Ba-rich magma beneath the roof wa about 100 m, and it must have ascended from a z below that tapped by the preceding ash flow,

i.e., 400 m. The time interval of this phase can be estimated as follows: The Ruplax Tuff is the compositional, and possibly therefore temporal, end-member of this phase, dated at about 10,000 years B.P. The second ignimbrite was erupted before 12,850 years B.P. Making generous allowance for error, this suggests a period of 1000-5000 years, at which time compositional zonation began to be reestablished in the chamber by liquid state processes.

The compositional spectrum of the postcaldera and tuffs reached its full development in less than 10,000 years, though highly evolved magma was available for eruption after a few (4-5?) thousand years. The dimensions of the zoned part of the system cannot be realistically estimated. The thickness of the tuff-forming zone was some tens to hundreds of meters. The thickness of the lava-producing zone is unknown, because its bottom layers were not tapped, according to our petrogenetic speculations.

We feel, however, that it is firmly established at Menengai that extreme compositional zonations, with observed enrichment factors >5 for some elements, were developed repeatedly through tens of cubic kilometers of magma in times of 10^2-10^4 years. These are very high rates, in terms of the hierarchy of large-volume silicic systems, and must be related to the high-halogen, high-Fe, relatively low viscosity nature of the melts.

Menengai Ash Flows: Enrichment and Depletion Factors

On the basis of published chemical data for compositionally zoned, silicic ash flow tuffs, the following generalizations may be made: (1) certain elements are always upward concentrating, namely, Na, Cl, F, Cs, Nb, Pb, Rb, Ta, Th, U, Y, and the HREE; (2) others are always downward concentrating, namely, Al, Mg, Ca, K, Ti, P, Ba, Cu, and Sr; (3) others exhibit variable behavior from one system to another which is at least partly related to the alkalinity of the system, namely, Fe, Co, Hf, Zn, Zr, LREE; (4) some elements, notably Sc and Mn, also show apparently nonsystematic behavior; (5) the zonation usually involved fractionation of the LREE from the HREE and of Eu from the trivalent REE.

In the light of these generalizations, aspects of the chemistry of the Menengai ash flow tuffs are worth mentioning in that they provide a little more information on the relationships between bulk composition and elemental behavior in silicic systems.

1. In common with other peralkaline, halogen-rich systems, Fe, Hf, Zn, Zr, and the LREE were enriched roofward.

2. While Mn concentrated upward in both sheets, Sc was a clear down element. It might be argued (Hildreth, 1981, p. 10,167) that Sc behavior was related to settling of small amounts of ferromagnesian minerals, but it is difficult, at Menengai, to reconcile that with upward enrichment of Ni.

3. Development of the zonations of the Menengai ash flows resulted in virtually no change in the ratios of LREE/HREE, though the concentrations increased roofward. This unusual behavior of the REE is compounded by the upward enrichment of Eu, though this could have been predicted by its constant distribution in the mildly peralkaline Tala Tuff (Mahood, 1981, Figure 3). Note, however, the much lower enrichment factors for Eu than for the other REE.

4. In the Bandelier (Smith, 1979) and Bishop (Hildreth, 1981) tuffs, Cu was a down element. In the second Menengai ash flow tuff, Cu concentrated roofward, while it remained almost constant in the first sheet, despite generally higher enrichment factors for most elements.

5. Another unusual feature of the Menengai sheets is the upward enrichment of Ni. The rocks thus show the uncommon relationship in igneous geochemistry of a negative correlation between Mg and Ni in a differentiated suite.

Development of Peralkalinity in Menengai Trachytes

It was noted earlier that the second Menengai ash flow is zoned from a strongly peralkaline, early erupted part to (barely) subalkalic. Peralkalinity is thus interpreted to have developed mainly by the action of liquid state differentiation processes on subalkalic magma. A comparable situation, though in a different bulk composition, has been described from the high-silica rhyolitic Tala Tuff, Mexico (Mahood, 1981), where a mildly peralkaline, first erupted portion is associated with a metaluminous last erupted portion. We agree with Hildreth (1981) that liquid state differentiation is probably a common, perhaps even ubiquitous, way of generating peralkaline silicic melts.

This study has provided no evidence of the origin of the subalkalic trachytes. While it is likely that they were formed by the partial melting, or fractional crystallization, of mafic materials, the parental trachytes have not been recognized at Menengai. The most primitive rocks, the high Ba tuffs, have compositions at least partly controlled by liquid state differentiation processes and thus cannot be used to model likely mafic source rocks or possible liquid lines of descent from basaltic magma. Evidence for the origin of the trachytes will have to come from elsewhere in the province.

Acknowledgments. We thank L. A. J. Williams for help and encouragement, J. O. Bowman and K. S. Waterhouse for analytical assistance, and Jackie Dixon for typing the script. P.T.L. gratefully acknowledges receipt of a Natural Environment Research Council (U.K.) research studentship.

References

Bacon, C. R., R. Macdonald, R. L. Smith, and P. A. Baedecker, Pleistocene high-silica rhyolites of the Coso volcanic field, Inyo County, California, J. Geophys. Res., 86, 10,223-10,241, 1981.

Bailey, D. K., Volcanism, earth degassing and replenished lithosphere mantle, Philos. Trans. R. Soc. London Ser. A, 297, 309-322, 1980.

Bailey, D. K., and R. Macdonald, Petrochemical variations among mildly peralkaline (comendite) obsidians from the oceans and continents, Contrib. Mineral. Petrol., 28, 340-351, 1970.

Bailey, D. K., and R. Macdonald, Fluorine and

chlorine in peralkaline liquids and the need for magma generation in an open system, Mineral. Mag., 40, 405-414, 1975.

Baker, B. H., Geology and geochemistry of the Ol Doinyo Nyokie trachyte ignimbrite vent complex, South Kenya Rift Valley, Bull. Volcanol., 39, 420-440, 1975.

Baker, B. H., and L. H. Henage, Compositional changes during crystallization of some peralkaline silicic lavas of the Kenya Rift Valley, J. Volcanol. Geotherm. Res., 2, 17-28, 1977.

Blake, S., Eruptions from zoned magma chambers, J. Geol. Soc. London, 138, 281-287, 1981.

Bottinga, Y., and D. F. Weill, Densities of liquid silicate systems calculated from partial molar volumes of oxide components, Am. J. Sci., 269, 169-182, 1970.

Dietrich, R. V., Behaviour of zirconium in certain artificial magmas under diverse P-T conditions, Lithos, 1, 20-29, 1968.

Gibson, I. L., A pantelleritic welded ash-flow from the Ethiopian Rift Valley, Contrib. Mineral. Petrol., 28, 89-111, 1970.

Gibson, I. L., The chemistry and petrogenesis of a suite of pantellerites from the Ethiopian Rift, J. Petrol., 13, 31-44, 1972.

Hildreth, W., The Bishop Tuff: Evidence for the origin of compositional zonation in silicic magma chambers, Spec. Pap. Geol. Soc. Am., 180, 43-75, 1979.

Hildreth, W., Gradients in silicic magma chambers: Implications for lithospheric magmatism, J. Geophys. Res., 10,153-10,192, 1981.

Hildreth, W., R. L. Christiansen, and J. R. O'Neil, Catastrophic isotopic modification of rhyolitic magma by creation of the Yellowstone caldera, Geol. Soc. Am. Abstr. Programs, 12, 111, 1980.

Jones, W. B., Chemical effects of deuteric alteration in some Kenyan trachyte lavas, Mineral. Mag., 44, 279-285, 1981.

Leat, P. T., The structural and geochemical evolution of Menengai caldera volcano, Kenya Rift Valley, Ph. D. thesis, Univ. of Lancaster, Lancaster, United Kingdom, 1983.

Leeman, W. P., and D. W. Phelps, Partitioning of rare earths and other trace elements between sanidine and coexisting volcanic glass, J. Geophys. Res., 86, 10,193-10,199, 1981.

Macdonald, R., Nomenclature and petrochemistry of the peralkaline oversaturated extrusive rocks, Bull. Volcanol., 38, 498-516, 1974.

Macdonald, R., and D. K. Bailey, The chemistry of the peralkaline oversaturated obsidians, U.S. Geol. Surv. Prof. Pap., 440-N-1, 1-37, 1973.

Macdonald, R., D. K. Bailey, and D. S. Sutherland, Oversaturated peralkaline glassy trachytes from Kenya, J. Petrol., 11, 507-517, 1970.

Macdonald, R., R. L. Smith, and J. E. Thomas, Chemistry of the subalkalic silicic obsidians, U.S. Geol. Surv. Prof. Pap., in press, 1984.

Mahood, G. A., Chemical evolution of a Pleistocene rhyolitic centre: Sierra La Primavera, Jalisco, Mexico, Contrib. Mineral. Petrol., 77, 129-149, 1981.

Mahood, G. A., and W. Hildreth, Large partition coefficients for trace elements in high-silica rhyolites, Geochim. Cosmochim. Acta, 47, 11-30, 1983.

Noble, D. C., Loss of sodium from crystallized comendite welded tuffs of the Miocene Grouse Canyon Member of the Belted Range Tuff, Nevada, Geol. Soc. Am. Bull., 81, 2677-2688, 1970.

Philpotts, A. R., Compositions of immiscible liquids in volcanic rocks, Contrib. Mineral. Petrol., 80, 201-218, 1982.

Pitcher, W. S., The nature, ascent and emplacement of granitic magmas, J. Geol. Soc. London, 136, 627-662, 1979.

Sceal, J. S. C., and S. D. Weaver, Trace element data bearing on the origin of salic rocks from the Quaternary volcano Paka, Gregory Rift, Kenya, Earth Planet. Sci. Lett., 12, 327-331, 1971.

Scott, S. C., The geology of Longonot volcano, central Kenya: A question of volumes, Philos. Trans. R. Soc. London Ser. A, 296, 437-465, 1980.

Shaw, H. R., R. L. Smith, and W. Hildreth, Thermogravitational mechanisms for chemical variations in zoned magma chambers, Geol. Soc. Am. Abstr. Programs, 8, 1102, 1976.

Smith, R. L., Ash flow magmatism, Spec. Pap. Geol. Soc. Am., 180, 5-27, 1979.

Smith, R. L., and R. A. Bailey, The Bandelier Tuf: A study of ash-flow cycles from zoned magma chambers, Bull. Volcanol., 29, 83-104, 1966.

Smith, R. L., and R. Macdonald, Rhyolitic volcani and its relationship to granitic plutonism, Geol. Soc. Am. Abstr. Programs, 11, 520, 1979.

Storey, M., Trachyte pyroclastics from Agua de Pa volcano, Sao Miguel, Azores: Evolution of magm body over 4,000 years, Contrib. Mineral. Petrol., 78, 423-432, 1981.

Turner, J. S., A fluid-dynamical model of differentiation and layering in magma chambers Nature, 285, 213-215, 1980.

Turner, J. S., and L. B. Gustafson, The flow of hot saline solutions from vents in the sea floor-some implications for exhalative massive sulfide and other ore deposits, Econ. Geol., 73, 1082-1100, 1978.

Turner, J. S., and L. B. Gustafson, Fluid motions and compositional gradients produced by crystallization or melting at vertical boundaries, J. Volcanol. Geotherm. Res., 11, 93-125, 1981.

Villemant, B., H. Jaffrezic, J. L. Joron, and M. Treuil, Distribution coefficients of major and trace elements: Fractional crystallizatio in the alkali basalt series of Chaine des Puy (Massive Central, France), Geochim. Cosmochim Acta, 45, 1997-2016, 1981.

Watson, E. B., Zircon saturation in felsic liquids: Experimental results and application to trace element geochemistry, Contrib. Miner Petrol., 70, 407-419, 1979.

Watson, E. B., and C. J. Capobianco, Phosphorus and the rare earth elements in felsic magmas: An assessment of the role of apatite, Geochim Cosmochim. Acta, 45, 2349-2358, 1981.

Wilson, A. D., A new method for the determinatic of ferrous iron in rocks and minerals, Bull. Geol. Surv. G. B., 9, 56-58, 1955.

Wright, J. V., and G. P. L. Walker, The ignimbrite source problem: Significance of a co-ignimbrite lag-fall deposit, Geology, 5, 729-732, 1977.

Wright, J. V., and G. P. L. Walker, Eruption, transport and deposition of ignimbrite: A case study from Mexico, J. Volcanol. Geotherm. Res., 9, 111-131, 1981.

P. T. Leat and R. Macdonald, Department of Environmental Sciences, University of Lancaster, Lancaster LA1 4YQ, England.
R. L. Smith, U.S. Geological Survey, Reston, VA 22092.

(Received September 29, 1983;
revised January 18, 1984;
accepted February 8, 1984.)

RETAIN THIS SET

Magmatic Processes: Physicochemical Principles
© The Geochemical Society, Special Publication No. 1, 1987
Editor B. O. Mysen

Dry peralkaline felsic liquids and carbon dioxide flux through the Kenya rift zone

D. K. BAILEY
Department of Geology, The University, Whiteknights, Reading RG6 2AB, Berkshire, U. K.

and

R. MACDONALD
Department of Environmental Sciences, University of Lancaster, Lancaster LA1 4YQ, U. K.

Preamble—When Hat Yoder was in London to receive the Wollaston Medal of the Geological Society the chance arose for him to see the Michaelangelo Tondo in the Royal Academy. His reaction, naturally, was to marvel that such beauty could be wrought from stone. Along with other participants at the meeting we pay tribute to Hat, who in his own way has continually given petrologists new perceptions of rocks.

Abstract—Around Lake Naivasha, at the topographic culmination of the Kenya rift, a wide range of peralkaline felsic magmas erupted in the Holocene. Glassy samples are abundant. Volcanological and petrographic evidence indicates that these glasses reflect characteristically low concentrations of H_2O in the melts, and this relationship is confirmed by experimental and chemical information.

Distinct magma types, trachytes, comendites and pantellerites, erupted almost exclusively from different centres, even though these are sufficiently close for intercalation of the erupted products from adjacent volcanoes. This individuality is maintained in chemical variation diagrams where the products from different centres form separate groups, with no gradational compositions. In some diagrams smaller clusters appear within the main groups. These distinctive patterns indicate that there is no continuous evolution of the melts below the rift, and that each centre represents the outpouring of a different melt. Batches within the same centre could also represent different episodes of melt generation.

Generation of these melts in a *regional* context can best be explained by melting of different sources during the influx of a CO_2-rich fluid. Trachytes, pantellerites and comendites could then be the products of a flux/melting cycle as it climbs progressively through mantle, mafic deep crust, and sialic crust. The high concentrations of sodium and iron in the melts call for enhancement of these elements in the source rocks: this could be achieved by regional metasomatism resulting from prolonged activity through the rift segment over the past 23 Ma. Incompatible trace element variations cannot be attributed to solid-melt interactions but could be imparted by the fluid during melting.

INTRODUCTION

FOR A VARIETY of reasons alkaline rocks have always held a fascination for igneous petrologists, but in recent years have assumed extra significance as it has emerged that their richness in incompatible elements and radio-isotopes are signalling special conditions of source, or melt-forming processes, or both. In most alkaline provinces peralkalinity has developed in varying degrees. Paradoxically, peralkalinity is strongest when magma penetrates continental lithosphere, where the crustal rocks are typically peraluminous. Such magmatism is especially evident in stable plate interiors where igneous activity of any kind must call for special explanation. Even where eruption is localised by an evident split in the lithosphere, there is still no ready explanation of why, for instance, continental fissuring may give vent to tholeiite floods in one region or epoch, and alkaline magmatism in another.

Aphyric volcanic glasses provide the closest samples to the composition of peralkaline melts, where it is clear that crystallisation, and indeed devitrification or hydration, leads notably to alkali and halogen losses (NOBLE *et al.*, 1967; MACDONALD and BAILEY, 1973). Glasses may also provide extra insight into the gases associated with strongly alkaline volcanism. This information is of value because the only direct, high temperature volcanic gas collection available is from the melilite nephelinite volcano of Mount Nyiragongo (CHAIGNEAU *et al.*, 1960): no direct, high temperature collections have been made of an oversaturated peralkaline volcano. The aim here is to examine and explore the potential information content of a range of oversaturated volcanic glasses from the central part of Kenya (Gregory) rift valley. All the samples are fresh, unaltered glasses; most are obsidians in which phenocrysts are absent or less than 2 percent in the mode; vesicles, if present, are widely sepa-

B8776 T. 106,107 Art. 2 (240)

rated. Pumice samples are excluded because of their susceptibility to post-eruptive hydration and alteration.

INTRINSIC H_2O CONTENTS OF PERALKALINE GLASSES

With one exception all peralkaline glass analyses in the compilation by MACDONALD and BAILEY (1973) have H_2O^+ contents of 0.67 weight percent or less. Many more analyses (published and unpublished) have since been added (BAILEY, 1978; 1980) and it is clear that the vast bulk of the H_2O^+ values are around the limit of detection (~0.1%): hence, most glasses are virtually anhydrous. These data are in complete accord with the case put forward earlier by NICHOLLS and CARMICHAEL (1969) that oversaturated peralkaline liquids are essentially dry. Other studies (see EWART, 1979) seem to indicate consistently low f_{O_2} and high temperatures in calc-alkaline rhyolites and dacites, which would be in keeping with the generally low H_2O^+ values in the glasses. Recently, however, TAYLOR *et al.* (1983) have reported H_2O contents up to 3.1% in fresh calc-alkaline rhyolite tephra, leading to the suggestion that these are the general levels in such melts, and that glasses with low H_2O are degassed. They propose that the main degassing of the melt takes place during foaming within the vent, so that later flows and domes with low H_2O represent extrusion of the collapsed foam. They report that there appear to be no differences in the compositions of the calc-alkaline glasses except for H_2O^+ and deuterium contents. In view of the manifest compositional changes in peralkaline glasses during devitrification and hydration, and during high temperature fusion experiments (HAMPTON and BAILEY, 1985), any massive loss of several percent H_2O from a high temperature peralkaline melt would render the consequent anhydrous glass suspect as a sample of the natural melt composition. It is essential, therefore, to examine the evidence with this in mind before considering the chemical variations among the glasses from the Kenya rift province.

General relationships and field evidence

The case presented here is part of a continuing study of alkaline glasses, encompassing the widest possible range of bulk compositions and samples from all regions and all different modes of eruption. The following list outlines the range and scope.

(1) Bulk compositions range from nephelinite through phonolite to comendite, *i.e.*, the maximum range of silica values.

(2) Samples are from all geographic and tectonic settings.

(3) Wide variations in vesicularity, and in phenocryst types and contents, are represented.

(4) Eruptive mode varies widely. Samples come from flow margins (top and bottom); flow interiors; angular blocks in agglomerate; angular fragments in pumice deposits; fiamme from welded ash flows; splatter; and agglutinated spatter.

Significantly, tephra fragments ranging from small chips in pumice deposits to large blocks in agglomerates are all low in H_2O^+; there is no evidence of high speed ejectamenta that could represent an H_2O-rich melt.

Experimental crystallisation and comparative petrography

In marked contrast with calc-alkaline rhyolites, which fail to crystallise in the laboratory when dry, pantellerite glasses start to crystallise in as little as thirty minutes at appropriate temperatures without addition of water. Experimental study of the melting and crystallisation of peralkaline glasses under a range of conditions is, therefore, possible (COOPER, 1975; BAILEY and COOPER, 1978) with results as shown in Figure 1. Details of the experimental conditions and the phases developed were given in BAILEY and COOPER (1978), which also contains a discussion of the consequences of the contrasting behaviour of wet and dry pantellerite melts. Relevant points from this discussion are summarised below.

(1) The exsolution of vapour under near-liquidus conditions in the dry experiments (Figure 1) indicates that some natural volatiles were quenched in at partial pressures at least as high as 0.3 kbar. A synthetic rhyolite melt would contain 2.5 weight percent of H_2O at an equivalent pressure (LUTH, 1976). Addition of H_2O to the natural pantellerite profoundly changes the melting behaviour indicating that it is capable of dissolving a similar quantity of H_2O at 0.3 kbar. As H_2O is one of the most soluble gases in silicate melts it hardly seems credible that a pantellerite melt could lose 2–3% H_2O whilst effectively retaining other gases at 0.3 kbar solubility levels. Hence, although there must have been some degassing from some samples (in decompression) this gas was not simply H_2O.

(2) Crystallisation of an H_2O-rich pantellerite results in acmitic pyroxenes and potassic feldspars quite different from those observed as natural phenocrysts, and in the wrong sequence.

(3) Kenyan obsidians with modal phenocryst

B8776 T. 107 Art. 2 2 Al

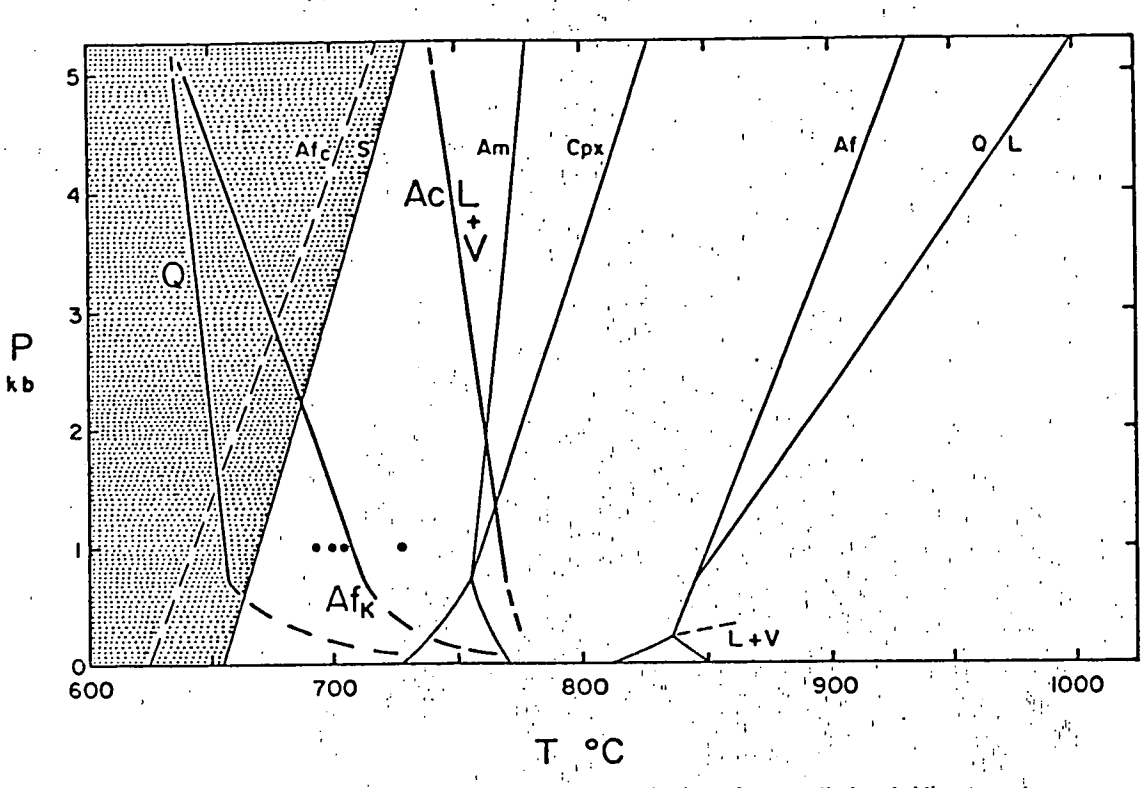

FIG. 1. Comparison of hydrous and anhydrous crystallisation of a pantellerite obsidian (sample KE12: Eburru, Kenya). Hydrous boundaries heavy lines: anhydrous boundaries light. The dry subsolidus region is shaded. V = fluid, L = liquid; Q = quartz; Af = alkali feldspar; Af_K = K-rich alkali feldspar; Af_c = alkali feldspar critical line (LUTH, 1976); Cpx = sodic hedenbergite; Am = arfvedsonitic amphibole; Ac = acmitic pyroxene; S = dry solidus. The points shown at 1 kb are the range of liquidus minima (quartz + feldspar + liquid) in related synthetic systems at P_{H_2O} = 1 kbar (CARMICHAEL and MACKENZIE, 1963; THOMPSON and MACKENZIE, 1967). Taken from BAILEY and COOPER (1978).

contents greater than 5% are rare: most have less than 2% and, hence, have a near-liquidus aspect. This characteristic, combined with low H_2O^+ contents, effectively rules out an origin from a magma at, or below, the H_2O-saturated liquidus in Figure 1. Firstly, the large differences in temperature between the wet and dry systems, require that subvolcanic degassing of any wet pantellerite magma should have been accompanied by extensive crystallisation. Secondly, the negative slopes of the phase field boundaries in the wet system would imply that any wet pantellerite magma at depth could get to the surface only as a pyroclastic eruption composed of H_2O-saturated glass, or as degassed crystalline lava.

If pantelleritic melts ever were wet at depth then some special conditions of eruption would be called for to account for the dry, near-liquidus aspect of the glasses. Suppose the original melt had previously contained as much as 3 weight percent H_2O (*e.g.*, approximately saturated at 2 km depth) and had somehow lost H_2O at a lower pressure. To achieve a dry near-liquidus condition its required starting temperature would be at least 50°C above the wet liquidus. Alternatively, it might have risen towards the surface from a point on a 3 weight percent H_2O liquidus, requiring a starting pressure of greater than 5 kbar. To make the transition from wet to dry melt therefore would seem to require an unusual eruption or thermal history. Non-systematic (vagarious) variation within the sample population would be expected in H_2O contents, oxidation states, alkalis and halogens. Furthermore, when crystals are present, at least some should carry a record of this eruption history. In fact, they are remarkably consistent in composition (NICHOLLS and CARMICHAEL, 1969; SUTHERLAND, 1974) even to the extent of showing scarcely any sign of zoning in the feldspars, the dominant phenocryst phase.

Peralkaline glasses are still puzzling in the light of their laboratory behaviour. Dry pantellerite held

B8776 T.106,107 Art. 2 3 Al
(242)

just above its solidus temperature for about an hour starts to crystallise; if taken to the liquidus temperature it bubbles. But both these states seem to have been largely missed out in the cooling of natural glass samples. In order to preserve such a glass it must somehow pass through the vesiculation and crystallisation temperature range (below about 700°C at low pressure) in a short time. Whereas this cooling history can be envisaged for particular instances such as flow margins, it is less easy in other cases. Glass clasts in pumice deposits are typically non-vesicular, non-porphyritic and *angular*. Hence, they were "through" this temperature range before incorporation in the pumice eruption. Our experiments with gas extraction indicate that foaming is a near-liquidus phenomenon (HAMPTON and BAILEY, 1984). It is difficult, therefore, to see how the obsidian clasts could have come from the part of the melt that was foaming. If they are chilled melt from the border zone of the foaming mass they should presumably record the highest H_2O contents available for peralkaline liquids.

Glass fiamme in welded ash flows also pose problems if, as suggested by TAYLOR *et al.* (1983), they "remain at magmatic temperatures for weeks or months". According to our experiments pantellerite fiamme could not survive as glass under such conditions. Almost wholly glassy flows and domes are also extruded from peralkaline silicic volcanoes and must pose similar problems. There is a need for some means of super-cooling peralkaline melts prior to eruption such that the viscosity is sufficiently high to inhibit crystallisation and bubbling, but flow is permitted.

Chemical variations and H_2O^+ levels

If peralkaline magmas have previously contained several percent H_2O, they must clearly have suffered massive vapour loss prior to glass formation. This must leave its mark on the melt composition, as other volatile species should be partitioned into the vapour. In high-temperature, gas extractions from glasses in the laboratory, H_2O is always accompanied by other species, either in the form of gases, or precipitated as sublimates. Most typically, the high-temperature sublimates include alkali halides (HAMPTON and BAILEY, 1985). These products mirror those observed at high temperature fumaroles on volcanoes. Similarly UNNI and SCHILLING (1978) have recorded that concentrations of Cl and H_2O in submarine basalts correlate with ocean depth, and are dependent on degree of vesiculation and loss of vapour on eruption at different pressures. In contrast to these observations, peralkaline silicic obsidians show no correlation between H_2O and Cl (Figure 2). In fact, no correlation between H_2O and any other variable has been found in these rocks, certainly not with alkalis and halogens where it might be most expected. Present evidence offers no case for massive sub-volcanic loss of water-rich vapour from peralkaline melts. The low and variable H_2O levels in the glasses may be essentially "accidental", *i.e.*, unrelated to the melt generation process. On this basis it is appropriate to treat the glasses as melt samples, in an attempt to unravel their chemical relationships and try to discern their petrogenesis.

PERALKALINE VOLCANOES IN THE CENTRAL KENYA RIFT

Volcanism has been active along the Kenya rift for the past 23 Ma, ranging from carbonatites and nephelinites to rhyolites (Figure 3). Felsic rocks constitute about half the total erupted volume, about 150,000 km³ (WILLIAMS, 1982). The bulk of the Tertiary-Recent felsic rocks are peralkaline making it the most voluminous and variegated peralkaline province in the world. Holocene activity in the central part of the rift, around its topographic culmination in the vicinity of Lake Naivasha, has been largely expressed by felsic central volcanoes on the rift floor. Figure 4 shows the largely monotonic magma compositions emitted from the main centres. Eruptives from adjacent centres may interfinger around the margins, but are always petrographically distinct. The general geology around Lake Naivasha has been described by THOMPSON and DODSON (1963), and there have been individual descriptions of Suswa (JOHNSON, 1969); Longonot

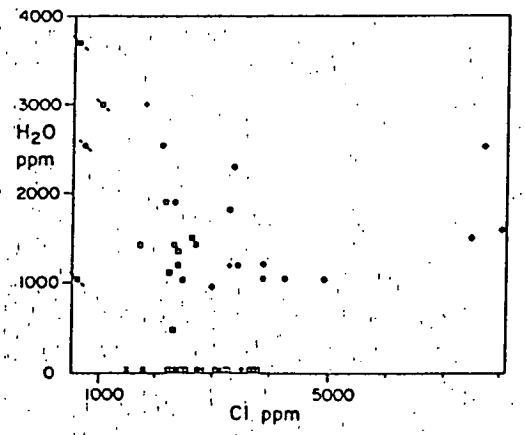

FIG. 2. Variation of Cl with H_2O in oversaturated peralkaline glasses. Diamonds indicate samples from Pantelleria, all other samples from the Kenya rift (for details see Figure 4).

B8776 T.106,107,108 Art. 2 4 Ql
(243)

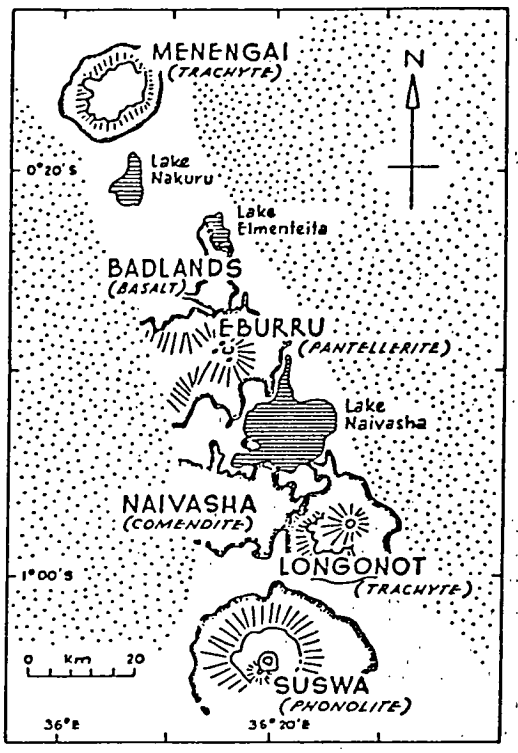

FIG. 3. Sketch map showing the chief Holocene volcanic centres in the Lake Naivasha section of the Kenya rift. Rift shoulders indicated by stipple.

(SCOTT, 1980); and south west Naivasha (MACDONALD *et al.*, in press). In addition to the felsic volcanoes, there is a small basalt field forming the Badlands, north east of Eburru (MCCALL, 1957). Small basalt cones pepper the fringes of the comendite field of south west Naivasha, and mixed basalt/felsic lavas have been erupted from Longonot (SCOTT and BAILEY, 1984) and Eburru. North of the Badlands the next major central volcano is Menengai, erupting only trachyte (LEAT, 1984).

Lake Naivasha is located on the crest of the classic continental rift valley first described by GREGORY (1894) and its volcanism has a special place in igneous petrogenesis. Many of the lavas used by BOWEN (1937) to illustrate his concept of Petrogeny's Residua System (nepheline–kalsilite–silica) were from this region. The Holocene volcanism around Lake Naivasha is an almost perfect case for a petrographic province, fulfilling all the criteria laid down by WILCOX (1979).

The Lake Naivasha region has the added advantage that glassy samples, covering most of the range of oversaturated peralkaline compositions are abundant. The first pantelleritic trachyte glasses were recognised at Menengai and Longonot (MCCALL, 1967; MACDONALD *et al.*, 1970), and the East African rift valley has so far provided the only samples of this melt. Trachyte glasses having clear chemical affinities with comendites are absent.

The extent and persistence of peralkaline activity through the East African lithosphere make it imperative to look for the causes, and the wide range of geology and sample compositions offer hope for eventual solutions to the questions of petrogenesis. It is appropriate first to look at chemical variations in the glasses with changing levels of peralkalinity.

Major element variations with peralkalinity

Some distinctions are seen immediately. For instance, the comendites from south west Naivasha separate from the pantellerites and the pantelleritic trachytes in terms of SiO_2, TiO_2, FeO, MnO and total iron (Figures 4 and 6). They also appear as a distinct group on most other variation diagrams. Like all other continental comendites, they appear to fall close to the quartz-feldspar cotectic, as extended into the peralkaline region (BAILEY and MACDONALD, 1970, Figure 5; MACDONALD *et al.*, in press, Figure 7), with the implication that the source contained free quartz. This characteristic, together with many other features of their major element composition would be most obviously satisfied by a crustal or sialic source (BAILEY and MACDONALD, 1970) and more detailed studies on trace elements and isotopes are consistent with this interpretation (MACDONALD *et al.*, in press; DAVIES and MACDONALD, in press).

Figure 4 also reveals separate clustering of trachytes and pantellerites, which persists in Al_2O_3 (Figure 5). As might be anticipated, there is a general negative correlation between alumina and peralkalinity, but the comendites, pantellerites and trachytes form separate groups. This separation is emphasized when molecular Al_2O_3 is plotted; the comendites and pantellerites appear to define one trend, while the trachytes form parallel trends at higher levels. This feature might be taken to reflect different series of liquids with various levels of silica, but it is noteworthy that trachyte liquids show no direct connection with rhyolites.

Just as it might be anticipated that Al_2O_3 would correlate negatively with peralkalinity, so a positive correlation might be expected for the alkalies (Figure 5). In comendites and pantellerites, K_2O is almost constant around 4.4%, but there are signs of slight negative distributions, which are emphasised when the trachytes are taken into account. The general fall in K_2O levels with increasing peralkalinity may be linked in some way to the "orthoclase effect"

B8716 T.106,108 Art. 2 S QL

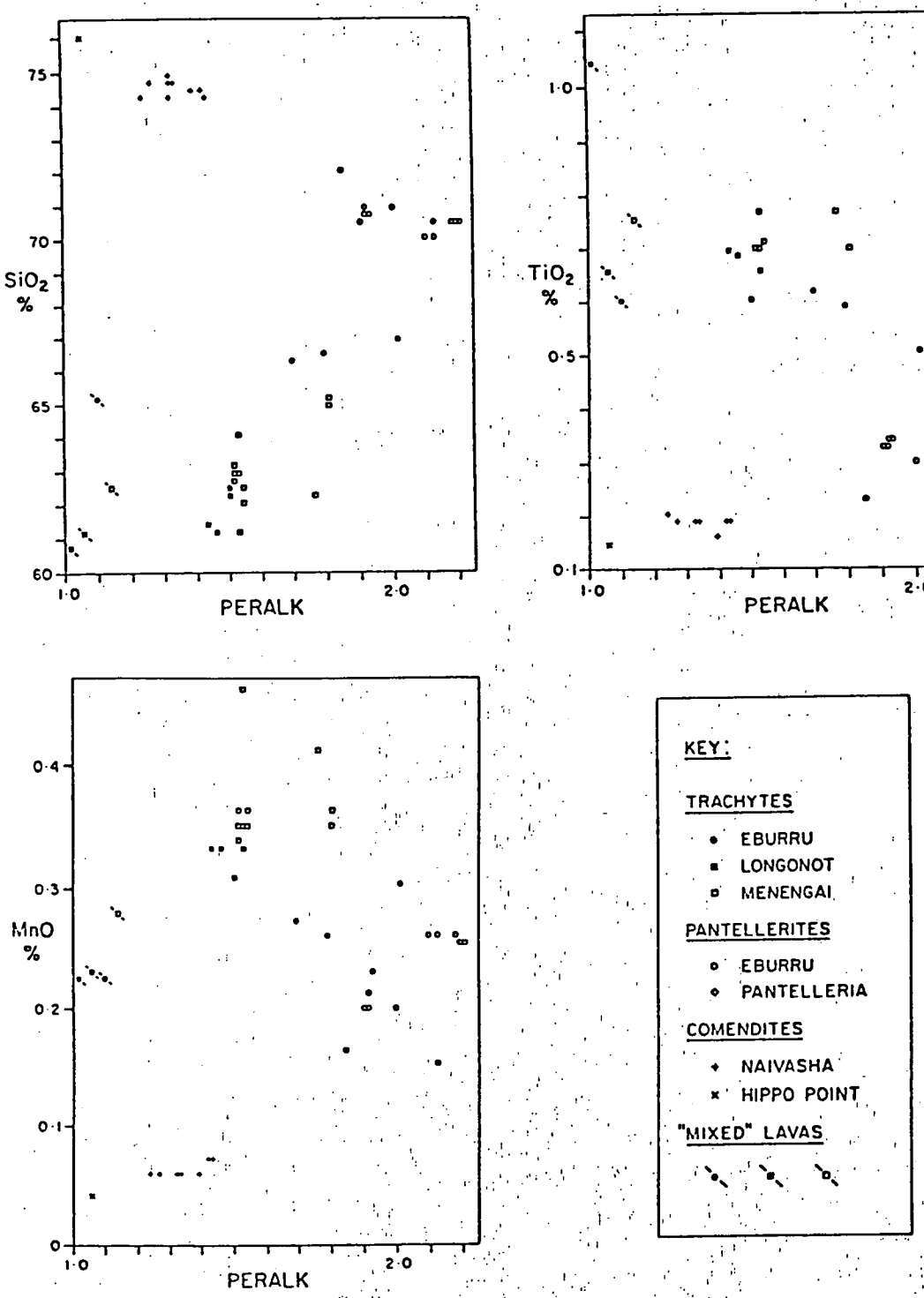

FIG. 4. Variations of SiO_2, TiO_2, and MnO with peralkalinity [Mol $(Na_2O + K_2O/Al_2O_3)$] in glassy samples from the Naivasha region. Plus signs, comendites from the main Naivasha field; cross, indicates tight group of comendites from the Hippo Point area on Lake Naivasha; open circles, pantellerites, closed circles, trachytic pantellerites from Eburru; filled squares, trachytes from Longonot; open squares, trachytes from Menengai; symbols with diagonal line indicate mixed lavas (possibly accumulitic in the case of Menengai).

B8T16 T.106 Art. 2 6 de
(245)

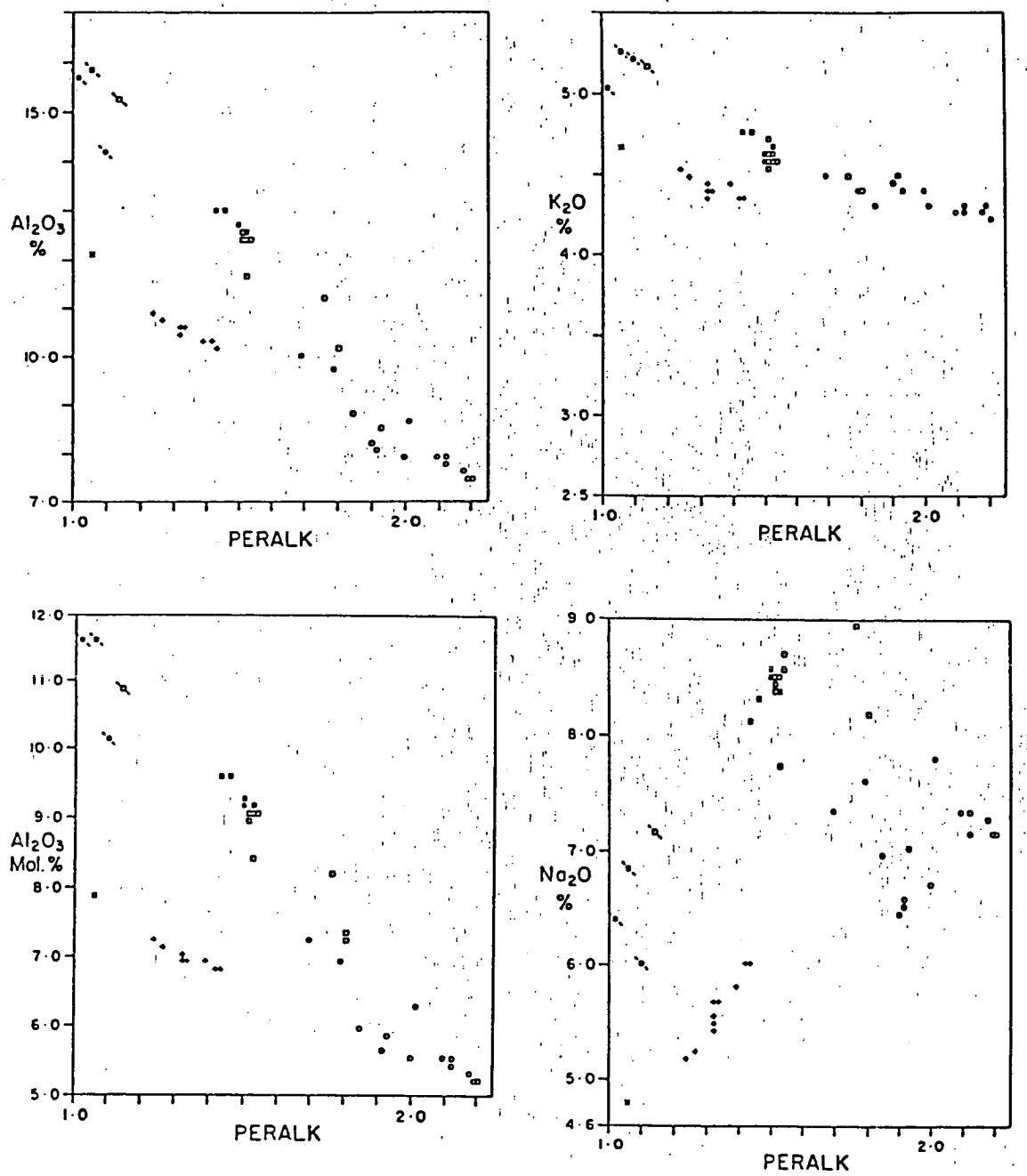

FIG. 5. Variations of Al_2O_3 (weight percent and mol percent), Na_2O and K_2O with peralkalinity. Mol percent Al_2O_3 can be used as an indication of variation in potential feldspar in the samples. Symbols as in Figure 4.

(BAILEY and SCHAIRER, 1964) whereby alkali feldspars tend to be richer in K_2O than their coexisting melts. It is not easy, however, to reconcile the relatively constant K_2O in the comendites and the pantellerites with this effect if indeed they represent series of liquids controlled by closed-system fractionation.

An even more striking pattern emerges for Na_2O (Figure 5). Trachytes from Longonot and Eburru fall on quite separate positive trends, which them-

B8776 T.106,108 Art. 2 7 Ql
(246)

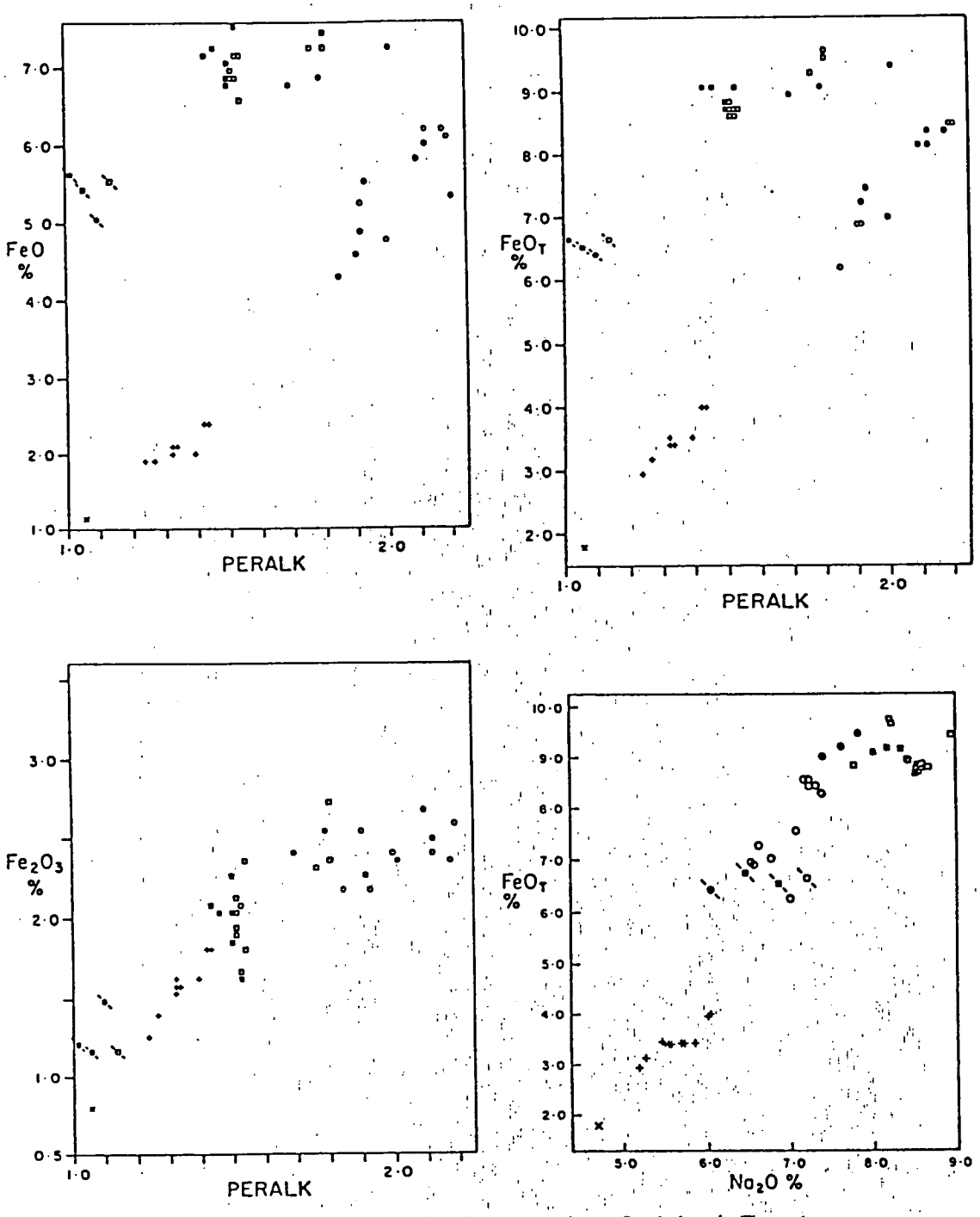

FIG. 6. Variations of soda and iron for Kenyan glasses. Symbols as in Figure 4.

selves are distinct from the distributions of pantellerites and comendites. This emphasizes the distinctions seen in Al_2O_3 and is mirrored by variation in other major elements, particularly FeO and total iron (Figure 6). Discrete populations of liquids are identified, some of which have been erupted even from the same volcano (Eburru). Within any series there is a general positive correlation between Na_2O and total iron, which may reflect some internal consistency in melt generation within that series,

B8776 T.106,108 ART. 2 8 DL
(247)

but the separation of the series, especially trachytes from rhyolites, would seem to require generation at least in distinct batches. Increasing soda correlates with iron content, and *within* each group with peralkalinity. Between trachytes and pantellerites, however, there is a broad negative distribution which seems to defy explanation in terms of interactions between melts and their observed phenocryst phases.

Where these rocks are not aphyric, the ubiquitous phenocryst is alkali feldspar, and the bulk compositions of the melts require that this phase must dominate in any crystallisation sequence. Separation of potassic feldspar from the trachytic liquids must lead to increasing sodicity beyond that actually observed in the pantellerites (MACDONALD *et al.*, 1970). Therefore, *if* these liquids were linked in a crystallisation sequence, a sodic phase was removed from the magma system as crystallisation progressed: no appropriate composition appears as a phenocryst in the trachytes.

The distribution of soda and iron (Figures 5 and 6), confirm the earlier suspicion that there is no chemical continuum between trachytes and pantellerites, and that they developed under different conditions. Pantellerite may represent a quartz-feldspar cotectic composition for a specific range of source rock compositions and pressures. At higher pressures (and in different source compositions?) the cotectic melt is closer to trachyte, as with increasing pressure in the "granite system" (TUTTLE and BOWEN, 1958). The special requirement in the "pantellerite system" would be that there is a phase boundary (marking the appearance of a phase rich in soda and iron) imposing a limit on the peralkalinity of the liquid that can be reached at any given pressure (see BAILEY, 1974).

A plot of Fe_2O_3 vs peralkalinity (Figure 6) reveals a steady progression through the comendites that could reflect an increasing contribution of acmite to the melts. There is no such regular variation of ferric iron and peralkalinity in the trachytes or pantellerites, and the latter appear to mark a "ceiling" in the possible levels of Fe_2O_3 in peralkaline melts. As the trachytes also have more iron than comendites or pantellerites, it is not possible to appeal simply to an acmitic component to account for the Fe_2O_3 variations in this part of the array. Melting of a source containing a combination of phases similar to the observed phenocrysts (feldspar, fayalite, sodic hedenbergite, aenigmatite, and oxide) could produce the trachytes. As discussed later, pantellerite melt generation may need to involve an arfvedsonitic amphibole in addition.

Formation of these peralkaline trachyte and pantellerite liquids seems to require melting of appropriate source compositions. This is indicated by the marked composition gaps, which have persisted despite intensive sampling, and must depict a real distribution of natural melts. The gaps must militate also against generation of trachytes and pantellerites by progressive melting of a single source. The separation of the trachytes from Longonot, Menengai and Eburru in various diagrams also renders unlikely the possibility of fractional melting at separate trachyte and rhyolite invariant points, for which there is no experimental evidence in any case. The separation of trachytic and pantelleritic liquids is further emphasized by the fact that in many diagrams the variations within the groups run *across* any expected trend from trachyte to pantellerite (Figure 4, 5 and 6). Further discussion of the questions of melt generation is best deferred until trace element variations have been examined.

Trace element versus major element functions

When variation in incompatible trace element concentrations is compared with peralkalinity the patterns are different (Figure 7). The main Naivasha comendites show a positive variation, but no other simple relationship emerges between trace elements and peralkalinity. Patterns in the trachytes are not well defined but some signs of positive trends may be detected within groups. The pantellerites, however, are scattered, with the highest levels of incompatible elements near the lowest levels of peralkalinity. Essentially, the trachytes, pantellerites and comendites form separate populations (c.f., the major element data), but distributions within groups are hinting at further differences between them. One major difference becomes clear when traces are compared with soda and iron. For the comendites there is a positive correlation of trace elements with Na_2O, but in the pantellerites the broad distribution is negative (Figure 8). Because FeO and FeO_T correlate positively with Na_2O, their relationships with trace elements are similar. What also emerges in Figure 8 is distinct clustering of different parts of the pantellerite population.

Variations between trace elements

Trace element correlations are much stronger. The strong correlation of Zr with Rb and F that was first noted for Eburru pantellerites (BAILEY and MACDONALD, 1975) appears in all groups of liquids even though they may separate from each other in the diagrams (Figure 9). This relationship has been found also in sample suites from the Azores and from Pantelleria (BAILEY, unpubl.).

B8776 T.108,109 Art. 2 9 QL
(248)

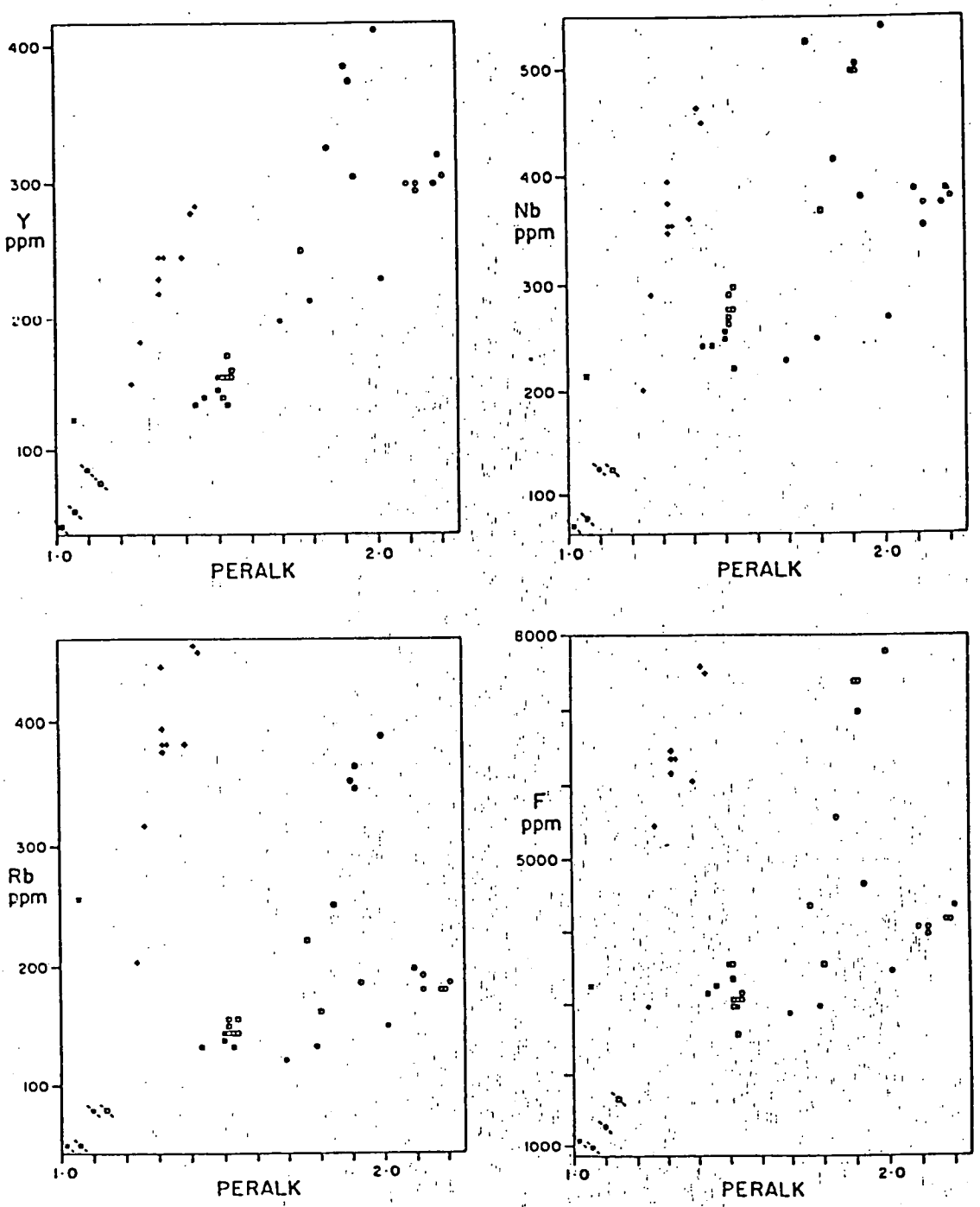

FIG. 7. Variations with peralkalinity for a selection of trace elements, Y, Nb, Rb and F, in Kenyan glasses. Symbols as in Figure 4.

Coherence also exists for Nb and Y through all the groups, and it had been noted previously (BAILEY and MACDONALD, 1975) that in the Eburru obsidians these two elements were more strongly correlated with Cl, as distinct from the strong covariance in F, Zr and Rb. When all groups of glasses are compared, the pattern of Cl distribution is less clear-cut, and there is a strong suggestion in Figure 9 of decoupling of the Cl distribution from variations in the other trace elements in the higher con-

B8776 T.106,109 Art. 2 10 QQ
(249)

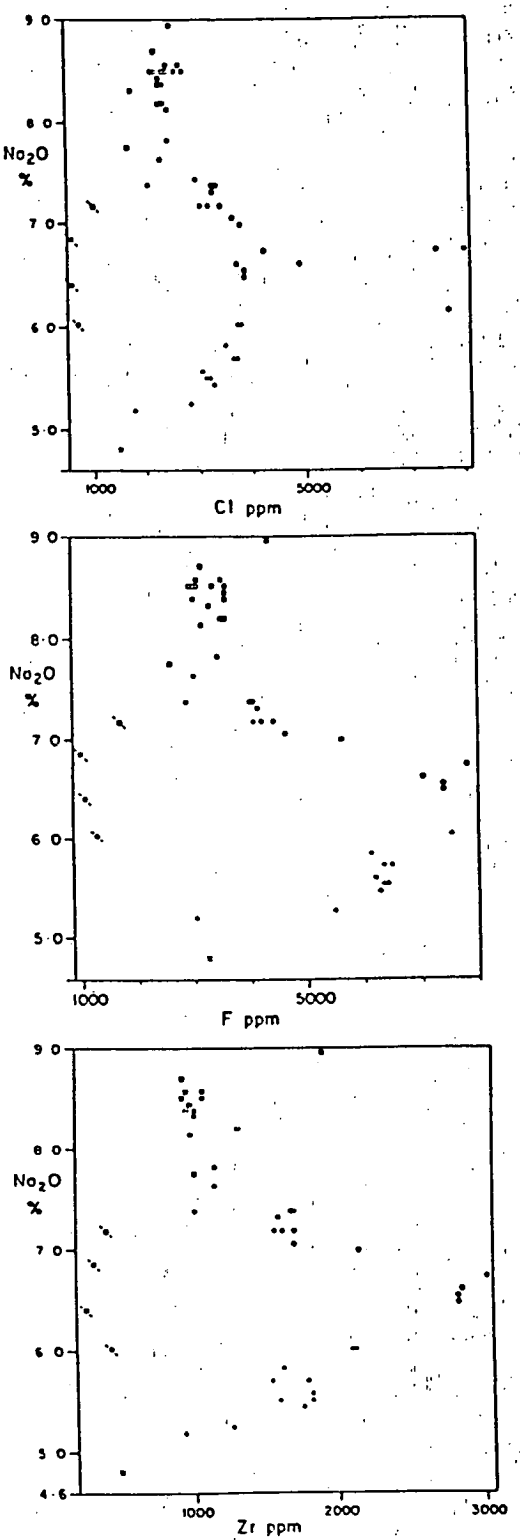

FIG. 8. Variations between different trace elements and Na_2O for peralkaline glasses from Kenya. Diamonds indicate samples from Pantelleria. Other symbols as in Figure 4.

centration ranges. There appears to be a "ceiling" for Cl in Kenyan glasses, which also shows up dramatically in the plot of Na_2O vs. Cl (Figure 8), where the negative distribution of the pantellerites and the positive distribution in the comendites appear to curve towards a common maximum. This contrasts with the Na_2O vs F diagram in which the more linear distributions might be pointing to a maximum outside the observed range. This limitation in the chlorine appears to be a regional effect because liquids from Pantelleria achieve much higher levels of Cl, describing a linear array with no obvious "ceiling" (Figures 8 and 9). The Kenyan rift liquids point to a limit in available Cl, but not F, in the source. The simple conclusion reached previously for the Eburru pantellerites that F, Zr and Rb formed one chemically coherent group, whilst Nb, Y and Cl formed another, therefore needs modification. A more reasonable conclusion would be that Zr and Rb cohere very strongly with F, whereas Nb and Y partly cohere with F, with part of their distribution connected with availability of Cl.

Summary of the chemical distributions

Comendites, pantellerites and trachytes form distinct populations, and for some elements, subgroups of these populations emerge. Three recurring sub-groups in the trachytes relate directly to the source volcanoes, Menengai, Longonot and Eburru. Eburru trachytes are distinct from Eburru pantellerites in most plots. *Within* individual groups there is a general trend of increasing soda and iron with peralkalinity, with the pantellerite groups lying on the extension of the comendite trend (Figure 6). Superimposed on this, however, there is a broad negative distribution from trachyte to pantellerite. Furthermore, although incompatible elements show positive covariance *within* the groups, they correlate negatively with soda and iron in the pantellerites, in contrast with trachytes and comendites. Viewed as a whole, it is clear that more than one process has been at work in generating these liquids. Soda (and iron) and peralkalinity seemingly can vary independently of incompatible trace elements.

THE SIGNIFICANCE OF SEPARATE POPULATIONS OF FELSIC LIQUIDS

The chemical variation diagrams emphasise the individuality of different volcanic centres by showing that each has erupted distinct and separate felsic magmas. Furthermore, there are contemporaneous basalts and hawaiites, but no extruded rocks with silica percentages between 54 and 61 weight percent that are not mixed lavas.

Different volcanoes have, therefore, erupted products that are not only chemically distinct, but

B8776 T.106, 109 Art. 2 11 (250)

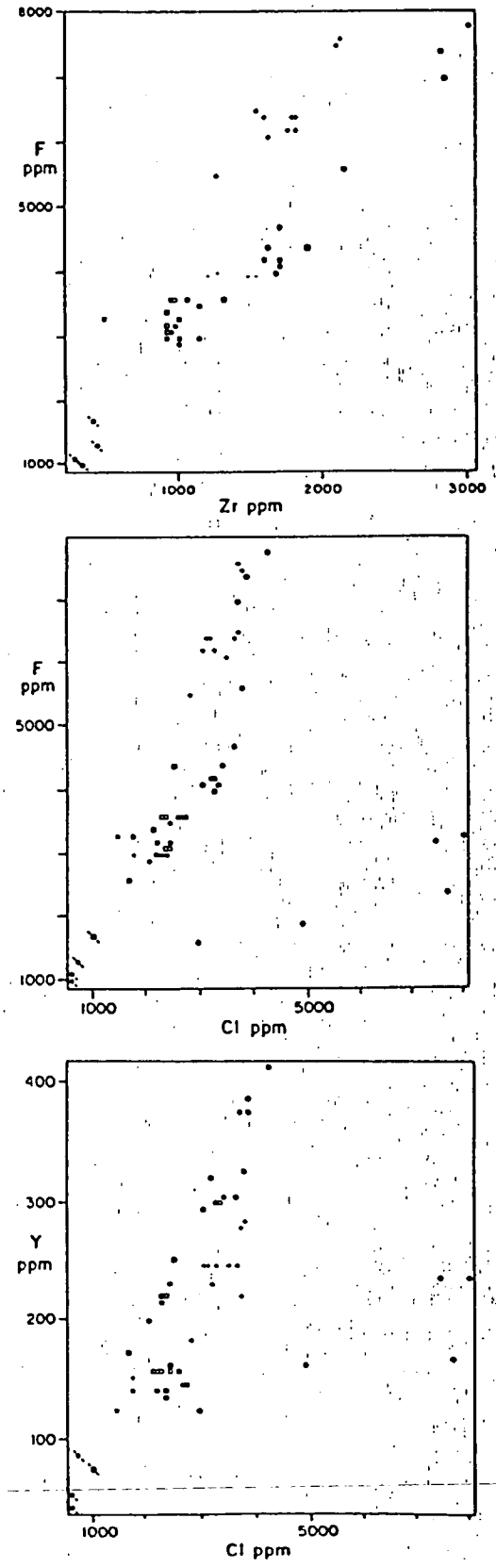

between which there are no bridging compositions. These distinct felsic magmas are all products of a major igneous cycle working through this segment of lithosphere. They are coeval and share some distinctive chemical features, especially peralkalinity. What is their relationship? If a basaltic parent were to be invoked, then each felsic batch has to evolve quite separately to produce the batches under the different volcanoes. In all cases the parent and the process must lead to strong peralkalinity and great enrichment in incompatibles. But if each magma type represents merely a stage in a common evolutionary process why should any one stage be restricted to one volcano? The most ready alternative is that the different volcanoes do not represent various degrees of melt differentiation but *are different melts.*

Closed-system magma evolution can be discounted even for single complexes, such as Eburru, where Rb varies as if it were an incompatible element (BAILEY and MACDONALD, 1975). This relationship cannot be reconciled with generation of the liquids solely by crystal–liquid interactions because the distribution coefficient for Rb in alkali feldspar is greater than 0.3. The behaviour of Rb in a series of liquids in equilibrium with alkali feldspar, based on measured distribution coefficients for Rb and Zr and the Rayleigh fractionation law is shown for the Eburru sequence in Figure 10. Also shown are the actual and calculated distributions for the Naivasha comendites and pantellerite glasses from Pantelleria. In all three cases the predicted curves depart from the actual distributions, and it must be assumed that in each series some factor other than evolution by feldspar–liquid interaction is necessary to give the observed distribution pattern for rubidium. As halogen contents typically rise above one weight percent in the more siliceous liquids, no mineral seen in the rocks could provide the source for incompatible elements. One possibility is that a halogen-rich fluid was contributing to the source region from the onset of melting.

Alternatively the high levels of incompatible elements might perhaps be attributed to late-stage processes after the melt had filled a shallow magma chamber. Some limited variation is possible by crystal fractionation, as inferred for Longonot (SCOTT, 1980) but the Rb factor rules this process out for Eburru (BAILEY and MACDONALD, 1975) and for Naivasha comendites (MACDONALD *et al.*, in press). Diffusion, or "liquid state" processes, may account for part of the variation, as suggested from

FIG. 9. Variations between trace elements for peralkaline glasses. Diamonds indicate samples from Pantelleria. Other symbols as in Figure 4.

B8776 T.106,109 Art. 2 12 Ae
(251)

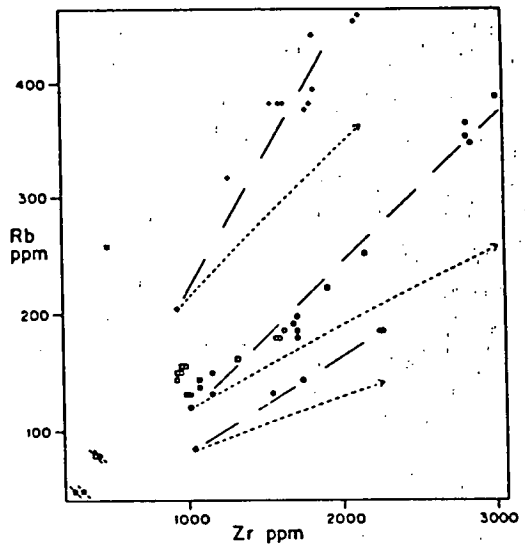

FIG. 10. Variation between Rb and Zr in peralkaline glasses. For three groups (comendites, and pantellerites from Eburru and from Pantelleria) the calculated alkali feldspar fractionation curves are shown by short dashed lines with arrows. The distribution coefficient for Rb (D = 0.3) is a mean from values given in BAILEY and MACDONALD (1975) and additional determinations, in which the distribution of Zr (D = 0.046) was also measured (using separated feldspars and glass matrices: Eburru samples; BAILEY, unpubl.). Symbols as in Figure 4.

the evidence of zoned ash flows on Menengai (LEAT *et al.*, 1984), but if such a process has given rise to zoned magma chambers, the products lie within the range for the magma type, which itself still remains tightly constrained in any one complex. Concentration of incompatible elements solely by diffusion also runs into difficulty with low and non-systematic variations of H_2O, and the apparent ceiling on Cl levels in the Kenya province. Difficulties are further compounded by the fact that the distribution pattern between Na, Fe, and incompatible elements is reversed in pantellerites compared with trachytes and comendites.

High level, magma chamber processes offer no solutions to the fundamental *geological* questions of how these distinct felsic magma types have been produced, how they have preserved their individuality, and what *regional* conditions have led to *all* the individual centres developing such striking richness in volatile and incompatible elements. An explanation that aims to encompass these factors must consider melt sources and the possible influence of fluids in magma generation.

CARBON DIOXIDE FLUX THROUGH THE RIFT

In previous papers attention has been drawn to the evidence for massive emission of CO_2 through the Kenya rift zone (BAILEY, 1978, 1980). The main points, with some additions, may be briefly summarised as follows.

(1) Igneous activity was initiated by nephelinite/carbonatite volcanism, which has continued intermittently for the past 23 Ma. An example of the early activity is the nephelinite volcano of Tinderet, with associated Miocene carbonatite ashes (DEANS and ROBERTS, 1984) 50 km to the west of the trachyte volcano of Menengai. The active carbonatite volcano of Oldonyo Lengai at the southern end of the rift is also part of regional igneous activity that includes felsic volcanism. In nephelinite volcanic gases, CO_2 dominates over H_2O; in nephelinite glasses from Nyiragongo, CO_2 is about ten times as abundant as H_2O; and carbonatite lavas from Oldonyo Lengai are anhydrous (but rich in F and Cl) (BAILEY, 1980).

(2) At the present time, all along the rift there is escape of CO_2, which is sufficiently abundant to be exploited in commercial wells at several places. This CO_2 flux has led to the suggestion by Kenyan geologists that present day geothermal fields along the rift are the result of heating of the ground water by hot juvenile CO_2 (WALSH, 1969).

(3) Due to the low solubility of CO_2 in salic magmas, evidence of the former presence of CO_2 in Kenyan peralkaline rocks is bound to be scarce, nevertheless, high-temperature carbonates are recorded in small pockets in some of the trachyte lavas on Longonot (SCOTT, 1982). A mixed carbonate/glass ash flow and carbonate lapillae tuffs have been discovered on Suswa (SKILLING and MACDONALD, personal communication, 1986). The main commercial CO_2 well also happens to be on the edge of the rift just to the east of Suswa.

The Kenya rift is fizzing with CO_2 and has been for at least the past 23 million years. This narrow gash in the lithosphere acts as a release channel for volatiles escaping from a large mantle volume below, analogous to the function of a pie funnel (BAILEY, 1980). The general thermal, chemical, and geodynamic consequences of such fluid focussing have been explored elsewhere (BAILEY, 1983).

SYNTHESIS

In the absence of any evidence for continuous melt evolution, the objective procedure would be to treat each magma batch as an entity, or the product of a separate event. Any links within or between the major groups, trachytes, pantellerites, and comendites, must then be attributable to common features in the melt generating regime. From this starting point, the following deductions are possible for the melting system:

B8716 T.106,109,110 Art. 2 13 GL
(252)

(1) Comendites show regular increase in Fe_2O_3 with peralkalinity, consistent with control by melting of an acmitic pyroxene in the source. A sodic pyroxene could exert some influence on the trachyte variations. Any such pyroxenes could be formed by metasomatism prior to melting.

(2) By contrast, pantellerites show no regular variation in Fe_2O_3, even though Na_2O and FeO_T rise steadily through the range. This relationship could describe an increasing contribution from a stable amphibole (fluor-arfvedsonite?) at increased melt levels. Such a melting pattern would give rise to higher sodium and iron with greater melt volumes, consistent with the negative correlation between Na_2O and incompatible elements in the pantellerites. It would imply also that any fluorine contribution from the amphibole was insufficient to produce a noticeable effect on the distribution pattern of F in the pantellerites as a whole.

(3) Halogens and other incompatible elements are mainly contributed from a fluid entering the melt zone. The anticipated general result would be higher concentrations in earlier, smaller melt volumes, but some variations in the melt samples could be due to varying amounts of fluid flux through the melt zone (see 4.d).

(4) Part of the fluid has very low solubility in siliceous liquids, with the effect that it is not wholly consumed in the initial melt. Consequently:

(a) Elements are partitioned between melt and fluid.

(b) Partitioning is dependent on melt composition, *e.g.*, trachyte or rhyolite.

(c) Partitioning is dependent on pressure-temperature conditions, and source mineralogy.

(d) Because part of the fluid is insoluble in the melt there can be fluid flux *through the melt region.*

Thus each melt may be buffered for incompatible elements by the fluid.

(5) The fluid is essentially anhydrous and CO_2-rich. It also carries other volatile elements such as alkalies (which can be contributed to the melt) but its most striking effect is on the incompatible element budget of the melt. Partitioning works both ways and the fluid scavenges alkaline earths (notably Ba and Sr) from the more siliceous melts. This would account for the extremely low Ba and Sr concentrations in these melts, which defy explanation by closed-system crystal fractionation or partial melting hypotheses.

(6) The three main magma types are determined by three types of metasomatised source rocks:

(a) comendite from metasomatised sialic rocks;

(b) pantellerite from metasomatised basic rocks;

(c) trachyte from metasomatised mantle containing felsic minerals (BAILEY, 1986).

(7) Different magma types show major differences in their chemical patterns. These might simply reflect fundamental differences in the fluid source, but there is a strong possibility that some of the differences may be a consequence of interaction between the fluid and rocks in its path before entering the melt zone. For instance, the higher Rb in comendites may be related to earlier scavenging of this element as the fluid moved through crustal rocks before entering the melt zone. On the other hand, the generally lower levels of incompatible elements in the trachytic melts may be more a function of variations in the partitioning between the CO_2-rich fluid and a less siliceous melt at higher pressures.

(8) Individual magma types erupt from distinct centres depending on the source level in the lithosphere. Trachyte centres tap a melt source in metasomatised mantle. As the trachyte source is exhausted, and the melting cycle climbs higher in the lithosphere, pantellerite can become the dominant eruptive. Comendite represents the ultimate stage of the rifting/melting process, when the melting cycle finally impinges on metasomatised sialic crust. Where an igneous cycle is well established, a range of sources, from mantle to crust, may be providing melts to a series of contemporaneous volcanoes. This scenario is consistent with the late development of the Lake Naivasha felsic magma centres, almost symmetrically disposed around the topographic culmination of the Gregory Rift.

Acknowledgments—We thank our friends and colleagues in the Department of Geology, University of Reading, whose skills and cooperation have been vital in this study. Fieldwork in Kenya was made possible by grants from the Natural Environment Research Council.

REFERENCES

BAILEY D. K. (1974) Experimental petrology relating to oversaturated peralkaline volcanics: a review. *Bull. Volcanol. Special Vol.* 38, 635–652.

BAILEY D. K. (1978) Continental rifting and mantle degassing. In *Petrology and Geochemistry of Continental Rifts.* (eds. E. -R. NEUMANN and I. B. RAMBERG), pp. 1–13 Reidel.

BAILEY D. K. (1980) Volcanism, earth degassing and replenished lithosphere mantle. *Philos. Trans. Roy. Soc. London* A297, 309–322.

BAILEY D. K. (1983) The chemical and thermal evolution of rifts. *Tectonophys.* 94, 585–597.

BAILEY D. K. (1986) Fluids, melts, flowage and styles of

B8776 T.110, 111 Art. 2 14 QQ
(253)

eruption in alkaline ultramafic magmatism. *Trans. Geol. Soc. S.A.* (in press). 88 (2), 449–457

BAILEY D. K. and SCHAIRER J. F. (1964) Feldspar–liquid equilibria in peralkaline liquids—the orthoclase effect. *Amer. J. Sci.* 262, 1198–1206.

BAILEY D. K. and MACDONALD R. (1970) Petrochemical variations among mildly peralkaline (comendite) obsidians from the oceans and continents. *Contrib. Mineral. Petrol.* 28, 340–351.

BAILEY D. K. and MACDONALD R. (1975) Fluorine and chlorine in peralkaline liquids and the need for magma generation in an open system. *Mineral. Mag.* 40, 405–14.

BAILEY D. K. and COOPER J. P. (1978) Comparison of the crystallisation of pantelleritic obsidian under hydrous and anhydrous conditions. In *Progress in Experimental Petrology, NERC Publications Series D* 11, 230–233 Eaton Press.

BOWEN N. L. (1937) Recent high-temperature research on silicates and its significance in igneous geology. *Amer. J. Sci.* 33, 1–21.

CARMICHAEL I. S. E. and MACKENZIE W. S. (1963) Feldspar–liquid equilibria in pantellerites: an experimental study. *Amer. J. Sci.* 261, 382–396.

CHAIGNEAU M., TAZIEFF H. and FABRE R. (1960) Composition des gaz volcaniques du lac de lave permanent du Nyiragongo. *Acad. Sci., Paris, C. R.* 250, 2482–8.

COOPER J. C. (1975) Experimental melting and crystallization of oversaturated peralkaline glassy rocks. Ph.D. Thesis, University of Reading.

DAVIES G. R. and MACDONALD R. (1986) Crustal influences in the petrogenesis of the Naivasha basalt-rhyolite complex: combined trace elements and Sr–Nd–Pb isotope constraints. (Submitted to *J. Petrol.*).

DEANS T. and ROBERTS B. (1984) Carbonatite tuffs and lava clasts of the Tinderet foothills, western Kenya: a study of calcified natrocarbonatites. *J. Geol. Soc. London* 141, 3, 563–580.

EWART A. (1979) A review of the mineralogy and chemistry of Tertiary-Recent dacitic, latitic, rhyolitic, and related salic volcanic rocks. In *Trondhjemites, dacites, and related rocks* (ed. F. BARKER), pp. 13–121 Elsevier.

GREGORY J. W. (1894) Contributions to the physical geography of British East Africa. *Geogr. J.* 4, 290.

HAMPTON C. M. and BAILEY D. K. (1984) Gas extraction experiments on volcanic glasses. *J. Non-Cryst. Solids* 67, 147–168.

HAMPTON C. M. and BAILEY D. K. (1985) Sublimates obtained during fusion of volcanic glasses. *J. Volcanol. Geotherm. Res.* 25, 145–155.

JOHNSON R. W. (1969) Volcanic geology of Mt. Suswa, Kenya. *Philos. Trans. Roy. Soc. London* 265A, 383–412.

LEAT P. T. (1984) Geological evolution of the trachytic caldera volcano Menengai, Kenya Rift Valley. *J. Geol. Soc. London* 141, 6, 1057–1069.

LEAT, P. T., MACDONALD R. and SMITH R. L. (1984) Geochemical evolution of the Menengai Caldera Volcano, Kenya. *J. Geophys. Res.* 89, 8571–8592.

LUTH W. C. (1976) Granitic rocks. In *The Evolution of the Crystalline Rocks*, (eds. D. K. BAILEY and R. MACDONALD), pp. 335–417 Academic Press.

MCCALL G. J. H. (1957) Geology and groundwater conditions in the Nakuru area. *Tech. Rept. 3*, Hydraulic Branch, M.O.W. Nairobi.

MCCALL G. J. H. (1967) Geology of the Nakuru-Thomson's Falls—Lake Hannington area. *Geol. Surv. Kenya, Report No. 78.*

MACDONALD R. and BAILEY D. K. (1973) The chemistry of the peralkaline oversaturated obsidians. *U.S. Geol. Surv. Prof. Paper 440N-1.*

MACDONALD R., BAILEY D. K. and SUTHERLAND D. S. (1970) Oversaturated peralkaline glassy trachytes from Kenya. *J. Petrol.* 11, 507–17.

MACDONALD R., BLISS C. M., LEAT P. T., BAILEY D. K. and SMITH R. L. (1986) Geochemical evolution of the Naivasha peralkaline rhyolitic complex, Kenya: I. Mineralogy and Geochemistry. (submitted to *J. Geol.*).

NICHOLLS J. and CARMICHAEL J. S. E. (1969) Peralkaline acid liquids: a petrological study. *Contrib. Mineral. Petrol.* 20, 268–294.

NOBLE D. C., SMITH V. C. and PECK L. C. (1967) Loss of halogens from crystallized and glassy silicic volcanic rocks. *Geochim. Cosmochim. Acta* 31, 215–223.

SCOTT S. C. (1980) The geology of Longonot volcano, Central Kenya: a question of volumes. *Philos. Trans. Roy. Soc. London* 296, 437–465.

SCOTT S. C. (1982) Evidence from Longonot volcano, Central Kenya, lending further support to the argument for a coexisting CO_2 rich vapour in peralkaline magma. *Geol. Mag.* 119, 215–217.

SCOTT S. C. and BAILEY D. K. (1984) Coeruption of contrasting magmas and temporal variations in magma chemistry at Longonot Volcano, Central Kenya. *Bull. Volcanol.* 47, 849–873.

SUTHERLAND D. (1974) Petrography and mineralogy of the peralkaline silicic rocks. *Bull. Volcanol. Special Vol.* 38, 517–547.

TAYLOR B. E., EICHELBERGER J. C. and WESTRICH H. R. (1983) Hydrogen isotopic evidence of rhyolitic magma degassing during shallow intrusion and eruption. *Nature* 306, 541–545.

THOMPSON A. O. and DODSON R. G. (1963) Geology of the Naivasha area. *Geol. Surv. Kenya Report No. 55.*

THOMPSON R. N. and MACKENZIE W. S. (1967) Feldspar–liquid equilibria in peralkaline acid liquids: an experimental study. *Amer. J. Sci.* 265, 714–34.

TUTTLE O. F. and BOWEN N. L. (1958) Origin of granite in the light of experimental studies in the system $NaAlSi_3O_8$–$KAlSi_3O_8$–H_2O. *Geol. Soc. Amer. Mem.* 74, 153 pp.

UNNI C. K. and SCHILLING J.-G. (1978) Cl and Br degassing by volcanism along the Reykjanes Ridge and Iceland. *Nature* 272, 19–23.

WALSH J. (1969) Mineral and thermal waters of Kenya. *XXIII International Geol. Cong.* 19, 105–110.

WILCOX R. E. (1979) The liquid line of descent and variation diagrams. In *The Evolution of the Igneous Rocks: Fiftieth Anniversary Perspectives*, (ed. H. S. YODER, JR.), Chap. 7, pp. 205–232, Princeton University Press.

WILLIAMS L. A. J. (1982) Physical aspects of magmatism in continental rifts. *Continental and Oceanic Rifts Geodynamics*, Series 8, 193–222.

B8776 T.111 Art. 2 15 Qe

(254)

Contr. Mineral. and Petrol. 24, 239—244 (1969)

Pantelleritic Obsidians from the Volcano Chabbi (Ethiopia)

R. MACDONALD
Dept. of Geology, Reading University

I. L. GIBSON
Dept. of Earth Sciences, Leeds University

Received June 30, 1969

Abstract. Chabbi, a Quaternary volcano in the Ethiopian Rift, appears to be unique in having erupted only non-porphyritic pantelleritic obsidians showing a very restricted range in composition. Petrogenetic schemes for deriving these lavas are discussed, and it is suggested that some degree of effective superheating, followed by failure of the magmas to crystallise because of their dryness (and hence high viscosity) can account at least for the absence of phenocrysts.

Introduction

The volcano Chabbi (Lat. 7°10′ N, Long. 38°27′ E) is one of a series of Quaternary peralkaline silicic centres lying within the Main Ethiopian Rift. This active volcano was not recognised as such until 1959 and the only account of the centre is by Mohr (1966), who showed Chabbi to be a shield-like mass of silicic obsidian flows. One of us (I.L.G.) visited Chabbi briefly during the summer of 1967 and made the additional field observations noted below while collecting a small suite of samples.

Field Relations

The field relations and tectonic setting of Chabbi have been described by Mohr, who was correct in stressing the complexity of this centre. There are several separate vents (Fig. 1) each of which is fairly steep-sided, and which coalesce to give a dome-shape to the volcano. There is almost no dissection of Chabbi, and the total thickness of flows is not known. It is possible that the volcano is a basaltic shield veneered with rhyolite, but we consider this extremely unlikely. Judging from the relative states of erosion of the various vents and from the amounts of pumice cover, the volcanic activity can be estimated to have continued over several thousands of years.

Mohr (1966) drew attention to one very important facet of the geology, namely that all the flows examined and sampled in the field are non-porphyritic obsidians. Although an extensive search was made, no porphyritic flows were found. Certainly the visible lavas from the Main, East, Northeast, North and Hot Cone centres of Mohr (1966) are all non-porphyritic, while reconnaissance suggests that those from the West centre are similar. Pumice layers between the lavas, and rhyolite fragments in the pyroclastic units, also appear to be aphyric.

The non-porphyritic character of the lavas is not typical of silicic peralkaline centres in the Ethiopian Rift. Fantale (Gibson, 1967) and the Gariboldi Pass complex (Cole, 1968), the only other two centres examined in any detail, are composed

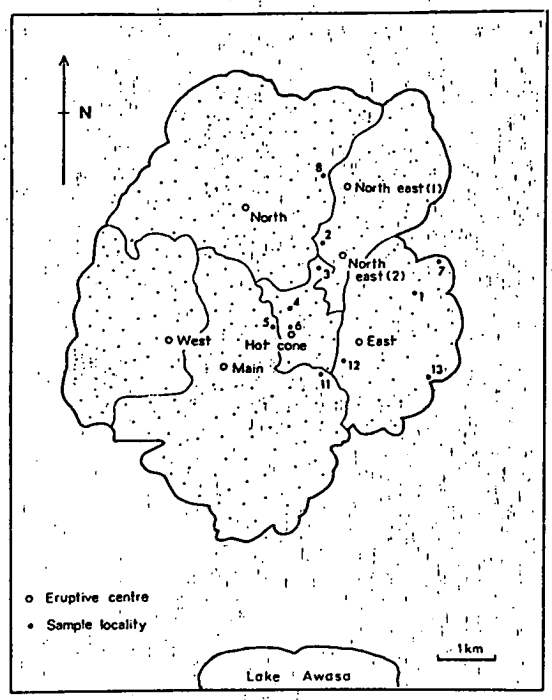

Fig. 1. Outline map of Chabbi volcano, after Mohr (1966). The area of Quaternary obsidians is shown stippled, and also indicated are the major eruptive centres and the sample localities

predominantly of porphyritic lavas and tuffs, with pure obsidians comprising probably less than 5% of the total effusive products. Reconnaissance suggests that other Rift centres are comparable to Fantale in this respect.

In view of this unusual characteristic of the Chabbi lavas, an attempt was made to assess whether the peculiar composition of the lavas had in any way influenced the character of the volcanism.

As stated by Mohr (1966), the vast majority of the products of this centre are normal silicic flows. These typically are 10—20 m thick, with steep, sharp flow-terminations, and rough uneven upper surfaces. These features indicate that the magma on eruption was viscous. It has recently been suggested (Schmincke and Swanson, 1967) that peralkaline lavas such as these might be unusually fluid on account of the high alkali and low alumina contents. We wish to stress that the field evidence from this centre indicates that the viscosity of these flows was, on eruption, similar to that of many calc-alkaline obsidians, such as those from central Iceland (Walker, 1965).

Associated with the obsidian lavas are intercalated beds of air-fall tuffs and agglomerates. No ash-flow tuffs have been identified with certainty. The units described by Mohr (1966, p. 12) as pyroclastic "flows" are more readily explained as normal viscous silicic flows veneered by airfall pumice.

There appears to be a relative scarcity of pumice deposits associated with the obsidians, and many eruptions had virtually no explosive phase. A similar situation exists at Fantale, and we suggest that this indicates low volatile contents of the magmas. The significance of this is discussed later.

Table. *Analyses of non-porphyritic pantelleritic obsidians from Chabbi volcano. Sample localities are shown in Fig. 1*

	1	2	3	4	5	6	7	8	11	12	13
SiO_2	74.4	74.4[a]	74.2	74.3	74.3	74.3	73.8	74.0	74.1	74.9	74.8
ZrO_2	0.25	0.25	0.25	0.25	0.25	0.25	0.25	0.25	0.24	0.24	0.25
TiO_2	0.35	0.27	0.27	0.26	0.27	0.27	0.26	0.27	0.29	0.27	0.28
Al_2O_3	9.42	9.41	9.40	9.35	9.44	9.48	9.54	9.46	9.62	9.46	9.69
Fe_2O_3	1.77	1.65	1.74	1.28	1.61	1.79	1.73	1.91	1.76	1.53	1.61
FeO	2.88	2.90	2.90	3.34	2.82	2.90	2.97	2.65	2.84	2.87	2.92
MnO	0.22	0.21	0.21	0.22	0.21	0.20	0.23	0.21	0.22	0.22	0.22
MgO	0.16	0.13	0.15	0.20	0.12	0.16	0.19	0.23	0.20	0.17	0.14
CaO	0.20	0.24	0.21	0.20	0.28	0.18	0.23	0.25	0.20	0.20	0.30
Na_2O	5.33	5.49	5.23	5.66	5.29	5.52	5.62	5.42	5.53	5.49	5.53
K_2O	4.29	4.39	4.26	4.44	4.39	4.48	4.43	4.41	4.37	4.47	4.38
H_2O^+	0.47	0.41	0.40	0.32	0.36	0.31	0.49	0.30	0.29	0.40	0.37
F	0.25	0.25	0.24	0.25	0.23	0.23	0.25	0.25	0.25	0.25	0.24
Cl	0.16	0.16	0.16	0.17	0.16	0.16	0.17	0.16	0.16	0.16	0.16
	100.05	100.16	99.62	100.24	99.73	100.23	100.16	99.77	100.07	100.63	100.89
O≡F, Cl	0.15	0.15	0.14	0.15	0.14	0.14	0.15	0.15	0.15	0.15	0.14
Total	99.90	100.01	99.48	100.09	99.59	100.09	100.01	99.62	99.92	100.48	100.75
Q	34.3	34.1	34.1	33.9	34.4	33.5	32.9	33.3	33.1	34.5	33.7
Or	25.6	26.1	25.6	26.1	26.1	26.7	26.1	26.1	26.1	26.7	26.1
Ab	24.1	23.6	24.1	23.6	23.6	23.6	24.1	24.1	24.6	23.6	25.2
Ac	5.1	5.1	5.1	3.7	4.6	5.1	5.1	5.5	5.1	4.2	4.6
Ns	3.3	3.8	3.1	4.4	3.4	3.8	3.8	3.3	3.5	4.0	3.5
Hy	5.5	5.4	5.5	6.4	5.3	5.5	5.9	5.4	5.5	5.5	5.5
	0.6	0.6	0.6	0.6	0.6	0.6	0.6	0.6	0.6	0.6	0.6
	0.4	0.4	0.4	0.4	0.4	0.4	0.4	0.4	0.4	0.4	0.4
CaF_2	0.3	0.3	0.3	0.3	0.4	0.3	0.3	0.4	0.3	0.3	0.4
Il	0.3	0.3	0.3	0.3	0.3	0.3	0.3	0.3	0.3	0.3	0.3

[a] SiO_2 by difference. Samples all dried at 105° C. P_2O_5 in all samples $< 0.05\%$. Analysts: R. MacDonald and S. A. Malik (SiO_2, F, Cl).

Analytical Data

Eleven analyses of non-porphyritic, non-hydrated obsidians are given in the Table. Chemically the rocks are transitional between comendites and pantellerites (Noble, 1968), but using the arbitrary division between these groups established by Lacroix (1927) and adopted by Noble (1968) namely, 12.5% normative femic constituents, the Chabbi lavas are classified as pantellerites. The analysed specimens are thought to be representative of all the flows of the volcano, and it is therefore striking that these flows have virtually identical compositions.

Origin of the Chabbi Lavas

Two features of the Chabbi flows are particularly interesting petrogenetically.

1. It is clear from the Table that the composition of the Chabbi obsidians, erupted probably over several thousands of years, has remained virtually constant.

2. There appears to be a complete lack of phenocryst minerals.

In conventional terms, these features are difficult to reconcile. Liquids formed by *fractional crystallisation* should contain and be in equilibrium with crystals, except in the case of complete crystal removal. This aphyric condition can normally be expected to persist over only a small temperature interval, unless the magmas become, and remain during ascent and eruption, either appreciably superheated or rapidly cooled below the stage of labile crystallisation. Porphyritic magmas might become aphyric by being rapidly moved to a lower pressure regime, with subsequent resorption of phenocrysts. Assuming that the liquids were brought quickly to the surface, they may have been erupted in an aphyric condition, since they will remain effectively superheated due to pressure release.

However, we consider it extremely unlikely that the fractional crystallisation of batches of basaltic magma over a longer period of time could have so accurately reproduced the same rhyolitic composition, and prefer to consider further alternatives.

A modification of this scheme is that a single superheated rhyolitic magma derived ultimately from basic magma was intruded into a sub-volcanic magma chamber and was able to exist for a long time without crystallising i.e. it passed from superheated to supercooled. Crystallisation was thus unable to destroy the uniformity of composition and the magma was available for periodic eruption at the surface. Alternatively intrusion of a porphyritic magma at its liquidus temperature, followed by pressure relief during tectonism, may have resulted in the whole mass being raised above the liquidus. In both cases, further crystallisation must have been delayed for a considerable period of time. We suggest that crystallisation in the Chabbi magmas was inhibited by their high viscosity, itself a function of their relatively anhydrous nature. It is known from experimental work on rhyolitic compositions that rates of crystallisation are exceedingly slow in dry systems, and several authors (Tuttle, 1952; Luth *et al.*, 1964; Nicholls and Carmichael, 1969; Bailey and Macdonald, 1969) have suggested that certain peralkaline rhyolites have evolved under dry conditions. These observations are consistent with the field evidence at Chabbi, where pyroclastic material is relatitively scarce, and where, on eruption at least, the magmas were very viscous.

Partial Melting of Basic Material

Since the source material is likely to have remained constant, and provided that pressure-temperature conditions were not too variable, it is possible that partial fusion of a basic rock could have produced the series of Chabbi obsidians (cf. Bailey, 1964; Bailey and Schairer, 1966). Such magmas, however, cannot have been formed with appreciable superheat and would be expected to have crystallised during ascent to the surface. Again, crystallisation may have been inhibited by the high viscosities of the liquids. Alternatively, a rhyolite magma may have been held at depth (? in the mantle) and was kept above its liquidus temperature by the regional geothermal gradient. Such a body may have been tapped only during periods of tectonic disturbance.

Complete Fusion of Peralkaline Granite

This is a possible mechanism for producing homogeneous rhyolite magmas, if it is assumed that they were superheated and remained so. Blocks of microgranite

have been recorded in the flows and tuffs from the Fantale (Lacroix, 1930) and Gariboldi Pass volcanoes, but none has so far been found at Chabbi, even in the pyroclastic materials.

Liquid Immiscibility

There may be some form of liquid immiscibility relationship between basalt and rhyolite at temperatures above the rhyolite liquidus, whereby the silicic liquids were separated from the basalt and brought to the surface in a superheated condition. In the case of Chabbi, where there are no basalts in the exposed volcanic pile, the possibility of the former co-existence of rhyolitic and basaltic magmas is questionable.

Conclusions

We feel that some combination of superheating, derived either at the site of magma genesis, or by relatively rapid movement into the crustal environment, followed by supercooling due to dryness, can explain the lack of crystals in the Chabbi rocks. Whether their composition could have been so accurately reproduced by a recurrent process involving a "eutectic" composition, e.g. fractional crystallisation or partial fusion of basic material, or whether the lavas have been derived from a single magma batch, is not known.

In the nature of its products, Chabbi appears to be a unique volcano. When the tectonic setting and petrology of the other Quaternary Ethiopian volcanoes are better known, some further clues as to the evolution of Chabbi may be found.

Acknowledgments. We wish to thank S. A. Malik of the Geochemistry Unit, Department of Geology, University of Reading, for the determination of SiO_2, F and Cl in the analysed specimens, and M. J. Saunders of the Grant Institute of Geology, University of Edinburgh for aid in determining the other elements. Drs. D. K. Bailey, K. G. Cox, P. G. Harris, B. G. Jamieson and B. G. J. Upton kindly read the manuscript and offered several useful suggestions for its improvement.

References

Bailey, D. K.: Crustal warping — a possible tectonic control of alkaline magmatism. J. Geophys. Res. 69, 1103—1111 (1964).

— Macdonald, R.: Alkali-feldspar fractionation trends and the derivation of peralkaline liquids. Am. J. Sci. 267, 242—248 (1969).

— Schairer, J. F.: The system Na_2O—Al_2O_3—Fe_2O_3—SiO_2 at 1 atmosphere, and the petrogenesis of alkaline rocks. J. Petrol. 7, 114—170 (1966).

Cole, J. W.: Gariboldi volcanic complex, Ethiopia. 12th Ann. Rep. Res. Inst. African Geol. Univ. Leeds, 30—32 (1968).

Gibson, I. L.: Preliminary account of the volcanic geology of Fantale, Shoa. Bull. Geophys. Obs. Addis Ababa 10, 59—67 (1967).

Lacroix, A.: Les rhyolites et les trachytes hyperalcalins quartzifères, à propos de ceux de la Corée. Compt. Rend. 185, 1410—1415 (1927).

— Les roches hyperalcalines du massif du Fantale et du col de Balla (Abyssinie). Soc. Geol. France Mem. 14, 89—102 (1930).

Luth, W. C., Jahns, R. H., Tuttle, O. F.: The granite system at pressure of 4 to 10 kilobars. J. Geophys. Res. 69, 759—773 (1964).

Mohr, P. A.: Chabbi volcano (Ethiopia). Bull. Volcanol. 29, 797—816 (1966).

Nicholls, J., Carmichael, I. S. E.: Peralkaline acid liquids: a petrological study. Contr. Mineral. and Petrol. 20, 268—294 (1969).

Noble, D. C.: Systematic variation of major elements in comendite and pantellerite glasses. Earth and Planet. Sci. Letters 4, 167—172 (1968).

Schmincke, H. U., Swanson, D. A.: Laminar viscous flowage structures in ash-flow tuffs from Gran Canaria, Canary Islands. J. Geol. 75, 641—664 (1967).

Tuttle, O. F.: Origin of the contrasting mineralogy of extrusive and plutonic salic rocks. J. Geol. 60, 107—124 (1952).

Walker, G. P. L.: Some aspects of Quaternary volcanism in Iceland. Trans. Leices. Lit. Phil. Soc. 59, 25—40 (1965).

Dr. R. Macdonald
Department of Geology
University of Reading
Reading, Great Britain

GENERAL STUDIES OF ALKALINE AND PERALKALINE ROCKS

Data of Geochemistry
Sixth Edition

MICHAEL FLEISCHER, *Technical Editor*

Chapter N. Chemistry of Igneous Rocks

Part 1. The Chemistry of the Peralkaline Oversaturated Obsidians

By RAY MACDONALD *and* D. K. BAILEY

GEOLOGICAL SURVEY PROFESSIONAL PAPER 440-N-1

Tabulation and discussion of chemical analyses of peralkaline, quartz-normative obsidians, the nature of chemical variation within these rocks, and a revised nomenclature

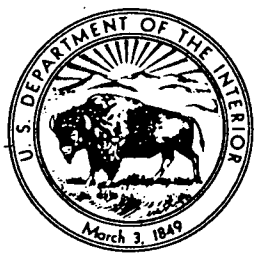

UNITED STATES GOVERNMENT PRINTING OFFICE, WASHINGTON : 1973

CONTENTS

	Page
Abstract	N1
Introduction	1
Petrogenetic importance of peralkaline rocks	1
Aims of the compilation	1
Acknowledgments	2
Secondary hydration and crystallization of peralkaline silicic glasses	2
Data selection	3
Compilation of analyses	5
Nomenclature	5
Petrochemistry	N6
Chemical variation in comendites and pantellerites	7
Subgroups within the comendites	12
Subgroups within the pantellerites	14
Trachyte obsidians	14
Trace elements	16
Variations in comendites and pantellerites	16
Trace elements in peralkaline trachytes	18
Discussion	18
References	19
Explanation to tables 2–8	22

ILLUSTRATIONS

		Page
FIGURE	1. Part of a molecular SiO_2–Al_2O_3–(Na_2O+K_2O) diagram showing some of the effects of hydration and devitrification on peralkaline glasses	N3
	2. Quadrilateral diagram showing loss of some original sodium in glassy rocks as a result of devitrification or hydration	4
	3. Frequency diagram showing volume percent of modal phenocrysts in samples of porphyritic obsidian	4
	4. Graph showing relations between volume percent of modal phenocrysts and agpaitic index in samples of porphyritic obsidian having >8 percent of phenocrysts	4
	5. Graph showing classification scheme for peralkaline silicic obsidians	5
	6. Part of a molecular SiO_2–Al_2O_3–(Na_2O+K_2O) diagram showing available analyses of comendites, pantellerites, comenditic trachytes, and pantelleritic trachytes	7
	7. Quadrilateral diagram showing variation in $Na_2O/(Na_2O+K_2O)$ in comenditic and pantelleritic obsidians (including trachytic varieties)	8
	8. Graphs showing the sum of normative femics plotted against agpaitic index for all analyses of comenditic and pantelleritic obsidians (including trachytic varieties)	8
	9. Graph showing the sum of normative femics plotted against normative quartz for all analyses of comenditic and pantelleritic obsidians (including trachytic varieties)	9
	10–12. Variation diagrams for pantellerites and comendites using the agpaitic index as abscissa	10
	13. Variation diagrams showing the subgroups within the pantellerites	15
	14. Variation diagrams for trace elements in comendites and pantellerites	17
	15. Variation diagrams showing trace element associations in pantellerites	18

TABLES

		Page
TABLE	1. Effect of hydration and devitrification on glassy peralkaline silicic rocks	N2
	2–4. Chemical analyses and norms of—	
	2. Comenditic obsidians	26
	3. Pantelleritic obsidians and separated glasses	28
	4. Comenditic and pantelleritic trachyte obsidians	33
	5. Trace element contents of comendite and pantellerite obsidians, compiled from published data	34
	6. Additional rare-earth-element data	35
	7. New determinations of trace elements in comendite and pantellerite obsidians	35
	8. Trace element contents of peralkaline trachyte obsidians from central Kenya	35
	9. Coefficients of correlation for various element and element ratio pairs	36
	10. Chemical analyses and norms of two obsidians	37

DATA OF GEOCHEMISTRY

CHEMISTRY OF IGNEOUS ROCKS

PART 1. THE CHEMISTRY OF THE PERALKALINE OVERSATURATED OBSIDIANS

By RAY MACDONALD[1] and D. K. BAILEY[2]

ABSTRACT

Peralkaline rocks are one of the characteristic products of nonorogenic magmatism, and the development of peralkaline silicic magmas continues to be a problem of special interest to petrologists. The problem is complicated by the fact that crystallization of these highly alkaline melts commonly results in significant chemical changes, such that the study of quenched liquids (glasses) is probably the only reliable approach to magma compositions. In this report, all acceptable analyses of oversaturated peralkaline obsidians are listed and compared in an attempt to provide a sound basis for further studies of peralkaline silicic magmatism.

One hundred and thirteen analyses of peralkaline silicic obsidians are tabulated, along with CIPW norms, modal data, and trace element analyses where available. The rocks are classified using a scheme slightly modified from that of Lacroix into comendites, pantellerites, comenditic trachytes, and pantelleritic trachytes. Though there is a continuous chemical transition between comendites and pantellerites, several parameters may be used to distinguish the two groups, including the agpaitic index and the FeO and Al_2O_3 contents. Variations in the comendites are discussed. Within the pantellerites, there are two subgroups: high-silica types, and varieties closely similar to those from the type area, Pantelleria. Though data are still very scarce, it is possible to characterize individual volcanoes by their trace element contents.

INTRODUCTION

PETROGENETIC IMPORTANCE OF PERALKALINE ROCKS

In the rocks of the earth's crust, molecular excess of Al_2O_3 over Na_2O+K_2O is prevalent, and the generation and survival of melts with the opposite characteristic present special problems. Peralkaline magmas are characteristically, if not exclusively, developed in nonorogenic magmatism and are frequently associated with magmas of mantle origin. An understanding of peralkaline petrochemistry is an essential prerequisite to unraveling the relations between the magma types and eventually to deciphering magma generation and development in the deep crust and mantle. The results given here are an attempt to define the present limits of knowledge in one group of peralkaline rocks—those containing normative quartz.

[1] Department of Environmental Sciences, University of Lancaster, United Kingdom.
[2] Department of Geology, University of Reading, United Kingdom.

AIMS OF THE COMPILATION

In order to define critical experimental studies, we began in 1967 to collect all the available analytical data on peralkaline silicic rocks to form a comprehensive picture of their chemistry and phase relations. It soon became clear that the volcanic rocks had undergone posteruptive changes in composition, especially loss of alkalis on crystallization or during hydration of glass, and precise interpretation of their interrelationships was very difficult. Several chemical features of the nonhydrated obsidians suggest that they are probably close to magmatic compositions.

Peralkaline silicic obsidians are uncommon, especially those with less than 20 percent normative quartz. We have attempted to collect suitable specimens from as many localities as possible. Thanks to the generosity of several geologists, we now have a wide range of samples, of which 32 have been analyzed in the Geochemistry Unit of the Geology Department, University of Reading, United Kingdom.

By choosing only obsidian, we may be imposing a selective bias in favor of certain compositions. It could be argued that the glassy condition is a result of some chemical peculiarity not found in magmas that have crystallized. At the present time, however, our compilation covers a wide range of composition; we have been unable to detect systematic differences from crystalline lavas; and experiments show that many of the obsidians are not difficult to crystallize. We suggest that this compilation of obsidian analyses is the logical first step towards quantifying the bases of comparison and that we shall be able to elucidate the more complex crystalline varieties only when the nature of the chemical variation within the obsidians is understood.

By confining our study to oversaturated peralkaline rocks we have adopted two arbitrary composition boundaries; no petrogenetic significance is implied. In particular, metaluminous rhyolites with agpaitic index close to 1 are excluded though they are obviously closely connected with comenditic rocks. On Easter Island, for

mple, some of the rhyolitic obsidians have small ounts of normative acmite; others have small ounts of normative anorthite, though they belong to same phases of volcanic activity. Similarly, we have included here any discussion of the geographical ribution, geology, or petrography of the analyzed imens, as these features can be properly evaluated when all peralkaline silicic rocks are considered.

ACKNOWLEDGMENTS

A. Malik, D. A. Bungard, J. M. C. Palmer, and L. Porteous of the Geochemistry Unit, Depart- t of Geology, University of Reading, made many of analyses quoted here. The chemical analytical pro- res and controls were largely developed by J. E. mas. Unpublished analyses of obsidians from ada were kindly made available by the U.S. Geo- al Survey. Dr. D. S. Sutherland allowed us to use e unpublished analyses of pantellerites from Kenya cted under the auspices of the East African Geo- al Research Unit. Dr. G. A. R. Till and the staff of Computer Unit, Department of Geology, University Reading, computed the correlation coefficients. nith and J. Watkins helped in producing the dia- s, and Miss V. Fulford and Miss L. Johnson ntly typed versions of the manuscript. Drs. Felix es, Michael Fleischer, and R. L. Smith suggested detailed and valuable improvements to the manu- t. To all these people we express our grateful ks. Ray Macdonald acknowledges with thanks re- of a University of Reading research fellowship g the period 1967–70.

SECONDARY HYDRATION AND CRYSTALLIZATION OF PERALKALINE SILICIC GLASSES

lowing the earlier work of Ross and Smith (1955) riedman and Smith (1958), D. C. Noble and his rkers in the U.S. Geological Survey have shown he compositions of peralkaline silicic glasses can ensively modified on secondary hydration and on llization. The major chemical changes so far igated are tabulated below:

dary hydration:

- -----Almost invariably lost to some degree (Noble, 1967, 1970).
- -----Generally lost, but may be gained on prolonged contact with ground water (Noble, 1967).
- -----May be leached from porous hydrated glasses (Noble, 1967).
- l-----Significant amounts may be added or removed by ground water (Noble and others, 1967).
- Mg-----Added by ground water (Noble, 1966).

Crystallization (including devitrification):

- Na-----Lost in variable amounts, roughly dependent on the peralkalinity of the glass (Carmichael, 1962; Noble, 1965, 1970; Ewart and others, 1968; Romano, 1969).
- F, Cl-----On average, 50 percent of F and 80 percent of Cl lost from the specimens studied (Noble and others, 1967; Carmichael, 1962; Noble, 1965; Romano, 1969).
- Fe-----More or less oxidized (Romano, 1969; Rosholt and Noble, 1969).
- U-----Some 20–60 percent lost, probably removed by ground water (Rosholt and Noble, 1969).

The three sets of analyses given in table 1 (A–E, 1–2, and 3–5) can be used to demonstrate some of the effects of secondary hydration and crystallization on peralkaline volcanic rocks, using projections in the system Na_2O–K_2O–Al_2O_3–SiO_2 developed by Bailey and Macdonald (1969). The glassy parts of the flows show a range of peralkalinity (fig. 1) from the mildly peralkaline comendite (table 1, No. 3) through the comendite (table 1, No. 1) to the strongly peralkaline pantellerites (table 1, D and E). It is clear from table 1 and from figures 1 and 2 that both crystallization and hydration

TABLE 1.—*Effect of hydration and devitrification on glassy, peralkaline silicic rocks*

[Data in percent except for ratios]

	A	B	C	D	E	1	2	3	4	5
SiO_2	68.25	68.80	68.50	68.60	68.00	73.98	71.70	75.37	73.32	71.94
Al_2O_3	10.90	11.15	10.96	10.64	11.34	11.28	10.94	11.95	11.76	11.89
Fe_2O_3	5.80	5.50	4.20	2.88	3.16	1.71	2.00	0.84	0.95	1.28
FeO	1.15	1.29	2.58	3.59	2.42	1.80	1.48	0.99	0.81	0.60
MgO	0.73	0.75	0.76	0.45	0.45	-----	-----	-----	-----	-----
CaO	0.49	0.49	0.49	0.49	0.53	-----	-----	-----	-----	-----
Na_2O	5.28	5.24	6.00	6.36	7.76	5.33	4.63	4.43	4.29	4.02
K_2O	4.92	4.90	4.86	4.80	4.72	4.55	4.85	4.82	4.66	4.52
H_2O-	0.42	0.31	0.09	0.25	0.00	0.02	0.10	0.04	0.17	0.82
H_2O+	0.57	0.53	0.33	1.18	0.56	0.16	2.90	0.45	2.77	3.32
TiO_2	0.65	0.57	0.53	0.65	0.65	-----	-----	-----	-----	-----
P_2O_5	0.05	0.08	0.07	0.05	0.06	-----	-----	-----	-----	-----
MnO	0.25	0.22	0.25	0.27	0.21	-----	-----	-----	-----	-----
Cl	0.26	0.22	0.31	0.35	0.51	-----	-----	-----	-----	-----
F	0.15	0.12	0.12	0.20	0.20	-----	-----	-----	-----	-----
Na_2O/K_2O	1.07	1.07	1.23	1.33	1.64	1.17	0.95	0.92	0.92	0.89
Na_2O+K_2O	10.20	10.14	10.86	11.16	12.48	9.88	9.48	9.25	8.95	8.54
$FeO/(FeO+Fe_2O_3)$	0.17	0.19	0.38	0.55	0.43	0.51	0.43	0.54	0.46	0.32
Fe as FeO	6.38	6.24	6.36	6.18	5.27	3.34	3.28	1.75	1.67	1.75

A–E. From pantelleritic lava, Fossa della Pernice, Pantelleria (Romano, 1969, table 1, A–E). A, from lower part of flow; B, interior, holocrystalline part of flow; C, transitional between glassy and crystalline parts of flow; D, from glassy crust, partly hydrated; E, from glassy crust, but removed along flow from D.

1, 2. Nonhydrated glass and hydrated dense glass from the comenditic Grouse Canyon Member of the Belted Range Tuff, Nevada (Noble, 1967, table 1, laboratory Nos. D100317, D100393).

3–5: Nonhydrated glass, hydrated dense glass, and hydrated porous glass from the comenditic Spearhead Member of the Thirsty Canyon Tuff, Nevada (Noble, 1967, table 1, laboratory Nos. D100320, D100394, D100454).

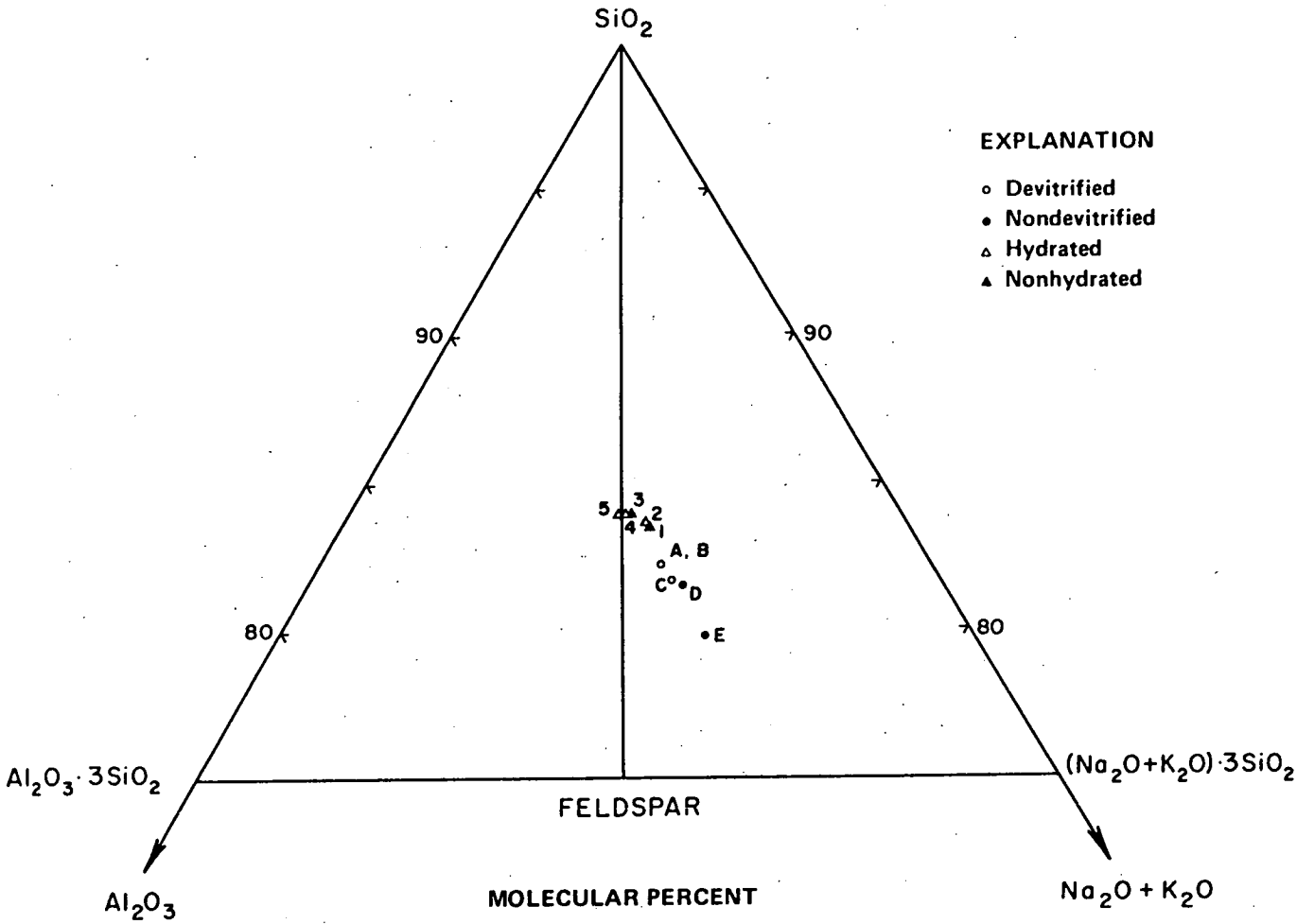

FIGURE 1.—Part of a molecular SiO_2–Al_2O_3–(Na_2O+K_2O) diagram showing some of the effects of hydration and devitrification on peralkaline glasses. Specimens identified as in table 1. In all cases, the rocks have become less peralkaline when hydrated or devitrified.

have had marked effects on the compositions of the rocks; the altered facies are less peralkaline and the sodium-potassium ratios are strikingly different. The more peralkaline glasses obviously show the greatest changes. We do not, however, suggest that all the variation in the Pantellerian specimens (table 1, A–E) is necessarily a result of these processes. For example, specimen E, which has the highest content of alkalis and may thus be considered as a "control" sample, contains 0.9 weight percent less Fe as FeO and has a lower Fe^{+2}/Fe^{+3} ratio than the partly hydrated specimen D. Since iron is not normally added or removed and the oxidation ratio normally increases during crystallization or hydration, the figures may indicate that there is a small but real chemical variation within this flow due to other processes.

DATA SELECTION

The compilation includes all published analyses of peralkaline silicic obsidians and glass separates known to us, and which we considered reliable, plus 20 unpublished analyses. The total number of analyses is 113.

During the data collection, analyses were rejected for the following reasons:

1. The total did not lie within the limits 99–101 percent.
2. Any one of the oxides SiO_2, Al_2O_3, Fe_2O_3, FeO, Na_2O, and K_2O was not reported.
3. Three or more of the oxides TiO_2, MnO, MgO, CaO, H_2O+, and P_2O_5 were not reported.
4. The analysis has been shown to be untrustworthy. For example Zies (1960) has found that Washington's (1913) original analyses of Pantellerian hyalopantellerites are partly in error, especially in the TiO_2 figures.

In this compilation we compare the compositions of volcanic rocks from various localities. In doing so, we assume that the analyses being examined represent magmatic liquid compositions. About 70 percent of the analyses are of porphyritic obsidians, however, and Noble (1965, p. B88) has stressed, with special refer-

486-965 O - 72 - 2

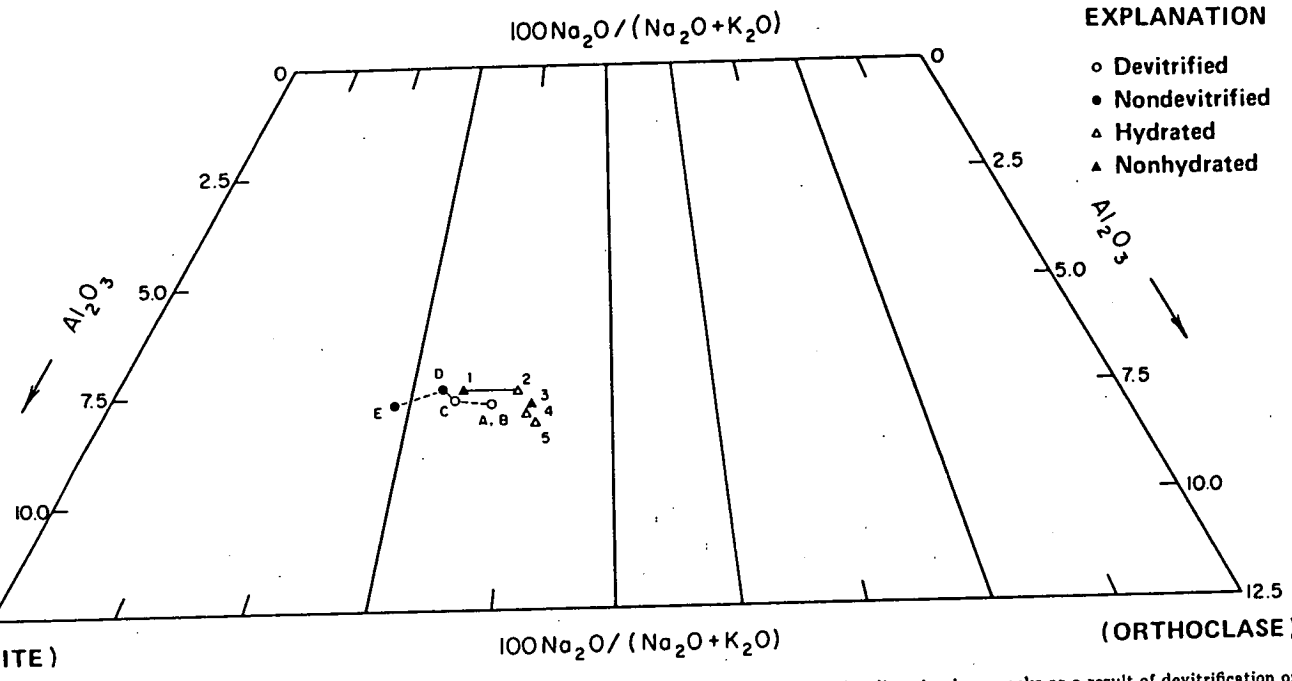

2.—Quadrilateral diagram, as devised by Bailey and Macdonald (1969), showing loss of some original sodium in glassy rocks as a result of devitrification or hydration. Specimens identified as in table 1.

o pantellerites, that porphyritic rocks will not lly represent liquid compositions because of "the es of crystal accumulation and separation." This ient assumes that segregation of crystals is a l process—we would argue that this segregation to be proven for rhyolite magmas. Our examina- uggests that segregation may have only minor . Of all porphyritic obsidians for which modal re available, only 14 have >8 percent phenocrysts lume and none has >20 percent (fig. 3). It might pected that if those obsidians with high crystal content were partly accumulitic, they would tend to show low values of the agpaitic index, because they have been diluted mainly with alkali feldspar. Yet those phenocryst-rich rocks occur at all values of agpaitic index (fig. 4).

We do not exclude the possibility that crystal accumulation has occurred in some of these lavas and indeed have suggested (Macdonald and others, 1970) the possibility for one trachyte from Kenya (analysis 107), but the data suggest that this is not typical.

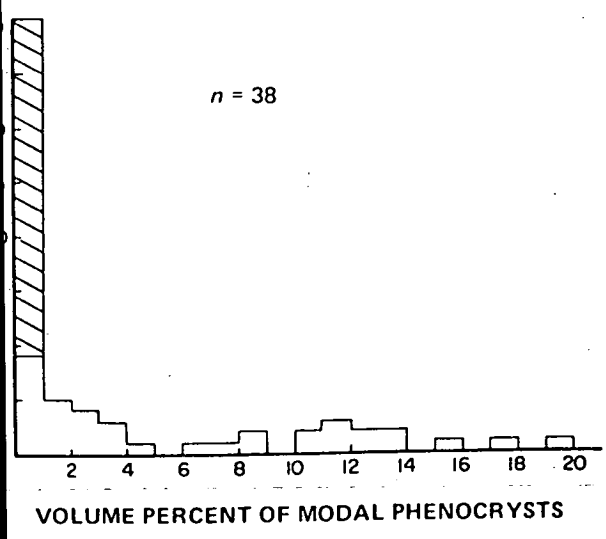

3.—Frequency diagram showing volume percent of modal phenocrysts mples of porphyritic obsidian. The patterned area represents the number hyric samples.

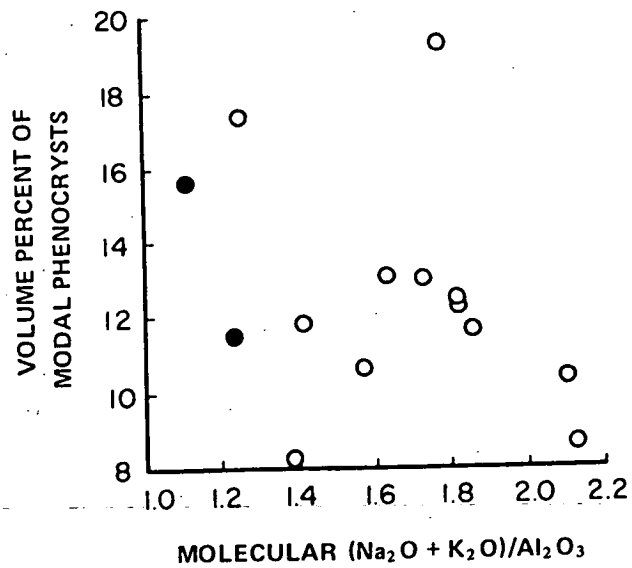

FIGURE 4.—Relations between volume percent of modal phenocrysts and agpaitic index in samples of porphyritic obsidian having >8 percent of phenocrysts.

COMPILATION OF ANALYSES

The major element analyses are compiled in tables 2–4 using the revised nomenclature of figure 5. Within each table, the analyses are grouped geographically. Analyses of two obsidians which lack adequate geographic information are given in table 10. Trace element data are given in tables 5–8. Details of individual specimens, including modal analyses where available, are given on pages N22–25. Here the rock names are those applied by the original authors.

All published norms have been checked before incorporation into the tables, and where adjustments have been made, the adjustment is mentioned in the specimen description. In several cases, the di and hy molecules had to be recalculated to wo+en+fs and en+fs, respectively.

The calculation of normative NaCl, NaF, and CaF_2 involves discarding part of the oxygen content of the analysis when the molecular weights of the pure molecules are used. The part discarded is insignificant for most rocks but is important in the fluorine- and chlorine-rich peralkaline lavas, as it results in low totals for the norm. For example, 0.5 and 1.0 percent (by weight) chlorine in an analysis, when calculated as normative hl, results in a lowering of the weight total of the norm by 0.11 and 0.22 percent, respectively. Also, 0.5 and 1.0 percent (by weight) fluorine, calculated as CaF_2 or NaF, lower the total by 0.21 and 0.42 percent, respectively. We have not included this excess oxygen in the norms, but it has resulted in some cases in a fairly large discrepancy between percent oxides (by weight) and the norm.

NOMENCLATURE

The terminology of peralkaline silicic extrusive rocks is fortunately quite uncomplicated, and it is possible to group the rocks simply into (1) peralkaline trachytes with $q < 10$ percent and (2) rhyolites of the comendite and pantellerite groups (Lacroix, 1927, 1930; Noble, 1968). The old term "quartz-keratophyre," as used for alkali rhyolites, refers to altered rocks (Johannsen, 1932). Noble (1968) has distinguished a group of volcanic rocks intermediate between peralkaline trachytes and rhyolites as "trachytic soda rhyolites," but for simplicity we have preferred to extend the terms "comendite" and "pantellerite" to cover these intermediate types.

Pantellerite was coined by Foerstner (1881) for alkali rhyolites from the island of Pantelleria in the Mediterranean, and Washington (1913), in a redescription of the rocks from the island, introduced the term "hyalopantellerite" for the glassy varieties. In recent literature the term "pantellerite" has tended to become synonymous with hyalopantellerite (Noble, 1965, p. B88). Comendite is a name devised by Bertolio (1895) for alkali rhyolites from Le Comende, San Pietro Island, Sardinia. Both comendites and pantellerites from the type areas are one-feldspar rhyolites, normally containing phenocrysts of alkali feldspar in the range anortho-

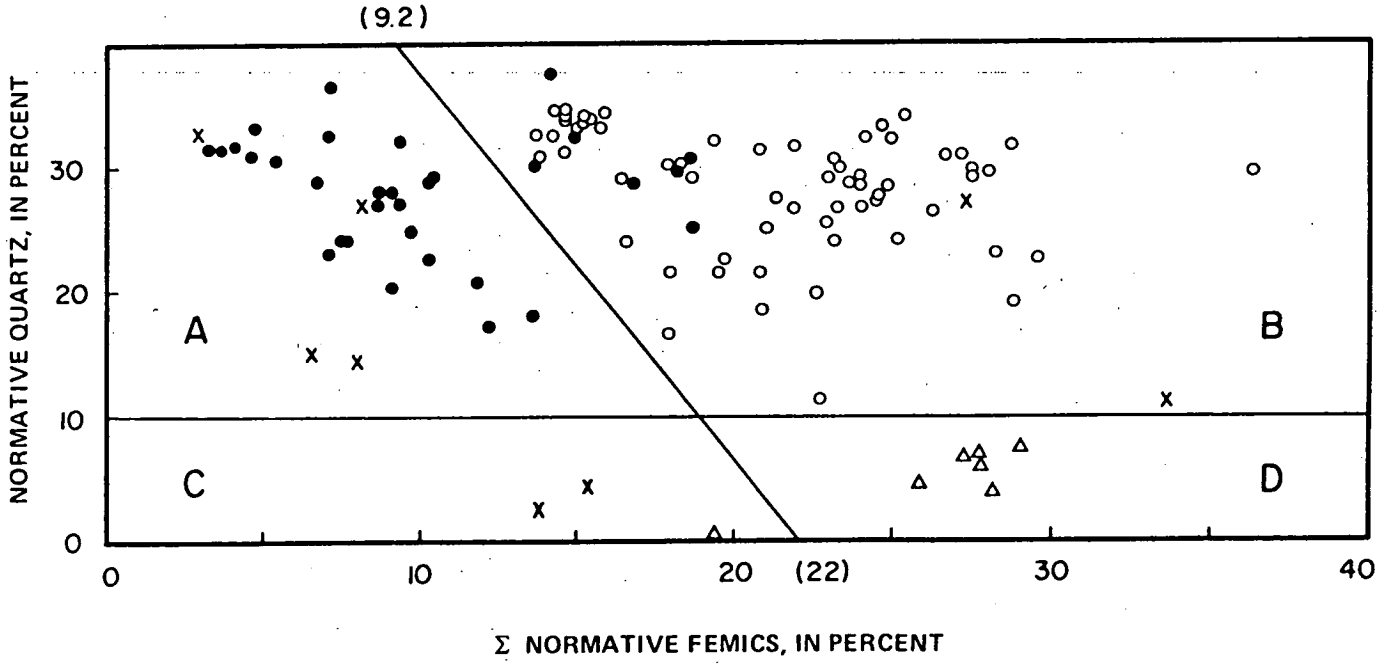

FIGURE 5.—Classification scheme for peralkaline silicic obsidians, modified from Lacroix (1927) and Noble (1968) to include trachytic varieties. The boundary line is arbitrary. Specimens are plotted using the nomenclature of the original authors: ●, comendite; ○, pantellerite; △, pantelleritic trachyte; ×, rocks termed simply rhyolite, trachyte, obsidian, and so forth. In our terminology: A, comendite; B, pantellerite; C, comenditic trachyte; and D, pantelleritic trachyte.

to sanidine ± green pyroxene (which, when
zed, appears to be sodic hedenbergite), aenigma-
nd quartz in a groundmass of the same minerals ±
ne, riebeckite to arfvedsonite, biotite, and acces-
minerals. Fayalite and iron oxides are scarce
crysts in some of the Pantellerian pantellerites.
nineralogy of the type specimens from the two
seemed to Johannsen (1932) to be so similar that,
he agreement of Washington (Johannsen, 1932,
, he suggested that the term "comendite" be
ed in preference to the older term "pantellerite."
pite the petrographic similarities, Lacroix (1927,
1934) was able to show that significant chemical
nces existed between the more typical members
two groups, but he also stressed that there was a
uous chemical transition between comendites and
lerites and that any division made between them
se grounds would be purely arbitrary.

ne petrologists might question, from the evidence
petrography and chemistry, whether it is neces-
o separate the two groups. We feel that there are
ent important differences to make such a distinc-
ecessary: in particular, the feldspar-liquid rela-
ips seem to be rather different, and this difference
be of importance in the petrogenesis of the two
(Bailey and Macdonald, 1969, and unpub. data;
lls and Carmichael, 1969, p. 273). Similarly, the
'comendite" as used by us includes rocks which
trivially peralkaline that some workers would call
alkali rhyolites. However, we prefer to retain the
term for high-SiO_2 metaluminous compositions
retain comendite for peralkaline rhyolites. This
is not really an abuse of the original rock name.
pe specimens from Sardinia cover a range in com-
n from those near pantellerite to metaluminous
es (Johnsen, 1912).

oix (1927) suggested that 12.5 percent normative
minerals be used as an arbitrary division between
dites (<12.5 percent) and pantellerites. Noble
has adopted this figure in a recent study of
aline rhyolite glasses. In order to incorporate the
aline trachytes into this classification, we have
slightly modified version of Lacroix's division,
on normative femic minerals and normative
(fig. 5). The boundary line is arbitrary. In the
etween 25 and 35 percent normative quartz, the
vision is effectively the same as that of Lacroix
oble, but in less siliceous compositions—that is,
ching Noble's (1968) trachytic soda rhyolites—
oundary is increasingly displaced towards
ingly femic compositions.

division between trachyte and rhyolite is taken
conventional 10 percent normative quartz, and

the composition field can now be split into the following four areas (fig. 5): A, comendites; B, pantellerites; C, comenditic trachytes; and D, pantelleritic trachytes. The analyses are compiled in tables 2–8 under these headings. These analyses are plotted in figure 5, the symbols representing the terminology used by the original authors. The old and new names agree fairly well, though compositions lying near the boundary line show some overlap. An example of this overlap is the suite of lavas (table 3, Nos. 91–103) from Mayor Island, New Zealand, which, according to figure 5, forms a series in the pantellerite field, spreading from types near the boundary to types well into the field. While Ewart, Taylor, and Capp (1968), on the basis of the report by Chayes and Zies (1962), and Noble (1968) have preferred to call the Mayor Island lavas pantellerites, Nicholls and Carmichael (1969) have termed them "comendites" and pointed out the differences between them and the type pantellerites. Chayes and Zies (1962) had implied that normative sodium metasilicate (ns) might be used to distinguish pantellerites from comendites because it seemed to be rare or absent in comendites but ubiquitous in (hyalo-) pantellerites. Subsequently, Ewart, Taylor, and Capp (1968, p. 123) termed the Mayor Island lavas "pantellerites" rather than comendites because of the presence in them of "a significant proportion of the normative ns molecule." This distinction is verified by the collection of analyses in tables 2–4. Of the comendites, 13 have no ns; the other 16 have <2 percent. All but three pantellerites have >2 percent ns, of which one from Sardinia (analysis 46) may be altered (p. N14). The low value in another, from Nevada (analysis 90), is due to making abnormally large amounts of NaF. It should be stressed here that this distinction applies to obsidians only. On crystallization, both comendites and pantellerites tend to lose alkalis, and ns is rare in crystalline varieties.

PETROCHEMISTRY

The chemical features which distinguish peralkaline rhyolites, especially pantellerites, from alkaline and calc-alkaline rhyolites were clearly recognized by Lacroix (1927, 1930) and include high contents of Na, Fe, Mn, Ti, and Zr and low contents of Ca, Mg, and P. Most striking are the low molecular Al_2O_3 contents, which by definition are less than the sum of molecular Na_2O+K_2O. More recent work has also shown that peralkaline rhyolite obsidians are strongly enriched in fluorine and chlorine (Bowen, 1937; Zies, 1960; Carmichael, 1962; Lovering, 1966; Noble, 1965, 1968; Noble and Haffty, 1969) and in the residual trace elements and are very depleted in certain other trace metals.

CHEMICAL VARIATION IN COMENDITES AND PANTELLERITES

Since rhyolite and trachyte magmas are largely composed of SiO_2, Al_2O_3, Na_2O, and K_2O, systematic chemical differences between comendites and pantellerites would be revealed most clearly in the proportions of these elements. In figures 6 and 7 the analyses are plotted in the system (Na_2O+K_2O)–Al_2O_3–SiO_2, using simple projections devised by Bailey and Macdonald (1969).

The more peralkaline nature of the pantellerites is easily shown in figure 6 by projecting lines from the SiO_2 apex through the sample points towards the alkali–alumina baseline. Such a line, with alkali–alumina ratio 55.5:44.5, separates the two groups with almost no overlap.

The variation in alkali ratios is shown in figure 7. As the pantellerites are consistently more peralkaline than the comendites, the plotting of all the analyses in this single projection (Bailey and Macdonald, 1969) involves the loss of the dimension of SiO_2 content. The value 100 $Na_2O/(Na_2O+K_2O)$ and the alumina content are, however, unambiguously represented. Both groups show a range of values of 100 $Na_2O/(Na_2O+K_2O)$, the pantellerites between 64 and 77, and the comendites between 56 and 72. All those comendites with values >66 are from three localities—New Guinea, Easter Island, and Iceland. They are only marginally peralkaline: their alkali ratios are more akin to those of metaluminous rhyolites. Eleven of the thirteen pantellerites with values <66 are from one volcano at Chabbi, Ethiopia (table 3, Nos. 69–79) (Macdonald and Gibson, 1969), and one is a Sardinian lava which is possibly altered (Noble and Haffty, 1969, p. 508). With the exception of these specimens, there is a general tendency for the pantellerites to show higher Na_2O/K_2O ratios (fig. 11).

In the rhyolites the progression from comendite to pantellerite is marked by an increase in peralkalinity, and since, during normal fractionation processes more evolved liquids are usually increasingly peralkaline (Carmichael and MacKenzie, 1963; Bailey and Schairer,

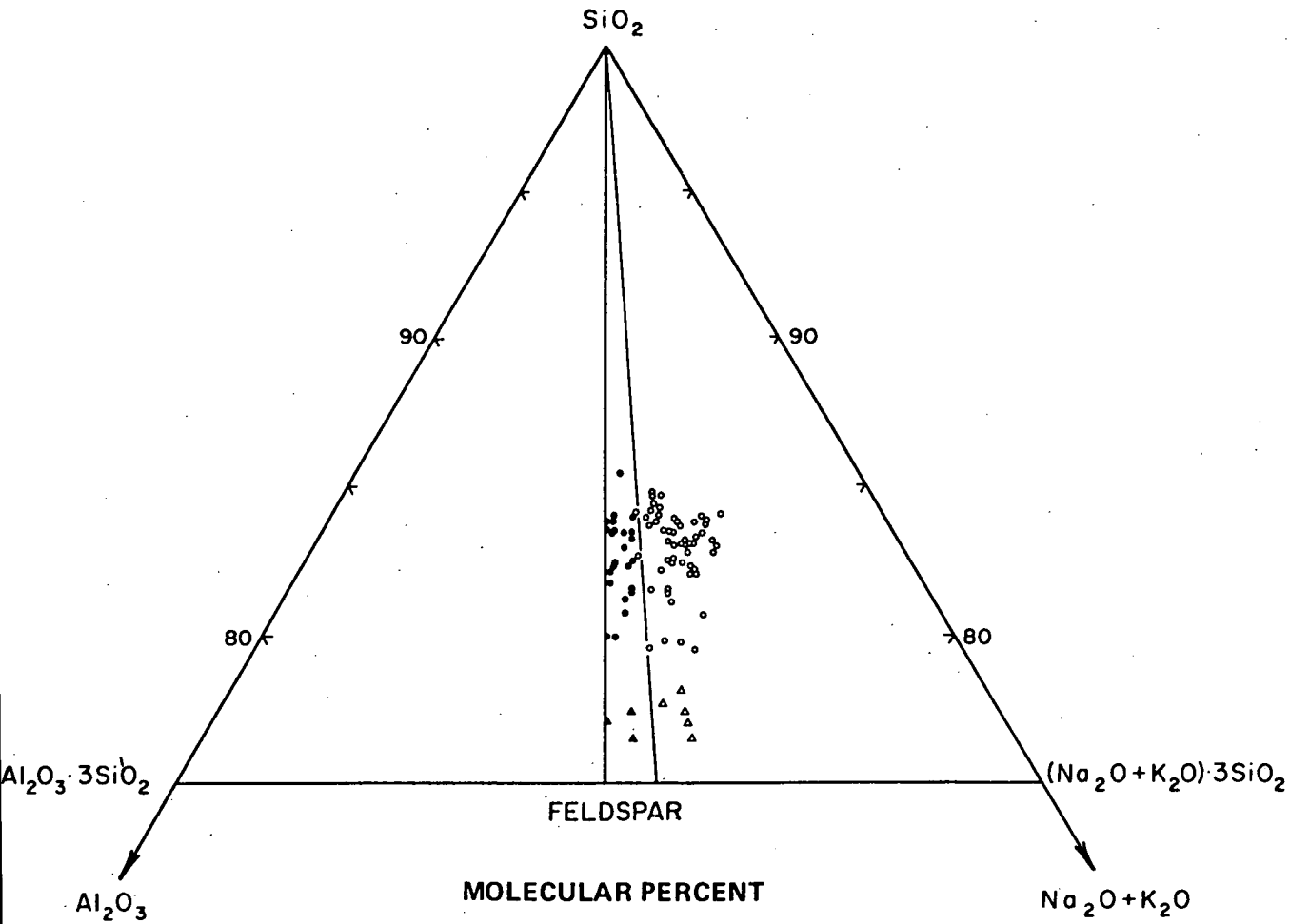

FIGURE 6.—Part of a molecular SiO_2–Al_2O_3–(Na_2O+K_2O) diagram showing available analyses of comendites (●), pantellerites (○), comenditic trachytes (▲), and pantelleritic trachytes (△). The thin line that is radial from the SiO_2 apex represents the agpaitic index $(Na_2O+K_2O):Al_2O_3$::55.5:44.5 and effectively separates comenditic from pantelleritic rocks.

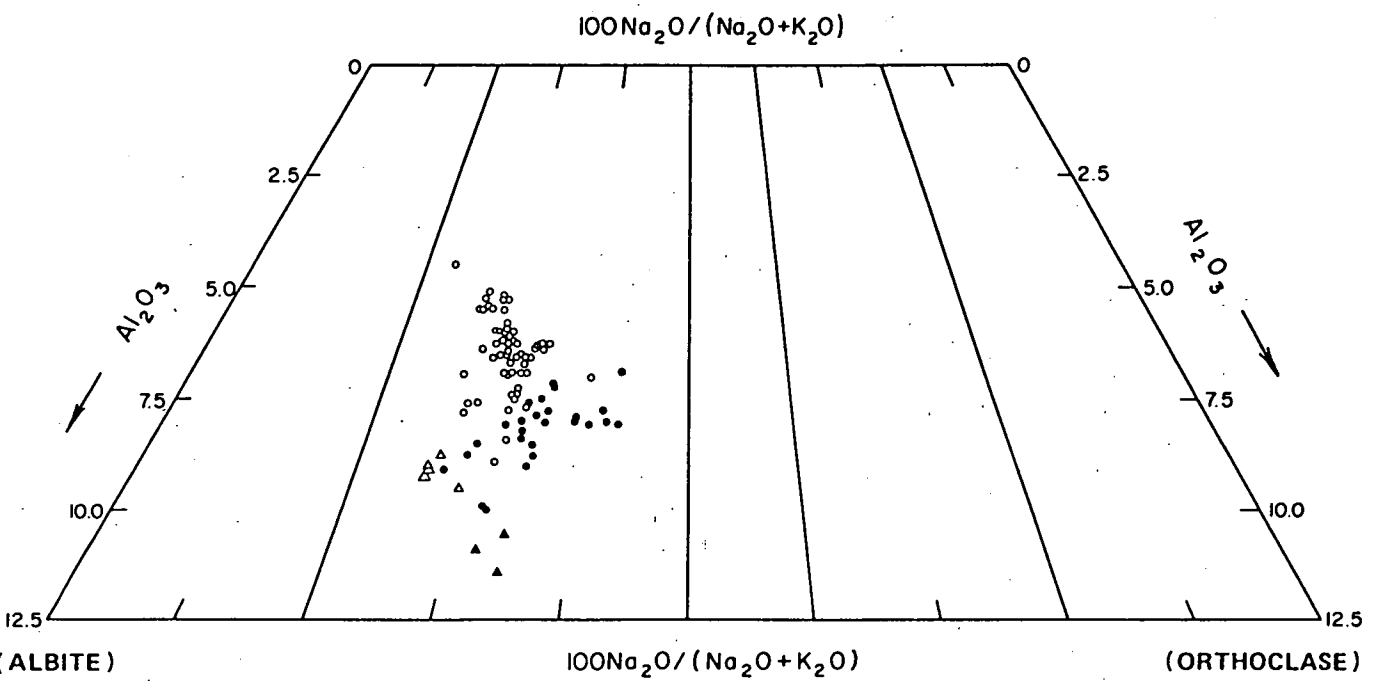

IGURE 7.—Variation in $Na_2O/(Na_2O+K_2O)$ in comenditic and pantelleritic obsidians (including trachytic varieties). Symbols as in figure 6. See text for explanation. The pantellerite having $100Na_2O/(Na_2O+K_2O)=59.8$ is from Sardinia (analysis 46) and has possibly lost some of its original sodium content.

64), the most useful representation of the chemical riation between the two groups is in terms of increas- g peralkalinity, of which the simplest measure is the paitic index $(Na_2O+K_2O)/Al_2O_3$.

In the series peralkaline trachyte to rhyolite, the riation in q is more marked than change in agpaitic index. To describe the chemical variation over the whole range of oversaturated peralkaline obsidians then requires three variables: agpaitic index, normative quartz, and the unknown (for example, element or element ratio). This involves the use of three-axes diagrams, the contouring of rectilinear diagrams, or the placing of rela-

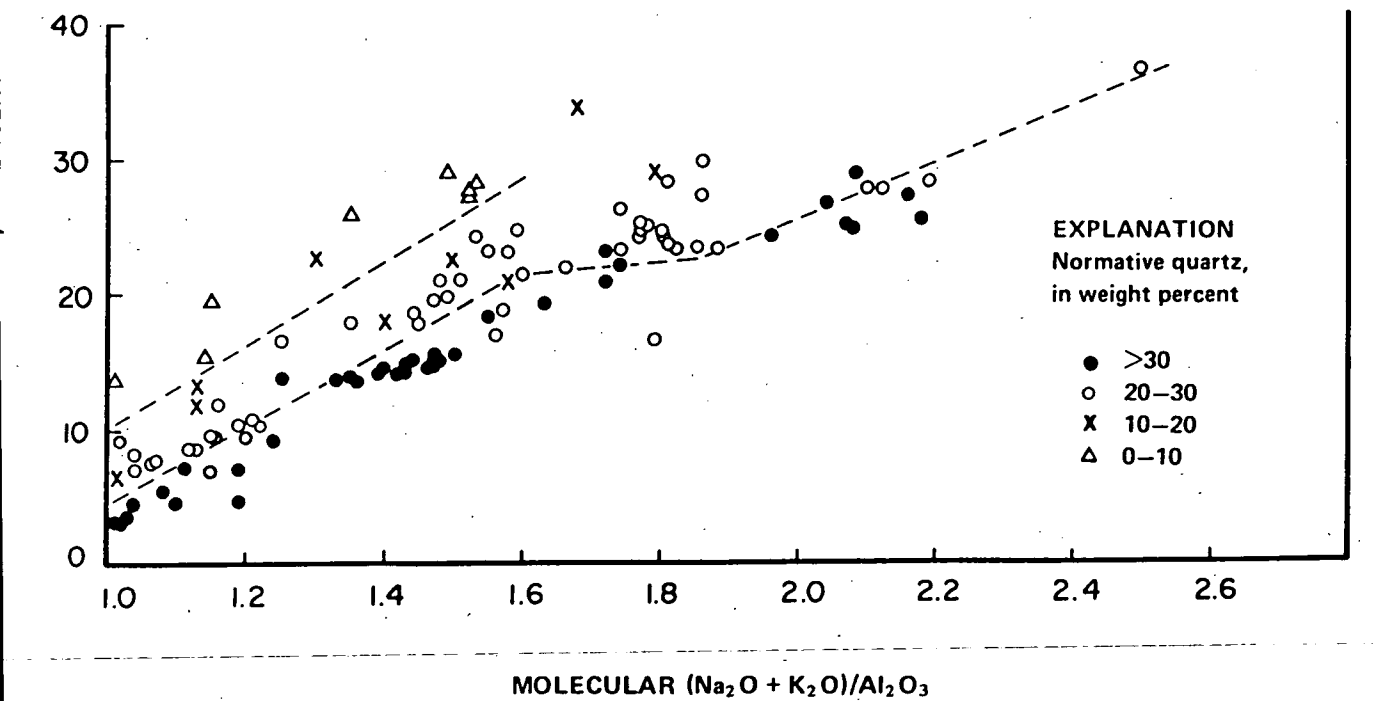

URE 8.—Sum of normative femics plotted against agpaitic index $(Na_2O+K_2O)/Al_2O_3$ for all analyses of comenditic and pantelleritic obsidians (including trachytic varieties). Dashed lines show approximate boundaries of normative quartz contents.

tively narrow limits on the range of quartz contents shown in any diagram. The contouring method has been used with reasonable success in figures 8 and 9, but the scarcity of analysis of rocks with less than 20 percent q makes it difficult to extend the contours towards the trachytic rocks. We have, therefore, chosen the third alternative to display the variation in chemistry of comendites and pantellerites and have plotted in figures 10, 11, 14, and 15 only those analyses where the q content is greater than 20 percent. Only 9 trachytes and 10 specimens with $10<q<20$ have been omitted by this scheme.

Correlation coefficients for all pairs of the following variables have been computed (table 9): all major elements, agpaitic index, Fe as FeO, $FeO/(FeO+Fe_2O_3)$, and Na_2O/K_2O. All analyses were used for these calculations, such that the maximum degrees of freedom were 111. Any correlation >0.25 is significant at the 1-percent level. As the relationships between agpaitic index and various elements and element ratios shown diagrammatically in figures 10 and 11 are based only on rocks with normative quartz >20 percent, their correlation coefficients will be slightly different (and usually higher) than those given in table 9.

Silicon.—Though comendites have generally higher values of SiO_2 than the pantellerites, there is a considerable scatter within each group. Part of the scatter may be a result of variable quartz fractionation (Ewart and others, 1968; Bailey and Macdonald, 1969), but the free SiO_2 content does appear to show a nonsystematic variation (Noble, 1968). A group of high silica pantellerites may be distinguished from those from the type area (p. N14).

Titanium.—The increase in TiO_2 with increasing agpaitic index is irregular, but statistically significant (table 9). The highest values are between 0.6 and 0.7 percent.

Aluminum.—The regular decrease in Al_2O_3 from comendite to pantellerite has already been stressed by Noble (1968). It is notable that 11 percent Al_2O_3 effectively separates the two groups, only four rocks being exceptional in this case, one of them being the Sardinian

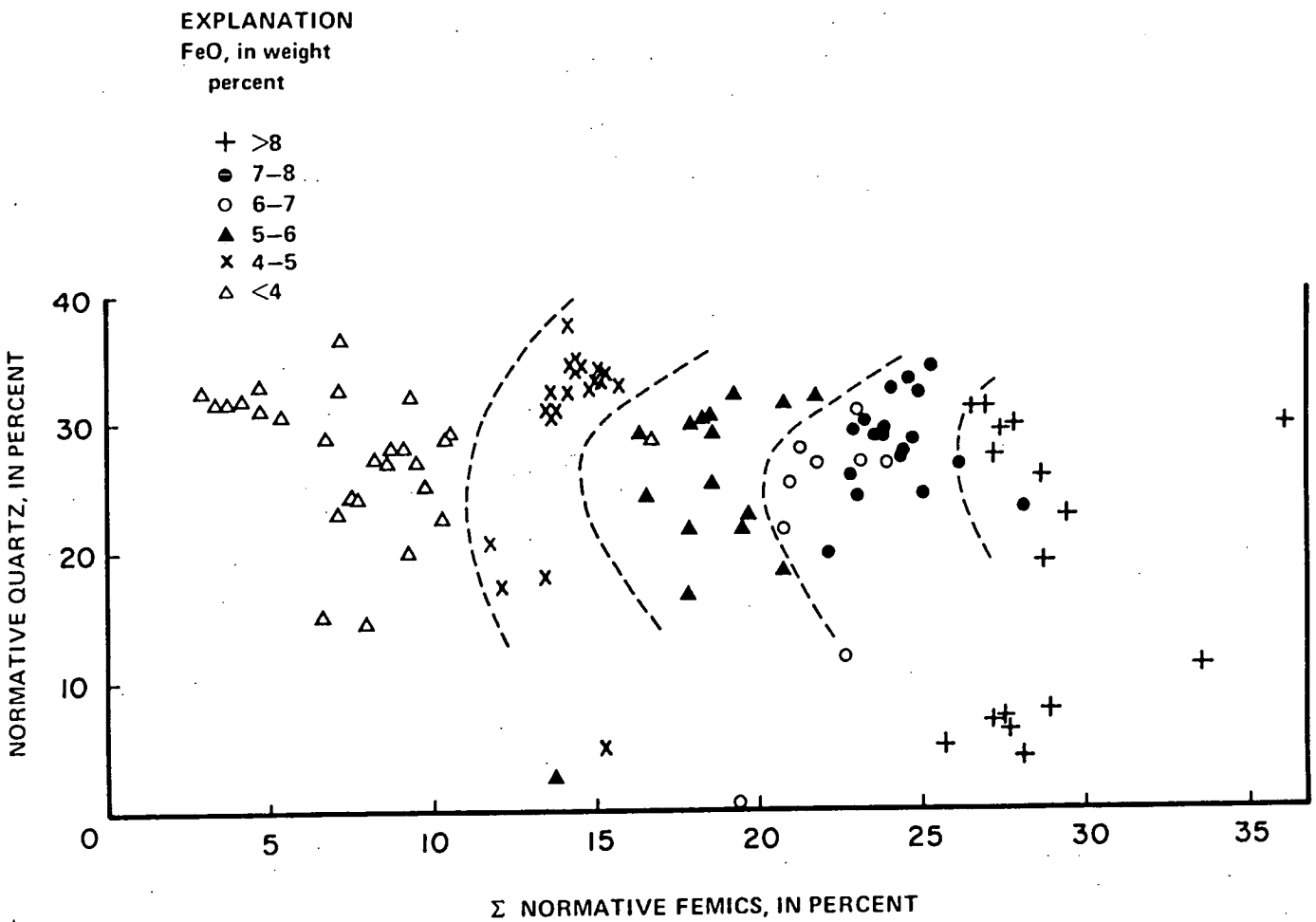

FIGURE 9.—Sum of normative femics plotted against normative quartz for all analyses of comenditic and pantelleritic obsidians (including trachytic varieties). Dashed lines show approximate boundaries of FeO values.

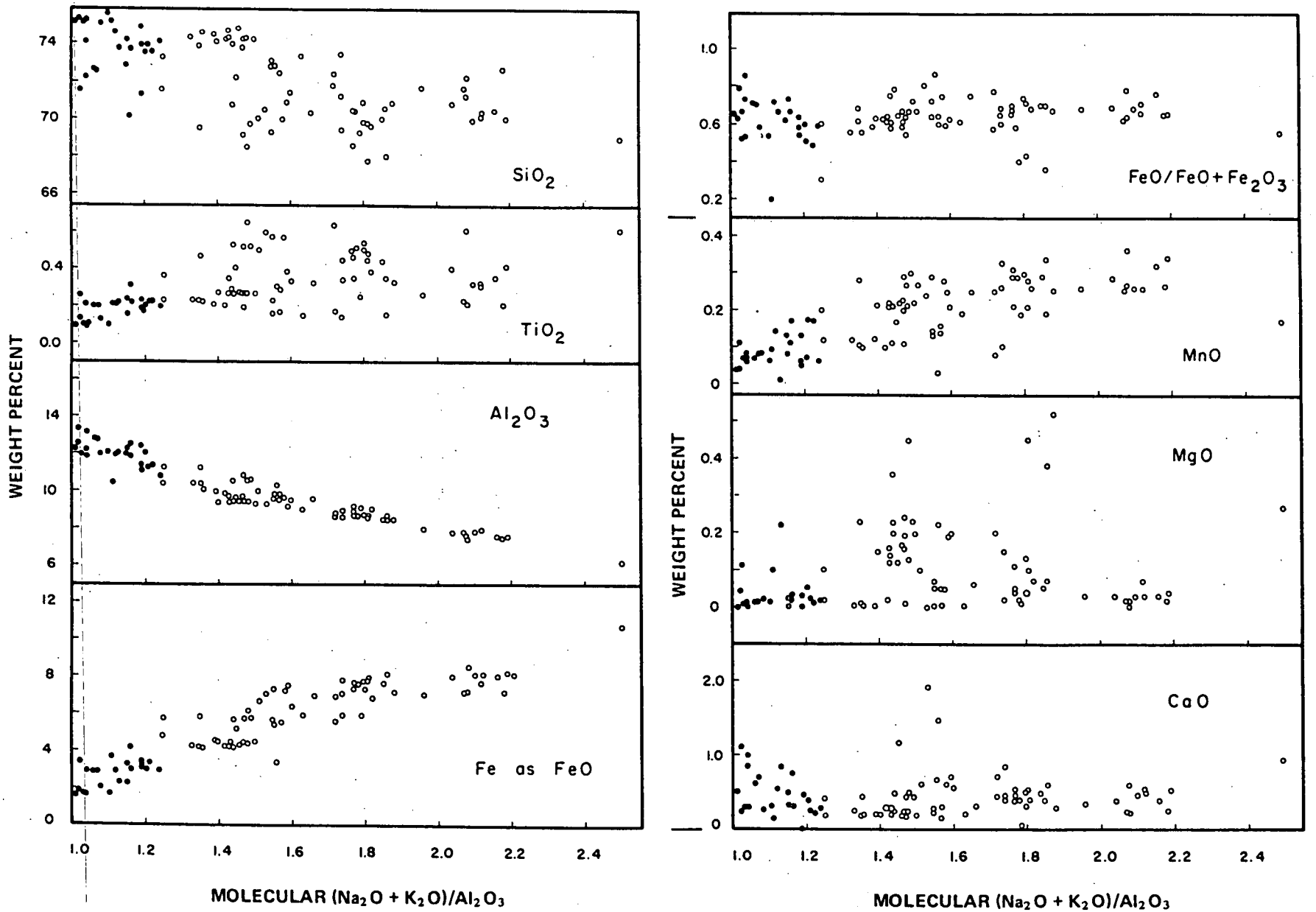

FIGURE 10.—Variation diagrams for SiO_2, TiO_2, Al_2O_3, FeO, $FeO/(FeO+Fe_2O_3)$, MnO, MgO, and CaO versus agpaitic index in comendites (●) and pantellerites (○). Only rocks with >20 percent normative quartz have been plotted.

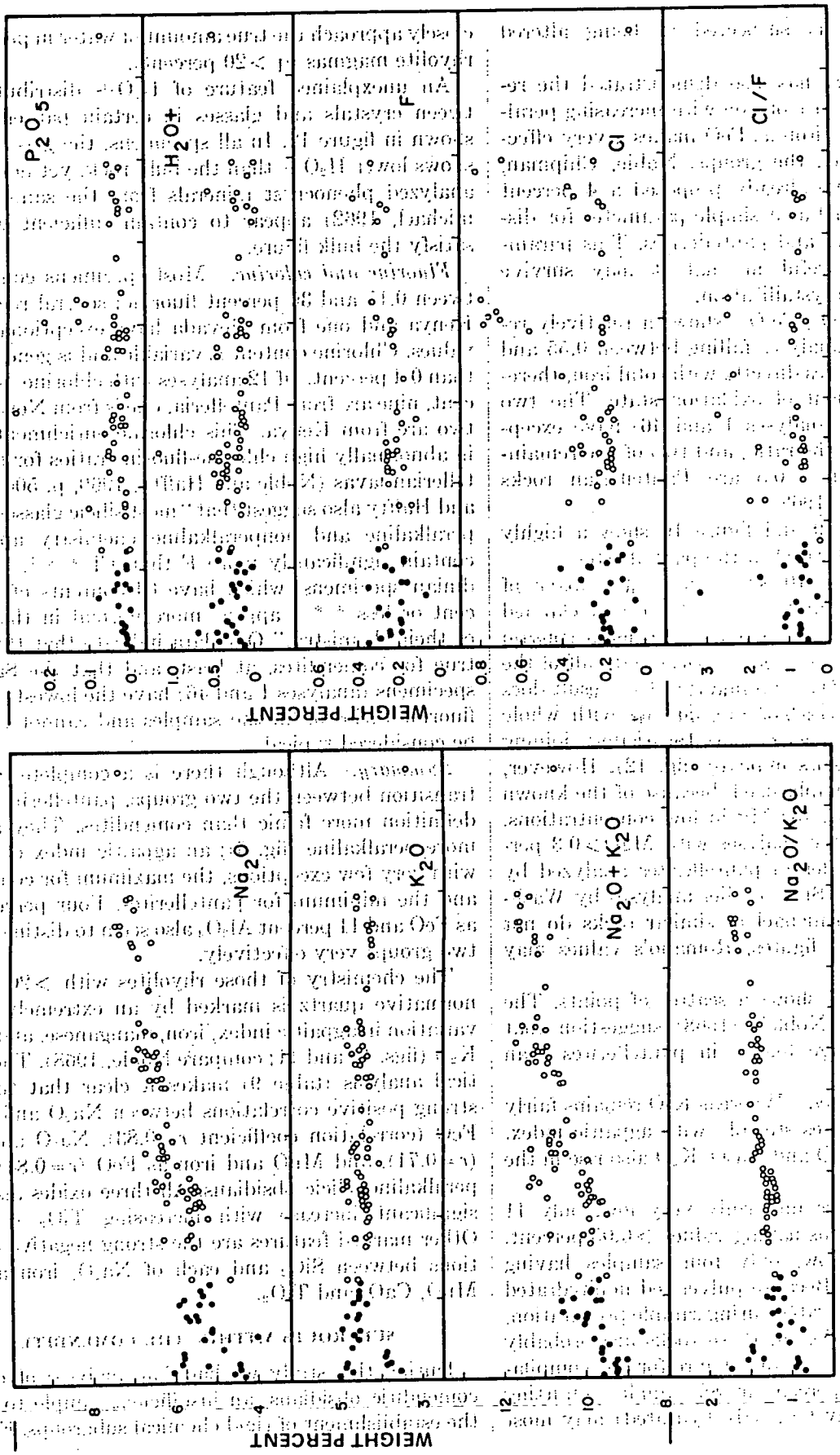

FIGURE 11.—Variation diagrams for Na_2O, K_2O, Na_2O+K_2O, Na_2O/K_2O, P_2O_5, H_2O+, F, Cl, and Cl/F versus agpaitic index in comendites (●) and pantellerites (○). A pantellerite from Nevada (analysis 90) with F = 1.30 percent, has been omitted from the fluorine diagram. Only rocks with >20 percent normative quartz have been plotted.

ndite (analysis 1) suspected of being altered 14).

n.—Noble (1968) has also demonstrated the re- ably regular increase of iron with increasing peral- ty and 4 percent iron as FeO makes a very effec- oundary between the groups. Noble, Chipman, Giles (1968) have already proposed a 4 percent of FeO and MnO as a simple parameter for dis- shing comendites and pantellerites. This param- is potentially useful in that it may survive ification and recrystallization.

e ratio $FeO/(FeO+Fe_2O_3)$ shows a relatively re- ed range, most analyses falling between 0.55 and Peralkalinity varies directly with total iron, there- but is independent of oxidation state. The two ian specimens (analyses 1 and 46) have excep- ly low values of the ratio, and two of the remain- hree rocks with <0.5 are Pantellerian rocks zed by Romano (1968).

nganese.—Table 9 and figure 10 show a highly cant increase of MnO in the pantellerites.

gnesium.—Figure 10 shows a wide scatter of . Noble, Haffty, and Hedge (1969) have claimed most comenditic and pantelleritic glasses contain 5 percent MgO. Our data indicate that half of the llerites have MgO > 0.05 percent. This result does ccur simply because of our dealing with whole rather than with glasses, as the tielines joining ble rock-glass pairs indicate (fig. 12). However, oint cannot be emphasized, because of the known lties of analyzing for Mg in low concentrations. xample, of the five analyses with MgO > 0.3 per- three are Pantellerian pantellerites analyzed by no (1968, 1969). Since earlier analyses by Wash- n, Zies, and Carmichael of similar rocks do not such high MgO figures, Romano's values may ly be too high.

cium.—Figure 10 shows a scatter of points. The do not support Noble's (1968) suggestion that is on the average higher in pantellerites than nendites.

ium and potassium.—Whereas K_2O remains fairly ant, Na_2O increases steadily with agpaitic index. esult, Na_2O+K_2O and Na_2O/K_2O also rise in the llerites (fig. 7).

sphorus.—P_2O_5 is uniformly very low, only 11 nt of the specimens having values >0.05 percent.

ter.—Water is low, only four samples having - >0.5 percent. Because pulverized nonhydrated s tend to adsorb water during sample preparation, analyses of H_2O+ in these rocks are probably y high. Thus, the average figure for our compila- (H_2O+ =0.23 percent in 88 samples, omitting sis 44 which may be partly hydrated) may most closely approach the true amount of water in peralkaline rhyolite magmas (q >20 percent).

An unexplained feature of H_2O+ distribution between crystals and glasses in certain pantellerites is shown in figure 12. In all specimens, the glass analysis shows lower H_2O+ than the bulk rock, yet none of the analyzed phenocryst minerals from the sample (Carmichael, 1962) appear to contain sufficient water to satisfy the bulk figure.

Fluorine and chlorine.—Most specimens contain between 0.15 and 30 percent fluorine; several rocks from Kenya and one from Nevada have exceptionally high values. Chlorine content is variable and is generally less than 0.4 percent. Of 12 analyses with chlorine >0.4 percent, nine are from Pantelleria, one is from Nevada, and two are from Kenya. This chlorine enrichment results in abnormally high chlorine-fluorine ratios for the Pantellerian lavas (Noble and Haffty, 1969, p. 506). Noble and Haffty also suggest that "most silicic glasses of both peralkaline and nonperalkaline chemistry appear to contain significantly more F than Cl * * *. The Sardinian specimens, which have Cl contents of 0.1 percent or less * * * appear more normal in this aspect of their chemistry." Our data indicate that this is not true for comendites, at least, and that the Sardinian specimens (analyses 1 and 46) have the lowest chlorine-fluorine ratios of all the samples and cannot therefore be considered typical.

Summary.—Although there is a complete chemical transition between the two groups, pantellerites are by definition more femic than comendites. They are also more peralkaline (fig. 6); an agpaitic index of 1.25 is, with very few exceptions, the maximum for comendites and the minimum for pantellerites. Four percent iron as FeO and 11 percent Al_2O_3 also seem to distinguish the two groups very effectively.

The chemistry of those rhyolites with >20 percent normative quartz is marked by an extremely regular variation in agpaitic index, iron, manganese, and Na_2O/K_2O (figs. 10 and 11; compare Noble, 1968). The statistical analysis (table 9) makes it clear that there are strong positive correlations between Na_2O and iron as FeO (correlation coefficient $r=0.83$), Na_2O and MnO ($r=0.71$), and MnO and iron as FeO ($r=0.84$) for all peralkaline silicic obsidians. All three oxides also show significant increase with increasing TiO_2 ($r>0.66$). Other marked features are the strong negative correlations between SiO_2 and each of Na_2O, iron as FeO, MnO, CaO, and TiO_2.

SUBGROUPS WITHIN THE COMENDITES

During this study we had full analyses of only 29 comenditic obsidians, an insufficient sample to justify the establishment of rigid chemical subgroups. Further-

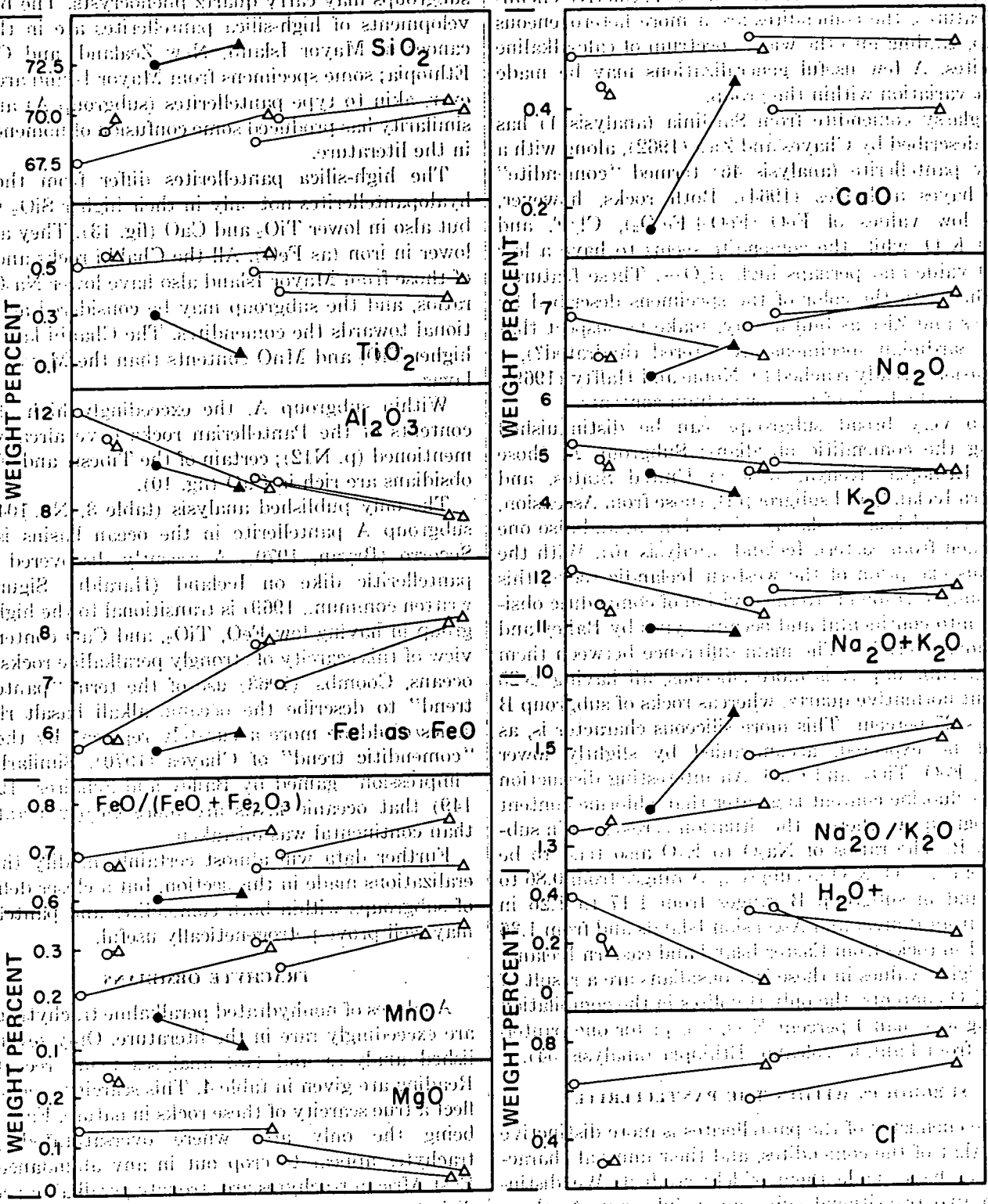

FIGURE 12.—Variation diagrams using agpaitic index $(Na_2O+K_2O)/Al_2O_3$ as abscissa. Tielines connect whole-rock (circles) and glass (triangles) pairs. ○—△, Pantelleria (analyses 33–40). ●—▲, Mayor Island, New Zealand (analyses 97, 98).

more, whereas the pantellerites have distinctive chemical features, the comendites are a more heterogeneous group, grading into the wider spectrum of calc-alkaline rhyolites. A few useful generalizations may be made about variation within the group.

A glassy comendite from Sardinia (analysis 1) has been described by Chayes and Zies (1962), along with a glassy pantellerite (analysis 46) termed "comendite" by Chayes and Zies (1964). Both rocks, however, have low values of $FeO/(FeO+Fe_2O_3)$, Cl/F, and Na_2O/K_2O, while the comendite seems to have a low Na_2O value and perhaps high H_2O-. These features, together with the color of the specimens described by Chayes and Zies as bluish gray, make us suspect that these Sardinian specimens are altered (hydrated?), a conclusion already reached by Noble and Haffty (1969), partly on the basis of the low sodium contents.

Two very broad subgroups can be distinguished among the comenditic obsidians: Subgroup A, those from Ethiopia, Kenya, western United States, and western Iceland, and subgroup B, those from Ascension, Bouvet, and Easter Islands, New Guinea, and also one specimen from eastern Iceland (analysis 16). With the obvious exception of the western Icelandic rocks, this grouping corresponds to the division of comenditic obsidians into continental and oceanic types by Bailey and Macdonald (1970). The main difference between them is that subgroup A is more siliceous, all having >25 percent normative quartz, whereas rocks of subgroup B have <25 percent. This more siliceous character is, as might be expected, accompanied by slightly lower Al_2O_3, FeO, TiO_2, and CaO. An interesting distinction is that fluorine content is greater than chlorine content in subgroup A, whereas the situation is reversed in subgroup B. The ratios of Na_2O to K_2O also tend to be different; Na_2O/K_2O in subgroup A ranges from 0.86 to 1.24 and in subgroup B ranges from 1.17 to 1.26 in rocks from Bouvet and Ascension Islands and from 1.36 to 1.71 in rocks from Easter Island and eastern Iceland. The higher values in these last obsidians are a result of low K_2O contents, the only rhyolites in the compilation having less than 4 percent K_2O, except for one pantellerite from Fantāle volcano, Ethiopia (analysis 54).

SUBGROUPS WITHIN THE PANTELLERITES

The chemistry of the pantellerites is more distinctive than that of the comendites, and their unusual characteristics have made them widely studied. We distinguish two transitional subgroups: Subgroup A, those from the type area, Pantelleria, and closely similar rocks from Chad, Ethiopia, Kenya, Nevada, and Socorro Island and subgroup B, a high-silica group. The high-silica group is not the same as the "quartz-pantellerite" subdivision of Johanssen (1932). Rocks from both of our subgroups may carry quartz phenocrysts. The best developments of high-silica pantellerites are in the volcanoes of Mayor Island, New Zealand, and Chabbi, Ethiopia; some specimens from Mayor Island are, however, akin to type pantellerites (subgroup A) and this similarity has produced some confusion of nomenclature in the literature.

The high-silica pantellerites differ from the type hyalopantellerites not only in their higher SiO_2 values, but also in lower TiO_2 and CaO (fig. 13). They are also lower in iron (as FeO). All the Chabbi rocks and some of those from Mayor Island also have lower Na_2O/K_2O ratios, and the subgroup may be considered as transitional towards the comendites. The Chabbi lavas have higher TiO_2 and MnO contents than the Mayor Island lavas.

Within subgroup A, the exceedingly high chlorine contents of the Pantellerian rocks have already been mentioned (p. N12); certain of the Tibesti and Fantāle obsidians are rich in CaO (fig. 10).

The only published analysis (table 3, No. 104) of a subgroup A pantellerite in the ocean basins is from Socorro (Bryan, 1970). A recently discovered glassy pantelleritic dike on Iceland (Haraldur Sigurdsson, written commun., 1969) is transitional to the high silica group in having low FeO, TiO_2, and CaO contents. In view of this scarcity of strongly peralkaline rocks in the oceans, Coombs' (1963) use of the term "pantellerite trend" to describe the oceanic alkali basalt–rhyolite series could be more accurately replaced by the term "comenditic trend" of Chayes (1970). Similarly, the "impression" gained by Bailey and Schairer (1966, p. 149) that oceanic lavas are more clearly peralkaline than continental was mistaken.

Further data will almost certainly modify the generalizations made in this section, but a closer definition of subgroups within both comendites and pantellerites may well prove petrogenetically useful.

TRACHYTE OBSIDIANS

Analyses of nonhydrated peralkaline trachytic glasses are exceedingly rare in the literature. Only seven published analyses and two analyses made recently at Reading are given in table 4. This scarcity seems to reflect a true scarcity of these rocks in nature, East Africa being the only area where oversaturated glassy trachytes appear to crop out in any abundance. The East African trachytes are strongly peralkaline; comenditic trachyte magma may be rarer still if comendites can be derived from metaluminous trachytes. For petrogenetic purposes it might have been instructive to include analyses of these metaluminous types in the compilation, but this inclusion would have widened the scope of the work far beyond our original intentions.

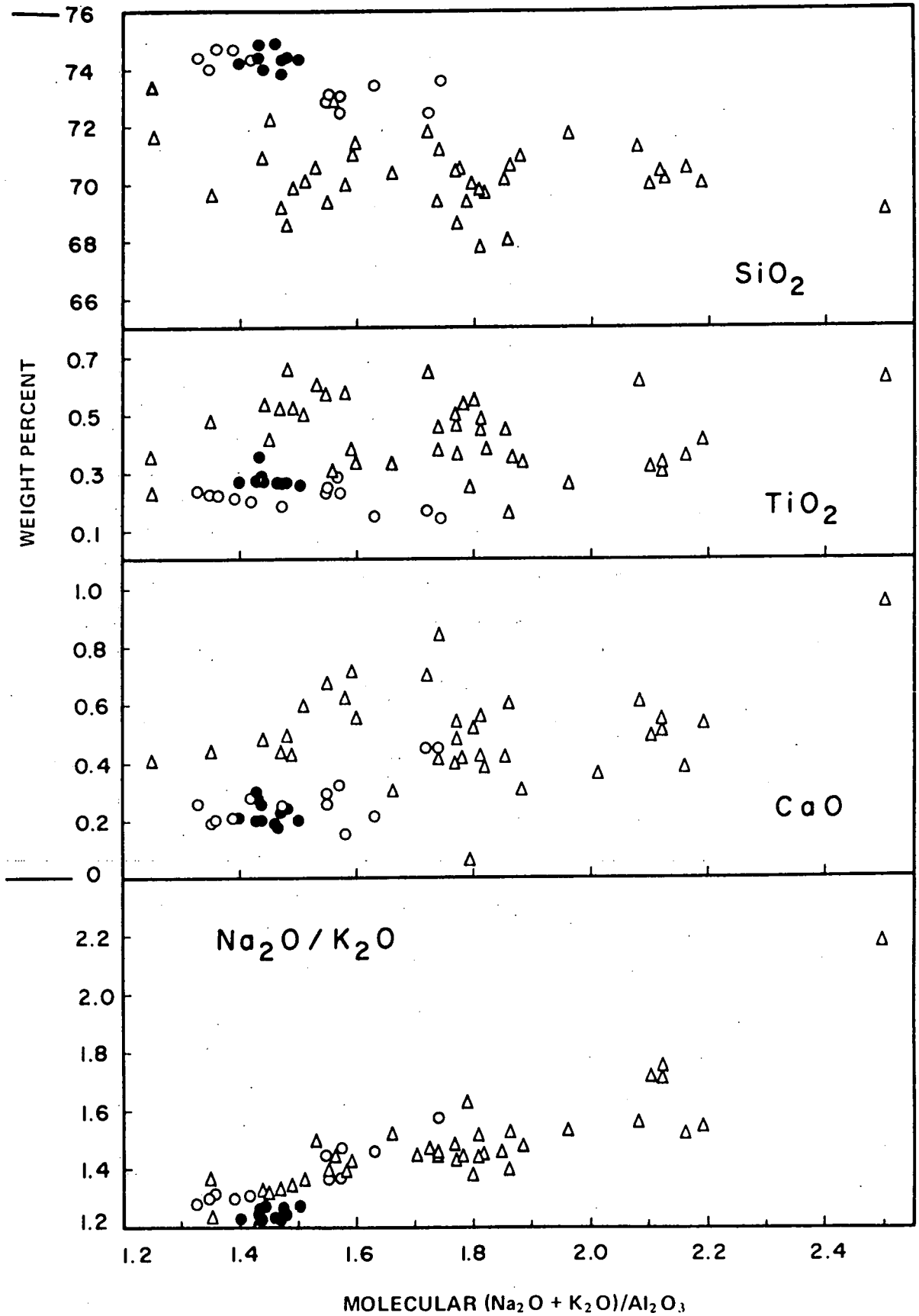

FIGURE 13.—Variation diagrams showing the subgroups within the pantellerites. High-silica pantellerites: ●, Chabbi, Ethiopia; ○, Mayor Island, New Zealand. △, Pantellerian pantellerites and similar types. The Sardinian specimen (analysis 46) has been omitted. Rocks having CaO >1 percent were also omitted from the CaO diagram to preserve the scale.

of the importance of trachytes in the study of ine rhyolites (Carmichael and MacKenzie, ailey and Schairer, 1964), we prefer merely to ne paucity of data on peralkaline trachytic nd to single out this field of research as requir- ediate attention.

e three analyses plotting in the comenditic field (fig. 5), one (analysis 107) is almost cer- pantellerite trachyte which has lost alkalis on lization and which has been enriched in cumulus phenocrysts (Macdonald and others, 1970). remaining analyses (analysis 105 from Ker- nd 106 from Pitcairn Island) are both of oceanic s.

pantelleritic trachytes are all from central Compared to the pantellerites with which they dly associated, they are enriched predictably in TiO_2, Fe_2O_3+FeO, MnO, MgO, and CaO. surprisingly perhaps, these trachytes are only lly less peralkaline than the pantellerites; the nce of this feature has been discussed by ald, Bailey, and Sutherland (1970).

TRACE ELEMENTS

im of the geochemist is to determine as accu- possible the behavior of trace elements during ic processes, and it is important, therefore, that s studied be representative of the composition agmas from which they were formed. Available icate that this is not normally the case in crys- peralkaline silicic rocks, because various minor may be lost during devitrification and (or) n (Noble, 1968; Rosholt and Noble, 1969) or the slower cooling of plutonic bodies, losses tly connected with the high mobility of the traces in fugitive alkaline solutions. As was the the major elements, it is necessary to use only ated glasses to estimate the true magmatic ces. Very few trace element analyses have been d, especially of comenditic obsidians, and we ordingly started an analytical program to try to of the more critical gaps. The results for 13 ele- aken from Ray Macdonald, D. K. Bailey, and ngell (unpub. data) are given in table 7, and d data are compiled in table 5. Table 5 is not ve, as we have used only those specimens for cceptable major element analyses are also .

mited data available (table 5) indicate that, o the "average granite" (Taylor, 1964; Taylor te, 1966) and calc-alkaline rhyolites from New (Ewart and others, 1968) and Arran, Scotland and Carmichael, 1969), the comendites and ites show strong enrichment in Hf, La, Mo, Nb, Ta, Y, Yb, Zn, and Zr, and moderate to strong enrichment in B, Be, Cd, Ga, Li, Sn, and perhaps Th and U. This enrichment is accompanied by a very marked depletion in Ba, Cr, Sr, V, and probably Sc. Concentrations of Co, Cs(?), Cu, Ni, Pb, and Rb seem to be similar to those in calc-alkaline types, except for those pantellerites with high agpaitic index, which may show enrichment in rubidium. Data from Mayor Island (Ewart and others, 1968) also indicate a strong enrichment in rare earths (analyses 91–95, tables 5 and 6).

VARIATIONS IN COMENDITES AND PANTELLERITES

As a result of the scarcity of data for the comendite obsidians, this discussion must be restricted to barium, copper, nickel, strontium, lead, rubidium, thorium, yttrium, cerium, lanthanum, niobium, zinc, and zirconium. Figures 14 and 15 show the variations of some of these elements with respect to the agpaitic index.

Barium.—Most pantellerites are strongly depleted in barium, except for those from Gariboldi volcano, Ethiopia, where barium values reach 680 ppm (parts per million). Barium values as high as 600 ppm from the vitreous parts of a pantelleritic welded ash-flow tuff which erupted from the nearby volcano Fantalē (Gibson, 1970) indicate that the Fantalē rocks may also be relatively barium-rich. On the other hand, Chabbi volcano, part of the same chain of Quaternary pantellerite volcanoes on the Ethiopian Rift Valley floor, is more "normal," with barium values in the pantellerites between 50–60 ppm.

The oceanic comendites of Bouvet and Easter Islands also show relative barium enrichment.

Copper.—All specimens are uniformly low in copper. Only a comendite from Nevada (analysis 12) contains >12 ppm.

Nickel.—All specimens are also low in nickel; 10 ppm is the maximum value recorded, and most rocks contain <5 ppm.

Strontium.—The pantellerites have strontium values as high as 12 ppm. The higher values in the comendites, as much as 42 ppm, might be expected as these rocks are transitional to calc-alkaline rhyolites (table 5). The claim by Noble, Haffty, and Hedge (1969) that most peralkaline glasses have <5 ppm strontium is only partly true, even for the pantellerites. Using this figure as the normal maximum amount, they noted that some Pantellerian specimens then had "anomalously" high strontium values, but the new data show that this feature is shared by many of the Gariboldi flows, whereas Gibson (1970) reports strontium values as high as 40 ppm from glassy lenses in the Fantalē welded tuff. Barberi, Borsi, Ferrara, and Innocenti (1969) have given values of 13 and 14 ppm for two pantellerites from Pantelleria. The spread of strontium concentra-

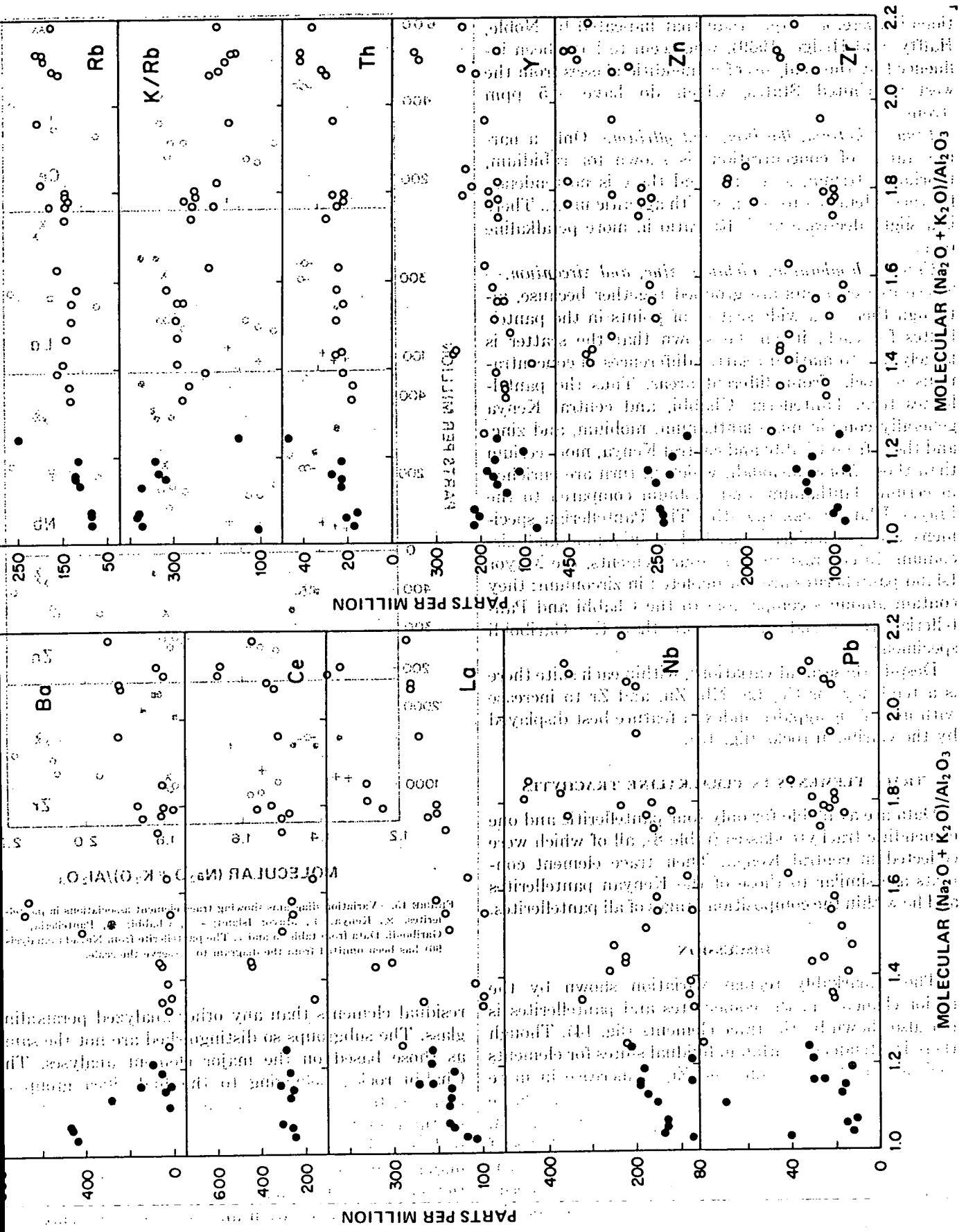

FIGURE 14.—Variation diagrams for trace elements in comendites and pantellerites. ●, comendite; ○, pantellerite. To preserve the scale, analysis 90 has been omitted from all but the barium diagram, analysis 11 from the zirconium diagram, and analysis 15 from the niobium diagram.

is therefore larger than that indicated by Noble, y, and Hedge (1969), who seem to have been in-ced by the analyses of comenditic glasses from the ern United States, which do have <5 ppm tium.

ad, rubidium, thorium, and yttrium.—Only a nar-range of concentrations is shown for rubidium, um, yttrium, and lead, and there is no tendency ese elements to co-vary with agpaitic index. There light decrease in K/Rb ratio in more peralkaline

rium, lanthanum, niobium, zinc, and zirconium.— e five elements are grouped together because, al-gh there is a wide scatter of points in the pantel-s for each, it can be shown that the scatter is y due to marked relative differences in concentra-in rocks from different areas. Thus the pantel-s from Pantelleria, Chabbi, and central Kenya ally contain more lanthanum, niobium, and zinc, hose from Chabbi and central Kenya, more cerium those from Gariboldi, which in turn are enriched rium, lanthanum, and niobium compared to the or Island rocks (fig. 15). The Pantellerian speci-are particularly enriched in niobium and zir-m. In contrast to these four elements, the Mayor d pantellerites are not depleted in zirconium; they in amounts comparable to the Chabbi and Pan-ian rocks and rather more than the Gariboldi mens.

spite these areal variations, within each suite there endency for Ce, La, Nb, Zn, and Zr to increase increasing agpaitic index, a feature best displayed e Gariboldi rocks (fig. 15).

RACE ELEMENTS IN PERALKALINE TRACHYTES

ta are available for only four pantelleritic and one nditic trachyte glasses (table 8), all of which were ted in central Kenya. Their trace element con-are similar to those of the Kenyan pantellerites e within the composition ranges of all pantellerites.

DISCUSSION

e remarkably regular variation shown by the elements in the comendites and pantellerites is so shown by the trace elements (fig. 14). Though is a tendency within individual suites for elements as Ce, La, Nb, Zn, and Zr to increase in more aline rocks, superimposed on the trends are large nces in abundances due to geographical location. possible, for example, to distinguish the lavas of oldi volcano from those of Pantelleria on the basis ir trace element contents, whereas the pantellerite Nevada has considerably higher values of the

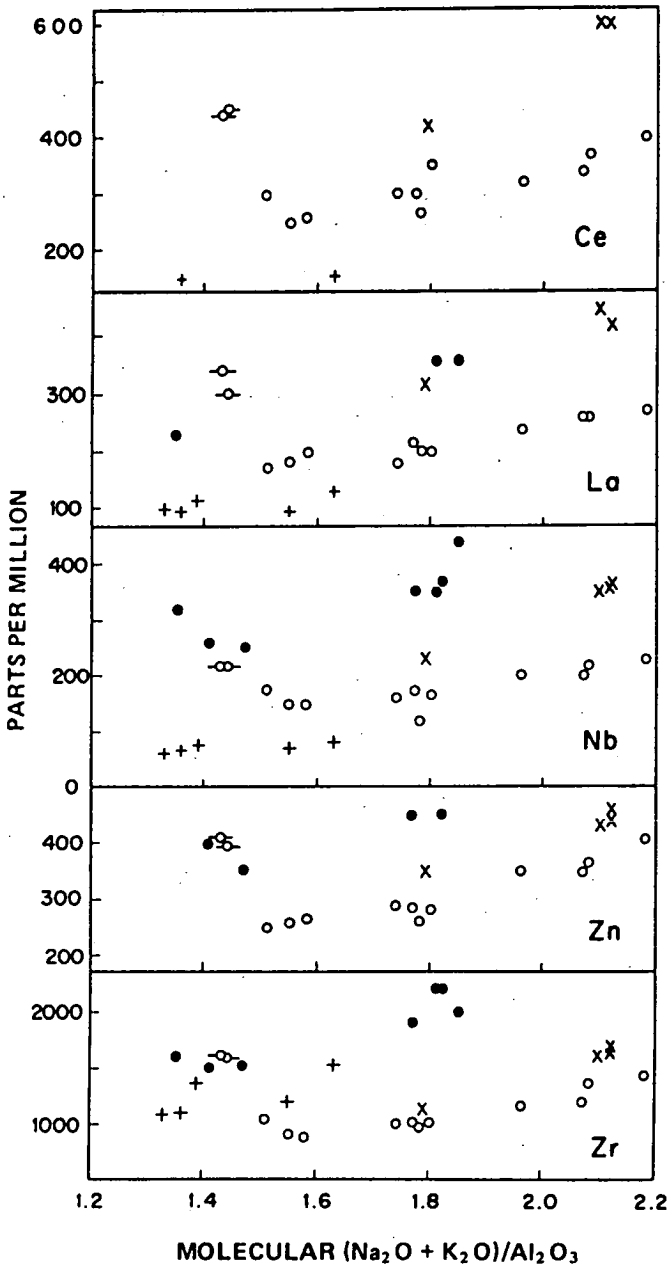

FIGURE 15.—Variation diagrams showing trace element associations in pantellerites. ×, Kenya; +, Mayor Island; -○-, Chabbi; ●, Pantelleria; ○, Gariboldi. Data from tables 5 and 7. The pantellerite from Nevada (analysis 90) has been omitted from the diagram to preserve the scale.

residual elements than any other analyzed peralkaline glass. The subgroups so distinguished are not the same as those based on the major element analyses. The Chabbi rocks, belonging to the high-silica group of pantellerites, have a trace element suite broadly similar to those of the type pantellerites, and the Gariboldi rock was classed as a type pantellerite on the basis of major elements. The preliminary data seem to indicate the possibility that each volcano is characterized by its trace element association and that the differences be-

tween volcanoes mark real differences in the minor-element chemistry of the source materials.

REFERENCES

Bailey, D. K., and Macdonald, Ray, 1969, Alkali-feldspar fractionation trends and the derivation of peralkaline liquids: Am. Jour. Sci., v. 267, p. 242–248.

——— 1970, Petrochemical variations among mildly peralkaline (Comendite) obsidians from the oceans and continents: Contr. Mineralogy and Petrology, v. 28, p. 340–351.

Bailey, D. K., and Schairer, J. F., 1964, Feldspar-liquid equilibria in peralkaline liquids—the orthoclase effect: Am. Jour. Sci., v. 262, p. 1198–1206.

——— 1966, The system Na_2O–Al_2O_3–Fe_2O_3–SiO_2 at 1 atmosphere, and the petrogenesis of alkaline rocks: Jour. Petrology, v. 7, p. 114–170.

Barberi, Franco, Borsi, S., Ferrara, G., and Innocenti, F., 1969, Strontium isotopic composition of some recent basic volcanites of the southern Tyrrhenian Sea and Sicily Channel: Contr. Mineralogy and Petrology, v. 23, p. 157–172.

Bertolio, Sollmann, 1895, Sulle comenditi, nuovo gruppo di rioliti con aegirina: Accad. Lincei Roma, Rend., v. 4, p. 48–50.

Bowen, N. L., 1937, Recent high-temperature research on silicates and its significance in igneous geology: Am. Jour. Sci., 5th ser., v. 33, p. 1–21.

Broch, O. A., 1946, Two contributions to Antarctic petrography: Norske Vidensk.-Acad. Oslo, Norwegian Antarctic Exped. Sci. Results, v. 2, no. 25, 32 p.

Bryan, W. B., 1970, Alkaline and peralkaline rocks of Socorro Island, Mexico: Carnegie Inst. Washington Year Book 68, 1968–69, p. 194–200.

Butler, J. R., and Smith, A. Z., 1962, Zirconium, niobium and certain other trace elements in some alkali igneous rocks: Geochim. et Cosmochim. Acta, v. 26, p. 945–953.

Butler, J. R., and Thompson, A. J., 1967, Cadmium and zinc in some alkali acidic rocks: Geochim. et Cosmochim. Acta, v. 31, p. 97–105.

Carmichael, I. S. E., 1962, Pantelleritic liquids and their phenocrysts: Mineralog. Mag., v. 33, No. 257, p. 86–113.

——— 1967, The iron-titanium oxides of salic volcanic rocks and their associated ferromagnesian silicates: Contr. Mineralogy and Petrology, v. 14, p. 36–64.

Carmichael, I. S. E., and MacKenzie, W. S., 1963, Feldspar-liquid equilibria in pantellerites—an experimental study: Am. Jour. Sci., v. 261, p. 382–396.

Chayes, Felix, 1970, Rhyolites of the oceanic islands. Carnegie Inst. Washington Year Book 68, 1968–69, p. 177.

Chayes, Felix, and Zies, E. G., 1962, Sanidine phenocrysts in some peralkaline volcanic rocks: Carnegie Inst. Washington Year Book 61, 1961–62, p. 112–118.

——— 1964, Notes on some Mediterranean comendite and pantellerite specimens: Carnegie Inst. Washington Year Book 63, 1963–64, p. 186–190.

Coombs, D. S., 1963, Trends and affinities of basaltic magmas and pyroxenes as illustrated on the diopside-olivine-silica diagram: Mineralog. Soc. America Spec. Paper 1, p. 227–250.

Edwards, A. B., 1938, Tertiary lavas from the Kerguelen archipelago: British, Australian, New Zealand Antarctic Research Exped. 1929–1931, Repts., ser. A, v. 2, no. 5, p. 69–100.

Ewart, Anthony, Taylor, S. R., and Capp, A. C., 1968, Geochemistry of the pantellerites of Mayor Island, New Zealand: Contr. Mineralogy and Petrology, v. 17, p. 116–140.

Foerstner, Enrico, 1881, Nota preliminare sulla geologia dell'Isola di Pantelleria secondo gli studii fatti negli anni 1874 e 1881: Com. Geol. Italiano Boll., v. 12, p. 523–556.

Friedman, Irving, and Smith, R. L., 1958, The deuterium content of water in some volcanic glasses: Geochim. et Cosmochim. Acta, v. 15, p. 218–228.

Gibson, I. L., 1970, A pantelleritic welded ash-flow tuff from the Ethiopian Rift Valley: Contr. Mineralogy and Petrology, v. 28, p. 89–111.

Hieke Merlin, Oplinia, 1953, Le vulcaniti acide dell'Africa orientale: Padova Univ. Ist. Geologia e Mineralogia Mem. v. 18, [no. 1], 46 p.

Johannsen, Albert, 1932, The quartz bearing rocks, Volume 2 *of* A descriptive petrography of the igneous rocks: Chicago, Ill., Univ. Chicago Press, 428 p.

Johnsen, Arrien, 1912, Die Gesteine der Inseln S. Pietro und S. Antioco (Sardinien): Akad. Wiss. Preuss., Abh. 2, Phys-Math Kl, p. 1–82.

Lacroix, Alfred, 1927, Les rhyolites et les trachytes hyperalcalins quartzifères, à propos de ceux de la Corée: Acad. Sci. [Paris] Comptes Rendus, v. 185, p. 1410–1415.

——— 1930, Les roches hyperalcalines du massif du Fantale et du col de Balla: Soc. Géol. France Mém., v. 14, p. 89–102.

——— 1934, Volcanisme et lithologie. Mission au Tibesti (1930–1931) dirigee par M. Dalloni: Acad. Sci. Paris, Mém., v. 61, p. 169–366.

——— 1936a, Composition minéralogique des roches volcaniques de l'Ile de Pâques: Acad. Sci. [Paris] Comptes Rendus, v. 202, p. 527–530.

——— 1936b, Composition chimique des laves de l'Ile de Pâques: Acad. Sci. [Paris] Comptes Rendus, v. 202, p. 601–605.

Lovering, J. F., 1966, Electron microprobe analyses of chlorine in two pantellerites: Jour. Petrology, v. 7, p. 65–67.

McCall, G. J. H., 1967, Geology of the Nakuru-Thomson's Falls-Lake Hannington area: Kenya Geol. Survey Rept. 78, 122 p.

Macdonald, Ray, Bailey, D. K. and Sutherland, D. S., 1970, Oversaturated peralkaline glassy trachytes from Kenya: Jour. Petrology, v. 11, p. 507–517.

Macdonald, Ray, and Gibson, I. L., 1969, Pantelleritic obsidians from the volcano Chabbi (Ethiopia): Contr. Mineralogy and Petrology, v. 24, p. 239–244.

Morgan, W. R., 1966, A note on the petrology of some lava types from east New Guinea: Geol. Soc. Australia Jour., v. 13, pt. 2, p. 583–591.

Nicholls, John, and Carmichael, I. S. E., 1969, Peralkaline acid liquids—a petrological study: Contr. Mineralogy and Petrology, v. 20, p. 268–294.

Noble, D. C., 1965, Gold Flat Member of the Thirsty Canyon Tuff—a pantellerite ash-flow sheet in southern Nevada: U.S. Geol. Survey Prof. Paper 525-B, p. B85–B90.

——— 1966, Comenditic volcanic rocks in the western United States [abs.]: Geol. Soc. America Spec. Paper 87, p. 117–118.

——— 1967, Sodium, potassium, and ferrous iron contents of some secondarily hydrated natural silicic glasses: Am. Mineralogist, v. 52, p. 280–286.

——— 1968, Systematic variation of major elements in comendite and pantellerite glasses: Earth and Planetary Sci. Letters, v. 4, p. 167–172.

——— 1970, Loss of sodium from crystallized comendite welded tuffs of the Miocene Grouse Canyon Member of the Belted Range Tuff, Nevada: Geol. Soc. America Bull., v. 81, p. 2677–2687.

Noble, D. C., Chipman, D. W., and Giles, D. L., 1968, Peralkaline silicic volcanic rocks in northwestern Nevada: Science, v. 160, p. 1337–1338.

D. C., and Haffty, Joseph, 1969, Minor-element and re-
ed major-element contents of some Mediterranean pantel-
ites and comendites: Jour. Petrology, v. 10, p. 502–509.
D. C., Haffty, Joseph, and Hedge, C. E., 1969, Strontium
d magnesium contents of some natural peralkaline silicic
sses and their petrogenetic significance: Am. Jour. Sci.,
267, p. 598–608.
D. C., Smith, V. C. and Peck, L. C., 1967, Loss of halogens
m crystallized and glassy silicic volcanic rocks: Geochim.
Cosmochim. Acta, v. 31, p. 215–223.
G. T., 1903, Contributions to the petrology of British East
rica: Mineralog. Mag., v. 13, p. 228–263.
er, H. P. T., and Hitchen, C. S., 1930, Vulkanologische
obachtungen längs der Bahnlinie Adis Abeba–Djibouti
bessinien): Zeitschr. Vulkanologie, v. 12, p. 269–289.
o, Romolo, 1958, New petrochemical data of volcanites
m the Island of Pantelleria (Channel of Sicily): Geol.
ndschau, v. 57, p. 773–783.
1969, Sur l'origine de l'éxcès de sodium (ns) dans certaines
es de l'Île de Pantelleria: Bull. Volcanol., v. 33, p. 694–700.

Rosholt, J. N., and Noble, D. C., 1969, Loss of uranium from crystallized silicic volcanic rocks: Earth and Planetary Sci. Letters, v. 6, p. 268–270.

Ross, C. S., and Smith, R. L., 1955, Water and other volatiles in volcanic glasses: Am. Mineralogist, v. 40, p. 1071–1089.

Taylor, S. R., 1964, Abundance of chemical elements in the continental crust—a new table: Geochim. et Cosmochim. Acta, v. 28, p. 1273–1285.

Taylor, S. R., and White, A. J. R., 1966, Trace element abundances in andesites: Bull. Volcanol., v. 29, p. 177–194.

Washington, H. S., 1913, The volcanoes and rocks of Pantelleria—Part 2, Petrography: Jour. Geology, v. 21, p. 683–713.

——— 1917, Chemical analyses of igneous rocks: U.S. Geol. Survey Prof. Paper 99, 1201 p.

——— 1921, Obsidian from Copan and Chichen Itza: Washington Acad. Sci. Jour., v. 11, p. 481–487.

Zies, E. G., 1960, Chemical analysis of two pantellerites: Jour. Petrology, v. 1, p. 304–308.

TABLES 2–10

EXPLANATION TO TABLES 2–8

No attempt has been made to specify the composition of the eldspar and pyroxene phenocrysts because, except where the henocrysts have actually been analyzed, sufficient data are rarely iven, especially in older papers, to accurately identify the mineral pecies. Abbreviations for phenocrysts are as follows: F is alkali eldspar; Q, quartz; P, pyroxene; O, olivine; A, aenigmatite (including cossyrite); AB, amphibole; IO, opaque ores; and AP, patite. Figures in parentheses, for example F(2), refer to modal ercentages; tr. in parentheses indicates trace. Colln. is collection umber; lab., laboratory number. Rock names used below are hose applied by the original authors.

COMENDITES

EUROPE

Sardinia

. Comendite, Le Fontane, Isola San Pietro. Analyst: E. G. Zies (fluorine by V. C. Smith). Phenocrysts: F(9.3), Q(6.0), tridymite and others (0.3). References: Chayes and Zies, 1962, table 7, colln. 40B5. Analysis of feldspar phenocrysts given in same paper. Trace element data from Noble and Haffty, 1969.

AFRICA

Chad

. Comendite obsidian, Tarso Toussidé, Tibesti Mountains. Analyst: F. Raoult. Phenocrysts: F, P, O, IO. Reference: Lacroix, 1934, p. 190, No. 1.

Ethiopia

. Comendite obsidian, Sardo, Afar. Analyst: O. Hieke Merlin. Phenocrysts: None. Reference: Hieke Merlin, 1953, table 2.

Belongs to Aden Series Volcanics.

Kenya

Rhyolite obsidian, south shore, Lake Naivasha. Analyst: A. Willman (fluorine by E. S. Shepherd). Phenocrysts: F, rare; O, very rare. Reference: Bowen, 1937, table 1, No. 6, colln. NLB 248.

Comendite obsidian, top of flow, north portal of Njorowa Gorge, Lake Naivasha. Analyst: A. Willman (fluorine by E. S. Shepherd). Phenocrysts: None. Reference: Bowen, 1937, table 1, No. 8, colln. NLB 246.

Rhyolite obsidian (comenditic), south shore, Lake Naivasha. Analyst: S. Goldich (fluorine by E. S. Shepherd). Phenocrysts: None. Reference: Bowen, 1937, table 1, No. 9, colln. NLB 249.

Comendite obsidian, exact locality unknown, Rift Valley. Analysts: S. A. Malik, D. A. Bungard, J. M. C. Palmer. Phenocrysts: None. Reference: Bailey and Macdonald, 1970, table 1, No. 11, colln. EAK 7.

Comendite obsidian, Kongoni farm, Naivasha. Analysts: S. A. Malik, D. A. Bungard, L. Porteous. Phenocrysts: F, including F–Q intergrowths (10.2), Q(1.3), P(tr.), vesicular specimen 29.2% pores, by volume. Reference: Bailey and Macdonald, 1970, table 1, No. 10, colln. 43/3/S/85.

UNITED STATES

Idaho

Comendite glass, Big Southern Butte. Analysts: V. C. Smith, J. Haffty. Reference: Noble, 1968, table 1, No. 1, lab. D101042.

Nevada

10. Comendite glass, Spearhead Member, Thirsty Canyon Tuff, Black Mountain volcanic center, Nye County. Analysts: V. C. Smith, J. Haffty, H. Neiman. Reference: Noble, 1968, table 1, No. 2, lab. D100737.
11. Comendite glass, basal glassy zone of Grouse Canyon Member, Belted Range Tuff, Silent Canyon volcanic center, Nye County. Analysts: V. C. Smith, J. Haffty, H. Nieman. Phenocrysts: None. References: Noble, 1968, table 1, No. 3, lab. D100317. Trace element data from Noble, 1970.
12. Comendite glass, lowermost part of Grouse Canyon Member, Belted Range Tuff, Silent Canyon volcanic center, Nye County. Analyst: E. S. Daniels. Phenocrysts: None. Reference: Noble, 1970, table 1, No. 2, lab. D100209.
13. Comendite glass, lowermost part of Grouse Canyon Member, Belted Range Tuff, Silent Canyon volcanic center, Nye County. Analyst: E. L. Munson. Phenocrysts: None. Reference: Noble, 1970, table 1, No. 3, lab. D101090.
14. Comendite glass separate, basal glassy zone of Spearhead Member, Thirsty Canyon Tuff, Black Mountain Volcanic center, Nye County. Analysts: V. C. Smith and others. References: Partial analysis in Noble, 1967, table 1, No. 2A, lab. D100320. Complete analysis from U.S. Geological Survey files.
15. Comendite glass separate, basal glassy zone of Spearhead Member, Thirsty Canyon Tuff, Black Mountain volcanic center, Nye County. Analysts: C. L. Parker and others. References: Partial analysis in Noble, 1967, table 1, No. 2B, lab. D100437. Complete analysis from U.S. Geological Survey files, trace element data from Noble and Haffty, 1969.

ATLANTIC OCEAN

Iceland

16. Obsidian, Oraefajokull, Eastern Iceland. Analyst: I. S. E. Carmichael, Phenocrysts: P(0.3), O(0.3), IO(0.1), plagioclase (2.1). Reference: Carmichael, 1967, table 5, No. 2. Analyses of pyroxene, olivine, and iron-titanium oxides given in same paper.

    This rock and perhaps that from Ljosufjoll (analysis 17) are the only ones in this compilation that contain plagioclase phenocrysts.
17. Comendite obsidian, Ljosufjoll. Analysts: S. A. Malik, D. A. Bungard, L. Porteous. Phenocrysts: F(1), P(tr.), O(tr.), plagioclase(?). Reference: Bailey and Macdonald, 1970, table 1, No. 7, colln. 491.

    See comment for specimen 16.
18. Comendite obsidian, Midhyrna. Analysts: S. A. Malik, D. A. Bungard, L. Porteous. Phenocrysts: F(<1), P(tr.), IO(tr.). Reference: Bailey and Macdonald, 1970, table 1, No. 8, colln. 295.

    Composition of feldspar phenocrysts is Or_{35}.
19. Comendite obsidian, Hrafntinnusker. Analysts: S. A. Malik, D. A. Bungard, L. Porteous. Phenocrysts: None. Reference: Bailey and Macdonald, 1970, table 1, No. 9, colln. 423.

Ascension Island

20. Comendite obsidian, Middleton's Ridge. Analysts: S. A. Malik, D. A. Bungard, J. M. C. Palmer. Phenocrysts: F, very scarce (<1). Reference: Bailey and Macdonald, 1970, table 1, No. 1, colln. 15375.

Bouvet Island

21. Comendite obsidian, Lars islet. Analyst: E. Klüver. Phenocrysts: F. Reference: Broch, 1946, p. 16.
Broch's norm in error; the corrected norm is given in table 2.
22. Comendite obsidian, Lars islet. Analysts: S. A. Malik, D. A. Bungard, J. M. C. Palmer. Phenocrysts: F(2.5). Reference: Bailey and Macdonald, 1970, table 1, No. 3, colln. WJ18B.
23. Comendite obsidian, Lars islet. Analysts: S. A. Malik, D. A. Bungard, J. M. C. Palmer. Phenocrysts: F(<1). Reference: Bailey and Macdonald, 1970, table 1, No. 2, colln. B2.

PACIFIC OCEAN

Easter Island

24. Banded hyperalkaline obsidian, Rana Kau. Analyst: F. Raoult. Phenocrysts: F, P, O. References: Analysis from Lacroix, 1936b, p. 603, phenocryst assemblage from Lacroix, 1936a, p. 529.
25. Comendite obsidian, slopes of Rana Kau. Analysts: S. A. Malik, D. A. Bungard, J. M. C. Palmer. Phenocrysts: Very scarce(?) zircon. Reference: Bailey and Macdonald, 1970, table 1, No. 5, colln. 17518.
26. Comendite obsidian, Motu Iti islet. Analysts: S. A. Malik, D. A. Bungard, J. M. C. Palmer. Phenocrysts: None. Reference: Bailey and Macdonald, 1970, table 1, No. 4, colln. 17525.
27. Comendite obsidian, northwest side of Cerro Orito. Analysts: S. A. Malik, D. A. Bungard, J. M. C. Palmer. Phenocrysts: None. Reference: Bailey and Macdonald, 1970, table 1, No. 6, colln. 17691.

New Guinea

28. Aegirine obsidian, southeast floor of Lamonai crater, Fergusson Island. Analysts: L. Castanelli, R. L. Bruce. Phenocrysts: Sparse, F, P. Reference: Morgan, 1966, table, No. 29.
29. Pumiceous aegirine obsidian, close to crater, Oian cone, Fergusson Island. Analysts: L. Castanelli, R. L. Bruce. Phenocrysts: Sparse F, P. Reference: Morgan, 1966, table, No. 30.

PANTELLERITES
EUROPE

Pantelleria

30. Hyalopantellerite, Gelkhamar. Analyst: E. G. Zies (fluorine by V. C. Smith). Phenocrysts: F(10.7), Q(0.8), P(0.2), A(0.8). Reference: Zies, 1960, p. 307, colln. PRC 2000.
Re-analysis of Washington's (1913) specimen A. Further revised analysis given by Noble and Haffty (1969) including fluorine figure. New Al_2O_3 (corrected for trace element interference) = 8.29, MgO = 0.07, Na_2O = 6.48, K_2O = 4.44, ZrO_2 = 0.27. Analysis of feldspar phenocrysts in Chayes and Zies (1962, table 8); trace element data from Noble and Haffty (1969).
31. Hyalopantellerite, Costa Zeneti. Analyst: E. G. Zies (fluorine by V. C. Smith). Phenocrysts: F(ca. 2). Reference: Zies, 1960, p. 307, colln. PRC 2007.
Re-analysis of Washington's (1913) specimen D. Further revised analysis and trace element data given by Noble and Haffty (1969), including fluorine figure. New Al_2O_3 (corrected for trace element interference) = 11.08, Na_2O = 6.34, K_2O = 4.61, ZrO_2 = 0.17.
32. Hyalopantellerite, Cuddia Gadir. Analyst: E. G. Zies (fluorine by V. C. Smith). Phenocrysts: F(8.8), Q(2.2), P(0.1), A(0.4), IO(0.1). Reference: Chayes and Zies, 1964, table 19, colln. 44B5.
Slightly revised analysis and trace element data given by Noble and Haffty, 1969, including fluorine figure. New Al_2O_3 (corrected for trace element interference) = 8.15, NA_2O = 6.60, K_2O = 4.41, ZrO_2 = 0.29. Analysis of feldspar phenocrysts in Chayes and Zies, 1964.
33, 34. Porphyritic pantellerite obsidian and separated (residual) glass, exact locality not given. Analyst: I. S. E. Carmichael. Phenocrysts: F(10.7), P(0.5), O(0.4), A(tr.), IO(0.2). References: Carmichael, 1962, table 6, Nos. 1R and 1G, colln. 5748; trace element data for 33 from Nicholls and Carmichael, 1969.
Chlorine computed from mode and analyzed chlorine content of glass. Analyses of feldspar, pyroxene, and olivine given in Carmichael (1962), with revised feldspar and pyroxene values in Nicholls and Carmichael (1969).
35, 36. Porphyritic pantellerite obsidian and separated (residual) glass, exact locality not given. Analyst: I. S. E. Carmichael. Phenocrysts: F(18.0), Q(0.1), P(0.3), O(tr.), A(0.9), IO(tr.). References: Carmichael, 1962, table 6, Nos. 2R and 2G, colln. 3112; trace element data for 35 from Nicholls and Carmichael, 1969.
Chlorine computed from mode and analyzed chlorine content of glass. Analyses of feldspar, pyroxene, and aenigmatite given in Carmichael (1962), with revised feldspar and pyroxene values in Nicholls and Carmichael (1969).
37, 38. Porphyritic pantellerite obsidian and separated (residual) glass, exact locality not given. Analyst: I. S. E. Carmichael. Phenocrysts: F(9.4), Q(2.0), P(tr.), A(0.9). References: Carmichael, 1962, table 6, Nos. 3R and 3G, colln. 5749; trace element data for 37 from Nicholls and Carmichael, 1969.
Chlorine computed from mode and analyzed chlorine content of glass. Analyses of feldspar and aenigmatite given in Carmichael (1962), with slightly revised feldspar values in Nicholls and Carmichael (1969).
39, 40. Porphyritic pantellerite obsidian and separated (residual) glass, exact locality not given. Analyst: I. S. E. Carmichael. Phenocrysts: F(1.2), P(tr.), O(tr.). References: Carmichael, 1962, table 6, Nos. 4R and 4G, colln. 3114; trace element data for 39 from Nicholls and Carmichael, 1969.
Chlorine computed from mode and analyzed chlorine content of glass. Analysis of feldspar phenocrysts given in Carmichael (1962), with a slightly revised value in Nicholls and Carmichael (1969).
41. Pantellerite, Cuddia Attalora. Analyst: R. Romano. Phenocrysts: No data. Reference: Romano, 1968, table 1, No. 28.
42. Pantellerite, Cuddia da Khamma. Analyst: R. Romano. Phenocrysts: No data. Reference: Romano, 1968, table 1, No. 29.
43. Pantellerite, Cala di Tramontana. Analyst: C. Sturiale. Phenocrysts: No data. Reference: Romano, 1968, table 1, No. 31.
44. Pantellerite, Fossa della Pernice (same flow as analysis 39). Analyst: R. Romano. Phenocrysts: No data. Reference: Romano, 1969, table 1, analysis D.
45. Pantellerite, Fossa della Pernice (same flow as analysis 38). Analyst: R. Romano. Phenocrysts: No data. Reference: Romano, 1969, table 1, analysis E.

Same analysis given in Romano (1968, table 1, No. 27), but with different values of MnO (0.25) and P_2O_5 (0.19). No explanation of this difference offered.

Sardinia

6. Comendite, Capo Sandolo, San Pietro. Analyst: E. G. Zies (fluorine by V. C. Smith). Phenocrysts: F(13.7), Q(3.6), P(<0.1), A(<0.1), AB(0.1). References: Chayes and Zies, 1964, table 19, colln. 39B3; fluorine and trace element data from Noble and Haffty, 1969. Analysis of feldspar given in Chayes and Zies (1964).

AFRICA

Chad

7. Pantellerite obsidian, Wantagoi, Tibesti Mountains. Analyst: F. Raoult. Phenocrysts: No data. Reference: Lacroix, 1934, p. 191, No. 7.
8. Pantellerite obsidian, western flank, Emi Koussi. Analyst: F. Raoult. Phenocrysts: No data. Reference: Lacroix, 1934, p. 191, No. 8.
9. Pantellerite obsidian, fragments, Enneri Gonoa. Analyst: F. Raoult. Phenocrysts: F. Reference: Lacroix, 1934, p. 191, No. 9.

Ethiopia

0. Comendite obsidian, Entotto, Shoa. Analyst: O. Hieke Merlin. Phenocrysts: None. Reference: Hieke Merlin, 1953, table 2.

Belongs to Trap Series Volcanics, Magdala group.

Aden Series Volcanics:

1. Comendite obsidian, Monte Agelu, near Gauani, Hararge. Analyst: O. Hieke Merlin. Phenocrysts: None. Reference: Hieke Merlin, 1953, table 2.
2. Pantellerite obsidian, south side of Fantālē volcano, Shoa. Analyst: F. Raoult. Phenocrysts: F, Q, P, A. Reference: Lacroix, 1930, p. 95, analysis A.
3. Porphyritic pantellerite obsidian, south side of Fantālē volcano, Shoa. Analyst: F. Raoult. Phenocrysts: F, Q, Q–F intergrowths, A, AB. Reference: Lacroix, 1930, p. 95, analysis B.
4. Opaque pantellerite obsidian, north side of Fantālē volcano, Shoa. Analyst: F. Raoult. Phenocrysts: No data. Reference: Lacroix, 1930, p. 97, analysis D.
5. Pantellerite, Fantālē volcano, Shoa. Analyst: C. S. Hitchen. Phenocrysts: No. data. Reference: Rohleder and Hitchen, 1930, p. 281, No. 6.
6. Pantelleritic obsidian bomb, Mojjo, Shoa. Analyst: C. S. Hitchen. Phenocrysts: No data. Reference: Rohleder and Hitchen, 1930, p. 281, No. 8.
7–68. Pantellerite obsidians, Gariboldi volcanic complex. Analysts: S. A. Malik, D. A. Bungard, J. M. C. Palmer, L. Porteous. Phenocrysts: 57—F, Q, P, A, AB; 58—F very scarce; 59—F(2.6), P(0.1), O(<0.1), IO(<0.1); 60—none; 61—F(6.7), P(0.4), O(tr.), IO(0.5); 62—F(1.5), P(0.1), O(tr.), IO(tr.); 63—F(1.8), P(0.2), IO(0.1); 64—F(0.2), P(tr.); 65—none; 66—F(1.4), P(0.1), A(0.1); 67—F(1.0), P(tr.), O(tr.); 68—F(4.1), Q(1.8), P(0.1), A(0.4), AB(0.1). Reference: Unpublished analyses of specimens collected by Dr. J. W. Cole and supplied to us by courtesy of Dr. I. L. Gibson (colln. G69, G77, G110, G320, G414, G417, G427, G429, G437, G444, G446, and G445, respectively).
9–79. Pantellerite obsidians, Chabbi volcano. 69, 75, 78, and 79—east vent; 71, 72, and 74—hot cone; 73 and 77—main vent; 76—north vent; 70—northeast vent. Analysts: R. Macdonald and S. A. Malik. Phenocrysts: None. Reference: Macdonald and Gibson, 1969, table, Nos. 1–8, 11–13.

Kenya

80. Phonolitic obsidian, Lake Nakuru. Analyst: G. T. Prior. Phenocrysts: F, P, O (all very scarce). Reference: Prior, 1903, p. 245.
81. Soda rhyolite (pantellerite) obsidian, Eburru. Analyst: A. Willman (fluorine by E. S. Shepherd). Phenocrysts: None. Reference: Bowen, 1937, table 1, No. 7, colln. NLB 230.
82. Pantellerite obsidian (Plr_3), east of Cedar Hill, Eburru. Analysts: S. A. Malik, D. A. Bungard, J. M. C. Palmer. Phenocrysts: F, P, A, AB. Reference: Dr. D. S. Sutherland, unpub. analysis, colln. 43/3/S/12.
83. Pantellerite obsidian (Plr_3), south of Cedar Hill, Eburru. Analysts: S. A. Malik, D. A. Bungard, J. M. C. Palmer. Phenocrysts: F(10.0), P(0.3), A(tr.), AB(0.1). Reference: Dr. D. S. Sutherland, unpub. analysis, colln. 43/3/S/36.
84. Pantellerite obsidian, block in agglomerate (Qvf), about 1 mile east of Cedar Hill, Eburru. Analysts: S. A. Malik, D. A. Bungard, J. M. C. Palmer. Phenocrysts: F(3.7), P(tr.), A(tr.). Reference: Dr. D. S. Sutherland, unpub. analysis, colln. 43/3/S/44.
85. Pantellerite obsidian (Plr_1), Eburru-Gilgil road. Analyst: H. Lloyd. Phenocrysts: F, Q–F intergrowths, A, AB. Reference: Dr. D. S. Sutherland, unpub. analysis, colln. 43/3/S/56.
86. Pantellerite obsidian, lens in pumiceous deposit, Kinangop escarpment. Analyst: M. Thind. Phenocrysts: P, very scarce. Reference: Dr. D. S. Sutherland, unpub. analysis, colln. 43/3/S/20.
87. Glassy soda-rhyolite (pantellerite), Lake Naivasha. Analyst: G. T. Prior. Phenocrysts: None. Reference: Prior, 1903, p. 246.
88. Pantellerite obsidian, south shore, Lake Naivasha. Analyst: I. S. E. Carmichael, J. Hampel. Phenocrysts: F(5.5), Q(0.7), P(0.3), A(0.3), AB(1.8). Reference: Nicholls and Carmichael, 1969, table 1, colln. 121–R. Analyses of feldspar, aenigmatite, amphibole, and residual glass calculated from mode given in same paper.
89. Pantellerite obsidian, band intercalated in pumice (Qvf), quarry, south of Masai Gorge, South Lake Road, Naivasha. Analyst: M. Thind. Phenocrysts: None. Reference: Dr. D. S. Sutherland, unpub. analysis, colln. 43/3/S/2.

UNITED STATES

Nevada

90. Pantellerite glass separate, ash-flow sheet, Gold Flat Member, Thirsty Canyon Tuff, Black Mountain volcanic center, Nye County. Analysts: D. F. Powers and others. Reference: Noble, 1965, table 1, No. 1, lab. D100126.

Slightly revised trace element data for this(?) rock (lab. not specified) given by Noble and Haffty (1969, table 1, No. 6). In parts per million—Be 5.6, Co <5, Cr 1, Cu 3, Ga 44, La 58, Mo 9, Nb 67, Ni 5, Pb 210, Sc 7, Sn 52, Sr 1.5, Y 490, Yb 55.

NEW ZEALAND

Mayor Island

91. Glassy pantellerite, flow 1a, young dome. Analyst: K. Bose. Phenocrysts: F(9.2), P(0.2), A(0.5), IO(tr.). Reference: Ewart, Taylor, and Capp, 1968, table 4, No. 1, colln. P29537.

Chlorine content computed from mode and analyzed chlorine content of glass. Analyses of pyroxene and aenigmatite given in same paper.

Pantellerite obsidian, Opo Bay. Analyst: K. Bose. Phenocrysts: F(6.3), Q(1.5), P(0.1), A(0.2). Reference: Ewart, Taylor, and Capp, 1968, table 4, No. 2, colln. P29553.

Chlorine content computed from mode and analysed chlorine content of glass. Analysis of aenigmatite given in same paper.

Pantellerite obsidian, northwest of Tarewakoura. Analyst: K. Bose. Phenocrysts: F(3.3), P(<0.1), A(<0.1). Reference: Ewart, Taylor, and Capp, 1968, table 4, No. 3, colln. P29543.

Pantellerite obsidian, Te Marawhero Point. Analyst: K. Bose. Phenocrysts: F(0.6), P(<0.1), A(<0.1). Reference: Ewart, Taylor, and Capp, 1968, table 4, No. 4, colln. P29560.

Pantellerite obsidian, Oira Bay. Analyst: K. Bose. Phenocrysts: F(0.6), P(tr.), A(tr.), IO(tr.). Reference: Ewart, Taylor, and Capp, 1968, table 4, No. 5, colln. P29532.

Glassy pantellerite, flow 2, young dome. Analyst: J. A. Ritchie. Phenocrysts: F(8.9), Q(3.7), P(<0.1), A(0.4). Reference: Ewart, Taylor, and Capp, 1968, table 4, No. 7, colln. 29117. Analysis of feldspar given in same paper.

98. Pantellerite obsidian and separated (residual) glass, flow 3, young dome. Analyst: J. A. Ritchie. Phenocrysts: F(8.1), Q(2.0), P(0.3), A(0.2). Reference: Ewart, Taylor, and Capp, 1968, table 4, Nos. 8R and 8G, colln. P29118. Analysis of feldspar phenocrysts given in same paper.

Glassy pantellerite, north shore of Opo Bay. Analyst: E. E. Munson, J. Haffty. Phenocrysts: <1 percent total, mainly F. Reference: Noble, 1968, table 1, No. 4, lab. D100406.

Sample collected in 1956 for R. L. Smith (who provided phenocryst data) and used in study of D/H ratios by Friedman and Smith (1958). Probably same flow as analysis 94 from Te Marawhero Point.

0, 101. Comendite obsidian and separated (residual) glass, Omapu Bay. Analysts: I. S. E. Carmichael, J. Hampel. Phenocrysts: F(3.5), Q(0.8), P(0.1), A(0.1). Reference: Nicholls and Carmichael, 1969, table 1, colln. NZC-2R and 2G.

Published norm of 2R in error; the corrected norm is given in table 3.

2, 103. Comendite obsidian and separated (residual) glass, young dome lavas, south side of island. Analysts: I. S. E. Carmichael, J. Hampel. Phenocrysts: F(3.1), A(tr.). Reference: Nicholls and Carmichael, 1969, table 1, colln. NZC-7R and 7G. Analysis of feldspar given in same paper.

MEXICO

4. Pantellerite obsidian, Socorro Island. Analyst: H. B. Wiik. Phenocrysts: F, P, A, IO. Reference: Bryan, 1970, table 13, No. 1, colln. S138. Analyses of feldspar, pyroxene and aenigmatite phenocrysts given in same paper.

COMENDITIC TRACHYTES

OCEANIC ISLANDS

Kerguelen, Indian Ocean

105. Obsidian trachyte, Baie de la Mouche, Ile de Cormorans. Analyst: F. Raoult. Phenocrysts: F, P. Reference: de la Rue, in Edwards, 1938, table 17, No. 2.

Pitcairn Island, Pacific Ocean

106. Trachyte obsidian, exact locality not given. Analyst: I. S. E. Carmichael. Phenocrysts: F(0.6), P(0.1), O(tr.), IO(tr.). Reference: Carmichael, 1962, table 6, No. 6R, colln. 12095.

AFRICA

Kenya

107. Glassy trachyte, block in agglomerate, northeast of Menengai. Analysts: S. A. Malik, D. A. Bungard, J. M. C. Palmer. Phenocrysts: F(about 10), P(0.3), O(0.3), IO(0.2). Reference: Macdonald, Bailey, and Sutherland, 1970, table 1, colln. 43/1/S/6a. Highly vesicular specimen (38.6 percent pores, by volume), thought to be partially accumulitic.

PANTELLERITIC TRACHYTES

AFRICA

Kenya

108. Pantellerite trachyte, caldera floor, Menengai. Analyst: Mineral Resources Division (Overseas Geol. Survey). Phenocrysts: No data. Reference: McCall, 1967, table 2, analysis N, colln. 43/1192.

109. Pantelleritic trachyte obsidian, block in agglomerate, northeast of Menengai. Analysts: S. A. Malik, D. A. Bungard, J. M. C. Palmer. Phenocrysts: F(1–3), AP. Reference: Macdonald, Bailey, and Sutherland, 1970, table 1, colln. 43/1/S/5.

110. Pantelleritic trachyte obsidian, block in agglomerate, northeast of Menengai. Analysts: S. A. Malik, D. A. Bungard, J. M. C. Palmer. Phenocrysts: F(1). Reference: Macdonald, Bailey, and Sutherland, 1970, table 1, colln. 43/1/S/6.

111. Pantelleritic trachyte obsidian, lava exposed in caldera wall below Valley Farm, west side of Menengai. Analysts: S. A. Malik, D. A. Bungard, J. M. C. Palmer. Phenocrysts: F, scarce. Reference: Macdonald, Bailey, and Sutherland, 1970, table 1, colln. 43/1/S/11.

112. Pantelleritic trachyte obsidian, crater rim, Longonot volcano. Analysts: S. A. Malik, D. A. Bungard, L. Porteous. Phenocrysts: F(0.5), P(0.4). Reference: Macdonald and Bailey, unpub. analysis, colln. LON 1.

113. Trachyte obsidian, Ol Doinyo Nyegi volcano. Analysts: S. A. Malik, D. A. Bungard, L. Porteous. Phenocrysts: F, P, O, IO. Reference: Unpublished analysis of specimen collected by Dr. L. A. J. Williams (colln. W486).

TABLE 2.—*Chemical analyses and norms of comendilic obsidians*

[Details of the specimens are given on p. N22. Data in weight percent except for ratios and indices. Tr. indicates trace]

	1	2	3	4	5	6	7	8	9	10	11	12	13	14	15
Chemical analyses															
SiO_2	75.31	74.70	73.80	75.55	75.03	73.96	72.9	74.2	75.33	75.25	73.98	73.84	73.69	75.37	75.29
Al_2O_3	10.43	11.97	12.10	12.31	11.10	11.40	12.33	10.84	12.29	11.99	11.28	11.80	11.28	11.95	12.12
Fe_2O_3	3.22	.83	.82	.69	1.31	1.65	1.30	1.23	.59	.90	1.71	1.01	1.83	.84	.88
FeO	.80	2.13	1.56	1.17	1.84	1.95	2.14	1.86	1.09	1.25	1.80	2.07	1.74	.99	.99
MgO	.10	Tr.	.22	.04	None	.03	.02	.02	.00	.02	.02	.03	.01	.00	.01
CaO	.13	.54	.84	.23	None	None	.50	.30	.48	.27	.24	.29	.21	.33	.33
Na_2O	3.99	5.12	5.10	4.55	5.09	5.41	5.66	5.17	4.29	4.79	5.33	5.40	5.35	4.43	4.42
K_2O	4.65	4.51	4.95	4.69	4.56	4.36	4.56	4.53	4.98	4.67	4.55	4.50	4.53	4.82	4.88
H_2O-	.38	------	.09	None	.01	.02	------	.09	.04	.05	.02	.01	.01	.04	.04
H_2O+	.51	.38	.22	.15	.08	.13	.05	.80	.09	.15	.16	.17	.43	.45	.36
TiO_2	.21	.21	.22	.13	.19	.17	.24	.20	.10	.13	.22	.22	.22	.11	.11
ZrO_2	.18	------	------	------	------	------	.18	------	.04	.09	.14	------	------	------	------
CeO_2	------	------	------	------	------	------	------	------	.00	------	.02	.01	------	------	------
P_2O_5	.03	------	.08	.01	Tr.	Tr.	.04	.01	.00	------	.01	.01	.01	.02	.01
MnO	------	------	------	.01	.01	.01	------	------	------	------	------	------	------	------	------
	.09	.14	.01	.04	.06	.05	.18	.06	.04	.08	.17	.17	.17	.07	.07
	.05	------	.19	.21	.27	.41	.26	.18	.19	.18	.13	.11	.11	.18	.18
	.18	------	.06	.28	.42	.68	.22	.30	.34	.25	.17	.16	.17	.25	.24
Subtotal	100.26	100.53	100.26	100.06	99.97	100.23	100.53	99.29	99.89	100.07	99.95	99.80	99.76	99.85	99.93
$\equiv(F,Cl)_2$	.09	------	.07	.16	.24	.38	.15	.17	.18	.14	.10	.10	.10	.15	.14
Total	100.17	100.53	100.19	99.90	99.73	99.85	100.38	99.12	99.71	99.93	99.85	99.70	99.66	99.70	99.79
Agpaitic index [1]	1.11	1.12	1.13	1.02	1.19	1.19	1.15	1.24	1.01	1.08	1.21	1.16	1.22	1.04	1.03
Mas FeO [2]	3.70	2.88	2.30	1.79	3.02	3.44	3.31	2.97	1.62	2.06	3.34	2.98	3.39	1.75	1.78
$FeO/(FeO+Fe_2O_3)$ [3]	.20	.72	.66	.63	.58	.54	.62	.60	.65	.58	.51	.67	.49	.54	.53
Na_2O/K_2O [3]	.86	1.14	1.03	.97	1.12	1.24	1.24	1.14	.86	1.03	1.17	1.20	1.18	.92	.91
Molecular:															
SiO_2	85.4	83.4	82.9	83.6	83.9	83.4	82.3	83.9	83.8	83.6	83.4	83.0	83.3	84.0	83.8
Al_2O_3	6.9	7.8	8.0	8.1	7.3	7.6	8.2	7.2	8.1	7.9	7.5	7.9	7.6	7.8	8.0
Na_2O+K_2O	7.7	8.8	9.1	8.2	8.8	9.0	9.5	8.9	8.1	8.5	9.1	9.1	9.1	8.2	8.2
100 $Na_2O/(Na_2O+K_2O)$	56.6	63.4	60.7	59.3	63.1	65.4	65.5	63.4	56.6	60.6	64.2	64.4	64.2	58.2	57.7
CIPW norms															
	36.5	28.2	27.0	32.7	32.5	33.1	24.9	31.9	31.4	30.4	29.2	28.0	28.9	31.7	31.4
	27.5	26.7	29.5	27.8	27.2	26.1	26.7	26.7	29.5	27.8	27.2	26.7	26.7	28.4	28.9
	27.6	36.7	34.6	35.1	31.4	33.5	33.3	30.4	35.1	35.6	32.5	35.6	33.0	34.6	35.1
	3.4	2.3	2.3	------	3.7	------	3.7	3.7	------	2.4	5.1	2.3	5.1	1.4	.9
	------	.9	1.1	------	------	------	.8	1.5	------	------	1.3	1.6	1.5	------	------
wo	------	1.2	1.3	------	------	------	.2	------	------	------	------	.1	------	------	------
en	------	------	.2	------	------	------	.1	------	------	------	------	------	------	------	------
fs	------	1.3	1.2	------	------	------	.2	------	------	------	------	.1	------	------	------
en	.3	------	.3	.1	------	.1	------	.1	------	.1	.1	.1	------	------	------
fs	------	2.6	1.3	1.3	2.9	2.0	3.6	3.2	1.5	2.1	3.2	3.6	3.0	1.5	1.3
	2.1	------	------	.9	------	2.3	------	------	.9	.2	------	------	------	.5	.3
	.5	.4	.5	.3	.5	.3	.5	.4	.2	.3	.5	.5	.5	.2	.2
	.1	------	.2	------	------	------	.1	------	------	------	------	------	------	Tr.	Tr.
	.3	------	------	------	------	------	.3	------	------	.2	.2	------	------	------	------
Fe_2	.1	------	.2	.3	------	------	.5	.4	.7	.3	.3	.3	.3	.5	.5
Cl	.1	------	.3	.4	.5	.7	.4	.3	.3	.3	.2	.2	.2	.3	.3
F	.3	------	------	.3	.8	1.4	------	.8	------	.2	------	------	------	------	------
ner	------	------	------	------	------	------	------	------	------	------	------	Tr.	------	------	------
emics [4]	(5) 7.1	------ 8.7	------ 8.6	(5) 2.9	------ 7.1	------ 4.7	------ 9.7	------ 9.3	(5) 3.3	------ 5.4	------ 10.5	------ 9.1	------ 10.4	------ 4.1	------ 3.7

See footnotes at end of table.

TABLE 2.—*Chemical analyses and norms of comenditic obsidians*—Continued

	16	17	18	19	20	21	22	23	24	25	26	27	28	29
Chemical analyses—Continued														
iO_2	71.52	74.3	75.8	73.6	71.4	69.47	69.5	70.2	74.22	72.6	72.3	72.7	69.80	69.60
l_2O_3	13.95	12.01	12.14	12.04	12.40	12.84	13.25	12.55	12.25	12.78	13.18	12.87	14.90	14.60
e_2O_3	.74	.88	.80	1.26	1.22	1.41	1.05	1.14	.40	.88	.82	.86	1.17	.84
eO	2.72	1.46	.94	1.87	2.14	3.70	3.21	3.10	2.52	2.02	2.25	2.06	1.98	2.10
lgO	.05	.00	.01	.05	.03	.17	.02	.02	Tr.	.01	.01	.01	.20	.20
aO	1.12	.32	.30	.38	.47	.71	.88	.77	.98	.69	.84	.62	.59	.48
a_2O	5.97	5.86	5.22	5.74	5.90	5.66	5.87	5.72	5.21	5.77	5.83	5.76	6.15	6.25
K_2O	3.49	4.58	4.48	4.51	4.70	4.83	4.93	4.82	3.82	3.84	3.78	3.89	4.50	4.50
H_2O-	.05	.22	.14	.18	------	.04	------	------	.16	------	------	------	.08	.11
H_2O+	.42	.23	.12	.00	.20	.35	.13	.25	.67	.31	.22	.27	.26	.52
iO_2	.26	.15	.09	.20	.23	.29	.32	.31	.09	.20	.21	.20	.30	.29
rO_2	------	------	------	------	.18	------	.20	.21	------	.14	.11	.14	------	------
O_2	------	------	------	------	------	.12	------	------	------	------	------	------	.06	.07
rO_4	.02	.00	.00	.01	.03	.03	.03	.03	Tr.	.02	.01	.01	.03	.04
	------	------	------	------	------	.01	------	------	------	------	------	------	------	------
nO	.11	.08	.06	.07	.18	.13	.12	.11	.06	.08	.08	.07	.10	.10
	------	.17	.25	.19	.26	.28	.25	.31	.05	.21	.20	.20	------	------
	------	.34	.29	.26	.23	------	.16	.18	------	.19	.18	.18	------	------
Subtotal	99.82	100.10	100.64	100.36	99.52	100.04	99.92	99.72	100.43	99.74	100.02	99.84	100.12	99.70
$\equiv(F,Cl)_2$	------	.18	.18	.15	.16	.06	.12	.15	.01	.13	.12	.12	------	------
Total	99.82	99.92	100.46	100.21	99.36	99.98	99.80	99.57	100.42	99.61	99.90	99.72	100.12	99.70
gpaitic index [1]	1.01	1.15	1.10	1.20	1.19	1.13	1.13	1.16	1.04	1.07	1.04	1.06	1.01	1.04
e as FeO [2]	3.39	2.25	1.66	3.00	3.24	4.97	4.16	4.13	2.88	2.81	2.99	2.83	3.03	2.86
$eO/(FeO+Fe_2O_3)$ [2]	.79	.62	.54	.60	.64	.72	.76	.73	.86	.70	.73	.71	.63	.71
Na_2O/K_2O [2]	1.71	1.17	1.16	1.27	1.26	1.17	1.19	1.19	1.36	1.50	1.54	1.48	1.37	1.39
lolecular:														
SiO_2	81.9	83.0	83.4	82.6	81.6	81.2	80.7	81.4	83.4	82.4	82.1	82.8	79.9	79.9
Al_2O_3	9.0	7.9	7.9	7.9	8.4	8.8	9.1	8.6	8.1	8.5	8.8	8.6	10.0	9.9
Na_2O+K_2O	9.1	9.1	8.7	9.5	10.0	10.0	10.2	10.0	8.5	9.1	9.1	9.1	10.1	10.3
$100\ Na_2O/(Na_2O+K_2O)$	72.1	63.7	63.7	66.0	65.5	64.1	64.6	64.3	67.2	69.4	70.1	69.4	67.3	67.8
CIPW norms—Continued														
	20.3	28.9	31.0	27.0	22.7	17.9	17.1	20.5	27.1	24.1	23.0	24.1	15.0	14.4
	20.6	27.2	26.7	26.7	27.8	28.4	28.9	28.4	22.5	22.8	22.2	22.8	26.6	26.6
b	49.3	36.2	37.2	36.7	37.7	39.3	40.9	37.7	41.7	44.0	46.6	44.5	51.6	50.0
c	1.4	2.8	2.3	3.7	3.7	4.2	3.2	3.2	1.2	2.5	.9	2.3	.4	2.4
s	------	.7	.1	1.3	1.5	.4	.9	1.1	.2	.1	------	------	------	------
i:														
wo	2.8	------	------	------	.2	1.0	1.4	1.1	2.0	.8	1.2	.8	1.0	.7
en	.1	------	------	------	.1	.1	.1	.1	------	------	------	------	.2	.1
fs	2.5	------	------	------	.1	1.1	1.5	1.2	2.3	.9	1.3	.9	.9	.7
y:														
en	------	------	------	.1	------	.4	------	------	------	------	------	------	.3	.4
fs	2.0	2.5	1.7	3.2	3.7	5.5	4.2	4.2	2.8	2.6	2.2	2.6	1.6	2.9
	------	------	------	------	------	------	------	------	------	------	.7	------	1.5	------
t	.3	------	------	------	------	------	------	------	------	------	------	------	------	------
	.6	.8	.2	.5	.5	.5	.6	.6	.2	.4	.4	.5	.6	.6
	------	------	------	------	------	.1	------	------	------	------	------	------	.1	.1
p	------	------	------	------	------	.8	------	.8	------	.2	.2	.2	------	------
	------	------	------	------	------	------	.3	.4	.1	.4	.4	.4	------	------
CaF_2	------	.5	.4	.6	.5	------	.3	.4	.1	.4	.4	.4	------	------
NaCl	------	.2	.5	.4	.4	.5	.4	.5	.1	------	------	------	------	------
NaF	------	.3	.3	------	------	------	------	------	------	------	------	------	------	------
c	------	------	------	------	------	.3	------	------	------	------	------	------	.1	.2
Other	------	------	------	------	------	------	------	------	------	------	------	------	------	------
femics [6]	9.2	6.8	4.7	9.4	10.3	13.6	12.2	11.8	8.2	7.7	7.1	7.5	6.6	8.0

[1] Molecular $(Na_2O+K_2O)/Al_2O_3$.
[2] By weight.
[3] Normative hematite, 0.6 percent.
[4] Normative corumdum, 0.4 percent.
[5] Normative corumdum, 0.1 percent.
[6] Sum of normative femic constituents, as defined by Washington (1917).

TABLE 3.—*Chemical analyses and norms of pantelleritic obsidians and separated glasses*

Details of the specimens are given on p. N23. Asterisk indicates residual glass separated from the whole rock sample having the preceding number. Tr. indicates trace. Data in weight percent except for ratios and indices]

	1 30	1 31	1 32	33	* 34	35	* 36	37	* 38	39	* 40	41	42	43	44
Chemical analyses															
O_2	69.81	69.56	70.07	67.5	69.9	68.6	70.1	69.7	70.5	69.2	69.8	68.00	67.75	69.40	68.60
$_2O_3$	8.59	11.27	8.40	12.0	8.8	9.2	7.6	9.1	7.6	10.9	10.7	8.73	8.80	8.66	10.64
$_2O_3$	2.28	1.87	2.29	1.8	2.1	2.7	2.9	2.2	2.0	2.0	2.0	5.60	4.75	2.75	2.88
O	5.76	4.18	5.62	4.0	5.9	5.3	5.6	4.9	6.3	4.0	4.0	3.19	3.69	5.38	3.59
gO	.10	.23	.05	.13	.13	.11	.04	.07	.03	.24	.23	.38	.45	.15	.45
aO	.42	.44	.42	.50	.52	.54	.53	.39	.39	.44	.43	.60	.56	.84	.49
a_2O	6.46	6.28	6.50	6.9	6.5	6.8	7.1	6.9	7.0	6.5	6.5	6.74	6.74	6.34	6.36
$_2O$	4.49	4.60	4.47	5.2	4.7	4.6	4.6	4.8	4.6	4.9	4.8	4.82	4.46	4.34	4.80
$_2O-$	.05	.02	.03	.02	Nil	.03	.04	.01	Nil	.02	.01	.06	.00	------	.25
$_2O+$	.14	.13	.08	.38	.04	.32	.23	.33	.05	.22	.17	------	------	.44	1.18
O_2	.45	.47	.44	.49	.54	.46	.41	.38	.35	.52	.52	.35	.48	.37	.65
O_2	.25	.12	.31	.22	.20	.24	.28	.30	.27	.21	.20	------	------	------	------
$_2$	------	------	------	------	------	------	------	------	------	------	------	------	------	------	------
O_5	.13	.10	.11	.04	.04	.04	.05	.04	.04	.04	.05	.13	.21	.05	.05
$_2$	.06	.06	.02	------	------	------	------	------	------	------	------	------	------	------	------
	------	------	------	------	------	------	------	------	------	------	------	------	------	------	------
nO	.28	.28	.29	.21	.30	.31	.34	.26	.32	.29	.30	.19	.21	.33	.27
	.76	.37	.79	.62	.70	.56	.69	.72	.82	.30	.31	------	------	------	.35
	.30	.19	.32	------	------	------	------	------	------	------	------	------	------	------	.20
Subtotal	100.33	100.17	100.21	100.01	100.37	99.81	100.51	100.10	100.27	99.78	100.02	98.79	98.10	99.05	100.76
$\equiv(F,Cl)_2$	.30	.16	.31	.14	.16	.13	.16	.16	.18	.07	.07	------	------	------	.16
Total	100.03	100.01	99.90	99.87	100.21	99.68	100.35	99.94	100.09	99.71	99.95	2 98.79	2 98.10	99.05	100.60
paitic index 4	1.81	1.35	1.85	1.41	1.80	1.77	2.19	1.82	2.16	1.47	1.49	1.86	1.81	1.74	1.48
as FeO 5	7.81	5.86	7.68	5.62	7.79	7.78	8.21	6.88	8.10	5.80	5.80	8.24	7.97	7.86	6.18
$O/(FeO+Fe_2O_3)$ 5	.72	.69	.71	.69	.74	.66	.66	.69	.76	.67	.67	.36	.44	.66	.55
$_2O/K_2O$ 5	1.44	1.37	1.45	1.33	1.38	1.48	1.54	1.44	1.52	1.33	1.35	1.40	1.51	1.46	1.33
olecular:															
SiO_2	83.1	81.6	83.3	79.8	82.8	82.1	83.0	82.2	83.2	81.4	81.6	82.1	82.3	83.2	81.6
Al_2O_3	6.0	7.8	5.9	8.4	6.2	6.5	5.3	6.3	5.3	7.5	7.4	6.2	6.3	6.1	7.4
Na_2O+K_2O	10.9	10.6	10.9	11.8	11.0	11.4	11.7	11.5	11.5	11.1	11.0	11.6	11.3	10.7	11.0
100 $Na_2O/(Na_2O+K_2O)$	68.4	67.3	69.1	66.9	67.7	69.2	70.1	68.5	69.8	66.9	67.3	68.1	69.9	68.9	66.9
CIPW norms															
	28.7	21.5	29.8	16.6	27.5	24.2	29.6	26.7	30.8	21.4	22.6	22.6	23.2	26.3	21.5
	26.7	27.2	26.1	30.6	27.8	27.2	27.2	28.4	27.2	28.9	28.4	28.4	26.1	25.6	28.4
	18.9	32.5	18.3	33.0	18.9	21.5	13.6	19.9	13.6	28.8	28.3	18.3	20.4	20.4	27.8
	6.5	5.5	6.5	5.1	6.0	7.8	8.3	6.5	6.0	6.0	6.0	16.2	13.9	7.9	8.3
	4.9	2.7	5.1	3.5	5.6	5.4	7.4	6.0	7.7	4.0	4.2	4.8	4.9	5.6	3.3
wo	------	.2	------	.9	.9	1.0	1.0	.7	.7	.8	.8	.9	.6	1.6	.3
en	------	.1	------	.1	.1	.1	Tr.	.1	.1	.1	.1	.2	.1	.1	.1
fs	------	.1	------	1.0	1.0	1.2	1.1	.7	.7	.8	.9	.9	.6	1.7	.3
	.3	.6	.1	.3	.3	.2	.1	.2	.1	.5	.5	.8	1.0	.3	1.0
en	10.4	7.3	10.1	6.0	9.4	8.4	9.2	8.1	10.9	6.8	6.2	4.8	5.7	8.2	5.8
fs	------	------	------	------	------	------	------	------	------	------	------	------	------	------	------
	.8	.9	.8	.9	1.1	.9	.8	.8	.8	.9	.9	.6	.9	.7	1.2
	.3	.2	.3	.1	.1	.1	.1	.1	.1	.1	.1	.3	.5	.1	.1
	.4	.2	.5	.4	.4	.4	.4	.4	.4	.4	.4	------	------	------	------
F_2	.4	.3	.4	------	------	------	------	------	------	------	------	------	------	------	.4
Cl	1.3	.6	1.3	.9	1.2	.9	1.2	1.2	1.3	.5	.5	------	------	------	.6
F	.3	------	.3	------	------	------	------	------	------	------	------	------	------	------	------
	------	------	------	------	------	------	------	------	------	------	------	------	------	------	------
emics 6	23.6	17.9	23.3	17.9	24.5	25.1	28.0	23.2	27.1	19.5	19.7	29.5	28.2	26.2	20.8

See footnotes at end of table.

TABLE 3.—*Chemical analyses and norms of pantelleritic obsidians and separated glasses*—Continued

	45	46	47	48	49	50	51	52	53	54	55	56	57	58	59
Chemical analyses—Continued															
SiO_2	68.00	73.34	72.24	65.78	71.82	70.88	72.82	71.30	70.52	69.06	70.99	71.63	72.8	71.7	69.9
Al_2O_3	11.34	10.41	9.68	12.45	8.65	10.59	10.30	7.42	9.30	6.30	9.18	11.31	7.57	7.94	9.70
Fe_2O_3	3.16	3.57	1.10	2.65	1.53	1.42	.44	1.96	1.38	4.98	3.15	2.41	2.54	2.33	1.86
FeO	2.42	1.60	4.24	3.61	5.55	4.41	2.99	6.79	5.72	6.26	4.67	3.56	4.96	4.98	5.58
MgO	.45	.10	.12	.96	Tr.	.36	.22	.00	.00	.27	.19	.02	.02	.03	.05
CaO	.53	.20	1.16	1.64	.70	.48	1.48	.60	1.92	.94	.71	.41	.26	.36	.62
Na_2O	7.76	4.68	5.72	6.64	6.26	6.21	6.69	6.63	5.98	7.37	6.07	5.61	7.20	6.64	6.32
K_2O	4.72	4.82	4.37	4.82	4.28	4.75	4.67	4.26	4.01	3.39	4.24	4.56	4.22	4.34	4.55
H_2O-	.00	.18	.14	.17	.08	.07	.04	.03	.14	Tr.	.02	------	.06	------	------
H_2O+	.56	.41	.30	.04	.44	.16	.10	.19	.18	.47	.22	.25	.02	.17	.13
TiO_2	.65	.23	.41	1.07	.64	.53	.30	.61	.60	.61	.38	.36	.21	.26	.57
ZrO_2	------	.24	.21	------	------	------	------	------	------	------	------	------	------	.17	.13
CO_2	------	------	.26	------	------	------	------	------	------	------	------	------	------	------	------
P_2O_5	.06	.00	------	.07	------	.05	------	.00	.06	.07	.28	.07	.03	.03	.04
SO_3	------	------	------	------	------	------	------	------	------	.47	------	------	------	------	------
S	------	------	------	------	------	------	------	------	------	------	------	------	------	------	------
MnO	.21	.12	.17	------	.25	.11	.03	.36	.24	.17	.25	.20	.27	.26	.28
Cl	.51	.07	.18	.13	------	.18	.30	------	------	.06	------	------	.25	.20	.16
F	.20	.26	------	------	------	.17	.11	------	------	------	------	------	.34	.26	.20
Subtotal	100.57	100.23	100.30	100.03	100.20	100.37	100.49	100.15	100.05	100.42	100.35	100.39	100.75	99.67	100.09
$O\equiv(F,Cl)_2$	.20	.13	.04	.03	------	.11	.11	------	------	.01	------	------	.20	.15	.12
Total	100.37	100.10	100.26	100.00	100.20	100.26	100.38	100.15	100.05	100.41	100.35	100.39	100.55	99.52	99.97
Agpaitic index [4]	1.58	1.25	1.45	1.30	1.72	1.44	1.56	2.08	1.53	2.50	1.59	1.25	2.18	1.96	1.58
Fe as FeO [5]	5.27	4.82	5.24	6.00	6.93	5.69	3.39	8.56	6.96	10.75	7.51	5.73	7.25	7.08	7.26
$FeO/(FeO+Fe_2O_3)$ [5]	.43	.31	.79	.68	.78	.76	.87	.78	.81	.56	.60	.60	.66	.68	.75
Na_2O/K_2O [5]	1.64	.97	1.31	1.38	1.46	1.31	1.43	1.56	1.49	2.17	1.43	1.23	1.71	1.53	1.39
Molecular:															
SiO_2	79.8	84.2	83.8	79.6	83.8	82.2	82.4	84.0	83.6	84.1	83.5	82.7	83.8	83.8	82.6
Al_2O_3	7.8	7.0	6.6	8.9	6.0	7.3	6.9	5.2	6.5	4.5	6.4	7.7	5.1	5.5	6.7
Na_2O+K_2O	12.3	8.8	9.6	11.5	10.2	10.5	10.7	10.8	9.9	11.3	10.1	9.6	11.1	10.7	10.7
100 $Na_2O/(Na_2O+K_2O)$	71.4	59.8	66.7	67.7	69.2	66.7	68.4	70.4	69.1	76.8	68.5	65.5	72.0	69.9	68.0
CIPW norms—Continued															
Q	18.5	30.1	29.9	11.4	30.6	25.1	28.6	31.7	26.7	29.5	27.2	24.0	34.2	32.3	25.4
or	27.8	28.4	26.1	28.4	25.6	28.4	27.8	25.6	23.4	20.0	25.0	27.2	25.0	25.6	26.7
ab	32.0	26.7	25.2	37.2	20.4	27.8	26.7	14.2	25.7	13.6	23.6	32.5	15.2	16.8	24.6
ac	9.3	9.7	3.2	7.9	4.2	4.2	1.4	6.0	4.2	14.3	9.2	6.9	7.4	6.5	5.3
ns	4.5	------	4.0	2.1	6.5	4.4	6.1	8.2	4.9	7.4	4.0	1.6	7.7	7.0	5.3
di:															
wo	.4	------	1.7	3.2	1.4	.2	2.8	1.3	3.9	1.8	.7	.6	------	------	.6
en	.1	------	.1	1.1	------	.1	.3	------	------	.1	.1	.1	------	------	.1
fs	.3	------	1.8	2.2	1.6	.2	2.8	1.5	4.5	1.9	.7	.7	------	------	.6
hy:															
en	1.0	.3	.2	1.3	------	.9	.2	------	------	.6	.4	.1	.1	.1	.1
fs	3.5	2.6	5.5	2.7	8.2	7.1	2.4	10.5	5.3	8.8	7.8	5.7	9.3	9.4	9.3
mt	------	.2	------	------	------	------	------	------	------	------	------	------	------	------	------
il	1.2	.5	.8	2.0	1.2	1.1	.6	1.2	1.2	1.2	.8	.8	.4	.5	1.1
ap	.1	------	------	.2	------	------	------	------	------	.2	.7	.2	Tr.	.1	.1
z	------	.4	.3	------	------	------	------	------	------	------	------	------	------	.2	.2
CaF_2	.4	.3	------	------	------	.4	.2	------	------	------	------	------	.4	.5	.4
NaCl	.8	.1	.3	.2	------	.3	.5	------	------	.1	------	------	.4	.4	.3
NaF	------	.3	------	------	------	------	------	------	------	------	------	------	.4	.1	------
cc	------	------	.6	------	------	------	------	------	------	------	------	------	------	------	------
Σ femics [4]	20.8	13.6	17.9	22.7	28.1	18.6	16.8	28.7	24.0	36.3	24.4	16.6	25.3	24.1	22.9

See footnotes at end of table.

TABLE 3.—*Chemical analyses and norms of pantelleritic obsidians and separated glasses*—Continued

	60	61	62	63	64	65	66	67	68	69	70	71	72	73	74
Chemical analyses—Continued															
----------	71.7	70.1	71.0	70.5	70.4	71.2	70.9	69.3	72.3	74.4	74.4	74.2	74.3	74.3	74.3
----------	7.86	10.00	8.81	8.76	8.70	8.95	7.86	9.88	7.74	9.42	9.41	9.40	9.35	9.44	9.48
----------	2.76	2.31	2.28	2.21	3.24	2.26	2.63	1.99	2.61	1.77	1.65	1.74	1.28	1.61	1.79
----------	4.69	4.63	5.40	5.37	4.68	5.05	5.82	5.50	4.92	2.88	2.90	2.90	3.34	2.82	2.90
----------	.02	.10	.04	.04	.02	.02	.03	.07	.02	.16	.13	.15	.20	.12	.16
----------	.26	.60	.36	.40	.41	.41	.40	.67	.24	.20	.24	.21	.20	.28	.18
----------	7.07	6.19	6.68	6.44	6.43	6.49	6.94	6.82	7.08	5.83	5.49	5.23	5.66	5.29	5.52
----------	4.21	4.55	4.41	4.52	4.47	4.52	4.24	4.54	4.16	4.29	4.39	4.26	4.44	4.39	4.48
----------	.07	------	.16	------	------	------	.08	------	.03	------	------	------	------	------	------
----------	.00	.14	.00	.20	.14	.15	.04	.14	.10	.47	.41	.40	.32	.36	.31
----------	.24	.50	.51	.50	.52	.45	.41	.57	.22	.35	.27	.27	.26	.27	.27
----------	------	.16	------	.15	.13	.14	------	.13	------	.25	.25	.25	.25	.25	.25
----------	------	------	------	------	------	------	------	------	------	------	------	------	------	------	------
----------	.03	.04	.04	.03	.03	.02	.05	.04	.03	------	------	------	------	------	------
----------	------	------	------	------	------	------	------	------	------	------	------	------	------	------	------
----------	------	------	------	------	------	------	------	------	------	------	------	------	------	------	------
----------	.26	.27	.29	.29	.29	.26	.29	.29	.27	.22	.21	.21	.22	.21	.20
----------	.21	.19	.19	.20	.20	.20	.28	.15	.23	.16	.16	.16	.17	.16	.16
----------	.26	.21	.24	.23	.22	.22	.80	.18	.29	.25	.25	.24	.25	.23	.23
Subtotal----------	99.64	99.99	100.41	99.84	99.88	100.34	100.17	99.77	100.24	100.15	100.16	99.62	100.24	99.73	100.23
$F,Cl)_2$----------	.16	.13	.14	.14	.14	.14	.19	.12	.17	.15	.15	.14	.15	.14	.14
Total----------	99.48	99.86	100.27	99.70	99.74	100.20	99.98	99.68	100.07	100.00	100.01	99.48	100.09	99.59	100.09
itic index [4]----------	2.07	1.51	1.80	1.77	1.78	1.74	2.04	1.55	2.08	1.43	1.48	1.40	1.50	1.43	1.47
FeO [5]----------	7.18	6.71	7.45	7.86	7.60	7.09	8.10	7.29	7.27	4.47	4.39	4.47	4.49	4.27	4.51
$(FeO+Fe_2O_3)$ [5]----------	.63	.67	.73	.71	.59	.69	.70	.73	.65	.62	.64	.63	.72	.64	.62
$/K_2O$ [5]----------	1.68	1.36	1.51	1.42	1.44	1.44	1.64	1.39	1.70	1.24	1.25	1.23	1.27	1.21	1.23
ular:															
iO_2----------	83.5	82.6	83.1	83.1	83.2	83.1	83.5	82.4	83.7	84.7	84.4	84.8	84.3	84.7	84.8
l_2O_3----------	5.4	6.9	6.0	6.1	6.0	6.2	5.4	6.9	5.3	6.3	6.3	6.3	6.3	6.3	6.3
Na_2O+K_2O----------	11.1	10.5	10.9	10.8	10.8	10.7	11.1	10.7	11.0	9.0	9.3	8.9	9.4	9.0	9.4
$00\ Na_2O/(Na_2O+K_2O)$----------	71.7	67.6	69.7	68.4	68.9	68.6	71.3	68.0	72.2	65.2	65.4	65.1	65.9	64.4	65.0
CIPW norms—Continued															
----------	32.2	25.1	29.1	28.6	28.3	29.0	30.9	23.9	33.2	34.3	34.1	34.1	33.9	34.4	33.5
----------	25.0	26.7	26.1	26.7	26.1	26.7	25.0	26.7	24.5	25.6	26.1	25.6	26.1	26.1	26.7
----------	16.8	26.2	20.4	19.9	19.9	21.0	16.8	25.7	16.8	24.1	23.6	24.1	23.6	23.6	23.6
----------	7.9	6.5	6.5	6.5	9.7	6.5	7.4	6.0	7.4	5.1	5.1	5.1	3.7	4.6	5.1
----------	7.3	4.1	6.2	6.0	5.1	5.9	7.1	4.6	7.2	3.3	3.8	3.1	4.4	3.4	3.8
----------	------	.5	------	.1	.1	.1	------	.8	------	------	------	------	------	------	------
----------	------	.1	------	.1	.1	.1	------	.1	------	------	------	------	------	------	------
----------	------	.5	------	.1	.1	.1	------	.8	------	------	------	------	------	------	------
----------	.1	.2	.1	.1	------	------	.1	.2	.1	.4	.3	.4	.5	.3	.4
----------	8.7	7.7	9.6	9.6	8.2	8.9	10.6	9.0	9.2	5.1	5.1	5.1	5.9	5.0	5.1
----------	.5	.9	1.0	.9	1.0	.9	.8	1.1	.4	.6	.6	.6	.6	.6	.6
----------	Tr.	.1	.1	------	------	------	.1	.1	Tr.	------	------	------	------	------	------
----------	------	.2	------	.2	.2	.2	------	.2	------	.4	.4	.4	.4	.4	.4
----------	.4	.4	.4	.5	.5	.5	.5	.4	.3	.3	.3	.3	.3	.4	.3
----------	.4	.3	.3	.4	.4	.4	.5	.2	.4	.3	.3	.3	.3	.3	.3
----------	.2	------	.1	------	------	------	.2	------	.3	------	------	------	------	------	------
ies [4]----------	24.9	21.0	23.9	23.9	24.8	23.0	26.6	23.1	24.6	14.8	15.2	14.6	15.4	14.3	15.3

footnotes at end of table.

TABLE 3.—*Chemical analyses and norms of pantelleritic obsidians and separated glasses*—Continued

	75	76	77	78	79	80	81	82	83	84	85	86	87	88	89
Chemical analyses—Continued															
SiO_2	73.8	74.0	74.1	74.9	74.8	64.00	70.36	70.4	70.0	66.4	70.45	71.39	70.61	70.13	70.86
Al_2O_3	9.54	9.46	9.62	9.46	9.69	10.43	9.63	7.95	7.92	9.73	8.99	9.57	8.59	7.97	8.48
Fe_2O_3	1.73	1.91	1.76	1.53	1.61	6.80	1.72	2.47	2.68	2.53	2.33	2.48	2.52	2.77	2.40
FeO	2.97	2.65	2.84	2.87	2.92	8.86	5.42	5.97	5.78	6.83	5.22	4.22	5.96	5.27	5.02
MgO	.19	.23	.20	.17	.14	.34	.06	.03	.03	.02	.05	.20	.07	.07	.52
CaO	.23	.25	.20	.20	.30	1.45	.30	.50	.48	.77	.48	.55	.61	.55	.30
Na_2O	5.62	5.42	5.53	5.49	5.53	7.59	6.73	7.35	7.37	7.60	6.71	6.39	6.77	7.46	6.68
K_2O	4.43	4.41	4.37	4.47	4.38	4.69	4.43	4.31	4.28	4.41	4.55	4.40	4.46	4.24	4.50
H_2O-	------	------	------	------	------	} .17	{ .01	------	------	------	------	Nil	} 0.10	{ .06	Nil
H_2O+	.49	.30	.29	.40	.87		.10	.18	.23	.19	.07	.35		.54	.20
TiO_2	.26	.27	.29	.27	.28	.78	.33	.32	.32	.59	.35	.33	.15	.30	.33
ZrO_2	.25	.25	.24	.24	.25	------	------	.26	.26	.16	------	------	------	.22	------
CO_2	------	------	------	------	------	------	------	------	------	------	------	.00	------	------	.00
P_2O_5	------	------	------	------	------	------	.03	.04	.03	.06	.01	.02	------	.04	.02
SO_3	------	------	------	------	------	------	------	------	------	------	------	------	------	------	------
S	------	------	------	------	------	------	------	------	------	------	------	------	------	------	------
MnO	.23	.21	.22	.22	.22	.87	.25	.26	.26	.26	.21	.21	.34	.26	.25
Cl	.17	.16	.16	.16	.16	------	.40	.33	.34	.23	------	.32	------	.37	.42
F	.25	.25	.25	.25	.24	------	.17	.40	.41	.30	------	.41	------	------	.69
Subtotal	100.16	99.77	100.07	100.63	100.89	99.88	99.94	100.77	100.39	100.08	99.42	100.84	100.18	100.25	100.67
$O \equiv (F,Cl)_2$	.15	.15	.15	.15	.14	------	.16	.24	.25	.18	------	.25	------	.08	.39
Total	100.01	99.62	99.92	100.48	100.75	99.88	99.78	100.53	100.14	99.90	99.42	100.59	100.18	100.17	100.28
Agpaitic index [4]	1.47	1.44	1.44	1.46	1.43	1.68	1.66	2.12	2.10	1.79	1.77	1.60	1.86	2.12	1.88
Fe as FeO [5]	4.53	4.37	4.43	4.25	4.37	9.54	6.97	8.20	8.19	9.11	7.32	6.45	8.23	7.77	7.18
$FeO/(FeO+Fe_2O_3)$ [5]	.63	.58	.62	.65	.64	.88	.76	.71	.68	.73	.69	.63	.70	.66	.68
Na_2O/K_2O [5]	1.27	1.23	1.27	1.23	1.26	1.65	1.52	1.71	1.72	1.72	1.47	1.45	1.52	1.76	1.48
Molecular:															
SiO_2	84.1	84.4	84.3	84.4	84.3	79.6	82.4	82.8	82.8	80.7	82.8	83.0	83.0	82.8	83.1
Al_2O_3	6.4	6.4	6.4	6.3	6.4	7.6	6.6	5.5	5.5	6.9	6.2	6.5	6.0	5.5	5.8
Na_2O+K_2O	9.5	9.2	9.3	9.3	9.3	12.8	11.0	11.7	11.7	12.4	11.0	10.5	11.0	11.7	11.1
100 $Na_2O/(Na_2O+K_2O)$	65.9	64.9	65.9	65.4	65.4	71.3	69.9	72.1	72.6	72.4	69.2	68.7	69.9	72.7	69.2
CIPW norms—Continued															
Q	32.9	33.3	33.1	34.5	33.7	11.0	26.6	29.5	29.0	19.2	27.1	27.7	27.1	28.8	30.0
or	26.1	26.1	26.1	26.7	26.1	27.2	26.1	25.6	25.0	26.1	26.7	26.1	26.1	25.1	26.7
ab	24.1	24.1	24.6	23.6	25.2	27.8	24.6	16.8	17.3	25.2	21.0	24.6	19.4	17.4	18.3
ac	5.1	5.5	5.1	4.2	4.6	18.0	5.1	7.2	7.9	7.4	6.7	7.4	7.4	8.0	6.9
ns	3.8	3.3	3.5	4.0	3.5	3.7	5.6	8.0	7.6	6.8	6.5	4.3	6.8	7.9	4.8
di:															
wo	------	------	------	------	------	3.0	------	------	------	.5	1.0	------	1.3	1.0	------
en	------	------	------	------	------	.4	------	------	------	.1	.1	------	Tr.	Tr.	------
fs	------	------	------	------	------	3.0	------	------	------	.5	1.1	------	1.4	1.2	------
hy:															
en	.5	.6	.5	.4	.4	.5	.2	.1	.1	------	.1	.5	.2	.2	1.3
fs	5.4	4.8	5.0	5.1	5.1	3.5	9.8	10.9	10.6	11.6	8.3	7.7	9.9	8.5	9.2
mt	------	------	------	------	------	------	------	------	------	------	------	------	------	------	------
il	.6	.6	.6	.6	.6	1.5	.6	.6	.6	1.2	.7	.6	.8	.6	.6
ap	------	------	------	------	------	------	.1	.1	Tr.	.1	------	------	------	.1	------
z	.4	.4	.4	.4	.4	------	------	.4	.4	.2	------	------	------	.3	------
CaF_2	.3	.4	.3	.3	.4	------	.4	.6	.7	.6	------	.8	------	------	.4
NaCl	.3	.3	.3	.3	.3	------	.6	.5	.6	.4	------	.5	------	.6	.7
NaF	------	------	------	------	------	------	------	.2	.2	------	------	.1	------	------	1.1
cc	------	------	------	------	------	------	------	------	------	------	------	------	------	------	------
Σ femics [6]	15.7	15.2	15.0	14.6	14.6	33.6	21.8	27.5	27.5	28.8	24.5	21.3	27.3	27.5	23.2

See footnotes at end of table.

TABLE 3.—*Chemical analyses and norms of pantelleritic obsidians and separated glasses*—Continued

	90	91	92	93	94	95	96	97	98	99	100	101	102	103	104
Chemical analyses—Continued															
₂	69.25	73.4	74.6	73.1	74.4	74.7	72.4	72.5	73.5	74.00	74.30	74.29	72.79	73.02	68.91
O₃	9.10	9.05	9.95	9.60	10.4	10.1	8.8	9.8	8.9	10.41	9.88	9.73	9.77	9.56	10.83
O₂	3.70	2.35	1.96	2.15	1.94	1.93	2.5	2.3	2.4	1.68	1.65	1.91	2.04	2.00	2.91
	2.61	3.80	2.80	3.75	2.50	2.45	3.4	3.5	3.8	2.74	2.81	2.71	3.57	3.75	4.56
O	.01	<.01	<.01	<.01	<.01	<.01	.2	<.1	.15	.01	.02	.01	.05	.05	.22
	.06	.21	.21	.26	.26	.20	.45	.15	.45	.19	.28	.25	.29	.32	.24
O	7.00	6.20	5.60	6.20	5.55	5.60	6.3	6.3	6.6	5.69	5.68	5.80	6.39	6.32	6.96
O	4.29	4.25	4.30	4.30	4.35	4.25	4.3	4.6	4.2	4.37	4.32	4.38	4.36	4.30	4.46
	.01	------	------	------	------	------	------	.10	------	.05	Nil	Nil	Nil	Nil	.10
O−	.14	.15	.18	.16	.16	.29	------	.15	------	.18	.32	.18	.08	Tr.	.26
O+	.25	.15	.21	.23	.24	.22	.17	.29	.14	.23	.20	.19	.25	.23	.40
₂	.78	.21	.18	.16	.15	.15	------	------	------	.14	.20	.22	.16	.17	------
₂	.00	.21	.10	.11	<.01	.05	------	------	------	------	------	------	------	------	------
	.01	.01	.01	.01	.01	.01	.06	.04	.03	.01	.02	.01	.02	.02	.02
₅	.08	------	------	------	------	------	------	------	------	------	------	------	------	------	------
	------	.02	.02	.01	.02	.03	------	------	------	------	------	------	------	------	------
O	.19	.19	.12	.14	.12	.10	.08	.16	.10	.10	.10	.11	.13	.14	.25
	.78	.24	.23	------	------	------	------	------	------	.21	.22	.22	.21	.17	------
	1.30	------	------	------	------	------	------	------	------	.13	------	------	------	------	------
Subtotal	99.56	100.44	100.47	100.18	100.10	100.08	98.66	99.89	100.27	100.09	100.00	100.01	100.11	100.05	100.12
(F,Cl)₂	.72	.05	.05	------	------	------	------	------	------	.10	.05	.05	.05	.04	------
Total	98.84	100.39	100.42	100.18	100.10	100.08	98.66	99.89	100.27	99.99	99.95	99.96	100.06	100.01	100.12
aitic index [4]	1.79	1.63	1.39	1.55	1.33	1.36	1.72	1.57	1.74	1.35	1.42	1.47	1.55	1.57	1.50
as FeO [5]	5.94	5.92	4.57	5.69	4.25	4.19	5.65	5.57	5.96	4.25	4.30	4.43	5.41	5.55	7.18
)/(FeO+Fe₂O₃) [5]	.41	.62	.59	.64	.56	.56	.58	.60	.61	.62	.63	.59	.64	.65	.61
O/K₂O [5]	1.63	1.46	1.30	1.44	1.28	1.82	1.47	1.87	1.57	1.30	1.31	1.32	1.47	1.47	1.56
lecular:															
SiO_2	82.3	83.9	84.2	83.5	83.9	84.1	83.7	83.0	83.7	83.7	84.0	84.0	83.2	83.4	81.2
Al_2O_3	6.4	6.1	6.6	6.5	6.9	6.7	6.0	6.6	6.0	6.9	6.6	6.5	6.6	6.4	7.5
Na_2O+K_2O	11.3	10.0	9.2	10.0	9.2	9.2	10.3	10.4	10.3	9.4	9.4	9.5	10.2	10.2	11.3
100 $Na_2O/(Na_2O+K_2O)$	71.1	69.0	66.2	68.5	66.2	66.7	68.9	67.5	70.2	66.7	66.7	67.1	69.1	68.9	70.4
CIPW norms—Continued															
	28.9	32.1	32.4	30.2	31.1	32.5	31.3	29.1	31.7	30.7	32.6	32.6	29.6	30.3	19.8
	25.6	25.0	25.6	25.4	25.7	25.1	25.6	27.2	26.0	26.1	25.5	25.9	25.8	25.4	26.4
	22.5	23.1	27.2	25.4	29.3	28.3	21.0	24.6	22.0	28.8	26.8	25.7	26.0	25.2	30.9
	10.6	6.9	5.5	6.2	5.6	5.6	7.4	6.5	6.9	5.1	4.8	5.5	5.9	5.8	8.4
	.4	4.6	2.8	4.6	2.6	3.0	5.6	5.0	6.1	2.8	3.3	3.6	4.6	4.8	4.3
wo	------	------	.2	.2	.5	.3	.8	.2	.9	------	.5	.5	.5	.6	.5
en	------	------	------	------	------	------	.1	------	.1	------	.1	------	------	------	.1
fs	------	------	.3	.3	.6	.3	.8	.3	1.0	------	.5	.6	.6	.7	.4
	------	------	------	------	------	------	.4	------	.4	------	------	------	.1	.1	.5
en	4.8	7.1	4.8	6.3	3.8	4.0	5.3	5.9	6.0	5.1	4.5	4.3	5.9	6.0	7.6
fs	------	------	------	------	------	------	------	------	------	------	------	------	------	------	------
	.5	.3	.4	.4	.5	.4	.3	.6	.3	.5	.4	.4	.5	.4	.8
	------	Tr.	Tr.	Tr.	Tr.	Tr.	.1	.1	.1	------	.1	Tr.	.1	.1	Tr.
	1.1	.3	.3	.2	.2	.2	------	------	------	.2	.3	.3	.2	.3	------
₂	.1	------	------	------	------	------	------	------	------	.3	------	------	------	------	------
Cl	1.3	.4	.4	------	------	------	------	------	------	.4	.4	.4	.4	.3	------
F	2.8	------	------	------	------	------	------	------	------	------	------	------	------	------	------
	------	.4	.2	.3	------	.1	------	------	------	------	------	------	------	------	------
emics [6]	16.4	19.3	14.2	18.3	13.6	13.7	20.8	18.6	21.8	13.8	14.2	14.9	18.2	18.5	22.6

Additional analytical data on this sample given he explanation to tables 2–8.
Also loss on ignition, 0.46 percent.

[3] Also loss on ignition 0.95 percent.
[4] Molecular $(Na_2O+K_2O)/Al_2O_3$.
[5] By weight.

[6] Sum of normative femic constituents, as defined by Washington (1917).

TABLE 4.—*Chemical analyses and norms of comenditic and pantelleritic trachyte obsidians*

[Details of the specimens are given on p. N25. Tr. indicates trace. Data in weight percent except for ratios and indices]

	Comenditic			Pantelleritic					
	105	106	107	108	109	110	111	112	113
Chemical analyses									
SiO_2	64.96	63.0	62.5	63.40	63.1	62.7	62.8	61.1	62.3
Al_2O_3	15.06	15.8	15.21	12.06	12.41	12.50	12.36	12.59	12.99
Fe_2O_3	.65	2.6	1.15	3.50	2.05	2.04	2.11	1.64	3.87
FeO	4.32	3.3	5.55	5.70	6.97	6.90	6.94	7.54	4.67
MgO	Nil	.42	.33	.31	.16	.18	.18	.23	.35
CaO	1.58	1.9	1.45	.99	1.12	1.20	1.13	1.20	1.28
Na_2O	6.79	6.4	7.18	7.95	8.43	8.52	8.42	8.56	7.44
K_2O	5.45	5.1	5.20	4.55	4.57	4.72	4.54	4.68	4.80
H_2O-	.26	.03	-----	.03	-----	-----	-----	.13	.14
H_2O+	.52	.24	.30	.24	.14	.19	.05	.00	.03
TiO_2	.59	.60	.75	.73	.69	.69	.70	.65	.82
ZrO_2	-----	.11	.03	-----	.13	.12	.13	-----	-----
P_2O_5	.05	.12	.14	.10	.09	.10	.09	.11	.12
MnO	.15	.18	.28	.40	.35	.35	.36	.33	.28
Cl	-----	-----	.10	-----	.23	.22	.23	.24	.13
F	-----	-----	.17	-----	.36	.34	.36	.30	.26
Subtotal	100.38	99.8	100.34	99.96	100.80	100.77	100.40	99.30	99.48
$O \equiv (F,Cl)_2$	-----	-----	.09	-----	.20	.19	.20	.18	.14
Total	100.38	99.8	100.25	99.96	100.60	100.58	100.20	99.12	99.34
Agpaitic Index [1]	1.14	1.01	1.15	1.49	1.52	1.52	1.52	1.53	1.35
Fe as FeO [2]	4.91	5.64	6.59	8.85	8.82	8.74	8.84	9.02	8.16
$FeO/(FeO+Fe_2O_3)$ [2]	.87	.56	.83	.62	.77	.77	.77	.82	.55
Na_2O/K_2O [2]	1.25	1.25	1.38	1.75	1.84	1.81	1.85	1.83	1.55
Molecular:									
SiO_2	77.4	77.1	76.5	78.2	77.4	77.1	77.4	76.6	77.7
Al_2O_3	10.6	11.4	10.9	8.7	9.0	9.1	9.0	9.2	9.5
Na_2O+K_2O	12.0	11.5	12.6	13.1	13.6	13.8	13.5	14.2	12.8
$100\ Na_2O/(Na_2O+K_2O)$	65.5	65.6	67.8	72.7	73.5	73.3	73.9	73.4	70.2
CIPW norms									
Q	4.7	2.6	0.3	7.5	6.8	6.0	6.7	4.2	4.8
or	32.2	30.0	30.6	26.7	27.2	27.8	26.7	27.8	28.4
ab	47.2	52.9	49.3	37.2	38.3	38.3	38.8	38.3	39.8
ac	1.8	.9	3.2	10.2	6.0	6.0	6.0	4.6	11.1
ns	2.0	-----	1.7	4.4	5.7	5.9	5.5	6.3	2.2
di:									
wo	3.1	3.6	2.2	1.9	.9	1.0	.9	1.2	1.5
en	-----	.8	.2	.2	.1	.1	.1	.1	.2
fs	3.6	3.0	2.2	1.9	.9	1.0	.9	1.3	1.5
hy:									
en	-----	.2	.6	.7	.3	.3	.3	.5	.7
fs	3.7	.6	7.3	8.1	11.4	11.1	11.2	12.1	6.3
mt	-----	3.2	-----	-----	-----	-----	-----	-----	-----
il	1.1	1.2	1.4	1.4	1.4	1.4	1.4	1.2	1.5
ap	.1	.3	.3	.2	.3	.3	.3	.3	.3
z	-----	.2	Tr.	-----	.2	.2	.2	-----	-----
CaF_2	-----	-----	.3	-----	.7	.7	.7	.6	.6
NaCl	-----	-----	.2	-----	.4	.4	.4	.4	.2
Σ femics [3]	15.4	13.8	19.4	29.0	27.7	27.8	27.3	28.2	25.9

[1] Molecular $(Na_2O+K_2O)/Al_2O_3$.
[2] By weight.
[3] Sum of normative femic constituents, as defined by Washington, 1917.

TABLE 5.—*Trace element contents, in parts per million, of comendite and pantellerite obsidians, compiled from published data*

[Specimen numbers are those used for major element analyses (tables 2 and 3). A, Average granite, from Taylor (1964), Taylor and White (1966). B, average rhyllitic volcanic rock, Taupo volcanic zone, New Zealand, from Ewart, Taylor, and Capp (1968). C, Average Arran pitchstone from Nicholls and Carmichael (1969). N.d. indicates not detected]

	Comendites				Pantellerites						
	1	11	12	15	30	31	32	33	35	37	39
	40	10	N.d.	30	30	10	30	-------	-------	-------	-------
	10	90	10	<5	50	50	50	-------	-------	-------	-------
	10	80	10	6	11	5	10	-------	-------	-------	-------
	-------	-------	-------	-------	-------	-------	-------	.70	.67	.48	.36
	<5	N.d.	N.d.	<2	<5	<5	<5	.9	.2	1.0	.2
	<1	1	1	<1	<1	<1	<1	-------	-------	-------	-------
	-------	-------	-------	<5	-------	-------	-------	-------	-------	-------	-------
	8	2	16	<1	5	3	7	4.5	2.5	7.5	1.5
	28	39	36	80	45	43	44	-------	-------	-------	-------
	-------	-------	-------	-------	-------	-------	-------	-------	-------	-------	-------
	170	210	240	110	360	230	360	-------	-------	-------	-------
	-------	-------	-------	78	-------	-------	-------	-------	-------	-------	-------
	2	5	4	5	22	22	18	19.2	14.1	17.3	16.8
	150	70	70	70	450	320	440	260	350	370	250
	2	N.d.	N.d.	<2	3	4	3	.4	1.0	3.5	.7
	70	30	30	40	30	20	40	14	16	20	12
	-------	-------	-------	390	-------	-------	-------	150	180	200	140
	2	4	6	<2	4	6	4	-------	-------	-------	-------
	16	7	7	6	24	14	24	-------	.8	-------	.8
	6	<5	6	2	7	3	9	<5	<5	<5	<5
	-------	-------	-------	-------	-------	-------	-------	12.0	23.7	18.5	17.7
	-------	-------	-------	-------	-------	-------	-------	-------	-------	-------	-------
	-------	-------	-------	-------	-------	-------	-------	-------	-------	-------	-------
	<5	N.d.	N.d.	<5	<5	<5	<5	-------	-------	-------	-------
	140	100	110	73	220	140	230	85	180	160	130
	14	8	8	6	20	10	19	-------	-------	-------	-------
	-------	-------	-------	-------	-------	-------	-------	400	450	450	350
	1300	100	860	-------	2200	1600	2000	1500	1900	2200	1500
Rb	-------	-------	-------	104	-------	-------	-------	290	210	200	290
[1]	1.11	1.21	1.16	1.03	1.81	1.35	1.85	1.41	1.77	1.82	1.47

	Pantellerites										
	46	88	[2] 90	[3] 91	92	93	94	[3] 95	A	B	C
	80	-------	100	-------	-------	-------	-------	-------	15	-------	-------
	20	-------	5	31	27	18	20	8.6	600	870	-------
	9	-------	60	11	9.8	8.5	8.1	8.2	5	N.d.	-------
	-------	-------	-------	-------	-------	-------	-------	-------	.2	N.d.	.08
	<5	-------	<2	N.d.	N.d.	N.d.	N.d.	N.d.	2	N.d.	1.4
	<1	-------	<1	N.d.	N.d.	N.d.	N.d.	N.d.	10	1.7	-------
	-------	-------	10	6.6	6.4	4.9	4.5	5.2	5	3.3	-------
	6	-------	[4] 17	5.5	3.3	3.4	3.4	5.6	10	6	5
	36	-------	42	40	86	84	86	82	20	16	-------
	-------	-------	<100	23.5	-------	-------	-------	15.5	4	4.5	-------
	280	-------	610	180	118	93	97	95	50	28.4	-------
	-------	-------	260	79	71	56	67	59	30	35	-------
	7	-------	6	24	-------	-------	-------	12.6	2	2.6	1.6
	220	365	640	81	76	71	63	69	20	5.6	17
	2	-------	<2	N.d.	N.d.	N.d.	N.d.	N.d.	4	N.d.	1.1
	80	-------	220	41	-------	-------	-------	21	30	18	18
	-------	225	950	162	160	129	130	134	145	108	160
	3	-------	<5	1.0	1.0	.6	.7	.7	6	4.7	-------
	20	-------	50	7.2	-------	-------	-------	5.7	3	1.3	-------
	7	10	2	4.7	1.9	1.1	1.8	.3	285	125	85
	-------	-------	-------	-------	-------	-------	-------	-------	3.5	-------	-------
	-------	-------	-------	23.6	21.8	-------	17.9	17.4	17	11.3	-------
	-------	-------	-------	6.9	6.4	-------	5.4	5.1	4.8	2.5	-------
	<5	-------	<5	N.d.	N.d.	N.d.	N.d.	N.d.	40	8.5	-------
	190	160	450	190	165	145	140	145	40	27.5	32
	19	-------	54	16.1	-------	-------	-------	9.2	0.18	3.55	-------
	-------	460	-------	-------	-------	-------	-------	-------	40	-------	52
	1700	1650	6300	1520	1360	1190	1090	1100	180	160	230
Rb	-------	156	37	218	223	277	278	263	240	249	230
[1]	1.25	2.12	1.79	1.63	1.39	1.55	1.33	1.36	-------	-------	-------

[1] Additional trace element data given in explanation to tables.
[2] Includes I, n.d.; In, 0.23; Tl, 0.93.
[3] Includes I, 0.47; In, 0.18.
[4] Probably reflects contamination (Noble, 1965).
[5] Agpaitic index is molecular $(Na_2O+K_2O)/Al_2O_3$.

TABLE 6.—*Additional rare-earth-element data, in parts per million, for Mayor Island pantellerites (91, 95), average granite (A), and average Taupo volcanic zone rhyolite (B)*

[From Ewart, Taylor, and Capp (1968)]

	91	95	A	B
Ce	158	150	100	43.5
Pr	30	32.5	10	6.4
Nd	125	89	31	18.2
Sm	26	17.8	5.0	5.5
Eu	1.89	1.12	.47	1.0
Gd	22.5	14.4	2.9	4.3
Tb	4.6	3.18	.15	1.15
Dy	21	14.4	.90	4.8
Ho	7.7	4.75	.17	1.4
Er	16.8	11.3	.45	3.9
Tm	1.82	1.13	.08	.46

TABLE 8.—*Trace element contents, in parts per million, of peralkaline trachyte obsidians from central Kenya*

[Specimen numbers are those used for major element analyses (table 4). Analyst, G. R. Angell, Grant Institute of Geology, Univ. of Edinburgh. All analyses by X-ray fluorescence]

	107	109	110	111	112
Ba	30	<20	<20	<20	20
Ce	230	470	440	430	360
Cu	5	5	10	7	12
La	145	390	380	380	280
Nb	130	285	270	285	220
Ni	<5	<5	7	5	7
Pb	15	27	17	30	25
Rb	90	170	160	170	155
Sr	<5	<5	<5	<5	5
Th	20	40	37	40	35
Y	90	190	180	180	150
Zn	150	275	300	305	290
Zr	385	960	930	975	1010
K/Rb	480	223	245	222	251
A.I.[1]	1.15	1.52	1.52	1.52	1.53

[1] Agpaitic index is molecular $(Na_2O+K_2O)/Al_2O_3$.

TABLE 7.—*New determinations, in parts per million, of trace elements in comendite and pantellerite obsidians*

[Specimen numbers are those used for major element analyses (tables 2 and 3). Analyst: G. R. Angell, Grant Institute of Geology, Univ. of Edinburgh. All analyses by X-ray fluorescence]

	Comendites							
	7	8	20	22	23	25	26	27
Ba	35	<20	50	285	150	470	440	460
Ce	250	280	260	260	310	300	240	250
Cu	10	10	10	7	10	12	12	12
La	165	210	160	170	210	170	130	160
Nb	190	210	180	175	190	130	135	130
Ni	<5	7	<5	<5	<5	<5	<5	5
Pb	15	32	12	17	25	10	12	15
Rb	120	250	115	110	120	85	85	85
Sr	<5	5	<5	15	12	25	42	25
Th	22	47	22	22	27	15	17	20
Y	170	160	170	160	185	210	210	200
Zn	220	180	215	250	270	240	235	235
Zr	1250	930	1235	1300	1410	960	870	1000
K/Rb	315	150	339	372	333	375	369	380
A.I.[1]	1.15	1.24	1.19	1.13	1.16	1.07	1.04	1.06

	Pantellerites							
	57	58	59	60	61	62	63	64
Ba	295	250	660	240	420	165	140	60
Ce	400	320	260	340	300	350	300	270
Cu	10	7	<5	10	5	7	7	5
La	270	240	200	260	170	200	220	200
Nb	280	200	150	200	175	165	175	120
Ni	<5	7	5	5	<5	7	<5	<5
Pb	50	22	20	22	17	20	30	22
Rb	175	210	120	160	130	145	145	135
Sr	7	10	10	5	7	5	5	<5
Th	37	27	25	30	25	22	25	22
Y	240	190	170	210	170	180	180	160
Zn	405	350	265	350	250	280	285	260
Zr	1440	1160	895	1200	1055	1005	1025	970
K/Rb	200	172	315	218	290	252	259	275
A.I.[1]	2.18	1.96	1.58	2.07	1.51	1.80	1.77	1.78

	Pantellerites							
	65	67	68	77	79	82	83	84
Ba	75	680	245	60	50	80	50	<20
Ce	300	250	370	450	440	590	600	420
Cu	10	7	5	<5	<5	10	12	5
La	180	180	260	300	340	420	450	320
Nb	160	150	220	220	220	360	350	230
Ni	5	5	5	10	<5	5	<5	<5
Pb	27	22	25	25	30	32	35	25
Rb	145	130	175	125	125	210	195	145
Sr	<5	12	10	<5	<5	7	<5	<5
Th	30	22	32	22	25	42	42	27
Y	160	160	240	255	260	350	340	240
Zn	290	260	365	395	410	440	430	350
Zr	1010	915	1370	1600	1605	1670	1600	1120
K/Rb	259	290	197	290	291	170	182	252
A.I.[1]	1.74	1.55	2.08	1.44	1.43	2.12	2.10	1.79

[1] Agpaitic index is molecular $(Na_2O+K_2O)/Al_2O_3$.

TABLE 9.—*Coefficients of correlation for various element and element ratio pairs*

[The number of analyses used for each variable was as follows: SiO_2 113, ZrO_2 62, TiO_2 113, Al_2O_3 113, Fe_2O_3 113, FeO 113, MnO 112, MgO 113, CaO 113, Na_2O 113, K_2O 113, P_2O_5 95, H_2O+ 109, H_2O- 68, F 68, Cl 88, agpaitic index 113, Fe as FeO 118, $FeO/(FeO+Fe_2O_3)$ 113, Na_2O/K_2O 113. CO_2 has been omitted because the number of analyses (15) is too small to be statistically meaningful]

	SiO_2	ZrO_2	TiO_2	Al_2O_3	Fe_2O_3	FeO	MnO	MgO	CaO	Na_2O
ZrO_2	0.1098									
TiO_2	−.8332	−0.1937								
Al_2O_3	−.2410	−.4656	0.0672							
Fe_2O_3	−.4244	.4413	.4138	−0.4666						
FeO	−.6546	−.0300	.6382	−.4246	0.3711					
MnO	−.6192	.1215	.7023	−.4057	.5049	0.8266				
MgO	−.4861	−.0772	.5849	.1377	.3977	.1144	0.2642			
CaO	−.6868	−.3978	.6357	.4064	.0489	.3553	.2087	0.3856		
Na_2O	−.8148	.0710	.6606	−.1839	.4879	.8176	.7057	.3050	0.4231	
K_2O	−.3250	−.1588	.2726	.4113	−.0612	−.0685	.0519	.2766	.1606	−0.0049
P_2O_5	−.3753	−.1383	.4002	−.1616	.4970	.3369	.2104	.3611	.3406	.3312
H_2O+	.1021	.1620	−.0351	.1131	−.0325	−.2493	−.1191	.1600	−.0059	−.2275
H_2O-	−.0366	−.0935	.1125	.2747	−.0735	−.1711	−.1672	.0628	.2290	−.2043
F	−.1110	.8121	−.0712	−.2193	.3508	.0844	.0906	−.0277	−.2342	.2070
Cl	−.2478	.5209	.1269	−.2982	.2206	.3357	.3367	−.0403	−.1012	.3613
Agpaitic index	−.2194	.4081	.2582	−.8582	.6008	.7295	.6409	.0347	−.0891	.6235
Fe as FeO	−.6789	.1110	.6620	−.5208	.7045	.9205	.8439	.2548	.2924	.8303
$FeO/(FeO+Fe_2O_3)$	−.2103	−.2916	.1910	.0876	−.5489	.4976	.2103	−.1907	.3788	.2925
Na_2O/K_2O	−.5892	.1285	.4705	−.3396	.4690	.7580	.5872	.1517	.3239	.8907

	K_2O	P_2O_5	H_2O+	H_2O-	F	Cl	Agpaitic index	Fe as FeO	$\frac{Fe}{FeO+Fe_2O_3}$
P_2O_5	−0.1801								
H_2O+	−.0242	0.0968							
H_2O-	.1612	−.1258	0.3185						
F	−.1743	−.1399	−.1475	−0.2169					
Cl	.1663	−.0446	−.1170	−.3806	0.5485				
Agpaitic index	−.2796	.3322	−.1918	−.2924	.2795	0.4252			
Fe as FeO	−.0781	.4590	−.2053	−.1609	.1810	.3400	0.8103		
$FeO/(FeO+Fe_2O_3)$	−.0693	−.0510	−.1583	−.1254	−.2144	.1240	.0781	0.1494	
Na_2O/K_2O	−.4490	.4294	−.1788	−.2391	.2465	.2438	.6842	.7767	0.2866

TABLE 10.—*Chemical analyses and norms of two obsidians*

[Not included in tables 2–4 because the localities at which the flows crop out are not known, and thus the specimens cannot be related to any geologic information. Tr. indicates trace. Data in weight percent except for ratios and indices]

	A1	A2
SiO_2	75.88	75.2
Al_2O_3	9.67	11.7
Fe_2O_3	2.23	1.7
FeO	.83	.5
MgO	.21	.1
CaO	.72	.4
Na_2O	5.13	5.2
K_2O	4.56	4.6
H_2O-	.38	.04
H_2O+		.13
TiO_2	.10	.19
ZrO_2	-----	.16
P_2O_5	-----	.04
MnO	Tr.	.15
Total	99.71	100.11
Agpaitic Index	1.38	1.16
Fe as FeO	2.84	2.03
$FeO/(FeO+Fe_2O_3)$	.27	.77
Na_2O/K_2O	1.13	1.13

	A1	A2
Molecular:		
SiO_2	84.8	83.5
Al_2O_3	6.4	7.7
Na_2O+K_2O	8.8	8.8
$Na_2O/(Na_2O+K_2O)$	63.4	63.2
Q	35.2	29.7
or	26.7	27.2
ab	24.6	34.6
ac	6.5	5.1
ns	2.7	.9
di:		
wo	1.5	.7
en	.4	.3
fs	1.2	.5
hy:		
en	.1	-----
fs	.3	.3
il	.2	.5
ap	-----	.1
Z	-----	.2
Σ femics	12.9	8.4

A1. Pantelleritic obsidian bead, found as an artifact, Chichen Itza, Mexico. Analyst: H. S. Washington. Phenocrysts: None. Reference: Washington (1921, table 2, No. 1).

A2. Comenditic obsidian, Caucasus, U.S.S.R. Analyst: R. Thomas. Phenocrysts: No data. Reference: Butler and Smith (1962, table 2, colln. 6059). Also contains, in parts per million, Rb 220, Y 90, Nb 70, Ta 5.5, K/Rb 170 (Butler and Smith, 1962, table 1), Zn 225, Cd 0.22 (Butler and Thompson, 1967, table 1).

U.S. GOVERNMENT PRINTING OFFICE : 1972 O - 486-965

Recommendations for Further Studies on the Peralkaline Oversaturated Volcanic Rocks

R. MACDONALD *, D. K. BAILEY ** and F. BARBERI ***

Introduction

The large-scale involvement of normal sialic crust in the generation of peralkaline silicic rocks seems to be ruled out on the following grounds:

(*i*) Sr isotope ratios and the characteristic pattern of trace elements in these rocks.

(*ii*) The formation of peralkaline rocks in truly oceanic settings.

Acceptable petrogenetic theories seem, then, to fall into two groups:

A *derivative* origin, whereby peralkaline liquids are formed by differentiation of more basic, non-peralkaline magmas. This is currently the most widely accepted hypothesis among petrologists.

An *independent* origin, whereby peralkaline silicic rocks can be formed directly by melting of pre-existing rocks, with or without the partecipation of an active volatile phase. Hypotheses of this sort command rather less following than the first.

We have tried in our recent work to be careful not to expound the merits of one theory or origin to the exclusion of any other, and we urge petrologists to exercise similar caution. Whether one or both, or neither, of these hypotheses is valid, we feel that in very few examples has the case for a particular made of origin been proven. The evidence from the various field and laboratory studies gathered together in this volume suggests to us that several different modes of origin may be possible.

* Dept. of Environmental Sciences, University of Lancaster, U.K.
** Dept. of Geology, University of Reading, U.K.
*** Istituto di Mineralogia e Petrografia, Università di Pisa, Italy.

Bull. Volcanol. 38 (1974)

The following comments are meant to act as guide-lines to the sort of problems which still remain.

Tectonics

In preparing this chapter, Macdonald was struck, firstly by how little information on many critical aspects of this topic was available in the literature, and secondly by the way in which all natural tectonic settings and magma associations are to some degree unique, making categorization extremely difficult.

One important contributory factor to the first of these points is that many of the most important peralkaline terrains, both volumetrically and in range of rock type, occur in Africa, in areas where large-scale geological maps either do not exist or are of a preliminary nature, or where the available information has not been collated, *e.g.*: the extensive outcrops of peralkaline rocks on the Ethiopian plateau, the volcanics of the Tibesti Massif, and the Plio-Pleistocene trachytes of central and southern Kenya.

It is clear that full-scale mapping programmes, coupled with relevant age determinations, are still necessary to provide basic geological information in many areas, and we should stress the need for careful field observation.

It has long been appreciated that peralkaline rocks are most abundantly developed in continental rift valleys settings. Happily, information is slowly accumulating in some regions on the fine details of the relationships between magmatism and structural evolution of the rifts. For example, BAKER *et al.* (1972) have summarized available data on the relationship between episodes of doming, faulting and salic magmatism in the East African Rift System. The control of major fault planes in localizing peralkaline volcanism in several provinces is discussed by SØRENSEN (1970) and UPTON (1974) for the Gardar province, BLACK and GIROD (1970) for Niger-Nigeria, VINCENT (1970) for the Tibesti Massif, Chad, and CHAPMAN (1968) for the White Mountain Magma Series. Several other relevant contributions may be found in SØRENSEN (1974). Radiometric age dates are clarifying the long-term eruptive sequences in these and other provinces, *e.g.* VON BREEMEN and UPTON (1972), BAKER *et al.* (1972), FAIRHEAD *et al.* (1972), BARBERI *et al.* (1972 *a*; 1975 *b*).

In time one should be able to construct very sophisticated models of the structural and magmatic evolution of these peralkaline

provinces, especially where geophysical studies are providing information relevant to the interpretation of the deep structures, and these will undoubtedly help to refine our petrogenetic models. An intriguing glimpse of the possibilities is offered by the work of Barberi and his colleagues in the Afar triangle, where several magmatic series, each leading to peralkaline residuum, have been recognized. Each is related to a rather different tectonic setting within the broad rift environment, and their nature is perhaps controlled by the nature and thickness of the crust through which they penetrate, or by the rate of the related extensional process.

Magma Associations

The broad outlines of the various magma associations involving peralkaline rocks are now known. Further work should include:

Estimate of Relative Abundances of Rock Types

It cannot be doubted that derivation of peralkaline magma by crystal fractionation of basaltic liquids is a viable mechanism (WILKINSON, 1965; LINDSLEY *et al.*, 1971). It is a rather more speculative matter as to which volcanic rock series this mode of origin also applies. Among the criteria which should be used is that the observed or reasonably inferred volume relationships of the various rock types in the serie should at least be of the right order of magnitude. Though one obviously cannot expect a volcano to be a precise sampler of its products, and though a concentration of more salic materials might occur as volcanoes tap the more differentiated, upper parts of magma columns, we persist in feeling that if large amounts of certain types of magma are available in a petrographic province, then somewhere and at some time, this magma will be erupted.

We stress the need for vigorous sampling programmes from two main points of view; firstly, to cover the complete range of rock types, in terms of both composition and eruptive style, and their relative abundances; and secondly, to relate these features to the structural development of the eruptive centres and to the volcanic cycle of which they are part.

In this connection, we feel that the bimodal basalt-trachyte/pantellerite association and the volcanic sequences of areas of dominantly

salic magmatism described by MACDONALD (this volume) require explanations other than standard crystal fractionation models.

Association with Subalkaline Rocks

Small volumes of peralkaline silicic rocks occur in orogenic belts, island arcs and at continental margins (MACDONALD, this volume), in areas largely dominated by sub-alkaline or calcalkaline volcanism. The tectonic significance of these occurrences is unknown, though it is possible that they formed during extensional episodes in a compressional framework. Thus they might be useful indicators of stress regimes. In detail, the genetic relationships to the associated calcalkaline rocks deserve study, especially relative ages and volumes, fine differences in tectonic environment and comparisons of major and trace-element chemistries, including isotope contents.

Volcanology

We have been impressed by the way in which the detailed volcanological studies of Schmincke have enabled him to make estimates of such important factors as the volatile contents, temperatures of eruption and viscosities of peralkaline magmas. We reiterate his plea for more quantitative information on the volcanological aspects of those rocks, *e.g.* proportions of pyroclastic rocks to lavas and of extrusive to intrusive rocks within provinces; petrographic differences between ignimbrites and lavas in volcanic series; the need to search for and explain vertical zonation within flow units.

One of the best ways to test petrogenetic schemes will be to quantify our knowledge of the rheologies of the magmas by careful volcanological studies, and to couple this with accurate determinations of liquid and crystal densities and experimental determinations of crystallisation sequences and viscosities.

Petrography

The need for detailed petrographical and mineralogical studies of peralkaline volcanic rocks has not always been sufficiently recognized by recent works, and there are still many fields of study requiring a

much more exhaustive coverage than is currently available. The following three seem to us to be among the more important.

(*a*) Trachytes. Since trachytes occupy a critical position in most genetic schemes of peralkaline rocks, we stress the need for much more information on these rocks, whose data are especially scarce.

(*b*) Phenocrysts and modal data. Large numbers of analyses are still presented with no mineralogical data. The value of such analyses is thus considerably reduced. It is impossible, for example, to use the rocks in studies of the natural phase equilibria involved in their evolution. It is also impossible to quantitatively test models involving crystal extraction or addition.

(*c*) Mineral analyses. Such phenocryst analyses as are available come mainly from pantellerites. Data are extremely scarce for comendites and trachytes. Again, such data must be available to critically test any petrogenetic models involving crystal-liquid equilibria, while the information to be gained about the physical conditions of magma generation and evolution is invaluable (*e.g.* NICHOLLS and CARMICHAEL, 1969; LINDSLEY *et al.*, 1971).

Major-element Geochemistry

(*a*) We are encouraged that petrologists, as exemplified by the contributors to this volume, are now fully aware of the possible post-eruption alteration processes affecting peralkaline rocks, and that they are prepared to take account of such processes in discussing rock chemistry.

(*b*) There is still a need for more analyses of non-hydrated obsidians, of comenditic trachytes in particular, but of comendites and pantelleritic trachytes also.

(*c*) We must not study peralkaline rocks in isolation from the rest of the rock spectrum. In many provinces, peralkaline rocks are only one end of a continuous compositional range to subalkaline types, and the passage between the varieties should be fully explored. From this point of view, the Great Basin volcanics and those of the Tibesti Massif would seem to us fruitful ground.

(*d*) Recognition in detail of magmatic lineages leading to peralkaline rocks. Although many studies (*e.g.* NOBLE and PARKER, this vol.) refer to a spectrum of basalts leading to a spectrum of silicic residua, little comparative work has yet been done in identifying the specific links with peralkaline types. Of particular interest here

would be an understanding of why only *some* suites have peralkaline members, when, as BAILEY (this volume) points out, virtually all basaltic rocks, even of tholeiitic affinity, have peralkaline potential.

(*e*) Recognition of specific links may lead on to relating such associations to specific tectonic settings.

Minor-element Geochemistry

In general terms, the characteristic patterns of minor- and trace-element distribution are now reasonably well known (FERRARA and TREUIL, this vol.), though it should be stressed that for many extensive areas and groups of peralkaline rocks, *e.g.* the Tibesti Massif, the Ethiopian plateau and the Plio-Pleistocene plateau trachytes in Kenya, trace element data are still completely lacking.

Peralkaline silicic rocks appear to contain large amounts of F, Cl, Hf, La, Mo, Nb, Ta, Y, Zn, Zr, B, Be, Cd, Ga, Li and Sn (and perhaps Th, U), and very low contents of Ba, Cr, Sr, V and Sc, compared to subalkaline and calc-alkaline varieties. Considerable variations in abundances of these elements exist between centres, however, even within the same petrographic province. This has been variously interpreted as indicating minor-element heterogeneity of source and/or evolutionary differences of the magmas.

There is no doubt that trace element distributions in volcanic series can be an invaluable petrogenetic tool, more sensitive in some respects than the major-elements, *e.g.* during the early stages of partial melting of source materials. Interpretations of the significance of trace element contents of peralkaline rocks may differ, but an essential pre-requisite for any interpretation is careful sampling, in terms of both locality and rock types. When reliable data are available, and when they are used in as quantitative a way as possible, they can provide extra insight into magmatic processes, and we recommend the continuation and extension of minor-element geochemical programmes directed at peralkaline rocks.

Petrogenesis

Crystal Fractionation of Basaltic Magma

We have mentioned earlier some of the field criteria which can be used to test this model. The geochemistry of the rocks should also

be consistent with the model. In particular, series with peralkaline silicic residua should be explicable in terms of the removal of the observed phenocryst phases, or of phenocrysts reasonably inferred to exist in the appropriate compositions at higher pressures. This thesis should be tested as closely as possible in every case, though inevitably difficulties will arise in that we are not normally looking at unique parent-daughter pairs in volcanic series, because crystal fractionation is never likely to be a completely closed-system process, and because of lack of information about the high-pressure equilibria controlling the evolution of peralkaline rocks and the partition of elements between the various solid-liquid-gas phases over a range of pressures. Readers of this volume are reminded, however, that there is, as yet, no *primary* field evidence for the generation of peralkaline rhyolites (granites) by fractional crystallization of magmas more basic than trachyte. Some evidence may be perfectly consistent with other mechanisms.

When all these criteria are applied, some suites do provide strong evidence consistent with this mode of origin, such as the centres on the axial ranges of the Afar triangle (BARBERI, *et al.*, this volume and 1975 *a*). This latter example illustrates the power of a combined field, petrographic, geochemical and isotope approach to these problems.

Independent Origin by Partial Melting

The theory that peralkaline liquids can be generated by direct fusion of deep crustal or upper mantle rocks has been promoted in recent years mainly by D. K. Bailey, who has also stressed the important role of volatiles in their genesis. The concept has not proved to be universally popular among petrologists, perhaps in part because it is not so simple as closed-system crystal fractionation models. The concept of open-system, volatile-fluxed magma generation invokes the use of a phase whose effects are difficult to quantify because it leaves only a partial record in the rocks.

Nonetheless, data now available from several carefully studied volcanoes in the Kenya rift (Menengai, Eburru, West Naivasha and Longonot) MACDONALD *et al.*, 1970; BAILEY and MACDONALD, in press) indicate that the magmas at each centre cannot be related by a close system process. Readers are reminded that this is the type area for the fractional crystallisation hypothesis (trachyte to rhyolite) of BOWEN (1937).

A model of open-system melting is attractive in many ways; it obviates the need for large volumes of (unseen) basic liquids in provinces dominated by salic volcanism; composition gaps are almost a requisite feature of the melting process; and it relates magma genesis to the field and analytical evidence of the importance of an active volatile phase. The model is still in its infancy and much more research is needed before it can be quantified in detail. In particular, the nature of the source materials and of the partial melts formed from them, and the phase relations controlling the process have been outlined only in general terms by BAILEY (1972 and 1974). Clearly, an important, though dauntingly complex, series of experiments is required to clarify the partial melting model. Some idea of the complexity has already been demonstrated by the experimental studies at Reading (BAILEY *et al.*, this volume) where for instance quartz becomes the liquidus phase in pantellerites at relatively low pressure. This finding presents serious problems for the generation of pantellerite by the melting of basic rocks in the deep crust. But it is worth noting that it presents even more difficult problems for a model based on closed system fractional crystallisation.

Final Thoughts

There are many volcanic series where crystal fractionation of a mildly alkaline basaltic magma has possibly been the dominant genetic process in the production of the peralkaline silicic rocks. BAKER (this volume) ascribes the origin of most of the oceanic island suites to this mechanism, though the genesis of the pantellerites of Socorro Island and Gran Canaria is still a matter of debate. The volcanoes on the Aden Volcanic Line (COX *et al.*, 1970), the centres on the axial ranges of the Afar Rift (BARBERI *et al.*, this vol.) and the Nandewar volcano, NSW (ABBOTT, 1969) all show features consistent with a crystal fractionation origin.

There are, on the other hand, many series where such a mechanism has not yet been convincingly demonstrated; the Plio-Pleistocene plateau trachytes of Kenya (BAKER *et al.*, 1972), the peralkaline silicic rocks of the central Kenyan Rift (BAILEY and MACDONALD, in press), the Pleistocene flood ignimbrites of the Ethiopian plateaux (BAKER *et al.*, 1972), the bimodal basalt-comendite association in the Afar Rift described by BARBERI *et al.* (this vol.), the wide range of silicic rocks

in the Great Basin of the western USA (NOBLE and PARKER, this vol.), the Tibesti volcanic rocks (VINCENT, 1970), and the Younger Granite complexes of Nigeria (BLACK and GIROD, 1970), are just some examples of suites whose petrogenesis is still a matter of debate. Here an independent origin for the peralkaline magmas is at least as likely as a derivative origin, and in many respects, is more likely.

The geological and petrological information which we gather from these rocks may not, in the end, give an unequivocal answer to their mode of origin, but until such times as the data are available, we should be open-minded on this subject. Continuous critical appraisal of all existing petrogenetic theory must eventually provide greater insight into the real processes of magma generation and evolution.

Manuscript available for the press March 1975

Nomenclature and Petrochemistry of the Peralkaline Oversaturated Extrusive Rocks

R. MACDONALD
Dept. of Environmental Sciences, University of Lancaster, U.K.

Abstract

Four-hundred and twenty-one analyses of quartz-normative, peralkaline, extrusive rocks have been collected from the literature and from unpublished sources and are used to examine chemical variation in this group of rocks. Comparisons are particularly made between the full body of data and the variations recorded in the non-hydrated obsidians alone by MACDONALD and BAILEY (1973). It is argued that the compositions of the magmas which formed these obsidians and those which subsequently crystallised were similar as regards the major oxides SiO_2, Al_2O_3, $FeO + Fe_2O_3$, Na_2O and K_2O.

Marked variations in the abundances of the minor oxides CaO and TiO_2 are shown to be a result of geographical location. Small but significant differences in the distribution of Al and Fe as a function of normative quartz can be recognised between various pantelleritic suites.

A new classificatory scheme is proposed, based on the iron (as FeO) and Al_2O_3 contents. This is simpler than previously employed normative classifications, is more applicable to crystalline rocks, and, happily, in 95 % of cases gives the same rock name as the normative system.

Introduction

By definition, peralkaline rocks have a molecular excess of $(Na_2O + K_2O)$ over Al_2O_3. This feature is found almost exclusively in salic rocks such as rhyolites, phonolites and their trachytic associates, and has not, to the author's knowledge, been recorded in more basic rocks such as benmoreites or mugearites. Important exceptions are the ijolites and certain potassic mafic lavas, such as the wyomingites, orendites and madupites of the Leucite Hills, Wyoming, and the jumillites of southern Spain, which maybe quite strongly peral-

BULL. VOLCANOL. 38 (1974)

kaline (CARMICHAEL, 1967*b*; BORLEY, 1967). These rare rocks are not directly related to the peralkaline salic types, however, and are not treated further in this account.

Peralkaline rocks are usually marked, and are often defined, by the presence of normative acmite (*ac*). This may not be the case in certain mildly peralkaline, Cl or F rich rocks. Calculations of large amounts of normative NaCl or NaF may result in there being insufficient Na_2O for allocating available Al_2O_3 to albite. Perversely, some CaO — poor peralkaline rocks may be calculated as containing normative corundum (*e. g.* BOWEN, 1937, table 1, no. 6; NOBLE, 1968*c*, table 1, no. 1). Absence of *ac* in an analysis containing F and Cl should not, therefore, be taken as evidence that the rock is not peralkaline.

The most obvious indication of peralkalinity is the modal presence of certain index minerals, of which alkali pyroxenes, alkali amphiboles and aenigmatite are the most common. These minerals may be found in rocks as basic as basalt, where they normally occur, for example, as reaction rims on pyroxene or in pegmatoids or segregation veins, but they are abundant only in salic rocks. In rocks which are not strictly peralkaline by definition, the presence of these minerals is said to confer on the host rock a « peralkaline tendency » or « potential », the assumption being that the crystallisation of melts of this composition would produce peralkaline residual liquids.

Metaluminous rocks with high peralkaline potential are closely associated with peralkaline rocks in many alkaline volcanic provinces, and so the compositional boundary used in this paper is clearly arbitrary in geological terms. A further restriction is that the papers in this volume are largely concerned with extrusive, rather than intrusive, varieties, even though peralkaline granites and syenites form many important and famous occurrences in the study of peralkaline rocks (MURTHY and VENKATARAMAN, 1965). The main reason for this restriction is that the extrusive volcanic rocks may normally be considered the nearest available approach to magmatic liquid compositions. This may not be true for porphyritic rocks in that mechanical sorting of crystals during flowage may cause departures from original magma composition. However, in a study of the chemical variation in peralkaline oversaturated obsidians, MACDONALD and BAILEY (1973) found no evidence of systematic differences in chemistry between porphyritic and non-porphyritic varieties. The assumption is therefore made below that all the analyses being examined represent liquid compositions.

An important proviso must be made in the case of crystalline (including devitrified) and secondarily hydrated specimens. Recent work, summarised by NOBLE (1970*b*) and MACDONALD and BAILEY (1973), has shown that the compositions of peralkaline rocks can be quite severely modified during these processes. The most important effects appear to be the loss, in variable amounts, of Na, F and Cl, loss or gain of K, gain of Mg, loss of Si, and oxidation of Fe^{2+} to Fe^{3+}. Previous reviews (NOBLE, 1968*c*; MACDONALD and BAILEY, 1973) of the chemistry of the peralkaline rocks have concentrated on the non-hydrated glassy variaties.

Nomenclature

A remarkably small number of varietal names has been in common use for the extrusive peralkaline *q*-normative rocks. The majority of samples have been referred to the comendite and pantellerite groups, or given a more general name, *e. g.* riebeckite rhyolite, aenigmatite trachyte, with reference being made to similarities with the comendites and pantellerites.

Pantellerite and *comendite* were terms introduced by FOERSTNER (1881) and BERTOLIO (1895) for rocks from Pantelleria and S. Pietro island, Sardinia, respectively. Brief descriptions of the type of rocks may be found in JOHANNSEN (1932). A. LACROIX was impressed by the close mineralogical and chemical similarities between these type rocks and rocks he had studied from several localities, notably Madagascar (1903), Korea (1927), Ethiopia (1930) and Tibesti (1934), and he extended the use of the terms to cover all peralkaline extrusive rhyolites. He was fully aware that a complete chemical transition existed between the two groups and that any division made between them would be on a fairly arbitrary basis. He chose 12.5 % normative femic minerals as his division, separating comendites (< 12.5) from pantellerites. This value was later adopted by NOBLE (1968*c*) in a study of the major element variation in peralkaline oversaturated obsidians.

Lacroix's arbitrary division separates two groups of rhyolites. In order to incorporate peralkaline trachytes into the scheme, MACDONALD and BAILEY (1973) modified it slightly by using a plot of normative femic minerals against *q*-contents (Fig. 1). The composition field is split into four — (a) comendites, (b) pantellerites, (c) comenditic trachytes, (d) pantelleritic trachytes. The trachyte-rhyolite boundary is taken at the conventional 10 % *q*, while the line separating comen-

ditic and pantelleritic rocks is arbitrary. In effect, this boundary in high silica compositions is very similar to that used by Lacroix and Noble, though at lower *q*-contents it becomes increasingly displaced towards higher normative femics contents.

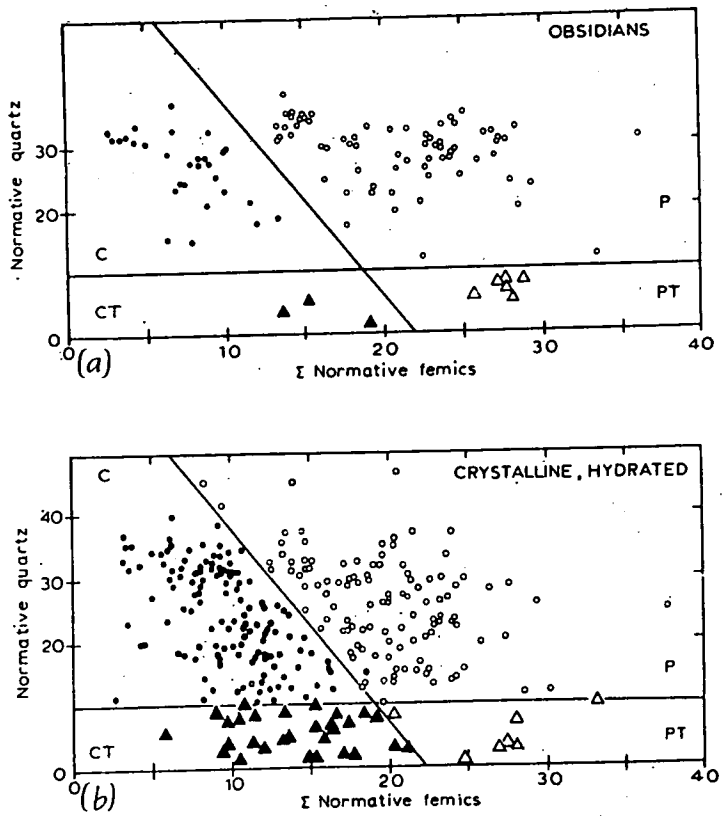

FIG. 1 - Classificatory scheme for peralkaline, quartz-normative extrusive rocks, from MACDONALD and BAILEY (1973).
(a) non-hydrated obsidians, (b) crystalline (including devitrified) and secondarily hydrated specimens. CT (closed triangles) = comenditic trachytes; PT (open triangles) = pantelleritic trachytes; C (closed circles) = comendites; P (open circles) = pantellerites.

The term *comenditic trachyte* was first used by MACDONALD and BAILEY (1973) and refers to mildly peralkaline, oversaturated trachyte. According to SMITH (1931, p. 224) *pantelleritic trachyte* was coined by Rosenbusch in 1908, for certain East African rocks; it refers to more strongly peralkaline and more mafic rocks than the comenditic varieties.

This modified scheme was originally proposed for glassy rocks, and it would be convenient to adopt it for all peralkaline, quartz-normative extrusive rocks. There are, however, difficulties involved in classifying certain crystalline and secondarily hydrated rocks by this method. As a result of both these post-eruptive processes, peralkaline rocks may undergo marked chemical changes (see above). The loss of Na, for example, minimizes the Fe contribution to the femic minerals, and also means a reduction in the potential *ns*, so that the usual result is a decrease in the content of normative femic minerals. At the same time, normative quartz may either increase or decrease.

Specimens whose compositions originally lay close to, but on the pantelleritic side of the boundary line in Fig. 1, may, as a result of post-eruptive processes, have normative compositions lying within the comendite field. Some rocks classified as « comendites » may actually have been derived from « pantelleritic » magmas. Examples of this are available in the literature; a pantellerite from Addis Ababa analysed by ROHLEDER and HITCHEN (1930, p, 281, no. VII), which must surely have lost 2-3 % wt. Na_2O at some stage, plots as a comendite in Fig. 1.

Thus the normative classification scheme gives in certain cases an inaccurate picture of the rock's true magmatic affinities, and for this reason, a new scheme is outlined below. The author accepts that it is generally undesirable to add further confusion to the confused world of rock nomenclature, but the greater accuracy achieved in this simple scheme merits its introduction. Furthermore, in only 6 % of cases is a change in rock name required by adoption of the proposed scheme.

MACDONALD and BAILEY (1973) noticed that, once the arbitrary boundary in Fig. 1 had been employed in subdividing the rhyolitic obsidians with $q > 20$ %, it was found to have other chemical characteristics, *e. g.* that comendites could be distinguished very effectively from pantellerites in having < 4 % total Fe (as FeO) and > 11 % Al_2O_3.

When all the available data are examined, it is found that this distinction becomes rather blurred. Rocks classified as comendites ($q > 20$ %) on a normative basis may have total Fe (as FeO) > 4 % and $Al_2O_3 < 11$ %, while certain pantellerites may also show a reversal of the obsidian situation (Fig. 2). Clearly, any division made between the groups on the basis of Fe and Al contents must be arbitrary, but these elements are particularly useful for this purpose, since

they appear to be largely unaffected by post-eruptive devitrification and hydration.

An attempt has been made to find in Fig. 3 a simple discriminant which can be employed to distinguish comenditic and pantelleritic rocks (including trachytic varieties), and which gives, in as many cases as possible, a similar result to the normative classification.

In a rectilinear diagram, Fe (as FeO) is abscissa and Al_2O_3 the ordinate. A line with equation $Al_2O_3 = 1.33$ Fe (as FeO) + 4.40 effectively separates comenditic and pantelleritic rocks: of 421 samples

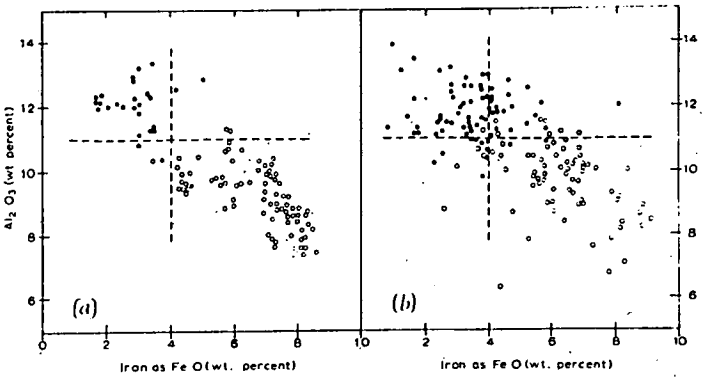

FIG. 2 - Iron (as Fe0) plotted against Al_2O_3 for comenditic (closed circles) and pantelleritic (open circles) rocks having normative quartz > 20 %.
(a) non-hydrated obsidians, (b) crystalline (including devitrified) and secondarily hydrated specimens.

tested, 94 % gave the same result by the new scheme as by the normative classification of MACDONALD and BAILEY (1973).

Further division into trachytic and rhyolitic varieties should strictly be made by calculating the C.I.P.W. norm (trachytes < 10 % norm. quartz). However, it is found that 96 % of the specimens allocated to the trachytic or rhyolitic classes by the normative classification are similarly allocated by a line on the diagram with the equation $Al_2O_3 = -0.68$ Fe (as FeO) + 17.65 (trachytes on Al_2O_3-rich side). Thus for most purposes the oxides FeO and Al_2O_3 can be used to divide all the *quartz-normative, peralkaline extrusive* rocks into the four groups in the heading. The italicized words indicate the application limits.

While the proposed classification may reasonably be applied to fine and perhaps medium-grained intrusive rocks, it would be unjustified to extend it to coarse-grained varieties. In such cases, it is

suggested that the rocks be given a general name, followed by the chemical affinity as deduced from the normative or modal mineralogy, *e. g.* riebeckite granite of pantelleritic affinity, aenigmatite syenite of comenditic trachyte affinity.

The terminology can be illustrated by using as examples the peralkaline oversaturated intrusions of the Oslofjord province, to which BRØGGER (1894) gave several varietal names. Thus the type *lestiwarite* and *sölvsbergite* dykes would be either comenditic trachytes or mi-

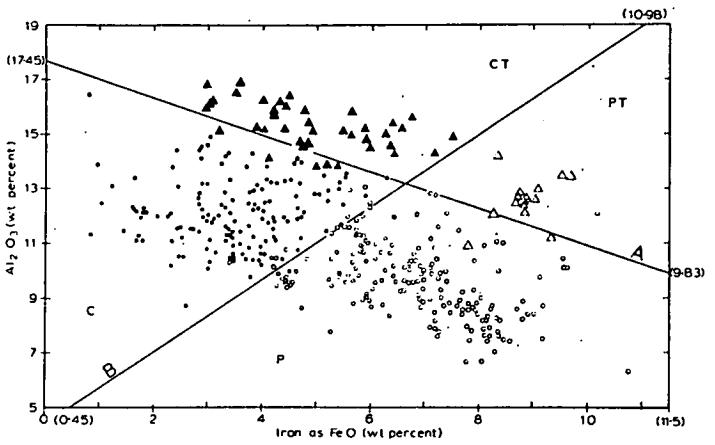

FIG. 3 - New classificatory scheme for peralkaline, quartz-normative extrusive rocks, based on Al_2O_3 and iron (as FeO) contents. The boundary lines were drawn to separate trachytes from rhyolites (A) and comenditic from pantelleritic rocks (B). Their equations may be found in the text. Symbols refer to rock names derived from the normative classification of Fig. 1, viz. closed circles = comendites (C); open circles = pantellerites (P); closed triangles = comenditic trachytes (CT); open triangles = pantelleritic trachytes (PT).

crosyenites of comenditic trachytic affinity, depending on the grain size. Similarly, the *lindöites* are comenditic, while the type *grorudite* is pantelleritic. The aegirine-riebeckite granites called ekerite by BRØGGER, are of comenditic affinity.

Four other rock names may be briefly discussed here. *Paisanite* was coined by OSANN (1893) for microgranites of comenditic affinity from Paisano Pass, S. W. Texas. Hakutoite is a term given by Yamanari (see LACROIX, 1927) to certain quartz trachytes from the volcano Hakuto-san, Manchuria. Of the three analyses given in LACROIX (1927, Nos. 9-11), two are comenditic trachytes and one a comendite. *Rockallite* was applied by JUDD (1897) to aegirine enriched veinlets and

segregations in the aegirine granite of Rockall. Comparable enclaves, this time enriched in riebeckite-arfvedsonite and found in the granite mass of Evisa, Corsica were called lindinosite by LACROIX (1923*b*). In both cases, the accumulation of the Na-Fe minerals was presumably mechanical, or by chemical segregation within the intruded masses, or perhaps by metasomatism of xenolithic country rock.

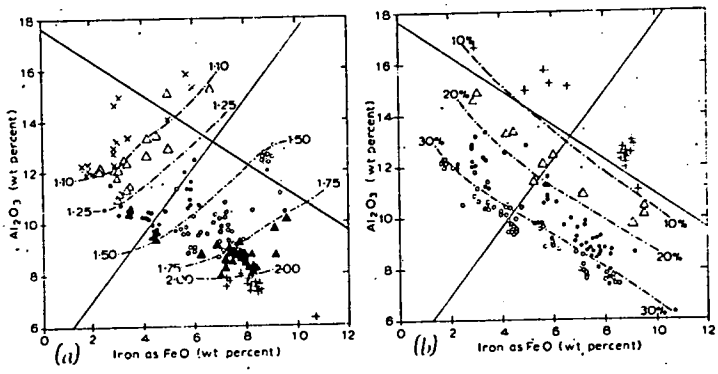

FIG. 4 - Iron (as FeO) plotted against Al_2O_3 for peralkaline, quartz-normative, non hydrated obsidians. The boundary lines from the classificatory scheme in Fig. 3 are also shown.
(a) This diagram is contoured for values of agpaitic index (mol. $(Na_2 + K_2O) / Al_2O_3$), the symbols representing the following ranges of the index: multiplication signs = 1.00-1.09, open triangles = 1.10-1.24, closed circles = 1.25-1.49, open circles = 1.50-1.74, closed triangles = 1.75-2.00, crosses = > 2.00. (b) Contoured for normative quartz values; crosses = < 10 %, open triangles = 10-19 %, closed circles = 20-29 %, open circles = > 30 %. Contours for 10, 20 and 30 % normative quartz are shown.

Analytical Data

Four hundred and twenty one analyses of extrusive, peralkaline, *q*-normative rocks have been collected from the literature and from various unpublished sources. The selection procedures applied were those of MACDONALD and BAILEY (1973), *i. e.* analyses were rejected for the following reasons:

a) the total did not lie within the limits 99-101 %;

b) any one of the oxides SiO_2, Al_2O_3, Fe_2O_3, FeO, Na_2O, and K_2O was not reported;

c) three or more of the oxides TiO_2, MnO, MgO, CaO, H_2O+, or P_2O_5 were not reported;

d) the analysis has subsequently been shown to be untrustworthy.

The *numbers* of rocks found in each classificatory division, along with a division into (*a*) non-hydrated obsidians, (*b*) crystallised, including devitrified rocks, and (*c*) hydrated obsidians, are given below. The separation of the hydrated obsidians from the crystalline rocks is only approximate, since in many cases, published analyses are not accompanied by petrographic descriptions. A similar lack of information prevented a further breakdown of the numbers into textural varieties, *e. g.* primary crystallised, devitrified, lens in ignimbrite etc. Average compositions are given in Table 1.

	Obsidians	*Crystalline*	*Hydrated Obsidians*
Comenditic trachyte	4	38	0
Comendite	43	119	4
Pantelleritic trachyte	16	5	0
Pantellerite	106	80	6

The spread of analyses in the normative classification diagram is shown in Fig. 1, and together with Table 1, it can be seen that the general range of compositions is very similar to that established for the glassy rocks by MACDONALD and BAILEY (1973). The *number* of analyses of comenditic trachyte is considerably increased while pantelleritic trachyte remains a relatively rare rock type, all but two of the analyses being of rocks from central Kenya. There are also many more analyses in the range 10-20 % *q*, allowing more detailed examination to be made of the chemical transition between the trachytic rocks and the more siliceous rhyolites.

Discussion of Data

It will be apparent that rocks classified here as rhyolitic cover a considerable range of *q*-contents, from 10 % to over 40 %, and that fairly marked chemical differences may exist between rocks of higher and those of lower SiO_2 contents. NOBLE (1968*c*) has in fact

TABLE 1 - Average analyses and composition ranges of quartz-normative, extrusive rocks.

Obs. = non-hydrated obsidians. - *CR, SH* = crystalline (including devitrified) and secondarily hydrated specimens. Dashes indicate insufficient data available.

COMENDITIC

	TRACHYTES (Norm. quartz < 10%)				*COMENDITES (10% < norm. quartz < 20%)*				*COMENDITES (Norm quartz > 20%)*			
	Average Obs.	*Range*	*Average CR, SH*	*Range*	*Average Obs.*	*Range*	*Average CR, SH*	*Range*	*Average Obs.*	*Range*	*Average CR, SH*	*Range*
SiO_2	63.0	62.5-65.0	64.1	59.4-67.5	69.3	68.6-69.8	67.9	63.8-70.7	74.0	69.4-75.9	73.2	69.5-79.1
TiO_2	0.64	0.59-0.75	0.66	0.0-1.30	0.31	0.29-0.34	0.51	0.05-1.27	0.21	0.09-0.87	0.32	0.05-1.25
Al_2O_3	15.69	15.06-16.82	15.28	13.80-16.86	14.01	13.25-14.90	13.64	11.59-16.46	11.59	10.18-13.35	11.50	8.72-14.16
Fe_2O_3	1.42	0.65-2.60	3.17	0.44-7.50	1.12	0.84-1.40	3.16	0.05-6.00	1.25	0.40-3.22	2.61	0.40-4.91
FeO	3.74	1.82-5.55	2.00	0.30-3.78	2.63	1.98-3.24	1.57	0.09-3.60	1.88	0.80-3.70	1.13	0.0-3.23
MnO	0.20	0.15-0.28	0.22	0.05-0.80	0.13	0.10-0.18	0.17	0.0-0.62	0.08	0.01-0.17	0.11	0.02-0.86
MgO	0.28	0.0-0.42	0.56	0.0-2.45	0.13	0.02-0.20	0.32	0.0-1.40	0.04	0.0-0.22	0.22	0.0-0.99
CaO	1.39	0.63-1.90	1.09	0.36-2.38	0.63	0.48-0.88	0.90	0.08-2.57	0.36	0.0-1.12	0.50	0.04-2.57
Na_2O	7.02	6.40-7.74	6.71	5.32-8.18	6.28	5.87-6.87	6.18	4.63-7.89	5.35	3.99-6.39	4.78	0.39-7.16
K_2O	5.33	5.10-5.59	5.00	3.04-7.01	4.66	4.50-4.93	4.60	3.70-6.10	4.46	3.49-4.98	4.62	1.48–11.51
P_2O_5	0.10	0.05-0.14	0.16	0.0-0.93	0.03	0.02-0.04	0.12	0.0-1.58	0.02	0.0-0.08	0.10	0.0-0.76
H_2O+	0.31	0.18-0.52	1.06	0.09-5.24	0.25	0.10-0.52	0.88	0.04-3.40	<0.20	0.0-0.67	0.62	0.01-3.55
F	0.17	(0.17)	—	—	0.23	0.16-0.29	—	—	0.37	0.06-0.76	0.15	0.02-0.38
Cl	0.16	0.10-0.21	—	—	0.28	0.25-0.31	—	—	0.24	0.05-0.41	0.09	0.01-0.44
No. of Specimens	4	4	38	38	4	4	45	45	39	39	78	78

Continued: TABLE 1 - Average analyses and composition ranges of quartz-normative, extrusive rocks.

Obs. = non-hydrated obsidians. - *CR, SH* = crystalline (including devitrified) and secondarily hydrated specimens. Dashes indicate insufficient data available.

PANTELLERITIC

	TRACHYTES (Norm. quartz < 10%)				*PANTELLERITES (10% < norm. quartz < 20%)*				*PANTELLERITES (Norm. quartz > 20%)*			
	Average Obs.	*Range*	*Average CR, SH*	*Range*	*Average Obs.*	*Range*	*Average CR, SH*	*Range*	*Average Obs.*	*Range*	*Average CR, SH*	*Range*
SiO_2	62.4	61.1-63.4	60.7	59.3-61.6	66.1	64.0-69.0	65.8	60.20-68.3	71.2	67.4-74.9	70.6	64.4-75.2
TiO_2	0.66	0.28-0.77	0.89	0.65-1.34	0.67	0.40-1.07	0.68	0.27-1.10	0.37	0.14-0.65	0.50	0.10-1.20
Al_2O_3	12.47	11.14-12.98	12.84	10.84-14.13	10.83	9.73-12.45	11.55	8.43-12.81	9.11	6.30-11.27	9.61	6.68-11.54
Fe_2O_3	2.10	1.64-3.50	3.75	2.39-5.11	3.04	1.80-6.30	4.98	2.51-7.69	2.38	0.44-5.60	5.05	1.66-8.95
FeO	6.96	5.70-7.54	5.35	3.75-7.38	4.97	2.42-7.46	2.78	0.37-4.89	4.52	1.60-6.73	2.04	0.10-4.83
MnO	0.35	0.31-0.41	0.39	0.24-0.65	0.29	0.21-0.37	0.27	0.0-0.77	0.21	0.03-0.36	0.25	0.06-1.32
MgO	0.19	0.12-0.32	0.90	0.44-1.36	0.29	0.02-0.96	0.81	0.10-4.71	0.09	0.0-0.75	0.37	0.0-2.06
CaO	1.02	0.73-1.20	2.61	1.39-3.74	0.83	0.24-1.64	1.00	0.40-2.73	0.45	0.06-2.04	0.67	0.17-2.16
Na_2O	8.49	7.95-8.97	6.41	5.60-7.10	7.46	6.64-8.22	5.80	4.10-7.73	6.44	4.68-7.83	4.89	2.42-7.04
K_2O	4.63	4.51-4.77	4.03	2.80-5.01	4.61	4.41-5.20	4.53	1.58-6.30	4.40	3.39-4.90	4.32	2.24-5.37
P_2O_5	0.08	0.07-0.11	0.47	0.04-1.06	0.06	0.02-0.07	0.15	0.0-1.62	0.05	0.0-0.28	0.09	0.0-0.73
H_2O+	0.12	0.0-0.24	1.58	0.11-4.05	0.25	0.04-0.56	0.61	0.50-3.76	<0.22	0.0-1.18	1.14	0.0-5.43
F	0.34	0.30-0.44	—	—	0.30	0.20-0.36	—	—	0.30	0.11-1.30	0.24	0.0-0.88
Cl	0.24	0.18-0.28	0.03	0.01-0.05	0.33	0.13-0.62	—	—	0.28	0.06-0.82	0.22	0.01-0.51
No. of Specimens	16	16	5	5	8	8	21	21	98	98	65	65

stressed this problem by distinguishing a group intermediate between the trachytes which he has called « trachytic soda rhyolites ». For sake of simplicity, the two-fold division has been preferred here, and for most geological purposes, it will be perfectly adequate. In comparing sets of analytical data, however, it is necessary to stipulate fairly narrow limits of *q*-content, to ensure correct comparison of like data. In the following sections, the limits of *q*-contents employed are stated wherever relevant.

Distinctive Chemical Features of Peralkaline Oversaturated Rocks

The chemical features which distinguish peralkaline from non-peralkaline rhyolites may be seen in Table 2 where the average compositions of the more mildly peralkaline (comenditic) and strongly

Table 2 - Average compositions of pantelleritic and comenditic obsidians (q > 20 %), and of certain non-peralkaline rhyolites from Iceland, New Zealand and the United States.

	Pantell.	*Com.*	*Rhy. Obs.*	*Iceland*	*Taupo*	*Cascades*
SiO_2	71.2	74.0	74.06	71.6	74.22	73.23
TiO_2	0.37	0.21	0.19	0.30	0.28	0.24
Al_2O_3	9.11	11.59	13.37	12.9	13.27	14.03
Fe_2O_3	2.38	1.25	0.70	1.40	0.88	0.60
FeO	4.52	1.88	1.11	1.76	0.92	1.70
MnO	0.21	0.08	0.07	0.08	0.05	0.02
MgO	0.09	0.04	0.13	0.32	0.28	0.35
CaO	0.45	0.36	0.82	1.60	1.59	1.32
Na_2O	6.44	5.35	4.50	4.34	4.24	3.94
K_2O	4.40	4.46	4.36	2.95	3.18	4.08
P_2O_5	0.05	0.02	0.03	0.11	0.05	0.05
H_2O+	<0.22	<0.20	0.39	1.70	0.80	0.49
F	0.30	0.37	0.11	—	—	—
Cl	0.28	0.24	0.12	—	—	—

Pantell. and com. = average compositions of pantellerite and comendite obsidians having normative quartz > 20 %, taken from Table 1.

Rhy. obs. = average of 30 non-peralkaline rhyolite obsidians from various localities, collected from the literature.

Iceland = average of 58 Icelandic acid rocks (Walker, 1966, Table 3).

Taupo = average rhyolitic eruptive, Taupo volcanic zone, New Zealand (Ewart *et al.*, 1968, Table 5).

Cascades = average Cascades rhyolite lava (Carmichael, 1964, Table 8).

peralkaline (pantelleritic) obsidians are listed, together with average values for rhyolites from two calc-alkaline provinces (Taupo, Cascades), a tholeiitic province (Iceland), and with an average of thirty non-peralkaline obsidians collected from the literature.

The most striking features of pantelleritic chemistry are the relatively high iron (as FeO), MnO, Na_2O, TiO_2, F, Cl and the low Al_2O_3, CaO and MgO. The *comendites* are generally transitional towards the non-peralkaline rhyolites in respect of these elements.

Comparison of the compositions of peralkaline trachyte with met- and per-aluminous varieties must await compilation and examination of analysis of the latter groups. Compared to the peralkaline rhyolites with which they are associated, however, pantelleritic and comenditic trachytes are on average richer in TiO_2, Al_2O_3, iron (as FeO), MnO, MgO, CaO and Na_2O, and poorer in SiO_2.

Chemical variation in the peralkaline oversaturated extrusive rocks

The Non-hydrated Obsidians

Macdonald and Bailey (1973) have presented correlation coefficients for all pairs of major oxides in 113 analyses of peralkaline, *q*-normative (0.3 to 37.6 %) obsidians. There are strong positive correlations between Na_2O and iron (as FeO) ($r = 0.83$), Na_2O and MnO (0.71) and MnO and iron (as FeO) (0.84). Na_2O, iron (as FeO) and MnO also show strong positive correlation with TiO_2 (> 0.66 in each case). All four oxides, plus CaO, have marked negative correlation with SiO_2. Al_2O_3 shows a significant correlation only with iron (as FeO) (-0.53).

Important positive correlations were also found between agpaitic index [molecular $(Na_2O + K_2O) / Al_2O_3$] and each of iron (as FeO) (0.81), MnO (0.64), and Na_2O/K_2O ratio (0.68), and between Na_2O/K_2O ratio and iron (as FeO) (0.78). Thus the major variations within the group appear to be increase in iron (as FeO), TiO_2, Na_2O, CaO, Na_2O/K_2O ratio and agpaitic index with decrease in SiO_2 and Al_2O_3. These results are in agreement with the observations of Lacroix (1927, 1930) and Noble (1965, 1968*c*) that pantellerites are generally more peralkaline and sodic, and richer in Fe and Mn than the more aluminous comendites.

All Peralkaline, Oversaturated, Extrusive Rocks

A question of some interest in the study of peralkaline rocks is, whether by concentrating attention on obsidians only, as has been the case in most recent studies, one is imposing a selective bias in favour of certain compositions. It is possible that the glassy nature of certain specimens represents a chemical peculiarity not found in magmas that have crystallised. Comparison of the accumulated analyses of the various textural types should indicate whether or not there are any significant chemical differences between glassy and non-glassy rocks, but interpretation of the data is complicated by two factors. Firstly, the crystalline peralkaline rocks are likely to have suffered post-eruptive chemical changes, and secondly, for some minor elements such as Ca and Ti, there are large differences in abundance due to geographical location. Some of these effects are discussed below.

1) *Silicon, iron and aluminium*

Although Si may be leached from porous hydrated glasses (NOBLE, 1967), the abundance of Si, Al and Fe is normally little affected during crystallisation and hydration processes. It is therefore informative to compare the averages for these elements in obsidians and crystalline rocks. (Table 1) Although the number of specimens is in some cases rather small, it is clear that the abundances of SiO_2, Al_2O_3 and iron (as FeO) are sufficiently similar in both textural varieties to suggest that there are no systematic differences between glassy and crystalline peralkaline oversaturated rocks. This infers that the glassy condition is a result of some other factor, such as the water content of the magmas, or is an accident of the eruptive process.

Despite the generally good correlation between iron (as FeO) and agpaitic index shown by the obsidians (MACDONALD and BAILEY, 1973, Table 9) and here inferred for the full body of data, it should be pointed out that within individual suites of peralkaline rocks, there is sometimes a reverse relationship. BARBERI *et al.* (this vol.), for example, show, in certain Afar rocks, that while agpaitic index increases in increasingly silica-rich rocks, iron drops quite sharply. In fact, the distribution of iron in various suites is rather complicated. Iron (as FeO) is plotted against normative quartz for some *pantel-*

leritic suites in Fig. 5, where it can be seen that, with increasing *q*-content, iron may also increase (Gran Canaria, Mayor Island), decrease (Erta'Ale, Tugtutôq dykes), or define a maximum (central Kenya) or minimum (Pantelleria) at intermediate *q*-values.

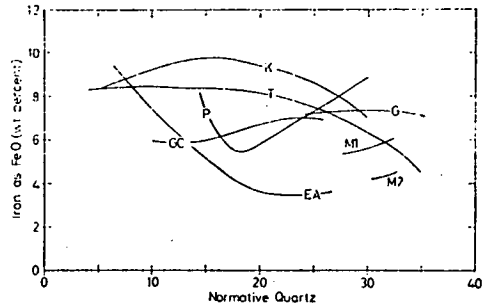

FIG. 5 - Normative quartz plotted against iron (as FeO) for various pantelleritic suites, and for the comenditic rocks of the Erta'Ale range. T = Tûgtutôq dykes, S. Greenland (MACDONALD, 1969), G.C. = Gran Canaria (SCHMINCKE and SWANSON, 1967; SCHMINCKE, 1969*a* and unpublished data), P = Pantelleria (various sources given in VILLARI, this volume), M1 = Mayor Island post-caldera lavas, M2 = Mayor Island pre-caldera lavas (EWART *et al.*, 1968), G = Gariboldi Pass volcano, Ethiopia (MACDONALD and BAILEY, 1973, table 3, nos 57-68), K = central Kenyan rift (MACDONALD and BAILEY, 1973, tables 3 and 4, and unpubl. data), EA = Erta'Ale range, Afar (various sources given in BARBERI *et al.*, this vol.).

Slight differences in the chemistry of various trachyte-rhyolite suites may also be distinguished in Al_2O_3 contents. For a given *q*-value (Fig. 6), there is a sequence of increasing Al_2O_3 content from the Ken-

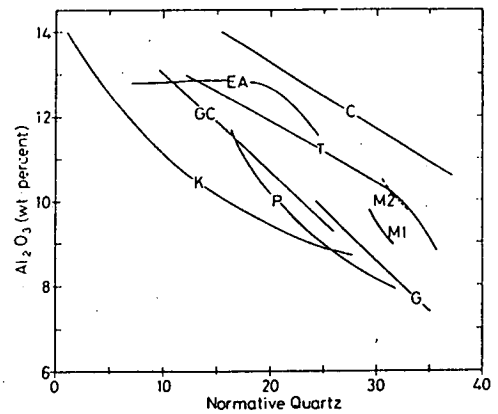

FIG. 6 - Normative quartz plotted against Al_2O_3 for various pantelleritic suites and for the comenditic rocks of the Erta'Ale range. Explanation as for Fig. 5, with the addition of C = generalised comendite trend.

yan rocks through the Tugtutôq and Mayor Island suites to the generalised comendite trend. Thus the degree of Al_2O_3-undersaturation shown by the rhyolites reflects the Al_2O_3 contents of the associated peralkaline trachytes (*c. f.* NOBLE, 1968*c*, Fig. 1).

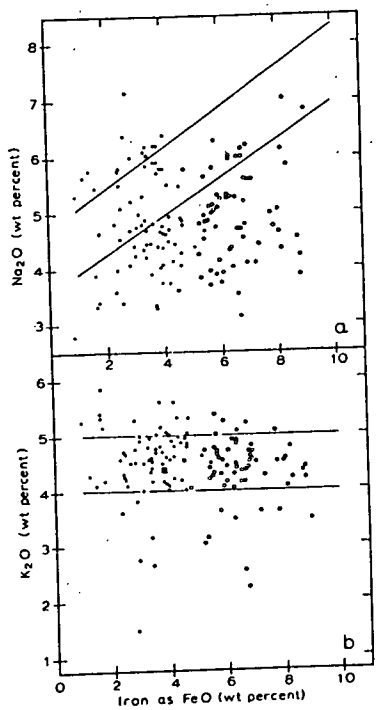

FIG. 7 - Iron (as FeO) plotted against (a) Na_2O and (b) K_2O for crystalline (including devitrified) and secondarily hydrated peralkaline extrusive rocks having normative quartz > 20 %. The solid lines in both (a) and (b) enclose 95 % of non-hydrated obsidian analyses. Closed circles = comendites; open circles = pantellerites.

2) *Sodium, potassium, fluorine and chlorine*

In the obsidians, Na_2O shows a very strong positive correlation with iron (as FeO) (r = 0.83, MACDONALD and BAILEY, 1973, Table 9). Variations in Na_2O in the crystalline rocks can thus be usefully summarised diagrammatically using iron as a basis of comparison. As might have been predicted from the work of Noble and his colleagues, summarised in NOBLE (1970*b*), Na_2O shows a considerable scatter when plotted against iron (as FeO) (Fig. 7a). Only 23 % of the Na_2O anal-

yses of crystalline and hydrated specimens fall within the limits defined by 95 % of the obsidians, the vast majority of the others falling on the Na_2O poor side (*cf.* averages in Table 1). Though some of this scatter may represent the occurrence in nature of peralkaline rhyolite magmas having Na_2O contents outside the range of those represented by glassy rocks, the main factor causing it is undoubtedly loss of Na_2O during crystallisation and hydration processes. A similar diagram and conclusions have previously been presented by NOBLE (1970*b*,

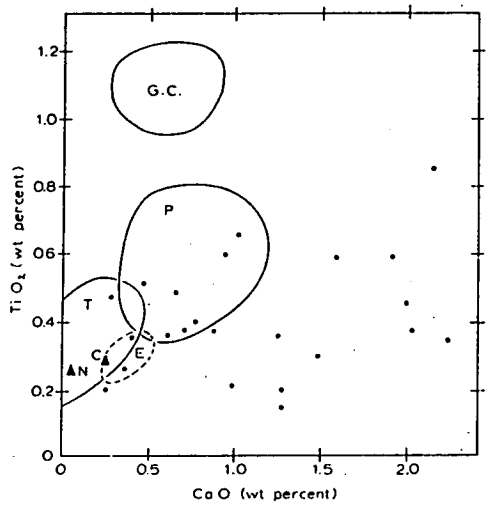

FIG. 8 - CaO plotted against TiO_2 for pantellerites (q > 20 %) from various localities. G.C., P, T, E represent fields occupied by rocks from Gran Canaria, Pantelleria, Tûgtutôq and the Eburru massif, central Kenya, respectively. Sources of information as for Fig. 5. Solid triangle marked C is the average obsidian from Chabbi volcano, Ethiopia (MACDONALD and GIBSON, 1969), and that marked N is a pantelleritic obsidian from Nevada (NOBLE, 1965). Closed circles are pantellerites from Ethiopia, compiled from various sources.

Fig. 4): one obvious use of such a diagram is that it allows a rough estimate to be made of the amount of Na_2O lost from a particular specimen during post-eruptive cooling.

The scatter of K_2O analyses (Fig. 7b) is much less marked, only 25 % of the analyses falling outside the 95 % obsidian limits. The relative amount by which they are «aberrant » also tends to be lower than for Na_2O, and the points are roughly equally distributed above and below the limits set by the obsidians. Again this is in accord with Noble's earlier conclusions that K_2O values are not so readily modi-

fied as those for Na_2O, and that K_2O may be either lost or gained, during crystallisation and hydration.

Similar processes have probably also modified the F and Cl contents of these peralkaline rocks. Average values for non-hydrated obsidians and for crystalline and hydrated samples (Table 1) indicate a general loss of substantial amounts of these elements from the latter types.

3) *Calcium and titanium*

MACDONALD and BAILEY (1973) recognised certain chemical characteristics which distinguished groups of pantellerites from various

TABLE 3 - Average CaO and TiO_2 contents of comendites ($q > 20$ %) from various localities.

	CaO	*TiO_2*	*No. of specimens*
Sardinia	0.13	0.33	13
Aden	0.65	0.24	7
Naivasha area, Kenya	0.18	0.18	16
Tibesti massif, Chad	0.59	0.35	7
Nevada	0.27	0.19	12
Nandewar volcano, Australia	0.10	0.21	3
Japan	0.30	0.33	8
Gran Canaria	0.68	0.77	3
Ascension Island	0.56	0.24	3
Bouvet Island	0.70	0.30	3
Easter Island	0.84	0.18	6

localities. The type rocks from Pantelleria were shown to be extremely Cl-rich, while many of the Ethiopian and Tibesti obsidians were thought to be high in CaO. A graph of CaO versus TiO_2 using all available analyses (Fig. 8) reveals some further differences between suites of rocks from various localities. Again by using a fairly limit-

ed composition range ($q > 20$ %), it is possible to show that the geographical differences are real. Thus, relative to the type pantellerites, those from Gran Canaria are very Ti-rich (SCHMINCKE, 1969*a* p. 10), while the Tugtutôq pantellerite dykes (included here for comparative purposes) and the Nevada pantellerite are apparently Ca-poor. The Ca-enriched nature of many of the Ethiopian samples is confirmed. The average partial analyses of comenditic ($q > 20$ %) rocks from various localities are in accord with the results from the pantellerites (Table 3).

MACDONALD and BAILEY (1973) have earlier pointed out that the concentrations of certain trace elements vary widely in pantelleritic obsidians due to geographical locations, and it would now appear that these variations also apply to some of the minor elements. It remains to be shown whether the variations reflect differences in the compositions of the source materials or different evolutionary histories of similar parental magmas, or both.

Manuscript available for the press Nov. 1974.

Tectonic Settings and Magma Associations

R. MACDONALD
Department of Environmental Sciences, University of Lancaster
Lancaster, U.K.

Abstract

The largest volumes of peralkaline silicic rocks are found in areas of epeirogenic uplift and rift formation on the continents, but they may also form in several other tectonic settings, such as the oceanic islands, during the later stages of orogenic cycles, as isolated occurrences in active mobile belts, and in areas of extensional tectonics at or near continental plate margins. Their emplacement is effected during periods of dominantly tensional stresses.

The peralkaline silicic rocks are typically members of the transitional, mildly alkaline basalt-trachyte association. Associated salic rocks are commonly feldspathoidal and/or anorthite-normative, as well as peralkaline. Two main types of association are distinguished: firstly, provinces where the peralkaline rocks are mainly of comenditic type, where the salic rocks are in relatively low abundance compared to basic, and where the intermediate (Daly) composition gap is not present; secondly, provinces of pantelleritic or mixed pantelleritic-comenditic volcanism, where the basic : acid volume relationships are reversed and where the Daly gap is usually markedly developed.

Introduction

It is intended in this chapter to outline the types of tectonic environments in which peralkaline silicic rocks occur, and to mention the range of rock types with which they are associated. The scope is clearly very large, and the account is necessarily generalised. Since every petrographic province is to some extent unique, any grouping of tectonic environments, such as that employed below, must be arbitrary. Many workers would undoubtedly choose other structural criteria as a basis of subdivision. The format adopted here should, however, help to stress that peralkaline silicic rocks occur in a wide range of tectonic settings, and will also serve to acquaint readers with the major outcrops of these rocks presently known.

Bull. Volcanol. 38 (1974)

Tectonic Settings

CONTINENTAL AREAS OF RIFT FORMATION AND/OR EPEIROGENIC UPLIFT

a) *Not Consequent upon Previous Orogeny*

Many of the world's most important outcrops of peralkaline oversaturated rocks may be conveniently described by reference to the « intercontinental belt of the world rift system » of ILLIES (1969). This is a system of rift valleys or grabens extending over western Europe through the Mediterranean into northern and eastern Africa. It consists of several segments, not in complete structural continuity, which have been active at various times from the Permian to Recent, and is mostly developed on continental crust.

In the *Oslofjord* province, mildly peralkaline granites, ekerites, (DIETRICH *et al.*, 1965) were intruded as part of this classic alkaline suite in Lower Permian times (276 ± 7 m. y., HEIER and COMPSTON, 1969). No extrusive equivalents are preserved, but some of the abundant dykes of comenditic and pantelleritic affinity may have acted as surface feeders. The structure of the Oslo graben, and its relation to the volcanic rocks, have been described by RAMBERG (1972), and RAMBERG and SMITHSON (1971).

Intrusive rocks of both comenditic and pantelleritic affinity are exposed in the area around *Frankfurt*, that is, at the junction of the Upper Rhine, Lower Rhine and the Hessen Depression. They are minor members of an igneous province dominated by basic undersaturated rocks (WIMMENAUER, 1974). Peralkaline trachyte and rhyolite intrusions have been described by BROUSSE and VARET (1966) from Cantal and Mont Dore in the French Massif Central, an area of uplift and graben formation, *e. g.* the Limagne and Forez grabens (WIMMENAUER, 1974, p. 238).

In the Mediterranean region, riebeckite granites are known in *N. W. Corsica* (LACROIX, 1923; QUIN, 1962) in close proximity to a system of buried rifts west of the island (GLANGEAUD *et al.*, 1966). The type area of comendite is in the island of *San Pietro* in S. W. Sardinia, some 50 km S. W. of the Campidano graben which traverses the island from N. W. to S. E. Here the peralkaline rocks are, however, coeval with calc-alkaline varieties, and the tectono-magmatic situation is clearly complex (ARAÑA *et al.*, this vol.). Pantelleria, the type locality of pantellerite, lies on an easterly extension of the graben

system, the so-called Channel of Sicily, one of a series of rift structures recognised between Tunisia and Sicily. According to geophysical evidence, the island has developed on continental crust about 20 km thick (VILLARI, this vol.) ILLIES (1969) suggests that the Hon graben in Libya marks a continuation of the western European grabens, thus forming a link between the European and African segments. The Hon structure disappears southwards but a zone of basic volcanic rocks may connect it to the Tibesti massif in Chad. Tibesti is a zone of epeirogenic uplift and faulting that has been the site of intensive volcanism from early Tertiary to Recent times (VINCENT, 1963, 1970). Alkali olivine basalts and peralkaline rhyolitic ignimbrites formed an essentially bimodal association during the earliest activity, while in a later (third) phase, thick pantelleritic and comenditic ignimbrites covered an area of 3200 km^2, with a volume of about 150 km^3. (VINCENT, 1970).

Structural links connect Tibesti with the alkaline provinces of western Africa, where BLACK and GIROD (1970) have separated two phases of alkaline activity in a region of uplift and faulting. The late Palaezoic to Tertiary ring-complexes of Nigeria, Niger and the Cameroons are high-level non-orogenic intrusions, with associated extrusives. Rock-types include quartz-syenite, hastingsite granites, biotite granites and peralkaline granites and rhyolites of comenditic affinity. Basic rocks form only 5 % of the exposed volume. The Tertiary to Recent volcanic rocks of Senegal, Hoggar, Air, Nigeria and the Cameroons all belong to the alkali olivine basalt-trachyte association, many of the basic rocks being notably undersaturated. BLACK and GIROD (1970) claim that many of the salic members (oversaturated and undersaturated), are peralkaline and that intermediate compositions (« trachyandesites ») are poorly represented. See also PIPER (1970) and PIPER and RICHARDSON (1972).

Probably the most important area in the world for peralkaline silicic volcanism, in terms of volumetric abundance and for the range of rock types, is the East African rift system, especially the Ethiopian and Kenyan sectors. In Arabia, the best known peralkaline localities are the comenditic strato-volcanoes of the Aden volcanic line (GASS and MALLICK, 1968; COX *et al.*, 1969, 1970), though the analyses and discussion presented by MOHR (1970, 1971, 1972) reveal the presence of important occurrences of pantelleritic rocks in Yemen.

BARBERI *et al.* (this vol.) describe peralkaline silicic rocks in three tectonic settings in the Afar depression of Ethiopia:

1) comenditic rhyolites occurring as late members of the dominantly basic assemblages in the axial volcanic ranges such as Erta'Ale,

2) comenditic and pantelleritic rocks forming important members of centres marginal to the rift walls,

3) pantellerites and comendites in essentially bimodal assemblages with basic rocks erupted from fissures in central and southern Afar.

Further south, comendites are minor members of the Miocene Shield Group of MOHR (1968), who also drew attention to the voluminous fissure and central eruptions of trachytic and pantelleritic ignimbrites which covered much of southern Ethiopia and filled the Main Ethiopian Rift in upper Pliocene times. These had their sources at the rift margins, where they are up to 500 m thick, though greater thicknesses probably exist on the rift floor.

GIBSON (this vol.) describes the caldera volcano Fantale, one of a series of dominantly silicic Quaternary centres situated along the Wonji Fault Belt, an en échelon series of faults running along the axis of the Main Ethiopian Rift. Basalts, hawaiites and mugearites were contemporaneously erupted from fissures between these discrete centres.

The earliest Cenozoic peralkaline rhyolites so far recorded in Kenya are lavas and ignimbrites outcropping in Turkana and provisionally assigned to the lower Pliocene (WALSH and DODSON, 1969; BAKER *et al.*, 1972). An extensive phase of peralkaline volcanism occurred in the late Pliocene and early Pleistocene when flood trachytes (lavas and ignimbrites, many of which are pantelleritic and comenditic), locally more than 900 m thick, flooded the floor of the central Kenyan rift and in places flowed onto the plateaux (WILLIAMS, 1970; BAKER *et al.*, 1972).

Perhaps the most spectacular array of peralkaline rocks in Kenya, however, is found in the series of Quaternary central volcanoes situated along the rift floor. These include Ol Doinyo Nyegi, Longonot and Menengai, all largely made of pantelleritic trachytes, the Eburru massif (pantellerites and comendites), the group of comenditic flows and domes south of Naivasha and the minor comenditic rocks at Pakka volcano (BAKER, 1958; THOMPSON and DODSON, 1963; MCCALL, 1967; SUTHERLAND, 1970, 1971; SCEAL and WEAVER, 1971).

Included here for reasons of geographical proximity may be the pantelleritic and comenditic rocks which form an important part

of the Ampasindava petrographic province of northern Madagascar (LACROIX, 1903). These sub-volcanic rocks were emplaced over the Mesozoic-Tertiary boundary and overlap in time with the development of the Sambirano graben (SAINT OURS, 1960).

b) *Consequent upon Previous Orogeny*

The emplacement of alkaline rocks during the late, cratogenic stages of the orogenic cycle is well established. Here an arbitrary distinction is made between areas where such rocks are associated with graben formation, and those where graben development is absent. (See « Complex tectonic » below). In the cases discussed here, the rift systems are developed within, and strike parallel to the regional grain of previously active orogenic belts.

The term « *Gardar igneous province* » refers to the series of volcanic and subvolcanic alkaline rocks emplaced during the final stages of the Ketilidian-Sanerutian orogeny in S. W. Greenland approx. 1100 m. y. ago (BRIDGWATER and WALTON, 1964; BRIDGWATER, 1965; BRIDGWATER and HARRY, 1968; SØRENSEN, 1970; UPTON, 1974; VAN BREEMEN and UPTON, 1972). Much of the original extrusive volcanic cover has been stripped off, but an alkali olivine basalt-hawaiite-trachyte succession at least 1500 m thick has been preserved in a down-faulted block near Ilimaussaq. The Gardar area is penetrated by several large central complexes and by dense dyke swarms. Comenditic and pantelleritic trachytes and rhyolites (and their coarse-grained equivalents) are important members of these intrusions (*e. g.*, MACDONALD, 1969; MACDONALD *et al.*, 1973; UPTON *et al.*, 1971), other components of which include oversaturated and feldspathoidal syenites, calc-alkaline granites, agpaitic syenites and relatively less abundant gabbros and syenogabbros.

Emplacement of the Gardar rocks accompanied regional faulting. In contrast to, say, the East African Rifts, the Gardar faulting had a large compressional component: two major sets of transcurrent faults are recognised (UPTON, 1974), intermittently active throughout the period, with net horizontal displacements measurable in some cases in tens of kilometres. However, large vertical displacements, over 1 km, can also be demonstrated for some of these wrench faults, which resulted in the development of subsiding fault-blocks or grabens. SØRENSEN (1970, p. 309) has suggested that the Gardar area may

represent a deep section through a rift zone, and also cites rather slender evidence that the rifting may have been preceded by arching. The alternating compressional and tensional tectonics point, however, to clear differences with the classical areas of epeirogenic uplift and rifting.

Likewise, *the Midland Valley of Scotland* is frequently referred to as a graben or rift, though structural analyses of its tectonic evolution indicate that the stress field for long periods of its active history was compressional (KENNEDY, 1958; GEORGE, 1960; FRANCIS, 1965 (*a*), (*b*), 1967). During the Lower Carboniferous, peralkaline trachytes and rhyolites of comenditic affinity were erupted as minor members of volcanic suites dominated by basalts and hawaiites.

The White Mountain Magma Series, intruded during the Mesozoic in New England (FOLAND *et al.*, 1971; ARMSTRONG and STUMP, 1971) includes granites and syenites of mildly peralkaline type. These intrusions post-date the Appalachian orogeny; they also post-date but may be genetically related to the Triassic key-stone graben which runs along the crest of the Appalachians (RODGERS, 1970).

c) *The British Tertiary Province*

Eruption of mainly basic rocks in the *British Tertiary Province* was apparently connected with the opening of the North Atlantic about 60 million years ago. The island of Rockall is made up of granite of pantelleritic affinity, and is believed to be intruded into a fragment of continental crust left stranded by the various rifting episodes accompanying the continental separation (JONES *et al.*, 1972). Some of the eastern Redhills intrusions of southern Skye are mildly peralkaline granites, though the majority are calc-alkaline (THOMPSON, 1969). Ailsa Craig and Holy Island are isolated peralkaline intrusions also belonging to this province.

COMPLEX-TECTONIC

Set out below are a series of occurrences of peralkaline silicic rocks which are not easily categorized. Their connection is that either they outcrop in orogenic belts, having been emplaced during, or slightly after, the main orogenic activity, or they occur in areas of prob-

able crustal extension which are in some way genetically related to the development of contemporaneous orogenic belts.

As might be expected, the peralkaline rocks are associated with calc-alkaline varieties, and are, with the possible exception of the Circum-Japan Sea alkaline province, subordinate in volume to them in each case.

i) Upper Palaeozoic silicic igneous rocks, thought to have been derived by anatexis within the Palaeozoic Tasman Geosynclinal zone, are exposed over a wide area in the *Georgetown Inlier* in North Queensland (BRANCH, 1966). Emplacement of the various plutonic and extrusive rocks was accompanied by the formation of cauldron subsidence blocks and ring-complexes. The volcanic rocks are predominantly rhyodacite (welded tuffs) with subordinate rhyolite, trachyandesite, andesite and basalt, forming a mainly calc-alkaline suite. As pointed out by NOBLE (1970), at least one of the analysed samples has pantelleritic chemistry, while several others may have originally been peralkaline prior to post-depositional alteration.

The post-orogenic Caledonian granite of Ronas Hill on the mainland of Shetland, off Scotland, is cut by a series of dykes, which include spessartine, microdiorite, porphyrite, quartz-feldspar porphyry and felsites, mainly of calc-alkaline affinity. The latest dykes however are riebeckite- and aegirine-bearing felsites of comenditic affinity (PHEMISTER, 1950). Though no definite evidence of the age of the dykes is available, it is likely that they are Devonian, broadly coeval with the granite.

Both these examples are occurrences of peralkaline rocks being emplaced in a late-orogenic environment, but with no associated graben formation.

ii) Late Orogenic in Association with Thrust Movements

Intrusion of rocks of comenditic affinity found as dykes and sills and as members of plutonic bodies, was associated with movements on major thrust planes in the marginal thrust zone of the Scottish Caledonides (SABINE, 1953; TILLEY, 1958; WOOLLEY, 1970).

iii) Other occurrences of peralkaline silicic rocks have been reported from certain orogenic areas where the magmatism is dominantly calc-alkaline. Little is known about their relationship with neighbouring

outcrops, either as a result of geographical separation (Mayor Island, Fergusson and Dobu Islands) or lack of information.

Mayor Island is an isolated volcano lying at the edge of the continental shelf in the Bay of Plenty, North Island, New Zealand. It is composed entirely of recent pantelleritic rocks, though the presence of trachyandesite inclusions may indicate a more basic volcanic substructure. The nature of the volcanics contrasts sharply with the calc-alkaline affinities of the eruptive rocks exposed on the immediately adjacent mainland areas (EWART *et al.*, 1968).

Specimens studied by MORGAN (1966) from the islands of Fergusson and Dobu, lying to the east of the Papuan mainland, are almost entirely comenditic rhyolites and obsidians, though a basaltic andesite has been recorded from Dobu. Once again, the volcanism of adjacent mainland areas is of calc-alkaline type.

WASHINGTON (1917) lists two analyses of rocks from Timor, one a comenditic trachyte, the other a pantellerite. The author has not yet been able to trace much geological information about these occurrences.

iv) Sardinia. (See ARAÑA *et al.*, this vol.).

v) The Basin-and-Range province of the western U.S.A. is a Cenozoic system of horsts and grabens formed by up to 90 km of crustal extension along normal faults (SCOTT *et al.*, 1971). Cenozoic volcanism in the Great Basin portion of the province alone resulted in at least 100,000 km^3 of erupted rock, silicic volcanism being dominant. Comenditic and pantelleritic rhyolites are, however, subordinate to calc-alkaline varieties (NOBLE, and PARKER, this vol.). NOBLE (1972) discusses, with full reference to the abundant literature on the subject, the complex tectono-magmatic evolution of the area, and its relationship to possible lithospheric subduction zone development during the Cenozoic.

vi) The Circum-Japan Sea alkaline province (AOKI, 1959; TIBA, 1966) contains many important occurrences of peralkaline silicic rocks, most notably in the Oki islands, Japan (TOMITA, 1935), and in the Hakuto volcano and Meissen district of Manchuria (LACROIX, 1927; TOMITA, 1935). Other occurrences include the Iki islands (AOKI, 1959), Morotu (YAGI, 1953), the Oga peninsula (YAGI and CHIHARA, 1963) and

the Tokati plain, Hokkaido (NEMOTO, 1934). The spatial distribution of the tholeiitic, calc-alkaline and alkaline series in this province is well-known (KUNO, 1966), though the details of the relationship between the magmatology and possible plate movements are less clear. It may be, however, that the alkaline (and peralkaline) rocks were generated in a zone of extensional tectonics on the landward side of a descending lithospheric plate, and as such may be compared to the Basin-and-Range province (NOBLE and PARKER, this vol.).

OCEANIC ENVIRONMENT

A comprehensive review of the occurrence of peralkaline silicic rocks in the ocean basins is provided by BAKER (this vol.). Attention is especially drawn to Baker's attempts to distinguish between the petrological and tectonic situations in two different oceanic environments: islands formed over the crestal zone of oceanic rises and those rising from extensive submarine plateaux.

Generalisations about Tectonic Settings

The foregoing discussion will have helped to stress an important feature of the distribution of peralkaline silicic rocks. Firstly there is the overwhelming tendency for these rocks to occur in the continental rift environment, or in rift-like settings such as the Basin-and-Range province (GILLULY, 1972, p. 412), and the Gardar area (SØRENSEN, 1970). Estimates of volumetric abundances are available for only a few areas and it is impossible to be specific on this point, but the author would estimate that more than 90 % of peralkaline silicic rocks occur in this setting, the majority of those being found in areas of uplift and rifting on the African continent. LE BAS (1971) has already discussed the relationship between areas of crustal swelling and rifting and peralkaline volcanism, and he mentions some further African localities, not specifically referred to above, in which peralkaline rocks occur viz. Angola, Chilwa-Zambesi, and the Hoggar.

Secondly, though their production is apparently favoured by rift tectonics, peralkaline silicic magmas are capable of generation in other settings, such as the oceanic islands where the salic rocks are characteristically if not exclusively peralkaline, and as (usually mi-

nor) members of late orogenic volcanic suites where associated rifting is absent.

There is one factor which links all these various tectonic environments: they are characterised by crustal tensional conditions. Most geologists appear to agree that rift structures and the periods of uplift which often accompany them are the results of extension of the crust (ILLIES, 1969), while the major ocean basins also provide evidence of extensional tectonics and strike-slip faulting, possibly related to sea-floor spreading. With the possible exception of the Assynt alkaline suite (emplaced during movements on the Moine Thrust Zone; WOOLLEY, 1970), there is no clear example of a suite of peralkaline silicic rocks having been emplaced under compressional stresses. Thus, these rock types may well be indicators of « palaeotension », that is, in ancient areas where the tectonic history is difficult to decipher, such as reworked orogenic belts, they may represent periods of tension in a dominantly compressional framework (BASS, 1970; MARTIN and PIWINSKI, 1972).

Martin and Piwinski have argued that there are two fundamentally different tectonic settings on the earth, in which contrasted kinds of magmatism occur: compressional tectonics and associated orogenic (calc-alkaline) volcanics, and tensional environments, producing tholeiitic and alkali olivine basalt volcanic associations. The nature of the crust within the non-orogenic zones *i. e.*, continental or oceanic, is adjudged to be of lesser importance than the overall stress patterns. There are, however, important and possibly fundamental differences, especially of scale, between peralkaline magmatism in the oceans and continents (see below). Until the influence of the continental crust on the generation of silicic magmas, in either a physical or chemical way, is fully understood, it seems more reasonable to maintain the traditional distinction between the continental and oceanic environments, though accepting that it may be the tensional conditions (or more likely, the factors causing them) which are the dominating influence in peralkaline magmatism.

Magma Associations

In terms of *magma associations*, implying a close relationship in space and in time between the various members of volcanic suites, the peralkaline silicic rocks may be regarded as the salic end-mem-

bers of an approximately silica-saturated olivine basalt - hawaiite - mugearite - (benmoreite) - trachyte - rhyolite lineage. This association seldom occurs within *petrographic provinces* independently, but usually is more or less closely related to more strongly undersaturated suites of basanitic and nephelinitic type (*e. g.* East African Rifts, BAKER *et al.*, 1972; Gardar, UPTON, 1974) or to tholeiite suites (*e. g.* Tibesti, VINCENT, 1970; Iceland, SIGURDSSON, 1971; Great Basin, NOBLE and PARKER, this vol.). In several individual centres and oceanic islands, however, it is possible to find only the transitional basalt-trachyte series, *e. g.* Easter Island, Ascension, Socorro (BAKER, this vol.), Pantelleria (VILLARI, this vol.), Nandewars (ABBOT, 1969) and Pakka volcano (SCEAL and WEAVER, 1971). It will be clear, though, that the question of the origin of peralkaline rocks and their basic associates cannot generally be considered in isolation, but in the context of long-term volcanic episodes which commonly produced a much wider spectrum of rock types.

There are only a few recorded instances of peralkaline silicic rocks not occurring as members of the transitional alkali basalt association. Mayor Island, New Zealand, and Fergusson and Dobu Islands in New Guinea, represent isolated peralkaline centres in dominantly calc-alkaline fields in active mobile belts, though it is possible that alkali basalts form the deeper, unexposed parts of these centres. The riebeckite bearing dykes of Shetland and the peralkaline rocks of the Georgetown inlier belong to post-orogenic acid series also of calc-alkaline affinity. In the eastern Redhills of Skye, a suite of granites of both subalkaline and peralkaline type were intruded shortly after the emplacement of the tholeiitic gabbros of the Cuillin and Blaven masses. There is still some doubt as to the origin of the granites; the possibilities suggested are products of refusion of sialic crustal material and the residua of fractional crystallisation of the gabbros (THOMPSON, 1969, and discussion of his paper). In the latter case, these rocks would be the only record of a true tholeiite - peralkaline rhyolite magmatic lineage.

THE ALKALI OLIVINE BASALT ASSOCIATION

The Basic Rocks

In the past ten years or so, following on the work of COOMBS (1963), it has been increasingly appreciated that the basalts closely

associated with peralkaline rocks are of the mildly alkaline or transitional types, containing only small amounts of either normative hypersthene or nepheline. Slight differences occur in the degrees of silica-saturation of these basalts; those from the younger suite of the northern Kenyan Rift Valley (KING and CHAPMAN, 1972), the Aden Volcanic Line (COX *et al.*, 1970) and the Tibesti Plateau Series (VINCENT, 1970) tend to be slightly silica-undersaturated, while those from such suites as the Nandewar volcano (ABBOTT, 1969), Socorro Island (BRYAN, 1970) and Erta'Alé (BARBERI *et al.*, this vol.) are more commonly *hy* normative. The basalts of Bouvet Island appear to be quartz-normative (BAKER, this vol.). LINDSLEY *et al.* (1971) report the development of approximately silica-saturated syenitic pegmatoids with peralkaline tendencies as the residual products of crystallisation of the Picture Gorge basalt in Oregon. This basalt has about 15 % normative hypersthene, and plots just inside the field of Hawaiian tholeiites defined by MACDONALD and KATSURA (1960), but its mineralogy indicates that it has affinities with the « transitional » basalts of COOMBS (1963). Other areas where the transitional nature of the basalts has been recognised include western Iceland (SIGURDSSON 1971), Pantelleria (VILLARI, this vol.), Kerguelen (BAKER, this vol.) and the Gardar province (UPTON, 1974). In the Basin and Range province of the western U.S.A., there is a wide range of basalt compositions, from nepheline-normative varieties to strongly oversaturated types. NOBLE and PARKER (this vol.) report that many of the basalts are rather potassic, while VITALIANO (1970) refers to many of the Upper Cenozoic « capping » basic rocks of west-central Nevada as belonging to a « calc-alkaline series ».

Within the range of « transitional » basalts, chemical differences other than the degree of silica-saturation must surely exist but little comparative work has yet been done on this aspect. As one example, UPTON (1974) notes that the basic rocks which he considers parental to the intermediate and salic varieties in the Gardar province are high-Al_2O_3, low MgO types. Similarly, little is known about the influence which such chemical features might have on the evolutionary trends of possible derivative liquids. For example, within restricted ranges of pressure, slight differences in chemistry or in oxygen fugacity might influence the order of crystallisation or melting of the major phases, thereby controlling the nature of the derived melts. BARBERI *et al.*, (1972, and this vol.) argue that in the Erta'Ale basalts plagioclase crystallisation proceeded that of clinopyroxene, and the

fractionation of the aluminous phase initiated a trend towards peralkalinity in the final products. BRYAN (1970) has suggested that the Ti-rich nature of basic magmas at Pantelleria and Socorro led to the early precipitation of aluminous titanaugite and titaniferous magnetite, whose removal left liquids of pantelleritic composition.

Further detailed work of this kind will undoubtedly reveal that there are several magmatic lineages leading to peralkaline silicic rocks, and an understanding of the relationship between the crystallisation sequences of the major mineral phases and the detailed chemistry of individual suites will eventually enable us to test various petrogenetic models. Unfortunately, comparison of the chemical variation in volcanic suites ranging from basic through to peralkaline silicic is complicated by the absence or relatively low abundance of the intermediate (in gen. « trachyandesitic », see below) members in several such suites.

Association with Subalkaline and Feldspathoidal Rocks

In many of the alkaline provinces discussed here, peralkaline silicic rocks are closely associated with subalkaline (*i. e.* anorthite-normative) types, a feature repeatedly stressed by NOBLE (1965, 1966, 1970). Examples are the Niger-Nigeria ring complexes (BLACK and GIROD, 1970), the Afar triangle and the Main Ethiopian Rift (BARBERI *et al.* this vol.), the Oslofjord complexes (OFTEDAHL, 1960, 1967), the White Mountain Magma Series (BILLINGS, 1928; CHAPMAN and WILLIAMS, 1935), the Great Basin (NOBLE and PARKER, this vol.), the Gardar province, S. Greenland (WATT, 1966; UPTON, 1974), the Nandewar volcano (ABBOTT, 1969), the Aden Volcanic Line (COX *et al.*, 1970), Iceland (SIGURDSSON, 1971), and several other oceanic islands (Ascension, Bouvet, Easter Island, Kerguelen and Samoa; BAKER, this vol.). The association is in fact, almost ubiquitous, though there are several centres or areas dominated by strongly peralkaline (pantelleritic) magmatism where no subalkaline rhyolites or granites have yet been recorded. These include the Quaternary volcanoes of the central Kenyan rift (BAILEY, this vol.), Socorro (BRYAN, 1964, 1966), Pantelleria (VILLARI, this vol.), and Fantalé (GIBSON, this vol.).

The association with feldspathoidal salic rocks (of both peralkaline and anorthite-normative type) is virtually as common as the association with subalkaline silicic rocks. Among the trachytic Qua-

ternary volcanoes of the central Kenyan rift, Mount Suswa has erupted mildly undersaturated lavas (NASH *et al.*, 1969), while the other major centres tend to be oversaturated (BAILEY, this vol.). Further north the Quaternary volcanoes of the northern Kenyan rift valley (Group V(b) of KING and CHAPMAN, 1972) have erupted both over- and under-saturated salic lavas. In the Tibesti mountains of Chad, feldspathoidal rocks are also present, but are minor compared to the silicic eruptives (VINCENT, 1970). Eruption of an undersaturated peralkaline suite rapidly followed that of an oversaturated series in Gran Canaria during Miocene times (SCHMINCKE, 1969). Plutonic equivalents of the association are the Oslofjord and Gardar provinces (OFTEDAHL, 1960, 1967; and WATT, 1966; UPTON, 1974), the White Mountain Magma Series (CHAPMAN and WILLIAMS, 1935), Ampasindava, Madagascar (LACROIX, 1903), and the Assynt alkaline suite (SABINE, 1953; TILLEY, 1958).

There are, however, areas where no undersaturated rocks have yet been recorded, and these may be distinguished from the « mixed provinces » listed above. They include the Great Basin (NOBLE and PARKER, this vol.), the Aden Volcanic Line (COX *et al.*, 1970), Pantelleria (VILLARI, this vol.), the Cenozoic volcanics of the Ethiopian Rift (LE BAS and MOHR, 1969), Iceland, Nandewar volcano (ABBOTT, 1969), Socorro (BRYAN, 1964) and several oceanic islands, such as Bouvet, Ascension and Easter Island (BAKER, this vol.).

RELATIVE ABUNDANCES AND SILICA-GAPS

A notable feature of many of the peralkaline rock series is the absence or relative scarcity of intermediate (trachyandesitic *s. l.*) members, a feature reported even from areas where rigorous sampling has been carried out. These « silica-gaps » (or the classical Daly gap) are particularly noticeable in pantelleritic terrains, and may be coupled in many centres with an absence or scarcity of basaltic material.

Among areas or centres of pantelleritic or pantelleritic plus comenditic volcanism displaying composition gaps *at the present level of erosion* are Pantelleria (VILLARI, this vol.), Socorro (BRYAN, 1964), Gran Canaria (SCHMINCKE, 1969), Tibesti (VINCENT, 1970), western Iceland (SIGURDSSON, 1971), the stratoid series of central Afar and the Marginal centres of Afar (BARBERI *et al.*, this vol.), the Quaternary central volcanoes of the central Kenyan rift (BAILEY, this vol.) and

the Great Basin (NOBLE and PARKER, this vol.). Ascension Island, where the silicic volcanism is comenditic, also displays a pronounced silica gap (BAKER, this vol.). Among intrusive suites, the Gardar rocks (UPTON, 1974) and the Niger-Nigerian younger « granites » have a similar lack of intermediate compositions.

There are, on the other hand, several suites where « trachyandesitic » compositions are well represented *e. g.* Nandewar volcano (ABBOTT, 1969), the Aden Volcanic Line (COX *et al.*, 1969, 1970), the Erta' Ale range (BARBERI *et al.*, this vol.), Easter Island and possibly Pitcairn Island (BAKER, this vol.), and the Carboniferous volcanics of the Midland Valley of Scotland (TOMKEIEFF, 1937). It is noticeable that the silicic rocks in these cases are all of comenditic type.

Recent research has also pointed out some other examples of compositional gaps in volcanic rock series. THOMPSON (1972) draws attention to the presence in several anorogenic suites of a chemical discontinuity roughly at the boundary between basaltic and « andesitic » (*e. g.* hawaiitic) types. Aden, Dogo-Iki islands in Japan and Erta'Ale are three of his examples which include peralkaline silicic members. UPTON (1974), following upon the work of WATT (1966) and MACDONALD (1969), records the scarcity of compositions intermediate between quartz syenite and granite (SiO_2 65-70 %) in the Gardar province.

It is probable that further documentation will reveal that few volcanic suites are truly continuous, and that most of them will show chemical « hiatuses » over certain ranges of SiO_2 content. Discussion of the significance of these, and the Daly gap mentioned above, is referred to the final paper in this volume.

One further point may be made here. In several suites, the most common basic rocks are not true basalts, but hawaiites. This has been noted, for example, at Aden and Little Aden (COX *et al.* 1970), Nandewar volcano (ABBOTT, 1969) and Ascension Island (BAKER, this vol.). Though BRYAN (1970) and VILLARI (this vol.) refer to the basic rocks of Socorro and Pantelleria (normative plagioclase, An < 50) respectively as basalts, many petrologists would refer to them as hawaiites (COOMBS and WILKINSON, 1969; THOMPSON, 1972). The scarcity of true basalts may simply reflect the present level of exposure of these volcanoes, or be a result of inefficient sampling of available magmas by them. COX *et al.* (1970) point out that though basalts are relatively scarce at Aden and Little Aden, they are abundant at other centres on the Aden Volcanic Line, such as Jebel Khariz.

Relative Abundances

Studies concerning the relative abundance of the various rock types in petrographic provinces were given fresh impetus during the « granite controversy », when it was accepted by the majority of geologists that the vast volumes of intermediate and acid plutonic rocks exposed in many orogenic belts could not have been derived by fractional crystallisation of basic magma, judging from the very small amounts of gabbroic and basaltic rocks associated with them. It is now an integral part of the study of volcanic terrains that workers consider the abundances of the various rock types and that any petrogenetic models proposed should take account of these observations.

The reference point to which most studies are directed is whether or not the observed volumes of the more salic rocks could be derived by fractional crystallisation of the *observed or reasonably inferred* volumes of associated basic rocks. It is here that the concept becomes speculative and open to personal prejudice. This may be illustrated with reference to a basalt-peralkaline trachyte suite. As a first and major imponderable, we still have very little idea of how much trachyte is likely to be produced by fractionation of basaltic magmas in a closed system crystallising under perfect fractionation conditions. As a result, it is impossible to predict how much would be generated under the varying degrees of imperfect fractionation likely to operate in nature. Furthermore, there is no reason to suppose that volcanoes are particularly efficient samplers of available magmas, and the volumes of the various erupted materials may be only a very crude approximation of the actual volumes of each type produced during the magmatic episode. It may be that for some physical reason or other, one type of magma (say, the peralkaline trachyte) is preferentially erupted, leading to a completely false impression of the relative importance of trachyte magma.

Other difficulties exist in providing accurate volumetric data for a volcanic centre. These include (*a*) preferential removal of certain rock types by erosion, (*b*) difficulties of estimating volumetric abundances in, in some cases, virtually non-dissected centres, (*c*) lack of knowledge of the nature and composition of the volcanic substructure.

Such are the problems involved in providing quantitative data on the relative abundances of the different rock (and magma) types in volcanic areas, that one's interpretation of available data must be

based at least in part on prejudice. SCEAL and WEAVER (1971) provide the following information for Pakka, a virtually undissected central volcano of Quaternary age in the Kenyan rift valley: basalt 25 %, mugearite 5 %, trachyte 70 %. That the trachytes are about three times as abundant as the basalts, and some fourteen times as abundant as the mugearites can be viewed either as of fundamental petrogenetic importance, or as an accident of the present level of exposure, depending on the petrogenetic model currently favoured by the individual.

Despite the obvious drawbacks in interpreting volumetric abundance data. I felt that it would be worthwhile to accumulate available information on the subject, as a basis for further discussion. Immediately a further difficulty was encountered in providing these figures, how does one decide on just which groups of rocks within a given province should be compared? Within such a province, there exists a range of rocks erupted perhaps over a considerable period of time and in geographically separate areas, and genetically related in only the broadest sense. For example, during later Pleistocene and Holocene times in Kenya, a string of trachytic and rhyolitic volcanoes developed on the floor of the Rift Valley, accompanied by only minor basic rocks, while to the east of the Rift, more than four times their volume of basaltic material was erupted in large multicentre fields (WILLIAMS, 1972, p. 87). Locally there are two associations — one basic, one salic —, while on a *regional* basis, the volcanism could be considered as essentially bimodal, with a predominance of basalt over trachyte and rhyolite.

In the Main Ethiopian Rift, a series of Quaternary volcanoes lies on or close to the Wonji Fault Belt (GIBSON, this vol.). Each is dominantly silicic, with basic rocks rare or absent, yet the areas *between* centres have been characterised by the eruption from fissures of basalts, hawaiites and mugearites. Are the fissure and central volcanic materials to be considered as independent or related phenomena in this case? The point to be made is that in providing volumetric abundance data for a petrographic province, one may well be lumping together data on rocks of different ages erupted in rather different tectonic environments. More meaningful in this respect may be data for individual centres, where a close genetic relationship between the various eruptive products may be more reasonably assumed, but in concentrating on a geographically restricted area, one may be overlooking important information on the regional availability of the var-

ious magma types. In both cases, petrogenetic models based on the basic : salic ratio should be made with caution.

The data below are grouped into, firstly, those for igneous provinces, and secondly, those for discrete centres of activity. The term salic includes in many cases rocks which are over- and under-saturated with respect to both alumina and silica, where data are not available to distinguish volumes of the peralkaline silicic fraction.

Association	Ratio of basic: salic rocks	Reference
Provinces		
Caenozoic volcanic rocks, Kenya.	~ 1 : 1	Williams, 1972.
Caenozoic volcanic rocks, Ethiopia.	6 : 1	Mohr, 1968.
Caenozoic volcanic rocks, Tibesti, Chad.	61 : 37	Vincent, 1970.
Carboniferous volcanic rocks, Scottish Midland Valley.	92.5 : 4.5	Tomkeieff, 1937.
Centres		
Socorro Island	< 1 : 9	Bryan, 1964.
Pantelleria	< 1 : 9	Rittmann, 1967.
Pakka, northern Kenya (« basic » includes mugearite)	3 : 7	Sceal and Weaver, 1971.
Mayor Island, New Zealand. (trachyandesite as inclusions only)	0 : 100	Ewart *et al.*, 1968.
Menengai, Kenya.	0 : 100	Williams, 1972.

From the foregoing discussion, two situations may be rathe arbitrarily distinguished in peralkaline terrains. (*a*) Provinces wher the salic rocks bulk relatively low compared to the basic types, an where the intermediate (Daly) composition gap is usually absent. The include the oceanic islands (excluding Socorro and Gran Canaria Nandewar volcano, the Erta' Ale range, the Midland Valley of Sco land, and the centres on the Aden Volcanic Line. The Caenozoic vc canoes of the northern Kenyan Rift Valley, such as Pakka, may al

belong in this group. It is noteworthy that the peralkaline silicic rocks of these provinces are normally of comenditic affinity.

b) Provinces of pantelleritic or mixed pantelleritic-comenditic type, where the Daly gap is usually prominent, and where the basic rocks are either in relatively low abundance or are completely absent. Examples are the Tibesti massif in Chad, the Basin-and-Range alkaline series, the centres of the Main Ethiopian Rift, the Marginal series of Afar, the Caenozoic volcanics of central Kenya, Mayor Island, New Zealand, and Socorro Island. Plutonic equivalents include the Gardar province, south Greenland, the Younger Granites of Niger-Nigeria, and the Oslofjord alkaline province.

Manuscript available for the press Nov., 1974.

The Alkaline Rocks

Edited by

H. Sørensen
Institut for Petrologi
Universitetets Mineralogisk-Geologiske Instituter, Copenhagen

A Wiley–Interscience Publication

JOHN WILEY & SONS
LONDON · NEW YORK · SYDNEY · TORONTO

358

distribution and constitution of the mantle. *Rev. Geophys.*, 2, 35–88.

von Eckermann, H., 1948. The alkaline district of Alnö Island. *Sverig. Geol. Undersök.*, 36.

von Herzen, R. P., 1967. Surface heat flow and some implications for the mantle. *The Earth's Mantle*, T. F. Gaskell, Ed., Academic Press, London, 197–230.

Hodgson, J. H., 1964. *Earthquakes and Earth Structure*. Prentice-Hall, New Jersey.

Ito, K., and Kennedy, G. C., 1971. 'An experimental study of the basalt–garnet granulite–eclogite transition', in Heacock, J. G., Ed., The structure and physical properties of the Earth's crust. *Am. Geophys. Union, Geophys. Mon.*, 14, 383–427.

James, D. E., Smith, T. J., and Steinhart, J. S., 1968. Crustal structure of the Middle Atlantic States. *J. Geophys. Res.*, 73, 1983–2007.

Luth, W. C., Jahns, R. H., and Tuttle, O. F., 1964. The granite system at pressures of 4 to 10 kb. *J. Geophys. Res.*, 69, 759–73.

McKie, D., 1966. 'Fenitization', in Tuttle, O. F., and Gittins, J., Eds., *The Carbonatites*. John Wiley and Sons, New York, 261–94.

Ringwood, A. E., and Green, D. H., 1966. An experimental investigation of the gabbro-eclogite transformation and some geophysical implications. *Dept. Geophys. Geochem. Austral. Nat. Univ. Publn.*, 444, 61–103.

Shackleton, R. M., 1970. On the origin of some African granites. *Proc. Geol. Ass.*, 81, 549–59.

Verwoerd, W. J., 1966. 'Fenitization of basic igneous rocks', in Tuttle, O. F., and Gittins, J., Eds., *The Carbonatites*. John Wiley and Sons, New York, 295–308.

Wright, J. B., 1969. Olivine nodules in trachyte from the Jos Plateau, Nigeria. (in press).

Yoder, H. S., Jr., and Tilley, C. E., 1962. Origin of basalt magmas. *J. Petrology*, 3, 342–532.

VI.2. THE RÔLE OF FRACTIONAL CRYSTALLIZATION IN THE FORMATION OF THE ALKALINE ROCKS

R. Macdonald

VI.2.1. Introduction

Bowen (1937) showed that when the normative salic compositions of certain East African alkaline lavas were projected into the system Quartz–Nepheline–Kalsilite (Q–Ne–Ks) they were restricted to the thermal valley on the liquidus surface, and interpreted this as evidence that crystal-liquid equilibria and hence fractional crystallization, had been the dominant process in the origin of these rocks. There is now a large body of experimental data to show that the residual liquids of fractionation of basic magma are enriched in the alkali–alumino silicates. This, and the direct evidence of differentiated intrusions, glassy residua and groundmass assemblages have convinced perhaps the majority of petrologists that fractional crystallization of basaltic magmas is the major cause of differentiation of alkaline rocks. In this chapter some aspects of recent work on the nature and evolution by fractional crystallization of the more common alkaline salic magmas are reviewed.

VI.2.2. Basic Parental Magmas

Coombs (1963) has shown that the fractional crystallization paths of alkali basaltic magma are dependent mainly on its initial composition. A mildly alkaline, transitional group showing neither appreciable hypersthene or nepheline in the norm, differentiates close to the critical plane of SiO_2-undersaturation (Yoder and Tilley, 1962 and II.4*) and leads via hawaiitic and mugearitic types to trachytic residua which straddle the feldspar join in the system Q–Ne–Ks. Under conditions of strong fractionation, the trachytic magma may itself yield phonolitic or alkali rhyolitic residua. Basanitic and nephelinitic magmas follow more strongly undersaturated

* Readers are referred to the relevant Chapters of this book where similarly cited.

crystallization paths, and may produce phonolitic derivatives without an intermediate trachytic stage. In southern Kenya and northern Tanzania two contrasted volcanic associations were supposed by Wright (1963) and Saggerson and Williams (1964) to have followed different fractionation paths: melanephelinite–nephelinite–phonolite and alkali basalt–trachyte(–comendite). Wilkinson (1966) has presented analytical data on the glassy residua of Tertiary basic lavas from New South Wales; the residua of an alkali olivine basalt and a nepheline basanite were trachyte and phonolite respectively. A similar relationship between degrees of SiO_2- undersaturation of parent and daughter magmas has been described from the Atlantic Ocean by de Almeida (1961), who divided the islands into two groups, a hyperalkaline group comprising Trinidade, Fernando de Noronha, Cape Verde, Sao Tomé, Principe and the Canaries, and a mioalkaline group consisting of the islands on the Mid-Atlantic Ridge and Madeira (see IV.7). The hyperalkaline group with the exception of part of the Canaries succession is strongly undersaturated and is approximately equivalent to the continental nephelinite–phonolite series, whereas the mioalkaline group is comparable to Coombs' transitional group of alkali basalts.

Kuno (1968) and Coombs and Wilkinson (1969) have recently provided comprehensive reviews of the possible fractionation trends of alkaline basic magmas. Expanding on their earlier work (see above), Coombs and Wilkinson have shown that there is a continuous spectrum of lineages from basic → salic liquids, depending on the composition of the parental magma. They distinguish the following general series.

Sodic

1. Alkali basalt–hawaiite–mugearite–benmoreite–trachyte.
2. Basanite–nepheline hawaiite–nepheline mugearite–nepheline benmoreite–phonolite.
3. Nephelinite series—? (insufficient data available).

Potassic

4. Trachybasalt–trachyandesite–tristanite–trachyte.
5. Sanidine basanite–nepheline trachyandesite–nepheline tristanite–phonolite.

Before discussing the nature of the residual liquids of these various basic magmas, it is necessary to review a current point of controversy in igneous petrology which bears directly on the rôle of fractional crystallization of basalt magma in the origin of alkaline rocks.

VI.2.3. Silica Gaps

Chayes (1963) has convincingly demonstrated the scarcity on oceanic islands of published analyses of lavas in the range $53\% < SiO_2 < 57\%$, the so-called 'Daly gap'. Although statistical data are not available the Daly gap also appears to exist in continental provinces, such as the Gardar (Upton, IV.3) and Kenya (Wright, 1965). The existence of this silica-gap was considered by Chayes to be of considerable petrogenetic importance since it casts doubt on the origin of basalt → trachyte series by conventional methods of crystal fractionation, where more evolved rocks should continuously occur in progressively smaller bulk.

In reply to Chayes (1963), Harris (1963), Baker (1968) and Cann (1968) have suggested that oceanic trachytes have been oversampled relative to trachyandesites due to their mode of occurrence as erosion-resistant domes and plugs, and to their distinctive, striking appearance in hand-specimen, leading to a bias in the geologist's collecting. Trachyandesites are commonly of dull and uninteresting appearance, may not be distinguishable from basalt in the field, and are more readily eroded than trachyte. These factors may have led to an undersampling of trachyandesites, especially on islands where the volume of intermediate and salic rocks is low. Recent detailed work on Hawaii (Macdonald, 1963) the Tristan da Cunha group (Harris, 1963) and St. Helena (Baker, 1968), the latter long regarded as a classic example of an island showing the Daly gap, has shown that intermediate lavas are

actually more abundant than trachytic and has prompted Baker (1968) to doubt whether the Daly gap would be substantiated during study of other islands. On the other hand, Bryan (1964) has found a distinctly bimodal distribution of lavas on the island of Socorro, with a minimum in the intermediate composition range. Further quantitative data are evidently required to determine whether the apparent scarcity of intermediate lavas is real or a result of sampling error.

Le Maitre (1968, p. 240) has pointed out that the paucity of intermediate lavas in basalt→trachyte sequences may be due to a discrimination in the eruptive process, and not to the scarcity of intermediate magmas, i.e. that trachyandesitic magma formed at depth has not been erupted at the surface as readily as more basic and more salic magma. For any given temperature and pressure acid magmas are more viscous than basic. Conversely, viscosity will decrease in the fractionation sequence basalt→trachyte due to volatile build-up. Intermediate magmas may therefore actually be more viscous than basaltic or trachytic magmas, and during the volcanic cycle may not reach the surface. A bimodal distribution of lavas, though not of magmas, would result.

A striking example of discrimination by a volcano has been given by Gass and Mallick (1968), from the Jebel Khariz volcano west of Aden, which consists of an older cone series of rhyolites, trachytes and basalts, and a younger caldera sequence of dominantly intermediate lavas. A similar relationship has been noted in the Aden and Little Aden volcanoes. Gass and Mallick (1968, p. 79) suggest that the acid magmas, being spatially nearest the surface in the differentiating magma chamber, and the relatively non-viscous basalts, were most readily extruded during the formation of the cone series, whereas the viscous intermediate magma, mainly as pyroclastic material, was erupted on caldera collapse. Had the volcanic cycle not produced caldera collapse, a perfectly good Daly gap would have been reported from the cone series.

A further explanation of silica-gaps may lie in the mechanics of crystallization. Chayes (1963) supposed that the existence of the Daly gap was incompatible with the formation of the basalt→trachyte association by simple fractional crystallization, arguing that successive residual liquids should occur in progressively smaller amounts. Bryan (1964) and Wilkinson (1966) have pointed out, however, that silica-gaps are characteristic of differentiated intrusions which provide some of the best evidence for fractional crystallization. Wyllie (1963) has presented models where apparent silica-gaps can be produced in a crystallization sequence as a result of the geometry of the phase equilibria. A continuous series of compositions from basalt→trachyte may not therefore be a requisite of fractional crystallization, and a combination of this effect, plus some sort of physical control and poor sampling as outlined above, may account for the oceanic Daly gap.

The scarcity of intermediate rocks in continental alkaline provinces is linked with the high ratio of salic: basic lavas, the salic lavas being too voluminous to be considered residual liquids of fractional crystallization of the observed volumes of basalt. This problem will be discussed in the next section.

VI.2.4. Fractionation of Salic Magmas

Alkali feldspar is the dominant mineral in trachytes, rhyolites and phonolites derived by fractionation of alkali basalt, accompanied by lesser amounts of quartz or feldspathoid. Generally the felsic minerals constitute more than 80% of the rocks and obviously their crystallization must have a strong influence on the nature of residual liquids. Fractionation of the other phenocrysts which are present in much smaller amounts, will be less influential. Among this latter group of minerals fayalitic olivine, Fe–Ti oxides, clinopyroxene, apatite and fluorite are common cumulus minerals in layered syenites, and have the effect of removing Mg, Ca, Fe, Ti, Mn, P and F from the melts. The status of biotite and calc-sodic amphiboles as fractionating phases has yet to be established, though both, being relatively undersaturated, could initiate a trend towards SiO_2-saturation in mildly under-

saturated magmas. Both minerals, for example, tend to be absent from the mafic cumulates of the Gardar complexes. In trachytic and phonolitic magmas, Na–Fe minerals may be fractionated: cumulitic aegirine, riebeckite-arfvedsonite and aenigmatite have been recorded in kakortokites from the Ilímaussaq intrusion (Ferguson, 1964), accompanied by the Na–Ca–Zr-silicate, eudialyte. Though these minerals are present in much smaller amounts than alkali feldspar and feldspathoid, their crystallization has influenced the alkali:alumina balance and the Na_2O/K_2O ratios of the melts to some degree. Generally, aegirine is a phenocryst in volcanic salic rocks only rarely, if ever, the primary pyroxene being aegirine-augite or diopside-hedenbergite (Yagi, 1966). The late crystallization of the femic minerals in strongly undersaturated peralkaline liquids is the basis of the 'agpaitic order of crystallization'.

Similarly, the author is unaware of any unequivocal evidence that fractionation of riebeckite-arfvedsonite has occurred in *acid* alkaline magma. The demonstration of Noble (1968), Nicholls and Carmichael (1969) and Bailey and Macdonald (1969) that more evolved pantelleritic liquids have increasingly higher Na/K ratios (cf. Fig. 6) may suggest that crystallization of primary aenigmatite in pantellerites has had little effect in influencing the evolutionary trends of the magmas. It is suggested that the alkali: alumina ratio in alkaline *acid* rocks is determined almost entirely by crystallization of alkali feldspar (assuming fractional crystallization as the only operative process).

The salic residual liquids of fractionation of basaltic magma are conveniently considered in terms of the system Q–Ne–Ks, petrogeny's residua system, the main features of which have been discussed by Tuttle and Bowen (1958), Fudali (1963) and Hamilton and MacKenzie (1965). Fractionation of alkali feldspar from trachytic liquids lying on either side of the alkali feldspar thermal divide must drive the residual liquids away from the divide into the so-called low-temperature trough or thermal valley on the liquidus surface. Slight SiO_2-deficiency or excess in the initial magmas is accentuated on progressive fractionation, with the ultimate production of phonolitic and rhyolitic liquids whose compositions are similar to the under- and over-saturated minima respectively.

Although this system has been useful in describing trends in salic magmas, it is not strictly a residua system for peraluminous or peralkaline rocks, i.e. those where molar $Na_2O + K_2O \neq Al_2O_3$ (Bailey and Schairer, 1964). Peralkaline magmas do not fractionate, for example, towards the minima in Q–Ne–Ks, but towards natural eutectics considerably richer in excess alkali (expressed as normative acmite and sodium metasilicate), analogous to those found experimentally in Na_2O–Al_2O_3–Fe_2O_3–SiO_2 by Bailey and Schairer (1966) (q+ab+ac+sodium disilicate and ne+ab+ac +sodium disilicate). Strongly peralkaline liquids such as pantellerites and agpaites cannot be plotted in terms of Q, Ne and Ks without gross distortion, especially in the Na_2O/K_2O ratios and feldspar/liquid relationships. The salic end members of the alkali basalt–trachyte association are typically peralkaline, carrying normative acmite, or have peralkaline tendencies as shown by the presence of alkali amphiboles and pyroxenes. To examine composition trends in these rocks, Bailey and Macdonald (1969) have devised two simple plots based on the molecular proportions of SiO_2, Al_2O_3, Na_2O and K_2O. The derivation of these projections is summarized in Fig. 1, and they are used in subsequent diagrams to illustrate several features of magmatic evolution. Though the projection has been used successfully for oversaturated salic rocks, success in plotting undersaturated rocks has been limited mainly because nepheline and feldspar are the common felsic phenocrysts of phonolites. The composition of both minerals cannot lie in any one plane whose alkali:alumina ratio is greater than 1. Fractionation trends involving crystallization of both feldspar and nepheline (or any feldspathoid) cannot therefore be shown without distortion in the projection. There is an urgent need for more sophisticated methods of plotting the compositions of undersaturated, peralkaline rocks, because until these are available, we will be unable to describe quantitatively

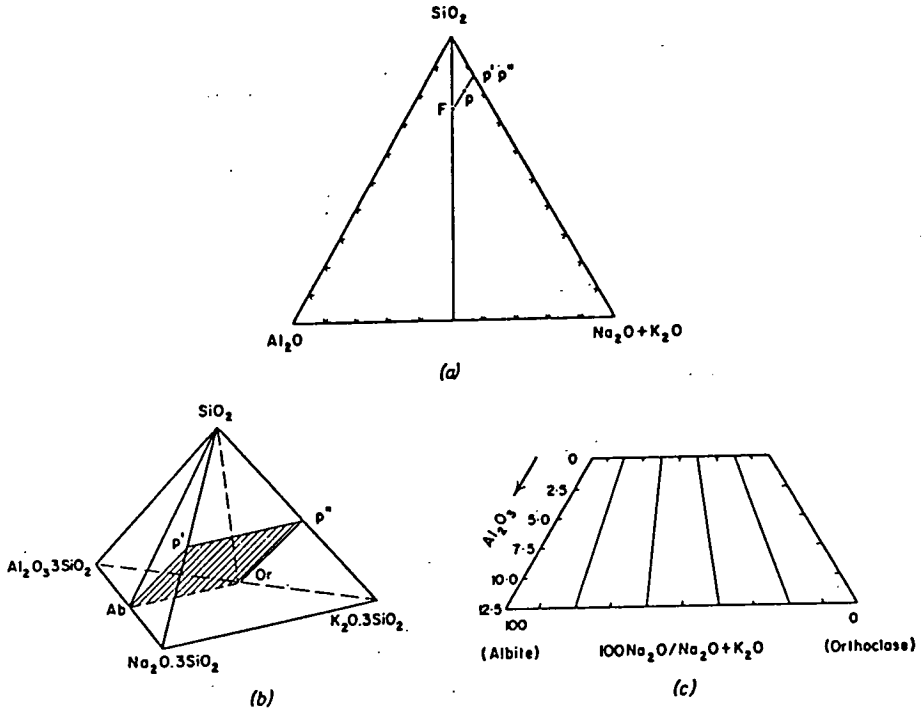

Fig. 1 (a) SiO_2–Al_2O_3–($Na_2O + K_2O$) diagram. Alkali feldspar projects as a point, F. P—hypothetical peralkaline composition. P′P″, the intersection of line Feldspar–P on alkali–silica sideline, measures the alkali–silica index of composition P. An infinite number of these planes may be drawn radiating from F.

(b) The oversaturated volume of the system Na_2O–K_2O–Al_2O_3–SiO_2, showing the plane Ab–Or–P″–P′. This plane is equivalent to F–P–P′P″ in (a).

(c) Quadrilateral representing any plane in the peralkaline volume of (b), such as Ab–Or–P″P′

the crystallization histories of the magmas.

The development of peralkaline residua is possible in any suite where feldspar is fractionating and where there is a deficiency of Al_2O_3 with respect to Na_2O, K_2O and CaO (expressed as normative diopside and/or wollastonite). Molar deficiency of this type will permit the 'plagioclase effect' of Bowen (1945) to operate. This effect depends on the fact that pure albite cannot precipitate from a liquid containing Ca, and means that precipitation of Ca-bearing plagioclase from suitable melts will tend to leave potential alkali silicate in the liquid. A kenyte from South Victoria Land, Antarctica analysed by Carmichael (1964) carries phenocrysts of anorthoclase (20%), olivine (0·6%), pyroxene (0·8%), iron ore (0·6%) and nepheline (trace). The feldspar phenocrysts have the composition $Or_{17}Ab_{63·2}An_{19·8}$ while the normative feldspar is $Or_{36·2}Ab_{55·6}An_{8·2}$. The rock has no normative acmite whereas the residual liquid (groundmass) carries 4·16% of that component. Carmichael (1964, p. 56) has pointed out that this is a natural example of the plagioclase effect operating to produce peralkaline residua. The degree of peralkalinity achieved by a given magma series will depend on the initial composition of the basaltic parents, but also on the magma crystallization history. For example, fractionation from basic melts of unusually large amounts of calcic plagioclase relative to olivine and clinopyroxene would rapidly deplete Al relative to alkalis and promote the passage to peralkaline residual liquids. In this respect it is tempting to

link the quite strongly peralkaline nature of several continental provinces, e.g. Gardar, New Hampshire, Oslo and Niger, with the occurrence in them of large bodies of anorthosite (cf. IV.3 and IV.8).

A peralkaline trend could also be initiated by fractionation of biotite (Carmichael, 1967), aluminous pyroxene (Schairer and Yoder, 1960), spinel, garnet or Al-bearing iron oxide (Bailey and Schairer, 1966), or of non-stoichiometric alkali feldspar (Luth and Tuttle, 1966). When a condition of Al_2O_3-deficiency has been achieved, further feldspar fractionation must accentuate this tendency, and successive residual liquids will be increasingly peralkaline. Similarly, if the trachytic liquid has even a slight excess of Al_2O_3, feldspar crystallization will promote a miaskitic trend. It was pointed out earlier that SiO_2-saturation or undersaturation in trachytic magma is also accentuated by feldspar fractionation. Bailey and Schairer (1964) have therefore suggested that trachytes lie near a 'cross-roads', which may lead to four kinds of residua, peralkaline or peraluminous oversaturated and peralkaline or peraluminous undersaturated liquids.

VI.2.4.1. Oversaturated Liquids

An excellent demonstration of the strong fractionation of saturated trachytic magma towards a rhyolitic end-point is provided by the western lower layered series of the Kûngnât complex, South Greenland (Upton, 1960). This thick series of syenites and quartz syenites showing rhythmic and cryptic layering, as well as igneous lamination, is thought to have developed by the gravitative settling of alkali feldspars in the range Or_{34-42} wt. %, Fe-olivines and clinopyroxenes, with subordinate amounts of apatite and Fe–Ti oxides. During fractionation the feldspars, originally sanidines which subsequently unmixed to perthites, showed an increase in Or relative to Ab while An decreased. Olivines became increasingly Fe-rich, and the pyroxenes showed a trend from ferroaugites to hedenbergites containing some aegirine-augite in solid solution. The other minerals present in the syenites, including quartz, hastingsitic amphiboles and biotite are of intercumulus origin.

The syenites are cut by a series of microgranite sheets which Upton (1960) has interpreted as the low-temperature residues from the layered succession. These peralkaline sheets consist essentially of alkali feldspar, quartz, riebeckite-arfvedsonite, aegirine and astrophyllite. Relative to the syenites they are depleted in Ti, Al, Fe, Mn, Mg, Ca and P, but enriched in Si, F, H_2O and in alkalis relative to Al_2O_3.

The geological relationships at Kûngnât make an origin of the microgranites by fractionation of trachytic magma seem very convincing. In the volcanic environment, however, attempts to describe the origin of peralkaline rhyolitic liquids have had mixed results, as might be expected. Most recent studies have tried to show that peralkaline rhyolites (i.e. the pantellerites and the comendites) are derived from peralkaline or peraluminous trachytes dominantly by fractionation of alkali feldspar (e.g. Carmichael and MacKenzie, 1963, Thompson and MacKenzie, 1967, Noble, 1968, Abbott, 1969, Macdonald, 1969). A simplified example of this process is shown diagrammatically in Fig. 2, where it can be seen that removal of feldspar (F) must restrict liquids (such as X) to a plane (Feldspar-X-X′) until a second phase crystallizes. This plane has a unique value of the ratio alkali:silica measured as the intercept on the SiO_2–alkalis side-line, dependent on the initial composition of the trachyte (Bailey and Macdonald, 1969) and a series of peralkaline liquids connected solely by alkali feldspar fractionation should have constant alkali:silica index.

Liquids evolving in a plane such as Feldspar-X-X′ will eventually reach the quartz–feldspar cotectic curve, and quartz becomes a phenocryst phase. Composition trends in that zone are controlled by removal of feldspar + quartz, and are approximately at right angles to any earlier feldspar trend. Their goal is presumably a natural eutectic analogous to the oversaturated eutectic (q + ab + ac + Na-disilicate) determined at 728 °C at 1 atmosphere in the system Na_2O–Al_2O_3–Fe_2O_3–SiO_2 by Bailey and Schairer (1966).

An example of a series which may have

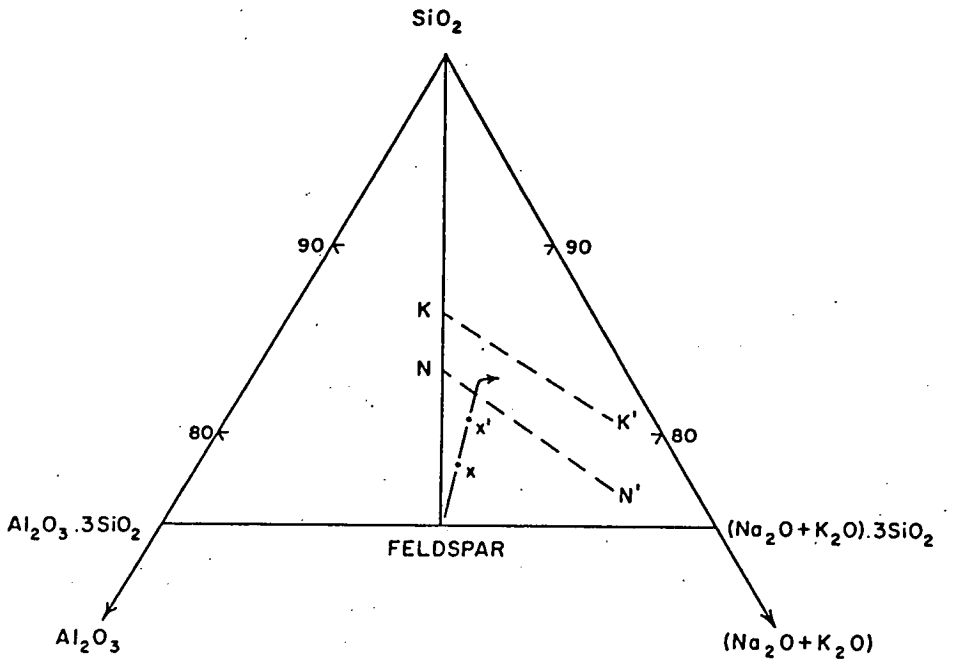

Fig. 2 SiO_2–Al_2O_3–(Na_2O + K_2O) diagram. X—hypothetical peralkaline trachyte, X′—peralkaline rhyolite. K–K′ is the quartz–potash feldspar cotectic and N–N′ the quartz-albite cotectic from the systems K_2O–Al_2O_3–SiO_2 and Na_2O–Al_2O_3–SiO_2 at 1 atmosphere (Schairer and Bowen, 1955, 1956). The zone defined by these lines is termed the quartz–feldspar cotectic zone. A possible fractionation trend of magmas of composition comparable to X is shown

evolved in this way is a peralkaline dyke swarm of Gardar age from the Tugtutôq area, South Greenland (Macdonald, 1969), which is a series passing from hastingsite microsyenites with small amounts of normative acmite to aegirine rhyolites and microgranites of comenditic affinity (Upton, 1964a). The phenocryst assemblages are:

Hastingsite microsyenites: Alkali feldspar, minor amounts of olivine, clinopyroxene, apatite, ore.

Riebeckite microsyenites: Alkali feldspar, minor amounts of ore.

Riebeckite microgranites: Alkali feldspar, quartz, minor amounts of riebeckite-arfvedsonite (or aegirine pseudomorphs), ore.

Aegirine microgranites: Alkali feldspar, quartz, minor hedenbergite, fayalite.

Analyses of the dykes have been plotted in Fig. 3; the trend is consistent with fractionation of the most abundant phenocryst minerals, i.e. feldspar from the trachytic magmas, and feldspar + quartz from the rhyolitic magmas. The analyses in the quartz–feldspar cotectic zone are rather scattered, a feature due at least partly to devitrification of the acid dykes (Macdonald, 1969).

Carmichael (1962), Carmichael and MacKenzie (1963) and Thompson and MacKenzie (1967) have specifically seen the evolution of peralkaline acid magmas as along a natural low-temperature zone analogous to the thermal valley in petrogeny's residua system. As determined experimentally the axis of this zone projects from the unique fractionation curve in Q–Or–Ab into the peralkaline volume of the system Na_2O–K_2O–Al_2O_3–SiO_2 and is strongly

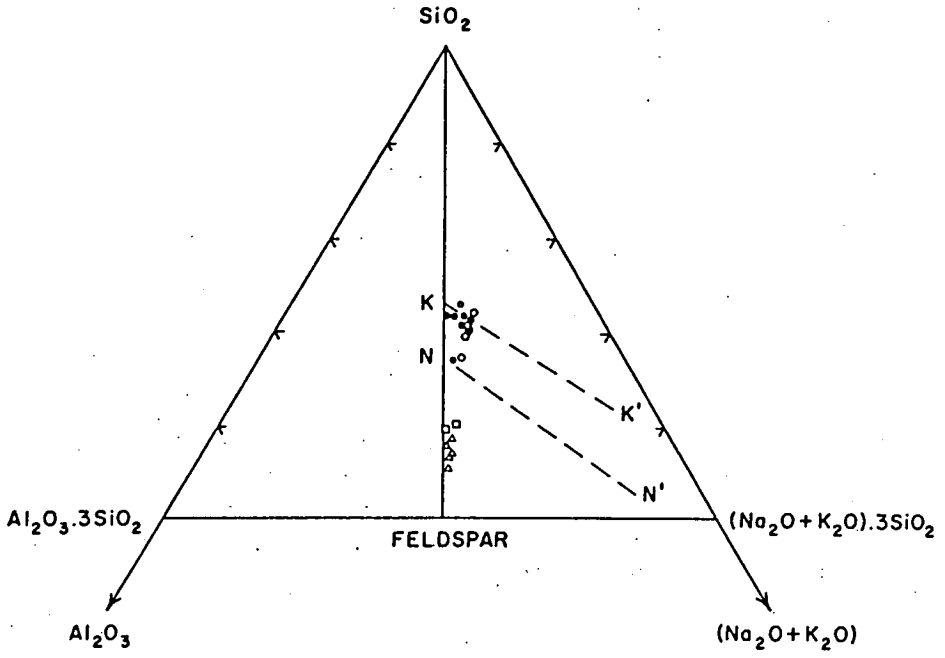

Fig. 3 Analyses of peralkaline microsyenite, rhyolite and microgranite dykes from Tugtutôq, South Greenland plotted in a SiO_2–Al_2O_3–(Na_2O + K_2O) diagram. Triangles—hastingsite microsyenites, squares—riebeckite microsyenites, closed circles—riebeckite microgranites, open circles—aegirine microgranites

inclined towards the NaO_2–Al_2O_3–SiO_2 plane (Fig. 4, from Thompson and MacKenzie, 1967). Depending on the initial composition, the equilibrium feldspar can be more or less sodic than the trachytic liquids, and its separation will drive residual liquids towards the low-temperature zone, when further separation of a feldspar of narrow composition range (Or_{30-35}) will restrict the residual liquids to the zone. Once the liquid composition projects into the zone, this liquid must, on further feldspar fractionation, become progressively more sodic (cf. the orthoclase effect of Bailey and Schairer, 1964. See Fig. 5).

The concept of the 'low-temperature zone', based on the experimental study of synthetic material, is not so easily applied to natural peralkaline rock assemblages. Macdonald, Bailey and Sutherland (1970) were unable to relate a series of pantelleritic trachyte and pantellerite obsidians from the Kenyan Rift Valley to a natural analogue of the zone, and could not explain the chemical features of the series by simple crystal fractionation. Nicholls and Carmichael (1969, p. 273) have shown that the feldspar-residual glass relationships in comendites (transitional to pantellerites) from Mayor Island, New Zealand, are rather different from those of rocks from Pantelleria and from Kenya and stated that 'The comenditic feldspar phenocrysts cannot be so readily incorporated into Thompson and MacKenzie's picture of feldspar crystallization.' By recalculation of the experimental data of Carmichael and MacKenzie (1963), Macdonald, Bailey and Sutherland (1970) found that the axis of the proposed low-temperature zone could not be straight or even gently curved, unless some complex feldspar–liquid–vapour-relationship had not been recognized during the experiments. Until many more

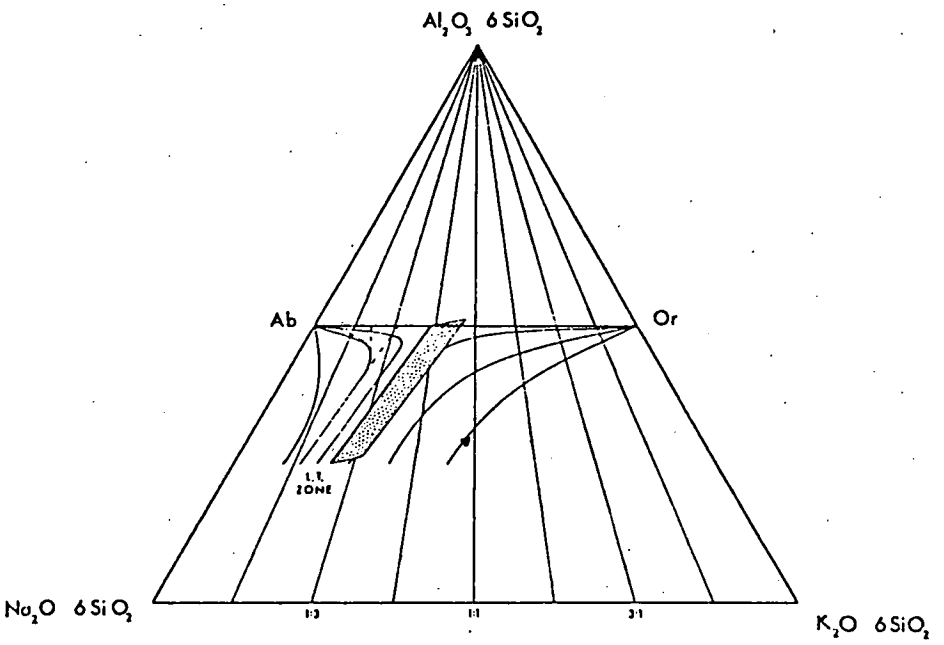

Fig. 4 The low-temperature zone (stippled) and associated fractionation curves in part of the system Na_2O–K_2O–Al_2O_3–SiO_2–H_2O, from Thompson and MacKenzie (1967, Fig. 7). The relations have been projected from SiO_2, on to the plane Al_2O_3 . $6SiO_2$–Na_2O . $6SiO_2$–K_2O . $6SiO_2$; lines radiating from the apex represent equal Na_2O/K_2O ratio. The hypothetical fractionation curves are shown as full lines

data are available on phenocryst–peralkaline siliceous glass pairs, the problem as to the existence of the natural analogue of the zone will persist. If, however, it does exist, it must be considerably more complex than envisaged from the experimental studies.

Using various continental alkaline suites as examples, Bailey and Schairer (1966), Wright (1966, 1969), Macdonald and Gibson (1969) and Bailey and Macdonald (1970) have also questioned the series basalt → peralkaline or peraluminous trachyte → peralkaline rhyolite as a product of continuous fractional crystallization. The disproportionately large volumes of salic relative to basic lavas in certain parts of the African Rifts caused Bailey and Schairer (1966) to suggest that alkaline trachytes and rhyolites are formed by partial melting in the deep crust or upper mantle, while Wright (1966, 1969) has found ultrabasic nodules in certain phonolites and trachytes from New Zealand and Nigeria which he has interpreted as indicating a direct mantle origin of these rocks. Chabbi volcano, Ethiopia, appears to have erupted only aphyric pantellerites of almost identical composition for several thousands of years, and Macdonald and Gibson (1969) found it difficult to see this as a result of recurrent fractional crystallization of basic magma. The mildly peralkaline comendites and comenditic trachytes have recently been reviewed by Bailey and Macdonald (1970). Whereas the oceanic rhyolites show chemical features consistent with their derivation from trachytic magmas dominantly by alkali feldspar fractionation, the continental comendites lie on a trend parallel to the quartz–feldspar minima in the peralkaline oversaturated volume of the system Na_2O–K_2O–Al_2O_3–SiO_2 as determined experimentally by Carmichael and MacKenzie (1963), rather than a distribution away from the minimum on the Or–Ab join (i.e. simplified alkali trachyte composition). Bailey and Mac-

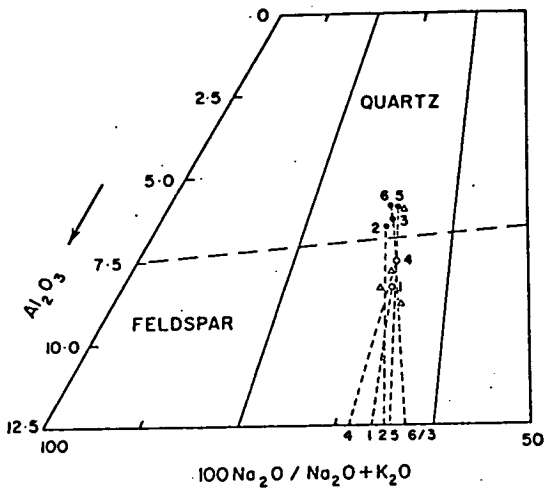

Fig. 5 Analyses of pantellerite obsidians from Pantelleria plotted in a quadrilateral representing the plane of alkali : silica index 7 : 93 (Bailey and Macdonald, 1969, Fig. 5). The quartz–feldspar cotectic has been interpolated between the intercepts of the Na_2O side-line with the quartz–feldspar cotectic, and the K_2O side-line with the quartz–potash feldspar side-line. Lavas on which there are petrographic data are shown by circles (filled where quartz-phyric) and those on which there are no data by triangles. Tie-lines connect rocks and their feldspar phenocrysts (in terms of mol. per cent Or/Or + Ab). With one exception, the feldspar phenocrysts are more potassic than the rocks, thus demonstrating the 'orthoclase effect' of Bailey and Schairer (1964). Data from Washington (1914), Zies (1960), Carmichael (1962), Chayes and Zies (1962, 1964)

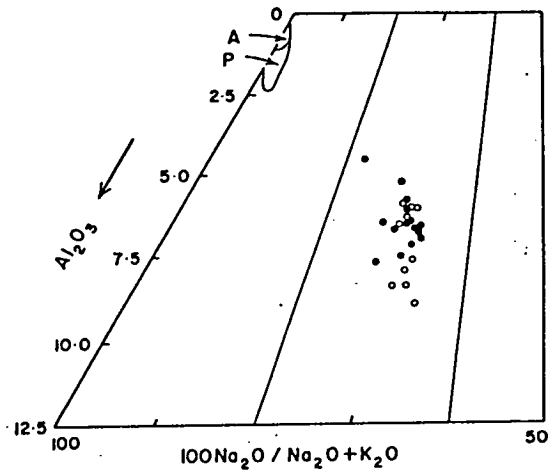

Fig. 6 Quadrilateral in which have been plotted pantellerite analyses taken from the literature. Note that the overall trend is towards increase in Na_2O/K_2O ratio with decreasing Al_2O_3. A = field of aenigmatite phenocrysts, P = field of pyroxene phenocrysts from pantellerite lavas, recalculated from data in Carmichael (1962), Zies (1966) and Ewart *et al.* (1968)

donald suggested that the continental comendites may represent partial fusion products, rather than fractional crystallization products, of basic material.

In summary, it is reasonable to assume that saturated alkaline trachytes and rhyolites may be formed by two or more processes. Where the volumes of basic and salic magmas are of the right order, and where the chemical trends are explicable by fractionation of the observed phenocryst assemblages, there is no strong case for doubting a derivation of the salic liquids by fractionation of basic magma, e.g. in the Gardar province (Upton, Chapter IV.3), in the majority of the oceanic islands, and in such volcanoes as Nandewar (Abbott, 1969) and those of the Aden Peninsula (Gass and Mallick, 1968). Where either of these conditions is unfulfilled, as in central Kenya (Macdonald *et al.*, 1970), it may be necessary to critically re-examine our petrogenetic theories. In any specific case, fractional crystallization must be proven, rather than assumed, to be the operative process.

VI.2.4.2. Undersaturated Liquids

Undersaturated trachytic magma may evolve in a rather similar way to oversaturated trachyte, i.e. dominantly by fractionation of feldspar, until the nepheline–feldspar cotectic is reached. The alkaline intrusions of the Gardar province, S. Greenland, where highly efficient crystal fractionation has produced rhythmically and cryptically layered syenites, provide excellent examples of this trend (see IV.3). The Hviddal giant dyke, a 550 m broad composite dyke in the Tugtutôq area, has a central intrusion of syenite and a narrow marginal zone of syeno-gabbro (Upton, 1964b). The syenite varies continually along its length from a larvikitic augite syenite to

a soda-rich foyaite, and this differentiation is believed by Upton to be due to cryptic and phase layering in an accumulitic suite of syenites, of which some 2000 m are exposed. Details of the mineralogical and chemical changes may be found in the original paper; of particular interest here is the sequence of cumulus phases. In the lower 800 m or so, the principal cumulus minerals were alkali feldspar, clinopyroxene, olivine, ilmenomagnetite and minor fluorapatite. Upton stresses the similarity of this assemblage to that in the more basic syenites of the Kûngnât complex, an intrusion which has fractionated from syenite → peralkaline granite. Olivine disappeared in the next 2000 m and from 1000 to ~ 1400 m cumulitic pyroxene, ore and apatite decreased in amount. Feldspar was possibly the only cumulate mineral for some 100 m. Nepheline eventually joined feldspar and the ratio of cumulus feldspar:nepheline was approximately 3:1 (Upton, 1964b, p. 77). The fractionation trend of the Hviddal dyke is shown in Fig. 7 a, b. The trachytic magma evolved in a metaluminous condition and became peralkaline only in the later stages of the exposed succession. With further fractionation, involving removal of both feldspar and nepheline the residual liquids would have moved towards a composition enriched in alkali silicate, similar to the quaternary invariant point (ne+ab+ac+sodium disilicate) found experimentally at 715 °C and 1 atm by Bailey and Schairer (1966) in the system Na_2O–Al_2O_3–Fe_2O_3–SiO_2.

Strong fractionation of undersaturated trachytic magma is displayed in the classic agpaitic complex of Ilímaussaq, some 15 km east of the eastern outcrops of the Hviddal dyke, but considerably younger than it. The following outline of the petrochemical evolution of the agpaites is based on the relationship demonstrated by a Si_2O–Al_2O_3–(Na_2O + K_2O) diagram (Fig. 8) and incorporates suggestions made by Ussing (1912), Sørensen (1958), Ferguson (1964), and Hamilton (1964). The parental magma was a larvikitic augite syenite closely comparable to that of the Hviddal dyke (Fig. 7), and it differentiated *in situ*, mainly by fractionation of feldspar with lesser amounts of clinopyroxene, olivine, ore, apatite, along a similar trend to that of the Hviddal syenites, to give a foyaite. *In situ* differentiation of this foyaite led to a gravity accumulated series of layered nepheline syenites (kakortokites) and to a flotation accumulitic series of sodalite-rich syenites (naujaites, cf. II.2).

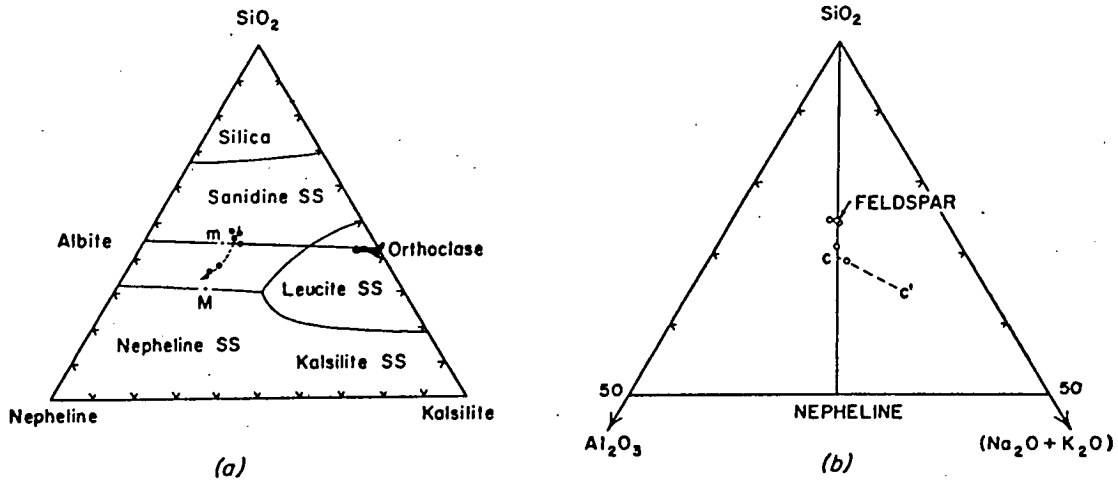

Fig. 7 Analyses of nepheline syenites from the Hviddal dyke, Tugtutôq, South Greenland plotted (a) in the system Q–Ne–Ks (after Upton, 1964b). m = alkali feldspar minimum, M = temperature minimum in Ab–Or–Ks–Ne (from Hamilton and MacKenzie, 1965). (b) in SiO_2–Al_2O_3–(Na_2O + K_2O) diagram. C–C', albite–nepheline cotectic from Schairer and Bowen (1956)

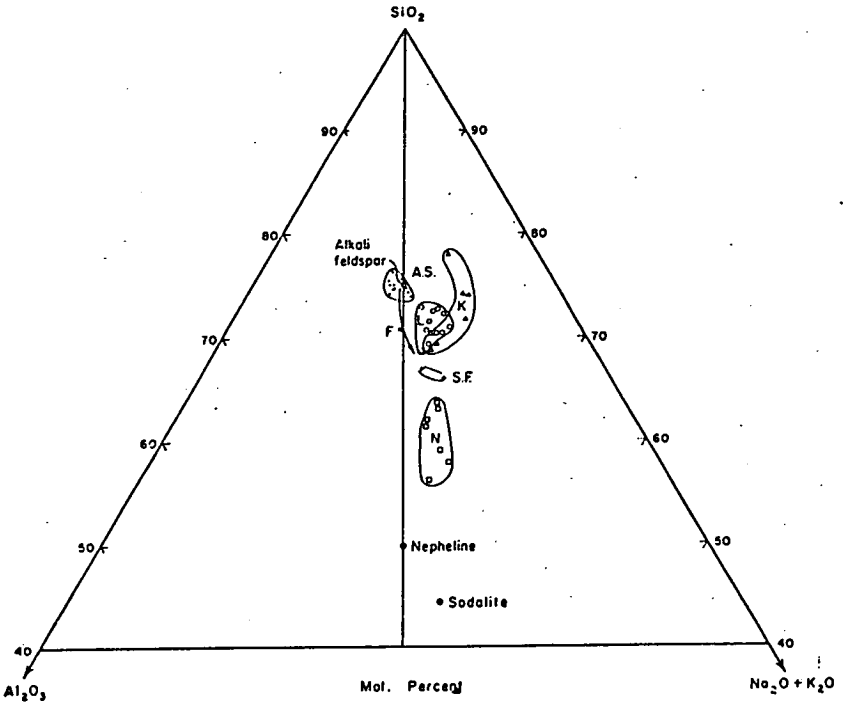

Fig. 8 Augite syenites and agpaites from the Ilímaussaq complex, South Greenland. A.S. = field of augite syenites (analyses given by solid circles), F = foyaite multiplication sign), S.F. = sodalite foyaites (crosses), N = naujaites (squares), K = kakortokites (triangles, filled for black kakortokites, half-filled for red, open for white), L = lujavrites (open circles). Data from Ussing (1912), Ferguson (1964), Hamilton (1964), Gerasimovsky and Kuznetsova (1967). Heavy line—trend of Hviddal nepheline syenites from Fig. 7

Three major types of kakortokites have been distinguished, consisting of various proportions of cumulus perthite, aegirine, riebeckite-arfvedsonite, eudialyte and nepheline (Ferguson, 1964, 1970; Sørensen, 1969).

The naujaites have formed by accumulation of floated sodalitic crystals from a sodalite foyaite, and their trend in Fig. 8, showing a range in composition between the sodalite composition point and the sodalite foyaites is consistent with this proposal. The residual liquids trapped between the downward crystallizing naujaites and the kakortokites were the lujavrites, highly peralkaline nepheline syenites consisting essentially of microcline, albite, arfvedsonite, aegirine, nepheline and eudialyte. The lujavrites show no distinct trend in Fig. 8 since their composition has been determined by fractionation of at least six cumulus phases from the immediately parental sodalite foyaite.

Agpaitic rocks such as those of Ilímaussaq are very scarce (Sørensen, 1960) and extrusives of lujavrite compositions, for example, have not been recorded. This possibly reflects the absence of the special conditions especially high volatile content necessary for the strong fractionation of foyaitic magma. Certain phonolites from the island of Trinidade have compositions comparable to the Ilímaussaq sodalite foyaites, and also carry phenocrysts of sodalite (de Almeida, 1961). Further fractionation of these magmas may eventually have led to lujavrite-like liquids, but the situation is complicated by the fact that various heteromorphic felsic assemblages may be developed in these salic liquids (Wilkinson, 1965), and by the possibility that other alkali rich

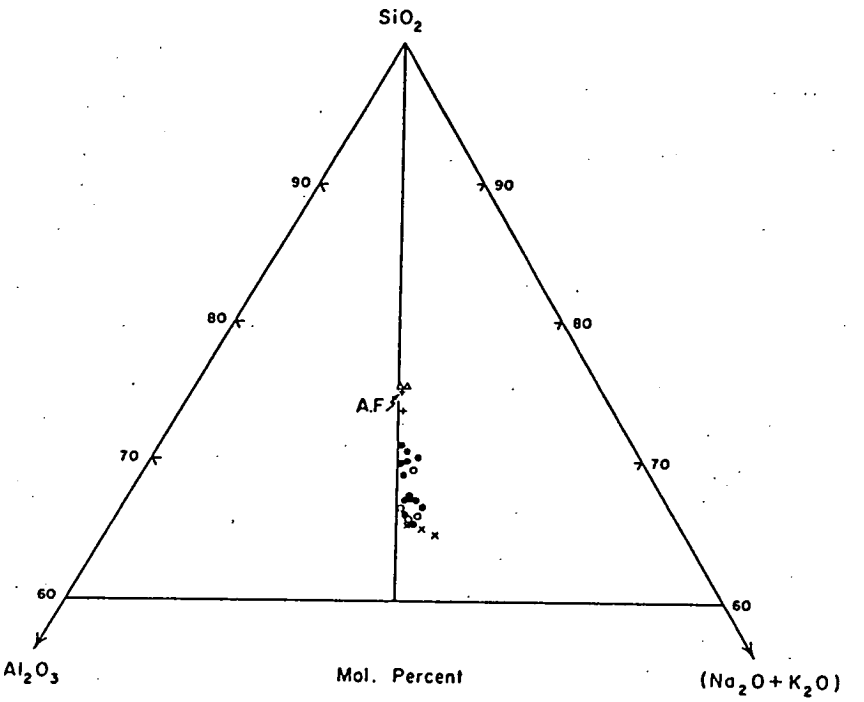

Fig. 9 Analyses of peralkaline phonolites from Atlantic islands. Triangles—St. Helena, crosses—Azores, solid circles—Principe, open circles—S. Tomé, multiplication signs—Trinidade

minerals such as aegirine or alkali amphibole may be fractionated.

The Trinidade phonolites (de Almeida, 1961) are more strongly undersaturated and more peralkaline than the phonolites of other Atlantic islands, some of which are plotted in Fig. 9. Those from St. Helena are mildly undersaturated and plot near the feldspar composition, whereas those on Principe, associated with basanites, are more strongly undersaturated and peralkaline. On Trinidade very strongly undersaturated and peralkaline phonolites occur with nephelinites and though seemingly stemming from different parental types, the phonolites of Principe and Trinidade overlap slightly in terms of SiO_2, Al_2O_3 and alkalis. It seems probable that continued fractionation of the Principe magmas would eventually produce residua comparable to those of Trinidade, though it should be possible to distinguish the two types of phonolite by their bulk chemistry, e.g. FeO, MgO and CaO contents, as they have evolved along different trends. In the general case, nepheline in strongly undersaturated series may have been crystallizing as phenocrysts in the most basic magmas, whereas in mildly alkaline basalt–phonolite suites, primary nepheline follows alkali feldspar in the crystallization sequence.

It seems clear that undersaturated basic magmas can evolve towards a phonolitic composition along several magmatic trends. One lineage descends near the critical plane of silica-undersaturation to the trachyte stage, but by continued feldspar fractionation can evolve towards a more undersaturated end-point, e.g. Ilímaussaq, St. Helena (Baker, 1969), Gough (Le Maitre, 1962) and Mt. Suswa, Kenya (Nash, Carmichael and Johnson, 1969). At the other extreme, phonolitic liquids may form from nephelinitic parents with only a small intermediate crystallization history, e.g. Trinidade. In the intermediate case, basanites may eventually fractionate towards phonolite,

via feldspathoidal trachybasalts (Coombs and Wilkinson, 1969).

VI.2.5. Transitions between Undersaturated and Oversaturated Compositions

Since the discovery that the alkali feldspar join in Q–Ne–Ks is a barrier preventing the passage of quartz- or nepheline-normative liquids to the other side, several mechanisms for crossing the barrier plane have been suggested. As mentioned earlier, the degree of SiO_2-saturation of residual liquids of fractional crystallization of basalt seems to be mainly dependent on the composition of the parent. Strongly oversaturated (i.e. with appreciable normative hypersthene) and strongly undersaturated (high in normative nepheline) basalts cannot normally give rise on fractionation to undersaturated or oversaturated residua, respectively. It is apparent too that the critical plane of SiO_2 undersaturation in basalts, Fo–Di–Pl, Yoder and Tilley (1962), is generally effective in controlling fractionation trends in the mildly alkaline, transitional group of basalts (Coombs, 1963). On the islands of the Mid-Atlantic Ridge two (Ascension and Bouvet) have hypersthene-normative basalts and rhyolitic derivatives, and three (St. Helena, Tristan de Cunha and Gough) have nepheline-normative basalts and phonolitic derivatives. However in the Azores, where the average basalt is nepheline-normative, both phonolites and rhyolites are found (Baker *et al.*, 1964). In some provinces such as the Gardar and Oslo provinces, larvikitic syenite (with small amounts of normative nepheline) was parental to oversaturated and undersaturated trends, leading to quartz syenite and granite on one hand, and to nepheline syenite and foyaite on the other (Barth, 1954). If it can be assumed that the thermal barrier Or–Ab has an equivalent crystallization barrier in these more complex natural compositions, then it might be crossed by any of several mechanisms.

VI.2.5.1. Undersaturated → oversaturated

Acmite melts incongruently to hematite plus a liquid enriched in NaO_2 and SiO_2; failure of the hematite to be resorbed from a suitable range of nepheline-normative liquids could result in passage of the liquids to an oversaturated condition, (Tilley, 1958). However, acmite crystallizes only from a liquid with excess sodium silicate (Bailey and Schairer, 1966), i.e. in the natural case where $Na_2O+K_2O > Al_2O_3+Fe_2O_3$. The effect could work only in strongly peralkaline liquids, yet in the majority of cases, magmas are thoroughly committed to either an under- or oversaturated trend before sodium metasilicate becomes a normative component. The incongruent melting of acmite probably is of minor importance in petrology, and it is significant that Nolan (1966) was unable to find any petrographic evidence of its occurrence in nature.

Bowen (1928) suggested from experience in Q–Ne–Ks at 1 atmosphere that the incongruent melting of orthoclase to leucite plus SiO_2-rich liquid could permit passage of undersaturated magmas over the join Ab–Or. The field of leucite is restricted at higher water vapour pressures, however, and incongruent melting of Or is eliminated at 2·6 kb and 900°C, (Goranson, 1938). The field of compositions which could show this effect is very small under normal magmatic conditions and Tilley (1958) and Fudali (1963) have suggested that the importance of this mechanism has probably been overemphasized.

Alkali feldspar is the most abundant phenocryst in the majority of trachytic rocks, and its composition strongly controls the fractionation paths that these rocks can follow. Even small departures from stoichiometry might influence the evolution of magma critically balanced with respect to SiO_2. For example, slight deficiency of SiO_2 from the ideal 1:1:6 formula might initiate an oversaturated from an undersaturated trend. In this respect it is interesting that the analyses of feldspars from Oslo larvikite reported by Oftedahl (1948) and Muir and Smith (1956) contain SiO_2 deficiences equivalent to 1–7% by wt. nepheline solid solution. Fractionation of SiO_2-deficient hydrous minerals such as biotite or certain amphiboles may also drive mildly undersaturated trachytic liquids through the feldspar divide. Biotite, for example, is a phenocryst in microsyenites from the Gardar and in trachytes from

Gough Island (Le Maitre, 1962) but its status as a cumulus phase has not yet been established.

VI2.5.2. Oversaturated→ undersaturated

This transition is considerably more difficult to achieve than the reverse, though again it must be questioned whether the process has more than theoretical significance in petrology. Bailey and Schairer (1966, p. 154) have suggested a possible mechanism, based on observations in the synthetic system NaO_2–Al_2O_3–Fe_2O_3–SiO_2, namely substitution of Fe^{3+} for Al in feldspar. The effect is to use Fe to make the molecule $NaFe^{3+}Si_3O_8$ rather than the acmite molecule $NaFe^{3+}Si_2O_6$, thereby using more silica. A trachytic magma plotting just on the silica-rich side of a natural crystallization barrier, such as Ab–Or–Ac–Alkali Disil., might be pushed through the plane towards the SiO_2 undersaturated side by separation of alkali feldspar carrying small amounts of Fe in its structure.

VI.2.6. Concluding Remarks

The fractionation of alkali feldspar from trachytic magma showing only a small range in the degree of SiO_2-saturation and alkali:alumina ratio can produce at least four series of residual liquids. Crystallization of feldspar is accompanied in peralkaline rhyolites by quartz, and in phonolites by a feldspathoid, and though the effect of feldspar fractionation alone is to make the slightly different parental peralkaline magmas diverge, crystallization of the second phase tends to make the different trends converge towards common eutectic compositions. In the phonolitic end-members of strongly undersaturated volcanic series, feldspathoid may be the dominant fractionating phase, and there may be an increase in the ratio feldspar:feldspathoid in residual liquids.

So far as is known the alumina:alkalis balance is not seriously affected by the crystallization of other phenocrysts in acid alkaline magmas. In undersaturated parageneses, other alkali-bearing minerals may be cumulus phases, but as they occur in relatively minor amounts the effect of fractionating them seems to be minor compared to the crystallization of the felsic minerals.

The demonstration by Coombs (1963) that the degree of undersaturation of salic alkaline magmas varies closely with that of the associated basic rocks is strong evidence that fractional crystallization has played the major rôle in the origin of the alkaline salic rocks. However, where the volume relationships of basic, intermediate and salic rocks can be shown to be totally inconsistent with such an origin, as is probable in parts of the East African Rifts, then partial melting of basic material may have contributed some part of the observed alkaline magma. One task of petrologists is to devise methods of distinguishing liquids formed by partial melting from those produced by fractionation (cf. VI. 1a. 5).

Further work should include chemical and modal analyses of phenocrysts and glass of alkaline obsidians, especially undersaturated types, coupled with relevant experimental studies, in order to establish the various evolutionary paths followed by these magmas. The direct evidence afforded by layered syenite intrusions must also be employed. Particularly large gaps exist in our knowledge of the trachytes and phonolites associated with strongly undersaturated basic rocks.

ACKNOWLEDGEMENT

I would like to thank Dr. D. K. Bailey for reading the manuscript, and for many lively discussions on the origin of alkaline rocks.

VI.2. REFERENCES

Abbott, M. J., 1969. Petrology of the Nandewar volcano, N.S.W., Australia. *Contr. Miner. Petrology*, **20**, 115–34.

Almeida, F. F. M. de, 1961. *Brazil, Div. de Geol. e Miner., Dept. Nac. de Prod. Mineral*, Monograph 18.

Bailey, D. K., 1964. Crustal warping—a possible tectonic control of alkaline magmatism. *J. Geophys. Res.*, **69**, 1103–11.

Bailey, D. K., and Macdonald R., 1969. Alkali feldspar fractionation trends and the derivation of peralkaline liquids. *Am. J. Sci.*, **267**, 242–8.

Bailey, D. K., and Macdonald, R., 1970. Petrochemical features of mildly peralkaline (comenditic) rhyolite glasses from the continents and ocean basins. *Contr. Miner. Petrology*, **28**, 340–51.

Bailey, D. K., and Schairer, J. F., 1964. Feldspar–liquid equilibria in peralkaline liquids—the orthoclase effect. *Am. J. Sci.*, **262**, 1198–206.

Bailey, D. K., and Schairer, J. F., 1966. The system Na_2O–Al_2O_3–Fe_2O_3–SiO_2 at 1 atmosphere, and the petrogenesis of alkaline rocks. *J. Petrology*, **7**, 114–70.

Baker, I., 1968. Intermediate oceanic volcanic rocks and the 'Daly gap'. *Earth Planet. Sci. Let.*, **4**, 103–6.

Baker, I., 1969. Petrology of the volcanic rocks of Saint Helena Island, South Atlantic. *Bull. geol. Soc. Am.*, **80**, 1283–310.

Baker, P. E., Gass, I. G., Harris, P. G., and Le Maitre, R. W., 1964. The volcanological report of the Royal Society expedition to Tristan da Cunha, 1962. *Phil. Trans. Roy. Soc. Lond.*, **256**, 439–578.

Barth, T. F. W., 1954. Studies on the igneous rock complex of the Oslo region 14: Provenance of the Oslo magmas. *Skr. norske Vidensk Akad., Mat.–naturv. Kl.*, 4.

Bowen, N. L., 1928. *The Evolution of the Igneous Rocks*. 332 pp. Princeton Univ. Press.

Bowen, N. L., 1937. Recent high-temperature research on silicates and its significance in igneous geology. *Am. J. Sci.*, **33**, 1–21.

Bowen, N. L., 1945. Phase equilibria bearing on the origin and differentiation of the alkaline rocks. *Am. J. Sci.*, **243A**, 75–89.

Bryan, W. B., 1964. Relative abundance of intermediate members of the oceanic basalt–trachyte association: evidence from Clarion and Socorro Islands, Revillagigedo Islands, Mexico. *J. Geophys. Res.*, **69**, 3047–9.

Cann, J. R., 1968. Bimodal distribution of rocks from volcanic islands. *Earth Planet. Sci., Lett.*, **4**, 479–80.

Carmichael, I. S. E., 1962. Pantelleritic liquids and their phenocrysts. *Mineralog. Mag.*, **33**, 86–113.

Carmichael, I. S. E., 1964. Natural liquids and the phonolitic minimum. *Geol. J.*, **4**, 55–60.

Carmichael, I. S. E., 1967. The iron–titanium oxides of salic volcanic rocks and their associated ferromagnesian silicates. *Contr. Miner. Petrology*, **14**, 36–64.

Carmichael, I. S. E., and MacKenzie, W. S., 1963. Feldspar–liquid equilibria in pantellerites: an experimental study. *Am. J. Sci.*, **261**, 382–96.

Chayes, F., 1963. Relative abundance of intermediate members of the oceanic basalt–trachyte association. *J. Geophys. Res.*, **68**, 1519–34.

Chayes, F., and Zies, E. G., 1962. Sanidine phenocrysts in some peralkaline volcanic rocks. *Carnegie Inst. Wash. Yearbook*, **61**, 112–18.

Chayes, F., and Zies, E. G., 1964. Notes on some Mediterranean comendite and pantellerite specimens. *Carnegie Inst. Wash. Yearbook*, **63**, 186–90.

Coombs, D. S., 1963. Trends and affinities of basaltic magmas and pyroxenes as illustrated on the diopside–olivine–silica diagram. *Min. Soc. Am. Spec. Pap.*, **1**, 227–50.

Coombs, D. S., and Wilkinson, J. F. G., 1969. Lineages and fractionation trends in undersaturated volcanic rocks from the East Otago Volcanic Province (New Zealand) and related rocks. *J. Petrology*, **10**, 440–501.

Ewart, A., Taylor, S. R., and Capp, A. C., 1968. Geochemistry of the pantellerites of Mayor Island, New Zealand. *Contr. Miner. Petrology*, **17**, 116–40.

Ferguson, J., 1964. Geology of the Ilímaussaq intrusion, South Greenland. *Meddr. Grønland*, **172**, 4.

Ferguson, J., 1970. The significance of the kakortokite in the evolution of the Ilímaussaq intrusion, South Greenland. *Meddr. Grønland*, **190**, 1, 193 pp.

Fudali, R. F., 1963. Experimental studies bearing on the origin of pseudoleucite and associated problems of alkalic rock systems. *Bull. geol. Soc. Am.*, **74**, 1101–26.

Gass, I. G., and Mallick, D. I. J., 1968. Jebel Khariz: an Upper Miocene strato-volcano of comenditic affinity on the South Arabian coast. *Bull. Volcan.*, **32-1**, 33–88.

Gerassimovsky, V. I., and Kuznetsova, S. Ya., 1967. On the petrochemistry of the Ilímaussaq intrusion, South Greenland. *Geochem. Int.*, **4**, 236–46.

Goranson, R. W., 1938. Silicate–water systems. Phase equilibria in the $NaAlSi_3O_8$–H_2O and $KAlSi_3O_8$–H_2O systems at high temperatures and pressures. *Am. J. Sci.*, **35-A**, 71–91.

Hamilton, E. I., 1964. The geochemistry of the northern part of the Ilímaussaq intrusion, S.W. Greenland. *Meddr. Grønland*, 162, 10.

Hamilton, D. L., and MacKenzie, W. S., 1965. Phase-equilibrium studies in the system $NaAlSiO_4$ (nepheline)–$KAlSiO_4$ (Kalsilite)–SiO_2–H_2O. *Mineralog. Mag.*, 34, 214–31.

Harris, P. G., 1963. Comments on a paper by F. Chayes, 'Relative abundances of intermediate members of the oceanic basalt–trachyte association'. *J. Geophys. Res.*, 68, 5103–7.

Kuno, H., 1968. 'Differentiation of basalt magmas', in Hess H. H. and Poldervaart, A, Eds., *Basalts: the Poldervaart Treatise on Rocks of Basaltic Composition, vol. 2*, 623–88. Interscience, New York.

Le Maitre, R. W., 1962. Petrology of volcanic rocks, Gough Islands, South Atlantic. *Bull. geol. Soc.*, 73, 1309–40.

Le Maitre, R. W., 1968. Chemical variations between and within volcanic rock series—a statistical approach. *J. Petrology*, 9, 220–52.

Luth, W. C., and Tuttle, O. F., 1966. The alkali feldspar solvus in the system Na_2O–K_2O–Al_2O_3–SiO_2–H_2O. *Am. Miner.*, 51, 1359–73.

Macdonald, G. A., 1963. Relative abundance of intermediate members of the oceanic basalt–trachyte association—a discussion. *J. Geophys. Res.*, 68, 5100–2.

Macdonald, R., 1969. The petrology of alkaline dykes from the Tugtutôq area, South Greenland. *Bull. geol. Soc. Denmark*, 19, 257–82.

Macdonald, R., Bailey, D. K., and Sutherland, D. S., 1970. Oversaturated peralkaline glassy trachytes from Kenya. *J. Petrology*, 11, 507–17.

Macdonald, R., and Gibson, I. L., 1969. Pantelleritic obsidians from the Volcano Chabbi (Ethiopia). *Contr. Miner. Petrology*, 24, 239–44.

Muir, I. D., and Smith, J. V., 1956. Crystallisation of feldspars in larvikite. *Zeit. Krist.*, 107, 182–95.

Nash, W. P., Carmichael, I. S. E., and Johnson, R. W., 1969. The mineralogy and petrology of Mount Suswa, Kenya. *J. Petrology*, 10, 409–39.

Nicholls, J., and Carmichael, I. S. E., 1969. Peralkaline acid liquids: a petrological study. *Contr. Miner. Petrology*, 20, 268–94.

Noble, D. C., 1965. Gold Flat member of the Thirsty Canyon Tuff—a pantellerite ash-flow sheet in southern Nevada. *U.S. geol. Survey, Prof. Paper.*, 525-B, 85–90.

Noble, D. C., 1967. Sodium, potassium, and ferrous iron contents of some secondarily hydrated natural silicic glasses. *Am. Miner.*, 52, 280–6.

Noble, D. C., 1968. Systematic variation of major elements in comendite and pantellerite glasses. *Earth Planet. Sci. Let.*, 4, 167–72.

Noble, D. C., Smith, V. C., and Peck, L. C., 1967. Loss of halogens from crystallised and glassy silicic volcanic rocks. *Geochim. cosmochim. Acta*, 31, 215–24.

Nolan, J., 1966. Melting relations in the system $NaAlSi_3O_8$–$NaAlSiO_4$–$NaFeSi_2O_6$–$CaMgSi_2O_6$–H_2O and their bearing on the genesis of alkaline undersaturated rocks. *Q. J. geol. Soc. Lond.*, 122, 119–57.

Oftedahl, C., 1948. Studies on the igneous rock complex of the Oslo region. 9: The feldspars. *Skr. norske Vidensk Akad., Mat.-naturv. Kl*, 3.

Romano, R., 1968. New petrochemical data of volcanites from the Island of Pantelleria (Channel of Sicily). *Geol. Rundschau*, 57, 773–83.

Saggerson, E. P., and Williams, L. A. J., 1964. Ngurumanite from Southern Kenya and its bearing on the origin of rocks in the northern Tanganyika alkaline district. *J. Petrology*, 5, 40–81.

Schairer, J. F., and Bowen, N. L., 1955. The system K_2O–Al_2O_3–SiO_2. *Am. J. Sci.*, 253, 681–746.

Schairer, J. F., and Bowen, N. L., 1956. The system Na_2O–Al_2O_3–SiO_2. *Am. J. Sci.*, 254, 129–195.

Schairer, J. F., and Yoder, H. S., 1960. The nature of residual liquids from crystallisation, with data on the system nepheline–diopside–silica. *Am. J. Sci.*, 258A, 273–83.

Sørensen, H., 1958. The Ilímaussaq batholith. A review and discussion. *Meddr. Grønland*, 162, 3.

Sørensen, H., 1960. On the agpaitic rocks. *Rep. Int. geol. Congr. 21st Session, Norden*, Pt. 13, 319–27.

Sørensen, H., 1969. Rythmic igneous layering in peralkaline intrusions. *Lithos*, 2, 261–83.

Thompson, R. N., and MacKenzie, W. S., 1967. Feldspar–liquid equilibria in peralkaline acid liquids: an experimental study. *Am. J. Sci.*, 265, 714–34.

Tilley, C. E., 1958. Problems of alkali rock genesis: *Q.J. geol. Soc. Lond.*, 113, 323–60.

Tuttle, O. F., and Bowen, N. L., 1958. Origin of granite in the light of experimental studies in the system $NaAlSi_3O_8$–$KAlSi_3O_8$–SiO_2–H_2O. *Geol. Soc. Am. Mem.*, 74, 153 pp.

Upton, B. G. J., 1960. The alkaline igneous complex of Kûngnât Fjeld, South Greenland. *Bull. Grønlands geol. Unders.*, 27 (also *Meddr Grønland*, 169, 8).

Upton, B. G. J., 1964a. The geology of Tugtutôq and neighbouring islands, South Greenland. Part 2. Nordmarkitic syenites and related alkaline rocks. *Meddr. Grønland*, 169, 2.

Upton, B. G. J., 1964b. The geology of Tugtutôq and neighbouring islands, South Greenland. Part 4. The nepheline syenites of the Hviddal composite dyke. *Meddr. Grønland*, 169, 3.

Ussing, N. V., 1912. The geology of the country around Julianehaab, Greenland. *Meddr. Grønland*, 38.

Villari, L., 1968. On the geovolcanological and morphological evolution of an endogenous dome (Pantelleria, Mt. Gelkhamar). *Geol. Rundschau*, 57, 784–95.

Washington, H. S., 1914. The volcanoes and rocks of Pantelleria. *J. Geol.*, 22, 16–27.

Wilkinson, J. F. G., 1965. Some feldspars, nepheline and analcimes from the Square Top Intrusion, Nundle, N. S. W. *J. Petrology*, 6, 420–44.

Wilkinson, J. F. G., 1966. Residual glasses from some alkali basaltic lavas from New South Wales. *Mineralog. Mag.*, 35, 847–60.

Wright, J. B., 1963. A note on possible differentiation trends in Tertiary to Recent lavas of Kenya. *Geol. Mag.*, 100, 164–80.

Wright, J. B., 1965. Petrographic sub-provinces in the Tertiary to Recent volcanics of Kenya. *Geol. Mag.*, 102, 541–57.

Wright, J. B., 1966. Olivine nodules in a phonolite of the East Otago alkaline province, New Zealand. *Nature*, 210, 519.

Wright, J. B., 1969. Olivine nodules and related inclusions in trachyte from the Jos Plateau, Nigeria. *Mineralog. Mag.*, 37, 370–4.

Wyllie, P. J., 1963. Effects of the changes of slope on liquidus and solidus paths in the system diopside–anorthite–albite. *Min. Soc. Am. Spec. Pap.*, 1, 204–12.

Yagi, K., 1966. The system acmite–diopside and its bearing on the stability relations of natural pyroxenes of the acmite–hedenbergite–diopside series. *Am. Miner.*, 15, 976–1000.

Yoder, H. S., and Tilley, C. E., 1962. Origin of basalt magmas: An experimental study of natural and synthetic rock systems. *J. Petrology*, 3, 342–532.

Zies, E. G., 1960. Chemical analysis of two pantellerites. *J. Petrology*, 1, 304–8.

Zies, E. G., 1966. A new analysis of cossyrite from the island of Pantelleria. *Am. Miner.*, 51, 200–5.

VI.3. LIMESTONE ASSIMILATION

Peter J. Wyllie

VI.3.1. Introduction

Limestone assimilation by subalkaline magma as a process for generating desilicated alkaline magma was proposed by Daly in 1910. It has remained on the petrological scene as a healthy hypothesis ever since, although in the past twenty years its strength has been waning. From the very beginning, the idea has been avidly supported by ardent advocates and vigorously contested by sceptical adversaries.

The two opposing views persist into the sixth decade. Schuiling (1964b) considered the limestone assimilation theory to be 'the only theory which really has been demonstrated in the field with a degree of certainty, scarcely ever achieved by petrological observation'. On the other hand, Turner and Verhoogen (1960, p. 396) concluded that 'Several decades of investigation have failed to confirm the efficacy of limestone assimilation as a significant factor in the development of nepheline-syenite magma.'

In the following account I have adopted a historical approach, in which I have attempted to trace certain aspects of the controversy through successive time periods. The three selected time periods of twenty-five, twenty, and fifteen years do appear to represent rather distinct stages. The first, 1910–35, is the period during which the stimulating hypothesis was launched. Arguments for and against were based mainly on interpretation of field data. The second period, 1936–55, was one during which the lines of attack and defense became deeply entrenched, and experimental study of silicate systems revealed the thermal barrier on the liquidus of silicate systems, rearing its ugly hump between subalkaline and feldspathoidal liquids. During the third period, 1956–70, the study of carbonatites disrupted the field evidence for limestone assimilation, and additional experimental data made it even more difficult to support the hypothesis.

PERMO-CARBONIFEROUS VOLCANISM IN NORTHERN BRITAIN

REVIEW ARTICLE

Petrochemistry of the Early Carboniferous (Dinantian) Lavas of Scotland

R. MACDONALD
Department of Environmental Sciences, University of Lancaster.

SYNOPSIS

This review is focussed on the early Carboniferous (Dinantian) stage of the complex Carboniferous-Permian volcanic cycle in central and southern Scotland (The "Midland Valley petrographic province"). Stress is particularly laid on aspects of the petrochemistry and petrogenesis not previously recognized or sufficiently discussed in the literature. The scarcity of analytical data for rocks from critical parts of the province means that much of the discussion must be of a preliminary nature; areas where further research is required are indicated.

The Dinantian lavas, dominated by a range of mildly undersaturated and hypersthene-normative (transitional) alkaline basalts, have associated nepheline or hypersthene-normative hawaiites, mugearites, benmoreites, quartz-trachytes and rhyolites. Several geographically distinct magmatic lineages are recognized, varying in such parameters as degree of silica undersaturation, Fe/Mg ratios and Na_2O/K_2O ratios at comparable values of differentiation index. TiO_2 and P_2O_5 contents also vary from suite to suite.

The proportions of each lava type are variable in different areas, but three volcanic associations are rather arbitrarily distinguished; one showing a spectrum of rocks from ankaramitic basalt to trachytes and rhyolites: a second dominated by plagioclase-phyric basalts and hawaiites: and thirdly, an association consisting largely of olivine-clinopyroxene-phyric basalts, with more differentiated rocks scarce or absent. Though data are very scarce for post-Dinantian lavas, it is suggested that there has been a progressive change in basic magma chemistry with time during the Carboniferous, later alkaline magmas being increasingly silica-undersaturated. This change was accompanied by a change in the nature of the volcanism, which became more explosive, tuffs and agglomerates representing an increasing proportion of the eruptive products.

Some aspects of the petrogenesis of the Dinantian basic lavas are examined. A high-pressure (>10 kb) stage of fractionation variably involving clinopyroxene or olivine + clinopyroxene is required to explain the chemical variation in the basalts and hawaiites. More differentiated rocks may have evolved by crystal fractionation at lower pressures (within crustal magma reservoirs?) but insufficient data are available to test this hypothesis.

INTRODUCTION

Published nearly forty years ago, Tomkeieff's (1937) influential review still stands as the main source of information on the petrochemistry of the Carboniferous-Permian alkaline rocks of central and southern Scotland ("The Midland Valley petrographic province"), while the only attempt to provide a comprehensive volcano-tectonic

Scott. J. Geol. 11, (4), 269–314, 1975

synthesis of the province is that by MacGregor (1948). During the last three decades or so, it would appear that interest in the petrology of these rocks has been generally low.

It is saddening that the province which, through the work of, *inter alia*, Hatch, Bailey, Tyrrell, Flett, MacGregor and Tomkeieff contributed so much to petrological thought in the first half of this century, does not now merit a single mention in such important new texts as that by Carmichael, Turner and Verhoogen (1974).

This review is meant to be a first step towards coordinating a renewed interest in the petrochemistry of the Scottish Carboniferous-Permian volcanic rocks. Concentration is focussed on the Dinantian volcanism which was only one part, albeit the most important volumetrically, of a complex magmatic and tectonic cycle, which also included later Carboniferous and Permian alkaline magmatism, a late Carboniferous phase of tholeiitic dyke and sill intrusion and a Permian suite of camptonitic intrusions in northern Scotland (MacGregor 1948). Little modern petrological work has been published on these post-Dinantian rocks, however, and the papers by MacGregor (1948, 1955) and Walker (1965) summarize most of the available information.

The specific aims of this review are:

(a) to provide a chemical classification of the alkaline rocks which slightly modifies existing classifications, but which is more in line with modern usage.

(b) to indicate the range of rock types present in terms of such chemical characteristics as degrees of silica-saturation and relative iron-enrichment and Na_2O/K_2O ratios. To this end, 49 new whole-rock analyses of lavas and intrusions from several localities are presented.

(c) to draw attention to the existence of several volcanic lineages within the Dinantian lava successions.

(d) to make some preliminary observations on the origin and evolution of the Dinantian basic magmas.

(e) to make some recommendations as to those fields where further petrochemical research is most needed.

A comment on the freshness of the rocks

It may be suspected that extrusive rocks of Carboniferous age would be sufficiently altered to make detailed petrochemical studies unrewarding. As MacGregor (1937) has pointed out, however, many of the Midland Valley rocks are very fresh, and relatively unaltered material is quite common over much of the ground. The intrusions are often in completely fresh condition. Among the lavas, basalts containing fresh, or only partially altered, olivine can often be found after diligent search, while in many other basic rocks, all the minerals except for the olivine are unaltered. Fresh trachytes are also fairly common, e.g. in the Clyde Plateau and East Lothian outcrops.

In my experience, the rocks most persistently found in an altered state are the mugearites, benmoreites and rhyolites. Again, careful search can usually reveal fairly clean material of intermediate composition, though olivine is seldom found unaltered in such rocks. Unfortunately, the rhyolites are almost invariably thoroughly altered.

In this study, analyses of rocks which have obviously been chemically altered have not been used in diagrams or in calculations and an attempt has been made to take account of the secondary oxidation affecting many samples by calculating CIPW norms with standard Fe_2O_3 values. The chemical variations within, and between, the various lava suites described below are, I feel, a true reflection of magmatic differences and not significantly due to secondary alteration processes.

Dinantian Volcanic Activity

Dinantian activity resulted in the formation of lava fields covering about 12,000 km², with a maximum thickness of just under 1 km (Francis 1967). The main outcrops are shown in Figure 1, while Francis (1967, figs. 3 and 5) has drawn cross-sections across the Midland Valley demonstrating the unusually clear picture of the three-dimensional distribution of the volcanic strata afforded by mining operations, boreholes and geophysical surveys.

Details of the overall distribution of the Dinantian sediments and volcanics, of local successions and of the relationships between sedimentation and volcanism have been summarized by Francis (1965a, 1965b, 1967, 1968, 1970) and will not be repeated here. Extra relevant references published since 1970 include Hall (1973), Davies (1974), McAdam (1974), Whyte and J. G. MacDonald (1974) and Craig and Hall (1975).

Sources of the volcanic rocks

Extrusion of the Dinantian magmas was relatively quiet. Though tuffs and agglomerates are common at the base of some local successions, perhaps due to phreatomagmatic activity as magmas were erupted into shallow lagoonal areas (McAdam *et al.* 1969; Whyte and J. G. MacDonald 1974), pyroclastic rocks are notably scarce compared to lavas in the main piles. The sources from which the basic lavas were emitted are not always identifiable. Black (1966) describes many of the centres which probably acted as the sources for the various sequences exposed in Edinburgh. In the Campsie Fells and Kilpatrick Hills, an impressive line of vents extending from Dumbarton to Dungoil almost certainly fed the lower parts of the local successions (MacGregor *et al.*, 1925; Whyte and J. G. MacDonald 1974; Craig and Hall 1975). Eruption of the more densely porphyritic basic rocks and more differentiated lavas of the Upper Group of the Campsie Fells seems to have been related to the growth of a substantial central volcano (Craig and Hall 1975). Further east, nearer Stirling, the lava pile has been interpreted as being of fissure origin (Francis *et al.*, 1970).

Little is known about eruptive sources or mechanisms in the area of the Clyde Plateau lavas south of the River Clyde. As in the Campsie Fells, eruption of trachytic lavas accompanied the growth of complex vents or centres (composite volcanoes?) in Renfrewshire (Johnstone 1965), and of a remarkable line of smaller vents extending ESE. though the Lanarkshire Block (Richey 1928, pp. 254–5).

In East Lothian, lack of inland exposure makes identification of source conduits

extremely difficult. Clough *et al.* (1910), followed by McAdam *et al.* (1969), have suggested that the two basaltic necks at Burning Mount, Kippielaw [NT 581 752] and St. Baldred's Cradle [NT 637 813] may represent feeder pipes to the lavas. Chemically, though, the St. Baldred's rock is much more silica-undersaturated than any analyzed East Lothian basic lava (Day 1930a), and may be of late, rather than early, Carboniferous, age (see pp. 296–9). Perhaps, as McAdam *et al.* (1969 p. 36) suggest, the feeders to the basalts are hidden in the poorly exposed ground near East Linton, where the basic lava succession is thickest.

The same authors suggest that the thick trachytic flows (and cumulo-domes?) of the Garleton Hills were of very local derivation, and probably conceal their source vents. These viscous magmas probably did not flow very far, an idea apparently supported by the much thinner sequence of trachytes in the Spilmersford borehole lava pile some 7 km further west (McAdam, 1974).

Earlier workers in the Birrenswark lavas of the Scottish Borders suggested, mainly on petrographical grounds, that the Tournaisian lavas issued from some of the many vents and plugs exposed along the lava outcrop (see Greig 1971, for summary). More recently, Leeder (1974) has drawn isopach maps for these lavas and has shown that they form a narrow strip elongated along the northern edge of the Northumberland Basin. He suggests that they were erupted either from aligned fissures or from small vents located along fissures and were related to the formation of the sedimentary basin in a tensional stress regime. A similar mode of eruption is proposed by Leeder (1974) for the Kelso Traps, located in a similar tectonic environment some 50 km further east.

Somewhat younger, Visean, activity in Dumfriesshire resulted in a rather different type of volcanism. The Glencartholm Volcanic Beds are dominantly pyroclastic in nature, while some of the sources of these rocks may be identified in agglomerate-filled necks near Langholm (Lumsden *et al.*, 1967). Thus the south-west Border country shows evidence of an evolution towards an increasingly explosive type of magmatic activity during the early Dinantian. The process is similar to the longer-term trend in the Midland Valley (see pp. 272–3).

Eruptive sequences

Tomkeieff (1937; see also Upton 1969) has noted a tendency for a long-term change of magma type from basic to acid in the Dinantian volcanic cycle. He would seem to be referring to the field evidence that, in many areas, trachytic and trachyandesitic rocks were erupted relatively late in the history of local successions, e.g. in the Upper Groups established by Survey Officers in the Campsie Fells (MacGregor *et al.*, 1925) and the Renfrewshire–Ayrshire Hills (Richey *et al.*, 1930).

This tendency should perhaps not be too widely applied. Evidence from the Renfrewshire Hills suggests that trachytic magma was available at a relatively early stage of the Dinantian activity (Johnstone 1965), while in the Cleish Hills, Fife (Francis 1967, p. 226) and in the eastern part of the Machrihanish outcrop, Kintyre (R. Macdonald,

unpublished mapping), rhyolitic rocks occur near the base of the local successions, overlain by basalts in both cases. There is much other evidence that basic and salic magmas were simultaneously available in some areas (Richey 1928; Francis 1967, p. 240). If the formation of the highly differentiated magmas reflected the growth of high-level magma chambers (see p. 306), then the formation of these chambers may have been dictated more by the details of local tectonics than by a decline in the vigour of the Dinantian volcanic activity (Upton 1969, p. 5).

Nature of the post-Dinantian volcanism

Several important points regarding the nature of the Midland Valley alkaline volcanism have recently been stressed by Francis (1967, 1968), following on the work of MacGregor (1948) and Tomkeieff (1937).

(i) The total volume of erupted materials decreased during the Carboniferous, so that the greatest accumulations of material (>80%?) were during the Dinantian.

(ii) The proportions of pyroclastic rocks to lava increased in the Upper, compared to the Lower, Carboniferous, though overall the volume of lavas is much greater than that of the fragmental materials.

(iii) The volumes of intrusive alkaline rocks are of the same order as those of the tuffs and agglomerates.

Thus post-Dinantian volcanism continued only spasmodically from scattered centres and the typical mode of eruption was from relatively short-lived ashcones. Small lava fields of Westphalian and Stephanian age in western Scotland appear to have been fed by a series of vents, possibly aligned along a NW.–SE. striking major line of weakness (Simpson and Richey 1936, p. 85).

Francis (1968) has argued that the change from the relatively quiet extrusion of lava to increasingly explosive volcanism was a function of sedimentation. In the early Carboniferous, continental conditions generally prevailed and no thick sequences of low density sediments had accumulated. Thick lava piles grew by extrusion onto the continental surface. Gradual marine incursion during the Carboniferous resulted in some areas in thick, poorly consolidated sedimentary sequences, which prevented the rise of the magma columns to the surface, forcing them instead to spread out as sills or sill-complexes. Francis (1968), following Daly (1933), believes that these sills commonly acted as reservoirs from which magmas punched their way to the surface as vents, though he points out that such a mechanism cannot be applied to all the examples of late Carboniferous vents, many of which were demonstrably fed by dykes (MacGregor 1948).

Francis's hypothesis is apparently confirmed by the close geographical relationship between vents and alkaline sills in the Midland Valley, and by the observation that post-Dinantian lavas commonly occur in areas where underlying Carboniferous sediments are thin or which were undergoing contemporary uplift at the time of eruption, for example the Namurian lavas in Ayrshire (Francis 1968, p. 166).

It is suggested later (pp. 296–9) that, as well as a change of character of the volcanism during the Carboniferous, there was an overall change in chemistry, the Dinantian magmas being of mildly alkaline or transitional type, while those of late Carboniferous age are more strongly silica-undersaturated, in extreme cases bordering on nephelinites chemically. This type of change of magma chemistry has been reported from such oceanic islands as the Hawaiian chain (G. A. MacDonald 1968) and Anjouan in the Comores (Flower 1973), and is also associated with an increasingly explosive type of eruption. In these islands it is clearly impossible to relate this change of physical character to contemporary sedimentation; rather the high volatile content of the magmas and their strongly undersaturated nature probably reflect the conditions of formation and evolution at elevated pressures. It may well be that the increasing pyroclastic proportion of the Midland Valley extrusives in the later Carboniferous finds a partial explanation in the changing magma compositions, as well as in Francis's (1968) model of sedimentation control.

Rock types and volcanic associations

The various rock types found in the Midland Valley province have been tabulated by MacGregor and MacGregor (1948), with summaries of the main petrographical features. These authors also provide a comprehensive bibliography up to 1948 of petrographical papers dealing with the Dinantian lavas and associated intrusions; relevant papers published since that time include the following:

Clyde Plateau: Hamilton (1956), Anderson (1963), Whyte (1966), J. G. MacDonald (1967) and Francis *et al.* (1970).

Arthur's Seat: Oertel (1952), Rutledge (1952), Clark (1952, 1956), Smith (1959) and Black (1966).

East Lothian: Tomkeieff (1952), McAdam (1974) and Livingstone and McKissock (1974).

Kelso Traps: Tomkeieff (1953).

Birrenswark lavas: Pallister (1952), Elliott (1960) and Lumsden *et al.* (1967). The latter two papers also contain information on the Kershopefoot Basalt and the Glencartholm Volcanic Beds.

The range of rock types found as Dinantian lavas and as associated intrusions include various olivine-basalts, trachybasalts (i.e. hawaiites and mugearites), various of types trachyandesite, trachytes and rhyolites. Phonolitic trachyte and phonolite occur as intrusions of probable Dinantian age, but all the extrusive trachytes analysed so far have been silica-oversaturated.

The proportion of each rock type found in the main outcrops is variable, but an attempt has been made in Figure 1 to indicate the main volcanic associations. The choice of association is sometimes rather arbitrary, as in the Kilpatrick Hills example described below. Furthermore, the associations as defined relate to products erupted possibly over a considerable period of time and from many different sources, and as such they refer to only the overall characteristics of the lavas. Richey (1928), for example,

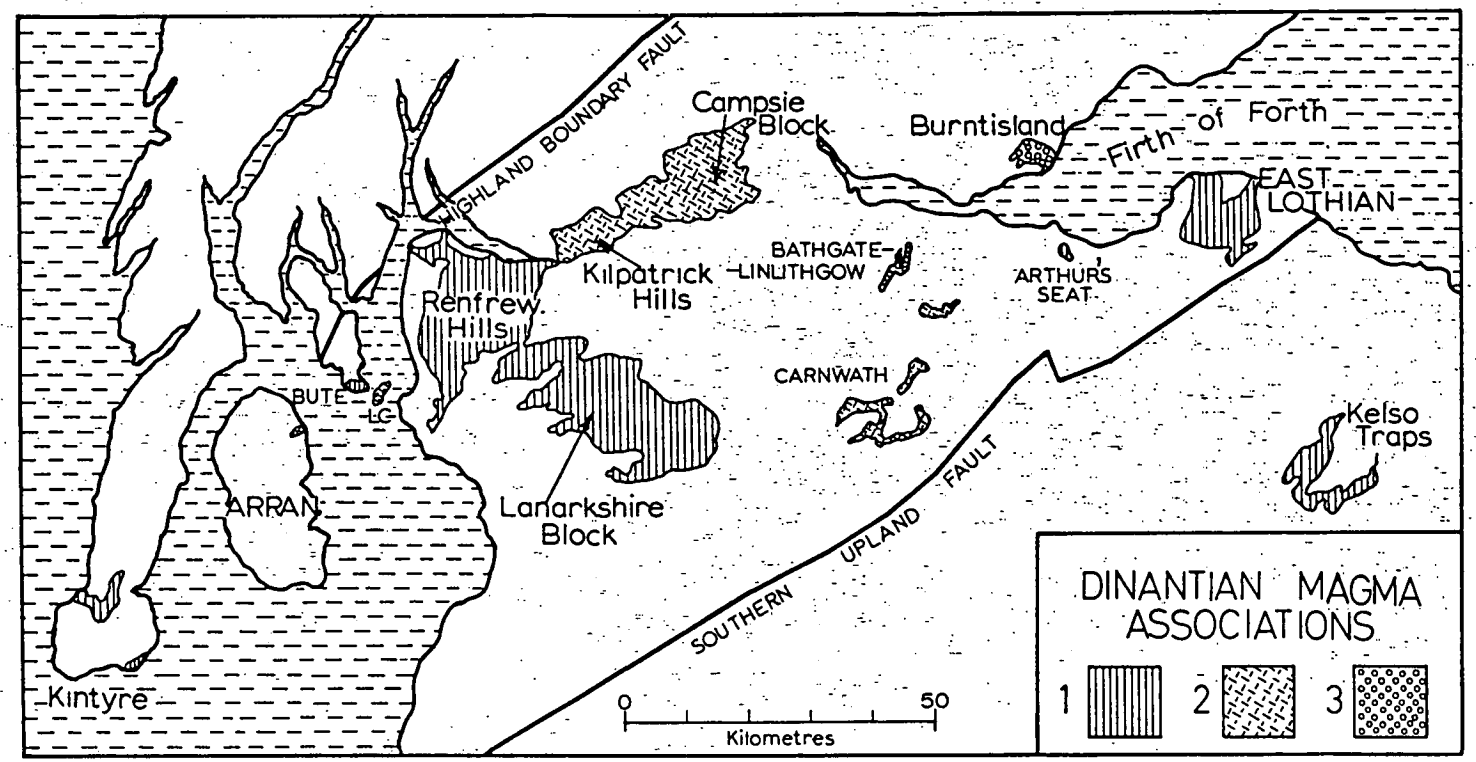

FIG. 1. Magma (volcanic) associations (p. 276) for the major Dinantian lava outcrops. The terms "Campsie Block" and "Lanarkshire Block" follow the usage of J. G. MacDonald (1965). To preserve the scale, the Birrenswark, Kershopefoot and Glencartholm volcanic rocks, all of uncertain magmatic affinity, are not shown.

has divided the volcanic succession of the Kilbirnie Hills into a Lower Group, dominated by feldspar-phyric basalts and hawaiites and similar to Association 2, and an Upper Group consisting largely of olivine-rich basalts, more akin to Association 3. The *total* association of the area is, however, that of type 1.

Association 1 is characterized by the occurrence of a wide range of alkaline rocks, but always shows a fair development of the more basic, olivine- and clinopyroxene-phyric varieties. Macroporphyritic flows, with phenocrysts >2 mm, are abundant. A typical series would be ankaramitic basalt → olivine-augite-plagioclase-phyric basalt → feldspar-phyric hawaiite → mugearite → (benmoreite) → trachyte, though seldom erupted in that order. Examples of areas with this type of Association are East Lothian, Kintyre and Arthur's Seat, Edinburgh.

Typically, basalts carrying microphenocrysts of olivine $\pm$ augite (Hillhouse basalts of local nomenclature) and microphyric hawaiites (Jedburgh basalts) are not common in this Association. The role of the olivine-phyric Dalmeny basalts (similar to, but more feldspathic than Hillhouse basalts) is variable; they appear to be absent as flows in East Lothian, confined to the lowest part of the Kintyre succession, but very abundant in the Lanarkshire block, locally dominating the succession. This latter feature show similarities with Association 3, though the rocks of 3 tend to be more basic and probably more silica-undersaturated, with feldspar-phyric rocks poorly represented.

Association 2 is dominated by feldspar-phyric hawaiites, with less abundant feldspar-phyric basalts, mugearites, and in the case of the Upper Campsies lavas, trachytes and rhyolites. Clinopyroxene-phyric basalts are uncommon. The Association is best represented in the Campsie Fells, the Strathblane Hills, the Fintry, Touch and Gargunnock Hills and Little Cumbrae, all of which are part of the Clyde Plateau Lavas.

In the Kilpatrick Hills, clinopyroxene-phyric basalts form 7% by volume of the exposed pile, according to Whyte and MacDonald (1974). This succession clearly has affinities with Association 1, but is included in 2 because of the predominance of feldspar-phyric basic lavas.

Association 3 characteristically shows a relatively restricted range of compositions, with olivine $\pm$ clinopyroxene-microphyric flows prevalent. Ankaramites are locally present, but feldspar-phyric flows are apparently uncommon. The main outcrops in the Association are in the Bathgate–Linlithgow Hills, at Burntisland, Fife and possibly in Arran.

This is the most poorly known Association geochemically; not one complete analysis is yet available.

Composite flows and intrusions

An intimate form of magma Association is that provided by the numerous examples of composite bodies found in the province. Composite flows are known from near Greenock (Kennedy 1931), Kilmacolm, Renfrewshire (Kennedy 1933), near Kelso (Tomkeieff 1945), the Strathblane Hills (J. G. MacDonald 1967), the Stirling area (Francis *et al.*, 1970) and Kintyre (R. Macdonald, unpublished mapping), while composite

intrusions, thought to be of Dinantian age, occur in the Tweed Basin (Tomkeieff 1945), at the Dasses, Royal Park, Edinburgh (Black 1966) and as the St. Leonard's Sill, Edinburgh (Black 1966).

The rock types involved in these bodies are variable but normally include a macroporphyritic and a microporphyritic (or aphyric) member, either of which may be the more basic. Field relationships vary from fairly simple, where one variety overlies or intrudes the other with a more or less planar contact, to complex and intimate admixtures of the two. Where relative ages of emplacement can be deduced, the microporphyritic member usually appears to be earlier.

Though the compositional ranges in the composite bodies are variable, the majority of examples include a hawaiite member, for example basaltic hawaiite and alkali olivine basalt near Greenock (Kennedy 1931), hawaiite and doleritic basalt at Lurgie Craigs, near Kelso (Table 6), hawaiite and mugearite at Mellerstain Hill, near Kelso (Table 6) and hawaiite occurring as two components at Hareheugh Craigs, also near Kelso (Table 6). An interesting flow outcropping near Kilmacolm, Renfrewshire (Kennedy, 1933) consists of a central portion of porphyritic trachyte flanked by an aphyric rock on the hawaiite-mugearite boundary compositionally.

The examples described above essentially contain two separate components. A hawaiite flow from the Strathblane Hills shows continuous chemical and petrographic variation from top to bottom (J. G. MacDonald 1967). The least basic material (Thornton-Tuttle Differentiation Index = 55) occurs at the base, and the most basic rock (DI = 46), which is also rather richer in plagioclase phenocrysts, is found at the top of the flow.

These composite bodies provide clear evidence of the coexistence of two magmas of differing composition, and in the case of the Strathblane Hills lava, of the apparent existence of a magma column differentiated prior to eruption. Detailed study of those bodies will give information on the mechanisms of differentiation within the Dinantian magma chambers and conduits which will be of wider relevance to the genesis of the Carboniferous lavas. J. G. MacDonald (1967), for example, has proposed that conventional crystal fractionation models cannot account for the variations in the Strathblane hawaiite. He suggests that the flow resulted from the progressive fusion of a gabbroic parent, and extends this hypothesis to all the lavas of the Strathblane succession.

A doctoral thesis containing information on certain Midland Valley composite bodies has recently been completed by W. W. Boyd (1974).

Petrochemistry

Nomenclature

The Scottish Carboniferous-Permian basic rocks have traditionally been classified on the basis of their phenocryst assemblages. In 1928 MacGregor standardized basalt nomenclature, distinguishing six groups, each named after a type locality, by the nature and size of the phenocrysts (Table 1). This nomenclature, introduced primarily as a

TABLE 1.

Comparison of the basalt nomenclature of MacGregor (1928), based mainly on phenocryst type and size, with the chemical classification adopted in this paper for the mildly alkaline and transitional basic rocks.

	Basalt type of MacGregor, 1928	Phenocrysts: Essential	Phenocrysts: Sometimes present	This paper
Microphyric (<2 mm)	Jedburgh	Plag, Ol		Microphyric Ol-plag. ± Fe-oxides-phyric (basaltic) hawaiites (occasionally basalt)
	Dalmeny	Ol	Cpx, Plag,	Microphyric Ol- or Ol + cpx −phyric basalt
	Hillhouse	Ol	Cpx	Microphyric Ol ± cpx−phyric basalt
Macroporphyritic (>2mm)	Markle	Plag. Ol		Macroporphyritic Ol−plag ± Fe-oxides-phyric basalts, basaltic hawaiites or hawaiites
	Dunsapie	Plag, Ol, Cpx		Macroporphyritic Ol-cpx-pl -Fe-oxides-phyric basaltic hawaiites, or Ol-cpx-pl-phyric basalts
	Craiglockhart	Ol + Cpx		Ankaramite

Ol = olivine, cpx = clinopyroxene, plag. = plagioclase.

field classification, is still used by virtually every student of Midland Valley volcanism, a remarkable tribute to its proposer. Nevertheless a modified nomenclature is used in this paper, for the following reasons:

(i) to bring the nomenclature more nearly into line with current petrological usage. Thus the feldspar-phyric Jedburgh and Markle basalts of MacGregor's (1928) terminology would be termed hawaiites by most modern petrographers, for example G. A. MacDonald (1968), Coombs and Wilkinson (1969), Thompson *et al.* (1972), Upton and Wadsworth (1972), Wilkinson (1974) and Best and Brimhall (1974). Certain aspects of the nomenclature have already been introduced to Midland Valley petrography by Upton (1969).

(ii) by using a chemical classification, it is hoped to stress parameters not implicit in MacGregor's scheme, especially the degree of silica-saturation.

The basic rocks of the Carboniferous-Permian alkaline suites show a broad spectrum of compositions, which is here rather arbitrarily divided into hypersthene-normative basalts, alkali-olivine-basalts (nepheline-normative) and basanites. The distinction between the latter two is drawn more or less at the conventional 5% *ne*, though in detail the actual limit of *ne* varies with DI, in the manner proposed by Coombs and Wilkinson (1969, Fig. 13).

These categories are further used as a three fold grouping of the suites of lineages of which they are members. While the hy-normative basalts and the basanites are normally associated with intermediate and salic rocks with high contents of *hy* and *ne* respectively, the alkali olivine basalts are almost invariably associated with hy-normative

intermediate products. Thus the latter suites cross through the low-pressure critical plane of silica saturation located near the plane Diopside-Olivine-Plagioclase, and the various alkali olivine basalt series in the area contain both *ne*- and *hy*-normative members.

An alkalis-silica diagram (Fig. 2) clearly demonstrates the wide range of compositions covered by the basic rocks of the three trends. Some of the Dinantian *hy*-normative basalts also contain normative quartz (q) and some plot in the field of Hawaiian tholeiites as defined by G. A. MacDonald (1968). This early Carboniferous phase of silica saturated basic volcanism has gone largely unnoticed, and it is worth stressing that at least part of this activity, concentrated in the Border Counties, had tholeiitic tendencies.

The diagram also reveals that the most "evolved" suites, in terms of the range of associated salic rocks, are those of mildly alkaline type. The more and less undersaturated basic rocks, that is the basanites and basalts rich in normative *hy*, were evidently not parental to strongly differentiated residua, and are normally associated only with hawaiites.

A comparison of the new basalt terminology with that of MacGregor (1948) is given in Table 1. Dunsapie basalts span the boundary between basalts and basaltic hawaiites chemically. Thompson (1972, p. 925) has pointed out that if a normative plagioclase composition of An = 50 is used to discriminate between basalts and hawaiites, then crystallization of magnetite as a phenocryst phase seems to occur only in the hawaiites. This observation also applies to the Scottish Dinantian suites (Fig. 4). Thus the phenocryst assemblage olivine-clinopyroxene-plagioclase usually indicates a basaltic rock in the revised nomenclature, while the same assemblage plus an oxide phase normally represents a basaltic hawaiite.

The overall similarity of Jedburgh and Markle basalts has long been appreciated (MacGegor 1928), but the latter term has in fact been applied to a rather wider range of rocks, including a mafic basanite from Auchineden Hill in the Kilpatrick Hills (Tyrrell 1912), through *ne*- and *hy*-normative basalts to acid hawaiites.

The nomenclature adopted for the more evolved members of each suite (Fig. 3) is based on the correlation of DI and normative plagioclase composition, as proposed by Coombs and Wilkinson (1969, Fig. 15), but with the addition of "basaltic hawaiite" for rocks with normative plagioclase composition in the range $45 < An < 50$. Coombs and Wilkinson made a further classificatory distinction between suites on the basis of their Na_2O–K_2O relationships. Relatively sodic suites they refer to basalt-hawaiite-mugearite-benmoreite-trachyte lineages (or feldspathoidal equivalents), while potassic suites are termed trachybasalt-trachyandesite-tristanite-trachyte (or feldspathoidal equivalents). The Scottish Dinantian lavas tend to occupy an intermediate position between typically sodic and typically potassic series (Fig. 13), making classification of their intermediate members rather difficult in terms of Coombs and Wilkinson's (1969) nomenclature. In particular, many of the Midland Valley mugearites have Na_2O/K_2O ratios falling below the minimum value of 2 recommended by these authors. The Scottish intermediate rocks appear to be much more akin mineralogically to the type

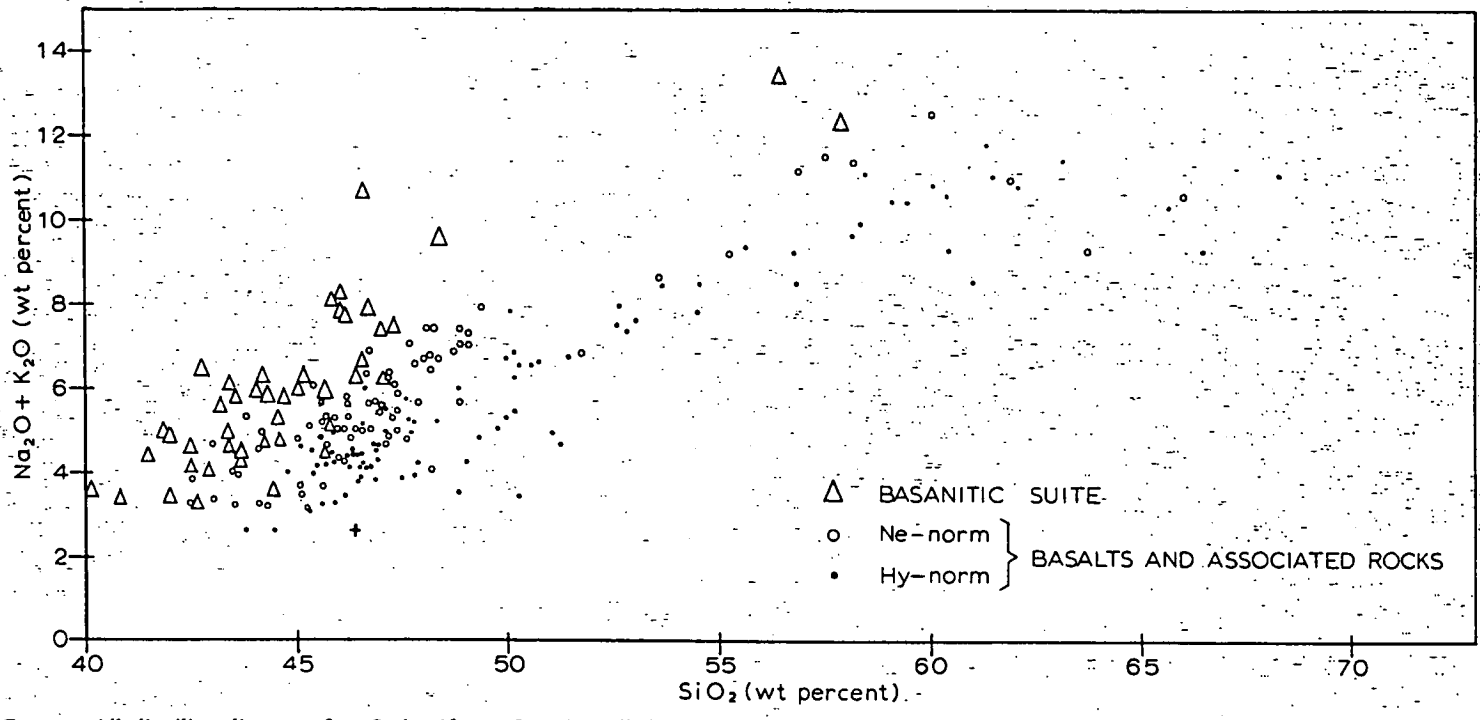

FIG. 2. Alkalis-silica diagram for Carboniferous-Permian alkaline rocks of the Midland Valley province. All available reliable analyses used. Cross=low-potassium, hypersthene-normative basalt from Kintyre (Table 2, no. 1).

389

mugearites than to the trachyandesites described by Coombs and Wilkinson, especially in their ferromagnesian minerals, and the former term, whose use has been established for more than seventy years in Midland Valley petrology (MacGregor 1928, pp. 345–6) is retained here.

An exception is a group of rocks which seems to be restricted to the Dunlop-Eagle-

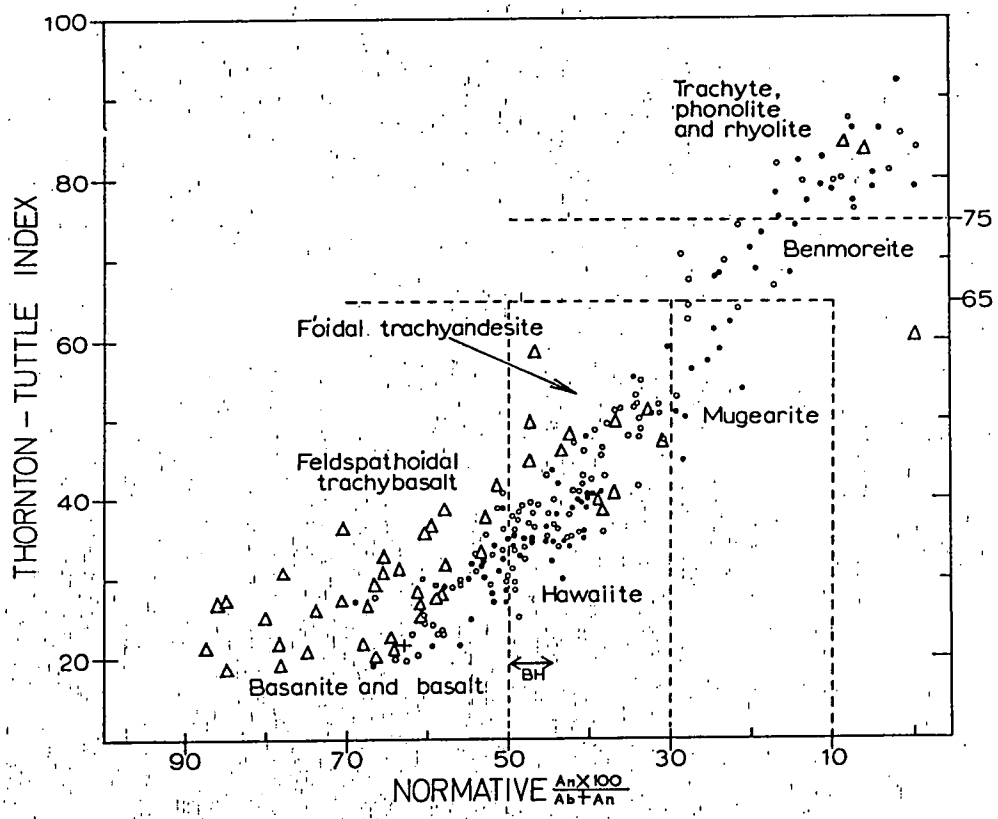

FIG. 3. Thornton-Tuttle Differentiation Index against normative plagioclase composition for Carboniferous-Permian alkaline rocks of the Midland Valley province. Boundaries after Coombs and Wilkinson (1969, fig. 15). Rock names are those employed in this paper. BH = basaltic hawaiite. Other symbols as in Figure 2.

sham-Strathaven Uplands (the 'Lanarkshire' Block of Fig. 1). These "trachybasalts" and "trachyandesites" (MacGregor and MacGregor 1948, p. 55) appear to differ from the mugearites mainly in the presence of amphibole phenocrysts, a usage in accord with the observations of Coombs and Wilkinson (1969). They are not, however, notably potassic, Na_2O/K_2O ratios being in general similar to those of mugearitic lavas of similar DI or Fe/Mg ratio. There are doubtless several magmatic lineages represented in this important area, and a final decision on the nomenclature of the intermediate rocks must await a thorough petrochemical study.

Phenocryst assemblages in relation to rock chemistry

Part of the success of MacGregor's (1928) classification of the olivine-basalts lay in the fact that there is a close relationship between phenocryst assemblages and the major-element chemistry of the rocks. Thus a rock name based on phenocryst content normally also implied a fairly restricted range of chemical composition (cf. Fig. 5). The occurrence of the various phenocrysts as a function of normative plagioclase composition in lavas from Kintyre and from the Early Campsie sequence is shown in Figure 4. An important distinction may be made; *while in the Kintyre rocks clinopyroxene persists as a phenocryst phase into the hawaiites, it is completely absent as phenocrysts in the basic Campsie lavas, even in the basalts.* This feature can be distinguished in other successions: the East Lothian and Arthur's Seat rocks appear to be of "Kintyre-type", while the Late Campsie, Strathblane Hills and Little Cumbrae rocks are more akin to the "Early Campsie-type".

Clearly there is a relationship between this grouping of the suites and the volcanic associations discussed earlier. Thus the Kintyre-type rocks mentioned above all belong

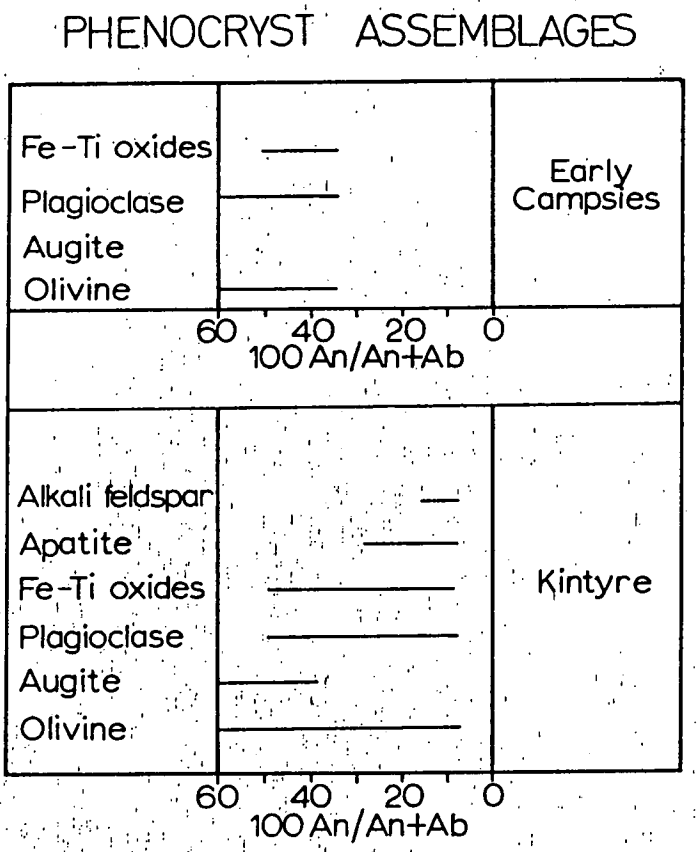

FIG. 4. Phenocryst occurrence plotted against normative plagioclase composition for Early Campsie lavas and Kintyre lavas. Data sources: Early Campsie—Table 4, this paper, and P. M. Craig and R. Macdonald (unpubl.): Kintyre—Table 2, this paper, and R. Macdonald (unpubl.)

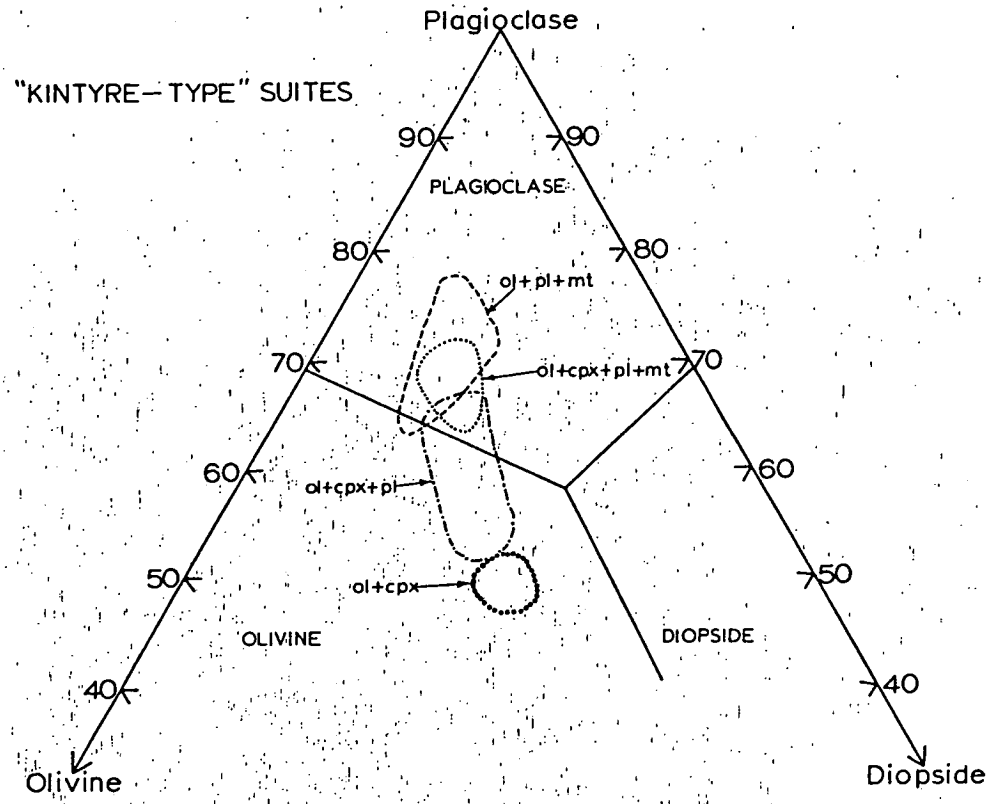

FIG. 5. Generalized relationship between phenocryst assemblages and rock chemistry in Kintyre-type suites, as demonstrated on an Olivine-Diopside-Plagioclase normative projection. Phase boundaries for 1-atmosphere pressure taken from Cox and Bell (1972). ol=olivine, cpx = clinopyroxene, pl = plagioclase, mt = Fe-Ti oxides. Data from Kintyre, East Lothian and Arthur's Seat lavas.

to Association 1 and the Early Campsie types to Association 2. There are exceptions, however; the Lanarkshire Block Lavas, assigned to Association 1, belong to neither group. There are only 15 available analyses of rocks from this area, and, furthermore, the presence of more than one magmatic lineage may be suspected, but judging from the analyzed specimens (for example Richey *et al.*, 1930), pyroxene may be present as phenocrysts throughout the basalt-trachyte composition range.

Figure 5 shows the sequence of phenocryst assemblages in the Kintyre-type suites as the rocks become increasingly feldspathic. The relationship is fairly general in these rocks, but certain basalts containing only olivine phenocrysts (Dalmeny type) present a slight complication. As Hamilton (1956, pp. 288–9) appreciated, this is a problem familiar to Midland Valley petrologists. While MacGregor (1928) considered that the Dalmeny basalts are chemically equivalent to Craiglockhart basalts (ankaramites), Tomkeieff (1937) grouped them with the olivine-augite-plagioclase-phyric basalts of Dunsapie type.

In fact there appear to be at least two types of Dalmeny basalt. There are firstly those which chemically and petrographically are the microphyric equivalents of the ankaramites, for example the type specimen from Dalmeny, and an intrusion at High Binn, Burntisland (MacGregor 1928, table, nos. ix and xi). A second type would normally contain only olivine microphenocrysts. Paradoxically they are not *more* primitive than the first group, but rather are more evolved, being chemically equivalent to the plagioclase-phyric basalts of Dunsapie type. Examples include the basalt forming the Lion's Head intrusion, Arthur's Seat (Clark 1952, p. 80) and the Tinnis Hill vent intrusion near Langholm (Elliott 1960). It is suggested later (p. 305) that the phenocrysts in the "Dunsapie" basalts and their microphyric equivalents represent a relatively high pressure assemblage, crystallizing in an olivine-clinopyroxene-plagioclase equilibrium. The compositions of these rocks lie, however, either in the primary phase field of olivine or very close to the olivine-plagioclase cotectic boundary at one atmosphere pressure. Thus it appears that the more evolved type of olivine-microphyric basalts represent compositions which have equilibrated at very low pressure before eruption, probably within a sub-volcanic reservoir. This interpretation is in accord with textural evidence in the olivine-augite-plagioclase-phyric (Dunsapie) basalts; the phenocrysts commonly show spectacular resorption features, and were clearly out of equilibrium with the host magmas (MacGregor 1932).

There is a scarcity of rocks containing only olivine phenocrysts and which are more magnesian than the ankaramites. As MacGregor (1928, p. 345) points out, the Hillhouse type of basalt, chemically the most primitive found in the Dinantian suites, almost always contains some phyric clinopyroxene, as well as olivine. It would appear that the Dinantian magmas had generally evolved to a state of olivine + clinopyroxene coprecipitation before eruption. Exceptions to this may possibly be found in the Bathgate-Linlithgow Hills and in the Burntisland lavas, where there are reports of basalts rich in clinopyroxene but carrying only olivine phenocrysts; as yet these are not analyzed chemically (Falconer 1906; Allan 1924).

One further point may be made here. Chemical analyses are provided in Table 2 of three flows from southern Kintyre. Petrographically, they are an essentially aphyric basalt, containing scattered olivine microphenocrysts (Dalmeny type); an ankaramite (Craiglockhart type) with some 30% by volume of olivine + augite phenocrysts; and an olivine-augite-plagioclase-phyric (Dunsapie) basalt, containing about 35% of phenocrysts. The analyses of these rocks are almost identical (Table 2, nos. 3, 4 and 2), despite the different phenocryst assemblages. It appears that these three specimens represent differing degrees of protracted *in situ* crystallization of similar, magnesian "ankaramitic" liquids.

This is not a general situation; most plagioclase-phyric basalts in the Midland Valley are much less magnesian than this particular Kintyre specimen (Table 2, no. 4). Nevertheless, the example serves as a timely warning that the phenocryst assemblages in basalts is controlled not only by the chemical composition of the host magmas, but also by their degree of crystallization.

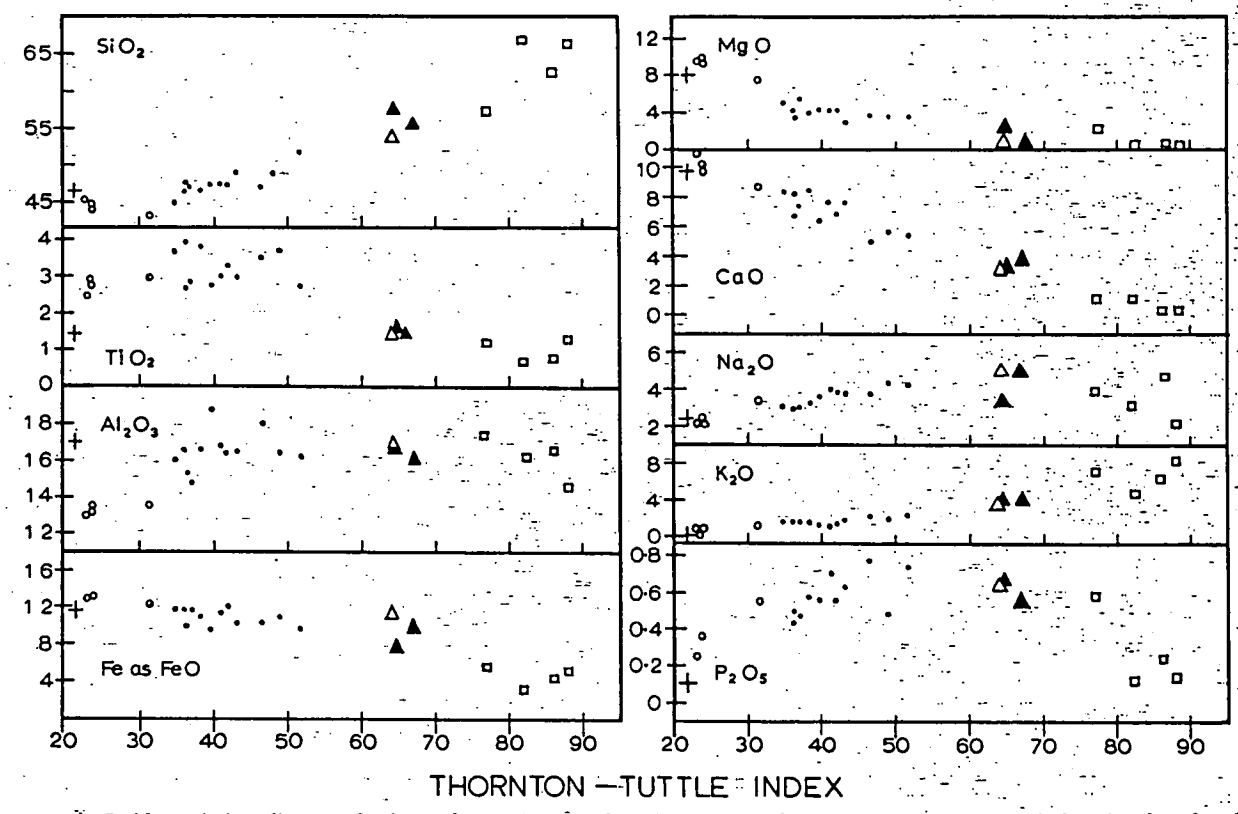

FIG. 6. Oxide variation diagram for lavas from Kintyre, plotted against Differentiation Index. Open circles—basalts, closed circles—hawaiites, open triangle—mugearite, closed triangles—benmoreites, squares—trachytes and rhyolites. Cross—low-potassium, hypersthene-normative basalt. Data sources; Table 2, this paper and R. Macdonald (unpubl.).

394

Identification of magmatic liquid compositions

Knowledge of the chemical compositions of the relevant magmas is necessary for understanding of the origin and evolution of volcanic series. In an area like the Midland Valley, where many of the rocks are markedly porphyritic, the possibility exists that the magma compositions have been modified by crystal accumulation. Two of the petrogenetic schemes proposed for the local rocks (Clark 1956; O'Hara 1968, p. 122) connect the basalt types by processes of selective crystal accumulation. Both workers, Clark for the Arthur's Seat volcanic rocks and O'Hara on a provincial basis, see the olivine-clinopyroxene-plagioclase-phyric (Dunsapie) basalts as being parental to the other main types, by plagioclase flotation to give the olivine-plagioclase-phyric (Markle) basalts and hawaiites, and by olivine-clinopyroxene sinking to give the ankaramitic (Craiglockhart) basalts. Recognition that chemically equivalent non-porphyritic representatives of these lava types exist (see below), shows that these models do not represent the controlling evolutionary process.

As MacGregor (1928) and Tomkeieff (1937) clearly recognised, the differences between the macro- and micro-porphyritic varieties of Scottish basalts are purely textural; chemically they are identical (for example the Kintyre specimens discussed above). Sparsely microphyric or aphyric rocks span the complete compositional range of the Dinantian alkaline rocks and there is no compelling reason to disbelieve that the majority of analyzed rocks represent liquid or near-liquid compositions, at least when they are in fresh condition. The one exception to this may be certain densely plagioclase-phyric basalts and hawaiites of Markle type. The type flow in East Lothian, for example, has demonstrably suffered plagioclase segregation (MacGregor 1960), but it should be stressed that this rock is considerably richer in phenocrysts than most rocks to which the term Markle basalt has been applied.

General petrochemical features of the Dinantian lavas

No systematic investigation of chemical variation in the Dinantian suites of central and southern Scotland has yet been attempted. Earlier studies by Tomkeieff (1937), MacGregor (1948) and Francis (1967) have tended to group the suites together into one series, called by MacGregor and MacGregor (1948, p. 53) an "alkaline (sodic) series". A more detailed examination, outlined below, reveals that there are several magmatic lineages in the Dinantian lavas.

The general petrochemical features of a suite of lavas from southern Kintyre are summarized in Figure 6. The rocks form a fairly coherent series, though there is some scatter in the more salic rocks for certain elements, almost certainly a result of deuteric alteration. It can be inferred that the Kintyre magmas lay on or close to a single "liquid line of descent" or magmatic lineage, a coherence further suggested by the close correlation of DI and normative plagioclase composition (Fig. 7). Suites of lavas from the

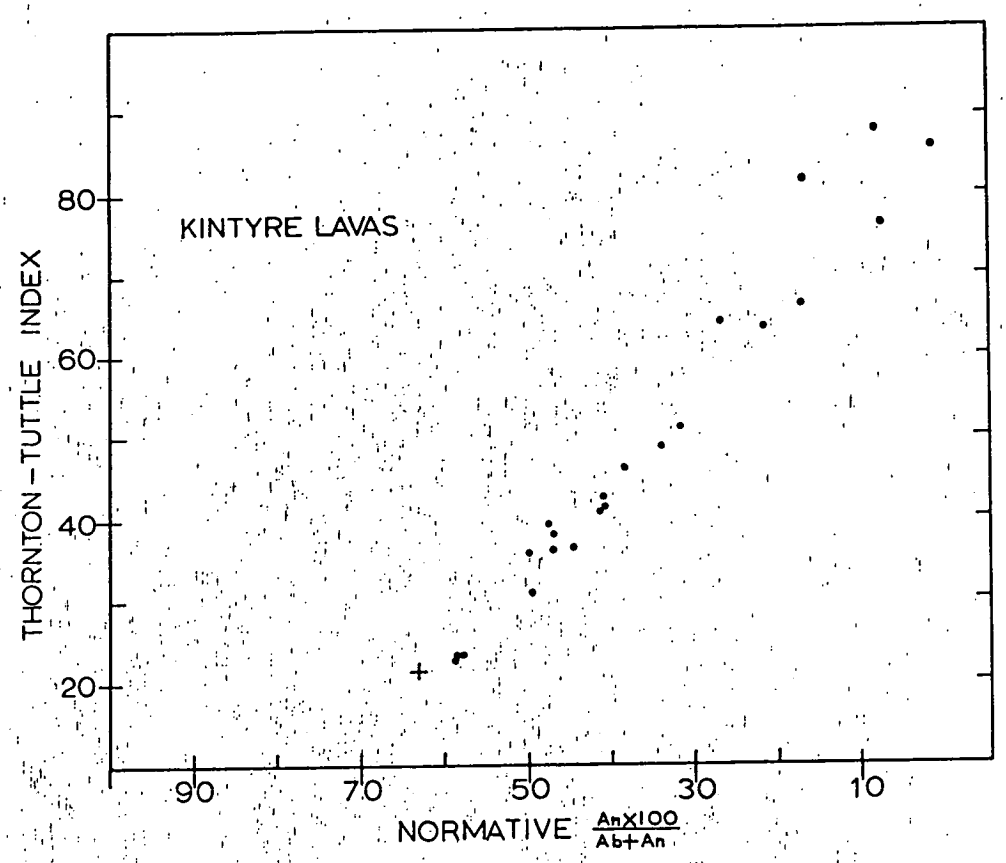

FIG. 7. Correlation of Differentiation Index and normative plagioclase composition in Kintyre lavas (*cf.* Coombs and Wilkinson 1969, figs. 14 and 15) Cross = low-potassium, hypersthene-normative basalt. Data sources as for Figure 6.

other main Dinantian outcrops show patterns similar to, but differing in detail from, the Kintyre trend. Each geographically distinct sequence has in fact a characteristic pattern of major-element variation, and the suites comprise a bundle of lineages. It should be noted, though, that more than one lineage may be represented in some areas; in the Campsie Fells, the Upper Group lavas differ slightly in certain features from those of the Lower Group (J. G. MacDonald and Whyte 1969, p. 19), though both groups are also distinguishable from other sequences in the Clyde Plateau. In East Lothian, the kulaite flows outcropping near the base of the lava succession are not typical members of the East Lothian lineage (see p. 295).

Taken as a whole, the Dinantian lavas range from being mildly silica-undersaturated to silica-saturated (q-normative) and the terms mildly alkaline, or transitional, basalts might be appropriate for the majority of flows. They have a character intermediate between typically "sodic" sequences, e.g. the Skye high-iron lavas (Thompson *et al.*, 1972), the Aden series (Cox *et al.*, 1970), the Erta'Ale volcanics (Barberi and Varet 1970),

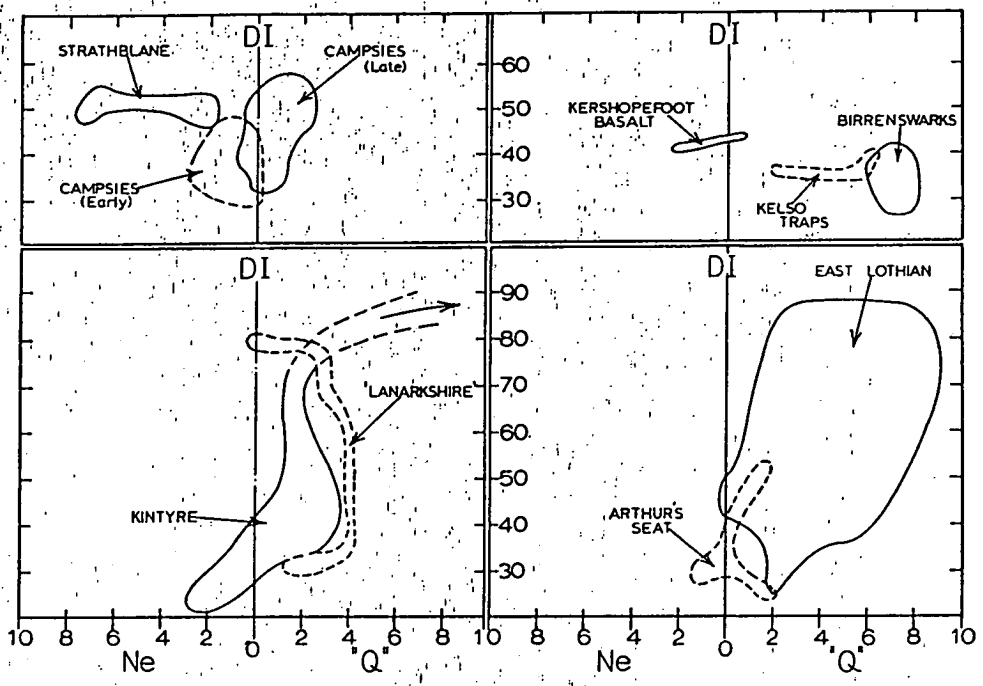

FIG. 8. Differentiation Index plotted against degree of silica saturation for various Dinantian lava suites. Ne = normative nepheline, "Qz" = normative quartz plus quartz in hypersthene (cf. Thompson *et al.* 1972, fig. 9). Data sources—Kintyre, as for Figure 6: Lanarkshire Block—Guppy and Thomas (1931, nos. 53, 86, 94, 96, 102, 104, 159–165, 264, 307); Arthur's Seat—Clark (1952, 1956); East Lothian—Table 3, Livingstone and McKissock (1974, Flows 5 and 16), Day (1928b, 1930c), Clough *et al.* (1910); Birrenswark Lavas and Kershopefoot Basalt—Pallister (1952), Elliot (1960) and Table 6; Kelso Traps—Tomkeieff (1945) and Table 6; Early and Late Campsies—as for Figure 4, plus J. G. MacDonald and Whyte (1969); Guppy and Thomas (1931, nos. 158, 300 and 302); Strathblane—data from differentiated hawaiite flow, J. G. MacDonald (1967).

and the Hawaiian alkaline lavas (G. A. MacDonald 1969) and typically "potassic" suites, e.g. Gough Island (Le Maitre 1962) and Tristan da Cunha (Baker *et al.*, 1964). Series showing trends towards both Fe-enrichment and Fe-depletion may also be recognised. All these series do have in common the fact that they appear to be high in TiO_2 and P_2O_5 compared to similar suites elsewhere and this may be a feature which characterized the Midland Valley volcanism.

Comparative petrochemistry of the Dinantian lavas

49 new major-element analyses of alkaline lavas and intrusions from the province are reported in Tables 2, 3, 4 and 6. Also available for this study were 231 reliable analyses gathered from the literature, 23 unpublished analyses courtesy of P. M. Craig, and 12 unpublished analyses of the author's. This makes a total of 315, which is quite

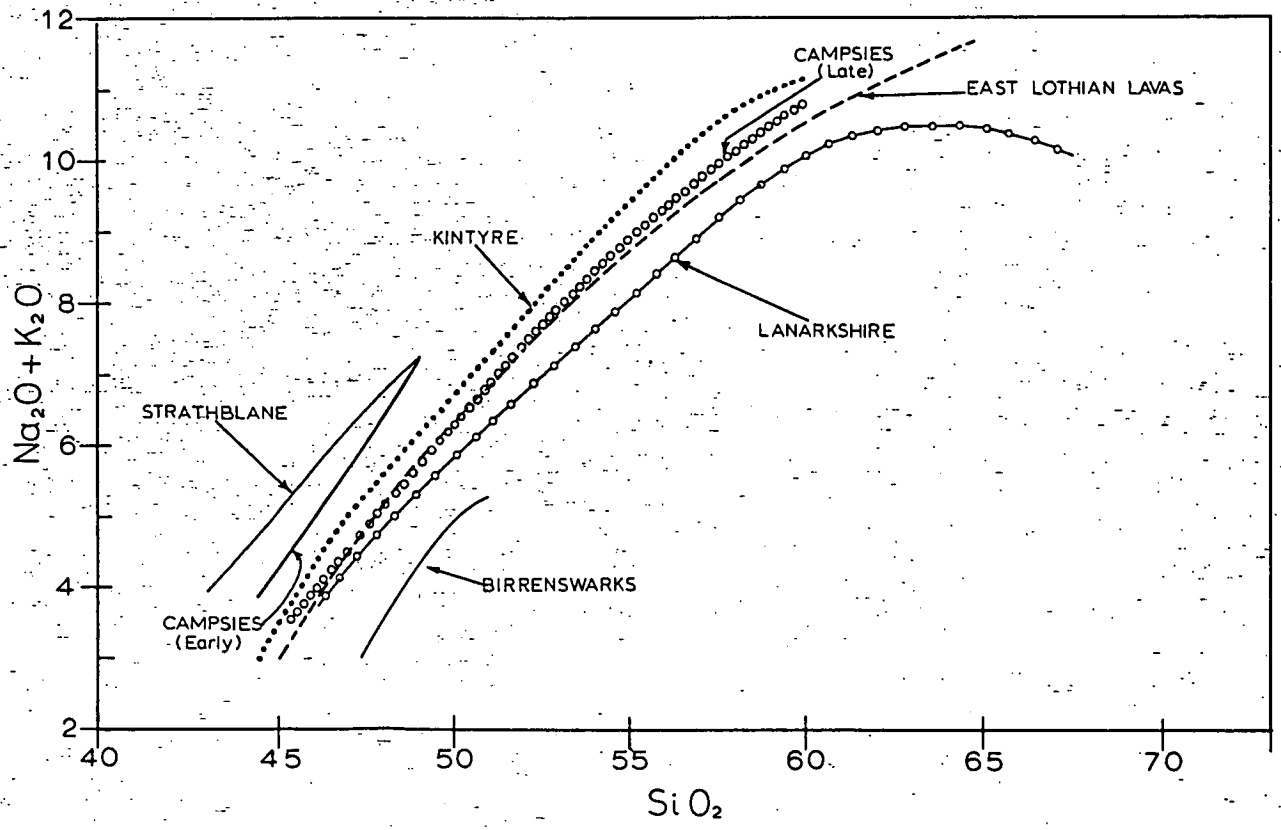

FIG. 9. Alkalis-silica diagram for various Dinantian lava suites, showing generalized distribution curves. Data sources as for Figure 8.

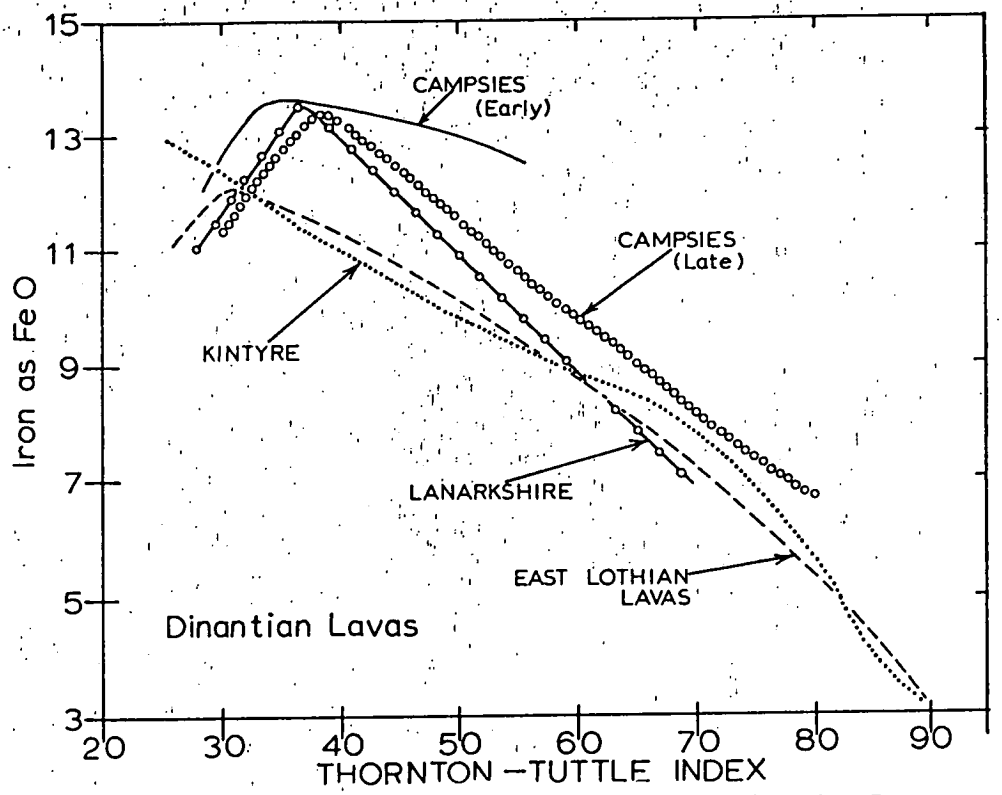

FIG. 10. Differentiation Index against iron (as FeO) for selected Dinantian lava suites. Data sources as for Figure 8.

inadequate for a province of this size and duration of activity. Of the major Dinantian lava successions, published data for the Kintyre and East Lothian suites are barely adequate, and for the others, totally inadequate. Only four analyses of post-Dinantian lavas are available in the literature. Clearly much remains to be done before a complete picture of the Midland Valley petrochemistry can be drawn, and it is stressed that much of the discussion which follows is based on scanty data. More detailed studies will help to refine and modify, or may even reject, some of the theories presented.

The various Dinantian magmatic lineages are best distinguished by the following parameters: degree of silica-saturation, Na_2O/K_2O ratios and relative degree of iron enrichment. These parameters are plotted in variation diagrams against Thornton-Tuttle DI in Figures 8, 10, 12. Several points may be made concerning these diagrams.

(a) The differences between various suites in terms of silica-saturation are slight, but probably real (Fig. 8) and can also be seen on an alkalis-silica diagram (Fig. 9). The basalts and hawaiites range from *ne*-normative to $hy \pm q$ normative, but *ne*-normative mugearites and benmoreites are virtually unknown among the Dinantian lavas, a possible exception being a basic mugearite from the Fintry Hills (Table 4, no. 10).

The suites thus transgress the critical plane of silica-undersaturation, a feature already

recorded from the Hawaiian alkaline suite (G. A. MacDonald 1968), the differentiated series of Piton des Neiges, Reunion (Upton and Wadsworth 1972), the volcanic rocks of the Takakusayama district, Japan (Tiba 1966) and the basalt-quartz rhyolite sequence on Dogo, Oki Islands, Japan (Uchimuzu 1966).

(b) The lineages may be divided into two on the basis of the iron-distribution. In the "peaked-curve" trends, a maximum Fe content occurs usually at a value of DI between 35–40, while in the "flat-curve" type, Fe falls steadily throughout the series. These differences are also reflected on an AFM diagram (Fig. 11).

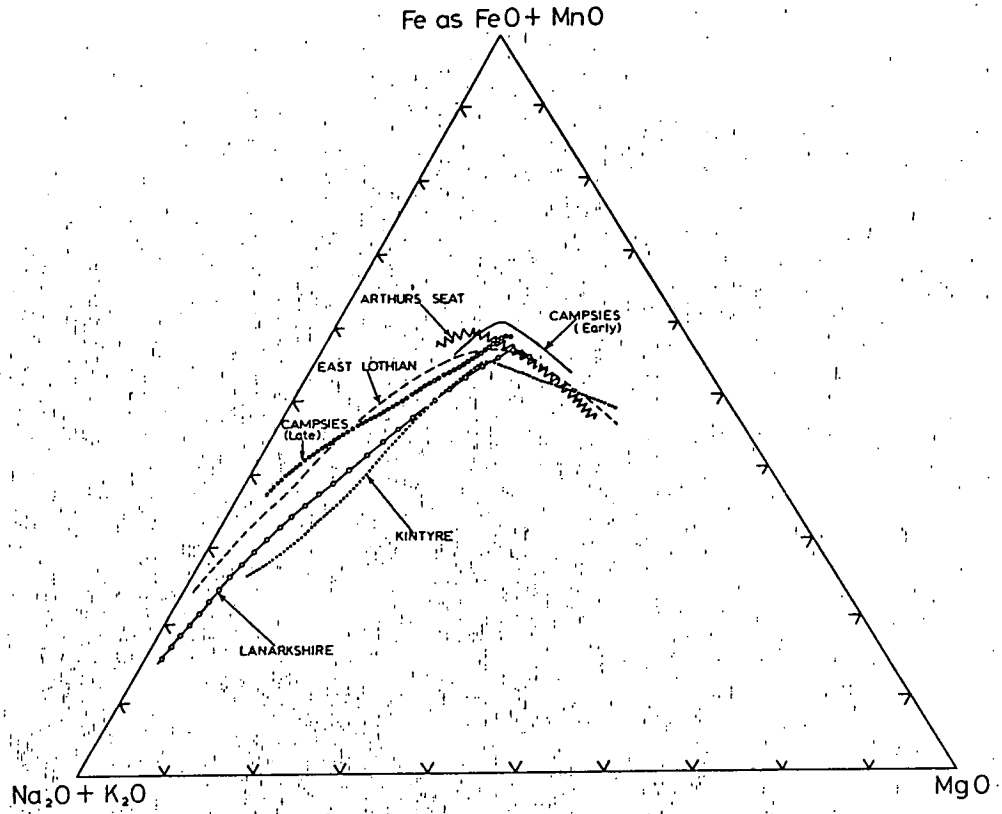

FIG. 11. AFM diagram for various Dinantian lava suites. Data sources as for Figure 8.

(c) Small variations can also be detected in the Na_2O/K_2O ratios (Fig. 12). At DI = 35, for example, the ratio ranges from about 2 to 3. While most of the lavas have a mildly sodic nature, the East Lothian lavas are notably potassic, as Bailey (*in* Clough *et al.*, 1910) recognized long ago. The range in alkali ratios is reflected in the normative plagioclase contents and is well displayed on a ternary feldspar plot (Fig. 13).

(d) Whilst it is a characteristic of the Dinantian lavas that they have rather high contents of TiO_2 and P_2O_5, the concentrations of these oxides vary from suite to suite (Figs. 14, 15). There is no significant correlation between Ti and P in the Dinantian lavas, and each suite has its own Ti and P characteristics. Maximum concentrations of

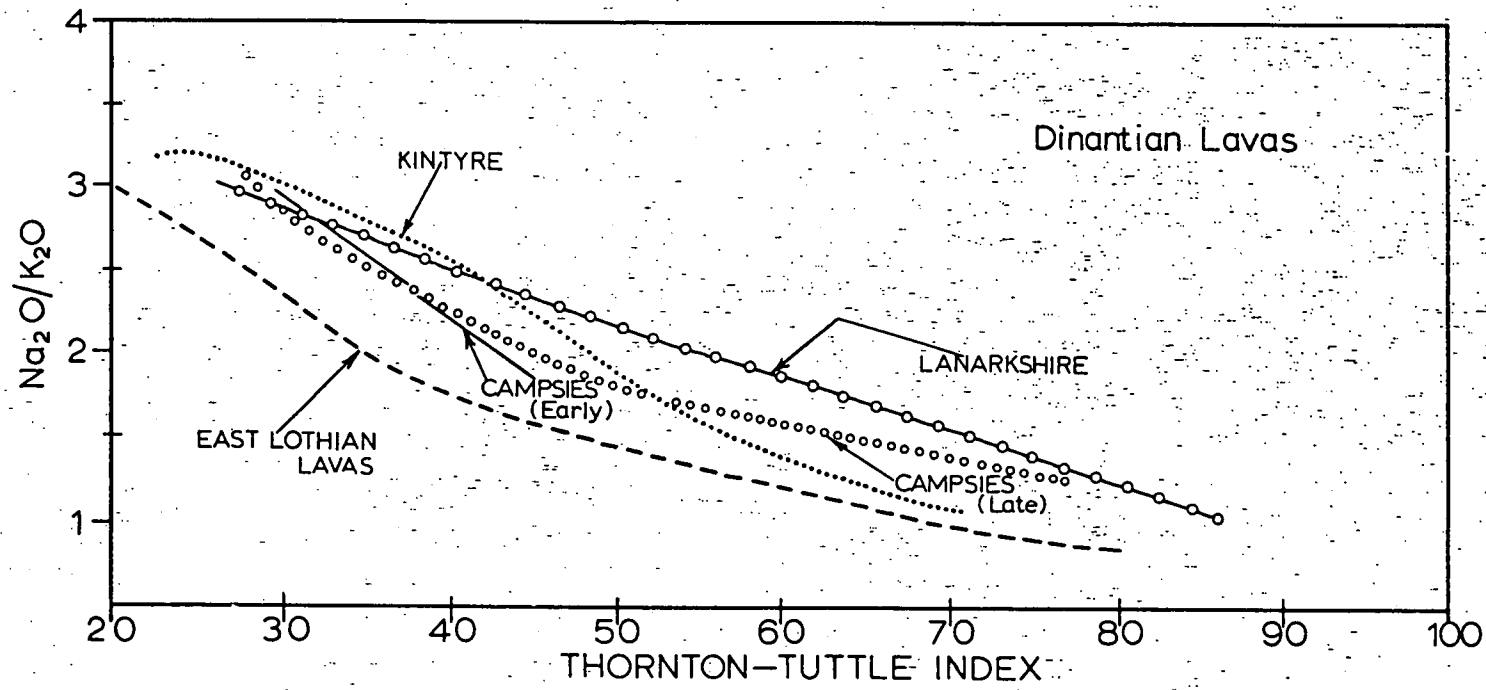

FIG. 12. Differentiation Index against Na_2O/K_2O ratio for various Dinantian lava suites. Data sources as for Figure 8.

P_2O_5 are attained at quite variable DI values; about 40 in the Arthur's Seat rocks, with a P_2O_5 content of about 0·5% and 55 in the East Lothian suite, with P_2O_5 some 0·95%. TiO_2 reaches maximum concentrations within a somewhat smaller range, between DI 35 and 45 in almost every case, but, as for P_2O_5, the maximum concentrations reached are variable.

It is worth stressing the point, made by Coombs and Wilkinson (1969, table 9), that the parameters discussed above vary independently in the Midland Valley lineages, so that all combinations of them are possible.

The following notes summarize the chemical characteristics of the main Dinantian suites. They are made with the proviso that they refer to the gross features of each succession. Further study will enable us to define major-element variations with more accuracy, and will almost certainly reveal the presence of more than one lineage in some of the areas.

It is a somewhat arbitrary business deciding whether a particular volcanic series is sodic or potassic, or a high or low Fe variant. The terms used here are based as closely as possible on their usage by Coombs and Wilkinson (1969).

Arthur's Seat lavas. Critically undersaturated with respect to silica. High Fe-variants. Mildly sodic. Moderate to low P_2O_5 enrichment. Moderately strong TiO_2 enrichment.

East Lothian lavas. Hypersthene-normative, low-Fe variants, mildly potassic. Very strong P_2O_5 enrichment, strong TiO_2 enrichment.

Early Campsie lavas. Alkali-olivine-basalts, mildly undersaturated. High-Fe variants. Mildly sodic. Very strong P_2O_5 enrichment, moderately strong TiO_2 enrichment.

Late Campsie lavas. Hypersthene-normative and alkali-olivine-basalts present. High-Fe variants. Mildly-moderately sodic. Strong P_2O_5 enrichment. Moderate TiO_2 enrichment.

Strathblane lavas. Mildly undersaturated, alkali-olivine-basalts. Mildly sodic. High-Fe variants. Moderate P_2O_5 enrichment, moderate TiO_2 enrichment. Based on compositional variation in a differentiated hawaiite flow (J. G. MacDonald 1967).

Lanarkshire Block lavas. Hypersthene-normative basalts. High-Fe variants. Generally moderately sodic, though potassic types also occur. Rather weak P_2O_5 enrichment. Very strong TiO_2 enrichment.

Kintyre lavas. Alkali-olivine-basalts, mildly undersaturated. Low Fe-variants, mildly sodic. Strong P_2O_5 enrichment, strong TiO_2 enrichment.

Kelso lavas. Hypersthene-normative basalts, mildly sodic. Both high- and low-Fe variants present? Moderate P_2O_5 enrichment? Strong TiO_2 enrichment.

Birrenswark lavas. Hypersthene $\pm$ quartz-normative basalts, mildly sodic. Low-Fe variants. Moderate P_2O_5 enrichment? Moderate or strong TiO_2 enrichment.

There are, among the Dinantian lavas, some restricted occurrences of rather unusual rock types. Of some interest is a flow outcropping at the base of the lava succession south of Machrihanish, Kintyre (Table 2, no. 1). Compared to the other analyzed Kintyre basalts (Fig. 6), this rock has very low TiO_2 and P_2O_5 and high Al_2O_3 and SiO_2 contents, while the K_2O value of 0·20% is the lowest recorded for a fresh alkali

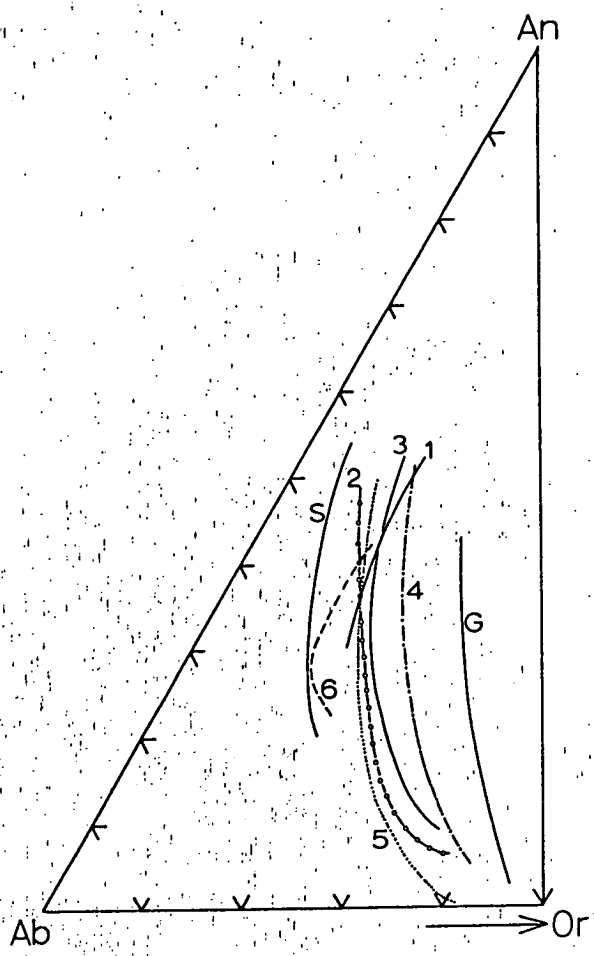

FIG. 13. Ternary feldspar diagram, showing generalized trends for six Dinantian suites, for the Skye basalt → high Fe—benmoreite series (S) (Thompson *et al.*, 1972) and for the Gough Island volcanic rocks (G) (Le Maitre, 1962). 1 = Early Campsies, 2 = Late Campsies, 3 = Kintyre, 4 = East Lothian, 5 = Lanarkshire Block, 6 = Kelso Traps.

basalt from the Midland Valley province. The flow is in many ways analogous to the low-alkali tholeiites discovered by Thompson *et al.* (1972) near the top of the Skye Eocene lava sequence, but shows some differences geochemically; in particular, CaO is not unusually high, as it is in the Skye examples, while the Skye rocks are not notably aluminous. Nevertheless, the low K, Ti and P contents of the lavas from both localities seem to require either that the appropriate magmas were formed by substantial partial melting of peridotitic mantle, followed by only minor (if any) fractionation during ascent to the surface, of, if phlogopite ± apatite were important phases in the Carboniferous mantle, that they did not contribute significant amounts of those elements to the melts (Flower *et al.*, 1975).

The Kintyre low-K flow is one of a series of aphyric or microphyric basaltic flows

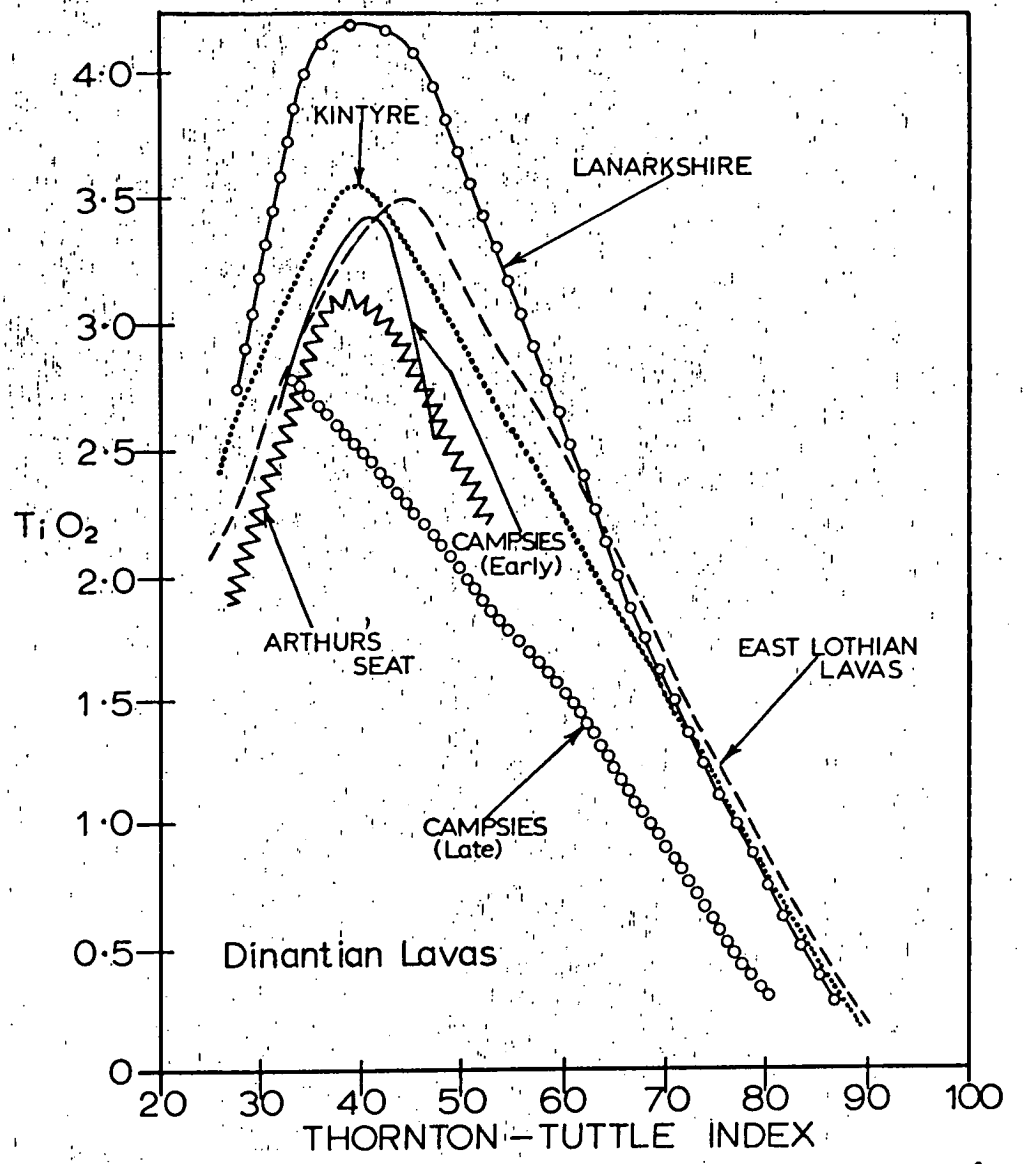

FIG. 14. Differentiation Index against TiO_2 for various Dinantian lava suites. Data sources as for Figure 8.

which everywhere forms the base to the local succession. This part of the sequence is not well known geochemically, but the only other analyzed rock (Table 2, no. 5) is also unusual among the Dinantian lavas in being basanitic. Clearly, further study of this interesting group of rocks is required.

Another rock type atypical in the Dinantian suite occurs as at least four flows and as blocks in an agglomerate in East Lothian (Bennett 1945). These rocks have affinities with the feldspathoidal hawaiites and have been distinguished as leucite-kulaites in

the literature (Bailey, *in* Clough *et al.*, 1910; Bennett 1945), though the leucite has been entirely pseudomorphed. Certain basic intrusions in East Lothian also appear to have carried leucite (Bennett 1945), but their age of emplacement remains uncertain. The genetic relationships of the strongly silica-undersaturated leucite-kulaites to the main transitional basalt → trachyte lineage of East Lothian is uncertain. Their restricted occurrences, however, seem to indicate a very localized melting and/or cooling crystallization anomaly.

Variation of basic magma compositions with time

In 1948, MacGregor (pp. 143–4) pointed out "that the average early Calciferous Sandstone magma was richer than the average later magmas in silica and poorer in magnesia and lime", thus providing the first firm statement of a change in magma chemistry with time during the Carboniferous. This view was apparently not accepted by Francis (1967, 1968), who felt "that there was little change in the composition of the parent magmas continuously available almost throughout the Carboniferous (1967, p. 238), and that "the Carboniferous alkaline parent magma gave rise to a suite of extrusive rocks . . . . which shows little significant variation with time or place . . . ." (1968, p. 164).

Considering the possible petrogenetic importance of a time-controlled change of magma chemistry, an attempt has been made in Figure 16 to plot the stratigraphical age of analyzed basic lavas (with normative $\frac{An \times 100}{Ab + An}$ between 45 and 60) against their degree of silica-saturation. The position of individual points within the diagram, especially in the Dinantian, has been estimated from the stratigraphical spread for each sequence shown by Francis (1968, Fig. 1) and from their approximate stratigraphic level within local successions as judged from published cross-sections. Since there are still major uncertainties of correlation between the main lava outcrops, and since the period of time represented by local successions is likely to be highly variable, there are undoubtedly substantial errors in the placing of many points. However, the *overall* distribution pattern is unlikely to change as radiometric dates continue to refine the lava stratigraphy. Also shown on Figure 16 are analyzed basic intrusions for which reliable radiometric age dates are available.

Two points are clear from the diagram; hypersthene-normative basalts (excluding those of the quartz-dolerite suite) are almost entirely restricted to the Dinantian, while strongly undersaturated basic rocks, with normative $ne > 5\%$ are largely of Westphalian and Stephanian age. It is impossible to judge whether the trend towards increasing silica-undersaturation is continuous from Lower to Upper Carboniferous (and perhaps Permian) times because of the almost complete absence of published analyses of late Dinantian and Namurian lavas. The results shown on Figure 16 are, nevertheless, taken to confirm MacGregor's (1948) view that Midland Valley alkaline volcanism became progressively more undersaturated with time. Such a trend is, of course, already well

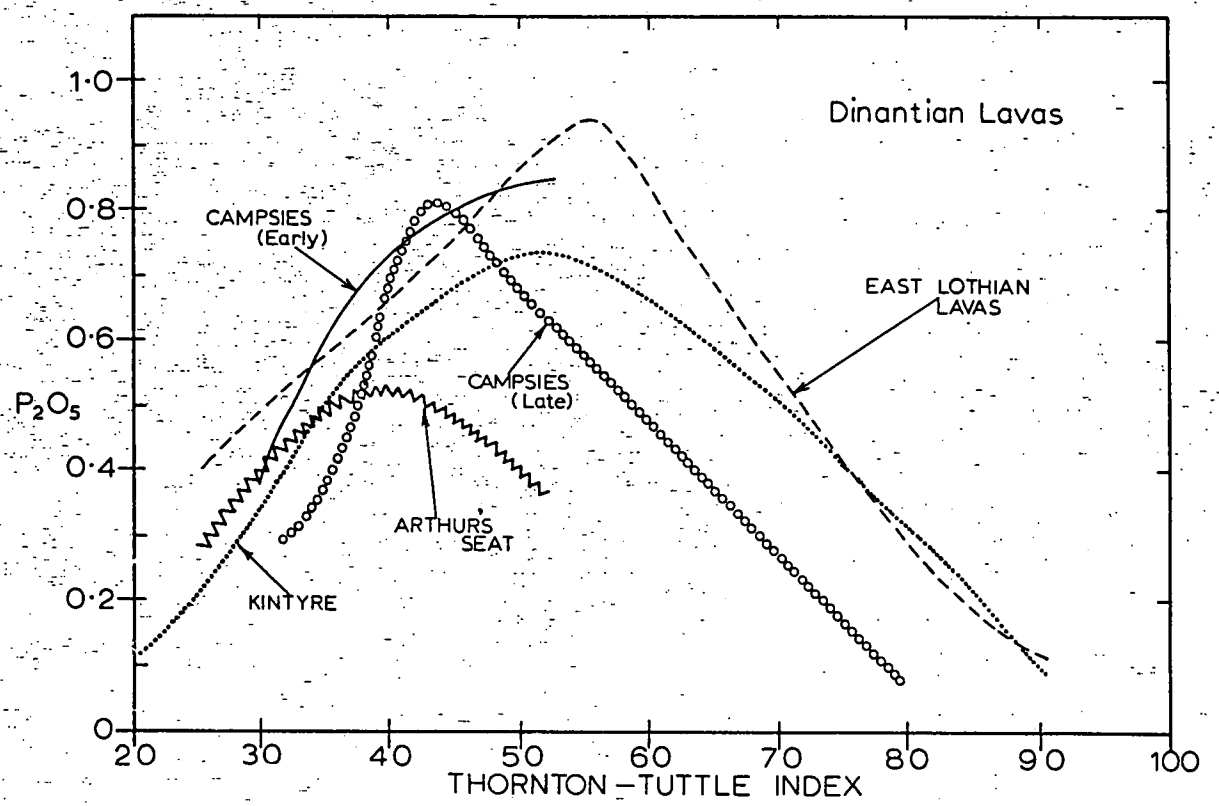

FIG. 15. Differentiation Index against P_2O_5 for various Dinantian lava suites. Data sources as for Figure 8.

904

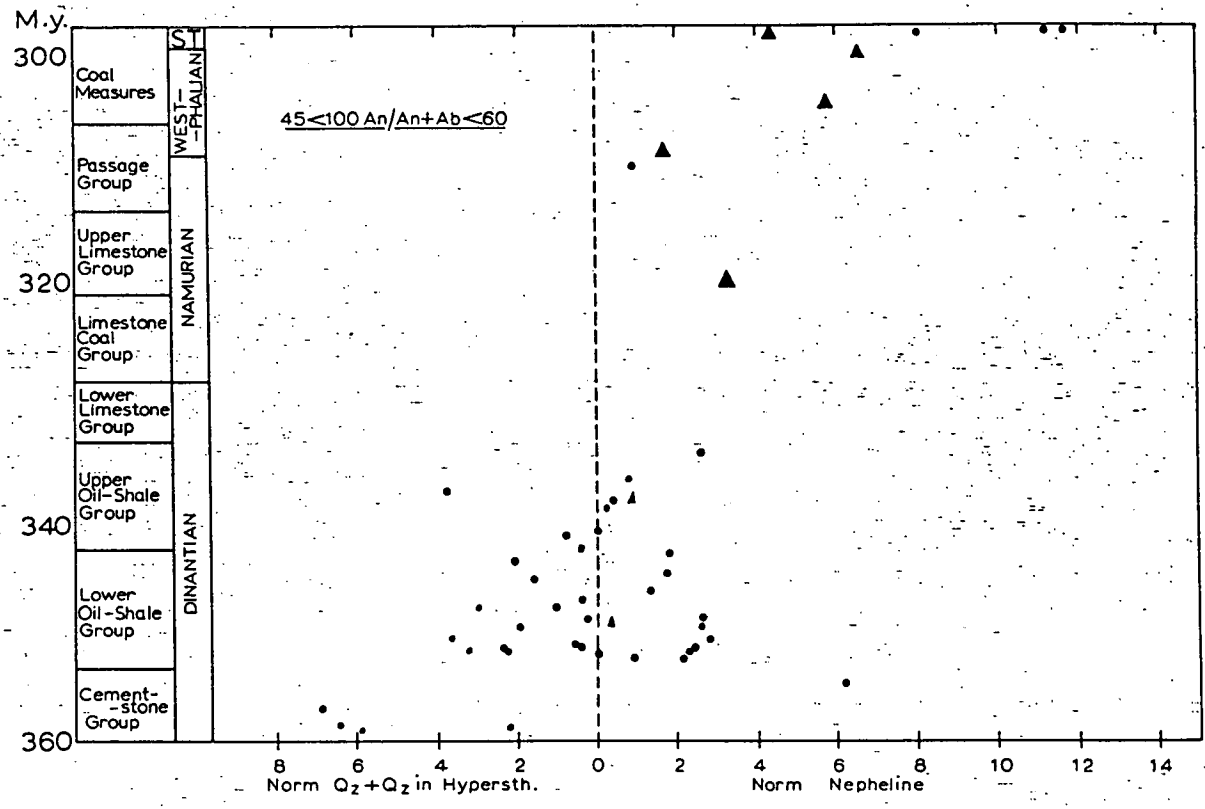

FIG. 16. Degree of silica-saturation of Carboniferous alkaline basalts and basaltic hawaiites plotted as a function of stratigraphical age. The stratigraphical column is from Francis (1967) and the absolute time scale adapted from Fitch *et al.* (1970). Circles represent lavas; triangles are intrusions for which reliable age dates are available (standard error not indicated)—data from Fitch *et al.* (1970) and H. A. F. de Souza (pers. comm.).

known from the Hawaiian Islands (G. A. MacDonald, 1968). A further similarity between the two areas is that volcanism occurred on a much reduced scale as time progressed, and also became increasingly explosive.

If the long-term trend towards silica-undersaturation in the Midland Valley was real, then it is possible to speculate on its causes. For example, early Dinantian volcanism may have been related to a major thermal event which promoted comparatively shallow melting within the mantle and produced the mildly alkaline and transitional basalts. This was followed by a long post-Dinantian cooling, marked, spasmodically, by magma formation at increasingly deeper levels, resulting in basanitic and more undersaturated magma types. This phase was replaced in the Stephanian by a second major thermal rise, marked by the quartz dolerite-tholeiite intrusive suite.

Models of this kind can be satisfactorily tested only when we have a fuller understanding of the melting and cooling crystallization histories of the various lava groups, since the Dinantian lavas, at least, appear to have suffered some degree of high-pressure crystal fractionation (see Petrogenesis section). In combination with tectonic analyses, they will eventually help to decipher the evolution of the graben.

Minor and trace element geochemistry

Very few minor and trace element determinations have been published for rocks from the Midland Valley province. Patterson (1945) and Higazy (1952) have presented data on differentiated intrusions of uncertain age in Ayrshire and Fife respectively. Determinations of 10 trace elements in 16 Dinantian flows, a tuff and an analcite basalt intrusion from the Spilmersford borehole, East Lothian, have been provided by Livingstone and McKissock (1974). Unfortunately the extrusive rocks have been extensively altered by post-eruptive processes and interpretation of the element distribution patterns in terms of magma evolution is very difficult.

There is a need for a large scale trace element study of Midland Valley volcanics, with the following aims:

(a) to provide further evidence of the co-generic nature of individual suites, or to subdivide suites into smaller, distinguishable units,

(b) to point to the existence of larger scale units within the province, such as the Firth of Forth volcanic group proposed by Francis (1965),

(c) as a potential aid in relating flow sequences to source vents,

(d) as a petrogenetic tool, firstly to help identify correct models of origin, and secondly to help quantify these models.

Petrogenesis

Basalts and hawaiites

Many of the features of the Dinantian suites lead one to suspect that they have evolved by continuous fractional crystallization of basaltic parental magmas. There are, for example, no major composition gaps in the series as a whole (Fig. 17), or where data are fullest, in individual sequences such as Kintyre or East Lothian. Tomkeieff

(1937) showed that volumetrically the various series are dominated by basaltic rocks, more differentiated types occurring in progressively smaller bulk, as might be expected from standard fractionation models. The generally close relationship between the chemistry of the basalts and hawaiites and their phenocryst assemblages (Fig. 5) also seems to indicate that crystal–liquid equilibria have controlled the evolution of the series.

The simplest petrogenetic model is to envisage the generation within the mantle of a range of basic liquids approximating in composition to the most basic Dinantian rocks (DI $\sim$ 22, MgO = 10–11%). These liquids rose into crustal magma reservoirs and generated the more salic magmas by fractional crystallization, separating cumulus phases now represented by the phenocrysts in the rocks.

Recent experimental work has emphasized the need for the close examination and refinement of such models. In a review of 1-atmosphere melting experiments on various basic rocks, Thompson (1972) stresses that much of the chemical variation in natural basalts and hawaiites is derived over a range of high pressures (> 10 kb), often involving crystal phases no longer represented as phenocrysts in the rocks. Sometimes, evidence of the polybaric history of the basic magmas is preserved as basic and ultrabasic nodules and as xenocrysts of various sorts carried up in the magmas; in the Midland Valley, the rich crop of nodules associated with the later Carboniferous lavas and vents will certainly provide detailed information on the evolution of their host rocks (Chapman 1974). Where such nodules and xenocrysts are almost entirely lacking, as in the Dinantian suites, evidence regarding the higher pressure stages of magma evolution must be sought either in experiment or by assessing chemical variations in the rocks in relation to the observed and inferred phenocryst assemblages. In the following section, both approaches are used to make some preliminary observations on the possible high-pressure fractionation of the Scottish basalts.

The large body of experimental data now available for low-variancy basic liquids indicates that, in a basalt fractionating at low pressures, any one of olivine, clinopyroxene and plagioclase may be the first phase to separate. Within a fairly small temperature interval, all three phases will eventually separate together from the liquid. In *tholeiitic* magmas, olivine may eventually cease to crystallize as a result of a low-pressure reaction relationship with pyroxene. No similar reaction is known to exist for clinopyroxene at low pressures in anhydrous basic magmas. Thus the disappearance of clinopyroxene from the phenocryst assemblage in the hawaiites in the Kintyre-type suites and its failure to appear in the Campsie lavas (Fig. 4) suggest that the evolution of these basic rocks is not simply a low-pressure process.

Added weight to this suggestion comes from simple crystal-extract calculations of the normative minerals required to produce average Early Campsie basaltic hawaiite from average basalt. This extract (Fig. 18) contains about 20% of normative diopside, yet as mentioned above, the basalts in question contain no phenocryst pyroxene.

A similar situation was found by Thompson *et al.* (1972) and Thompson (1974a) in Eocene lavas from Skye. High-pressure experiments on two Skye basalts, neither carrying phyric clinopyroxene, by Thompson (1974a) showed that clinopyroxene joined,

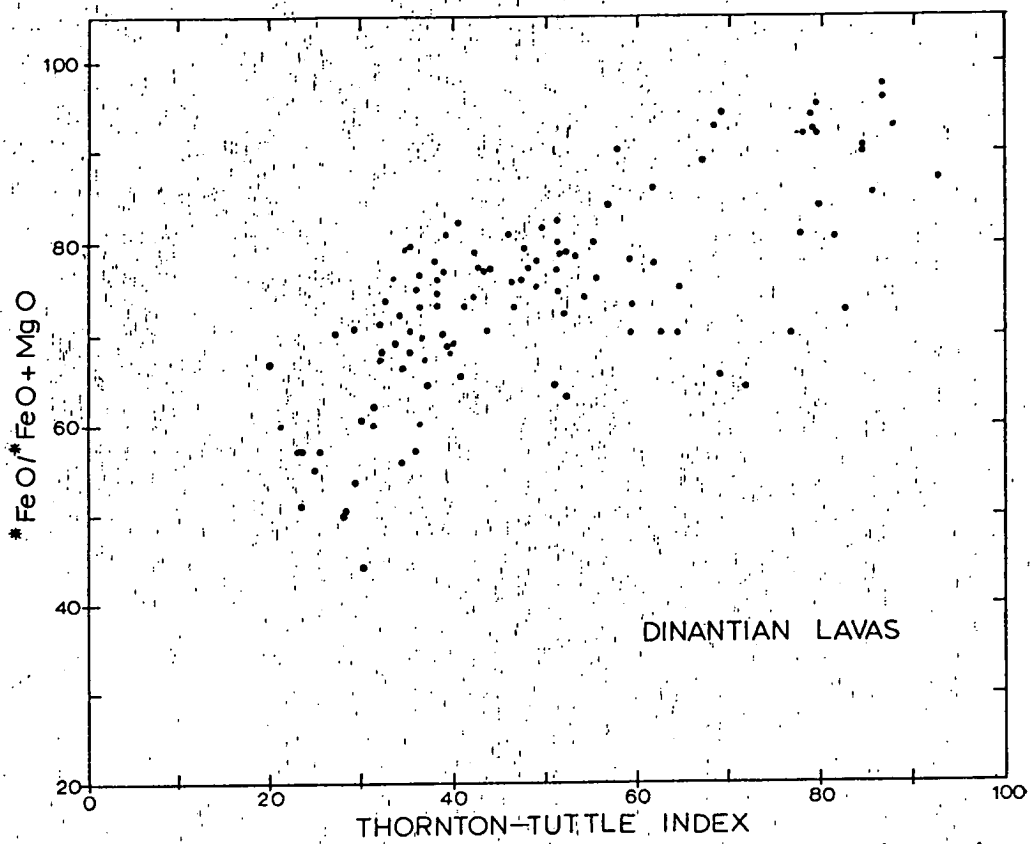

FIG. 17. Differentiation Index plotted against FeO/FeO + MgO ratio for Dinantian lavas, to show that there are no major compositional gaps. Asterisks indicate that total Fe is reported as FeO.

or replaced, olivine and plagioclase on the liquidus at pressures in the range 10·5 to 16·5 kb, and led him to suggest that the chemical variation now seen in the Skye basalt and hawaiite flows was at least partly derived by separation of pyroxene in this pressure range.

Replacement of olivine by clinopyroxene on the liquidus of olivine-plagioclase-phyric basic rocks has also been reported for rocks from the Gardar province, south Greenland, by Upton (1971), and there would seem to be no real experimental difficulties in proposing that the Early Campsie basalts would show similar behaviour.

The crystal-extract required to produce average early Campsie hawaiite from average basaltic hawaiite does not, on the contrary, contain significant amounts of pyroxene (1·5%). The major normative minerals are olivine (23·5%) plagioclase (67·4%) and Fe-Ti oxides (7·5%), which are the actual phenocryst phases in these rocks. Thus it would appear that this particular phase of differentiation may simply have involved removal of the low-pressure assemblages.

Some general features of the lower—and higher—pressure fractionation trends can be examined on a normative Olivine–Diopside–Plagioclase projection (Fig. 18). The

compositional fields of Early Campsie basalts, basaltic hawaiites and hawaiites are shown, as are the 1-atmosphere phase boundaries for natural basalts constructed by Cox and Bell (1972). These authors make the point (op. cit., p. 5) that the diagram can be used to give reasonably accurate predictions of the stability fields for natural basalts lying close to the composition plane Ol-Cpx-Pl.

It can be seen that the majority of the Early Campsie basalts and hawaiites forms a fairly coherent group lying almost entirely within the primary phase field of plagioclase, though almost all these rocks are olivine- and plagioclase-phyric. The low-pressure cotectics do not allow liquids derived from olivine-phyric magmas to enter into the plagioclase field, and the trend must then be interpreted in one of two ways. Either it is not a 1-atmosphere liquid line of descent or there has been preferential accumulation of feldspar phenocrysts into olivine-plagioclase ± clinopyroxene-phyric liquids (cf. Cox and Bell 1972, pp. 8–9). The important observation here is that many of the Early Campsie basalts and hawaiites are phenocryst-poor or even aphyric, demonstrating that *liquid* compositions lay within the low-pressure plagioclase field. Thus movement of magma compositions into this field by selective plagioclase accumulation or olivine ± clinopyroxene removal cannot be maintained for the Early Campsie suite. Rather, the projection seems to provide further evidence for the suggestion made above, namely that the earlier part of the trend is controlled by higher-pressure equilibria.

This stage can be thought of as follows. The magmas immediately parental to the basalts were crystallizing in an olivine-plagioclase-clinopyroxene equilibrium at pressures greater than 9–10 kb, and separated a bulk crystal extract of the composition shown on Figure 18. This drove residual liquid compositions through to basaltic hawaiite. During their progress to the surface, the magmas must have ascended sufficiently slowly or paused at shallow depth (in crustal magma reservoirs?) sufficiently long for the high-pressure phases to be resorbed and replaced by the currently observed low-pressure phenocrysts.

Such a hypothesis requires that the natural olivine-plagioclase cotectic lay at rather more plagioclase-rich compositions than the 1-atmosphere cotectic of Cox and Bell (1972), that is, that the plagioclase field had contracted relative to that of olivine. This feature is most commonly attributed to elevated water vapour pressures (Yoder 1969). The presence of biotite, analcite and amphibole in the groundmass of many Dinantian basic rocks may indicate that important amounts of water were present during crystallization.

Furthermore, the presence of both plagioclase and olivine as phenocrysts in the Early Campsie hawaiites appears to suggest that removal at higher pressures of clinopyroxene-bearing assemblages drove the residual liquids *by coincidence* to compositions approximating to the low pressure olivine-plagioclase (±Fe-oxides) cotectic. One might predict, however, that certain hawaiites from this series would have re-equilibrated entirely within the plagioclase stability field, such that their phenocryst assemblage would now be plagioclase ±Fe-oxides. Discovery of such rocks would lend a certain credence to the above speculations.

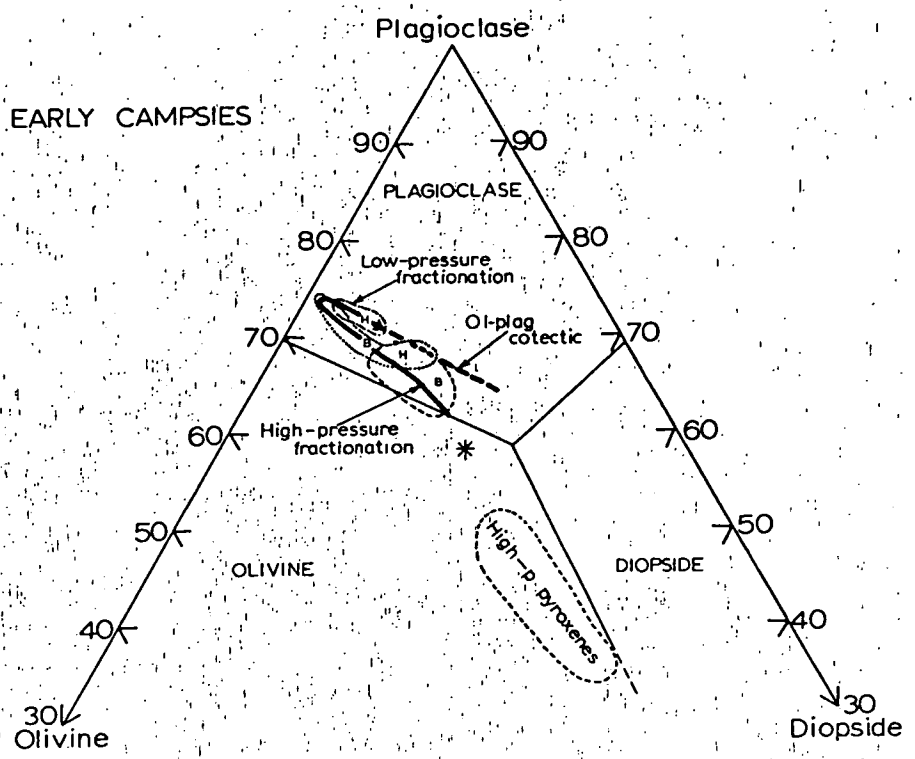

FIG. 18. Olivine-Diopside-Plagioclase normative projection, showing the suggested evolutionary scheme for the Early Campsie basic lavas. B, BH and H are the compositional fields of basalt, basaltic hawaiite and hawaiite respectively. The 1-atmosphere phase boundaries are taken from Cox and Bell (1972). Heavy full line is the high pressure liquid line-of-descent; the partly full, partly dashed, heavy line is the low-pressure trend, taken to be (near-) coincident with the natural low-pressure olivine-plagioclase cotectic. The asterisk indicates the crystal extract required to produce the average basaltic hawaiite from average basalt (Actual normative composition of this extract, at $P_2O_5 = 0{\cdot}0\%$, is plagioclase 55·3%, olivine 19·0% diopside 21·1%, Fe-Ti-oxides 4·6%. The "high-p pyroxenes" field represents the compositions, recalculated on a normative basis, of liquidus or near-liquidus pyroxenes crystallized from Skye basalts SK 971 and 66018 in the pressure range 13 to 31 kb, by Thompson (1974a, 1974b).

Where magma resided in shallow reservoirs sufficiently long before extrusion for appreciable crystal fractionation to take place, separation of olivine-plagioclase ± Fe-oxides produced hawaiitic residual liquids. It is suggested that the spread of compositions of the appropriate lavas, which projects into the Ol-Di-Pl system as a roughly linear zone trending away from the olivine-plagioclase sideline, marks the position of the low pressure olivine-plagioclase ± Fe-oxides cotectic, and that the cooling magmas proceeded down the natural analogue of this boundary. The overall fractionation of the Early Campsie basic magmas, shown in Figure 18 as a heavy line, involves a sharp v-turn, as the higher-pressure equilibria were replaced by low-pressure equilibria.

An interesting alternative to the higher-pressure history outlined above is suggested by the data of Thompson (1974b) on pyroxenes crystallized from various basalts at pressures up to 31 kb. The pyroxenes from the Skye rocks mentioned earlier are markedly

aluminous: recalculated on a normative basis, the range of compositions shown by liquidus or near-liquidus pyroxenes in the pressure range 13 to 26 kb projects as a roughly linear zone in Figure 18, where it is approximately colinear with the fields of basalts and basaltic hawaiites. This raises the possibility that the high-pressure stage of fractionation involved not olivine-clinopyroxene-plagioclase assemblages, but an aluminous clinopyroxene only, a suggestion easily open to experimental test. One implication of such a scheme is that, if the basic magmas have been derived from a peridotitic mantle, then olivine has in some way been reacted off the liquidus.

It should be noted that the postulated clinopyroxene should have to be *ne*-normative, rather than the normally hy-normative variety found by Thompson (1974a) in the Skye rocks, because the intermediate rocks of the Midland Valley suites are almost invariably less undersaturated than the associated basalts. (for example Fig. 19). It is interesting to

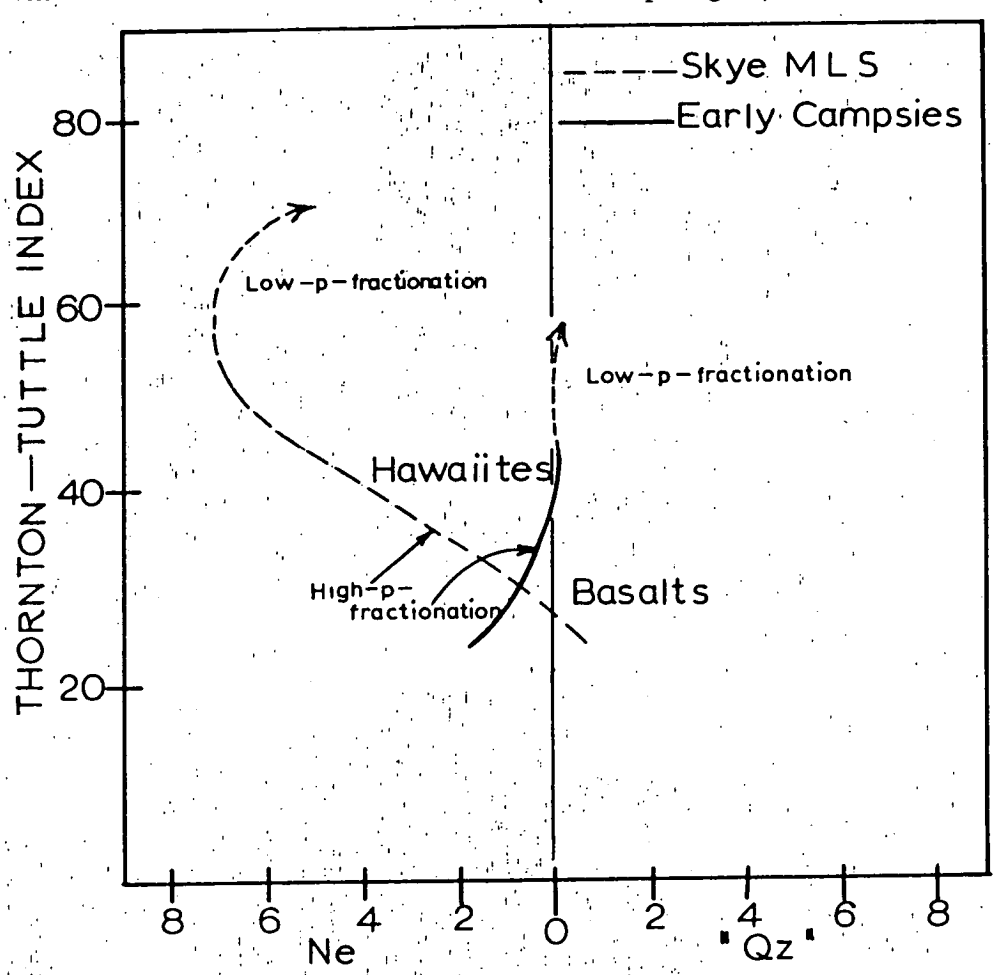

FIG. 19. Differentiation Index plotted against degree of silica saturation for the Skye Main Lava Series (Thompson 1974a, fig. 8), and the Early Campsie lavas. Suggested high-and low-pressure stages of the fractionation histories of both suites are indicated.

note in this respect that Thompson's (1974b) pyroxenes in spec. SK 971 become in fact increasingly silica-poor with increasing pressure, actually becoming *ne*-normative at >20 kb. The composition of these high-pressure pyroxenes is very dependent on magma composition, however, and the postulated Early Campsie liquidus pyroxenes may actually have become nepheline-normative at pressures less than 20 kb.

If these speculations are correct, the Early Campsie lavas seem to provide another example of the *clinopyroxenite stage* of basalt evolution of the experimental petrologists (for example O'Hara 1968, fig. 7A).

The compositions of the basic members of the Kintyre-type suites project into the Ol-Di-Pl system as a fairly coherent, linear zone, ranging from the olivine field into that of plagioclase (Fig. 5). This trend is at an angle to that of the Early Campsie rocks and does not lie on a clinopyroxene control. Following the earlier discussion, it is suggested that this is again a partly high-pressure trend, this time reflecting a *wehrlite* stage of fractionation (O'Hara 1968, fig. 7A). Examples of compositions of this type which have been arrested at low pressures sufficiently long for the magmas to precipitate new phenocryst assemblages are the olivine-phyric (Dalmeny) basalts described on p. 284.

In summary, a high-pressure stage of basalt evolution seems to be recognizable in the Dinantian lavas, though there is a need for experimental verification and quantification of the predictions made about the order of crystallization and chemistry of the major phases. Until such data are available, little can be positively stated about the ultimate origin of the basalts, in particular as to whether the most basic rocks represent primary magmas (cf. Thompson, 1974a) or liquids already modified by crystal fractionation before reaching the evolutionary stages described above.

Similarly, the slight petrochemical differences between the various Dinantian successions may reflect minor differences in the source mantle and/or the melting process, or variable fractionation histories during magma ascent. Validation or rejection of the primary magma hypothesis will prove of value in this case. In the case of the East Lothian field, however, the mildly potassic character of the Dinantian lavas also pertains to much of the later, intrusive activity, many of the (post-Namurian?) basanites analyzed by T. C. Day (for example 1928, p. 51, no. 2, 1932, p. 381, no 3) being notably potassic. This geochemical feature may reflect a compositional characteristic of the mantle, with the peridotites of the source zone containing rather larger amounts of K relative to Na (in phlogopite?) than, say, the Campsie source zone, whose products are more sodic in character. On a provincial basis, the mantle may be slightly inhomogeneous with respect to the large-ion elements such as K, Na, Ti and P. Equally well, in view of the complications which are emerging with respect to the melting behaviour of phlogopite-bearing peridotites (Flower *et al.*, 1975), inter-suite variations may represent slightly different depths or degrees of melting of a homogeneous source material.

Mugearites, benmoreites and trachytes

Appraisal of the crystallization histories of the intermediate members of the Dinantian suites is complicated either by lack of chemical data, as in the Lanarkshire Block where

perhaps the most important range of these rocks exists, or by the uncertainties of magma compositions brought about by the slightly altered nature of many specimens. Variation diagrams (Fig. 6) for the Kintyre lavas indicate considerable spread in MgO and Na_2O values in the intermediate and salic compositions, and while this *may* partly be due to the existence of more than one magmatic lineage, it more likely is caused by combinations of leaching, albitization and carbonation. The following discussion should be regarded as preliminary; a more detailed analysis awaits more complete data.

In most recent studies of alkali basalt → trachyte sequences, the intermediate and salic members are thought to have formed by low-pressure fractionation of the hawaiitic magmas (for example Barberi and Varet 1970; G. A. MacDonald 1968; Cox *et al.*, 1970; Thompson *et al.*, 1972; Upton and Wadsworth 1972; Flower 1973; Thompson 1974a; Upton 1974.) It was suggested earlier (p. 303) that the Early Campsie hawaiites were also formed by low-pressure fractionation of basaltic hawaiites, and this mode of origin is here cautiously extended to all the Midland Valley intermediate and salic rocks.

Such a model is generally in agreement with the field evidence. It has long been recognized that eruption of the trachytic lavas in the Clyde Plateau was related to the growth of large central volcanoes. It may be inferred that substantial magma chambers underlay these centres, and that the formation of the salic magmas was by crystal fractionation of mugearitic and benmoreitic parents within these chambers.

Future research

An attempt has been made in this contribution to point out some previously unrecorded or insufficiently stressed features of the petrochemistry of the Dinantian volcanic rocks. The overall chemical characteristics of the lavas have been summarized. Several magmatic lineages have been recognized, differing only in detail but lending to each major outcrop its own chemical "fingerprint". The possible role of high-pressure (> 10 kb) processes on the evolution of the basalts has been discussed, and an argument made for the importance of clinopyroxene fractionation within the mantle.

It is worth repeating, however, that much of the discussion is of a preliminary nature, and is based on chemical data which are at best barely adequate. Many of the areas where further petrochemical research is required have been indicated in the text; the more important points are summarized below.

(a) The petrography of the Dinantian lavas, especially the basic varieties, is known in great detail. The chemical mineralogy, on the other hand, is very poorly known. The few available determinations of mineral compositions in the lavas have all been made optically, to the best of my knowledge. It will be impossible to quantify and test petrogenetic models until the range of compositions, at least of the phenocryst phases, is known. In particular the composition of the texturally complex clinopyroxene, plagioclase and olivine phenocrysts in the clinopyroxene-phyric basalts will provide information on the polybaric evolution of these rocks.

(b) A major whole-rock, major element programme should be instigated to provide

information on the chemical variation *within* and *between* the main Dinantian suites. Specifically, (i) the lineages recognized in this paper are in some cases based on too few analyses and need to be amplified and modified; (ii) in certain areas, more than one lineage almost certainly exists, though they cannot be separated using existing data; (iii) more analyses will increase confidence in proposing petrogenetic schemes.

From these points of view, the area of the Clyde Plateau south of the River Clyde will prove rewarding ground, judging from published petrographic accounts.

(c) The need for, and aims of, an extensive trace-element analytical programme have been outlined on p. 299.

(d) Many of the suggestions made here regarding the high-pressure evolution of the Scottish basalts and hawaiites are directly open to experimental test. Sir James Hall, the "Father of Experimental Petrology", used rocks from the Midland Valley province in his pioneering experiments on the melting and crystallization of basalt (1805). These remain the first and last local rocks to have been accorded the privilege of such study.

(e) Considering the known complexities of stratigraphical correlation within the Carboniferous strata of the Midland Valley, the continuation and expansion of age-dating programmes on the lavas (for example Fitch *et al.*, 1970) is absolutely necessary. Furthermore, the relationships between lavas and intrusions, especially as regards firstly the identification of possible lava feeders and secondly, a more detailed knowledge of the changes of magma chemistry with time, need to be clarified by reliable age-dates.

(f) The Dinantian volcanism is only part of a much broader spectrum of activity during the Carboniferous and Permian in Scotland. A complete understanding of the relationships between the graben tectonics of the Midland Valley and the associated magmatism will be possible only when the petrogenesis of not only the Dinantian lavas, but also the later Carboniferous and Permian alkaline rocks, the quartz-dolerite suite and the camptonite suite of the Highlands, is better known. There can be no doubt, however, that significant contributions to petrology remain to be made in this fascinating province.

Acknowledgments

My colleague, Sheila Rizzello, made most of the new chemical analyses reported here. P. M. Craig and H. A. F. de Souza kindly allowed me to use unpublished information. A. D. McAdam and other officers of the I.G.S. (Edinburgh) helped me with details of local geology and localities. Various undergraduates from this Department have had part of their labours incorporated in this report, namely B. Beddoe-Stephens, A. D. Curtis, W. F. Price, I. C. Rowlands, M. Scott and V. A. Sugden. H. Willis and Mrs. M. Hartup helped me to produce the manuscript. Peter Craig, Bob Thompson and Brian Upton provided stimulating reviews of the script. Financial support for my Midland Valley work comes from the Department of Environmental Sciences, University of Lancaster.

To all these people, and especially to Douglas Fettes for his encouragement and patience, I offer my warmest thanks.

References

ALLAN, D. A. 1924. The igneous geology of the Burntisland district. *Trans. R. Soc. Edinb.* **53**, 479–501.

ANDERSON, F. W. 1963. The Geological Survey bore at Rashiehill, Stirlingshire (1951). *Bull. geol. Surv. Gt. Br.* **20**, 43–106.

BAKER, P. E., GASS, I. G., HARRIS P. G. and LE MAITRE, R. W. 1964. The volcanological report of the Royal Society expedition to Tristan da Cunha, 1962. *Phil. Trans. R. Soc.* **256**, 439–578.

BARBERI, F. and VARET, J. 1970. The Erta Ale volcanic range (Danakil Depression, Northern Afar, Ethopia). *Bull. Volcan.* **34**, 848–917.

BENNETT, J. A. E. 1945. Some occurrences of leucite in East Lothian. *Trans. Edinb. geol. Soc.* **14**, 34–52.

BEST, M. G. and BRIMHALL, W. H. 1974. Late Cenozoic alkalic basaltic magmas in the western Colorado plateaus and the Basin and Range transition zone, U.S.A., and their bearing on mantle dynamics. *Bull. geol. Soc. Am.* **85**, 1677–1690.

BLACK, G. P. 1966. *Arthur's Seat*, Edinburgh and London.

BOYD, W. W. 1974. Geochemical investigation of composite bodies involving intermediate members of the alkali basalt-trachyte suite. *Univ. Edinburgh Ph.D. thesis* (unpubl.)

CARMICHAEL, I. S. E., TURNER, F. J. and VERHOOGEN, J. 1974. *Igneous Petrology* New York.

CHAPMAN, N. A. 1974. Ultrabasic inclusions from the Coalyard Hill Vent, Fife. *Scott. J. Geol.* **10**, 223–227.

CLARK, R. H. 1952. The significance of flow-structure in the microporphyritic ophitic basalts of Arthur's Seat. *Trans. Edinb. geol. Soc.* **15**, 69–83.

——, 1956. A petrological study of the Arthur's Seat volcano. *Trans. R. Soc. Edinb.* **63**, 37–70.

CLOUGH, C. T., BARROW, G., CRAMPTON, C. B., MAUFE, H. B., BAILEY, E. B. and ANDERSON, E. M. 1910. The Geology of East Lothian (2nd ed.). *Mem. geol. Surv. U.K.*

COOMBS, D. S. and WILKINSON, J. F. G. 1969. Lineages and fractionation trends in undersaturated volcanic rocks from the East Otago Volcanic Province (New Zealand) and related rocks. *J. Petrology* **10**, 440–501.

COX, K. G. and BELL, J. D. 1972. A crystal fractionation model for the basaltic rocks of the New Georgia Group, British Solomon Islands. *Contr. Mineral. Petrol.* **37**, 1–13.

——, GASS, I. G. and MALLICK, D. I. J. 1970. The peralkaline volcanic suite of Aden and Little Aden, South Arabia. *J. Petrology* **11**, 433–461.

CRAIG, P. M. and HALL, I. H. S. 1975. The Lower Carboniferous rocks of the Campsie-Kilpatrick area. *Scott. J. Geol.* **11**, 171–174.

DALY, R. A. 1933. *Igneous rocks and the depth of the earth* (2nd ed.), New York.

DAVIES, A. 1974. The Lower Carboniferous (Dinantian) sequence at Spilmersford, East Lothian, Scotland. *Bull. geol. Surv. Gt. Br.* **45**, 1–38.

DAY, T. C. 1928(a). The volcanic vents on the shore between North Berwick and Tantallon Castle. *Trans. Edinb. geol. Soc.* **12**, 41–52.

——, 1928(b). Metasomatism in basalt near Eel Burn, North Berwick. *Trans. Edinb. geol. Soc.* **12**, 117–121.

——, 1930(a). Volcanic vents on the coast from Tantallon Castle eastwards to Peffer Sands, and at Whitberry Point. *Trans. Edinb. geol. Soc.* **12**, 213–233.

——, 1930(b). An igneous dyke in the quartz-banakite of Bangly Quarry near Haddington. *Trans. Edinb. geol. Soc.* **12**, 256–259.

——, 1930(c). Chemical analyses of thirteen igneous rocks of East Lothian. *Trans. Edinb. geol. Soc.* **12**, 263–266.

——, 1932. Volcanic vents at Longskelly Rocks, and at Yellow Craig Plantation, west of North Berwick. *Trans. Edinb. geol. Soc.* **12**, 376–381.

ELLIOTT, R. B. 1960. The Carboniferous volcanic rocks of the Langholm district. *Proc. Geol. Ass.* **71**, 1–24.

FALCONER, J. D. 1906. The igneous geology of the Bathgate–Linlithgow Hills. Part 2. Petrography. *Trans. R. Soc. Edinb.* **45**, 133–150.

FITCH, F. J., MILLER, J. A. and WILLIAMS, S. C. 1970. Isotopic ages of British Carboniferous rocks. *C.R. 6ème Congr. Int. Stratigr. Geol. carbonif., Sheffield, 1967* Pt. **2**, 771–789.

FLOWER, M. F. J. 1973. Evolution of basaltic and differentiated lavas from Anjouan, Comores Archipelago. *Contr. Mineral. Petrol.* **38**, 237–260.

——, SCHMINCKE, H.-U. and THOMPSON, R. N. 1975. Phlogopite stability and the Sr^{87}/Sr^{86} step in basalts along the Reykjanes Ridge. *Nature* **254**, 404–406.

FRANCIS, E. H. 1965(a). *In* Craig, G. Y. (ed), *The Geology of Scotland*, 309–357, Edinburgh and London.

——, 1965(b). Carboniferous-Permian igneous rocks. *In* Craig, G. Y. (ed), *The Geology of Scotland* 359–382, Edinburgh and London.

——, 1967. Review of Carboniferous-Permian volcanism in Scotland. *Geol. Rdsch.* **57**, 219–46.

——, 1968. Effect of sedimentation on volcanic processes, including neck-sill relationships, in the British Carboniferous. *23rd Intern. geol. Congress* **2**, 163–174.

——, 1970. Review of Carboniferous volcanism in England and Wales. *J. Earth Sci. Leeds* **8**, 41–56.

——, FORSYTH, I. H., READ, W. A. and ARMSTRONG, M. 1970. The geology of the Stirling district. *Mem. geol. Surv. U.K.*

GREIG, D. C. 1971. The south of Scotland. *Br. reg. Geol.* (3rd ed.).

GUPPY, E. M. and THOMAS, H. H. 1931. Chemical analyses of igneous rocks, metamorphic rocks and minerals. *Mem. geol. Surv. U.K.*

HALL, J. 1805. Experiments on whinstone and lava. *Trans. R. Soc. Edinb.* **5**, 43–75.

HALL, J. 1973. A seismic reflection survey of the Clyde Plateau Lavas in North Ayrshire and Renfrewshire. *Scott. J. Geol.* **9**, 253–279.

HAMILTON, J. 1956. Mineralogy of basalts from the western Kilpatrick Hills and its bearing on the petrogenesis of Scottish Carboniferous olivine basalts. *Trans. Edinb. geol. Soc.* **16**, 280–298.

HIGAZY, R. A. 1952. The distribution and significance of the trace elements in the Braefoot Outer Sill, Fife. *Trans. Edinb. geol. Soc.* **15**, 150–186.

JOHNSTONE, G. S. 1965. The volcanic rocks of the Misty Law–Knockside Hills district, Renfrewshire. *Bull. geol. Surv. Gt. Br.* **22**, 53–64.

KENNEDY, W. Q. 1931. On composite lava flows. *Geol. Mag.* **68**, 166–181.

——, 1933. Composite auto-intrusion in a Carboniferous lava flow. *Mem. geol. Surv. Summ. Prog. for* 1932 Pt. **2**, 83–93.

LEEDER, M. R. 1974. The origin of the Northumberland basin. *Scott. J. Geol.* **10**, 283–296.

LE MAITRE, R. W., 1962. Petrology of volcanic rocks, Gough Island, South Atlantic. *Bull. geol. Soc. Am.* **73**, 1309–1340.

LIVINGSTONE, A. and McKISSOCK, G. M. 1974. The geochemistry of the igneous rocks in the Lower Carboniferous (Dinantian) sequence at Spilmersford, East Lothian, Scotland. *Bull. geol. Surv. Gt. Br.* **45**, 47–61.

LUMSDEN, G. I., TULLOCH, W., HOWELLS, M. F. and DAVIES, A. 1967. The Geology of the neighbourhood of Langholm. *Mem. geol. Surv. U.K.*

McADAM, A. D. 1974. The petrography of the igneous rocks in the Lower Carboniferous (Dinantian) at Spilmersford, East Lothian, Scotland. *Bull. geol. Surv. Gt. Br.* **45**, 39–46.

——, HOWELLS, M. F. and UPTON, B. G. J. 1969. East Lothian. *In* Upton, B. G. J. (ed), *Field excursion guide to the Carboniferous volcanic rocks of the Midland Valley of Scotland*, 36–43. Edinburgh.

MACDONALD, G. A. 1968. Composition and origin of Hawaiian lavas. *Geol. Soc. Am. Mem.* **116**, 477–522.

MACDONALD, J. G. 1965. The petrology of the Clyde Plateau Lavas of the Campsie and Kilpatrick Hills. *Univ. Glasgow Ph.D. thesis* (unpubl.)

——, 1967. Variations within a Scottish Lower Carboniferous lava flow. *Scott. J. Geol.* **3**, 34–45.

—— and WHYTE, F. 1969. The Campsie Fells area, Stirlingshire. *In* Upton, B. G. J. (ed), *Field excursion guide to the Carboniferous volcanic rocks of the Midland Valley of Scotland*, 16–22. Edinburgh.

MACGREGOR, A. G. 1928. The classification of Scottish Carboniferous olivine basalts and mugearites. *Trans. geol. Soc. Glasg.* **18**, 324–360.

——, 1932. Note on corroded ferromagnesian phenocrysts in a Scottish basalt. *Trans. Edinb. geol. Soc.* **12**, 329–333.

MACGREGOR, A. G. 1937. The Carboniferous and Permian volcanoes of Scotland. *Bull. Volcan.* (2)1, 41–58.
——, 1948. Problems of Carboniferous-Permian volcanicity in Scotland. *Q. Jl geol. Soc. Lond.* 104, 133–153.
——, 1955. Xenolithic monchiquite. *Geol. Mag.* 92, 82–83.
——, 1960. Garleton Hills and Traprain Law. *In Edinburgh Geology: an excursion guide*, 61–69, Edinburgh and London.
MACGREGOR, M., DINHAM, B. A., BAILEY, E. B. and ANDERSON, E. M. 1925. The geology of the Glasgow district (2nd ed.). *Mem. geol. Surv. U.K.*
—— and MACGREGOR, A. G., 1948. The Midland Valley of Scotland. *Br. reg. Geol.* (2nd ed.).
MUIR, I. D. and TILLEY, C. E. 1961. Mugearites and their place in alkali igneous rocks series. *J. geol.* 69, 186–203.
OERTEL, G. 1952. A structural investigation of the porphyritic basalts of Arthur's Seat, Edinburgh. *Trans. Edinb. geol. Soc.* 14, 360–378.
O'HARA, M. J. 1968. The bearing of phase equilibrium studies in synthetic and natural systems on the origin and evolution of basic and ultrabasic rocks. *Earth. Sci. Rev.* 4, 69–133.
PALLISTER, J. W. 1952. The Birrenswark Lavas, Dumfriesshire. *Trans. Edinb. geol. Soc.* 14, 336–348.
PATTERSON, E. M. 1945. The distribution of trace-elements in a Scottish Permo-Carboniferous teschenite and its lugaritic differentiate. *Geol. Mag.* 82, 230–234.
RICHEY, J. E. 1928. The North Ayrshire sequence of Calciferous Sandstone volcanic rocks. *Trans. geol. Soc. Glasg.* 18, 247–257.
——, ANDERSON, E. M. and MACGREGOR, A. G. 1930. The geology of North Ayrshire. *Mem. geol. Surv. U.K.*
RUTLEDGE, H. 1952. A petrological note on a composite sill, The Dasses, Arthur's Seat. *Trans. Edinb. geol. Soc.* 14, 379–388.
SIMPSON, J. B. and RICHEY, J. E. 1936. The geology of the Sanquhar Coalfield and the adjacent basin of Thornhill. *Mem. geol. Surv. U.K.*
SMITH, W. W. 1959. Pseudomorphs after olivine in Markle basalt. *Mineralog. Mag.* 32, 324–331.
THOMPSON, R. N. 1972. The 1-atmosphere melting patterns of some basaltic volcanic series. *Am. J. Sci.* 272, 901–932.
——, 1974(a). Primary basalts and magma genesis. I. Skye, North-West Scotland. *Contr. Mineral. Petrol.* 45, 317–341.
——, 1974(b). Some high-pressure pyroxenes. *Mineralog. Mag.* 39, 768–787.
——, ESSON, J. and DUNHAM, A. C. 1972. Major element chemical variation in the Eocene lavas of the Isle of Skye, Scotland. *J. Petrology* 13, 219–253.
TIBA, T. 1966. Petrology of the alkaline rocks of the Takakusayama district, Japan. *Sci. Rep. Tohoku Univ.*, Ser. III, 9, 541–610.
TOMKEIEFF, S. I., 1937. Petrochemistry of the Scottish Carboniferous-Permian igneous rocks. *Bull. volcan.* (2) 1, 59–87.
——, 1945. Petrology of the Carboniferous igneous rocks of the Tweed Basin. *Trans. Edinb. geol. Soc.* 14, 53–75.
——, 1952. Analcite-trachybasalt inclusions in the phonolite of Traprain Law. *Trans. Edinb. Geol. Soc.* 16, 360–373.
——, 1953. The Carboniferous igneous rocks of the Kelso district. *Proc. Univ. Durham Phil. Soc.* 11, 95–101.
TYRRELL, G. W., 1912. The petrology of the Kilpatrick Hills, Dunbartonshire. *Trans. geol. Soc. Glasg.* 14, 219–257.
UCHIMUZU, M., 1966. Geology and petrology of alkali rocks from Dogo, Oki Islands. *J. fac. Sci. Tokyo Univ.* Sec. 2, 16, 85–159.
UPTON, B. G. J., 1969. *Field excursion guide to the Carboniferous volcanic rocks of the Midland Valley of Scotland*, Edinburgh.
——, 1971. Melting experiments on chilled gabbros and syenogabbros. *Carnegie Instn. Wash. Yb.* 70, 112–118.

UPTON, B. G. J. 1974. The alkaline province of South-West Greenland. *In* Sørensen, H. (ed), *The Alkaline Rocks*, 221–238, London.

——, and WADSWORTH, W. J. 1972. Aspects of magmatic evolution on Réunion Island. *Phil. Trans. R. Soc.* **271A**, 105–130.

WALKER, F. 1965. The part played by tholeiitic magma in the Carbo-Permian vulcanicity of central Scotland. *Mineralog. Mag.* **34**, 498–516.

WHYTE, F. 1966. Dumbarton Rock. *Scott. J. Geol.* **2**, 107–121.

——, and MACDONALD, J. G. 1974. Lower Carboniferous vulcanicity in the northern part of the Clyde Plateau. *Scott. J. Geol.* **10**, 187–198.

WILKINSON, J. F. G. 1974. The mineralogy and petrography of alkali basaltic rocks. *In* Sørensen, H. (ed), *The Alkaline Rocks*, 67–95, London.

YODER, H. S. 1969. Calcalkaline andesites: experimental data bearing on the origin of their assumed characteristics. *In* McBirney, A. R. (ed), Proceedings of the Andesite Conference. *Oregon Dept. Geol. Mineral Ind. Bull.* **65**, 77–89.

MS received 16th September 1975

Tables 2—6 have been deposited with the British Library Lending Division, Boston Spa, Wetherby, Yorkshire, LS 23 7BQ. Copies can be obtained from the library by quoting SUP 24001. The explanations to the tables are given below.

Explanation to Table 2

Chemical analyses and C.I.P.W. norms of lavas from southern Kintyre. Analyses by Sheila Rizzello (1, 2, 7, 8, 13, 16, 19 and 19—with I. C. Rowlands; 6, 12, 14, 20—with M. Scott). n.d. = not detected. Asterisks = dried for 2 hrs. at 105°C. Norms calculated using standard Fe_2O_3 values and on a CO_2-free basis.

Abbreviations used for modal data in this and subsequent tables are: Ol, olivine; Cpx, clinopyroxene; Pl, plagioclase; IO, iron oxides; Ap, apatite; AF, alkali feldspar; Am, amphibole.

1. Aphyric, low-potassium basalt, flow, south of Skerry Fell, Machrihanish. [NR 635 178] (Fresh) MV 261.

2. Alkali olivine basalt, macroporphyritic flow, Drumlemble. [NR 664 193] (Fresh) MV267. Phenocrysts: Ol(10·1), Cpx(11·4), Pl(13·4).

3. Alkali olivine basalt, sparsely microphyric flow?, Kilbride, Southend, [NR 718 088] (Fresh). MV 201. Phenocrysts: Ol(tr.).

4. Ankaramitic basalt, flow, Eudan nan Gallan, Uisaed, Machrihanish. [NR 624 204] (Fresh) MV 222. Phenocrysts: Ol(14·9), Cpx (14·4).

5. Alkali olivine basalt (basanite?), aphyric or sparsely microphyric flow, Achnaclach. [NR 693 151] (olivine pseudomorphed, otherwise fresh). MV 207. Phenocrysts: Ol (tr.).

6. Basaltic hawaiite, macroporphyritic flow, Cullan Doon, Chiscan Water. [NR 698 168] (olivine pseudomorphed). MV 256. Phenocrysts: Ol(0·6), Cpx (0·3), Pl(6·1).

7. Basaltic hawaiite, microphyric flow, west of Skerry Fell Fad, Machrihanish. [NR 630 185] (Fairly fresh). MV 329. Phenocrysts: Ol(1·3), Cpx(3·5), Pl(2·3).

8. Hawaiite, sparsely microphyric or aphyric flow, south of Skerry Fell Fad, Machrihanish. [NR 638 178] (olivine pseudomorphed) MV 311. Phenocrysts: Ol(tr.).

9. Basaltic hawaiite, microphyric flow, south of Black Hill. [NR 695 159] (olivine pseudomorphed) MV 210. Phenocrysts: Ol(tr), Pl(6·2), IO(tr).

10. Hawaiite, Macroporphyritic flow, shore section, Machrihanish. [NR 634 208] (olivine pseudomorphed). MV 226. Phenocrysts: Ol(4·4), Pl(9·9), IO(1·0).

11. Hawaiite, macroporphyritic flow, shore section, Machrihanish. [NR 627 208] (olivine pseudomorphed). MV 218. Phenocrysts: Ol(4·5), Cpx(tr), Pl(25·2), IO(1·9).

12. Hawaiite, upper macroporphyritic component of composite flow, Laggs Farm. [NR 689 167] (Flow somewhat oxidized) MV 213. Phenocrysts: Cpx(0·1), Pl(21·8) IO(0·1).

13. Hawaiite, microphyric flow, 100 m north-west of lifeboat house, shore section Uisaed, Machrihanish. [NR 629 209] MV 307(a) Phenocrysts: Ol(0·7), Pl(13·5), IO(2·3).

14. Hawaiite, microphyric flow, Black Hill scarp, near Uigle Farm. [NR 697 164] (olivine pseudomorphed) MS 34. Phenocrysts: Ol(tr), Pl(tr).

15. Mugearite, microphyric flow, crags at top of Black Hill. [NR 695 161] (Highly oxidized). MV 211. Phenocrysts: Ol(tr), Pl(tr), IO(tr), Ap(tr), AF(tr).

16. Benmoreite, sparsely microphyric flow, south of Skerry Fell Fad, Machrihanish. [NR 633 182] (Fresh) MV 328. Phenocrysts: Pl(tr), IO(tr), Ap(tr), AF(3·1).

17. Trachyte, microphyric flow, shore west of Carrick Caban, Machrihanish. [NR 637 207] (Not fresh) MV 215. Phenocrysts: Ol(1·1), Pl(10·3), IO(0·2), Ap(0·7) AF(1·4).

18. Rhyolite, sparsely microphyric flow, small disused quarry north of High Tirfergus Farm. [NR 655 186] (Not fresh). MV 265. Phenocrysts: Pl(0·9), IO(0·4), AF(0·5).

19. Quartz trachyte, microphyric flow, north-east slope of Skerry Fell Fad, Machrihanish. [NR 638 183] (Not very fresh). MV 203. Phenocrysts: AF(7·7).

20. Rhyolite, microphyric flow in Chiscan Water. [NR 702 168] (Highly oxidized). MS 124. Note: for norm calculation, mol. FeO was arbitrarily made equal to mol TiO_2. Phenocrysts: Ol(0·3), AF(13·8).

The standard Fe_2O_3 values used in the norm calculations are slightly modified from those of Thompson *et al.* (1972), viz.
where

$Na_2O + K_2O < 4\%$, $Fe_2O_3 = 1{\cdot}50\%$
$Na_2O + K_2O$ 4–7%, $Fe_2O_3 = 2{\cdot}00\%$
$Na_2O + K_2O$ 7–10%, $Fe_2O_3 = 2{\cdot}50\%$
$Na_2O + K_2O > 10\%$, Fe_2O_3 not standardized.

Explanation to Table 3

Chemical analyses and C.I.P.W. norms and lavas and intrusions from the East Lothian volcanic field. 1–9 and 14–15 are new analyses by Sheila Rizzello and 13 a new analysis by C. M. Lamb. n.d. = not detected. Asterisks = dried for 2 hrs. at 105°C. Norms have been calculated using standard Fe_2O_3 values and on a CO_2-free basis.

1. Hypersthene-normative basalt, macroporphyritic flow, railway cutting (under A1 road), East Linton. [NT 595 771]. (Flow somewhat oxidized, olivines pseudomorphed). MV 48. Phenocrysts: Ol(8·2), Cpx(4·1), Pl(6·2).

2. Hypersthene-normative basalt, macroporphyritic flow, Kippielaw Quarry [NT 584 755]. (Flow somewhat chloritized). MV 72. Phenocrysts: Ol(3·3), Cpx(0·8), Pl(9·1).

3. Hypersthene-normative basalt, microphyric flow, Kippielaw scarp. [NT 585 755]. (olivines pseudomorphed, otherwise fresh). MV 71(a). Phenocrysts: Ol(1·4) Cpx(0·4), Pl(6·4).

4. Basaltic hawaiite, microphyric flow, southern end of Whitekirk Hill. [NT 594 816]. (Flow oxidized). MV 128. "Mugearite" of Clough *et al.* (1910, p. 71). Phenocrysts: Ol(0·5), Pl(4·1).

5. Aphyric hawaiite, flow forming small scarp, Lawhead Farm. [NT 599 796] (Fresh). MV 42. "Mugearite" of Clough *et al.* (1910, p. 74).

6. Hawaiite, microphyric flow, railway cutting, East Linton. [NT 597 771]. (Flow oxidized). MV 47. "Mugearite" of Clough *et al.* (1910, p. 72). Phenocrysts: Ol, Pl, IO, Ap (all tr).

7. Mugearite, sparsely microphyric flow, Kippielaw scarp. [NT 587 756]. (Flow oxidized). MV 70. Phenocrysts: Pl(tr), IO(tr).

8. Mugearite, sparsely microphyric flow, Brownrigg Farm. [NT 553 809]. (Flow oxidized). MV 126(b). Phenocrysts: Ol(1·3), Pl(4·4), IO(0·2).

9. Benmoreite, sparsely microphyric flow, roadside, Kingston. [NT 543 823]. (Flow oxidized). MV 24. Phenocrysts: Pl(0·4), IO(0·2).

10. Benmoreite, Congalton Mains. Muir and Tilley (1961, table 4). (mugearite-trachyte, spec. no. 66120).

11. Trachyte (Quartz-banakite), flow, Bangly Quarry. Day (1930b, p. 257). Phenocrysts: Cpx, Pl, IO, AF.

12. Trachyte, flow, Skid Hill Quarry. Day (1930c, p. 266). Phenocrysts: Ol, Cpx, Pl, IO, AF.

13. Hypersthene-normative basalt, macroporphyritic intrusion in vent, Burning Mount. [NT 581 752]. (olivines partially pseudomorphed). MV 74. Phenocrysts: Ol(7·5). Cpx(1·6), Pl(20·7).

14. Alkali olivine basalt, macroporphyritic intrusion, Cairndinnis Farm. [NT 572 745]. (Fresh). MV 167. Phenocrysts: Ol(4·2), Cpx(5·6), Pl(10·9).

15. Olivine analcite dolerite, sill, Gosford Bay. [NT 442 779]. (Fresh) MV 164. (see Clough *et al.*, 1910, p. 115). Essentially aphyric, though some of larger olivine grains are probably microphenocrysts.

Explanation to Table 4.

Chemical analyses and C.I.P.W. norms of lavas and intrusions from the Clyde Plateau Lavas north of the River Clyde. 1–6, lavas and possible feeders of the stratigraphically Lower Group of MacGregor *et al.* (1925), Whyte and J. G. MacDonald (1974) and Craig and Hall (1975). 7–12, lavas and intrusion of the same authors' Upper Group. Asterisks = dried for 2 hrs. at 105°C. Norms calculated using standard Fe_2O_3 values and on a CO_2-free basis.

1. Basaltic hawaiite (Jedburgh basalt), flow, Aldessan Burn, Campsie. [NS 697 808]. J. G. MacDonald and Whyte (1969, table 3, no. 2).

2. Basaltic hawaiite (Jedburgh basalt), flow, Almeel Burn, Campsie. [NS 594 822]. J. G. MacDonald and Whyte (1969, table 3, no. 3).

3. Basaltic hawaiite (Jedburgh basalt), plug, Little Caldon Neck, north of Kilpatrick Hills. MacGregor *et al.* (1925, p. 182) and Guppy and Thomas (1931, no. 270). Phenocrysts: Ol, Pl.

4. Microphyric basaltic hawaiite, intrusion in Dumgoyne vent, Strathblane. [NS 540 827]. New analysis by A. D. Curtis and S. A. Rizzello. Phenocrysts: Ol, Pl.

5. Aphyric hawaiite, intrusion in vent, quarry, Dumbuck, Bowling. [NS 419 746]. New analysis by B. Beddoe-Stephens and S. A. Rizzello.

6. Microphyric hawaiite, plug in vent, Dumbarton Rock. Whyte (1966, table 2, no. 4). Phenocrysts: Ol, Pl.

7. Macroporphyritic basaltic hawaiite (Markle basalt), flow, south cairn of Dunbrach, Fintry. J. G. MacDonald and Whyte (1969, table 3 no. 4).

8. Microphyric hawaiite (Jedburgh basalt), flow, Alnwick Burn, below Shearer's Burn, Campsie. J. G. MacDonald and Whyte (1969, table 3, no. 5).

9. Mugearite, flow, Alnwick Burn, upstream from Shearer's Burn, Campsie. J. G. MacDonald and Whyte (1969, table 3, no. 6).

10. Aphyric mugearite, flow, Balhennan Farm, Fintry Hills. MacGregor *et al.* (1925, p. 182) and Guppy and Thomas (1931, no. 302).

11. Microphyric trachyte (trachyandesite), plug in neck, Meikle Bin, Campsie Fells. MacGregor *et al.* (1925, p. 183) and Guppy and Thomas (1931, no. 158). Phenocrysts: Ol, Cpx, Pl, IO.

12. Trachyte, flow, north face of Dunbrach, Fintry. J. G. MacDonald and Whyte, (1969, table 3, no. 7).

Explanation to Table 5.

Chemical analyses and C.I.P.W. norms of lavas and intrusions from the 'Lanarkshire' Block. All specimens belong stratigraphically to the Upper Group of Richey (1928). Data from Guppy and Thomas (1931) and Richey *et al.* (1930). Norms have been calculated using standard Fe_2O_3 values, and on a CO_2-free basis.

1. Hypersthene-normative basalt, flow, Little Calder water, Avondale, Lanarkshire. Guppy and Thomas (1931, no. 264). Phenocrysts: Ol, Cpx, Pl.

2. Hypersthene-normative basalt, flow, Winkingfield, Ayrshire. Guppy and Thomas (1931, no. 307). Phenocrysts: Ol, Cpx, Pl.

3. Mugearite, marginal facies of plug, Loudon Hill, Ayrshire. "Trachyandesite" of Guppy and Thomas (1931, no. 164). Phenocrysts: Cpx, Pl, Am.

4. Mugearite (hornblende trachyandesite), lava, Cleuchearn Burn, East Kilbride, Lanarkshire. Guppy and Thomas (1931, no. 162). Phenocrysts: Pl, Am.

5. Benmoreite, plug, Black Law, near Dunlop, Ayrshire. "Trachyandesite" of Guppy and Thomas (1931, no. 161).

6. Benmoreite, flow, Ballagioch Hill, near Eaglesham, Renfrewshire. "Trachyandesite" of Guppy and Thomas (1931, no. 160). Phenocrysts: Ol, Cpx, Pl, IO.

7. Benmoreite, probably a plug, East Browncastle, Avondale, Lanarkshire. "Trachyandesite" of Guppy and Thomas (1931, no. 159). Phenocrysts: Cpx, Pl.

8. Trachyte, flow, Drumreevough, Avondale, Lanarkshire. Guppy and Thomas (1931, no. 96). Phenocrysts: Cpx, Pl, AF.

9. Trachyte, flow, near Winkingfield Farm, Ayrshire. Guppy and Thomas (1931, No. 94).

10. Rhyolite, altered flow, Loganswell, near Eaglesham, Renfrewshire. Guppy and Thomas (1931, no. 53). Phenocrysts: AF.

Explanation to Table 6.

Chemical analyses (some partial) and C.I.P.W. norms of lavas and intrusions from the Kelso and Langholm areas. 1–4, lavas from the Kelso traps; 5–13, intrusions (and separated groundmasses) associated with Kelso Traps; 14– lava flow, Birrenswark Lavas; 15– plug in vent, near Langholm. All new analyses by Sheila Rizzello (1–4 with W. F. Price). n.d. = not detected. Asterisks = dried for 2 hrs. at 105°C. Norms calculated using standard Fe_2O_3 values and on a CO_2-free basis.

1. Basaltic hawaiite, microphyric flow, railway cutting, Lintmill, near Duns. [NT 732 463] (Olivine pseudomorphed) MV 180. Phenocrysts: Ol? Cpx? Pl, IO.

2. Basaltic hawaiite, macroporphyritic flow, south bank of Blackadder Water, Lintmill, near Duns. [NT 734 463] (Not very fresh). MV 179.

3. Hawaiite, microphyric flow, Baillieknowe Quarry, Stichill. [NT 709 382] (Olivine pseudomorphed) MV 184. Phenocrysts: Ol, Cpx, Pl, IO.

4. Basaltic hawaiite, microphyric flow, River Tweed section, Makerstoun House. [NT 673 315] (olivine pseudomorphed) MV 192.

5. Sparsely microphyric mugearite (or hawaiite), west end of quarry in composite intrusion, Mellerstain Hill. [NT 639 394]. (Fresh) MV 51. Phenocrysts: Pl(<0·1).

6. Macroporphyritic basaltic hawaiite, central part of quarry in composite intrusion, Mellerstain Hill. [NT 639 394]. (Fresh) MV 52. Phenocrysts: Ol, (1·3).

7. Microphyric hawaiite, plug, quarry, Dunion Hill, Jedburgh. [NT 626 191] (Fresh) MV 13. Phenocrysts: Ol(1·3), Pl(4·3).

8. Macroporphyritic hawaiite, porphyritic member of composite intrusion, quarry, Hareheugh Craigs. [NT 688 399] (Fresh). MV 39A. Phenocrysts: Ol(2·3), Cpx(5·0), Pl(17·0).

9. Hawaiite, groundmass separated from MV 39A. Iron determined as Fe_2O_3 only. H_2O^+ not determined. MV 39A.(G).

10. Hawaiite, aphyric member of composite intrusion, quarry, Hareheugh Craigs. [NT 688 399] (Fresh) MV 39B.

11. Hawaiite, macroporphyritic member of composite intrusion, southern end of Lurgie Craigs. [NT 674 396]. (Fresh) MV 40A. Phenocrysts: Ol(2·0), Cpx(0·8), Pl(26·0).

12. Hawaiite, groundmass separated from MV 40A. Iron determined as Fe_2O_3 only. H_2O^+ not determined. MV 40A(G).

13. Hypersthene-normative basalt, aphyric member of composite intrusion, north side of Lurgie Craigs. [NT 673 397] (Fresh) MV 40B.

14. Hypersthene-normative basalt, macroporphyritic flow forming scarp feature, Watch Hill, Langholm. [NY 434 905]. (olivines pseudomorphed) MV 122. (see also Lumsden *et al.* (1967, p. 74 and p. 195)). Phenocrysts: Ol, Cpx, Pl.

15. Microphyric hypersthene-normative basalt, plug, immediately east of fault between vent agglomerate and plug, Howgill Sike vent, Langholm. [NY 436 917]. (Fresh) MV 121. Phenocrysts: Ol(1·2), Cpx(1·7), Pl(1·3), IO(tr). Also contains 0·6% orthopyroxene xenocrysts.

Variations in basalt chemistry with time in the Midland Valley province during the Carboniferous and Permian

R. Macdonald,[1] J. E. Thomas[2] and S. A. Rizzello[1]

[1] *Department of Environmental Sciences, University of Lancaster*

[2] *Department of Geology, University of Reading*

SYNOPSIS

New chemical data for lavas from the sequences at Burntisland, the Bathgate-Linlithgow Hills, the Passage Group succession of Ayrshire, Mauchline and Thornhill are used to examine changes in chemistry of basic magmas emplaced in the Midland Valley petrographic province during the Carboniferous and early Permian. These lava groups contain basic magma types not yet recorded from the earlier Dinantian suites, especially moderately to strongly silica-undersaturated varieties.

The Carboniferous-Permian alkaline magmatism is related to two thermal cycles, each of which produced a similar trend of magma compositions (towards increasing silica-undersaturation) with time; one cycle was early Dinantian to early Namurian, the other mid-Namurian to early Permian in age. Each cycle developed, however, under different tectonic conditions.

INTRODUCTION

Progressive changes in the composition of basic magmas emplaced within a petrographic province reflect either changing conditions at the site of generation or differing evolutionary paths of the magmas. Since both are controlled to some degree by regional tectonics, the recognition of patterns of basalt chemistry within a province may in turn allow the geologist to provide information on the tectonic-magmatic cycle initiating the volcanism.

During the Carboniferous, the formation of rocks ranging in composition from tholeiitic to nephelinitic accompanied the tectonic development of the Midland Valley graben in Scotland. Macdonald (1975) has recently reviewed the evidence relating to time-controlled changes in basic magma chemistry of the *alkaline* rocks of the province. While pointing out that data for post-Dinantian lavas were very scarce, he accepted MacGregor's (1948) suggestion that the later Carboniferous basic rocks were, on average, more basic and more silica-undersaturated than those emplaced in the early Carboniferous.

In this paper, we provide 39 new analyses of basalts, basanites and basaltic hawaiites from the Midland Valley petrographic province, chosen to fill data gaps in the literature, especially those in post-Dinantian sequences. The new data permit a firmer statement to

Scott. J. Geol. 13, (1), 11–22, 1977

be made of the chemical affinities of certain Carboniferous lava sequences and a generalized model of the magmatic evolution of the province is proposed.

Methods

Prior to this study, only four analyses of post-Dinantian lavas from this province were available in the literature, while there were *no* analyses of the important late Dinantian sequences at Burntisland, Fife and in the Bathgate-Linlithgow Hills. Our collecting has been concentrated in these areas; brief details of sample localities are given below. We also give five new analyses of lavas from the Campsie Block, which approximately span the stratigraphic range of the sequence.

The new analyses were made at the Universities of Reading and Lancaster. Two rocks were analysed in both laboratories, with satisfactory agreement. C.I.P.W. norms were calculated using the standard Fe_2O_3 values of Macdonald (1975). All references to the normative character of the lavas in this respect are based on these modified norms. Rock nomenclature is that used by Macdonald (1975).

The total number of lava analyses used here (Fig. 1) is 76, 51 being of Dinantian, and 25 of post-Dinantian, rocks. The remaining points plotted in Figure 1 represent intrusions for which reliable radiometric age dates are available, viz. Hillhouse (Miller and Brown 1965), Spilmersford (McAdam 1974), Lomond Hills (Fitch *et al.* 1970 and this paper, Table, nos. 37–9) and various East Lothian intrusions (H. A. F. de Souza, pers. comm.).

The complete body of data provides a reasonably full coverage of the extrusive Carboniferous alkaline magmatism of the province. The time period covered by the fewest analyses is the lower Namurian, reflecting the scarcity of lavas of this age in Scotland. Any refinement of petrogenetic models for the Midland Valley will depend, however, on more detailed sampling of individual successions and on assessments of basalt chemistry within these successions as functions of time and local tectonic conditions.

Details of Sampling

The Burntisland lavas

The volcanic rocks of the Burntisland area lie almost entirely within the Dinantian, though Francis (1968, Fig. 1) shows the succession as extending just into the Namurian. A detailed flow-by-flow stratigraphy was established by Geikie (1900), while Allan (1924) has provided petrographical details of the lavas.

The Burntisland volcanic group is dominated by basalt lavas, with subordinate tuffs. The lavas appear to be mainly olivine-pyroxene-phyric basalts of Dalmeny and Hillhouse type, though some flows also contain scarce plagioclase phenocrysts (Allan 1924). Our collecting has been concentrated in the lower part of the sequence, because the upper flows (north of Kinghorn Bay) are badly weathered (Allan 1924). The six analysed specimens were chosen firstly to span as completely as possible the stratigraphical range

and secondly, for their freshness; all are relatively fresh and two contain only partially pseudomorphed olivine phenocrysts.

Five of the six analysed lavas are ol — or ol + cpx — phyric, hypersthene-normative basalts, the sixth being an ol + cpx — phyric alkali olivine basalt. A range of basalt types clearly exists and further analyses will be required to define the complete compositional spectrum. However, it appears from the new data that the Burntisland sequence is dominated by hypersthene-normative basalts of transitional type.

The Bathgate-Linlithgow lavas

These lavas and associated pyroclastic rocks span the Dinantian-Namurian boundary (Francis 1967, 1968); details of the stratigraphy and field relationships may be found in MacGregor and Haldane (1933) and Mitchell and Mykura (1962). The petrography has been described by Falconer (1906) and Flett (1910).

The analysed specimens all carry phenocrysts of ol + cpx. While one is a critically-undersaturated basalt, the others are notably silica-undersaturated, in three cases justifying use of the term basanite. Thus these lavas provide the earliest *clear* examples of basanitic magma in the Midland Valley during the Carboniferous.

Also given in the Table (no. 36) is an analysis of an intrusion in the Binns Vent, which cuts Upper Oil-Shale Group strata north-east of Linlithgow. This, and other geographically related centres, are normally thought of as being coeval with the lavas to the west. The analysed rock, however, is a hypersthene-normative variety and is not comparable to any of the analysed lavas. Either the Binns basalt did not feed surface extrusions, or there is a wider range of compositions in the lavas than our six analyses indicate.

Passage Group lavas, Ayrshire

Extrusive rocks of Namurian to Westphalian age occur in Ayrshire and Fife. Our eight analysed specimens, plus one from the literature (Richey *et al.* 1930) comprise: five from the Main Outcrop, three from the Barassie Inlier and one from the Southern Outcrop of northern Ayrshire (Richey *et al.* 1930). There are at present no analyses of rocks from the Northern Outcrop, the outcrops in central Ayrshire (Eyles *et al.* 1949) or the Fife lavas.

The Passage Group lavas are dominantly microphyric ol ± cpx — phyric basalts of Dalmeny type. The flow recorded in Richey *et al.* (1930) has 1·8 per cent normative nepheline, but the eight rocks analysed for this study are all hypersthene-normative, with "Q" values ranging from 0·4 to 4·8. This suggests that the Passage Group basic volcanism in Ayrshire was largely of silica-saturated type.

Lavas of the Mauchline and Thornhill basins

These Stephanian lavas are the youngest Carboniferous extrusive rocks in the Midland Valley province and are therefore of particular relevance to this study. There are three published analyses of Mauchline lavas (Tyrrell 1928; Eyles *et al.* 1929), to which we have

added six from Mauchline and four from the Thornhill area, all of relatively fresh material. This number gives only a minimal coverage, both stratigraphically and geographically; for example, there are no analyses of rocks from the important Lugar Water section in the southern part of the Mauchline outcrop.

According to Tyrrell (1928) and MacGregor (1948), the majority of the flows are ol ± cpx − phyric basalts of Dalmeny type, though analcite—and nepheline—basanites have also been recorded. The new data confirm these observations and also indicate that hypersthene-normative (transitional) basaltic magmatism made an important, if secondary contribution to the dominantly silica-undersaturated activity.

Petrochemistry

Macdonald (1975) has shown that the nature of the chemical variation within certain Dinantian lava sequences indicates that the original magmas lay on, or close to, individual liquid lines of descent. Each magmatic lineage was taken to be a result of continuous fractionation of basic parental magmas over an extended pressure range. Within each of the suites for which we provide new data in this paper, the variations in such parameters as degree of silica-saturation, Na_2O/K_2O ratios, TiO_2 and P_2O_5 contents are such that the rocks cannot be considered to represent single magmatic lineages. They more probably result from separate fusion events of mantle lherzolite, involving varying degrees of partial melting under differing pressure conditions.

The late Dinantian and post-Dinantian lavas belong to Magmatic Association 3, as defined by Macdonald (1975) for the main Dinantian outcrops. Chemically, they are *broadly* similar to the more basic members of Association 1 as, for example, the Kintyre and Lanarkshire successions. In detail, however, certain differences may be noted. The Burntisland lavas are richer in normative hypersthene (for DI $<$ 30) than any analysed earlier Dinantian lava, while the basanitic lavas of the Bathgate-Linlithgow Hills and the Mauchline and Thornhill suites also have no older Carboniferous equivalents.

The overall picture, therefore, as appreciated by MacGregor (1948) and Francis (1967) is one of a much restricted range of differentiation in the post-Oil Shale Group lavas, such that only the more basic types were generated and erupted. At the same time, a wider spectrum of basic compositions was developed and, in particular, strongly silica-undersaturated magmas became increasingly important at the expense of hypersthene-normative magmatism.

Variations in Basic Magma Chemistry with Time

The degrees of silica-saturation of basic alkaline rocks (100 An/(An + Ab) $>$ 45) from the Midland Valley petrographic province are plotted against time in Figure. 1 (cf. Macdonald 1975, Fig. 16). The relationship between magma composition and time is by no means simple but our preferred interpretation is outlined below.

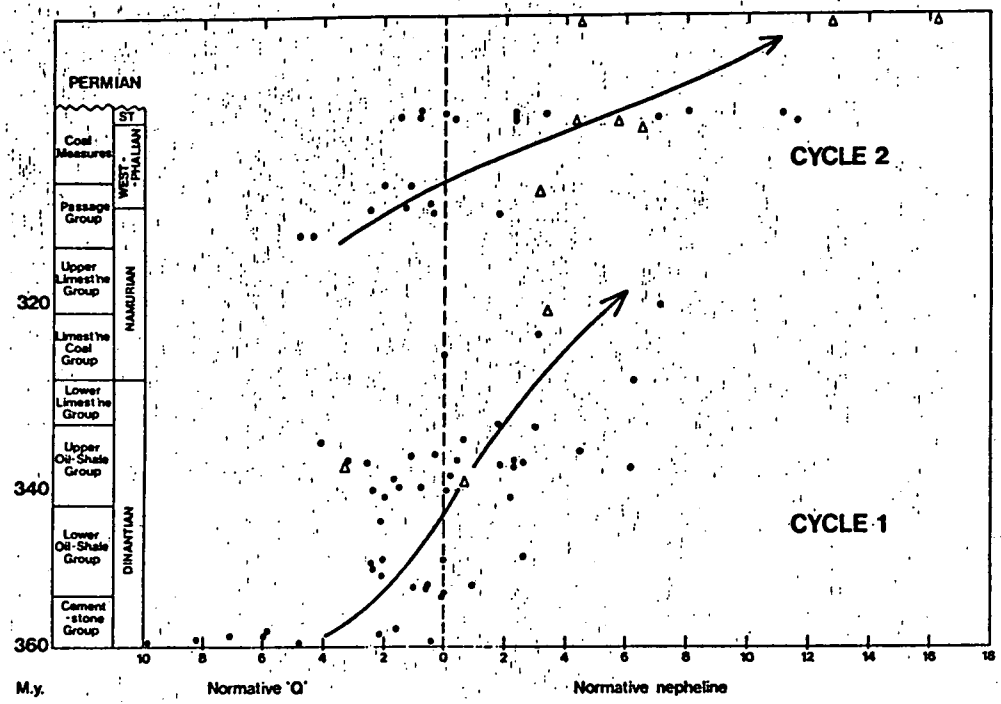

FIG. 1. Degree of silica-saturation of Carboniferous-Permian alkaline basic rocks (100 An/An + Ab > 45) plotted as a function of stratigraphical age. The stratigraphical column is from Francis (1967) and the absolute time scale freely adapted from Fitch *et al.* (1970). Circles are lavas; triangles are radiometrically-dated intrusions (sources in text). "Q" = normative quartz + quartz in normative hypersthene. The trend lines indicate the inferred changes of basic magma compositions during each thermal cycle.

Available analyses cover reasonably well the Dinantian volcanic piles and those plotted in Figure. 1 probably provide a true picture of the chemical affinities of those lavas. Thus, early Dinantian basic magmatism was, on a regional scale, predominantly hypersthene (± quartz) normative, while in the later Dinantian both hypersthene—and nepheline—normative basalts were common eruptive products. More strongly undersaturated (basanitic) magmas were very rare in the Dinantian.

We recognize that in some areas, e.g. Strathblane (MacDonald 1967; Macdonald 1975), nepheline—normative basalts were erupted early in the succession, but, overall, these examples are volumetrically subordinate to silica saturated varieties.

The analyses plotted in Figure. 1 give a false impression of the relative importance of silica-saturated and undersaturated magmatism in post-Dinantian times in the province. There is in the literature a large number of analyses of strongly undersaturated basic intrusions known on stratigraphical grounds to be of post-Dinantian age, but as yet not dated radiometrically (e.g. Tyrrell 1928; Guppy and Thomas 1931; Eyles *et al.* 1949; Drever and MacDonald 1967; Forsyth and Chisholm; 1976). Furthermore, petrographical

information on lavas and fragments in agglomerates of post-Dinantian age in Ayrshire (Tyrrell 1928; Eyles *et al.* 1949) confirms the silica-undersaturated nature of much of this activity.

It is reasonable to infer, therefore, that post-Dinantian activity was dominated by silica-undersaturated magmatism, basanitic and even more strongly undersaturated varieties (tending towards nephelinites) being particularly notable in late Carboniferous and possibly early Permian times. Hypersthene-normative basic rocks belonging to the alkaline suite are not common in post-Dinantian sequences, with the notable exception of the Passage Group lavas of Ayrshire.

The Magmatic Evolution of the Midland Valley Alkaline Series

The data summarized in Figure 1 do not completely clarify the question as to whether or not the Midland Valley alkaline basic lavas became increasingly silica-undersaturated with time during the Carboniferous. To assume that they did, one would have either to ignore the Passage Group lavas of Ayrshire, or to relegate their hy-normative character to a position of local importance only.

In the speculative model outlined below, we prefer a role of much wider, regional significance for these lavas, suggesting that they indicate the initiation of a second thermal cycle during the Carboniferous.

Dinantian activity in the province was related to the development of a rapidly-propagating thermal cycle. Tectonically, this cycle was expressed by a regional tensional stress regime, with normal faulting and differential relative subsidence of fault-bounded blocks of the Midland Valley graben floor. High geothermal gradients promoted melting of mantle peridotite at shallow depths (< 50 km?), such that the basic magmas generated were hypersthene (rarely plus quartz) normative. Compared to later Carboniferous times, melting was pervasive and it was during the Dinantian that the greatest thickness of lavas accumulated.

In later Dinantian times, the thermal cycle began to wane. The increasing proportion of silica-undersaturated magmas is interpreted as indicating that melting of the mantle proceeded at greater depths (60–100 km?), while the volumes of lava erupted were much smaller than during the earlier plateau-building activity. By the early Namurian, the province was experiencing a time of relative volcanic quiescence, though pyroclastic activity related to the waning of the cycle continued in Fife and West Lothian (Francis 1967).

The second cycle was initiated in mid- to late-Namurian times. The hypersthene-normative nature of the Passage Group lavas of Ayrshire attests to high-level fusion of the mantle and it may be significant that the Midland Valley experienced a regional uplift during this period (Francis 1965). As in the first cycle, the basic magmatism became increasingly silica-undersaturated with time, though, in the Stephanian and early Permian, very strongly undersaturated magmas of a type unknown in the Dinantian were being emplaced (Fig. 1). The trend of magma compositions is consistent with a waning of the

energy of the activity and with a depression of the regional pattern of isotherms as the second cycle proceeded.

As Francis (1967, 1968) has clearly pointed out, the post-Dinantian volcanism was on a much reduced scale compared to the first cycle activity and was dominated by explosive volcanism. This may be related to the different tectonic situation in the later Carboniferous. Compressional forces, probably connected with the Hercynian orogeny which reached a climax at about 295 m years ago (Fitch *et al.* 1970), were the dominant stresses acting during the second thermal cycle (George 1965), perhaps intermittent in some places with tensional stress and continued normal faulting (Leeder 1972). Easy access of magma to the surface may have been prevented by the nature of those stresses, and, during the waning stages of the second cycle, magma was erupted only when high gas pressures had been generated by protracted deep-level fractionation.

Such a model leaves unexplained one very important facet of the later Carboniferous magmatism: the quartz dolerite suite. The emplacement of these tholeiitic basalts in a relatively short time during the Stephanian (about 296 m years, Fitch *et al.* 1970) indicates a period of high-level melting of the mantle and of extensional tectonics, in sharp contrast to the general conditions outlined above for the second thermal cycle. A renewed study of the conditions of generation and differentiation of these rocks is necessary for a more complete understanding of the complex late Carboniferous–early Permianmagmagmaism within the province.

Acknowledgements

We thank S. A. Malik and D. A. Bungard for analyses made at the University of Reading, and P. M. Craig, F. J. Fitch and H. A. F. de Souza for kindly providing specimens. E. H. Francis and M. R. Leeder read the manuscript and cheerfully reminded us of its speculative nature.

References

ALLAN, D. A. 1924. The igneous geology of the Burntisland district. *Trans. R. Soc. Edinb.* 53, 479–501.

DREVER, H. I. and MACDONALD, J. G. 1967. Some new data on "kylitic" sills and associated picrites in Ayrshire, Scotland. *Proc. R. Soc. Edinb. B*, 70, 31–48.

EYLES, V. A., SIMPSON, J. B. and MACGREGOR, A. G. 1929. The igneous geology of central Ayrshire. *Trans. geol. Soc. Glasg.* 18, 361–87.

——, ——, —— 1949. The geology of central Ayrshire. *Mem. geol. Surv. U.K.*

FALCONER, J. D. 1906. The igneous geology of the Bathgate-Linlithgow Hills. Part 2. Petrography. *Trans. R. Soc. Edinb.* 45, 133–50.

FITCH, F. J., MILLER, J. A. and WILLIAMS, S. C. 1970. Isotopic ages of British Carboniferous rocks. *C. R. 6ème Congr. Int. Stratigr. Geol. carbonif., Sheffield*, 1967, Pt. 2, 771–89.

FLETT, J. S. 1910. *In* The geology of the neighbourhood of Edinburgh. *Mem. geol. Surv. U.K.*

FORSYTH, I. H. and CHISHOLM, J. I. 1977. The geology of East Fife. *Mem. geol. Surv. U.K.* (in press).

FRANCIS, E. H. 1965. Carboniferous. *In* Craig, G. Y. (ed.), *The Geology of Scotland*, 309–57, Edinburgh and London.

—— 1967. Review of Carboniferous-Permian volcanism in Scotland. *Geol. Rdsch.* 57, 219–46.
—— 1968. Effect of sedimentation on volcanic processes, including neck-sill relationships, in the British Carboniferous. *23rd Intern. geol. Congress* 2, 163–74.
GEIKIE, A. 1900. The geology of central and western Fife and Kinross. *Mem. geol. Surv. U.K.*
GEORGE, T. N. 1965. The geological growth of Scotland. *In* Craig, G. Y. (ed.) *The Geology of Scotland*, 1–48, Edinburgh and London.
GUPPY, E. M. and THOMAS, H. H. 1931. Chemical analyses of igneous rocks, metamorphic rocks and minerals. *Mem. geol. Surv. U.K.*
LEEDER, M. R. 1972. Discussion of Russell, M. J. *Scott. J. Geol.* 8, 283–7.
McADAM, A. D. 1974. The petrography of the igneous rocks in the Lower Carboniferous (Dinantian) at Spilmersford, East Lothian, Scotland. *Bull. geol. Surv. Gt. Br.* 45, 39–46.
MACDONALD, R. 1975. Petrochemistry of the Early Carboniferous (Dinantian) lavas of Scotland. *Scott. J. Geol.* 11, 269–314.
MACGREGOR, A. G. 1948. Problems of Carboniferous-Permian volcanicity in Scotland. *Q. Jl geol. Soc. Lond.* 104, 133–53.
MACGREGOR, M. and HALDANE, D. 1933. The economic geology of the Central Coalfield, Area III. *Mem. geol. Surv. U.K.*
MACGREGOR, M. and MACGREGOR, A. G. 1948. The Midland Valley of Scotland. *Br. reg. Geol.* (2nd ed.).
MILLER, J. A. and BROWN, P. E. 1965. K-Ar age studies in Scotland. *Geol. Mag.* 102, 106–34.
MITCHELL, G. H. and MYKURA, W. 1962. The geology of the neighbourhood of Edinburgh. 3rd ed. *Mem. geol. Surv. U.K.*
RICHEY, J. E., ANDERSON, E. M. and MACGREGOR, A. G. 1930. The geology of North Ayrshire, *Mem. geol. Surv. U.K.*
TYRRELL, G. W. 1928. A further contribution to the petrography of the late Palaeozoic igneous suite of the west of Scotland. *Trans. geol. Soc. Glasg.* 18, 259–94.

MS accepted for publication 8th November 1976

	SiO_2	TiO_2	Al_2O_3	Fe_2O_3	FeO	MnO	MgO	CaO	Na_2O	K_2O	P_2O_5	H_2O+	CO_2	Total
Campsie Block														
1	46·5	2·84	18·59	9·15	2·92	0·19	3·98	7·31	3·91	1·45	0·34	1·88	0·31	99·37
2	46·0	3·04	16·21	5·48	8·68	0·18	5·77	7·55	3·32	1·24	0·45	1·84	0·12	99·88
3	45·5	3·59	16·58	6·93	6·78	0·20	5·32	8·06	3·14	1·08	0·45	2·29	0·08	100·00
4	45·0	3·45	15·18	5·15	8·63	0·23	5·40	9·61	2·74	1·13	0·41	2·32	0·48	99·73
5	48·6	2·29	19·77	8·68	2·36	0·11	3·13	7·93	3·62	1·26	0·28	1·48	<0·05	99·51
Burntisland lavas														
6	43·9	2·65	14·77	5·02	6·59	0·28	8·92	10·68	1·55	1·48	0·55	3·57	—	99·96
7	47·7	2·27	15·73	5·34	6·22	0·17	4·61	11·41	2·68	0·90	0·45	1·80	0·67	99·95
8	46·6	1·83	13·96	2·60	8·51	0·17	11·07	7·37	2·54	0·92	0·31	3·68	—	99·56
9	44·4	3·08	14·05	4·61	6·45	0·14	9·38	10·07	2·04	0·48	0·54	4·29	—	99·53
10	44·3	2·82	14·17	4·62	7·07	0·20	8·54	8·82	3·35	1·26	0·60	4·11	—	99·86
11	46·5	1·93	14·02	4·04	7·98	0·21	9·19	8·99	2·08	0·82	0·30	3·46	—	99·52
Bathgate-Linlithgow lavas														
12	42·9	2·60	13·69	4·52	6·62	0·18	9·49	11·65	2·08	0·74	0·49	3·78	1·07	99·81
13	42·2	3·14	13·97	4·99	6·95	0·23	7·28	11·54	2·79	0·70	0·81	3·19	1·13	98·92
14	42·3	2·82	13·72	5·41	6·70	0·18	8·38	11·90	2·80	0·49	0·63	2·95	1·67	99·95
15	44·6	2·53	14·47	2·69	8·12	0·18	8·27	9·00	2·91	0·76	0·56	3·49	1·83	99·41
16	46·4	2·30	14·96	3·47	7·88	0·18	7·29	8·07	3·85	1·20	0·62	3·59	0·14	99·95
17	43·4	2·55	12·99	3·01	8·61	0·20	10·18	10·44	3·13	0·94	0·81	2·42	0·73	99·41
Passage Group lavas														
18	47·0	2·18	14·11	5·35	6·59	0·17	7·72	10·07	2·35	1·07	0·46	2·85	0·17	100·09
19	47·1	2·18	14·51	5·38	6·43	0·16	7·06	10·02	2·55	1·03	0·39	2·55	0·10	99·46
20	48·1	1·86	14·06	5·03	6·95	0·14	7·89	8·61	2·57	0·86	0·28	3·16	0·08	99·59
21	50·0	1·92	14·71	5·94	4·97	0·11	6·57	9·72	2·82	0·88	0·28	2·15	0·20	100·27
22	48·1	2·28	15·78	3·88	6·19	0·28	5·83	9·69	3·01	1·64	0·45	1·81	0·33	99·27
23	46·6	2·36	14·05	5·30	6·69	0·30	8·27	10·08	2·46	0·96	0·42	2·29	0·05	99·83
24	45·6	2·34	14·13	10·11	3·04	0·15	7·49	9·74	2·34	1·09	0·42	2·92	0·29	99·66
25	47·0	2·45	16·82	3·32	7·13	0·19	5·73	9·23	3·15	1·34	0·63	2·35	<0·05	99·34

	SiO_2	TiO_2	Al_2O_3	Fe_2O_3	FeO	MnO	MgO	CaO	Na_2O	K_2O	P_2O_5	H_2O+	CO_2	Total
Thornhill lavas														
26	42·6	2·44	13·96	8·59	2·42	0·24	11·14	9·77	2·88	1·14	0·52	3·65	—	99·74
27	46·3	2·16	14·89	8·74	2·26	0·16	8·35	8·91	2·64	1·28	0·45	3·35	—	99·49
28	46·4	2·17	14·81	8·91	2·45	0·12	8·54	8·60	2·68	1·38	0·42	2·97	—	99·55
29	46·0	2·03	13·66	8·61	2·93	0·18	9·10	10·25	2·74	1·27	0·40	2·01	0·38	99·56
Mauchline lavas														
30	45·5	1·98	13·87	9·64	1·81	0·20	9·34	9·04	3·09	1·00	0·42	3·45	0·13	99·47
31	44·0	2·12	13·90	10·43	1·81	0·19	10·53	9·81	2·17	1·20	0·39	3·24	0·10	99·89
32	47·1	1·88	13·79	9·07	2·38	0·16	9·72	9·02	2·66	0·91	0·31	2·65	0·06	99·71
33	45·5	1·75	14·81	9·29	2·28	0·20	7·96	10·57	2·41	1·58	0·31	2·47	0·17	99·30
34	44·9	1·59	13·94	9·96	1·45	0·14	9·59	9·75	2·22	1·05	0·28	3·60	0·76	99·23
35	44·4	1·71	14·97	10·75	1·12	0·14	8·98	9·64	1·92	1·48	0·30	3·64	0·76	99·81
Intrusions														
36	46·6	2·86	15·17	4·54	7·20	0·17	6·84	9·05	2·35	1·45	0·48	2·73	0·15	99·51
37	42·8	2·46	13·00	3·58	8·74	0·22	9·32	10·58	3·88	1·12	1·01	2·80	0·08	99·59
38	42·9	2·50	12·88	3·41	8·99	0·23	9·21	10·27	4·09	1·87	0·98	1·94	0·05	99·32
39	47·6	2·28	14·54	1·93	8·76	0·18	7·59	9·49	3·40	1·98	0·68	1·52	0·06	100·01

New analyses of Carboniferous-Permian lavas and intrusions from the Midland Valley petrographic province. Analysts: Specs. 6, 8–11, 26–28, S. A. Rizzello and R. Macdonald; others, S. A. Malik and D. A. Bungard

EXPLANATION TO TABLE

Campsie Block

1. Macroporphyritic basaltic hawaiite, NW of Loup of Fintry, 810m E 04°S from Walton Bridge, east of Fintry (NS 6607 8632). Spec. no. ZP 479, supplied by P. M. Craig. *Phens*: Ol (tr.), Pl (30·9), IO (tr.).
2. Microphyric hypersthene-normative basaltic hawaiite, crags, north bank of R. Endrick, 670m E 10°S from Walton Bridge, east of Fintry (NS 6592 8626). Spec. no. ZP 478, supplied by P. M. Craig. *Phens*: Ol (2·9), Cpx (0·1), Pl (7·8), IO (tr.).
3. Sparsely microphyric or aphyric hypersthene-normative basalt, basal flow, east bank of burn at Spout of Ballochleam, 1,560m S 13°E from Eastern Glinns, NE Fintry Hills (NS 65318998). Spec. no. ZP 463, supplied by P. M. Craig. *Phens*: Ol (tr.).
4. Macroporphyritic alkali olivine basalt, outcrop on north slope of Laird's Hill, 1,410m N 27°E from Corrie Farm, NW of Kilsyth (NS 6968 8036). Spec. no. ZP 474, supplied by P. M. Craig. *Phens*: Ol (2·9), Pl (6·8).
5. Macroporphyritic hypersthene-normative basalt, trap feature, 280m N 45°E from Easter Langhill, west of Denny on R. Carron (NS 7736 8435). Spec. no. ZP 470, supplied by P. M. Craig. *Phens*: Ol (tr.), Pl (37·8), IO (0·2).

Burntisland lavas

6. Macroporphyritic hypersthene-normative basalt, King Alexander's Craig, Pettycur. (NT 253 865). Spec. no. MV 400. *Phens*: Ol (8·8).
7. Microphyric hypersthene-normative basalt, roadside cutting, Pettycur (NT 258 864). Spec. no. MV 402. *Phens*: Ol (7·8), Cpx (1·9).
8. Microphyric hypersthene-normative basalt, cutting in caravan site, Pettycur (NT 257 864). Spec. no. MV 403. *Phens*: Ol (8·0).
9. Microphyric hypersthene-normative basalt, hillside above western end of United Glass Co. works, Pettycur (NT 265 863). Spec. no. MV 106. *Phens*: Ol (6·3), Cpx (0·5).
10. Microphyric alkali olivine basalt, shore east of Pettycur harbour. Flow No. 27 of Geikie, 1900 (NT 267 861). Spec. no. MV 406. *Phens*: Ol (13·3), Cpx (1·8).
11. Microphyric hypersthene-normative basalt, just east of Kinghorn Ness (NT 270 862). Spec. no. MV 407. *Phens*: Ol (10·2).

Bathgate-Linlithgow lavas

12. Microphyric alkali olivine basalt, quarry, Longmuir Plantation (NT 023 739). Spec. no. HS 91, supplied by H. A. F. de Souza. *Phens*: Ol (9·9), Cpx (8·8).
13. Macroporphyritic basanite, by fence in stream, west of Broomyknowes Farm (NT 015 744). Spec. no. HS 88, supplied by H. A. F. de Souza. *Phens*: Ol (6·2), Cpx (6·6).
14. Microphyric basanite, small stream NW of Beecraigs, south of Linlithgow (NT 009 742). Spec. no. HS 87, supplied by H. A. F. de Souza. *Phens*: Ol (4·2), Cpx (4·0), IO (tr.).
15. Microphyric basalt (critically silica-undersaturated), Hiltly, near Linlithgow (NT 005 757). Spec. no. MV 200. *Phens*: Ol (3·5), Cpx (1·2).
16. Microphyric hawaiite, small east-facing quarry, hill behind Craigmailing Farm (NS 995 727). Spec. no. HS 92, supplied by H. A. F. de Souza. *Phens*: Ol (1·8), Cpx (0·8).
17. Microphyric basanite, near top of Kipps Hill. (NS 985 738). Spec. no. HS 94, supplied by H. A. F. de Souza. *Phens*: Ol (7·8), Cpx (1·3).

Passage Group lavas, Ayrshire

18. Microphyric hypersthene-normative basalt, quarry, Auchenharvie Castle, NE of Irvine (NS 363 443). Spec. no. HS 52, supplied by H. A. F. de Souza. *Phens*: Ol (3·4). (Phenocryst size taken as > 0·75 mm).
19. Microphyric hypersthene-normative basalt, mill, west bank of Annick Water, west of Kilmaurs (NS 374 423). Spec. no. HS 51, supplied by H. A. F. de Souza. *Phens* (> 0·75 mm): Ol (3·8).

20. Microphyric hypersthene-normative basalt, small quarry by roadside, east bank of Carmel Water, near Kilmaurs (NS 425 417). Spec. no. HS 50, supplied by H. A. F. de Souza. *Phens*: Ol (8·1), Cpx (5·2).
21. Microphyric hypersthene-normative basalt, east bank of Carmel Water, NE of Buntonhill Farm, near Kilmaurs (NS 428 418). Spec. no. HS 49, supplied by H. A. F. de Souza. *Phens*: Ol (9·3), Cpx (6·1).
22. Microphyric basaltic hawaiite, northern end of Stinking Rocks, Barassie. (NS 322 335.) Spec. no. MV 500. *Phens*: Ol (5·1), Cpx (7·5), Pl (1·6).
23. Sparsely microphyric hypersthene-normative basalt, stream bank, 30m west of railway line, golf course, Barassie (NS 326 339). Spec. no. MV 501. *Phens*: Ol (tr.).
24. Aphyric hypersthene-normative basalt, rock knob, left bank of stream, near Laigh Hillhouse, Loans (NS 340 328). Spec. no. MV 502.
25. Sparsely microphyric hypersthene-normative basalt, small scarp, Townhead private estate, Symington (NS 376 315). Spec. no. MV 506. *Phens*: Ol (tr.), Cpx (tr.).

Thornhill lavas

26. Sparsely microphyric basanite, Enterkin Burn lava scarp, NW of Chapel Farm (NS 877 064). Spec. no. MV 412. *Phens*: Ol (tr.).
27. Microphyric hypersthene-normative basalt, dip slope of Enterkin Burn lava scarp, west of Chapel Farm (NS 876 059). Spec. no. MV 413. *Phens*: Ol (7·1), Cpx (0·5).
28. Macroporphyritic hypersthene-normative basalt, east bank of Carron Water, north of Jenny Hare's Bridge, near Durisdeer (NS 883 029). Spec. no. Mu 409. *Phens*: Ol (10·9), Cpx (0·3).
29. Microphyric alkali olivine basalt, NE corner of Morton Loch (NX 892 993). Spec. no. MV 410. *Phens*: Ol (10.9), Cpx (9·6).

Mauchline lavas

30. Microphyric alkali olivine basalt, middle of railway cutting, Tarbolton Station (NS 443 252). Spec. no. HS 43, supplied by H. A. F. de Souza. *Phens* (>1 mm): Ol (3·2).
31. Microphyric alkali olivine basalt, old quarry, east of Altonburn, Tarbolton (NS 436 267). Spec. no. MV 510. *Phens* (>0·75 mm): Ol (1·8).
32. Microphyric hypersthene-normative basalt, old quarry, north end of Mauchline Hill (NS 511 275). Spec. no. MV 507. *Phens*: Ol (9·9), Cpx (0·5).
33. Microphyric alkali olivine basalt, east bank of R. Ayr, 150m east of Howford Bridge (NS 517 254). Spec. no. HS 36, supplied by H. A. F. de Souza. *Phens:* Ol (8·1), Cpx (5·0).
34. Microphyric basalt (critically silica-undersaturated), high up on cliff, east bank of R. Ayr, 200m east of Howford Bridge (NS 518 255). Spec. no. HS 33, supplied by H. A. F. de Souza. *Phens*: Ol (5·3), Cpx (2·3).
35. Microphyric alkali olivine basalt, east bank of R. Ayr, 800m east of Howford Bridge (NS 519 257). Spec. no. HS 32, supplied by H. A. F. de Souza. *Phens*: Ol (7·3), Cpx (2·4).

Intrusions

36. Microphyric hypersthene-normative basalt, by footpath north of Binns Tower, near Linlithgow (NS 053 786). Spec. no. HS 96, supplied by H. A. F. de Souza. *Phens*: Ol (2·7), Cpx (1·0).
37. Nepheline basanite, Maiden Castle Camp, Green Hill, Lomond Hills, Kinross-shire (NO 223 068). Spec. no. FM 476, supplied by F. J. Fitch. Fitch *et al.* (1970) obtained a K-Ar age of 278 ±8 m. y. for this specimen.
38. Nepheline basanite, SE slopes of Green Hill, Lomond Hills. (NO 225 070). Spec. no. FM 477, supplied by F. J. Fitch. Fitch *et al.* (1970) report a K-Ar age of 274 ± 5 m. y. for this specimen.
39. Alkali olivine dolerite, crags near summit of East Lomond, Lomond Hills. (NO 244 063). Spec. no. FM 475, supplied by F. J. Fitch. Fitch *et al.* (1970) give a K-Ar age of 271 ± 6 m. y. for this rock.

Phil. Trans. R. Soc. Lond. A **297**, 245–257 (1980)
Printed in Great Britain

Trace element evidence for mantle heterogeneity beneath the Scottish Midland Valley in the Carboniferous and Permian

By R. Macdonald
Department of Environmental Sciences, University of Lancaster, Bailrigg, Lancaster LA1 4YQ, U.K.

The alkaline rocks of Carboniferous to Permian age in the Midland Valley province range in composition from hypersthene-normative, transitional basalts to strongly undersaturated basanitic and nephelinitic varieties. They were formed by varying degrees of equilibrium partial melting of a phlogopite peridotite mantle. Ba, Ce, Nb, P, Sr and Zr were strongly partitioned into the liquid during melting; K and Rb were retained by residual phlogopite for small degrees of melting only.

The composition of the mantle source is inferred to have been broadly similar to that from which oceanic alkaline basalts are currently being generated. It was, however, heterogeneous as regards distribution of the incompatible trace elements, with up to fourfold variations in elemental abundances and ratios. The mantle beneath the province may be divisible into several areas, of some hundreds of square kilometres each, which retained a characteristic incompatible element chemistry for up to 50 Ma and which imparted a distinctive chemistry to all the basic magmas generated within them.

Introduction

The main outcrops of Carboniferous and Permian igneous rocks in Scotland lie within the Midland Valley graben. Small outliers occur in the Highlands and Southern Uplands, while sequences of flows up to 120 m thick lie discontinuously along the Scottish borders. The border outcrops are not included in this report because of a lack of relevant chemical data.

The area of the Midland Valley province, defined as the rectangle enclosing the main outcrops, is some 30000 km^2, within which rather more than 12000 km^2 of lava currently crop out. The volume of alkaline lavas is about 6000 km^3, 80% of which is basaltic (Francis 1967), though the original volumes may have been nearer 10000 km^3. An estimated 1200–1500 km^3 of alkaline magma is also present as intrusions of various ages covering the range of the extrusive activity.

The rocks of the province range in age from earliest Carboniferous to Permian, a span of some 80 Ma being indicated by available age dates (Fitch *et al.* 1970). An estimated minimum of 80% of the total volume of igneous material was, however, emplaced during the Dinantian (Macdonald 1975), say a 25–30 Ma period, mainly as a series of individual lava piles showing partial overlap. The terminology and distribution of the main lava sequences are described by Francis (1967, 1968). Major element characteristics of each have been discussed by Macdonald (1975) and Macdonald *et al.* (1977). Macdonald (1975) concluded that the Dinantian lava successions represented several magmatic lineages, each differing in such parameters as the degree of silica undersaturation, Na_2O/K_2O and $FeO/(FeO+MgO)$ ratios and TiO_2 and P_2O_5 contents.

The Midland Valley alkaline basic rocks range in composition from hypersthene (hy.)-normative, transitional basalts to basanitic and nephelinitic varieties. For simplicity two

TABLE 1. REPRESENTATIVE TRACE ELEMENT (micrograms per gram) AND MAJOR ELEMENT (percentages by mass) ANALYSES OF ALKALI BASALTS (1–6) AND BASANITES (7–11), AND OF A LOW-K THOLEIITE (12), FROM THE MIDLAND VALLEY PROVINCE

	(1) ZP 423	(2) MV 501	(3) MV 400	(4) MV 222	(5) HS 36	(6) MV 27	(7) MV 520	(8) FM 476	(9) MV 105	(10) HS 94	(11) MV 703	(12) MV 261
trace elements												
Ba	170	505	665	480	810	960	740	1115	1115	1160	550	105
Ce	18	35	58	42	31	44	34	132	86	87	25	8
Nb	14	39	38	25	34	28	46	132	52	69	28	3
Rb	26	33	27	18	42	25	48	15	11	21	19	2
Sr	618	537	635	460	594	575	545	1716	1130	1283	690	140
Y	27	30	19	21	22	30	30	38	27	36	26	21
Zn	88	70	93	103	130	73	70	103	88	89	71	65
Zr	118	172	200	170	136	186	155	300	306	301	180	72
major elements												
K_2O	0.70	0.96	1.30	0.74	1.58	1.71	1.92	1.12	1.31	0.94	1.35	0.20
TiO_2	1.52	2.36	2.65	2.82	1.75	2.54	2.37	2.46	2.78	2.55	3.22	1.45
P_2O_5	0.27	0.42	0.55	0.36	0.31	0.47	0.83	1.01	0.73	0.81	0.37	0.11
Mg no.	69	61	63	62	61	65	63	63	66	66	62	60

Specimen localities. (Din., Dinantian; Nam., Namurian; Steph., Stephanian.) ZP 423: hy.-norm. ankaramitic basalt, sheet, Kilsyth Hills; Din; specimen courtesy of P. M. Craig. MV 501: hy.-norm. basalt, Passage Group lavas, Ayrshire; Nam. (Macdonald *et al.* 1977, no. 23). MV 400: hy.-norm. basalt, Burntisland lavas, Fife; Din. (Macdonald *et al.* 1977, no. 6). MV 222: ne.-norm. ankaramitic basalt, flow, Kintyre; Din. (Macdonald 1975, table 2, no. 4). HS 36: ne.-norm. basalt, Mauchline lavas, Ayrshire; Steph. (Macdonald *et al.* 1977, no. 33). MV 27: ne.-norm. basalt, Dalmeny; Din. (Guppy & Thomas 1931, no. 272). MV 520: essexite, intrusion, Crawfordjohn; late Carb.–Permian? (Scott 1915). FM 476: nepheline basanite, intrusion, Lomond Hills; Permian (Macdonald *et al.* 1977, no. 37). MV 105: ?nepheline basanite, Chapel Ness intrusion, Elie, Fife; late Carb.–Permian (Forsyth & Chisholm 1977, table 10, no. V). HS 94: basanite, Bathgate–Linlithgow lavas; Din.–Nam. (Macdonald *et al.* 1977, no. 17). MV 703: basanite, plug, Kersewell, Carnwath; age uncertain (Guppy & Thomas 1931, no. 290). MV 261: low-K tholeiite, Kintyre lavas; Din. (Macdonald 1975, table 2, no. 1).

groups are distinguished in this paper: an *alkali basalt* group, consisting of hy.-normative basalts and alkali olivine basalts with normative nepheline (ne.) < 5%, and a *basanitic* group, consisting of those basic rocks with ne. > 5%.

Major element compositions appear to have evolved rather systematically with time, such that two thermal cycles may be distinguished (Macdonald *et al.* 1977), each starting with hy.-normative magmatism and progressing towards increasingly silica-undersaturated types. Details of the magma types and their relations to extrusive and intrusive sequences may be found in MacGregor (1948), MacGregor & MacGregor (1948), Francis (1967, 1968), Macdonald (1975) and Macdonald *et al.* (1977).

TABLE 2. RANGES AND AVERAGES OF TRACE ELEMENTS (micrograms per gram) AND SELECTED MAJOR ELEMENTS (percentages by mass) IN MIDLAND VALLEY BASIC ROCKS (Mg no. ≥ 60)

	alkali basalts				basanites			
	hy.-norm.		ne. 0–5%		ne. 5–10%		ne. > 10%	
	range	average	range	average	range	average	range	average
trace elements								
Ba	170–665	449	260–1230	686	550–2213	1046	740–1150	912
Ce	18–69	40	16–70	42	15–107	71	34–132	96
Nb	14–47	31	9–79	41	28–73	55	28–132	72
Rb	3–37	21	8–45	25	3–50	20	11–48	25
Sr	275–680	540	342–1636	708	555–1283	809	545–1716	939
Y	13–34	25	13–36	25	12–36	28	20–40	31
Zn	64–106	84	70–147	96	62–246	110	70–174	109
Zr	105–322	182	108–285	179	130–301	212	142–330	243
major elements								
K_2O	0.48–1.38	0.99	0.45–1.71	1.06	0.49–2.10	1.15	0.80–1.92	1.48
TiO_2	1.52–3.08	2.22	1.57–3.12	2.38	2.44–3.22	2.83	2.30–2.93	2.68
P_2O_5	0.27–0.55	0.39	0.25–0.79	0.45	0.37–1.10	0.69	0.58–1.92	1.09
n(max.)	17		25		11		11	

The majority of the basic rocks with Mg number ≥ 60 are either aphyric or carry phenocrysts of ol. + cpx. and rarely, plag. ± oxide. There is no evidence that a significant number of these rocks represent low-pressure accumulative types. Generalized petrographic descriptions of relevant rock types are provided by MacGregor & MacGregor (1948, pp. 54 and 65).

Ba, Ce, Nb, Rb, Sr, Y, Zn and Zr have been determined by analysis by X-ray fluorescence in 64 samples of basic alkaline rock (Mg number† ≥ 60) from the Midland Valley province. Representative analyses are presented in table 1. Estimated analytical precisions are: Sr and Zr 2%, other elements 5%.

K_2O, TiO_2 and P_2O_5 determinations given in table 1 are taken from the references cited in the table or are previously unpublished data (ZP 423).

Ranges and means for the same elements are given in table 2, the complete range of basic compositions being arbitrarily divided into four on the basis of normative composition. It is apparent that each element shows considerable variations in abundance, both within and between the normative groups.

† Mg number = 100 Mg/(Mg + Fe^{2+}), atomic ratio; Fe_2O_3/FeO ratio taken to be 0.25 (Kesson 1973).

Trace element variations

Four different processes may have acted to produce variations in trace element distribution in the Midland Valley basic rocks.

(i) *Deuteric alteration.* As Macdonald (1975, p. 270) has stressed, many of the Midland Valley alkaline rocks are remarkably fresh, despite their Upper Palaeozoic age. A large majority of the specimens used in this study have mineralogies unaltered, or only slightly altered, by deuteric processes. Olivine is commonly fresh or only partially serpentinized. Plagioclase and pyroxene are ubiquitously fresh. Certain specimens show minor amounts of secondary carbonate but there is no evidence of extensive zeolitization.

The elements most likely to have been mobilized by deuteric effects are Ba, K, Rb and Sr. The strong correlations (table 3), not only between these elements but between them and such reputedly immobile elements as Ce and Nb suggest, however, that any such mobilization must have been slight. It may be assumed that the observed trace element contents normally represent the primary magmatic abundances.

(ii) *Crustal contamination.* In the absence of relevant isotopic data, it is difficult to assess the possible importance of this process. Two lines of evidence suggest, however, that the basalts have not been significantly affected by crustal rocks.

(*a*) It will be shown later that the mantle sources of the alkaline rocks had values of Rb/Sr and K/Rb comparable to those inferred for the source areas of Recent alkaline basalts of oceanic islands. Since the trace element composition of the Midland Valley mantle was deduced from the basalts, the implication is that their K, Rb and Sr contents have not been substantially modified by crustal contamination.

(*b*) There is no significant correlation between K and Rb and the degree of silica-saturation of the alkali basalts of the Midland Valley. Such a correlation would seem to be a necessary result of the contamination of basic magma by significant amounts of sialic material.

(iii) *Fractional crystallization.* Polybaric fractional crystallization tends to obscure those chemical features of basic magmas derived from their mantle sources. Certain features of the trace element variations within certain Midland Valley sequences very probably result from high to moderate pressure fractionation of the parental magmas. To minimize these effects, the compositions of *primary* magmas only should be used to infer mantle compositions. Perversely, the assignment of a primary status to a magma depends on the composition chosen for its mantle source. A widely accepted criterion is that only basalts with Mg number > 66–67 are likely primary basalts, implying a mantle olivine of composition Fo > 87. However, Wilkinson & Binns (1977) have made a case for a more heterogeneous mantle, containing relatively Fe-rich lherzolitic areas capable of generating basic magmas with Mg numbers $\leqslant$ 50.

In view of this uncertainty, attention here is largely restricted to basic rocks with Mg number $\geqslant$ 60. These may be termed 'near-primary' magmas, i.e. they have suffered only modest (less than 20%) amounts of fractionation of ferromagnesian phases during ascent from their sources. This is in accord with the suggestion of Macdonald (1975), based on major element chemistry, that the majority of the Midland Valley Dinantian basalts had experienced a recognizable polybaric fractionation history, involving the removal of wehrlitic (ol.+cpx.) or clinopyroxenitic (Al-cpx.) assemblages at pressures greater than 10 kbar (1 MPa) and ol.+plag.+oxide assemblages at lower pressures.

While such fractionation will have affected the absolute abundances of the incompatible

elements, it will not have seriously modified the ratios of two elements with similar, low, solid–liquid partition coefficients.

(iv) *Primary magmatic variations.* Trace element variations that persist *after* removal of possible fractionation events are taken to represent variable conditions of magma genesis. These are of two types: variations related to the degree of partial melting and those resulting from variations in mantle source composition.

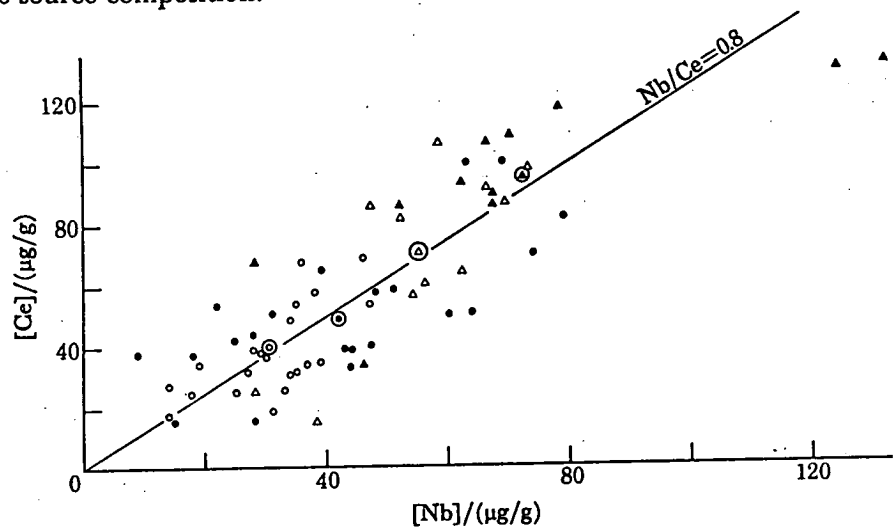

FIGURE 1. Ce–Nb graph for alkaline basic rocks with Mg number ≥ 60. Open circles, hy.-normative basalts; closed circles, basalts with ne. 0–5 %; open triangles, basanites with ne. 5–10 %; closed triangles, basanites with ne. > 10 %. Circled symbols represent the averages for each group.

PETROGENETIC MODEL

The main groups of basic rocks may be taken, as a first approximation, to represent the products (or the derivatives thereof) of variable degrees of closed-system, partial melting of a fertile mantle source over a limited range of pressures. Thus the basanites resulted from the smallest degrees of melting (say not more than 7 %; Sun & Hanson 1975), the ne.-normative alkali basalts from intermediate degrees (7–15 %?) and the hy.-normative alkali basalts the most extensive mantle fusion (15–20 %?). This model is based on the following kinds of interpretation.

Figure 1 is a plot of Ce against Nb for all available analyses of Midland Valley basic rocks having Mg number ≥ 60. Different symbols distinguish four groups of rocks on the basis of their degree of silica-undersaturation. Averages for each group are shown. The data form a collinear display extending through the origin and scattering about a Nb/Ce ratio of 0.8. The bulk distribution coefficients of Ce and Nb for the residual mantle mineralogies may be taken to be very low, i.e. these elements have been essentially incompatible during the melting process. The Nb/Ce ratio of 0.8 thus approximates that of the mantle source and the amounts of Ce and Nb are inversely proportional to the degrees of partial melting.

Graphical analysis of this sort, plus the correlation coefficients presented in table 3 suggest that Ba, P, Sr and Zr also behaved essentially as incompatible elements. If those elements were ever major constituents of an accessory phase in the source peridotites (e.g. P in apatite or Zr in zircon), then those phases melted or were reacted out during the first 1–2 % of melting and were not present in the residual mineralogies at any stage. Y apparently was retained by

clinopyroxene ± garnet, though the partition coefficients can be shown to have been less than unity for both phases.

It appears, on the other hand, that K, Rb, Ti and Zn were not incompatible over the full melting range. A plot of Ce against TiO_2 (figure 2) reveals the following:

(i) The alkali basalts show a positive correlation between those elements, approximately collinear with the origin. As will be shown, the scatter is mainly due to minor differences in the source materials, though removal of Ti in clinopyroxene during high pressure fractionation may well have been a contributory factor.

(ii) The basanites generally have higher Ce contents and Ce/Ti ratios than the alkali basalts and are not collinear with them.

TABLE 3. CORRELATION MATRIX FOR TRACE AND SELECTED MAJOR ELEMENTS

Ba												
Ce	0.47											
Nb	0.43	0.83										
Rb	−0.06	−0.13	−0.04									
Sr	0.45	0.65	0.77	−0.28								
Y	0.34	0.48	0.53	−0.03	0.46							
Zn	0.15	0.18	0.12	0.09	−0.08	0.10						
Zr	0.46	0.83	0.69	−0.27	0.65	0.56	0.19					
K_2O	0.20	0.21	0.15	0.73	−0.11	0.16	0.19	0.09				
TiO_2	0.43	0.57	0.38	−0.41	0.37	0.32	0.25	0.67	−0.03			
P_2O_5	0.30	0.69	0.56	−0.07	0.49	0.37	0.15	0.71	0.30	0.47		
d.s.u.	0.21	0.63	0.58	0.15	0.39	0.47	0.15	0.53	0.46	0.39	0.56	
	Ba	Ce	Nb	Rb	Sr	Y	Zn	Zr	K_2O	TiO_2	P_2O_5	d.s.u.

d.s.u., Degree of silica-undersaturation.

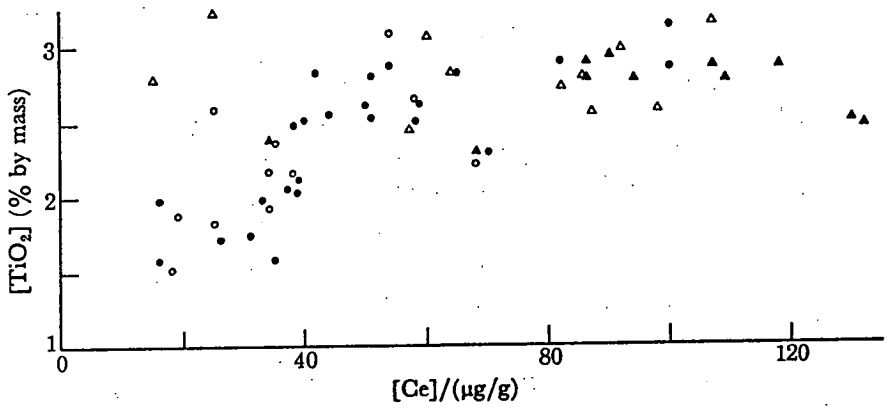

FIGURE 2. Ce–TiO_2 graph for alkaline basic rocks (Mg number ≥ 60). Symbols as in figure 1.

The interpretation most consistent with the model used in this paper is that a mineral in which Ti is a major component was residual for the basanites but not for the alkali basalts.

By similar reasoning, residual phases concentrating K, Rb and Zn can be inferred to have remained in the mantle after generation of the basanites. The collinearity of these elements with each other and with the incompatible elements in the alkali basalts suggests, however, that the accessory minerals had disappeared from the residue by this stage of melting and that

those elements remaining in the residual mantle (e.g. Y in clinopyroxene) had low bulk distribution coefficients.

Nature of accessory phases

The K/Rb ratios of the Midland Valley alkaline basic rocks (Mg number ⩾ 60) show a wide range, with a mode at about 350 (figure 3). The basanites have average K/Rb ratios rather higher than those of the alkali basalts. The pattern is similar to that described from oceanic alkali basalts by Sun & Hanson (1975), and following their line of argument and that of Arth (1976), it may be inferred that *phlogopite* was the residual phase concentrating K and Rb during the earliest stages of melting. The constraint of the present model is that phlogopite should have completely melted during the first 7% of melting such that it was not a residual phase during formation of the alkali basalts (cf. Hofmann & Hart 1978).

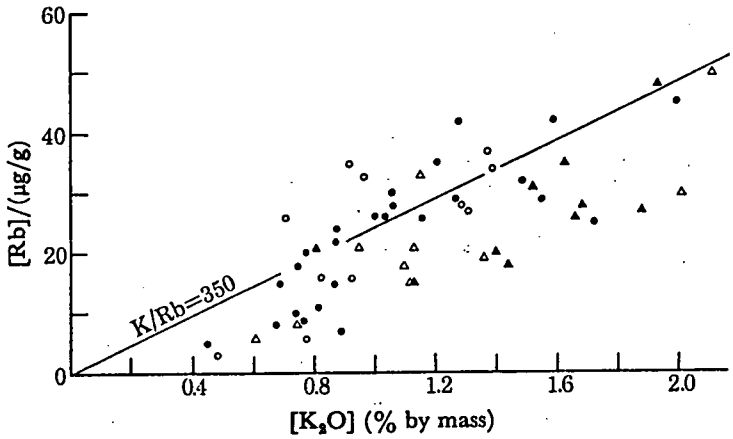

FIGURE 3. K_2O–Rb graph for alkaline basic rocks (Mg number ⩾60). Symbols as in figure 1.

It is tempting to suggest that the mica phase was in fact *titanphlogopite*, thereby finding a suitable residual phase to concentrate Ti. The lack of significant correlation between K and Ti (table 3) renders this doubtful, however. Neither is there any unequivocal evidence for another likely mantle host, e.g. titanclinohumite, ilmenite or Ti-rich clinopyroxene.

Zn shows only a restricted range of compositions though the strongly undersaturated varieties are on average richer in Zn. Zn is apparently partitioned into the melt though less strongly than Ba and the other incompatible elements and is possibly being retained by a sulphide phase ± clinopyroxene. This assumes closed-system fusion: alternatively, Zn contents were perhaps being buffered by a volatile phase.

The general model applied here is that the Midland Valley basic rocks or their parental magmas were formed by varying degrees of partial melting of a phlogopite-bearing peridotitic mantle. Phlogopite was completely consumed by the melt at about the point when the melt became critically undersaturated with respect to silica. Ba, Ce, Nb, P, Sr, Y and Zr were either incompatible or had very low bulk distribution coefficients for the relevant residual mineralogies. K and Rb concentrations were initially buffered by phlogopite. Zn may have been partially retained by a sulphide phase while the nature of the accessory Ti-mineral (if any) is uncertain.

Recognition of mantle heterogeneity

A good correlation between Ce and Nb in the alkaline rocks of the Midland Valley was noted in figure 1. In figure 4, Ce and Nb data are presented for two of the lava suites: the Mauchline and Thornhill lavas (Stephanian) and the North Ayrshire lavas of Dinantian age. The suites clearly have different Nb/Ce ratios.

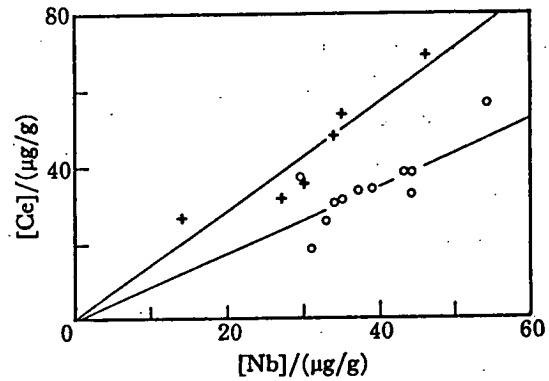

Figure 4. Ce plotted against Nb for basic rocks (Mg number ⩾60) of the N Ayrshire (crosses) and Mauchline–Thornhill (circles) sequences.

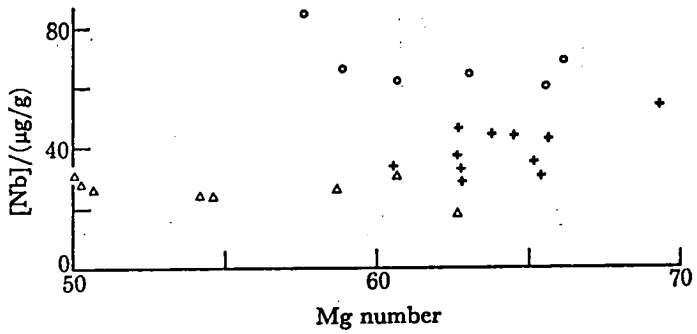

Figure 5. Mg number – Nb graph for lavas of the East Lothian (triangles), Bathgate–Linlithgow (circles) and Mauchline–Thornhill (crosses) sequences.

Table 4. Estimated abundances of incompatible trace elements at Mg number = 60 in various lava sequences

eruptive sequence	age	normative character	Ba	Ce	Nb	P	Sr	Zr	Σ (Ba→Zr)
Burntisland	Din.	hy.	650	60	40	2617	550	225	4142
East Lothian	Din.	hy.	600	30	24	1963	675	160	3452
N. Ayrshire	Din.	hy.	465	50	30	—	555	235	—
Arthur's Seat	Din.	c.u.	530	43	35	1701	700	170	3179
Campsie Block	Din.	c.u.	220	25	20	1527	500	140	2432
Kintyre	Din.	ne.	450	60	30	1527	550	210	2827
Bathgate–Linlithgow	Din.–Nam.	ne.	1000?	65	65	3053	900	250	5333
Passage Group, Ayrshire	Nam.–West.	hy.	400	15	30	1527	400	150	2522
Mauchline–Thornhill	Steph.	ne.	650	35	37	1876	600	150	3348
estimated maximum error	—	—	±50	±5	±5	±220	±50	±10	

c.u., Critically undersaturated with respect to silica. Din., Dinantian; Nam., Namurian; Steph., Stephanian; West., Westphalian.

The point may be stressed from a different viewpoint. Nb is plotted against Mg number for three volcanic sequences in figure 5. Clear differences exist between them at comparable Mg numbers.

The abundances of the incompatible elements at Mg number = 60 in several of the major lava sequences are given in table 4. These were estimated either directly, or by extrapolation, from incompatible element – Mg number graphs. Error estimates reflect the degree of scatter for each element.

The table clearly shows the wide range of elemental abundances and ratios which exists in rocks of identical Mg number. Nb, for example, varies by a factor of 3.3, Zr/Nb ratio by 1.8. The variations in the elemental *ratios* preclude the possibility that they were caused by varying degrees of fractional crystallization. The differences must have been derived at source.

It was noted earlier that, on a regional scale, the abundances of the incompatible elements, except K, Rb and Ti, correlated positively with the degree of silica-undersaturation. The lavas used in table 4 belong, with the exception of only three samples, to the alkali basalt group (normative ne. < 5%). Within this more restricted major element compositional range, there is little or no correlation between the incompatible elements and the degree of silica-saturation. Regional variations apparently override the effects of major element composition (cf. Kesson 1973). If basic rocks with comparable major element chemistry may be taken to have had comparable evolutionary histories, then the variations in trace element chemistry in the lava sequences reflect local variations in the source material, i.e. mantle heterogeneity. In the following sections, two scales of differences between individual lava sequences will be examined. The other is a less well defined, larger-scale variation, involving groups of lava suites and related intrusions.

Nature of the mantle heterogeneity

By totalling the incompatible elements at Mg number = 60 in the lava sequences, two types of suite may be arbitrarily distinguished: those with values of Σ (Ba+Ce+Nb+P+Sr+Zr) > 3400 μg/g and those with less than 3400 μg/g. These may be termed the 'high' and 'low' groups respectively.

Within each group, however, there is a wide range in abundances of the individual elements. For example, Nb in the 'high' group varies from 24 to 65 μg/g at Mg number 60; the P_2O_5/Ce ratio in the same group ranges from 100 to 150. Thus the observation that the basalts of a certain suite are relatively depleted in one incompatible trace element carries no implication that they are depleted in all such elements.

Neither can there be any implication that the basalts are reflecting their generation in areas of relatively *primitive* or *depleted* mantle. The ratios of Zr/Nb and K/Ba have been used by Erlank & Kable (1976) to define such areas in the suboceanic mantle. They suggest that tholeiitic basalts with low values of both ratios represent melts of relatively primitive, undepleted mantle, while basalts with high ratios have been generated in areas which had undergone previous mantle fusion events, depleting them in Ba relative to K and Nb relative to Zr.

In the Midland Valley alkali basalts, however, no such simple relation exists (figure 6). Figure 6 is a plot of Zr/Nb against K/Ba ratios. Only alkali basalts have been plotted, since it is likely that these elements were not being retained in substantial amounts by a residual phase in the mantle during generation of those basalts. The Bathgate–Linlithgow lavas, belonging to the 'high' group, have a low Zr/Nb ratio (a 'primitive' characteristic) and a

high K/Ba ratio (a 'depleted' characteristic). The Passage Group lavas of Ayrshire, one of the 'low' incompatible element suites, have a very low Zr/Nb ratio and a low K/Ba ratio. If the lower elemental abundances of the 'low' group point to a lower incompatible element content of their mantle sources, then that depletion has not been caused by a previous melting event within an originally homogeneous mantle.

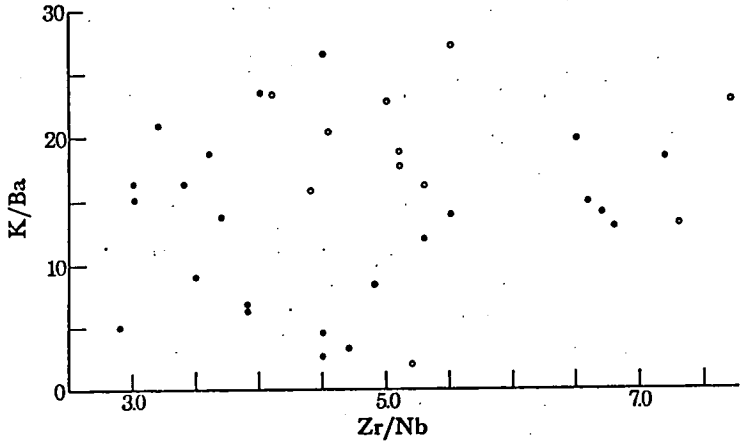

FIGURE 6. Zr/Nb ratio plotted against K/Ba ratio in alkali basalts (Mg number ≥ 60) of the Midland Valley province. Open circles, hy.-norm. basalts; closed circles, basalts with ne. < 5%.

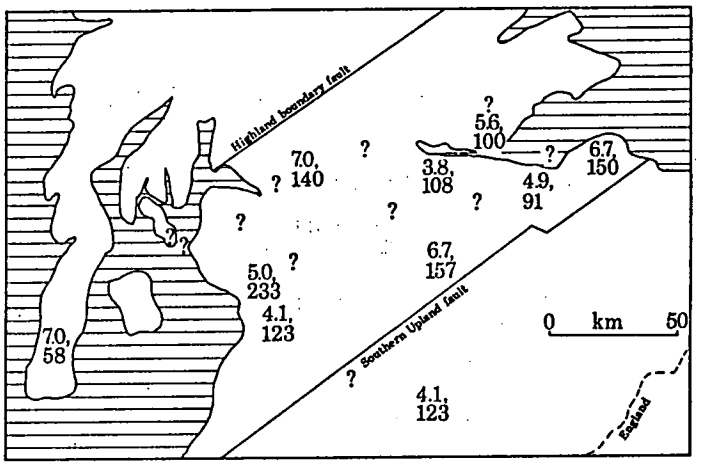

FIGURE 7. Inferred Zr/Nb (upper figures) and P_2O_5/Ce (lower figures) ratios of the mantle sources of the various Midland Valley lava suites. Question marks indicate sequences for which insufficient data are currently available.

These points are summarized in figure 7, where the average Zr/Nb and P_2O_5/Ce ratios at Mg number 60 for the main lava sequences and thus their inferred mantle sources are shown.

It appears, therefore, that the incompatible elements were not uniformly distributed in the Midland Valley mantle sources. They showed apparently non-systematic variations both in their absolute and relative concentrations.

Larger-scale heterogeneities

The inter-suite characteristics described above may, in some instances, be extended to cover geographical areas that include several phases of magmatism. In a K–Ti–2P diagram

(Schmincke & Flower 1974), the composition fields for basic rocks from East Lothian and Ayrshire show very little overlap (figure 8). Both fields contain data for rocks varying in age from Dinantian to late Carboniferous or early Permian and ranging in character from hy-. normative to strongly silica-undersaturated (ne. > 10%). The source volume of the Ayrshire rocks appears to have been rather different from that underlying East Lothian for a considerable period of time (more than 50 Ma?).

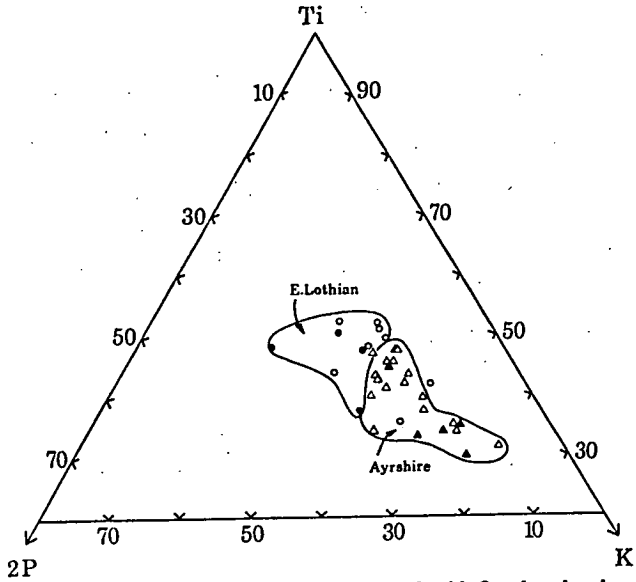

FIGURE 8. Ti–K–2P plot (atom percentages) for alkaline basic rocks (defined as having normative 100 An/(An+Ab) ≥ 50) of Permo-Carboniferous age from Ayrshire (triangles) and East Lothian (circles). Open symbols, ne. < 5%; closed symbols, ne. ≥ 5%.

It seems likely that several distinct areas of this type, each covering some hundreds of square kilometres, exist within the Midland Valley province but the lack of data currently precludes their clear definition. It follows from the preceding discussion, however, that within each of these larger areas, smaller-scale variations, involving different elements, also occur.

CAUSES OF MANTLE HETEROGENEITY

One consequence of the petrogenetic model used in this paper is that the ratios of the incompatible elements in the hy.-normative basalts reflect those of their mantle sources. Certain inferred ratios are presented in table 5 and compared with the estimated ratios in other sources of alkaline basalts, mainly based on data from oceanic islands. The Midland Valley ratios are, of course, modes; source heterogeneity provides variable ranges of these ratios.

The Permo-Carboniferous mantle beneath the Midland Valley appears to have been rather similar to the present sub-oceanic mantle in its relative abundances of K, Nb, P, Rb, Sr and Zr. It was apparently rather richer in Ba and poorer in Ce.

Sun & Hanson (1975) and Hanson (1977) have recently discussed the relations between oceanic island basalts and oceanic ridge basalts, outlining the need for a process or processes that can effectively enrich in the incompatible elements the sources of the alkaline basalts and/or deplete those of the low-K tholeiites. Enrichment of mantle by metasomatic fluids

(Lloyd & Bailey 1975) or by a network of basaltic to ultrabasic veins are possibilities cited by Hanson (1977).

Of some interest in this respect is the incompatible element chemistry of a low-K tholeiite from the base of the Dinantian lava succession in Kintyre (Macdonald 1975). Allowing that such rocks are formed by moderate (20–25%) degrees of melting of mantle peridotite, leaving a residue of harzburgitic composition, then the ratios of the incompatible elements should reflect the mantle source, perhaps even more accurately than those of the hy.-normative members of the alkaline suite.

TABLE 5. INFERRED ELEMENT RATIOS OF CERTAIN MANTLE SOURCE AREAS

	Rb/Sr	K/Sr	K/Rb	K/Ba	Ba/Nb	Zr/Nb	P_2O_5/Ce	K/Ce	references
sources of Midland Valley alkaline rocks	0.05	19	350	19	~9	5	90	219	this paper
sources of oceanic alkaline basic rocks	0.04	18	400	28	16	6.6	75	140	Sun & Hanson (1975), Langmuir *et al.* (1977)
low-K tholeiite, Kintyre	0.014	12	830	16	35	24	138	208	this paper

The Rb and Sr contents of the Kintyre low-K tholeiite are 2 and 140 μg/g respectively, with an Rb/Sr ratio of 0.0143. These data are consistent with the suggestion that the rock formed by 20% partial melting, with up to 20% subsequent fractional crystallization, of a mantle source containing 23–28 μg Sr/g and 0.3–0.4 μg Rb/g. These figures compare closely with those used by Hofmann & Hart (1978, p. 49) for the sub-oceanic mantle. The K content of the Kintyre source would be 266–332 μg/g and the K/Rb ratio 830, again consistent with Hofmann & Hart's estimates.

Certain other inferred geochemical parameters of the source of the Kintyre low-K tholeiite are given in table 5 and compared with those deduced for the volumetrically much more abundant Kintyre alkaline lavas. The tholeiite source was depleted in Ce, Nb and Rb relative to the source of the alkaline basalts. The situation thus mirrors that of the present day ocean basalts.

Several interesting possibilities are raised by this unique flow among the Midland Valley lavas.

(i) It was generated in a different pressure régime from the alkaline rocks. The mantle would then be vertically heterogeneous chemically.

(ii) It represents the products of fusion of an area of mantle not affected by the metasomatic event which effectively 'rejuvenated' the incompatible element chemistry of the mantle source.

(iii) It represents fusion of a mantle source, depletion of which had contributed at some earlier stage to the enrichment of the eventual sources of the alkaline basalts.

My grateful thanks are due to J. Bowman, Helen Coyle and K. Waterhouse for chemical analyses; N. Chapman and P. Aspen for kindly providing specimens from East Fife and allowing me access to unpublished chemical data; R. Banks and B. Robinson for computer programmes and Carolyn Amos and W. Pye for help in the production of the manuscript.

This research is financed by the Department of Environmental Sciences, University of Lancaster.

References (Macdonald)

Arth, J. G. 1976 *J. Res. U.S. geol. Surv.* **4**, 41–47.
Erlank, A. J. & Kable, E. J. D. 1976 *Contr. Miner. Petr.* **54**, 281–291.
Fitch, F. J., Miller, J. A. & Williams, S. C. 1970 In *C.r. 6ème Congr. Int. Stratigr. Geol. Carbonif.*, Sheffield, 1967, pt 2, pp. 771–789.
Forsyth, I. H. & Chisholm, J. I. 1977 *The geology of East Fife.* (*Mem. geol. Surv. U.K.*)
Francis, E. H. 1967 *Geol. Rdsch.* **57**, 219–246.
Francis, E. H. 1968 In *23rd Int. Geol. Congress*, vol. 2, pp. 163–174.
Guppy, E. M. & Thomas, H. H. 1931 *Chemical analyses of igneous rocks, metamorphic rocks and minerals.* (*Mem. geol. Surv. U.K.*).
Hanson, G. N. 1977 *J. geol. Soc. Lond.* **134**, 235–253.
Hofmann, A. W. & Hart, S. R. 1978 *Earth planet. Sci. Lett.* **38**, 44–62.
Kesson, S. E. 1973 *Contr. Miner. Petr.* **42**, 93–108.
Langmuir, C. H., Bender, J. F., Bence, A. E. & Hanson, G. N. 1977 *Earth planet. Sci. Lett.* **36**, 133–156.
Lloyd, F. E. & Bailey, D. K. 1975 *Phys. Chem. Earth* **9**, 389–416.
Macdonald, R. 1975 *Scott. J. Geol.* **11**, 269–314.
Macdonald, R., Thomas, J. E. & Rizzello, S. A. 1977 *Scott. J. Geol.* **13**, 11–22.
MacGregor, A. G. 1948 *Q. Jl geol. Soc. Lond.* **104**, 133–153.
MacGregor, M. & MacGregor, A. G. 1948 *The Midland Valley of Scotland*, 2nd edn. (*British Regional Geology.*)
Schmincke, H.-U. & Flower, M. J. F. 1974 *Naturwissenschaften* **61**, 288–297.
Scott, A. 1915 *Geol. Mag.* **52**, 455–461.
Sun, S. S. & Hanson, G. N. 1975 *Contr. Miner. Petr.* **52**, 77–106.
Wilkinson, J. F. G. & Binns, R. A. 1977 *Contr. Miner. Petr.* **65**, 199–212.

Transactions of the Royal Society of Edinburgh: Earth Sciences, **72**, 57–74, 1981

Geochemistry of a continental tholeiite suite: late Palaeozoic quartz dolerite dykes of Scotland

R. Macdonald, D. Gottfried, M. J. Farrington, F. W. Brown and N. G. Skinner

ABSTRACT: The late Carboniferous quartz dolerite suite of Scotland consists mainly of quartz tholeiites, with subordinate olivine tholeiites and tholeiitic andesites. The low pressure evolution of the magmas was controlled by fractionation of olivine–plagioclase–pyroxene–oxides assemblages from more magnesian compositions and plagioclase–pyroxene–oxides–apatite removal from intermediate compositions. A higher pressure stage dominated by olivine fractionation is suggested by the presence of olivine nodules in a magnesian basalt dyke from Fife.

The suite is of high-Fe-Ti type, closely comparable to certain basalts erupted in areas of active lithospheric spreading or "hot spots", such as Iceland and Hawaii. The ppO_2 can be inferred to have been rather higher in the Scottish rocks than in comparative suites, promoting earlier separation of Fe-Ti oxides, with the consequent effects on trace element distribution.

Apart from varying degrees of fractionation, chemical variations in the dykes are of three types: rather minor variations *along* individual dykes, variations *across* certain thicker dykes, and minor and trace element variations reflecting chemical heterogeneities in the mantle sources. The dykes and sills are inferred to have been fed from a plexus of small, partly independent, magma reservoirs.

New trace element data on tholeiitic lavas from the Oslo Rift confirm recently revived suggestions that the Scottish and northern English quartz dolerites are part of a larger province extending into Scandinavia.

KEY WORDS: Carboniferous continental tholeiites, high Fe-Ti basalts, low-temperature remobilization,mantle heterogeneity, olivine nodules, polybaric fractionation.

The NE-SW orientated structural trends and inferred basement controls which had dominated early and mid-Carboniferous tectonism in central Scotland were briefly replaced by an intense E-W fracturing in late Carboniferous times. This in turn gave way in Permian times to NW- or NNW-trending rift structures (Francis 1978). The magmatic history of the area was no less complex. Alkaline volcanism occurred throughout much of the Carboniferous. Permian magmatism was also of alkaline type and, although generally more silica-undersaturated, was closely related to the Carboniferous activity. In sharp contrast, magmatism accompanying the late Carboniferous fracturing was of quartz tholeiitic affinity.

Stratigraphic, structural and radiometric evidence indicates that the E-W fracturing and associated tholeiitic magmatism represented a very short-lived event, probably less than 5 m.y. (Francis 1978, p. 144). Explanations for the sudden changes in the nature of the stress system and of the magmatism have recently been sought in plate tectonic models of the European region (Francis 1978).

As a contribution towards knowledge of the late Palaeozoic continental magmatism in Britain, this paper presents geochemical data on the dykes and discusses the rocks in terms of their magmatic affinities, geochemical evolution and source characteristics.

1. Age and field relationships

K-Ar age determinations on sill and dyke rocks from Scotland and Northern England have confirmed long-established stratigraphical evidence that they were emplaced during late Carboniferous times, 292–295 m.y. ago (Francis 1978). Though locally the dykes may be disposed into geographical groups, such as those distinguished in the Stirling area of the Midland Valley of Scotland (Francis *et al.* 1970), there is no petrographic, geochemical or radiometric evidence that they represent discrete swarms of varying ages.

The dykes range in width from 1–2 m to ~50 m, averaging some 20 m, and vary in length up to 130 km. The dominant trend is E-W, although there is a major change in direction to ENE-WSW from Strathmore to Buchan (Fig. 1). Local deviations in trend occur near the Highland Boundary fault in Perthshire and in relatively short dykes in the Stirling area which were emplaced *en échelon* (Francis *et al.* 1970). There is some direct, and much circumstantial, evidence that the dykes acted as feeders for the quartz dolerite sill complex, which is almost entirely restricted to Carboniferous strata within the Midland Valley. The complex covers an area of 1500 km^2 and attains a thickness of 180 m (Francis 1978).

Petrography, chemistry and age-relations have long been used to link the Scottish rocks with the Whin sills and dykes of Northern England. Walker (1964) has referred to this association as the Central British tholeiitic province, and estimated the volume of magma to be 492 km^3. Francis (1978) has revived the suggestion (Hjelmqvist 1939) that the suite may also be traced into southern Norway and Sweden. The British rocks may, therefore, be part of a much larger tholeiitic province extending across the North Sea.

This paper concentrates on the chemical composition of the dykes although four samples from the sill complex have been analyzed to confirm consanguinity with the dykes and

to consider the lower-pressure, geochemical evolution of the dyke magmas. Earlier analyses of the sill complex (Guppy & Sabine 1956, nos 676, 677, 680, 681, 682) are also used but new analyses of the Northfield (Stirling) sill are used rather than those of Walker (1952).

Sample localities are listed after Table 1. There is a wide variety of host rocks: Archaean gneisses in Barra, greywacke-shale metasediments in the Scottish Highlands, Devonian sediments and volcanic rocks in the Midland Valley and southern Highlands and a range of Carboniferous volcanic rocks and sediments in the Midland Valley. This permits an assessment of the role of high-level assimilation in the development of this tholeiitic suite.

2. Nomenclature

The nomenclature employed here is that of Wilkinson and Binns (1977) for tholeiitic rocks. *Olivine tholeiites* and *tholeiites* contain normative An/(An+Ab)>50, differentiation index generally <30 and M values often >60, where $M = 100\,Mg/(Mg+Fe^2)$. *Tholeiitic andesites* have normative andesine (An/(An+Ab) = 30–50), normative quartz <10, differentiation index >35 and M values usually <50.

The Scottish late Carboniferous dykes and equivalent sill rocks have consistently been referred to as quartz dolerites and tholeiites, on the basis of mineralogy. The new chemical data are entirely consistent with this, with the exception of 4 analyzed specimens from 3 dykes (sample nos 63, 88, 87, 72) which are sufficiently evolved to justify use of the term tholeiitic andesite. This number represents only about 5% of the total number of analyzed rocks and it probably gives a reasonable estimate of the relative proportions of each type among the Scottish dyke swarms.

3. Magma type

All but one of the fresh (see 5.1) specimens are quartz-normative, the amount of "q+q in hy" increasing with increasing differentiation index. The chemical data thus confirm the mineralogical evidence (such as instability of olivine and the presence of free quartz) that these rocks belong predominantly to the quartz tholeiite magma type.

The olivine-normative specimen (11, ol = 2·6) is one of the most magnesian of the dykes and it seems likely that the parental magmas to the suite were in fact olivine tholeiites. It seems likely that analysis of more, Mg-rich Scottish rocks will reveal the presence of further olivine-normative specimens.

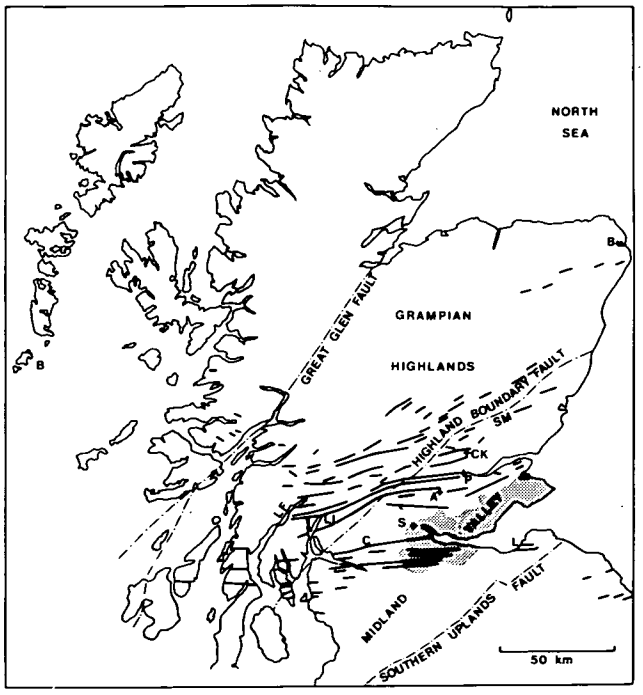

Figure 1 Sketch map showing distribution of quartz dolerite dykes; stippled area is region underlain by Midland Valley sill complex; B Barra, Bu Buchan, SM Strathmore, CK Craigmakerran, P Perth, A Auchterarder, S Stirling, C Campsie Fells, LF Loch Fyne, LL Loch Long, L Longniddry.

4. Petrography

Petrographic descriptions of the Scottish quartz dolerites may be found in Walker (1934, 1935, 1952, 1964, 1965), MacGregor and MacGregor (1948), Walker *et al.* (1952), Francis (1963), Francis *et al.* (1970) and Forsyth and Chisholm (1977). The mineralogy of the dykes is fairly simple. The dominant minerals are plagioclase, augite and Fe-Ti oxides. Ca-poor pyroxene (hypersthene and pigeonite), olivine, hornblende, biotite, chlorophaeite, pyrite and apatite are common, but not invariable, minor constituents. The dykes either contain micropegmatite or a mesostasis of more or less devitrified glass. Despite the wealth of petrographic detail, it must be noted that studies of mineral chemistry are, as yet, almost totally lacking.

Olivine is, with one exception, found pseudomorphed and this is also the normal case with the Ca-poor pyroxenes. Apparently all petrologists who have studies the dykes, including the present authors, have found considerable difficulty in distinguishing the original nature of the pseudomorphs in many specimens and records of the former presence of olivine and hypersthene are commonly accompanied by question marks. The difficulties of determining the former presence in the dykes of olivine and/or Ca-poor pyroxenes make it impossible to be categorical about the compositional range over which each occurs or to establish the order of appearance of the main phases. Thus in the same paper Walker (1965) states: "... olivine ... was the first mineral to separate, being closely followed by augite or lime-poor pyroxene and plagioclase..." (p. 504) and "The sequence of crystallization ... is ... olivine, plagioclase, hypersthene (where present), augite, and iron-ores ..." (p. 515). The differences are slight but indicative of some uncertainty. Similar problems faced Dunham and Kaye (1965) in their study of the Little Whin sill. "The order of crystallization was probably olivine, followed after non-reaction by two pyroxenes and plagioclase... The iron-titanium ores probably formed early" (p. 266).

Our observations are subject to the same uncertainties. However, we have identified pseudomorphs thought to be after olivine only in rocks with MgO ≥ 6% wt. While Ca-poor pyroxene appears to have crystallized in the central portions of the dykes over the complete spectrum from the most magnesian basalt to the tholeiitic andesites, its former presence as a *phenocryst* phase has been suspected only in rocks with MgO < 6% wt. The following sequence of assemblages characterizing the intratelluric stages is therefore inferred for the Scottish dykes:

Assemblage	Approximate MgO Content (wt %)
ol	
ol + pl + aug	7
(ol) + pl + aug + Ca-poor px + oxides	
pl + aug + Ca-poor px + oxides	5

This sequence has overall similarities to that found during crystallization of the Alae lava lake, Hawaii (Wright & Peck

1978) and of tholeiitic lavas from Eastern Iceland (Wood 1978). Ca-poor pyroxene and oxides make a first appearance at more magnesian compositions than in the Hawaiian and Icelandic examples. Walker (1965) has remarked on the relatively early appearance of oxides in the Scottish rocks, a feature perhaps attributable to crystallization under relatively high ppO_2. It appears that the assemblage oxides + Ca-poor pyroxene was thus stabilized relative to olivine.

5. Chemical composition

5.1. Post-magmatic chemical changes

Members of the quartz dolerite suite show varying degrees of alteration from almost totally fresh to completely decomposed. Marginal zones in particular are invariably altered, even in dykes where the interiors are fairly fresh. As can be judged from the H_2O analyses (Table 2), all samples have been secondarily hydrated to some degree, resulting in variable replacement of the ferromagnesian minerals and groundmass glass by serpentine-chlorite assemblages and alteration of the plagioclase to sericite ± clay minerals. Certain specimens additionally, or alternatively, show partial replacement by carbonate, the ferromagnesian minerals being especially prone to this type of alteration. Albitization of the plagioclase is a rather less common effect.

Not surprisingly, there has been considerable mobility of certain elements during alteration. Inspection of data on margin-centre pairs (Table 4) indicates that Mg, Ca, Na, K, Ba, Cs, Sr, Rb, Zn and Pb have variably been added to, or removed from, the dyke margins during low-temperature alteration processes. Petrographic evidence further indicates that similar chemical changes are likely to have modified the dyke centres. Such modifications create difficulties in establishing the original, magmatic abundances of the mobile elements in the dykes but, fortunately, a sufficient number of fresh dykes is available that, for almost all elements, reasonable estimates of magmatic abundance can be made.

In a typical case (Fig. 2), the total body of data shows considerable scatter. The different symbols employed reveal, however, that most of the scatter is the result of plotting data for altered as well as unaltered rocks. Thus sericitised and albitised specimens commonly contain low CaO proportions, while high CaO/MgO ratios occur invariably in altered rocks. *Fresh* rocks, taken to be those only a few per cent modally altered, define a coherent trend of decreasing CaO with decreasing MgO which is inferred to be the magmatic trend. It must be noted, however, that even in fresh rocks, as so defined, the most mobile trace elements show significant scatter on variation diagrams (Fig. 5) which probably results, at least in part, from remobilization processes. The term 'fresh' should be read with this qualification in mind.

A summary of the behaviour of the mobile elements during each main alteration process is given in Table 5. It should be noted, however, that the amount of chemical modification resulting from each process varies from dyke to dyke. Furthermore, in those dykes where two or more low-temperature processes have operated, it may be impossible to distinguish the chemical effects of each.

MgO is used as the abscissa in several variation diagrams. It is acknowledged that in several specimens MgO has either been added or subtracted relative to its magmatic abundance and therefore provides some scatter in these diagrams. Nevertheless, the use of MgO permits a ready comparison of the British data with published data on comparable tholeiitic suites.

5.2. Chemical variations along dykes

Loch Long-Auchterarder dyke. A long dyke may be traced with modest confidence through discontinuous outcrops from west of Loch Long to Auchterarder in Perthshire (MacGregor & MacGregor 1948, plate VI). This body has been sampled at six localities. Data for selected stable elements (Table 6) indicate that chemical variation within this dyke is negligible, confirming the field evidence that it constitutes a single mass.

Campsie dyke. Three samples have been collected from this dyke in that part of its outcrop, the Campsie Fells, where its continuity is most clearly established. As for the previous dyke, variations in stable element abundances (Table 6) are largely within analytical error. The most westerly sample (60) does have significantly lower Zr, however, a difference checked independently in the Lancaster and Reston laboratories. Further sampling of the dyke may reveal other, small variations.

Loch Fyne-Perth dyke. A dyke running parallel to, but some 8 km to the north of, the Loch Long-Auchterarder intrusion, has also been sampled at six localities. Here a slightly more complicated picture emerges (Table 6). Specimens from west of the Highland Boundary Fault are very slightly less evolved than those further east. If the dyke represents one magma pulse, then that magma was differentiated either prior to intrusion (and intruded W → E) or post-intrusion (the geographical differences representing different vertical horizons in the mass). Alternatively, two dyke segments may be involved.

These examples indicate that long (tens of km) segments of the dykes may be chemically homogeneous. Even where apparent variations *along* strike are recorded, these variations are very much smaller than those *between* dykes.

5.3. Differentiation within dykes

Specimens from the marginal and central zones of eight dykes were collected primarily to test for the degree of mobility of certain elements. An unexpected result was that two of the dykes showed systematic compositional differences between margins and centres. While it has long been known (Walker 1934, 1935) that *in situ* differentiation has produced acid veins and patches in certain dykes, this appears to be the first record of a compositional variation *across* the dykes.

Longniddry dyke (84, 85). This dyke exhibits internal differentiation from a mafic chill zone to a rather more evolved centre approaching tholeiitic andesite composition. We have not systematically sampled across this intrusion and thus cannot describe the differentiation in detail. However, the two analyzed samples indicate, with the exception of Al_2O_3, chemical variations identical to those of the whole body of data. Fractionation *within* the dyke appears to have largely mimicked that producing the main variations in the dyke suite. The higher Al_2O_3 proportion in the more evolved facies is in contrast to the normal situation (Fig. 3). It may be that plagioclase fractionation was less marked in the Longniddry magma than during the evolution of the main reservoirs.

Craigmakerran dyke (22, 23). This dyke shows rather more complex variations. The marginal zone has the higher concentrations of the stable incompatible elements consistent with its being a differentiation product of the magma represented by the central zone. The SiO_2 and MgO abundances apparently indicate a more *mafic* composition but it seems probable that silica-leaching and magnesium metasomatism have occurred in this highly altered chill rock.

Table 1 Trace element data for dyke and sill rocks

Sample No.	*1*	*2*	*3*	*4*	*5*	*6*	*7*	*8*	*9*	*10*	*11*	*12*	*13*	*14*	*15*	*16*	*17*	*18*
Rb	16	8	12	7	7	9	8	20	6	4	10	49	92	113	28	15	16	18
Cs	—	—	0·7	0·7	0·7	—	1·2	—	—	—	—	0·6	0·9	1·0	0·9	—	0·4	0·8
Ba	180	140	338	254	185	215	313	365	180	160	220	430	500	640	554	240	259	332
Sr	305	280	276	264	284	284	273	390	305	300	395	560	820	445	380	350	476	361
Pb	18	27	32	19	7	16	23	4	2	7	8	6	5	15	35	3	17	17
Th	1·1	1·2	2·1	2·2	1.3	1·7	2·1	1·9	1·2	1·4	1·0	3.1	3·2	3·9	3·2	1·4	1·1	1·8
U	—	—	0·5	0·7	—	0·6	—	—	—	—	—	0·6	1·0	0·8	0·9	—	—	—
Zr	142	139	187	189	139	138	189	133	128	127	113	175	186	188	180	131	116	150
Hf	3·6	3·5	5·2	5·5	3·7	3·9	5·2	5·0	3·5	3·4	3·3	4·5	4·6	4·9	4·7	3·8	3·3	4·2
Nb	16	16	24	23	17	16	21	21	16	17	14	19	18	20	21	16	17	20
Ta	0·96	0·96	1·32	1·49	1·02	0·96	1·24	1·40	1·13	1·10	1·01	1·21	1·17	1·16	1·18	1·09	1·03	1·23
La	12	12	21	22	14	15	21	20	14	14	13	24	26	28	25	15	13	19
Ce	31	29	47	46	31	30	43	42	29	30	28	51	52	50	51	31	29	42
Nd	21	20	25	36	22	17	33	27	22	27	17	29	30	36	29	22	21	26
Sm	4·4	5·2	8·0	7·8	5·4	5·0	7·2	7·0	5·0	5·3	4·8	7·1	7·3	7·3	7·4	5·7	5·0	6·6
Eu	1·64	1·55	2·13	2·21	1·65	1·63	1·92	2·07	1·60	1·68	1·46	1·94	1·97	2·07	1·99	1·66	1·59	1·88
Gd	4·4	3·8	6·0	7·1	4·6	3·1	4·2	5·7	3·5	3·3	4·0	5·6	5·8	6·6	6·1	4·4	3·9	5·2
Tb	0·87	0·85	1·4	1·4	0·92	0·83	1·2	1·2	0·85	0·83	0·83	1·2	1·1	1·0	1·2	0·90	0·95	0·98
Tm	0·29	0·28	0·58	0·57	0·31	0·32	0·44	0·40	—	0·29	0·26	0·40	0·39	0·38	0·43	0·28	0·33	0·43
Yb	2·1	2·3	3·3	3·5	2·2	2·4	3·2	2·7	2·0	2·1	2·0	2·5	2·9	2·8	2·6	2·4	2·0	2·5
Lu	0·29	0·28	0·45	0·50	0·33	0·34	0·43	0·41	0·28	0·26	0·25	0·67	0·44	0·36	0·37	0·30	0·26	0·34
Y	30	32	36	36	31	30	36	36	20	18	23	—	34	32	34	—	24	28
Co	47·3	45.3	43·7	45·5	44·5	45·4	45·5	51·1	47·6	48·7	49·7	41·1	40·0	40·2	38·2	44·5	57·9	41·8
Ni	73	—	35	—	—	—	—	—	—	—	98	—	—	—	—	—	—	49
Zn	49	94	108	101	84	96	94	78	87	91	58	88	82	100	77	70	69	73
Sc	32·1	32·1	32·4	33·4	31·9	31·6	32·7	30·6	30·3	30·7	31·2	27·8	27·2	27·0	25·3	30·9	30·6	27·0
MgO	6·2	6·4	5·1	5·2	5·8	6·0	5·0	6·2	5·4	5·5	7·3	5·4	5·2	5·2	5·5	6·4	6·8	5·9
Nature of alteration	F	F	F	F	F	F	F	S, Sp	C	C, Sp	F	S, Sp	S, Sp	S, A, Sp	S, Sp	S, Sp	S	S, Sp

Sample No.	*19*	*20*	*21*	*22*	*23*	*24*	*25*	*26*	*27*	*28*	*29*	*30*	*31*	*32*	*33*	*34*	*35*	*36*
Rb	—	14	33	15	10	12	18	10	21	13	8	4	11	33	6	5	11	12
Cs	—	0·4	0·5	0·6	0·9	—	0·6	0·6	0·7	0·5	0·4	—	0·4	0·6	—	—	0·5	—
Ba	210	340	445	150	235	295	204	198	290	260	230	370	260	380	140	130	500	277
Sr	275	305	265	383	235	310	378	303	320	245	340	315	300	410	270	271	245	298
Pb	<1	20	<1	6	20	12	4	7	<1	7	—	9	10	3	37	9	3	22
Th	1·7	2·2	2·1	1·1	1·5	2·2	1·3	0·8	2·9	3·3	1·1	1·5	1·4	1·5	1·5	1·7	1·4	1·3
U	—	—	0·8	—	—	—	—	—	1·3	1·4	—	—	—	—	—	0·5	—	0·4
Zr	164	203	212	143	158	184	137	127	156	160	119	150	144	142	167	156	153	144
Hf	4·2	5·1	5·3	3·3	4·2	4·9	3·7	3·2	3·8	4·0	3·2	3·9	3·9	3·8	4·4	4·1	3·8	3·9
Nb	15	20	20	14	20	23	17	17	15	15	17	19	19	19	19	16	19	19
Ta	1·17	1·17	1·22	0·84	1·00	1·43	1·00	0·91	1·02	0·85	1·04	1·16	1·17	1·17	1·26	1·15	1·07	1·20
La	16	23	24	13	25	21	14	13	18	19	14	17	17	17	28	16	16	16
Ce	33	48	55	29	46	43	30	28	36	39	29	36	36	36	45	35	33	35
Nd	20	43	41	22	31	31	23	20	20	24	17	25	29	23	27	23	28	26
Sm	5·8	8·8	9·0	4·7	8·0	7·1	4·8	5·0	5·8	5·9	5·4	5·4	6·5	6·0	5·9	5·9	5·8	6·1
Eu	1·66	2·65	2·79	1·44	2·14	2·11	1·63	1·54	1·48	1·50	1·54	1·73	1·78	1·81	1·72	1·75	1·71	1·75
Gd	4·8	7·3	6·7	4·0	4·7	5·9	4·6	4·3	4·8	4·9	4·2	4·6	5·2	4·3	3·5	5·2	4·7	4·9
Tb	1·0	1·3	1·7	0·80	1·3	1·2	0·90	0·97	0·85	0·94	1·1	0·92	0·84	0·80	1·1	1·0	0·94	0·92
Tm	0·31	0·52	0·50	0·22	0·38	0·45	0·36	0·43	0·36	0·37	0·30	0·31	0·38	0·39	0·32	0·35	0·40	0·39
Yb	2·7	3·4	3·3	2·3	3·0	2·6	2·2	2·4	2·5	2·3	1·9	2·2	2·3	2·2	2·3	2·9	2·7	2·1
Lu	0·38	0·47	0·59	0·31	0·36	0·38	0·34	0·33	0·58	0·53	0·33	0·30	0·30	0·30	0·31	0·50	0·36	0·27
Y	31	40	39	28	35	34	29	27	28	32	20	34	26	30	26	33	35	29
Co	44·5	44·9	43·7	44·6	44·3	46·7	47·0	44·6	37·7	38·4	49·7	44·9	45·7	45·6	40·9	47·9	45·2	45·2
Ni	—	36	—	—	—	—	93	80	74	—	115	92	—	—	—	—	—	120
Zn	84	93	80	54	180	79			67	81	80	88	90	100	164	99	104	79
Sc	32·9	34·8	33·2	32·0	35·3	32·3	33·2	30·8	28·6	29·6	32·3	28·9	31·0	30·6	37·5	36·2	34·7	29·3
MgO	6·1	5·7	5·0	6·6	8·6	6·3	6·5	6·5	7·1	7·7	6·8	6·8	6·6	7·8	7·7	6·2	6·0	6·7
Nature of alteration	F	S, A, Sp	S, A, Sp	F	C	F	S	F	F	Sp	F	F	F	S, C	C, S	F	F	F

Table 1 (*continued*)

Sample No.	*37*	*38*	*39*	*40*	*41*	*42*	*43*	*44*	*45*	*46*	*47*	*48*	*49*	*50*	*51*	*52*	*53*	*54*
Rb	7	12	15	34	15	19	25	24	12	7	7	12	13	10	34	45	21	15
Cs	—	—	0·6	0·7	0·3	1·0	0·8	—	—	—	0·2	—	—	—	0·6	0·5	0·4	0·5
Ba	230	245	360	338	610	390	435	251	206	244	180	197	218	256	466	1241	373	387
Sr	320	265	325	369	470	425	355	289	271	279	285	284	282	206	398	448	411	356
Pb	7	3	26	5	9	4	6	24	14	16	<1	20	14	12	19	9	21	8
Th	1·1	1·4	3·0	3·2	3·0	3·0	2·9	1·8	2·0	2·0	1·7	1·3	1·7	1·2	3·1	2·1	1·4	3·0
U	—	0·7	—	—	0·9	—	0·7	—	0·7	—	—	—	—	0·7	1·0	—	—	0·7
Zr	140	154	184	184	186	198	186	—	130	156	157	—	149	168	182	163	133	187
Hf	3·6	3·7	5·1	4·5	4·5	4·6	4·6	4·5	4·2	4·4	3·8	4·4	4·1	4·7	4·9	4·2	3·5	4·8
Nb	19	14	20	16	20	21	19	18	18	18	18	19	20	20	21	18	19	20
Ta	1·08	1·13	1·24	1·21	1·19	1·16	1·15	1·15	1·03	1·15	1·06	1·20	1·39	1·32	1·18	1·16	0·99	1·17
La	16	14	32	25	26	25	23	17	17	18	15	18	18	19	26	20	15	25
Ce	36	32	60	49	52	51	48	34	31	34	35	35	38	38	52	39	32	53
Nd	21	19	43	28	28	36	19	28	24	26	26	32	25	30	38	26	21	28
Sm	6·1	5·7	8·0	6·8	7·3	7·1	6·7	6·1	6·2	5·9	5·5	6·8	6·6	7·1	6·9	6·2	5·4	7·3
Eu	1·76	1·57	2·28	1·88	1·96	2·06	1·91	1·73	1·59	1·70	1·66	1·86	1·83	1·96	2·07	1·82	1·62	2·02
Gd	4·9	4·8	6·6	5·6	5·9	6·0	5·2	4·4	2·9	2·1	4·6	3·6	4·6	3·7	5·6	5·2	4·4	6·0
Tb	0·98	0·88	1·2	1·1	1·1	1·1	1·2	1·1	1·0	1·1	0·89	1·0	1·0	1·1	1·2	1·0	0·86	1·3
Tm	0·36	0·28	0·45	0·40	0·39	0·35	0·40	0·36	0·25	0·45	0·27	0·41	—	0·41	0·58	0·33	0·35	0·35
Yb	2·0	1·9	2·9	2·7	2·6	2·8	2·5	2·6	2·6	2·7	2·4	2·4	2·3	2·6	2·6	2·7	2·0	2·8
Lu	0·69	0·29	0·39	0·39	0·45	0·72	0·52	0·37	0·33	0·33	0·33	0·32	0·33	0·34	0·36	0·34	0·29	0·39
Y	33	24	38	27	32	33	30	27	30	30	34	25	28	30	35	28	21	34
Co	48·2	43·7	39·9	40·9	38·2	44·7	42·1	44·2	46·6	47·2	44·0	49·9	49·7	50·2	38·8	43·2	46·7	41·2
Ni	—	—	—	—	49	50	59	—	—	—	—	—	—	—	—	—	—	—
Zn	87	44	220	93	105	93	74	72	83	86	90	78	85	89	80	70	77	98
Sc	30·0	24·3	28·5	27·1	25·8	27·5	28·3	31·5	32·0	31·8	31·9	30·9	30·4	31·6	26·6	28·6	31·3	26·6
MgO	6·4	6·6	6·1	5·4	5·4	5·8	5·6	6·1	6·3	4·9	6·1	6·3	6·1	6·0	5·5	5·8	6·8	5·6
Nature of alteration	F	F	C, Sp	F	S, A?, Sp	F	F	F	Fg	F	Fg	F	F	Fg	S, A?, Sp	S, Sp	S	Sp, C, S

Sample No.	*55*	*56*	*57*	*58*	*59*	*60*	*61*	*62*	*63*	*64*	*65*	*66*	*67*	*68*	*69*	*70*	*71*	*72*
Rb	18	50	77	22	26	26	21	25	28	5	5	35	40	106	43	7	38	40
Cs	—	0·9	0·3	—	—	—	0·4	0·3	0·9	0·5	—	0·7	0·6	0·9	0·7	—	10·2	0·9
Ba	270	540	640		487	470	323	641	772	235	250	418	547	775	754	293	440	482
Sr	400	375	165	474	490	446	369	388	647	285	290	451	498	287	504	330	365	200
Pb	26	38	38	17	24	12	28	20	12	5	1	26	26	33	17	7	<1	5
Th	2·8	6·8	12·6	2·7	2·5	2·7	2·4	3·1	3·9	1·9	1·6	2·8	3·0	9·5	2·7	2·1	1·1	4·4
U	—	1·6	2·7	—	—	0·7	0·8	—	0·9	—	—	0·9	0·7	2·4	0·6	—	—	1·2
Zr	160	370	745	189	194	229	184	223	256	165	172	172	179	493	181	212	107	233
Hf	4·2	9·5	16·1	5·1	5·1	5·4	5·0	5·0	6·3	4·2	3·8	4·2	4·5	12·1	4·6	5·6	3·1	6·1
Nb	19	41	21	20	22	24	24	25	23	19	19	19	20	20	20	23	14	22
Ta	1·07	2·20	2·24	1·31	1·27	1·30	1·25	1·53	1·35	1·22	1·17	1·09	1·07	1·78	1·18	1·55	1·11	1·60
La	22	44	55	27	26	30	28	31	40	17	17	23	24	47	25	23	13	32
Ce	46	92	103	50	54	54	58	63	78	36	36	47	49	94	50	46	27	65
Nd	25	53	50	33	33	33	31	29	46	30	27	29	33	43	30	29	18	38
Sm	6·5	12·4	10·9	7·6	7·9	8·1	7·5	8·1	9·8	6·1	6·4	6·3	6·8	8·8	6·0	7·6	5·1	9·1
Eu	1·86	3·29	1·85	2·17	2·20	2·25	2·45	2·65	2·75	1·79	1·79	1·84	1·94	1·61	1·90	2·17	1·49	2·34
Gd	6·1	12·3	10·1	6·1	5·4	5·7	6·9	7·3	7·5	4·9	5·2	4·8	5·6	6·8	5·7	6·0	3·7	6·9
Tb	0·70	2·0	1·8	1·4	1·1	1·2	1·5	1·4	1·5	1·0	0·98	0·96	1·0	1·4	1·1	1·2	0·88	1·4
Tm	0·41	0·93	0·92	0·48	0·46	0·36	0·48	0·50	0·46	0·31	0·49	0·36	0·52	0·67	0·43	0·36	0·34	0·48
Yb	2·4	5·0	5·9	2·7	2·9	3·2	2·8	3·0	3·5	2·7	2·4	2·5	2·6	4·1	2·5	3·0	1·6	3·4
Lu	0·33	0·64	0·81	0·38	0·36	0·43	0·38	0·42	0·45	0·38	0·36	0·32	0·33	0·55	0·34	0·41	0·29	0·44
Y	38	60	65	38	30	36	32	36	42	32	33	31	31	50	31	31	27	37
Co	38·7	13·2	1·6	43·9	42·8	35·4	43·7	32·6	38·3	45·9	46·3	40·8	29·3	16·5	30·1	46·8	49·0	30·1
Ni	46	4·2	3·1	—	—	—	33	—	—	—	95	—	—	—	—	—	—	—
Zn	90	108	20		100	77	94	133	108	77	70	97	103	42	55	97	65	103
Sc	28·4	14·9	3·5	26·3	26·2	24·8	26·8	24·5	26·5	32·9	32·8	27·2	26·2	11·2	25·7	30·3	29·3	23·3
MgO	5·5	2·9	0·38	5·8	5·5	4·6	6·0	4·7	4·4	6·1	6·4	5·6	5·5	2·3	5·5	5·1	7·1	3·2
Nature of alteration	Sp	Sp, S	Sp	S, A?, Sp	S, A, Sp	S, Sp	S, A	S, A	Fg	F	Fg	S, A?	S, A?, Sp	Sp, S	S, A, Sp	Fg	S, A	C, S

Table 1 (*continued*)

Sample No.	*73*	*74*	*75*	*76*	*77*	*78*	*79*	*80*	*81*	*82*	*83*	*84*	*85*	*86*	*87*	*88*	*89*	*90*
Rb	21	38	29	16	14	12	35	35	8	22	2	24	13	14	21	26	22	21
Cs	0·4	1·0	0·5	—	—	—	0·4	0·5	—	—	—	0·4	—	0·3	—	0·7	1·0	1·5
Ba	1190	460	220	400	505	290	435	624	260	330	160	400	270	350	566	575	560	435
Sr	345	290	310	370	362	345	365	502	330	350	215	420	330	329	377	390	765	410
Pb	36	6	16	20	27	13	2	6	12	4	1	80	16	3	5	19	7	12
Th	3·1	3·9	2·5	1·9	1·8	1·5	2·5	2·9	1·3	2·7	1·6	2·8	2·0	2·5	3·3	3·6	1·7	1·7
U	1·0	0·9	—	—	—	0·7	—	0·9	—	—	—	0·7	—	—	0·9	0·9	—	0·6
Zr	171	214	168	148	166	140		191	124	187	164	211	160	180	249	280	156	156
Hf	4·5	5·9	4·3	3·9	4·2	3·8	3·9	4·3	3·0	4·7	3·8	5·1	3·9	4·3	6·0	6·7	4·1	3·9
Nb	17	22	17	19	16	18	18	16	16	20	13	22	18	16	24	24	18	19
Ta	1·20	1·42	1·06	1·15	1·05	1·11	1·01	1·00	1·04	1·21	1·07	1·47	1·03	1·07	1·28	1·44	0·95	1·10
La	24	31	20	20	21	17	23	22	14	23	17	27	18	22	30	33	24	22
Ce	46	61	47	36	42	36	45	43	30	46	33	55	39	41	65	78	46	47
Nd	29	35	25	29	26	28	30	29	24	29	21	35	29	29	35	42	26	32
Sm	6·8	8·3	5·6	6·0	6·5	5·6	6·6	6·3	5·1	6·8	6·1	8·1	6·3	6·9	7·3	7·7	6·1	6·6
Eu	1·79	2·31	1·90	1·72	2·02	1·82	1·82	1·68	1·61	1·87	1·65	2·46	1·85	1·70	2·34	2·73	2·02	2·09
Gd	4·9	6·7	5·5	3·7	5·4	4·8	5·0	4·4	4·2	5·4	4·6	6·8	4·9	4·6	6·5	7·1	5·8	5·4
Tb	1·1	1·4	0·98	1·0	1·0	0.86	0·97	0·97	0·75	1·1	1·0	1·4	0·87	0·92	1·3	1·5	1·2	1·1
Tm	0·32	0·45	0·35	0·30	0·34	0·33	0·39	0·30	0·37	0·38	0·33	0·27	0·42	0·30	0·37	0·52	0·31	0·49
Yb	2·8	3·2	2·3	2·5	2·7	2·2	2·4	2·5	2·1	2·7	2·2	3·1	2·3	2·6	3·0	3·0	2·6	2·7
Lu	0·37	0·44	0·30	0·35	0·35	0·30	0·36	0·32	0·24	0·38	0·32	0·48	0·32	0·35	0·37	0·39	0·44	0·62
Y	32	38	33	26	31	30	32	30	21	33	21	39	28	27	33	40	38	32
Co	37·2	36·7	40·4	35·5	39·9	40·8	39·1	37·0	51·2	38·3	41·7	28·6	54·0	37·8	36·7	37·8	43·9	45·9
Ni	—	—	—	—	—	—	65	—	93	—	—	33	56	—	—	—	—	—
Zn	100	107	85	76	112	80	41	73	85	84	42	224	88	63	107	116	122	122
Sc	26·4	25·7	26·9	26·9	28·7	28·4	32·0	26·1	30·5	26·6	27·3	22·6	28·3	26·4	24·2	24·5	28·2	28·8
MgO	5·1	5·1	7·4	3·5	4·5	5·5	6·0	5·5	5·5	5·4	5·1	2·1	5·1	5·6	4·5	3·7	6·0	6·2
Nature of alteration	F	S, Sp	S, Sp	C	Sp, C	Sp, C	A, S, Sp	S, A, Sp	C	Fg	C, Sp	C, Sp	C, Sp	F	C, Sp	C	S, A, Sp?	F

Explanation of Table 1

F fresh, S sericitised, A albitised, Sp serpentinised, C carbonated, Fg fresh but with substantial amount of glassy (or devitrified) matrix. Cs, Th, U, Hf, Ta, REE, Co and Sc determined by INAA (analysts; P. A. Baedecker & L. J. Schwarz, Reston); Nb determined spectrophotometrically (analyst: E. Y. Campbell, Reston) and Ni by d.c. arc emission spectroscopy (analyst: C. S. Annell, Reston); techniques outlined by Gottfried *et al.* (1978).

Rb, Ba, Sr, Pb, Zr, Y and Zn determined by XRF on rock powder packed against mylar film (analyst: J. R. Bowman, Lancaster).

Estimated precisions (1σ) are: Cs 5%, Th 10%, U 11%, Hf 4%, Ta 6%, La 7%, Ce 4%, Nd 8%, Sm 8%, Eu 4%, Gd 17%, Tb 8%, Tm 18%, Yb 6%, Lu 6%, Co 2%, Sc 2%, Nb 10%, Ni 15%, Rb 10%, Ba 5%, Sr 2%, Pb 10%, Zr 4%, Y 5%, Zn 5%.

Specimen localities (field numbers (in brackets) refer to collections housed in the Department of Environmental Sciences, University of Lancaster):

Invernesshire 1, 2 (MO 21, MO 34) marginal facies of dyke, North Barra, Outer Hebrides [NF 72250361 & NF 67910523 respectively].

Aberdeenshire 3 (MV 635) dyke, Boddam [NK 132418]; 4 (MV 638) dyke, Haddo [NK 871339]; 5 (MV 639) dyke, Ythan [NJ 792363]; 6 (MV 640) dyke, Coshelly [NJ 730352]; 7 (MV 642) dyke, Largie [NJ 611317].

Argyllshire 8 (MV 585) dyke, Loch Fyne [NN 088154]; 9–11 (MV 582, 583 and 584) northern, southern margins and centre of dyke, Strachur [NN 085012]; 12, 13 (MV 579, 580) centre and 14 (MV 581) margin of dyke, Larach Hill [NN 160915]; 15 (MV 632) dyke, Tayvallich [NS 725872]; 16 (MV 578) dyke, Dunoon Castle [NS 164761]; 17 (MV 633) dyke, Ellary [NR 740762]; 18 (MV 634) dyke, Cretshengan [NR 708666].

Perthshire 19 (MV 610) dyke, Broadgreen [NO 136358]; 20 (MV 608) dyke, Campsie Linn [NO 125340]; 21 (MV 609) dyke, Wolfhill [NO 156337]; 22, 23 (MV 559, 560) centre and margin of dyke, Craigmakerran [NO 142322]; 24 (MV 611) dyke, Bridge of Dalcrue [NO 045280]; 25 (MV 624) dyke, Monachyle Glen [NN 465221]; 26 (MV 625) dyke, Stobinian [NN 439219]; 27, 28 (MV 604, 605) centre and margin of dyke, Twenty-shilling Wood, Comrie [NN 763227]; 29 (MV 601) dyke, Loch Lubnaig [NN 586128]; 30 (MV 597) dyke, Muthill [NN 863190]; 31 (MV 606) dyke, Crossgates, Perth [NO 048209]; 32 (MV 607) dyke, Friarton Quarry, Perth [NO 117212]; 33–35 (MV 561, 562, 563) margin, centre medium-grained and centre coarse-grained of dyke, Corsiehill Quarry, Perth [NO 134234]; 36 (MV 649) dyke, Glen Artney [NN 691153]; 37 (MV 602) dyke, Tighnablair [NN 778168]; 38 (MV 603) dyke, Culloch [NN 776178]; 39, 40 (MV 557, 558) margin and centre of dyke, quarry, Auchterarder Station [NN 956122]; 41 (MV 599) dyke, Loch Ard [NN 451018]; 42 (MV 600) dyke, Pass of Leny [NN 602087]; 43 (MV 598) dyke, Titus Well, near Braco [NN 817123]; 44 (MV 646) dyke, near Doune [NN 700058]; 45 (MV 645) dyke, Lundie [NN 730049]; 46 (MV 644) dyke, Kilbryde [NN 750039]; 47 (MV 569) dyke, Lairhill, Sheriffmuir [NN 836025]; 48, 49 (MV 647, 648) centre coarse-grained and centre medium-grained, dyke, Braco Castle [NN 822114].

Angus 50 (MV 643) dyke, Tannadice [NO 474582].

Dunbartonshire 51 (MV 631) dyke, Inverbeg [NS 347973]; 52 (MV 556) dyke, near Dullatur Station [NS 748772].

Stirlingshire 53 (MV 629) dyke, Cruinn a'Bheinn [NN 366057]; 54 (MV 630) dyke, Rowardennan [NS 368988]; 55–57 (MV 570, 572, 574) "normal" grey facies, pink-mottled intermediate type and aplitic vein, sill, Northfield Quarry [NS 800854]; 58 (MV 626) dyke, Meikle Binn [NS 674817]; 59 (MV 627) dyke, Meikle Binn [NS 676816]; 60 (MV 522) dyke, Campsie Glen [NS 617804]; 61 (MV 628) dyke, Lecket Hill [NS 635805]; 62 (MV 623) dyke, Myot Hill [NS 775823]; 63 (MV 553) dyke, Kinkell [NS 632761].

Clackmannanshire 64 (MV 613) dyke, Burn of Sorrow [NN 935006]; 65 (MV 614) dyke, Broich Burn [NN 920013]; 66–69 (MV 618, 619, 620, 621) very coarse and less coarse central facies, aplite and margin, Ochil Fault Intrusion, Gloom Hill Quarry, Dollar [NS 963990].

Fife 70 (MV 565) quarry, Newton Hill [NO 399243]; 71 (MV 616) dyke, Norman's Law [NO 304198]; 72 (MV 566) dyke, Kinnaird [NO 421158]. 73 (MV 567) sill, Craiglumphart Quarry [NO 424139]; 74 (MV 568) dyke, quarry, Bankhead [NO 436107].

Renfrewshire 75 (AF 32) dyke, Wemyss Station [NS 193685].

Lanarkshire 76–78 (MV 550, 551, 552) margin, grey centre and dark centre of dyke, Cleddens, Bishopbriggs [NS 618706]; 79 (MV 596) dyke, Mollinsburn [NS 717718].

West Lothian 80 (MV 534) dyke, Beecraigs [NS 998736].

Midlothian 81 (MV 595) dyke, St Bernard's Well, Edinburgh [NT 244741].

East Lothian 82 (MV 586) dyke, Preston Grange [NT 371738]; 83 (MV 588) margin of dyke, Port Seton [NT 404759]; 84–85 (MV 589, 590) centre and margin of dyke, Longniddry [NT 438768]; 86 (MV 68) dyke, Bangly Hill [NT 493758].

Ayrshire 87 (AF 19) dyke, Auchenames [NS 180491]; 88 (AF 4) same dyke as 87, Auchenames [NS 175492].

Norway 89 (MV N1) B1 Lava, Sundvollen, S end of Steinfjord (40 Km W of Oslo); 90 (MV N2) B1 Lava, Knabberud, Baerumcauldron, S of Breijøer (N of Oslo).

Table 2 Analyses of dyke and sill rocks

Sample No.	*1*	*2*	*3*	*4*	*5*	*6*	*8*	*9*	*10*	*11*	*15*	*16*	*17*	*18*	*20*	*21*	*22*
SiO_2	49·8	49·9	49·9	50·1	50·3	50·3	48·5	47·3	47·5	48·6	50·3	48·3	48·1	49·0	48·0	48·8	49·3
Al_2O_3	13·3	13·4	13·5	13·0	14·0	14·4	13·4	13·8	13·8	13·5	13·0	13·0	13·8	13·4	11·9	11·9	13·1
Fe_2O_3	3·1	2·9	3·4	3·7	2·8	3·0	4·9	3·7	3·4	4·5	4·9	4·9	4·5	5·8	6·1	5·6	3·2
FeO	10·0	10·0	10·2	10·8	9·0	9·1	8·3	8·2	7·6	7·3	7·4	7·8	8·0	7·3	8·8	8·6	9·1
MgO	6·2	6·4	5·1	5·2	5·8	6·0	6·2	5·4	5·5	7·3	5·5	6·4	6·8	5·9	5·7	5·0	6·6
CaO	10·2	10·2	8·7	8·9	10·8	10·4	8·6	11·0	11·8	10·5	8·1	9·1	9·1	8·9	7·3	7·6	9·6
Na_2O	2·6	2·5	2·6	2·6	2·3	2·4	2·7	2·1	2·1	2·3	2·4	2·4	2·2	2·4	2·6	2·7	2·7
K_2O	0·63	0·43	0·93	0·44	0·47	0·51	1·1	0·43	0·39	0·63	1·7	0·83	1·1	1·1	0·80	1·4	1·1
H_2O	1·2	1·2	2·0	1·9	1·4	1·6	3·0	1·7	2·5	2·5	3·0	3·1	2·9	2·8	3·4	3·4	2·3
TiO_2	2·4	2·4	2·8	2·9	2·1	2·1	3·0	2·4	2·5	2·3	2·5	2·5	2·5	2·5	3·8	3·5	2·2
P_2O_5	0·28	0·26	0·35	0·35	0·25	0·24	0·36	0·26	0·27	0·26	0·37	0·28	0·26	0·33	0·59	0·62	0·25
MnO	0·16	0·15	0·22	0·20	0·13	0·18	0·18	0·21	0·19	0·19	0·17	0·16	0·16	0·16	0·24	0·19	0·18
CO_2	0·02	0·02	0·02	0·02	0·35	0·01	0·01	2·1	1·3	0·07	0·03	0·06	0·02	0·04	0·55	0·04	0·03
TOTAL	100	100	100	100	100	100	100	99	99	100	99	99	99	99	100	99	100
Nature of alteration	F	F	F	F	F	F	S, Sp	C	C, Sp	F	S, Sp	S, Sp	S	S, Sp	S, A, Sp	S, A, Sp	F

Sample No.	*23*	*24*	*25*	*26*	*27*	*28*	*29*	*30*	*32*	*33*	*34*	*36*	*38*	*39*	*40*	*42*	*43*
SiO_2	41·4	48·7	48·5	48·6	52·3	52·4	48·1	48·7	46·5	45·1	47·7	48·7	48·7	44·7	50·0	49·9	50·0
Al_2O_3	13·8	12·9	13·0	13·7	12·5	12·5	13·4	13·2	13·1	13·9	13·5	13·0	15·0	13·6	13·4	13·0	13·1
Fe_2O_3	8·4	4·2	3·8	4·3	3·4	2·3	4·4	4·6	4·4	4·6	4·5	3·6	4·0	5·0	4·8	5·5	4·4
FeO	4·2	9·1	8·5	8·3	6·3	6·9	7·8	8·0	8·6	6·5	8·6	9·0	5·7	7·2	7·4	7·4	7·7
MgO	8·6	6·3	6·5	6·5	7·1	7·7	6·8	6·8	7·8	7·7	6·2	6·7	6·6	5·6	5·4	5·8	5·6
CaO	7·5	9·7	10·1	10·2	9·6	8·0	10·6	9·8	6·4	7·1	9·9	10·5	10·6	9·1	8·8	8·1	8·7
Na_2O	2·5	2·3	2·4	2·3	1·8	2·4	2·1	2·2	2·0	2·7	2·4	2·1	2·2	2·4	2·3	2·3	2·5
K_2O	0·67	0·61	0·75	0·65	0·78	0·68	0·48	0·30	1·6	0·34	0·33	0·55	0·53	0·65	1·0	0·78	1·2
H_2O	5·9	2·6	2·3	2·8	3·0	3·9	2·3	2·7	4·6	6·1	2·8	2·1	3·5	4·1	2·3	3·2	2·6
TiO_2	2·6	3·0	2·3	2·2	1·6	1·6	2·5	2·6	2·7	2·7	2·5	2·6	1·7	2·5	2·4	2·5	2·3
P_2O_5	0·29	0·34	0·28	0·26	0·20	0·20	0·26	0·29	0·32	0·32	0·31	0·29	0·27	0·36	0·37	0·35	0·33
MnO	0·16	0·19	0·18	0·20	0·13	0·16	0·16	0·20	0·19	0·28	0·21	0·19	0·12	0·11	0·18	0·13	0·16
CO_2	3·1	0·07	0·01	0·02	0·23	0·22	0·09	0·31	1·0	1·1	0·30	0·07	0·09	4·3	0·43	0·21	0·10
TOTAL	99	100	99	100	99	99	99	100	99	99	99	99	99	100	99	99	99
Nature of alteration	C	F	S	F	F	Sp	F	F	S, C	C, S	F	F	F	C, Sp	F	F	F

Sample No.	*45*	*47*	*50*	*52*	*53*	*55*	*56*	*57*	*60*	*61*	*62*	*63*	*65*	*66*	*68*	*69*	*70*
SiO_2	50·3	50·5	48·8	49·4	48·7	50·7	59·8	75·0	49·7	49·7	49·8	48·9	49·9	49·5	64·2	50·0	48·1
Al_2O_3	13·8	12·9	13·5	12·8	13·8	13·6	12·9	12·0	13·0	12·7	12·9	12·2	13·1	13·3	12·3	13·7	12·3
Fe_2O_3	3·9	3·4	4·7	4·0	3·8	3·4	2·0	0·58	6·0	5·7	5·2	5·3	3·3	4·3	2·4	1·6	4·3
FeO	8·3	7·9	8·1	9·4	8·6	8·5	6·2	1·3	6·8	7·9	7·6	8·2	8·3	8·0	3·6	9·5	9·6
MgO	6·3	6·1	6·0	5·8	6·8	5·5	2·9	0·38	4·6	6·0	4·7	4·4	6·4	5·6	2·3	5·5	5·1
CaO	9·8	9·9	9·3	7·5	10·2	8·8	2·8	0·36	8·1	5·4	5·6	8·3	10·0	8·4	4·4	6·3	9·6
Na_2O	2·4	2·3	2·3	3·0	2·1	2·5	3·9	4·1	2·9	4·7	4·3	2·2	2·4	2·9	2·9	3·6	2·3
K_2O	0·42	0·48	0·66	1·2	0·82	0·71	2·6	4·3	1·4	1·2	2·1	1·7	0·44	1·5	4·4	2·1	0·75
H_2O	2·0	2·3	2·3	3·4	1·7	3·0	3·5	1·5	2·9	3·2	2·6	3·0	2·3	2·6	1·9	2·9	2·5
TiO_2	2·2	2·2	2·9	2·7	2·6	2·3	1·8	0·28	2·7	3·0	3·0	3·3	2·2	2·4	0·98	2·5	3·2
P_2O_5	0·24	0·25	0·34	0·34	0·27	0·32	0·63	0·08	0·46	0·46	0·49	0·63	0·25	0·34	0·15	0·36	0·37
MnO	0·24	0·19	0·12	0·20	0·19	0·15	0·09	0·01	0·15	0·18	0·17	0·20	0·16	0·16	0·10	0·19	0·18
CO_2	0·01	0·20	0·01	0·33	0·06	0·06	0·02	0·04	0·11	0·02	0·65	0·61	0·17	0·04	0·24	0·27	0·67
TOTAL	100	99	99	100	100	100	99	100	99	100	99	99	99	99	100	99	99
Nature of alteration	Fg	Fg	Fg	S, Sp	S	Sp	Sp, S	Sp	S, Sp	S, A	S, A	Fg	Fg	S, A?	Sp, S	S, A, Sp	F

Key as in Table 1; analyses by N. G. Skinner (Reston) using rapid-rock methods of Shapiro (1975).

Table 2 (*continued*)

Sample No.	*71*	*72*	*73*	*74*	*75*	*76*	*77*	*79*	*80*	*81*	*84*	*85*	*86*	*87*	*88*
SiO_2	47·1	47·8	49·5	50·2	49·0	44·8	46·6	49·4	49·9	45·7	46·5	47·0	49·9	49·9	48·1
Al_2O_3	13·4	12·2	13·3	12·9	13·5	12·5	13·8	12·7	13·5	12·9	14·6	13·2	13·0	12·4	12·9
Fe_2O_3	4·2	5·0	6·0	6·6	5·4	2·2	4·0	1·5	4·5	3·9	4·4	5·4	6·8	6·6	5·6
FeO	8·5	7·2	6·4	6·9	7·5	9·7	7·9	12·2	8·0	7·4	5·4	7·4	5·1	7·1	7·6
MgO	7·1	3·2	5·1	5·1	7·4	3·5	4·5	6·0	5·5	5·5	2·1	5·1	5·6	4·5	3·7
CaO	7·5	6·9	8·8	5·5	5·5	11·0	9·1	4·9	6·2	11·5	12·2	8·8	9·1	8·0	8·1
Na_2O	3·5	1·8	2·3	3·1	2·6	2·0	2·0	3·8	3·5	1·9	2·8	2·4	2·6	2·5	2·8
K_2O	1·7	3·1	0·87	1·6	1·2	0·60	0·66	1·3	1·6	0·47	1·1	0·68	0·7	1·2	2·0
H_2O	3·4	3·4	3·9	4·0	4·6	2·3	5·2	3·2	3·3	2·8	2·0	2·9	3·5	3·1	2·4
TiO_2	2·7	2·6	2·5	2·9	2·6	2·4	2·4	3·1	2·4	2·1	2·3	2·6	2·2	2·9	2·7
P_2O_5	0·30	0·44	0·34	0·42	0·34	0·33	0·33	0·30	0·34	0·27	0·39	0·32	0·31	0·45	0·49
MnO	0·16	0·17	0·17	0·21	0·15	0·17	0·10	0·14	0·18	0·17	0·20	0·17	0·24	0·15	0·26
CO_2	0·07	5·5	0·43	0·06	0·01	7·8	3·4	0·07	0·23	4·3	6·0	3·0	0·44	1·1	2·7
TOTAL	100	99	100	99	100	99	100	99	99	99	100	99	99	100	99
Nature of alteration	S, A	C, S	F	S, Sp	S, Sp	C	Sp, C	A, S, Sp	S, A, Sp	C	C, Sp	C, Sp	F	C, Sp	C

Table 3 Analyses of dyke rocks

Sample No.	*7*	*13*	*37*	*46*	*49*	*54*
SiO_2	49·4	49·6	48·9	49·6	49·4	49·2
Al_2O_3	12·73	13·72	14·09	13·80	13·30	13·64
Fe_2O_3	4·12	5·52	4·83	4·16	4·36	4·38
FeO	10·98	8·28	8·96	8·89	9·63	9·00
MgO	5·00	5·58	6·40	6·63	6·41	6·33
CaO	9·13	6·17	10·35	9·51	9·57	7·77
Na_2O	2·34	2·88	1·93	2·18	2·03	2·19
K_2O	0·66	3·06	0·39	0·47	0·46	0·79
H_2O	0·74	2·29	1·93	1·73	2·08	2·68
TiO_2	2·91	2·41	2·59	2·20	2·71	2·42
P_2O_5	0·29	0·32	0·24	0·20	0·25	0·31
MnO	0·17	0·15	0·16	0·16	0·20	0·16
CO_2	1·9	0·06	0·08	0·06	0·05	0·33
TOTAL	100·37	100·04	100·85	99·59	100·45	99·20
Nature of alteration	F	S, Sp	F	F	F	Sp, C, S?

Analyses made using XRF and wet-chemical methods (analysts; K. S. Waterhouse & J. Bowman, Lancaster).

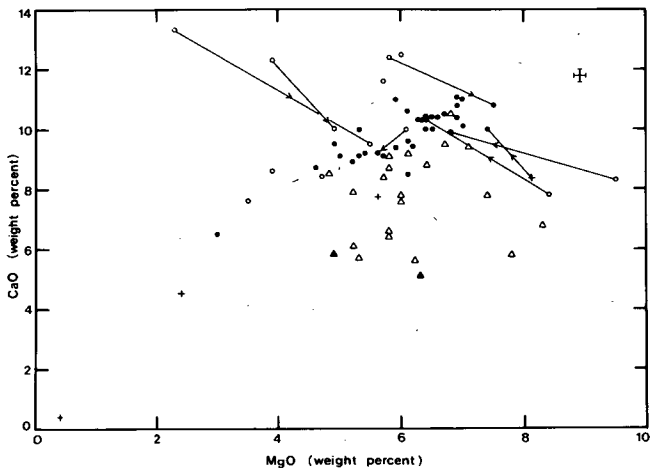

Figure 2 CaO-MgO variation diagram showing the effects of various secondary mobilization processes; tie-lines connect margins and centres of certain dykes, arrows towards centres; ● fresh, ○ carbonated, △ sericitised, ▲ albitised, + serpentinised, the terms referring to the dominant characteristic of each specimen. Analyses recalculated 100% volatile-free before plotting; cross denotes estimated analytical imprecision.

Table 4 Margin/centre concentration ratios involving mobile elements and H_2O and CO_2 analyses (weight per cent)

Margin sample	*39*	*28*	*76*	*10*	*33*
Centre sample	*40*	*27*	*77*	*11*	*34*
SiO_2	0·89	1·01	0·98	1·00	0·99
MgO	1·09	1·09	0·80	0·77	1·31
CaO	1·09	0·84	1·23	1·15	0·76
Na_2O	1·08	1·26	1·00	0·92	1·20
K_2O	0·71	0·88	0·93	0·63	1·09
Ba	1·07	0·90	0·79	0·73	1·08
Cs	0·86	0·71	—	—	—
Pb	5·20	>7	0·74	0·88	4·11
Rb	0·44	0·62	1·14	0·40	1·20
Sr	0·88	0·77	1·02	0·76	1·00
Zn	2·37	1·21	0·68	1·57	1·66
H_2O margin	4·1	3·9	2·3	2·5	6·1
H_2O centre	2·3	3·0	5·2	2·5	2·8
CO_2 margin	4·3	0·22	7·8	1·3	1·1
CO_2 centre	0·43	0·23	3·4	0·07	0·30

Table 5 Chemical effects of remobilization processes

	Sericitisation (of feldspar)	*Hydration* (Leaching of glass, serpentinisation)	*Carbonation*	*Albitisation*
Na	+	−	−	+
K	+		+, −	+
Mg	(+)		−	(+)
Ca	−		+	−
Ba	+			+
Cs	−	−	−	−
Rb	+		(−)	+
Sr	+		−	(+)
Pb	+, −	−	+, −	
Zn			+	

Blank no discernible effect, ( ) minor effects, + added (or unchanged), − subtracted (or unchanged).

Table 6 Test of chemical homogeneity along dykes

	Loch Long–Auchterarder						*Campsie*			*Loch Fyne–Perth*						Estimated analytical error
Sample No.	*13*	*51*	*54*	*41*	*42*	*40*	*60*	*61*	*62*	*11*	*53*	*29*	*30*	*31*	*32*	
Zr	186	182	187	186	198	184	184	229	223	113	133	119	150	144	142	±4%
Hf	4·6	4·9	4·8	4·5	4·6	4·5	5·0	5·4	5·2	3·3	3·5	3·2	3·9	3·9	3·8	±4%
Nb	18	21	20	20	21	20	24	24	25	14	19	17	19	19	19	±5%
Ta	1·17	1·18	1·17	1·19	1·16	1·21	—	1·30	1·83	1·01	0·99	1·04	1·16	1·17	1·17	±6%
Th	3·2	3·1	3·0	3·0	3·0	3·2	2·4	2·7	2·8	1·0	1·4	1·1	1·5	1·4	1·5	±10%
TiO_2	2·5	—	2·5	—	2·6	2·5	2·8	3·1	3·1	2·4	2·6	2·6	2·7	—	2·9	±0·05 abs.
P_2O_5	0·32	—	0·31	—	0·37	0·39	0·48	0·47	0·51	0·27	0·28	0·27	0·30	—	0·34	±0·04 abs.

Zr–Th in p.p.m. TiO_2, P_2O_5 in wt% (100%, volatile-free).
Samples arranged in W-E order within each dyke.
In the Loch Fyne dyke, samples 29 and 30 are from W and E of the Highland Boundary fault respectively.

Assuming that the incompatible elements are more reliable indicators of the path of differentiation, then that path is the reverse of that in the Longniddry dyke, where the central zone is more evolved.

Judging from these examples, a minority of the (thicker?) dykes demonstrate compositional variations, perpendicular to the strike, which may be symmetrical about the dyke centre. Further work is required to determine the nature of the fractionation, whether it occurred *in situ* or prior to intrusion and how it was related to the major differentiation processes affecting the dyke magmas.

5.4. Major element variation

The dykes show major element variations broadly comparable to those in other continental and oceanic island tholeiite suites (Carmichael *et al.* 1974). Using MgO as a measure of differentiation (Fig. 3), SiO_2, FeO_t, TiO_2 and P_2O_5 show

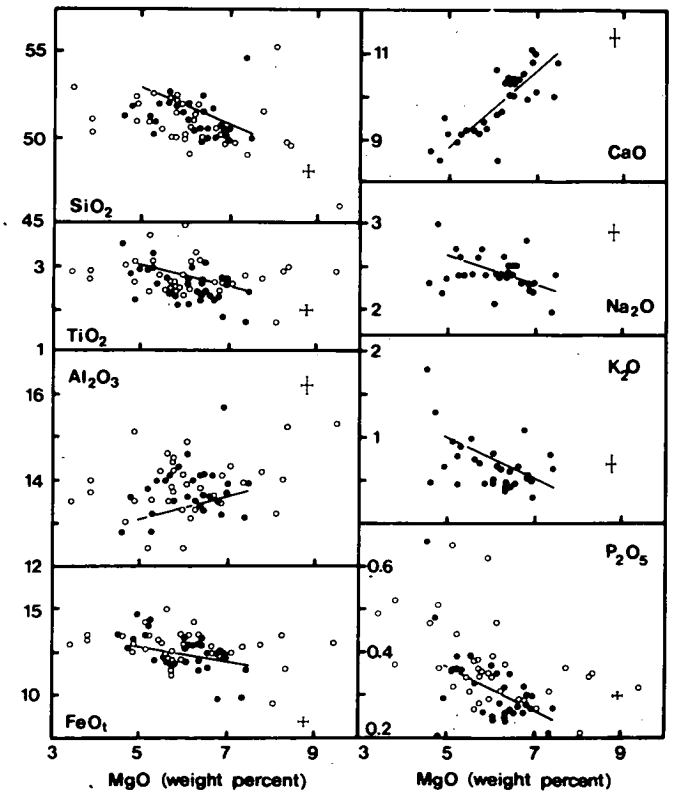

Figure 3 MgO variation diagrams for major oxides in the dykes; ● fresh rocks, ○ altered rocks; fresh rocks only plotted for mobile elements (Ca, Na, K); crosses denote estimated analytical imprecision. Solid lines represent the compositional range modelled in the fractionation calculations. Analyses calculated 100% volatile-free before plotting.

muted increases, CaO a rather regular decrease and Al_2O_3 a scattered, overall decrease in more fractionated rocks. Na_2O and K_2O show overall increases against decreasing MgO.

The geochemical similarity of dyke compositions to those of the *in situ* differentiation trends of the sill complex suggests that low-pressure fractionation was an important factor in magmatic evolution. There are also close similarities (Fig. 4) between the Scottish rocks and the compositional trends in the differentiated Alae lava lake, Hawaii (Wright & Peck 1978), which evolved, in more magnesian compositions, by fractionation of olivine-plagioclase-pyroxene assemblages.

It may be inferred that the more magnesian Scottish basalts separated the same minerals, with the addition of early crystallizing Fe-Ti oxides. This has been tested quantitatively using the linear programming model of Banks (1979). In the absence of relevant data for the Scottish rocks, the mineral analyses employed are those from the Alae lava lake basalts (Wright & Peck 1978, table 7, excluding pigeonite and magnetite analyses) and the parent and residual magma compositions are estimates of median compositions of the dykes at 7·5 and 5% (Table 7).

The model shows that the compositional variation within the dykes in the range 7·5 to 5% MgO can be satisfactorily

Table 7 Estimated median compositions and C.I.P.W. norms of the dyke rocks at varying MgO contents

	A	B	C			A	B	C
SiO_2	50·3	52·9	53·0		q	1·0	5·9	4·3
Al_2O_3	13·8	13·1	12·8		or	2·2	6·1	8·8
FeO_t	11·7	12·7	13·6		ab	18·9	22·0	23·4
MgO	7·5	5·0	4·5		an	26·4	21·1	17·9
CaO	11·1	8·9	8·7	di	wo	11·3	8·6	9·1
Na_2O	2·2	2·6	2·8	di	en	6·1	3·9	3·7
K_2O	0·4	1·0	1·5	di	fs	4·8	4·6	5·5
TiO_2	2·4	3·0	3·2	hy	en	12·5	8·5	7·4
P_2O_5	0·24	0·37	0·45	hy	fs	9·5	10·4	10·7
MnO	0·17	0·21	0·21		mt	2·1	2·1	2·1
					il	4·6	5·8	6·0
					ap	0·6	0·9	1·1
Rb	9	27	29		Nd	18	40	45
Cs	0·3	0·9	1·0		Sm	4·8	8·3	9·2
Ba	200	450	500		Eu	1·5	2·3	2·5
Sr	310	320	?		Gd	4·0	6·7	7·4
Pb	8	22	25		Tb	0·8	1·3	1·4
Th	1·0	3·0	3·5		Tm	0·23	0·50	0·55
U	0·4	1·0	1·1		Yb	1·9	2·9	3·0
Zr	120	200	220		Lu	0·25	0·44	0·48
Hf	3·0	5·0	5·5		Y	24	36	38
Nb	14	22	24		Co	50	37	34
Ta	0·95	1·4	1·5		Ni	115	35	20
La	13	32	37		Zn	65	100	108
Ce	26	56	58		Sc	33	26	24

Analyses presented volatile-free and with all Fe as FeO (FeO_t); for norm calculations, Fe_2O_3 assumed to be 1·5% (wt).

modelled by extracting an assemblage of 5% olivine, 21% pyroxene, 22·5% plagioclase and 1·5% Fe-Ti oxide, the total amount of crystallization being some 50%. The tested fractionation trend is shown as solid lines on Figure 3.

This is not, of course, a unique solution: other assemblages, especially involving Ca-poor pyroxene, are perfectly acceptable. Furthermore, the spread of the data in the variation diagrams indicates that the dykes do not belong to a unique liquid line of descent. Nevertheless, the calculation shows that the compositional range may be expressed in terms of the observed early-separating phases and that is is consistent with a low-pressure fractionation history.

5.5. Evolution at low pressure

The most evolved dykes are tholeiitic andesites having MgO between 4 and 5%. Information on the further stages of differentiation must be sought in the sill complex. In Figure 4, major element data for sill rocks ranging from dolerite to aplitic granites are compared to the composition field of the fresh dykes and to the liquid line of descent of the Alae lava lake. The analyses confirm the consanguinity of the dyke and sill magmas. They also suggest that the Hawiian example is a good analogue of the crystallization of the sill complex. It can be inferred, therefore, that the fractionating assemblage in the more differentiated sill members was plagioclase-pyroxene–Fe-Ti oxides–apatite (Wright & Peck 1978).

One important difference between the Scottish tholeiites and the Alae magma may be noted. As a result of the earlier crystallization of ilmenite, FeO_t and TiO_2 show only a muted increase in the composition range 8 → 5% MgO and the maximum values attained are lower than in the Alae magma. Predictably, SiO_2 increased rather more rapidly as a consequence (Fig. 4).

5.6. Evolution at higher pressures

Available evidence (Frey *et al.* 1978) suggests that fertile peridotite mantle has an Mg-value (100 Mg/(Mg+Fe)) of ⩾88–89. Mafic magmas derived from such a source will have Mg-values of 68–75 for up to about 30% melting. Unless the sources of the more magnesian members of the dyke suite (Mg-values ~58–59) were considerably more Fe-rich than normally considered to be the case (c.f. Wilkinson & Binns 1977), it must be assumed that those melts are *not* primary magmas but have been modified by polybaric fractional crystallization.

Though normative olivine has been recorded in only one of the fresh dykes, a trend of decreasing "q+q in hy" with increasing MgO makes it likely that the dyke magmas were derived from olivine tholeiite parents. It may be inferred that olivine-dominated fractionation at pressures <8 kb (Yoder 1976) drove the magmas from olivine- to quartz-normative type, a suggestion in line with the presence of olivine nodules in a dyke from Norman's Law (71). This phase of evolution drove the magmas close to a low-pressure, low-variancy condition involving ol+aug+pl+Ca-poor px+Fe-Ti oxides.

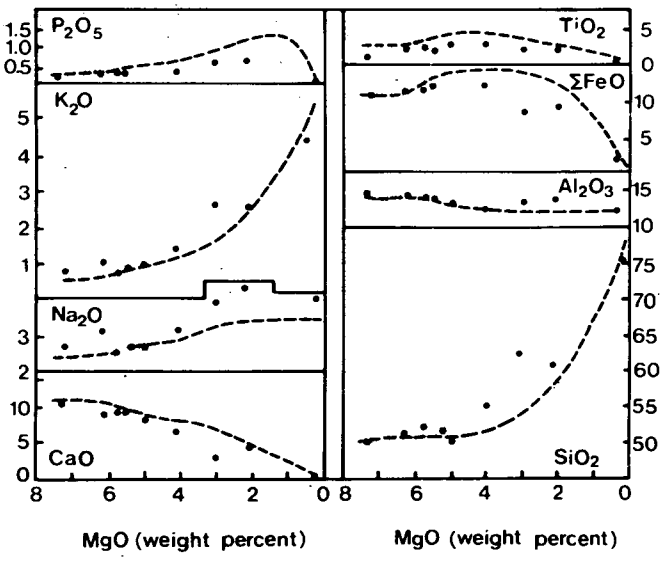

Figure 4 MgO—major oxides variation diagrams (c.f. Wright & Peck 1978, Fig. 4); field of Scottish dykes >4·5% MgO. ● analyses of rocks from the Midland Valley sill complex (this paper, Table 2, nos 56, 56, 57 and Guppy & Sabine 1956, nos 676, 677, 680, 681, 682). Dashed line—liquid line of descent, Alae lave lake, Hawaii (Wright & Peck 1978).

6. Trace element geochemistry

6.1. Mobile elements

The processes which resulted in remobilization of these elements have been discussed earlier (5.1). Data for fresh samples only are plotted against MgO in Figure 5.

The value of the estimated median magmatic abundances (Table 7) can be judged against the degree of scatter for each element. Thus, in the case of Pb, remobilization has been sufficiently intense that the magmatic abundances can be estimated only to within several factors. Generally, the alkali earth metals, where the estimated abundances are probably within 5 to 25% of the real value, appear to have been less mobile than the alkali metals (40–50%).

6.2. Stable elements

Th, U, Zr, Hf, Nb, Ta and the REE all behaved relatively incompatibly during crystallization of the dyke magmas, while Co, Ni and Sc were compatible. It is possible to model the trace element behaviour satisfactorily using the mineral assemblage deduced from major element compositions and the partition coefficients listed in Table 8. Graphical examples of the modelling are given in Figures 9 and 12.

Certain aspects of the stable element chemistry deserve further comment. For example, the fresh dykes show a trend of increasing Th/U ratio with increasing differentiation (Fig.

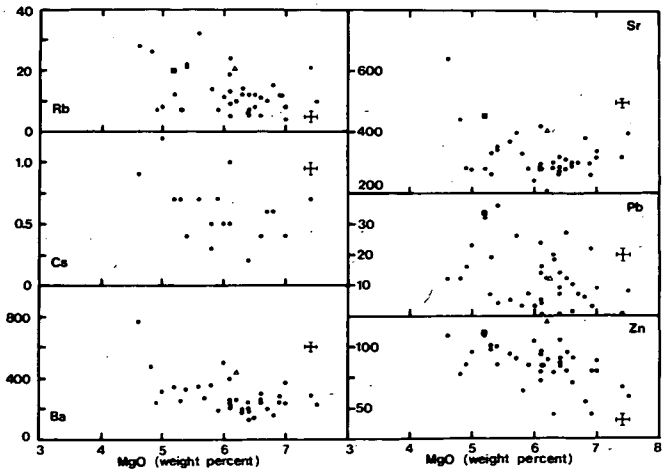

Figure 5 MgO-mobile trace element variation diagrams for fresh dyke rocks only; △ Norwegian tholeiitic lava (89); ■ average, Little Whin sill (Dunham & Kaye 1965); crosses denote estimated analytical imprecision. Analyses nos 90 and 73 have been omitted from the Cs and Ba diagrams respectively, to preserve the scales.

6), a trend continued by the acid residua of the sill complex (Th/U in 57 = 4·7), Previous evidence from differentiated tholeiitic suites has invariably found that this ratio remains constant (Gottfried *et al.* 1968). Two explanations seem possible to explain this anomaly. Firstly, the spread of Th/U ratios in the Scottish rocks may be a result of the poor analytical precision of U at such low concentrations. Secondly, the higher ppO_2 inferred to have operated during magmatic evolution may have resulted in oxidation of U to uranyl ions and promoted an increased mobility relative to otherwise comparable tholeiitic suites. More precise U analyses, especially of margin-centre pairs, are required to permit an unequivocal interpretation of the data.

Table 8 Values of mineral-liquid partition coefficients used in fractionation trend calculations

	Ol	Cpx	Pl	Fe-Ti oxides	Reference(s)
Zr	0·01	0·1	0·01	0·28	Pearce & Norry (1979, table 1)
Nb	0·01	0·1	0·01	2·0	Pearce & Norry (1979, table 1) except oxide—arbitrary
Ti	0·02	0·3	0·04	4	Pearce & Norry (1979, table 1) except oxide—assumed
Co	2·5	2·2	0·05	10	Irving (1978)
Ce	0·0005	0·098	0·12	0·007	Arth (1976); Hanson (1977); Irving (1978); values used to 40% crystallization only
Yb	0·0015	0·28	0·067	0·06	
Ni	14	2·5	0	12	Irving (1978)

Mineral assemblage: olivine (Ol) 0·105, clinopyroxene (Cpx) 0·417, plagioclase (Pl) 0·446, Fe-Ti oxides 0·033.
Equation used in calculations is that given by Arth (1976, eq. 8).
In some cases, the values have been selected from ranges given in the source reference.

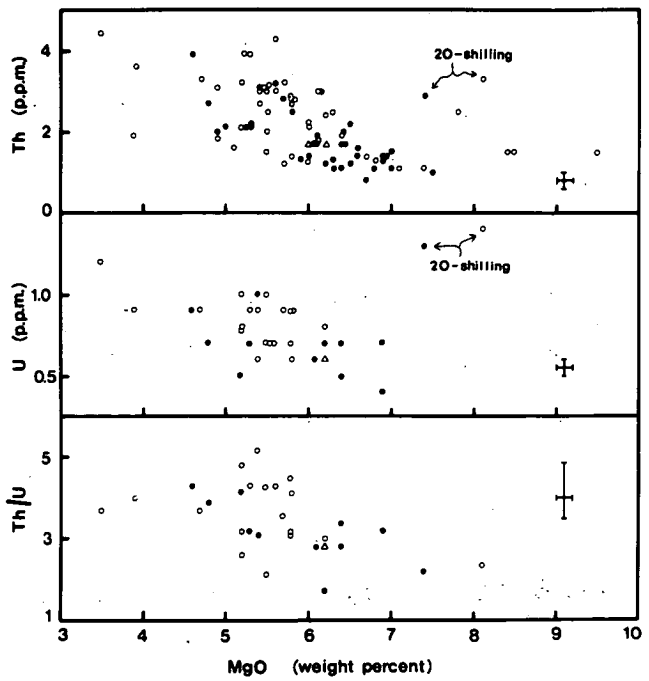

Figure 6 MgO-Th, U, Th/U variation diagrams for dyke rocks; ● fresh rocks, ○ altered rocks, △ Norwegian tholeiitic lavas; crosses denote estimated analytical imprecision.

The graphical method of Pearce and Norry (1979) is used to explore Zr-TiO_2 and Zr-Y relationships in the dykes in Figure 8. These are qualitatively explicable in terms of ol + cpx ± pl ± mt ± opx fractionation in the compositional range basalt to tholeiitic andesite, while *appreciable* oxide removal in more differentiated magmas is demanded by the sharp decrease in TiO_2 abundances.

It is probable that the main solid phases into which Nb and Ta were partitioning were pyroxene and Fe-Ti oxides. It was pointed out earlier (5.5) that oxides separated relatively early during crystallization of the dyke magmas, resulting in a muted increase in FeO_t and TiO_2 to maxima between 5–6% MgO. Nb and Ta mimic this behaviour (Fig. 7).

Nb-TiO_2 distributions are modelled in Figure 9 (details in Table 8). The rather good fit is consistent with the simple fractionation scheme applied in this paper. The fit is least successful at the high Nb end of the trend, when increased proportions of oxide precipitation are required to account for the approximately constant TiO_2 contents.

Data from the more differentiated members of the sill complex (Fig. 4) indicate that FeO_t and TiO_2 drop sharply to low abundances in the most silicic rocks. It may be noted, however, that during these later stages of evolution, Ti was more strongly partitioned into the crystalline phases than either Nb or Ta. This can be demonstrated by examining 100.Nb/Ti ratios (Fig. 10). The 100.Nb/Ti ratio remains constant, or perhaps increases slightly, through the range of differentiation exhibited by the dykes. There is an abrupt increase towards the aplitic residua of the Northfield (Stirling) and Dollar sheets, to values >1. This behaviour is

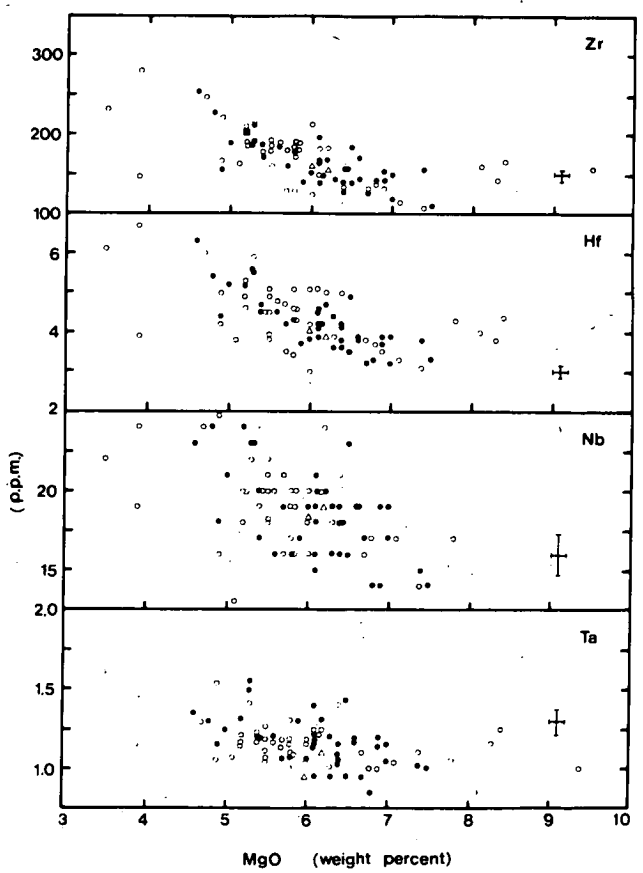

Figure 7 MgO-Zr, Hf, Nb and Ta variation diagrams for dyke rocks; ● fresh rocks, ○ altered rocks, △ Norwegian tholeiitic lavas; ■ average, Little Whin sill (Dunham & Kaye 1965); crosses denote estimated analytical imprecision.

similar to that in other tholeiitic masses (Gottfried *et al.* 1968).

For most suites (Fig. 10), the 100.Nb/Ti ratio in mafic rocks approximates closely to 0·13. This suggests that the mantle sources of these tholeiites are fairly uniform in Nb-Ti geochemistry and that higher-pressure evolution does not notably alter the ratio. The Hangnest intrusion in South Africa is a notable exception; its 100.Nb/Ti ratio of <1 reflects an unusually low Nb content. In this respect, the range of 100.Nb/Ti ratios in the more magnesian members of the Scottish suite (from <0·1 to 0·15) lies outside experimental error and almost certainly reflects small variations in the ratio in the source rocks.

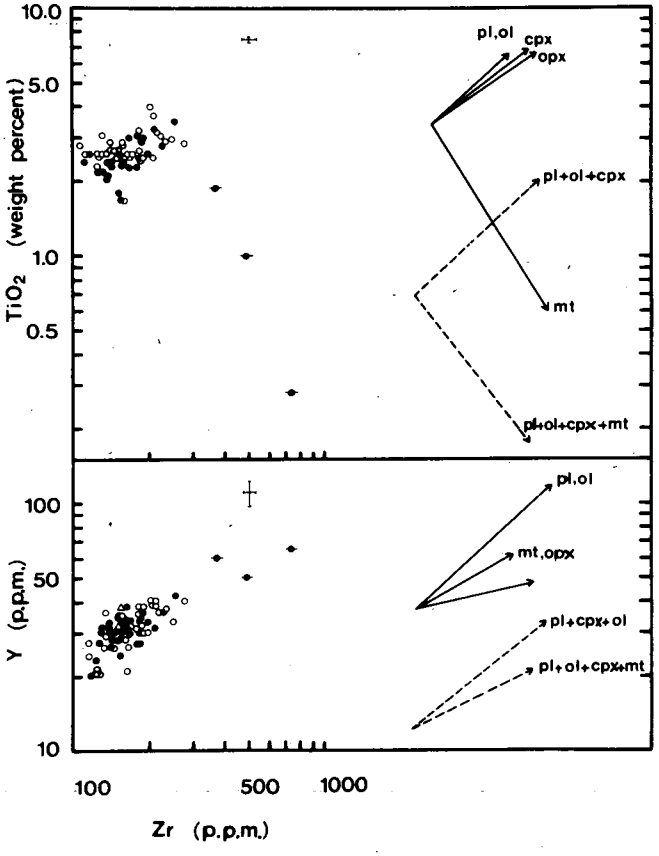

Figure 8 Compositional trends in the Scottish tholeiites compared to the modelled fractionation trends of Pearce and Norry (1979); selected mineral and assemblage vectors are those most relevant to the Scottish rocks; ● fresh rocks, ○ altered rocks, △ Norwegian tholeiitic lavas, –●– intermediate and silicic samples from Northfield (Stirling) and Dollar sheets; crosses denote estimated analytical imprecision.

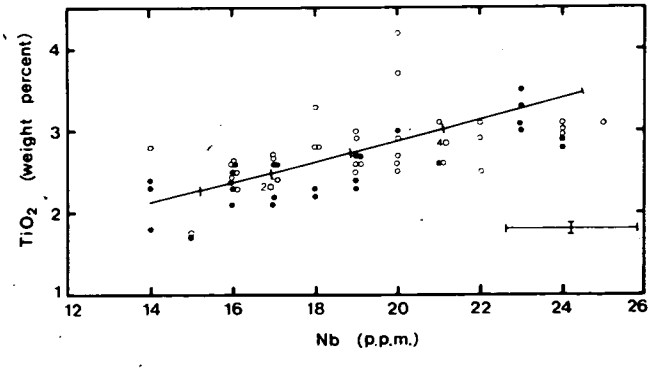

Figure 9 Nb-TiO_2 variation diagram for the dyke rocks; ● fresh rocks, ○ altered rocks; cross denotes estimated analytical imprecision. Numbers and ticks on the modelled Rayleigh fractionation curve (solid line) represent per cent crystallization of the assumed parental magma.

Divergence of the various trends in more differentiated compositions (Fig. 10) results from varying amounts of oxide fractionation. Relatively early separation of oxides in the Scottish tholeiites resulted in sharp increases in the Nb/Ti ratio at more magnesian compositions than in the comparative suites.

As the comparisons in Table 9 show, the Scottish rocks are "typical" continental tholeiites as regards REE.

A commonly sought explanation for the HREE-depleted pattern of continental tholeiites is that garnet± clinopyroxene were residual phases in the source mantle after fusion (Helmke & Haskin 1973; Lo & Goles 1976; Leeman 1976). It may be noted, however, that the more magnesian Scottish rocks have Al_2O_3/CaO ratios of about 1·2, i.e. close to those of chondrites. It has been argued that such basalts must be, or be derived from, liquids generated

Table 9 Comparison of REE profile characteristics of the Scottish tholeiites with those of continental basalts compiled by Leeman (1977)

Locality	$[La/Sm]_{E.F.}$	$[Yb]_{E.F.}$
Snake River Plain		
McKinney Basalt pillow glass	1·9	19
low REE tholeiite	1·4	11·5
high REE tholeiite	1·9	20
Columbia River Plateau		
lower Picture Gorge	1·4	12·5
upper Picture Gorge	1·7	14·5
high-Mg lower Yakima	2·5	14
low-Mg lower Yakima	2·4	19
middle Yakima	2·3	17
Steens Mountain		
average of 52	2·0	16·5
Deccan		
miscellaneous (range of 18)	1·8–2·5	12–20
Scottish, late Palaeozoic		
Magnesian basalt (71)	1·4	8·2
Tholeiitic andesite (63)	2·1	16·9

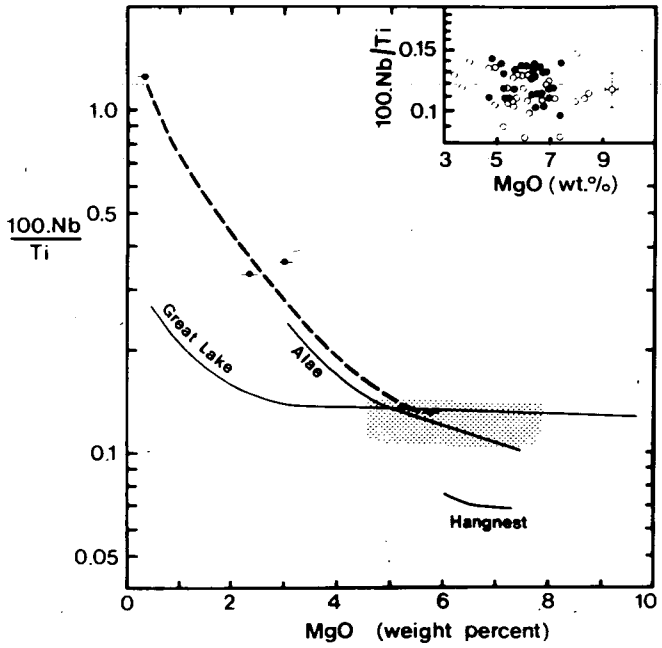

Figure 10 MgO-(100. Nb)/Ti variation diagram for the dyke rocks (● fresh rocks, ○ altered rocks), samples from the differentiated sheets (–●–) and comparative tholeiitic suites from the Alae lava lake (Wright & Peck 1978), Great Lake, Tasmania (Gottfried *et al.* 1968) and Hangnest, Karroo (le Roex & Reid 1978). Dashed line is inferred trend for the Midland Valley sill complex. Shaded area is field of dyke compositions; individual data points shown in inset; cross on symbol denotes estimated analytical imprecision.

by sufficiently high degrees of mantle fusion that neither garnet or clinopyroxene were significant residual phases (Frey *et al.* 1978, p. 473). It seems unlikely, therefore, that garnet or clinopyroxene retained HREE relative to LREE after generation of the tholeiite precusor magmas.

A more recent explanation for the LREE-enriched pattern is that the source regions were already enriched in LREE prior to the melting event. Hanson (1977), Frey *et al.* (1978), Mysen (1978), Wood (1979), and Hawkesworth and Vollmer (1979) have produced models, relating to a variety of basalts, whereby LREE-enriched fluids or melts migrate through the mantle, enriching some areas and depleting others, in LREE. Such a mechanism may have been applicable to the Scottish case and indeed Macdonald (1980) has invoked mantle metasomatism as a partial explanation for trace element variations in the *alkaline* members of the Permo-Carboniferous magmatism.

Whatever the cause of the REE-pattern in the more magnesian Scottish basalts, the further enrichment of LREE relative to HREE (Fig. 11) apparently requires continued clinopyroxene ± oxide fractionation, which would be in accord with other major and trace element data discussed above. This is modelled in Figure 12 (details in Table 8). The variations in Ce and Yb are satisfactorily duplicated by the model conditions over the range 7·5 to 5% MgO. A heavily increased partitioning of the HREE into the solid phases is indicated for more differentiated compositions, however. The trend in Figure 12 was calculated using $D_{Yb}^{px/l} = 1{\cdot}5$ and $D_{Yb}^{ox/l} = 2$ and a fractionating assemblage of px = 0·42, pl = 0·48 and ox = 0·1. These partition coefficients are higher than those compiled by Irving (1978) though Schock (1979, table iv) reports $D_{Yb}^{mt/l}$ up to 1·8 for titanomagnetites from ocean-floor basalts.

The question must be raised as to why the plagioclase fractionation apparently demanded by the major element data produced no Eu-anomaly in the magmas until very advanced stages of fractionation. The entry of Eu^{2+} into plagioclase is strongly dependent on fo_2 (Weill & McKay 1975) and it might be argued that relatively high values of ppO_2 in the Scottish magmas tended to keep Eu in the Eu^{3+} state, thus preventing its entry into plagioclase (cf. Thompson *et al.* 1980, p. 284).

The situation is not unique, however, in that other tholeiitic suites, such as the Tertiary lavas of Eastern Iceland, which developed under conditions of low ppO_2, show the same lack of a Eu anomaly (Wood 1978, p. 425). Wood points out that K_{Eu} is dependent on factors other than ppO_2, e.g. bulk liquid composition and temperature, and that these factors may have acted to prevent Eu entry into plagioclase.

A possible alternative lies in the data of Schock (1979), who showed that titanomagnetites separated from various basaltic rocks all demonstrate marked, negative Eu anomalies. Coprecipitation of plagioclase and oxides may have counteracted any tendency towards the development of an anomaly in residual magmas.

The development of a large Eu anomaly in the silicic liquids, as exemplified by the aplites (57, 68) indicates that K_{Eu} was significantly higher in the later stages of crystallization, whatever the critical factor, e.g. falling ppO_2, changing bulk liquid or feldspar compositions or changing temperatures (Wood 1978).

Mention should also be made of the relative depletion of the other intermediate REE in the aplitic rocks. Since apatite may concentrate intermediate REE relative to the L- and H-members, this effect may be ascribed to apatite fractionation in more evolved compositions (c.f. Wood 1978).

Of some interest is to compare the Ni/Co ratio of the Scottish tholeiites with those of comparable suites. The decrease of Ni/Co ratio with increasing differentiation of tholeiitic magma has been documented by Fleischer (1968), K_{Ni} clearly being $>K_{Co}$ as regards the ferromagnesian phases. Fleischer (1968) also noted the range of Ni/Co ratios at constant mafic index within such suites. This is elaborated in Figure 14. The ratio ranges from ~0·1 in the strongly

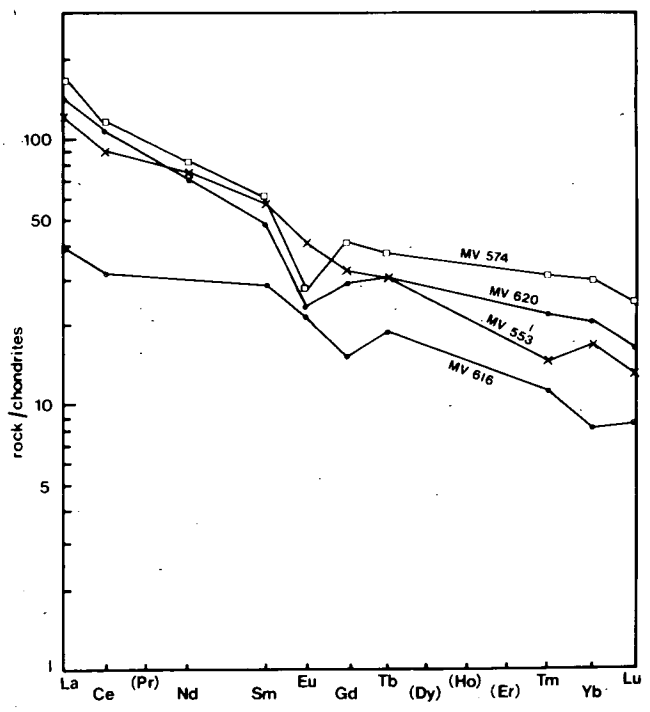

Figure 11 Chondrite-normalized REE patterns for a magnesian basalt (71), a tholeiitic andesite (63) and two aplite veins (57, 68). Chondrite concentrations are taken from Haskin *et al.* (1968). The basalt compositions were chosen to bracket all others not shown.

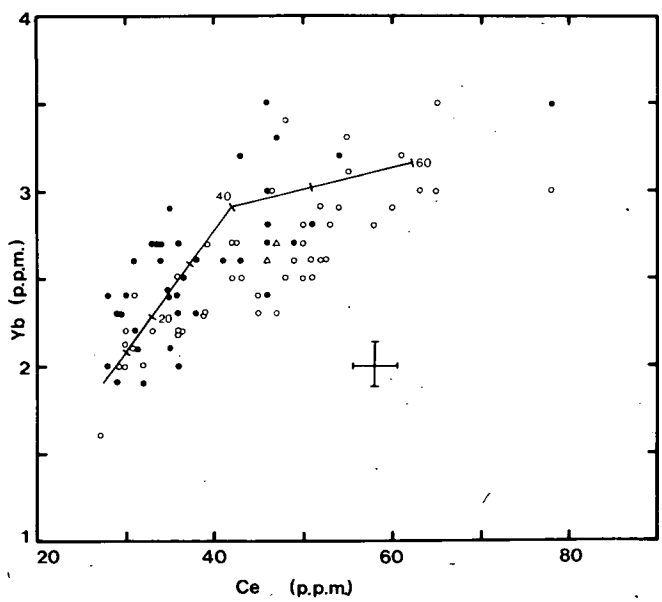

Figure 12 Ce-Yb variation diagram for the dyke rocks; ● fresh rocks, ○ altered rocks, △ Norwegian tholeiitic lavas; cross denotes estimated analytical imprecision. Numbers and ticks on the modelled Rayleigh fractionation curve (solid line) represent per cent crystallization of the assumed parental magma.

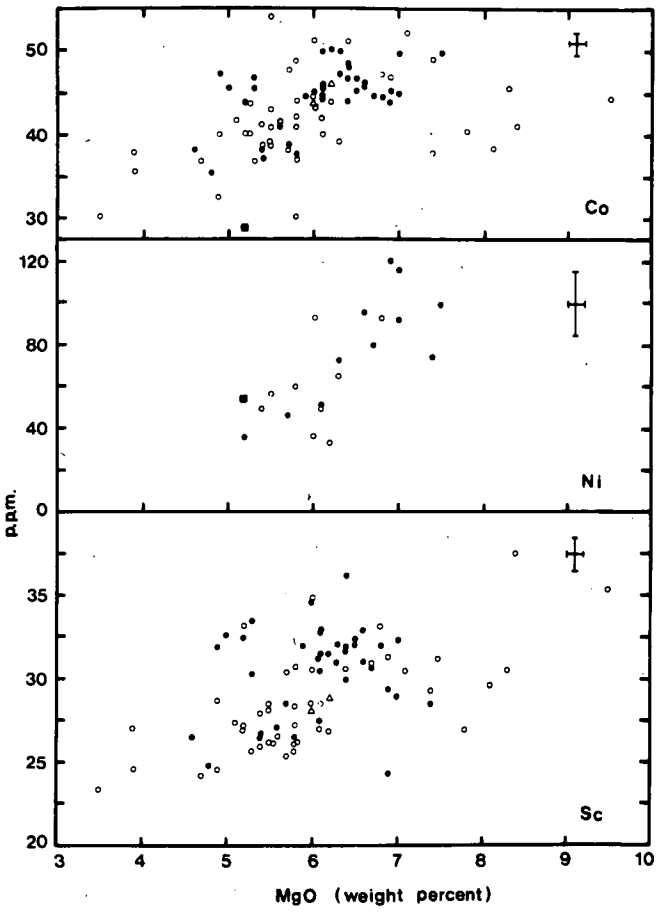

Figure 13 MgO-Co, Ni and Sc variation diagrams for the dyke rocks; ● fresh rocks, ○ altered rocks, △ Norwegian tholeiitic lavas; ■ average, Little Whin sill (Dunham & Kaye 1965); crosses denote estimated analytical imprecision.

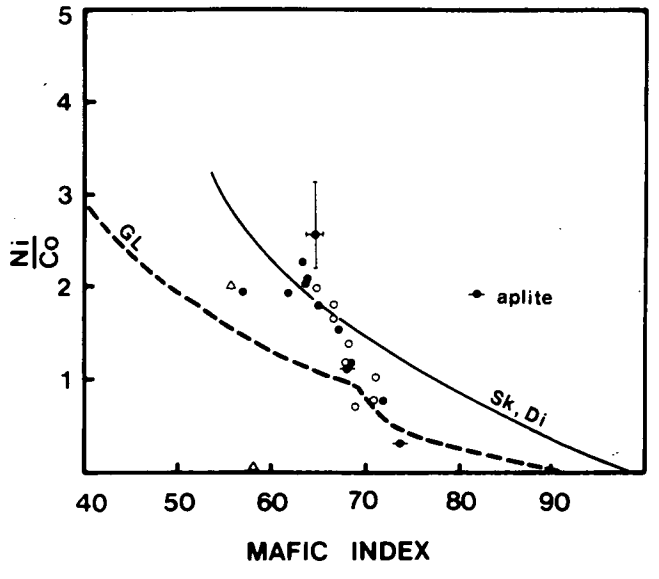

Figure 14 Ni/Co ratio-mafic index ((100. $FeO+Fe_2O_3$)/($FeO+Fe_2O_3+MgO$)) variation diagram for dyke rocks (● fresh, ○ altered) and specimens from the Northfield (Stirling) sill —●—; ▲, △ bulk, compositions of the Blaauwkrans and Hangnest sills, Karroo, S. Africa (le Roex & Reid 1978). Solid line—Skaergaard and Dillsburg intrusions, dashed line—Great Lake intrusion (Fleischer 1968, fig. 2); cross denotes estimated analytical imprecision for Scottish rocks.

Ni-depleted Hangnest intrusion to >3 for certain Skaergaard rocks.

Considering the major element similarities between these rocks, it seems improbable that widely differing fractionation histories have caused the spread in Ni/Co ratios. A more likely explanation is that Ni has been removed, prior to eruption, from the Ni-depleted varieties by sulphide fractionation (Desborough *et al.* 1968; Czamanske & Moore 1977; Duke 1979), or that the source mantle rocks have been heterogeneous as regards Ni and Co geochemistry.

The more magnesian Scottish dykes scatter around the trend for the Skaergaard and Dillsburg intrusions (Fig. 14) but more differentiated samples follow an apparent trend of rather sharply decreasing Ni/Co ratios to meet the Great Lake dolerite trend. This does not necessarily indicate a gross change in Ni-Co relationships compared to other tholeiitic sequences; rather, in suites such as the Scottish tholeiites where Fe-enrichment is muted during fractionation, the mafic index changes less over a given crystallization interval than in Fe-enriched sequences.

It is probably no coincidence that there is a kink in the Great Lake trend at that point (mafic index about 70) where the Scottish rocks join it. It may be surmised that the Great Lake magma reached a critical value of ppO_2 whereby either Ni-Co partitioning into the fractionating phases changed or a new phase began to separate.

7. Discussion

7.1. Inter-relationships between the trace elements

The various "incompatible elements" showed varying degrees of incompatibility during crystallization of the dyke magmas, as is shown by the following enrichment factors over the limiting composition range 7·5 to 4·5% of MgO:

K, Rb, Th, ?Cs	>3
Zr, Hf, LREE, Ba?	~2·5
Nb, Ta, P, HREE	~2.

The K-related elements show maximum enrichment factors of >3. From this it is inferred that the most evolved, tholeiitic andesite dykes represent greater than 65% crystallization of the magnesian parental magmas.

Between-dyke variations. The relationships between the stable elements may be used to comment upon geochemical variations between the dykes. Graphical analysis shows that, for all elements, the majority of dykes fall within a relatively restricted compositional range. This range is here termed the *Main Dyke series* (MDS); examples are shown on P-Nb and P-Zr diagrams (Fig. 15). On both diagrams, three dykes, from Campsie Linn, Wolfhill and Kinkell, fall outside the MDS range and it may be inferred that they are variants of the MDS in being rather P-rich. The Twenty-shilling dyke is a high Th-U variant (Fig. 6).

Compositional spread within the dykes is also indicated on variation diagrams using Zr as abscissa (Figs 8, 16). The scatter for most elements is outside that expected from analytical error and it must be assumed that it represents real between-dyke variations.

The ratio Zr/Nb (Fig. 16) is particularly informative in this respect since it is insensitive to the extent of partial melting of the mantle sources (Pearce & Norry 1979). This is because the minor phases which concentrate these elements are almost certainly absent from the residual mineralogy in equilibrium with tholeiitic magma. Variations in the ratio can, therefore, be confidently attributed to source heterogeneity.

Considerations of this sort, involving all the geochemical data, lead to the further conclusion that dykes which show anomalous (relative to the MDS) concentrations of one or more elements need not necessarily show anomalous concentrations of any other element. A specific dyke may have element concentrations within the MDS for all but 1 or 2 elements. Examples of the complexities of the anomalies are tabulated below.

Dyke	Sample Nos	Relative to MDS	
		High	*Low*
Culloch	38	Al	Fe, Ti, Sc
Twenty-shilling	27, 28	Si, Th, U, 100. Nb/Ti	Al, Fe, Ti, Co
Boddam	3	Sc, Co	
Dalcrue	24	Nb, Ta	
Wolfhill	21	P	100. Nb/Ti
Campsie Linn	20	HREE, Y	

The point to be stressed is that superimposed on the spectrum of major-element compositions, there is a small but real variation in trace elements which is largely non-systematic. Some dykes can be shown to be uniquely fingerprinted by their chemical composition. Probably all the dykes are to some extent unique though this may normally be within the limits of analytical error.

The dykes do not represent, therefore, the simple infilling of fissures by homogeneous magma. Rather, a plexus of small, partly independent, magma reservoirs, each contributing to the filling of segments of the dyke system must be envisaged.

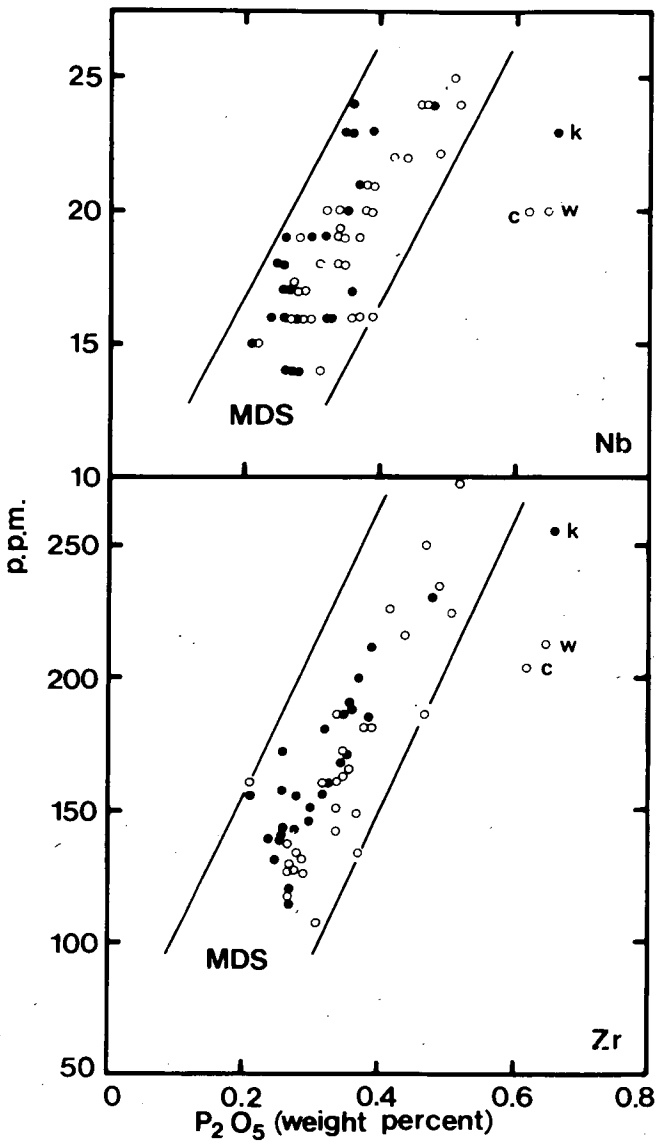

Figure 15 P_2O_5-Nb, Zr variation diagrams for the dyke rocks; ● fresh rocks, ○ altered rocks. MDS = Main Dyke Series. C = Campsie Linn, W = Wolfhill, K = Kinkell dykes (20, 21, 63, respectively).

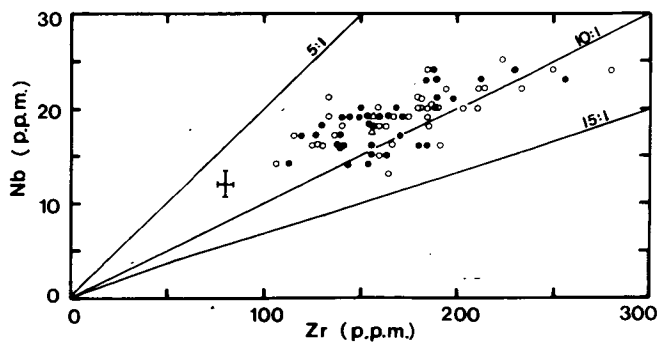

Figure 16 Zr-Nb variation diagram for the dyke rocks; ● fresh rocks, ○ altered rocks, △ Norwegian tholeiitic lavas; cross denotes estimated analytical imprecision. Solid lines are lines of constant Zr:Nb ratio.

7.2. Correlations with English and Scandinavian tholeiites

The most modern geochemical data for the Whin sill rocks of Northern England are those of Dunham and Kaye (1965) and Harrison (1968) for the Little and Great Whin sills respectively. The average compositions of these intrusions compare very closely with Scottish rocks of comparable MgO content, except for higher Al_2O_3 and lower SiO_2 contents. The Al_2O_3 determinations in the Little Whin rocks may be too high (Dunham & Kaye 1965, p. 255) and the inter-suite differences may not be significant. The rather lower SiO_2 abundances may be real.

The tholeiitic affinities of the B1 "Permian" lavas of the Krokskogen area in the Oslo Rift were first noted by Weigand (1975), who suggested that these lavas were not genetically related to the basalts of alkaline affinity of equivalent stratigraphic age elsewhere in the Rift. In correlating the lavas with the British intrusions, Francis (1978) points out that the Norwegian rocks are perhaps the only surface expression of the tholeiitic magmas.

Two lava samples from Krokskogen have been analyzed for certain trace elements (Table 1), to supplement the major and trace element data of Weigand (1975). Again, these compositions prove to be indistinguishable from the Scottish rocks when plotted on variation diagrams (Figs 5–8, 12, 13, 16) and the correlation of Francis (1978) seems to be fully justified.

The Central British province (Walker 1964) now appears to be part of a larger, North Sea province and an explanation for its development probably has to be sought (Francis 1978) in relative plate motions during late Carboniferous times.

7.3. Role of sialic contamination

The view that sialic contamination has played a significant role in the evolution of continental tholeiite magmas (Engel *et al.* 1965; Compston *et al.* 1968; Ragland *et al.* 1971; Faure *et al.* 1974; Smith *et al.* 1975) has not received universal support (Gottfried *et al.* 1968; Jamieson & Clarke 1970; Weigand & Ragland 1970; McDougall 1976; Leeman 1977; le Roex & Reid 1978). In particular, Leeman (1977) has interpreted Sr- and Pb-isotopic evidence to show that continental tholeiites have been derived, without crustal

Table 10 Comparison of selected oxide and element concentrations in the Scottish tholeiites with those in various tholeiitic suites

	MgO	FeO_t	TiO_2	Zr	Nb	P_2O_5	Sr	K_2O	Rb	Th	U	Rb/Sr	Reference
High-Fe-Ti type													
1 Alae lava lake, Hawaii	7·50	10·9	2·72	150	16·2	0·27	380	0·56	20	—	—	0·05	Wright & Peck (1978)
2 FETI-basalts, N Atlantic	5·58	15·0	2·47	180	—	0·23	182	0·56	13	1·6	0·47	0·07	Brooks & Jakobsson (1974)
3 Scottish late Palaeozoic tholeiites	7·5	11·7	2·4	120	14	0·24	310	0·4	9	1·0	0·4	0·03	This paper, Table 7.
4 Average low-Mg basalt, Karroo, Rhodesia	5·81	12·1	2·85	450	—	0·46	636	1·53	42	—	—	0·07	Jamieson & Clarke (1970)
5 FG-1 dyke D, Kangerdlugssuaq	5·79	14·7	4·36	290	—	0·36	202	0·58	13·2	—	0·53	0·07	Brooks & Nielsen (1978, table 1(a))
Low-Fe-Ti type													
6 Eastern N America high Ti, q-norm	7·41	10·4	1·12	92	9·5	0·13	186	0·66	21	2·2	—	0·11	Gottfried *et al.* (1978); D. Gottfried (unpubl.)
7 ENA high-Fe, q-norm	5·53	12·5	1·14	90	8·0	0·13	180	0·64	22	2·4	—	0·12	Gottfried *et al.* (1978); D. Gottfried (unpubl.)
8 Tasmanian dolerites	6·72	8·8	0·59	55	5	0·08	130	0·91	33	3·2	0·8	0·25	Gottfried *et al.* (1978); D. Gottfried (unpubl.); McDougall (1964)
9 Hy-norm, Antarctic dolerites	6·64	9·6	0·70	—	—	0·18	125	0·81	31	3·8	1·6	0·25	Compston *et al.* (1968)
10 Blaauwkrans, Karroo	7·55	10·1	0·90	77	4·2	0·14	167	0·56	29	—	—	0·17	le Roex & Reid (1978)
11 Hangnest, Karroo	6·18	9·4	1·18	168	5·7	0·25	194	0·87	22	—	—	0·11	le Roex & Reid (1978)
12 Birds River, Karroo	8·4	9·4	0·9	69	12	0·17	251	0·62	13	—	—	0·05	Eales & Robey (1976)

contamination, from ancient, lithospheric mantle sources characterized by higher Rb/Sr and U/Pb ratios than typical sub-oceanic mantle sources.

Apart from isotopic evidence, those elements which should most readily denote crustal contamination are those which do not readily fit into the lattice sites of the stable phases in the country rocks, e.g. K, Rb, Cs, Ba, U, Th, Ti, P and LREE (Green & Ringwood 1967). Secondary mobilization of the first 4-named of these in the Scottish dykes makes it impossible to assess their variation as a function of contamination. It should be noted, however, that there is no apparent relationship in the dykes between the contents of Th, Ti, P or LREE and the tectonic setting or country-rock lithology, despite the wide range of country rocks (gneisses of the Lewisian complex to essentially contemporaneous Carboniferous sediments). Perhaps more critical is that the Scottish rocks are so closely comparable to basalts from Hawaii and Iceland (Table 10), where continental crust is lacking. The chemical features of the dyke suite seem undoubtedly to be mantle related.

7.4. Comparisons with other continental and oceanic tholeiites

Chemical features of the dykes are compared in Table 10 to those of several other quartz-normative continental and oceanic tholeiites. The data broadly show two end-members, a high-Fe-Ti member also relatively high in P, Sr, Zr and Nb and a lower-Fe-Ti member enriched in K, Rb, Th and U and with higher Rb/Sr ratios.

Using data for q- and ol-norm tholeiites from 43 provinces, Jamieson and Clarke (1970) showed that K and Rb are broadly coherent with P, Sr, Ti and Zr. Their results are not at variance with the above suggestions: here we are dealing with a more restricted sample population and, therefore, with a different level of inter-suite variation. In fact, it is relevant that Jamieson and Clarke (1970, p. 187) noted the lower correlation coefficient of Rb with the other LIL-elements. While they ascribe it to analytical uncertainty, we stress that, in detail, Rb does not always follow the Ti-group in tholeiitic basalts.

Rather, the data are interpreted as clearly showing that enrichment or depletion of tholeiites in certain LIL-elements does not mean similar behaviour of all such elements (Gottfried *et al.* 1968). Thus, the Antarctic and Tasmanian dolerites are relatively high in the K-related elements and low in the Ti-related set. Since all these are incompatible, or nearly so, during the partial melting of the mantle and subsequent high-pressure fractionation, such variations may be taken to represent geochemical variability of the source regions of continental and oceanic island tholeiites.

A finer-scale variability is shown by individual suites. Thus, the Hangnest intrusion shows distinct Nb depletion (100.Nb/Ti = 0·08) but relative Zr enrichment. The Alae lava lake basalt is rather lower in FeO_t than other high-Fe-Ti basalts of similar MgO content. Clearly, a second-order type of source heterogeneity is superimposed on the broad pattern of element distribution described above.

The Scottish tholeiites are of high-Fe-Ti type. Their closest analogues chemically are basalts from Hawaii and those rocks from the North Atlantic Tertiary province termed FETI-basalts by Brooks and Jakobsson (1974). These authors (p. 145) point out that FETI-basalts tend to occur in areas of active lithospheric spreading and regions of excess basalt discharge ("hot spots"). The Midland Valley tholeiites, emplaced in relatively large volume over a short time period in a tensional environment, would thus appear to be normal in their tectonomagmatic affinities.

8. Acknowledgments

We thank C. S. Annell, P. A. Baedecker, E. Y. Campbell and L. J. Schwarz (U.S.G.S., Reston) and J. Bowman and K. S. Waterhouse (University of Lancaster) for analytical data; E. H. Francis and D. J. Fettes kindly provided samples from Norway and Barra, respectively.

References

Arth, J. G. 1976. Behavior of trace elements during magmatic processes—a summary of theoretical models and their applications. J RES U S GEOL SURV **4**, 41–7.

Banks, R. J. 1979. The use of linear programming in the analysis of petrological mixing problems. CONTRIB MINERAL PETROL **70**, 237–44.

Brooks, C. K. & Jakobsson, S. P. 1974. Petrochemistry of the volcanic rocks of the North Atlantic ridge system. *In* Kristjansson, L. (ed) *Geodynamics of Iceland and the North Atlantic Area*, 139–154. Dordrecht: Reidel.

Brooks, C. K. & Neilsen, T. F. D. 1978. Early stages in the differentiation of the Skaergaard magma as revealed by a closely related suite of dyke rocks. LITHOS **11,** 1–14.

Carmichael, I. S. E., Turner, F. J. & Verhoogen, J. 1974. *Igneous Petrology*. New York: McGraw-Hill.

Compston, W., McDougall, I. & Heier, K. S. 1968. Geochemical comparison of the Mesozoic basaltic rocks of Antarctica, South Africa, South America and Tasmania. GEOCHIM COSMOCHIM ACTA **32,** 129–49.

Czamanske, G. K. & Moore, J. G. 1977. Composition and phase chemistry of sulfide globules in basalt from the Mid-Atlantic Ridge rift valley near 37°N lat. BULL GEOL SOC AM **88,** 587–99.

Desborough, G. A., Anderson, A. T. & Wright, T. L. 1968. Mineralogy of sulfides from certain Hawaiian basalts. ECON GEOL **63,** 636–44.

Duke, J. M. 1979. Computer simulation of the fractionation of olivine and sulfide from mafic and ultramafic magmas. CAN MINERAL **17,** 507–14.

Dunham, A. C. & Kaye, M. J. 1965. The petrology of the Little Whin Sill, County Durham. PROC YORKSHIRE GEOL SOC **35,** 229–76.

Eales, H. V. & Robey, J. van A. 1976. Differentiation of tholeiitic Karroo magma at Birds River, South Africa. CONTRIB MINERAL PETROL **56,** 101–17.

Engel, A. E. J., Engel, C. G. & Havens, R. G. 1965. Chemical characteristics of oceanic basalts and the upper mantle. BULL GEOL SOC AM **76,** 719–34.

Faure, G., Bowman, J. R., Elliot, D. H. & Jones, L. M. 1974. Strontium isotope composition and petrogenesis of the Kirkpatrick Basalt, Queen Alexandra Range, Antarctica. CONTR MINERAL PETROL **48,** 153–69.

Fleischer, M. 1968. Variation of the ratio Ni/Co in igneous rock series. WASHINGTON ACAD SCI J **58,** 108–17.

Forsyth, I. H. & Chisholm, J. I. 1977. The Geology of East Fife. MEM GEOL SURV G B.

Francis, E. H. 1963. Quartz-dolerite sill. *In* Anderson, F. W. *The Geological Survey bore at Rashiehill, Stirlingshire (1951).* BULL GEOL SURV G B **20,** 43–106.

Francis, E. H. 1978. The Midland Valley as a rift, seen in connection with the late Palaeozoic European rift system. *In* Ramberg, I. B. & Neumann, E-R. (eds) *Tectonics and Geophysics of Continental Rifts*, 133–47. Dordrecht: Reidel.

Francis, E. H., Forsyth, I. H., Read, W. A. & Armstrong, M. 1970. The Geology of the Stirling District. MEM GEOL SURV G B.

Frey, F. A., Green, D. H. & Roy, S. D. 1978. Integrated models of basalt petrogenesis: a study of quartz tholeiites to olivine melilitites from south eastern Australia utilizing geochemical and experimental petrological data. J PETROL **19,** 463–513.

Gottfried, D., Greenland, L. P. & Campbell, E. Y. 1968. Variation of Nb-Ta, Zr-Hf, Th-U and K-Cs in two diabase–granophyre suites. GEOCHIM COSMOCHIM ACTA **32,** 925–47.

Gottfried, D., Annell, C. S. & Schwarz, L. J. 1978. Geochemistry of subsurface basalt from the deep corehole (Clubhouse Crossroads Corehole 1) near Charleston, South Carolina—magma type and tectonic implications. PROF PAP U S GEOL SURV **1028-G.**

Green, D. H. & Ringwood, A. E. 1967. The genesis of basaltic magmas. CONTRIB MINERAL PETROL **15,** 103–90.

Guppy, E. M. & Sabine, P. A. 1956. Chemical analyses of igneous rocks, metamorphic rocks and minerals. MEM GEOL SURV G B.

Hanson, G. N. 1977. Geochemical evolution of the suboceanic mantle. J GEOL SOC LONDON **134,** 235–53.

Harrison, R. K. 1968. Petrology of the Little and Great Whin sills in the Woodland Borehole, Co. Durham. BULL GEOL SURV G B **28,** 38–54.

Haskin, L. A., Haskin, M. A., Frey, F. A. & Wildeman, T. R. 1968. Relative and absolute terrestrial abundances of the rare earths. *In* Ahrens, L. H. (ed) *Origin and Distribution of the Elements*, 889–912. Oxford: Pergamon.

Hawkesworth, C. J. & Vollmer, R. 1979. Crustal contamination versus enriched mantle: $^{143}Nd/^{144}Nd$ and $^{87}Sr/^{86}Sr$ evidence from the Italian volcanics. CONTRIB MINERAL PETROL **69,** 151–65.

Helmke, P. A. & Haskin, L. A. 1973. Rare-earth elements, Co, Sc and Hf in the Steens Mountain basalts. GEOCHIM COSHOCHIM ACTA **37,** 1513–29.

Hjelmqvist, S. 1939. Some post-Silurian dykes in Scania and problems suggested by them. SVER GEOL UNDERS C. **430.**

Irving, A. J. 1978. A review of experimental studies of crystal/liquid trace element partitioning. GEOCHIM COSMOCHIM ACTA **42,** 743–70.

Jamieson, B. G. & Clarke, D. B. 1970. Potassium and associated elements in tholeiitic basalts. J PETROL **11,** 183–204.

Leeman, W. P. 1976. Petrogenesis of McKinney (Snake River) olivine tholeiite in light of rare-earth element and Cr/Ni distributions. BULL GEOL SOC AM **87,** 1582–86.

Leeman, W. P. 1977. Comparison of Rb/Sr, U/Pb, and rare earth characteristics of sub-continental and sub-oceanic mantle regions. BULL OREGON DEP GEOL MIN IND **96,** 149–68.

le Roex, A. P. & Reid, D. L. 1978. Geochemistry of Karroo dolerite sills in the Calvinia district, Western Cape Province, South Africa. CONTRIB MINERAL PETROL **66,** 351–60.

Lo, H. H. & Goles, G. G. 1976. Compositions of Formosan basalts and aspects of their petrogeneses. Lithos **9,** 149–59.

Macdonald, R. 1980. Trace element evidence for mantle heterogeneity beneath the Scottish Midland Valley in the Carboniferous and Permian. PHIL TRANS R SOC LONDON A **297,** 245–57.

MacGregor, M. & MacGregor, A. G. 1948. *The Midland Valley of Scotland.* BRITISH REGIONAL GEOLOGY. Edinburgh: H.M.S.O.

McDougall, I. 1964. Differentiation of the Great Lake dolerite sheet, Tasmania: J GEOL SOC AUSTRALIA **11,** 107–132.

McDougall, I. 1976. Geochemistry and origin of basalt of the Columbia River Group, Oregon and Washington. BULL GEOL SOC AM **87,** 777–92.

Mysen, B. O. 1978. Experimental determination of crystal-vapor partition coefficients for rare earth elements to 30 Kbar pressure. CARNEGIE INST WASHINGTON YEARB **77,** 689–95.

Pearce, J. A. & Norry, M. J. 1979. Petrogenetic implications of Ti, Zr, Y and Nb variations in volcanic rocks. EARTH PLANET SCI LETT **69,** 33–47.

Ragland, P. C., Brunfelt, A. O. & Weigand, P. W. 1971. Rare-earth abundances in Mesozoic dolerite dykes from Eastern United States. *In* Brunfelt, A. O. & Steinnes, E. (eds) *Activation Analysis in Geochemistry and Cosmochemistry*, 227–35. Oslo: Universitetsforlaget.

Schock, H. H. 1979. Distribution of rare-earth and other trace elements in magnetites. CHEM GEOL **26,** 119–33.

Shapiro, L. 1975. Rapid analysis of silicate, carbonate and phosphate rocks. U S GEOL SURV BULL **1401.**

Smith, R. C. II, Rose, A. W. & Lanning, R. M. 1975. Geology and geochemistry of Triassic diabase in Pennsylvania. BULL GEOL SOC AM **86,** 943–55.

Thompson, R. N., Gibson, I. L., Marriner, G. F., Mattey, D. P. & Morrison, M. A. 1980. Trace-element evidence of multistage mantle fusion and polybaric fractional crystallization in the Palaeocene lavas of Skye, NW Scotland. J PETROL **21,** 265–93.

Walker, F. 1934. A preliminary account of the quartz-dolerite dykes of Perthshire. TRANS PROC PERTHSHIRE SOC NAT SCI **9,** 109–17.

Walker, F. 1935. The late Palaeozoic quartz-dolerites and tholeiites of Scotland. MINERAL MAG **24,** 131–59.

Walker, F. 1952. Differentiation in a quartz-dolerite sill at Northfield Quarry, Stirlingshire. TRANS EDINBURGH GEOL SOC **15,** 393–405.

Walker F, 1964. A comparative survey of four tholeiitic magma provinces. *In* Subramanian, A. P. & Balakrishna, S. (eds) *Advancing Frontiers in Geology and Geophysics*, 309–26. Hyderabad: Indian Geophysical Union.

Walker, F. 1965. The part played by tholeiitic magma in the Carbo-Permian vulcanicity of central Scotland. MINERAL MAG **34,** 498–516.

Walker, F., Vincent, H. C. G. & Mitchell, R. L. 1952. The chemistry and mineralogy of the Kinkell tholeiite, Stirlingshire. MINERAL MAG **29,** 895–908.

Weigand, P. W. 1975. Geochemistry of the Oslo basaltic rocks. SKR NORSKE VIDENSK-AKAD OSLO. I. MAT-NATURV KL, N. S. No. 34.

Weigand, P. W. & Ragland, P. C. 1970. Geochemistry of Mesozoic dolerite dykes from Eastern North America. CONTRIB MINERAL PETROL **29,** 195–214.

Weill, D. F. & McKay, G. A. 1975. The partitioning of Mg, Fe, Sr, Ce, Sm, Eu and Yb in lunar igneous systems and a possible origin of KREEP by equilibrium partial melting. Proc. Sixth Lunar Sci Conf., 1143–58. GEOCHIM COSMOCHIM ACTA SUPPL 6.

Wilkinson, J. F. G. & Binns, R. A. 1977. Relatively iron-rich lherzolite xenoliths of the Cr-diopside suite; a guide to the primary nature of anorogenic tholeiitic andesite magmas. CONTRIB MINERAL PETROL **65,** 199–212.

Wood, D. A. 1978. Major and trace element variations in the Tertiary lavas of Eastern Iceland and their significance with respect to the Iceland geochemical anomaly. J PETROL **19,** 393–436.

Wood, D. A. 1979. Dynamic partial melting: its application to the petrogeneses of basalts erupted in Iceland, the Faeroe Islands, the Isle of Skye (Scotland) and the Troodos Massif (Cyprus). GEOCHIM COSMOCHIM ACTA **43,** 1031–46.

Wright, T. L. and Peck, D. L. 1978. Crystallization and differentiation of the Alae magma, Alae Lava Lake, Hawaii. PROF PAP U S GEOL SURV **935-C**.

Yoder, H. S., Jr. 1976. *Generation of basaltic magma.* Washington D.C.: National Academy of Sciences.

R. MACDONALD and M. J. FARRINGTON, Department of Environmental Sciences, University of Lancaster, Bailrigg, Lancaster LA1 4YQ, England.
D. GOTTFRIED, F. W. BROWN and N. G. SKINNER, U.S. Geological Survey, National Center, Reston, Va 22092, U.S.A.

MS received 7 November 1980. Accepted for publication 19 March 1981.

J. geol. Soc. London, Vol. 141, 1984, pp. 147–159, 11 figs., 4 tables. Printed in Northern Ireland.

Geochemistry and petrogenesis of the Derbyshire Carboniferous basalts

R. Macdonald, K. N. Gass, R. S. Thorpe & I. G. Gass

SUMMARY: Dinantian volcanism in Derbyshire was associated with minor phases of isostatic uplift of a shallow carbonate platform on the northern margin of the St. George's Land E–W land mass. The mainly tholeiitic magmas were generated by varying degrees of partial melting of heterogeneous mantle sources followed by fractional crystallization and final equilibration mainly within the lower crust. Large, high-level magma chambers were not established. Even single lava sequences, such as the Miller's Dale Lava, represent several, isolated magmatic phases. Volcanism was of within-plate type. Magmas generated in isolated mantle pockets rose to the surface through crust attenuated by lithospheric stretching.

The existence of basaltic lavas, sills; dykes, breccias, tuffs and ashes within the Carboniferous Limestone of Derbyshire has been known for well over a century (Fig. 1). During this time these basaltic rocks have been described petrographically (e.g. Bemrose 1894, 1907; Tomkeieff 1928), their stratigraphy synthesized (Walters & Ineson 1981), their palaeogeography identified (Walkden 1977) and their regional setting and significance discussed (Francis 1978; Upton 1982). Yet, although they are the subject of numerous publications, no one, so far as we are aware, has attempted a detailed examination of their geochemistry, or proposed magmatic processes to explain their composition; this paper attempts to fill the gap.

As detailed descriptions of field relations, age, petrography and regional setting are given elsewhere, only those aspects relevant to our geochemical and petrogenetic discussion will be summarized below.

Within the accepted age span (*c.* 360–280 Ma) of the Carboniferous Period (Francis & Woodland 1964; Fitch *et al.* 1970), volcanism seems to have been most intense and widespread in the Dinantian (345–325 Ma), whereas sill emplacement occurred principally during the Namurian (325–310 Ma). Fitch *et al.* (1970) quote minimum K-Ar ages for several Derbyshire basalts. For instance, they date the Lower Miller's Dale Lava (LMDL) at 276 ± 17 (282 ± 17; this and subsequent dates on 1976 decay constants) the Upper Miller's Dale Lava (UMDL) at 318 ± 9, the Tideswell Dale Sill at 287 ± 13 and an olivine basalt intrusion at Calton Hill at 295 ± 14. Fitch and his colleagues considered some of these dates were 'discrepantly low' due to argon loss, with which Walters & Ineson (1981) agree. Stratigraphically, the Lower Miller's Dale Lava is taken as occurring near the top of the Asbian stage (former D_1 zone) in the area, whereas the Upper Miller's Dale Lava was erupted at or very close to the Brigantian-Asbian stage boundary (D_2/D_1 zones); some 70 m of limestone separate the two lava groups.

Throughout the Carboniferous Period the British Isles lay in tropical latitudes between 0–10°N (Turner & Tarling 1975). In Upper Visean times the Derbyshire Block was a roughly circular, level carbonate platform of some 500 km^2 that lay either on, or just off, the northern edge (Fig. 2) of an E–W land barrier (St. George's Land). Walkden (1977) has suggested that the area was subjected to numerous (12–15) cycles of uplift, during which the platform rose just above sea-level, together with subsequent submergence when it was mainly covered by shallow seas. Walkden (1977) showed that during periods of emergence the recently deposited limestones were eroded and karst surfaces developed. He also made the interesting suggestion that volcanism is temporally associated with periods of uplift; the significance of this relation is discussed further below.

This broad palaeogeographic scenario fits, not only with our field data, but with the observations of others. For instance, the Upper Miller's Dale lavas flowed out over an eroded surface between D_1 & D_2 that had long been recognized as such (Cope 1933, 1937). Also, Walkden (1977) and Walters & Ineson (1981) identified the widespread tuff and K-bentonite horizons as the products of air-fall ash deposits on palaeokarst surfaces. An exception to the uplift-volcanism correlation is at Calton Hill, where field evidence suggests to us that a phreatic tuff-ring of subaqueous basaltic agglomerates and ashes was formed before the effusion of the associated alkali basalts. Even when the lavas were above sea-level, it is evident that the elevation was not great, for the spatially very variable vesicularity of most lavas indicates that at times they flowed over wet sediments and sometimes terminated in shallow water (Cheshire & Bell 1977; Walkden 1977). Borehole data (Walters & Ineson 1981) show that most of these volcanic products occur at depths within Carboniferous sediments and that only a minor fraction are exposed at the surface.

Poor exposure and lack of continuous outcrop make the regional correlation of basalt units difficult. Despite this, however, Walters & Ineson (1981), in

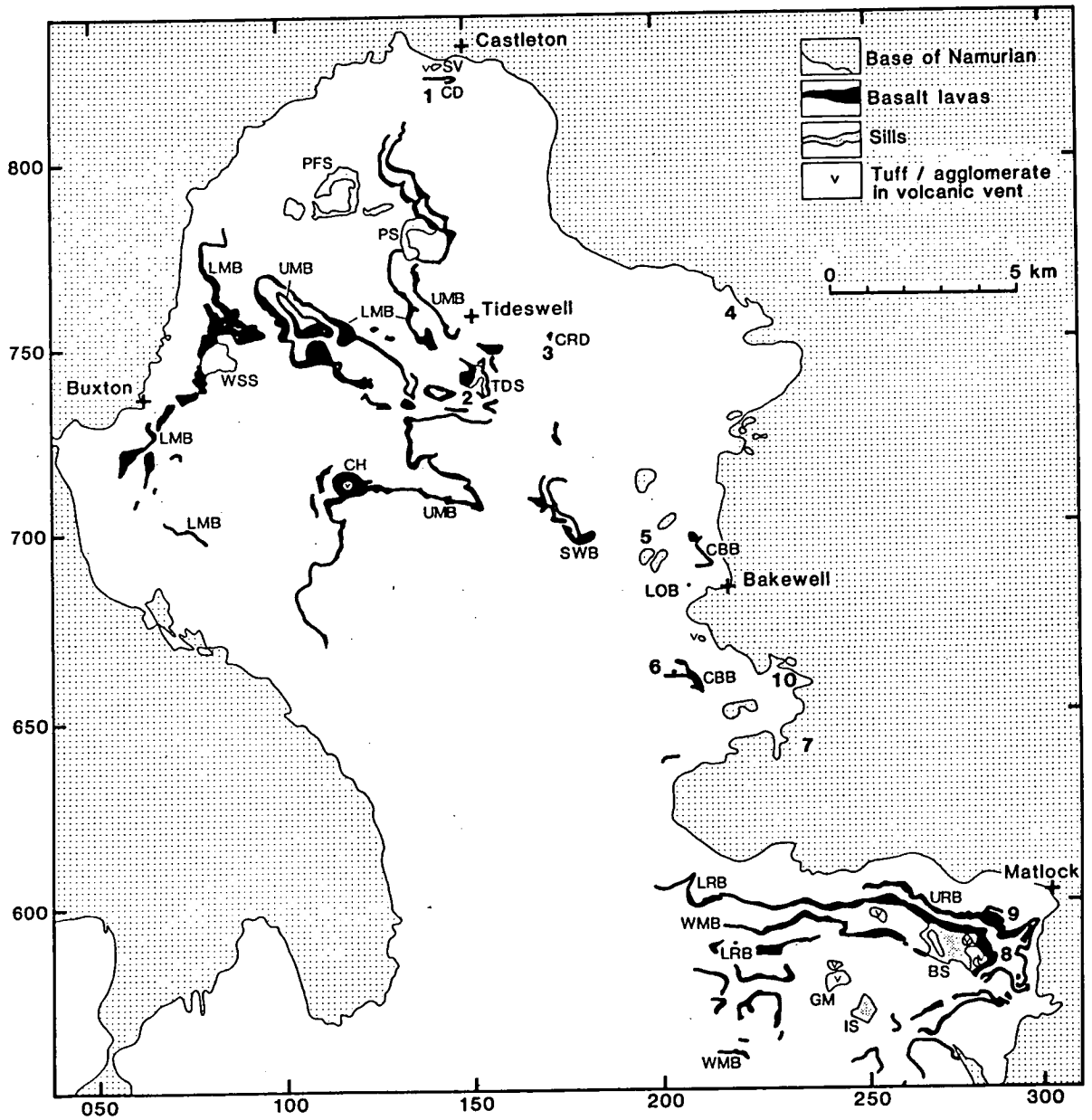

FIG. 1. Distribution of Carboniferous lavas, intrusions and volcanic vents showing locations of analysed samples. *Lavas:* UMB, Upper Miller's Dale; LMB, Lower Miller's Dale; CD, Cave Dale; CRD, Cressbrook Dale; SWB, Shacklow Wood; CBB, Conksbury Bridge; LOB, Lathkill Lodge; LRB, Lower Matlock; WMB, Winstermoor; URB, Upper Matlock; R. Rowsley boreholes. *Sills:* PFS, Peak Forest; PS, Potluck; WSS, Water Swallows; TDS, Tideswell; BS, Bonsall; IS, Ible. *Volcanic vents:* SV, Speedwell; CH, Calton Hill; GM, Grangemill. The numbers refer to the stratigraphic sections shown in Fig. 3, and 10 = location of Rowsley borehole.

their recent stratigraphic synthesis using mine and borehole data as well as surface exposures, recognized 30 distinct lava and tuff horizons and identified that there were two main eruptive centres at Matlock and Miller's Dale. They also suggested that the volcanic products were erupted from short-lived central vent volcanoes and that the volcanic rocks extend eastward under the Namurian cover. Fig. 3 is based on stratigraphic sections by Walters & Ineson (1981) and shows the relationships between the major extrusive

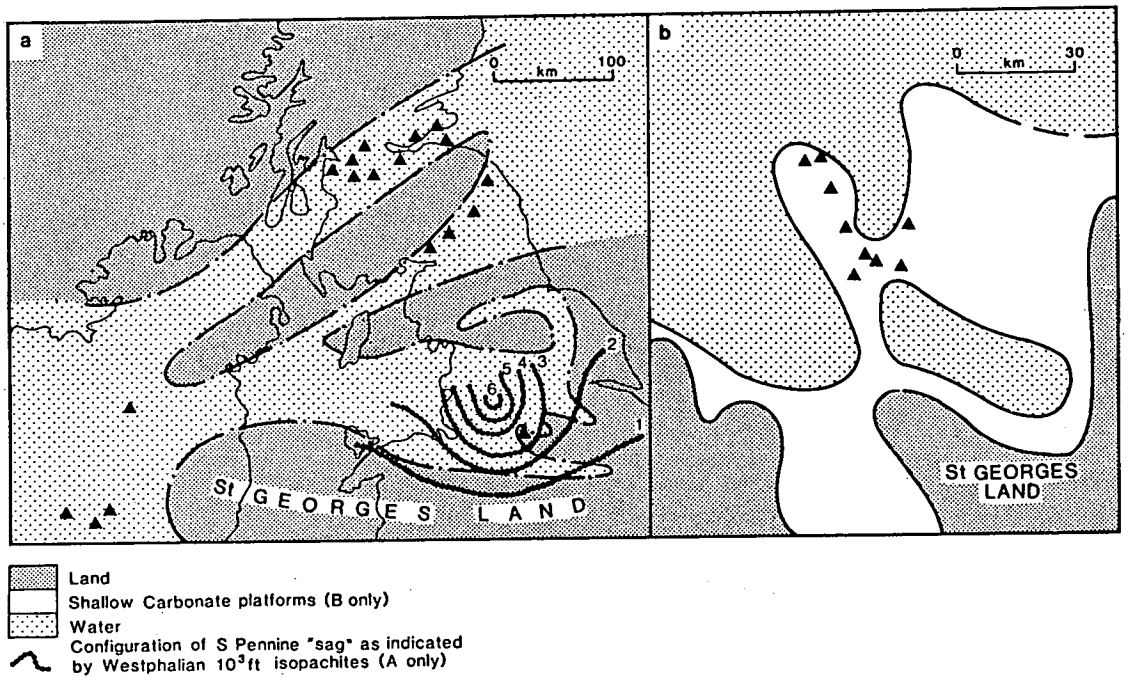

FIG. 2. Palaeogeographical setting of the Derbyshire volcanism. (*a*) The block-basin topography of the British Dinantian, with an indication of the main volcanic areas. The configuration of the late Carboniferous sag, which was superimposed on the earlier structures, is after Leeder's fig. 5 (1982). (*b*) Detail of the northern edge of St. George's Land during Dinantian times, showing the relationship of the Derbyshire volcanic centres to shallow carbonate platforms varyingly above or below sea-level.

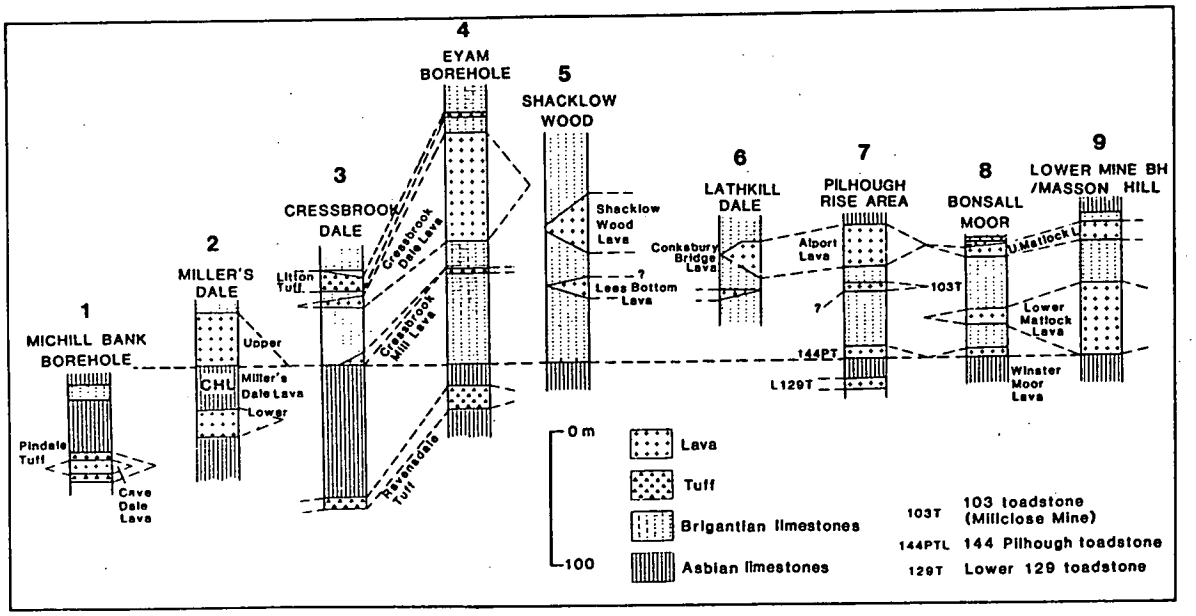

FIG. 3. Stratigraphical positions of selected Carboniferous volcanic rocks in Derbyshire, constructed from sections in Walters & Ineson (1981). CHL indicates the approximate stratigraphic position of the Calton Hill lava. The sections are numbered as shown on Fig. 1 and are drawn relative to a horizontal line at the Asbian–Brigantian boundary.

units. One feature deserves special mention: unlike some previous workers, we recognize the lavas at Calton Hill Quarry as a sequence separated from the overlying Upper Miller's Dale Lava by some 15 m of limestone.

The Derbyshire Carboniferous basalts occur in stratigraphic units that are usually between 3 and 30 m thick. Normally, exposures are so small or overgrown that it is not possible to identify whether such units represent single or multiple flows. Even in larger outcrops, it has not been possible to identify the single or multiple nature of the Lower and Upper Miller's Dale lavas. Walters & Ineson (1981) showed conclusively from borehole evidence that many of the lava units were multiple but they followed tradition in referring to them as 'Lava', e.g. the Upper Miller's Dale Lava and the Cressbrook Dale Lava; the terms are used in the same sense in this paper. Multiple flows can be seen at Calton Hill quarry where, in the outcrop that has not been covered by rubbish, it is possible to identify five flow units. Here, the massive centres of each flow unit are of fresh alkali basalt in which only olivine has been partly altered. In contrast, the rock-forming minerals of the rubbly and vesicular tops and bottoms of these flows have been totally replaced by secondary minerals. The relation between alteration and vesicularity (the more vesicular the rock the more extensive the alteration) suggests that the main agents of alteration were percolating ground waters and hydrothermal solutions.

Petrography and mineralogy of lavas and intrusions

Petrographic descriptions of igneous rocks of Derbyshire have been given by Bemrose (1894, 1907), Tomkeieff (1928), Smith *et al.* (1967), and Stevenson & Gaunt (1971). This section is based on these accounts, on microscopic studies of specimens we collected and on electron microprobe analyses of selected samples.

The lavas are usually highly altered, commonly vesicular, fine-grained, olivine-phyric and aphyric basalts containing amygdales of carbonate, chlorite, chalcedony or albite. The primary igneous mineralogy is generally completely replaced by secondary minerals. Olivine is altered to combinations of serpentine, iddingsite, Fe-Ti oxide, chlorite and carbonate. Fresh clinopyroxene occurs in several lavas, although it is generally replaced by chlorite. Altered pyroxene is commonly assumed to be clinopyroxene (augite) but orthopyroxene, altered to carbonate (calcite), chlorite, serpentine (bastite) and haematite, has been recorded from the Upper Matlock Lava (Smith *et al.* 1967, p. 262). Plagioclase varies widely in the degree of preservation: whereas some lavas contain fresh calcic labradorite, it is commonly recrystallized and altered to albite, carbonate and epidote. Accessory minerals include Fe-Ti oxide and apatite set in a microcrystalline groundmass of chlorite, carbonate and chalcedony. The lavas are frequently brecciated and veined by carbonate minerals.

In contrast, the lavas erupted from the Calton Hill vent are distinctive in being petrographically fresh and in containing spinel-lherzolite and harzburgite xenoliths (Tomkeieff 1928; Hamad 1963; Donaldson 1978). The lavas contain phenocrysts of olivine (Fo_{80-85}), clinopyroxene (augite; $Wo_{45}En_{45}Fs_{10}$), abundant Fe-Ti oxide grains and plagioclase (An_{64}) subophitically enclosed by augite with a higher Fe/Mg ratio ($Wo_{50}En_{36}Fs_{14}$), analcite and calcite (Donaldson 1978, p. 365). In addition to olivine phenocrysts, the lava contains larger xenocrysts of olivine (Fo_{88}) that are clearly derived from the xenoliths, but apparently no xenocrysts of pyroxene or spinel. The xenoliths consist mainly (64–85%) of partially serpentinized Mg-rich olivine (Fo_{91-92}), 8–24% orthopyroxene ($Wo_1En_{91}Fs_8$) with minor (1–2%) clinopyroxene (chrome-diopside, $Wo_{47}En_{49}Fs_4$) and <4% spinel (all data from Donaldson 1978).

The sills are dominantly medium- to coarse-grained olivine dolerites, which differ from the lavas in being coarser grained, having altered olivine phenocrysts, ophitic intergrowths of clinopyroxene and plagioclase, and an absence or rarity of vesicles and amygdales. Petrographic descriptions are given by Smith *et al.* (1967, pp. 263–4) for the Ible and Bonsall Sills and by Stevenson & Gaunt (1971, pp. 293–9) for the Waterswallows, Peak Forest, Potluck, Mount Pleasant and Tideswell Dale Sills. These sills commonly have serpentinized olivine phenocrysts set in a sub-ophitic or ophitic intergrowth of generally fresh clinopyroxene (augite) and plagioclase (labradorite). Accessory minerals include Fe-Ti oxide and apatite in a microcrystalline matrix that contains plagioclase and secondary chlorite. Accessory nepheline has been recorded from the Bonsall Sill (Smith *et al.* 1967, p. 264) and accessory orthopyroxene, altered to chlorite, has been reported in the Pot Luck Sill (Stevenson & Gaunt 1971, p. 298).

To determine the magmatic affinities of the lavas, electron microprobe analyses (Table 1) have been determined for the cores of clinopyroxenes in representative fresh samples selected from the range of lava compositions. These are a Lower Miller's Dale lava (sample D2, 7.7% normative 'Q' ('Q' = normative quartz plus the quartz component of normative hypersthene)), a Lower Matlock lava (sample D21, 4.9% normative 'Q') and a Calton Hill lava (sample KG31, 1.1% normative nepheline). The Lower Miller's Dale lava has coexisting salite ($Wo_{38}En_{46}Fs_{16}$ –$Wo_{39}En_{42}Fs_{20}$) and magnesian pigeonite ($Wo_8En_{61}Fs_{31}$). The Lower Matlock lava has augite ($Wo_{42}En_{44}Fs_{14}$) and the Calton Hill lava has salite ($Wo_{48}En_{40}Fs_{12}$). The chemical compositions of the

TABLE 1. *Representative chemical analyses of clinopyroxenes from Derbyshire lavas*

	1	*2*	*3*	*4*
SiO_2	54.20	52.52	52.12	49.50
TiO_2	0.41	0.95	1.18	1.65
Al_2O_3	0.51	2.28	2.51	5.54
Cr_2O_3	0.00	0.58	0.43	0.57
FeO	19.29	9.67	8.72	6.85
MnO	0.51	0.27	0.25	0.14
MgO	21.59	15.73	14.85	13.18
CaO	3.99	18.14	19.96	22.20
Na_2O	0.07	0.33	0.31	0.55
Total	100.57	100.20	100.33	100.18
atomic %				
Mg	61.2	46.0	43.6	40.0
Fe	30.7	15.9	14.4	11.6
Ca	8.1	38.1	42.1	48.4

1. Pigeonite Lower Miller's Dale Lava (D2)
2. Salite Lower Miller's Dale Lava (D2)
3. Augite Lower Matlock Lava (D21)
4. Salite Calton Hill Lava (KG31)

clinopyroxenes are compared in terms of SiO_2 and Al_2O_3 (Fig. 4a) and tetrahedral Al (Al_z) and TiO_2 (Fig. 4b; *cf.* Le Bas 1962, figs 2 & 5 respectively). These diagrams confirm that the clinopyroxenes from each rock sample are distinctive, indicating a range of magmatic compositions. The clinopyroxenes from the Lower Miller's Dale and Lower Matlock rocks are relatively SiO_2-rich and TiO_2- and Al_2O_3-poor and plot within the fields of 'non-alkaline' (specifically, in this case, tholeiitic) pyroxenes. The Lower Miller's Dale pyroxene has more 'tholeiitic' characteristics, consistent with chemical features to be described later. The Calton Hill clinopyroxenes have higher contents of Al_2O_3 (>4%) and TiO_2 (>1.5%) and plot within the field of normal alkaline rocks, again consistent with the silica-undersaturated composition of the host basalt.

In spite of the alteration suffered by the Derbyshire lavas, the overall petrological characteristics therefore indicate that they form a series ranging from 'tholeiitic' types containing minor olivine, relict orthopyroxene and clinopyroxene, to alkaline varieties containing more abundant olivine together with analcime. The existence of this range is fully confirmed by analyses of clinopyroxenes, since these range from pigeonite and SiO_2-rich, Al_2O_3- and TiO_2-poor clinopyroxene in the most 'tholeiitic' representatives (e.g. Lower Miller's Dale) to the salites in the more alkaline lavas of Calton Hill. The sills also range between relatively 'tholeiitic' (e.g. the Pot Luck Sill) and relatively 'alkaline' (e.g. the Bonsall Sill) dolerites, but the overall compositional range of the sills is smaller than that represented by the lavas.

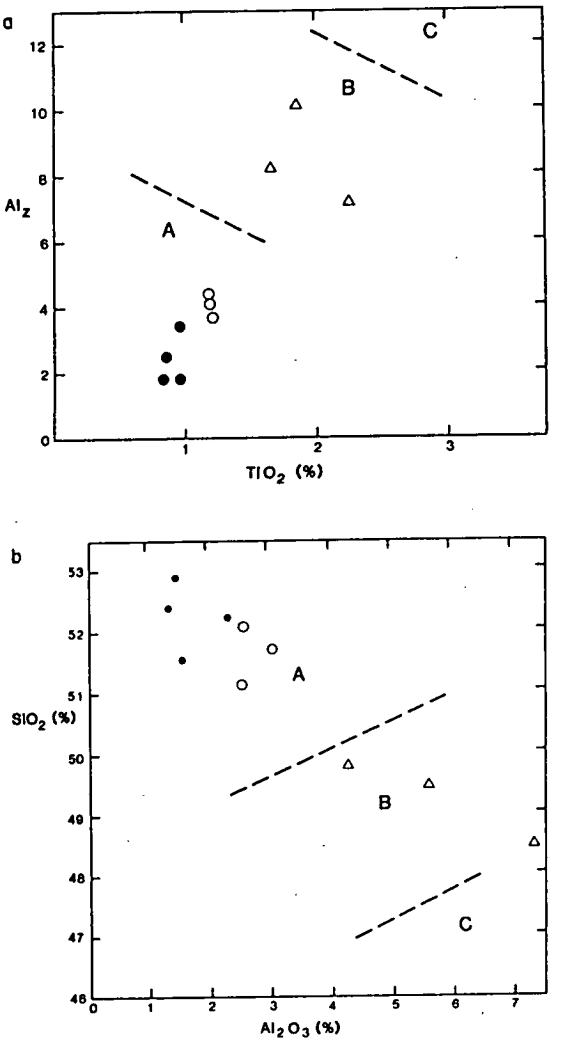

FIG. 4. (a) Plot of Al_z against TiO_2 and (b) Plot of SiO_2 against Al_2O_3 for clinopyroxenes from lavas. Open circles, UMB; closed circles, LMB; and open triangles, CH. Abbreviations as in Fig. 1. The broken lines separate three groups of clinopyroxene composition: A, non-alkaline (tholeiitic, high alumina and calc-alkaline) lavas; B, alkaline lavas and C, peralkaline lavas (from Le Bas 1962).

Geochemistry

60 rocks were analysed, mainly by standard X-ray fluorescence methods using U.S.G.S. standard rocks, for major elements and Ba, Cr, Nb, Ni, Rb, Sr, Y and Zr. Six were also analysed by instrumental neutron activation analysis for Hf, REE, Ta and Th, following the procedure of Potts *et al.* (1981). The specimens represent the various stratigraphic lava sequences as

TABLE 2. *Representative analyses of Carboniferous lavas and sills in Derbyshire*

	L. Miller's Dale Lava D2	U. Miller's Dale Lava KG55U	Calton Hill Lava KG31	Calton Hill Lava KG34	Calton Hill Lava KG33	U. Matlock Lava D17	U. Matlock Lava D20	Conksbury Bridge Lava SK143	Ible Sill D23	Tideswell Dale Sill KG51H
SiO_2	51.5	47.6	46.0	47.8	44.8	48.7	48.9	47.4	49.9	51.2
TiO_2	1.70	1.92	2.28	2.22	2.42	1.92	1.93	2.25	1.77	1.98
Al_2O_3	15.26	13.82	13.27	14.58	13.53	16.12	12.74	14.46	16.01	15.36
Fe_2O_3	3.89	2.53	2.83	3.22	5.23	3.55	5.27	4.65	4.34	4.14
FeO	6.86	8.73	9.12	7.14	6.93	4.85	3.61	7.34	5.57	6.24
MnO	0.16	0.16	0.17	0.09	0.37	0.06	0.09	0.12	0.09	0.12
MgO	6.47	9.69	10.96	9.88	9.82	4.84	4.79	8.65	7.53	6.47
CaO	8.92	7.10	9.37	9.14	10.14	9.04	8.63	8.36	8.83	8.59
Na_2O	2.93	2.80	2.55	2.21	2.02	2.74	2.04	2.29	2.71	2.82
K_2O	0.62	0.78	1.12	0.80	0.92	1.44	1.92	0.94	0.54	0.73
P_2O_5	0.17	0.25	0.49	0.31	0.44	0.30	0.33	0.34	0.22	0.27
H_2O^+	0.92	3.60	2.46	1.83	2.74	2.62	3.34	2.91	1.81	1.46
CO_2	—	0.11	0.05	0.10	0.06	3.33	5.62	0.20	—	—
Total	99.40	99.09	100.67	99.32	99.42	99.51	99.21	99.91	99.32	99.38
Ba	140	209	574	239	387	288	455	249	129	214
Cr	265	—	—	—	—	222	357	—	398	—
Nb	11	24	42	29	42	28	33	33	16	18
Ni	89	—	—	—	—	87	107	—	276	—
Rb	13	18	22	16	16	20	29	12	10	14
Sr	274	238	522	337	495	442	321	533	266	291
Y	25	23	23	22	21	22	22	22	22	26
Zr	99	117	178	140	180	129	133	151	100	121

follows: Lower Miller's Dale Lava 8, Cave Dale Lava 1, Upper Miller's Dale Lava 9, Calton Hill Lava 7, Cressbrook Mill Lava 1, Shacklow Wood Lava 1, Cressbrook Dale Lava 1, Lower Matlock Lava 4, Upper Matlock Lava 4, Conksbury Bridge Lava 2, with a further two specimens from an unnamed lava in a borehole near Rowsley. One sample came from each of the Peak Forest, Waterswallows, Pot Luck, Bonsall and Ible Sills and 15 from a systematic collection through the Tideswell Dale Sill.

TABLE 3. *Additional trace element data for selected lavas*

	Lower Miller's Dale Lava KG14	Lower Miller's Dale Lava KG25	Upper Miller's Dale Lava KG40	Upper Miller's Dale Lava KG55L	Calton Hill Lava KG34	Calton Hill Lava KG33
La	7.7	9.3	8.3	18.8	18.8	29.9
Ce	16.3	17.8	19.2	34.5	39.8	59.6
Nd	11.0	11.9	13.1	21.1	23.8	32.8
Sm	3.1	3.1	3.7	5.1	5.3	6.6
Eu	1.22	1.17	1.42	1.63	1.87	2.3
Gd	3.0	4.0	4.4	4.9	5.3	7.4
Tb	0.56	0.62	0.74	0.78	0.90	1.01
Tm	0.22	0.25	0.32	0.32	0.39	0.32
Yb	1.25	1.54	1.77	1.70	1.96	1.89
Lu	0.18	0.23	0.25	0.25	0.27	0.25
Hf	2.47	2.82	2.40	3.06	3.33	4.40
Ta	0.64	0.77	0.57	1.42	1.68	2.82
Th	1.24	1.56	1.15	2.11	2.35	3.94

Representative analyses are given in Table 2 and the INAA data in Table 3. The complete body of data and details of analytical procedures are available from the authors on request. These data are also available in machine-readable form from the recently established UK-IGBA data base housed in the National Geochemical Data Bank of the Institute of Geological Sciences, London.

Problems of interpretation of chemical data

All the analysed samples show varying degrees of alteration, from those largely retaining original igneous mineralogy to others in which the original minerals are completely replaced. Secondary hydration is ubiquitous, resulting in variable replacement of the ferromagnesian minerals by serpentine–chlorite assemblages and alteration of the plagioclase to sericite ± clay minerals. Many samples show partial replacement and sometimes veining by carbonate ± silica minerals, and albitization of plagioclase is a common feature. An indication of the types of alteration in the analysed rocks is given with the chemical data.

During secondary alteration, mobility of Si, Ca, Mg, Na, K, Ba, Rb and Sr is likely. Such mobility may be evaluated by plotting data for a reputedly stable incompatible trace element, such as Zr, against another stable element and an element of suspected

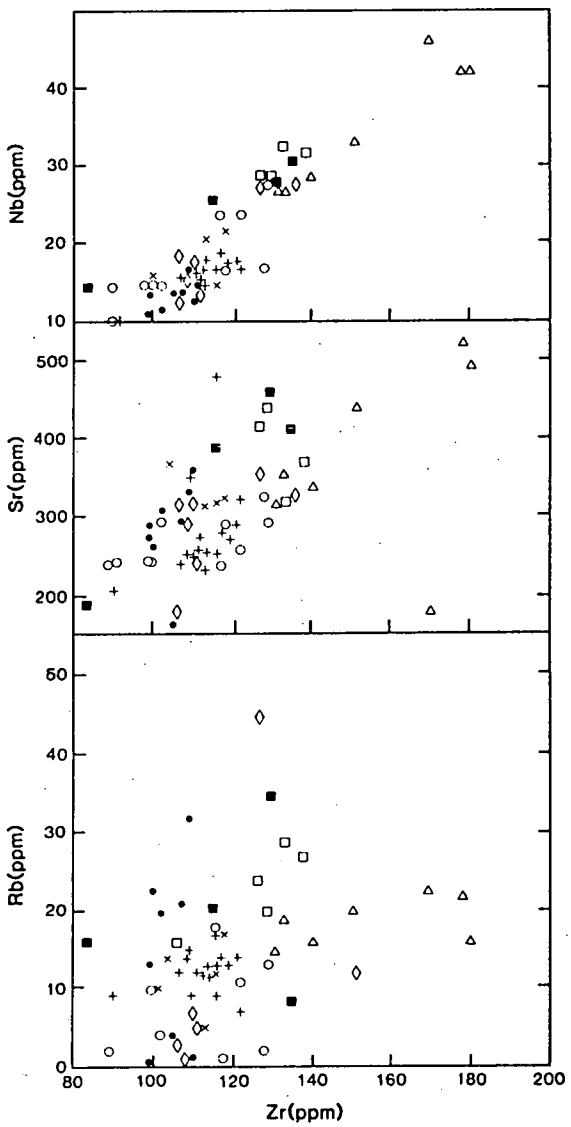

FIG. 5. Plot of Nb, Sr and Rb against Zr for analysed lavas and sills. Symbols used are as follows: Closed circles, LMB; open circles, UMB; open triangles, CH; closed squares, LRB; open squares, URB; open diamonds, other lavas; Tideswell sill = +, other sills = X. Abbreviations of lavas as in Fig. 1.

mobility. Graphs of Zr against Nb, Sr and Rb (Fig. 5) indicate that Nb was stable and that Rb was secondarily mobilized in the Derbyshire rocks, as indicated by the varying degrees of scatter of the data. Although the scatter for Sr suggests some mobilization, it was not sufficiently intense to obscure the positive correlation with Zr. Further discussion in this section is concentrated on those elements, Zr, Nb, Y, Ti and P, considered to be stable during alteration of basaltic rocks (e.g. Pearce & Cann 1973; Floyd & Winchester 1975; Pearce & Norry 1979) and on those rocks deemed to be 'fresh'. In the following discussion, the term 'fresh' is applied to 29 specimens (14 from lavas, 15 from sills) where the pyroxene and plagioclase are almost wholly fresh, although the olivine may be partly or totally serpentinized.

Magmatic affinities

A Zr-Nb plot (Fig. 5) permits three important observations:

(i) The sills and some of the extrusive rocks have comparable compositions and, despite the age difference, may be discussed together.

(ii) The sills and extrusive rocks show a significant range of incompatible trace element abundances (more than a factor of four for some stable elements).

(iii) Individual volcanic sequences, such as the Upper Miller's Dale and Calton Hill Lavas, may cover up to about half the compositional spectrum. The geochemistry thus provides additional evidence that at least the main lava sequences consist of several chemically distinct flows. The Tideswell Dale Sill shows internal chemical differentiation.

Such inter- and intra-sequence variation, especially in incompatible trace element abundances, may result from several factors: varying degrees of partial melting of the source rocks, heterogeneity of the source, differing degrees of fractional crystallization (perhaps involving different mineral assemblages) of a parental, or series of parental, magma(s) and crustal contamination of mantle-derived melts. It is difficult to assess the degree to which the Derbyshire rocks have been affected by crustal contamination, but positive correlation between the degree of silica-undersaturation and such lithophile elements as K, Ba and Rb suggests that such contamination, if it occurred, must have been slight.

We first use the geochemical and mineralogical data to establish the magmatic affinities of the lavas. Here, four lines of evidence are particularly relevant:

(1) C.I.P.W. norms have been calculated for the fresh samples only, on a volatile-free basis and with Fe_2O_3 arbitrarily set at 1.5 wt%. The range is from q- to ne-normative, but the majority are ol + hy-normative.

(2) The stable incompatible elements Nb, Y and Zr are particularly useful in assessing magmatic affinity in that they are assumed to be unaffected by alteration processes. Zr/Nb ratio decreases and Zr/Y and Nb/Y ratios increase with increasing alkalinity of basalts (e.g. Pearce & Cann 1973; Floyd & Winchester 1975; Pearce & Norry 1979). In Fig. 6, the Zr/Y ratio is plotted against the

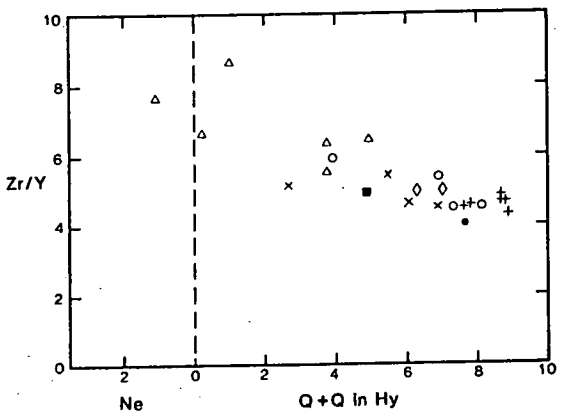

FIG. 6. Plot, for fresh samples only, of Zr/Y against normative nepheline (Ne) or normative quartz (Q) plus quartz in normative hypersthene (Hy). Symbols as in Fig. 5.

degree of silica-undersaturation (expressed as normative nepheline or normative quartz plus quartz in normative hypersthene, termed 'Q'). The good negative correlation of Zr/Y with 'Q' is taken to confirm that the range in magmatic affinities suggested by the norms is real. Similar conclusions are reached by using Zr/Nb and Y/Nb ratios instead of Zr/Y.

(3) There are significant, negative correlations between Ti, P, Zr, Hf, Nb, Ta, Th, the LREE abundances and 'Q' in all samples and between those elements and Ba and Rb in fresh samples. The range from ne- to q-normative compositions must therefore be related to magmatic variations rather than to hydrothermal alteration.

(4) Six lavas covering the range of lava compositions have been analysed for REE (Fig. 7). All samples are light-REE (LREE) enriched with chondrite-normalized $Ce(Ce_N) = 19–70$, and $Yb_N = 6–8$. The REE patterns are characterized by large

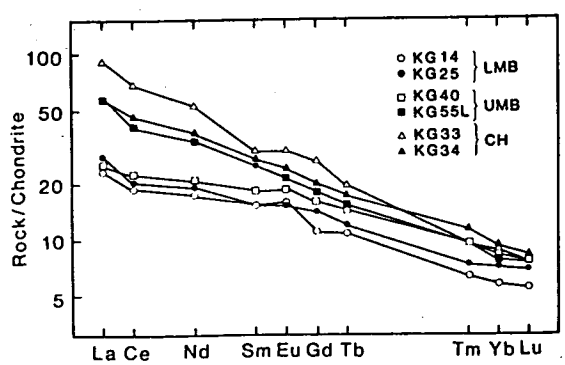

FIG. 7. Chondrite-normalized REE plot for lavas. Abbreviations of lavas as in Fig. 1.

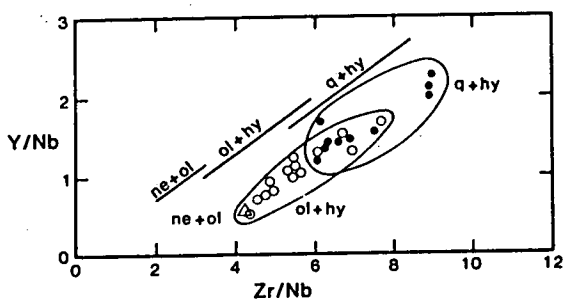

FIG. 8. Plot of Y/Nb against Zr/Nb. Symbols, as in Fig. 5, indicate the normative characteristics calculated for fresh rocks only. Fields are for q + hy and ol + hy normative rocks. The generalized ranges (full lines) were then used to determine the magmatic affinities of altered samples; those in areas of overlap assigned on overall characteristics of their lava sequence.

variation in the LREE in comparison with the heavy REE (HREE). The Ce_N/Yb_N ratio ranges from 2.9–8.0, with the Lower and Upper Miller's Dale showing lower REE contents and significantly varied Ce_N/Yb_N (2.9–5.2) in comparison with the Calton Hill lavas ($Ce_N/Yb_N = 5.2$ and 8.0). Noting the higher Ce_N/Yb_N ratios of alkaline in comparison with tholeiitic lavas (e.g. Kay & Gast 1973) and the relative stability of the REE to hydrothermal alteration, these data confirm that the lavas form a spectrum between relatively tholeiitic and alkaline types.

A plot of Zr/Nb against Y/Nb (Fig. 8) allows the determination of the affinities of altered specimens since both ratios correlate with degree of silica-undersaturation. The range of normative characteristics of each sequence is shown in Table 4, and

TABLE 4: *Magmatic affinities of Derbyshire lavas and sills.*

Unit	*Normative characteristics*
Conksbury Bridge Lava	ol + hy: some near CPSU*
Upper Matlock Lava	some near CPSU*
Lower Matlock Lava	some near CPSU*
Unnamed Lava	q + hy
Shacklow Wood Lava	q + hy
Cressbrookdale Lava	ol + hy: close to CPSU
Upper Miller's Dale Lava	ol + hy, q + hy
Cressbrook Mill Lava	q + hy or ol + hy
Calton Hill Lava	ol + ne, ol + hy
Lower Miller's Dale Lava	q + hy
Cave Dale Lava	q + hy
Ible, Tideswell Dale and Waterswallows Sills	q + hy
Bonsall, Pot Luck and Peak Forest Sills	ol + hy

*CPSU = critical plane of silica-undersaturation.

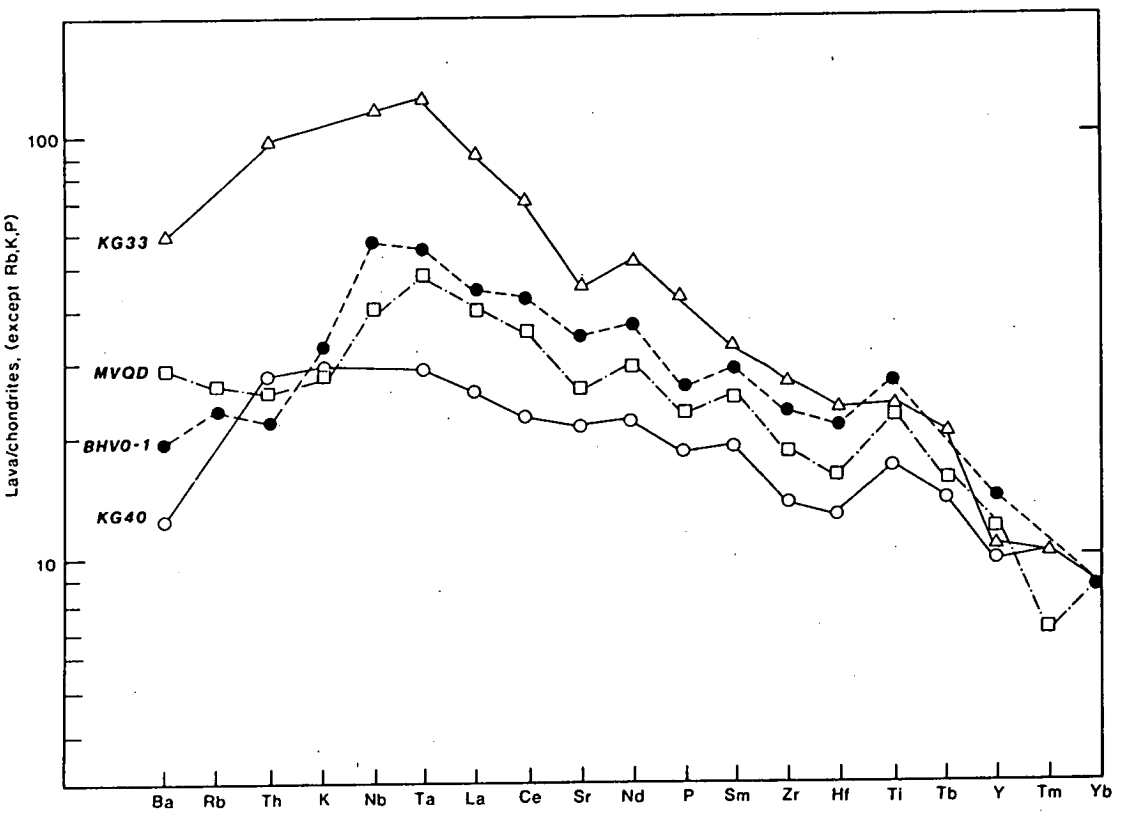

FIG. 9. Chondrite-normalized (except for Rb, K and P), incompatible element patterns for: Calton Hill lava (KG 33); Upper Miller's Dale lava (KG 40); olivine tholeiite (BHVO-1), Kilauea, Hawaii (Thompson 1982, fig. 15); median composition at 7.5% MgO, late Carboniferous quartz dolerite suite, Scotland (MVQD; Macdonald *et al.* 1981, table 7). Normalizing factors from Thompson (1982, p. 105).

indicates that the bulk of the Derbyshire volcanism was tholeiitic, in the sense of containing normative hy. This is confirmed by trace element abundances (Fig. 9); the Derbyshire rocks are compositionally similar to such typically tholeiitic suites such as the late Carboniferous quartz dolerites of the Midland Valley and Whin Sill(s).

Petrogenesis

A widely accepted criterion (e.g. Frey *et al.* 1978) is that only basalts with Mg number >66–67 are likely to be primary basalts, assuming a mantle olivine of composition Fo >87. On this basis, only certain of the Calton Hill lavas would be possible primary magmas. Following the interpretation of Thompson (1982) for British Tertiary Volcanic Province lavas, it would seem that the Derbyshire rocks plotting within field A (Fig. 10) have compositions related to cotectic equilibria at about 9 kbar, whereas those in field B reached their final compositions at lower pressures, within the upper crust. Undoubtedly, this is why some of the basalts straddle the CPSU (critical plane of silica-undersaturation) in the natural basalt system, which is a thermal divide only at low pressures.

It may be noted that the Derbyshire basalts, considered either *in toto* or as individual sequences such as the Calton Hill lavas, do not show decreasing MgO, Ni or Cr concentrations along the down-temperature direction of the 9 kbar cotectic. They do not represent a simple fractionation series at this pressure. Chemical variation within the rocks is related either to higher-pressure fractionation events or to partial melting conditions.

The REE data may be used to comment on relevant models. As noted earlier, the REE patterns are characterized by large variation in the LREE in comparison with the HREE. Such variation is incompatible with low-pressure fractional crystallization of olivine and plagioclase, which generates lavas with sub-parallel REE patterns with different abundances. Extensive fractional crystallization of clinopyroxene might cause LREE enrichment but this seems unlikely, as clinopyroxene has $D^{Cr}_{cpx/l} = 10$ and the lavas with

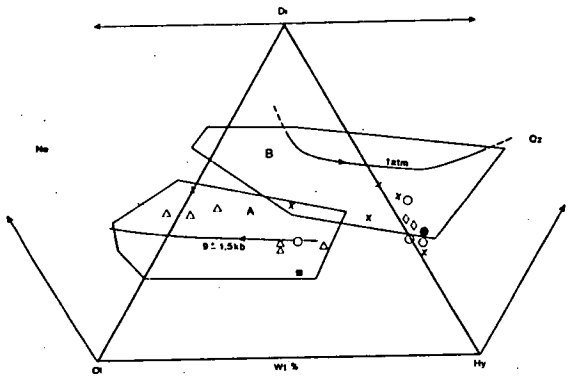

FIG. 10. Compositions of fresh Derbyshire basalts plotted in terms of normative di, ol, hy, ne and q. Symbols as in Fig. 5. The cotectic curves at 1 atm, and 9 kbar (anhydrous) represent the equilibria olivine + plagioclase + clinopyroxene + natural basaltic liquid (Thompson 1982, fig. 2). Arrows mark direction of falling temperature. Field A is slightly enlarged over that which encloses Tertiary Plateau-type mafic rocks from Skye and Mull. B encloses representative Non-Porphyritic Central magma type mafic rocks from throughout the British Tertiary Volcanic Province (from data plotted in Thompson (1982, fig. 2)).

the highest Ce_N/Yb_N do not show any depletion of Cr in comparison with lavas with lower Ce_N/Yb_N. Further, the apparent rarity of clinopyroxene phenocrysts and textural evidence for near-simultaneous crystallization of plagioclase and clinopyroxene argues against extensive fractionation of clinopyroxene. We therefore conclude that the REE data do not reflect low-pressure fractional crystallization of mineral phases present within the basalts.

The characteristic large variation of LREE in relation to HREE has been observed in other basaltic volcanic provinces and has been analysed by Shimizu & Arculus (1975) for a suite of basanitoids and alkali basalts from Grenada, which have similar REE characteristics to the Derbyshire basalts. The small variation in HREE in relation to LREE indicates the presence of a mineral with high HREE partition coefficients such as garnet. Assuming that the mantle source may have 2–3 times chondritic REE abundances (e.g. Kay & Gast 1973; Sun & Hanson 1975) the formation of lavas with HREE (e.g. Yb_N) concentrations of 6–8 × chondritic implies formation by partial melting or fractional crystallization involving garnet or some other mineral(s) with high HREE partition coefficients.

In their analysis, Shimizu & Arculus (1975) excluded low-pressure fractional crystallization (*cf.* above) and investigated high-pressure fractional crystallization and partial melting models. The high-pressure fractionation might have involved garnet-bearing assemblages such as those involved in eclogite-fractionation (e.g. O'Hara 1968). However, as emphasized by Shimizu & Arculus (1975), the high D_{Ga}^{Yb} in garnet means that different degrees of such high pressure fractional crystallization would be unlikely to generate almost constant HREE concentrations. Also, the high values of D_{Ga}^{Cr} and D_{Ga}^{Yb} would generate an inverse correlation between Ce_N/Yb_N and Cr as a result of eclogite fractionation. Such a correlation is not observed. However, the presence of garnet through varying degrees of partial melting is consistent with constant HREE abundances (Shimizu & Arculus 1975) and this model is preferred for the Derbyshire lavas. This is consistent with the conclusion of Donaldson (1978) that the source of the Calton Hill xenoliths was 'probably close to the spinel/garnet transition which would have been crossed by either a small pressure increase or a small temperature decrease' (Donaldson 1978, p. 371).

It appears, therefore, that the Derbyshire rocks had a complicated genesis, *viz*, variable degrees of partial melting of the source rocks generated a range of silica-undersaturation in the parental melts and variable amounts of subsequent moderate-pressure fractional crystallization produced the ranges in Cr, Ni and MgO contents. This is consistent with the observations of Donaldson (1978, p. 372), who noted the lack of evidence for differentiation of the Calton Hill magmas, at least at depths <45 km. It follows that in those sequences which show a substantial range of silica-undersaturation, such as the Upper Miller's Dale Lava, the eruptive rocks represent equilibration over a range of pressures. Unfortunately, the scarcity of data for fresh rocks makes it impossible to analyze the Derbyshire volcanics in terms of parent-daughter relationships.

It is possible to use the incompatible trace element data to comment on the heterogeneity of the mantle sources of the Derbyshire volcanic rocks. Particular use is made of Zr and Nb, which are insensitive to the degree of partial melting or fractional crystallization because of low partition coefficients for likely solid phases (Pearce & Norry 1979).

Zr/Nb ratios (Fig. 8) vary overall from 3.6 to 9. Even in the rocks of one sequence there is considerable variation, e.g. 4.6 to 8.9 in the Upper Miller's Dale Lava. These ranges are quite outside those possible from varying degrees of partial melting or differing fractionation histories, if the mineral–liquid distribution coefficients compiled by Pearce & Norry (1979) for mantle rocks and basalt phenocryst phases are at all representative. This indicates that the Derbyshire volcanics were derived from source mantle rocks which were heterogeneous as regards Zr and Nb distribution. The significance is that each lava or sill, even within a single stratigraphic sequence, represents a discrete melting event.

It may also be noted that within sequences where a

stratigraphy can be established, e.g. Calton Hill, there is no tendency for composition to vary systematically with time, nor can any simple relationship between compositional and geographical location be established, e.g. in the Upper Miller's Dale Lava. These lines of evidence are consistent with the eruption of the Derbyshire extrusive rocks from relatively short-lived small-sized vents. This in turn suggests that high-level magma chambers of substantial size or longevity were never developed during Carboniferous volcanism in Derbyshire. Rather, the melts may have passed through the crust in a system of small conduits, dykes and sills which were largely unconnected between the vents erupting lavas within (and between) each lava sequence (*cf.* Thompson *et al.* 1972 for Skye volcanism and Moore *et al.* 1976 for the San Francisco volcanic field, Arizona).

Discussion

During the period of Carboniferous volcanism the British Isles lay well within the Laurasian continent whose northern, western and eastern margins were many hundreds of kilometres away whilst its southern boundary lay just to the S of the British Isles. Although during the late Devonian–early Carboniferous the ocean separating Laurasia from a more southerly continent was closing (Dewey 1982, fig. 38), Upton (1982, p. 256) maintained that this volcanism was 'thoroughly intraplate in character' and 'not influenced directly by any subduction processes'. Upton's conclusions are confirmed by the geochemical results of this study (Fig. 11).

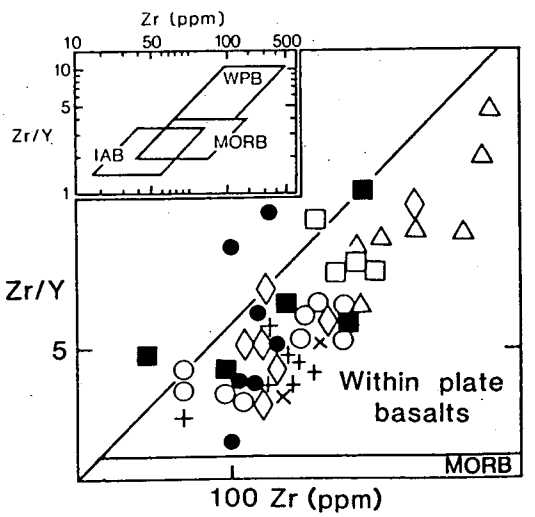

FIG. 11. Zr/Y-Zr plot (Pearce & Norry 1979) indicating the within-plate character of the Derbyshire basalts. Symbols as in Fig. 5. In inset, WPB, within plate basalts; MORB, mid-ocean ridge basalts; and IAB, island arc basalts.

Excluding the far-fetched concept of membrane tectonics (Turcotte & Oxburgh 1973) and the unlikely relationship to a fossil subduction zone in this area (*cf.* Elston 1982), two principal mechanisms have been invoked to explain within-plate Cenozoic volcanism. The first (Gass *et al.* 1978; Pollack *et al.* 1981) proposes that a slow-moving and/or thermally susceptible lithospheric plate is partially fused over a mantle thermal high. Melts produced in this way are alkalic and commonly use faults as lines of easy egress to the surface. However, they are usually also associated with areas of marked topographic uplift, reflecting the production by partial melting of zones of anomalous mantle within the thicker continental lithosphere. In the case of the Derbyshire magmatism, it is relevant to note that there is no evidence for *major* uplift before, during or after the volcanic activity.

The second mechanism is related to tensional stresses produced by the irregular impaction of two continental plates. Upton (1982) has suggested, with particular reference to the Midland Valley and Northumberland Basins, that stresses produced by continental impingement could have produced tensional stresses that reactivated lines of weakness in the underlying basement, thereby controlling the site of volcanic activity and initiating trough formation. In Derbyshire, however, the volcanic activity does not lie along a Caledonide trend. Indeed, Wilkinson (1967) has noted that intrusive bodies and volcanic vents tend to coincide with WNW–ESE anticlinal axes. The lack of evidence that the Derbyshire area was a zone of major lithospheric weakness during the Carboniferous (Leeder 1982) apparently requires at least some modifications to Upton's (1982) proposals.

Noting the seismic evidence for crustal thinning of some 6 km beneath the central Carboniferous basin, Leeder (1982) has attempted to apply McKenzie's (1978) model of lithospheric stretching to Carboniferous basin formation in a continental lithosphere rendered inhomogeneous by the presence of granitic plutons in the upper crust (*cf.* aspects of Francis's (1978) model). The driving force for the stretching was taken to be plate motions and stresses caused by subduction to the S of Britain. Leeder (1982) envisaged that the lithosphere N of St. George's Land was subjected to stretching during the Dinantian, causing regional tension and rift formation in areas of less buoyant (i.e. granite-free) crust.

The status of the Derbyshire area during this stage is uncertain; the northern margin of St. George's Land was not a fault, though it may have been the flexured margin of a half-graben (Leeder 1982, fig. 7B). It is perhaps no coincidence that the Derbyshire volcanism was volumetrically much smaller than that in the Midland Valley of Scotland and the Northumberland trough, where reactivated lines of Caledonian weakness allowed melts easier access to the surface.

Leeder (1982) further suggested that there was an important change in tectonic behaviour in northern Britain during Namurian times. The fault-bounded rifting of the Dinantian was replaced by a general crustal sagging, centred in N Lancashire, caused by asthenospheric cooling. Derbyshire was on the southern limb of this sag and the renewed Namurian volcanism (expressed as sills) might be related to uplift of a rejuvenated St. George's Land, for which there is good sedimentary evidence. It may be noted that, whereas a different style of magmatic emplacement accompanied this transition from rift to sag, the change is not reflected in the chemistry of the volcanic rocks. Magmatic processes during both episodes were apparently identical.

We conclude, therefore, that the Derbyshire Carboniferous volcanism, unlike the Midland Valley of Scotland and Northumberland Trough occurrences, was not associated with any major lithospheric fracturing. The lack of associated isostatic uplift precludes the production of extensive partial melting in the underlying upper mantle. The S Pennine crustal sag of Leeder (1982), associated as it is with underlying crustal attenuation, could well have resulted from lithospheric stretching as invoked by McKenzie (1978). If these inferences are correct, then it seems most probable that no major zone of partial melting underlay Carboniferous Derbyshire but that the mantle was sufficiently fertile for minor quantities of magma to be generated in isolated pockets and that some of these came to the surface along fractures in the attenuated crust and in later Carboniferous times along the flanks of the S Pennine sag.

Walkden's (1977) correlation of minor phases of isostatic uplift with volcanism is interesting, in that Gasse (1975) and Faure (1976) indicated similar temporal correlations for the 0–30 Ma Cenozoic volcanics of the Afar depression. It appears that the energy in these volcanogenic lithothermal systems produces either uplift or volcanism. When volcanism occurs, uplift stops. The 12–15 cycles of uplift identified by Walkden (1977) are not all associated with volcanic products but, as only minor quantities of basalt were erupted and the amount of uplift was limited in both vertical and surface extent, it seems likely that the mantle processes that triggered these effects were also minor and restricted as is also indicated by the geochemically-based magmatic mechanisms we describe.

ACKNOWLEDGMENTS. We are grateful to Dr P. J. Potts, Dr O. Williams Thorpe, A. Tindle, J. Bowman, K. Waterhouse and L. Griffiths for help with sample preparation and analysis, to J. Taylor & H. Boxall for drawing the diagrams and to P. A. Budd for typing the manuscript.

References

BEMROSE, H. H. A. 1894. On the microscopical structure of the Carboniferous dolerites and tuffs of Derbyshire. *Q. J. geol. Soc. London,* **50,** 603–44.

—— 1907. The toadstones of Derbyshire. Their field relations and petrography. *Q. J. geol. Soc. London,* **63,** 241–81.

CHESHIRE, S. G. & BELL, J. D. 1977. The Speedwell vent, Castleton, Derbyshire; a Carboniferous litteral cone. *Proc. Yorks. geol. Soc.* **41,** 173–84.

COPE, F. W. 1933. A tholeiite dyke near Buxton, Derbyshire. *Geol. Mag.* **70,** 414–22.

—— 1937. Some features of the D_1-D_2 limestones of the Miller's Dale region, Derbyshire. *Proc. Yorks. geol. Soc.* **23,** 178–95.

DEWEY, J. F. 1982. Plate tectonics and the evolution of the British Isles. *J. geol. Soc. London,* **139,** 371–414.

DONALDSON, C. H. 1978. Petrology of the uppermost upper mantle deduced from spinel lherzolite and harzburgite nodules at Calton Hill, Derbyshire. *Contrib. Mineral. Petrol.* **65,** 363–77.

ELSTON, G. P. 1982. The basin and range province: origin and tectonic significance. *Ann. Rev. Earth planet. Sci.* **10,** 409–40.

FAURE, H. 1976. Les deformations des cotes et le modele geodynamique de l'Afar. *In:* PILGER, A. & ROSLER, A. (eds). *Afar Between Continental and Oceanic Rifting.* Nagele u. Obermiller, Stuttgart, 148–55.

FITCH, F. J., MILLER, J. A. & WILLIAMS, S. C. 1970. Isotopic ages of British Carboniferous rocks. *C.R. 6th Int. Congr. Carb. Strat. Geol.* (Sheffield, 1967) **2,** 771–90.

FLOYD, P. A. & WINCHESTER, J. A. 1975. Magma type and tectonic setting discrimination using immobile elements. *Earth planet. Sci. Lett.* **27,** 211–18.

FRANCIS, E. H. 1978. The Midland Valley as a rift, seen in connection with the late Palaeozoic European rift system. *In:* RAMBERG, I. B. & NEUMANN, E. R. (eds). *Tectonics and Geophysics of Continental Rifts.* Reidel, Dordrecht, 133–47.

—— & WOODLAND, A. W. 1964. The Carboniferous period. HARLAND, W. B., GILBERT SMITH, A. & WILCOCK, B. (eds) *In: The Phanerozoic Time-scale.* Spec. Publ. geol. Soc. London, **1,** 221–32.

FREY, F. A., GREEN, D. H. & ROY, S. D. 1978. Integrated models of basalt petrogenesis: a study of quartz tholeiites to olivine melilitites from south eastern Australia utilizing geochemical and experimental petrological data. *J. Petrol.* **19,** 463–513.

GASS, I. G., POLLACK, H., THORPE, R. S. & CHAPMAN, D. S. 1978. Geophysical and geochemical parameters of mid-plate magmatism. *Philos. Trans. R. Soc. London,* **288A,** 581–96.

GASSE, F. 1975. Fluctuation in Afar lake levels during the late Quaternary period. *In:* PILGER, A. & ROSLER, A. (eds). *Afar Depression of Ethiopia.* Nagele u. Obermiller, Stuttgart, 184–288.

HAMAD, S. EL D. 1963. The chemistry and mineralogy of the

olivine nodules of Calton Hill, Derbyshire. *Mineralog. Mag. London*, **33**, 483–97.

KAY, R. W. & GAST, P. W. 1973. The rare earth content and origin of alkali-rich basalts. *J. Geol. Chicago*, **81**, 653–82.

LE BAS, M. J. 1962. The role of aluminium in igneous clinopyroxenes with relation to their parentage. *Am. J. Sci.* **260**, 267–88.

LEEDER, M. R. 1982. Upper Palaeozoic basins of the British Isles—Caledonide inheritance versus Hercynian plate margin processes. *J. geol. Soc. London*, **139**, 479–91.

MACDONALD, R., GOTTFRIED, D., FARRINGTON, M. J., BROWN, F. W. & SKINNER, N. G. 1981. Geochemistry of a continental tholeiite suite: late Palaeozoic quartz dolerite dykes of Scotland. *Trans. R. Soc. Edinburgh; Earth Sci.* **72**, 57–74.

MCKENZIE, D. P. 1978. Some remarks on the development of sedimentary basins. *Earth planet. Sci. Lett.* **40**, 25–32.

MOORE, R. B., WOLFE, E. W. & ULRICH, G. E. 1976. Volcanic rocks of the eastern and northern parts of the San Francisco volcanic field, Arizona. *J. Research U.S. geol. Surv.* **4**, 549–60.

O'HARA, M. J. 1968. The bearing of phase equilibrium studies in synthetic and natural systems on the origin and evolution of basic and ultrabasic rocks. *Earth Sci. Rev.* **4**, 69–133.

PEARCE, J. A. & CANN, J. R. 1973. Tectonic setting of basic volcanic rocks determined by using trace element analyses. *Earth planet. Sci. Lett.* **19**, 290–300.

—— & NORRY, M. J. 1979. Petrogenetic implications of Ti, Zr, Y and Nb variations in volcanic rocks. *Contrib. Mineral. Petrol.* **69**, 33–47.

POLLACK, H. N., GASS, I. G., THORPE, R. S. & CHAPMAN, D. S. 1981. On the vulnerability of lithospheric plates to Mid-plate volcanism (reply to comments by P. R. Vogt). *J. geophys. Res.* **86**, 961–6.

POTTS, P. J., THORPE, O. W. & WATSON, J. S. 1981. Determination of the rare-earth element abundances in 29 international rock standards by instrumental neutron activation analysis: a critical reappraisal of calibration errors. *Chem. Geol.* **34**, 331–52.

SHIMIZU, N. & ARCULUS, R. J. 1975. Rare earth element concentrations in a suite of basanitoids and alkali olivine basalts from Grenada, Lesser Antilles. *Contrib. Mineral. Petrol.* **50**, 231–40.

SMITH, E. G., RHYS, G. H. & EDEN, R. A. 1967. Geology of the country around Chesterfield, Matlock and Mansfield. *Mem. geol. Surv. G.B.*

STEVENSON, I. P. & GAUNT, G. D. 1971. Geology of the country around Chapel en le Frith. *Mem. geol. Surv. G.B.*

SUN, S.-S. & HANSON, G. H. 1975. Origin of Ross Island basanitoids and limitations upon the heterogeneity of mantle sources for alkali basalts and nephelinites. *Contrib. Mineral. Petrol.* **52**, 77–106.

THOMPSON, R. N. 1982. Magmatism of the British Tertiary Volcanic Province. *Scott. J. Geol.* **18**, 49–107.

——, ESSON, J. & DUNHAM, A. C. 1972. Major element chemical variation in the Eocene lavas of the Isle of Skye, Scotland. *J. Petrol.* **13**, 219–53.

TOMKEIEFF, S. I. 1928. The volcanic complex of Calton Hill. *Q. J. geol. Soc. London*, **84**, 703–18.

TURCOTTE, D. L. & OXBURGH, E. R. 1973. Mid-plate tectonics. *Nature, London*, **244**, 337–9.

TURNER, P. & TARLING, D. H. 1975. Implications of new palaeomagnetic results from the Carboniferous system of Britain. *J. geol. Soc. London*, **131**, 469–88.

UPTON, B. G. J. 1982. Carboniferous to Permian volcanism in the stable foreland. *In:* SUTHERLAND, D. S. (ed.). *Igneous Rocks of the British Isles*, John Wiley & Sons, 255–75.

WALKDEN, G. M. 1977. Volcanic and erosive events on an Upper Viséan carbonate platform, north Derbyshire. *Proc. Yorks. geol. Soc.* **41**, 347–67.

WALTERS, S. G. & INESON, P. R. 1981. A review of the distribution and correlation of igneous rocks in Derbyshire, England. *Mercian Geol.* **8**, 81–132.

WILKINSON, P. 1967. Volcanic rocks in the Peak District. *In:* NEVES, R. & DOWNIE, C. (eds). *Geological Excursions in the Sheffield Region and the Peak District National Park*. Univ. Sheffield Press, 47–53.

Received 3 February 1983; revised typescript received 8 June 1983.

R. MACDONALD & K. N. GASS, Department of Environmental Sciences, University of Lancaster, Bailrigg, Lancaster LA1 4YQ.

R. S. THORPE, & I. G. GASS, Department of Earth Sciences, The Open University, Walton Hall, Milton Keynes, MK7 6AA.

PROCEEDINGS OF THE YORKSHIRE GEOLOGICAL SOCIETY, VOL. 45, PART 3, PP. 141-146, 1985

Geochemistry and tectonic significance of the Lower Carboniferous Cockermouth lavas, Cumbria

R. MACDONALD and B. H. WALKER

SUMMARY: Dinantian volcanism in the Cockermouth area was associated with the initiation of the Northumberland Basin and was related to crustal attenuation resulting from lithospheric stretching. The sequence consists mainly of basalts of tholeiitic (quartz-normative) affinity, with minor tholeiitic andesites. The basaltic magmas were generated by variable degrees of partial melting of homogeneous mantle source rocks followed by fractional crystallization and final equilibration at high crustal levels. The tholeiitic andesites probably indicate the establishment of high level magma chambers. The intrusive basalts of Little Mell Fell are confirmed on chemical grounds as likely outliers of the Cockermouth lavas. There are also close compositional similarities with Dinantian lavas in Derbyshire and south and central Scotland, and with the Whin Sill magma type, indicating that changing tectonic conditions during the Carboniferous are not reflected in magma compositions. There is no evidence in magma chemistry that the Iapetus suture underlies the Northumberland Basin.

Eruption of the Dinantian Cockermouth lavas coincided with the initiation of the Northumberland Basin and heralded a major period of marine transgression onto the Cumbrian/Alston Block (Leeder 1974). Mantle melting, subsidence and uplift were undoubtedly closely related. Leeder (1982) has suggested that basin subsidence resulted from lithospheric stretching which caused regional tension, rift formation and volcanism in areas of less buoyant crust. A special feature of early Dinantian magmatism in the Northumberland Basin is that it occurred in an area of the lithosphere which may contain the remnant Iapetus suture (Leeder 1982). Petrological studies of the Cockermouth lavas, while providing important general information on Dinantian volcanism in northern Britain, may also indicate any possible influence of the ancient plate boundary on later magmagenetic processes.

The Cockermouth lavas (Eastwood 1928) crop out from near Cockermouth to Bothel, a distance of about 13 km (Fig. 1). They lie within the Basement Beds; spore assemblages from sediments below and above the lavas belong to the CM zone of the Courceyan stage (Mitchell 1978, p. 171). There is no good evidence to suggest whether or not the lavas thin out to zero in any direction. Associated extrusive rocks may have been erupted to the south. Capewell (1954) suggested, on petrographical grounds, that basaltic intrusions and vent tuffs at Little Mell Fell, some 32 km to the south-east of the lava outcrop, represent an outlier of the early Dinantian activity. This suggestion is tested geochemically in this paper.

Exposure of the lavas is poor over much of the outcrop, which makes the mapping of individual flows and the erection of a lava stratigraphy very difficult. At some localities, e.g. around Wood Hall and in Ullerance Gill, five or perhaps six separate flows can be distinguished on the basis of topography and/or the presence of scoriaceous flow tops. A maximum total thickness of about 100 m occurs towards the west of the outcrop (Fig. 1). There is a general easterly thinning to 30 - 40 m in the Bothel area, while the number of flows is reduced to two or three.

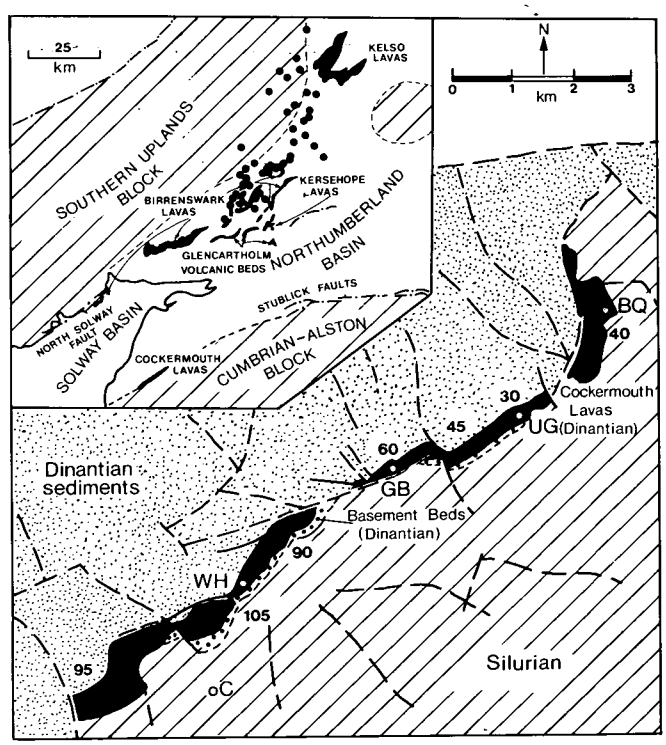

Fig. 1. Sketch map (after Eastwood 1928 and Geological Survey maps) showing the distribution of the Cockermouth lavas. Approximate thicknesses (in metres) of the sequence also shown. BQ – Bothelcrags Quarry; UG – Ullerance Gill; GB – Gill Beck; WH – Wood Hall. Inset shows the general tectonic setting of the Lower Carboniferous lavas of the Northumberland Basin (after Leeder 1974). Filled circles are volcanic necks.

Relatively quiet extrusion of the Cockermouth lavas is suggested by the apparent absence of pyroclastic materials and by the presence of bole-like material between certain flows (e.g. 300 m NE of Wood Hall: Eastwood 1928). As proposed by Leeder (1974) for the closely similar Birrenswark lavas at the northern margin of the Northumberland Basin, the Cockermouth lavas may have been erupted as successive flows from a fissure line or from a series of vents aligned along the present line of outcrop. Eruptive sources have not yet been recognised in the field, however, and Eastwood *et al.* (1968, p. 152) have suggested that the sources may have lain further west. A basaltic dyke cutting Skiddaw Slates at [NY 1232 3206] has been discounted as a possible lava feeder on the basis of size (thickness = 1.5 m) by Eastwood *et al.* (1968).

1. PETROGRAPHY

The Cockermouth lavas are not so 'remarkably consistent' in petrological character as thought by Eastwood (1928, p. 17). While the dominant rock type is basaltic, the presence of *tholeiitic andesites* is also noted here. This appears to be the first record of intermediate rocks among the Dinantian lavas of England, though they are common in the Scottish Midland Valley (MacGregor 1928).

The *fresh basalts* are typically sparsely microphyric, with variable amounts of olivine microphenocrysts. The phenocryst assemblages olivine + plagioclase (specimens F2, 37) and olivine + plagioclase + augite (F3, F4) are less common. Cognate olivine-augite-plagioclase xenoliths are found in specimen F4. The groundmass consists of the same phases plus Fe-Ti-oxides. Textures are most commonly ophitic, trachyophitic, and, less often, intergranular.

A notable feature of the basalts, however, is their ubiquitous secondary alteration. Olivine is invariably replaced by serpentine-chlorite-green mica-silica-ore-carbonate assemblages. Augite may be preserved in partially fresh condition (F3, F4, 35) but is more normally altered to serpentine ± carbonate. Of the major silicate phases, plagioclase is most frequently found fresh; where altered, it is carbonated and/or slightly albitised.

One possible result of the pervasive alteration is that no positive identification of Ca-poor pyroxene has been made in the lavas, though its presence may be suspected from its occurrence in compositionally similar Dinantian lavas from Derbyshire (Macdonald *et al.* 1984).

Tholeiitic andesites have been found in Gill Beck (G1, G2), in the quarry at Bothelcrags (BQ1) and possibly as an altered xenolith in a basalt flow in Ullerance Gill. The Gill Beck rocks are fine-grained, with a strong flow texture defined by the plagioclase laths. Granular augite is partially serpentinised; equant ore grains are abundant. Quartz, alkali-feldspar and chlorite are late-crystallising minerals. The Bothelcrags rock is rather similar, except that albitisation, carbonation and sericitisation of the plagioclase and replacement of the ferromagnesian minerals by carbonate and serpentine are ubiquitous.

Petrographic descriptions of the Little Mell Fell rocks are given by Capewell (1954), whose likening of them to the olivine basalts of Cockermouth is confirmed here. However, these rocks are notably fresh.

2. GEOCHEMISTRY

Analyses have been made of twenty-two Cockermouth lavas and of two rocks from Little Mell Fell, using standard XRF and wet-chemical techniques. The lavas were chosen to cover the stratigraphic and lateral ranges and to be as fresh as possible. Representative analyses are given in Table 1; the full body of data is available from the authors and has also been placed in the YGS library.

Table 1

Representative analyses of Cockermouth lavas

Locality	Home Wood	Mily Scroggs	Redmain	Gill Beck	Ullerance Gill	Little Fell
Grid ref. (NY-)	127328	131332	136336	149342	170351	429240
Spec. No.	44A	F3	RF2	G1	U3	LMF1
SiO_2	51.9	50.4	50.0	57.7	42.2	49.5
TiO_2	2.08	2.35	1.97	0.90	1.51	3.02
Al_2O_3	14.66	14.64	15.22	18.40	13.27	14.27
FeO*	10.05	10.49	10.57	7.68	11.54	11.58
MnO	0.10	0.13	0.16	0.23	0.22	0.14
MgO	5.81	4.14	7.35	2.43	3.75	7.12
CaO	9.28	9.85	9.21	6.11	14.03	8.08
Na_2O	2.29	2.73	2.38	2.96	1.87	2.71
K_2O	0.83	1.26	0.47	1.12	0.29	1.48
P_2O_5	0.29	0.47	0.29	0.24	0.21	0.54
H_2O+	2.87	1.62	2.24	2.18	3.16	1.01
Total	100.16	98.08†	99.86	99.95	92.05†	99.45
(ppm)						
Ba	195	314	214	348	62	408
Ce	46	65	42	62	28	63
Nb	22	28	18	17	11	32
Rb	14	21	3	24	9	30
Sr	264	215	315	271	167	510
Y	25	28	21	27	17	30
Zr	159	215	145	141	85	258

Analyses by XRF; major elements on fusion discs using a Philips PW 1400 spectrometer (University of Lancaster).
†low totals in F3 and U3 due to non-determination of CO_2.

As noted above, the rocks show varying degrees of alteration, between those largely retaining igneous mineralogy to those where original minerals have been totally pseudomorphed. Mobility of such elements as Si, Ca, Mg, Na, K, Ba, Rb and Sr is very likely during carbonation, hydration and silicification. Employing the methods used by Macdonald *et al.* (1981, table 5) to assess chemical changes during alteration of Carboniferous quartz dolerites in Scotland, it can be shown that the most important major element effects in

the Cockermouth lavas were addition of Ca and loss of Mg and Na during carbonation and loss of Na during secondary hydration. Trace element mobility may be evaluated by plotting element concentrations against data for stable incompatible elements such as Zr, with another stable element as a monitor. Plots of Zr against Nb, Sr and Rb (Fig. 2) indicate a situation similar to that

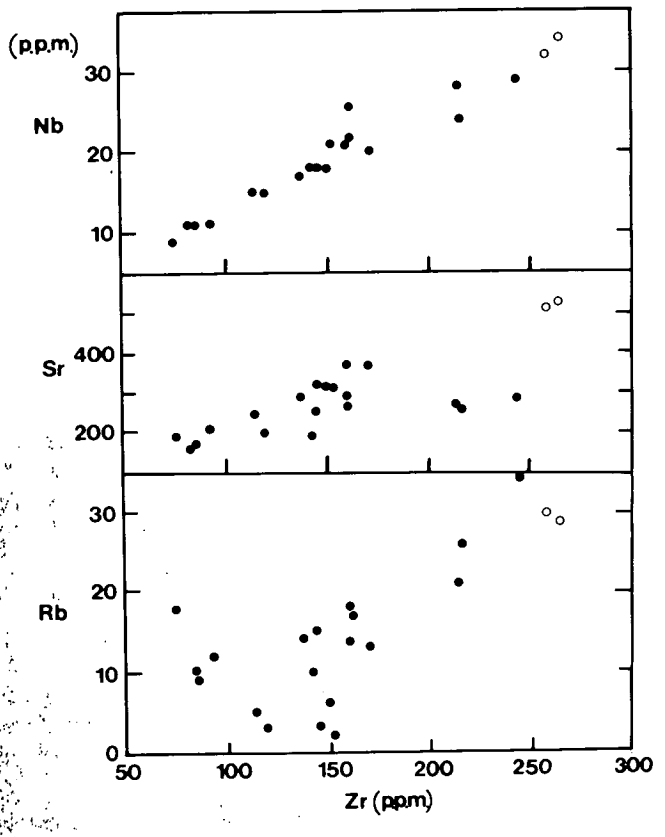

Fig. 2. Plot of Nb, Sr and Rb against Zr for analyzed lavas (solid circles) and Little Mell Fell intrusions (open circles).

in the Dinantian basalts of Derbyshire (Macdonald *et al.* 1984). Nb was stable, and Rb was secondarily mobilized, during the various alteration processes. Sr data are scattered, suggesting some mobilisation, but this was not strong enough to obscure the positive relationship with Zr.

Certain important features may be noted in the Zr-Nb plot:

(a) The basalts show a significant range of incompatible trace element abundances (x 3 for some stable elements).
(b) The Cockermouth basaltic lavas form a very coherent, genetically related group of rocks.
(c) The Little Mell Fell intrusions are almost certainly related to the lavas, confirming the suggestion (Capewell 1954) of Dinantian magmatism on the Lake District Block.

The range in incompatible trace element abundances may result from several factors; varying degrees of melting of (possibly heterogeneous) mantle source rocks, polybaric fractional crystallization of the parental magmas and crustal contamination of mantle-derived melts. Positive correlations between the degree of silica-undersaturation and such lithophilic elements as K (Fig. 3) and Ba suggest that any crustal contamination must have been slight and such effects are ignored in the following discussion.

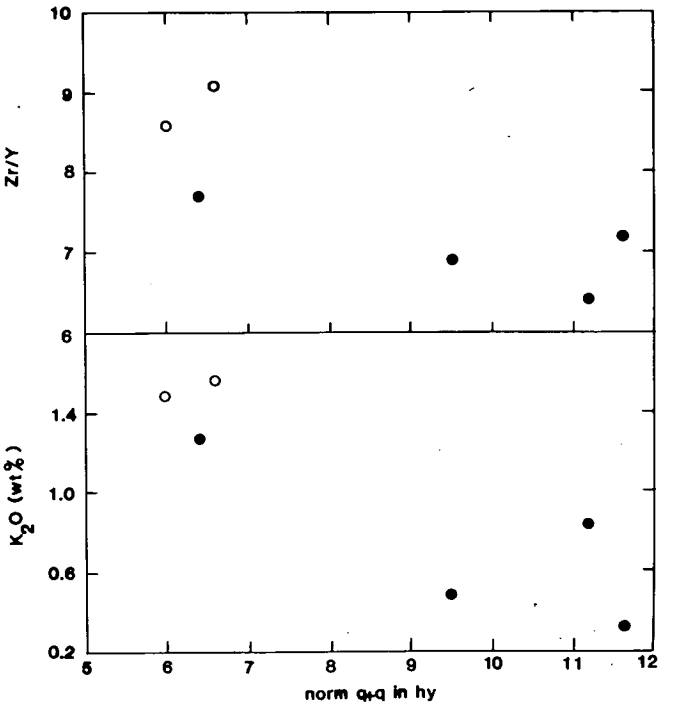

Fig. 3. Degree of silica – saturation plotted against K_2O and Zr/Y for 'fresh' Cockermouth lavas (solid circles) and Little Mell Fell intrusions (open circles). Note the negative correlation in both cases. 'Fresh' rocks are 44A, F3, RF2, 35, LMF1, and LMF8.

The incompatible trace element data provide some information on the degree of heterogeneity of the mantle sources of the Cockermouth rocks. Zr and Nb are particularly useful, since low partition coefficients for likely solid phases in the mantle make them insensitive to the degree of partial melting or fractional crystallization (Pearce & Norry 1979). Zr/Nb ratios in the basalts vary only from 7.2 to 8.4, a range within that of possible analytical error. Other relevant ratios, such as Zr/Y and Ce/P_2O_5, give similar results and it may be concluded that there is no evidence that the mantle sources were chemically heterogeneous.

An important first step in assessing the petrogenesis of the lavas is to establish their magmatic affinities. In this respect, the following lines of evidence may be noted:

(a) CIPW norms have been calculated, on a volatile-free basis and with Fe_2O_3 arbitrarily set according to the limits of Macdonald (1975), for fresh basalts only (with fresh rocks defined as having a substantial proportion of augite and plagioclase unaltered). The samples are quartz-normative, with the exception of one Little Mell Fell rock, which is barely olivine-normative ($ol = 1.3\%$).

(b) The ratios Zr/Y and Nb/Y increase, and the ratio Zr/Nb decreases, with increasing alkalinity of basalts (Pearce & Cann 1973; Floyd & Winchester 1975; Pearce & Norry 1979). The Cockermouth rocks show negative correlation of Zr/Y (Fig. 3) and Nb/Y ratios, and positive correlation of Zr/Nb ratio, with the degree of silica-saturation. This suggests that the range in silica-saturation, though small, is real. Furthermore, significant negative correlations between the degree of silica-saturation and the abundances of Ti, K, P, Ba, Ce, Nb and Zr indicate that the chemical variations are *magmatic* and not a result of hydrothermal alteration.

Cockermouth magmatism appears, therefore, to have been predominantly of quartz tholeiitic type, in the sense of containing $q + hy$. They form a group chemically transitional between the *hy*-norm, alkaline rocks of the Midland Valley of Scotland (Macdonald 1980) and the late Carboniferous quartz dolerite

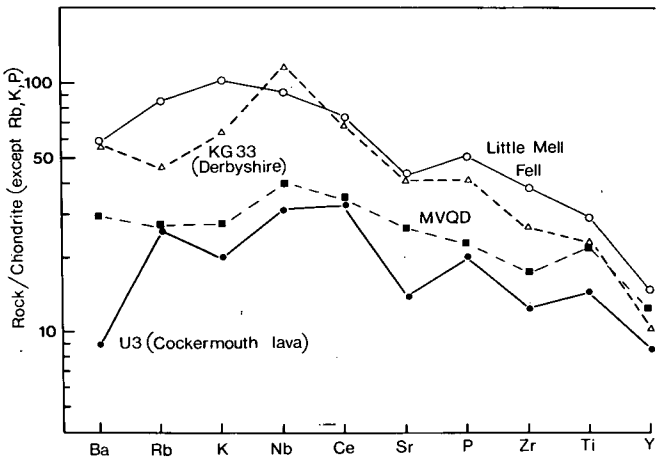

Fig. 4 Chondrite-normalized (except for Rb, K and P) element patterns for: Cockermouth lava (U3), Little Mell Fell intrusion (LMF1), Calton Hill lava, Derbyshire (KG33) (Macdonald *et al.* 1984), and median composition at 7.5% MgO, late Carboniferous quartz dolerite suite, Scotland (MVQD, Macdonald *et al.* 1981, table 7), which is analogous to the Whin Sill magma composition. Normalizing factors from Thompson (1982, p. 105).

dyke-sill complex of northern Britain (Macdonald *et al.* 1981). In this respect, they are closely similar to the Dinantian basaltic lavas of Derbyshire (Fig. 4) which show, however, a somewhat broader range of alkalinity, from *ne*-normative to *q*-normative types (Macdonald *et al.* 1984), and to the Birrenswark basalts of the northern part of the Northumberland Basin (Macdonald 1975).

A note is required on the terminology applied to the compositionally intermediate members of the Cockermouth sequence, since this is the first time that tholeiitic andesite has been used for a British Carboniferous lava, as far as we are aware. Though the rocks in question are somewhat altered, their major element concentrations must be reasonably close to magmatic. This is clearly shown in Figure 5, where the

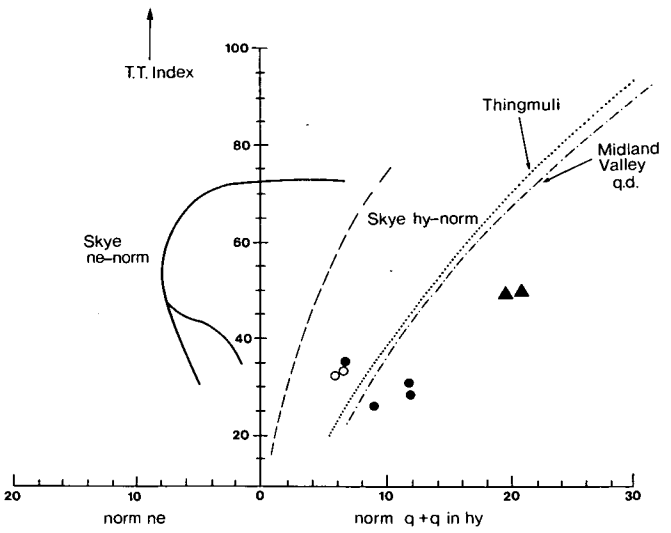

Fig. 5. Degree of silica-saturation plotted against Thornton-Tuttle Differentiation Index to show the tholeiitic affinity of the Cockermouth lavas. Solid circles – basalts, closed triangles – tholeiitic andesites, open circles – Little Mell Fell intrusions. Data for Skye series from Thompson *et al.* (1972), Thingmuli, Iceland from Carmichael (1964) and the Midland Valley quartz dolerite suite from Macdonald *et al.* (1981).

two freshest samples plot in comparable positions to the intermediate members of such tholeiitic suites as the Antrim lavas, Thingmuli lavas and the Midland Valley quartz dolerite suite. It follows that a tholeiitic nomenclature should be adopted for these rocks. A similar case has recently been argued by Lyle and Thompson (1983) for Tertiary intermediate lavas in Antrim.

3. PETROGENESIS OF BASALTS

The problems of establishing the magmatic composition of the majority of Cockermouth specimens makes it difficult to assess their petrogenesis. The following comments are based on the discussion of the Derbyshire basalts (Macdonald *et al.* 1984)

The low Mg number (100 Mg/(Mg + Fe) $\leqslant$60) of the Cockermouth and Little Mell Fell basalts makes it unlikely that they are primary basalts, since only basalts with Mg number >66 are taken to be in equilibrium with mantle olivine of composition Fo >87. It would seem that the lavas have reached their final compositions at lower pressures, within the upper crust. On a normative basalt projection (Fig. 6), they are related to cotectic equilibria close to 1 atm. (cf. Thompson 1982). $Hy \pm q$–normative basalts from Derbyshire plot in the same field and have also been interpreted as showing low-pressure control (Macdonald *et al.* 1984).

An important observation is that the basalts do not show a simple relationship between MgO and the abundances of the incompatible trace elements. In fact, the most magnesian rocks also contain the highest abundances of such elements, and of K, Ti and P. The basalts do not represent, therefore, a simple low-

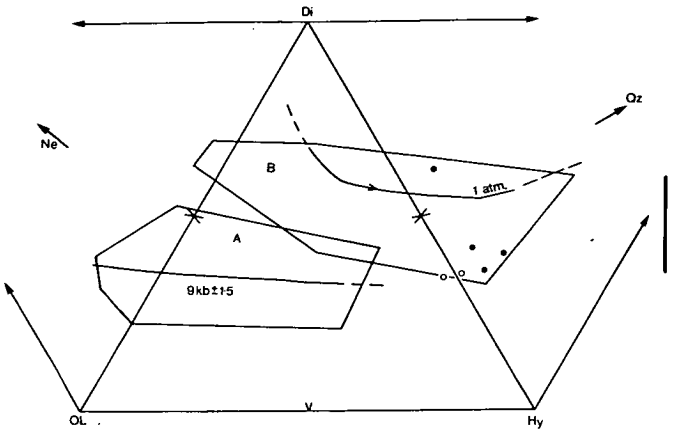

Fig. 6. Compositions of fresh Cockermouth basalts plotted in terms of di, ol, hy, ne and qz. Symbols as in Fig. 2. The cotectic curves at 1 atm. and 9 Kb (anhydrous) represent the equilibria olivine + plagioclase + clinopyroxene + natural basaltic liquid (Thompson 1982, Figure 2). Arrows mark direction of falling temperature.
Field A is slightly enlarged over that which encloses Tertiary Plateau-type mafic rocks from Skye and Mull. B encloses representative Non-Porphyritic Central magma-type mafic rocks from throughout the British Tertiary Volcanic Province (from data plotted in Thompson 1982, Figure 2). Note how the Cockermouth rocks seem to be related to low-pressure equilibria.

pressure fractionation series. Chemical variation within the basalts must be due either to variable partial melting conditions or to higher-pressure fractionation. It is not possible to judge between these on available evidence but, again using Derbyshire as a model, it is probable that the Cockermouth rocks evolved as follows: variable degrees of partial melting of the source rocks generated the slight range of silica-saturation in parental melts and then variable amounts of subsequent moderate to low pressure fractional crystallization produced the range of MgO content.

4. DISCUSSION

The tholeiitic affinity of the Cockermouth lavas matches that of part of the Derbyshire Dinantian lavas, the Birrenswark-Kelso lavas and of part of the central Scottish sequences (Macdonald 1975; Macdonald *et al.* 1977; Macdonald *et al.* 1984). Their composition is also more closely similar to that of the Whin Sill than has been previously recognized, indicating that although the magmas were generated in different structural regimes (Leeder 1982, Johnson 1982), this was not reflected in the magma chemistry. Leeder (1982) has suggested that Dinantian volcanism of the Northumberland Basin was a result of the partial melting of the upper mantle along the line of the supposed Iapetus suture, as a result of the thinning of weak lithosphere. We accept (cf. Macdonald *et al.* 1984) that the magmatism is in some way related to lithospheric stretching. It is important to note, however, that if the suture lies beneath the Northumberland Basin, its presence had no detectable influence on magma composition. Dinantian magmatism throughout the stable foreland produced a rather restricted range of basaltic magma compositions (tholeiitic to mildly undersaturated), suggesting uniform conditions of genesis within compositionally similar mantle sources.

The presence of intermediate lavas in the Cockermouth suite points to the establishment, at least locally, of high-level magma chambers in which fractionation of the basaltic parental magmas took place. The Northumberland Basin thus marks a transitional stage between the Midland Valley, where intermediate to silicic volcanics are relatively common, and Derbyshire, where they are apparently completely absent.

Acknowledgements. Professor E. H. Francis and Dr M. R. Leeder kindly commented on the manuscript and J. O. Bowman and K. S. Waterhouse provided analytical assistance. P. D. Iles and W. F. Price contributed field observations from unpublished mapping.

References

CAPEWELL, J. G. 1954. The basic intrusions and an associated vent near Little Mell Fell, Cumberland. *Trans. Leeds Geol. Assoc.* **6**, 243-248.

CARMICHAEL, I. S. E. 1964. The petrology of Thingmuli, a Tertiary volcano in eastern Iceland. *J. Petrol.* **5**, 435-460.

EASTWOOD, T. 1928. The Cockermouth lavas, Cumberland – a Carboniferous volcanic episode. *Summ. Prog. Geol. Surv. G. B.*, Pt. 2, 15-22.

EASTWOOD, T., HOLLINGWORTH, S. E., ROSE, W. C. C. & TROTTER, F. M. 1968. Geology of the country around Cockermouth and Caldbeck. *Mem. Geol. Surv. G. B.*

FLOYD, P. W. & WINCHESTER, J. A. 1975. Magma type and tectonic setting discrimination using immobile elements. *Earth Planet. Sci. Lett.* **27**, 211-218.

JOHNSON, G. A. L. 1982. Geographical change in Britain during the Carboniferous Period. *Proc. Yorkshire Geol. Soc.* **44**, 181-203.

LEEDER, M. R. 1974. The origin of the Northumberland basin. *Scott. J. Geol.* **10**, 283-296.

LEEDER, M. R. 1982. Upper Palaeozoic basins of the British Isles – Caledonide inheritance versus Hercynian plate margin processes. *J. Geol. Soc.* **139**, 479-491.

LYLE, P. & THOMPSON, S. J. 1983. The classification and chemistry of the Tertiary intermediate lavas of Northeast Ireland. *Scott. J. Geol.* **19**, 17-27.

MACDONALD, R. 1975. Petrochemistry of the early Carboniferous (Dinantian) lavas of Scotland. *Scott. J. Geol.* **11**, 269-314.

MACDONALD, R. 1980. Trace element evidence for mantle heterogeneity beneath the Scottish Midland Valley in the Carboniferous and Permian. *Phil. Trans. R. Soc., Ser. A*, **297**, 245-257.

MACDONALD, R., GASS, K. N., THORPE, R. S. & GASS, I. G. 1984. Geochemistry and petrogenesis of the Derbyshire Carboniferous basalts. *J. Geol. Soc.* **141**, 147-159.

MACDONALD, R., GOTTFRIED, D., FARRINGTON, M. J., BROWN, F. W. & SKINNER, N. G. 1981. Geochemistry of a continental tholeiite suite: late Palaeozoic quartz dolerite dykes of Scotland. *Trans. R. Soc. Edinburgh Earth Sci.* **72**, 57-74.

MACDONALD, R. THOMAS, J. E. & RIZZELLO, S. A. 1977. Variations in basalt chemistry with time in the Midland Valley province during the Carboniferous and Permian. *Scott. J. Geol.* **13**, 11-22.

MACGREGOR, A. G. 1928. The classification of Scottish Carboniferous olivine basalts and mugearites. *Trans. Geol. Soc. Glasgow* **18**, 324-360.

MITCHELL, M. 1978. Dinantian. pp. 168-177 in MOSELEY, F. (editor): *The geology of the Lake District.* Yorkshire Geol. Soc.

PEARCE, J. A. & CANN, J. R. 1973. Tectonic setting of basic volcanic rocks determined by using trace element analyses. *Earth Planet. Sci. Lett.* **19**, 290-300.

PEARCE, J. A. & NORRY, M. J. 1979. Petrogenetic implications of Ti, Zr, Y and Nb variations in volcanic rocks. *Contrib. Mineral. Petrol.* **69**, 33-47.

THOMPSON, R. N. 1982. Magmatism of the British Tertiary Volcanic Province. *Scott. J. Geol.* **18**, 49-107.

THOMPSON, R. N., ESSON, J. & DUNHAM, A. C. 1972. Major element chemical variation in the Eocene lavas of the Isle of Skye, Scotland. *J. Petrol.* **13**, 219-253.

R. MACDONALD, Ph.D.
Department of Environmental Sciences
University of Lancaster,
LANCASTER
LA1 4YQ.

B. H. WALKER, B.Sc.
Department of Earth Sciences
University of Leeds
LEEDS
LS2 9JT.

Revised manuscript received: 9th October, 1984.

Mag. 122 (4), 1985, Pp. 389–396. Printed in Great Britain

Geochemical evidence for the emplacement of the Whin Sill complex of northern England

R. S. THORPE* & R. MACDONALD†

* Department of Earth Sciences, The Open University, Milton Keynes, MK76AA, England
† Department of Environmental Sciences, University of Lancaster, Lancaster, LA1 4YQ, England

(*Received* 5 September 1984; *accepted* 7 January 1985)

Abstract – The Whin Sill comprises a major quartz tholeiite sill of late Carboniferous age underlying an area of *c.* 5000 km² and with a volume of *c.* 200 km³, associated with contemporaneous dykes emplaced within Carboniferous sedimentary rocks in northeast England. New trace element analyses of chilled margins, sill interiors and dykes indicate that the Whin Sill complex magmas show significant chemical variations in terms of the relatively stable trace elements Th, Ce, Y, Zr, Nb and Ni. These data indicate that the complex was fed by a large number of compositionally distinct magma pulses, and that certain of the dykes may have formed feeder channels for the sill. The chemical characteristics of the sill and dyke samples are consistent with derivation by extensive polybaric fractional crystallization of olivine tholeiite magma derived by partial melting of compositionally heterogeneous mantle peridotite and/or crustal contamination of mantle-derived magmas.

ntroduction

e Whin Sill complex comprises a number of basaltic and a suite of dykes of late Carboniferous age placed into Carboniferous sedimentary rocks in theast England. It is probably the type example of form of intrusion (Randall, 1980) and has been nsively studied for more than a century (summaries Randall, 1980; Dunham & Strasser-King, 1982 and ncis, 1982). Despite this, many problems remain cerning magma sources and the mode of emplace- nt of the complex. Here, we use geochemical data comment on two such problems: the number of gmatic pulses involved in sill development and the tionships between the sill and associated dykes.

Geological setting

e largest sill, termed the Great Whin Sill, is broadly cordant with the eastward-dipping geological cture of the region, and underlies *c.* 4000–5000 km² area, and has a volume variously estimated at 120 km³ (Dunham & Strasser-King, 1982) and km³ (Francis, 1982). However, the sill thickens ards the east, as it dips below the North Sea, so that se values represent only a fraction of the total ume of the Whin Sill.

The outcrop of the Whin Sill forms a semi-continuous crop pattern determined by the regional geological ctures (Fig. 1). The outcrop of the sill forms the oe Hills in the north, then runs to Bamburgh Castle the Farne Islands and forms the coastline between nstanburgh and Cullernose Point. These outcrops n an arc around the Devonian Cheviot granite. th of the granite, a discontinuous outcrop trends thwest from Alnwick through Wards Hill and rasford to the River North Tyne and then to the westernmost outcrop near Denton Fell. The southernmost outcrops include those in upper Teesdale, where the sill is *c.* 73 m in thickness and responsible for the picturesque waterfalls of High Force and Cauldron Snout. The sill has been penetrated in several boreholes (Fig. 1), including the Harton borehole (Ridd, Walker & Jones, 1970), which has the maximum recorded thickness of the sill; the aggregate thickness of three leaves of the sill is *c.* 90 m. The stratigraphic horizons at which the sills are emplaced range from Dinantian in the north (Kyloe Hills) and southwest (Teesdale) to Coal Measures (Westphalian) in the Midgeholme district (Fig. 1). The geological features of the Whin Sill have recently been described in detail by Francis (1982).

In some boreholes (e.g. Harton, see above) and in Weardale west of Stanhope (Fig. 1) the sill occurs as a number of leaves at different stratigraphic horizons. In Weardale (including the Rookhope borehole) a leaf *c.* 2 m in thickness and termed the Little Whin Sill (Dunham, 1948) occurs 120 m above the main sill; the leaf has been studied in detail by Dunham & Kaye (1965). The sill samples analysed for the present study are from the undivided 'Great Whin Sill' and are therefore relevant to the emplacement of a single sheet of magma.

The dykes associated with the Whin Sill occur in four spatially distinct groups (or echelons), each with a NE–SW to ENE–WSW strike. From north to south these are (i) the Holy Island dyke echelon, which is slightly north of the known exposures of the Whin Sill (Randall & Farmer, 1970); (ii) the High Green dyke echelon, which includes some dykes up to *c.* 65 m in width and reaches the coast at Boulmer; (iii) the St Oswald's Chapel dyke echelon; and (iv) the Hett dyke system, and the Wackerfield dyke which occurs

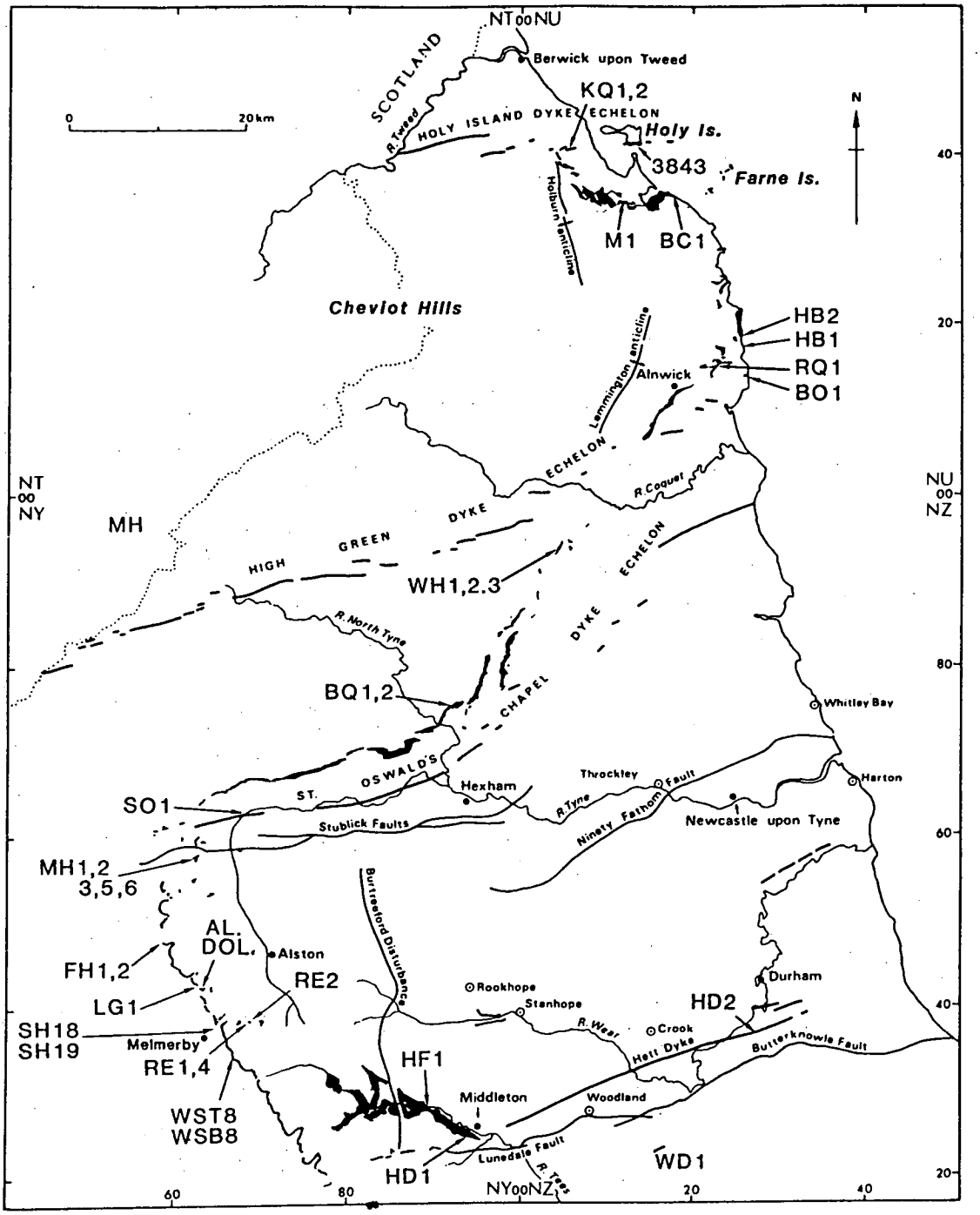

Figure 1. The outcrop of the Whin Sill and associated dykes showing locations of analysed samples (circles show locations of boreholes which have penetrated the Whin Sill).

c. 8 km to the south. Contemporaneous dykes also occur close to the outcrop of the sill, near Melmerby, between the St Oswald's Chapel and Hett dyke systems (Wadge, Harrison & Snelling, 1972).

The Whin Sill and associated dykes intrude Upper Carboniferous (Westphalian) rocks, but do not penetrate the Permian. Pebbles of Whin Sill dolerite are known from Permian continental breccias ('brockram') on the west of the Pennines (Dunham, 1932). The age of emplacement is therefore bracketed between the Upper Carboniferous and Lower Permian, and this is confirmed by K–Ar dating, which suggests an age of 295 ± 6 Ma (Fitch & Miller, 1967). Dykes near Melmerby (Fig. 1) have yielded an almost identical age of 296 ± 8 Ma (Wadge, Harrison & Snelling, 1972), indicating that they are contemporaneous with the Whin Sill (ages uncorrected from original references).

The mechanism of emplacement of the Whin Sill has been the subject of much speculation. Many workers have suggested that the sill has been emplaced through fissures now represented by the Whin dykes. For example, Holmes & Harwood (1928, p. 531) argued that it is 'highly probable' that 'the visible dykes are

feeders of the Whin Sill', but that 'in the Pennines, eems probable that... there are also hidden feeders t represented at the surface'. In addition to the main ke echelons (see above), the area of the monoclinal d termed the Burtreeford 'disturbance' has been ggested as the possible site of a feeder channel unham, 1948; Burgess and Holliday, 1979). Objec- ns to the concept of dyke feeders are that, at the e of intrusion, the sill was at a lower elevation than level of emplacement of the dykes (Dunham & asser-King, 1982), and that the thickness of the sill es not correlate with the location of the dykes rancis, 1982). However, the concept of dyke feeders the Whin Sill has been elegantly developed by ancis (1982), who argued that the sill was emplaced hin stratigraphically low areas of the Carboniferous ccession by gravitational flow down-dip from feeder kes which were emplaced to within 0.5–1 km of the ntemporary land surface.

Petrography

e petrography and petrology of the Whin Sill has en described by, *inter alia*, Holmes & Harwood 28); Tomkeieff (1929); Dunham (1948); Dunham, pley & Strasser-King (1972); Harrison (1968); and nham & Strasser-King (1982). This account is sed upon data within these references and on a study the analysed samples. The sill has a fine-grained crocrystalline or tachylitic margin which may be ıyric or may contain microphenocrysts of plagioclase l pyroxene and aggregates of serpentine and Fe–Ti de which have been interpreted as pseudomorphs er olivine (Allport, 1874; Tomkeieff, 1929). Fresh vine (Fo_{85}) has been found only in the margin of the tle Whin Sill (Dunham & Kaye, 1965). The main ss of the sill is a medium-grained dolerite, nposed typically of 50% plagioclase (zoned from $_{68}$–An_{25}), 37% clinopyroxene (augite, subcalcic gite and pigeonite), 0.5% orthopyroxene, 7% Fe–Ti ide, 1.5% quartz, 2.5% micropegmatite, and a small ıount of secondary carbonate, biotite and hornblende unham & Strasser-King, 1982).

Locally, the Whin Sill feldspars are altered to white ca and clay minerals and the ferromagnesian nerals are altered to amphibole, chlorite and rbonates (Ineson, 1972; Dunham & Strasser-King, 82) The end-product of such alteration is the rmation of a rock termed the 'White Whin' in which primary igneous mineralogy is replaced by a ıt-coloured microcrystalline aggregate composed of ite micas, clay minerals, quartz and carbonates with amd Fe–Ti oxides. Such White Whin may form in lled margins or within the sill interior.

n addition to the dominant andesitic–labradorite gioclase, Holmes & Harwood (1928), Heslop & ıythe (1910) and Dunham (1948) recorded the currences of glomerporphyritic aggregates and phenocrysts of more highly calcic plagioclase (bytownite–anorthite) within the Whin dykes and within some samples of the sill. The equigranular ophitic texture of the sill is consistent with simultaneous crystallization of plagioclase and clinopyroxene, followed by quartz and micropegmatite. This is confirmed by a one-atmosphere melting experiment upon a sample of the sill from Barrasford quarry, which showed simultaneous crystallization of plagioclase, augite and pigeonite at 1156 °C (Tilley, Thompson & Lovenbury, 1972).

4. Geochemistry

Published major element analyses of the Whin Sill complex and the contemporaneous Midland Valley tholeiite suite (e.g. Harrison, 1968; Macdonald *et al.* 1981; Dunham & Strasser-King, 1981) indicate that these rocks were derived from a relatively Fe-, Ti-rich quartz–tholeiite magma.

A major aim of this study was to assess the degree of compositional homogeneity of the magmas feeding the sill complex. The extreme possibilities are, firstly, that the mass was completely homogeneous and thus fed from a single source or, secondly, that it was heterogeneous, having been derived from a large number of compositionally distinct sources.

A problem in assessing these possibilities is that the sill was differentiated *in situ* after emplacement, the chemical variations resulting from this tending to mask any original compositional variations. Our collecting was concentrated, therefore, on the chilled margins, the assumption being that these would preserve most closely the magma composition at the time of emplacement. Seventeen samples were collected, to achieve coverage of the major outcrops, including five pairs of upper and lower contacts. Nine specimens of sill interiors were used to examine the effects of low-pressure fractionation. Samples of the associated dykes were collected from the four main dyke echelons, together with two contemporaneous dykes from Melmerby (Wadge, Harrison & Snelling, 1972; see Fig. 1). Due to the non-availability of chills at most localities, the dyke samples are generally interiors. We have assumed that compositional variations within these bodies are slight and that the samples are close to magmatic compositions. The similarity of the two analyses of the Hett dyke (HD1 and HD2, Table 1), collected *c.* 40 km apart, suggests that this assumption is valid.

All 35 samples were analysed for nine trace elements by standard methods at the University of Lancaster. However, in order to detect small variations within rocks of superficially similar composition, the trace element analyses were performed six times, and the results presented in Table 1 are the mean and standard deviation (1-sigma) of six determinations.

The trace element data confirm suspicions, raised by

Table 1. Trace element analyses for (*a*) chilled margins, (*b*) sill interiors and (*c*) dykes from the Whin Sill complex

	Rb	Ba	Sr	Th	Ce	Y	Zr	Nb	Ni
				(*a*) Chilled margins					
KQ1	25.0±0.5	171.6±0.7	34.7±1.6	5.3±0.8	50.9±1.1	25.5±0.9	207.2±1.0	20.1±0.3	54.5±0.9
M1	57.9±1.0	431.2±1.3	314.7±1.3	6.3±0.8	65.2±1.0	34.1±0.3	172.2±0.4	17.8±0.5	40.1±0.9
BC1	23.9±1.0	400.3±1.9	439.4±0.9	4.8±0.4	54.8±1.0	34.7±0.6	173.8±0.9	17.5±1.0	61.6±1.2
HB2	4.7±0.4	38.0±0.7	52.6±1.0	5.4±0.6	61.4±0.8	39.8±0.8	183.8±1.0	18.6±0.3	46.7±0.6
RQ1	24.3±0.6	239.5±1.0	380.8±0.8	3.7±0.8	42.4±0.9	29.5±0.9	150.2±0.5	15.6±0.7	29.7±1.0
WH1	23.5±0.7	351.3±1.3	344.3±0.7	5.8±0.8	56.5±0.7	24.6±0.7	170.0±1.1	17.5±0.9	35.6±1.1
WH2	24.1±0.3	387.2±1.3	367.2±1.0	6.8±0.5	61.5±1.7	28.2±0.5	180.3±0.9	18.1±0.4	25.0±0.5
BQ1	25.3±0.7	348.7±2.6	361.6±0.8	4.1±0.6	53.8±0.6	29.4±0.8	161.6±1.2	16.1±2.4	42.0±1.4
MH3	21.3±0.7	546.4±1.0	700.9±2.1	5.7±0.6	54.4±0.5	28.9±0.5	164.7±1.3	16.6±1.0	39.8±1.3
MH5	19.4±0.6	330.0±1.2	332.2±1.0	4.5±0.4	59.5±0.6	27.1±0.9	161.9±1.0	15.3±0.8	41.2±1.5
FH1	18.3±0.8	329.2±1.1	209.5±1.0	4.2±0.3	54.6±0.9	30.1±0.7	177.6±1.1	19.2±1.1	51.1±1.6
FH2	23.4±0.4	447.9±1.6	410.7±0.9	5.2±0.5	56.7±1.4	29.4±0.9	173.1±0.8	17.3±0.8	42.9±1.1
RE1	8.6±0.5	118.1±1.0	404.3±0.6	5.5±0.5	53.8±1.0	30.2±0.6	175.1±1.7	16.4±0.9	43.6±1.1
RE4	11.5±0.6	147.0±1.1	438.5±1.0	4.8±0.6	56.1±0.9	26.8±0.8	161.0±1.1	16.5±0.7	42.1±0.9
WST8	22.4±0.6	341.1±1.0	341.8±1.1	4.7±0.4	53.6±1.1	26.5±0.6	158.6±1.1	15.6±0.5	52.8±1.2
WSB8	21.8±0.9	258.7±1.1	339.2±1.1	4.9±0.3	51.8±1.0	26.8±0.6	159.6±0.7	15.7±0.5	38.8±0.9
HF1	10.1±0.3	163.1±0.9	326.1±0.9	4.7±0.5	49.4±1.7	28.9±0.9	161.3±0.9	16.7±0.8	41.9±1.0
				(*b*) Sill interiors					
KQ2	21.5±0.7	359.0±0.8	338.2±1.0	6.5±0.4	51.2±1.7	26.8±0.7	157.5±0.7	15.7±0.8	39.7±1.2
WH3	22.1±0.6	334.9±0.8	344.1±2.6	3.8±0.8	51.4±1.3	28.2±1.2	163.3±0.6	15.5±0.4	39.7±1.2
BQ2	23.5±1.5	335.3±1.1	348.2±1.2	5.3±0.3	57.7±1.1	26.6±1.2	157.4±0.4	15.3±0.5	37.6±1.1
MH1	28.4±1.1	486.1±1.3	364.5±0.6	4.0±0.4	55.1±1.0	27.8±1.1	159.9±1.3	14.2±0.8	38.8±1.1
MH2	22.1±0.6	451.3±1.3	358.1±0.9	3.3±0.4	51.3±1.2	28.5±1.0	162.9±1.2	15.6±0.8	39.5±1.0
MH6	28.2±1.0	388.6±1.1	335.9±0.9	4.6±0.6	65.1±2.0	28.8±0.5	162.3±1.1	16.3±0.6	43.8±1.0
LG1	20.0±0.7	367.2±1.6	351.1±0.8	6.2±0.3	57.5±0.6	27.6±1.4	161.6±1.8	13.9±0.7	39.8±0.8
RE2	16.4±0.4	276.2±1.4	357.7±1.7	5.5±0.4	55.2±1.3	27.8±0.4	161.8±0.9	16.9±0.6	40.8±1.4
AL.DOL.	21.6±0.4	404.8±1.5	363.9±1.2	3.0±0.5	53.2±1.2	28.3±0.9	160.9±0.6	15.0±0.4	39.1±0.9
				(*c*) Dykes					
HB1	12.9±0.5	279.7±1.3	446.3±1.2	2.7±0.4	47.7±1.2	28.1±0.7	150.9±0.8	16.0±0.8	36.4±0.8
BO1	19.3±0.9	302.6±1.3	337.3±1.3	4.5±0.6	41.8±1.2	29.9±0.6	151.4±0.9	15.9±0.8	27.5±1.3
SO1	19.9±0.5	376.4±0.9	383.9±1.3	6.1±0.4	62.3±2.1	28.4±0.8	159.3±1.0	15.2±0.6	40.7±0.9
HD1	20.1±0.7	326.5±0.8	340.6±0.9	5.6±0.5	56.5±1.2	27.2±0.5	161.8±0.7	14.7±0.9	38.5±0.9
HD2	19.9±0.4	354.1±1.1	358.2±1.1	3.2±0.4	48.8±1.4	26.5±0.8	154.9±0.9	15.5±0.9	39.3±0.8
WD1	28.8±0.7	392.1±1.5	382.2±1.4	4.7±0.3	59.4±0.6	27.5±0.5	160.8±1.2	15.5±0.5	40.1±1.1
SH18	6.5±0.5	184.3±1.2	270.9±1.2	2.8±0.2	33.9±1.1	33.0±0.6	124.1±1.1	6.8±1.0	72.4±1.2
SH19	4.8±0.7	95.4±1.1	235.0±1.1	2.4±0.4	28.2±0.9	32.1±0.9	129.8±0.5	7.5±0.7	65.4±1.5
3843	26.0±0.7	330±0.7	287.9±0.8	6.0±0.73	64.3±0.8	39.8±0.7	170.6±0.9	17.8±0.4	48.7±0.6

The data are means of 6 determinations ±1 standard deviation (1-sigma).

the petrographic evidence of low-temperature alteration, that certain elements, especially Ba, Rb and Sr, have been secondarily remobilized. Large variations in abundances in the chills at specific locations (e.g. MH3/MH5, FH1/FH2) and on a regional basis almost certainly reflect hydrothermal alteration. However, there is better agreement between Th, Ce, Y, Zr, Nb and Ni concentrations within the pairs of analysed chilled margins (Fig. 2a–e), confirming that those elements are generally stable, or immobile during low-temperature alteration of basaltic rocks (Pearce & Cann, 1973; Pearce, 1982, 1983). The concentrations in pairs of chilled margins provide clues about the likely relative element migrations. Thus for Zr–Nb, Zr–Y and Zr–Th the chilled margins show relatively small differences or show changes in abundance consistent with variation due to minor differences in hydration and/or carbonation of the chilled margin samples. Assuming that Zr is relatively immobile during such processes, the less systematic behaviour of Ce and Ni in relation to Zr in the chilled margins indicates minor migration (up to *c.* 10% of these elements within these samples.

The plots in Figure 2a–e may now be used to evaluate the relative chemical variations within the chilled margins and interiors of the Whin Sill, and the dykes, and their significance for sill emplacement.

5. Magma sources

(i) The chemical data may be used to evaluate the magmatic affinities of the Whin Sill magma. In this respect, the overall similarity in chemical composition of sill and dykes (excluding the Melmerby dykes) shown by Fig. 2 indicates that the association is likely to be co-magmatic. However, the precisely determined trace element data (Table 1 and Fig. 2) show that real trace element variations exist, particularly within the chilled margin samples. For example, the analysed samples have Zr/Nb = *c.* 10, but show small but significant variation of Zr/Nb between 9.25 (chilled margin, FH1) and 11.63 (sill interior, LG1). The significance of such variations is emphasized by fig. 2a, which shows that, at Zr = *c.* 160 (1-sigma precision = *c.* 1 ppm), Nb varies from *c.* 14 to 17 ppm (1-sigma precision < *c.* 1 ppm), and that at Nb = *c.* 16 ppm, Zr

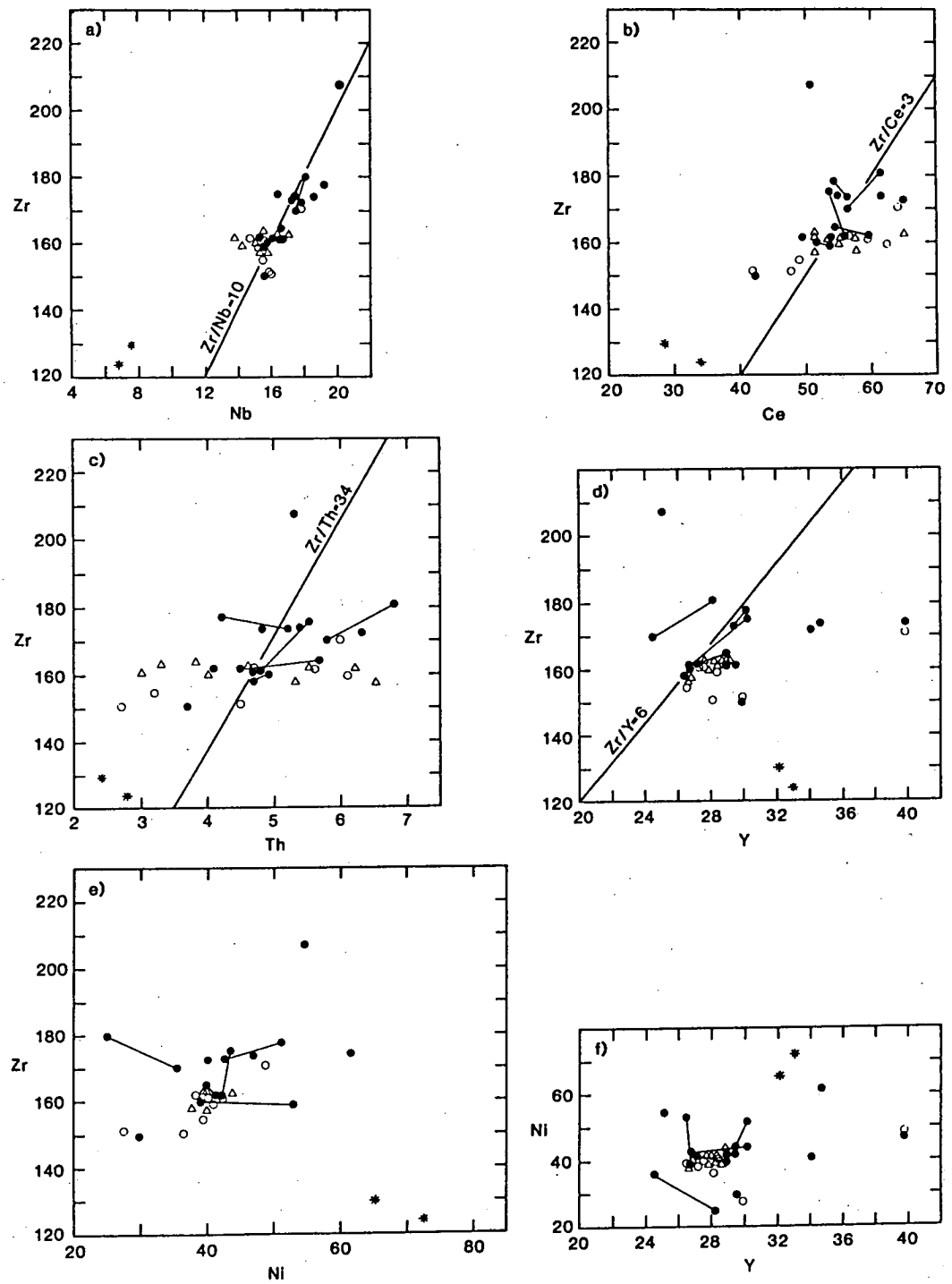

gure 2. Trace element variation diagrams for samples of chilled margins, sill interiors and dykes from the Whin Sill complex; Zr–Nb, (*b*) Zr–Ce, (*c*) Zr–Th, (*d*) Zr–Y, (*e*) Zr–Ni and (*f*) Ni–Y. Solid circles = chilled margins, open triangles = sill interiors d open circles = dyke samples. The Melmerby dyke samples are indicated by asterisks. Chilled margin samples from the ne location are joined by a line.

ries from *c.* 150 to 175 ppm. Further, the association high Zr with high Ni in certain chilled margin mples (Fig. 2e) is significant, as discussed below.

Before using these chemical data to evaluate magma urces for the Whin Sill complex we consider the ssibility of internal crystal settling/flowage differen- tion and/or multiple intrusion within the sill. though there is no evidence for crystal settling within the sill (see above and Dunham & Strasser-King, 1981, pp. 27–8), evidence of concentration and increasing size of phenocrysts towards the centre of the sill (e.g. Harrison, 1968; Dunham & Strasser-King, 1981, 1982) has been used to argue that 'flow differentiation could have been operative during the emplacement of the Whin Sill Complex' (Dunham & Strasser-King, 1981, p. 30). However, the chilled

margins are aphyric and phenocryst-poor, and margins at individual localities show significant variations in element concentrations and ratios (e.g. Zr and Nb), which are incompatible with variations in concentration of phenocrysts and microphenocrysts present within the emplaced magma. We therefore suggest that flow differentiation cannot explain chemical variations reported in Table 1, and that chemical variations between chilled margins and sill interiors (cf Fig. 2) are more likely to reflect multiple intrusion, as explained below.

The chemical data in Table 1 and Figure 2 therefore indicate that the sill complex was not fed by a simple homogeneous, parental magma. Neither is there a simple relationship between composition and either geographical distribution or stratigraphic level, as might result from the differentiation during cooling of a magma as it moved vertically and/or laterally from its source. Rather, the trace element evidence suggests the sill was fed by many pulses of magma showing compositional variations along short (of the order of a few kilometres) section of strike. The data are also consistent with the majority of the sill complex having been emplaced through dykes belonging to the dyke echelons described above.

(ii) The chilled margin samples with higher Zr, Nb and Ni cannot have been fed by magma represented by the dolerite present within the dykes. These samples may have been derived from a different magma batch emplaced at a slightly earlier time, through the major dyke echelons, or from magma emplaced through unidentified dykes (or other feeders) within the area of the Whin Sill.

(iii) The two Melmerby dykes (SH 18 and SH 19) are characterized by lower Rb, Ba, Sr, Th, Ce, Zr and Nb, and higher Ni than all other analysed samples. This is consistent with major element evidence (Wadge, Harrison & Snelling, 1972) of the relatively magnesian nature of these rocks. They appear to represent the least evolved magmas in the complex, and their compositions indicate that they cannot have acted as feeders to the sill at the present level of exposure, as suggested by Wadge, Harrison & Snelling (1972). The different ratios of Zr/Nb and Zr/Y to the other specimens (Figs 2*a* and *d*) further suggest that the Melmerby dykes are unlikely to be co-genetic with the rest of the complex (cf. Dunham & Strasser-King, 1981).

(iv) The chemical variations may reflect low- or high-pressure fractional crystallization or variation in mantle source composition. Although fractional crystallization is likely to be responsible for some of the chemical variations summarized in Figure 2, the wide variations in concentrations of Zr and Nb and low values of D^{Zr} and D^{Nb} for the possible and observed crystallizing phases (olivine, pyroxene and plagioclase, generally between 0.01 and 0.1; Pearce & Norry, 1979), indicate that these variations are unlikely to represent low-pressure fractional crystallization of such phases. High-pressure fractional crystallization of the Whin Sill parent magma may have involved garnet-bearing olivine and pyroxene assemblages such as those involved in eclogite fractionation (e.g. O'Hara, 1968). The high values of D^{Ni}_{ol} (*c.* 10), D^{Ni}_{pyx} (*c.* 2–4) and D^{Zr}_{ga} (*c.* 0.3) suggest that such fractional crystallization processes would generate a negative correlation of Ni–Zr. However, Figure 2*e* indicates that the chilled margins and dyke samples with high Zr are also characterized by high Ni (cf. Fig. 2). Accordingly, it is unlikely that the chemical variation observed within the Whin Sill has resulted from high-pressure fractional crystallization (cf. arguments in Macdonald *et al.* 1984).

The chemical variations are therefore interpreted in terms of small but significant variations in the composition of the mantle peridotite and/or small amounts of crustal contamination. Zr and Nb are known to be fractionated during the formation of subduction-related magmas (e.g. Pearce, 1982, 1983). Variations in mantle composition may therefore reflect migration and extraction of melts of different Zr/Nb ratios within the mantle during Caledonian subduction. Alternatively, small degrees of Caledonian partial melting of mantle rocks could have yielded magmas with high Zr and Nb contents and high Zr/Nb ratios. Some of the heterogeneity within the Whin Sill/dyke magmas may reflect small degrees of contamination by such crustal rocks. The relationship of high Zr and high Ni abundances in the Whin rocks seems to require that the more magnesian rocks had suffered the highest degrees of contamination. In either case it is significant that the chill (KQ1) and dyke (3843) samples with the highest Zr–Nb–Ni abundances both occur at the northern end of the complex, since this may indicate the regional scale of heterogeneity within the source of the Whin Sill/dyke magmas.

6. Petrogenesis

The data summarized above may be used to comment on the petrogenesis of the Whin Sill complex. The Whin Sill is an olivine-free quartz tholeiite with an evolved chemical composition (Mg number < 60) and a phenocryst mineralogy consistent with equilibration at crustal pressure and is therefore likely to be derived from more mafic olivine tholeiite magma (cf. Macdonald *et al.* 1981). Such a parent magma would experience fractional crystallization within the lower crust (cf. Cox, 1980) and during subsequent uprise through dyke feeders.

The fractional crystallization of olivine tholeiite magma within the crust may be evaluated in terms of the fosterite (Fo)–anorthite (An)–silica (Q) system (Presnall *et al.* 1979). At pressures appropriate to the

ver crust (*c.* 10 kbar), fractional crystallization of +enstatite (En) initially causes enrichment of the gma in An parallel to the plane of silica saturation tween An–En), but does not lead to the crossing of An–En plane until crystallization and removal of gioclase occurs (cf. Presnall *et al.* 1979). The occur-ce of glomerporphyritic aggregates and xenocrysts bytownite–anorthite composition (Heslop & ythe, 1910; Holmes & Harwood, 1928) indicates occurrence of a high-pressure fractional crystalli-ion event in the evolution of the Whin Sill complex. is process was proposed by Holmes & Harwood 28), who argued that 'the phenocrysts must have stallized with a magma of such composition that the gioclase could begin at An_{90}... the Whin sill gma, in which the plagioclase begins at about An_{70}, tself a product of a deep-seated partial differentia-n from a more mafic parental magma' (Holmes & rwood, 1928, p. 503).

The arguments and data above are consistent with occurrence of high-pressure fractional crystalliza-n. At pressures between 10 kbar and 1 atm the pansion of the olivine phase field into compositions re silica-rich than the An–En plane enables ctional crystallization of Fo alone to move the mposition of the magma to the Fo–En cotectic, lowed by fractional crystallization of En to move magma to the An–Fo–Q eutectic. Macdonald *et al.* 81) reported olivine nodules from Scottish dykes ich are part of the same province as the Whin Sill. actional crystallization of An + Fo may then cause magma to move to the 1 atm ternary En–An–Q tectic. With the addition of diopside (Di) this tectic composition is equivalent to the mineralogy of Whin sill. Consideration of the relative volumes of lt and crystals during such a fractionation scheme dicates that production of Whin Sill quartz tholeiite m parental olivine tholeiite may involve up to 80% ctional crystallization (cf. Morse, 1980, p. 173). mulates from such fractionation may be underplated the base of the crust as proposed in the model of x (1980) and contained within dykes emplaced in lower crust.

We see the Whin Sill complex, therefore, as the oduct of extensive polybaric fractional crystal-ation of many batches of mantle-derived olivine oleiite magma. Such magma may have been rived by partial melting of compositionally terogeneous mantle peridotite, and/or may have perienced minor crustal contamination during ascent thin the lower crust. The magmas rose high into the ust (< 1 km depth) and then flowed down-dip to atigraphic levels controlled by magma density rancis, 1982), where the various pulses aggregated. nvection within the expanding mass, associated th *in situ* differentiation, tended to mask the primary gmatic differences now best recorded in the chilled rgins.

Acknowledgements. We thank Dr J. W. Gaskarth for providing several sill and dyke samples and Dr B. A. O. Randall for providing the sample of the Holy Island dyke. This study was financed by the University of Lancaster and the Open University. We are grateful to the referees and Dr R. S. J. Sparks for constructive comments on the manuscript, to Kim Gurney and Marilyn Leggett for typing assistance, and to John Taylor for drawing the diagrams.

References

ALLPORT, S. 1874. On the microscopic structure and composition of British Carboniferous dolerites. *Quarterly Journal of the Geological Society of London* **30**, 529–67.

BURGESS, I. C. & HOLLIDAY, D. W. 1979. *Geology of the country around Brough-under-Stainmore*. Memoir. Geological Survey of Great Britain. 131 pp.

COX, K. G. 1980. A model for flood basalt volcanism. *Journal of Petrology* **21**, 629–50.

DUNHAM, K. C. 1932. Quartz–dolerite pebbles (Whin Sill) in the Upper Brockram. *Geological Magazine* **69**, 425–7.

DUNHAM, K. C. 1948. *The geology of the Northern Pennine Orefield*, I. Memoir. Geological Survey of Great Britain. 457 pp.

DUNHAM, A. C. & KAYE, M. J. 1965. The petrology of the Little Whin Sill, County Durham. *Proceedings of the Yorkshire Geological Society* **35**, 229–76.

DUNHAM, A. C., COPLEY, P. A. & STRASSER-KING, V. H. 1972. Submicroscopic exsolution lamellae in pyroxenes in the Whin Sill, northern England. *Contributions to Mineralogy and Petrology* **37**, 211–20.

DUNHAM, A. C. & STRASSER-KING, V. H. 1981. *Petrology of the Great Whin Sill in the Throckley borehole, Northumberland*. Report no. 81/4, Institute of Geological Sciences.

DUNHAM, A. C. & STRASSER-KING, V. H. 1982. Late Carboniferous intrusions of northern Britain. In *Igneous Rocks of the British Isles* (ed. D. S. Sutherland), pp. 277–83. Chichester: Wiley.

FITCH, F. J. & MILLER, J. A. 1967. The age of the Whin Sill. *Geological Journal* **5**, 233–50.

FRANCIS, E. H. 1982. Magma and sediment. I. Emplacement mechanism of late Carboniferous tholeiite sills in northern Britain. *Journal of the Geological Society of London* **139**, 1–20.

HARRISON, R. K. 1968. Petrology of the Little and Great Whin Sills in the Woodland borehole, Co. Durham. *Bulletin of the Geological Survey of Great Britain* **28**, 38–54.

HESLOP, M. K. & SMYTHE, J. A. 1910. On the dyke at Crookdene (Northumberland) and its relationship to the Collywell, Tynemouth, and Morpeth dykes. *Quarterly Journal of the Geological Society of London* **66**, 1–18.

HOLMES, A. & HARWOOD, H. F. 1928. The age and composition of the Whin Sill and the related dykes of the north of England. *Mineralogical Magazine* **21**, 493–542.

INESON, P. R. 1972. Alteration of the Whin Sill adjacent to baryte–witherite mineralisation, Settlingstones mine, Northumberland. *Transactions of the Institute of Mining and Metallurgy* **81**, B 67–72.

MACDONALD, R., GOTTFRIED, D., FARRINGTON, M. J., BROWN, F. W. & SKINNER, N. G. 1981. Geochemistry of a continental tholeiite suite: late Palaeozoic quartz

dolerite dykes of Scotland. *Transactions of the Royal Society of Edinburgh; Earth Science* **72**, 57–74.

MACDONALD, R., GASS, K. N., THORPE, R. S. & GASS, I. G. 1984. Geochemistry and petrogenesis of the Derbyshire Carboniferous basalts. *Journal of the Geological Society of London* **141**, 147–59.

MORSE, S. A. 1980. *Basalts and Phase Diagrams*. Heidelberg: Springer. 493 pp.

O'HARA, M. J. 1968. The bearing of phase equilibrium studies in synthetic and natural systems on the origin and evolution of basic and ultra-basic rocks. *Earth Science Reviews* **4**, 69–133.

PEARCE, J. A. 1982. Trace element characteristics of lavas from destructive plate boundaries. In *Andesites* (ed. R. S. Thorpe), pp. 525–48. Chichester: Wiley.

PEARCE, J. A. 1983. Role of the sub-continental lithosphere in magma genesis at active continental margins. In *Continental Basalts and Mantle Xenoliths* (ed. C. J. Hawkesworth & M. J. Norry), pp. 230–49. Shiva Publishing Limited.

PEARCE, J. A. & CANN, J. R. 1973. Tectonic setting of basic volcanic rocks determined using trace element analyses. *Earth and Planetary Science Letters* **19**, 290–300.

PEARCE, J. A. & NORRY, M. J. 1979. Petrogenetic implications of Ti, Zr, Y and Nb variations in volcanic rocks. *Contributions to Mineralogy and Petrology* **69**, 33–47.

PRESNALL, D. C., DIXON, J. R., O'DONNEL, T. H. & DIXON, S. A. 1979. Generation of mid-ocean ridge tholeites. *Journal of Petrology* **20**, 3–36.

RANDALL, B. A. O. & FARMER, N. 1970. The Holy Island dyke. *Transactions of the Natural History Society of Northumberland* **17**, 79–91.

RANDALL, B. A. O. 1980. Lower Carboniferous igneous rocks. In *The Geology of Northeast England* (ed. D. A. Robson), pp. 65–75. The Natural History Society of Northumbria.

RIDD, M. F., WALKER, D. B. & JONES, J. M. 1970. A deep borehole at Harton on the margin of the Northumbrian trough. *Proceedings of the Yorkshire Geological Society* **38**, 75–103.

TILLEY, C. E., THOMPSON, R. N. & LOVENBURY, P. A. 1972. Melting relations of some oceanic basalts. *Geological Journal* **8**, 59–64.

TOMKEIEFF, S. I. 1929. A contribution to the petrology of the Whin Sill. *Mineralogical Magazine* **22**, 100–20.

WADGE, A. J., HARRISON, R. K. & SNELLING, N. J. 1972. Olivine–dolerite intrusions near Melmerby, Cumberland, and their age determination by the potassium–argon method. *Proceedings of the Yorkshire Geological Society* **39**, 59–70.